Volume 76,2025

Neutrosophic Sets and Systems

An International Journal in Information Science and Engineering

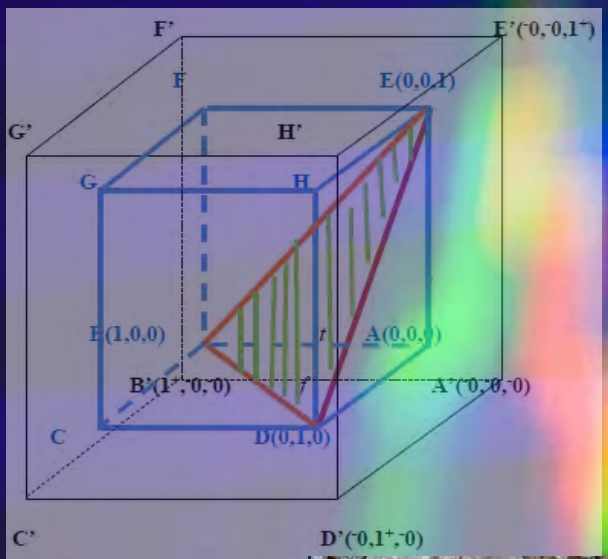

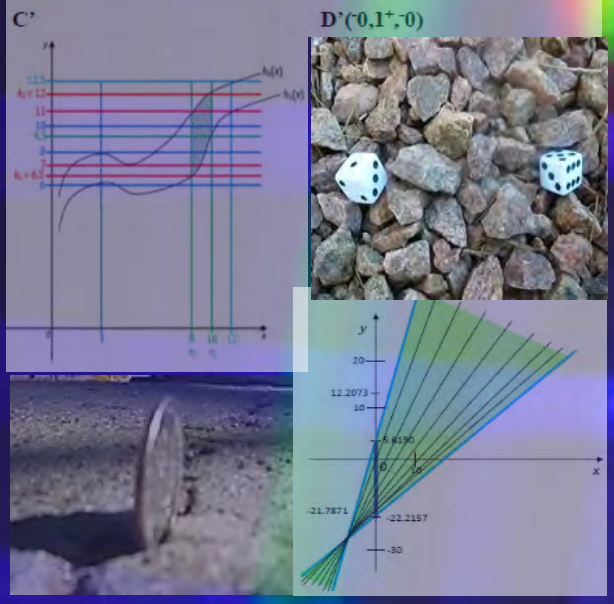

Editors-in-Chief
Florentin Smarandache
Mohamed Abdel-Baset
Maikel Leyva-Vázquez

ISSN 2331-6055 (Print)
ISSN 2331-608X (Online)

<A> <neutA> <antiA>

Neutrosophic Science
International Association (NSIA)

ISSN 2331-6055 (print) *ISSN 2331-608X (online)*

Neutrosophic Sets and Systems

An International Journal in Information Science and Engineering

University of New Mexico

ISSN 2331-6055 (print) ISSN 2331-608X (online)

University of New Mexico

Neutrosophic Sets and Systems

An International Journal in Information Science and Engineering

Copyright Notice

Copyright @ Neutrosophics Sets and Systems

All rights reserved. The authors of the articles do hereby grant Neutrosophic Sets and Systems non-exclusive, worldwide, royalty-free license to publish and distribute the articles in accordance with the Budapest Open Initiative: this means that electronic copying, distribution and printing of both full-size version of the journal and the individual papers published therein for non-commercial, academic or individual use can be made by any user without permission or charge. The authors of the articles published in Neutrosophic Sets and Systems retain their rights to use this journal as a whole or any part of it in any other publications and in any way they see fit. Any part of Neutrosophic Sets and Systems howsoever used in other publications must include an appropriate citation of this journal.

Information for Authors and Subscribers

*"*Neutrosophic Sets and Systems*"* has been created for publications on advanced studies in neutrosophy, neutrosophic set, neutrosophic logic, neutrosophic probability, neutrosophic statistics that started in 1995 and their applications in any field, such as the neutrosophic structures developed in algebra, geometry, topology, etc.

The submitted papers should be professional, in good English, containing a brief review of a problem and obtained results.

Neutrosophy is a new branch of philosophy that studies the origin, nature, and scope of neutralities, as well as their interactions with different ideational spectra.

This theory considers every notion or idea <A> together with its opposite or negation <antiA> and with their spectrum of neutralities <neutA> in between them (i.e. notions or ideas supporting neither <A> nor <antiA>). The <neutA> and <antiA> ideas together are referred to as <nonA>.

Neutrosophy is a generalization of Hegel's dialectics (the last one is based on <A> and <antiA> only).

According to this theory every idea <A> tends to be neutralized and balanced by <antiA> and <nonA> ideas - as a state of equilibrium.

In a classical way <A>, <neutA>, <antiA> are disjoint two by two. But, since in many cases the borders between notions are vague, imprecise, Sorites, it is possible that <A>, <neutA>, <antiA> (and <nonA> of course) have common parts two by two, or even all three of them as well.

Neutrosophic Set and *Neutrosophic Logic* are generalizations of the fuzzy set and respectively fuzzy logic (especially of intuitionistic fuzzy set and respectively intuitionistic fuzzy logic). In neutrosophic logic a proposition has a degree of truth (*T*), a degree of indeterminacy (*I*), and a degree of falsity (*F*), where *T, I, F* are standard or non-standard subsets of $]^{-}0, 1^{+}[$.

Neutrosophic Probability is a generalization of the classical probability and imprecise probability.

Neutrosophic Statistics is a generalization of the classical statistics.

What distinguishes the neutrosophics from other fields is the <neutA>, which means neither <A> nor <antiA>.

<neutA>, which of course depends on <A>, can be indeterminacy, neutrality, tie game, unknown, contradiction, ignorance, imprecision, etc.

All submissions should be designed in MS Word format using our template file:

http://fs.unm.edu/NSS/NSS-paper-template.doc.

A variety of scientific books in many languages can be downloaded freely from the Digital Library of Science:

http://fs.unm.edu/ScienceLibrary.htm.

To submit a paper, mail the file to the Editor-in-Chief. To order printed issues, contact the Editor-in-Chief. This journal is non-commercial, academic edition. It is printed from private donations.

Information about the neutrosophics you get from the UNM website:

http://fs.unm.edu/neutrosophy.htm. The

home page of the journal is accessed on

http://fs.unm.edu/NSS.

ISSN 2331-6055 (print) ISSN 2331-608X (online)

University of New Mexico

Neutrosophic Sets and Systems

An International Journal in Information Science and Engineering

**** NSS has been accepted by SCOPUS. Starting with Vol. 19, 2018, the NSS articles are indexed in Scopus.**

NSS ABSTRACTED/INDEXED IN
SCOPUS,
Google Scholar,
Google Plus,
Google Books,
EBSCO,
Cengage Thompson Gale (USA),
Cengage Learning (USA),
ProQuest (USA),
Amazon Kindle (USA),
University Grants Commission (UGC) - India,
DOAJ (Sweden),
International Society for Research Activity (ISRA),
Scientific Index Services (SIS),
Academic Research Index (ResearchBib),
Index Copernicus (European Union),
CNKI (Tongfang Knowledge Network Technology Co.,
Beijing, China),
Baidu Scholar (China),
Redalyc - Universidad Autonoma del Estado de Mexico (IberoAmerica),
Publons,
Scimago, etc.

Google Dictionaries have translated the neologisms "**neutrosophy**" (1) and"**neutrosophic**" (2), coined in 1995 for the first time, into about 100 languages.
FOLDOC Dictionary of Computing (**1, 2**), Webster
Dictionary (**1, 2**), Wordnik (**1**),Dictionary.com, The Free
Dictionary (**1**), Wiktionary (**2**), YourDictionary (**1, 2**),OneLook Dictionary (**1, 2**), Dictionary / Thesaurus (**1**), Online Medical Dictionary (**1,2**), Encyclopedia (**1, 2**), Chinese Fanyi Baidu Dictionary (**2**), Chinese Youdao Dictionary (**2**) etc. have included these scientific neologisms.

Copyright © Neutrosophic Sets and Systems, 2025

ISSN 2331-6055 (print) NSS **Editorial Board** *ISSN 2331-608X (online)*

University of New Mexico

Editors-in-Chief

Prof. Emeritus Florentin Smarandache, PhD, Postdoc, Mathematics, Physical and Natural Sciences Division, University of New Mexico, Gallup Campus, NM 87301, USA, Email: smarand@unm.edu.

Dr. Mohamed Abdel-Baset, Head of Department of Computer Science, Faculty of Computers and Informatics, Zagazig University, Egypt, Email: mohamedbasset@ieee.org.

Prof. Dr. Maikel Leyva-Vázquez, Instituto Superior Tecnológico Bolivariano de Tecnología, Ecuador: maikel.leyvav@ug.edu.ec.

Associate Editors

Dr. Said Broumi, Laboratory of Information Processing, Faculty of Science Ben M'Sik, University of Hassan II, Casablanca, Morocco, Email: s.broumi@flbenmsik.ma.

Assoc. Prof. Alok Dhital, Mathematics, Physical and Natural Sciences Division, University of New Mexico, Gallup Campus, NM 87301, USA, Email: adhital@unm.edu.

Dr. S. A. Edalatpanah, Department of Applied Mathematics, Ayandegan Institute of Higher Education, Tonekabon, Iran, Email: saedalatpanah@gmail.com.

Charles Ashbacker, Charles Ashbacher Technologies, Box 294, 118 Chaffee Drive, Hiawatha, IA 52233, United States, Email: cashbacher@prodigy.net.

Prof. Dr. Xiaohong Zhang, Department of Mathematics, Shaanxi University of Science &Technology, Xian 710021, China, Email: zhangxh@shmtu.edu.cn.

Prof. Dr. W. B. Vasantha Kandasamy, School of Computer Science and Engineering, VIT, Vellore 632014, India, Email: vasantha.wb@vit.ac.in.

Editors

Yanhui Guo, University of Illinois at Springfield, One University Plaza, Springfield, IL 62703, United States,Email: yguo56@uis.edu.

Giorgio Nordo, MIFT - Department of Mathematical and Computer Science, Physical Sciences and Earth Sciences, Messina University, Italy,Email: giorgio.nordo@unime.it.

Mohamed Elhoseny, American University in the Emirates,Dubai,UAE,
Email: mohamed.elhoseny@aue.ae.

Le Hoang Son, VNU Univ. of Science, Vietnam National Univ. Hanoi, Vietnam, Email: sonlh@vnu.edu.vn.

Huda E. Khalid, Head of Scientific Affairs and Cultural Relations Department, Nineveh Province, Telafer University, Iraq, Email: dr.huda-ismael@uotelafer.edu.iq.

A. A. Salama, Dean of the Higher Institute of Business and Computer Sciences, Arish, Egypt, Email: ahmed_salama_2000@sci.psu.edu.eg.

Young Bae Jun, Gyeongsang National University, South Korea, Email: skywine@gmail.com.

Yo-Ping Huang, Department of Computer Science and Information, Engineering National Taipei University, New Taipei City, Taiwan, Email: yphuang@ntut.edu.tw.

Tarek Zayed, Department of Building and Real Estate, The Hong Kong Polytechnic University, Hung Hom, 8 Kowloon, Hong Kong, China, Email: tarek.zayed@polyu.edu.hk.

Vakkas Ulucay, Kilis 7 Aralık University, Turkey, Email: vulucay27@gmail.com.

Peide Liu, Shandong University of Finance and Economics, China, Email: peide.liu@gmail.com.

Jun Ye, Ningbo University, School of Civil and Environmental Engineering, 818 Fenghua Road, Jiangbei District, Ningbo City, Zhejiang Province, People's Republic of China, Email: yejun1@nbu.edu.cn.

Memet Şahin, Department of Mathematics, Gaziantep University, Gaziantep 27310, Turkey, Email: mesahin@gantep.edu.tr.

Muhammad Aslam & Mohammed Alshumrani, King Abdulaziz Univ., Jeddah, Saudi Arabia, Emails magmuhammad@kau.edu.sa, maalshmrani @kau.edu.sa.

Mutaz Mohammad, Department of Mathematics, Zayed University, Abu Dhabi 144534, United Arab Emirates. Email: Mutaz.Mohammad@zu.ac.ae.

Abdullahi Mohamud Sharif, Department of Computer Science, University of Somalia, Makka Al-mukarrama Road, Mogadishu, Somalia, Email: abdullahi.shariif@uniso.edu.so.

.

Copyright © Neutrosophic Sets and Systems, 2025

Katy D. Ahmad, Islamic University of Gaza, Palestine,Email: katyon765@gmail.com.
NoohBany Muhammad, American University of Kuwait,Kuwait,Email: noohmuhammad12@gmail .com.
Soheyb Milles, Laboratory of Pure and Applied Mathematics, University of Msila, Algeria, Email: soheyb.milles@univ-msila.dz.
Pattathal Vijayakumar Arun, College of Science and Technology,Phuentsholing,Bhutan,
Email: arunpv2601@gmail.com.
Endalkachew Teshome Ayele, Department of Mathematics, Arbaminch University, Arbaminch, Ethiopia,Email: endalkachewteshome83@yahoo. com.
A. Al-Kababji, College of Engineering, Qatar University,Doha,Qatar,
Email: ayman.alkababji@ieee.org.
Xindong Peng, School of Information Science and Engineering, Shaoguan University, Shaoguan 512005, China, Email: 952518336@qq.com.
Xiao-Zhi Gao, School of Computing, University of Eastern Finland, FI-70211 Kuopio, Finland, xiao-zhi.gao@uef.fi.
Madad Khan, Comsats Institute of Information Technology,Abbottabad,Pakistan,
Email: madadmath@yahoo.com.
G. Srinivasa Rao, Department of Statistics, The University of Dodoma, Dodoma, PO. Box: 259, Tanzania,Email: gaddesrao@gmail.com.
Ibrahim El-henawy, Faculty of Computers and Informatics,ZagazigUniversity,Egypt,
Email: henawy2000@yahoo.com.
Muhammad Saeed, Department of Mathematics, University of Management and Technology, Lahore, Pakistan,
Email: muhammad.saeed@umt.edu.pk.
A. A. A. Agboola, Federal University of Agriculture, Abeokuta, Nigeria,
Email: agboolaaaa@funaab.edu.ng.
Abduallah Gamal, Faculty of Computers and Informatics, Zagazig University, Egypt,
Email: abduallahgamal@zu.edu.eg.
Ebenezer Bonyah, Department of Mathematics Education, Akenten Appiah-Menka University of Skills Training and Entrepreneurial Development, Kumasi 00233, Ghana,
Email: ebbonya@gmail.com.
Roan Thi Ngan, Hanoi University of Natural Resources and Environment, Hanoi, Vietnam,
Email: rtngan@hunre.edu.vn.
Sol David Lopezdomínguez Rivas, Universidad Nacional de Cuyo, Argentina.
Email: sol.lopezdominguez@fce.uncu.edu.ar.
Maikel Yelandi Leyva Vázquez, Universidad Regional Autónoma de los Andes (UNIANDES), Avenida Jorge Villegas, Babahoyo, Los Ríos, Ecuador,
Email: ub.c.investigacion@uniandes.edu.ec.
Arlen Martín Rabelo, Exxis, Avda. Aviadores del Chaco N° 1669 c/ San Martin, Edif. Aymac I, 4to. piso, Asunción, Paraguay,
Email: arlen.martin@exxis-group.com.
Carlos Granados, Estudiante de Doctorado en Matematicas, Universidad del Antioquia, Medellın, Colombia,
Email: carlosgranadosortiz@outlook.es.
Tula Carola Sanchez Garcia, Facultad de Educacion de la Universidad Nacional Mayor de San Marcos, Lima, Peru,
Email: tula.sanchez1@unmsm.edu.pe.
Carlos Javier Lizcano Chapeta, Profesor - Investigador de pregrado y postgrado de la Universidad de Los Andes, Mérida 5101, Venezuela, Email: lizcha_4@hotmail.com.
Noel Moreno Lemus, Procter & Gamble International Operations S.A., Panamá,
Email: nmlemus@gmail.com.
Asnioby Hernandez Lopez, Mercado Libre, Montevideo, Uruguay.
Email: asnioby.hernandez@mercadolibre.com.
Muhammad Akram, University of the Punjab, New Campus, Lahore, Pakistan,
Email: m.akram@pucit.edu.pk.
Tatiana Andrea Castillo Jaimes, Universidad de Chile, Departamento de Industria, Doctorado en Sistemas de Ingeniería, Santiago de Chile, Chile,
Email: tatiana.a.castillo@gmail.com.
Irfan Deli, Muallim Rifat Faculty of Education, Kilis 7 Aralik University, Turkey,
Email: irfandeli@kilis.edu.tr.
Ridvan Sahin, Department of Mathematics, Faculty of Science, Ataturk University, Erzurum 25240, Turkey, Email: mat.ridone@gmail.com.
Ibrahim M. Hezam, Department of computer, Faculty of Education, Ibb University, Ibb City,

Yemen, Email: ibrahizam.math@gmail.com.
Moddassir khan Nayeem, Department of Industrial and Production Engineering, American International University-Bangladesh, Bangladesh; nayeem@aiub.edu.
Aiyared Iampan, Department of Mathematics, School of Science, University of Phayao, Phayao 56000, Thailand, Email: aiyared.ia@up.ac.th.
Ameirys Betancourt-Vázquez, 1 Instituto Superior Politécnico de Tecnologias e Ciências (ISPTEC), Luanda, Angola, Email: ameirysbv@gmail.com.
H. E. Ramaroson, University of Antananarivo, Madagascar, Email: erichansise@gmail.com.
G. Srinivasa Rao, Department of Mathematics and Statistics, The University of Dodoma, Dodoma PO. Box: 259, Tanzania.
Onesfole Kuramaa, Department of Mathematics, College of Natural Sciences, Makerere University, P.O Box 7062, Kampala, Uganda, Email: onesfole.kurama@mak.ac.ug.
Karina Pérez-Teruel, Universidad Abierta para Adultos (UAPA), Santiago de los Caballeros, República Dominicana, Email: karinaperez@uapa.edu.do.
Neilys González Benítez, Centro Meteorológico Pinar del Río, Cuba, Email: neilys71@nauta.cu.
Jesus Estupinan Ricardo, Centro de Estudios para la Calidad Educativa y la Investigation Cinetifica, Toluca,Mexico,Email: jestupinan2728@gmail.com
Victor Christianto, Malang Institute of Agriculture (IPM), Malang, Indonesia, Email: victorchristianto@gmail.com.
Wadei Al-Omeri, Department of Mathematics, Al-Balqa Applied University, Salt 19117, Jordan, Email: wadeialomeri@bau.edu.jo.
Ganeshsree Selvachandran, UCSI University, Jalan Menara Gading, Kuala Lumpur, Malaysia, Email: Ganeshsree@ucsiuniversity.edu.my.
Ilanthenral Kandasamy, School of Computer Science and Engineering (SCOPE), Vellore Institute of Technology (VIT), Vellore 632014, India, Email: ilanthenral.k@vit.ac.in
Kul Hur, Wonkwang University, Iksan, Jeollabukdo, South Korea, Email: kulhur@wonkwang.ac.kr.
Kemale Veliyeva & Sadi Bayramov, Department of Algebra and Geometry, Baku State University, 23 Z. Khalilov Str., AZ1148, Baku, Azerbaijan, Email: kemale2607@mail.ru,
Email: baysadi@gmail.com.
Irma Makharadze & Tariel Khvedelidze, Ivane Javakhishvili Tbilisi State University, Faculty of Exact and Natural Sciences, Tbilisi, Georgia.
Inayatur Rehman, College of Arts and Applied Sciences, Dhofar University Salalah, Oman, Email: irehman@du.edu.om.
Mansour Lotayif, College of Administrative Sciences, Applied Science University, P.O. Box 5055, East Al-Ekir, Kingdom of Bahrain.
Riad K. Al-Hamido, Math Department, College of Science, Al-Baath University, Homs, Syria, Email: riad-hamido1983@hotmail.com.
Saeed Gul, Faculty of Economics, Kardan University, Parwan-e- Du Square, Kabil, Afghanistan, Email: s.gul@kardan.edu.af.
Faruk Karaaslan, Çankırı Karatekin University, Çankırı, Turkey, Email: fkaraaslan@karatekin.edu.tr.
Morrisson Kaunda Mutuku, School of Business, Kenyatta University, Kenya
Surapati Pramanik, Department of Mathematics, Nandalal Ghosh B T College, India, Email: drspramanik@isns.org.in.
Suriana Alias, Universiti Teknologi MARA (UiTM) Kelantan, Campus Machang, 18500 Machang, Kelantan, Malaysia, Email: suria588@kelantan.uitm.edu.my.
Arsham Borumand Saeid, Dept. of Pure Mathematics, Faculty of Mathematics and Computer, Shahid Bahonar University of Kerman, Kerman, Iran, Email: arsham@uk.ac.ir.
Ahmed Abdel-Monem, Department of Decision support, Zagazig University, Egypt, Email: aabdelmounem@zu.edu.eg.
Çağlar Karamasa, Anadolu University, Faculty of Business,
Turkey, Email: ckaramasa@anadolu.edu.tr.
Mohamed Talea, Laboratory of Information Processing, Faculty of Science Ben M'Sik, Morocco, Email: taleamohamed@yahoo.fr.
Assia Bakali, Ecole Royale Navale, Casablanca, Morocco, Email: assiabakali@yahoo.fr.
V.V. Starovoytov, The State Scientific Institution «The United Institute of Informatics Problems of the National Academy of Sciences of Belarus»,

Copyright © Neutrosophic Sets and Systems, 2025

Minsk, Belarus, Email: ValeryS@newman.bas-net.by.
E.E. Eldarova, L.N. Gumilyov Eurasian National University, Nur-Sultan, Republic of Kazakhstan, Email: Doctorphd_eldarova@mail.ru. Mukhamed iyeva Dilnoz Tulkunovna & Egamberdiev Nodir Abdunazarovich, Science and innovation center for information and communication technologies, Tashkent University of Information Technologies (named after Muhammad Al-Khwarizmi), Uzbekistan.
Mohammad Hamidi, Department of Mathematics, Payame Noor University (PNU), Tehran, Iran. Email: m.hamidi@pnu.ac.ir.
Lemnaouar Zedam, Department of Mathematics, Faculty of Mathematics and Informatics, University Mohamed Boudiaf, M'sila, Algeria, Email: l.zedam@gmail.com.
M. Al Tahan, Department of Mathematics, Lebanese International University, Bekaa, Lebanon, Email: madeline.tahan@liu.edu.lb.
Mohammad Abobala, Tishreen University, Faculty of Science, Department of Mathematics, Lattakia, Syria,Email" mohammad.abobala@tishreen.edu.sy
Rafif Alhabib, AL-Baath University, College of Science, Mathematical Statistics Department, Homs, Syria, Email: ralhabib@albaath-univ.edu.sy.
R. A. Borzooei, Department of Mathematics, Shahid Beheshti University, Tehran, Iran, borzooei@hatef.ac.ir.
Selcuk Topal, Mathematics Department, Bitlis Eren University, Turkey, Email: s.topal@beu.edu.tr.
Qin Xin, Faculty of Science and Technology, University of the Faroe Islands, Tórshavn, 100, Faroe Islands.
Sudan Jha, Pokhara University,Kathmandu, Nepal, Email: jhasudan@hotmail.com.
Mimosette Makem and Alain Tiedeu, Signal, Image and Systems Laboratory, Dept. of Medical and Biomedical Engineering, Higher Technical Teachers' Training College of EBOLOWA, PO Box 886, University of Yaoundé, Cameroon, E-mail: alain_tiedeu@yahoo.fr.
Mujahid Abbas, Department of Mathematics and Applied Mathematics, University of Pretoria Hatfield 002, Pretoria, South Africa, Email: mujahid.abbas@up.ac.za.
Željko Stević, Faculty of Transport and Traffic Engineering Doboj, University of East Sarajevo, Lukavica, East Sarajevo, Bosnia and Herzegovina, Email: zeljko.stevic@sf.ues.rs.ba.
Michael Gr. Voskoglou, Mathematical Sciences School of Technological Applications, Graduate Technological Educational Institute of Western Greece, Patras, Greece, Email: voskoglou@teiwest.gr.
Saeid Jafari, College of Vestsjaelland South, Slagelse, Denmark, Email: sj@vucklar.dk.
Angelo de Oliveira, Ciencia da Computacao, Universidade Federal de Rondonia, Porto Velho - Rondonia, Brazil, Email: angelo@unir.br.
Valeri Kroumov, Okayama University of Science, Okayama, Japan, Email: val@ee.ous.ac.jp.
Rafael Rojas, Universidad Industrial de Santander, Bucaramanga, Colombia, Email: rafael2188797@correo.uis.edu.co.
Walid Abdelfattah, Faculty of Law, Economics and Management, Jendouba, Tunisia, Email: abdelfattah.walid@yahoo.com.
Akbar Rezaei, Department of Mathematics, Payame Noor University, P.O.Box 19395-3697, Tehran, Iran, Email: rezaei@pnu.ac.ir.
John Frederick D. Tapia, Chemical Engineering Department, De La Salle University - Manila, 2401 Taft Avenue, Malate, Manila, Philippines, Email: john.frederick.tapia@dlsu.edu.ph.
Darren Chong, independent researcher, Singapore, Email: darrenchong2001@yahoo.com.sg.
Galina Ilieva, Paisii Hilendarski, University of Plovdiv, 4000 Plovdiv, Bulgaria, Email: galili@uni-plovdiv.bg.
Paweł Pławiak, Institute of Teleinformatics, Cracow University of Technology, Warszawska 24 st., F-5, 31-155 Krakow, Poland, Email: plawiak@pk.edu.pl.
E. K. Zavadskas, Vilnius Gediminas Technical University, Vilnius, Lithuania, Email: edmundas.zavadskas@vgtu.lt.
Darjan Karabasevic, University Business Academy, Novi Sad, Serbia, Email: darjan.karabasevic@mef.edu.rs.
Dragisa Stanujkic, Technical Faculty in Bor, University of Belgrade, Bor, Serbia, Email: dstanujkic@tfbor.bg.ac.rs.
Katarina Rogulj, Faculty of Civil Engineering,

Architecture and Geodesy, University of Split, Matice Hrvatske 15, 21000 Split, Croatia; Email: katarina.rogulj@gradst.hr.
Luige Vladareanu, Romanian Academy, Bucharest, Romania, Email: luigiv@arexim.ro.
Hashem Bordbar, Center for Information Technologies and Applied Mathematics, University of Nova Gorica, Slovenia, Email: Hashem.Bordbar@ung.si.
N. Smidova, Technical University of Kosice, SK 88902, Slovakia, Email: nsmidova@yahoo.com.
Quang-Thinh Bui, Faculty of Electrical Engineering and Computer Science, VŠB-Technical University of Ostrava, Ostrava-Poruba, Czech Republic, Email: qthinhbui@gmail.com.
Mihaela Colhon & Stefan Vladutescu, University of Craiova, Computer Science Department, Craiova, Romania,Emails: colhon.mihaela@ucv.ro, vladutescu.stefan@ucv.ro.
Philippe Schweizer, Independent Researcher, Av. de Lonay 11, 1110 Morges, Switzerland, Email: flippe2@gmail.com.
Madjid Tavanab, Business Information Systems Department, Faculty of Business Administration and Economics University of Paderborn, D-33098 Paderborn, Germany, Email: tavana@lasalle.edu.
Rasmus Rempling, Chalmers University of Technology, Civil and Environmental Engineering, Structural Engineering, Gothenburg, Sweden.
Fernando A. F. Ferreira, ISCTE Business School, BRU-IUL, University Institute of Lisbon, Avenida das Forças Armadas, 1649-026 Lisbon, Portugal, Email: fernando.alberto.ferreira@iscte-iul.pt.
Julio J. Valdés, National Research Council Canada, M-50, 1200 Montreal Road, Ottawa, Ontario K1A 0R6, Canada, Email: julio.valdes@nrc-cnrc.gc.ca.
Tieta Putri, College of Engineering Department of Computer Science and Software Engineering, University of Canterbury, Christchurch, New Zeeland.
Phillip Smith, School of Earth and Environmental Sciences, University of Queensland, Brisbane, Australia, phillip.smith@uq.edu.au.
Sergey Gorbachev, National Research Tomsk State University, 634050 Tomsk, Russia, Email: gsv@mail.tsu.ru.
Sabin Tabirca, School of Computer Science, University College Cork, Cork, Ireland, Email: tabirca@neptune.ucc.ie.
Umit Cali, Norwegian University of Science and Technology, NO-7491 Trondheim, Norway, Email: umit.cali@ntnu.no.
Willem K. M. Brauers, Faculty of Applied Economics, University of Antwerp, Antwerp, Belgium, Email: willem.brauers@uantwerpen.be.
M. Ganster, Graz University of Technology, Graz, Austria, Email: ganster@weyl.math.tu-graz.ac.at.
Ignacio J. Navarro, Department of Construction Engineering, Universitat Politècnica de València, 46022 València, Spain, Email: ignamar1@cam.upv.es.
Francisco Chiclana, School of Computer Science and Informatics, De Montfort University, The Gateway, Leicester, LE1 9BH, United Kingdom, Email: chiclana@dmu.ac.uk.
Jean Dezert, ONERA, Chemin de la Huniere, 91120 Palaiseau, France, Email: jean.dezert@onera.fr.

.

Copyright © Neutrosophic Sets and Systems, 2025

ISSN 2331-6055 (print) NSS *ISSN 2331-608X (online)*

University of New Mexico

Contents

Samar Wazir, M.M. Sufyan Beg, Tanvir Ahmad, Shahab Saquib Sohail, On Neutrosophy logic for Multiple Correlation Analysis in Fuzzy Uncertain Database……..……1-17
Wentao Li, Qiuyan Zhao, ExpTODIM-VIKOR Framework for Quality Evaluation of University Educational Management Using Linguistic Neutrosophic Numbers……..……18-39
Cheng Yang, Grey Relational Analysis Framework with 2-Tuple Linguistic Neutrosophic Set for Building Material Supplier Selection……40-58
Qiuyan Zhao, Wentao Li, Incorporating Intelligence in Multiple-Attribute Decision-Making using Algorithmic Framework and Double-Valued Neutrosophic Sets: Varied Applications to Employment Quality Evaluation for University Graduates……59-78
Roliza Md Yasin, Nurul Izzah Wardah Salim, Nik Fakhira Nik Ahmad Fuad, Noorzahirah Mohd Zahali, Suriana Alias and Norzieha Mustapha, Average Distance Measure for TOPSIS-Sine Trigonometric Single-valued Neutrosophic Weighted Aggregation Operator and Its Application in Decision Making……79-98
Musallam M. AlZubi, Mohamed A. Mohamed, Hanan M. Amer and A. A. Salama, Neutrosophic Fuzzy Power Management (NFPM): Tackling Uncertainty in Energy Harvesting for Sensor Networks……..99-114
Yue Wang, Jiawei Zhao, Neutrosophic Set-Based PSNN-TOPSIS Framework for Multi-Attribute Decision Making: Applications in Evaluating the Quality of Environmental Art Design in Green Building Contexts……115-134
Bin Xie, An Effective Neutrosophic Approach for Group Decision-Making in College English Teaching Quality Evaluation……135-153
R. M. Abou alzahab, Amr Ismail, S. H. Abd Elkhalik, M. Y. Shams, H. M. El-Bakry and A. A. Salama, A Novel Framework for Gauging Information Extracted from Smartphones Using Neutrosophic Logic……154-171
Quansong Qi, Evaluating University Crisis Management: A Neutrosophic LogTODIM Framework for Public Opinion…….172-188
Norzieha Mustapha, Suriana Alias, Roliza Md Yasin, Alia Nur Izzah Zulkifli, Noorazliyana Shafii and Florentin Smarandache, A generalized hybrid distance measure for SVNS with an application in medical diagnosis……189-204
Alaa Elmor, NSDTL: A Robust Malware Detection Framework Under Uncertainty……205-220
Xiaobin Zheng, Guiqing Chen, Shita Huang, Lunsen Zou, Single-Valued Neutrosophic ExpTODIM Technique for Quality Evaluation of MPPT Controller Design for Photovoltaic Systems……221-240
A.Almutairi, Hamiden Abd El- Wahed Khalifa and Basma E. El- Demerdash, Incorporating Neutrosophic Uncertainty in Data Envelopment Analysis……241-252
Kai Guo, Enhanced EDAS Framework for Landscape Planning and Design Quality Evaluation under Single-Valued Neutrosophic Sets……253-274
Poonam Singh, Sooraj Gupta, Combining Two Auxiliary Variables for Elevated Estimation of Finite Population Mean under Neutrosophic Framework……..275-287
Ahmed Mohamed Shitaya, Mohamed El Syed Wahed, Saied Helemy Abd El khalek, Amr Ismail, Mahmoud Y. Shams, A. A. Salama, Predicting Student Behavior Using a Neutrosophic Deep Learning Model……..288-310
Rui Wang, Mingjie Li, Fangwei Zhang, Yiying Pan and Zongao Zhang, An Evaluation Method for University Classroom Education Quality under Machine Vision and Single-Valued Neutrosophic Hesitant Fuzzy Set Environment……311-329
Peide Liu, Qaisar Khan, Rashid Ali, Hidayat ULLAH, Rashid Jan, Multiple-Attribute Decision Making Based on Novel Single Valued Neutrosophic Aczel-Alsina Power Muirhead Mean Operators……330-359
Prasanta Kumar Raut, Sakya Singh Satapathy, Siva Prasad Behera, Said Broumi, Ajay Kumar Sahoo, Solving the shortest path Problem in an interval-valued Neutrosophic Pythagorean environment using an enhanced A* search algorithm……360-374
Xiaoying Liu, Intelligent Framework for Regional Tourism Ecological Efficiency Evaluation under High-Quality Development with Single-Valued Neutrosophic Information……375-399
A. Meenakshi, S. Dhanushiya, Optimizing Network Structures Through Neutrosophic Graph Product Operations and its Coloring: A Comprehensive Approach for Enhanced Connectivity and Robustness……..400-429
Kelei Shi, An efficient Model for Satisfaction Evaluation of College Students' Online Ideological and Political Education with Single-Valued Neutrosophic Numbers……..430-448
Rajesh Singh, Anamika Kumari, Florentin Smarandache and Shobh Nath Tiwari, Construction Of Almost Unbiased Estimator For Population Mean Using Neutrosophic Information……..449-463
Mengjun Wu, Yonghui Feng, Cross-Entropy Method Adapted for Evaluating the Teaching Quality of University Physical Education Utilizing 2-Tuple Linguistic Neutrosophic Sets……464-484
Lu Luo, Cong Wang, Improving Teaching Quality Assessment in Smart Classrooms for English Majors: An Integrated Double-Valued Neutrosophic Decision-Making Model……485-499
Lorenzo Affe, Giorgio Nordo and Florentin Smarandache, A Python Class for Neutrosophic Morphology……500-519
Wenbao Qiao, Comprehensive Framework for Collaborative Decision-Making in Evaluating Computer Network Security Using Interval Neutrosophic Information……..520-537
Juan Wang, Integrated Decision-Making Framework for Employment and Entrepreneurship Abilities Evaluation of Vocational College Students Under Double-Valued Neutrosophic Sets……538-550
Norah Mousa Alrayes, Mayada Abualhomos, Mutaz Mohamed Abbas Ali, Amani Shatarah, Mai Mousa Mahmoud Alhejoj, Abdallah Al-Husban, On Some Novel Results About the Behavior of Some Numerical Solutions of a Neutrosophic Generalized Half – Linear Second Order Differential Equation……551-569

Copyright © Neutrosophic Sets and Systems, 2025

NSS
Neutrosophic Sets and Systems, Vol. 76, 2025
University of New Mexico

On Some Novel Results About the Behavior of Some Numerical Solutions of a Neutrosophic Generalized Half – Linear Second Order Differential Equation

Norah Mousa Alrayes[1*] Mayada Abualhomos[2], Mutaz Mohamed Abbas Ali[3], Amani Shatarah[4], Mai Mousa Mahmoud Alhejoj[5], Abdallah Al-Husban[6, 7],

[1]Department of Mathematics, College of Science, Taibah University, Al-Madinah, Saudi Arabia, Nrees@taibahu.edu.sa

[2]Applied Science Private University Amman,11931,Jordan, abuhomos@asu.edu.jo

[3]Zayed Military College, Department of General Science, UAE, Mesh451144@gmail.com

[4]Department of Mathematics, College of Science, Taibah University, Al-Madinah, Saudi Arabia, ashatarah@taibahu.edu.sa

[5]Department of Basic Sciences and Informatics, Al-Balqa Applied University, Jordan, Mai.hjouj@bau.edu.jo

[6]Department of Mathematics, Faculty of Science and Technology, Irbid National University, P.O. Box: 2600 Irbid, Jordan, dralhosban@inu.edu.jo

[7]Jadara Research Center, Jadara University, Irbid 21110, Jordan,

Abstract: The generalized neutrosophic differential equation is a differential equation with neutrosophic real variable $x + yI$ instead of classical real variable x. This research is devoted to studying the oscillation of generalized neutrosophic half linear second order differential equation with the negative and delayed neutral term as follows:

$$\left(r(k+mI)z^{'}(k+mI)\right)^{'} + c(k+mI)f\left(x\left(\theta(k+mI)\right), r(k+mI)z^{'}(k+mI)\right) = 0\,.$$

Also, the generalized neutrosophic half–linear differential equation of the second order with max term featured by the following from:

$$\left[r(k+mI)z^{'}(k+mI)\right]^{'} + c(k+mI)\ \ MAX_{s\in[\theta(k+mI),k+mI]}\, f\left(x(s), r(k+mI)z^{'}(k+mI)\right) = 0\,,$$

with

$$z(k+mI) = x(k+mI) - a(k+mI)x\big(\theta(k+mI)\big),$$

Where we illustrate a numerical approach for the oscillation with indeterminacy element that represents the neutrosophic approach.

Keywords: Generalized Half, Linear, Riccati Transformation, neutrosophic generalized differential equation, neutrosophic variable.

Introduction

The importance of differential equations in our daily life is not limited to a specific application, phenomenon or example because they help us describe, present and explain the mechanism of these phenomena, including the spread of diseases, the mechanism of electrical work, climate change, nuclear explosions and many phenomena, all expressed in mathematical images. In particular, semi–linear differential equations with a negative neutral limit are a generalization of the linear Sturm-Liouville problem, which has been the subject of study for many researchers in the field of physics, as well as maximum-limit differential equations, as they are solved in the work of automatic control systems and in electronic networks. The second-order semi-linear differential equation is given in the following form:

$$\Big(r(t)\phi\left(x^{'}(t)\right)\Big)^{'} + \mathrm{c}(t)\phi\big(x(t)\big) = 0. \qquad (1)$$

Since r(t) >0 no matter what $t \in \mathbb{R}$ and $c(t)$ are continuous dependencies, $\phi(x) = |x|^{p-1}sgn(x)$ for $p > 1$. Equation (1) is called the classical equation with dependent x and independent transform t, and is a linear differential equation with respect to the dependent $\phi(x)$ that is nonlinear with respect to x, thus, it is nonlinear with respect to the dependent x. The researcher Bihari is the first to develop a second-order semi-linear differential equation in [1] in 1966, focusing on the space of solutions to this equation, so if $x(t)$ is a solution to Equation (2), $\lambda x(t)$ is also solved. In 1987, Elbert [2] came up with some criteria by which

such an equation is subjected to become oscillatory [3]. The generalized equation is oscillatory if the following is true:

$$c(t) > 0\,, \int_0^{\infty} c(t) = +\infty\,, \int_0^{\infty} \frac{1}{r(t)}\,dt = +\infty\,.$$

The generalized second-order semi-linear differential equation is given in the following Form: [5]

$$\left[r(t)x'(t)\right]' + c(t)f\left(x(t)\,, r(t)x'(t)\right) = 0\,, \qquad (2)$$

$$f\left(x\,, rx'\right) \coloneqq \emptyset(x)\left|rx'\right|^{2-p}; r(t) > 0\,, \forall t \in \mathbb{R}.$$

Researchers *Došlý* and *Řezníčková* studied the basic solutions of Equation (2) in [4] and then researchers *Došlý* and *Bognár* set important parameters in [5] for the oscillation of Equation (2).

Researchers *Marík* and *Fišnarová* studied in [7] the oscillation of the classical half-linear differential equation with a delayed limit and then with a neutral limit and developed criteria for the oscillation of this equation through the oscillation of the classical equation in 2013.

The equation $\left[\emptyset\left(\dot{x}(t)\right)\right]' + \lambda c(t)\emptyset\left(x\left(\tau(t)\right)\right) = 0$ oscillates when the equation:

$$\left[\phi\left(\dot{x}(t)\right)\right]' + \lambda c(t)\left(\frac{\tau(t)}{t}\right)^{p-1}\phi\left(x(t)\right) = 0\,.$$

Thus, it is oscillation.

Then, in [6], the researchers worked on finding a standard for the oscillation of equations with a delayed limit using the Riccati transform. Neutrosophic logic as an important new tool was used by many authors to study many different areas of pure and applied mathematics, such as algebra [9-11], and mathematical analysis [12-13]. One of the most important

applications of neutrosophic logic was in the field of differential equations, were we can see many differential neutrosophic equations and their solutions [13-40].

The importance of this research comes from the fact that it gives an analytical study of the behavior of the solutions of the neutrosophic generalized version of Equation (2), which is a generalized neutrosophic second-order semi-linear differential equation with a neutral limit. This study plays an important role in knowing the behavior of the phenomena described by this equation and therefore the possibility of controlling the results of these phenomena, and therefore this research is of great importance for researchers in the theoretical and applied scientific fields. The aim of this research is to study the infinite behavior of solutions of a generalized second-order semi-linear differential equation with a negative and maximal neutral limit, in terms of oscillation.

Results and discussion:

1. The study of the oscillation of a generalized second-order semi-linear differential equation with a neutral and delayed limit

The generalized neutrosophic second-order semi-linear differential equation with a delayed and neutral limit is given by the following relation:

$$[r(k+mI)\acute{z}(k+mI)]' + c(k+mI)f\left(x\left(\tau(k+mI)\right), r(k+mI)\acute{z}(k+mI)\right) \quad (3)$$

with a negative neutral limit $z(k+mI) = x(k+mI) - a(k+mI)x\left(\theta(k+mI)\right)$, where we will study the case $\tau(t+mI) = \theta(k+mI)$, whatever $k+mI \geq T$ so that $k+mI \in [k_0+m_0I, +\infty[$ and T starting point.

Equation (3), satisfies the following conditions:

1) $\theta(k+mI) \in \acute{C}([k_0+m_0I, +\infty[, \mathbb{R})$,

2) $\theta(k+mI) \leq k+mI$,

3) $\lim_{t\to+\infty} \theta(k+mI) = +\infty$,

4) $0 \leq a(k+mI) < 1$.

2. Riccati's neutrosophic transform:

Studying the oscillation of generalized equations using the Riccati transform is an effective method, since the equation transforms from the second to the first order. For $x(k+mI)$ solution of Equation (2) the Riccati transform of Equation (2) is given in the following Form [5]:

$$\acute{v}(k+mI)+c(k+mI) \quad +\frac{H(v)}{r(k+mI)} \tag{4}$$

where $H(v)$ is defined by the relation $H(v)=\acute{g}\left(g^{-1}(v)\right)\left(g^{-1}(v)\right)^{2}$, which is absolutely increasing for $u>0$, and also completely decreasing for $u<0$, and achieves $H(0)=0$, so is a completely convex dependent, Since

$$u(k+mI)=\frac{r(k+mI)\,\acute{x}(k+mI)}{x(k+mI)}.$$

The dependent is also given by the following relation:

$$g(u)=\begin{cases}\int_{\frac{1}{u}}^{+\infty}\frac{ds}{F(s)} & if\ u>0\\ \frac{1}{u} & \\ \int_{-\infty}^{\frac{1}{u}}\frac{ds}{F(s)} & if\ u<0\\ 0 & if\ u=0\end{cases}, \tag{5}$$

where g is completely increasing, thus $\lim_{t\to-\infty} g(u)=-\infty \ \ and \ \lim_{t\to+\infty} g(u)=+\infty$.

Remark 1.1.

If Equation (2) is non-oscillatory, then there exists $v(k+mI)$ a finite solution of Equation (4) on the domain $[T,+\infty[$ the following cases are equivalent:

1- Equation (2) is non-oscillatory,

2- There exists $v(k+mI)$ a finite solution of Equation (4) on the domain $[T,+\infty[$,

3- There is a finite dependent $v(t)$ on the domain $[T,+\infty[$ achieves the following:

$$\acute{v}(k+mI)+c(k+mI)+\frac{H(v)}{r(k+mI)}\leq 0.$$

Lemma 1.1.

Let $x(k+mI)>0$be a solution of Equation (3), then $z(t+mI)$ fulfills one of the two cases:

1) $\acute{z}(k+mI)>0\,;z(k)>0$ and $[r(k+mI)\acute{z}(k+mI)]^{\acute{}}\leq 0$,

2) $\acute{z}(k+mI)>0;z(k+mI)<0$ and $[r(k+mI)\acute{z}(k+mI)]^{\acute{}}\leq 0$.

Proof.

Since $x(k+mI)>0$, whatever$k+mI>T$ is the solution of Equation (3) then, we have:

$$[r(k+mI)\acute{z}(k+mI)]^{\acute{}}=-c(k+mI)f\left(x\big(\theta(k+mI)\big),r(k+mI)\acute{z}(k+mI)\right)\leq 0.$$

Suppose that $\acute{z}(k+mI)\leq 0$, and here we distinguish two cases:

The first case: $z(k+mI)\geq 0$, and since $[r(t)\acute{z}(t)]^{\acute{}}\leq 0$whatever$k+mI>T$, then there is $m>0$.

Check $r(k+mI)\acute{z}(k+mI)<-m$ regardless of $k+mI>T_1>T$, from which $\acute{z}(k+mI)<-\frac{m}{r(k+mI)}$, and by integration, we find:

$$m\int_T^t\frac{1}{r(s)}ds\leq z(k+mI)+m\int_T^t\frac{1}{r(s)}ds<z(T),$$

and when $k+mI$ strives towards $+\infty$, we find that $z(T)=+\infty$, and this is a contradiction.

The second case: $z(k)<0$, and since $[r(k+mI)\acute{z}(k+mI)]^{\acute{}}\leq 0$, whatever $k+mI>T$, there is a number $k>0$ such that for $T_1>T$, then, $r(k+mI)\acute{z}(k+mI)<-k$, that is, $\acute{z}(k+mI)<-\frac{k}{r(k+mI)}$, and by complementing from T to t we find that:

$$z(T)-k\int_T^{t+mI}\frac{1}{r(s)}ds>z(k+mI)\,,$$

and when seeking t towards $+\infty$ we find $\lim_{t\to+\infty}z(k)=-\infty$.

But we have $x\big(\theta(k+mI)\big)=\frac{x(k+mI)-z(t+mI)}{a(k+mI)}>\frac{-z(k+mI)}{a(t+mI)}$, and from it we find $\lim_{t\to+\infty}x\big(\theta(k+mI)\big)=+\infty$,

and since $\lim_{t\to+\infty} \theta(k+mI) = +\infty$, we find $\lim_{t\to+\infty} x(k+mI) = +\infty$.

Now, we notice that: $z(k+mI) < 0$, thus:

$x(k+mI) < a(k+mI)x\big(\theta(k+mI)\big) < x\big(\theta(k+mI)\big)$, we form a sequence $\theta(k_n) = k_{n-1}$such that $k_0, k_1, k_2, \ldots$

and $\boldsymbol{k_{n-1} < k_n}$, now considering $x(k_0) = \eta$, and since $x(t+mI) < x\big(\theta(t+mI)\big)$, from which we find that:

$x(k_n) < x\big(\theta(k_n)\big)$, thus, $x(k_n) < x(k_{n-1})$ and from it we find that $x(t_n) < \eta$ is whatever n is a natural number, and this means:

$\lim_{t\to+\infty} x(k+mI) < \eta$ and this is a contradiction.

From it, $\acute{z}(k+mI) > 0$, and here we find that $z(k+mI) < 0$ or that there exists $T_2 > T$ such that $z(k+mI) > 0$.

Lemma 1.2

Let $x(k+mI)$ be a solution of Equation (3) achieves that $x(k+mI) > 0$ for $0 < T < k + mI$ and let be

$$\int_T^{\infty} \frac{dk+mI}{r(k+mI)},$$

then $x\big(\theta(k+mI)\big) \geq z\big(\theta(k+mI)\big)$ for every $T < k+mI$ in the case of $z(k+mI) > 0$.

Lemma 1.3

Let $x(t+mI)$ be a solution of Equation (3) achieves that $x(k+mI) > 0$ for $0 < T < k + mI$ and let

$$\int_T^{\infty} \frac{dk+mI}{r(k+mI)},$$

and $\acute{r}(k+mI) > 0$, as well as

$$\int_T^{\infty} c(k+mI)\theta(k+mI)^{p-1}dt + mI = \infty.$$

Then

$$\frac{z\big(\theta(t+mI)\big)}{z(t+mI)} \geq \frac{\theta(t+mI)}{t+mI},$$

for each $T < k + mI$. In the case of $z(k + mI) > 0$.

Proof.

We impose $x(k + mI) > 0$ for each $T < k + mI$ solution of Equation (3), where $\acute{r}(k + mI) > 0$ and considering $z(k + mI) > 0$, we find from the preliminary (3) that $\acute{z}(k + mI) > 0$, and now let's prove that $\left(\frac{z(k+mI)}{k+mI}\right)'$ thus, $\acute{z}(k + mI)k - z(k + mI) \leq 0$ and that in a way that the assumption.

We assume by argument that $\left(\frac{z(k+mI)}{k+mI}\right)' \geq 0$, that is, the dependent $\frac{z(k+mI)}{k+mI}$ is completely increasing, and therefore $z(k + mI) > (k + mI)k$, from which the following is achieved:

$$[r(k + mI)\acute{z}(k + mI)]' = -c(k + mI)\frac{\left(x\left(\theta(k + mI)\right)\right)^{p-1}}{\left(r(k + mI)\acute{z}(k + mI)\right)^{p-2}},$$

and from it we get

$$\left(r(k + mI)\acute{z}(k + mI)\right)^{p-2}[r(k + mI)\acute{z}(k + mI)]' = -c(k + mI)\left(x\left(\theta(k + mI)\right)\right)^{p-1},$$

By integrating the two sides from T to $k + mI$, we get

$$\left(r(k + mI)\acute{z}(k + mI)\right)^{p-1} = \left(r(T)\acute{z}(T)\right)^{p-1} - (p - 1)\int_{T}^{k+mI} c(s)\left(x\left(\theta(s)\right)\right)^{p-1} ds\,.$$

We have $\acute{z}(k + mI) > 0$ and $p - 1$ are even, then we find that $\left(r(k + mI)\acute{z}(k + mI)\right)^{p-1} \geq 0$, therefore

$$\left(r(T)\acute{z}(T)\right)^{p-1} - (p - 1)\int_{T}^{t} c(s)\left(x\left(\theta(s)\right)\right)^{p-1} ds \geq 0\,,$$

and so, we find the following:

$$\left(r(T)\acute{z}(T)\right)^{p-1} \geq (p - 1)\int_{T}^{t} c(s)z\left(\theta(s)\right)^{p-1} ds \geq k^{p-1}(p - 1)\int_{T}^{t} c(s)\theta(s)^{p-1} ds\,,$$

and when *t* seeks toward ∞, then $\left(r(T)\acute{z}(T)\right)^{p-1} \geq \infty$, and this is a contradiction because $r(T)\,\acute{z}(T)$ is a neutrosophic real number that cannot be infinite, that is, $\acute{z}(k + mI)(k + mI) - z(k + mI) \leq 0$for every $T < t + mI$ and therefore, we find:

$$\frac{z\big(\theta(k+mI)\big)}{\theta(k+mI)} \geq \frac{z(k+mI)}{k+mI} \tag{6}$$

Lemma 1.4

Let $x(k+mI)$ be a solution of Equation (3) achieves that $x(k+mI) > 0$ for $0 < T < k + mI$ and let

$$\int_{T}^{\infty} \frac{dk+mI}{r(k+mI)} = +\infty .$$

Then $\left(\frac{x\big(\theta(k+mI)\big)}{z(k+mI)}\right)^{p-1} \geq 1.$

For every $T < k + mI$ in the case of $z(k+mI) < 0,\ p > 1$ is an odd number.

Lemma 1.5.

The Riccati transform of Equation (3) gives us the following form:

$$\acute{v}(k+mI) + c(k+mI)\left(\frac{x\big(\theta(k+mI)\big)}{z(k+mI)}\right)^{p-1} + \frac{H(v)}{r(k+mI)} = 0, \tag{7}$$

where $p > 1$is an odd number.

Proof.

Suppose that $x(k+mI) \neq 0$ is a solution of Equation (2) for every $T \leq t + mI$ is a solution of Equation (3) and $v(t+mI) = g\big(u(k+mI)\big)$, and the dependent $u(k+mI) = \frac{r(k+mI)\acute{z}(k+mI)}{z(k+mI)}$ by deriving the dependent $v(k+mI)$, we get:

$$\acute{v}(k+mI) = \acute{g}(u)\acute{u}(k+mI)$$

$$= \acute{g}(u)\left[\frac{[r(k+mI)\acute{z}(k+mI)]'z(k+mI) - r(k+mI)\acute{z}^2(k+mI)}{z^2(k+mI)}\right],$$

$$\acute{v}(k+mI) = \acute{g}(u)\left[\frac{-c(k+mI)f\left(x\big(\theta(k+mI)\big), r(k+mI)\acute{z}(k+mI)\right)}{z(k+mI)} - \frac{r(k+mI)\acute{z}^2(k+mI)}{z^2(k+mI)}\right],$$

$$\acute{v}(k+mI) = -\acute{g}(u)c(k+mI)\left(\frac{x\big(\theta(k+mI)\big)}{z(k+mI)}\right)^{p-1}\left(\frac{z(k+mI)}{r(k+mI)\acute{z}(k+mI)}\right)^{p-2}$$

$$-\frac{\acute{g}(u)}{r(k+mI)}\left(\frac{r(k+mI)\acute{z}(k+mI)}{z(k+mI)}\right)^{2},$$

$$\acute{v}(k+mI) = -\acute{g}(u)c(k+mI)\left(\frac{x\big(\theta(k+mI)\big)}{z(k+mI)}\right)^{p-1}u^{2-p}(k+mI)$$

$$-\frac{\acute{g}(u)}{r(k+mI)}u^{2}(k+mI)\,.$$

By choosing the dependent g, so that $\acute{g}(u)u^{2-p}(k+mI)=1$, the equation turns into the following form:

$$\acute{v}(k+mI)+c(k+mI)\left(\frac{x\big(\theta(k+mI)\big)}{z(k+mI)}\right)^{p-1}+\frac{H(v)}{r(k+mI)}=0\,,$$

$$H(v)=u^{2}\acute{g}(u)\,.$$

Theorem 1.1

Let's have the following equation:

$$[r(t+mI)\acute{x}(t+mI)]^{\acute{}}$$

$$+c(t+mI)\left(\frac{\theta(t+mI)}{t+mI}\right)^{p-1}\quad f\big(x(t+mI)\,,r(t+mI)\acute{x}(t+mI)\big)$$

$$=0\,,\qquad(8)$$

where $\acute{r}(t+mI)\geq 0$ and

$$\int_{T}^{\infty}\frac{dt}{r(t+mI)}=+\infty\,,$$

then if equation (8) is oscillatory, thus, equation (3) is oscillatory.

Proof.

To complete the required we have to prove that Equation (3) is oscillatory.We will use the method of reversing the assumption, suppose that equation (8) is oscillatory, and Equation (3) is non-oscillatory, then there is $x(t+mI)$ solution of Equation (3), so that $x(t+mI)>0$ for each $T<t+mI$, and here, by lemma 1.1, we distinguish two cases:

The first case: in the case of $z(t) > 0$where p is an odd number for each $T < t + mI$,

By Lemma1.5, we have a Riccati transform of Equation (3) is:

$$\acute{v}(t + mI) + c(t + mI)\left(\frac{x\big(\theta(t + mI)\big)}{z(t + mI)}\right)^{p-1} + \frac{H(v)}{r(t + mI)} = 0$$

Since $v(t + mI)$ is a finite dependent because $x(t + mI) \neq 0$, therefore, taking advantage of the primality of 1.3 and the primality of 1.2, we find that:

$$\acute{v}(t) + c(t + mI)\left(\frac{\theta(t + mI)}{t + mI}\right)^{p-1} + \frac{H(v)}{r(t + mI)}$$

$$\leq \acute{v}(t + mI) + c(t + mI)\left(\frac{z\big(\theta(t + mI)\big)}{z(t + mI)}\right)^{p-1} + \frac{H(v)}{r(t + mI)}$$

$$\leq \acute{v}(t + mI) + c(t + mI)\left(\frac{x\big(\theta(t + mI)\big)}{z(t + mI)}\right)^{p-1} + \frac{H(v)}{r(t + mI)} = 0\,.$$

Hence

$$\acute{v}(t + mI) + c(t + mI)\left(\frac{\theta(t + mI)}{t + mI}\right)^{p-1} + \frac{H(v)}{r(t + mI)} \leq 0\,.$$

According to proposition 1.1, we find that equation (8) is non-oscillatory, which contradicts the assumption.

The second case: in the case of $z(t + mI) < 0$ for every$t + mI > T$,

We will take the Riccati transform of Equation (3), where:

$$u(t + mI) = \frac{r(t + mI)\acute{z}(t + mI)}{z(t + mI)} \qquad \text{and} \qquad v(t + mI) = g\big(u(t + mI)\big)\,.$$

According to lemma1.5, we have

$$\acute{v}(t + mI) + c(t + mI)\left(\frac{x\big(\theta(t + mI)\big)}{Z(t + mI)}\right)^{p-1} + \frac{H(v)}{r(t + mI)} = 0\,.$$

Since $v(t + mI)$ is a finite dependent, therefore, taking advantage of the lemma1.4, we have:

$$\acute{v}(t+mI)+c(t+mI)\left(\frac{\theta(t+mI)}{t+mI}\right)^{p-1}+\frac{H(v)}{r(t+mI)}$$

$$\leq \acute{v}(t+mI)+c(t+mI)+\frac{H(v)}{r(t+mI)}$$

$$\leq \acute{v}(t+mI)+c(t+mI)\left(\frac{x(\theta(t+mI))}{z(t+mI)}\right)^{p-1}+\frac{H(v)}{r(t+mI)}=0\,.$$

Therefore

$$\acute{v}(t+mI)+c(t+mI)\left(\frac{\theta(t+mI)}{t+mI}\right)^{p-1}+\frac{H(v)}{r(t+mI)}\leq 0\,.$$

According to lemma1.1, equation (8) is non-oscillatory, which contradicts the assumption.

2. The study of the oscillation of a generalized neutrosophic second-order semi-linear differential equation with a maximal limit

In this paragraph, we study the oscillation of a generalized neutrosophic semi-linear differential equation that contains a neutral and a maximal limit, and this equation has the following form:

$$[r(t+mI)\acute{z}(t+mI)]^{'}+c(t+mI)\ \boldsymbol{Max}_{s\in[\theta(t+mI),t+mI]}f\big(x(s)\,,r(t+mI)\acute{z}(t+mI)\big)$$
$$=0\,, \qquad (9)$$

where $f(x,y)$ is defined as in Equation (2) provided p is an odd natural number, thus, $p\geq 1$, then: $r(t+mI)\cdot c(t+mI)$ are absolutely positive dependents and the dependent $z(t)$ given by the relation $z(t)=x(t+mI)-a(t+mI)x\big(\theta(t+mI)\big)$ fulfills the following conditions:

1) $a(t+mI)\leq a0\leq 1$,

2) $\theta(t+mI)\leq t+m,$,

3) $]\infty+, Limt+mI\to+\infty\ \theta(t+mI)=+\infty[$

Lemma 1.2: The Riccati transform of equation (9) gives us the following form:

$$\acute{v}(t+mI)+c(t+mI)max_{s\in[\theta(t+mI),t+mI]}\left(\frac{x(s)}{z(t+mI)}\right)^{p-1}+\frac{H(v)}{r(t+mI)}=0 \quad (10)$$

where $p \geq 1$ is an odd number.

Proof.

We assume that $x(t+mI) \neq 0$ for every $T < t+mI$ solution of equation (9) and that $v(t+mI) = g\big(u(t+mIt+mI)\big)$,

And the dependent $u(t) = \frac{r(t+mI)\acute{z}(t+mI)}{z(t+mI)}$ by deriving $v(t+mI)$, we get:

$$\acute{v}(t) = \acute{g}(u)\acute{u}(t) = \acute{g}(u)\left[\frac{[r(t)\acute{z}(t)]^{'}z(t) - r(t)\acute{z}^2(t)}{z^2(t)}\right],$$

$$\acute{v}(t) = \acute{g}(u)\left[\frac{-c(t)max_{s\in[\theta(t),t]}f\big(x(s),r(t)\acute{z}(t)\big)}{z(t)} - \frac{r(t)\acute{z}^2(t)}{z^2(t)}\right],$$

$$\acute{v}(t) = -\acute{g}(u)c(t)\left[\frac{max_{s\in[\theta(t),t]}x(s)}{z(t)}\right]^{p-1}\left[\frac{z(t)}{r(t)\acute{z}(t)}\right]^{p-2} - \frac{\acute{g}(u)}{r(t)}\left[\frac{r(t)\acute{z}(t)}{z(t)}\right]^2,$$

$$\acute{v}(t) = -\acute{g}(u)c(t)\left[\frac{max_{s\in[\theta(t),t]}x(s)}{z(t)}\right]^{p-1}[u(t)]^{2-p} - \frac{\acute{g}(u)}{r(t)}[u(t)]^2 .$$

By choosing the dependent g so that $\acute{g}(u)u^{2-p}(t) = 1$, we get the equation:

$$\acute{v}(t+mI) + c(t+mI)\left[\frac{max_{s\in[\theta(t+mI),t+mI]}x(s)}{z(t+mI)}\right]^{p-1} + \frac{H(v)}{r(t+mI)} = 0,$$

Theorem 2.2 Let's have the following equation:

$$[r(t+mI)\acute{x}(t+mI)]^{'} + c(t+mI)\left(\frac{\theta(t+mI)}{t+mI}\right)^{p-1} f\big(x(t+mI), r(t+mI)\acute{x}(t+mI)\big) = 0\,, \qquad (11)$$

where $\acute{r}(t+mI) \geq 0$ and $\int^{\infty} \frac{dt}{r(t+mI)} = +\infty$, then if equation (11) is oscillatory, equation (9) is oscillatory.

Proof.

We will use the method of reversing the assumption, suppose that equation (11) is oscillatory, and equation (9) is non-oscillatory, then there is $x(t+mI)$ solution to equation (9), so that it achieves that $x(t+mI)>0$ for each $T<t+mI$, and here we distinguish two cases:

The first case: in the case of $z(t+mI)>0$ by introductory 1.1 where p is an odd number for every $T<t+mI$.

Taking the Riccati transform of the given equation (9), where $v(t+mI)=g\big(u(t+mI)\big)$ is a finite solution and $u(t+mI)=\frac{r(t+mI)\acute{z}(t+mI)}{z(t+mI)}$.

Defined over the entire domain $]T,+\infty[$ where $T<t+mI$, and by introductory 1.2 and introductory 1.3 where p is an odd number for each $T<t$, and by introductory 1.5, we find that:

$$\acute{v}(t+mI)+c(t+mI)\left(\frac{\theta(t+mI)}{t+mI}\right)^{p-1}+\frac{H(v)}{r(t+mI)}$$

$$\leq \acute{v}(t+mI)+c(t+mI)\left(\frac{z\big(\theta(t+mI)\big)}{z(t+mI)}\right)^{p-1}+\frac{H(v)}{r(t+mI)}$$

$$\leq \acute{v}(t+mI)+c(t+mI)\left(\frac{x\big(\theta(t+mI)\big)}{z(t+mI)}\right)^{p-1}+\frac{H(v)}{r(t+mI)}$$

$$\leq \acute{v}(t+mI)+c(t+mI)\left(\frac{max_{s\in[\theta(t),t]}x(s)}{z(t+mI)}\right)^{p-1}+\frac{H(v)}{r(t+mI)}\leq 0\,,$$

thus

$$\acute{v}(t+mI)+c(t+mI)\left(\frac{\theta(t+mI)}{t+mI}\right)^{p-1}+\frac{H(v)}{r(t+mI)}\leq 0\,.$$

According to lemma1.1, equation (11) is non-oscillatory, which contradicts the assumption.

The second case: in the case of $z(t+mI)<0$ and $x(t+mI)>0$ by introductory 1.4 where p is an odd number for each $T<t+mI$.

Taking the Riccati transform of equation (9) where $v(t+mI)=g\big(u(t+mI)\big)$ is a finite solution of equation (10) and $u(t+mI)=\frac{r(t+mI)\acute{z}t+mI}{z(t+mI)}$ is defined over the entire domain $]T,+\infty[$ and using the lemma 1.4 we have the following relation:

$$\left(\frac{x\big(\theta(t+mI)\big)}{z(t+mI)}\right)^{p-1} \geq 1,$$

and according to the lemma 1.5, we have:

$$\acute{v}(t+mI)+c(t+mI)\left(\frac{\theta(t+mI)}{t+mI}\right)^{p-1}+\frac{H(v)}{r(t+mI)}$$

$$\leq \acute{v}(t+mI)+c(t+mI)+\frac{H(v)}{r(t+mI)}$$

$$\leq \acute{v}(t+mI)+c(t+mI)\left(\frac{x(\theta(t+mI))}{z(t+mI)}\right)^{p-1}+\frac{H(v)}{r(t+mI)}$$

$$\leq \acute{v}(t+mI)+c(t+mI)\left[\frac{max_{s\in[\theta(t+mI),t+mI]}x(s)}{z(t+mI)}\right]^{p-1}+\frac{H(v)}{r(t+mI)}.$$

From it, we find that:

$$\acute{v}(t+mI)+c(t+mI)\left(\frac{\theta(t+mI)}{t+mI}\right)^{p-1}+\frac{H(v)}{r(t+mI)}$$

$$\leq \acute{v}(t+mI)+c(t+mI)\left[\frac{max_{s\in[\theta(t+mI)t+mI]}x(s)}{z(t+mI)}\right]^{p-1}+\frac{H(v)}{r(t+mI)}=0.$$

thus,

$$\acute{v}(t+mI)+c(t+mI)\left(\frac{\theta(t+mI)}{t+mI}\right)^{p-1}+\frac{H(v)}{r(t+mI)}\leq 0\,.$$

According to lemma 1.1, the condition is equivalent to the fact that equation (11) is non-oscillatory, and this is a contradiction.

Numerical Results:

In the following tables, we show how the improved method gives better numerical results than the classical approaches.

Variables values for classical equation	**M1**	**E1**	**M2**	**E2**	**M3**	**E3**
1.00000	$2.68e^{-002}$	$2.46e^{-002}$	$1.32e^{-002}$	$1.20e^{-002}$	1.01806	1.03393
0.39811	$2.68e^{-002}$	$2.66e^{-002}$	$1.32e^{-002}$	$1.01e^{-002}$	1.02214	1.03627

0.12589	$1.93e^{-002}$	$1.70e^{-002}$	$9.57e^{-003}$	$8.29e^{-003}$	1.00972	1.03642
0.03981	$1.56e^{-002}$	$1.59e^{-002}$	$7.72e^{-003}$	$7.83e^{-003}$	0.99062	1.01896
0.01585	$1.53e^{-002}$	$1.62e^{-002}$	$7.75e^{-003}$	$8.05e^{-003}$	0.98424	1.00995
0.00631	$1.54e^{-002}$	$1.66e^{-002}$	$7.77e^{-003}$	$8.24e^{-003}$	0.98034	1.00599
0.00251	$1.54e^{-002}$	$1.68e^{-002}$	$7.79e^{-003}$	$8.35e^{-003}$	0.97986	1.00662
0.00100	$1.54e^{-002}$	$1.69e^{-002}$	$7.80e^{-003}$	$8.40e^{-003}$	0.97965	1.00664
0.00040	$1.54e^{-002}$	$1.70e^{-002}$	$7.80e^{-003}$	$8.43e^{-003}$	0.97957	1.00662
0.00016	$1.54e^{-002}$	$1.70e^{-002}$	$7.80e^{-003}$	$8.44e^{-003}$	0.97956	1.00661
0.00006	$1.54e^{-002}$	$1.70e^{-002}$	$7.80e^{-003}$	$8.44e^{-003}$	0.97954	1.00660
0.00001	$1.54e^{-002}$	$1.70e^{-002}$	$7.78e^{-003}$	$8.45e^{-003}$	0.97954	1.00660

The values of the variables with indeterminacy						
	M1	E1	M2	E2	M3	E3
1.00000+I	$5.96e^{-004}$+I	$2.10e^{-003}$+I	$2.20e^{-004}$+I	$1.28e^{-002}$+I	1.43755+I	0.71812+I
0.39811+0.6765I	$6.98e^{-004}$+I	$2.41e^{-003}$+I	$4.05e^{-004}$+I	$1.68e^{-002}$+I	1.28634+I	0.70181+I
0.12589+0,11234I	$7.56e^{-004}$+I	$1.23e^{-003}$+I	$3.10e^{-004}$+I	$1.11e^{-003}$+I	1.47698+I	1.00965+I
0.03981+0.765I	$9.12e^{-004}$+I	$4.22e^{-003}$+I	$5.06e^{-004}$+I	$1.10e^{-003}$+I	1.80228+I	1.94442+I
0.01585+0.00876I	$1.15e^{-003}$+I	$5.76e^{-003}$+I	$6.27e^{-004}$+I	$2.46e^{-003}$+I	1.10448+I	1.15208+I
0.00631+0.6543I	$1.26e^{-003}$+I	$6.28e^{-003}$+I	$6.61e^{-004}$ + I	$3.08e^{-003}$+I	0.97539+I	1.02933+I
0.00251+0.7205I	$1.26e^{-003}$+I	$6.41e^{-003}$+I	$6.68e^{-004}$ + I	$3.25e^{-003}$+I	0.92225+I	0.97894+I
0.00100+I	$1.26e^{-003}$+I	$6.44e^{-003}$+I	$6.70e^{-004}$ + I	$3.30e^{-003}$+I	0.91116+I	0.96771+I
0.00040+0.15094I	$1.26e^{-003}$+I	$6.45e^{-003}$+I	$6.70e^{-004}$ + I	$3.30e^{-003}$+I	0.90910+I	0.96551+I
0.00016+0,00013I	$1.26e^{-003}$+I	$6.45e^{-003}$+I	$6.70e^{-004}$+I	$3.30e^{-003}$+I	0.90872+I	0.96508+I
0.00006+0.876093409I	$1.26e^{-003}$+I	$6.45e^{-003}$+I	$6.70e^{-004}$+I	$3.31e^{-003}$+I	0.90863+I	0.96503+I
0.00001+0.000012I	$1.26e^{-003}$+I	$6.45e^{-003}$ + I	$6.70e^{-004}$+I	$3.31e^{-003}$+I	0.90862+I	0.96502+I

Conclusion and future applications:

In this research, we studied the oscillation of Equation (3), which is a generalized neutrosophic second-order semi-linear differential equation with a negative and delayed limit, as it was compared with equation (8), which is a generalized neutrosophic second-order semi-linear differential equation; we used the Riccati transform technique to reach our results. And then, in the second section, we studied the oscillation of the neutrosophic second-

order semi-linear differential equation, which contains a negative neutral limit and another maximum, and we came to condition (11) is useful in proving whether equation (9) is oscillatory or non-oscillatory. We recommend that our novel approach to be used for the same equation generalized in terms of refined neutrosophic real numbers, where it can be defined by using a refinement of the indeterminacy element.

References

1. BIHARI.I., 1964, An oscillation theorem concerning the half-linear differential equation of second order, Magy, Tud, Akad, Mat, Kut, intéz, PP 275-280**.**
2. ELBERT. A., On the half – linear second order differential equation, Hungar , A cta Math .Hungar. 49(1987), 487-508
3. DOšLÝ. O., REHAK. P., 2005, Half-linear differential equations, Acta Math.
4. DOšLÝ. O., $\check{R}EZN\acute{I}\check{C}KOV\acute{A}$. J., 2012, Conjugacy and principal solution of generalized half-linear second order differential equations, Qual, PP 1-13.
5. DOšL$\acute{Y}$.O., BOGN$\acute{A}R$.G.,2013, Conditional oscillation and principal solution of generalized half- linear differential equation, Debrecen, PP 451-459.
6. MAR$\acute{I}K$. R., FIšNAROVÁ. S., Oscillation of half-linear differential equations with delay, Mendel University in Brno, Zem ^ ed ^ elsk ´ A 1,613 00 Brno, Czech Republic, 2013
7. FIšNAROVÁ. S., MAR$\acute{I}K$.R., 2014, Modified Riccati technique for half- linear differential equations with delay, Electronic journal of Qualitative Theory of Differential Equations, pp. 1-14.
8. SELVARANGAM. S., RANI. B., THANDAPANI, E. Oscillation results for second order half- linear neutral delay differential equations with "maxima". Tamkang Journal of Mathematics, Volume 48, Number 3, 289-299, sept 2017.
9. Sankari, H., and Abobala, M., " On The Group of Units Classification In 3-Cyclic and 4-cyclic Refined Rings of Integers And The Proof of Von Shtawzens' Conjectures", International Journal of Neutrosophic Science, 2023.
10. Sankari, H., and Abobala, M., " On The Classification of The Group of Units of Rational and Real 2-Cyclic Refined Neutrosophic Rings", Neutrosophic Sets and Systems, 2023.
11. Katy D. Ahmad, Mikail Bal, Arwa A. Hajjari, Rozina Ali. (2021). Novel Applications Of Neutrosophic AH-Isometries To The Group Of Units Problem In Neutrosophic Rings and Refined Neutrosophic Rings. Journal of Neutrosophic and Fuzzy Systems, 1 (2), 89-98 (**Doi :** https://doi.org/10.54216/JNFS.010205).
12. Dima Alrwashdeh , Talat Alkhouli , Ahmed Soiman Rashed Alhawiti , Ali Allouf , Hussein Edduweh , Abdallah Al-Husban, On Two Novel Generalized Versions of Diffie-Hellman Key Exchange Algorithm Based on Neutrosophic and Split-Complex Integers and their Complexity Analysis, International Journal of Neutrosophic Science, Vol. 25 Issue. 2 PP. 01-10, (2025), Doi:https://doi.org/10.54216/IJNS.250201.
13. Salama, A. Dalla, R. Al, M. Ali, R. (2022). On Some Results About The Second Order Neutrosophic Differential Equations By Using Neutrosophic Thick Function. Journal of Neutrosophic and Fuzzy Systems, (), 30-40. **DOI:** https://doi.org/10.54216/JNFS.040104.

14. Salama, A. Al, M. Dalla, R. Ali, R. (2022). A Study of Neutrosophic Differential Equations By Using the One-Dimensional Geometric AH-Isometry Of NeutrosophicLaplace Transformation. Journal of Neutrosophic and Fuzzy Systems, (), 08-25. **DOI:** https://doi.org/10.54216/JNFS.040201.
15. Hazaymeh, Ayman. "Time Effective Fuzzy Soft Set and Its Some Applications with and Without a Neutrosophic." International Journal of Neutrosophic Science 23.2 (2023): 129-29.
16. A. S. Heilat, H. Zureigat, R. Hatamleh, B. Batiha, New Spline Method for Solving Linear Two-Point Boundary Value Problems European Journal of Pure and Applied Mathematics 14 (4), 1283-1294, 2021
17. Al-Husban, A., Djenina, N., Saadeh, R., Ouannas, A., & Grassi, G. (2023). A new incommensurate fractional-order COVID 19: modelling and dynamical analysis. Mathematics, 11(3), 555.
18. Hamadneh, T., Hioual, A., Alsayyed, O., Al-Khassawneh, Y. A., Al-Husban, A., & Ouannas, A. (2023). The FitzHugh–Nagumo Model Described by Fractional Difference Equations: Stability and Numerical Simulation. Axioms, 12(9), 806.
19. Heilat, A. S., Karoun, R. C., Al-Husban, A., Abbes, A., Al Horani, M., Grassi, G., & Ouannas, A. (2023). The new fractional discrete neural network model under electromagnetic radiation: Chaos, control and synchronization. Alexandria Engineering Journal, 76, 391-409.
20. Al-Husban, A., Karoun, R. C., Heilat, A. S., Al Horani, M., Khennaoui, A. A., Grassi, G., & Ouannas, A. (2023). Chaos in a two dimensional fractional discrete Hopfield neural network and its control. Alexandria Engineering Journal, 75, 627-638.
21. Abu Falahah, I., Hioual, A., Al-Qadri, M. O., Al-Khassawneh, Y. A., Al-Husban, A., Hamadneh, T., & Ouannas, A. (2023). Synchronization of Fractional Partial Difference Equations via Linear Methods. Axioms, 12(8), 728.
22. Hamadneh, T., Abbes, A., Falahah, I. A., Al-Khassawneh, Y. A., Heilat, A. S., Al-Husban, A., & Ouannas, A. (2023). Complexity and chaos analysis for two-dimensional discrete-time predator–prey Leslie–Gower model with fractional orders. Axioms, 12(6), 561.
23. Hamadneh, T., Hioual, A., Alsayyed, O., Al-Khassawneh, Y. A., Al-Husban, A., & Ouannas, A. (2023). Finite Time Stability Results for Neural Networks Described by Variable-Order Fractional Difference Equations. Fractal and Fractional, 7(8), 616.
24. Abubaker, A. A., Abualhomos, M., Matarneh, K., & Al-Husban, A. (2025). A Numerical Approach For The Algebra of Two-Fold. Neutrosophic Sets and Systems, 75, 181-195.
25. Al-Husban, A., Djenina, N., Saadeh, R., Ouannas, A., & Grassi, G. (2023). A new incommensurate fractional-order COVID 19: modelling and dynamical analysis. Mathematics, 11(3), 555.
26. Hatamleh, R. (2003). On the Form of Correlation Function for a Class of Nonstationary Field with a Zero Spectrum. Rocky Mountain Journal of Mathematics, 33(1)159-173. https://doi.org/10.1216/rmjm/1181069991.
27. Hatamleh, R., Zolotarev, V. A. (2014). On Two-Dimensional Model Representations of One Class of Commuting Operators. Ukrainian Mathematical Journal, 66(1), 122–144. https://doi.org/10.1007/s11253-014-0916-9.

28. Hatamleh, R., Zolotarev,V. A. (2015). On Model Representations of Non-Selfadjoint Operators with Infinitely Dimensional Imaginary Component. Journal of Mathematical Physics, Analysis, Geometry,11(2), 174–186. https://doi.org/10.15407/mag11.02.174 .
29. Hatamleh, R., Zolotarev, V. A. (2016). Triangular Models of Commutative Systems of Linear Operators Close to Unitary Operators.Ukrainian Mathematical Journal,68(5),791–811. https://doi.org/10.1007/s11253-016-1258-6.
30. T.Qawasmeh, A. Qazza, R. Hatamleh, M.W. Alomari, R. Saadeh, Further accurate numerical radius inequalities, Axiom-MDPI, 12 (8), 801, 2023
31. Raed Hatamleh, Ayman Hazaymeh.(2024). Finding Minimal Units In Several Two-Fold Fuzzy Finite Neutrosophic Rings, Neutrosophic Sets and Systems, Vol. 70, pp.1-16. DOI: 10.5281/zenodo.13160839
32. Abdallah Shihadeh, Khaled Ahmad Mohammad Matarneh, Raed Hatamleh, Mowafaq Omar Al-Qadri, Abdallah Al-Husban,(2024), On The Two-Fold Fuzzy n-Refined Neutrosophic Rings For $2\leq n\leq 3$, Neutrosophic Sets and Systems, Vol. 68,pp.8-25.
33. Raed Hatamleh , Ayman Hazaymeh.(2025),On Some Topological Spaces Based On Symbolic n-Plithogenic Intervals, International Journal of Neutrosophic Science, Vol. 25 Issue. 1 PP. 23-37. Doi: https://doi.org/10.54216/IJNS.250102.
34. Raed Hatamleh , Ayman Hazaymeh,(2025),On The Topological Spaces of Neutrosophic Real Intervals, International Journal of Neutrosophic Science, Vol. 25 Issue. 1 PP. 130-136, (Doi: https://doi.org/10.54216/IJNS.250111.
35. Raed Hatamleh , Ayman Hazaymeh.(2025),The Properties of Two-Fold Algebra Based on the n-standard Fuzzy Number Theoretical System, International Journal of Neutrosophic Science, 25 (1) ,172-178.(Doi: https://doi.org/10.54216/IJNS.250115).
36. Ahmad A. Abubaker , Raed Hatamleh , Khaled Matarneh , Abdallah Al-Husban,(2025), On the Irreversible k-Threshold Conversion Number for Some Graph Products and Neutrosophic Graphs, International Journal of Neutrosophic Science,25(2), 197-205. (Doi: https://doi.org/10.54216/IJNS.250217).
37. Abdallah Shihadeh, Khaled Ahmad Mohammad Matarneh, Raed Hatamleh, Randa Bashir Yousef Hijazeen, Mowafaq Omar Al-Qadri, Abdallah Al-Husban.(2024). An Example of Two-Fold Fuzzy Algebras Based On Neutrosophic Real Numbers, Neutrosophic Sets and Systems,vol.67, pp. 169-178.(DOI:10.5281/zenodo.11151930).
38. Abubaker, Ahmad A, Hatamleh, Raed, Matarneh, Khaled, Al-Husban, Abdallah.(2024). On the Numerica Solutions for Some Neutrosophic Singular Boundary Value Problems by Using (LPM) Polynomials, Inernational Journal of Neutrosophic Science,25(2),197-205. (Doi: https://doi.org/10.54216/IJNS.250217).
39. Raed Hatamleh (2024). On the Compactness and Continuity of Uryson's Operator in Orlicz Space, International Journal of Neutrosophic Science, 24 (3), 233-239.
40. Ayman Hazaymeh, Ahmad Qazza, Raed Hatamleh, Mohammad W Alomari, Rania Saadeh, On Further Refinements of Numerical Radius Inequalities, Axiom-MDPI,12(9),807,2023.

Received: July 24, 2024. Accepted: Oct 25, 2024

NSS
Neutrosophic Sets and Systems, Vol. 76, 2025
University of New Mexico

Integrated Decision-Making Framework for Employment and Entrepreneurship Abilities Evaluation of Vocational College Students Under Double-Valued Neutrosophic Sets

Juan Wang*
Zhejiang Financial College, Hangzhou,310018, Zhejiang, China
*Corresponding author, E-mail: 20040002@zfc.edu.cn

Abstract: The evaluation of vocational college students' employment and entrepreneurship abilities is a comprehensive assessment of their professional skills, job adaptability, innovation capabilities, and entrepreneurial qualities. The goal is to examine students' practical abilities, alignment with market demands, innovative thinking, and entrepreneurial spirit, helping them identify their strengths and weaknesses to enhance their competitiveness in the job market. This evaluation also provides insights for schools to improve their teaching methods, fostering students' overall development and better alignment with societal needs. The employment and entrepreneurship abilities evaluation of vocational college students is multi-attribute decision-making (MADM) problem. Recently, methods such as the MABAC approache have been applied to tackle these challenges. Double-Valued Neutrosophic Sets (DVNSs) are used to represent uncertainty data in the evaluation process. In this study, a Double-Valued Neutrosophic Number MABAC (DVNN- MABAC) approach is proposed to address MADM problems involving DVNSs. Finally, a numerical case study on the employment and entrepreneurship abilities evaluation of vocational college students is provided to demonstrate the effectiveness of the DVNN- MABAC approach.

Keywords: MADM; DVNSs; MABAC approach; employment and entrepreneurship abilities evaluation

1. Introduction

The evaluation of employment and entrepreneurship abilities of vocational college students holds significant practical importance, serving as both an assessment of students' individual professional competencies and a feedback mechanism to align school teaching quality with societal needs. First, by evaluating students' employment abilities, the assessment helps gauge their performance in areas such as professional skills, job adaptability, and teamwork, enabling students to identify their strengths and weaknesses, and thus improve their competitiveness in

the job market. Second, the evaluation of entrepreneurship abilities helps stimulate students' innovative thinking and entrepreneurial spirit, cultivating their problem-solving and independent thinking abilities in complex market environments, which are essential for future entrepreneurial success. Furthermore, this systematic evaluation allows schools to adjust their teaching methods and curricula in a timely manner, ensuring that the skills and qualities they cultivate in students align with market demands. Through this evaluation mechanism, schools can more effectively improve the quality of education and produce highly skilled individuals with practical abilities, innovative thinking, and entrepreneurial potential. This not only fosters students' personal career development but also provides strong support for social economic innovation and industry upgrading. The employment and entrepreneurship abilities evaluation of vocational college students is MADM problem. Recently, the TODIM approach [1, 2] and TOPSIS approach [3] have been applied to handle such problems.

It creates a method that can be employed in complex system evaluations, such as in education or technology assessments, and can be easily implemented using common computational tools, making it practical for real-world applications.

Double-Valued Neutrosophic Sets (DVNSs) [4] have been employed to represent fuzzy data during the quality evaluation process. DVNSs offer significant advantages in evaluating the effectiveness of multimedia. First, they handle uncertainty and ambiguity, accurately representing fuzzy data in the evaluation process. Second, DVNS simultaneously considers truth, indeterminacy, and falsity, providing more comprehensive evaluation results. Lastly, DVNS is flexible and applicable to complex evaluation scenarios, assisting decision-makers in making more rational judgments when faced with uncertainty and ambiguous information. In this study, we propose the DVNN- MABAC approach to solve MADM problems with DVNSs. Finally, a numerical study on the employment and entrepreneurship abilities evaluation of vocational college students is presented to validate the effectiveness of the DVNN- MABAC model.

The structure of this paper is as follows: Section 2 provides an introduction to DVNSs. In Section 3, the DVNN- MABAC method, is proposed within the DVNS framework. Section 4 presents a case study illustrating the employment and entrepreneurship abilities evaluation of vocational college students, accompanied by a comparative analysis. Finally, Section 5 offers concluding remarks.

2. Literature review

The evaluation of employment and entrepreneurship abilities of vocational college students is a comprehensive assessment of their overall competencies, aimed at enhancing their competitiveness in the job market and their potential for entrepreneurship. First, the employment ability evaluation focuses on professional skills, job adaptability, and communication and teamwork skills. This helps students understand their performance in real work environments, identify areas for improvement, and strengthen their competitiveness in

the job market. At the same time, the evaluation provides feedback to the school, encouraging the optimization of curriculum design to ensure that talent development aligns with industry needs. Secondly, the entrepreneurship ability evaluation emphasizes students' innovative thinking, market sensitivity, risk management, and resource integration abilities. Through this evaluation, students can better grasp the core skills needed for entrepreneurship, while fostering an entrepreneurial mindset and the ability to respond to market changes. Additionally, schools can use the evaluation data to adjust the content and approach of entrepreneurship education, providing better support for students' entrepreneurial aspirations. Overall, the evaluation of employment and entrepreneurship abilities is not only crucial for students' individual development but also provides a scientific basis for schools to improve education quality and cultivate highly skilled, application-oriented talent. Duan and Wang [5] were the first to propose a method for evaluating college students' employment and entrepreneurship abilities based on the grey relational matrix and ideal point method. Subsequently, Chu, Chu and Fang [6] conducted a study on the employment and entrepreneurship abilities of graduates from applied universities, particularly those facing employment difficulties. Through a questionnaire survey, they developed a self-evaluation index system and identified three key factors influencing employment and entrepreneurship: professional ability, development ability, and basic ability. Based on these findings, they proposed relevant strategies from both the university and personal perspectives to improve employment and entrepreneurship capabilities. Li [7] explored ways to enhance college students' employment and entrepreneurship abilities through an educational system. He pointed out that the current employment and entrepreneurship education systems were ineffective and needed improvement. The article emphasized that a more robust educational system should be developed to comprehensively enhance students' abilities in alignment with the "mass entrepreneurship, mass innovation" strategy for social and economic development. In the same year, Xin and Han [8] researched how to cultivate college students' employment and entrepreneurship abilities using a smart classroom cloud platform. Through the integration of the "cloud-network-terminal" smart classroom platform and "Internet+" technology, they established a "four-precision" education model that focused on precise data collection, analysis, evaluation, and presentation. This was aimed at improving the capability of higher education institutions to foster employment and entrepreneurship and providing data support for decision-making. Tang [9] analyzed the current state of employment and entrepreneurship education in vocational colleges under the "Double High Plan" and proposed measures to enhance students' overall competence and employability. She argued that improving the comprehensive qualities of vocational college students is essential for promoting market-driven economic development in the context of innovation and entrepreneurship. Zhang [10] further explored the cultivation of college students' employment and entrepreneurship abilities from a market-demand perspective. He identified existing problems in universities' employment and entrepreneurship education and proposed enhancing

students' abilities by improving educational support mechanisms, revising evaluation models, and strengthening collaborative education. Finally, Qin, Gao, Jia, Zhang and Yue [11] proposed a comprehensive model for cultivating college students' employment and entrepreneurship abilities based on the "1+5T integration theory." They developed the "PPD" evaluation system and, through the "9P" cycle process, trained diversified T-shaped talents. The "1119N" model they proposed aimed to fully enhance students' employability and entrepreneurial skills, introducing significant innovations in higher education teaching theories.

MADM refers to a class of decision-making methods used to evaluate and select among multiple alternatives based on several attributes or criteria [12, 13]. It is widely applied in complex decision-making scenarios such as project evaluation, supplier selection, and investment decisions, assisting decision-makers in making optimal choices when faced with multidimensional information [14, 15]. The core of MADM lies in how to manage the importance of various attributes and the performance of alternatives under different attributes [16, 17]. First, decision problems typically involve multiple attributes (or criteria) that need to be considered, which can be either quantitative or qualitative. Second, different attributes may carry different levels of importance, so each attribute needs to be assigned a weight to reflect its relative significance in the decision-making process. Several methods are commonly used in MADM, including TOPSIS [3] and TODIM [18]. TOPSIS [3] ranks alternatives.

One key advantage of MADM is its flexibility, as it can handle different types of information (such as quantitative and qualitative data) and incorporate the subjective preferences of decision-makers. However, MADM also faces challenges, especially when dealing with a large number of attributes or conflicting opinions among decision-makers, which can increase the complexity of the decision-making process. In summary, MADM provides a systematic decision-making approach, helping decision-makers make rational choices in complex, multi-dimensional environments. In 1986, Atanassov [19] developed the intuitionistic fuzzy sets, incorporating hesitation into the existing membership and non-membership degrees. Later, Kandasamy [4] introduced Double-Valued Neutrosophic Sets (DVNSs) to enhance the representation of fuzziness with help of Neutrosophic Sets [20-22].

3. Preliminaries

Kandasamy [4] put forward the DVNSs.

Definition 2 [4]. The DVNSs is put forward:

$$UA=\left\{\left(x,UT_A(x),UIT_A(x),UIF_A(x),UF_A(x)\right)\middle|x\in X\right\} \tag{1}$$

with $UT_A(x)$ is truth-membership, $UIT_A(x)$ is listed as indeterminacy leaning for truth-membership, $UIF_A(x)$ is listed as indeterminacy leaning for falsity-membership indeterminacy-membership, $UF_A(x)$ is listed as falsity-membership,

$UT_A(x), UIT_A(x), UIF_A(x), UF_A(x) \in [0,1]$,
$0 \le UT_A(x) + UIT_A(x) + UIF_A(x) + UF_A(x) \le 4$.

The DVNN is listed as: $UA = (UT_A, UIT_A, UIF_A, UF_A)$, $DT_A, DIT_A, DIF_A, DF_A \in [0,1]$, $0 \le UT_A + UIT_A + UIF_A + UF_A \le 4$.

Definition 2. Let $UA = (UT_A, UIT_A, UIF_A, UF_A)$, the score value is constructed:

$$USV(DA) = \frac{(2 + UT_A + UIT_A - UIF_A - UF_A)}{4},\ DSV(UA) \in [0,1]. \quad (2)$$

Definition 3. Let $UA = (UT_A, UIT_A, UIF_A, UF_A)$, the accuracy value is constructed:

$$UAV(UA) = \frac{(UT_A + UIT_A + UIF_A + UF_A)}{4},\ UAV(UA) \in [0,1]\ . \quad (3)$$

The order between two DVNNs is put forward.

Definition 4. Let $UA = (UT_A, UIT_A, UIF_A, UF_A)$ and $UB = (UT_B, UIT_B, UIF_B, UF_B)$, let $USV(DA) = \frac{(2 + UT_A + UIT_A - UIF_A - UF_A)}{4}$ and $USV(UB) = \frac{(2 + UT_B + UIT_B - UIF_B - UF_B)}{4}$, and let $UAV(UA) = \frac{(UT_A + UIT_A + UIF_A + UF_A)}{4}$ and $UAV(UB) = \frac{(UT_B + UIT_B + UIF_B + UF_B)}{4}$, then if $USV(UA) < USV(UB)$, $UA < UB$; if $USV(UA) = USV(UB)$, Then (1)if $UAV(UA) = UAV(UB)$, $UA = UB$; (2) if $UAV(UA) < UAV(UB)$, $UA < UB$.

Definition 5[4]. $UA = (UT_A, UIT_A, UIF_A, UF_A)$, $UB = (UT_B, UIT_B, UIF_B, UF_B)$, the operations are constructed:

(1) $UA \oplus UB = (UT_A + UT_B - UT_A UT_B, UIT_A + UIT_B - UIT_A UIT_B, UIF_A UIF_B, UF_A UF_B)$;

(2) $UA \otimes UB = (UT_A UT_B, UIT_A UIT_B, UIF_A + UIF_B - UIF_A UIF_B, UF_A + UF_B - UF_A UF_B)$;

(3) $\lambda UA = \left(1 - (1 - UT_A)^{\lambda}, 1 - (1 - UIT_A)^{\lambda}, (UIF_A)^{\lambda}, (UF_A)^{\lambda}\right), \lambda > 0$;

(4) $(UA)^{\lambda} = \left((UT_A)^{\lambda}, (UIT_A)^{\lambda}, 1 - (1 - UIF_A)^{\lambda}, 1 - (1 - UF_A)^{\lambda}\right), \lambda > 0$.

Definition 6[4]. Let $UA = (UT_A, UIT_A, UIF_A, UF_A)$ and $UB = (UT_B, UIT_B, UIF_B, UF_B)$, then the normalized Euclidean distance between $UA = (UT_A, UIT_A, UIF_A, UF_A)$ and $UB = (UT_B, UIT_B, UIF_B, UF_B)$ is:

$$ED(UA, UB) = \sqrt{\frac{1}{4}\left(\begin{array}{l} |UT_A - UT_B|^2 + |UIT_A - UIT_B|^2 \\ + |UIF_A - UIF_B|^2 + |UF_A - UF_B|^2 \end{array}\right)} \quad (4)$$

4. DVNN-MABAC approach

This section shows the steps of the MABAC method under the DVNN environment. The MABAC method is used to rank the alternatives. It is used the decision matrix to obtain the rank of alternatives. The steps of the MABAC method are shown in Figure 1.

Step 1. Build the decision matrix.

$$\mathrm{X} = \begin{bmatrix} x_{11} & \cdots & x_{1n} \\ \vdots & \ddots & \vdots \\ x_{m1} & \cdots & x_{mn} \end{bmatrix} \tag{5}$$

Where $i = 1,2,\ldots,m; j = 1,2,..,n$

Step 2. Normalize the decision matrix.

$$e_{ij} = \frac{x_{ij} - \min x_i}{\max x_i - \min x_i} \tag{6}$$

$$e_{ij} = \frac{x_{ij} - \max x_i}{\min x_i - \max x_i} \tag{7}$$

Step 3. Compute the criteria weights.

The criteria weights are determined using average method

Step 4. Determine the weighted normalized decision matrix.

$$r_{ij} = w_j + e_{ij} * w_j \tag{8}$$

Step 5. Obtain the border approximation values.

$$g_j = \left(\prod_{i=1}^{m} r_{ij}\right)^{\frac{1}{m}} \tag{9}$$

Step 6. Compute the distance from the $\boldsymbol{g_j}$

$$\boldsymbol{u_{ij} = r_{ij} - g_i}$$

Step 7. Compute the total distance

$$\boldsymbol{D_i = \sum_{j=1}^{n} u_{ij}}$$

Step 8. Final rank of alternatives.

The alternatives are ranked based on the larges value in $\boldsymbol{D_i}$.

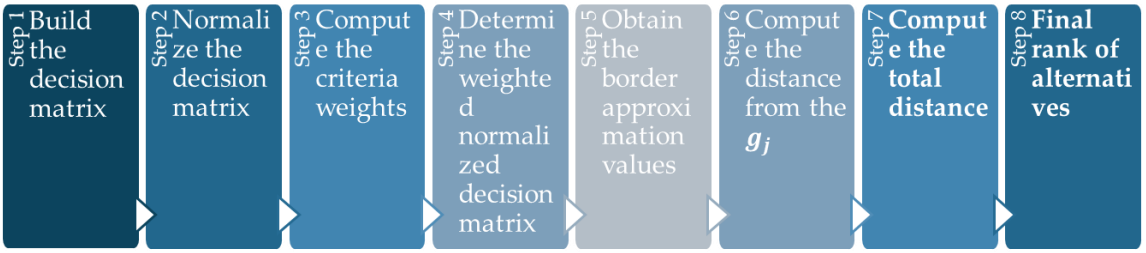

Figure 1. The stages of the DVNN-MABAC.

5. Data analysis

The evaluation of employment and entrepreneurship abilities of vocational college students is a systematic and comprehensive process aimed at assessing students' overall competencies in various areas, including professional skills, job adaptability, innovative thinking, and entrepreneurial capabilities. This evaluation not only focuses on students' academic performance but also emphasizes their practical abilities and adaptability in real work environments. By evaluating students' employment and entrepreneurship abilities, vocational colleges can better understand their professional competence and future potential, thereby providing more targeted teaching and support. Firstly, the evaluation of employment abilities helps assess students' performance in areas such as professional skills, communication, teamwork, and problem-solving. This process not only helps students recognize their strengths and weaknesses but also clarifies their future career development direction, enabling them to adjust their mindset and actions to enhance their competitiveness in the job market. At the same time, the results of the evaluation provide important feedback to the college, encouraging improvements in course design, teaching methods, and practical training to increase the precision and relevance of talent cultivation. Secondly, the evaluation of entrepreneurship abilities focuses on assessing students' innovation awareness, market sensitivity, risk management, and resource integration abilities. This evaluation not only stimulates students' entrepreneurial enthusiasm but also helps them accumulate entrepreneurial experience in practice, fostering confidence and resilience. With the increasing demand for innovative and entrepreneurial talent in society, cultivating entrepreneurship skills has become an essential part of vocational education. Overall, the evaluation of employment and entrepreneurship abilities provides students with a clear direction for improvement, while also offering schools scientific data to improve their teaching and curriculum design. This evaluation mechanism not only promotes students' comprehensive development but also helps society by producing high-quality, application-oriented talent that meets

market demands, contributing to social and economic innovation and sustainable development. The employment and entrepreneurship abilities evaluation of vocational college students are MADM. 13 potential vocational colleges are assessed with 12 attributes are shown in Figure 2.

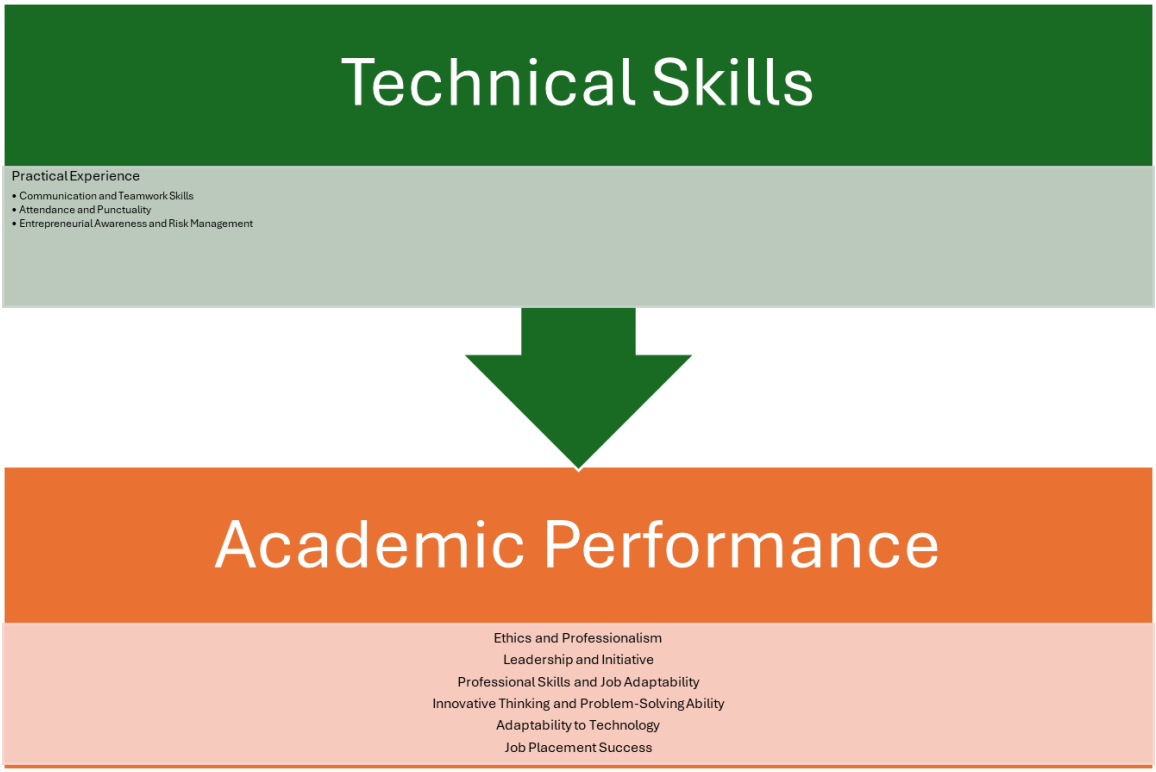

Figure 2. The 12 attributes.

Step 1. We built the decision matrix between criteria and alternatives using the DVNN through three experts as displayed in Table 1.

Step 2. Then we normalize the decision matrix between criteria and alternatives as displayed in Table 2.

Step 3. Then we used the average method to obtain the weights of criteria as shown in Figure 3.

Step 4. Then we determine the weighted normalized decision matrix as displayed in Table 3.

Step 5. Then we obtained the g_i values.

Step 6. Then we compute the distance from the g_i.

Step 7. Then we obtained the total distance

Step 8. Then we rank the alternatives as shown in Figure 4.

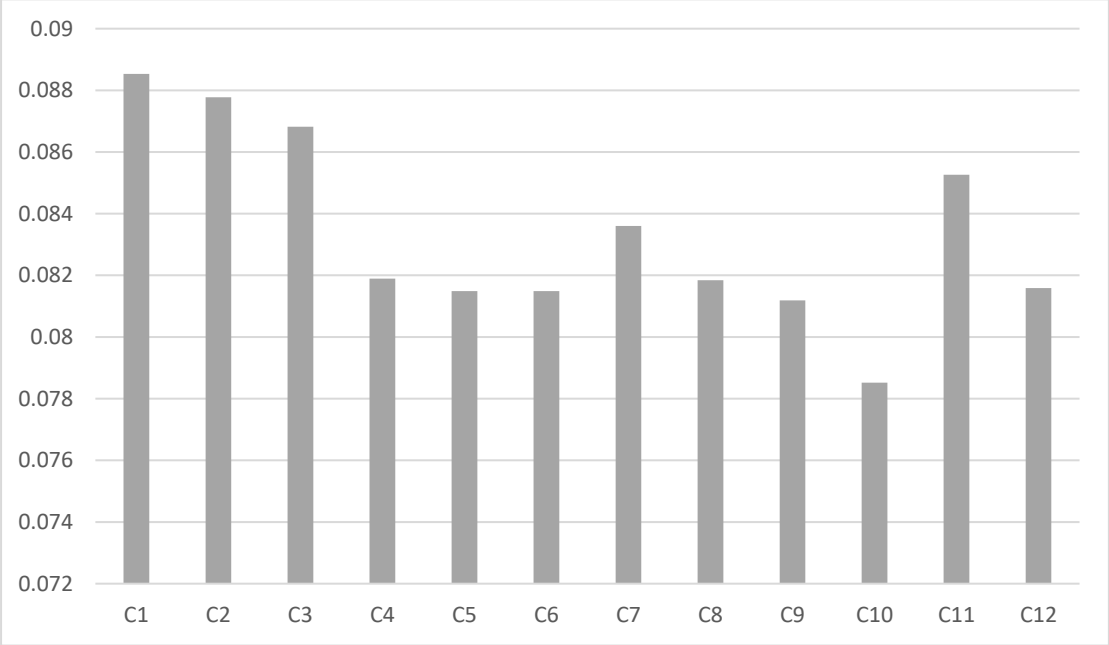

Figure 3. The criteria weights.

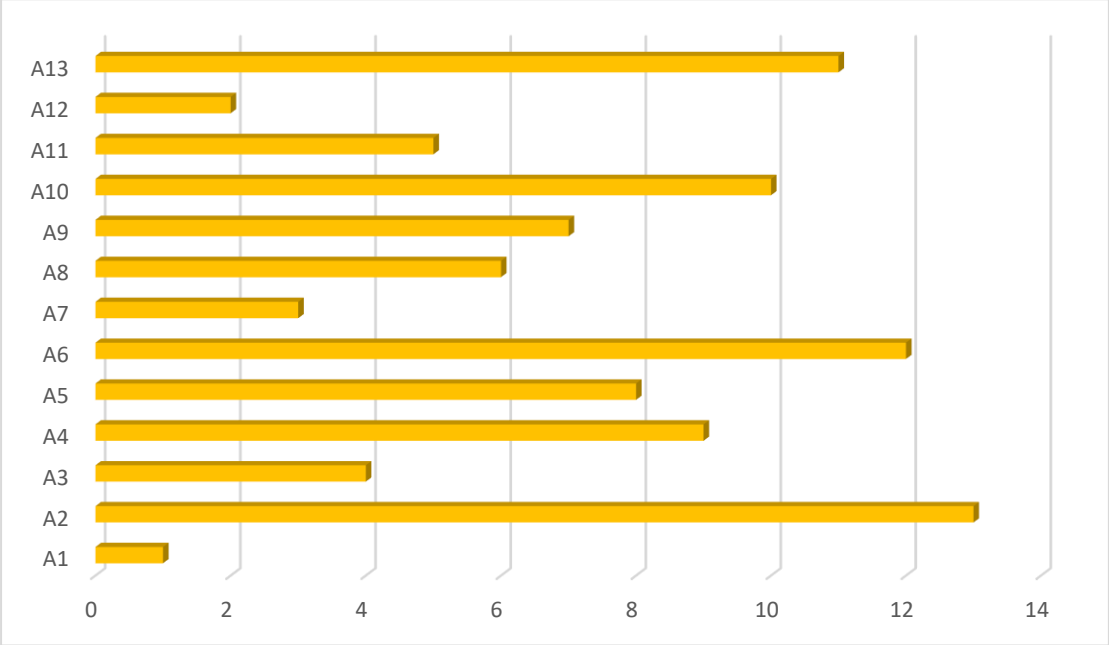

Figure 4. The rank of alternatives.

Table 1. The opinions of three experts.

	C_1	C_2	C_3	C_4	C_5	C_6	C_7	C_8	C_9	C_{10}	C_{11}	C_{12}
A_1	(0.2, 0.4, 0.4, 0.7)	(0.8, 0.1, 0.1, 0.1)	(0.6, 0.2, 0.2, 0.3)	(0.4, 0.3, 0.3, 0.5)	(0.2, 0.4, 0.4, 0.7)	(0.9, 0.05, 0.05, 0.05)	(0.8, 0.1, 0.1, 0.1)	(0.6, 0.2, 0.2, 0.3)	(0.4, 0.3, 0.3, 0.5)	(0.2, 0.4, 0.4, 0.7)	(0.9, 0.05, 0.05, 0.05)	(0.9, 0.05, 0.05, 0.05)
A_2	(0.9, 0.05, 0.05, 0.05)	(0.2, 0.4, 0.4, 0.7)	(0.4, 0.3, 0.3, 0.5)	(0.2, 0.4, 0.4, 0.7)	(0.9, 0.05, 0.05, 0.05)	(0.8, 0.1, 0.1, 0.1)	(0.6, 0.2, 0.2, 0.3)	(0.4, 0.3, 0.3, 0.5)	(0.2, 0.4, 0.4, 0.7)	(0.4, 0.3, 0.3, 0.5)	(0.2, 0.4, 0.4, 0.7)	(0.8, 0.1, 0.1, 0.1)
A_3	(0.8, 0.1, 0.1, 0.1)	(0.9, 0.05, 0.05, 0.05)	(0.4, 0.3, 0.3, 0.5)	(0.2, 0.4, 0.4, 0.7)	(0.8, 0.1, 0.1, 0.1)	(0.9, 0.05, 0.05, 0.05)	(0.9, 0.05, 0.05, 0.05)	(0.8, 0.1, 0.1, 0.1)	(0.6, 0.2, 0.2, 0.3)	(0.4, 0.3, 0.3, 0.5)	(0.4, 0.3, 0.3, 0.5)	(0.8, 0.1, 0.1, 0.1)
A_4	(0.4, 0.3, 0.3, 0.5)	(0.9, 0.05, 0.05, 0.05)	(0.8, 0.1, 0.1, 0.1)	(0.6, 0.2, 0.2, 0.3)	(0.4, 0.3, 0.3, 0.5)	(0.2, 0.4, 0.4, 0.7)	(0.9, 0.05, 0.05, 0.05)	(0.8, 0.1, 0.1, 0.1)	(0.6, 0.2, 0.2, 0.3)	(0.2, 0.4, 0.4, 0.7)	(0.2, 0.4, 0.4, 0.7)	(0.6, 0.2, 0.2, 0.3)
A_5	(0.2, 0.4, 0.4, 0.7)	(0.6, 0.2, 0.2, 0.3)	(0.9, 0.05, 0.05, 0.05)	(0.9, 0.05, 0.05, 0.05)	(0.8, 0.1, 0.1, 0.1)	(0.6, 0.2, 0.2, 0.3)	(0.4, 0.3, 0.3, 0.5)	(0.2, 0.4, 0.4, 0.7)	(0.4, 0.3, 0.3, 0.5)	(0.2, 0.4, 0.4, 0.7)	(0.2, 0.4, 0.4, 0.7)	(0.4, 0.3, 0.3, 0.5)
A_6	(0.8, 0.1, 0.1, 0.1)	(0.8, 0.1, 0.1, 0.1)	(0.8, 0.1, 0.1, 0.1)	(0.2, 0.4, 0.4, 0.7)	(0.4, 0.3, 0.3, 0.5)	(0.2, 0.4, 0.4, 0.7)	(0.4, 0.3, 0.3, 0.5)	(0.2, 0.4, 0.4, 0.7)	(0.2, 0.4, 0.4, 0.7)	(0.4, 0.3, 0.3, 0.5)	(0.4, 0.3, 0.3, 0.5)	(0.2, 0.4, 0.4, 0.7)
A_7	(0.9, 0.05, 0.05, 0.05)	(0.2, 0.4, 0.4, 0.7)	(0.8, 0.1, 0.1, 0.1)	(0.4, 0.3, 0.3, 0.5)	(0.9, 0.05, 0.05, 0.05)	(0.4, 0.3, 0.3, 0.5)	(0.9, 0.05, 0.05, 0.05)	(0.4, 0.3, 0.3, 0.5)	(0.4, 0.3, 0.3, 0.5)	(0.9, 0.05, 0.05, 0.05)	(0.9, 0.05, 0.05, 0.05)	(0.2, 0.4, 0.4, 0.7)
A_8	(0.8, 0.1, 0.1, 0.1)	(0.4, 0.3, 0.3, 0.5)	(0.2, 0.4, 0.4, 0.7)	(0.8, 0.1, 0.1, 0.1)	(0.4, 0.3, 0.3, 0.5)	(0.6, 0.2, 0.2, 0.3)	(0.8, 0.1, 0.1, 0.1)	(0.9, 0.05, 0.05, 0.05)	(0.4, 0.3, 0.3, 0.5)	(0.8, 0.1, 0.1, 0.1)	(0.8, 0.1, 0.1, 0.1)	(0.2, 0.4, 0.4, 0.7)
A_9	(0.6, 0.2, 0.2, 0.3)	(0.6, 0.2, 0.2, 0.3)	(0.4, 0.3, 0.3, 0.5)	(0.9, 0.05, 0.05, 0.05)	(0.4, 0.3, 0.3, 0.5)	(0.6, 0.2, 0.2, 0.3)	(0.8, 0.1, 0.1, 0.1)	(0.9, 0.05, 0.05, 0.05)	(0.2, 0.4, 0.4, 0.7)	(0.6, 0.2, 0.2, 0.3)	(0.6, 0.2, 0.2, 0.3)	(0.4, 0.3, 0.3, 0.5)
A_{10}	(0.4, 0.3, 0.3, 0.5)	(0.8, 0.1, 0.1, 0.1)	(0.6, 0.2, 0.2, 0.3)	(0.8, 0.1, 0.1, 0.1)	(0.9, 0.05, 0.05, 0.05)	(0.2, 0.4, 0.4, 0.7)	(0.4, 0.3, 0.3, 0.5)	(0.6, 0.2, 0.2, 0.3)	(0.8, 0.1, 0.1, 0.1)	(0.4, 0.3, 0.3, 0.5)	(0.4, 0.3, 0.3, 0.5)	(0.4, 0.3, 0.3, 0.5)
A_{11}	(0.8, 0.1, 0.1, 0.1)	(0.9, 0.05, 0.05, 0.05)	(0.8, 0.1, 0.1, 0.1)	(0.9, 0.05, 0.05, 0.05)	(0.2, 0.4, 0.4, 0.7)	(0.4, 0.3, 0.3, 0.5)	(0.6, 0.2, 0.2, 0.3)	(0.8, 0.1, 0.1, 0.1)	(0.9, 0.05, 0.05, 0.05)	(0.2, 0.4, 0.4, 0.7)	(0.9, 0.05, 0.05, 0.05)	(0.2, 0.4, 0.4, 0.7)

A_{12}	(0.9, 0.05, 0.05, 0.05)	(0.8, 0.1, 0.1, 0.1)	(0.9, 0.05, 0.05, 0.05)	(0.8, 0.1, 0.1, 0.1)	(0.2, 0.4, 0.4, 0.7)	(0.4, 0.3, 0.3, 0.5)	(0.2, 0.4, 0.4, 0.7)	(0.4, 0.3, 0.3, 0.5)	(0.8, 0.1, 0.1, 0.1)	(0.9, 0.05, 0.05, 0.05)	(0.8, 0.1, 0.1, 0.1)	(0.9, 0.05, 0.05, 0.05)
A_{13}	(0.9, 0.05, 0.05, 0.05)	(0.6, 0.2, 0.2, 0.3)	(0.8, 0.1, 0.1, 0.1)	(0.2, 0.4, 0.4, 0.7)	(0.4, 0.3, 0.3, 0.5)	(0.2, 0.4, 0.4, 0.7)	(0.4, 0.3, 0.3, 0.5)	(0.2, 0.4, 0.4, 0.7)	(0.2, 0.4, 0.4, 0.7)	(0.4, 0.3, 0.3, 0.5)	(0.6, 0.2, 0.2, 0.3)	(0.8, 0.1, 0.1, 0.1)
	C_1	C_2	C_3	C_4	C_5	C_6	C_7	C_8	C_9	C_{10}	C_{11}	C_{12}
A_1	(0.2, 0.4, 0.4, 0.7)	(0.8, 0.1, 0.1, 0.1)	(0.6, 0.2, 0.2, 0.3)	(0.4, 0.3, 0.3, 0.5)	(0.2, 0.4, 0.4, 0.7)	(0.9, 0.05, 0.05, 0.05)	(0.8, 0.1, 0.1, 0.1)	(0.6, 0.2, 0.2, 0.3)	(0.4, 0.3, 0.3, 0.5)	(0.2, 0.4, 0.4, 0.7)	(0.9, 0.05, 0.05, 0.05)	(0.4, 0.3, 0.3, 0.5)
A_2	(0.9, 0.05, 0.05, 0.05)	(0.2, 0.4, 0.4, 0.7)	(0.2, 0.4, 0.4, 0.7)	(0.2, 0.4, 0.4, 0.7)	(0.9, 0.05, 0.05, 0.05)	(0.8, 0.1, 0.1, 0.1)	(0.6, 0.2, 0.2, 0.3)	(0.4, 0.3, 0.3, 0.5)	(0.2, 0.4, 0.4, 0.7)	(0.4, 0.3, 0.3, 0.5)	(0.2, 0.4, 0.4, 0.7)	(0.2, 0.4, 0.4, 0.7)
A_3	(0.8, 0.1, 0.1, 0.1)	(0.9, 0.05, 0.05, 0.05)	(0.4, 0.3, 0.3, 0.5)	(0.2, 0.4, 0.4, 0.7)	(0.8, 0.1, 0.1, 0.1)	(0.9, 0.05, 0.05, 0.05)	(0.2, 0.4, 0.4, 0.7)	(0.8, 0.1, 0.1, 0.1)	(0.4, 0.3, 0.3, 0.5)	(0.4, 0.3, 0.3, 0.5)	(0.4, 0.3, 0.3, 0.5)	(0.8, 0.1, 0.1, 0.1)
A_4	(0.4, 0.3, 0.3, 0.5)	(0.2, 0.4, 0.4, 0.7)	(0.6, 0.2, 0.2, 0.3)	(0.4, 0.3, 0.3, 0.5)	(0.2, 0.4, 0.4, 0.7)	(0.2, 0.4, 0.4, 0.7)	(0.4, 0.3, 0.3, 0.5)	(0.2, 0.4, 0.4, 0.7)	(0.6, 0.2, 0.2, 0.3)	(0.2, 0.4, 0.4, 0.7)	(0.2, 0.4, 0.4, 0.7)	(0.6, 0.2, 0.2, 0.3)
A_5	(0.2, 0.4, 0.4, 0.7)	(0.4, 0.3, 0.3, 0.5)	(0.6, 0.2, 0.2, 0.3)	(0.6, 0.2, 0.2, 0.3)	(0.4, 0.3, 0.3, 0.5)	(0.6, 0.2, 0.2, 0.3)	(0.6, 0.2, 0.2, 0.3)	(0.4, 0.3, 0.3, 0.5)	(0.6, 0.2, 0.2, 0.3)	(0.4, 0.3, 0.3, 0.5)	(0.4, 0.3, 0.3, 0.5)	(0.4, 0.3, 0.3, 0.5)
A_6	(0.4, 0.3, 0.3, 0.5)	(0.6, 0.2, 0.2, 0.3)	(0.2, 0.4, 0.4, 0.7)	(0.6, 0.2, 0.2, 0.3)	(0.6, 0.2, 0.2, 0.3)	(0.2, 0.4, 0.4, 0.7)	(0.6, 0.2, 0.2, 0.3)	(0.6, 0.2, 0.2, 0.3)	(0.2, 0.4, 0.4, 0.7)	(0.6, 0.2, 0.2, 0.3)	(0.6, 0.2, 0.2, 0.3)	(0.2, 0.4, 0.4, 0.7)
A_7	(0.6, 0.2, 0.2, 0.3)	(0.6, 0.2, 0.2, 0.3)	(0.4, 0.3, 0.3, 0.5)	(0.2, 0.4, 0.4, 0.7)	(0.6, 0.2, 0.2, 0.3)	(0.4, 0.3, 0.3, 0.5)	(0.2, 0.4, 0.4, 0.7)	(0.6, 0.2, 0.2, 0.3)	(0.4, 0.3, 0.3, 0.5)	(0.6, 0.2, 0.2, 0.3)	(0.6, 0.2, 0.2, 0.3)	(0.4, 0.3, 0.3, 0.5)
A_8	(0.6, 0.2, 0.2, 0.3)	(0.2, 0.4, 0.4, 0.7)	(0.4, 0.3, 0.3, 0.5)	(0.4, 0.3, 0.3, 0.5)	(0.2, 0.4, 0.4, 0.7)	(0.6, 0.2, 0.2, 0.3)	(0.4, 0.3, 0.3, 0.5)	(0.2, 0.4, 0.4, 0.7)	(0.4, 0.3, 0.3, 0.5)	(0.2, 0.4, 0.4, 0.7)	(0.2, 0.4, 0.4, 0.7)	(0.6, 0.2, 0.2, 0.3)
A_9	(0.2, 0.4, 0.4, 0.7)	(0.4, 0.3, 0.3, 0.5)	(0.2, 0.4, 0.4, 0.7)	(0.4, 0.3, 0.3, 0.5)	(0.4, 0.3, 0.3, 0.5)	(0.6, 0.2, 0.2, 0.3)	(0.4, 0.3, 0.3, 0.5)	(0.4, 0.3, 0.3, 0.5)	(0.2, 0.4, 0.4, 0.7)	(0.4, 0.3, 0.3, 0.5)	(0.4, 0.3, 0.3, 0.5)	(0.6, 0.2, 0.2, 0.3)
A_{10}	(0.4, 0.3, 0.3, 0.5)	(0.4, 0.3, 0.3, 0.5)	(0.6, 0.2, 0.2, 0.3)	(0.2, 0.4, 0.4, 0.7)	(0.4, 0.3, 0.3, 0.5)	(0.2, 0.4, 0.4, 0.7)	(0.2, 0.4, 0.4, 0.7)	(0.4, 0.3, 0.3, 0.5)	(0.8, 0.1, 0.1, 0.1)	(0.4, 0.3, 0.3, 0.5)	(0.4, 0.3, 0.3, 0.5)	(0.2, 0.4, 0.4, 0.7)
A_{11}	(0.4, 0.3, 0.3, 0.5)	(0.2, 0.4, 0.4, 0.7)	(0.8, 0.1, 0.1, 0.1)	(0.9, 0.05, 0.05, 0.05)	(0.2, 0.4, 0.4, 0.7)	(0.4, 0.3, 0.3, 0.5)	(0.6, 0.2, 0.2, 0.3)	(0.2, 0.4, 0.4, 0.7)	(0.9, 0.05, 0.05, 0.05)	(0.2, 0.4, 0.4, 0.7)	(0.2, 0.4, 0.4, 0.7)	(0.4, 0.3, 0.3, 0.5)
A_{12}	(0.2, 0.4, 0.4, 0.7)	(0.8, 0.1, 0.1, 0.1)	(0.9, 0.05, 0.05, 0.05)	(0.8, 0.1, 0.1, 0.1)	(0.2, 0.4, 0.4, 0.7)	(0.4, 0.3, 0.3, 0.5)	(0.2, 0.4, 0.4, 0.7)	(0.4, 0.3, 0.3, 0.5)	(0.8, 0.1, 0.1, 0.1)	(0.9, 0.05, 0.05, 0.05)	(0.8, 0.1, 0.1, 0.1)	(0.4, 0.3, 0.3, 0.5)
A_{13}	(0.9, 0.05, 0.05, 0.05)	(0.6, 0.2, 0.2, 0.3)	(0.8, 0.1, 0.1, 0.1)	(0.2, 0.4, 0.4, 0.7)	(0.4, 0.3, 0.3, 0.5)	(0.2, 0.4, 0.4, 0.7)	(0.4, 0.3, 0.3, 0.5)	(0.2, 0.4, 0.4, 0.7)	(0.2, 0.4, 0.4, 0.7)	(0.4, 0.3, 0.3, 0.5)	(0.6, 0.2, 0.2, 0.3)	(0.2, 0.4, 0.4, 0.7)
	C_1	C_2	C_3	C_4	C_5	C_6	C_7	C_8	C_9	C_{10}	C_{11}	C_{12}
A_1	(0.2, 0.4, 0.4, 0.7)	(0.8, 0.1, 0.1, 0.1)	(0.6, 0.2, 0.2, 0.3)	(0.4, 0.3, 0.3, 0.5)	(0.2, 0.4, 0.4, 0.7)	(0.9, 0.05, 0.05, 0.05)	(0.8, 0.1, 0.1, 0.1)	(0.6, 0.2, 0.2, 0.3)	(0.4, 0.3, 0.3, 0.5)	(0.4, 0.3, 0.3, 0.5)	(0.9, 0.05, 0.05, 0.05)	(0.4, 0.3, 0.3, 0.5)
A_2	(0.9, 0.05, 0.05, 0.05)	(0.4, 0.3, 0.3, 0.5)	(0.4, 0.3, 0.3, 0.5)	(0.2, 0.4, 0.4, 0.7)	(0.9, 0.05, 0.05, 0.05)	(0.4, 0.3, 0.3, 0.5)	(0.4, 0.3, 0.3, 0.5)	(0.4, 0.3, 0.3, 0.5)	(0.2, 0.4, 0.4, 0.7)	(0.2, 0.4, 0.4, 0.7)	(0.4, 0.3, 0.3, 0.5)	(0.2, 0.4, 0.4, 0.7)
A_3	(0.4, 0.3, 0.3, 0.5)	(0.2, 0.4, 0.4, 0.7)	(0.4, 0.3, 0.3, 0.5)	(0.2, 0.4, 0.4, 0.7)	(0.8, 0.1, 0.1, 0.1)	(0.2, 0.4, 0.4, 0.7)	(0.2, 0.4, 0.4, 0.7)	(0.4, 0.3, 0.3, 0.5)	(0.4, 0.3, 0.3, 0.5)	(0.4, 0.3, 0.3, 0.5)	(0.2, 0.4, 0.4, 0.7)	(0.8, 0.1, 0.1, 0.1)
A_4	(0.2, 0.4, 0.4, 0.7)	(0.8, 0.1, 0.1, 0.1)	(0.6, 0.2, 0.2, 0.3)	(0.4, 0.3, 0.3, 0.5)	(0.4, 0.3, 0.3, 0.5)	(0.8, 0.1, 0.1, 0.1)	(0.8, 0.1, 0.1, 0.1)	(0.2, 0.4, 0.4, 0.7)	(0.2, 0.4, 0.4, 0.7)	(0.2, 0.4, 0.4, 0.7)	(0.8, 0.1, 0.1, 0.1)	(0.6, 0.2, 0.2, 0.3)
A_5	(0.8, 0.1, 0.1, 0.1)	(0.6, 0.2, 0.2, 0.3)	(0.4, 0.3, 0.3, 0.5)	(0.9, 0.05, 0.05, 0.05)	(0.2, 0.4, 0.4, 0.7)	(0.2, 0.4, 0.4, 0.7)	(0.6, 0.2, 0.2, 0.3)	(0.8, 0.1, 0.1, 0.1)	(0.8, 0.1, 0.1, 0.1)	(0.8, 0.1, 0.1, 0.1)	(0.6, 0.2, 0.2, 0.3)	(0.4, 0.3, 0.3, 0.5)
A_6	(0.6, 0.2, 0.2, 0.3)	(0.4, 0.3, 0.3, 0.5)	(0.2, 0.4, 0.4, 0.7)	(0.2, 0.4, 0.4, 0.7)	(0.8, 0.1, 0.1, 0.1)	(0.8, 0.1, 0.1, 0.1)	(0.4, 0.3, 0.3, 0.5)	(0.6, 0.2, 0.2, 0.3)	(0.6, 0.2, 0.2, 0.3)	(0.6, 0.2, 0.2, 0.3)	(0.4, 0.3, 0.3, 0.5)	(0.9, 0.05, 0.05, 0.05)
A_7	(0.4, 0.3, 0.3, 0.5)	(0.9, 0.05, 0.05, 0.05)	(0.8, 0.1, 0.1, 0.1)	(0.4, 0.3, 0.3, 0.5)	(0.6, 0.2, 0.2, 0.3)	(0.6, 0.2, 0.2, 0.3)	(0.9, 0.05, 0.05, 0.05)	(0.4, 0.3, 0.3, 0.5)	(0.4, 0.3, 0.3, 0.5)	(0.4, 0.3, 0.3, 0.5)	(0.9, 0.05, 0.05, 0.05)	(0.8, 0.1, 0.1, 0.1)
A_8	(0.9, 0.05, 0.05, 0.05)	(0.8, 0.1, 0.1, 0.1)	(0.6, 0.2, 0.2, 0.3)	(0.2, 0.4, 0.4, 0.7)	(0.4, 0.3, 0.3, 0.5)	(0.4, 0.3, 0.3, 0.5)	(0.8, 0.1, 0.1, 0.1)	(0.9, 0.05, 0.05, 0.05)	(0.9, 0.05, 0.05, 0.05)	(0.9, 0.05, 0.05, 0.05)	(0.8, 0.1, 0.1, 0.1)	(0.2, 0.4, 0.4, 0.7)
A_9	(0.8, 0.1, 0.1, 0.1)	(0.2, 0.4, 0.4, 0.7)	(0.4, 0.3, 0.3, 0.5)	(0.8, 0.1, 0.1, 0.1)	(0.9, 0.05, 0.05, 0.05)	(0.9, 0.05, 0.05, 0.05)	(0.2, 0.4, 0.4, 0.7)	(0.8, 0.1, 0.1, 0.1)	(0.8, 0.1, 0.1, 0.1)	(0.8, 0.1, 0.1, 0.1)	(0.2, 0.4, 0.4, 0.7)	(0.4, 0.3, 0.3, 0.5)
A_{10}	(0.2, 0.4, 0.4, 0.7)	(0.8, 0.1, 0.1, 0.1)	(0.9, 0.05, 0.05, 0.05)	(0.6, 0.2, 0.2, 0.3)	(0.8, 0.1, 0.1, 0.1)	(0.8, 0.1, 0.1, 0.1)	(0.2, 0.4, 0.4, 0.7)	(0.2, 0.4, 0.4, 0.7)	(0.2, 0.4, 0.4, 0.7)	(0.2, 0.4, 0.4, 0.7)	(0.4, 0.3, 0.3, 0.5)	(0.4, 0.3, 0.3, 0.5)
A_{11}	(0.8, 0.1, 0.1, 0.1)	(0.2, 0.4, 0.4, 0.7)	(0.8, 0.1, 0.1, 0.1)	(0.4, 0.3, 0.3, 0.5)	(0.2, 0.4, 0.4, 0.7)	(0.2, 0.4, 0.4, 0.7)	(0.6, 0.2, 0.2, 0.3)	(0.8, 0.1, 0.1, 0.1)	(0.9, 0.05, 0.05, 0.05)	(0.2, 0.4, 0.4, 0.7)	(0.9, 0.05, 0.05, 0.05)	(0.2, 0.4, 0.4, 0.7)
A_{12}	(0.9, 0.05, 0.05, 0.05)	(0.8, 0.1, 0.1, 0.1)	(0.2, 0.4, 0.4, 0.7)	(0.9, 0.05, 0.05, 0.05)	(0.2, 0.4, 0.4, 0.7)	(0.4, 0.3, 0.3, 0.5)	(0.2, 0.4, 0.4, 0.7)	(0.4, 0.3, 0.3, 0.5)	(0.8, 0.1, 0.1, 0.1)	(0.9, 0.05, 0.05, 0.05)	(0.8, 0.1, 0.1, 0.1)	(0.9, 0.05, 0.05, 0.05)
A_{13}	(0.9, 0.05, 0.05, 0.05)	(0.6, 0.2, 0.2, 0.3)	(0.2, 0.4, 0.4, 0.7)	(0.8, 0.1, 0.1, 0.1)	(0.4, 0.3, 0.3, 0.5)	(0.2, 0.4, 0.4, 0.7)	(0.4, 0.3, 0.3, 0.5)	(0.2, 0.4, 0.4, 0.7)	(0.2, 0.4, 0.4, 0.7)	(0.4, 0.3, 0.3, 0.5)	(0.6, 0.2, 0.2, 0.3)	(0.8, 0.1, 0.1, 0.1)

Table 2. The normalized decision matrix.

	C_1	C_2	C_3	C_4	C_5	C_6	C_7	C_8	C_9	C_{10}	C_{11}	C_{12}
A_1	1.246154	1	0.571429	0.32	0	1	1	0.813559	0.296296	0.098765	1	0.546875
A_2	1	0	0	0	1	0.691358	0.555556	0.40678	0	0.197531	0	0.25
A_3	0.615385	0.71875	0.142857	0	0.888889	0.666667	0.375	0.949153	0.395062	0.296296	0.109589	1
A_4	0	0.671875	0.857143	0.533333	0.197531	0.098765	0.819444	0.40678	0.395062	0	0.219178	0.625
A_5	0.123077	0.5	0.625	0.933333	0.395062	0.395062	0.555556	0.542373	0.592593	0.395062	0.219178	0.25
A_6	0.492308	0.625	0.142857	0.213333	0.592593	0.296296	0.444444	0.542373	0.197531	0.493827	0.328767	0.296875
A_7	0.538462	0.546875	0.714286	0.213333	0.728395	0.395062	0.75	0.542373	0.296296	0.62963	0.849315	0.375
A_8	0.784615	0.375	0.142857	0.426667	0.197531	0.493827	0.777778	0.915254	0.530864	0.62963	0.547945	0.125
A_9	0.369231	0.25	0	0.786667	0.530864	0.728395	0.444444	1	0.296296	0.592593	0.219178	0.375
A_{10}	0	0.75	0.767857	0.533333	0.728395	0.296296	0.111111	0.40678	0.592593	0.197531	0.219178	0.125
A_{11}	0.615385	0.296875	1	0.826667	0	0.197531	0.666667	0.813559	1	0	0.630137	0
A_{12}	0.584615	1	0.678571	1	0	0.296296	0	0.40678	0.888889	1	0.876712	0.84375
A_{13}	1	0.625	0.571429	0.32	0.296296	0	0.333333	0	0	0.296296	0.547945	0.625

Table 3. The weighted normalized decision matrix.

	C_1	C_2	C_3	C_4	C_5	C_6	C_7	C_8	C_9	C_{10}	C_{11}	C_{12}
A_1	0.198855	0.175553	0.136433	0.108097	0.081489	0.162978	0.167203	0.148424	0.105243	0.086276	0.170523	0.126209
A_2	0.177062	0.087777	0.086821	0.081891	0.162978	0.137827	0.130047	0.115132	0.081187	0.094031	0.085262	0.101987
A_3	0.143012	0.150866	0.099224	0.081891	0.153924	0.135815	0.114952	0.159521	0.113261	0.101787	0.094605	0.163179
A_4	0.088531	0.146752	0.161239	0.125567	0.097586	0.089537	0.152108	0.115132	0.113261	0.078521	0.103949	0.132583
A_5	0.099427	0.131665	0.141084	0.158323	0.113682	0.113682	0.130047	0.126229	0.129298	0.109542	0.103949	0.101987
A_6	0.132116	0.142637	0.099224	0.099362	0.129779	0.105634	0.120758	0.126229	0.097224	0.117297	0.113293	0.105811
A_7	0.136202	0.13578	0.148836	0.099362	0.140845	0.113682	0.146303	0.126229	0.105243	0.12796	0.157676	0.112186
A_8	0.157994	0.120693	0.099224	0.116832	0.097586	0.12173	0.148625	0.156746	0.124286	0.12796	0.13198	0.091788
A_9	0.12122	0.109721	0.086821	0.146313	0.124748	0.140845	0.120758	0.163682	0.105243	0.125052	0.103949	0.112186
A_{10}	0.088531	0.153609	0.153487	0.125567	0.140845	0.105634	0.092891	0.115132	0.129298	0.094031	0.103949	0.091788
A_{11}	0.143012	0.113835	0.173642	0.149588	0.081489	0.097586	0.139336	0.148424	0.162374	0.078521	0.138988	0.08159
A_{12}	0.140288	0.175553	0.145735	0.163783	0.081489	0.105634	0.083602	0.115132	0.153353	0.157042	0.160011	0.150431
A_{13}	0.177062	0.142637	0.136433	0.108097	0.105634	0.081489	0.111469	0.081841	0.081187	0.101787	0.13198	0.132583

5. Conclusion

The purpose of evaluating the employment and entrepreneurship abilities of vocational college students is to comprehensively understand their competencies in areas such as professional skills, job adaptability, innovative thinking, and entrepreneurial capabilities. This helps students identify their strengths and weaknesses, enabling them to enhance their

competitiveness in the job market. At the same time, the evaluation provides feedback to schools, encouraging them to optimize course design and teaching methods to better meet societal and market needs. Additionally, by evaluating entrepreneurial abilities, the process stimulates students' innovation awareness and entrepreneurial spirit, preparing them to navigate market changes and entrepreneurial challenges for future career success. The employment and entrepreneurship abilities evaluation of vocational college students are MADM. Recently, the MABAC approach has been applied to address MADM problems. DVNSs are used as an effective tool for representing fuzzy data in the employment and entrepreneurship abilities evaluation of vocational college students. In this study, the DVNN-MABAC approach is proposed to handle MADM under DVNSs. Finally, a numerical study on the employment and entrepreneurship abilities evaluation of vocational college students is conducted to validate the DVNN- MABAC model.

Based on the content of this study, future research can delve into the following three directions: (1) Expanding the application areas of the decision model: Although the DVNN-MABAC method performed well in the employment and entrepreneurship abilities evaluation of vocational college students, its application scope can be further expanded. Future studies could apply this model to other teaching quality evaluations, corporate management decision-making, healthcare optimization, and more, to verify its applicability and effectiveness in different contexts. This would provide richer data support for the model's use across a wide range of fields. (2) Incorporating additional uncertainty-handling methods: While DVNSs are effective at handling fuzzy information, more complex decision environments may involve even greater uncertainty or fuzziness. Future research could consider integrating other uncertainty-handling methods, such as interval numbers, grey system theory, or stochastic fuzzy sets, to further enhance the model’s ability to process complex information. These extended methods would improve the model's robustness in dynamic and uncertain environments. (3) Optimizing computational efficiency and algorithm performance: As the scale and complexity of decision problems increase, computational efficiency and performance become critical issues. Future studies could focus on improving the algorithm design of the DVNN- MABAC method, optimizing its computational complexity, and enhancing its ability to handle large-scale datasets. Additionally, leveraging machine learning and artificial intelligence techniques to develop intelligent optimization algorithms could further improve the method’s computational efficiency and decision-making speed. By pursuing these research directions, the DVNN-MABAC method can be further enhanced in terms of its broad applicability and decision-support capabilities, providing more comprehensive and efficient solutions for complex decision-making problems.

Acknowledgment

The work was supported by the Research Project on China Vocational Education in Zhejiang Province in 2023: Strategies for Enhancing the Employment and Entrepreneurial Abilities of Higher Vocational College Students Oriented Towards High-Quality Employment (Project Number: ZJCV2023C31).

References

[1] L. Gomes, M. Lima, Todim: Basics and apllication to multicriteria ranking of projects with environmental impacts, Foundations of Control Engineering, 16 (1991) 113-127.

[2] L.F.A.M. Gomes, M.M.P.P. Lima, From modeling individual preferences to multicriteria ranking of discrete alternatives: A look at prospect theory and the additive difference model, Foundations of Computing and Decision Sciences, 17 (1992) 171-184.

[3] Y.-J. Lai, T.-Y. Liu, C.-L. Hwang, Topsis for modm, European Journal of Operational Research, 76 (1994) 486-500.

[4] I. Kandasamy, Double-valued neutrosophic sets, their minimum spanning trees, and clustering algorithm, Journal of Intelligent Systems, 27 (2018) 163-182.

[5] S. Duan, X. Wang, Application of grey relational matrix and ideal point method in the evaluation of college students' employment and entrepreneurship ability, Journal of Shenyang Normal University (Natural Science Edition), 34 (2016) 109-112.

[6] Z. Chu, W. Chu, Y. Fang, Research on the employment and entrepreneurship ability of applied college graduates based on factor analysis: Taking relatively difficult graduates as samples, Journal of Taiyuan Normal University (Natural Science Edition), 17 (2018) 1-6.

[7] X. Li, Employment and entrepreneurship education system to improve college students' employment and entrepreneurship ability, Employment and Security, (2021) 80-81.

[8] H. Xin, S. Han, Research on the cultivation of college students' employment and entrepreneurship ability based on the smart classroom cloud platform, Modern Vocational Education, (2021) 44-46.

[9] L. Tang, Research on the evaluation of employment and entrepreneurship ability of vocational college students under the background of "double high plan", Shanxi Youth, (2022) 146-148.

[10] B. Zhang, Employment and entrepreneurship ability training of college students oriented by market demand, Employment and Security, (2023) 31-33.

[11] G. Qin, Y. Gao, D. Jia, P. Zhang, X. Yue, Research on the all-chain and diversified training mode of college students' employment and entrepreneurship ability based on "1+5t integration theory", Journal of Shandong Vocational College of Commerce and Technology, 23 (2023) 102-106.

[12] M. Mohamed, A. Elsayed, A novel multi-criteria decision making approach based on bipolar

neutrosophic set for evaluating financial markets in egypt, Multicriteria Algorithms with Applications, 5 (2024) 1-17.

[13] A. M.Ali, M. Muthuswamy, Neutrosophic multi-criteria decision-making framework for sustainable evaluation of power production systems in renewable energy sources, Sustainable Machine Intelligence Journal, 4 (2023) (3):1-10.

[14] A.A. Salama, M.Y. Shams, S. Elseuofi, H.E. Khalid, Exploring neutrosophic numeral system algorithms for handling uncertainty and ambiguity in numerical data: An overview and future directions, Neutrosophic Sets and Systems, 65 (2024) 253-295.

[15] A.A. Salama, H.E. Khalid, A.G. Mabrouk, Unveiling uncertainty: Neutrosophic set-based algorithms for robust decision-making, Neutrosophic Sets and Systems, 72 (2024) 222-243.

[16] M. Jdid, F. Smarandache, Neutrosophic vision of the expected opportunity loss criterion (neol) decision making under risk, Neutrosophic Sets and Systems, 65 (2024) 110-118.

[17] S.G. Quek, H. Garg, G. Selvachandran, M. Palanikumar, K. Arulmozhi, F. Smarandache, Vikor and topsis framework with a truthful-distance measure for the (t, s)-regulated interval-valued neutrosophic soft set, Soft Computing, (2023) 27.

[18] L. Gomes, L.A.D. Rangel, An application of the todim method to the multicriteria rental evaluation of residential properties, European Journal of Operational Research, 193 (2009) 204-211.

[19] K.T. Atanassov, More on intuitionistic fuzzy-sets, Fuzzy Sets and Systems, 33 (1989) 37-45.

[20] F. Smarandache, Foundation of revolutionary topologies: An overview, examples, trend analysis, research issues, challenges, and future directions, Neutrosophic Systems with Applications, 13 (2024) 45-66.

[21] F.A. Smarandache, Unifying field in logics. Neutrosophy: Neutrosophic probability, set and logic, American Research Press, Rehoboth, 1999.

[22] H. Wang, F. Smarandache, Y. Zhang, R. Sunderraman, Single valued neutrosophic sets, Infinite Study, 12 (2010) 20110.

Received: July 23, 2024. Accepted: Oct 25, 2024

NSS
Neutrosophic Sets and Systems, Vol. 76, 2025
University of New Mexico

Comprehensive Framework for Collaborative Decision-Making in Evaluating Computer Network Security Using Interval Neutrosophic Information

Wenbao Qiao*
Nanjing University of Finance and Economics, Nanjing, 210023, Jiangsu, China
Corresponding author, E-mail: qwb0404@163.com
https://orcid.org/0009-0001-7251-767X

Abstract: Computer network security (CNS) evaluation is crucial for protecting information assets and maintaining the stable operation of network systems. Through this evaluation, potential threats and vulnerabilities within the network can be systematically identified, effectively preventing possible cyber-attacks and data breaches. Additionally, network security evaluation helps enterprises and organizations allocate security resources appropriately, enhancing their ability to respond to emergencies and ensuring business continuity and data integrity. In summary, network security evaluation is one of the foundational tasks for achieving continuous, secure, and stable network operations. The CNS evaluation is multiple-attribute group decision making (MAGDM). Then, the generalized TODIM(GTODIM) approach has been developed to deal with MAGDM. The interval neutrosophic sets (INSs) are defined as an effective tool for representing uncertain data during the CNS evaluation. In this manuscript, the interval neutrosophic number generalized TODIM (INN-GTODIM) approach is proposed to put forward the MAGDM under INSs. Finally, numerical example study for CNS evaluation is introduced to validate the INN-GTODIM approach. The primary contributions of this study are outlined: (1) Deriving weight information through the application of average method, enhancing the robustness of the decision-making process; (1) Implementing the INN-GTODIM approach for MAGDM scenarios that utilize INSs, showcasing its adaptability to complex decision-making environments; (1) Applying the INN-GTODIM approach specifically to the domain of CNS evaluation, and comparing its performance against existing approaches to highlight its strengths and improvements; (4) Providing a detailed comparative analysis, which clearly demonstrates that the INN-GTODIM approach significantly enhances the effectiveness of CNS evaluations.

Keywords: Multiple-attribute group decision making (MAGDM); Interval neutrosophic sets (INSs); GTODIM approach; Computer network security evaluation

1. Introduction and background

Computer network security (CNS) evaluation refers to the systematic approach of assessing the security within a computer network, including identifying existing security threats and vulnerabilities, as well as evaluating the effectiveness of current security measures[1]. This process

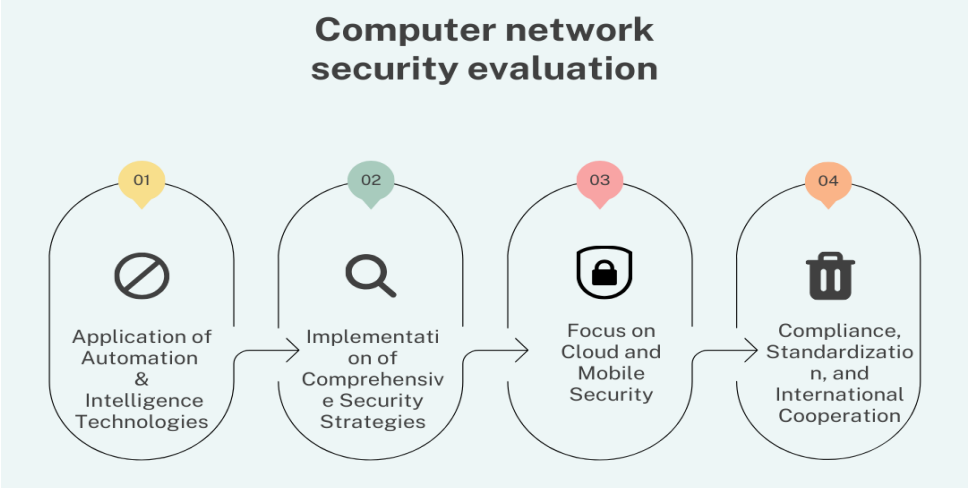

Figure 1. main elements of computer network security (CNS) evaluation

involves a comprehensive examination of various aspects of the network, such as hardware, software, data transmission and storage security, and network access controls[2]. The purpose of CNS evaluation is to ensure the security of network resources, prevent data breaches, and maintain the integrity and availability of the network system. The concept of CNS evaluation has evolved with the development of computer network technology and the increase in network security threats. Initially, network security focused primarily on the security of physical devices and basic access controls. However, as the Internet became widespread and network technology increased in complexity, the scope of network security evaluations also expanded, gradually including more dimensions of security checks[3]. The development of CNS evaluation can be summarized into four key points shown in Figure 1. First, the continuous advancements in artificial intelligence, network security evaluations increasingly rely on automated tools and intelligent algorithms. These technologies enhance the efficiency and accuracy of evaluations, automatically detecting abnormal behavior in the network and swiftly identifying potential security threats[4]. Second, network security no longer relies on single techniques or measures, but employs multi-level, multi-strategy comprehensive security measures. This includes physical security, system security, application security, data security, and other aspects, forming an all-around protection system[5]. Third, with the widespread adoption of cloud computing and mobile devices, cloud security and mobile security have become particularly important. Network security evaluations now incorporate considerations such as data encryption, access control, and endpoint protection to address the security challenges posed by these emerging technologies[6]. Forth, as global regulations on data protection and network security become stricter, such as the EU's GDPR, compliance has become a key component of network security evaluations. The application of various international and industry standards, along with cross-industry and cross-border cooperation, enhances the ability to withstand network threats. The aforementioned points outline the evolution of CNS evaluations from simple measures to the current comprehensive, multi-dimensional assessments, reflecting the continual updates and development in evaluation approaches and focuses as technology progresses and network threats increase.

MAGDM is a decision-making method involving multiple decision-makers who collaboratively evaluate a set of alternatives that perform differently across various attributes or criteria[7]. This method is widely used in complex decision scenarios such as policy formulation, business strategic

planning, and engineering management [8]. In the process of MAGDM, the first step is to define the objectives of the decision problem and identify the relevant evaluation criteria. These criteria might include dimensions such as cost, benefit, risk, sustainability, and more[9-11]. The group of decision-makers typically consists of experts from diverse backgrounds, providing a range of perspectives and expertise. The decision-making process usually involves several steps: defining the problem and decision criteria; collecting relevant data and information to assess each alternative against these criteria; and using appropriate decision-making methods like the Analytic Hierarchy Process (AHP), TOPSIS, entropy [28] or VIKOR method[12-16]. These methods help to quantify and integrate the preferences and evaluations of decision-makers. A key challenge in MAGDM is managing the consistency and divergence of opinions among decision-makers. This often requires coordination and negotiation to achieve a consensus or near-consensus decision. Additionally, fairness and transparency in the decision-making process are crucial to ensure that all key stakeholders' opinions are adequately considered. Ultimately, the decision outcomes formed through the group decision-making process not only reflect multi-dimensional data analysis but also integrate diverse human experiences and judgments, making the final decisions more comprehensive and reliable. The use of MAGDM tools enhances the efficiency and quality of decisions, helping decision-makers find optimal solutions in complex environments.

Neutrosophic theory [17] is particularly well-suited for handling unreliable, vague, or incomplete data. In the context of evaluating service performance in library and information institutions from the perspective of user experience, uncertainties often arise from factors like user feedback, service usage patterns, and satisfaction levels. By employing single-value neutrosophic sets (SVNSs) [18] and interval neutrosophic sets (INSs) [19], this theory offers a more flexible and comprehensive way to represent these uncertainties compared to traditional fuzzy sets. Smarandache [20] constructed a practical applications of Soft Set with extensions to HyperSoft Set, IndetermSoft Set, IndetermHyperSoft Set and TreeSoft Set. Mohamed and Elsayed [21] constructed the MADM approach based on bipolar Neutrosophic sets for evaluating financial markets in Egypt. Salem, Mohamed and Smarandache [22] integrated vague T2NSs with OWCM-RAM for intelligent medical 4.0 evaluator framework. The field of CNS evaluation is increasingly being addressed through MAGDM approaches. Notably, approaches such as GTODIM [23] and TOPSIS [15] have been adapted to tackle challenges inherent in MAGDM. The use of INSs[19], which are computed by three probabilistic components: truth-membership, indeterminacy-membership, and falsity-membership, effectively captures the vague and uncertain data often encountered in CNS evaluations, which include numerous qualitative assessments.

1.1. Contribution

This paper highlights the synergistic benefits of integrating GTODIM approach. This integration leverages the psychological insights into decision-makers' behavior provided by GTODIM in assessing the proximity to ideal solutions—both positive and negative. This manuscript introduces a novel approach, the INN-GTODIM approach, specifically tailored for handling MAGDM scenarios within the framework of INSs. A practical numerical study concerning CNS evaluations is demonstrating the efficacy of INN-GTODIM approach.

1.2. Research objective

The primary research objectives and motivations of this study are outlined:

- Deriving weight information through the application of average method, enhancing the

robustness of the decision-making process.

- Implementing the INN-GTODIM approach for MAGDM scenarios that utilize INSs, showcasing its adaptability to complex decision-making environments
- Applying the INN-GTODIM approach specifically to the domain of CNS evaluation, and comparing its performance against existing approaches to highlight its strengths and improvements.
- Providing a detailed comparative analysis, which clearly demonstrates that the INN-GTODIM approach significantly enhances the effectiveness of CNS evaluations. This comprehensive approach ensures that the proposed approach not only addresses the multifaceted nature of decision-making in network security but also advances the field by integrating nuanced psychological insights.

1.3.Paper outline

This work is organized as follows: Section 2 explains the fundamental concepts of INSs. Section 3 develops the INN-GTODIM approach within the framework of INSs, incorporating average method. Section 4 presents a practical example regarding CNS evaluation, along with a comparative analysis. Section 5 discusses managerial applications of the INN-GTODIM approach. Section 6 provides concluding remarks. Finally, Section 7 outlines future directions for research and application.

2. Fundamental Concepts and Definitions

In this section, we provide a foundational overview of INSs as presented by Wang et al.[19]. INS represent a significant advancement in neutrosophic theory, extending traditional neutrosophic sets by allowing for interval-valued representations of truth, indeterminacy, and falsity membership functions. The formal definitions and properties outlined in this section lay the groundwork for understanding the structure and application of INSs, which are instrumental to the theoretical and practical contributions of this work.

Definition 1. The INSs are expressed as follows:

$$LA=\left\{\left(\phi,LT_A(\phi),LI_A(\phi),LF_A(\phi)\right)\middle|\phi\in\Phi\right\} \tag{1}$$

where the $LT_A(\phi),LI_A(\phi),LF_A(\phi)$ depicts the truth-membership, indeterminacy-membership and falsity-membership, $LT_A(\phi),LI_A(\phi),LF_A(\phi)\subseteq[0,1]$ and satisfies $0\le\sup LT_A(\phi)+\sup LI_A(\phi)+\sup LF_A(\phi)\le 3$.

The INN) is depicted: $LA=([LTL_A,LTR_A],[LIL_A,LIR_A],[LFL_A,LFR_A])$, where $LT_A,LI_A,LF_A\subseteq[0,1]$, and $0\le LTR_A+LIR_A+LFR_A\le 3$ [19].

The evolution of INNs usually use score value to act as a practical measure of their "truth" degree across intervals [24]. The score value is essential in deciding the relative magnitude of INNs by taking into account the intervals of truth, indeterminacy, and falsity degrees (refer to definition 2). Additionally, the accuracy value was measured to give another perspective on INNs by seizing the

degree to which truth dominates over falsity within the neutrosophic intervals (refer to definition 3).

Definition 2. Let $LA=\left(\left[LTL_A, LTR_A\right],\left[LIL_A, LIR_A\right],\left[LFL_A, LFR_A\right]\right)$ be INN, score value is expressed as follows:

$$SV\left(LA\right)=\frac{\left(2+LTL_A-LIL_A-LFL_A\right)+\left(2+LTR_A-LIR_A-LFR_A\right)}{6},\ SV\left(LA\right)\in\left[0,1\right]. \tag{2}$$

Definition 3. Let $LA=\left(\left[LTL_A, LTR_A\right],\left[LIL_A, LIR_A\right],\left[LFL_A, LFR_A\right]\right)$ be INN, accuracy value is computed as follows:

$$AV\left(LA\right)=\frac{\left(LTL_A+LTR_A\right)-\left(LFL_A+LFR_A\right)}{2},\ AV\left(LA\right)\in\left[-1,1\right]. \tag{3}$$

Huang et al. [25] explored the concept of order relations between two INNs, providing a formal framework for comparing their values. interpreting the order relations is essential for applications where the ranking and preference of neutrosophic numbers are necessary (Refer to Definition 4). This framework facilitates decision-making processes by establishing criteria for determining which INN is greater or lesser, thereby enhancing the utility of neutrosophic methods in various domains.

Definition 4. Let $LA=\left(\left[LTL_A, LTR_A\right],\left[LIL_A, LIR_A\right],\left[LFL_A, LFR_A\right]\right)$ and $LB=\left(\left[LTL_B, LTR_B\right],\left[LIL_B, LIR_B\right],\left[LFL_B, LFR_B\right]\right)$ be INNs, $SV\left(LA\right)=\frac{\left(2+LTL_A-LIL_A-LFL_A\right)+\left(2+LTR_A-LIR_A-LFR_A\right)}{6}$ and $SV\left(LB\right)=\frac{\left(2+LTL_B-LIL_B-LFL_B\right)+\left(2+LTR_B-LIR_B-LFR_B\right)}{6}$, and $AV\left(LA\right)=\frac{\left(LTL_A+LTR_A\right)-\left(LFL_A+LFR_A\right)}{2}$ and $AV\left(LB\right)=\frac{\left(LTL_B+LTR_B\right)-\left(LFL_B+LFR_B\right)}{2}$, then if $SV\left(LA\right)<SV\left(LB\right)$, $LA<LB$; if $SV\left(LA\right)=SV\left(LB\right)$, (1) if $AV\left(LA\right)=AV\left(LB\right)$, $LA=LB$; (2) if $AV\left(LA\right)<AV\left(LB\right)$, $LA<LB$.

The operations on INNs are fundamental to leveraging their capabilities in modeling uncertainty and ambiguity **[26]**. These operations include addition, subtraction, multiplication, and division, each defined to preserve the inherent structure of the neutrosophic intervals (refer to Definition 5).

Definition 5. Let $LA=\left(\left[LTL_A, LTR_A\right],\left[LIL_A, LIR_A\right],\left[LFL_A, LFR_A\right]\right)$ and

$LB=\left(\left[LTL_B,LTR_B\right],\left[LIL_B,LIR_B\right],\left[LFL_B,LFR_B\right]\right)$ be INNs, the operations are expressed as follows:

$$(1)\ LA\oplus LB=\begin{pmatrix}\left(LTL_A+LTL_B-LTL_ALTL_B,LTR_A+LTR_B-LTR_ALTR_B\right),\\ \left[LIL_ALIL_B,LIR_ALIR_B\right],\left[LFL_ALFL_B,LFR_ALFR_B\right]\end{pmatrix};$$

$$(2)\ LA\otimes LB=\begin{pmatrix}\left[LTL_ALTL_B,LTR_ALTR_B\right],\\ \left[LIL_A+LIL_B-LIL_ALIL_B,LIR_A+LIR_B-LIR_ALIR_B\right],\\ \left[LFL_A+LFL_B-LFL_ALFL_B,LFR_A+LFR_B-LFR_ALFR_B\right]\end{pmatrix};$$

$$(3)\ \lambda LA=\begin{pmatrix}\left[1-\left(1-LTL_A\right)^{\lambda},1-\left(1-LTR_A\right)^{\lambda}\right],\\ \left[\left(LIL_A\right)^{\lambda},\left(LIR_A\right)^{\lambda}\right],\left[\left(LFL_A\right)^{\lambda},\left(LFR_A\right)^{\lambda}\right]\end{pmatrix},\lambda>0;$$

$$(4)\ \left(LA\right)^{\lambda}=\begin{pmatrix}\left[\left(LTL_A\right)^{\lambda},\left(LTR_A\right)^{\lambda}\right],\left[\left(LIL_A\right)^{\lambda},\left(LIR_A\right)^{\lambda}\right],\\ \left[1-\left(1-LFL_A\right)^{\lambda},1-\left(1-LFR_A\right)^{\lambda}\right]\end{pmatrix},\lambda>0.$$

Definition 6[27]. Let $LA=\left(\left[LTL_A,LTR_A\right],\left[LIL_A,LIR_A\right],\left[LFL_A,LFR_A\right]\right)$ and $LB=\left(\left[LTL_B,LTR_B\right],\left[LIL_B,LIR_B\right],\left[LFL_B,LFR_B\right]\right)$, the INN Hamming distance (INNHD) is expressed as follows:

$$INNHD\left(LA,LB\right)=\frac{1}{6}\begin{pmatrix}\left|LTL_A-LTL_B\right|+\left|LTR_A-LTR_B\right|+\left|LIL_A-LIL_B\right|+\\ \left|LIR_A-LIR_B\right|+\left|LFL_A-LFL_B\right|+\left|LFR_A-LFR_B\right|\end{pmatrix} \quad (4\text{-A})$$

Definition 6[27]. Let $LA=\left(\left[LTL_A,LTR_A\right],\left[LIL_A,LIR_A\right],\left[LFL_A,LFR_A\right]\right)$ and $LB=\left(\left[LTL_B,LTR_B\right],\left[LIL_B,LIR_B\right],\left[LFL_B,LFR_B\right]\right)$, the INN Euclidean distance (INNED) is computed as follows:

$$INNED\left(SA,SB\right)=\sqrt{\frac{1}{6}\begin{pmatrix}\left|LTL_A-LTL_B\right|^2+\left|LTR_A-LTR_B\right|^2+\left|LIL_A-LIL_B\right|^2+\\ \left|LIR_A-LIR_B\right|^2+\left|LFL_A-LFL_B\right|^2+\left|LFR_A-LFR_B\right|^2\end{pmatrix}} \quad (4\text{-B})$$

The INNWA approach [26] are expressed as follows:

Definition 7. Let $LA_j=\left(\left[LTL_j,LTR_j\right],\left[LIL_j,LIR_j\right],\left[LFL_j,LFR_j\right]\right)$ be INNs, the INNWA is expressed as follows:

$$\begin{aligned}&\mathrm{INNWA}\left(LA_1, LA_2, \ldots, LA_n\right)\\&= lw_1 LA_1 \oplus lw_2 LA_2 \ldots \oplus lw_n LA_n = \bigoplus_{j=1}^{n} lw_j LA_j \\&= \left(\begin{array}{c}\left[1-\prod_{j=1}^{n}\left(1-LTL_{ij}\right)^{lw_j}, 1-\prod_{j=1}^{n}\left(1-LTR_{ij}\right)^{lw_j}\right],\\ \left[\prod_{j=1}^{n}\left(LFL_{ij}\right)^{lw_j}, \prod_{j=1}^{n}\left(LFR_{ij}\right)^{lw_j}\right], \left[\prod_{j=1}^{n}\left(LTL_{ij}\right)^{lw_j}, \prod_{j=1}^{n}\left(LTR_{ij}\right)^{lw_j}\right]\end{array}\right)\end{aligned} \tag{5}$$

where $lw=\left(lw_1, lw_2, ..., lw_n\right)^T$ be weight of LA_j ,$lw_j > 0, \sum_{j=1}^{n} lw_j = 1$ [26].

3. Research Methodology

In this section, we introduce our proposed methodology for addressing MAGDM within the framework of INNs. The approach is designed to effectively handle uncertainty and ambiguity, making it well-suited for complex decision-making environments.

3.1. INN-MAGDM description

Then, INN-GTODIM approach is computed for MAGDM. Let $LA=\left\{LA_1, LA_2, \cdots, LA_m\right\}$ be alternatives and $LG=\left\{LG_1, LG_2, \cdots, LG_n\right\}$ be attributes with weight $l\omega=\left\{l\omega_1, l\omega_2, \cdots, l\omega_n\right\}$, $l\omega_j \in [0,1]$, $\sum_{j=1}^{n} l\omega_j = 1$ and experts $LE=\left\{LE_1, LE_2, \cdots, LE_q\right\}$ with weight $lw=\left\{lw_1, lw_2, \cdots, lw_t\right\}$. Then, INN-GTODIM approach is applied to MAGDM following the steps shown in Figure 2.

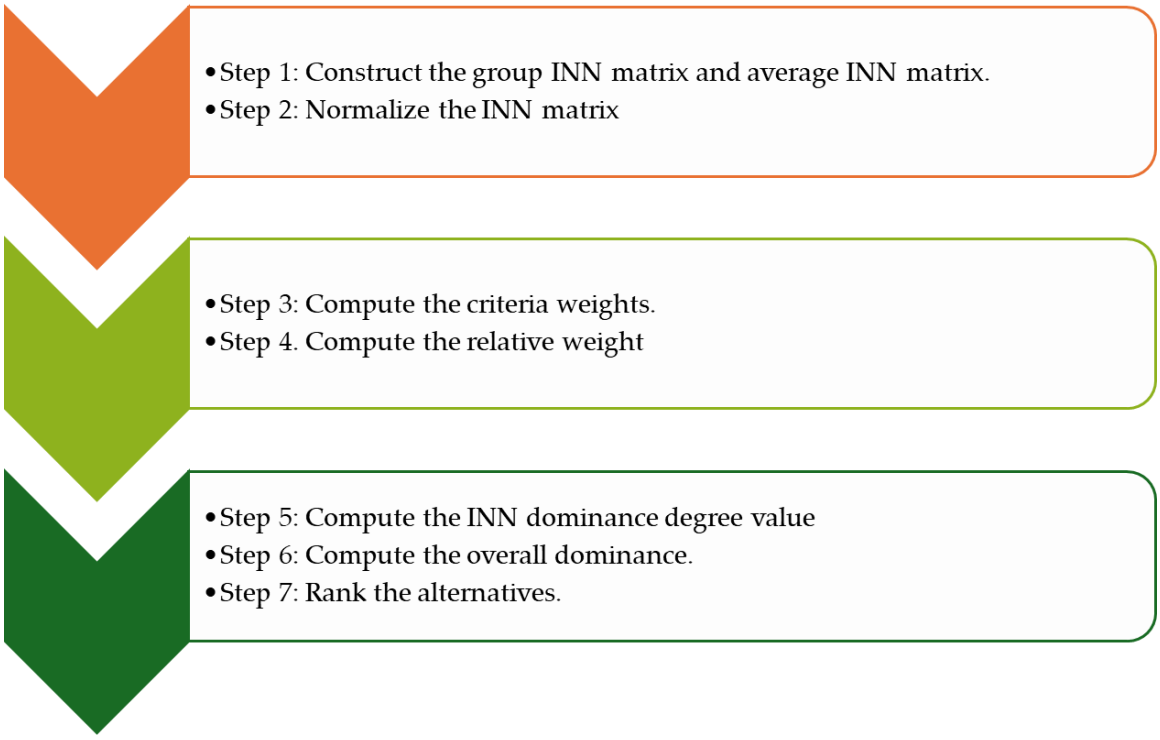

Figure. 2. The framework of INN-GTODIM approach for MAGDM.

Step 1. calculate the INN-matrix $LR^t = \left[LR_{ij}^t\right]_{m\times n} = \left(\left[LTL_{ij}^t, LTR_{ij}^t\right], \left[LIL_{ij}^t, LIR_{ij}^t\right], \left[LFL_{ij}^t, LFR_{ij}^t\right]\right)_{m\times n}$ and average-matrix $LR = \left[LR_{ij}\right]_{m\times n}$ based on INNWA approach:

$$\begin{aligned} LR_{ij} &= \left(\left[LTL_{ij}, LTR_{ij}\right], \left[LIL_{ij}, LIR_{ij}\right], \left[LFL_{ij}, LFR_{ij}\right]\right) \\ &= lw_1 LR_{ij}^1 \oplus lw_2 LR_{ij}^2 \oplus \cdots \oplus lw_t LR_{ij}^t \\ &= \left(\begin{array}{l} \left[1-\prod_{k=1}^{t}\left(LTL_{ij}^t\right)^{lw_j}, 1-\prod_{k=1}^{t}\left(LTR_{ij}^t\right)^{lw_j}\right], \\ \left[\prod_{k=1}^{t}\left(LFL_{ij}^t\right)^{lw_j}, \prod_{k=1}^{t}\left(LFR_{ij}^t\right)^{lw_j}\right], \\ \left[\prod_{k=1}^{t}\left(1-LTL_{ij}^t\right)^{lw_j}, \prod_{k=1}^{t}\left(1-LTR_{ij}^t\right)^{lw_j}\right] \end{array}\right) \end{aligned} \tag{6}$$

Step 2. Normalize the $LR = \left[LR_{ij}\right]_{m\times n}$ into $NLRSN = \left[NLR_{ij}\right]_{m\times n}$.

For benefit attributes:

$$\begin{aligned} NLR_{ij} &= \left(\left[LTL_{ij}^N, LTR_{ij}^N\right], \left[LIL_{ij}^N, LIR_{ij}^N\right], \left[LFL_{ij}^N, LFR_{ij}^N\right]\right) \\ &= LR_{ij} = \left(\left[LTL_{ij}, LTR_{ij}\right], \left[LIL_{ij}, LIR_{ij}\right], \left[LFL_{ij}, LFR_{ij}\right]\right) \end{aligned} \tag{7}$$

For cost attributes:

$$\begin{aligned} NLR_{ij} &= \left(\left[LTL_{ij}^{N}, LTR_{ij}^{N}\right], \left[LIL_{ij}^{N}, LIR_{ij}^{N}\right], \left[LFL_{ij}^{N}, LFR_{ij}^{N}\right]\right) \\ &= LR_{ij} = \left(\left[LFL_{ij}, LFR_{ij}\right], \left[LIL_{ij}, LIR_{ij}\right], \left[LTL_{ij}, LTR_{ij}\right]\right) \end{aligned} \tag{8}$$

Step 4. Illustrate relative weight:

$$rl\omega_j = l\omega_j \Big/ \max_j l\omega_j , \tag{12}$$

Step 5. Illustrate the INN dominance degree values (INNDDV).

(1) The INNDDV of LA_i over LA_t under LG_j is computed in light with INNHD and INNED:

$$INNDDV_j\left(LA_i, LA_t\right) = \begin{cases} \sqrt{\dfrac{rlw_j \times \dfrac{INNHD\left(NLR_{ij}, NLR_{tj}\right) + INNED\left(NLR_{ij}, NLR_{tj}\right)}{2}}{\sum_{j=1}^{n} rlw_j}} & \text{if } SV\left(NLR_{ij}\right) > SV\left(NLR_{tj}\right) \\ 0 & \text{if } SV\left(NLR_{ij}\right) = SV\left(NLR_{tj}\right) \\ -\dfrac{1}{\theta}\sqrt{\dfrac{\sum_{j=1}^{n} rl\omega_j \times \dfrac{INNHD\left(NLR_{ij}, NLR_{tj}\right) + INNED\left(NLR_{ij}, NLR_{tj}\right)}{2}}{rl\omega_j}} & \text{if } SV\left(NLR_{ij}\right) < SV\left(NLR_{tj}\right) \end{cases} \tag{13}$$

The values of θ is determined for Ref.[29].

(2)The $INNDDV_j\left(LA_i\right)\left(j = 1, 2, \cdots, n\right)$ under LG_j is computed as follows:

$$INNDDV_j\left(LA_i\right) = \left[INNDDV_j\left(LA_i, LA_t\right)\right]_{m\times m}$$

$$= \begin{array}{c} \\ LA_1 \\ LA_2 \\ \vdots \\ LA_m \end{array} \begin{array}{c} \begin{array}{cccc} LA_1 & LA_2 & \cdots & LA_m \end{array} \\ \begin{bmatrix} 0 & INNDDV_j\left(LA_1, LA_2\right) & \cdots & INNDDV_j\left(LA_1, LA_m\right) \\ INNDDV_j\left(LA_2, LA_1\right) & 0 & \cdots & INNDDV_j\left(LA_2, LA_m\right) \\ \vdots & \vdots & \cdots & \vdots \\ INNDDV_j\left(LA_m, LA_1\right) & INNDDV_j\left(LA_m, LA_2\right) & \cdots & 0 \end{bmatrix} \end{array}$$

(3) Illustrate the overall INNDDV of LA_i:

$$INNDDV_j\left(LA_i\right) = \sum_{t=1}^{m} INNDDV_j\left(LA_i, LA_t\right) \tag{14}$$

(4) The overall INNDDV matrix is computed as follows:

$$INNDDV = \left(INNDDV_{ij}\right)_{m\times n}$$

$$= \begin{bmatrix} & LG_1 & LG_2 & \cdots & LG_n \\ LA_1 & \sum_{t=1}^{m} INNDDV_1(LA_1, LA_t) & \sum_{t=1}^{m} INNDDV_2(LA_1, LA_t) & \cdots & \sum_{t=1}^{m} INNDDV_n(LA_1, LA_t) \\ LA_2 & \sum_{t=1}^{m} INNDDV_1(LA_2, LA_t) & \sum_{t=1}^{m} INNDDV_2(LA_2, LA_t) & \cdots & \sum_{t=1}^{m} INNDDV_n(LA_2, LA_t) \\ \vdots & \vdots & \vdots & \vdots & \vdots \\ LA_m & \sum_{t=1}^{m} INNDDV_1(LA_m, LA_t) & \sum_{t=1}^{m} INNDDV_2(LA_m, LA_t) & \cdots & \sum_{t=1}^{m} INNDDV_n(LA_m, LA_t) \end{bmatrix} \tag{15}$$

Step 6. Compute the overall dominance degree.

$$y_i = \frac{INNDDV_i - \min INNDDV_i}{\max INNDDV_i - \min INNDDV_i} \tag{16}$$

Step 7. Rank the alternatives.

4. Results and Discussions

In this section, we present and analyse the results obtained from each stage of our approach. Detailed tabular results illustrate the outcomes of key steps, providing a comprehensive view of the method's performance and intermediate calculations. In addition, we conduct comparative analysis to evaluate the efficiency of our approach (figure 2) relative to existing methods, enabling a deeper understanding of its strengths and potential areas for improvement.

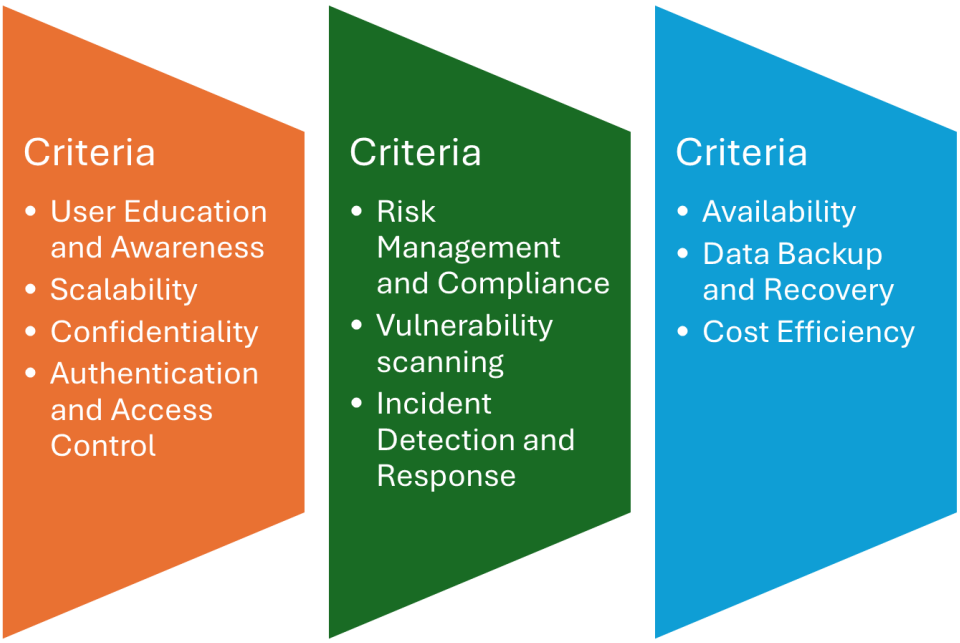

Figure 3. The ten attributes of the system.

As the fields of science and information technology continue to advance, the integration of internet and computer network technologies into critical sectors like politics, economics, and defense has

become more widespread. This increasing prevalence has emphasized the vital issue of network security. Today's information systems are exposed to significant risks and severe threats, with cyber \attackers taking advantage of the complexities and vulnerabilities within computer network architectures. In China, although there are numerous systems designed to assess the CNS, only a few are in active use, with most focusing primarily on detecting network vulnerabilities. These systems typically fall short in providing detailed risk assessments or predictive insights regarding the status of network security, leading to a gap in comprehensive protection against potential threats across various industries. The existing frameworks for network security assessment are not effectively integrated with detection technologies, resulting in a lack of solid infrastructure and supportive platforms for conducting thorough tests and evaluations of network information security. This gap underscores the pressing need for a holistic network security assessment system that embraces a wide range of detection methods and risk evaluation strategies. Network information security is an interdisciplinary domain that encompasses network technology, communication technology, cryptography, information security, applied mathematics, and information theory. Its primary objective is to protect the hardware, software, and data within network systems from both accidental and intentional threats, thereby maintaining their integrity and ensuring their consistent and dependable operation. The smooth functioning of a network system is contingent upon the reliability of various components, including hardware, operating systems, application software, the surrounding environment, and communication devices. Evaluating network security involves scrutinizing a plethora of qualitative indicators, as the compromise or failure of any single component can introduce vulnerabilities. Therefore, the selection of indicators for network security evaluation is an intricate task that requires an exhaustive and comprehensive analysis of numerous factors to ensure that the indicators chosen are both representative and all-encompassing. This meticulous approach is essential to effectively safeguard network systems against the evolving landscape of cyber threats and vulnerabilities. The CNS evaluation is MAGDM. Five potential computer network systems are chosen with four attributes, shown in Figure 3.

Table 1. Linguistic Terms and INNs

Linguistic Terms	INNs
Exceedingly Terrible - LET	([0.05, 0.2], [0.6, 0.7], [0.75, 0.9])
Very Terrible – LVT	([0.15, 0.3], [0.5, 0.6], [0.65, 0.8])
Terrible – LT	([0.25, 0.4], [0.4, 0.5], [0.55, 0.7])
Medium – LM	([0.4, 0.6], [0.1, 0.2], [0.4, 0.6])
Well – LW	([0.45, 0.6], [0.3, 0.4], [0.25, 0.5])
Very Well – LVW	([0.65, 0.8], [0.5, 0.6], [0.15, 0.3])
Exceedingly Well - LEW	([0.75, 0.9], [0.6, 0.7], [0.05, 0.2])

The approach known as INN-GTODIM is demonstrated as a method to address the evaluation of CNS.

In Step 1, we calculate the INN-matrix, based on Table 1 as with Ref.[30, 31], $R^t = \left[s\phi_{ij}^t\right]_{5\times4} = \left(\left[STL_{ij}^t, STR_{ij}^t\right], \left[SIL_{ij}^t, SIR_{ij}^t\right], \left[SFL_{ij}^t, SFR_{ij}^t\right]\right)_{5\times4}$, and the corresponding values is tabulated in Table 2.

Table 2. The decision matrix

	C_1	C_2	C_3	C_4	C_5	C_6	C_7	C_8	C_9	C_{10}
A_1	([0.05, 0.2], [0.6, 0.7], [0.75, 0.9])	([0.15, 0.3], [0.5, 0.6], [0.65, 0.8])	([0.25, 0.4], [0.4, 0.5], [0.55, 0.7])	([0.4, 0.6], [0.1, 0.2], [0.4, 0.6])	([0.45, 0.6], [0.3, 0.4], [0.25, 0.5])	([0.65, 0.8], [0.5, 0.6], [0.15, 0.3])	([0.65, 0.8], [0.5, 0.6], [0.15, 0.3])	([0.75, 0.9], [0.6, 0.7], [0.05, 0.2])	([0.05, 0.2], [0.6, 0.7], [0.75, 0.9])	([0.15, 0.3], [0.5, 0.6], [0.65, 0.8])
A_2	([0.45, 0.6], [0.3, 0.4], [0.25, 0.5])	([0.65, 0.8], [0.5, 0.6], [0.15, 0.3])	([0.75, 0.9], [0.6, 0.7], [0.05, 0.2])	([0.05, 0.2], [0.6, 0.7], [0.75, 0.9])	([0.15, 0.3], [0.5, 0.6], [0.65, 0.8])	([0.25, 0.4], [0.4, 0.5], [0.55, 0.7])	([0.4, 0.6], [0.1, 0.2], [0.4, 0.6])	([0.45, 0.6], [0.3, 0.4], [0.25, 0.5])	([0.65, 0.8], [0.5, 0.6], [0.15, 0.3])	([0.25, 0.4], [0.4, 0.5], [0.55, 0.7])
A_3	([0.4, 0.6], [0.1, 0.2], [0.4, 0.6])	([0.45, 0.6], [0.3, 0.4], [0.25, 0.5])	([0.65, 0.8], [0.5, 0.6], [0.15, 0.3])	([0.75, 0.9], [0.6, 0.7], [0.05, 0.2])	([0.05, 0.2], [0.6, 0.7], [0.75, 0.9])	([0.15, 0.3], [0.5, 0.6], [0.65, 0.8])	([0.25, 0.4], [0.4, 0.5], [0.55, 0.7])	([0.4, 0.6], [0.1, 0.2], [0.4, 0.6])	([0.75, 0.9], [0.6, 0.7], [0.05, 0.2])	([0.4, 0.6], [0.1, 0.2], [0.4, 0.6])
A_4	([0.25, 0.4], [0.4, 0.5], [0.55, 0.7])	([0.4, 0.6], [0.1, 0.2], [0.4, 0.6])	([0.05, 0.2], [0.6, 0.7], [0.75, 0.9])	([0.15, 0.3], [0.5, 0.6], [0.65, 0.8])	([0.25, 0.4], [0.4, 0.5], [0.55, 0.7])	([0.4, 0.6], [0.1, 0.2], [0.4, 0.6])	([0.45, 0.6], [0.3, 0.4], [0.25, 0.5])	([0.45, 0.6], [0.3, 0.4], [0.25, 0.5])	([0.05, 0.2], [0.6, 0.7], [0.75, 0.9])	([0.45, 0.6], [0.3, 0.4], [0.25, 0.5])
A_5	([0.75, 0.9], [0.6, 0.7], [0.05, 0.2])	([0.25, 0.4], [0.4, 0.5], [0.55, 0.7])	([0.75, 0.9], [0.6, 0.7], [0.05, 0.2])	([0.15, 0.3], [0.5, 0.6], [0.65, 0.8])	([0.65, 0.8], [0.5, 0.6], [0.15, 0.3])	([0.4, 0.6], [0.1, 0.2], [0.4, 0.6])	([0.65, 0.8], [0.5, 0.6], [0.15, 0.3])	([0.65, 0.8], [0.5, 0.6], [0.15, 0.3])	([0.15, 0.3], [0.5, 0.6], [0.65, 0.8])	([0.65, 0.8], [0.5, 0.6], [0.15, 0.3])
A_6	([0.05, 0.2], [0.6, 0.7], [0.75, 0.9])	([0.15, 0.3], [0.5, 0.6], [0.65, 0.8])	([0.65, 0.8], [0.5, 0.6], [0.15, 0.3])	([0.4, 0.6], [0.1, 0.2], [0.4, 0.6])	([0.25, 0.4], [0.4, 0.5], [0.55, 0.7])	([0.15, 0.3], [0.5, 0.6], [0.65, 0.8])	([0.75, 0.9], [0.6, 0.7], [0.05, 0.2])	([0.75, 0.9], [0.6, 0.7], [0.05, 0.2])	([0.25, 0.4], [0.4, 0.5], [0.55, 0.7])	([0.75, 0.9], [0.6, 0.7], [0.05, 0.2])
A_7	([0.75, 0.9], [0.6, 0.7], [0.05, 0.2])	([0.05, 0.2], [0.6, 0.7], [0.75, 0.9])	([0.45, 0.6], [0.3, 0.4], [0.25, 0.5])	([0.4, 0.6], [0.1, 0.2], [0.4, 0.6])	([0.25, 0.4], [0.4, 0.5], [0.55, 0.7])	([0.15, 0.3], [0.5, 0.6], [0.65, 0.8])	([0.05, 0.2], [0.6, 0.7], [0.75, 0.9])	([0.15, 0.3], [0.5, 0.6], [0.65, 0.8])	([0.4, 0.6], [0.1, 0.2], [0.4, 0.6])	([0.05, 0.2], [0.6, 0.7], [0.75, 0.9])
A_8	([0.65, 0.8], [0.5, 0.6], [0.15, 0.3])	([0.75, 0.9], [0.6, 0.7], [0.05, 0.2])	([0.45, 0.6], [0.3, 0.4], [0.25, 0.5])	([0.4, 0.6], [0.1, 0.2], [0.4, 0.6])	([0.25, 0.4], [0.4, 0.5], [0.55, 0.7])	([0.15, 0.3], [0.5, 0.6], [0.65, 0.8])	([0.05, 0.2], [0.6, 0.7], [0.75, 0.9])	([0.25, 0.4], [0.4, 0.5], [0.55, 0.7])	([0.45, 0.6], [0.3, 0.4], [0.25, 0.5])	([0.15, 0.3], [0.5, 0.6], [0.65, 0.8])
A_9	([0.15, 0.3], [0.5, 0.6], [0.65, 0.8])	([0.65, 0.8], [0.5, 0.6], [0.15, 0.3])	([0.45, 0.6], [0.3, 0.4], [0.25, 0.5])	([0.4, 0.6], [0.1, 0.2], [0.4, 0.6])	([0.25, 0.4], [0.4, 0.5], [0.55, 0.7])	([0.15, 0.3], [0.5, 0.6], [0.65, 0.8])	([0.05, 0.2], [0.6, 0.7], [0.75, 0.9])	([0.75, 0.9], [0.6, 0.7], [0.05, 0.2])	([0.65, 0.8], [0.5, 0.6], [0.15, 0.3])	([0.25, 0.4], [0.4, 0.5], [0.55, 0.7])
A_{10}	([0.15, 0.3], [0.5, 0.6], [0.65, 0.8])	([0.05, 0.2], [0.6, 0.7], [0.75, 0.9])	([0.75, 0.9], [0.6, 0.7], [0.05, 0.2])	([0.65, 0.8], [0.5, 0.6], [0.15, 0.3])	([0.45, 0.6], [0.3, 0.4], [0.25, 0.5])	([0.4, 0.6], [0.1, 0.2], [0.4, 0.6])	([0.25, 0.4], [0.4, 0.5], [0.55, 0.7])	([0.15, 0.3], [0.5, 0.6], [0.65, 0.8])	([0.05, 0.2], [0.6, 0.7], [0.75, 0.9])	([0.4, 0.6], [0.1, 0.2], [0.4, 0.6])
	C_1	C_2	C_3	C_4	C_5	C_6	C_7	C_8	C_9	C_{10}
A_1	([0.05, 0.2], [0.6, 0.7], [0.75, 0.9])	([0.15, 0.3], [0.5, 0.6], [0.65, 0.8])	([0.25, 0.4], [0.4, 0.5], [0.55, 0.7])	([0.4, 0.6], [0.1, 0.2], [0.4, 0.6])	([0.45, 0.6], [0.3, 0.4], [0.25, 0.5])	([0.65, 0.8], [0.5, 0.6], [0.15, 0.3])	([0.65, 0.8], [0.5, 0.6], [0.15, 0.3])	([0.75, 0.9], [0.6, 0.7], [0.05, 0.2])	([0.05, 0.2], [0.6, 0.7], [0.75, 0.9])	([0.15, 0.3], [0.5, 0.6], [0.65, 0.8])
A_2	([0.45, 0.6], [0.3, 0.4], [0.25, 0.5])	([0.65, 0.8], [0.5, 0.6], [0.15, 0.3])	([0.15, 0.3], [0.5, 0.6], [0.65, 0.8])	([0.05, 0.2], [0.6, 0.7], [0.75, 0.9])	([0.15, 0.3], [0.5, 0.6], [0.65, 0.8])	([0.15, 0.3], [0.5, 0.6], [0.65, 0.8])	([0.4, 0.6], [0.1, 0.2], [0.4, 0.6])	([0.15, 0.3], [0.5, 0.6], [0.65, 0.8])	([0.65, 0.8], [0.5, 0.6], [0.15, 0.3])	([0.25, 0.4], [0.4, 0.5], [0.55, 0.7])
A_3	([0.4, 0.6], [0.1, 0.2], [0.4, 0.6])	([0.15, 0.3], [0.5, 0.6], [0.65, 0.8])	([0.25, 0.4], [0.4, 0.5], [0.55, 0.7])	([0.75, 0.9], [0.6, 0.7], [0.05, 0.2])	([0.15, 0.3], [0.5, 0.6], [0.65, 0.8])	([0.25, 0.4], [0.4, 0.5], [0.55, 0.7])	([0.15, 0.3], [0.5, 0.6], [0.65, 0.8])	([0.25, 0.4], [0.4, 0.5], [0.55, 0.7])	([0.75, 0.9], [0.6, 0.7], [0.05, 0.2])	([0.4, 0.6], [0.1, 0.2], [0.4, 0.6])
A_4	([0.15, 0.3], [0.5, 0.6], [0.65, 0.8])	([0.25, 0.4], [0.4, 0.5], [0.55, 0.7])	([0.4, 0.6], [0.1, 0.2], [0.4, 0.6])	([0.15, 0.3], [0.5, 0.6], [0.65, 0.8])	([0.25, 0.4], [0.4, 0.5], [0.55, 0.7])	([0.4, 0.6], [0.1, 0.2], [0.4, 0.6])	([0.25, 0.4], [0.4, 0.5], [0.55, 0.7])	([0.4, 0.6], [0.1, 0.2], [0.4, 0.6])	([0.45, 0.6], [0.3, 0.4], [0.25, 0.5])	([0.25, 0.4], [0.4, 0.5], [0.55, 0.7])
A_5	([0.25, 0.4], [0.4, 0.5], [0.55, 0.7])	([0.4, 0.6], [0.1, 0.2], [0.4, 0.6])	([0.45, 0.6], [0.3, 0.4], [0.25, 0.5])	([0.25, 0.4], [0.4, 0.5], [0.55, 0.7])	([0.4, 0.6], [0.1, 0.2], [0.4, 0.6])	([0.45, 0.6], [0.3, 0.4], [0.25, 0.5])	([0.4, 0.6], [0.1, 0.2], [0.4, 0.6])	([0.45, 0.6], [0.3, 0.4], [0.25, 0.5])	([0.25, 0.4], [0.4, 0.5], [0.55, 0.7])	([0.65, 0.8], [0.5, 0.6], [0.15, 0.3])
A_6	([0.4, 0.6], [0.1, 0.2], [0.4, 0.6])	([0.45, 0.6], [0.3, 0.4], [0.25, 0.5])	([0.65, 0.8], [0.5, 0.6], [0.15, 0.3])	([0.4, 0.6], [0.1, 0.2], [0.4, 0.6])	([0.45, 0.6], [0.3, 0.4], [0.25, 0.5])	([0.65, 0.8], [0.5, 0.6], [0.15, 0.3])	([0.45, 0.6], [0.3, 0.4], [0.25, 0.5])	([0.65, 0.8], [0.5, 0.6], [0.15, 0.3])	([0.4, 0.6], [0.1, 0.2], [0.4, 0.6])	([0.75, 0.9], [0.6, 0.7], [0.05, 0.2])
A_7	([0.45, 0.6], [0.3, 0.4], [0.25, 0.5])	([0.65, 0.8], [0.5, 0.6], [0.15, 0.3])	([0.75, 0.9], [0.6, 0.7], [0.05, 0.2])	([0.45, 0.6], [0.3, 0.4], [0.25, 0.5])	([0.65, 0.8], [0.5, 0.6], [0.15, 0.3])	([0.75, 0.9], [0.6, 0.7], [0.05, 0.2])	([0.65, 0.8], [0.5, 0.6], [0.15, 0.3])	([0.75, 0.9], [0.6, 0.7], [0.05, 0.2])	([0.45, 0.6], [0.3, 0.4], [0.25, 0.5])	([0.05, 0.2], [0.6, 0.7], [0.75, 0.9])
A_8	([0.65, 0.8], [0.5, 0.6], [0.15, 0.3])	([0.75, 0.9], [0.6, 0.7], [0.05, 0.2])	([0.45, 0.6], [0.3, 0.4], [0.25, 0.5])	([0.65, 0.8], [0.5, 0.6], [0.15, 0.3])	([0.75, 0.9], [0.6, 0.7], [0.05, 0.2])	([0.15, 0.3], [0.5, 0.6], [0.65, 0.8])	([0.75, 0.9], [0.6, 0.7], [0.05, 0.2])	([0.25, 0.4], [0.4, 0.5], [0.55, 0.7])	([0.65, 0.8], [0.5, 0.6], [0.15, 0.3])	([0.15, 0.3], [0.5, 0.6], [0.65, 0.8])
A_9	([0.75, 0.9], [0.6, 0.7], [0.05, 0.2])	([0.65, 0.8], [0.5, 0.6], [0.15, 0.3])	([0.45, 0.6], [0.3, 0.4], [0.25, 0.5])	([0.75, 0.9], [0.6, 0.7], [0.05, 0.2])	([0.25, 0.4], [0.4, 0.5], [0.55, 0.7])	([0.15, 0.3], [0.5, 0.6], [0.65, 0.8])	([0.05, 0.2], [0.6, 0.7], [0.75, 0.9])	([0.75, 0.9], [0.6, 0.7], [0.05, 0.2])	([0.75, 0.9], [0.6, 0.7], [0.05, 0.2])	([0.25, 0.4], [0.4, 0.5], [0.55, 0.7])
A_{10}	([0.15, 0.3], [0.5, 0.6], [0.65, 0.8])	([0.05, 0.2], [0.6, 0.7], [0.75, 0.9])	([0.75, 0.9], [0.6, 0.7], [0.05, 0.2])	([0.65, 0.8], [0.5, 0.6], [0.15, 0.3])	([0.45, 0.6], [0.3, 0.4], [0.25, 0.5])	([0.4, 0.6], [0.1, 0.2], [0.4, 0.6])	([0.25, 0.4], [0.4, 0.5], [0.55, 0.7])	([0.15, 0.3], [0.5, 0.6], [0.65, 0.8])	([0.05, 0.2], [0.6, 0.7], [0.75, 0.9])	([0.4, 0.6], [0.1, 0.2], [0.4, 0.6])
	C_1	C_2	C_3	C_4	C_5	C_6	C_7	C_8	C_9	C_{10}
A_1	([0.05, 0.2], [0.6, 0.7], [0.75, 0.9])	([0.15, 0.3], [0.5, 0.6], [0.65, 0.8])	([0.25, 0.4], [0.4, 0.5], [0.55, 0.7])	([0.4, 0.6], [0.1, 0.2], [0.4, 0.6])	([0.45, 0.6], [0.3, 0.4], [0.25, 0.5])	([0.65, 0.8], [0.5, 0.6], [0.15, 0.3])	([0.4, 0.6], [0.1, 0.2], [0.4, 0.6])	([0.75, 0.9], [0.6, 0.7], [0.05, 0.2])	([0.05, 0.2], [0.6, 0.7], [0.75, 0.9])	([0.4, 0.6], [0.1, 0.2], [0.4, 0.6])
A_2	([0.45, 0.6], [0.3, 0.4], [0.25, 0.5])	([0.65, 0.8], [0.5, 0.6], [0.15, 0.3])	([0.4, 0.6], [0.1, 0.2], [0.4, 0.6])	([0.05, 0.2], [0.6, 0.7], [0.75, 0.9])	([0.15, 0.3], [0.5, 0.6], [0.65, 0.8])	([0.25, 0.4], [0.4, 0.5], [0.55, 0.7])	([0.05, 0.2], [0.6, 0.7], [0.75, 0.9])	([0.4, 0.6], [0.1, 0.2], [0.4, 0.6])	([0.4, 0.6], [0.1, 0.2], [0.4, 0.6])	([0.05, 0.2], [0.6, 0.7], [0.75, 0.9])
A_3	([0.4, 0.6], [0.1, 0.2], [0.4, 0.6])	([0.4, 0.6], [0.1, 0.2], [0.4, 0.6])	([0.05, 0.2], [0.6, 0.7], [0.75, 0.9])	([0.4, 0.6], [0.1, 0.2], [0.4, 0.6])	([0.4, 0.6], [0.1, 0.2], [0.4, 0.6])	([0.4, 0.6], [0.1, 0.2], [0.4, 0.6])	([0.75, 0.9], [0.6, 0.7], [0.05, 0.2])	([0.05, 0.2], [0.6, 0.7], [0.75, 0.9])	([0.05, 0.2], [0.6, 0.7], [0.75, 0.9])	([0.75, 0.9], [0.6, 0.7], [0.05, 0.2])
A_4	([0.05, 0.2], [0.6, 0.7], [0.75, 0.9])	([0.05, 0.2], [0.6, 0.7], [0.75, 0.9])	([0.75, 0.9], [0.6, 0.7], [0.05, 0.2])	([0.05, 0.2], [0.6, 0.7], [0.75, 0.9])	([0.05, 0.2], [0.6, 0.7], [0.75, 0.9])	([0.05, 0.2], [0.6, 0.7], [0.75, 0.9])	([0.15, 0.3], [0.5, 0.6], [0.65, 0.8])	([0.4, 0.6], [0.1, 0.2], [0.4, 0.6])	([0.75, 0.9], [0.6, 0.7], [0.05, 0.2])	([0.4, 0.6], [0.1, 0.2], [0.4, 0.6])
A_5	([0.4, 0.6], [0.1, 0.2], [0.4, 0.6])	([0.75, 0.9], [0.6, 0.7], [0.05, 0.2])	([0.15, 0.3], [0.5, 0.6], [0.65, 0.8])	([0.75, 0.9], [0.6, 0.7], [0.05, 0.2])	([0.75, 0.9], [0.6, 0.7], [0.05, 0.2])	([0.75, 0.9], [0.6, 0.7], [0.05, 0.2])	([0.4, 0.6], [0.1, 0.2], [0.4, 0.6])	([0.05, 0.2], [0.6, 0.7], [0.75, 0.9])	([0.15, 0.3], [0.5, 0.6], [0.65, 0.8])	([0.05, 0.2], [0.6, 0.7], [0.75, 0.9])
A_6	([0.05, 0.2], [0.6, 0.7], [0.75, 0.9])	([0.15, 0.3], [0.5, 0.6], [0.65, 0.8])	([0.15, 0.3], [0.5, 0.6], [0.65, 0.8])	([0.15, 0.3], [0.5, 0.6], [0.65, 0.8])	([0.15, 0.3], [0.5, 0.6], [0.65, 0.8])	([0.15, 0.3], [0.5, 0.6], [0.65, 0.8])	([0.05, 0.2], [0.6, 0.7], [0.75, 0.9])	([0.75, 0.9], [0.6, 0.7], [0.05, 0.2])	([0.15, 0.3], [0.5, 0.6], [0.65, 0.8])	([0.75, 0.9], [0.6, 0.7], [0.05, 0.2])
A_7	([0.75, 0.9], [0.6, 0.7], [0.05, 0.2])	([0.15, 0.3], [0.5, 0.6], [0.65, 0.8])	([0.4, 0.6], [0.1, 0.2], [0.4, 0.6])	([0.15, 0.3], [0.5, 0.6], [0.65, 0.8])	([0.15, 0.3], [0.5, 0.6], [0.65, 0.8])	([0.15, 0.3], [0.5, 0.6], [0.65, 0.8])	([0.75, 0.9], [0.6, 0.7], [0.05, 0.2])	([0.15, 0.3], [0.5, 0.6], [0.65, 0.8])	([0.4, 0.6], [0.1, 0.2], [0.4, 0.6])	([0.15, 0.3], [0.5, 0.6], [0.65, 0.8])
A_8	([0.15, 0.3], [0.5, 0.6], [0.65, 0.8])	([0.4, 0.6], [0.1, 0.2], [0.4, 0.6])	([0.45, 0.6], [0.3, 0.4], [0.25, 0.5])	([0.4, 0.6], [0.1, 0.2], [0.4, 0.6])	([0.4, 0.6], [0.1, 0.2], [0.4, 0.6])	([0.4, 0.6], [0.1, 0.2], [0.4, 0.6])	([0.15, 0.3], [0.5, 0.6], [0.65, 0.8])	([0.15, 0.3], [0.5, 0.6], [0.65, 0.8])	([0.15, 0.3], [0.5, 0.6], [0.65, 0.8])	([0.15, 0.3], [0.5, 0.6], [0.65, 0.8])
A_9	([0.15, 0.3], [0.5, 0.6], [0.65, 0.8])	([0.65, 0.8], [0.5, 0.6], [0.15, 0.3])	([0.45, 0.6], [0.3, 0.4], [0.25, 0.5])	([0.4, 0.6], [0.1, 0.2], [0.4, 0.6])	([0.25, 0.4], [0.4, 0.5], [0.55, 0.7])	([0.15, 0.3], [0.5, 0.6], [0.65, 0.8])	([0.15, 0.3], [0.5, 0.6], [0.65, 0.8])	([0.4, 0.6], [0.1, 0.2], [0.4, 0.6])	([0.4, 0.6], [0.1, 0.2], [0.4, 0.6])	([0.4, 0.6], [0.1, 0.2], [0.4, 0.6])
A_{10}	([0.4, 0.6], [0.1, 0.2], [0.4, 0.6])	([0.05, 0.2], [0.6, 0.7], [0.75, 0.9])	([0.75, 0.9], [0.6, 0.7], [0.05, 0.2])	([0.65, 0.8], [0.5, 0.6], [0.15, 0.3])	([0.45, 0.6], [0.3, 0.4], [0.25, 0.5])	([0.4, 0.6], [0.1, 0.2], [0.4, 0.6])	([0.4, 0.6], [0.1, 0.2], [0.4, 0.6])	([0.15, 0.3], [0.5, 0.6], [0.65, 0.8])	([0.05, 0.2], [0.6, 0.7], [0.75, 0.9])	([0.4, 0.6], [0.1, 0.2], [0.4, 0.6])

Step 2. We normalize the decision matrix as shown in Table 3.

Table 3. The normalized decision matrix.

	C_1	C_2	C_3	C_4	C_5	C_6	C_7	C_8	C_9	C_{10}
A_1	0.080046	0.085227	0.086538	0.098528	0.110727	0.12252	0.113532	0.122112	0.080233	0.091435
A_2	0.111369	0.119318	0.097222	0.078143	0.086505	0.092182	0.09289	0.094609	0.115116	0.08912
A_3	0.100928	0.097727	0.090812	0.116648	0.088812	0.094516	0.102064	0.086909	0.112791	0.109954
A_4	0.087007	0.089773	0.095085	0.082673	0.088812	0.094516	0.09633	0.09901	0.098837	0.107639
A_5	0.107889	0.105682	0.100427	0.100793	0.116494	0.114352	0.106651	0.09901	0.089535	0.107639
A_6	0.087007	0.093182	0.101496	0.093998	0.096886	0.099183	0.105505	0.119912	0.094186	0.128472
A_7	0.12297	0.094318	0.104701	0.097395	0.100346	0.101517	0.108945	0.09571	0.104651	0.082176
A_8	0.110209	0.117045	0.102564	0.105323	0.107266	0.092182	0.097477	0.086909	0.106977	0.086806
A_9	0.100928	0.119318	0.102564	0.107588	0.093426	0.087515	0.081422	0.113311	0.117442	0.096065
A_{10}	0.091647	0.078409	0.11859	0.118913	0.110727	0.101517	0.095183	0.082508	0.080233	0.100694

Step 3. We compute the criteria weights as shown in Figure 4.

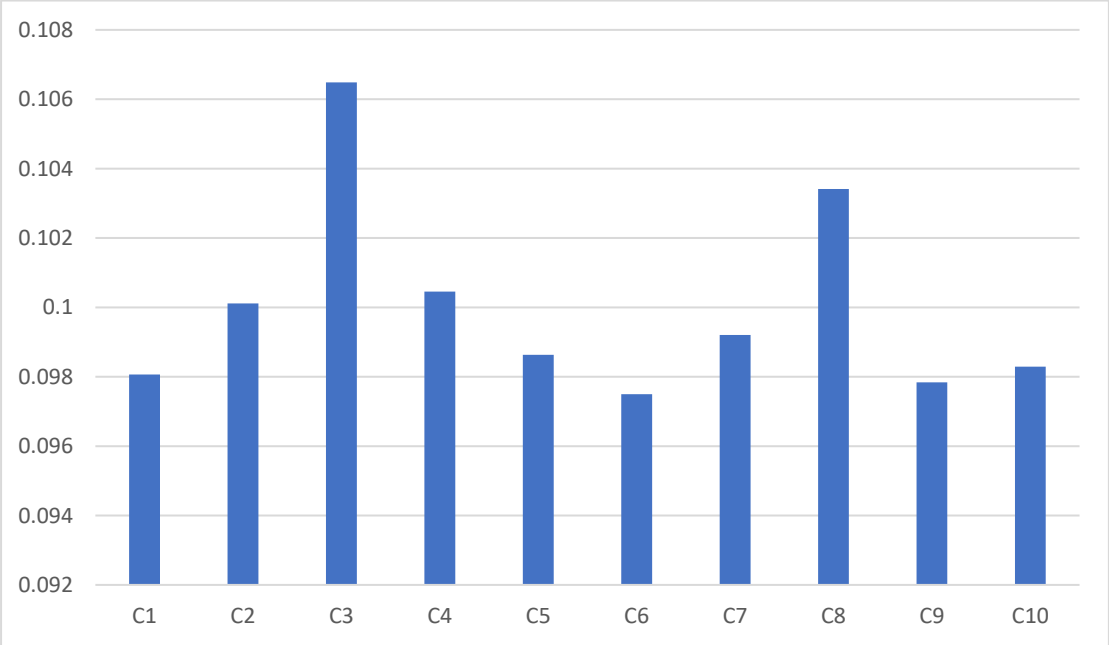

Figure 4. The criteria weights.

Step 4. We compute the relative weight.

Step 5. We compute the dominance degree.

Step 6. We compute the total dominance degree.

Step 7. We ordered alternatives as shown in Figure 5.

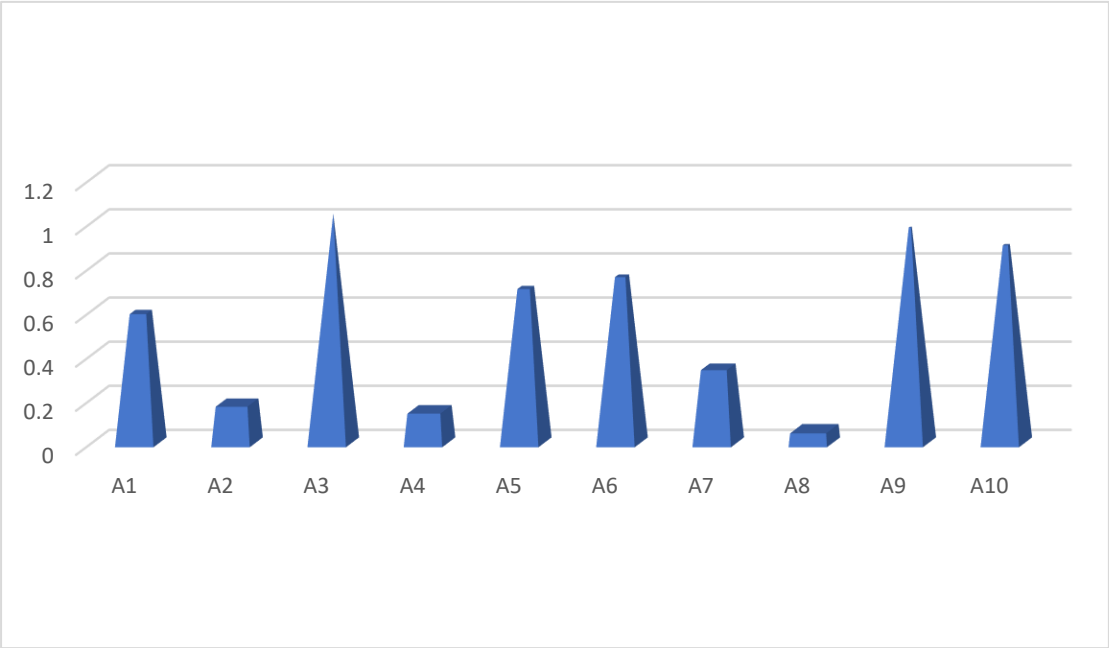

Figure 5. The rank of alternatives.

5. Managerial Applications

- The INN-GTODIM approach allows organizations to effectively assess network security risks, enabling better allocation of security resources. This ensures that critical areas receive the necessary attention and funding, maximizing protection against potential threats.
- By systematically identifying vulnerabilities and potential threats, the approach helps managers develop targeted risk management strategies. This proactive stance can significantly reduce the likelihood of cyber-attacks and data breaches.
- The integrated evaluation framework aids decision-makers by providing a structured method to analyze multiple attributes related to network security. This enhances their ability to make informed decisions in complex and uncertain environments.
- Organizations can use the results from the INN-GTODIM approach to benchmark their network security performance against industry standards and best practices. This can drive continuous improvement efforts and ensure compliance with regulatory requirements.
- The approach facilitates better emergency response planning by identifying potential security weaknesses. This preparation is crucial for maintaining business continuity and ensuring that data integrity is preserved during crises.
- Implementing the INN-GTODIM approach can serve as a basis for training programs aimed at enhancing employee awareness about network security risks and the importance of evaluation processes.
- The insights gained from network security evaluations can inform long-term strategic planning, helping organizations to adapt their security measures in response to evolving threats and technological advancements.

By incorporating the INN-GTODIM approach into managerial practices, organizations can enhance their overall security posture and resilience in the face of increasing cyber threats.

6. Conclusion

This research study introduces the INN-GTODIM approach, which synthesizes various techniques to effectively address the challenges of multiple-attribute group decision making (MAGDM) within the context of interval neutrosophic sets (INSs). This approach combines the strengths of INSs with the structured evaluation processes of GTODIM, creating a comprehensive framework for assessing computer network security (CNS).

To demonstrate the effectiveness of the INN-GTODIM approach, we present a detailed numerical case study focused specifically on evaluating CNS. This case study not only illustrates the application of the approach but also validates its effectiveness in providing a thorough and nuanced analysis of network security issues. The demonstration highlights how this integrated approach can adeptly manage the complexities and uncertainties inherent in network security evaluations, offering a valuable tool for decision-makers in the field.

7. Future Directions

- Explore the use of the INN-GTODIM approach in other fields beyond network security, such as healthcare, education, or environmental management, to evaluate its versatility.
- Investigate ways to refine the integration of INSs with decision-making techniques to further improve the robustness and reliability of the assessments.
- Develop mechanisms to integrate real-time data into the evaluation framework, allowing for dynamic assessments that adapt to changing conditions and uncertainties.
- Create intuitive software tools that implement the INN-GTODIM approach, making it accessible for practitioners and decision-makers who may not have technical expertise.
- Conduct comparative analyses with other decision-making models to benchmark the performance of the INN-GTODIM approach in various scenarios.
- Offer training programs and workshops to educate stakeholders on the application of this integrated approach, fostering a deeper understanding of its potential benefits.
- Initiate longitudinal studies to assess the long-term effectiveness of the approach in decision-making processes and its impact on outcomes over time.

These future directions aim to enhance the applicability and effectiveness of the INN-GTODIM approach in addressing complex decision-making challenges across various domains.

References

[1] A. Abraham, K. Smith, R. Jain, L. Jain, Network and information security: A computational intelligence approach special issue of journal of network and computer applications, Journal of Network and Computer Applications, 30 (2007) 1-3.

[2] A.S. Anagun, I. Cin, A neural network based computer access security system for multiple users, Computers & Industrial Engineering, 35 (1998) 351-354.

[3] C. Chen, R. Surette, M. Shah, Automated monitoring for security camera networks: Promise from computer vision labs, Security Journal, 34 (2021) 389-409.

[4] B. Xu, Methods for evaluating the computer network security with fuzzy number intuitionistic fuzzy dual hamy mean operators, Journal of Intelligent & Fuzzy Systems, 39 (2020) 4427-4441.

[5] J.W. Zhao, R. Masood, S. Seneviratne, A review of computer vision methods in network security, Ieee Communications Surveys and Tutorials, 23 (2021) 1838-1878.

[6] H.N. Wang, Big data security management countermeasures in the prevention and control of computer network crime, Journal of Global Information Management, 30 (2022) 16.

[7] B.Q. Ning, R. Lin, G.W. Wei, X.D. Chen, Edas method for multiple attribute group decision making with probabilistic dual hesitant fuzzy information and its application to suppliers selection, Technological and Economic Development of Economy, 29 (2023) 326-352.

[8] A. Kanchana, D. Nagarajan, S. Broumi, Multi-attribute group decision-making based on the neutrosophic bonferroni mean operator, Neutrosophic Sets and Systems, 57 (2023) 139-164.

[9] M. Akram, S. Naz, G. Santos-Garcia, M.R. Saeed, Extended codas method for magdm with 2-tuple linguistic spherical fuzzy sets, Aims Mathematics, 8 (2023) 3428-3468.

[10] F. Ahemad, M.K. Mehlawat, P. Gupta, A gra approach to a magdm problem with interval-valued -rung orthopair fuzzy information, Soft Computing, 27 (2023) 15793-15815.

[11] R.M. Zulqarnain, I. Siddique, S. Ei-Morsy, Einstein-ordered weighted geometric operator for pythagorean fuzzy soft set with its application to solve magdm problem, Mathematical Problems in Engineering, 2022 (2022) 14.

[12] S. Opricovic, G.H. Tzeng, Compromise solution by mcdm methods: A comparative analysis of vikor and topsis, European Journal of Operational Research, 156 (2004) 445-455.

[13] S. Opricovic, G.H. Tzeng, Extended vikor method in comparison with outranking methods, European Journal of Operational Research, 178 (2007) 514-529.

[14] E. Cevikcan, S. Cebi, I. Kaya, Fuzzy vikor and fuzzy axiomatic design versus to fuzzy topsis: An application of candidate assessment, Journal of Multiple-Valued Logic and Soft Computing, 15 (2009) 181-208.

[15] Y.-J. Lai, T.-Y. Liu, C.-L. Hwang, Topsis for modm, European Journal of Operational Research, 76 (1994) 486-500.

[16] C.T. Chen, Extensions of the topsis for group decision-making under fuzzy environment, Fuzzy Sets

and Systems, 114 (2000) 1-9.

[17] F.A. Smarandache, Unifying field in logics. Neutrosophy: Neutrosophic probability, set and logic, American Research Press, Rehoboth, 1999.

[18] H. Wang, F. Smarandache, Y.Q. Zhang, R. Sunderraman, Single valued neutrosophic sets, Multispace Multistruct, (2010) 410-413.

[19] H. Wang, F. Smarandache, Y.Q. Zhang, R. Sunderraman, Interval neutrosophic sets and logic: Theory and applications in computing, Hexis: Phoenix, AZ, USA, (2005).

[20] F. Smarandache, New types of soft sets “hypersoft set, indetermsoft set, indetermhypersoft set, and treesoft set”: An improved version, Infinite Study, 2023.

[21] M. Mohamed, A. Elsayed, A novel multi-criteria decision making approach based on bipolar neutrosophic set for evaluating financial markets in egypt, Multicriteria Algorithms with Applications, 5 (2024) 1-17.

[22] A. Salem, M. Mohamed, F. Smarandache, Im4.0ef: Tele-medical realization via integrating vague t2nss with owcm-ram toward intelligent medical 4.0 evaluator framework, Sustainable Machine Intelligence Journal, 9 (2024) 79-88.

[23] L. Gomes, M. Lima, Todim: Basics and apllication to multicriteria ranking of projects with environmental impacts, Foundations of Control Engineering, 16 (1991) 113-127.

[24] J.J. Peng, J.Q. Wang, J. Wang, H.Y. Zhang, X.H. Chen, Simplified neutrosophic sets and their applications in multi-criteria group decision-making problems, International Journal of Systems Science, 47 (2016) 2342-2358.

[25] Y.H. Huang, G.W. Wei, C. Wei, Vikor method for interval neutrosophic multiple attribute group decision-making, Information, 8 (2017) 144.

[26] H.Y. Zhang, J.Q. Wang, X.H. Chen, Interval neutrosophic sets and their application in multicriteria decision making problems, Scientific World Journal, 2014 (2014) 645953.

[27] J. Ye, Similarity measures between interval neutrosophic sets and their applications in multicriteria decision-making, Journal of Intelligent & Fuzzy Systems, 26 (2014) 165-172.

[28] C.E. Shannon, A mathematical theory of communication, Bell System Technical Journal, 27 (1948) 379-423.

[29] A. Tversky, D. Kahneman, Prospect theory: An analysis of decision under risk, Econometrica, 47 (1979) 263-291.

[30] A. Karasan, C. Kahraman, A novel interval-valued neutrosophic edas method: Prioritization of the united nations national sustainable development goals, Soft Computing, 22 (2018) 4891-4906.

[31] F. Li, Research and evaluation on comprehensive obstacle-avoiding behavior for unmanned vehicles based on the interval neutrosophic number multiple attribute group decision making, Journal of Intelligent & Fuzzy Systems, 44 (2023) 10721-10732.

Received: July 21, 2024. Accepted: Oct 24, 2024

NSS

Neutrosophic Sets and Systems, Vol. 76, 2025

University of New Mexico

A Python Class for Neutrosophic Morphology

Lorenzo Affè[1,*], Giorgio Nordo[2] and Florentin Smarandache[3]

[1]MIFT Department – Mathematical and Computer Science, Physical Sciences and Earth Sciences University of Messina, 98166 Sant'Agata, Messina, Italy; lorenzo.affe1@gmail.com

[2]MIFT Department – Mathematical and Computer Science, Physical Sciences and Earth Sciences University of Messina, 98166 Sant'Agata, Messina, Italy; giorgio.nordo@unime.it

[3]Mathematics, Physics, and Natural Science Division University of New Mexico 705 Gurley Ave., Gallup, NM 87301, USA; smarand@unm.edu

Abstract. In this work, we introduce a Python class, named `NSmorph`, developed to facilitate image manipulation through neutrosophic morphological operations. This innovative approach extends traditional image processing methods by leveraging the flexibility of neutrosophic logic to handle uncertainty, indeterminacy, and noise in digital images. The class offers implementations of essential morphological operators, such as neutrosophic dilation, erosion, opening, and closing, providing a robust tool for applications where image clarity is often compromised, like medical imaging and surveillance. We detail the class structure and functions and provide multiple examples to demonstrate its practical applications and comparative advantages over classical morphological methods.

Keywords: neutrosophic set; neutrosophic morphology; morphological image processing; Python programming; uncertainty in image analysis.

1. Introduction

In contemporary society, marked by increasing complexity and interconnected systems, classical mathematical theories face significant limitations when applied to real-world scenarios where vagueness, uncertainty, and indeterminacy are predominant. Such challenges are particularly pronounced in the field of image analysis, where accurate data interpretation plays a crucial role in diverse applications ranging from medical diagnostics to security surveillance. Traditional image processing techniques often struggle to handle these uncertainties effectively, necessitating alternative mathematical approaches capable of modeling and managing ambiguity [19].

Mathematical Morphology, originally developed by Matheron and Serra [13, 14], provides a powerful set of tools in nonlinear image analysis, primarily focusing on the geometric structure of images. Classical morphological operators, extensively discussed in Dougherty's works [2,3], have proven effective for tasks like noise filtering, shape extraction, and image segmentation. However, these operators are built on deterministic models of data, which can be limiting in applications where noise or uncertainty inherently affects image quality. Researchers have thus explored various generalizations, including Zadeh's fuzzy sets [20] and Atanassov's intuitionistic fuzzy sets [1], to accommodate situations where precise binary interpretations are insufficient. These theories laid the groundwork for the emergence of neutrosophic sets, introduced by Smarandache [17], which extend the representation of uncertainty by considering degrees of truth, indeterminacy, and falsehood independently, providing a nuanced framework suited to complex, real-world data.

Neutrosophic set theory has been applied successfully in various domains, including graph theory [4], decision-making [6], and soft topological spaces [7], where traditional mathematical approaches fall short. In image analysis, Neutrosophic Morphology applies Smarandache's principles to extend classical morphological operations, providing a framework that captures and preserves information about uncertainty and noise within images. This has proven especially beneficial in applications where data reliability varies significantly, allowing each pixel in an image to possess distinct degrees of membership, non-membership, and indeterminacy [18]. Studies have demonstrated that neutrosophic operators maintain structural transformations without losing important information about the underlying uncertainty, making them particularly effective for medical image analysis [12] and other fields requiring enhanced data fidelity [8, 16].

The importance of computational applications and frameworks developed in Python has significantly grown within neutrosophic studies. These frameworks facilitate practical implementations of neutrosophic concepts, making them more accessible to researchers and practitioners. Recent Python-based tools, such as those by El-Ghareeb [5] and Sleem et al. [16], have laid foundational work for performing neutrosophic operations efficiently. Nordo et al. [9] further extended this effort by developing a comprehensive Python framework specifically tailored for neutrosophic sets and mappings, highlighting the demand for adaptable and open-source tools in this field. Such frameworks not only simplify the computational aspects but also expand the applicability of neutrosophic methods across various disciplines, including image processing, where tools that address uncertainty and indeterminacy are crucial.

Despite these advancements, there remains a need for a comprehensive and user-friendly Python-based solution that can perform neutrosophic morphological operations in image analysis with flexibility and precision. Existing frameworks either focus narrowly on numerical

neutrosophic operations or lack the modular design needed for broader applicability [5, 16]. Recognizing this gap, we propose `NSmorph`, a Python class designed to implement fundamental neutrosophic morphological operators, including neutrosophic dilation, erosion, opening, and closing. These operators extend traditional morphological techniques into the neutrosophic domain, providing a versatile toolkit for image manipulation in environments with prevalent uncertainty, noise, and indeterminacy [11].

The structure of the paper is organized as follows: in Section 2, we delve into the data structure and the specific methods that constitute the `NSmorph` class, detailing each component's functionality. Section 3 presents practical examples that demonstrate the efficacy of the class in various scenarios, along with observations on the performance of neutrosophic operators relative to their classical counterparts. Finally, in Section 4, we provide our conclusions, underscoring the advantages of neutrosophic morphology in image analysis and the potential for future developments in this field [15].

2. The `NSmorph` class

The `NSmorph` class is designed for manipulating neutrosophic images using common morphological operators, including NS-dilation, NS-erosion, NS-opening, and NS-closing. The class constructor can initialize a neutrosophic image from various input types, such as a file path to a PNG or JPEG image, a NumPy array, or an instance of the `NSmorph` class itself. The following code shows how the constructor is implemented:

```
import os.path
import cv2 as cv
import numpy as np
from matplotlib import pyplot as plt

class NSmorph:
   def __init__(self, image, radius=0):
      if radius < 0:
      raise ValueError(f"The radius '{radius}' of the neighbourhood cannot be
    negative")
      if type(image) == np.ndarray:
         if image is None:
            raise ValueError("The image is not valid")
         (height, width)=image.shape
         self.__height = height
         self.__width = width
         self.__image_orig = image
         self.__radius = radius
         i_med = np.zeros((height, width), dtype = np.float32)
         for y in range(height):
            for x in range(width):
               md = 0
               n_pixel = 0
               for j in range(y - radius, y + radius + 1):
```

```
24                  for i in range(x - radius, x + radius +1):
25                     if (0<=i<width) and (0<=j<height) :
26                        md += image[j][i]
27                        n_pixel += 1
28               md /= n_pixel
29               i_med[y][x] = md
30         i_med_min = i_med.min()
31         i_med_max = i_med.max()
32         i_med_size = i_med_max - i_med_min
33         delta = np.zeros((height, width), dtype=np.float32)
34         for y in range(height):
35            for x in range(width):
36               delta[y][x] = abs(image[y][x] - i_med[y][x])
37         delta_min = delta.min()
38         delta_max = delta.max()
39         delta_size = delta_max - delta_min
40         ns_image = np.zeros((height, width, 3), dtype = np.float32)
41         for y in range(height):
42            for x in range(width):
43               ns_image[y][x][0] = (i_med[y][x] - i_med_min)/i_med_size if
   i_med_size !=0 else 0
44               ns_image[y][x][1] = (delta[y][x] - delta_min)/delta_size if
   delta_size !=0 else 0
45               ns_image[y][x][2] = 1 - ns_image[y][x][0]
46         self.__ns_image = ns_image
47      elif type(image) == str:
48         tmp_imgns = NSmorph(NSmorph.load(image), radius)
49         self.__ns_image = tmp_imgns.get()
50         self.__image_orig = tmp_imgns.getOrig()
51         self.__height = tmp_imgns.height()
52         self.__width = tmp_imgns.width()
53         self.__radius = radius
54      elif type(image) == NSmorph :
55         self.__ns_image = image.get()
56         self.__image_orig = image.getOrig()
57         self.__height = image.height()
58         self.__width = image.width()
59         self.__radius = image.radius()
60      else:
61         raise ValueError("The first parameter must be a matrix or a string")
```

Lines 1 to 4 import necessary libraries, including OpenCV and NumPy for image handling and `pyplot` for visualization. The constructor is defined in line 7, where the `radius` parameter is checked for validity in lines 8 and 9. The constructor can handle three types of input:

- NumPy array (lines 10–46): If `image` is a NumPy array, the image's height, width, and radius are stored. Then, from lines 18 to 32, the average intensity $\overline{I}$ for each pixel is computed by averaging the values within the kernel centered at each pixel. This forms the first channel of the neutrosophic image. In lines 33 to 39, the `delta` matrix, which measures intensity deviation from the local average (representing the homogeneity function), is computed and stored as the second channel. Finally, lines 40

to 46 construct the neutrosophic image by normalizing the intensity and delta values and calculating the non-membership degree as $1 - \texttt{membership}$.

- File path (string) (lines 47–53): If `image` is a file path, the constructor calls the `load` method to load the image as a grayscale NumPy array. The `NSmorph` instance for this image is then initialized, and the original image dimensions and radius are set.
- Existing `NSmorph` object (lines 54–59): If `image` is an existing `NSmorph` instance, the neutrosophic image and related attributes are directly copied.

Finally, in lines 60 and 61, if the input does not match any valid types, an error is raised.

The `NSmorph` class also includes several methods to retrieve the complete neutrosophic image or its individual components—membership, non-membership, and indeterminacy—or to convert it back to the original binary format. These functions provide flexible access and modification capabilities for each aspect of the neutrosophic image representation.

A particularly useful method is the static method `load(img_path)`, which loads an image from a specified file path `img_path`. This method reads the image in grayscale, thus simplifying conversion to the neutrosophic format. If the provided path is invalid, not found, or inaccessible, the method raises an error, leveraging `os.path.isfile()` to verify the file's existence. This ensures that only valid paths are processed, preventing runtime issues due to incorrect paths.

```
@staticmethod
def load(img_path):
    if img_path is None:
        raise ValueError("The path of the image is not valid")
    if not os.path.isfile(img_path):
        raise FileNotFoundError(f"The file '{img_path}' does not exist or it is not accessible.")
    image = cv.imread(img_path, cv.IMREAD_GRAYSCALE)
    if image is None:
        raise IOError(f"It has not been possible to read the image file '{img_path}'")
    return image
```

The `get()` method gives back the neutrosophic image.

```
def get(self):
    return self.__ns_image
```

Methods are also available for retrieving and assigning specific components of the neutrosophic image:

- Membership (`getM()` and `setM()`): `getM()` returns the membership degree for each pixel, while `setM(x, y, mu)` allows for setting the membership degree at a specific pixel location `(x, y)`.
- Non-membership (`getNM()` and `setNM()`): `getNM()` retrieves the non-membership degree matrix, and `setNM(x, y, omega)` sets the non-membership degree for the specified pixel.
- Indeterminacy (`getI()` and `setI()`): `getI()` returns the indeterminacy degree, while `setI(x, y, sigma)` assigns a new indeterminacy degree to a given pixel.

Each method supports fine-grained control over image processing, allowing users to either view or modify the neutrosophic image's distinct properties individually or as a composite.

```
def getM(self):
    return self.__ns_image[:,:,0]

def getI(self):
    return self.__ns.image[:,:,1]

def getNM(self):
    return self.__ns.image[:,:,2]


def setM(self, x, y, mu):
    self.__ns_image[y][x][0] = mu

def setI(self, x, y, sigma):
    self.__ns_image[y][x][1] = sigma

def setNM(self, x, y, omega):
    self.__ns_image[y][x][2] = omega
```

The `getOrig()` method returns the original grayscale image from which the neutrosophic image was derived. This can be useful for comparison purposes, allowing users to access the unprocessed version of the image alongside its neutrosophic representation. The method is implemented as follows:

```
def getOrig(self):
    return self.__image
```

The `width()` and `height()` methods return the width and height of the image, respectively. These methods are particularly useful when constructing other morphological operations, such as dilation and erosion, as they provide easy access to the dimensions of the image, which is essential for managing boundary conditions and kernel application across the entire image. The implementations are straightforward:

```
def width(self):
    return self.__width

def height(self):
    return self.__height
```

The `radius()` method returns the radius of the neighborhood associated with the uploaded image. This radius defines the size of the local region around each pixel that is used in various neutrosophic morphological operations, such as calculating local intensity averages or applying structuring elements in dilation and erosion. Accessing the radius through this method is particularly useful when the neighborhood size impacts processing or when adapting the morphological operators to different kernel sizes. The implementation is as follows:

```
def radius(self):
    return self.__radius
```

The `getBinary()` method performs thresholding on the current image, producing a binary image based on a threshold value specified by the user. The method returns a binary representation of the image as a NumPy matrix, where rows and columns are indexed from $(0, 0)$ at the top left corner. In this binary matrix, pixel values are set to 0 (black) for intensities below the threshold and 1 (white) for intensities equal to or above the threshold. The method is implemented as follows:

```
def getBinary(self, threshold):
    (ret, bin_image) = cv.threshold(self.__image_orig, threshold, 1, cv.
    THRESH_BINARY)
    return bin_image
```

The `getRepresentation()` method returns a grayscale image that represents an interpolation of the three neutrosophic levels: membership, indeterminacy, and non-membership. This interpolation combines the three levels based on customizable weights provided as optional parameters. By default, these weights prioritize the membership degree, reflecting its primary influence on the pixel intensity in the resulting grayscale image. The following code illustrates this implementation:

```
def getRepresentation(self, weightM=0.85, weightI=0.25, weightNM=-0.1, binary
    =False, limit_value=128):
    img_M = self.getM()
    img_I = self.getI()
    img_NM = self.getNM()
    mat_rap = np.zeros((self.__height, self.__width, 3), dtype = np.float32)
```

```
    for y in range(self.__height):
        for x in range(self.__width):
            mat_rap[y][x][0] = weightM*img_M[y][x] + weightI*img_I[y][x] +
     weightNM*img_NM[y][x]
    img_rap = cv.cvtColor(mat_rap, cv.COLOR_BGR2GRAY)
    if binary == True:
        (ret, img_rap) = cv.threshold(img_rap, limit_value, 1, cv.THRESH_BINARY)
    return img_rap
```

The method signature is as follows:

- `weightM`: Weight assigned to the membership degree. Default is 0.85.
- `weightI`: Weight assigned to the indeterminacy degree. Default is 0.25.
- `weightNM`: Weight assigned to the non-membership degree. Default is -0.1.
- `binary`: Boolean flag to enable binarization of the resulting image based on a threshold.
- `limit_value`: Threshold value used for binarization if `binary` is set to `True`. Default is 128.

The grayscale image is generated by combining the three components, emphasizing areas with higher membership and optionally applying thresholding if `binary` is `True`. If thresholding is active, the method uses `limit_value` to convert the grayscale image to a binary one, mapping values above the threshold to white and those below to black.

This function is particularly useful for visualizing the overall neutrosophic information in a single image, allowing for quick interpretation of complex neutrosophic properties in greyscale or binary format.

2.1. *Neutrosophic dilation*

The `dilation(self, kernel)` method performs the dilation operation on a neutrosophic image, using another neutrosophic image as the structuring element (kernel). The method returns the dilated neutrosophic image and it is implemented as follows:

```
def dilation(self, kernel):
    (height, width) = (self.__height, self.__width)
    (height_k, width_k) = (kernel.height(), kernel.width())

    img_M = self.getM()
    img_I = self.getI()
    img_NM = self.getNM()
    kernel_M = kernel.getM()
    kernel_I = kernel.getI()
    kernel_NM = kernel.getNM()

    mat_generating = np.zeros((height, width, 3), dtype=np.uint8)
    im_empty = cv.cvtColor(mat_generating, cv.COLOR_BGR2GRAY)
```

```
    im_dil = NSmorph(im_empty)

    for y in range(height):
        for x in range(width):

            width_sx = x - width_k//2
            if width_sx<0 :
                width_sx = 0
            width_dx = x + width_k//2 +1
            if width_dx > width - 1 :
                width_dx = width - 1
            height_up = y - height_k//2
            if height_up < 0 :
                height_up = 0
            height_down = y+ height_k//2 + 1
            if height_down > height - 1 :
                height_down = height - 1

            mat_M = img_M[height_up:height_down, width_sx:width_dx]
            mat_I = img_I[height_up:height_down, width_sx:width_dx]
            mat_NM = img_NM[height_up:height_down, width_sx:width_dx]

            (n_rows, n_columns) = mat_M.shape

            width_sx_kernel = width_k//2 - n_columns//2
            if width_sx_kernel > n_columns//2 - 1:
                width_sx_kernel = 0
            width_dx_kernel = width_k//2 + n_columns//2 + 1
            if width_dx_kernel > n_columns//2 + 1:
                width_dx_kernel = n_columns
            height_up_kernel = height_k//2 - n_rows//2
            if height_up_kernel > n_rows//2 - 1:
                height_up_kernel = 0
            height_down_kernel = height_k//2 + n_rows//2 + 1
            if height_down_kernel > n_rows//2 + 1 :
                height_down_kernel = n_rows

            mat_kernelM = kernel_M[height_up_kernel:height_down_kernel,
        width_sx_kernel:width_dx_kernel]
            mat_kernelI = kernel_I[height_up_kernel:height_down_kernel,
        width_sx_kernel:width_dx_kernel]
            mat_kernelNM = kernel_NM[height_up_kernel:height_down_kernel,
        width_sx_kernel:width_dx_kernel]

            minimum_M = np.minimum(mat_M, mat_kernelM)
            minimum_I = np.minimum(mat_I, mat_kernelI)
            maximum_NM = np.maximum(mat_NM, 1 - mat_kernelNM)

            mu = minimum_M.max()
            sigma = minimum_I.max()
            omega = maximum_NM.min()

            im_dil.setM(x, y, mu)
            im_dil.setI(x, y, sigma)
            im_dil.setNM(x, y, omega)
    return im_dil
```

In lines 2 and 3, the dimensions of both the input image and the kernel are stored in separate tuples. Then, in lines 5 to 10, the membership, indeterminacy, and non-membership matrices of the image and kernel are retrieved.

From lines 12 to 14, an empty matrix, `mat_generating`, is created using `np.zeros()` from the NumPy library. This matrix is converted into a grayscale image, `im_empty`, with OpenCV's `cv.cvtColor()` function and serves as the base for creating the dilated neutrosophic image `im_dil`.

Lines 16 and 17 use nested `for` loops to iterate through each pixel of the input image. Within each loop, lines 19 to 30 define the bounds for the image region centered on the current pixel (x, y), ensuring that the extracted region matches the size of the kernel. This is done by adjusting for any out-of-bounds areas along the edges of the image, where the kernel might partially exceed the image boundaries.

In lines 32 to 34, the membership, indeterminacy, and non-membership matrices are extracted for the region defined by these bounds, centered around (x, y). Line 36 then evaluates the actual dimensions of these matrices, accounting for cases where the region is truncated by image boundaries.

Lines 38 to 49 set up further bounds to ensure that the extracted kernel matrices align precisely with the region around (x, y) in the image. This step helps reduce the kernel dimensions to match those of the extracted region when scanning near boundaries.

The actual dilation operation occurs in lines 55 to 61, applying the following neutrosophic morphological formulas:

$$\begin{aligned}
\mu_{A\oplus B}(v) &= \sup_{u\in\mathbb{U}} \min\left\{\mu_A(v+u), \mu_B(u)\right\}, \\
\sigma_{A\oplus B}(v) &= \sup_{u\in\mathbb{U}} \min\left\{\sigma_A(v+u), \sigma_B(u)\right\}, \\
\omega_{A\oplus B}(v) &= \inf_{u\in\mathbb{U}} \max\left\{\omega_A(v+u), 1-\omega_B(u)\right\},
\end{aligned}$$

where $\mu_{A\oplus B}(v)$, $\sigma_{A\oplus B}(v)$, and $\omega_{A\oplus B}(v)$ represent the degrees of membership, indeterminacy, and non-membership, respectively, after dilation.

In lines 63 to 65, the calculated values for membership, indeterminacy, and non-membership are stored in the `im_dil` image at position (x, y). Finally, in line 66, the fully processed dilated neutrosophic image is returned.

2.2. *Neutrosophic erosion*

The `erosion(self, kernel)` method applies the neutrosophic erosion operation to the input image using a specified *kernel*, which is also a neutrosophic image. The method returns the eroded neutrosophic image and is implemented as follows:

```
def erosion(self, kernel):
   (height, width) = (self.__height, self.__width)
   (height_k, width_k) = (kernel.height(), kernel.width())

   img_M = self.getM()
   img_I = self.getI()
   img_NM = self.getNM()
   kernel_M = kernel.getM()
   kernel_I = kernel.getI()
   kernel_NM = kernel.getNM()

   mat_generating = np.zeros((height, width, 3), dtype=np.uint8)
   im_empty = cv.cvtColor(mat_generating, cv.COLOR_BGR2GRAY)
   im_er = NSmorph(im_empty)

   for y in range(height):
      for x in range(width):

         width_sx = x - width_k//2
         if width_sx<0 :
            width_sx = 0
         width_dx = x + width_k//2 +1
         if width_dx > width - 1 :
            width_dx = width - 1
         height_up = y - height_k//2
         if height_up < 0 :
            height_up = 0
         height_down = y+ height_k//2 + 1
         if height_down > height - 1 :
            height_down = height - 1

         mat_M = img_M[height_up:height_down, width_sx:width_dx]
         mat_I = img_I[height_up:height_down, width_sx:width_dx]
         mat_NM = img_NM[height_up:height_down, width_sx:width_dx]

         (n_rows, n_columns) = mat_M.shape

         width_sx_kernel = width_k//2 - n_columns//2
         if width_sx_kernel > n_columns//2 - 1:
            width_sx_kernel = 0
         width_dx_kernel = width_k//2 + n_columns//2 + 1
         if width_dx_kernel > n_columns//2 + 1:
            width_dx_kernel = n_columns
         height_up_kernel = height_k//2 - n_rows//2
         if height_up_kernel > n_rows//2 - 1:
            height_up_kernel = 0
         height_down_kernel = height_k//2 + n_rows//2 + 1
         if height_down_kernel > n_rows//2 + 1 :
            height_down_kernel = n_rows

         mat_kernelM = kernel_M[height_up_kernel:height_down_kernel,
   width_sx_kernel:width_dx_kernel]
         mat_kernelI = kernel_I[height_up_kernel:height_down_kernel,
   width_sx_kernel:width_dx_kernel]
         mat_kernelNM = kernel_NM[height_up_kernel:height_down_kernel,
   width_sx_kernel:width_dx_kernel]
```

```
54
55          maximum_M = np.maximum(mat_M, 1 - mat_kernelM)
56          maximum_I = np.maximum(mat_I, 1 - mat_kernelI)
57          minimum_NM = np.minimum(mat_NM, mat_kernelNM)
58
59          mu = maximum_M.min()
60          sigma = maximum_I.min()
61          omega = minimum_NM.max()
62
63          im_er.setM(x, y, mu)
64          im_er.setI(x, y, sigma)
65          im_er.setNM(x, y, omega)
66      return im_er
```

Similar to the neutrosophic dilation method, the dimensions of both the input image and kernel are stored in tuples (lines 2 and 3), and the membership, indeterminacy, and non-membership matrices of the input image and kernel are assigned to `img_M`, `img_I`, `img_NM` and `kernel_M`, `kernel_I`, `kernel_NM` respectively (lines 5 to 10).

Lines 12 to 14 create an empty matrix, `mat_generating`, which serves as the base for the output eroded image, `im_er`. The matrix is initialized as a grayscale image using `cv.cvtColor()` from the OpenCV library.

Nested `for` loops in lines 16 and 17 iterate over each pixel in the input image. Lines 19 to 30 define the region within the input image centered at each pixel (x, y), ensuring the extracted region matches the kernel size. These boundary checks ensure that when the kernel partially overlaps the image edges, the region adjusts accordingly to prevent out-of-bounds errors.

The membership, indeterminacy, and non-membership matrices for the region around (x, y) are extracted in lines 32 to 34. In line 36, the actual dimensions of these matrices are determined to account for potential edge clipping.

Lines 38 to 49 then adjust the kernel's size to match that of the extracted region, ensuring alignment during the operation.

The erosion operation is applied in lines 55 to 61, using the following formulas for neutrosophic morphological erosion:

$$\mu_{A\ominus B}(v) = \inf_{u\in\mathbb{U}} \max\left\{\mu_A(v+u), 1-\mu_B(u)\right\},$$
$$\sigma_{A\ominus B}(v) = \inf_{u\in\mathbb{U}} \max\left\{\sigma_A(v+u), 1-\sigma_B(u)\right\},$$
$$\omega_{A\ominus B}(v) = \sup_{u\in\mathbb{U}} \min\left\{\omega_A(v+u), \omega_B(u)\right\},$$

where $\mu_{A\ominus B}(v)$, $\sigma_{A\ominus B}(v)$, and $\omega_{A\ominus B}(v)$ represent the degrees of membership, indeterminacy, and non-membership, respectively, for the eroded image.

Finally, in lines 63 to 65, the computed membership, indeterminacy, and non-membership values are saved to `im_er` at (x, y). In line 66, the method returns the fully processed eroded neutrosophic image.

2.3. *Neutrosophic opening and closing*

The `opening(self, kernel)` method performs the neutrosophic opening operation on the image. This operation first applies the erosion operator, followed by the dilation operator, using the same *kernel*, which is also a neutrosophic image, passed as a parameter. The result is a neutrosophic image where small structures are removed, and larger shapes are preserved without altering their boundaries significantly. This method is especially useful for tasks where noise reduction or shape smoothing is required. The implementation is straightforward:

```
def opening(self, kernel):
    return self.erosion(kernel).dilation(kernel)
```

The `closing(self, kernel)` method, in contrast, performs the neutrosophic closing operation. This operation first applies the dilation operator to the image, followed by the erosion operator, using the same *kernel* provided. Closing is typically used to fill small holes and connect adjacent structures within an image without significantly altering their contours, making it useful in image enhancement tasks. The implementation is as follows:

```
def closing(self, kernel):
    return self.dilation(kernel).erosion(kernel)
```

The complete source code for this Python class has been released under the Open Source GNU General Public License version 3.0 (or GPL-3.0) and is freely accessible at the url github.com/lorenzoaffe/nsmorph.

3. **Examples and Observations**

In this section, we demonstrate the `NSmorph` class by using neutrosophic dilation, erosion, opening, and closing operations on an image affected by noise. These examples showcase how each neutrosophic morphological operator interacts with noisy data, specifically observing the effect on the image's brightness, clarity, and feature preservation. Such noise, often introduced as random variations in pixel values, can significantly compromise image quality in real-world applications.

```
from ns_morph import NSmorph
import cv2 as cv
```

```
import numpy as np
from matplotlib import pyplot as plt

path_image = "immagini/j_puntini.jpg"
image = NSmorph.load(path_image)
ns_image = NSmorph(image, 4)

path_kernel = "immagini/kernel_croce.jpg"
kernel = NSmorph.load(path_kernel)
ns_kernel = NSmorph(kernel, 1)

nsdil_image = ns_image.dilation(ns_kernel)

plt.suptitle("Neutrosophic dilation (M=membership, I=indeterminacy, NM=non-
    membership)")

plt.subplot(4,3,1)
plt.imshow(ns_image.getOrig(), cmap='gray')
plt.xticks([])
plt.yticks([])
plt.title("Original")

...

plt.subplot(4,3,11)
plt.imshow(nsdil_image.getRepresentation(), cmap='gray')
plt.xticks([])
plt.yticks([])
plt.title("dilation")

plt.subplot(4,3,12)
plt.imshow(nsdil_image.getRepresentation(binary=True, limit_value=0.04), cmap=
    'gray')
plt.xticks([])
plt.yticks([])
plt.title("binarized dilation")

plt.show()
```

In lines 1 to 4, we import necessary modules and libraries, including `NSmorph`, OpenCV-Python, NumPy, and `pyplot` from Matplotlib. Lines 6 to 8 generate the neutrosophic image from the specified path using the static method `load(img_path)`. Similarly, lines 10 to 12 initialize the kernel. Line 14 performs neutrosophic dilation on the image with the kernel, storing the result in `nsdil_image`. From lines 18 to 36, the images are plotted, showing the original, the dilated, and the binarized dilated images.

Figures 1, 2, 3, and 4 present the results of applying NS-dilation, NS-erosion, NS-opening, and NS-closing respectively. Each figure includes grayscale images of the membership, indeterminacy, and non-membership components, as well as the interpolated neutrosophic image and a binarized version obtained through thresholding.

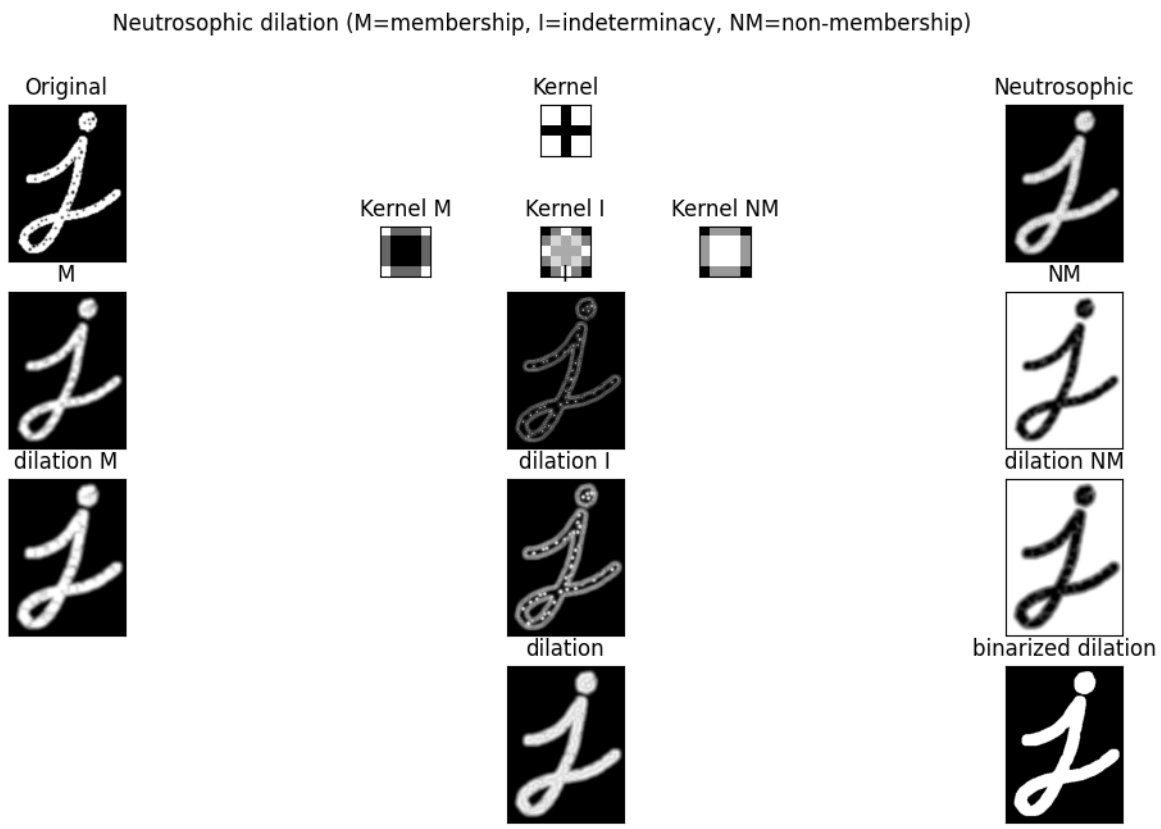

FIGURE 1. Example of the neutrosophic dilation of a neutrosophic image with image radius = 4 and kernel radius = 1

In Figure 1, we observe that the NS-dilation operator effectively smooths the shape of the image while filling in small holes. Notably, the indeterminacy component (I) retains the presence of noise, indicating areas where the operator's action is limited by the uncertainty inherent in the noisy regions.

Figure 2 shows the application of the NS-erosion operator, which reduces protrusions and expands holes. Similar to dilation, erosion captures noise effects, particularly in the membership (M) and non-membership (NM) components. This retention of noise highlights how neutrosophic operators can provide information on uncertainty while performing morphological transformations.

In Figure 3, the NS-opening operator, a sequence of erosion followed by dilation, preserves the indeterminacy and non-membership values in noisy areas but still manages to remove minor structures without disturbing the primary shape of the image. This operator is effective in refining shapes by reducing small-scale noise, emphasizing indeterminacy in regions with higher pixel variability.

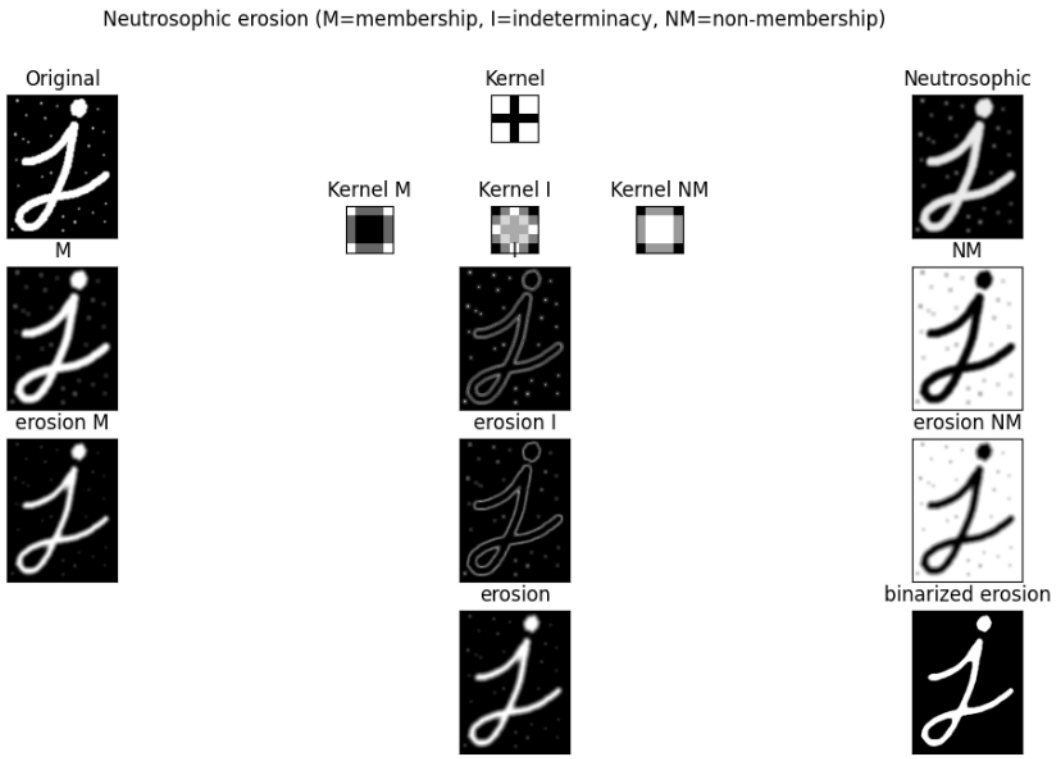

FIGURE 2. Example of the neutrosophic erosion of a neutrosophic image with image radius = 4 and kernel radius = 1

Finally, Figure 4 shows the NS-closing operation, which first applies dilation and then erosion. This operation fills small gaps and connects nearby features, with noise remaining visible in the indeterminacy component. The ability of NS-closing to smooth object boundaries without completely erasing uncertainty demonstrates its utility in applications where preserving ambiguous regions is important.

These examples illustrate the unique advantages of neutrosophic morphological operators, which maintain noise information through indeterminacy while effectively processing image structures. This dual capability of modification and noise retention makes neutrosophic morphology suitable for complex image processing tasks where uncertainty plays a significant role.

4. **Conclusions**

In this paper, we introduced `NSmorph`, a Python class designed for the manipulation of neutrosophic digital images through morphological operators specifically tailored to handle uncertainty and ambiguity. This class implements key neutrosophic operators, including NS-dilation, NS-erosion, NS-opening, and NS-closing, each serving as an extension of classical

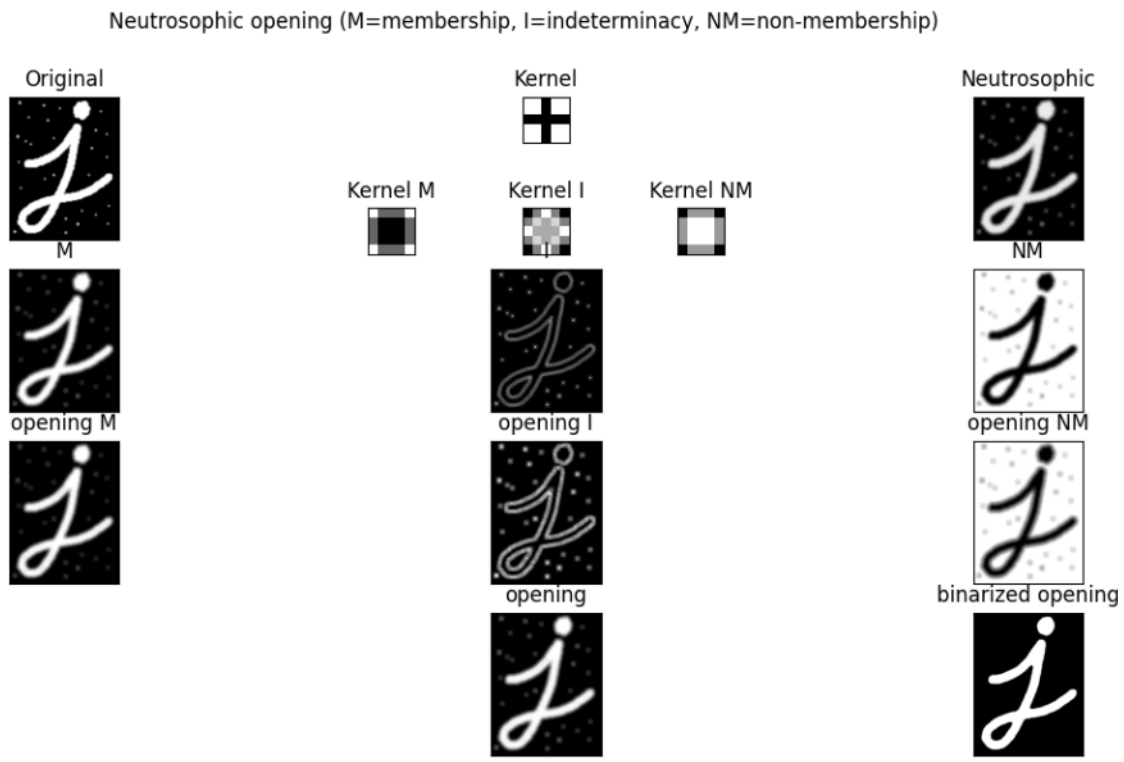

FIGURE 3. Example of the neutrosophic opening of a neutrosophic image with image radius = 4 and kernel radius = 1

morphology in a way that retains the core actions of these transformations while addressing noise and indeterminacy. The design of `NSmorph` includes a flexible constructor and a suite of methods that allow users to access, modify, and visualize the membership, indeterminacy, and non-membership components of an image, adding a layer of control that is essential for applications where uncertain data is prevalent.

The examples provided illustrate how neutrosophic operators differ from traditional morphology, showcasing their capacity to improve image processing outcomes in noisy environments. In particular, the neutrosophic dilation and erosion operations demonstrated a unique capability to maintain information on uncertainty in the indeterminacy component while performing standard morphological tasks, such as smoothing shapes and filling or reducing holes. This dual function of transforming image structures while retaining noise information in the indeterminacy channel provides a substantial advantage for applications that require both enhancement and detailed uncertainty analysis, such as medical imaging, remote sensing, and security surveillance.

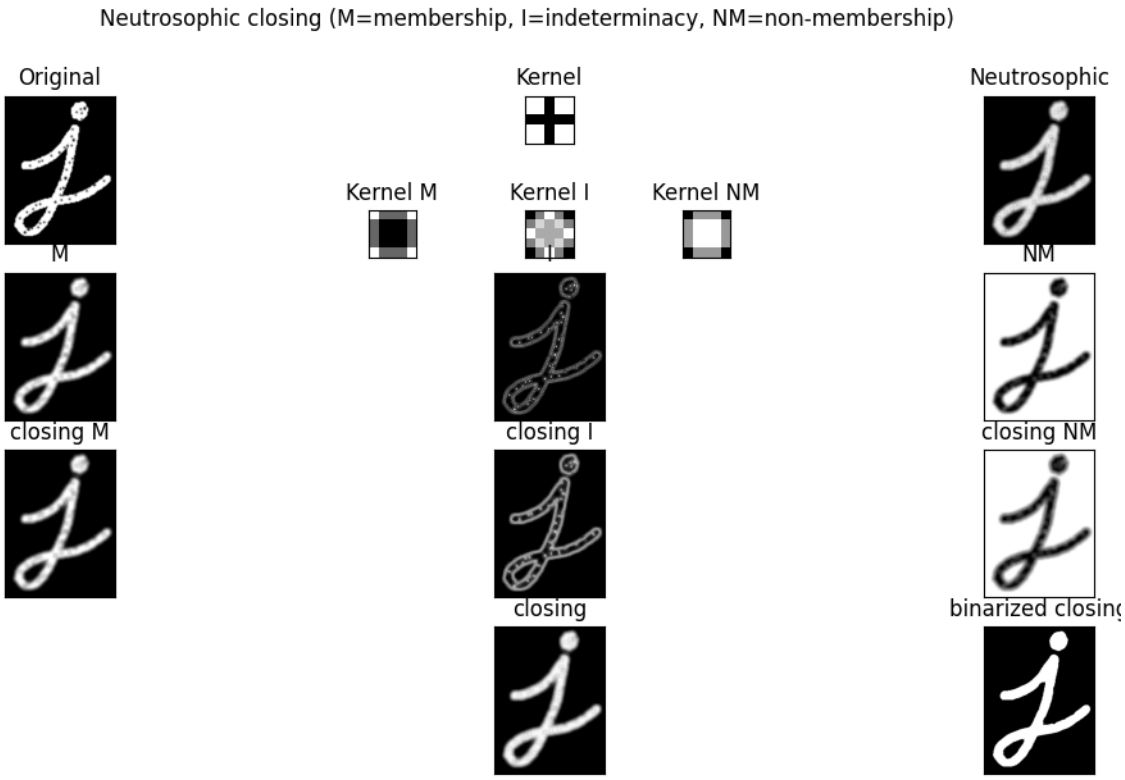

FIGURE 4. Example of the neutrosophic closing of a neutrosophic image with image radius = 4 and kernel radius = 1

Similarly, the neutrosophic opening and closing operations highlighted the class's capability to refine image structures. The NS-opening operator proved effective in reducing small-scale noise while sharpening key features, thus avoiding the loss of critical information. On the other hand, the NS-closing operator showed effectiveness in filling small gaps and connecting nearby structures without compromising the representation of ambiguous areas. These observations underscore how `NSmorph` enables users to adapt morphological operations to complex image processing needs, where standard morphological operators would typically smooth or discard valuable uncertain information.

Overall, the development of `NSmorph` contributes to the field of digital image processing by providing a robust tool for managing indeterminate data, preserving ambiguity, and enhancing the interpretability of images under uncertain conditions. The demonstrated effectiveness of neutrosophic morphological operators in retaining and processing noise information establishes `NSmorph` as a valuable asset for researchers and practitioners who require enhanced flexibility and control over image data affected by noise or uncertainty. Future work may explore

additional neutrosophic operators or adaptations of existing ones to further expand the class's utility across diverse image processing applications.

Acknowledgment

This research was supported by Gruppo Nazionale per le Strutture Algebriche, Geometriche e le loro Applicazioni (G.N.S.A.G.A.) of Istituto Nazionale di Alta Matematica (INdAM) "F. Severi", Italy.

References

1. Atanassov K.T. Intuitionistic Fuzzy Sets. *Fuzzy Sets and Systems* **20** (1), pp. 87-96, 1986.
2. Dougherty E.R. An Introduction to Morphological Image Processing. *SPIE Optical Engineering Press*, Bellingham, Washington (USA), 1992.
3. Dougherty E.R., Lotufo R.A. Hands-on Morphological Image Processing. *SPIE Press*, Bellingham, Washington (USA), 2003.
4. Broumi S., Talea M., Bakali A., Smarandache F. Single valued neutrosophic graphs. *Journal of New theory* **10**, pp. 86-101, 2016.
5. El-Ghareeb H.A. Novel Open Source Python Neutrosophic Package. *Neutrosophic Sets and Systems* **25**, pp. 136-160, 2019.
6. Mehmood A., Nadeem F., Nordo G., Zamir M., Park C.,Kalsoom H., Jabeen S., Khan M.Y. Generalized neutrosophic separation axioms in neutrosophic soft topological spaces. *Neutrosophic Sets and Systems* **32** (1), pp. 38–51, 2020.
7. Mehmood A., Nadeem F., Park C., Nordo G., Kalsoom H., Rahim Khan M., Abbas N. Neutrosophic soft alpha-open set in neutrosophic soft topological spaces. *Journal of Algorithms and Computation* **52**, pp. 37–66, 2020.
8. Nordo G., Mehmood A., Broumi S. Single Valued Neutrosophic Filters. *International Journal of Neutrosophic Science* **6**, pp. 8-21, 2020.
9. Nordo G., Jafari S., Mehmood A., Basumatary B. A Python Framework for Neutrosophic Sets and Mappings. *Neutrosophic Sets and Systems* **65**, pp. 199-236, 2024.
10. Salama A., El-Ghareeb H.A.. Manie A.M., Smarandache F. Introduction to develop some software programs for dealing with neutrosophic sets. *Neutrosophic Sets and Systems* **3**, pp. 51-52, 2019.
11. Salama A., Abd el-Fattah M., El-Ghareeb H.A.. Manie A.M. Design and Implementation of Neutrosophic Data Operations Using Object Oriented Programming. *International Journal of Computer Application* **4** (5), pp. 163-175, 2014.
12. Salama A.A., El-Hafeez S.A., El-Nakeeb A., El-Hassanein Eman M. Neutrosophic Approach for Mathematical Morphology. *Master's thesis*, Port Said University, 2018.
13. Serra J. Image Analysis and Mathematical Morphology. *Academic Press*, London (UK), 1982.
14. Serra J., Soille P. (Eds.) Mathematical Morphology and Its Applications to Image and Signal Processing. *Klwwer Academic Publishers*, Dordrecht (Netherlands), 1994.
15. Shih F.Y. Image processing and Mathematical Morphology: Fundamentals and Applications. *CRC Press*, New York (USA), 2009.
16. Sleem A., Abdel-Baset M., El-henawy I. PyIVNS: A python based tool for Interval-valued neutrosophic operations and normalization. *SoftwareX* **12**, pp. 1-7, 2020.
17. Smarandache F. A Unifying Field in Logics. Neutrosophy: Neutrosophic Probability, Set and Logic. Rehoboth: American Research Press, 1999.

18. Wang H., Smarandache F., Zhang Y.Q., Sunderraman R. Single Valued Neutrosophic Sets. *Technical Sciences and Applied Mathematics*, pp. 10-14, 2012.
19. Wilson J.N, Ritter G.X. Handbook of Computer Vision Algorithms in Image Algebra (2nd edition). *CRC Press*, New York (USA), 2000.
20. Zadeh L.A. Fuzzy Sets, *Information and Control* **8** (3), pp. 338-353, 1965.

Received: July 26, 2024. Accepted: Oct 25, 2024

NSS
Neutrosophic Sets and Systems, Vol. 76, 2025
University of New Mexico

Improving Teaching Quality Assessment in Smart Classrooms for English Majors: An Integrated Double-Valued Neutrosophic Decision-Making Model

Lu Luo[1], Cong Wang[2]*

[1]Huainan Vocational and Technical College, Huainan, 232001, Anhui, China (Lu Luo, E-mail: claire_luo668@sina.com)

[2]School of Foreign Languages, Huainan Normal University, Huainan, 232038, Anhui, China

*Corresponding author, E-mail: wangcong199@126.com; wangcong@huun.edu.cn

https://orcid.org/0009-0007-7649-1968

Abstract: The evaluation of multimedia-based college English teaching aims to assess the impact of multimedia technology on teaching quality and student learning outcomes. With the introduction of multimedia, classroom interactivity is enhanced, and students' interest and engagement are increased. Additionally, multimedia provides more opportunities for self-directed learning, helping students reinforce knowledge outside the classroom. However, the evaluation must focus on the alignment of technology with teaching objectives and whether the use of multimedia truly improves students' language skills and classroom efficiency. The evaluation of smart classroom teaching quality for English majors in universities is a multi-attribute decision-making (MADM) problem. Recently, methods such as the TOPSIS approach have been applied to tackle these challenges. Double-Valued Neutrosophic Sets (DVNSs) are used to represent fuzzy data in the evaluation process. In this study, a Double-Valued Neutrosophic Number TOPSIS (DVNN-TOPSIS) approach is proposed to address MADM problems involving DVNSs. Finally, a numerical case study on the quality evaluation of smart classroom teaching for English majors is provided to demonstrate the effectiveness of the DVNN-TOPSIS approach.

Keywords: MADM; DVNSs; TOPSIS approach; Smart classroom teaching

1. Introduction

The evaluation of multimedia-based college English teaching aims to comprehensively assess the impact of multimedia technology on teaching quality and student learning outcomes. By incorporating rich audio, video, and image resources, multimedia teaching makes the classroom more dynamic and engaging, enhancing students' interest and participation. Additionally, the interactive nature of multimedia fosters better communication between

teachers and students, optimizing the classroom feedback mechanism. Moreover, multimedia teaching offers students more opportunities for independent learning, allowing them to use online resources for review and further study, thereby reinforcing classroom knowledge. However, evaluating teaching effectiveness requires not only examining whether multimedia technology improves students' language skills but also considering its alignment with teaching objectives and its actual contribution to classroom efficiency. Effective multimedia teaching should seamlessly integrate technology with course content, avoiding distractions and ensuring that the desired teaching goals are achieved. The quality evaluation of smart classroom teaching for English majors in universities is MADM problem. Recently, the MCDM approach [1, 2] and TOPSIS approach [3] have been applied to handle such problems.

1.1 Motivation of this study

The TOPSIS method combines the advantages of both and TOPSIS, offering the following three key benefits:

I. I**t balances the decision-maker's subjective preferences with objective data analysis**. TOPSIS objectively evaluates the relative merits of alternatives by calculating their distances from the ideal and negative ideal solutions.

II. I**t excels in handling complex and uncertain decision-making environments**. TOPSIS, through the construction of ideal solutions, effectively resolves multi-dimensional decision problems, providing clear ranking results. This makes the TOPSIS method highly effective in complex scenarios, applicable to decision analysis across various fields.

III. I**t is easy to implement and widely applicable**. The computational process of TOPSIS is relatively simple, making it easy to understand and execute. Together, they create a method that can be employed in complex system evaluations, such as in education or technology assessments, and can be easily implemented using common computational tools, making it practical for real-world applications. Double-Valued Neutrosophic Sets (DVNSs) [4] have been employed to represent fuzzy data during the quality evaluation process.

DVNSs offer significant advantages in evaluating the effectiveness of multimedia-based college English teaching.

I. First, they handle uncertainty and ambiguity, accurately representing fuzzy data in the evaluation process.

II. Second, DVNS simultaneously considers truth, indeterminacy, and falsity, providing more comprehensive evaluation results.

III. Lastly, DVNS is flexible and applicable to complex evaluation scenarios, assisting decision-makers in making more rational judgments when faced with uncertainty and ambiguous information.

In this study, we propose the DVNN-TOPSIS approach to solve MADM problems with DVNSs. Finally, a numerical study on the quality evaluation of smart classroom teaching for English majors is presented to validate the effectiveness of the DVNN-TOPSIS model.

1.2 Organization of this study

The structure of this paper is as follows: Section 2 introduces DVNSs. In Section 3, the DVNN-TOPSIS method, incorporating entropy, is proposed within the DVNS framework. Section 4 presents a case study illustrating the quality evaluation of smart classroom teaching for English majors, accompanied by a comparative analysis. Finally, Section 5 offers concluding remarks.

2. Literature review

MADM refers to a class of decision-making methods used to evaluate and select among multiple alternatives based on several attributes or criteria [5, 6]. It is widely applied in complex decision-making scenarios such as project evaluation, supplier selection, and investment decisions, assisting decision-makers in making optimal choices when faced with multidimensional information [7, 8]. The core of MADM lies in how to manage the importance of various attributes and the performance of alternatives under different attributes [9, 10]. First, decision problems typically involve multiple attributes (or criteria) that need to be considered, which can be either quantitative or qualitative. Second, different attributes may carry different levels of importance, so each attribute needs to be assigned a weight to reflect its relative significance in the decision-making process. Several methods are commonly used in MADM, including TOPSIS [3] and MCDM [11]. TOPSIS [3] ranks alternatives by calculating their distances from the ideal and negative ideal solutions. One key advantage of MADM is its flexibility, as it can handle different types of information (such as quantitative and qualitative data) and incorporate the subjective preferences of decision-makers. However, MADM also faces challenges, especially when dealing with a large number of attributes or conflicting opinions among decision-makers, which can increase the complexity of the decision-making process. In summary, MADM provides a systematic decision-making approach, helping decision-makers make rational choices in complex, multi-dimensional environments. In 1986, Atanassov [12] developed the intuitionistic fuzzy sets, incorporating hesitation into the existing membership and non-membership degrees. Later, Kandasamy [4] introduced Double-Valued Neutrosophic Sets (DVNSs) to enhance the representation of fuzziness with help of Neutrosophic Sets [13-15].

The evaluation of multimedia-based college English teaching aims to comprehensively assess the impact of multimedia technology on the teaching process and learning outcomes. By incorporating multimedia, the traditional teaching model has been transformed, making the classroom more engaging and flexible. Multimedia allows teachers to present content in a more vivid manner, which significantly improves students' attention and motivation to learn. Additionally, the instant feedback and interactive features provided by multimedia enhance

communication and interaction between teachers and students, optimizing the dynamic feedback mechanism of the classroom. Multimedia teaching also offers students more opportunities for self-directed learning. With access to various online resources, students can engage in extracurricular study and review, reinforcing the content learned in class. Moreover, the use of multimedia broadens the channels through which knowledge is conveyed, exposing students to diverse language contexts and cultural backgrounds, thus improving their practical language skills. However, despite the many advantages of multimedia technology in teaching, evaluating its effectiveness requires considering its alignment with teaching objectives and the potential challenges or distractions it may introduce into the learning process. Ultimately, the improvement in teaching outcomes depends not only on the use of technology but also on how effectively it is integrated into the overall instructional design. Tang and Wu [16] explored how to combine multimedia teaching with differentiated teaching based on multiple intelligence theory to improve English learning efficiency in independent colleges and found that this combination effectively enhanced students' English proficiency in such institutions. Cui [17] examined how to create a good psychological environment in English classrooms under multimedia teaching, emphasizing its importance in improving teaching outcomes and suggesting relevant strategies. Liu and Niu [18] proposed optimizing multimedia teaching modes in college English based on constructivist theory. They argued that students are active constructors of knowledge, and teachers should promote autonomous learning through contextual teaching and collaborative activities. Li [19] pointed out that while multimedia teaching makes English classes more dynamic and effective, challenges remain in integrating it with traditional teaching methods. Wang [20] explored the application of metacognitive theory in network-based multimedia teaching, suggesting that metacognitive strategies help students monitor and regulate their learning, thereby improving outcomes. Liu [21] proposed combining traditional recitation strategies with multimedia teaching to optimize English instruction, particularly enhancing language retention. Zhang [22] studied innovative strategies for multimedia teaching in college English, highlighting that multimedia enhances student engagement and improves teaching efficiency but also poses challenges related to technology and teacher competence. Dai [23] analyzed the application of multimedia-based learning apps, using the "Gaci APP" as an example, and suggested that such tools can address shortcomings in traditional teaching by offering innovative features that improve learning outcomes. Ling [24] examined the reform of English teaching modes in the context of multimedia, arguing that multimedia technology can enrich teaching content, optimize the environment, and improve overall teaching quality. Gao [25] discussed the necessity of reforming college English teaching in the multimedia network environment, proposing innovative teaching methods to meet the modern demands of English education. Finally, Wang [26] analyzed the innovative paths for college English teaching from the perspective of new media technologies, suggesting that such technologies can drive teaching reforms and improve students' comprehensive English abilities.

3. Preliminaries

Kandasamy [4] put forward the DVNSs.

Definition 2 [4]. The DVNSs is put forward:

$$DA=\left\{\left(x,DT_A(x),DIT_A(x),DIF_A(x),DF_A(x)\right)\middle|x\in X\right\} \quad (1)$$

with $DT_A(x)$ is truth-membership, $DIT_A(x)$ is listed as indeterminacy leaning for truth-membership, $DIF_A(x)$ is listed as indeterminacy leaning for falsity-membership indeterminacy-membership, $DF_A(x)$ is listed as falsity-membership, $DT_A(x),DIT_A(x),DIF_A(x),DF_A(x)\in[0,1]$, $0\le DT_A(x)+DIT_A(x)+DIF_A(x)+DF_A(x)\le 4$.

The DVNN is listed as: $DA=\left(DT_A,DIT_A,DIF_A,DF_A\right)$, $DT_A,DIT_A,DIF_A,DF_A\in[0,1]$, $0\le DT_A+DIT_A+DIF_A+DF_A\le 4$.

Definition 2. Let $DA=\left(DT_A,DIT_A,DIF_A,DF_A\right)$, the score value is constructed:

$$DSV(DA)=\frac{\left(2+DT_A+DIT_A-DIF_A-DF_A\right)}{4},\ DSV(DA)\in[0,1]. \quad (2)$$

Definition 3. Let $DA=\left(DT_A,DIT_A,DIF_A,DF_A\right)$, the accuracy value is constructed:

$$DAV(DA)=\frac{\left(DT_A+DIT_A+DIF_A+DF_A\right)}{4},\ DAV(DA)\in[0,1]\ . \quad (3)$$

The order between two DVNNs is put forward.

Definition 4. Let $DA=\left(DT_A,DIT_A,DIF_A,DF_A\right)$ and $DB=\left(DT_B,DIT_B,DIF_B,DF_B\right)$, let $DSV(DA)=\frac{\left(2+DT_A+DIT_A-DIF_A-DF_A\right)}{4}$ and $DSV(DB)=\frac{\left(2+DT_B+DIT_B-DIF_B-DF_B\right)}{4}$, and let $DAV(DA)=\frac{\left(DT_A+DIT_A+DIF_A+DF_A\right)}{4}$ and $DAV(DB)=\frac{\left(DT_B+DIT_B+DIF_B+DF_B\right)}{4}$, then if $DSV(DA)<DSV(DB)$, $DA<DB$; if $DSV(DA)=DSV(DB)$, Then (1)if $DAV(DA)=DAV(DB)$, $DA=DB$; (2) if $DAV(DA)<DAV(DB)$, $DA<DB$.

Definition 5[4]. $DA=\left(DT_A,DIT_A,DIF_A,DF_A\right)$, $DB=\left(DT_B,DIT_B,DIF_B,DF_B\right)$, the operations are constructed:

(1) $DA\oplus DB=\left(DT_A+DT_B-DT_ADT_B,DIT_A+DIT_B-DIT_ADIT_B,DIF_ADIF_B,DF_ADF_B\right)$;

(2) $DA\otimes DB=\left(DT_ADT_B,DIT_ADIT_B,DIF_A+DIF_B-DIF_ADIF_B,DF_A+DF_B-DF_ADF_B\right)$;

(3) $\lambda DA=\left(1-\left(1-DT_A\right)^{\lambda},1-\left(1-DIT_A\right)^{\lambda},\left(DIF_A\right)^{\lambda},\left(DF_A\right)^{\lambda}\right),\lambda>0$;

(4) $\left(DA\right)^{\lambda}=\left(\left(DT_A\right)^{\lambda},\left(DIT_A\right)^{\lambda},1-\left(1-DIF_A\right)^{\lambda},1-\left(1-DF_A\right)^{\lambda}\right),\lambda>0.$

Definition 6[4]. Let $DA=\left(DT_A, DIT_A, DIF_A, DF_A\right)$ and $DB=\left(DT_B, DIT_B, DIF_B, DF_B\right)$, then the normalized Euclidean distance between $DA=\left(DT_A, DIT_A, DIF_A, DF_A\right)$ and $DB=\left(DT_B, DIT_B, DIF_B, DF_B\right)$ is:

$$ED\left(DA, DB\right)=\sqrt{\frac{1}{4}\left(\begin{array}{l}\left|DT_A-DT_B\right|^2+\left|DIT_A-DIT_B\right|^2 \\ +\left|DIF_A-DIF_B\right|^2+\left|DF_A-DF_B\right|^2\end{array}\right)} \tag{4}$$

4. DVNN-TOPSIS approach

In MCDM, several alternatives can be assessed using number of criteria. MCDM can support the experts in the decision-making process. There are decision making issues that have several conflict criteria. So, the TOPSIS method used to rank alternatives by using the positive ideal solution (PIS) and negative ideal solution (NIS). Figure 1 shows the framework of the proposed method. The steps of the neutrosophic TOPSIS method include as follows:

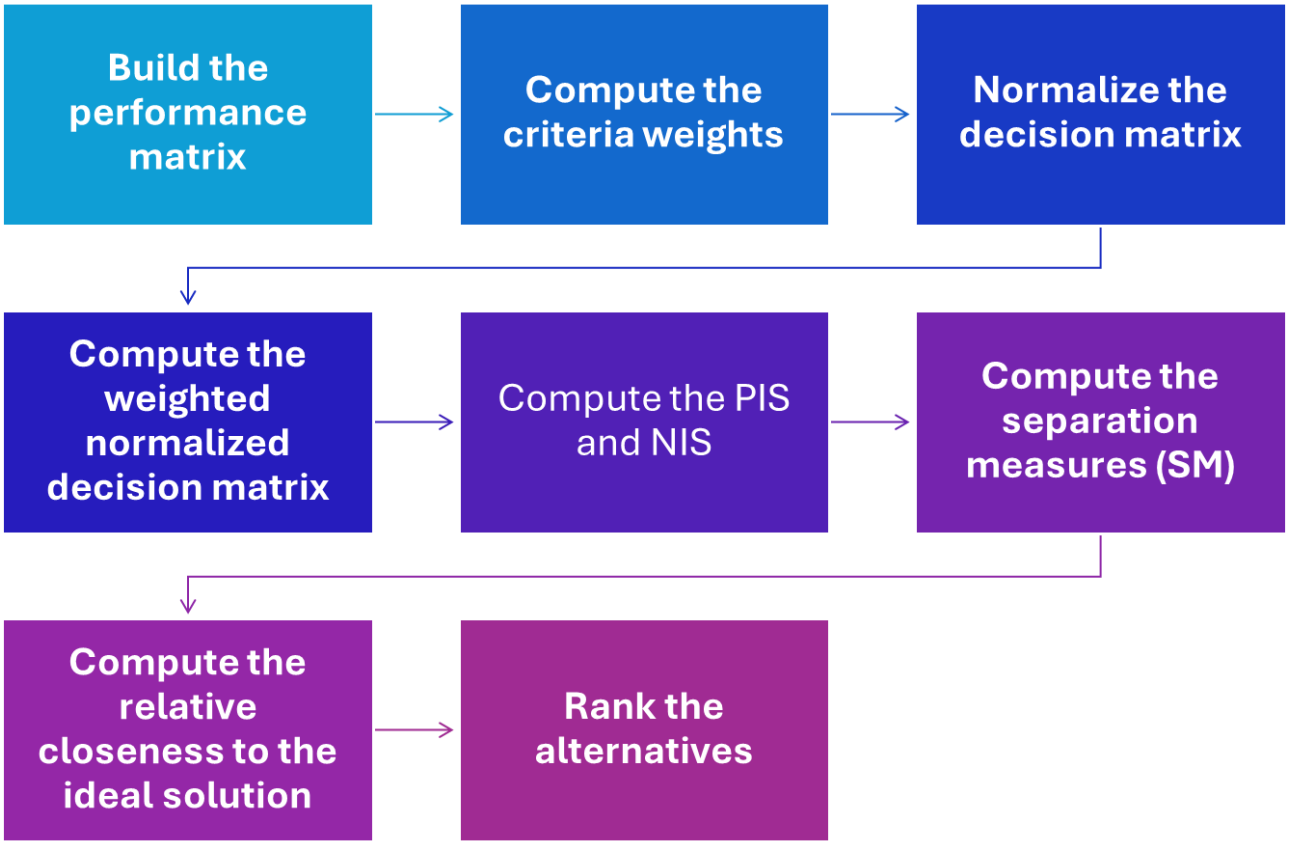

Figure 1. The steps of the TOPSIS method.

A. Build the performance matrix.

The performance matrix between criteria and alternatives $\boldsymbol{F_{ij}}$ where i refers to the number of alternatives and j refers to the number of criteria.

B. Compute the criteria weights.

The criteria weights are computed by using the average method.

C. Normalize the decision matrix.

The normalized performance matrix can be computed as:

$$\boldsymbol{u_{ij} = \frac{F_{ij}}{\sqrt{\sum_{j=1}^{m}(F_{ij})^2}},\ \ j = 1, 2, 3, \ldots n; i = 1, 2, \ldots, m}$$

(5)

D. Compute the weighted normalized decision matrix.

The criteria weights are multiplied by the normalized decision matrix to obtain the weighted normalized decision matrix such as:

$$\boldsymbol{r_{ij} = w_j * u_{ij}} \tag{6}$$

E. Compute the PIS and NIS.

$$\boldsymbol{B^+ = \{B_1^+, \ldots, B_n^+\} = \left\{\left(\max_i r_{ij}, j \in J\right)\left(\min_i r_{ij}, j \in J^*\right)\right\}}$$

(7)

$$\boldsymbol{B^- = \{B_1^-, \ldots, B_n^-\} = \left\{\left(\min_i r_{ij}, j \in J\right)\left(\max_i r_{ij}, j \in J^*\right)\right\}} \tag{8}$$

Where $\boldsymbol{J^*}$ refers to the cost criteria and $\boldsymbol{J}$ refers to the beneficial criteria.

F. Compute the separation measures (SM).

We compute the SM from PIS and NIS as:

$$\boldsymbol{d_i^+ = \left\{\sum_{j=1}^{n}\left(r_{ij} - r_j^+\right)^2\right\}^{\frac{1}{2}}} \tag{9}$$

$$\boldsymbol{d_i^-} = \left\{\sum_{j=1}^{n}\left(\boldsymbol{r_{ij}} - \boldsymbol{r_j^-}\right)^2\right\}^{\frac{1}{2}} \tag{10}$$

G. Compute the relative closeness to the ideal solution

$$\boldsymbol{T_i} = \frac{\boldsymbol{d_i^-}}{\boldsymbol{d_i^+ + d_i^-}} \tag{11}$$

H. Rank the alternatives.

Rank the best alternatives based on $\boldsymbol{T_i}$ in descending order.

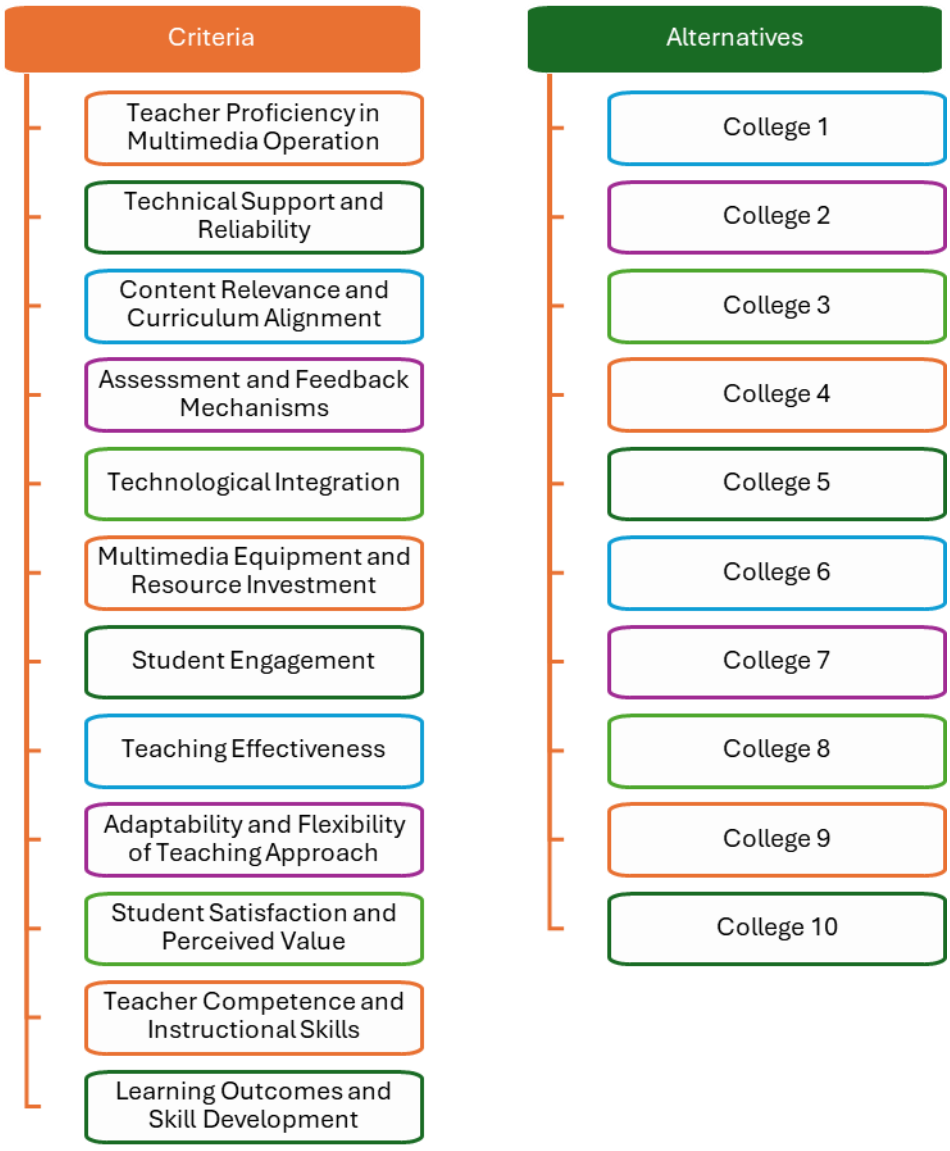

Figure 2. The criteria and alternatives.

5. Data analysis

This section shows the results of the proposed method under the neutrosophic sets.

5.1. Data analysis with quality evaluation of smart classroom teaching for English majors in universities

The evaluation of smart classroom teaching quality for college English is a systematic process designed to assess the effectiveness of multimedia technology in English instruction. With the rapid advancement of information technology, multimedia teaching has become a key tool in college English education, enriching content, enhancing classroom interaction, and stimulating students' interest in learning. However, to accurately and comprehensively evaluate its true effectiveness, a well-structured evaluation system is essential. At the core of evaluating smart classroom teaching quality is the establishment of clear and reasonable criteria. Common evaluation dimensions include the quality of teaching content (such as its depth and practicality), the innovation in teaching methods (including the effective use of multimedia and variety in instructional approaches), student engagement (such as participation in classroom activities and self-directed learning), resource utilization efficiency (such as the appropriate use of teaching materials, videos, and audio resources), teachers' instructional abilities (including pacing, communication, and classroom management), and students' learning outcomes (such as knowledge retention and language skill improvement). The selection of evaluation methods is equally critical. Common approaches include questionnaires, classroom observation, student feedback, and performance analysis. Questionnaires can capture students' perceptions and opinions on multimedia teaching, providing subjective insights. Classroom observation assesses how multimedia is practically implemented in teaching through both teacher behavior and student engagement. Additionally, analyzing students' exam performance offers a quantitative measure of multimedia's impact on learning outcomes. In practice, evaluation should blend both qualitative and quantitative methods. For instance, well-designed scoring standards can convert subjective student feedback into measurable data, while statistical analysis of academic performance offers an objective assessment of multimedia’s effects. Finally, the evaluation results should be shared with teachers and educational administrators, offering insights into the strengths and areas for improvement in current teaching practices. Teachers can use these results to refine their content and methods, optimizing their instructional design to further improve teaching quality. In conclusion, evaluating smart classroom teaching quality for college English is a comprehensive and systematic process. The goal is to apply scientific and effective evaluation methods to fully understand the impact of multimedia teaching, providing valuable insights for both educational decision-making and instructional enhancement. The quality evaluation of smart classroom teaching for English majors in universities is MADM.

A. We built the performance matrix between criteria and alternatives by using double valued neitrosophic number. Then we used the score function to obtain single number and combined into single matrix. We used 12 criteria and 10 alternatives as shown in Figure 2. Three experts are involved to evaluate the criteria and alternatives.

B. We compute the criteria weighs as shown in Figure 3. Criterion 8 has the highest weight and criterion 10 has the lowest weight.

C. Eq. (5) is used to normalize the decision matrix as shown in Table 1.

D. Eq. (6) is used to compute the weighted normalized decision matrix as shown in Table 2.

E. Eq. (7,8) are used to compute the PIS and NIS.

F. Eqs. (9 and 10) are used to compute the SM as shown in Table 3.

G. Eq. (11) is used to compute the relative closeness to the ideal solution

H. Rank the alternatives as shown in Figure 4.

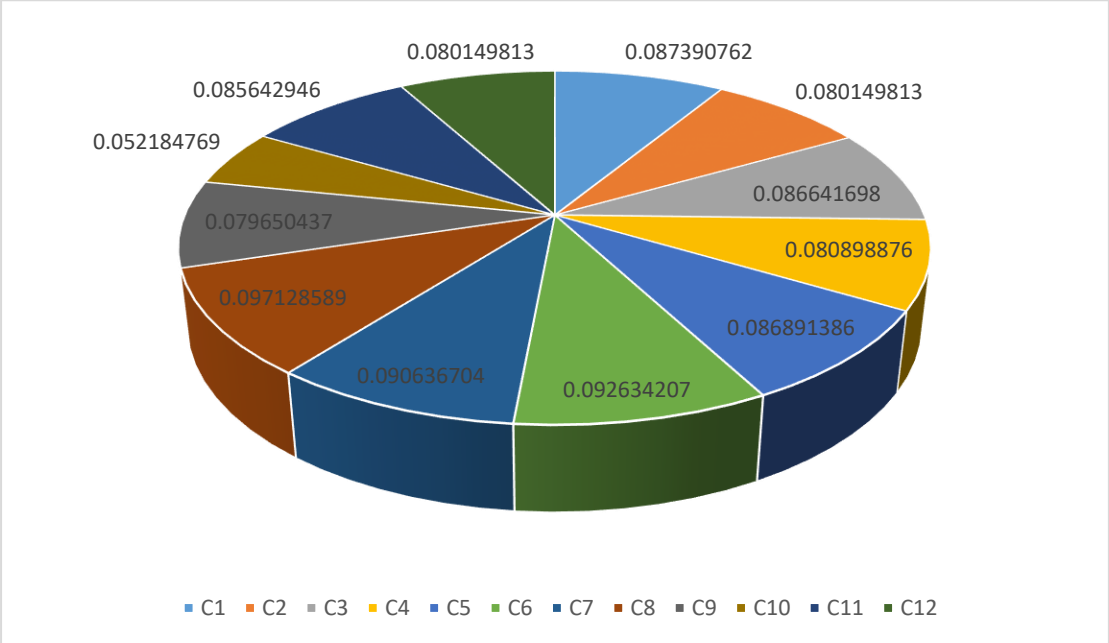

Figure 3. The criteria weights.

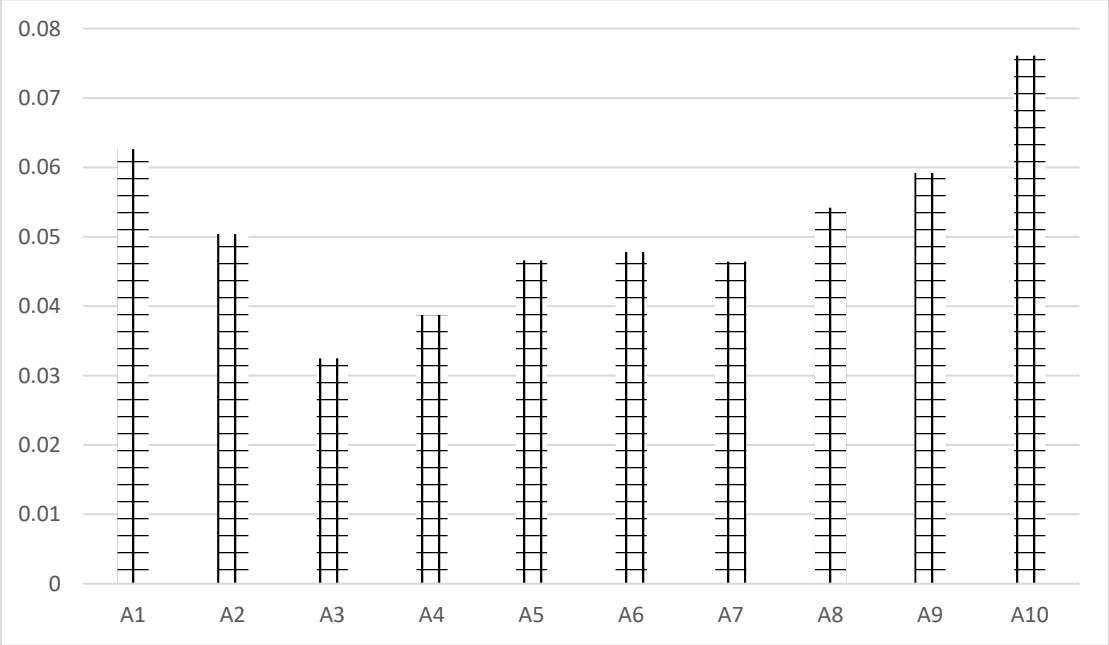

Figure 4. The rank of alternatives.

Table 1. The normalized decision matrix

	C_1	C_2	C_3	C_4	C_5	C_6	C_7	C_8	C_9	C_{10}	C_{11}	C_{12}
A_1	0.346043932	0.51032	0.30729	0.386478	0.35525	0.156332	0.123445	0.191364	0.027586	0.038922	0.488251	0.359253
A_2	0.354484028	0.24571	0.324849	0.046009	0.195388	0.436085	0.320958	0.398675	0.422981	0.428138	0.248408	0.479003
A_3	0.362924123	0.349664	0.30729	0.322065	0.310844	0.419629	0.427944	0.29502	0.321833	0.518956	0.334066	0.322406
A_4	0.295403356	0.330763	0.359968	0.441689	0.390775	0.279752	0.222202	0.310967	0.321833	0.441112	0.282671	0.442157
A_5	0.405124603	0.274061	0.482884	0.220844	0.195388	0.287981	0.419714	0.382728	0.285052	0.337321	0.188448	0.331618
A_6	0.337603836	0.321313	0.28973	0.358872	0.301963	0.353805	0.296269	0.29502	0.128733	0.285426	0.385461	0.193444
A_7	0.346043932	0.302412	0.30729	0.294459	0.2842	0.329121	0.213972	0.350834	0.3862	0.129739	0.334066	0.28556
A_8	0.354484028	0.24571	0.158035	0.285257	0.301963	0.287981	0.320958	0.310967	0.358614	0.090817	0.334066	0.239502
A_9	0.059080671	0.311862	0.324849	0.377276	0.381894	0.197472	0.197512	0.223258	0.285052	0.350295	0.316935	0.221078
A_{10}	0.092841055	0.141756	0.184374	0.24845	0.373013	0.304437	0.444403	0.342861	0.395395	0.090817	0.025697	0.082904

Table 2. The weighted normalized decision matrix

	C_1	C_2	C_3	C_4	C_5	C_6	C_7	C_8	C_9	C_{10}	C_{11}	C_{12}
A_1	0.030241043	0.040902	0.026624	0.031266	0.030868	0.014482	0.011189	0.018587	0.002197	0.002031	0.041815	0.028794
A_2	0.030978629	0.019694	0.028145	0.003722	0.016978	0.040396	0.029091	0.038723	0.033691	0.022342	0.021274	0.038392
A_3	0.031716216	0.028026	0.026624	0.026055	0.027001	0.038872	0.038787	0.028655	0.025634	0.027082	0.02861	0.025841
A_4	0.025815524	0.026511	0.031188	0.035732	0.033955	0.025915	0.02014	0.030204	0.025634	0.023019	0.024209	0.035439
A_5	0.035404148	0.021966	0.041838	0.017866	0.016978	0.026677	0.038041	0.037174	0.022705	0.017603	0.016139	0.026579
A_6	0.029503456	0.025753	0.025103	0.029032	0.026238	0.032774	0.026853	0.028655	0.010254	0.014895	0.033012	0.015504
A_7	0.030241043	0.024238	0.026624	0.023821	0.024695	0.030488	0.019394	0.034076	0.030761	0.00677	0.02861	0.022888
A_8	0.030978629	0.019694	0.013692	0.023077	0.026238	0.026677	0.029091	0.030204	0.028564	0.004739	0.02861	0.019196

A_9	0.005163105	0.024996	0.028145	0.030521	0.033183	0.018293	0.017902	0.021685	0.022705	0.01828	0.027143	0.017719
A_{10}	0.008113 45	0.011362	0.015974	0.020099	0.032412	0.028201	0.040279	0.033302	0.031493	0.004739	0.002201	0.006645

Table 3. The SM values.

	C_1	C_2	C_3	C_4	C_5	C_6	C_7	C_8	C_9	C_{10}	C_{11}	C_{12}
A_1	2.66577E-05	0	0.000231	1.99E-05	9.53E-06	0.000672	0.000846	0.000405	0.000992	0.000628	0	9.21E-05
A_2	1.95852E-05	0.00045	0.000187	0.001025	0.000288	0	0.000125	0	0	2.25E-05	0.000422	0
A_3	1.36008E-05	0.000166	0.000231	9.37E-05	4.82E-05	2.32E-06	2.23E-06	0.000101	6.49E-05	0	0.000174	0.000158
A_4	9.19417E-05	0.000207	0.000113	0	0	0.00021	0.000406	7.26E-05	6.49E-05	1.65E-05	0.00031	8.72E-06
A_5	0	0.000359	0	0.000319	0.000288	0.000188	5.01E-06	2.4E-06	0.000121	8.98E-05	0.000659	0.00014
A_6	3.48182E-05	0.000229	0.00028	4.49E-05	5.96E-05	5.81E-05	0.00018	0.000101	0.000549	0.000149	7.75E-05	0.000524
A_7	2.66577E-05	0.000278	0.000231	0.000142	8.58E-05	9.82E-05	0.000436	2.16E-05	8.58E-06	0.000413	0.000174	0.00024
A_8	1.95852E-05	0.00045	0.000792	0.00016	5.96E-05	0.000188	0.000125	7.26E-05	2.63E-05	0.000499	0.000174	0.000368
A_9	0.000914521	0.000253	0.000187	2.72E-05	5.96E-07	0.000489	0.000501	0.00029	0.000121	7.75E-05	0.000215	0.000427
A_{10}	0.000744782	0.000873	0.000669	0.000244	2.38E-06	0.000149	0	2.94E-05	4.83E-06	0.000499	0.001569	0.001008

The three advantages of DVNN-TOPSIS approach for evaluating the quality of smart classroom teaching for English majors are outlined:

(1) Enhanced ability to handle fuzzy information: Based on DVNSs, this method provides a more precise way to represent uncertainty and fuzziness. Compared to traditional methods, DVNSs can handle membership, non-membership, and hesitation information simultaneously, making decision-making in fuzzy environments more comprehensive and reasonable.

(2)Integration of the strengths of TOPSIS: The DVNN -TOPSIS method combines the strengths of both TOPSIS. TOPSIS evaluates alternatives based on their distances from ideal and negative-ideal solutions. The combination leads to more robust and rational results.

(3) High adaptability to complex decision environments: This method is particularly suited for multi-attribute, multi-criteria decision-making scenarios, such as smart classroom teaching evaluations. It can process fuzzy information under various attributes and preferences, producing reasonable results even in complex environments, making it highly adaptable and widely applicable.

5. Conclusion

The evaluation of smart classroom teaching quality in college English is a systematic process aimed at assessing the impact of multimedia technology in teaching. The evaluation involves multiple dimensions, including the richness and practicality of teaching content, the innovation of teaching methods, student engagement, and the efficiency of resource utilization. By combining qualitative and quantitative evaluation

methods, such as questionnaires, classroom observation, and student performance analysis, it provides a comprehensive reflection of the impact of multimedia teaching on student learning outcomes. Additionally, the evaluation must consider the investment in multimedia equipment and the teacher's technical proficiency to ensure the efficient use and optimal allocation of teaching resources. Ultimately, the evaluation of teaching effectiveness provides scientific evidence for improving instructional design and enhancing teaching quality, contributing to the continuous development of college English education. The quality evaluation of smart classroom teaching for English majors in universities is MADM. DVNSs are used as an effective tool for representing fuzzy data in the quality evaluation of smart classroom teaching for English majors in universities. In this study, the DVNN-TOPSIS approach is proposed to handle MADM under DVNSs. Finally, a numerical study on the quality evaluation of smart classroom teaching for English majors is conducted to validate the DVNN-TOPSIS model.

Based on the content of this study, future research can delve into the following three directions: (1) Expanding the application areas of the decision model: Although the DVNN-TOPSIS method performed well in evaluating the quality of smart classroom teaching for English majors, its application scope can be further expanded. Future studies could apply this model to other disciplines' smart teaching quality evaluations, corporate management decision-making, healthcare optimization, and more, to verify its applicability and effectiveness in different contexts. This would provide richer data support for the model's use across a wide range of fields. (2) Incorporating additional uncertainty-handling methods: While DVNSs are effective at handling fuzzy information, more complex decision environments may involve even greater uncertainty or fuzziness. Future research could consider integrating other uncertainty-handling methods, such as interval numbers, grey system theory, or stochastic fuzzy sets, to further enhance the model’s ability to process complex information. These extended methods would improve the model's robustness in dynamic and uncertain environments. (3) Optimizing computational efficiency and algorithm performance: As the scale and complexity of decision problems increase, computational efficiency and performance become critical issues. Future studies could focus on improving the algorithm design of the DVNN-TOPSIS method, optimizing its computational complexity, and enhancing its ability to handle large-scale datasets. Additionally, leveraging machine learning and artificial intelligence techniques to develop intelligent optimization algorithms could further improve the method’s computational efficiency and decision-making speed. By pursuing these research directions, the DVNN-TOPSIS method can be further enhanced in terms of its broad applicability and decision-support capabilities, providing more comprehensive and efficient solutions for complex decision-making problems.

References

[1] L. Gomes, M. Lima, Todim: Basics and apllication to multicriteria ranking of projects with environmental impacts, Foundations of Control Engineering, 16 (1991) 113-127.

[2] L.F.A.M. Gomes, M.M.P.P. Lima, From modeling individual preferences to multicriteria ranking of discrete alternatives: A look at prospect theory and the additive difference model, Foundations of Computing and Decision Sciences, 17 (1992) 171-184.

[3] Y.-J. Lai, T.-Y. Liu, C.-L. Hwang, Topsis for modm, European Journal of Operational Research, 76 (1994) 486-500.

[4] I. Kandasamy, Double-valued neutrosophic sets, their minimum spanning trees, and clustering algorithm, Journal of Intelligent Systems, 27 (2018) 163-182.

[5] M. Mohamed, A. Elsayed, A novel multi-criteria decision making approach based on bipolar neutrosophic set for evaluating financial markets in egypt, Multicriteria Algorithms with Applications, 5 (2024) 1-17.

[6] A. M.Ali, M. Muthuswamy, Neutrosophic multi-criteria decision-making framework for sustainable evaluation of power production systems in renewable energy sources, Sustainable Machine Intelligence Journal, 4 (2023) (3):1-10.

[7] A.A. Salama, M.Y. Shams, S. Elseuofi, H.E. Khalid, Exploring neutrosophic numeral system algorithms for handling uncertainty and ambiguity in numerical data: An overview and future directions, Neutrosophic Sets and Systems, 65 (2024) 253-295.

[8] A.A. Salama, H.E. Khalid, A.G. Mabrouk, Unveiling uncertainty: Neutrosophic set-based algorithms for robust decision-making, Neutrosophic Sets and Systems, 72 (2024) 222-243.

[9] M. Jdid, F. Smarandache, Neutrosophic vision of the expected opportunity loss criterion (neol) decision making under risk, Neutrosophic Sets and Systems, 65 (2024) 110-118.

[10] S.G. Quek, H. Garg, G. Selvachandran, M. Palanikumar, K. Arulmozhi, F. Smarandache, Vikor and topsis framework with a truthful-distance measure for the (t, s)-regulated interval-valued neutrosophic soft set, Soft Computing, (2023) 27.

[11] L. Gomes, L.A.D. Rangel, An application of the todim method to the multicriteria rental evaluation of residential properties, European Journal of Operational Research, 193 (2009) 204-211.

[12] K.T. Atanassov, More on intuitionistic fuzzy-sets, Fuzzy Sets and Systems, 33 (1989) 37-45.

[13] F. Smarandache, Foundation of revolutionary topologies: An overview, examples, trend analysis, research issues, challenges, and future directions, Neutrosophic Systems with Applications, 13 (2024) 45-66.

[14] F.A. Smarandache, Unifying field in logics. Neutrosophy: Neutrosophic probability, set and logic, American Research Press, Rehoboth, 1999.

[15] H. Wang, F. Smarandache, Y. Zhang, R. Sunderraman, Single valued neutrosophic sets,

Infinite Study, 12 (2010) 20110.

[16] G. Tang, L. Wu, Exploration of college english teaching reform in independent colleges: The combination of multimedia teaching and differentiated teaching based on multiple intelligence theory, Contemporary Educational Theory and Practice, 6 (2014) 110-111.

[17] Y. Cui, How to create a good psychological environment in college english classroom in the context of multimedia teaching, Journal of Mudanjiang University, 24 (2015) 184-185.

[18] M. Liu, Y. Niu, Exploration of college english multimedia teaching mode based on constructivist theory, Education Modernization, 3 (2016) 101-103.

[19] J. Li, Research on college english multimedia teaching and cooperation, Overseas English, (2017) 65-66.

[20] L. Wang, Exploration of the application of metacognitive theory in college english network multimedia teaching, Modern Communication, (2018) 191-192.

[21] P. Liu, Optimization of recitation strategy in college english multimedia teaching, Campus English, (2018) 37-38.

[22] M. Zhang, Innovative strategies for college english multimedia teaching, Overseas English, (2019) 117-118.

[23] J. Dai, Application research of app based on multimedia teaching in college english teaching: Taking gaci app as an example, Happy Reading, (2022) 91-93.

[24] J. Ling, Reform of college english teaching mode in the context of multimedia, Journal of Hubei Open Vocational College, 36 (2023) 185-187.

[25] J. Gao, Reflections on college english teaching reform in the multimedia network environment, Overseas English, (2023) 141-143.

[26] C. Wang, Research and practice of college english curriculum teaching in the perspective of new media, Modern Commerce and Industry, 45 (2024) 79-81.

Received: July 29, 2024. Accepted: Oct 28, 2024

NSS
Neutrosophic Sets and Systems, Vol. 76, 2025
University of New Mexico

Cross-Entropy Method Adapted for Evaluating the Teaching Quality of University Physical Education Utilizing 2-Tuple Linguistic Neutrosophic Sets

Mengjun Wu[1]*, Yonghui Feng[2]

[1]Guizhou Education University, Guiyang, 550018, Guizhou, China

[2]Liaodong University, Dandong, 118001, Liaoning, China(Yhms999@163.com)

*Corresponding author Email: wumengjun@gznc.edu.cn

Abstract: The evaluation of university physical education teaching quality helps measure the actual effectiveness of the courses and ensures the achievement of teaching objectives. Through evaluation, schools can identify deficiencies in teaching and make improvements, enhancing students' physical fitness and health. Additionally, evaluation provides data support for teaching reforms, aiding in curriculum optimization and strengthening faculty, thereby promoting the comprehensive development of physical education and fostering students' lifelong awareness of fitness and healthy lifestyles. The teaching quality evaluation of university physical education adopts the multiple-attribute group decision-making (MAGDM) approach. Currently, cross-entropy (CE) model was constructed to handle the MAGDM. To capture uncertain data for the teaching quality evaluation of university physical education, 2-tuple linguistic neutrosophic numbers (2TLNNs) are administrated as valuable decision tool. This study constructs the 2TLNN cross-entropy (2TLNN-CE) technique, which combines traditional cross-entropy and 2TLNSs. The 2TLNN-CE technique is applied to MAGDM in the context of teaching quality evaluation. Furthermore, numerical example for the teaching quality evaluation of university physical education is presented, and comparative analysis is administrated to validate the advantages of 2TLNN-CE technique. The contributions of this study are summarized:(1) Extension of cross-entropy technique to 2TLNSs, enabling its application in uncertain decision scenarios; (2) Introduction of 2TLNN-CE technique for MAGDM, specifically tailored for teaching quality evaluation; (3) Illustration of 2TLNN-CE technique through numerical example of teaching quality evaluation of university physical education accompanied by comparative analysis to highlight its benefits.

Keywords: Multiple-attribute group decision-making (MAGDM); 2TLNSs; 2TLNN-CE model; teaching quality evaluation

1. Introduction

The quality of university physical education teaching is a crucial standard for measuring the effectiveness of sports courses in higher education, directly impacting students' physical fitness, athletic skills, and health awareness. High-quality physical education requires that the teaching content meets the actual needs of students while also being scientific and systematic, ensuring that students can comprehensively grasp fundamental sports skills and theoretical knowledge. Additionally, diverse and flexible teaching methods are key; teachers should adopt personalized approaches based on students' physical conditions and interests to stimulate their enthusiasm for sports and enhance classroom participation. The quality of teaching is also reflected in student learning outcomes. Through regular assessments and tests, schools can track students' progress in physical education, including improvements in physical fitness, health levels, and mastery of sports skills. Quality physical education not only helps students develop good exercise habits during their time at university but also fosters lifelong awareness of physical activity, promoting a healthy lifestyle. Therefore, improving the quality of university physical education is essential for enhancing overall educational standards and plays a critical role in students' comprehensive development. The earliest research was conducted by Liang [1], who explored how to improve the teaching quality of university martial arts courses through a systematic and standardized teaching model. Liang [1] suggested that martial arts courses not only enhance students' physical fitness but also foster lifelong exercise habits, providing recommendations for the role of universities in promoting martial arts. Following this, Wang and Yan [2] studied the teaching efficacy of university physical education teachers and its impact on teaching quality. They found through surveys that the higher the teachers' sense of efficacy, the better the teaching quality, and proposed strategies to enhance teacher efficacy. Later, Zhang and He [3] proposed a reform plan to quantify and standardize the evaluation criteria for university physical education teaching quality. Their research showed that quantitative evaluation helps improve classroom teaching quality and increases the motivation of both teachers and students. In 2017, Zhou and Wu [4] constructed a satisfaction evaluation model to assess the quality of university physical education teaching. They used the Delphi method and the analytic hierarchy process to propose a satisfaction evaluation system composed of multiple indicators and verified its operability and reliability. Liu [5] pointed out that the deviation in modern university physical education quality evaluation standards is one of the reasons for the decline in students' physical fitness. He highlighted the issues in evaluating physical education quality and proposed strategies to improve classroom teaching. Following this, Wang, Ding and Zhang [6] studied the construction of an information-based teaching quality evaluation system, proposing a multi-level evaluation index system and verifying its scientific and practical applicability through actual courses. In 2020, Liu, Yin and Wang [7] established a university physical education quality assurance system, suggesting measures such as layered teaching, school-based curriculum development, and innovative teaching methods to enhance teaching quality. Their study

provided valuable insights for managing physical education. From the perspective of "students' core sports literacy," Zhao, Gong and Sheng [8] constructed a new classroom teaching quality evaluation system, adding a teaching reflection component and emphasizing the diversification and scientific nature of the evaluation system. In 2022, based on grey system theory and fuzzy evaluation, Zhou and Wang [9] proposed a new model for evaluating university physical education quality. They used the analytic hierarchy process to determine the weight of evaluation standards and suggested strategies to further improve teaching quality. Lastly, Ma [10] explored the standardization reform of university physical education teaching quality evaluation, emphasizing the importance of improving teaching quality through a scientific evaluation system and proposed specific measures for standardization reform.

The teaching quality evaluation of university physical education presents a MAGDM. To address this, the CE technique [11, 12] has been utilized as a means to manage MAGDM. In the context of teaching quality evaluation of university physical education, 2TLNSs [13] are administrated as valuable decision tool to handle uncertain information in light with neutrosophic sets [14-17]. While various techniques have been developed to optimize the traditional cross-entropy technique [18], there is a scarcity of methods that apply the entropy technique [19] and cross-entropy technique [18] to manage MAGDM using 2TLNSs. In this study, we propose the 2TLNN-CE approach, which combines the traditional CE approach along with 2TLNSs. The 2TLNN-CE approach is then applied to MAGDM for teaching quality evaluation of university physical education. To illustrate key advantages of proposed technique, numerical example concerning the teaching quality evaluation of university physical education is presented, accompanied by comparative analysis. The key contributions of this study are summarized: (1) Extension of cross-entropy technique to integrate with 2TLNSs, enhancing its applicability; (2) Development of the 2TLNN-CE technique for MAGDM using 2TLNSs; (3) Demonstration of the 2TLNN-CE technique through a specific numerical study on the teaching quality evaluation of university physical education, with comparisons made against existing techniques. (4) Comparative analysis confirms the effectiveness of 2TLNN-CE technique for teaching quality evaluation of university physical education.

To achieve this, the study follows a fundamental structure outlined: Sect. 2 provides the 2TLNSs. Sect. 3 presents the application of 2TLNN-CE technique for MAGDM. In Sect. 4, numerical example focusing on the teaching quality evaluation of university physical education is presented. Comparative analysis is administrated to further examine the results.

2. Preliminaries

Wang et al. [13] administrated the 2TLNSs.

Definition 1 [20, 21]. Let $ool = \{ool_1, ool_2, \ldots, ool_{oo}\}$ be LTSs. The label ool_i is linguistic variable, and ool is administrated:

$$ool=\begin{Bmatrix} ool_0=extremely\ poor, ool_1=very\ poor, ool_2=poor, ool_3=medium, \\ ool_4=good, ool_5=very\ good, ool_6=extremely\ good. \end{Bmatrix} \quad (1)$$

Definition 2[13]. Let $oos_j\left(j=1,2,3,\ldots,n\right)$ be 2TLSs. If $oos=\left\langle\left(ool_t,oo\xi\right),\left(ool_i,oo\psi\right),\left(ool_f,oo\zeta\right)\right\rangle$ is administrated for $ool_t,ool_i,ool_f\in ool$, $oo\xi,oo\psi,oo\zeta\in\left[-0.5,0.5\right)$, $\left(ool_t,oo\xi\right),\left(ool_i,oo\psi\right),\left(ool_f,oo\zeta\right)$ is the linguistic truth-membership, linguistic indeterminacy and linguistic falsity-membership, then the 2TLNSs are administrated:

$$oos_j=\left\langle\left(ool_{t_j},oo\xi_j\right),\left(ool_{i_j},oo\psi_j\right),\left(ool_{f_j},oo\zeta_j\right)\right\rangle \quad (2)$$

with condition $0\le\Delta^{-1}\left(ool_{t_j},oo\xi_j\right)\le oo$, $0\le\Delta^{-1}\left(ool_{i_j},oo\psi_j\right)\le oo$, $0\le\Delta^{-1}\left(ool_{f_j},oo\zeta_j\right)\le oo$, and $0\le\Delta^{-1}\left(ool_{t_j},oo\xi_j\right)+\Delta^{-1}\left(ool_{i_j},oo\psi_j\right)+\Delta^{-1}\left(ool_{f_j},oo\zeta_j\right)\le 3oo.$

Definition 3[13]. Let $oos=\left\langle\left(ool_t,oo\xi\right),\left(ool_i,oo\psi\right),\left(ool_f,oo\zeta\right)\right\rangle$, linguistic score function $LSF\left(oos\right)$ and linguistic accuracy function $LAF\left(o\delta\right)$ are $oos=\left\langle\left(ool_t,oo\xi\right),\left(ool_i,oo\psi\right),\left(ool_f,oo\zeta\right)\right\rangle$:

$$LSF\left(oos\right)=\frac{\left(2oo+\Delta^{-1}\left(ool_{t_j},oo\xi_j\right)-\Delta^{-1}\left(ool_{i_j},oo\psi_j\right)-\Delta^{-1}\left(ool_{f_j},oo\zeta_j\right)\right)}{3oo} \quad (3)$$

$$LAF\left(oos\right)=\frac{oo+\Delta^{-1}\left(ool_{t_j},oo\xi_j\right)-\Delta^{-1}\left(ool_{f_j},oo\zeta_j\right)}{3oo} \quad (4)$$

Definition 4[13]. Let $oos_1=\left\langle\left(ool_{t_1},oo\xi_1\right),\left(ool_{i_1},oo\psi_1\right),\left(ool_{f_1},oo\zeta_1\right)\right\rangle$, $oos_2=\left\langle\left(ool_{t_2},oo\xi_2\right),\left(ool_{i_2},oo\psi_2\right),\left(ool_{f_2},oo\zeta_2\right)\right\rangle$, then (1) If $LSF\left(oos_1\right)<LSF\left(oos_2\right)$, $oos_1<oos_2$; (2) If $LSF\left(oos_1\right)=LSF\left(oos_2\right), LAF\left(oos_1\right)<LAF\left(oos_2\right)$, $oos_1<oos_2$; (3)If $LSF\left(oos_1\right)=LSF\left(oos_2\right), LAF\left(oos_1\right)=LAF\left(oos_2\right), oos_1=oos_2$;

Definition 5[13]. Let $oos_1 = \left\langle \left(ool_{t_1}, oo\xi_1 \right), \left(ool_{i_1}, oo\psi_1 \right), \left(ool_{f_1}, oo\zeta_1 \right) \right\rangle$,

$oos_2 = \left\langle \left(ool_{t_2}, oo\xi_2 \right), \left(ool_{i_2}, oo\psi_2 \right), \left(ool_{f_2}, oo\zeta_2 \right) \right\rangle$,

$oos = \left\langle \left(ool_t, oo\xi \right), \left(ool_i, oo\psi \right), \left(ool_f, oo\zeta \right) \right\rangle$, then

$$oos_1 \oplus oos_2 = \left\{ \begin{array}{l} \Delta\left(oo\left(\dfrac{\Delta^{-1}\left(ool_{t_1}, oo\xi_1 \right)}{oo} + \dfrac{\Delta^{-1}\left(ool_{t_2}, oo\xi_2 \right)}{oo} - \dfrac{\Delta^{-1}\left(ool_{t_1}, oo\xi_1 \right)}{oo} \cdot \dfrac{\Delta^{-1}\left(ool_{t_2}, oo\xi_2 \right)}{oo} \right) \right), \\ \Delta\left(oo\left(\dfrac{\Delta^{-1}\left(ool_{i_1}, oo\psi_1 \right)}{oo} \cdot \dfrac{\Delta^{-1}\left(ool_{i_2}, oo\psi_2 \right)}{oo} \right) \right), \\ \Delta\left(oo\left(\dfrac{\Delta^{-1}\left(ool_{f_1}, oo\zeta_1 \right)}{oo} \cdot \dfrac{\Delta^{-1}\left(ool_{f_2}, oo\zeta_2 \right)}{oo} \right) \right) \end{array} \right\};$$

$$oos_1 \otimes oos_2 = \left\{ \begin{array}{l} \Delta\left(oo\left(\dfrac{\Delta^{-1}\left(ool_{t_1}, oo\xi_1 \right)}{oo} \cdot \dfrac{\Delta^{-1}\left(ool_{t_2}, oo\xi_2 \right)}{oo} \right) \right), \\ \Delta\left(oo\left(\dfrac{\Delta^{-1}\left(ool_{i_1}, o\psi_1 \right)}{oo} + \dfrac{\Delta^{-1}\left(ool_{i_2}, oo\psi_2 \right)}{oo} - \dfrac{\Delta^{-1}\left(ool_{i_1}, oo\psi_1 \right)}{oo} \cdot \dfrac{\Delta^{-1}\left(ool_{i_2}, oo\psi_2 \right)}{oo} \right) \right), \\ \Delta\left(oo\left(\dfrac{\Delta^{-1}\left(ool_{f_1}, oo\zeta_1 \right)}{oo} + \dfrac{\Delta^{-1}\left(ool_{f_2}, oo\zeta_2 \right)}{oo} - \dfrac{\Delta^{-1}\left(ool_{f_1}, oo\zeta_1 \right)}{oo} \cdot \dfrac{\Delta^{-1}\left(ool_{f_2}, oo\zeta_2 \right)}{oo} \right) \right) \end{array} \right\};$$

$$\xi oos = \left\{ \begin{array}{l} \Delta\left(oo\left(1 - \left(1 - \dfrac{\Delta^{-1}\left(ool_t, oo\xi \right)}{oo} \right)^{\xi} \right) \right), \\ \Delta\left(oo\left(\dfrac{\Delta^{-1}\left(ool_i, oo\psi \right)}{oo} \right)^{\xi} \right), \Delta\left(oo\left(\dfrac{\Delta^{-1}\left(ool_f, oo\zeta \right)}{oo} \right)^{\xi} \right) \end{array} \right\}, \xi > 0;$$

$$oos^{\xi}=\left\{\begin{array}{l}\Delta\left(oo\left(\left(\frac{\Delta^{-1}\left(ool_t,oo\xi\right)}{oo}\right)^{\xi}\right)\right),\Delta\left(oo\left(1-\left(1-\left(\frac{\Delta^{-1}\left(ool_i,oo\psi\right)}{oo}\right)^{\xi}\right)\right)\right),\\ \Delta\left(oo\left(1-\left(1-\left(\frac{\Delta^{-1}\left(ool_f,oo\zeta\right)}{oo}\right)^{\xi}\right)\right)\right)\end{array}\right\},\xi>0.$$

Definition 6[13]. Let $oos_j=\left\langle\left(ool_{t_j},oo\xi_j\right),\left(ool_{i_j},oo\psi_j\right),\left(ool_{f_j},oo\zeta_j\right)\right\rangle$, the 2TLNNWG is:

$$\begin{aligned}&2\text{TLNNWG}\left(oos_1,oos_2,\ldots,oos_n\right)\\&=\left(oos_1\right)^{ow_1}\otimes\left(oos_2\right)^{ow_2}\ldots\otimes\left(oos_n\right)^{ow_n}=\overset{n}{\underset{j=1}{\otimes}}\left(oos_j\right)^{ow_j}\\&=\left(\begin{array}{l}\Delta\left(oo\prod_{j=1}^{n}\left(\frac{\Delta^{-1}\left(ool_{t_j},oo\xi_j\right)}{oo}\right)^{ow_j}\right),\\ \Delta\left(oo\left(1-\prod_{j=1}^{n}\left(1-\frac{\Delta^{-1}\left(ool_{i_j},oo\psi_j\right)}{oo}\right)^{ow_j}\right)\right),\\ \Delta\left(oo\left(1-\prod_{j=1}^{n}\left(1-\frac{\Delta^{-1}\left(ool_{f_j},oo\zeta_j\right)}{oo}\right)^{ow_j}\right)\right)\end{array}\right)\end{aligned}\tag{5}$$

where ow_j is weight numbers of oos_j, $0\le ow_j\le 1,\sum_{j=1}^{n}ow_j=1.$

3. Cross-entropy with TFNNs

Bhandari and Pal [22] administrated the CE approach for probability distributions.

Definition 7[22]. Let $ou\alpha=\left(ou\alpha\left(ou_1\right),ou\alpha\left(ou_2\right),\cdots,ou\alpha\left(ou_n\right)\right)$ and $ou\beta=\left(ou\beta\left(ou_1\right),ou\beta\left(ou_2\right),\cdots,ou\beta\left(ou_n\right)\right)$ are two sets on the $\left(ou_1,ou_2,\cdots,ou_n\right)$. The cross-entropy of $ou\alpha=\left(ou\alpha\left(ou_1\right),ou\alpha\left(ou_2\right),\cdots,ou\alpha\left(ou_n\right)\right)$ and $ou\beta=\left(ou\beta\left(ou_1\right),ou\beta\left(ou_2\right),\cdots,ou\beta\left(ou_n\right)\right)$ is administrated:

$$CE\left(ou\alpha,ou\beta\right)=\sum_{j=1}^{n}\left(ou\alpha\left(ou_j\right)\ln\frac{ou\alpha\left(ou_j\right)}{ou\beta\left(ou_j\right)}+\left(1-ou\alpha\left(ou_j\right)\right)\ln\frac{1-ou\alpha\left(ou_j\right)}{1-ou\beta\left(ou_j\right)}\right) \quad (6)$$

which depicts the discrimination of $ou\alpha=\left(ou\alpha\left(ou_1\right),ou\alpha\left(ou_2\right),\cdots,ou\alpha\left(ou_n\right)\right)$ from $ou\beta=\left(ou\beta\left(ou_1\right),ou\beta\left(ou_2\right),\cdots,ou\beta\left(ou_n\right)\right)$.

Shang and Jiang [18] administrated the modified CE.

Definition 8[18]. Let $ou\alpha=\left(ou\alpha\left(ou_1\right),ou\alpha\left(ou_2\right),\cdots,ou\alpha\left(ou_n\right)\right)$ and $ou\beta=\left(ou\beta\left(ou_1\right),ou\beta\left(ou_2\right),\cdots,ou\beta\left(ou_n\right)\right)$ are two sets on the $\left(ou_1,ou_2,\cdots,ou_n\right)$. The cross-entropy of $ou\alpha=\left(ou\alpha\left(ou_1\right),ou\alpha\left(ou_2\right),\cdots,ou\alpha\left(ou_n\right)\right)$ from $ou\beta=\left(ou\beta\left(ou_1\right),ou\beta\left(ou_2\right),\cdots,ou\beta\left(ou_n\right)\right)$ is administrated:

$$CE\left(ou\alpha,ou\beta\right)=\sum_{j=1}^{n}\left(\begin{array}{l}ou\alpha\left(ou_j\right)\ln\dfrac{ou\alpha\left(ou_j\right)}{\frac{1}{2}\left(ou\alpha\left(ou_j\right)+ou\beta\left(ou_j\right)\right)}+\\ \left(1-ou\alpha\left(ou_j\right)\right)\ln\dfrac{1-ou\alpha\left(ou_j\right)}{1-\frac{1}{2}\left(ou\alpha\left(ou_j\right)+ou\beta\left(ou_j\right)\right)}\end{array}\right) \quad (7)$$

which depicts the discrimination degree of $ou\alpha=\left(ou\alpha\left(ou_1\right),ou\alpha\left(ou_2\right),\cdots,ou\alpha\left(ou_n\right)\right)$ from $ou\beta=\left(ou\beta\left(ou_1\right),ou\beta\left(ou_2\right),\cdots,ou\beta\left(ou_n\right)\right)$.

Then, 2TLNN-CE are administrated based on modified CE [18] and 2TLNNs[23].

Definition 9. Assume that $oos_1=\left\langle\left(ool_{t_1},oo\xi_1\right),\left(ool_{i_1},oo\psi_1\right),\left(ool_{f_1},oo\zeta_1\right)\right\rangle$, $oos_2=\left\langle\left(ool_{t_2},oo\xi_2\right),\left(ool_{i_2},oo\psi_2\right),\left(ool_{f_2},oo\zeta_2\right)\right\rangle$. The 2TLNN-CE is administrated between oos_1 and oos_2:

$$
\begin{aligned}
&\text{2TLNN-CE}\left(oos_1, oos_2\right)\\
&=\left(\begin{array}{l}
\dfrac{\Delta^{-1}\left(ool_{t_1}, oo\xi_1\right)}{oo}\ln\dfrac{\dfrac{\Delta^{-1}\left(ool_{t_1}, oo\xi_1\right)}{oo}}{\dfrac{1}{2}\left(\dfrac{\Delta^{-1}\left(ool_{t_1}, oo\xi_1\right)}{oo}+\dfrac{\Delta^{-1}\left(ool_{t_2}, oo\xi_2\right)}{oo}\right)}\\
+\left(1-\dfrac{\Delta^{-1}\left(ool_{t_1}, oo\xi_1\right)}{oo}\right)\ln\dfrac{1-\dfrac{\Delta^{-1}\left(ool_{t_1}, oo\xi_1\right)}{oo}}{1-\dfrac{1}{2}\left(\dfrac{\Delta^{-1}\left(ool_{t_1}, oo\xi_1\right)}{oo}+\dfrac{\Delta^{-1}\left(ool_{t_2}, oo\xi_2\right)}{oo}\right)}
\end{array}\right)\\
&+\left(\begin{array}{l}
\dfrac{\Delta^{-1}\left(ool_{i_1}, oo\psi_1\right)}{oo}\ln\dfrac{\dfrac{\Delta^{-1}\left(ool_{i_1}, oo\psi_1\right)}{oo}}{\dfrac{1}{2}\left(\dfrac{\Delta^{-1}\left(ool_{i_1}, oo\psi_1\right)}{oo}+\dfrac{\Delta^{-1}\left(ool_{i_2}, oo\psi_2\right)}{oo}\right)}\\
+\left(1-\dfrac{\Delta^{-1}\left(ool_{i_1}, oo\psi_1\right)}{oo}\right)\ln\dfrac{1-\dfrac{\Delta^{-1}\left(ool_{i_1}, oo\psi_1\right)}{oo}}{1-\dfrac{1}{2}\left(\dfrac{\Delta^{-1}\left(ool_{i_1}, oo\psi_1\right)}{oo}+\dfrac{\Delta^{-1}\left(ool_{i_2}, oo\psi_2\right)}{oo}\right)}
\end{array}\right)\\
&+\left(\begin{array}{l}
\dfrac{\Delta^{-1}\left(ool_{f_1}, oo\zeta_1\right)}{oo}\ln\dfrac{\dfrac{\Delta^{-1}\left(ool_{f_1}, oo\zeta_1\right)}{oo}}{\dfrac{1}{2}\left(\dfrac{\Delta^{-1}\left(ool_{f_1}, oo\zeta_1\right)}{oo}+\dfrac{\Delta^{-1}\left(ool_{f_2}, oo\zeta_2\right)}{oo}\right)}\\
+\left(1-\dfrac{\Delta^{-1}\left(ool_{f_1}, oo\zeta_1\right)}{oo}\right)\ln\dfrac{1-\dfrac{\Delta^{-1}\left(ool_{f_1}, oo\zeta_1\right)}{oo}}{1-\dfrac{1}{2}\left(\dfrac{\Delta^{-1}\left(ool_{f_1}, oo\zeta_1\right)}{oo}+\dfrac{\Delta^{-1}\left(ool_{f_2}, oo\zeta_2\right)}{oo}\right)}
\end{array}\right)
\end{aligned}
\tag{8}
$$

which portrays the act of discriminating against oos_2 based on their difference from oos_1.

In light with Shannon's inequality[24], it's validated that $\text{2TLNN-CE}\left(oos_1, oos_2\right)\geq 0$, and $\text{2TLNN-CE}\left(oos_1, oos_2\right)=0$ if and only if $\left(ool_{t_1}, oo\xi_1\right)=\left(ool_{t_2}, oo\xi_2\right), \left(ool_{i_1}, oo\psi_1\right)=\left(ool_{i_2}, oo\psi_2\right), \left(ool_{f_1}, oo\zeta_1\right)=\left(ool_{f_2}, oo\zeta_2\right)$.

4. 2TLNN-CE technique for MAGDM based on information entropy

The 2TLNN-CE technique is administrated for MAGDM. 2TLNN-CE technique for MAGDM is administrated (See Figure 1):

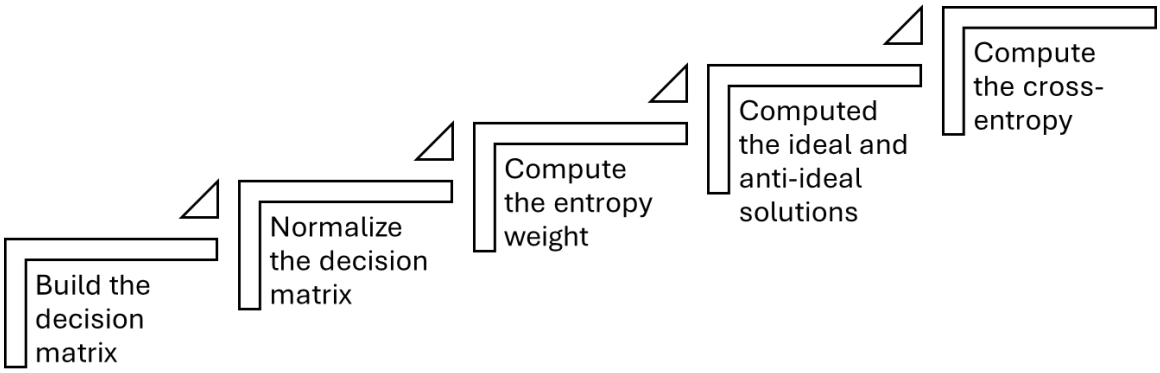

Figure 1. 2TLNN-CE model for MAGDM based on entropy with 2TLNNs

Step 1. Administrate the 2TLNN-matrix $OR=\left[OR_{ij}^{t}\right]_{m\times n}=\left\{\left(ool_{t_{ij}}^{t},oo\xi_{ij}^{t}\right),\left(ool_{i_{ij}}^{t},oo\psi_{ij}^{t}\right),\left(ool_{f_{ij}}^{t},oo\zeta_{ij}^{t}\right)\right\}_{m\times n}$ and average matrix $OR=\left[OR_{ij}\right]_{m\times n}$:

$$OR=\left[OR_{ij}^{t}\right]_{m\times n}=\begin{array}{c} \\ OA_1 \\ OA_2 \\ \vdots \\ OA_m \end{array}\begin{array}{c} \begin{array}{cccc} OB_1 & OB_2 & \cdots & OB_n \end{array} \\ \begin{bmatrix} OR_{11}^{t} & OR_{12}^{t} & \cdots & OR_{1n}^{t} \\ OR_{21}^{t} & OR_{22}^{t} & \cdots & OR_{2n}^{t} \\ \vdots & \vdots & \vdots & \vdots \\ OR_{m1}^{t} & OR_{m2}^{t} & \cdots & OR_{mn}^{t} \end{bmatrix} \end{array} \tag{9}$$

$$OR=\left[OR_{ij}\right]_{m\times n}=\begin{array}{c} \\ OA_1 \\ OA_2 \\ \vdots \\ OA_m \end{array}\begin{array}{c} \begin{array}{cccc} OB_1 & OB_2 & \cdots & OB_n \end{array} \\ \begin{bmatrix} OR_{11} & OR_{12} & \cdots & OR_{1n} \\ OR_{21} & OR_{22} & \cdots & OR_{2n} \\ \vdots & \vdots & \vdots & \vdots \\ OR_{m1} & OR_{m2} & \cdots & OR_{mn} \end{bmatrix} \end{array} \tag{10}$$

Based on 2TLNNWG technique, the $OR=\left[OR_{ij}\right]_{m\times n}=\left\{\left(ool_{t_{ij}},oo\xi_{ij}\right),\left(ool_{i_{ij}},oo\psi_{ij}\right),\left(ool_{f_{ij}},oo\zeta_{ij}\right)\right\}_{m\times n}$ is:

$$
\begin{aligned}
OR_{ij} &= \left(oos_{ij}^{1}\right)^{ow_1} \otimes \left(oos_{ij}^{2}\right)^{ow_2} \otimes \cdots \otimes \left(oos_{ij}^{t}\right)^{ow_t} \\
&= \left\{ \begin{array}{l}
\Delta\left(oo\prod_{d=1}^{t}\left(1-\frac{\Delta^{-1}\left(ool_{t_{ij}}, oo\xi_{ij}\right)^{t}}{oo} \right)^{ow_t} \right), \\
\Delta\left(oo\left(1-\prod_{d=1}^{t}\left(1-\frac{\Delta^{-1}\left(ool_{i_{ij}}, oo\psi_{ij}\right)^{t}}{oo} \right)^{ow_t} \right) \right), \\
\Delta\left(oo\left(1-\prod_{d=1}^{t}\left(1-\frac{\Delta^{-1}\left(ool_{f_{ij}}, oo\zeta_{ij}\right)^{t}}{oo} \right)^{ow_t} \right) \right)
\end{array} \right\},
\end{aligned} \tag{11}
$$

Step 2. Normalize the $OR = \left[OR_{ij} \right]_{m\times n}$ into $NOR = \left[NOR_{ij} \right]_{m\times n}$.

Aiming at benefit attributes:

$$
NOR_{ij} = OR_{ij} = \left\{ \left(ool_{t_{ij}}, oo\xi_{ij}\right), \left(ool_{i_{ij}}, oo\psi_{ij}\right), \left(ool_{f_{ij}}, oo\zeta_{ij}\right) \right\} \tag{12}
$$

Aiming at non-benefit attributes:

$$
\begin{aligned}
NOR_{ij} &= \left\{ \left(ool_{t_{ij}}, oo\xi_{ij}\right), \left(ool_{i_{ij}}, oo\psi_{ij}\right), \left(ool_{f_{ij}}, oo\zeta_{ij}\right) \right\} \\
&= \left\{ \Delta\left(oo - \Delta^{-1}\left(ool_{t_{ij}}, ool_{ij}\right) \right), \Delta\left(oo - \Delta^{-1}\left(ool_{i_{ij}}, oo\psi_{ij}\right) \right), \Delta\left(oo - \Delta^{-1}\left(ool_{f_{ij}}, oo\zeta_{ij}\right) \right) \right\}
\end{aligned} \tag{13}
$$

Step 3. Administrate the Weight. Entropy [19] is administrated to conduct weight values. Normalized 2TLNN-matrix is administrated based on $SF\left(NOR_{ij}\right)$ and $AF\left(NOR_{ij}\right)$:

$$
\begin{aligned}
N2TLNNM_{ij} &= \frac{SF\left(NOR_{ij}\right) + AF\left(NOR_{ij}\right)}{\sum_{i=1}^{m}\left(SF\left(NOR_{ij}\right) + AF\left(NOR_{ij}\right) \right)} \\
&= \frac{\left(\begin{array}{l}
SF\left\{ \left(ool_{t_{ij}}, oo\xi_{ij}\right), \left(ool_{i_{ij}}, oo\psi_{ij}\right), \left(ool_{f_{ij}}, oo\zeta_{ij}\right) \right\} \\
+AF\left\{ \left(ool_{t_{ij}}, oo\xi_{ij}\right), \left(ool_{i_{ij}}, oo\psi_{ij}\right), \left(ool_{f_{ij}}, oo\zeta_{ij}\right) \right\}
\end{array} \right)}{\sum_{i=1}^{m}\left(\begin{array}{l}
SF\left\{ \left(ool_{t_{ij}}, oo\xi_{ij}\right), \left(ool_{i_{ij}}, oo\psi_{ij}\right), \left(ool_{f_{ij}}, oo\zeta_{ij}\right) \right\} \\
+AF\left\{ \left(ool_{t_{ij}}, oo\xi_{ij}\right), \left(ool_{i_{ij}}, oo\psi_{ij}\right), \left(ool_{f_{ij}}, oo\zeta_{ij}\right) \right\}
\end{array} \right)}
\end{aligned} \tag{14}
$$

Then, the 2TLNN Shannon entropy (2TLNNSE) is administrated:

$$
2TLNNSE_j = -\frac{1}{\ln m}\sum_{i=1}^{m} N2TLNNM_{ij} \ln N2TLNNM_{ij} \tag{15}
$$

and $N2TLNNM_{ij}\ln N2TLNNM_{ij}=0$ if $N2TLNNM_{ij}=0$.

The weight $o\omega=\left(o\omega_1,o\omega_2,...,o\omega_n\right)$ is administrated:

$$o\omega_j=\frac{1-2TLNNSE_j}{\sum_{j=1}^{n}\left(1-2TLNNSE_j\right)} \tag{16}$$

Step 4. Administrate the 2TLNNPIDS (2TLNN positive ideal decision solution):

$$2TLNNPIDS=\left\{2TLNNPIDS_j\right\} \tag{17}$$

$$2TLNNPIDS_j=\left\{\left(ool_{t_j}^{+},oo\xi_j^{+}\right),\left(ool_{i_j}^{+},oo\psi_j^{+}\right),\left(ool_{f_j}^{+},oo\zeta_j^{+}\right)\right\} \tag{18}$$

$$\begin{aligned}&SF\left\{\left(ool_{t_j}^{+},oo\xi_j^{+}\right),\left(ool_{i_j}^{+},oo\psi_j^{+}\right),\left(ool_{f_j}^{+},oo\zeta_j^{+}\right)\right\}\\&=\max_i SF\left\{\left(ool_{t_{ij}},oo\xi_{ij}\right),\left(ool_{i_{ij}},oo\psi_{ij}\right),\left(ool_{f_{ij}},oo\zeta_{ij}\right)\right\}\end{aligned} \tag{19}$$

Step 5. Administrate the 2TLNN-CE between NOR_{ij} and 2TLNNPIDS:

$$
\begin{aligned}
&\text{2TLNN-CE}\left(NOR_{ij}, 2TLNNPIDS\right)\\
&=\sum_{j=1}^{n} o\omega_j \left(\frac{\Delta^{-1}\left(ool_{t_{ij}}, oo\xi_{ij}\right)}{oo} \ln \frac{\dfrac{\Delta^{-1}\left(ool_{t_{ij}}, oo\xi_{ij}\right)}{oo}}{\dfrac{1}{2}\left(\dfrac{\Delta^{-1}\left(ool_{t_{ij}}, oo\xi_{ij}\right)}{oo}+\dfrac{\Delta^{-1}\left(ool^{+}_{t_j}, oo\xi^{+}_{j}\right)}{oo}\right)} \right.\\
&\left. +\left(1-\frac{\Delta^{-1}\left(ool_{t_{ij}}, oo\xi_{ij}\right)}{oo}\right) \ln \frac{1-\dfrac{\Delta^{-1}\left(ool_{t_{ij}}, oo\xi_{ij}\right)}{oo}}{1-\dfrac{1}{2}\left(\dfrac{\Delta^{-1}\left(ool_{t_{ij}}, oo\xi_{ij}\right)}{oo}+\dfrac{\Delta^{-1}\left(ool^{+}_{t_j}, oo\xi^{+}_{j}\right)}{oo}\right)} \right)\\
&+\sum_{j=1}^{n} o\omega_j \left(\frac{\Delta^{-1}\left(ool_{i_{ij}}, oo\psi_{ij}\right)}{oo} \ln \frac{\dfrac{\Delta^{-1}\left(ool_{i_{ij}}, oo\psi_{ij}\right)}{oo}}{\dfrac{1}{2}\left(\dfrac{\Delta^{-1}\left(ool_{i_{ij}}, oo\psi_{ij}\right)}{oo}+\dfrac{\Delta^{-1}\left(ool^{+}_{i_j}, oo\psi^{+}_{j}\right)}{oo}\right)} \right.\\
&\left. +\left(1-\frac{\Delta^{-1}\left(ool_{i_{ij}}, oo\psi_{ij}\right)}{oo}\right) \ln \frac{1-\dfrac{\Delta^{-1}\left(ool_{i_{ij}}, oo\psi_{ij}\right)}{oo}}{1-\dfrac{1}{2}\left(\dfrac{\Delta^{-1}\left(ool_{i_{ij}}, oo\psi_{ij}\right)}{oo}+\dfrac{\Delta^{-1}\left(ool^{+}_{i_j}, oo\psi^{+}_{j}\right)}{oo}\right)} \right)\\
&+\sum_{j=1}^{n} o\omega_j \left(\frac{\Delta^{-1}\left(ool_{f_{ij}}, oo\zeta_{ij}\right)}{oo} \ln \frac{\dfrac{\Delta^{-1}\left(ool_{f_{ij}}, oo\zeta_{ij}\right)}{oo}}{\dfrac{1}{2}\left(\dfrac{\Delta^{-1}\left(ool_{f_{ij}}, oo\zeta_{ij}\right)}{oo}+\dfrac{\Delta^{-1}\left(ool^{+}_{f_j}, oo\zeta^{+}_{j}\right)}{oo}\right)} \right.\\
&\left. +\left(1-\frac{\Delta^{-1}\left(ool_{f_{ij}}, oo\zeta_{ij}\right)}{oo}\right) \ln \frac{1-\dfrac{\Delta^{-1}\left(ool_{f_{ij}}, oo\zeta_{ij}\right)}{oo}}{1-\dfrac{1}{2}\left(\dfrac{\Delta^{-1}\left(ool_{f_{ij}}, oo\zeta_{ij}\right)}{oo}+\dfrac{\Delta^{-1}\left(ool^{+}_{f_j}, oo\zeta^{+}_{j}\right)}{oo}\right)} \right)
\end{aligned}
\tag{20}
$$

Step 6. In light withthe $\text{2TLNN-CE}\left(NOR_{ij}, 2TLNNPIDS\right)$, the smaller $\text{2TLNN-CE}\left(NOR_{ij}, 2TLNNPIDS\right)$ is better alternative.

5. Numerical example and sensitivity analysis

We analysis the results with the sensitivity analysis to show the stability of the results.

5.1. Numerical example

The evaluation of university physical education teaching quality is an indispensable part of the higher education sports system, aimed at comprehensively assessing the effectiveness of physical education and ensuring the achievement of teaching objectives. Through a scientific evaluation system, universities can systematically assess various aspects, such as the teaching process, content, methods, and students' learning outcomes. This helps analyze the effectiveness and rationality of teaching, and provides critical reference points for educational reforms in physical education. Firstly, the evaluation of physical education teaching quality helps universities identify problems in the teaching process. For example, whether the curriculum design is reasonable, whether the content meets the actual needs of students, and if the teaching methods are diversified and targeted. By analyzing these issues, universities can promptly adjust teaching strategies, optimize the curriculum structure, and ensure that physical education is more closely aligned with students' real situations, effectively enhancing their learning interest and participation. Secondly, physical education teaching evaluation contributes to improving teachers' teaching skills and professional development. The evaluation results provide feedback to teachers, helping them identify shortcomings in their teaching and make improvements. Moreover, the evaluation system guides teachers in their professional growth, encouraging them to continually enhance their teaching abilities and innovation, thus promoting the overall development of the university's physical education faculty. Additionally, the evaluation of teaching quality is a powerful tool for driving reforms in university physical education. Through data analysis and comprehensive assessments, universities can identify flaws in the current teaching models and implement targeted reforms. For instance, in response to student dissatisfaction with certain courses or teaching methods, new teaching approaches can be introduced, or course content can be adjusted to improve teaching outcomes. In this process, the evaluation system provides objective data support, ensuring the scientific and rational direction of the reforms. Finally, physical education teaching quality evaluation helps foster students' lifelong awareness of physical fitness and healthy living. By evaluating students' learning outcomes in physical education, universities can better understand their physical development and adjust teaching accordingly. This not only improves students' athletic skills and physical health but also enhances their interest in exercise, cultivating a lifelong habit of physical activity. In summary, the evaluation of university physical education teaching quality plays a vital role in improving teaching standards, promoting educational reforms, and fostering students' health awareness. Through a scientific and systematic evaluation system, universities can continually optimize physical education, promoting the sustainable

development of university sports education. The teaching quality evaluation of university physical education is MAGDM.

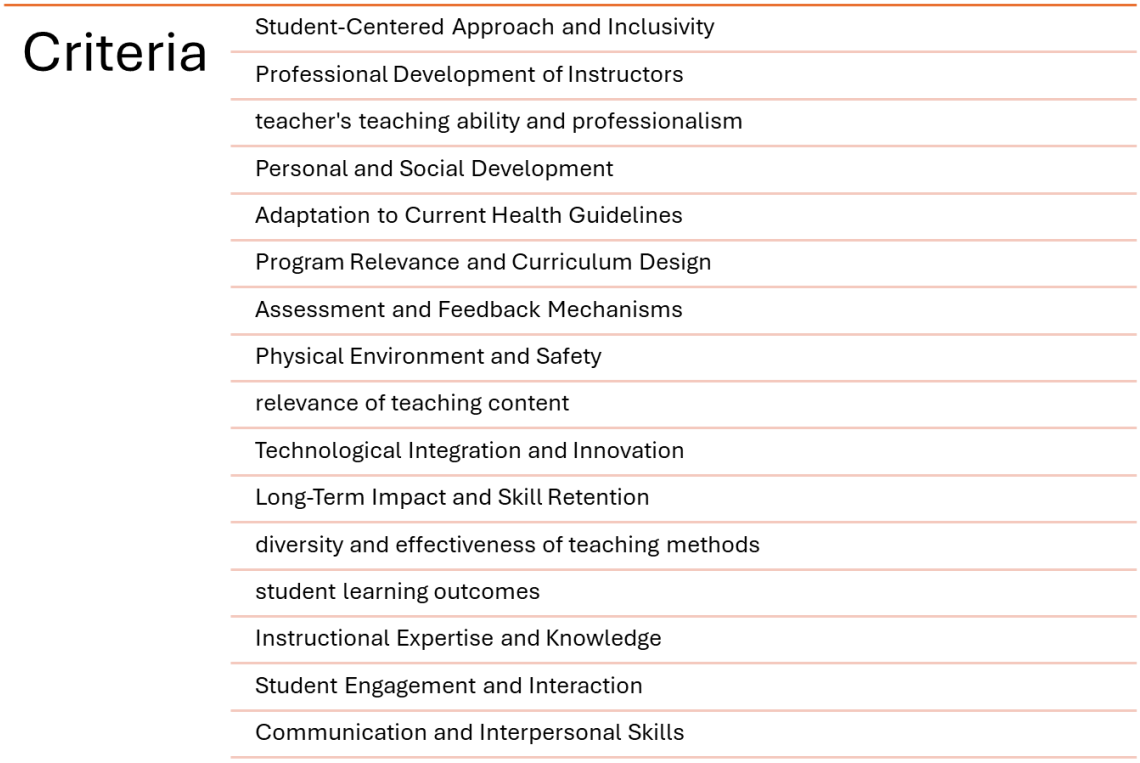

Figure 2. The criteria and alternatives.

Step 1. We used the neutrosophic numbers to evaluate the criteria and alternatives to build the decision matrix. Figure 2 shows the criteria and alternatives.

Step 2. Table 1 shows the normalized decision matrix between criteria and alternatives.

Step 3. We compute the entropy weight for each criterion as shown in Figure 3. We show the criterion 9 is the best and criterion 2 is the worst.

Step 4. We computed the ideal and anti-ideal solutions.

Step 5. Compute the cross-entropy for each entropy as shown in Table 2.

Step 6. Figure 4 shows the rank of alternatives. We show the alternative 13 is the best and alternative 14 is the worst.

Table 1. The normalized decision matrix.

	C_1	C_2	C_3	C_4	C_5	C_6	C_7	C_8	C_9	C_{10}	C_{11}	C_{12}	C_{13}	C_{14}	C_{15}	C_{16}
A_1	0.333333	0.692308	0.857143	1	0.4	0.2	0.4	0.846154	0.923077	1	0.933333	0.666667	0.866667	0.8	0.928571	0.933333

A_{14}	A_{13}	A_{12}	A_{11}	A_{10}	A_9	A_8	A_7	A_6	A_5	A_4	A_3	A_2
0.866667	0.866667	0.933333	0.6	0.466667	0.4	0.733333	1	0.733333	0.733333	0.6	1	0.8
0.461538	0.769231	1	1	0.692308	0.923077	0.692308	0.461538	0.538462	0.923077	0.769231	0.461538	0.230769
0.428571	0.785714	1	0.928571	0.571429	0.5	0.714286	0.928571	0.642857	0.714286	0.857143	0.642857	0.428571
0.2	1	0.6	0.733333	0.533333	0.733333	0.8	0.733333	0.733333	0.733333	0.8	0.666667	0.666667
0.4	0.4	1	0.666667	0.933333	0.866667	0.533333	0.466667	0.666667	0.8	0.866667	0.933333	0.8
0.6	0.6	0.733333	0.933333	0.933333	0.466667	0.733333	0.666667	0.733333	0.8	0.733333	0.866667	1
0.4	1	0.4	0.8	0.866667	0.6	0.466667	0.8	0.666667	0.6	0.6	0.866667	0.466667
0.230769	0.923077	0.461538	0.692308	0.769231	1	0.769231	0.769231	0.769231	0.615385	0.538462	0.692308	0.769231
0.692308	0.615385	1	0.615385	0.615385	0.846154	1	0.846154	0.923077	0.846154	0.538462	0.846154	0.769231
0.4	0.6	1	0.333333	0.866667	0.933333	0.733333	0.8	0.466667	0.733333	0.666667	0.6	0.866667
0.2	1	0.6	0.666667	0.866667	0.6	0.733333	0.533333	0.666667	0.666667	0.533333	0.666667	1
1	0.8	0.6	0.6	0.466667	0.666667	0.933333	0.666667	0.533333	0.466667	0.733333	0.866667	0.8
0.6	1	0.8	0.666667	0.666667	0.933333	0.866667	0.6	0.533333	0.6	0.733333	0.8	0.933333
0.666667	1	0.8	0.533333	0.733333	0.466667	0.533333	0.666667	0.866667	0.933333	0.666667	0.866667	0.6
0.714286	0.714286	1	0.785714	0.357143	0.857143	0.785714	0.642857	0.642857	0.642857	0.857143	0.428571	0.857143
0.6	0.933333	0.666667	0.866667	0.666667	0.333333	1	0.8	0.8	0.733333	0.533333	0.466667	0.866667

A_{15}	0.8	0.846154	0.714286	0.466667	0.4	0.866667	0.666667	0.538462	0.615385	0.466667	0.866667	0.666667	0.333333	0.333333	0.357143	0.466667

Table 2. The cross-entropy values.

	C_1	C_2	C_3	C_4	C_5	C_6	C_7	C_8	C_9	C_{10}	C_{11}	C_{12}	C_{13}	C_{14}	C_{15}	C_{16}
A_1	0.059034	0.06119	0.063417	0.061356	0.060138	0.057255	0.060396	0.061711	0.063611	0.063488	0.061183	0.062512	0.06271	0.062699	0.063377	0.236721
A_2	0.062466	0.05782	0.0602	0.060668	0.063331	0.061081	0.061142	0.061492	0.062705	0.06299	0.061276	0.063403	0.062964	0.061598	0.063075	0.235753
A_3	0.063234	0.060057	0.06211	0.060668	0.063995	0.060887	0.064042	0.061232	0.063182	0.061598	0.060598	0.063786	0.062428	0.06299	0.060222	0.226832
A_4	0.06139	0.061448	0.063417	0.061015	0.063679	0.060611	0.062348	0.060549	0.060893	0.062011	0.060104	0.06298	0.062113	0.062011	0.063075	0.22885
A_5	0.062149	0.061851	0.062596	0.060857	0.063331	0.060762	0.062348	0.060923	0.063182	0.062375	0.060598	0.060729	0.061357	0.063251	0.061933	0.233477
A_6	0.062149	0.060511	0.06211	0.060857	0.062516	0.060611	0.062844	0.061492	0.063611	0.060582	0.060598	0.0614	0.060898	0.06299	0.061933	0.234678
A_7	0.063234	0.060057	0.063767	0.060857	0.060862	0.060431	0.063684	0.061492	0.063182	0.062699	0.060104	0.062512	0.061357	0.062011	0.061933	0.234678
A_8	0.062149	0.06119	0.062596	0.061015	0.061487	0.060611	0.061142	0.061492	0.064001	0.062375	0.060785	0.064136	0.06271	0.061127	0.062739	0.237596
A_9	0.059775	0.061851	0.06093	0.060857	0.063679	0.05963	0.062348	0.062058	0.063182	0.063251	0.060375	0.062512	0.062964	0.060582	0.063075	0.221661
A_{10}	0.060397	0.06119	0.06156	0.060168	0.063995	0.060993	0.064042	0.061492	0.061575	0.06299	0.061072	0.060729	0.061758	0.062375	0.059437	0.232127
A_{11}	0.06139	0.062009	0.063767	0.060857	0.062516	0.060993	0.063684	0.061232	0.061575	0.059188	0.060598	0.061989	0.061758	0.061127	0.062739	0.235753
A_{12}	0.063004	0.062009	0.064086	0.060441	0.064283	0.060611	0.060396	0.060092	0.064001	0.063488	0.060375	0.061989	0.062428	0.062699	0.063649	0.232127

A_{13}	0.062749	0.061448	0.063028	0.061356	0.060138	0.060214	0.064663	0.061898	0.061575	0.061598	0.061276	0.063403	0.063193	0.063488	0.062361	0.236721
A_{14}	0.062749	0.060057	0.0602	0.057386	0.060138	0.060214	0.060396	0.057845	0.062174	0.059946	0.057347	0.064456	0.061357	0.062011	0.062361	0.230598
A_{15}	0.062466	0.061666	0.062596	0.059835	0.060138	0.060887	0.062844	0.060549	0.061575	0.060582	0.061072	0.062512	0.059009	0.059188	0.059437	0.226832

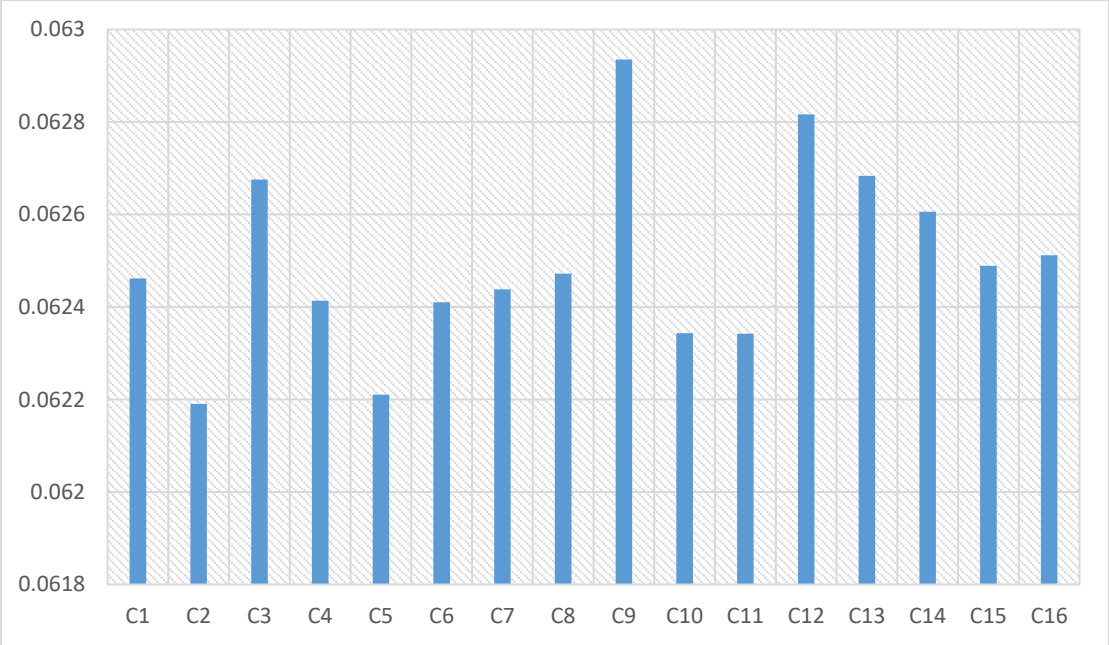

Figure 3. The criteria weights.

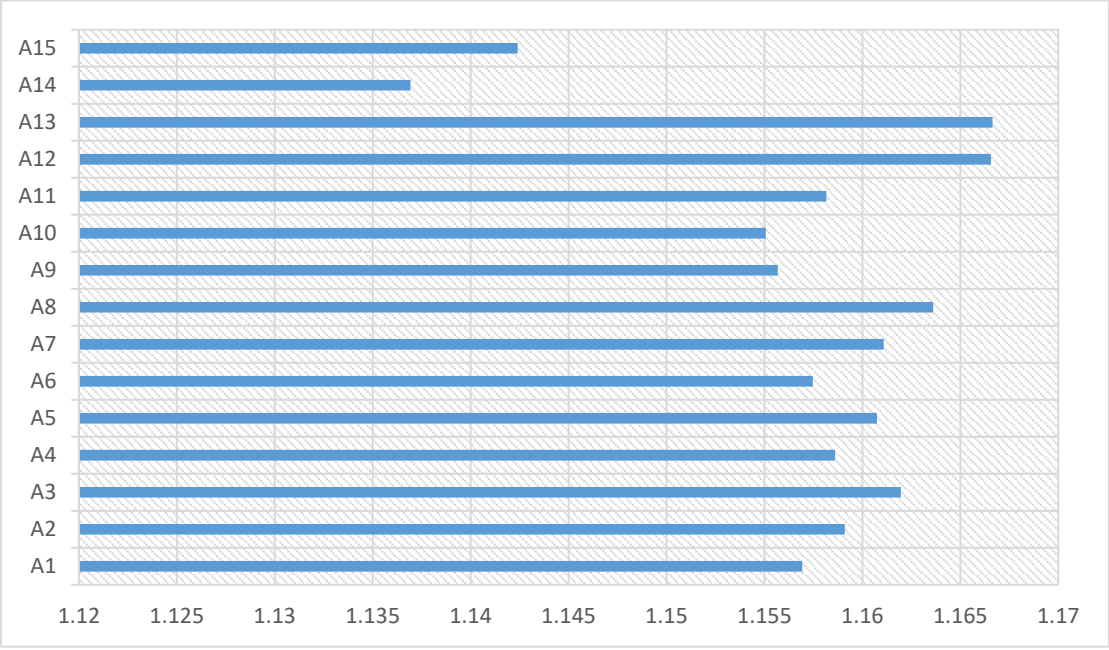

Figure 4. The rank of alternatives.

Sensitivity Analysis

We change the criteria weights with different values to show the different rank under different cases. We change the weights of criteria with 17 cases as shown in Figure 5. Then we applied the cross-entropy method. We show the cross-entropy values as shown in Figure 6. The results show the rank of alternatives stable in different cases. Then we show the rank of alternatives as shown in Figure 7.

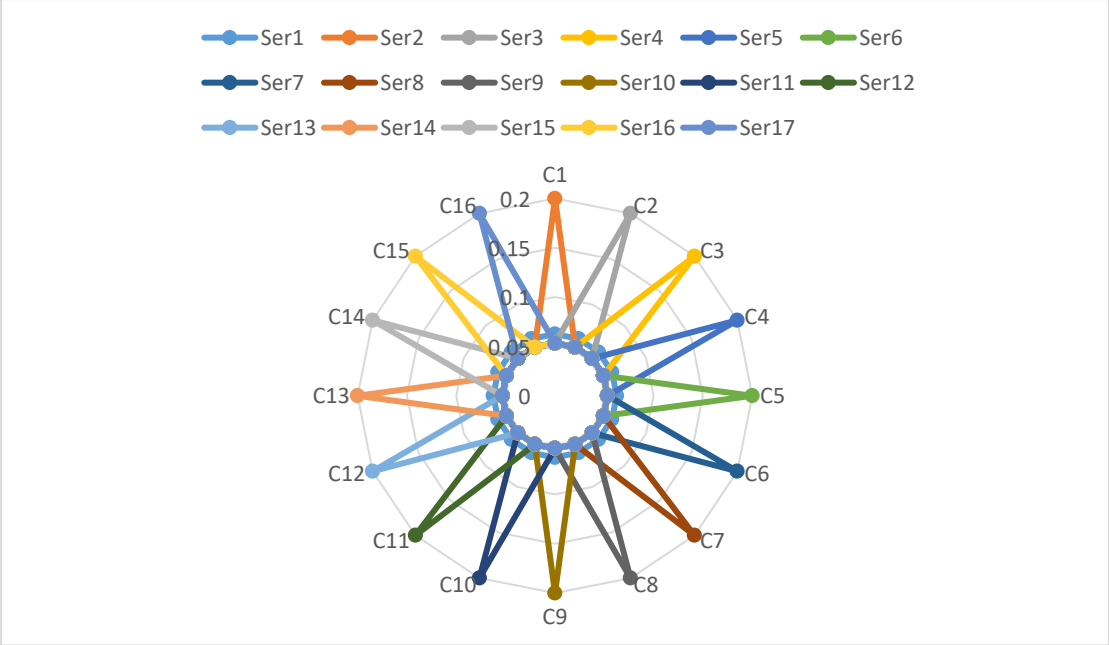

Figure 5. The different criteria weights.

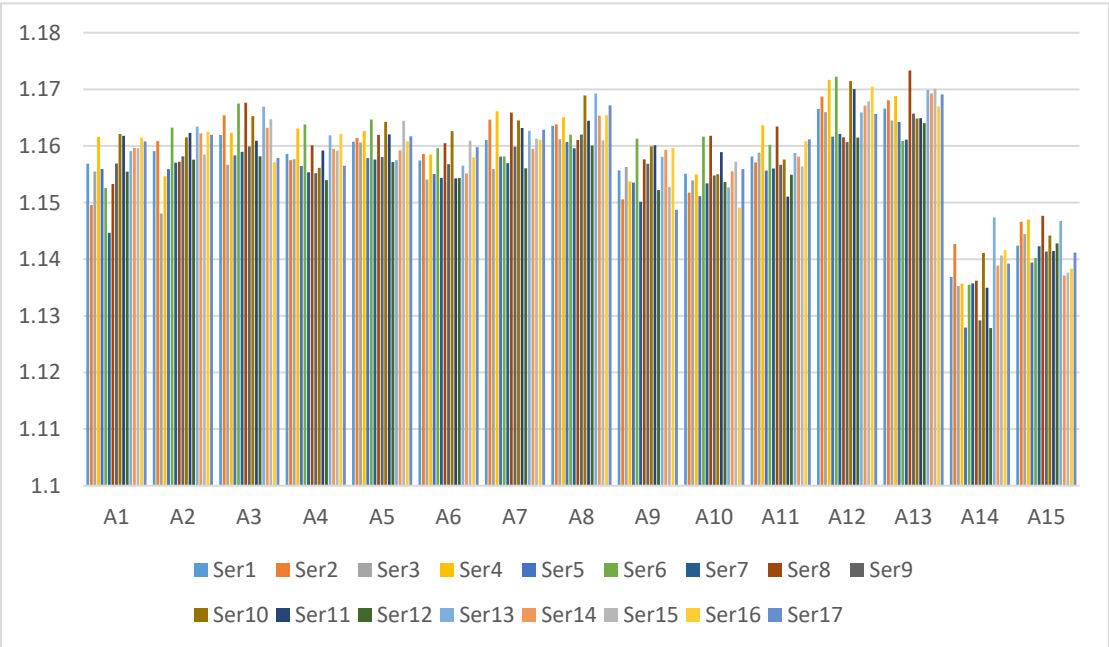

Figure 6. The cross-entropy values.

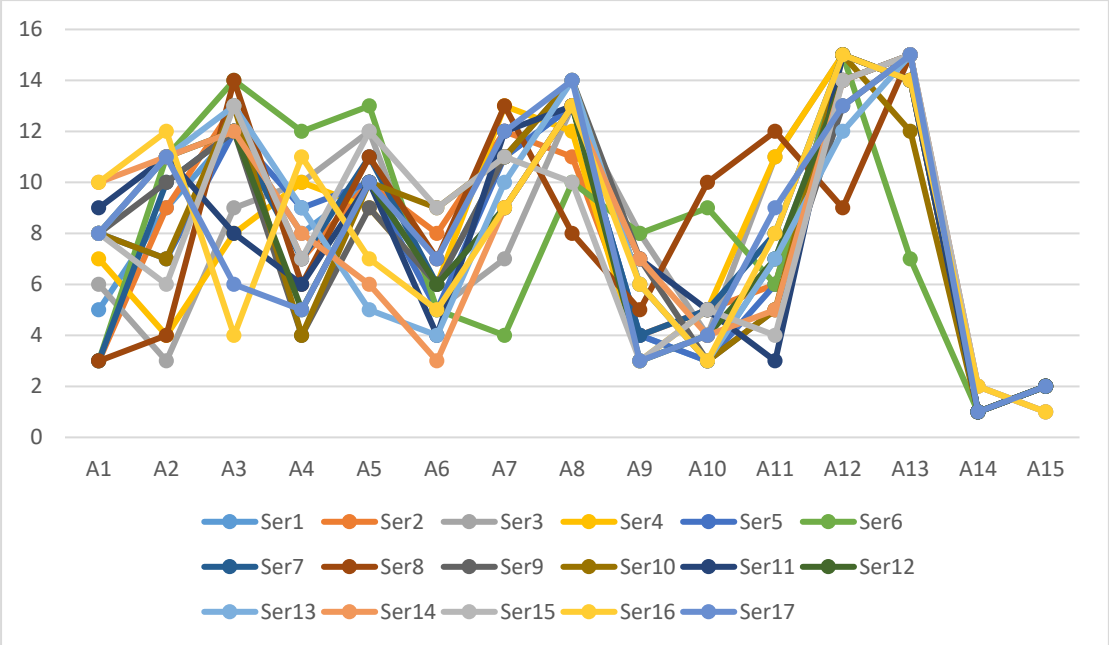

Figure 7. Rank of alternatives under different cases.

Upon comparing the final results of 2TLNN-CE model with existing models, it is observed that there are slight differences in the calculated results. However, both the best physical education college and the worst physical education college remain the same. This consistency indicates that the 2TLNN-CE technique is effective and reliable MAGDM approach. The subtle differences could be attributed to certain factors. The 2TLNNWG technique[13] copes with the individual's influence on the final outcome, while 2TLNN-TODIM model [23] copes with the psychological behavior of DMs. In contrast, the 2TLNN-CE technique encompasses the individual uncertainty and overall uncertainty under 2TLNNs.The 2TLNN-CE technique offers several key advantages: (1) It effectively addresses both individual and overall uncertainty within the framework of 2TLNNs; (2) The technique possesses a straightforward structure and exhibits strong differentiation capabilities; (3) It overcomes design flaws present in existing CE measures and could accurately reflect individual and overall differentiation among different 2TLNNs. However, it is important to note that the 2TLNN-CE technique does not account for the psychological behavior of DMs in MAGDM, which represents a limitation of the approach.

6. Conclusion

The evaluation of university physical education teaching quality is essential for ensuring teaching objectives are met. By assessing aspects like the teaching process, content, methods, and student outcomes, it reflects the effectiveness of physical education courses. Evaluation helps schools identify issues such as poor curriculum design or monotonous

methods, providing a basis for instructional improvement. A scientific evaluation system allows timely adjustments to strategies, enhancing students' interest, physical fitness, and skills. It also offers feedback for teacher development, optimizing faculty, and drives reforms in sports programs, fostering lifelong exercise habits and healthy living. The problem of teaching quality evaluation of university physical education is MAGDM. This study presents the application of 2TLNN-CE technique, which is based on the traditional CE technique with 2TLNSs. By incorporating CE technique along with 2TLNSs, 2TLNN-CE technique is implemented for MAGDM with 2TLNSs. Additionally, numerical example focusing on the teaching quality evaluation of university physical education is provided to validate the advantages of 2TLNN-CE. Comparative analysis is administrated to highlight the strengths of this technique. The key contributions of this study are summarized: (1) Extension of cross-entropy technique to encompass 2TLNSs, expanding its applicability; (2) Implementation of 2TLNN-CE technique for MAGDM, utilizing the advantages of 2TLNSs; (3) Demonstration of 2TLNN-CE technique through numerical example involving the teaching quality evaluation of university physical education. Comparative analysis is administrated to further illustrate the advantages of 2TLNN-CE technique.

References

[1] J. Liang, Research on ways to improve the teaching quality of university martial arts courses, Contemporary Sports Technology, 4 (2014) 85-86.

[2] H. Wang, F. Yan, Research on university physical education teachers' teaching efficacy and its impact on teaching quality, Journal of Nanjing Institute of Physical Education (Natural Science Edition), 14 (2015) 1-3.

[3] H. Zhang, H. He, Research on quantitative reform of university physical education classroom teaching quality evaluation indicators, Contemporary Sports Technology, 6 (2016) 120-122.

[4] S. Zhou, G. Wu, Construction of satisfaction evaluation system for university physical education teaching quality, Hubei Sports Science and Technology, 36 (2017) 1017-1021.

[5] Z. Liu, Discussion on issues in modern university physical education teaching quality evaluation, Contemporary Sports Technology, 8 (2018) 123-124.

[6] X. Wang, H. Ding, H. Zhang, Construction and practice research of information-based teaching quality evaluation system: A case study of theoretical courses in physical education at linyi university, Journal of Harbin Institute of Physical Education, 37 (2019) 6-10.

[7] J. Liu, J. Yin, X. Wang, Research on university physical education teaching quality assurance system, Zhejiang Sports Science, 42 (2020) 42-47.

[8] T. Zhao, J. Gong, J. Sheng, Research on university physical education classroom teaching quality evaluation system from the perspective of core physical literacy: A case study of hexi university, Journal of Hexi University, 37 (2021) 72-76.

[9] S. Zhou, Y. Wang, Fuzzy evaluation of university physical education teaching quality based on grey system theory, Ice and Snow Sports Innovation Research, (2022) 113-116.

[10] X. Ma, Research on standardized reform and practice of university physical education classroom teaching quality evaluation, Contemporary Sports Technology, 13 (2023) 156-161.

[11] H. Chockler, E. Farchi, B. Godlin, S. Novikov, Cross-entropy-based replay of concurrent programs, in: 12th International Conference on Fundamental Approaches to Software Engineering held in Conjuction with European Conference on Theory and Practice of Software, Springer-Verlag Berlin, York, ENGLAND, 2009, pp. 201-+.

[12] J. Ye, Multicriteria fuzzy decision-making method based on the intuitionistic fuzzy cross-entropy, in: International Conference on Intelligent Human-Machine Systems and Cybernetics, Ieee Computer Soc, Hangzhou, PEOPLES R CHINA, 2009, pp. 59-61.

[13] J. Wang, G.W. Wei, Y. Wei, Models for green supplier selection with some 2-tuple linguistic neutrosophic number bonferroni mean operators, Symmetry-Basel, 10 (2018) 36.

[14] V. Christianto, F. Smarandache, The convergence of ikigai and design thinking: Crafting a purposeful framework, Sustainable Machine Intelligence Journal, 7 (2024) (1):1-8.

[15] M. Mohamed, A. Elsayed, M. Voskoglou, Collaboration of vague theory and mathematical techniques for optimizing healthcare by recommending optimal blockchain supplier, Sustainable Machine Intelligence Journal, 6 (2024) (5):1-15.

[16] F.A. Smarandache, Unifying field in logics. Neutrosophy: Neutrosophic probability, set and logic, American Research Press, Rehoboth, 1999.

[17] H. Wang, F. Smarandache, Y. Zhang, R. Sunderraman, Single valued neutrosophic sets, Infinite Study, 12 (2010) 20110.

[18] X. Shang, W. Jiang, A note on fuzzy information measures, Pattern Recognition Letters, 18 (1997) 425-432.

[19] C.E. Shannon, A mathematical theory of communication, Bell System Technical Journal, 27 (1948) 379-423.

[20] F. Herrera, L. Martinez, A 2-tuple fuzzy linguistic representation model for computing with words, Ieee Transactions on Fuzzy Systems, 8 (2000) 746-752.

[21] F. Herrera, L. Martinez, An approach for combining linguistic and numerical information based on the 2-tuple fuzzy linguistic representation model in decision-making, International Journal of Uncertainty Fuzziness and Knowledge-Based Systems, 8 (2000) 539-562.

[22] D. Bhandari, N.R. Pal, Some new information measures for fuzzy sets, Information Sciences, 67 (1993) 209-228.

[23] J. Wang, G.W. Wei, M. Lu, Todim method for multiple attribute group decision making under 2-tuple linguistic neutrosophic environment, Symmetry-Basel, 10 (2018) 15.

[24] J. Lin, Divergence measures based on the shannon entropy, IEEE Transactions on Information theory, 37 (1991) 145-151.

Received: July 28, 2024. Accepted: Oct 26, 2024

NSS
Neutrosophic Sets and Systems, Vol. 76, 2025
University of New Mexico

Construction Of Almost Unbiased Estimator For Population Mean Using Neutrosophic Information

Rajesh Singh[1], Anamika Kumari[2], Florentin Smarandache[3] and Shobh Nath Tiwari[1*]
[1]Department of Statistics, Institute of Science, Banaras Hindu University, Varanasi-221005, Uttar Pradesh, India

[2]Department of Data Science and Computing, Manipal Academy of Higher Education

[3]Department of Mathematics, University of New Mexico, 705 Gurley Ave, Gallup, USA

rsinghstat@gmail.com, anamika.kumari@manipal.edu, fsmarandache@gmail.com, shobh7285@gmail.com;

*Corresponding: shobh7285@gmail.com

Abstract: In classical statistics, the population mean is estimated using determinate, crisp data value when auxiliary information is known. These estimates can often be biased. The main objective of this study is to introduce the neutrosophic estimator with the minimum mean squared error (MSE) for the unknown value of the population mean as well as overcome the limitations of classical statistics when dealing with ambiguous or indeterminate data. Neutrosophic statistics was introduced by Florentin Smarandache. It is a generalisation of classical statistics that addresses ambiguous, unclear, vague, and indeterminate data. In this study, we have proposed neutrosophic almost unbiased estimator that use known neutrosophic auxiliary parameters to estimate the neutrosophic population mean of the primary variable. Equations for bias and mean squared error are calculated for the suggested estimators up to the first order of approximation. The proposed estimator performs better than the other existing estimators with respect to the MSE and percent relative efficiency (PRE) criteria. The estimator with the highest PRE or lowest MSE is advised for practical utility in various kinds of application areas. The theoretical conclusions are validated by the empirical analysis, which made use of the real data sets.

Keywords: Classical statistics, neutrosophic statistics, auxiliary information, bias, mean squared error, percent relative efficiency.

1. Introduction

One of the purpose of sampling theory is to estimate study variable on the basis of auxiliary information with more precision. In sampling theory, we estimate population parameter on the basis of auxiliary variable that has a correlation with study variable. Some of the popular methods used to obtain these objectives to estimate population parameter using ratio, product, regression method of estimation.

Ratio and product estimators are frequently used in survey sampling for getting an improved estimator of population mean given that the auxiliary information is known. The concept of ratio estimator was introduced by [1] as a method for utilising auxiliary information. Ratio estimator compute ratios between the sample means of the study variable and the auxiliary variable and using

known auxiliary data on a variable that is linearly related to the variable under study, is used to estimate the population mean.

Whereas, the product estimator, an additional technique for adding auxiliary information into estimation, was put up by [2]. In the product method of estimation, the sample means of auxiliary variable and study variable are multiplied, and the result is used as the foundation for estimation. Over time, several improvements have been made to the classical ratio and product estimators.

One improvement was proposed by [3], they proposed exponential ratio and product type estimators for estimating unknown population mean of the study variable using auxiliary information.

Several researchers such as [1,5,6,7] accomplished some outstanding work in this area. However, our primary focus here is on proposing almost unbiased estimator using neutrosophic information.

Classical statistics deals with data form by crisp numbers and there is no uncertainty in measurement of the observation. But there are so many cases when indeterminacy, vagueness, ambiguousness exists in the data. In day-to-day life where we have indeterminate data, for illustration, the measurement of temperature anywhere, decision support systems, information systems, the weather forecast, economy growth and more. In such cases we need to introduce new techniques to handle with such type of indeterminate data. Fuzzy logic is one method for resolving these kinds of issues regarding ambiguous, imprecise or uncertain observation but still, it ignores indeterminacy. In this situation, neutrosophic techniques are more suitable which address both randomness and indeterminacy.

While classical statistics deals with determinate and crisp values, neutrosophic statistics deals with sets values. As an extension of classical statistics, neutrosophic statistics is identical as classical statistics in the absence of indeterminacy, [9]. The evaluation of both determinate and indeterminate components of the observations is possible with neutrosophic logic, which is an extension of fuzzy logic. It is particularly useful for analysing data that is imprecise or unclear, as noted by [9].

Neutrosophic statistics can be used to solve a number of real-world issues as neutrosophic statistics to the analysis of road traffic accidents, [10]. [11] introduced a goodness-of-fit test within the framework of neutrosophic statistics and [12] concentrated on using neutrosophic analysis of variance on data from university students. In neutrosophic statistics, the sample size may not be precisely determined and not known as the exact number, [13]. Methods based on fuzzy logic are rapidly evolving and frequently used in decision-making settings, [14]. Further advancement of fuzzy sets is complex fuzzy sets, and a complex neutrosophic set is their generalized form. Estimation using neutrosophic techniques are a relatively new and mostly unexplored area compared to estimation challenges in classical probability sampling designs with definite and well-defined data, [15].

Classical statistics struggled to handle indeterminacies that arise from ambiguous, imprecise or incomplete frequency-related data, because it involved values that were uncertain and could include a range of possible measurements. Therefore, neutrosophic statistics is used as a more adaptable and extension of classical statistics in uncertain or indeterminacy situations. However, there has been limited attention given to neutrosophic sampling as compare to classical statistics for estimating the population parameters.

Frame of our paper is constructed in the following manner: Section 1 mentioned Introduction. Section 2 discussed about observation and terminology of neutrosophic statistics. Section 3 outlines some existing neutrosophic estimators. Section 4 presents the proposed neutrosophic almost

unbiased estimator. Section 5 mentioned some member of the proposed estimator. Section 6 presents empirical study. Section 7 is devoted to discussion whereas section 8 discusses the conclusion.

2. Neutrosophic observation and terminology

Numerous kinds of neutrosophic observations were provided, such as quantitative neutrosophic data that suggested a number might fall within an unknown interval (a,b), [9]. There are several ways to represent the interval value of a neutrosphic number. [16] and [17] have used neutrosophic interval values as $Z_N = Z_L + Z_U I_N$, where, $I_N \in [I_L, I_U]$. In addition, we apply the same notations from [17] to the considered neutrosophic data, which are represented in the intervals form as $Z_N \in [Z_L, Z_U]$, where, 'Z_L'is the lower value and ‘ Z_U ’ is the upper value of the neutrosophic variable Z_N. We choose a neutrosophic sample of size $n_N \in [n_L, n_U]$ using the simple random sampling without replacement (SRSWOR) technique from a finite population of 'N' units $(P_1, P_2, ..., P_N)$. Let $y_N(i) \in [y_L, y_U]$ be the ith sample observation of our neutrosophic data. The auxiliary variable $x_N(i)$ is similarly represented as $x_N(i) \in [x_L, x_U]$.

Let $\bar{y}_N(i) \in [\bar{y}_L, \bar{y}_U]$ and $\bar{x}_N(i) \in [\bar{x}_L, \bar{x}_U]$ be sample mean for the neutrosophic y_N and x_N respectively and neutrosophic auxiliary variable x_N is correlated to our neutrosophic study variable y_N. The population means for the neutrosophic variables y_N and x_N, which represent the overall averages of the neutrosophic data set, are represented by $\bar{Y}_N \in [\bar{Y}_L, \bar{Y}_U]$ and $\bar{X}_N \in [\bar{X}_L, \bar{X}_U]$ respectively. For y_N and x_N, the neutrosophic coefficients of variation are $C_{yN} \in [C_{yNL}, C_{yNU}]$ and $C_{xN} \in [C_{xNL}, C_{xNU}]$ respectively. Furthermore, the neutrosophic correlation coefficient between neutrosophic variables x_N and y_N is denoted as $\rho_{yxN} \in \left[\rho_{yxL}, \rho_{yxU}\right]$. The neutrosophic coefficient of kurtosis for auxiliary variable x_N is denoted by $\beta_{2(x)N} \in [\beta_{2(x)\mathrm{L}}, \beta_{2(x)\mathrm{U}}]$. The neutrosophic mean errors are $\bar{\mathrm{e}}_{yN} \in [\bar{\mathrm{e}}_{yL}, \bar{\mathrm{e}}_{yU}]$ and $\bar{\mathrm{e}}_{xN} \in [\bar{\mathrm{e}}_{xL}, \bar{\mathrm{e}}_{xU}]$. In order to find the estimator's bias and MSE, we write

$$\bar{\mathrm{y}}_N(i) = \bar{Y}_N\left(1 + \bar{e}_{yN}(i)\right), \quad \bar{x}_N(i) = \bar{X}_N\left(1 + \bar{e}_{xN}(i)\right),$$

$$E(\bar{e}_{xN}) = E(\bar{e}_{yN}) = 0 \text{ and}$$

$$E(\bar{e}_{yN}^2) = \theta_N C_{yN}^2, \quad E(\bar{e}_{xN}^2) = \theta_N C_{xN}^2, \quad E(\bar{e}_{xN}\bar{e}_{yN}) = \theta_N \rho_{yxN} C_{yN} C_{xN} .$$

Where, $\bar{e}_{yN} \in [\bar{e}_{yL}, \bar{e}_{yU}]$, $\bar{e}_{xN} \in [\bar{e}_{xL}, \bar{e}_{xU}]$, $\bar{e}_{yN}\bar{e}_{xN} \in [\bar{e}_{yL}\bar{e}_{xL}, \bar{e}_{yU}\bar{e}_{xU}]$, $\bar{e}_{yN}^2 \in [\bar{e}_{yL}^2, \bar{e}_{yU}^2]$, $\bar{e}_{xN}^2 \in [\bar{e}_{xL}^2, \bar{e}_{xU}^2]$.

$$C_{xN}^2 = \frac{\sigma_{xN}^2}{\bar{X}_N^2} \quad , \quad C_{yN}^2 = \frac{\sigma_{yN}^2}{\bar{Y}_N^2}, \; C_{yxN} = \rho_{yxN} C_{yN} C_{xN},$$

where, $C_{xN}^2 \in [C_{xL}^2, C_{xU}^2]$, $C_{yN}^2 \in [C_{yL}^2, C_{yU}^2]$.

$$\rho_{yxN} = \frac{\sigma_{yxN}}{\sigma_{yN}\sigma_{xN}} \ , \ \rho_{yxN} \in [\rho_{yxL}, \rho_{yxU}],$$

$$\theta_N = \frac{(1-f_N)}{n_N}, \text{ where, } \theta_N \in [\theta_L, \theta_U], \ n_N \in [n_L, n_U] \ , \ \sigma_{xN}^2 \in [\sigma_{xL}^2, \sigma_{xU}^2], \ \sigma_{yN}^2 \in [\sigma_{yL}^2, \sigma_{yU}^2],$$

$$\sigma_{yxN} \in [\sigma_{yxL}, \sigma_{yxU}].$$

Likewise, in a neutrosophic environment, bias and MSE can be defined as $Bias(\bar{y}_N) \in [Bias_L, Bias_U]$, $MSE(\bar{y}_N) \in [MSE_L, MSE_U]$ respectively.

The graph below illustrates the flowchart of the proposed study employing neutrosophic numbers. The flowchart below has been recommended by [16].

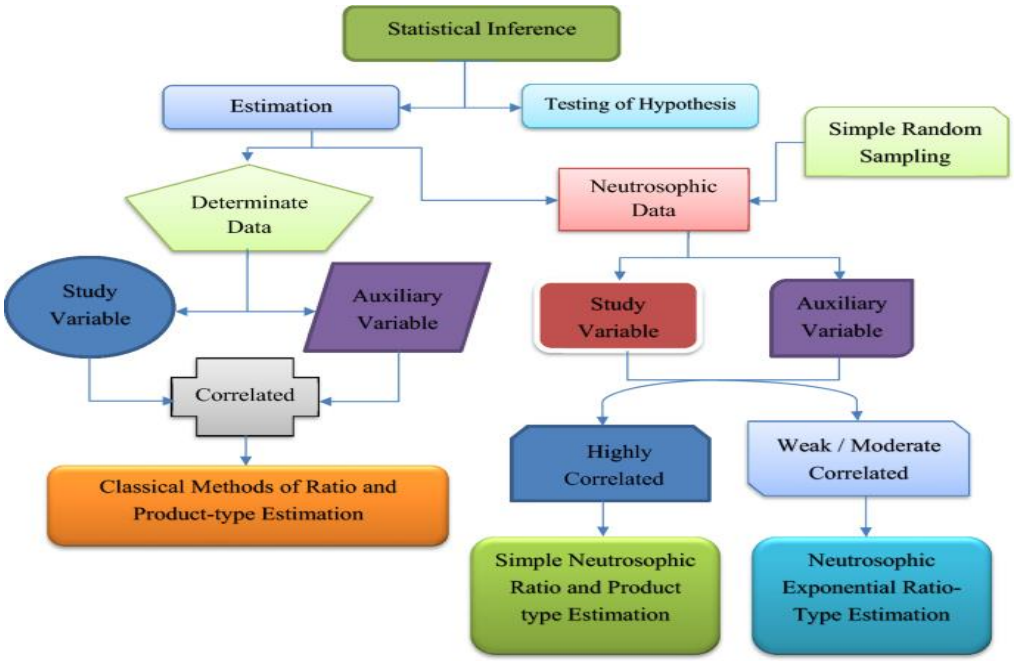

3. Some existing neutrosophic estimators

The estimation of neutrosophic population mean $\bar{Y}_N$ using neutrosophic sample mean which is provided by,

$$t_{1N} = \bar{y}_N \tag{3.1}$$

The variance of the estimator t_{1N} to the first order of approximation is provided by,

$$V(t_{1N}) = \theta_N \bar{Y}_N^2 C_{yN}^2 \ , \text{ where, } t_{1N} \in [t_{1L}, t_{1U}]. \tag{3.2}$$

[16] recommended the usual neutrosophic ratio estimator of neutrosophic population mean $\bar{Y}_N$ utilising the known neutrosophic population mean of X as,

$$t_{2N} = \bar{y}_N \left(\frac{\bar{X}_N}{\bar{x}_N} \right) \tag{3.3}$$

The bias term and MSE of the estimator t_{2N} are given by, respectively

$$Bias(t_{2N}) = \theta_N \bar{Y}_N (C_{xN}^2 - C_{yxN}) \tag{3.4}$$

$$MSE(t_{2N}) = \theta_N \bar{Y}_N^2 \left(C_{yN}^2 + C_{xN}^2 - 2C_{yxN} \right) \tag{3.5}$$

Where, $C_{yxN} = \rho_{yxN} C_{xN} C_{yN}$ and $t_{2N} \in [t_{2L}, t_{2U}]$.

Motivated by [2], the neutrosophic product estimators is given by,

$$t_{3N} = \bar{y}_N \left(\frac{\bar{x}_N}{\bar{X}_N} \right) \tag{3.6}$$

The bias and MSE of the estimator's (t_{3N}) are provided by,

$$Bias(t_{3N}) = \theta_N \bar{Y}_N C_{yxN} \tag{3.7}$$

$$MSE(t_{3N}) = \theta_N \bar{Y}_N^2 \left(C_{yN}^2 + C_{xN}^2 + 2C_{yxN} \right) \text{ , where, } t_{3N} \in [t_{3L}, t_{3U}]. \tag{3.8}$$

Inspired by [4], [16] proposed the following neutrosophic ratio estimator that utilises the coefficient of variation (CV) of the neutrosophic variable X as,

$$t_{4N} = \bar{y}_N \left(\frac{\bar{X}_N + C_{xN}}{\bar{x}_N + C_{xN}} \right) \tag{3.9}$$

The bias and MSE of the estimator t_{4N}, up to the first order of approximation are respectively,

$$Bias(t_{4N}) = \theta_N \bar{Y}_N (\lambda_{1N}^2 C_{xN}^2 - \lambda_{1N} C_{yxN}) \tag{3.10}$$

$$MSE(t_{4N}) = \theta_N \bar{Y}_N^2 \left(C_{yN}^2 + \lambda_{1N}^2 C_{xN}^2 - 2\lambda_{1N} C_{yxN} \right) \tag{3.11}$$

where, $\lambda_{1N} = \dfrac{\bar{X}_N}{\bar{X}_N + C_{xN}}$ and $t_{4N} \in [t_{4L}, t_{4U}]$.

Motivated by [3], [16] suggested the following neutrosophic exponential ratio-type estimator as follows:

$$t_{5N} = \bar{y}_N \exp\left(\frac{\bar{X}_N - \bar{x}_N}{\bar{x}_N + \bar{X}_N} \right) \tag{3.12}$$

The estimator's (t_{5N}) bias and MSE are provided by,

$$Bias(t_{5N}) = \theta_N \bar{Y}_N \left(\frac{3}{8} C_{xN}^2 - \frac{1}{2} C_{yxN} \right) \tag{3.13}$$

$$MSE(t_{5N}) = \theta_N \bar{Y}_N^2 \left(C_{yN}^2 + \frac{C_{xN}^2}{4} - C_{yxN} \right) \text{ , where, } t_{5N} \in [t_{5L}, t_{5U}]. \tag{3.14}$$

Motivated by [3], [18] suggested the neutrosophic product-type exponential estimator as,

$$t_{6N} = \bar{y}_N \exp\left(\frac{\bar{x}_N - \bar{X}_N}{\bar{x}_N + \bar{X}_N} \right) \tag{3.15}$$

The bias and MSE of the estimator t_{6N} are given by,

$$Bias(t_{6N}) = \theta_N \bar{Y}_N \left(\frac{3}{8} C_{xN}^2 + \frac{1}{2} C_{yxN} \right) \tag{3.16}$$

$$MSE(t_{6N}) = \theta_N \bar{Y}_N^2 \left(C_{yN}^2 + \frac{C_{xN}^2}{4} + C_{yxN} \right) \text{ , where, } t_{6N} \in [t_{6L}, t_{6U}]. \tag{3.17}$$

Motivated by [19], [17] suggested the neutrosophic ratio estimator t_{7N}, utilising the known population coefficient of correlation ρ_{yxN} is provided as,

$$t_{7N} = \bar{y}_N \left(\frac{\bar{X}_N + \rho_{yxN}}{\bar{x}_N + \rho_{yxN}} \right) \tag{3.18}$$

The bias and MSE of the estimator t_{7N} are respectively given as,

$$Bias(t_{7N}) = \theta_N \bar{Y}_N (\lambda_{2N}^2 C_{xN}^2 - \lambda_{2N} C_{yxN}) \tag{3.19}$$

$$MSE(t_{7N}) = \theta_N \bar{Y}_N^2 \left(C_{yN}^2 + \lambda_{2N}^2 C_{xN}^2 - 2\lambda_{2N} C_{yxN} \right) \tag{3.20}$$

where, $\lambda_{2N} = \dfrac{\bar{X}_N}{\bar{X}_N + \rho_{yxN}}$ and $t_{7N} \in [t_{7L}, t_{7U}]$.

Inspired by [20], [17] proposed the neutrosophic ratio estimators utilising CV and the coefficient of kurtosis of auxiliary variable X, expressed as follows:

$$t_{8N} = \bar{y}_N \left(\frac{\beta_{2(x)N} \bar{X}_N + C_{xN}}{\beta_{2(x)N} \bar{x}_N + C_{xN}} \right) \tag{3.21}$$

The estimator's (t_{8N}) bias and MSE are defined as,

$$Bias(t_{8N}) = \theta_N \bar{Y}_N (\lambda_{3N}^2 C_{xN}^2 - \lambda_{3N} C_{yxN}) \tag{3.22}$$

$$MSE(t_{8N}) = \theta_N \bar{Y}_N^2 \left(C_{yN}^2 + \lambda_{3N}^2 C_{xN}^2 - 2\lambda_{3N} C_{yxN} \right) \tag{3.23}$$

where, $\lambda_{3N} = \dfrac{\beta_{2(x)N}\bar{X}_N}{\beta_{2(x)N}\bar{X}_N + C_{xN}}$ and $t_{8N} \in [t_{8L}, t_{8U}]$.

Motivated by [8], [16] recommended the neutrosophic modified exponential ratio estimator defined as,

$$t_{9N} = \bar{y}_N \exp\left(\frac{(a\bar{X}_N + b) - (a\bar{x}_N + b)}{(a\bar{X}_N + b) + (a\bar{x}_N + b)}\right) \tag{3.24}$$

where a and b denotes the auxiliary neutrosophic parameters.

The bias and MSE of the neutrosophic exponential ratio estimator t_{9N} are respectively given as,

$$Bias(t_{9N}) = \theta_N \bar{Y}_N \left(\frac{3}{8}\lambda_{4N}^2 C_{xN}^2 - \frac{1}{2}\lambda_{4N} C_{yxN}\right) \tag{3.25}$$

$$MSE(t_{9N}) = \theta_N \bar{Y}_N^2 \left(C_{yN}^2 + \lambda_{4N}^2 C_{xN}^2 - 2\lambda_{4N} C_{yxN}\right) \tag{3.26}$$

where, $\lambda_{4N} = \dfrac{a\bar{X}_N}{2(a\bar{X}_N + b)}$ and $t_{9N} \in [t_{9L}, t_{9U}]$.

From (3.22) and (3.25), we see that the estimators t_{8N} and t_{9N} recommended by [17], [16] respectively, are biased estimator. Bias is disadvantageous in certain applications.

Motivated by [8] and [17], we have suggested an almost unbiased estimator for the population mean $\bar{Y}_N$ using neutrosophic auxiliary information in SRSWOR.

4. The proposed neutrosophic almost unbiased estimator

Suppose $t_0 = \bar{y}_N$, $t_1 = \left[\bar{y}_N \left(\dfrac{a\bar{X}_N + b}{a\bar{x}_N + b}\right)^K\right]$, $t_2 = \left[\bar{y}_N \exp\left(K\left(\dfrac{(a\bar{X}_N + b) - (a\bar{x}_N + b)}{(a\bar{X}_N + b) + (a\bar{x}_N + b)}\right)\right)\right]$

such that $t_0, t_1, t_2 \in A$, where A is the collection of all possible estimators for estimating the neutrosophic population mean $\bar{Y}_N$. Justification of using a and b in proposing estimators is given by [22]. By definition, the set A is a linear variety if

$$t^* = \sum_{i=0}^{2} \alpha_i t_i \in A. \tag{4.1}$$

$$\text{for } \sum_{i=0}^{2} \alpha_i = 1 \text{ and } \alpha_i \in R. \tag{4.2}$$

where $\alpha_i (i = 0,1,2)$ refers to the statistical constants, R stands for the set of real numbers and K takes distinct values, that is, $K = 1$ for the ratio estimators and $K = -1$ for the product estimators.

The bias and MSE of the estimators t_1 and t_2 are, respectively, given by (up to the first order of approximation)

$$B(t_1) = \theta_N \bar{Y}_N \left[\lambda^2 C_{xN}^2 \left(\frac{K(K+1)}{2} \right) - \lambda K \rho_{yxN} C_{yN} C_{xN} \right] \tag{4.3}$$

$$MSE(t_1) = \theta_N \bar{Y}_N^2 \left[C_{yN}^2 + \lambda^2 K^2 C_{xN}^2 - 2\lambda K \rho_{yxN} C_{yN} C_{xN} \right] \tag{4.4}$$

$$B(t_2) = \theta_N \bar{Y}_N \left[\lambda^2 C_{xN}^2 \left(\frac{2K + K^2}{8} \right) - \frac{\lambda K}{2} \rho_{yxN} C_{yN} C_{xN} \right] \tag{4.5}$$

$$MSE(t_2) = \theta_N \bar{Y}_N^2 \left[C_{yN}^2 + \frac{\lambda^2 K^2}{4} C_{xN}^2 - \lambda K \rho_{yxN} C_{yN} C_{xN} \right] \tag{4.6}$$

where, $\lambda = \dfrac{a\bar{X}_N}{a\bar{X}_N + b}$; a and b denotes the auxiliary neutrosophic parameters.

The bias and MSE of the estimator t^* are determined using,

$\bar{y}_N(i) = \bar{Y}_N \left(1 + \bar{e}_{yN}(i)\right)$, $\bar{x}_N(i) = \bar{X}_N \left(1 + \bar{e}_{xN}(i)\right)$.

Such that, $E(\bar{e}_{xN}) = E(\bar{e}_{yN}) = 0$.

Defining the estimator t^* in terms of $\bar{e}_{xN}$ and $\bar{e}_{yN}$, we obtain,

$$\begin{aligned} t^* &= \alpha_0 \bar{Y}_N \left(1 + \bar{e}_{yN}\right) + \alpha_1 \left[\bar{Y}_N \left(1 + \bar{e}_{yN}\right) \left(\frac{a\bar{X}_N + b}{a\bar{X}_N \left(1 + \bar{e}_{xN}\right) + b} \right)^K \right] \\ &+ \alpha_2 \left[\bar{Y}_N \left(1 + \bar{e}_{yN}\right) \exp\left(K \left(\frac{(a\bar{X}_N + b) - \left(a\bar{X}_N \left(1 + \bar{e}_{xN}\right) + b\right)}{(a\bar{X}_N + b) + \left(a\bar{X}_N \left(1 + \bar{e}_{xN}\right) + b\right)} \right) \right) \right] \\ &= \alpha_0 \bar{Y}_N \left(1 + \bar{e}_{yN}\right) + \alpha_1 \left[\bar{Y}_N \left(1 + \bar{e}_{yN}\right) \left(1 + \lambda \bar{e}_{xN}\right)^{-K} \right] \\ &+ \alpha_2 \bar{Y}_N \left(1 + \bar{e}_{yN}\right) \exp\left[K \left(-\frac{\lambda}{2} \bar{e}_{xN} \left(1 + \frac{\lambda}{2} \bar{e}_{xN} \right)^{-1} \right) \right] \end{aligned} \tag{4.7}$$

where, $\lambda = \dfrac{a\bar{X}_N}{a\bar{X}_N + b}$.

Expanding the terms on the right side of the equation (4.7) and having the terms up to the first order of approximation.

$$t^* = \bar{Y}_N \left[\begin{array}{l} (\alpha_0+\alpha_1+\alpha_2)+(\alpha_0+\alpha_1+\alpha_2)\bar{e}_{yN} - \lambda K \bar{e}_{xN}\left(\alpha_1+\frac{\alpha_2}{2}\right)+\alpha_1\lambda^2\bar{e}_{xN}{}^2\left(\frac{K(K+1)}{2}\right) \\ +\alpha_2\lambda^2\bar{e}_{xN}{}^2\left(\frac{2K+K^2}{8}\right)-K\alpha_1\lambda\bar{e}_{xN}\bar{e}_{yN}-\frac{K}{2}\alpha_2\lambda\bar{e}_{xN}\bar{e}_{yN} \end{array} \right] \tag{4.8}$$

The bias of the estimator t^*, up to the second power of $e's$, can be computed by subtracting $\bar{Y}_N$ from both sides of equation (4.8) after taking the expectation of each side.

$$B(t^*) = \theta_N \bar{Y}_N C_{xN}^2 \left[\alpha_1\lambda^2 \frac{K(K+1)}{2} + \alpha_2\lambda^2\left(\frac{2K+K^2}{8}\right) - \left(K\alpha_1\lambda+\frac{K}{2}\alpha_2\lambda\right)\rho_{yxN}\frac{C_{yN}}{C_{xN}}\right] \tag{4.9}$$

From equation (4.8), we have

$$t^* - \bar{Y}_N \cong \bar{Y}_N\left[\bar{e}_{yN} - \lambda\alpha K\bar{e}_{xN}\right] \tag{4.10}$$

where, $\alpha = \left(\alpha_1 + \frac{\alpha_2}{2}\right)$. (4.11)

By taking square of each side of (4.10) and then taking expectations, we get MSE of the estimator t^*, to the first order of approximation as,

$$MSE(t^*) = \theta_N \bar{Y}_N^2\left[C_{yN}^2 + C_{xN}^2\lambda K\alpha\left(\lambda K\alpha - 2\delta_N\right)\right] \tag{4.12}$$

where, $\delta_N = \rho_{yxN}\frac{C_{yN}}{C_{xN}}$.

Minimum MSE of the estimator t^* would occur when

$$\alpha = \frac{\delta_N}{\lambda K}. \tag{4.13}$$

Applying this value of $\alpha = \frac{\delta_N}{\lambda K}$ in equation (4.1), we get the optimum value of estimator t^* (optimum).

Hence, the minimum MSE of the estimator t^* is provided by

$$\min.MSE\left(t^*\right) = \theta_N \bar{Y}_N^2 C_{yN}^2\left(1-\rho_{yxN}^2\right) \tag{4.14}$$

This MSE is equivalent to the classical linear regression estimator.

By using equation (4.11) and (4.13) we have

$$\alpha_1 + \frac{\alpha_2}{2} = \alpha = \frac{\delta_N}{\lambda K}. \tag{4.15}$$

There are only two equations with three unknowns in equations (4.2) and (4.15). The unique values for $\alpha_i's$, $(i=0,1,2)$ can't be found. In order to get unique values for $\alpha_i's$, we will apply the linear constraint

$$\sum_{i=0}^{2}\alpha_i B(t_i)=0. \tag{4.16}$$

where $B(t_i)$ represents the bias of i^{th} estimator.

The matrix form of equations (4.2), (4.15), and (4.16) is as follows:

$$\begin{pmatrix}1 & 1 & 1\\ 0 & 1 & \frac{1}{2}\\ 0 & B(t_1) & B(t_2)\end{pmatrix}\begin{pmatrix}a_0\\ a_1\\ a_2\end{pmatrix}=\begin{pmatrix}1\\ \alpha\\ 0\end{pmatrix} \tag{4.17}$$

where, $\alpha=\dfrac{\delta_N}{\lambda K}$.

By using equation (4.17), The unique values of $\alpha_i's$ $(i=0,1,2)$ are obtained as,

$$\left.\begin{aligned}\alpha_0&=\frac{B(t_2)-\frac{B(t_1)}{2}-\alpha B(t_2)+\alpha B(t_1)}{B(t_2)-\frac{B(t_1)}{2}}\\ \alpha_1&=\frac{\alpha B(t_2)}{B(t_2)-\frac{B(t_1)}{2}}\\ \alpha_2&=\frac{-\alpha B(t_1)}{B(t_2)-\frac{B(t_1)}{2}}\end{aligned}\right] \tag{4.18}$$

such that,

$\sum_{i=0}^{2}\alpha_i=1$ and $\alpha_i\in R$.

By using these $\alpha_i's$, $\left(i=0,1,2\right)$ eliminate the bias up to terms of order $o(n^{-1})$ at (4.1).

5. Some member of the suggested estimator $'t^*'$

Several estimators of the population mean are provided by choosing the appropriate combination of constants a, b and $\alpha_i's$,$\left(i=0,1,2\right)$, as shown in the following scheme.

Estimator	Values of

	α_0	α_1	α_2	a	b	K
$t_{1N} = \bar{y}_N$ The mean per unit estimator	1	0	0	0	0	1
$t_{2N} = \bar{y}_N \left(\frac{\bar{X}_N}{\bar{x}_N} \right)$ [16] estimator	0	1	0	1	0	1
$t_{3N} = \bar{y}_N \left(\frac{\bar{x}_N}{\bar{X}_N} \right)$ Neutrosophic product estimator	0	1	0	1	0	-1
$t_{4N} = \bar{y}_N \left(\frac{\bar{X}_N + C_{xN}}{\bar{x}_N + C_{xN}} \right)$ [16] estimator	0	1	0	1	C_{xN}	1
$t_{5N} = \bar{y}_N \exp\left(\frac{\bar{X}_N - \bar{x}_N}{\bar{x}_N + \bar{X}_N} \right)$	0	0	1	1	0	1
$t_{6N} = \bar{y}_N \exp\left(\frac{\bar{x}_N - \bar{X}_N}{\bar{x}_N + \bar{X}_N} \right)$ [18] estimator	0	0	1	1	0	-1
$t_{7N} = \bar{y}_N \left(\frac{\bar{X}_N + \rho_{yxN}}{\bar{x}_N + \rho_{yxN}} \right)$	0	1	0	1	ρ_{yxN}	1
$t_{8N} = \bar{y}_N \left(\frac{\beta_{2(x)N} \bar{X}_N + C_{xN}}{\beta_{2(x)N} \bar{x}_N + C_{xN}} \right)$ [17] estimator	0	1	0	$\beta_{2(x)N}$	C_{xN}	1
$t_{9N} = \bar{y}_N \exp\left(\frac{(a\bar{X}_N + b) - (a\bar{x}_N + b)}{(a\bar{X}_N + b) + (a\bar{x}_N + b)} \right)$	0	0	1	a	b	1

In addition, the estimators mentioned above, by simply changing the values of a, b and $\alpha_i's$ ($i = 0,1,2$). From the proposed estimator t^* at (4.1), several estimators can be created.

6. Empirical Study

Population 1 : Here, we use the data provided by [21], which is birth rate and data on the natural growth rate obtained from the sample registration system (SRS)(2020) is used to demonstrate the performance of different estimators of neutrosophic study variable $Y_N \in [Y_L, Y_U]$. The neutrosophic auxiliary variable and neutrosophic study variable are given by,

X_N : Birth rate Y_N : Natural growth rate

The PRE formula is given by

$$PRE = \frac{MSE(\bar{y}_N)}{MSE(\text{estimator})} \times 100 \tag{6.1}$$

Table 1. Descriptive statistics of birth rate and natural growth rate data as per SRS 2020.

Parameter	Neutrosophic Value	Parameter	Neutrosophic Value
N_N	[36, 36]	n_N	[10, 10]
μ_{xN}	[14.472, 18.053]	C_{yN}	[0.333, 0.411]
μ_{yN}	[10.894, 10.631]	ρ_{yxN}	[0.620, 0.849]
C_{xN}	[0.213, 0.236]	$\beta_{2(x)N}$	[3.034, 2.173]

Table 2. Neutrosophic MSEs and PRE of the different estimators.

Estimator	MSE	I_N	PRE
t_{1N}	[0.951886, 1.378714]	[0, 0.31]	[100, 100]
t_{2N}	[0.490003, 0.586746]	[0, 0.16]	[194.26, 234.98]
t_{3N}	[2.092575, 3.174567]	[0, 0.34]	[43.43, 45.49]
t_{4N}	[2.070519, 3.145647]	[0, 0.34]	[43.83, 45.97]
t_{5N}	[0.672372, 0.820965]	[0, 0.18]	[141.57, 167.94]
t_{6N}	[1.425287, 2.163247]	[0, 0.34]	[63.73, 66.79]
t_{7N}	[0.510456, 0.586471]	[0, 0.13]	[186.48, 235.09]
t_{8N}	[0.492618, 0.586646]	[0, 0.16]	[193.23, 235.02]
t_{9N} $(a=1, b=1)$	[0.684577, 0.844600]	[0, 0.19]	[139.05, 163.24]
t^*	**[0.385639, 0.586416]**	[0, 0.34]	**[235.11, 246.83]**

Population 2 : Here, we use the data sets considered by [18]. Numerous data points, such as the minimum, maximum and mean temperatures over a wide time duration, are included in this dataset regarding the All India Seasonal and Annual Temperature Series. The neutrosophic auxiliary variable and neutrosophic study variable are given by,

X_N : Minimum and maximum temperatures in January and February.

Y_N : Temperatures from March through May.

Table 3. Descriptive statistics of the population 2.

Parameter	Neutrosophic Value	Parameter	Neutrosophic Value
N_N	[119, 119]	n_N	[20, 20]
μ_{xN}	[13.908,24.674]	C_{yN}	[0.0007, 00.0006]
μ_{yN}	[20.694, 31.560]	ρ_{yxN}	[0.6274, 0.7202]

C_{xN}	[0.0017, 0.0015]	$\beta_{2(x)N}$	[4.973, 5.583]

Table 4. Neutrosophic MSEs and PRE of the different estimators.

Estimator	MSE	I_N	PRE
t_{1N}	[8.87822E-06, 1.72193E-05]	[0, 0.48]	[100.00, 100.00]
t_{2N}	[3.39108E-05, 5.58304E-05]	[0, 0.39]	[26.18, 30.84]
t_{3N}	[8.78263E-05, 0.000173977]	[0, 0.50]	[10.11, 9.90]
t_{4N}	[3.39013E-05, 5.58219E-05]	[0, 0.39]	[26.19, 30.85]
t_{5N}	[8.39692E-06, 1.21037E-05]	[0, 0.31]	[105.73, 142.26]
t_{6N}	[3.53547E-05, 7.1177E-05]	[0, 0.50]	[25.11, 24.19]
t_{7N}	[3.06832E-05, 5.20435E-05]	[0, 0.41]	[28.94, 33.09]
t_{8N}	[3.39089E-05, 5.58288E-05]	[0, 0.39]	[26.18, 30.84]
t_{9N} $(a=1, b=1)$	[7.61584E-06, 1.13888E-05]	[0, 0.33]	[116.58, 151.19]
t^*	**[5.38372E-06, 8.28831E-06]**	[0, 0.35]	**[164.91, 207.75]**

7. Discussion

In Table 2, as can be shown that the sampling variance of the neutrosophic estimator t_{1N} is [0.951886, 1.378714] and the neutrosophic exponential ratio estimator's (t_{5N}) MSE is [0.672372, 0.820965] whereas the range of the neutrosophic MSEs (t_{4N}) is [2.070519, 3.145647]. The reason behind the higher MSEs of the neutrosophic estimators t_{4N} over the neutrosophic estimator t_{1N} is that the low value of the neutrosophic CV of the neutrosophic auxiliary variable x. In comparison to the other population mean $(\bar{Y}_N)$ estimators in competition, the MSE of the proposed class of neutrosophic estimators (t^*) is the lowest at [0.385639, 0.586416] with higher PRE.

Similarly, the proposed and existing estimators' MSEs and PRE are given by Table 4. Additionally, it has shown that the suggested estimators' MSEs and PREs are lower and higher respectively, in comparison to those of the other estimators already in use. Its value is highlighted by the bolded text. Hence, Tables 2 and 4 confirmed these results, showing that the suggested estimators are preferable to the existing ones.

8. Conclusion

In this paper, we have recommended an almost unbiased neutrosophic estimator to estimate the neutrosophic population mean $\bar{Y}_N$ using some known value of auxiliary information. In order to evaluate their precision, we computed bias and MSE for the suggested estimators, concentrating on first-order approximations. We evaluated our suggested estimator with existing estimators using data from a natural environment. Via conducting empirical study, we have identified strong evidence that our suggested estimator performs better than the existing ones within the context of neutrosophic sampling. It should be emphasised that in cases where the study variable's observations are nondeterministic or uncertain, the neutrosophic estimators are best suited for enhanced population mean estimate. Therefore, it might be advised to use the proposed class of estimators to

estimate the neutrosophic population mean $\overline{Y}_N$ in a variety of real-world settings, including those in the social sciences, economics, agriculture, biology and mathematics.

References

[1] W. G. Cochran, "The estimation of the yields of cereal experiments by sampling for the ratio of grain to total produce," J. Agric. Sci., vol. 30, no. 2, pp. 262–275, Apr. 1940, doi: 10.1017/S0021859600048012.

[2] M. N. Murthy, "Product method of estimation," Sankhyā Indian J. Stat. Ser. A. (1961-2002), Vol. 26, No. 1, pp. 69-74, Jul.1964, https://www.jstor.org/stable/25049308.

[3] S. Bahl and R. K. Tuteja, "Ratio and product type exponential estimators," J. Inf. Optim. Sci., vol. 12, no. 1, pp. 159–164, Jan. 1991, doi:10.1080/02522667.1991.10699058.

[4] B. V. S. Sisodia and V. K. Dwivedi, "A modified ratio estimator using coefficient of variation of auxiliary variable," J Indian Soc Agric Stat, 33(1), 13–18, 1981.

[5] C. Kadilar and H. Cingi, "Ratio estimators in simple random sampling," Appl. Math. Comput., vol.151, no. 3, pp. 893–902, Apr. 2004, doi:10.1016/S0096-3003(03)00803-8.

[6] R. Singh, R. Mishra, A. Kumari, and S. K. Yadav, "Almost unbiased estimators for population coefficient of variation using auxiliary information," Asian J. Probab. Stat., vol. 26, no. 5, pp. 1–18, May 2024, doi:10.9734/ajpas/2024/v26i5614.

[7] H. P. Singh and R. S. Solanki, "A new procedure for variance estimation in simple random sampling using auxiliary information," Stat. Pap., vol. 54, no. 2, pp. 479–497, May 2013, doi:10.1007/s00362-012-0445-2.

[8] R. Singh, P. Chauhan, F. Smarandache, and N. Sawan, "Auxiliary information and a priori values in construction of improved estimators," Infinite Study, 2007.

[9] F. Smarandache, "Introduction to neutrosophic statistics," Infinite Study, 2014.

[10] M. Aslam, "Monitoring the road traffic crashes using NEWMA chart and repetitive sampling," International Journal of Injury Control and Safety Promotion, 28(1), pp. 39–45. 2020, doi:10.1080/17457300.2020.1835990.

[11] M. Aslam, "A new goodness of fit test in the presence of uncertain parameters," Complex Intell. Syst., Oct. 2020, doi:10.1007/s40747-020-00214-8.

[12] M. Aslam, "Neutrosophic analysis of variance: application to university students," Complex Intell. Syst., vol. 5, no. 4, pp. 403–407, Dec. 2019, doi:10.1007/s40747-019-0107-2.

[13] F. Smarandache, "A unifying field in logics: Neutrosophic logic, neutrosophic set, neutrosophic probability, and statistics. arXiv preprint math/0101228 - 6th ed.". 2001.

[14] N. Jan, L. Zedam, T. Mahmood, K. Ullah, and Z. Ali, "Multiple attribute decision making method under linguistic cubic information," J. Intell. Fuzzy Syst., vol. 36, no. 1, pp. 253–269, Jan. 2019, doi:10.3233/JIFS-181253.

[15] R. Varshney, A. Pal, Mradula, and I. Ali, "Optimum allocation in the multivariate cluster sampling design under gamma cost function," J. Stat. Comput. Simul., vol. 93, no. 2, pp. 312–323, Jan. 2023, doi:10.1080/00949655.2022.2104845.

[16] Z. Tahir, H. Khan, M. Aslam, J. Shabbir, Y. Mahmood, and F. Smarandache, "Neutrosophic ratio-type estimators for estimating the population mean," Complex Intell. Syst., vol. 7, no. 6, pp. 2991–3001, Dec. 2021, doi:10.1007/s40747-021-00439-1.

[17] S. K. Yadav and F. Smarandache, "Generalized neutrosophic sampling strategy for elevated estimation of population mean," Neutrosophic Sets and Systems, Vol. 53, 2023 SSRN doi:10.2139/ssrn.4652035.

[18] V. K. Yadav and S. Prasad, "Neutrosophic estimators for estimating the population mean in survey sampling," Meas. Interdiscip. Res. Perspect., pp. 1–25, Mar. 2024, doi: 10.1080/15366367.2023.2267835.

[19] H. P. Singh and R. Tailor, "Estimation of finite population mean using known correlation coefficient between auxiliary characters," Statistica, vol. 65, no. 4, Art. no. 4, 2005, doi: 10.6092/issn.1973-2201/1300.

[20] L. N. Upadhyaya and H. P. Singh, "Use of transformed auxiliary variable in estimating the finite population mean," Biom. J., vol. 41, no. 5, pp. 627–636, 1999, doi: 10.1002/(SICI)1521-4036(199909)41:5<627::AID-BIMJ627>3.0.CO;2-W.

[21] R. Singh and A. Kumari, "Neutrosophic ranked set sampling scheme for estimating population mean: An application to demographic data," Neutrosophic Sets and Systems, Vol. 68, 2024, doi:10.5281/zenodo.11479519.

[22] R. Singh and M. Kumar, "A note on transformations on auxiliary variable in survey sampling," Model Assist. Stat. Appl., vol. 6, no. 1, pp. 17–19, Mar. 2011, doi: 10.3233/MAS-2011-0154.

Received: July 26, 2024. Accepted: Oct 25, 2024

Neutrosophic Sets and Systems, Vol. 76, 2025
University of New Mexico

An efficient Model for Satisfaction Evaluation of College Students' Online Ideological and Political Education with Single-Valued Neutrosophic Numbers

Kelei Shi
Shandong Women's University, Jinan, 250300, Shandong, China
Corresponding author: E-mail: 24004@sdwu.edu.cn

Abstract: Under the background of big data, the evaluation of college students' satisfaction with online ideological and political education (IAPE) is primarily achieved through data mining and analysis techniques, allowing for a more comprehensive and accurate reflection of students' attitudes and feedback. By collecting data through online surveys, social media interactions, and other channels, educators can adjust the content and methods of teaching in real-time to better meet students' needs and improve the effectiveness and satisfaction of IAPE. The satisfaction evaluation of college students' online IAPE in the context of big data is a multi-attribute group decision-making (MAGDM) problem. Recently, VIKOR method have been applied to address MAGDM challenges. Single-valued neutrosophic sets (SVNSs) are employed as a tool to represent uncertain data in the satisfaction evaluation of college students' online IAPE within the big data context. In this paper, we propose the single-valued neutrosophic number VIKOR (SVNN-VIKOR) method to solve MAGDM problems under SVNSs. Finally, a numerical case study is presented to validate the effectiveness of the proposed method in evaluating the satisfaction of college students' online IAPE in the context of big data.

Keywords: MAGDM; SVNSs; information entropy; VIKOR approach; satisfaction of college students' online IAPE

1. Introduction

In the context of big data, research on the satisfaction evaluation of college students' online ideological and political education has become an important topic in the field of education. With the rapid development of internet technology, online ideological and political education has become a crucial part of ideological and political education in universities. Through online

platforms, students can access learning resources anytime and anywhere, participate in interactions, and enhance their political literacy. However, scientifically and comprehensively evaluating students' satisfaction with online ideological and political education is key to improving the quality and effectiveness of education. First, the evaluation of satisfaction requires the establishment of a multidimensional evaluation index system. Common indicators include platform usability and ease of operation, richness and practicality of content, interactivity (such as communication between students and teachers, or among students), the timeliness and quality of educational resources, and the effectiveness of students' learning and ideological progress. Additionally, emotional experiences, such as students' interest in the course, level of participation, and recognition of the ideological content, are also critical dimensions. Second, big data technologies can be used to achieve comprehensive satisfaction analysis. By collecting data on students' learning behaviors on the platform, such as study duration, interaction frequency, and assignment submissions, combined with surveys and online feedback, a thorough evaluation that combines both quantitative and qualitative analysis can be conducted. Finally, the research results should provide guidance for improving online ideological and political education, helping educators optimize teaching content and methods to enhance the effectiveness of political education for students. The satisfaction evaluation of college students' online IAPE in the context of big data represents a classical MAGDM problem. Decision-makers (DMs) often utilize SVNSs [1] in the satisfaction evaluation of college students' online IAPE in the context of big data. The SVNSs [1] offer significant advantages in handling uncertainty and fuzzy information. First, SVNSs can simultaneously represent truth, falsity, and indeterminacy, providing a more flexible modeling approach compared to traditional fuzzy sets or intuitionistic fuzzy sets. This allows for a precise description of uncertainty in complex systems. Second, SVNSs effectively address common issues of uncertainty and incomplete information in decision-making, especially in cases where information is ambiguous or contradictory. Third, SVNSs offer greater flexibility by independently representing truth, falsity, and indeterminacy in a three-dimensional space, thereby improving the accuracy and rationality of decisions. Finally, SVNSs are widely applied in areas such as multi-criteria decision-making, risk assessment, and medical diagnosis,

making them particularly suitable for dealing with fuzzy and uncertain information in complex decision environments. Thus, SVNSs provide a powerful and flexible solution for uncertainty-related problems. However, due to limited knowledge about the decision domain and time constraints, the attribute weights are frequently unknown. This challenge motivated us to develop a novel decision-making approach to determine weight values based on entropy under SVNSs. Gomes and Lima [2] and Gomes and Lima [3] initially introduced the TODIM method for MADM under risk, and later, Leoneti and Gomes [4] proposed the Exponential TODIM (ExpTODIM). While many decision algorithms use ExpTODIM[4-6] and VIKOR[7, 8] methods independently to identify optimal decisions, few have explored the VIKOR under SVNSs. To address this gap, we propose an integrated SVNN-VIKOR method to solve the MAGDM problem. An illustrative example of satisfaction evaluation of college students' online IAPE in the context of big data, accompanied by a comparative analysis, is provided to validate the effectiveness and reliability of the SVNN-VIKOR approach.

The main contributions of this paper are:

(1) To design an information entropy method using SVNSs to derive weight information.

(2) To establish an integrated SVNN -VIKOR method to solve the MAGDM problem; and

(3) To present an illustrative example of satisfaction evaluation of college students' online IAPE in the context of big data to demonstrate the effectiveness of SVNN- -VIKOR method.

The structure of this paper is outlined: Section 2 introduces the literature review. Section 3 introduces the concept of SVNSs. In Section 4, the SVNN-VIKOR method, incorporating entropy, is developed under the SVNS framework. Section 5 presents an illustrative case study on the satisfaction evaluation of college students' online IAPE in the context of big data, along with a comparative analysis. Finally, concluding remarks are provided in Section 6.

2. Literature review

With the rapid development of internet technology, big data is injecting new vitality into IAPE in universities, driving powerful transformations in the field of higher education. The internet has become an essential domain for today's college students, which means that universities

need to leverage big data technology to innovate and advance IPE work. This approach not only focuses on students' genuine needs but also seeks to gain their recognition, thus effectively fulfilling President Xi Jinping's directive for universities to make IPE "contextualized, timely, and innovative" [9]. Universities primarily utilize platforms such as official websites, WeChat public accounts, and TikTok to deliver IPE content. The satisfaction of college students with online IPE refers to their evaluation of the effectiveness of these virtual educational activities [10]. Although the concept of "IAPE" does not exist in foreign countries, extensive research has been conducted in areas such as civic education, moral education, and legal education. In the United States, advanced network technologies have facilitated the emergence of online education as a new form of IPE [11]. Compared to foreign studies on online IPE, Chinese scholars have conducted more detailed research on the subject, exploring it from various perspectives. From the standpoint of online platforms, online IPE in China primarily uses live streaming platforms, the "Xuexi Qiangguo" app, and short videos on TikTok to achieve high interactivity and real-time engagement. By employing big data technology, universities have enhanced their ability to educate and guide students in ideological and political matters, thereby improving the overall effectiveness of IPE [12, 13]. From the perspective of the educational environment, universities are utilizing artificial intelligence, big data, and other digital technologies to comprehensively monitor internet public opinion related to their institutions, placing online public opinion management as a high priority in campus governance. This approach ensures that students are guided toward the correct values, enhances their critical thinking skills, and fully realizes the educational function of IPE [14]. At the same time, universities are utilizing online IPE platforms to organize various online cultural activities, encouraging student participation and interaction, thereby increasing students' engagement and sense of belonging [15].

MAGDM is a decision-making method where multiple decision-makers evaluate and select from multiple alternatives based on several attributes or criteria [16-18]. This method is widely used in complex decision-making scenarios, especially when multiple stakeholders are involved, and a variety of factors need to be considered, such as project evaluation, policy making, and supplier selection [19]. The core of MAGDM lies in balancing the weights of

different attributes and forming a rational decision outcome from the information provided by different DMs [20, 21]. In practice, there are two main challenges: first, how to handle the trade-offs between different attributes, and second, how to integrate the preferences and opinions of multiple DMs [22, 23]. To address these issues, common methods include weighted averaging, Analytic Hierarchy Process (AHP), fuzzy set theory, and entropy weighting methods. These approaches aim to assign appropriate weights to each attribute to comprehensively evaluate the advantages and disadvantages of each option. In situations with high uncertainty (such as incomplete or fuzzy information), methods like SVNS and grey system theory are widely used to better handle uncertain data. In recent years, hybrid decision-making models that combine various methods, such as VIKOR [7, 8], have become a research focus in MAGDM. These methods integrate different decision tools to provide more flexible and accurate decision support. The ultimate goal of MAGDM is to synthesize various pieces of information and the opinions of decision-makers to arrive at an optimal or near-optimal decision, ensuring fairness and rationality in the decision-making process[24, 25].

2. Preliminaries

Wang et al. [1] designed the SVNSs

Definition 1 [1]. The SVNSs is designed:

$$YA=\left\{\left(\phi,YT_A\left(\phi\right),YI_A\left(\phi\right),YF_A\left(\phi\right)\right)\middle|\phi\in\Phi\right\} \tag{1}$$

where $YT_A\left(\phi\right),YI_A\left(\phi\right),YF_A\left(\phi\right)$ designed the truth-membership, indeterminacy-membership and falsity-membership, $YT_A\left(\phi\right),YI_A\left(\phi\right),YF_A\left(\phi\right)\in\left[0,1\right]$ and satisfies $0\le YT_A\left(\phi\right)+YI_A\left(\phi\right)+YF_A\left(\phi\right)\le 3$.

The single-valued neutrosophic number (SVNN) is designed as $YA=\left(YT_A,YI_A,YF_A\right)$, where $YT_A,YI_A,YF_A\in\left[0,1\right]$, and $0\le YT_A+YI_A+YF_A\le 3$.

Definition 2 [26]. Let $YA=\left(YT_A,YI_A,YF_A\right)$ and $YB=\left(YT_B,YI_B,YF_B\right)$ be SVNN, score values are designed:

$$SV\left(YA\right)=\frac{\left(2+YT_A-YI_A-YF_A\right)}{3},\ S\left(YA\right)\in\left[0,1\right]. \tag{2-a}$$

$$SV\left(YB\right)=\frac{\left(2+YT_B-YI_B-YF_B\right)}{3},\ S\left(YB\right)\in\left[0,1\right]. \tag{2-a}$$

Definition 3[26]. Let $YA=\left(YT_A,YI_A,YF_A\right)$ and $YB=\left(YT_B,YI_B,YF_B\right)$ be SVNN, an accuracy value is designed:

$$HV\left(YA\right)=YT_A-YF_A,\ AV\left(YA\right)\in\left[-1,1\right]. \tag{3}$$

$$HV\left(YB\right)=YT_B-YF_B,\ AV\left(YB\right)\in\left[-1,1\right]. \tag{3}$$

Peng, Wang, Wang, Zhang and Chen [26] designed the order for SVNNs.

Definition 4[26]. Let $YA=\left(YT_A,YI_A,YF_A\right)$ and $YB=\left(YT_B,YI_B,YF_B\right)$ be two given SVNNs, $SV\left(YA\right)=\frac{\left(2+YT_A-YI_A-YF_A\right)}{3}$ and $SV\left(YB\right)=\frac{\left(2+YT_B-YI_B-YF_B\right)}{3}$, and $HV\left(YA\right)=YT_A-YF_A$ and $HV\left(YB\right)=YT_B-YF_B$, then if $SV\left(YA\right)<SV\left(YB\right)$, then $YA<YB$; if $SV\left(YA\right)=SV\left(YB\right)$, then (1)if $AV\left(YA\right)=AV\left(YB\right)$, then $YA=YB$; (2) if $AV\left(YA\right)<AV\left(YB\right)$, then $YA<YB$.

Definition 5[1]. Let $YA=\left(YT_A,YI_A,YF_A\right)$ and $YB=\left(YT_B,YI_B,YF_B\right)$ be SVNNs, basic operations are designed:

(1) $YA\oplus YB=\left(YT_A+YT_B-YT_AYT_B,YI_AYI_B,YF_AYF_B\right)$;
(2) $YA\otimes YB=\left(YT_AYT_B,YI_A+YI_B-YI_AYI_B,YF_A+YF_B-YF_AYF_B\right)$;
(3) $\lambda YA=\left(1-\left(1-YYT_A\right)^{\lambda},\left(YI_A\right)^{\lambda},\left(YF_A\right)^{\lambda}\right),\lambda>0$;
(4) $\left(YA\right)^{\lambda}=\left(\left(YT_A\right)^{\lambda},\left(YI_A\right)^{\lambda},1-\left(1-YF_A\right)^{\lambda}\right),\lambda>0.$

Definition 6[27]. Let $YA=\left(YT_A,YI_A,YF_A\right)$ and $YB=\left(YT_B,YI_B,YF_B\right)$, the SVNN Hamming distance (SVNNHD) is designed:

$$SVNNHD\left(XA,XB\right)=\frac{\left|YT_A-YT_B\right|+\left|YI_A-YI_B\right|+\left|YF_A-YF_B\right|}{3} \tag{4}$$

The SVNNWA and SVNNWG approach is designed:

Definition 7[26]. Let $YA_j=\left(YT_j,YI_j,YF_j\right)$ be SVNNs, the SVNNWA is designed:

$$\begin{aligned}&\mathrm{SVNNWA}\left(YA_1, YA_2, \ldots, YA_n\right)\\&=yw_1YA_1 \oplus yw_2YA_2 \ldots \oplus yw_nYA_n = \overset{n}{\underset{j=1}{\oplus}} yw_jYA_j\\&=\left(1-\prod_{j=1}^{n}\left(1-YT_{ij}\right)^{yw_j}, \prod_{k=1}^{l}\left(YF_{ij}\right)^{yw_j}, \prod_{k=1}^{l}\left(YT_{ij}\right)^{yw_j}\right)\end{aligned} \tag{5}$$

where $yw=\left(yw_1, yw_2, ..., yw_n\right)^T$ be weight of YA_j, $yw_j > 0, \sum_{j=1}^{n} yw_j = 1.$

Definition 8[26]. Let $YA_j = \left(YT_j, YI_j, YF_j\right)$ be SVNNs, the SVNNWG approach is designed:

$$\begin{aligned}&\mathrm{SVNNWG}\left(YA_1, YA_2, \ldots, YA_n\right)\\&=\left(YA_1\right)^{yw_1} \otimes \left(YA_2\right)^{yw_2}, \ldots \otimes \left(YA_n\right)^{yw_n} = \overset{n}{\underset{j=1}{\otimes}} \left(YA_j\right)^{yw_j}\\&=\left(\prod_{j=1}^{n}\left(YT_{ij}\right)^{yw_j}, 1-\prod_{j=1}^{n}\left(1-YF_{ij}\right)^{yw_j}, 1-\prod_{j=1}^{n}\left(1-YT_{ij}\right)^{yw_j}\right)\end{aligned} \tag{6}$$

where $yw=\left(yw_1, yw_2, ..., yw_n\right)^T$ be weight of YA_j, $yw_j > 0, \sum_{j=1}^{n} yw_j = 1.$

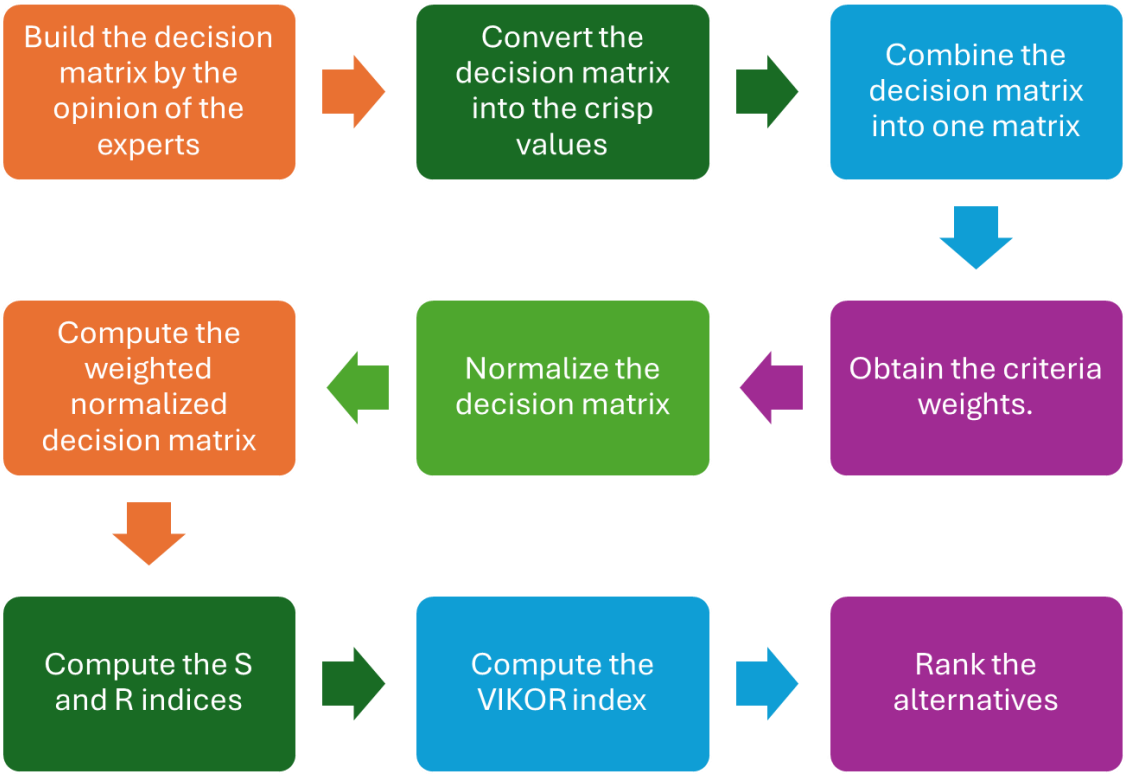

Figure 1. The steps of the SVNN-VIKOR.

3. Materials and Methods

3.1 SVNN-VIKOR Method

VIKOR method is a MAGDM method used to rank the alternatives. The criteria in this method are independent and the qualitative criteria are changed into quantitative criteria. The steps of the SVNN-VIKOR method are shown in Figure 1.

1. Build the decision matrix by the opinion of the experts

$$X^D = \begin{bmatrix} y_{11}^D & \cdots & y_{1n}^D \\ \vdots & \ddots & \vdots \\ y_{m1}^D & \cdots & y_{mn}^D \end{bmatrix} \tag{7}$$

Where $i = 1,2, \dots, n; j = 1,2, \dots m.$

2. Convert the decision matrix into the crisp values.

3. Combine the decision matrix into one matrix.

$$X = \begin{bmatrix} y_{11} & \cdots & y_{1n} \\ \vdots & \ddots & \vdots \\ y_{m1} & \cdots & y_{mn} \end{bmatrix} \tag{8}$$

4. Obtain the criteria weights.

The criteria weights are obtained using the average method.

5. Normalize the decision matrix

$$N_{ij} = \frac{\max y_{ij} - y_{ij}}{\max y_{ij} - \min y_{ij}} \tag{9}$$

6. Compute the weighted normalized decision matrix

$$U_{ij} = w_j * N_{ij} \tag{10}$$

7. Compute the S and R indices

$$S_i = \sum_{j=1}^{n} U_{ij} \tag{11}$$

$$R_i = \max U_{ij}$$

8. Compute the VIKOR index

$$G_i = L * \left(\frac{S_i - \min S_i}{\max S_i - \min S_i}\right) + (1 - L) * \left(\frac{R_i - \min R_i}{\max R_i - \min R_i}\right) \tag{12}$$

Where L refers to the strategic weight and value equal to 0.5.

4. Numerical example and comparative analysis

4.1. Numerical Example for satisfaction evaluation of college students' online IAPE

In the context of big data, the satisfaction evaluation of college students' online IAPE has undergone significant changes. Traditional satisfaction evaluations often relied on surveys or a limited number of interviews, which provided only a small amount of data and made it difficult to comprehensively reflect students' true feelings. The introduction of big data technology allows educators to obtain

information about students' learning behavior, interactions, and feedback from multiple channels and dimensions, enabling more accurate and dynamic satisfaction evaluations. Firstly, big data can collect and process data from various sources in real time, such as usage records from online course platforms, social media comments, and learning interactions. This data includes not only explicit feedback from students (such as ratings and comments) but also implicit behaviors (such as time spent on learning, click rates on pages, frequency of participation in discussions, etc.), providing a more comprehensive perspective for satisfaction evaluation. Secondly, big data analysis helps educators identify different needs and preferences among student groups. By performing statistical and clustering analysis on large datasets, it is possible to discover how students from different backgrounds and with varying learning habits respond differently to online IAPE, thus offering a basis for personalized teaching. This precise analysis can effectively enhance the relevance of education and students' sense of engagement, thereby improving overall satisfaction. Furthermore, big data technology allows educators to dynamically adjust teaching content and methods based on real-time feedback. In the past, evaluations often lagged behind actual teaching, but now, through real-time analysis of big data, educators can quickly understand students' attitudes and learning outcomes, and make timely adjustments to course settings and teaching strategies, thus improving the quality of education. In conclusion, with the support of big data technology, the satisfaction evaluation of college students' online IAPE is not only more comprehensive and accurate but also has the ability to make dynamic adjustments, providing strong support for the optimization and improvement of IAPE. The satisfaction evaluation of college students’ online IAPE in the context of big data is MAGDM.

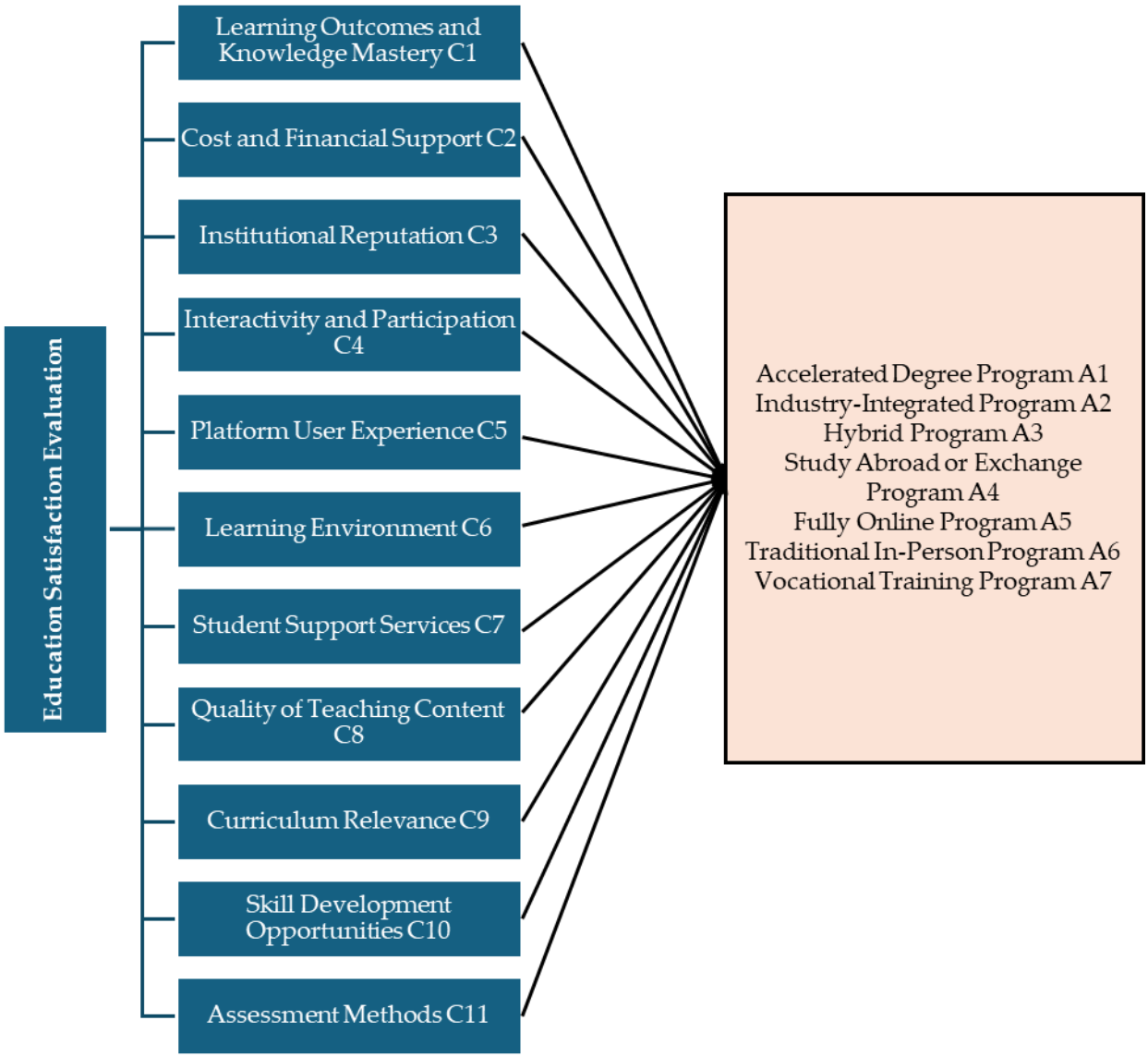

Figure 2. The criteria and alternatives.

We applied the SVNN-VIKOR with 11 criteria and 7 alternatives as shown in Figure 2.

1. Four experts evaluated the criteria and alternatives. They used SVNN. Tables A1-A4.
2. We converted SVNN into crisp values.
3. We combined the decision matrix into one matrix as shown in Table 1.

Table 1. The combined decision matrix.

	A_1	A_2	A_3	A_4	A_5	A_6	A_7
C_1	0.470833	0.620833	0.404167	0.225	0.691667	0.7125	0.7125
C_2	0.341667	0.641667	0.445833	0.508333	0.404167	0.270833	0.616667
C_3	0.445833	0.608333	0.620833	0.379167	0.579167	0.204167	0.5
C_4	0.570833	0.804167	0.466667	0.404167	0.65	0.754167	0.333333
C_5	0.591667	0.65	0.620833	0.445833	0.629167	0.804167	0.166667
C_6	0.720833	0.470833	0.529167	0.445833	0.629167	0.783333	0.066667
C_7	0.783333	0.320833	0.775	0.5875	0.4875	0.5875	0.066667

C_8	0.670833	0.508333	0.670833	0.629167	0.558333	0.570833	0.866667
C_9	0.691667	0.641667	0.4	0.375	0.3625	0.516667	0.783333
C_{10}	0.245833	0.629167	0.6	0.5375	0.491667	0.166667	0.783333
C_{11}	0.291667	0.558333	0.5375	0.4875	0.416667	0.616667	0.616667

4. Then we will compute the criteria weights as shown in Figure 3. we show the criterion 8 has the highest weight and criterion 2 has the lowest weight.

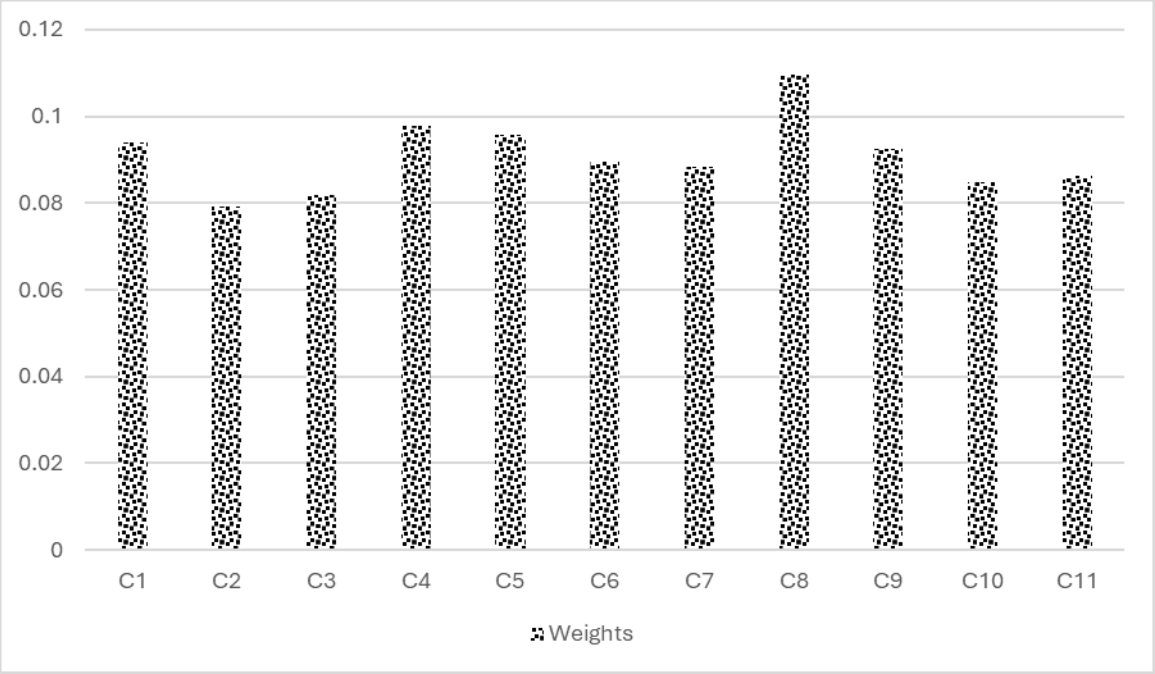

Figure 3. The criteria weights.

5. We normalized the decision matrix as shown in Table 2.

Table 2. The normalized decision matrix.

	A_1	A_2	A_3	A_4	A_5	A_6	A_7
C_1	0.495726	0.188034	0.632479	1	0.042735	0	1.03E-09
C_2	0.191011	1	0.47191	0.640449	0.359551	0	0.932584
C_3	0.42	0.03	0	0.58	0.1	1	0.29
C_4	0.495575	0	0.716814	0.849558	0.327434	0.106195	1
C_5	0.333333	0.24183	0.287582	0.562092	0.27451	0	1
C_6	0.087209	0.436047	0.354651	0.47093	0.215116	0	1
C_7	0	0.645349	0.011628	0.273256	0.412791	0.273256	1
C_8	0.546512	1	0.546512	0.662791	0.860465	0.825581	0
C_9	0.217822	0.336634	0.910891	0.970297	1	0.633663	0
C_{10}	0.871622	0.25	0.297297	0.398649	0.472973	1	0
C_{11}	1.625	0.291667	0.395833	0.645833	1	0	0

6. We compute the weighted normalized decision matrix as shown in Table 3.

Table 3. The weighted normalized decision matrix.

	A_1	A_2	A_3	A_4	A_5	A_6	A_7
C_1	0.046655	0.017697	0.059525	0.094114	0.004022	0	9.65E-11
C_2	0.015127	0.079195	0.037373	0.05072	0.028475	0	0.073856
C_3	0.034378	0.002456	0	0.047474	0.008185	0.081852	0.023737

C_4	0.048413	0	0.070026	0.082994	0.031987	0.010374	0.097691
C_5	0.03195	0.02318	0.027565	0.053877	0.026312	0	0.095851
C_6	0.007798	0.038988	0.031711	0.042107	0.019234	0	0.089413
C_7	0	0.057109	0.001029	0.024181	0.036529	0.024181	0.088494
C_8	0.059979	0.109749	0.059979	0.07274	0.094435	0.090606	0
C_9	0.020144	0.031132	0.084238	0.089732	0.092479	0.058601	0
C_{10}	0.073838	0.021178	0.025185	0.033771	0.040067	0.084713	0
C_{11}	0.140481	0.025215	0.03422	0.055832	0.08645	0	0

7. We compute the S and R indices.
8. We complete the VIKOR index we put the L with 0.5 as shown in Figure 4. We show the alternative 6 is the best and alternative 1 is the worst.

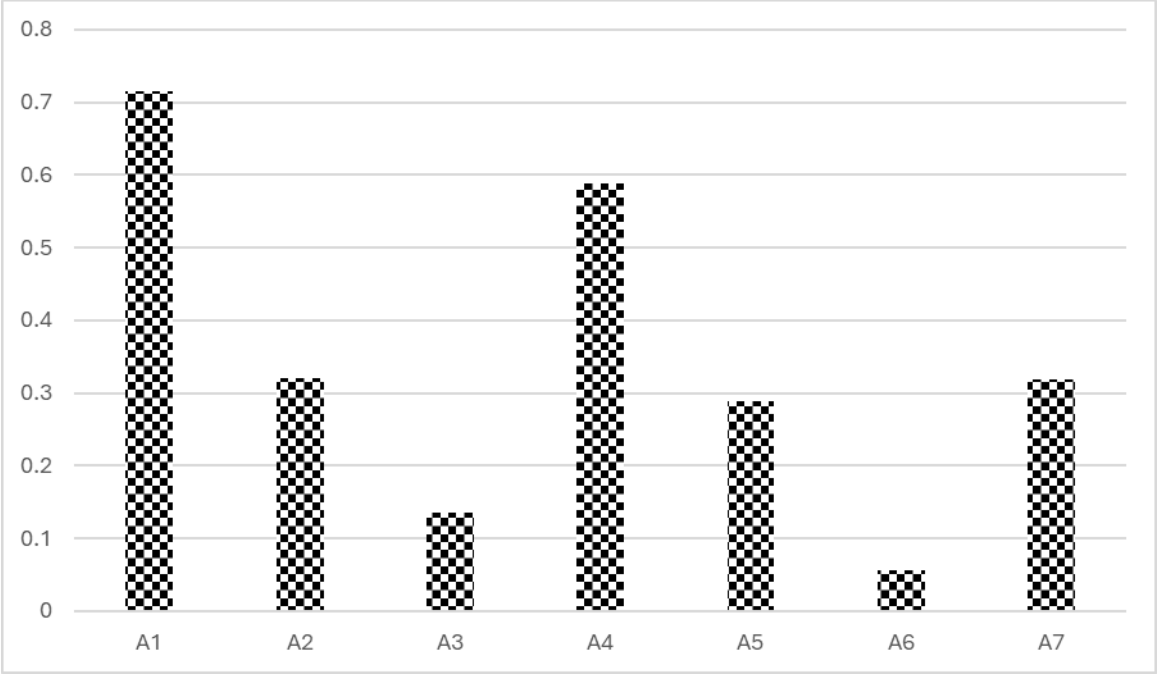

Figure 4. The values of VIKOR index.

4.2. Sensitivity analysis and discussion analysis

We adjust the L parameter in the VIKOR index. We put the values between 0 to 1 and show the rank of alternatives. We show alternative 6 is the best as shown in Figure 5. So, we show the rank of alternatives is stable.

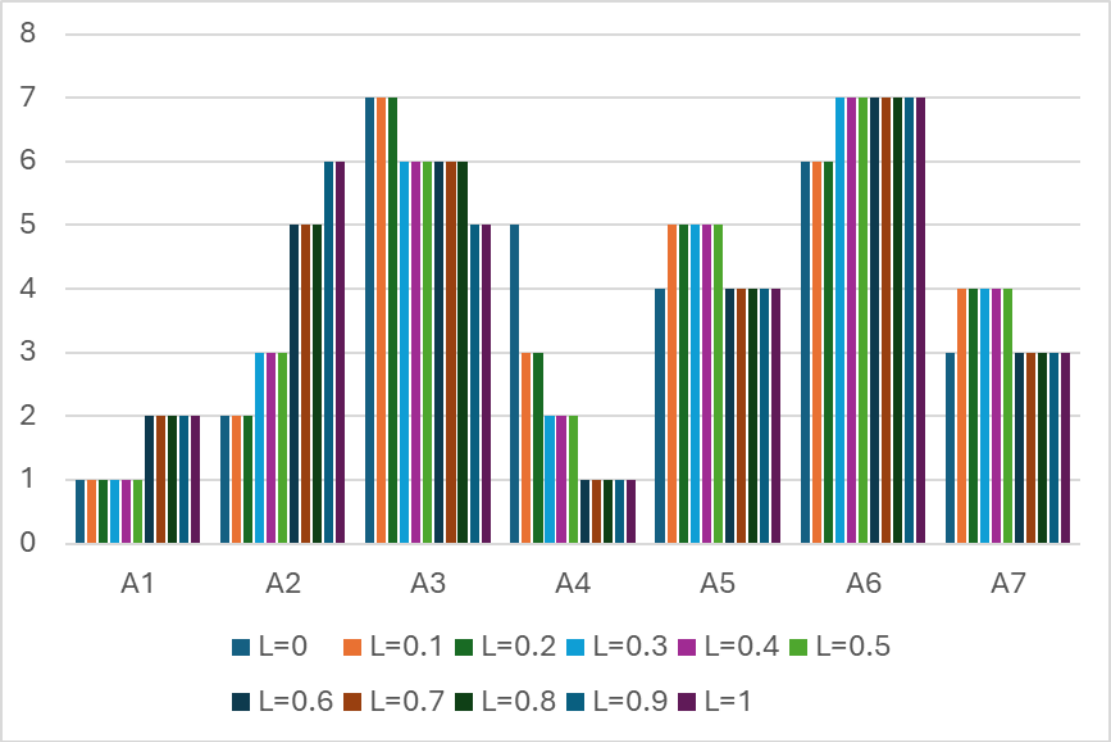

Figure 5. The rank of alternatives under different L parameters.

In contrast, the SVNN-VIKOR approach proposed in this paper offers the following three main advantages: **(1) High Flexibility**: This method effectively addresses MAGDM problems with uncertainty and fuzziness, particularly within the framework of SVNSs, providing a more accurate representation of uncertain information in decision-making. **(2) Improved Computational Efficiency**: Compared to some existing methods, SVNN-VIKOR exhibits relatively lower computational complexity when handling multiple decision-makers and attributes, maintaining high accuracy while reducing the computational burden. **(3) Good Consistency in Decision Results**: In comparison with other methods, SVNN-VIKOR demonstrates superior performance in terms of ranking consistency and rationality of results, confirming its effectiveness and reasonableness in solving MAGDM problems.

However, despite these advantages, the proposed method also has the following two limitations: (1) **High Sensitivity to Parameters**: Certain parameters in the SVNN-VIKOR method significantly impact the results, which may lead to instability in different decision-making scenarios, requiring parameter tuning to ensure optimal performance. (2) **Increased Complexity in Application**: Compared to some more straightforward methods, the theoretical framework and computational

process of this approach are relatively complex, which may demand higher levels of expertise and computational capacity from users, thus increasing the difficulty of practical application.

Overall, while the proposed method demonstrates notable advantages in flexibility, efficiency, and result consistency, there is still room for improvement in terms of parameter sensitivity and application complexity.

5. Conclusion and future research directions

In the context of big data, the satisfaction evaluation of college students' online IAPE is primarily achieved through advanced data collection and analysis techniques. By utilizing various channels such as online surveys, social media interactions, and learning platform data, comprehensive feedback and behavioral data from students can be gathered. Big data technology not only provides real-time feedback but also uncovers students' focal points, interests, and learning challenges through in-depth analysis. This data offers educators scientific insights, enabling them to optimize content and methods to better meet students' individual needs. Additionally, machine learning and AI technologies assist in analyzing students' satisfaction with online IAPE, predicting educational outcomes, and offering targeted improvement suggestions. Ultimately, big data-based satisfaction evaluation effectively enhances the quality of online IAPE and improves students' learning experiences. The satisfaction evaluation of college students' online IAPE in the context of big data is MAGDM. Recently, the VIKOR method has been utilized to address MAGDM problems, with SVNSs employed to represent uncertain information in satisfaction evaluations. In this paper, we introduce the SVNN-VIKOR model to solve MAGDM within the framework of SVNSs. Lastly, a numerical case study focused on the satisfaction evaluation of college students' online IAPE in the context of big data is presented to validate the effectiveness of the proposed method.

Although the SVNN-VIKOR method proposed in this paper demonstrates significant advantages in evaluating the satisfaction of college students' online IAPE in the context of big data, there are several research limitations that merit attention. First, **the complexity of the model is relatively high**. While the SVNN-VIKOR method effectively handles uncertain information, its computational process is complex. This complexity, especially when dealing with large datasets, results in high computational time and resource consumption, potentially making it less suitable for real-time decision-making scenarios. Second, **parameter tuning issues**. The SVNN-VIKOR model

is highly sensitive to the selection of certain parameters, which significantly affect the final outcome. The sensitivity to these parameters means that different parameter choices can lead to varying decision results, thereby impacting the model's stability and generalizability. Lastly, **a lack of extensive empirical validation**. Although the effectiveness of the method is verified through a numerical case study, it is limited to a specific scenario with simulated data. The model's applicability and robustness in other fields or real-world applications have not yet been fully tested, lacking broad empirical case support.

Based on the above research limitations, future studies can explore the following three directions:(1)**Optimizing the computational efficiency of the model:** To improve the applicability of the SVNN-VIKOR method for large datasets, further research can focus on incorporating parallel computing, distributed computing, and other techniques to optimize the algorithm's computational efficiency. This would reduce time and resource consumption, making the method more suitable for real-time decision-making, particularly in dynamic data environments. (2) **Parameter optimization and automatic tuning mechanisms:** To address the limitation of parameter sensitivity, future research could explore the use of intelligent optimization algorithms (such as genetic algorithms, particle swarm optimization, etc.) to automatically tune the parameters. This would reduce the subjectivity in parameter settings and improve the model's adaptability and stability across different scenarios. (3) **Empirical studies and application expansion across multiple fields:** Beyond the satisfaction evaluation of online IAPE, future research could apply the SVNN-VIKOR method in other educational or non-educational fields for broader empirical validation. By testing and verifying the method in various domains, the generalizability of the approach can be further evaluated, enhancing its application value across multiple fields and scenarios.

References

[1] H. Wang, F. Smarandache, Y.Q. Zhang, R. Sunderraman, Single valued neutrosophic sets, Multispace Multistruct, (2010) 410-413.

[2] L. Gomes, M. Lima, Todim: Basics and apllication to multicriteria ranking of projects with environmental impacts, Foundations of Control Engineering, 16 (1991) 113-127.

[3] L.F.A.M. Gomes, M.M.P.P. Lima, From modeling individual preferences to multicriteria ranking of discrete alternatives: A look at prospect theory and the additive difference model, Foundations of

Computing and Decision Sciences, 17 (1992) 171-184.

[4] A.B. Leoneti, L. Gomes, A novel version of the todim method based on the exponential model of prospect theory: The exptodim method, European Journal of Operational Research, 295 (2021) 1042-1055.

[5] Y. Deng, W.X. Zhang, An exptodim-gra based multiple attribute group decision-making method for development level evaluation of digital inclusive finance under intuitionistic fuzzy circumstances, Journal of Intelligent & Fuzzy Systems, 45 (2023) 10661-10673.

[6] H. Sun, Z. Yang, Q. Cai, G. Wei, Z. Mo, An extended exp-todim method for multiple attribute decision making based on the z-wasserstein distance, Expert Systems with Applications, 214 (2023) 119114.

[7] S. Opricovic, G.H. Tzeng, Compromise solution by mcdm methods: A comparative analysis of vikor and topsis, European Journal of Operational Research, 156 (2004) 445-455.

[8] S. Opricovic, G.H. Tzeng, Extended vikor method in comparison with outranking methods, European Journal of Operational Research, 178 (2007) 514-529.

[9] J. Wu, H. Hu, Incorporating ideological and political work throughout the entire education process to create a new situation in the development of higher education in china, Shanghai Education, 2017 (2017) 4-5.

[10] Y. Fang, L. Huang, N. Lan, et al., Research on enhancing college students' sense of gain in online ideological and political education based on the yiban platform, Western Journal, 2021 (2021) 107-109.

[11] X. Yu, The "five educations" and "three natures" of ideological and political education in the united states, Contemporary World and Socialism, 2011 (2011) 166-171.

[12] H. Geng, Feasibility analysis of ideological and political education for "post-95" college students based on online live streaming platforms, Journal of Changzhou Vocational Institute of Information Technology, 2017 (2017) 83-86.

[13] H. Zhang, Research on the role of network media in promoting ideological and political education for young people: A case study of the xuexi qiangguo platform and tiktok short videos, Media Forum, 2020 (2020) 166-167.

[14] C. Hu, J. He, Optimizing ideological and political education in universities from the perspective of online public opinion, Journal of Liaoning Open University, 2023 (2023) 62-65.

[15] J. Ma, Research on college students' satisfaction with university online ideological and political micro-platforms and countermeasures, Taste · Classics, 2023 (2023) 90-93,106.

[16] A.A. El-Douh, S. Lu, A. Abdelhafeez, A.M. Ali, A.S. Aziz, Heart disease prediction under machine learning and association rules under neutrosophic environment, Neutrosophic Systems with Applications, 10 (2023) 35-52.

[17] K. M. Sallam, A.W. Mohamed, Single valued neutrosophic sets for assessment quality of suppliers under uncertainty environment, Multicriteria Algorithms with Applications, 1 (2023) 1-10.

[18] N. N.Mostafa, A. Krishan Kumar, Y. Ali, A comparative study on x-ray image enhancement based on neutrosophic set, Sustainable Machine Intelligence Journal, 7 (2024) (2):1-10.

[19] M. Abdel-Baset, V. Chang, A. Gamal, Evaluation of the green supply chain management practices: A novel neutrosophic approach, Computers in Industry, 108 (2019) 210-220.

[20] L. Niu, J. Ye, Magdm technique based on linguistic neutrosophic tangent dombi aggregation operators and its application in selecting new energy design schemes, Neutrosophic Sets and Systems, 70 (2024) 137-154.

[21] A. Kanchana, D. Nagarajan, S. Broumi, Multi-attribute group decision-making based on the neutrosophic bonferroni mean operator, Neutrosophic Sets and Systems, 57 (2023) 139-164.

[22] X.D. Peng, J.G. Dai, F. Smarandache, Research on the assessment of project-driven immersion teaching in extreme programming with neutrosophic linguistic information, International Journal of Machine Learning and Cybernetics, 14 (2023) 873-888.

[23] L.T.H. Lan, D.T. Hien, N.T. Thong, F. Smarandache, N.L. Giang, An anp-topsis model for tourist destination choice problems under temporal neutrosophic environment, Applied Soft Computing, 136 (2023) 12.

[24] Z. Wang, Q. Cai, G. Wei, Modified todim method based on cumulative prospect theory with type-2 neutrosophic number for green supplier selection, Engineering Applications of Artificial Intelligence, 126 (2023) 106843.

[25] B. Chen, Q. Cai, G. Wei, Z. Mo, Novel aczel-alsina operations-based linguistic z-number aggregation operators and their applications in multi-attribute group decision-making process, Engineering Applications of Artificial Intelligence, 124 (2023) 106541.

[26] J.J. Peng, J.Q. Wang, J. Wang, H.Y. Zhang, X.H. Chen, Simplified neutrosophic sets and their

applications in multi-criteria group decision-making problems, International Journal of Systems Science, 47 (2016) 2342-2358.

[27] P. Majumdar, S.K. Samanta, On similarity and entropy of neutrosophic sets, Journal of Intelligent & Fuzzy Systems, 26 (2014) 1245-1252.

Appendix

Table A1. The first decision matrix.

	A_1	A_2	A_3	A_4	A_5	A_6	A_7
C_1	(0.1,0.9,1)	(0.4,0.7,0.7)	(0.2,0.8,0.9)	(0.1,0.9,1)	(0.9,0.2,0.1)	(0.9,0.2,0.1)	(0.85,0.3,0.2)
C_2	(0.2,0.8,0.9)	(0.5,0.5,0.5)	(0.4,0.7,0.7)	(0.2,0.8,0.9)	(0.2,0.8,0.9)	(0.1,0.9,1)	(0.65,0.4,0.4)
C_3	(0.4,0.7,0.7)	(0.65,0.4,0.4)	(0.4,0.7,0.7)	(0.1,0.9,1)	(0.9,0.2,0.1)	(0.1,0.9,1)	(0.5,0.5,0.5)
C_4	(0.5,0.5,0.5)	(0.85,0.3,0.2)	(0.5,0.5,0.5)	(0.2,0.8,0.9)	(0.9,0.2,0.1)	(0.9,0.2,0.1)	(0.4,0.7,0.7)
C_5	(0.5,0.5,0.5)	(0.9,0.2,0.1)	(0.65,0.4,0.4)	(0.4,0.7,0.7)	(0.85,0.3,0.2)	(0.9,0.2,0.1)	(0.2,0.8,0.9)
C_6	(0.65,0.4,0.4)	(0.1,0.9,1)	(0.85,0.3,0.2)	(0.5,0.5,0.5)	(0.65,0.4,0.4)	(0.85,0.3,0.2)	(0.1,0.9,1)
C_7	(0.85,0.3,0.2)	(0.2,0.8,0.9)	(0.9,0.2,0.1)	(0.65,0.4,0.4)	(0.5,0.5,0.5)	(0.65,0.4,0.4)	(0.1,0.9,1)
C_8	(0.9,0.2,0.1)	(0.4,0.7,0.7)	(0.9,0.2,0.1)	(0.85,0.3,0.2)	(0.5,0.5,0.5)	(0.5,0.5,0.5)	(0.9,0.2,0.1)
C_9	(0.9,0.2,0.1)	(0.5,0.5,0.5)	(0.1,0.9,1)	(0.2,0.8,0.9)	(0.4,0.7,0.7)	(0.4,0.7,0.7)	(0.85,0.3,0.2)
C_{10}	(0.1,0.9,1)	(0.65,0.4,0.4)	(0.85,0.3,0.2)	(0.9,0.2,0.1)	(0.1,0.9,1)	(0.2,0.8,0.9)	(0.85,0.3,0.2)
C_{11}	(0.1,0.9,1)	(0.2,0.8,0.9)	(0.2,0.8,0.9)	(0.4,0.7,0.7)	(0.5,0.5,0.5)	(0.65,0.4,0.4)	(0.65,0.4,0.4)

Table A2. The second decision matrix.

	A_1	A_2	A_3	A_4	A_5	A_6	A_7
C_1	(0.2,0.8,0.9)	(0.5,0.5,0.5)	(0.65,0.4,0.4)	(0.2,0.8,0.9)	(0.5,0.5,0.5)	(0.65,0.4,0.4)	(0.85,0.3,0.2)
C_2	(0.2,0.8,0.9)	(0.5,0.5,0.5)	(0.2,0.8,0.9)	(0.5,0.5,0.5)	(0.65,0.4,0.4)	(0.85,0.3,0.2)	(0.65,0.4,0.4)
C_3	(0.4,0.7,0.7)	(0.2,0.8,0.9)	(0.5,0.5,0.5)	(0.65,0.4,0.4)	(0.85,0.3,0.2)	(0.1,0.9,1)	(0.5,0.5,0.5)
C_4	(0.5,0.5,0.5)	(0.85,0.3,0.2)	(0.2,0.8,0.9)	(0.5,0.5,0.5)	(0.65,0.4,0.4)	(0.85,0.3,0.2)	(0.4,0.7,0.7)
C_5	(0.5,0.5,0.5)	(0.2,0.8,0.9)	(0.5,0.5,0.5)	(0.65,0.4,0.4)	(0.85,0.3,0.2)	(0.9,0.2,0.1)	(0.2,0.8,0.9)
C_6	(0.65,0.4,0.4)	(0.2,0.8,0.9)	(0.5,0.5,0.5)	(0.65,0.4,0.4)	(0.85,0.3,0.2)	(0.85,0.3,0.2)	(0.1,0.9,1)
C_7	(0.85,0.3,0.2)	(0.2,0.8,0.9)	(0.5,0.5,0.5)	(0.65,0.4,0.4)	(0.85,0.3,0.2)	(0.65,0.4,0.4)	(0.1,0.9,1)
C_8	(0.2,0.8,0.9)	(0.5,0.5,0.5)	(0.65,0.4,0.4)	(0.85,0.3,0.2)	(0.65,0.4,0.4)	(0.85,0.3,0.2)	(0.9,0.2,0.1)
C_9	(0.2,0.8,0.9)	(0.5,0.5,0.5)	(0.2,0.8,0.9)	(0.5,0.5,0.5)	(0.65,0.4,0.4)	(0.85,0.3,0.2)	(0.85,0.3,0.2)
C_{10}	(0.1,0.9,1)	(0.2,0.8,0.9)	(0.5,0.5,0.5)	(0.65,0.4,0.4)	(0.85,0.3,0.2)	(0.2,0.8,0.9)	(0.85,0.3,0.2)
C_{11}	(0.2,0.8,0.9)	(0.5,0.5,0.5)	(0.65,0.4,0.4)	(0.85,0.3,0.2)	(0.5,0.5,0.5)	(0.65,0.4,0.4)	(0.65,0.4,0.4)

Table A3. The third decision matrix.

	A_1	A_2	A_3	A_4	A_5	A_6	A_7
C_1	(0.9,0.2,0.1)	(0.85,0.3,0.2)	(0.5,0.5,0.5)	(0.5,0.5,0.5)	(0.85,0.3,0.2)	(0.5,0.5,0.5)	(0.5,0.5,0.5)
C_2	(0.9,0.2,0.1)	(0.85,0.3,0.2)	(0.5,0.5,0.5)	(0.5,0.5,0.5)	(0.5,0.5,0.5)	(0.1,0.9,1)	(0.65,0.4,0.4)
C_3	(0.4,0.7,0.7)	(0.9,0.2,0.1)	(0.85,0.3,0.2)	(0.5,0.5,0.5)	(0.5,0.5,0.5)	(0.1,0.9,1)	(0.5,0.5,0.5)

C_4	(0.5,0.5,0.5)	(0.85,0.3,0.2)	(0.9,0.2,0.1)	(0.85,0.3,0.2)	(0.5,0.5,0.5)	(0.5,0.5,0.5)	(0.4,0.7,0.7)
C_5	(0.9,0.2,0.1)	(0.85,0.3,0.2)	(0.5,0.5,0.5)	(0.5,0.5,0.5)	(0.85,0.3,0.2)	(0.9,0.2,0.1)	(0.2,0.8,0.9)
C_6	(0.9,0.2,0.1)	(0.85,0.3,0.2)	(0.5,0.5,0.5)	(0.5,0.5,0.5)	(0.5,0.5,0.5)	(0.85,0.3,0.2)	(0.1,0.9,1)
C_7	(0.85,0.3,0.2)	(0.2,0.8,0.9)	(0.9,0.2,0.1)	(0.85,0.3,0.2)	(0.5,0.5,0.5)	(0.5,0.5,0.5)	(0.1,0.9,1)
C_8	(0.9,0.2,0.1)	(0.4,0.7,0.7)	(0.9,0.2,0.1)	(0.85,0.3,0.2)	(0.5,0.5,0.5)	(0.5,0.5,0.5)	(0.9,0.2,0.1)
C_9	(0.9,0.2,0.1)	(0.85,0.3,0.2)	(0.5,0.5,0.5)	(0.5,0.5,0.5)	(0.4,0.7,0.7)	(0.4,0.7,0.7)	(0.85,0.3,0.2)
C_{10}	(0.1,0.9,1)	(0.9,0.2,0.1)	(0.85,0.3,0.2)	(0.5,0.5,0.5)	(0.5,0.5,0.5)	(0.2,0.8,0.9)	(0.85,0.3,0.2)
C_{11}	(0.9,0.2,0.1)	(0.85,0.3,0.2)	(0.5,0.5,0.5)	(0.5,0.5,0.5)	(0.5,0.5,0.5)	(0.65,0.4,0.4)	(0.65,0.4,0.4)

Table A4. The fourth decision matrix.

	A_1	A_2	A_3	A_4	A_5	A_6	A_7
C_1	(0.85,0.3,0.2)	(0.9,0.2,0.1)	(0.4,0.7,0.7)	(0.2,0.8,0.9)	(0.65,0.4,0.4)	(0.9,0.2,0.1)	(0.85,0.3,0.2)
C_2	(0.2,0.8,0.9)	(0.85,0.3,0.2)	(0.85,0.3,0.2)	(0.9,0.2,0.1)	(0.4,0.7,0.7)	(0.2,0.8,0.9)	(0.65,0.4,0.4)
C_3	(0.85,0.3,0.2)	(0.85,0.3,0.2)	(0.9,0.2,0.1)	(0.4,0.7,0.7)	(0.2,0.8,0.9)	(0.65,0.4,0.4)	(0.5,0.5,0.5)
C_4	(0.85,0.3,0.2)	(0.9,0.2,0.1)	(0.4,0.7,0.7)	(0.2,0.8,0.9)	(0.65,0.4,0.4)	(0.9,0.2,0.1)	(0.4,0.7,0.7)
C_5	(0.5,0.5,0.5)	(0.85,0.3,0.2)	(0.9,0.2,0.1)	(0.4,0.7,0.7)	(0.2,0.8,0.9)	(0.65,0.4,0.4)	(0.2,0.8,0.9)
C_6	(0.85,0.3,0.2)	(0.9,0.2,0.1)	(0.4,0.7,0.7)	(0.2,0.8,0.9)	(0.65,0.4,0.4)	(0.85,0.3,0.2)	(0.1,0.9,1)
C_7	(0.85,0.3,0.2)	(0.85,0.3,0.2)	(0.9,0.2,0.1)	(0.4,0.7,0.7)	(0.2,0.8,0.9)	(0.65,0.4,0.4)	(0.1,0.9,1)
C_8	(0.85,0.3,0.2)	(0.9,0.2,0.1)	(0.4,0.7,0.7)	(0.2,0.8,0.9)	(0.65,0.4,0.4)	(0.5,0.5,0.5)	(0.9,0.2,0.1)
C_9	(0.9,0.2,0.1)	(0.85,0.3,0.2)	(0.9,0.2,0.1)	(0.4,0.7,0.7)	(0.2,0.8,0.9)	(0.65,0.4,0.4)	(0.85,0.3,0.2)
C_{10}	(0.85,0.3,0.2)	(0.9,0.2,0.1)	(0.4,0.7,0.7)	(0.2,0.8,0.9)	(0.65,0.4,0.4)	(0.2,0.8,0.9)	(0.85,0.3,0.2)
C_{11}	(0.1,0.9,1)	(0.85,0.3,0.2)	(0.9,0.2,0.1)	(0.4,0.7,0.7)	(0.2,0.8,0.9)	(0.65,0.4,0.4)	(0.65,0.4,0.4)

Received: July 26, 2024. Accepted: Oct 22, 2024

NSS
Neutrosophic Sets and Systems, Vol. 76, 2025
University of New Mexico

Optimizing Network Structures Through Neutrosophic Graph Product Operations and its Coloring: A Comprehensive Approach for Enhanced Connectivity and Robustness

A. Meenakshi [1,*], S. Dhanushiya[2]

[1,2]Department of Mathematics, Vel Tech Rangarajan Dr. Sagunthala R&D Institute of Science and Technology; Chennai-600 062, India, meenakshiannamalai1@gmail.com[1], sdhanushiya488@gmail.com[2]

[*]Correspondence: meenakshiannamalai1@gmail.com, 9940070544

Abstract

Optimal network analysis requires advanced techniques to handle the inherent complexity and uncertainty of real-world systems. We have used vertex order coloring on neutrosophic graphs to find the most effective approach to improve network reliability and performance. Neutrosophic graphs($\mathcal{NG}$) offer a comprehensive framework for modelling real-world networks with inherent uncertainties by incorporating degrees of truth, falsity, and indeterminacy. In this paper, we have investigated various graph product operations as a means of optimizing network structures. We further investigated the applications of vertex order coloring to identify α, β and γ strong vertices within various graph operations of $\mathcal{NG}$. We examined several $\mathcal{NG}$ products with the goal of determining the most optimal network based on particular important metrics including the total number of alpha-strong vertices, the weight of alpha-strong vertices, the chromatic number, and the weight of the graph's minimum spanning tree. The objective of our research is to identify the best solutions that strike a balance between robustness and association by rigorously studying and comparing various product operations. Our research advances the subject of network theory and provides useful information for a variety of applications, including social networks, transportation, and telecommunications.

Keywords: Neutrosophic graph, vertex order coloring, co-normal, tensor, residue

Introduction

Graph theory, a foundational field in mathematics, originated in 1736 with Leonhard Euler's solution to the Königsberg bridge problem, marking the birth of graph theory. This field of study investigates the characteristics and uses of graphs, which are mathematical structures that represent pairwise relationships between objects [8]. The concept of graph coloring, which holds significant importance in graph theory, originated in the 19th century when Francis Guthrie proposed the four-color theorem in 1852[25], which was subsequently validated by Kenneth Appel and Wolfgang Haken in 1976. It entails giving network vertices distinct colors in order to differentiate between

neighboring vertices. This is a technique that has applications in resource allocation, scheduling, and map coloring. Lotfi A. Zadeh's 1965 invention of fuzzy set theory completely changed how mathematical models deal with imprecision and uncertainty [2]. This development led to the rise of fuzzy graph theory, introduced by Azriel Rosenfeld in 1975[22], It models networks with ambiguous or imprecise links by fusing the ideas of fuzzy sets with graph theory. Bhutani initially presented the idea of coloring in fuzzy graph theory in 1993[3, 4]. By extending the classic graph coloring problem to fuzzy graphs, Bhutani's work made it possible to investigate coloring techniques in graphs with edges that have different membership levels. Gong and zhang [11, 13] explored the concepts of adjacent vertex distinguishing proper edge coloring and adjacent vertex distinguishing total coloring within the context of fuzzy graphs. In addition to outlining the necessary and sufficient conditions for a vertex to be strong, Nagoor Gani et al. [12] established three different kinds of vertices namely α, β and γ strong vertices. Based on these principles, Krassimir Atanassov's intuitionistic fuzzy graph theory introduced in 1986 adds another level of complexity by taking into account both the degree of membership and the degree of non-membership. This method makes it possible to model uncertainty more thoroughly. Talebi et al. [26] introduced a new concept of coloring intuitionistic fuzzy graphs, which have good capabilities in handling vague and incompatible information, unlike traditional fuzzy graphs. This concept addresses problems where fuzzy graphs may not provide satisfactory results. Rosyida et al. presented an algorithm for coloring picture fuzzy graphs based on strong and weak adjacencies between vertices, which is an extension of the concepts from fuzzy graphs and intuitionistic fuzzy graphs ($\mathcal{IFGS}$)[23]. Rifayathali et al. [24] introduced the concept of chromatic excellence in intuitionistic fuzzy graphs, providing new insights into graph coloring. Florentin Smarandache, introduced the concept of neutrosophic fuzzy set ($\mathcal{NFS}$) by combining fuzzy set ($\mathcal{FS}$) with neutrosophic set ($\mathcal{NS}$), leading to the development of new concept and also proposed the single valued neutrosophic fuzzy set ($\mathcal{SVNFS}$) to address difficulties faced in dealing with real-life problems due to nonstandard intervals of neutrosophic components[13]. By permitting elements to have different degrees of membership, fuzzy set theory expands on conventional set theory and offers a more complex depiction of real-world situations. By adding a third parameter to indicate the degree of indeterminancy, Florentin Smarandache's 1998 development of $\mathcal{NG}$ expands on these ideas and provides an even more comprehensive framework for managing ambiguity and uncertainty. Meenakshi et al. [17,19,20] explored the use of neutrosophic graphs to model real-world problems containing inconsistent information, showcasing the versatility and applicability of this approach in various scenarios. They also developed an optimal algorithm to illustrate the applications of the proposed single-valued neutrosophic graph, providing a practical demonstration of its efficiency in information flow within networks Assigning colors to vertices under fuzzy constraints is known as coloring fuzzy graphs, which includes intuitionistic and neutrosophic graphs. This technique has applications in network design, resource

allocation, and decision-making processes. These developments demonstrate how mathematical modelling is always changing when it comes to solving challenging real-world issues. Meenakshi et al.'s (17) goal is to build a single-valued neutrosophic graph using the max product of graphs, which should increase the efficiency of the maximized network. Aparna et al. introduced the concept of Single Valued Neutrosophic R-dynamic Vertex Coloring, combining Single Valued Neutrosophic Vertex Coloring and r-dynamic coloring to address graph coloring problems [1, 3]. Graph products are procedures that create a new graph by joining two graphs. Graph product operations play a significant role in network design and optimization. The residue product of two fuzzy graphs was defined by K. Radha et al. [23] and its features, including efficiency, connectedness, and completeness, were examined. The co-normal product of IFG was first proposed by K. Kalaiarasi et al. [14, 15], who also examined its importance in relation to the completeness, regularity, and pseudo-regularity of fuzzy graphs. Mohanta et al. [22] presented various operations on $\mathcal{SVNG}$, including rejection, symmetric difference, maximal product, and residue product. These operations are accompanied by appropriate examples, enhancing understanding and application

This introductory section is followed by a detailed analysis of pertinent literature, and the article proceeds as follows: We have included the preliminary information for a better grasp of $\mathcal{NG}$ concepts and coloring ideas in Section 2. Section 3 deals with the approach used in this investigation. Single-Valued Neutrosophic Vertex Order Coloring is a concept that incorporates the idea of neutrosophic graphs into traditional vertex coloring. This method minimizes coloring conflicts based on neutrosophic logic by assigning colors to each vertex in a graph based on a certain order prioritizing α strong vertices followed by β and γ strong vertices. Section 4 summarizes our research's conclusions, including theorems and an analysis of different operations. In Section 5, different operations on $\mathcal{NG}$ are detailed and its coloring using Neutrosophic Vertex Order Coloring(NVOC) is demonstrated. We have critically discussed these findings in Section 6, examining possible mechanisms and providing an algorithm to determine the optimal network. The article concludes with a summary of its most important findings. By using this systematic approach, we offered an extensive understanding of various operations and identified the optimal network depending on specific factors.

2. Preliminaries

2.1 Single valued Neutrosophic set [4]

Let $\mathcal{X}$ be a universe of discourse.

$\mathcal{N}$= {(x, $\mathcal{T}_{\mathcal{N}}(x)$, $\mathcal{I}_{\mathcal{N}}(x)$, $\mathcal{F}_{\mathcal{N}}$ (x): x ∈ X} is a $\mathcal{SVNFS}$ on $\mathcal{X}$. The degree of truth membership value is given by $\mathcal{T}_{\mathcal{N}}$ (x): $\mathcal{X}$ → [0, 1], degree of indeterminancy value, and degree of falsity membership value of x on $\mathcal{N}$ are denoted by $\mathcal{I}_{\mathcal{N}}$ (x): $\mathcal{X}$ → [0, 1] and $\mathcal{F}_{\mathcal{N}}$ (x): $\mathcal{X}$ → [0, 1], respectively, meeting the criteria 0 < $\mathcal{T}_{\mathcal{N}}$ (x) + $\mathcal{I}_{\mathcal{N}}(x)$ + $\mathcal{F}_{\mathcal{N}}$ (x) ≤ 3, ∀ x ∈ $\mathcal{X}$.

2.2 Single valued Neutrosophic Graph [5]

The $\mathcal{SVNG}$, $\widetilde{\mathcal{N}_{\mathcal{G}}}$ of $\mathcal{N}_{\mathcal{G}}$=($\mathcal{V}_{\mathcal{G}}$, $\mathcal{E}_{\mathcal{G}}$) is denoted by $\widetilde{\mathcal{N}_{\mathcal{G}}}$ =($\mathcal{V}_{\mathcal{G}}$,$\zeta$,$\omega$) where ζ = ($\mathcal{T}_{\zeta}$, $\mathcal{I}_{\zeta}$, $\mathcal{F}_{\zeta}$) is a single-valued Neutrosophic set on $\mathcal{V}_{\mathcal{G}}$ and ω = ($\mathcal{T}_{\omega}$, $\mathcal{I}_{\omega}$, $\mathcal{F}_{\omega}$) is a single-valued Neutrosophic symmetric relation on $\mathcal{E}_{\mathcal{G}} \subseteq \mathcal{V}_{\mathcal{G}} \times \mathcal{V}_{\mathcal{G}}$ is defined as follows:

i) $\mathcal{T}_{\mu}$ $(x, y) \leq \mathcal{T}_{\zeta}$ $(x) \wedge \mathcal{T}_{\zeta}$ (y) , ∀ $(x, y) \in \mathcal{V}_{\mathcal{G}} \times \mathcal{V}_{\mathcal{G}}$.

ii) $\mathcal{I}_{\mu}$ $(x, y) \leq \mathcal{I}_{\zeta}$ $(x) \wedge \mathcal{I}_{\zeta}$ (y) , ∀ $(x, y) \in \mathcal{V}_{\mathcal{G}} \times \mathcal{V}_{\mathcal{G}}$.

iii) $\mathcal{F}_{\mu}$ $(x, y) \geq \mathcal{F}_{\zeta}$ $(x) \vee \mathcal{F}_{\zeta}$ (y) , ∀ $(x, y) \in \mathcal{V}_{\mathcal{G}} \times \mathcal{V}_{\mathcal{G}}$.

2.3 Complete single valued Neutrosophic Graph [5]

The $\mathcal{SVNG}$ $\widetilde{\mathcal{N}_{\mathcal{G}}}$ is said to be complete if ∀ $(x, y) \in \mathcal{E}_{\mathcal{G}}$,

$$\mathcal{T}_{\omega_{\widetilde{\mathcal{N}_{\mathcal{G}}}}}(x, y) = \mathcal{T}_{\zeta_{\widetilde{\mathcal{N}_{\mathcal{G}}}}}(x) \wedge \mathcal{T}_{\zeta_{\widetilde{\mathcal{N}_{\mathcal{G}}}}}(y),$$

$$\mathcal{I}_{\omega_{\widetilde{\mathcal{N}_{\mathcal{G}}}}}(x, y) = \mathcal{I}_{\zeta_{\widetilde{\mathcal{N}_{\mathcal{G}}}}}(x) \wedge \mathcal{I}_{\zeta_{\widetilde{\mathcal{N}_{\mathcal{G}}}}}(y),$$

$$\mathcal{F}_{\omega_{\widetilde{\mathcal{N}_{\mathcal{G}}}}}(x, y) = \mathcal{F}_{\zeta_{\widetilde{\mathcal{N}_{\mathcal{G}}}}}(x) \vee \mathcal{F}_{\zeta_{\widetilde{\mathcal{N}_{\mathcal{G}}}}}(y),$$

2.4 Strong single valued Neutrosophic Graph [5]

The $\mathcal{SVNG}$ $\widetilde{\mathcal{N}_{\mathcal{G}}}$ is known as strong single valued Neutrosophic graph if ∀ $(x, y) \in \mathcal{V}_{\mathcal{G}}$,

$$\mathcal{T}_{\omega_{\widetilde{\mathcal{N}_{\mathcal{G}}}}}(x, y) = \mathcal{T}_{\zeta_{\widetilde{\mathcal{N}_{\mathcal{G}}}}}(x) \wedge \mathcal{T}_{\zeta_{\widetilde{\mathcal{N}_{\mathcal{G}}}}}(y),$$

$$\mathcal{I}_{\omega_{\widetilde{\mathcal{N}_{\mathcal{G}}}}}(x, y) = \mathcal{I}_{\zeta_{\widetilde{\mathcal{N}_{\mathcal{G}}}}}(x) \wedge \mathcal{I}_{\zeta_{\widetilde{\mathcal{N}_{\mathcal{G}}}}}(y),$$

$$\mathcal{F}_{\omega_{\widetilde{\mathcal{N}_{\mathcal{G}}}}}(x, y) = \mathcal{F}_{\zeta_{\widetilde{\mathcal{N}_{\mathcal{G}}}}}(x) \vee \mathcal{F}_{\zeta_{\widetilde{\mathcal{N}_{\mathcal{G}}}}}(y).$$

2.5 Degree, neighborhood and Cardinality of a vertex in $\mathcal{SVNG}$ [5]

Let $\widetilde{\mathcal{N}_{\mathcal{G}}}$ =($\mathcal{V}_{\mathcal{G}}$,$\zeta$,$\omega$) be a $\mathcal{SVNG}$ and $\mathfrak{a}_i$ be a vertex in a $\widetilde{\mathcal{N}_{\mathcal{G}}}$. A vertex's degree, represented by $\mathcal{d}(\mathfrak{a}_i)$, is the total weight of the strong arcs that incident at it.

The neighborhood of $\mathfrak{a}_i$ is represented by the strong arc $\widetilde{\mathcal{N}_{\mathcal{G}}}$ ={$\omega_i \in \mathcal{V}_{\mathcal{G}}$/ ($\mathfrak{a}_i$, ω_i)}.

The minimum degree of $\widetilde{\mathcal{N}_{\mathcal{G}}}$ is given by $\delta(\widetilde{\mathcal{N}_{\mathcal{G}}}) = \min\{d_{\widetilde{\mathcal{N}_{\mathcal{G}}}}(\mathfrak{a}_i)/\ \mathfrak{a}_i \in \mathcal{V}_{\mathcal{G}}\}$.

The maximum degree of $\widetilde{\mathcal{N}_{\mathcal{G}}}$ is given by $\Delta(\widetilde{\mathcal{N}_{\mathcal{G}}}) = \max\{d_{\widetilde{\mathcal{N}_{\mathcal{G}}}}(\mathfrak{a}_i)/\ \mathfrak{a}_i \in \mathcal{V}_{\mathcal{G}}\}$.

The cardinality of a vertex $\mathfrak{a}_i \in \mathcal{V}$ in a $\mathcal{SVNG}$, $\mathcal{N}_{\mathcal{G}}$=($\mathcal{V}_{\mathcal{G}}$, $\mathcal{E}_{\mathcal{G}}$) is defined by

$$|\mathfrak{a}_i| = \mathcal{T}_{\zeta}(\mathfrak{a}_i) + \mathcal{I}_{\zeta}(\mathfrak{a}_i) + \mathcal{F}_{\zeta}(\mathfrak{a}_i).$$

The cardinality of an edge $\mathfrak{a}_i\mathfrak{a}_j \in \mathcal{E}$ in a $\mathcal{SVNG}$, $\mathcal{N}_{\mathcal{G}}$=($\mathcal{V}_{\mathcal{G}}$, $\mathcal{E}_{\mathcal{G}}$) is defined by

$$|\mathfrak{a}_i\mathfrak{a}_j| = \mathcal{T}_{\omega}(\mathfrak{a}_i\mathfrak{a}_j) + \mathcal{I}_{\omega}(\mathfrak{a}_i\mathfrak{a}_j) + \mathcal{F}_{\omega}(\mathfrak{a}_i\mathfrak{a}_j).$$

2.7 Adjacent Vertex of a fuzzy graph [10]

Let $\mathfrak{a}_i$ be the vertex of a fuzzy graph $\mathcal{F}_{\mathcal{G}} = (\mathbb{V}_{\mathcal{G}}, \mathbb{E}_{\mathcal{G}})$ then the adjacent vertices to the vertex $\mathfrak{a}_i$ is

$$\mathbb{A}\ (\mathfrak{a}_i) = \{\mathfrak{a}_i\ \epsilon\ \mathbb{V}_{\mathcal{G}}\ \exists\ \tfrac{1}{2}[\sigma(i) \wedge \sigma(j)] \leq \mu(ij)\}.$$

$$\mathbb{A}_s(\mathfrak{a}_i) = \{\mathfrak{a}_i \epsilon\ \mathbb{A}(\mathbb{V}_{\mathcal{G}}) | d(j) \geq d(i)\}$$

$$\mathbb{A}_w(\mathfrak{a}_i) = \{\mathfrak{a}_i \epsilon\ \mathbb{A}(\mathbb{V}_{\mathcal{G}}) | d(j) < d(i)\}.$$

3. Neutrosophic vertex order coloring

A sophisticated but effective development of conventional vertex coloring is NVOC. It is appropriate for situations where ambiguity and vagueness are crucial since it enables a more nuanced representation of these components. This approach offers a more advanced and adaptable solution to the vertex coloring problem by ensuring that the coloring complies with the rules of neutrosophic logic.

3.1 $\mathcal{K}$-vertex coloring of $\mathcal{SVNG}$

A family $\mathfrak{E} = \{e_1, e_2, \dots, e_{\mathcal{K}}\}$ of Neutrosophic sets on a set $\mathcal{V}$ is called a $\mathcal{K}$-vertex coloring of $\widetilde{\mathcal{N}_{\mathcal{G}}}: (\mathcal{V}_{\mathcal{G}}, \zeta, \omega)$ if

a) $\cup\ \mathfrak{E} = \zeta$

b)$e_i \wedge e_j = 0$

c) For every strong edge xy of $\mathcal{N}_{\mathcal{G}}$, min{ $e_i(\mu_1(x))$, $e_i(\mu_1(y))$}= 0 and max {$e_i(\gamma_1(x))$, $e_i(\gamma_1(x))$}= 1,$(1 \leq j \leq k)$

The least value of $\mathcal{K}$ for which the $\mathcal{N}_{\mathcal{G}}$ has a $\mathcal{K}$-vertex coloring denoted by $\chi^{\tau_0}(\widetilde{\mathcal{N}_{\mathcal{G}}})$, is called the chromatic number of the $\mathcal{NG}$ $\widetilde{\mathcal{N}_{\mathcal{G}}}$.

3.2 Adjacent Vertex of $\mathcal{SVNG}$

Let $\mathfrak{a}_i$ be the vertex of a $\mathcal{SVNG}$, $\widetilde{\mathcal{N}_{\mathcal{G}}}$ =$(\mathcal{V}_{\mathcal{G}},\zeta,\omega)$ then the adjacent vertices to the vertex $\mathfrak{a}_i$ is

$\mathbb{A}\ (\mathfrak{a}_i) = \{x\ \epsilon\ \mathcal{V}_{\mathcal{G}} \ni \frac{1}{2}[\sigma(x) \wedge \sigma(y)]\ \leq \mu(xy)\}$.

$\mathbb{A}_s(\mathfrak{a}_i) = \{x \epsilon\ \mathbb{A}(\mathfrak{a}_i) \ni \{d(y) \geq d(x)\}$ where $\mathbb{A}_s(\mathfrak{a}_i)$ denotes the strong adjacent vertices of a vertex $\mathfrak{a}_i$

$\mathbb{A}_w(\mathfrak{a}_i) = \{x \epsilon\ \mathbb{A}(\mathfrak{a}_i) \ni \{d(y) < d(x)\}$ where $\mathbb{A}_w(\mathfrak{a}_i)$denotes the weak adjacent vertices of a vertex $\mathfrak{a}_i$

$\mathbb{A}_{P_{S_T}}(\mathfrak{a}_i) = \{x \epsilon\ \mathbb{A}(\mathfrak{a}_i) \ni \{d(y) \geq d(x)\}$ and $\{x \epsilon\ \mathbb{A}\ (\mathfrak{a}_i) \ni \{d(y) < d(x)\}$ where

$\mathbb{A}_{P_{S_T}}(\mathfrak{a}_i)$ denotes the partially strong adjacent vertices of a vertex $\mathfrak{a}_i$.

3.3 α –Strong Vertex of $\mathcal{SVNG}$

A vertex $\mathfrak{a}_i\ \epsilon\ \zeta$ of an $\mathcal{SVNG}$, $\widetilde{\mathcal{N}_{\mathcal{G}}}: (\mathcal{V}_{\mathcal{G}}, \zeta, \omega)$ is said to be $\alpha -$ strong vertex,, if for every $\mathfrak{a}_i \epsilon\ \mathbb{A}(\zeta)$ satisfies $d_s(\mathfrak{a}_i) \geq d(\mathbb{A}_s(\mathfrak{a}_i))$. It is denoted by $\alpha_{sv}(\zeta)$.

3.4 γ –Strong Vertex of $\mathcal{SVNG}$

A vertex $\mathfrak{a}_i \in \zeta$ of an $\mathcal{SVNG}, \widetilde{\mathcal{N}}_{\mathcal{G}}: (\mathcal{V}_{\mathcal{G}}, \zeta, \omega)$ is said to be a $\gamma -$ strong or weak vertex, if for every $\mathfrak{a}_i \in \mathbb{A}(\zeta)$ satisfies $d_w(\mathfrak{a}_i) \leq d(\mathbb{A}_w(\mathfrak{a}_i))$. It is denoted by $\gamma_{wv}(\zeta)$.

3.5 $\beta -$ Strong Vertex of $\mathcal{SVNG}$

A vertex that satisfies both $\alpha - strong\ and\ \gamma - strong$ conditions is said to be $a\ \beta - strong\ Vertex$.

It is denoted by $\beta(\zeta)$.

3.5.1 All of Alpha's strong vertices are also weak ones, and vice versa.
3.5.2 All gamma strong vertices are strong silent .

3.6 Neutrosophic vertex order coloring of $\mathcal{SVNG}$

Neutrosophic vertex order colouring of $\widetilde{\mathcal{N}}_{\mathcal{G}}: (\mathcal{V}_{\mathcal{G}}, \zeta, \omega)$ is defined as a family ψ={$\mathfrak{S}_\alpha(\mathcal{V})$, $\beta(\mathcal{V})$, $\mathfrak{W}_\gamma(\mathcal{V})$} of strong vertices on a set $\mathcal{V}_{\mathcal{G}}$ if

i)$\cup\ \psi = \zeta$

ii)$\cap\ \psi = \phi$

iii)If $u, v \in \mathfrak{S}_\alpha(\mathcal{V})$ (or) $u, v \in \beta(\mathcal{V})$for each ($\mu(u, v) > 0$) of G, then $c(u) \neq c(v)$, where $c(u)$is the colour of u

iv)For every ($\mu(u, v) > 0$) of G, if $u, v \in \mathfrak{W}_\gamma(\mathcal{V})$, then $c(u)=c(v)$ and $\mu(u, v) = 0$

v)If $u, v \in \xi$, then $c(u)=c(v)$ and for every ($\mu(u, v) = 0$) of G.

The chromatic number of neutrosophic graph $\widetilde{\mathcal{N}}_{\mathcal{G}}$, $\chi^{\tau^*}(\widetilde{\mathcal{N}}_{\mathcal{G}})$ is the least number $\hbar$ for which a $\hbar$ -fuzzy vertex order colouring exists.

3.7 Illustration

Figure 1 is an example of a neutrosophic graph $\widetilde{\mathcal{N}}_{\mathcal{G}}$, where $\widetilde{\mathcal{N}}_{\mathcal{G}}=(\mathcal{V}_{\mathcal{G}}, \mathcal{E}_{\mathcal{G}})$ =(8,13) in the below example.

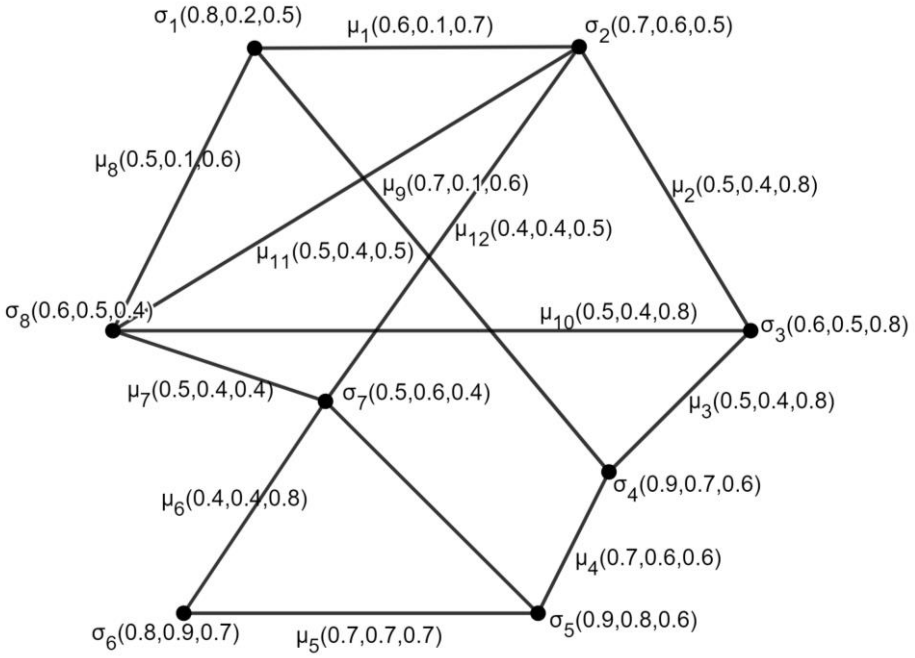

Figure 1: $\widetilde{\mathcal{N}_{\mathcal{G}}}$

Determine the degree of each vertex by definition 2.8. Sort vertices into α, β, and γ strong categories based on the criteria listed in definitions 3.2, 3.3, and 3.4. The degree and category of vertices are displayed in table 1. Use the fuzzy vertex order coloring approach to color the vertices so that no two neighboring vertices have the same color applied to them. Section 6 provides an algorithm for coloring $\mathcal{NG}$'s.

Table 1: Degree and category of vertices

Vertices	Degree of Vertices	Category
$d_{T,I,F}(\sigma_1)$	1.87	β *Strong*
$d_{T,I,F}(\sigma_2)$	2.06	α *Strong*
$d_{T,I,F}(\sigma_3)$	1.29	γ *Strong*
$d_{T,I,F}(\sigma_4)$	1.6	β *Strong*
$d_{T,I,F}(\sigma_5)$	1.4	β *Strong*
$d_{T,I,F}(\sigma_6)$	0.83	γ *Strong*
$d_{T,I,F}(\sigma_7)$	1.87	β *Strong*

$d_{T,I,F}(\sigma_8)$	2.06	α *Strong*

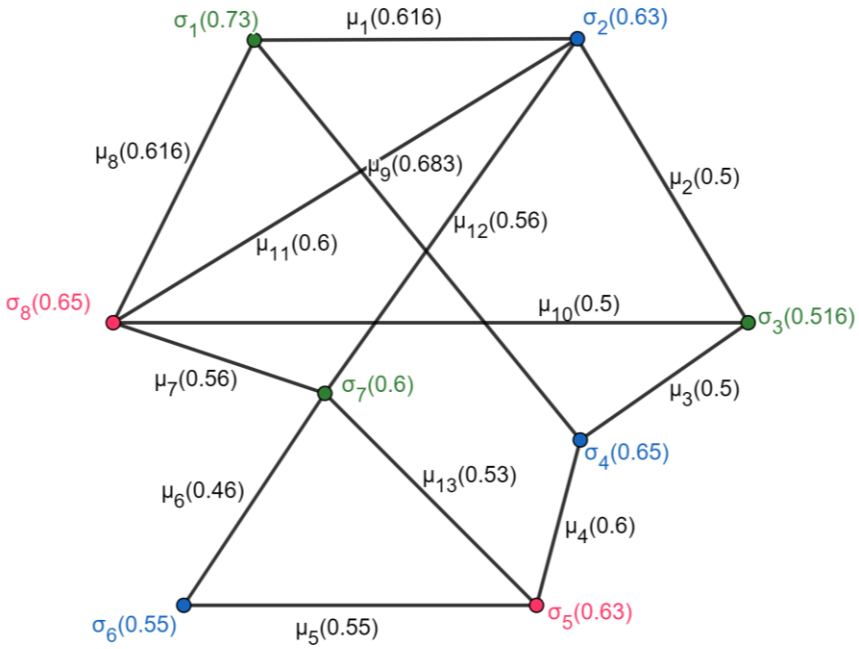

Figure 2: Vertex order coloring of $\widetilde{\mathcal{N}_{\mathcal{G}}}$

Vertex Category	Identification of color
α strong vertex	$\sigma_2 - 1,\ \sigma_8 - 3$
β strong vertex	$\sigma_1 - 2, \sigma_4 - 1, \sigma_5 - 3, \sigma_7 - 2$
γ strong vertex	$\sigma_3 - 2, \sigma_6 - 1$

For Figure 2, the chromatic number (χ^{τ^*}) is observed to be 3.

4. Results and discussion

The most recent developments in Neutrosophic vertex order coloring have been discussed in this section, along with several new theorems that broaden the scope of our research. These new theorems improve our theoretical knowledge of Neutrosophic vertex order coloring and present us with fresh avenues for practical applications in a variety of fields.

Theorem 4.1

Let $\widetilde{\mathcal{N}_{\mathcal{G}}}: (\mathcal{V}_{\mathcal{G}}, \zeta, \omega)$ be a regular neutrosophic graph. Then All the vertices of $\mathcal{NG}$ are α-strong vertices

Proof:

A neutrosophic graph $\widetilde{\mathcal{N}_{\mathcal{G}}}:(\mathcal{V}_{\mathcal{G}},\zeta,\omega)$ is regular if every vertex $\mathfrak{a}_i \in \mathcal{V}$ has the same degree. The degree $d(\mathfrak{a}_i)$ is the sum of the truth membership values of the edges incident to $\mathfrak{a}_i$

$$d(\mathfrak{a}_i)=\sum_{\mathfrak{a}_i\in\mathcal{V}}[\sigma((v,u))]$$

Since $\widetilde{\mathcal{N}_{\mathcal{G}}}$ is regular, for every vertex $\mathfrak{a}_i \in \mathcal{V}_{\mathcal{G}}$, we have $d(\mathfrak{a}_i) = d$.

As a result of their regularity, the edges incident to each vertex's total truth membership values must be equal to d. Each vertex $\mathfrak{a}_i$ has a uniformly high total of truth membership values for its incident edges, according to this consistent degree.

The truth membership values of the edges incident to σ_i must be sufficiently high for a vertex $\mathfrak{a}_i$ to maintain a degree d. All vertices $\mathfrak{a}_i$ in$\mathcal{V}_{\mathcal{G}}$ are α-strong since every vertex in a regular $\mathcal{NG}$ has low indeterminacy and falsity values and high truth membership values.

Therefore, All the vertices of $\mathcal{NG}$ are α-strong vertices if it is a regular neutrosophic graph.

Theorem 4.2

A complete $\mathcal{NG}$, $\widetilde{\mathcal{N}_{\mathcal{G}}}:(\mathcal{V}_{\mathcal{G}},\zeta,\omega)$must have at least one pair of α-strong vertices whose degrees are same.

Proof: Every vertex in a complete $\mathcal{NG}$ with n vertices is connected to every other vertex. As a result, every vertex $\mathfrak{a}_i$ has $n-1$ edges incident with it.

The degree $d(\mathfrak{a}_i)$ is the sum of the truth membership values of the edges incident to $\mathfrak{a}_i$

$$d(\mathfrak{a}_i)=\sum_{\mathfrak{a}_i\in\mathcal{V}}[\sigma((v,u))].$$

The degrees are constrained within a specified range due to the total connectivity of the graph and the limited range of truth membership values. Therefore, if we distribute the degrees across n vertices, there must be at least one pair of vertices with the same degree, according to the pigeonhole principle.

Therefore, A complete $\mathcal{NG}$, $\widetilde{\mathcal{N}_{\mathcal{G}}}:(\mathcal{V}_{\mathcal{G}},\zeta,\omega)$have at least one pair of α-strong vertices whose degrees are same.

Theorem 4.3

A vertex u is γ-strong in a neutrosophic graph $\widetilde{\mathcal{N}_{\mathcal{G}}}: (\mathcal{V}_{\mathcal{G}}, \zeta, \omega)$ if there is at least one distinct weakest arc among the edges incident to u.

Proof:

Consider of a vertex $\mathfrak{a}_i$ in the neutrosophic network $\widetilde{\mathcal{N}_{\mathcal{G}}}: (\mathcal{V}_{\mathcal{G}}, \zeta, \omega)$.

The set $\mathcal{E}_u = \{ e_i = (u, v_i) | v_i \in V \}$ represents the edges incident to u. The truth membership values of these edges are provided by $\sigma_{\mathcal{T}}(e_i)$.

In order for u to be γ-strong, there needs to be an edge $e_{min} = (u, v_{min}) \in \mathcal{E}_u$ such that $\sigma(e_{min})$ is the smallest truth membership value among all the edges in $\mathcal{E}_u$, and this value is unique, (i.e) no other edge in $\mathcal{E}_u$ shares this minimum value. This condition can be mathematically represented as follows: $\sigma(e_{min}) < \sigma(e) \; \forall \, e \in \mathcal{E}_u, \; e \neq e_{min}$.

The definition of a γ-strong vertex is satisfied by u if it has at least one unique weakest arc among its incident edges, which is indicated by the existence of the edge e_{min}. In contrast to other vertices that might not have such a unique weakest arc, this condition guarantees that the vertex u is distinct in having a uniquely minimal truth membership value for one of its incident edges. Therefore, the neutrosophic graph $\widetilde{\mathcal{N}_{\mathcal{G}}}'s$ unique weakest arc verifies that u is a γ-strong vertex.

Theorem 4.4

The degree of every γ-strong node in a $\mathcal{NG}$, $\widetilde{\mathcal{N}_{\mathcal{G}}}: (\mathcal{V}_{\mathcal{G}}, \zeta, \omega)$ with a crisp graph underlying $\mathcal{C}_{\mathcal{G}}$ that is regular is smaller than the minimum degree of any α-strong node $\mathfrak{a}_i$

$[d_{\gamma}(\mathfrak{v}) < \min \; d_{\alpha}(\mathfrak{v}_i)]$, where $i \in Z^{+}$.

Proof: Let $\mathcal{NG}$, $\widetilde{\mathcal{N}_{\mathcal{G}}}: (\mathcal{V}_{\mathcal{G}}, \zeta, \omega)$ be a neutrosophic graph. The underlying crisp graph $\mathcal{C}_{\mathcal{G}}$, is regular, (i.e) each vertex in $\mathcal{C}_{\mathcal{G}}$ has an equal number of edges. A vertex $\mathfrak{a}_i$ is considered γ-strong in $\mathcal{NG}$ if it is connected to at least one edge with a significantly lower truth membership value (i.e) there must be at least one unique weakest arc among the edges incident to σ_i. The total degree $d_{\gamma}(\mathfrak{a}_i)$ of $\mathfrak{a}_i$ is

decreased by this particular weakest arc because a vertex's degree is determined by the total truth membership values of its incident edges. Conversely, a vertex $\mathfrak{a}_i$ with high truth membership values ($\mathcal{T}$) and low indeterminacy ($\mathcal{I}$) and falsity ($\mathcal{F}$) is said to be α-strong because of constant and comparatively high truth membership values of its incident edges, resulting in a higher degree d_α ($\mathfrak{a}_i$).The degrees are uniform since $\mathcal{C}_\mathcal{G}$ is regular. However, the γ-strong condition lowers the truth membership value of γ-strong vertices, decreasing their degree of comparison in α-strong vertices. Because the α-strong vertices consistently maintain higher truth membership values across their incident edges, for any γ-strong vertex $\mathfrak{a}_i$, its degree $d_\gamma(\mathfrak{a}_i)$ is less than the minimum degree $\min(d_\alpha(\mathfrak{a}_i))$ of any α-strong vertex $\mathfrak{a}_i$. This is because α-strong vertices consistently maintain higher truth membership values across their incident edges.

Integrating other advanced techniques, such as machine learning models, could help improve scalability and efficiency, particularly in large networks. Some managerial implications include network optimization, resource allocation and in healthcare systems. This approach can significantly enhance patient referral systems by optimizing the flow between different healthcare providers, ultimately reducing waiting times and improving service efficiency.

5. Study of α, β *and* γ strong vertices in Neutrosophic graph Operations

Using vertex and edge cardinality (definitions 2.6), we can find the membership values for the $\mathcal{NG}$ represented in Figure 2. Determine each vertex's degree by definition 2.5, Sort vertices into α, β, and γ strong categories based on the criteria listed in definitions 3.3, 3.4, and 3.5. Use the neutrosophic vertex order coloring approach to color the vertices so that no two neighboring vertices have the same color applied to them. This section deals with an innovative technique for coloring $\mathcal{NG}$ networks.

5.1 α, β *and* γ strong vertices of Co-normal product

Consider two single-valued Neutrosophic graphs $\mathbb{N}_{\mathbb{G}_1}' = (\mathcal{V}_1, \mathcal{E}_1)$ and $\mathbb{N}_{\mathbb{G}_2}' = (\mathcal{V}_2, \mathcal{E}_2)$ whose $\mathbb{G}_{\mathcal{C}_{\mathcal{N}_1}} = (\mathcal{X}_1, \mathcal{Y}_1)$ and $\mathbb{G}_{\mathcal{C}_{\mathcal{N}_2}} = (\mathcal{X}_2, \mathcal{Y}_2)$ respectively.

Then the Co-normal product $\mathbb{N}_{\mathbb{G}_1}' \boxplus_{\mathcal{CN}} \mathbb{N}_{\mathbb{G}_2}' = (\mathcal{X}_1 \boxplus_{\mathcal{CN}} \mathcal{X}_2, \mathcal{Y}_1 \boxplus_{\mathcal{CN}} \mathcal{Y}_2)$ is defined as

i. $\forall (x, y) \in \mathcal{V}_1 \times \mathcal{V}_2$,

$\mathcal{T}_{x_1} \boxplus_{\mathcal{CN}} \mathcal{T}_{x_2}\ (u_1, u_2) = \mathcal{T}_{x_1}\ (u_1) \wedge\ \mathcal{T}_{x_2}\ (u_2)$;

$\mathcal{I}_{x_1} \boxplus_{\mathcal{CN}} \mathcal{I}_{x_2}\ (u_1, u_2) = \mathcal{I}_{x_1}\ (u_1) \wedge \mathcal{I}_{x_2}\ (u_2)$ and

$\mathcal{F}_{x_1} \boxplus_{\mathcal{CN}} \mathcal{F}_{x_2}(u_1, u_2) = \mathcal{F}_{x_1}\ (u_1) \vee \mathcal{F}_{x_2}\ (u_2)$

ii. $\mathcal{T}_{\mathcal{Y}}((u_1, u_2)\ (v_1, v_2)) = (\mathcal{T}_{\mathcal{Y}_1}(u_1 v_1) \wedge\ \mathcal{T}_{x_2}\ (v_1, v_2))$;

$\mathcal{I}_{\mathcal{Y}}((u_1, u_2)\ (v_1, v_2)) =\ (\mathcal{I}_{\mathcal{Y}_1}(u_1 v_1) \wedge\ \mathcal{I}_{x_2}\ (v_1, v_2))$;

$\mathcal{F}_{\mathcal{Y}}((u_1, u_2)\ (v_1, v_2)) = (\mathcal{F}_{x_1}(u_1 v_1) \vee\ \mathcal{F}_{\mathcal{Y}_2}\ (v_1, v_2))$; $\forall\ u_1 = u_2$ and $v_1, v_2 \in \mathcal{X}_2$ where

$u_1, u_2 \in \mathcal{X}_1$ *and* $v_1, v_2 \in \mathcal{X}_2$

iii. $\mathcal{T}_{\mathcal{Y}}((u_1, u_2)\ (v_1, v_2)) = (\mathcal{T}_{\mathcal{Y}_1}(u_1 v_1) \wedge\ \mathcal{T}_{x_2}\ (v_1, v_2))$;

$\mathcal{I}_{\mathcal{Y}}((u_1, u_2)\ (v_1, v_2)) =\ (\mathcal{I}_{\mathcal{Y}_1}(u_1 v_1) \wedge\ \mathcal{I}_{x_2}\ (v_1, v_2))$;

$\mathcal{F}_{\mathcal{Y}}((u_1, u_2)\ (v_1, v_2)) = (\mathcal{F}_{x_1}(u_1 v_1) \vee\ \mathcal{F}_{\mathcal{Y}_2}\ (v_1, v_2))$; $\forall\ u_1, u_2 \in \mathcal{X}_1$ and $v_1 = v_2$

where $u_1, u_2 \in \mathcal{X}_1$ *and* $v_1, v_2 \in \mathcal{X}_2$

The construction of the Co-normal product network $\mathbb{N}_{\mathbb{G}_1}' \boxplus_{\mathcal{CN}} \mathbb{N}_{\mathbb{G}_2}'$ is shown in the following steps.

Step 1: Construct the co-normal $\mathcal{SVNG}$ product network, $\mathbb{N}_{\mathbb{G}_1}' \boxplus_{\mathcal{CN}} \mathbb{N}_{\mathbb{G}_2}'$(figure 5) of two $\mathcal{NG}$ (Figure 3,4).

Step 2: The truth, indeterminancy and falsity membership values, makes up each vertex. The values are assigned in accordance with Table 2 using Vertex cardinality (definition 2.6).

Step 3: The values are assigned in accordance with Table 3 by using edge cardinality (definition 2.6).

Step 4: Determine each vertex's adjacent vertices and degree for each vertex. Table 4 provides the degree of each vertex in Figure 5.

Step 5: Sort the α, β, and γ strong vertices according to the conditions given in definition 3.3,3.4 and 3.5.

Figure 3 and 4 are the examples of neutrosophic graphs where $\mathbb{N}_{\mathbb{F}_{\mathbb{G}_1}}'$=(3,3) and $\mathbb{N}_{\mathbb{F}_{\mathbb{G}_2}}'$=(4,5) respectively.

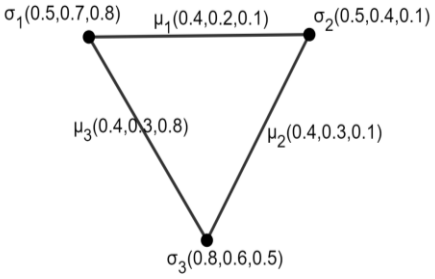

Figure 3: $\mathbb{N}_{\mathbb{F}_{\mathbb{G}_1}'}$

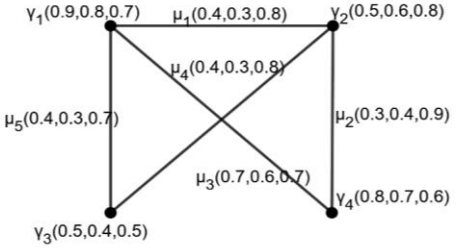

Figure 4: $\mathbb{N}_{\mathbb{F}_{\mathbb{G}_2}'}$

Figure 5 is the neutrosophic network, $\mathbb{N}_{\mathbb{G}_1'} \boxplus_{\mathcal{CN}} \mathbb{N}_{\mathbb{G}_2'}$ which is driven by applying co-normal product between $\mathbb{N}_{\mathbb{F}_{\mathbb{G}_1}'}$ and $\mathbb{N}_{\mathbb{F}_{\mathbb{G}_2}'}$.

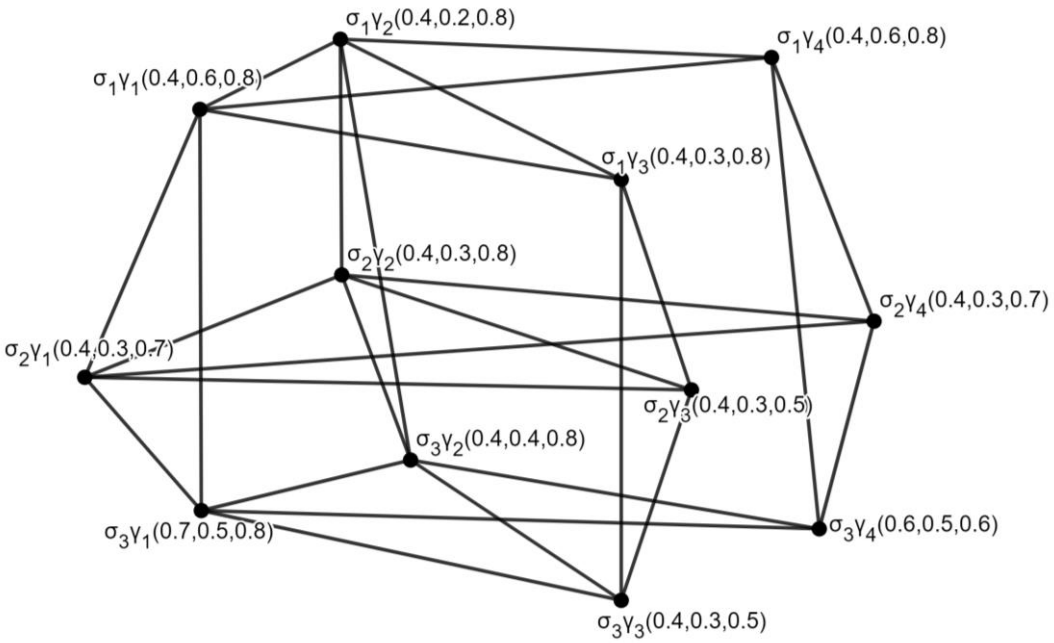

Figure 5: $\mathbb{N}_{\mathbb{G}_1'} \boxplus_{\mathcal{CN}} \mathbb{N}_{\mathbb{G}_2'}$

Table 2: Membership values of the vertices of $\mathbb{N}_{\mathbb{G}_1'} \boxplus_{\mathcal{CN}} \mathbb{N}_{\mathbb{G}_2'}$

Vertices	Membership Values	Vertex Cardinality $\lvert\mathbb{E}\rvert$

$\sigma(\sigma_1\gamma_1)$	(0.4,0.6,0.8)	0.33
$\sigma(\sigma_1\gamma_2)$	(0.4.0.2,0.8)	0.46
$\sigma(\sigma_1\gamma_3)$	(0.4,0.3,0.8)	0.43
$\sigma(\sigma_1\gamma_4)$	(0.4.0.6,0.8)	0.33
$\sigma(\sigma_2\gamma_1)$	(0.4,0.3,0.7)	0.46
$\sigma(\sigma_2\gamma_2)$	(0.4,0.3,0.8)	0.43
$\sigma(\sigma_2\gamma_3)$	(0.4,0.3,0.5)	0.53
$\sigma(\sigma_2\gamma_4)$	(0.4,0.3,0.7)	0.46
$\sigma(\sigma_3\gamma_1)$	(0.7,0.5,0.8)	0.46
$\sigma(\sigma_3\gamma_2)$	(0.4,0.4,0.8)	0.4
$\sigma(\sigma_3\gamma_3)$	(0.4,0.3,0.5)	0.53
$\sigma(\sigma_3\gamma_4)$	(0.6,0.5,0.6)	0.5

Table 3: Membership values of the edges of $\mathbb{N}_{\mathbb{G}_1}' \boxplus_{\mathcal{CN}} \mathbb{N}_{\mathbb{G}_2}'$

Edges	Membership Values	Edge Cardinality $\lvert\mathbb{E}\rvert$	Edges	Membership Values	Edge Cardinality $\lvert\mathbb{E}\rvert$
$\mu(\sigma_1\gamma_1\sigma_2\gamma_1)$	(0.3,0.1,0.7)	0.5	$\mu(\sigma_1\gamma_4\sigma_2\gamma_4)$	(0.3,0.1,0.6)	0.53
$\mu(\sigma_1\gamma_1\sigma_3\gamma_1)$	(0.3,0.2,0.7)	0.43	$\mu(\sigma_1\gamma_4\sigma_3\gamma_4)$	(0.3,0.2,0.8)	0.43
$\mu(\sigma_1\gamma_1\sigma_1\gamma_2)$	(0.3,0.1,0.7)	0.43	$\mu(\sigma_2\gamma_1\sigma_3\gamma_1)$	(0.3,0.2,0.7)	0.43
$\mu(\sigma_1\gamma_1\sigma_1\gamma_3)$	(0.3,0.2,0.8)	0.43	$\mu(\sigma_2\gamma_1\sigma_2\gamma_2)$	(0.3,0.2,0.8)	0.43

$\mu(\sigma_1\gamma_1\sigma_1\gamma_4)$	(0.4,0.5,0.8)	0.36	$\mu(\sigma_2\gamma_1\sigma_2\gamma_3)$	(0.3,0.2,0.7)	0.46
$\mu(\sigma_1\gamma_2\sigma_3\gamma_2)$	(0.3,0.2,0.8)	0.43	$\mu(\sigma_2\gamma_1\sigma_2\gamma_4)$	(0.4,0.3,0.7)	0.46
$\mu(\sigma_1\gamma_2\sigma_1\gamma_3)$	(0.3,0.2,0.8)	0.43	$\mu(\sigma_2\gamma_2\sigma_3\gamma_2)$	(0.3,0.2,0.8)	0.43
$\mu(\sigma_1\gamma_2\sigma_1\gamma_4)$	(0.2,0.3,0.9)	0.33	$\mu(\sigma_2\gamma_2\sigma_2\gamma_3)$	(0.3,0.2,0.8)	0.43
$\mu(\sigma_1\gamma_3\sigma_2\gamma_3)$	(0.3,0.1,0.5)	0.56	$\mu(\sigma_2\gamma_2\sigma_2\gamma_4)$	(0.2,0.3,0.9)	0.33
$\mu(\sigma_1\gamma_3\sigma_3\gamma_3)$	(0.3,0.2,0.8)	0.43	$\mu(\sigma_2\gamma_3\sigma_3\gamma_3)$	(0.3,0.2,0.5)	0.53
$\mu(\sigma_1\gamma_2\sigma_2\gamma_2)$	(0.3,0.1,0.8)	0.46	$\mu(\sigma_2\gamma_4\sigma_3\gamma_4)$	(0.3,0.2,0.6)	0.5
$\mu(\sigma_3\gamma_1\sigma_3\gamma_2)$	(0.3,0.2,0.8)	0.53	$\mu(\sigma_3\gamma_1\sigma_3\gamma_3)$	(0.3,0.2,0.7)	0.46
$\mu(\sigma_3\gamma_2\sigma_3\gamma_3)$	(0.3,0.2,0.8)	0.43	$\mu(\sigma_3\gamma_1\sigma_3\gamma_4)$	(0.5,0.4,0.7)	0.46
$\mu(\sigma_3\gamma_2\sigma_3\gamma_4)$	(0.2,0.3,0.9)	0.33			

Table 4: List of α strong, β strong, and γ strong vertices of $\mathbb{N}_{\mathbb{G}_1'} \boxplus_{\mathcal{CN}} \mathbb{N}_{\mathbb{G}_2'}$

Vertex	Adjacent vertices	Degree	α strong	β strong	γ strong
$\sigma_1\gamma_1$	$\sigma_2\gamma_1, \sigma_3\gamma_1, \sigma_1\gamma_2, \sigma_1\gamma_3, \sigma_1\gamma_4$	2.15	-	$\sigma_1\gamma_1$	-
$\sigma_1\gamma_2$	$\sigma_1\gamma_1, \sigma_2\gamma_2, \sigma_3\gamma_2, \sigma_1\gamma_3, \sigma_1\gamma_4$	2.08	-	$\sigma_1\gamma_2$	-
$\sigma_1\gamma_3$	$\sigma_1\gamma_1, \sigma_1\gamma_2, \sigma_2\gamma_3, \sigma_3\gamma_3$	1.85	-	$\sigma_1\gamma_3$	-
$\sigma_1\gamma_4$	$\sigma_1\gamma_1, \sigma_1\gamma_2, \sigma_2\gamma_4, \sigma_3\gamma_4$	1.65	-	-	$\sigma_1\gamma_4$
$\sigma_2\gamma_1$	$\sigma_1\gamma_1, \sigma_3\gamma_1, \sigma_2\gamma_2, \sigma_2\gamma_3, \sigma_2\gamma_4$	2.31	$\sigma_2\gamma_1$	-	-
$\sigma_2\gamma_2$	$\sigma_1\gamma_2, \sigma_3\gamma_2, \sigma_2\gamma_1, \sigma_2\gamma_3, \sigma_2\gamma_4$	2.08	-	$\sigma_2\gamma_2$	-
$\sigma_2\gamma_3$	$\sigma_2\gamma_1, \sigma_2\gamma_2, \sigma_1\gamma_3, \sigma_3\gamma_3$	1.98	-	$\sigma_2\gamma_3$	-
$\sigma_2\gamma_4$	$\sigma_2\gamma_1, \sigma_2\gamma_2, \sigma_1\gamma_4, \sigma_3\gamma_4$	1.82	-	$\sigma_2\gamma_4$	-

$\sigma_3\gamma_1$	$\sigma_1\gamma_1, \sigma_2\gamma_1, \sigma_3\gamma_2, \sigma_3\gamma_3, \sigma_3\gamma_4$	2.24	-	$\sigma_3\gamma_1$	-
$\sigma_3\gamma_2$	$\sigma_1\gamma_2, \sigma_2\gamma_2, \sigma_3\gamma_1, \sigma_3\gamma_3, \sigma_3\gamma_4$	2.15	-	$\sigma_3\gamma_2$	-
$\sigma_3\gamma_3$	$\sigma_1\gamma_3, \sigma_2\gamma_3, \sigma_3\gamma_1, \sigma_3\gamma_2$	1.85	-	$\sigma_3\gamma_3$	-
$\sigma_3\gamma_4$	$\sigma_1\gamma_4, \sigma_2\gamma_4, \sigma_3\gamma_1, \sigma_3\gamma_2$	1.72	-	$\sigma_3\gamma_4$	-

Table 5: Color identification of α, β, and γ strong vertices

Vertex	Identification of Color
α strong vertex	$\sigma_2\gamma_1 - 2$
β strong vertex	$\sigma_1\gamma_1 - 1, \sigma_1\gamma_2 - 2, \sigma_2\gamma_2 - 1, \sigma_3\gamma_2 - 3, \sigma_3\gamma_1 - 4, \sigma_1\gamma_3 - 4, \sigma_2\gamma_3 - 3,$ $\sigma_3\gamma_3 - 2, \sigma_2\gamma_4 - 4, \sigma_3\gamma_4 - 2$
γ strong vertex	$\sigma_1\gamma_4 - 3$

The minimum spanning tree of $\mathbb{N}_{\mathbb{G}_1'} \boxplus_{\mathcal{CN}} \mathbb{N}_{\mathbb{G}_2'}$ is computed using kruskal's algorithm and its weights is observed as $\mathcal{MST}_{\mathcal{W}_0}(\mathbb{N}_{\mathbb{G}_1'} \boxplus_{\mathcal{CN}} \mathbb{N}_{\mathbb{G}_2'}) = 4.36$

From Table 7, The chromatic number for $\mathbb{N}_{\mathbb{G}_1'} \boxplus_{\mathcal{CN}} \mathbb{N}_{\mathbb{G}_2'}$ is given by, $\chi^{\tau^*}(\mathbb{N}_{\mathbb{G}_1'} \boxplus_{\mathcal{CN}} \mathbb{N}_{\mathbb{G}_2'}) = 4$

5.2 α, β *and* γ strong vertices of Tensor product

Assume that the single-valued neutrosophic graphs of $\mathbb{G}_{\mathcal{T}_1} = (\mathcal{X}_1, \mathcal{Y}_1)$ and $\mathbb{G}_{\mathcal{T}_2} = (\mathcal{X}_2, \mathcal{Y}_2)$ are $\mathbb{N}_{\mathbb{G}_1'} = (\mathcal{V}_1, \mathcal{E}_1)$ and $\mathbb{N}_{\mathbb{G}_2'} = (\mathcal{V}_2, \mathcal{E}_2)$ are respectively. A pair $(\mathcal{X}, \mathcal{Y})$ is considered to be the tensor product $\mathbb{N}_{\mathbb{G}_1'} \star_{\mathcal{T}} \mathbb{N}_{\mathbb{G}_2'}$ if:

i. $\mathcal{T}_{\mathcal{X}}(u_1, u_2) = \mathcal{T}_{x_1}(u_1) \wedge \mathcal{T}_{x_2}(u_2)$;

$\mathcal{I}_{\mathcal{X}}(u_1, u_2) = \mathcal{T}_{x_1}(u_1) \wedge \mathcal{T}_{x_2}(u_2)$;

$\mathcal{F}_{\mathcal{X}}(u_1, u_2) = \mathcal{T}_{x_1}(u_1) \vee \mathcal{T}_{x_2}(u_2) \ \forall \ (u_1, u_2) \in \mathcal{V}_1 \times \mathcal{V}_2$

ii. $\mathcal{T}_{\mathcal{Y}}((u_1, u_2)(v_1, v_2)) = \mathcal{T}_{y_1}(u_1 v_1) \wedge \mathcal{T}_{x_2}(v_1, v_2)$;

$$\mathcal{I}_{\mathcal{y}}((u_1, u_2)(v_1, v_2)) = \mathcal{I}_{\mathcal{y}_1}(u_1 v_1) \wedge \mathcal{I}_{x_2}(v_1, v_2);$$

$$\mathcal{F}_{\mathcal{y}}((u_1, u_2)(v_1, v_2)) = \mathcal{F}_{x_1}(u_1 v_1) \vee \mathcal{F}_{\mathcal{y}_2}(v_1, v_2); \quad \forall\, u_1 u_2 \in X_1 \text{ and } v_1, v_2 \in X_2$$

The construction of the tensor product network $\mathbb{N}_{\mathbb{G}_1}' \star_{\mathcal{T}} \mathbb{N}_{\mathbb{G}_2}'$ is shown in the following steps.

Step 1: Construct the tensor $\mathcal{SVNG}$ product network, $\mathbb{N}_{\mathbb{G}_1}' \star_{\mathcal{T}} \mathbb{N}_{\mathbb{G}_2}'$(figure 6) of two $\mathcal{NG}$ (Figure 3,4).

Step 2: Three truth, indeterminancy and falsity membership values, make up each vertex. The values are assigned in accordance with Table 6 using Vertex cardinality (definition 2.6).

Step 3: The values are assigned in accordance with Table 7 by using edge cardinality (definition 2.7).

Step 4: Determine each vertex's adjacent vertices and degree for each vertex. Table 8 provides the degree of each vertex in Figure 6.

Step 5: Sort the α, β, and γ strong vertices according to the conditions given in definition 3.3,3.4 and 3.5.

Figure 6 is the neutrosophic network, $\mathbb{N}_{\mathbb{G}_1}' \star_{\mathcal{T}} \mathbb{N}_{\mathbb{G}_2}'$ which is driven by applying tensor product between $\mathbb{N}_{\mathbb{F}_{\mathbb{G}_1}}'$ and $\mathbb{N}_{\mathbb{F}_{\mathbb{G}_2}}'$.

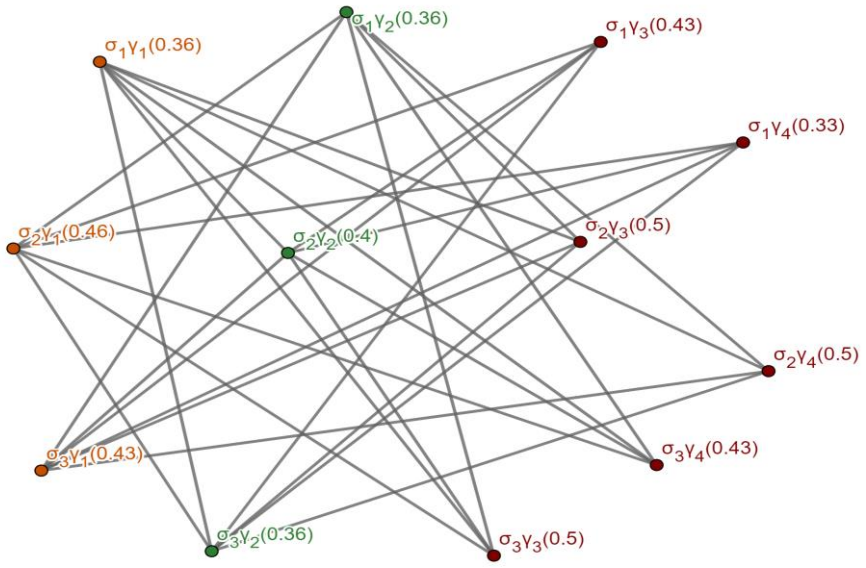

Figure 6: $\mathbb{N}_{\mathbb{G}_1}' \star_{\mathcal{T}} \mathbb{N}_{\mathbb{G}_2}'$

Table 6: Membership values of the vertices of $\mathbb{N}_{\mathbb{G}_1}' \star_{\mathcal{T}} \mathbb{N}_{\mathbb{G}_2}'$

Vertices	Membership Values	Vertex Cardinality $\lvert\mathbb{E}\rvert$

$\sigma(\sigma_1\gamma_1)$	(0.4,0.5,0.8)	0.36
$\sigma(\sigma_1\gamma_2)$	(0.3.0.4,0.8)	0.36
$\sigma(\sigma_1\gamma_3)$	(0.3,0.2,0.8)	0.43
$\sigma(\sigma_1\gamma_4)$	(0.3.0.5,0.8	0.33
$\sigma(\sigma_2\gamma_1)$	(0.3,0.2,0.7)	0.46
$\sigma(\sigma_2\gamma_2)$	(0.3,0.3,0.8)	0.4
$\sigma(\sigma_2\gamma_3)$	(0.3,0.3,0.5)	0.5
$\sigma(\sigma_2\gamma_4)$	(0.3,0.2.0.6)	0.5
$\sigma(\sigma_3\gamma_1)$	(0.5,0.5,0.7)	0.43
$\sigma(\sigma_3\gamma_2)$	(0.3,0.4,0.8)	0.36
$\sigma(\sigma_3\gamma_3)$	(0.3,0.3,0.5)	0.5
$\sigma(\sigma_3\gamma_4)$	(0.4,0.5,0.6)	0.43

Table 7: Membership values of the edges of $\mathbb{N}_{\mathbb{G}_1'} \star_{\mathcal{T}} \mathbb{N}_{\mathbb{G}_2'}$

Edges	Membership Values	Edge Cardinality $\lvert\mathbb{E}\rvert$	Edges	Membership Values	Edge Cardinality $\lvert\mathbb{E}\rvert$
$\mu(\sigma_1\gamma_1\sigma_2\gamma_2)$	(0.3,0.1,0.8)	0.46	$\mu(\sigma_1\gamma_4\sigma_3\gamma_1)$	(0.3,0.2,0.8)	0.43
$\mu(\sigma_1\gamma_1\sigma_2\gamma_3)$	(0.2,0.1,0.7)	0.46	$\mu(\sigma_1\gamma_4\sigma_3\gamma_2)$	(0.2,0.2,0.9)	0.36
$\mu(\sigma_1\gamma_1\sigma_2\gamma_4)$	(0.3,0.1,0.7)	0.5	$\mu(\sigma_2\gamma_1\sigma_3\gamma_2)$	(0.3,0.2,0.8)	0.43

$\mu(\sigma_1\gamma_1\sigma_3\gamma_2)$	(0.3,0.2,0.8)	0.43	$\mu(\sigma_2\gamma_1\sigma_3\gamma_3)$	(0.3,0.2,0.7)	0.46
$\mu(\sigma_1\gamma_1\sigma_3\gamma_3)$	(0.3,0.2,0.8)	0.43	$\mu(\sigma_2\gamma_1\sigma_3\gamma_4)$	(0.3,0.2,0.7)	0.46
$\mu(\sigma_1\gamma_1\sigma_3\gamma_4)$	(0.3,0.2,0.8)	0.43	$\mu(\sigma_2\gamma_2\sigma_3\gamma_1)$	(0.3,0.2,0.8)	0.43
$\mu(\sigma_1\gamma_2\sigma_2\gamma_1)$	(0.3,0.1,0.8)	0.46	$\mu(\sigma_2\gamma_2\sigma_3\gamma_3)$	(0.3,0.2,0.8)	0.43
$\mu(\sigma_1\gamma_2\sigma_2\gamma_3)$	(0.3,0.1,0.8)	0.46	$\mu(\sigma_2\gamma_2\sigma_3\gamma_4)$	(0.2,0.2,0.9)	0.36
$\mu(\sigma_1\gamma_2\sigma_2\gamma_4)$	(0.2,0.1,0.9)	0.4	$\mu(\sigma_2\gamma_3\sigma_3\gamma_1)$	(0.3,0.2,0.7)	0.46
$\mu(\sigma_1\gamma_2\sigma_3\gamma_1)$	(0.3,0.2,0.8)	0.43	$\mu(\sigma_2\gamma_3\sigma_3\gamma_2)$	(0.3,0.2,0.8)	0.43
$\mu(\sigma_1\gamma_2\sigma_3\gamma_3)$	(0.3,0.2,0.8)	0.43	$\mu(\sigma_2\gamma_4\sigma_3\gamma_1)$	(0.3,0.2,0.7)	0.43
$\mu(\sigma_1\gamma_2\sigma_3\gamma_4)$	(0.3,0.2,0.8)	0.43	$\mu(\sigma_2\gamma_4\sigma_3\gamma_2)$	(0.2,0.2,0.9)	0.46
$\mu(\sigma_1\gamma_3\sigma_2\gamma_1)$	(0.3,0.1,0.8)	0.5	$\mu(\sigma_1\gamma_3\sigma_3\gamma_2)$	(0.3,0.2,0.8)	0.43
$\mu(\sigma_1\gamma_3\sigma_2\gamma_2)$	(0.3,0.1,0.8)	0.46	$\mu(\sigma_1\gamma_4\sigma_2\gamma_1)$	(0.3,0.1,0.7)	0.43
$\mu(\sigma_1\gamma_3\sigma_3\gamma_1)$	(0.3,0.2,0.8)	0.43	$\mu(\sigma_1\gamma_4\sigma_2\gamma_2)$	(0.2,0.1,0.9)	0.4

Table 8: List of α strong, β strong, and γ strong vertices of $\mathbb{N}_{\mathbb{G}_1'} \star_{\mathcal{T}} \mathbb{N}_{\mathbb{G}_2'}$

Vertex	Adjacent vertices	Degree	α strong	β strong	γ strong
$\sigma_1\gamma_1$	$\sigma_2\gamma_2, \sigma_2\gamma_3, \sigma_2\gamma_4, \sigma_3\gamma_2, \sigma_3\gamma_3, \sigma_3\gamma_4$	2.71	$\sigma_1\gamma_1$	-	-
$\sigma_1\gamma_2$	$\sigma_2\gamma_1, \sigma_2\gamma_3, \sigma_2\gamma_4, \sigma_3\gamma_1, \sigma_3\gamma_3, \sigma_3\gamma_4$	2.61	-	$\sigma_1\gamma_2$	-
$\sigma_1\gamma_3$	$\sigma_2\gamma_2, \sigma_2\gamma_1, \sigma_3\gamma_2, \sigma_3\gamma_1$	1.82	-	-	$\sigma_1\gamma_3$

$\sigma_1\gamma_4$	$\sigma_2\gamma_1, \sigma_2\gamma_2, \sigma_3\gamma_1, \sigma_3\gamma_2$	1.62	-	-	$\sigma_1\gamma_4$
$\sigma_2\gamma_1$	$\sigma_1\gamma_2, \sigma_1\gamma_3, \sigma_1\gamma_4, \sigma_3\gamma_2, \sigma_3\gamma_3, \sigma_3\gamma_4$	2.81	$\sigma_2\gamma_1$	-	-
$\sigma_2\gamma_2$	$\sigma_1\gamma_1, \sigma_1\gamma_3, \sigma_1\gamma_4, \sigma_3\gamma_1, \sigma_3\gamma_3, \sigma_3\gamma_4$	2.54	-	$\sigma_2\gamma_2$	-
$\sigma_2\gamma_3$	$\sigma_1\gamma_1, \sigma_1\gamma_2, \sigma_3\gamma_2, \sigma_3\gamma_1$	1.81	-	-	$\sigma_2\gamma_3$
$\sigma_2\gamma_4$	$\sigma_1\gamma_1, \sigma_1\gamma_2, \sigma_3\gamma_2, \sigma_3\gamma_1$	1.72	-	-	$\sigma_2\gamma_4$
$\sigma_3\gamma_1$	$\sigma_1\gamma_2, \sigma_1\gamma_3, \sigma_1\gamma_4, \sigma_2\gamma_2, \sigma_2\gamma_3, \sigma_2\gamma_4$	2.64	$\sigma_3\gamma_1$	-	-
$\sigma_3\gamma_2$	$\sigma_1\gamma_1, \sigma_1\gamma_3, \sigma_1\gamma_4, \sigma_3\gamma_1, \sigma_3\gamma_3, \sigma_3\gamma_4$	2.44	-	$\sigma_3\gamma_2$	-
$\sigma_3\gamma_3$	$\sigma_2\gamma_2, \sigma_2\gamma_1, \sigma_1\gamma_1, \sigma_1\gamma_2$	1.75	-	-	$\sigma_3\gamma_3$
$\sigma_3\gamma_4$	$\sigma_2\gamma_2, \sigma_2\gamma_1, \sigma_1\gamma_1, \sigma_1\gamma_2$	1.68	-	-	$\sigma_3\gamma_4$

Table 9: Color identification of α, β, and γ strong vertices

Vertex	Identification of Color
α strong vertex	$\sigma_1\gamma_1 - 1, \sigma_2\gamma_1 - 1, \sigma_3\gamma_1$-1
β strong vertex	$\sigma_1\gamma_2 - 2, \sigma_2\gamma_2 - 2, \sigma_3\gamma_2 - 2$
γ strong vertex	$\sigma_1\gamma_3 - 3, \sigma_2\gamma_3 - 3, \sigma_3\gamma_3 - 3, \sigma_1\gamma_4 - 3, \sigma_2\gamma_4 - 3, \sigma_3\gamma_4 - 3$

The minimum spanning tree of $\mathbb{N}_{\mathbb{G}_1'} \star_{\mathcal{T}} \mathbb{N}_{\mathbb{G}_2'}$ is computed using kruskal's algorithm and its weights is observed as $\mathcal{MST}_{\mathcal{W}_0}(\mathbb{N}_{\mathbb{G}_1'} \star_{\mathcal{T}} \mathbb{N}_{\mathbb{G}_2'}) = 4.53$

From Table 7, The chromatic number for $\mathbb{N}_{\mathbb{G}_1'} \star_{\mathcal{T}} \mathbb{N}_{\mathbb{G}_2'}$ is given by, $\chi^{\tau^*}(\mathbb{N}_{\mathbb{G}_1'} \star_{\mathcal{T}} \mathbb{N}_{\mathbb{G}_2'}) = 3$

5.3 α, β and γ strong vertices of Residue product [15]

Consider two single-valued Neutrosophic networks of the graphs $\mathbb{N}_{\mathbb{G}_1'} = (\mathcal{V}_1, \mathcal{E}_1)$ and $\mathbb{N}_{\mathbb{G}_2'} = (\mathcal{V}_2, \mathcal{E}_2)$ with $\mathbb{G}_{\mathcal{R}_{\mathcal{P}_1}} = (\mathcal{X}_1, \mathcal{Y}_1)$ and $\mathbb{G}_{\mathcal{R}_{\mathcal{P}_2}} = (\mathcal{X}_2, \mathcal{Y}_2)$ respectively. Then the Residue product $\mathbb{N}_{\mathbb{G}_1'} \diamond_{\mathcal{R}_{\mathcal{P}}} \mathbb{N}_{\mathbb{G}_2'} = (\mathcal{X}_1 \diamond_{\mathcal{R}_{\mathcal{P}}} \mathcal{X}_2, \mathcal{Y}_1 \diamond_{\mathcal{R}_{\mathcal{P}}} \mathcal{Y}_2)$ is defined as

i) $\forall (x,y) \in \mathcal{V}_1 \times \mathcal{V}_2$,

$$\mathcal{T}_{x_1} \diamond_{\mathcal{R}_\mathcal{P}} \mathcal{T}_{x_2} (u_1, u_2) = (\mathcal{T}_{x_1} (u_1) \wedge \mathcal{T}_{x_2} (u_2);$$

$$\mathcal{I}_{x_1} \diamond_{\mathcal{R}_\mathcal{P}} \mathcal{I}_{x_2} (u_1, u_2) = \mathcal{I}_{x_1} (u_1) \wedge \mathcal{I}_{x_2} (u_2) \text{ and}$$

$$\mathcal{F}_{x_1} \diamond_{\mathcal{R}_\mathcal{P}} \mathcal{F}_{x_2} (u_1, u_2) = \mathcal{F}_{x_1} (u_1) \vee \mathcal{F}_{x_2} (u_2),$$

ii) $\forall (x,y) \in \mathcal{E}_1$ and $z \neq w \in \mathcal{V}_2$,

$$(\mathcal{T}_{y_1} \diamond_{\mathcal{R}_\mathcal{P}} \mathcal{T}_{y_2}) ((x, z), (y, w)) = \mathcal{T}_{y_1} (x,y);$$

$$(\mathcal{I}_{y_1} \diamond_{\mathcal{R}_\mathcal{P}} \mathcal{I}_{y_2}) ((x, z), (y, w)) = \mathcal{I}_{y_1} (x,y) \text{ and}$$

$$(\mathcal{F}_{y_1} \diamond_{\mathcal{R}_\mathcal{P}} \mathcal{F}_{y_2}) ((x, z), (y, w)) = \mathcal{F}_{y_1} (x,y).$$

The construction of the residue product network $\mathbb{N}_{\mathbb{G}_1}' \diamond_{\mathcal{R}_\mathcal{P}} \mathbb{N}_{\mathbb{G}_2}'$ is shown in the following steps.

Step 1: Construct the residue $\mathcal{SVNG}$ product network, $\mathbb{N}_{\mathbb{G}_1}' \diamond_{\mathcal{R}_\mathcal{P}} \mathbb{N}_{\mathbb{G}_2}'$(figure 7) of two $\mathcal{NG}$ (Figure 3,4).

Step 2: The truth, indeterminancy and falsity membership values, make up each vertex. Step 3: The values are assigned in accordance with Table 10 by using edge cardinality (definition 2.7).

Step 4: Determine each vertex's adjacent vertices and degree for each vertex. Table 8 provides the degree of each vertex in Figure 7.

Step 5: Sort the α, β, and γ strong vertices according to the conditions given in definition 3.3,3.4 and 3.5.

Figure 7 is the neutrosophic network, $\mathbb{N}_{\mathbb{G}_1}' \diamond_{\mathcal{R}_\mathcal{P}} \mathbb{N}_{\mathbb{G}_2}'$ which is driven by applying residue product between $\mathbb{N}_{\mathbb{F}_{\mathbb{G}_1}}'$ and $\mathbb{N}_{\mathbb{F}_{\mathbb{G}_2}}'$.

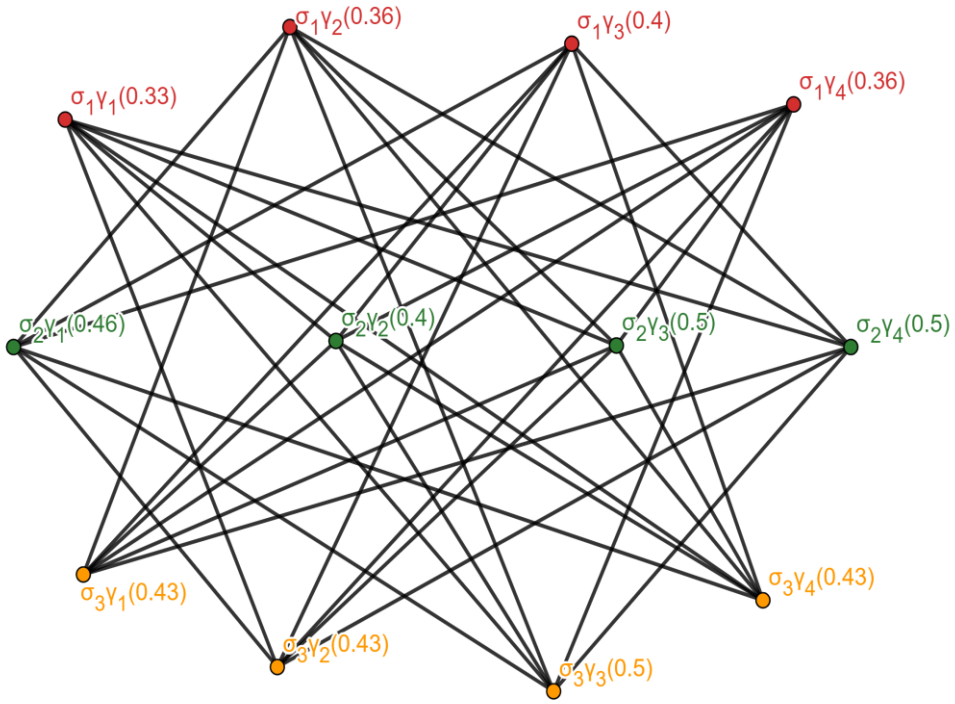

Figure 7: $\mathbb{N}_{\mathbb{G}_1'} \diamond_{\mathcal{R}_\mathcal{P}} \mathbb{N}_{\mathbb{G}_2'}$

Table 10: Membership values of the edges of $\mathbb{N}_{\mathbb{G}_1'} \diamond_{\mathcal{R}_\mathcal{P}} \mathbb{N}_{\mathbb{G}_2'}$

Edges	Membership Values	Edge Cardinality $\lvert\mathbb{E}\rvert$	Edges	Membership Values	Edge Cardinality $\lvert\mathbb{E}\rvert$
$\mu(\sigma_1\gamma_1\sigma_2\gamma_2)$	(0.3,0.1,0.8)	0.43	$\mu(\sigma_1\gamma_4\sigma_3\gamma_1)$	(0.3,0.2,0.8)	0.43
$\mu(\sigma_1\gamma_1\sigma_2\gamma_3)$	(0.3,0.1,0.7)	0.5	$\mu(\sigma_1\gamma_4\sigma_3\gamma_2)$	(0.2,0.2,0.9)	0.36
$\mu(\sigma_1\gamma_1\sigma_2\gamma_4)$	(0.3,0.1,0.7)	0.5	$\mu(\sigma_2\gamma_1\sigma_3\gamma_2)$	(0.3,0.2,0.8)	0.43
$\mu(\sigma_1\gamma_1\sigma_3\gamma_2)$	(0.3,0.2,0.8)	0.43	$\mu(\sigma_2\gamma_1\sigma_3\gamma_3)$	(0.3,0.2,0.7)	0.46
$\mu(\sigma_1\gamma_1\sigma_3\gamma_3)$	(0.3,0.2,0.8)	0.46	$\mu(\sigma_2\gamma_1\sigma_3\gamma_4)$	(0.3,0.2,0.7)	0.46
$\mu(\sigma_1\gamma_1\sigma_3\gamma_4)$	(0.3,0.2,0.8)	0.43	$\mu(\sigma_2\gamma_2\sigma_3\gamma_1)$	(0.3,0.2,0.8)	0.43
$\mu(\sigma_1\gamma_2\sigma_2\gamma_1)$	(0.3,0.1,0.8)	0.46	$\mu(\sigma_2\gamma_2\sigma_3\gamma_3)$	(0.3,0.2,0.8)	0.43

$\mu(\sigma_1\gamma_2\sigma_2\gamma_3)$	(0.3,0.1,0.8)	0.46	$\mu(\sigma_2\gamma_2\sigma_3\gamma_4)$	(0.2,0.2,0.9)	0.36
$\mu(\sigma_1\gamma_2\sigma_2\gamma_4)$	(0.2,0.1,0.9)	0.4	$\mu(\sigma_2\gamma_3\sigma_3\gamma_1)$	(0.3,0.2,0.7)	0.46
$\mu(\sigma_1\gamma_2\sigma_3\gamma_1)$	(0.3,0.2,0.8)	0.43	$\mu(\sigma_2\gamma_3\sigma_3\gamma_2)$	(0.3,0.2,0.8)	0.43
$\mu(\sigma_1\gamma_2\sigma_3\gamma_3)$	(0.3,0.2,0.8)	0.43	$\mu(\sigma_2\gamma_4\sigma_3\gamma_1)$	(0.3,0.2,0.7)	0.43
$\mu(\sigma_1\gamma_2\sigma_3\gamma_4)$	(0.3,0.1,0.8)	0.46	$\mu(\sigma_2\gamma_4\sigma_3\gamma_2)$	(0.2,0.2,0.9)	0.46
$\mu(\sigma_1\gamma_3\sigma_2\gamma_1)$	(0.3,0.1,0.7)	0.5	$\mu(\sigma_1\gamma_3\sigma_3\gamma_2)$	(0.3,0.2,0.8)	0.43
$\mu(\sigma_1\gamma_3\sigma_2\gamma_2)$	(0.3,0.2,0.8)	0.43	$\mu(\sigma_1\gamma_4\sigma_2\gamma_1)$	(0.3,0.1,0.7)	0.43
$\mu(\sigma_1\gamma_3\sigma_3\gamma_1)$	(0.3,0.2,0.8)	0.46	$\mu(\sigma_1\gamma_4\sigma_2\gamma_2)$	(0.2,0.1,0.9)	0.4
$\mu(\sigma_1\gamma_3\sigma_2\gamma_4)$	(0.4,0.2,0.1)	0.7	$\mu(\sigma_1\gamma_3\sigma_3\gamma_4)$	(0.4,0.3,0.8)	0.43
$\mu(\sigma_2\gamma_3\sigma_3\gamma_2)$	(0.3,0.2,0.8)	0.43	$\mu(\sigma_1\gamma_4\sigma_2\gamma_3)$	(0.4,0.2,0.1)	0.7
$\mu(\sigma_2\gamma_4\sigma_3\gamma_3)$	(0.4,0.3,0.1)	0.66	$\mu(\sigma_2\gamma_3\sigma_3\gamma_4)$	(0.4,0.3,0.1)	0.66

Table 11: List of α strong, β strong, and γ strong vertices of $\mathbb{N}_{\mathbb{G}_1'} \circ_{\mathcal{R}_p} \mathbb{N}_{\mathbb{G}_2'}$

Vertex	Adjacent vertices	Degree	α strong	β strong	γ strong
$\sigma_1\gamma_1$	$\sigma_2\gamma_2, \sigma_2\gamma_3, \sigma_2\gamma_4, \sigma_3\gamma_2, \sigma_3\gamma_3, \sigma_3\gamma_4$	2.75	-	$\sigma_1\gamma_1$	-
$\sigma_1\gamma_2$	$\sigma_2\gamma_1, \sigma_2\gamma_3, \sigma_2\gamma_4, \sigma_3\gamma_1, \sigma_3\gamma_3, \sigma_3\gamma_4$	2.64	-	-	$\sigma_1\gamma_2$
$\sigma_1\gamma_3$	$\sigma_2\gamma_1, \sigma_2\gamma_2, \sigma_2\gamma_4, \sigma_3\gamma_1, \sigma_3\gamma_2, \sigma_3\gamma_4$	2.95	-	$\sigma_1\gamma_3$	-
$\sigma_1\gamma_4$	$\sigma_2\gamma_1, \sigma_2\gamma_2, \sigma_2\gamma_3, \sigma_3\gamma_1, \sigma_3\gamma_2, \sigma_3\gamma_3$	2.82	-	$\sigma_1\gamma_4$	-
$\sigma_2\gamma_1$	$\sigma_1\gamma_2, \sigma_1\gamma_3, \sigma_1\gamma_4, \sigma_3\gamma_2, \sigma_3\gamma_3, \sigma_3\gamma_4$	2.81	-	$\sigma_2\gamma_1$	-
$\sigma_2\gamma_2$	$\sigma_1\gamma_1, \sigma_1\gamma_3, \sigma_1\gamma_4, \sigma_3\gamma_1, \sigma_3\gamma_3, \sigma_3\gamma_4$	2.48	-	-	$\sigma_2\gamma_2$
$\sigma_2\gamma_3$	$\sigma_1\gamma_1, \sigma_1\gamma_2, \sigma_1\gamma_4, \sigma_3\gamma_1, \sigma_3\gamma_2, \sigma_3\gamma_4$	2.91	$\sigma_2\gamma_3$	-	-

$\sigma_2\gamma_4$	$\sigma_1\gamma_1, \sigma_1\gamma_2, \sigma_1\gamma_3, \sigma_3\gamma_1, \sigma_3\gamma_2, \sigma_3\gamma_3$	3.08	$\sigma_2\gamma_4$	-	-
$\sigma_3\gamma_1$	$\sigma_1\gamma_2, \sigma_1\gamma_3, \sigma_1\gamma_4, \sigma_2\gamma_2, \sigma_2\gamma_3, \sigma_2\gamma_4$	2.67		$\sigma_3\gamma_1$	-
$\sigma_3\gamma_2$	$\sigma_1\gamma_1, \sigma_1\gamma_3, \sigma_1\gamma_4, \sigma_3\gamma_1, \sigma_3\gamma_3, \sigma_3\gamma_4$	2.44	-	-	$\sigma_3\gamma_2$
$\sigma_3\gamma_3$	$\sigma_1\gamma_1, \sigma_1\gamma_2, \sigma_1\gamma_4, \sigma_2\gamma_1, \sigma_2\gamma_2, \sigma_2\gamma_4$	2.87	-	$\sigma_3\gamma_3$	-
$\sigma_3\gamma_4$	$\sigma_1\gamma_1, \sigma_1\gamma_2, \sigma_1\gamma_3, \sigma_2\gamma_1, \sigma_2\gamma_2, \sigma_2\gamma_3$	2.8	-	$\sigma_3\gamma_4$	-

Table 12: Color identification of α, β, and γ strong vertices

Vertex	Identification of Color
α strong vertex	$\sigma_2\gamma_3 - 2\,, \sigma_2\gamma_4 - 2$
β strong vertex	$\sigma_1\gamma_1 - 1, \sigma_1\gamma_3 - 1, \sigma_1\gamma_4 - 1, \sigma_2\gamma_1 - 2, \sigma_3\gamma_1 - 3, \sigma_3\gamma_3 - 3, \sigma_3\gamma_4 - 3$
γ strong vertex	$\sigma_1\gamma_2 - 1, \sigma_2\gamma_2 - 2, \sigma_3\gamma_2 - 3$

The minimum spanning tree of $\mathbb{N}_{\mathbb{G}_1'} \diamond_{\mathcal{R}_\mathcal{P}} \mathbb{N}_{\mathbb{G}_2'}$ is computed using kruskal's algorithm and its weights is observed as $\mathcal{MST}_{\mathcal{W}_0}(\mathbb{N}_{\mathbb{G}_1'} \diamond_{\mathcal{R}_\mathcal{P}} \mathbb{N}_{\mathbb{G}_2'}) = 4.56$

From Table 7, The chromatic number for $\mathbb{N}_{\mathbb{G}_1'} \diamond_{\mathcal{R}_\mathcal{P}} \mathbb{N}_{\mathbb{G}_2'}$ is given by, $\chi^{\tau^*}(\mathbb{N}_{\mathbb{G}_1'} \diamond_{\mathcal{R}_\mathcal{P}} \mathbb{N}_{\mathbb{G}_2'}) = 3$

6. Applications of Neutrosophic product network- vertex order coloring

The fuzzy graph theory discipline has made great strides with the introduction of the NVOC method, which provides an advanced tool for network structure optimization under uncertainty. In this section, we have presented the algorithm for NVOC, a technique used to assign colors to vertices while accommodating uncertainty and vagueness. The NVOC algorithm makes use of the special qualities of neutrosophic graphs to offer practical recommendations for a variety of real-world applications, enhancing the effectiveness, dependability, and resilience of network systems.

Input: Neutrosophic graphs $\mathbb{N}_{\mathbb{F}_{\mathbb{G}_1}'}$ and $\mathbb{N}_{\mathbb{F}_{\mathbb{G}_2}'}$

Output: Optimal Neutrosophic network $\mathcal{O}^*_{\mathcal{N}_{\mathcal{F}_i}}$.

Step 1: using several kinds of network operations, construct a connected network $\widetilde{\mathcal{N}_{\mathcal{G}}}$, with the vertex set $\mathcal{V}_1 \times \mathcal{V}_2$

Step 2: Select the relevant operations and ascertain the effective edges in the $\mathcal{NG}$ $\widetilde{\mathcal{N}_{\mathcal{G}}}$ with n vertices.

Step 3: Determine the adjacent edges and make sure they are effective edges in order to construct an effective network. The condition to verify the effectiveness of the edge is given as follows.

$$\mu(uv) = \frac{1}{2}[\sigma(u) \wedge \sigma(v)] \leq \mu(uv).$$

Construct a new network with effective edges and eliminate the non-effective ones.

Step 4: Next, get the degree of each vertex using the formula $d(\sigma_i) = \sum_{i=1}^{n} d(\mathcal{A}(\sigma_i))$

Step 5: Based on the criteria listed in definitions 3.2, 3.3, and 3.4, evaluate the properties of vertices and categorize them as α strong, β strong, or γ strong vertices.

Step 6: Determine an m-coloring of the vertices in the $\mathcal{NG}$. Let $\{\sigma_1, \sigma_2, \ldots \sigma_n\}$ represent the vertices of $\widetilde{\mathcal{N}_{\mathcal{G}}}$: $(\mathcal{V}_{\mathcal{G}}, \zeta, \omega)$, and let {1, 2,..., m} represent the vertex colors in Z+.

Step 7: From $\mathbb{Z}^+$ to $\alpha_{str}(\mathcal{V})$, assign colors 1 to j.

Step 8: Assign each strong vertex a unique color that corresponds to $\alpha_{str}(\mathcal{V})$ if they are adjacent. If they are not adjacent, then assign the same color to each vertex.

Step 9: Assign color values j+1 to k for each $\beta(\mathcal{V})$, and then repeat step 7 for all $\beta(\mathcal{V})$.

Step 10: Give each vertex of γ_{str} $(\mathcal{V})$ the same value from $[\mathcal{K}+1, m]$. An edge that connects two γ strong vertices should be removed. If not, apply the same color to each vertex that is a member of $\gamma_{str}(\mathcal{V})$.

Step 11: For every product network, the weight of the minimum spanning tree $(\mathcal{MST}_{\mathcal{W}_0})$ has been calculated in order to evaluate the effective product graph. The chromatic number for each selected network can be obtained using χ^{τ^*}.

Step 12: $(|\alpha_{str}|)$ provides the cardinality of α strong vertices, and $(\mathcal{W}_0\ (\alpha_{str}))$ provides the weight of α strong vertices. The analysis of the most optimal network among the many networks will be done using the summation $(\mathcal{S}^*_{\mathcal{O}N_i})$ of all these parameters.

Step 13: To determine the optimal Neutrosophic product network ($\mathcal{O}^*_{\mathcal{N}_{\mathcal{F}_i}}$), the smallest value of $\mathcal{S}^*_{\mathcal{O}\mathcal{N}_i}$, where i=1,2,...,n. Therefore, $\mathcal{O}^*_{\mathcal{N}_{\mathcal{F}_i}} = \min\{\mathcal{S}^*_{\mathcal{O}\mathcal{N}_i}\}$

From Section 5.1, 5.2, 5.3, we arrived at the following,

Let $\mathbb{G}_{\mathcal{C}_\mathcal{N}}$ be the Co-normal product of Neutrosophic network and its sum of the values of χ^{τ^*}, $|\alpha_{str}|$, $\mathcal{W}_0$ (α_{str}) and $\mathcal{W}(\mathcal{MST}_{\mathcal{W}_0})$ say $\mathcal{S}^*_{\mathcal{O}\mathcal{N}_1}$=11.67.

Let $\mathbb{G}_\mathcal{T}$ be the Tensor product of Neutrosophic network and its sum of the values of χ^{τ^*}, $|\alpha_{str}|$, $\mathcal{W}_0$ (α_{str}) and $\mathcal{W}(\mathcal{MST}_{\mathcal{W}_0})$ say $\mathcal{S}^*_{\mathcal{O}\mathcal{N}_2}$=18.69.

Let $\mathbb{G}_{\mathcal{R}_\mathcal{P}}$ be the Residue product of Neutrosophic network and its sum of the values of χ^{τ^*}, $|\alpha_{str}|$, $\mathcal{W}_0$ (α_{str}) and $\mathcal{W}(\mathcal{MST}_{\mathcal{W}_0})$ say $\mathcal{S}^*_{\mathcal{O}\mathcal{N}_3}$=15.55.

Table 13: Comparison of optimal values of neutrosophic product networks

Operations on $\mathcal{NG}$'s	$\lvert\alpha_{str}\rvert$	$\mathcal{W}_0$ (α_{str})	$\mathcal{W}(\mathcal{MST}_{\mathcal{W}_0})$	χ^{τ^*}	$\mathcal{S}^*_{\mathcal{O}\mathcal{N}_i}$
Co- normal product	1	2.31	4.36	4	11.67
Tensor product	3	8.16	4.53	3	18.69
Residue product	2	5.99	4.56	3	15.55

The four elements that make up the ideal network are the identification of various node types, examination of the network's effective nodes, assessment of the effectiveness level, and calculation of the chromatic number. The Co-normal Neutrosophic product network is the most optimal network, according to Table 13. The proposed method effectively handles network structures using neutrosophic graph product operations and vertex order coloring, particularly in dealing with uncertainty and indeterminacy. However, the limitations may include scalability issues and applications scope. The complexity of neutrosophic graphs can increase significantly with the size of the network, which may lead to computational challenges in larger datasets. While neutrosophic graphs are well-suited for uncertain data, the method may not be optimal for networks where certainty and crisp values dominate.

7. Conclusion

Network optimization can be effectively achieved by examining several graph product operations, such as co-normal, tensor, and residue products, through vertex order coloring on neutrosophic graphs. With this approach, we could analyze network stability, performance, and relationship while taking into consideration the inherent uncertainties of real-world systems. This

research improves the ability to design more resilient, dependable, and efficient networks by discovering ideal configurations. The healthcare industry is one of the areas where this idea has the greatest influence. Neutrosophic graph theory optimization of patient referral networks can result in notable enhancements in the provision of healthcare services. Through efficient management of patient movement across several healthcare providers and institutions, this methodology guarantees prompt access to medical care. This strategy guarantees prompt access to medical care, lowers patient wait times, and maximizes the use of medical resources by efficiently regulating the flow of patients between different healthcare providers and facilities. Such developments show the significant societal benefits of this research by improving patient outcomes as well as the general sustainability and efficiency of healthcare systems. Future studies could explore the application of neutrosophic graph coloring in diverse areas such as financial networks, transportation logistics, and supply chain management. Development of more efficient algorithms to handle large-scale neutrosophic graphs and to improve computational performance is another important future direction.

References

1. Ahmed, H., & Alsharafi, M. (2024). Domination on Bipolar Fuzzy Graph Operations: Principles, Proofs, and Examples. *Neutrosophic Systems with Applications*, 17, 34-46. https://doi.org/10.61356/j.nswa.2024.17245
2. Akram, M., & Shahzadi, G. (2017). Operations on single-valued neutrosophic graphs. *Infinite Study*.
3. Aparna, V., Mohanapriya, N., & Broumi, S. (2022). Single valued neutrosophic R-dynamic vertex coloring of graphs. *Neutrosophic Sets and Systems*, 48, 306-317.
4. Bathusha, S. S., & Raj, S. A. K. (2024). A Novel Approach on Energy of λJ-dominating Single-Valued Neutrosophic Graph Structure. *Neutrosophic Systems With Applications*, 16, 48-66. https://doi.org/10.61356/j.nswa.2024.16215.
5. Bhutani, K. R. (1993). Fuzzy sets, fuzzy relations, and fuzzy groups: some interrelations. Information sciences, 73(1-2), 107-115.
6. Broumi, S., Bakali, A. and Bahnasse, A., 2018. Neutrosophic sets: An overview. *Infinite Study*.
7. Broumi, S., Talea, M., Bakali, A., & Smarandache, F. (2016). Operations on interval valued neutrosophic graphs. *Infinite Study*.
8. Bondy, John Adrian, and Uppaluri Siva Ramachandra Murty. *Graph theory with applications*. Vol. 290. London: Macmillan, 1976.
9. Das, S., Roy, B. K., Kar, M. B., Kar, S., & Pamucar, D. (2020). Neutrosophic fuzzy set and its application in decision making. *Journal of Ambient Intelligence and Humanized Computing*, *11*, 5017-5029.

10. Deo, N. (2016). *Graph theory with applications to engineering and computer science*. Courier Dover Publications.
11. Dey, A., Son, L. H., Kumar, P. K., Selvachandran, G., & Quek, S. G. (2018). New concepts on vertex and edge coloring of simple vague graphs. *Symmetry*, *10*(9), 373.
12. Gani, A. N., & Kani, B. F. (2016). Fuzzy vertex order colouring. *International Journal of Pure and Applied Mathematics*, *107*(3), 601-614.
13. Gong, Z., & Zhang, C. (2023). Adjacent Vertex Distinguishing Coloring of Fuzzy Graphs. *Mathematics*, *11*(10), 2233.
14. Kalaiarasi, K. and Mahalakshmi, L., On Co-normal product of Two IFGs, *International Journal of Pure and Applied Mathematics*, 2018, 120(5), pp.1321-1335.
15. Khalil, A.M., Cao, D., Azzam, A., Smarandache, F. and Alharbi, W.R., 2020. Combination of the single-valued neutrosophic fuzzy set and the soft set with applications in decision-making. *Symmetry*, *12*(8), p.1361.
16. Mahapatra, R., Samanta, S. and Pal, M., 2022. Edge colouring of neutrosophic graphs and its application in detection of phishing website. *Discrete Dynamics in Nature and Society*, *2022*(1), p.1149724.
17. Meenakshi, A., Mythreyi, O., Bramila, M., Kannan, A., & Senbagamalar, J. (2023). Application of neutrosophic optimal network using operations. *Journal of Intelligent & Fuzzy Systems*, *45*(1), 421-433.
18. Meenakshi, A., & Dhanushiya, S. (2023, October). Fuzzy Network using Vertex Order Coloring and Efficient Domination. In *2023 First International Conference on Advances in Electrical, Electronics and Computational Intelligence (ICAEECI)* (pp. 1-11). IEEE.
19. Meenakshi Annamalai & Mythreyi.O, Applications of Neutrosophic social network using max product networks. *Journal of Intelligent & Fuzzy Systems*, 2023, https://doi.org/10.3233/JIFS-223484
20. Meenakshi, A., Kannan, A., Cep, R., & Elangovan. M, Efficient Graph Network Using Total Magic Labeling and Its Applications, *Mathematics*, 2023, 11(19), 4132.
21. Meenakshi, A., Mythreyi, O., Čep, R., & Karthik, K. (2024). A Study on Optimizing the Maximal Product in Cubic Fuzzy Graphs for Multifaceted Applications. *Mathematics*, *12*(10), 1605.
22. Mohanta, K., Dey, A., & Pal, A. (2021). A note on different types of product of neutrosophic graphs. *Complex & Intelligent Systems*, *7*, 857-871.
23. Radha, K. and Arumugam, S., On residue product of two fuzzy graphs, *International Journal of Multidisciplinary Research and Development*, Volume 2; Issue 11; 2015; Page No. 221-227
24. Rifayathali, M. A., Prasanna, A., & Mohideen, S. I. (2018). Intuitionistic fuzzy graph coloring. *Int. J. Res. Anal. Rev*, *5*(3), 734-742.
25. Rosyida, I., & Indrati, C. R. (2023). An algorithm for coloring of picture fuzzy graphs based on strong and weak adjacencies, and its application. *Algorithms*, *16*(12), 551.

26. Talebi, A. A., Ghassemi, M., Rashmanlou, H., & Poroch, M. H. (2022). Range-Valued Fuzzy Colouring of Intuitionistic Fuzzy Graphs with Application. *Applied Mathematics E-Notes*, *22*, 460-475.
27. Wallis, Walter Denis. *A beginner's guide to graph theory*. Boston, MA: Birkhäuser

Funding: This research received no external funding.

Conflicts of Interest: "The authors declare no conflict of interest."

Received: July 20, 2024. Accepted: Oct 23, 2024

NSS
Neutrosophic Sets and Systems, Vol. 76, 2025
University of New Mexico

Intelligent Framework for Regional Tourism Ecological Efficiency Evaluation under High-Quality Development with Single-Valued Neutrosophic Information

Xiaoying Liu
College of Management, Shanxi Vocational University of Engineering Science and Technology, Taiyuan, 030619, Shanxi, China
*Corresponding author, E-mail: liuxiaoying@sxgkd.edu.cn; 13834661229@126.com

Abstract: The evaluation of regional tourism ecological efficiency (RTEE) under high-quality development aims to measure how the tourism industry promotes economic growth while minimizing resource consumption and environmental impact. By analyzing economic output per unit of carbon emissions, it assesses the sustainability and environmental performance of the tourism sector. This evaluation method considers resource utilization, energy efficiency, and ecological protection, helping decision-makers optimize tourism development models, achieve a balance between economic and ecological benefits, and promote the transition of tourism towards a low-carbon, green, and high-quality direction. The RTEE evaluation under high-quality development is MADM. The single-valued neutrosophic number generalized power geometric BM (SVNNGPGBM) technique is put forward and MADM decision techniques are put forward in line with SVNNGPGBM technique and power geometric (PG) technique. Finally, numerical example about RTEE evaluation under high-quality development and comparative analysis was put forward the SVNNGPGBM technique.

Keywords: MADM; SVNSs; GGBM technique; ecological efficiency evaluation

1. Introduction

The evaluation of regional tourism ecological efficiency under the context of high-quality development holds profound strategic significance. Firstly, it provides a scientific basis for balancing the economic benefits of the tourism industry with ecological protection. By quantifying environmental impacts such as resource consumption, carbon emissions, and waste management, this evaluation reveals whether the tourism sector is reducing its ecological burden while achieving economic growth. Such assessments not only help identify efficient, low-consumption tourism development models but also support decision-making

for optimizing resource allocation, thereby promoting the green transformation and sustainable development of the tourism industry.

Secondly, the evaluation offers crucial insights for policymakers and businesses in formulating environmentally friendly policies and strategies. Governments can leverage the evaluation results to implement targeted policies that encourage low-carbon, eco-friendly tourism practices, avoiding the inefficient "pollute first, clean up later" development model. Simultaneously, businesses can adjust their operational strategies based on the evaluation outcomes to improve resource efficiency and environmental awareness, thereby enhancing their market competitiveness. Furthermore, regional tourism ecological evaluation helps foster ecological collaboration between regions, driving a win-win situation for both economic growth and environmental protection. By guiding regions to prioritize ecological conservation in tourism development, the evaluation system encourages green competition and cooperation, improving overall ecological efficiency and supporting the achievement of a green, low-carbon, and sustainable high-quality economic growth, ultimately enhancing regional competitiveness and sustainable development capacity.

In today's increasingly fierce market competition, enterprises or individuals often face various decision-making [1-3]. As information technology continues to advance rapidly, individuals are encountering increasingly complex decision-making environments [4-7]. The complexity of the decision-making environment makes it increasingly unlikely for individual decision-makers to make multi-attribute decisions. In real life, it is often necessary to evaluate and choose from numerous alternative options (candidates, objects, etc.). Especially for major decision-making problems, it is necessary for experts from different fields to leverage each person's professional advantages, evaluate the solutions from different aspects, and then select or rank the solutions, which is commonly known as MADM problems[8-12]. Figure 1 shows the factors which affect the decisions' results.

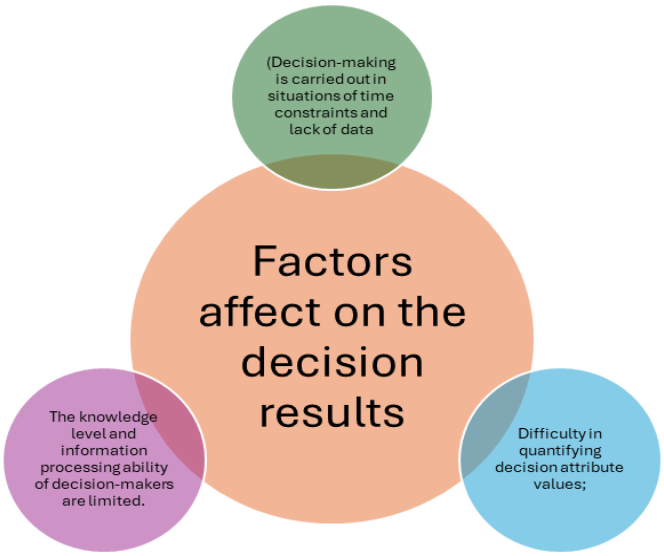

Figure 1. Factors that affect the decisions' results.

The complexity of the decision-making environment makes it sometimes difficult for decision experts to use precise numerical values to represent the evaluation information of solutions, while using a single value set to express the evaluation information is very convenient and feasible[13-18]. Therefore, the study of MADM problems based on single valued intermediate intelligence sets not only has significant theoretical significance for the development of management science, but also has significant practical significance for solving many complex decision-making problems.

The main contributions of this study are outlined:

- The SVNNGPGBM technique is constructed.
- The maximizing deviation technique is proposed to handle weight.
- The SVNNGPGBM technique is applied to MADM.
- A numerical example for RTEE evaluation under high-quality development is demonstrated using the SVNNGPGBM technique.

To conduct so, The SVNSs was constructed on Sec. 2. The SVNNGPGBM technique is conducted on Sec. 3. MADM approach based on SVNNGPGBM technique is conducted in Sec. 4. A numerical example for RTEE evaluation under high-quality development is conducted on Sec. 5. Conclusion is conducted for Sec. 6.

2. Literature review

The evaluation of regional tourism ecological efficiency under high-quality development aims to assess the balance between economic growth and ecological protection in the tourism

industry. The evaluation focuses on the equilibrium between resource utilization, environmental impact, and economic benefits, emphasizing the concepts of green and sustainable development. By analyzing environmental indicators such as energy consumption, carbon emissions, and waste management, alongside tourism output, it reveals whether regional tourism effectively reduces environmental burdens while achieving economic growth. This evaluation system provides a scientific basis for policymakers to optimize resource allocation, enhance ecological efficiency, and promote the green transformation and sustainable development of the tourism industry, thus supporting high-quality regional economic growth. The research on tourism ecological efficiency (TEE) has evolved significantly over the years, focusing on various regions and methodologies. In 2016, Yao, Chen, Yin and Li [19] conducted an empirical analysis on the TEE of Hainan Province, using a tourism ecological efficiency model to calculate the efficiency for different tourism activities. They concluded that optimizing the tourism model with "short distances, long stays, and high consumption" can improve TEE, while the opposite would reduce it. In 2018, Gao [20] studied the spatial effects of TEE in Jiangsu Province, using tools like MaxDEA and OpenGeoda to measure efficiency across 13 cities. The study revealed significant spatial imbalances in TEE and suggested policies for improvement. Lin and Lin [21] evaluated the eco-efficiency of the tourism industry in Jiangxi Province from 2011 to 2016 using a super-efficiency DEA model. They found that while the overall efficiency was high, there were notable spatial disparities, with regions in northern Jiangxi performing better than those in the south. In 2021, Wang [22] explored the relationship between tourism industry agglomeration and TEE in Shanxi Province from 2009 to 2018. The study showed that tourism agglomeration positively affected TEE, with spatial configuration evolving through different stages during the study period. Fang [23] examined the coordination between TEE and economic development in the Yangtze River Economic Belt from 2010 to 2018. The study revealed that while TEE generally improved, significant regional disparities persisted. The research proposed strategies to promote the coordinated development of tourism and the economy. Hong, Wang and Zhang [24] focused on the western regions of China from 2000 to 2017, analyzing the spatial and temporal evolution of TEE. They found that factors such as tourist scale, industrial structure optimization, and technological advancements contributed to increased TEE, while urbanization had a negative impact. In 2022, Li and Wu [25] investigated the spatial consistency between TEE and regional ecological security in the middle reaches of the Yangtze River from 2005 to 2018. Their study suggested that the relationship between TEE and

ecological security followed an inverted U-shaped pattern, with spatial consistency improving over time. Liu [26] examined the impact of regional innovation on TEE across 30 provinces in China from 2008 to 2017, finding that innovation significantly improved tourism efficiency, particularly in the eastern regions, though there was a downward trend in overall TEE. Focusing on Shandong Province, Tian and Zhao [27] used a three-stage DEA model to evaluate the TEE of 16 cities from 2010 to 2019. Their study showed that while Shandong's TEE was relatively high, regional differences persisted, largely influenced by natural environment factors and innovation in tourism models. Finally, in 2023, Deng [28] conducted a comprehensive study on the spatiotemporal differentiation of TEE in 30 provinces across mainland China from 2000 to 2019. Using a "tourism value-added coefficient" to estimate carbon emissions, Deng applied a spatial Durbin model to investigate the factors influencing TEE. The results indicated a significant increase in carbon emissions from tourism, but also a gradual improvement in ecological efficiency, with regional disparities diminishing over time. Across these studies, the common thread is the emphasis on balancing tourism development with environmental sustainability. Table 1 shows the previous works.

Across these studies, the common thread is the emphasis on balancing tourism development with environmental sustainability. The use of various models, including DEA, SBM, and spatial analysis, has allowed researchers to assess TEE's evolution across different regions and time periods, providing valuable insights for policymakers to promote low-carbon, green, and high-quality tourism development.

Table 1. Previously works on the same issue.

Authors	Study	Contributions and results
Yao, Chen, Yin and Li [19]	They conducted an empirical analysis on the TEE of Hainan Province, using a tourism ecological efficiency model to calculate the efficiency of different tourism activities.	They concluded that optimizing the tourism model with "short distances, long stays, and high consumption" can improve TEE, while the opposite would reduce it.
In 2018, Gao [20]	They studied the spatial effects of TEE in Jiangsu Province, using tools like MaxDEA and OpenGeoda to measure efficiency across 13 cities.	The study revealed significant spatial imbalances in TEE and suggested policies for improvement
Lin and Lin [21]	They evaluated the eco-efficiency of the tourism industry in Jiangxi Province from 2011 to 2016 using a super-efficiency DEA model.	They found that while the overall efficiency was high, there were notable spatial disparities, with regions in northern Jiangxi performing better than those in the south. In 2021,
Wang [22]	They explored the relationship between tourism industry agglomeration and TEE in Shanxi Province from 2009 to 2018.	The study showed that tourism agglomeration positively affected TEE, with spatial configuration evolving through different stages during the study period.
Liu [26]	They examined the impact of regional innovation on TEE across 30 provinces in China from 2008 to 2017,	They are finding that innovation significantly improved tourism efficiency, particularly in the eastern regions, though there was a downward trend in overall TEE.
Tian and Zhao [27]	They used a three-stage DEA model to evaluate the TEE of 16 cities from 2010 to 2019.	Their study showed that while Shandong's TEE was relatively high, regional differences persisted, largely

		influenced by natural environment factors and innovation in tourism models.
Deng [28]	They conducted a comprehensive study on the spatiotemporal differentiation of TEE in 30 provinces across mainland China from 2000 to 2019. Using a "tourism value-added coefficient" to estimate carbon emissions,	Deng applied a spatial Durbin model to investigate the factors influencing TEE. The results indicated a significant increase in carbon emissions from tourism, but also a gradual improvement in ecological efficiency, with regional disparities diminishing over time.

2. Preliminaries

Wang et al. [29] put forward the SVNSs.

Definition 1 [29]. The SVNSs are put forward:

$$EA=\left\{\left(\theta,ET_A\left(\theta\right),EI_A\left(\theta\right),EF_A\left(\theta\right)\right)\middle|\theta\in\Theta\right\} \tag{1}$$

where $ET_A\left(\theta\right),EI_A\left(\theta\right),EF_A\left(\theta\right)$ is the truth-membership, indeterminacy-membership and falsity-membership, $ET_A\left(\theta\right),EI_A\left(\theta\right),EF_A\left(\theta\right)\in\left[0,1\right]$, $0\le ET_A\left(\theta\right)+EI_A\left(\theta\right)+EF_A\left(\theta\right)\le 3$.

The SVNN is put forward as $EA=\left(ET_A,EI_A,EF_A\right)$, where $ET_A,EI_A,EF_A\in\left[0,1\right]$, and $0\le ET_A+EI_A+EF_A\le 3$.

Definition 2 [30]. Let $EA=\left(ET_A,EI_A,EF_A\right)$, the score function is put forward:

$$SF\left(EA\right)=\frac{\left(2+ET_A-EI_A-EF_A\right)}{3},\ SF\left(EA\right)\in\left[0,1\right]. \tag{2}$$

Definition 3[30]. Let $EA=\left(ET_A,EI_A,EF_A\right)$, the accuracy function is put forward:

$$AF\left(EA\right)=\frac{ET_A-EF_A+1}{2},\ AF\left(EA\right)\in\left[0,1\right]. \tag{3}$$

Peng et al.[30] put forward the order relation.

Definition 4[30]. Let $EA=\left(ET_A,EI_A,EF_A\right)$, $EB=\left(ET_B,EI_B,EF_B\right)$, let $SF\left(EA\right)=\frac{\left(2+ET_A-EI_A-EF_A\right)}{3}$ and $SF\left(EB\right)=\frac{\left(2+ET_B-EI_B-EF_B\right)}{3}$, and let $AF\left(EA\right)=\frac{ET_A-EF_A+1}{2}$ and $AF\left(EB\right)=\frac{ET_B-EF_B+1}{2}$, if $SF\left(EA\right)<SF\left(EB\right)$, $PA<PB$; if $SF\left(EA\right)=SF\left(EB\right)$, (1)if $AF\left(EA\right)=AF\left(EB\right)$, $EA=EB$; (2) if $AF\left(EA\right)<AF\left(EB\right)$, $EA<EB$.

Definition 5[29]. Let $EA=\left(ET_A,EI_A,EF_A\right)$ and $EB=\left(ET_B,EI_B,EF_B\right)$, the put forward operations are:

(1) $EA \oplus EB = \left(ET_A + ET_B - ET_A ET_B, EI_A EI_B, EF_A EF_B\right)$;

(2) $EA \otimes EB = \left(ET_A ET_B, EI_A + EI_B - EI_A EI_B, EF_A + EF_B - EF_A EF_B\right)$;

(3) $\lambda EA = \left(1-\left(1-ET_A\right)^{\lambda}, \left(EI_A\right)^{\lambda}, \left(EF_A\right)^{\lambda}\right), \lambda > 0$;

(4) $\left(EA\right)^{\lambda} = \left(\left(ET_A\right)^{\lambda}, \left(EI_A\right)^{\lambda}, 1-\left(1-EF_A\right)^{\lambda}\right), \lambda > 0.$

Definition 6[31]. Let $EA = \left(ET_A, EI_A, EF_A\right)$ and $EB = \left(ET_B, EI_B, EF_B\right)$, then the normalized Hamming distance between $EA = \left(ET_A, EI_A, EF_A\right)$ and $EB = \left(ET_B, EI_B, EF_B\right)$ is put forward:

$$HD\left(EA, EB\right) = \frac{1}{3}\begin{pmatrix} \left|ET_A - ET_B\right| \\ +\left|EI_A - EI_B\right| + \left|EF_A - EF_B\right| \end{pmatrix} \tag{4}$$

Definition 6[32]. Let $es, et, er > 0$, $ea_i (i = 1, 2, 3, \ldots, n)$ $\left(ea_i > 0\right)$ with weight $ew = (ew_1, ew_2, \ldots, ew_n)^T$, $ew_i \in [0,1]$, $\sum_{i=1}^{n} ew_i = 1$. The GWBM technique is put forward:

$$\begin{aligned} &\mathrm{GWBM}_{ew}^{es,et,er}(ea_1, ea_2, \ldots, ea_n) \\ &= \left(\sum_{i,j,k=1}^{n} ew_i ew_j ew_k ea_i^s ea_j^t ea_k^r\right)^{1/(es+et+er)} \end{aligned} \tag{5}$$

3. GSVNNPBM technique

Then, GSVNNWBM technique is put forward.

Definition 8. Let $es, et, er > 0$, $EA_i = (ET_i, EI_i, EF_i)$ $(i = 1, 2, 3, \ldots, n)$ be SVNNs with weight $ew_i = (ew_1, ew_2, \ldots, ew_n)^T$, $\sum_{i=1}^{n} ew_i = 1$. If

$$\begin{aligned} &\mathrm{GSVNNWBM}_{ew}^{es,et,er}(EA_1, EA_2, \cdots, EA_n) \\ &= \left(\bigoplus_{i,j,k=1}^{n} ew_i ew_j ew_k \left(EA_i^{es} \otimes EA_j^{et} \otimes EA_k^{er}\right)\right)^{1/(es+et+er)} \\ &= \begin{pmatrix} \left(1 - \prod_{i,j,k=1}^{n} \left(1 - ET_i^{es} ET_j^{et} ET_k^{er}\right)^{zw_i zw_j zw_k}\right)^{1/(es+et+er)}, \\ 1 - \left(1 - \prod_{i,j,k=1}^{n} \left(1 - \left(1-EI_i\right)^{es} \left(1-EI_j\right)^{et} \left(1-EI_k\right)^{er}\right)^{ew_i ew_j ew_k}\right)^{1/(es+et+er)}, \\ 1 - \left(1 - \prod_{i,j,k=1}^{n} \left(1 - \left(1-EF_i\right)^{es} \left(1-EF_j\right)^{et} \left(1-EF_k\right)^{er}\right)^{ew_i ew_j ew_k}\right)^{1/(es+et+er)}. \end{pmatrix} \end{aligned} \tag{6}$$

then $\mathrm{GSVNNWBM}_{ew}^{s,t,r}$ is called GSVNNWBM technique.

The GSVNNWBM technique has the same properties.

Property 1 (Idempotency). If $EA_i = (ET_i, EI_i, EF_i)(i = 1, 2, \ldots, n)$ are same, that is, $EA_i = EA = (ET, EI, EF)$, then

$$\mathrm{GSVNNWBM}_{ew}^{es,et,er}(EA_1, EA_2, \cdots, EA_n) = EA \tag{7}$$

Property 2 (Monotonicity). Let $EA_i = (ET_{A_i}, EI_{A_i}, EF_{A_i})(i = 1, 2, 3, \ldots, n)$ and $EB_i = (ET_{B_i}, EI_{B_i}, EF_{B_i})$ $(i = 1, 2, 3, \ldots, n)$ be SVNNs. If $ET_{A_i} \le ET_{B_i}$, $EI_{A_i} \ge EI_{B_i}$, $EF_{A_i} \ge EF_{B_i}$ holds for all i, then

$$\begin{aligned} &\mathrm{GSVNNWBM}_{ew}^{es,et,er}(EA_1, EA_2, \cdots, EA_n) \\ &\le \mathrm{GSVNNWBM}_{ew}^{es,et,er}(EB_1, EB_2, \cdots, EB_n) \end{aligned} \tag{8}$$

Property 3 (Boundedness). Let $EA_i = (ET_{A_i}, EI_{A_i}, EF_{A_i})(i = 1, 2, 3, \ldots, n)$ be SVNNS. If $PA^+ = (\max_i(PT_i), \min_i(PI_i), \min_i(PF_i))$ and $PA^- = (\min_i(PT_i), \max_i(PI_i), \max_i(PF_i))$ then

$$EA^- \le \mathrm{GSVNNWBM}_{ew}^{es,et,er}(EA_1, EA_2, \cdots, EA_n) \le EA^+. \tag{9}$$

Then, generalized single-valued neutrosophic number power BM (GSVNNPBM) technique is put forward in line with GSVNNWBM technique and PA technique [33].

Definition 9. Let $es, et, er > 0$, $EA_i = (ET_i, EI_i, EF_i)$ $(i = 1, 2, 3, \ldots, n)$ be SVNNs, The GSVNNPBM technique is put forward:

$$\begin{aligned} &GSVNNPBM^{es,et,er}((EA_1, EA_2, \cdots, EA_n) \\ &= \left(\bigoplus_{i,j,k=1}^{n} \frac{\left(1 + ET\left(EA_i\right)\right)}{\sum_{i=1}^{n}\left(1 + ET\left(EA_i\right)\right)} \frac{\left(1 + ET\left(EA_j\right)\right)}{\sum_{j=1}^{n}\left(1 + ET\left(EA_j\right)\right)} \frac{\left(1 + ET\left(EA_k\right)\right)}{\sum_{k=1}^{n}\left(1 + ET\left(EA_k\right)\right)} \left(EA_i^{es} \otimes EA_j^{et} \otimes EA_k^{er}\right) \right)^{1/(es+et+er)} \end{aligned} \tag{10}$$

where $ET\left(EA_a\right) = \sum_{\substack{j=1 \\ a \ne j}}^{m} Sup\left(EA_a, EA_j\right)$, $Sup\left(EA_a, EA_j\right)$ is the decision support for EA_a from EA_j, with given conditions: (1) $Sup\left(EA_a, EA_b\right) \in [0,1]$; (2) $Sup\left(EA_b, EA_a\right) = Sup\left(EA_a, EA_b\right)$; (3) $Sup\left(EA_a, EA_b\right) \ge Sup\left(EA_s, EA_t\right)$, if $HD\left(EA_a, EA_b\right) \le HD\left(EA_s, EA_t\right)$, HD is a distance.

The Theorem 1 is constructed.

Theorem 1. Let $es, et, er > 0$ and $EA_i = (ET_i, EI_i, EF_i)(i = 1, 2, 3, \ldots, n)$ be SVNNs. The aggregated value for SVNNGPGBM is SVNN and

$$SVNNGPGBM^{es,et,er}(EA_1, EA_2, \cdots, EA_n)$$

$$= \frac{1}{es+et+er} \overset{n}{\underset{i,j,k=1}{\otimes}} \left(esEA_i \oplus etEA_j \oplus erEA_k \right)^{\frac{(1+ET(EA_i))}{\sum_{i=1}^{n}(1+ET(EA_i))} \frac{(1+E(EA_j))}{\sum_{j=1}^{n}(1+ET(EA_j))} \frac{(1+ET(EA_k))}{\sum_{k=1}^{n}(1+ET(EA_k))}}$$

$$= \begin{pmatrix} \left(1 - \left(1 - \prod_{i,j,k=1}^{n} (1-(1-ET_i)^{es}(1-ET_j)^{et}(1-ET_k)^{er} \right)^{\frac{(1+ET(EA_i))}{\sum_{i=1}^{n}(1+ET(EA_i))} \frac{(1+E(EA_j))}{\sum_{j=1}^{n}(1+ET(EA_j))} \frac{(1+ET(EA_k))}{\sum_{k=1}^{n}(1+ET(EA_k))}} \right)^{1/(es+et+er)}, \\ \left(1 - \prod_{i,j,k=1}^{n} \left(1 - EI_i^{es} EI_j^{et} EI_k^{er} \right)^{\frac{(1+ET(EA_i))}{\sum_{i=1}^{n}(1+ET(EA_i))} \frac{(1+E(EA_j))}{\sum_{j=1}^{n}(1+ET(EA_j))} \frac{(1+ET(EA_k))}{\sum_{k=1}^{n}(1+ET(EA_k))}} \right)^{1/(es+et+er)}, \\ \left(1 - \prod_{i,j,k=1}^{n} \left(1 - EF_i^{es} EF_j^{et} EF_k^{er} \right)^{\frac{(1+ET(EA_i))}{\sum_{i=1}^{n}(1+ET(EA_i))} \frac{(1+E(EA_j))}{\sum_{j=1}^{n}(1+ET(EA_j))} \frac{(1+ET(EA_k))}{\sum_{k=1}^{n}(1+ET(EA_k))}} \right)^{1/(es+et+er)}. \end{pmatrix} \tag{11}$$

Proof:

$$\begin{aligned} esEA_i &= (1-(1-PT_i)^{es}, EI_i^{es}, EF_i^{es}), \\ etEA_j &= (1-(1-ET_j)^{et}, EI_j^{et}, EF_j^{et}), \\ erEA_k &= (1-(1-ET_k)^{er}, EI_k^{er}, EF_k^{er}). \end{aligned} \tag{12}$$

$$\begin{aligned} &esEA_i \oplus etEA_j \oplus erEA_k \\ &= \begin{pmatrix} 1-(1-ET_i)^{es}(1-ET_j)^{et}(1-ET_k)^{er}, \\ EI_i^{es} EI_j^{et} EI_k^{er}, EF_i^{es} EF_j^{et} EF_k^{er} \end{pmatrix} \end{aligned} \tag{13}$$

Thereafter,

$$\left(esEA_i \oplus etEA_j \oplus erEA_k \right)^{\frac{(1+ET(EA_i))}{\sum_{i=1}^{n}(1+ET(EA_i))} \frac{(1+ET(EA_j))}{\sum_{j=1}^{n}(1+ET(EA_j))} \frac{(1+ET(EA_k))}{\sum_{k=1}^{n}(1+ET(EA_k))}}_k$$

$$= \begin{pmatrix} (1-(1-ET_i)^{es}(1-ET_j)^{et}(1-ET_k)^{er})^{\frac{(1+ET(EA_i))}{\sum_{i=1}^{n}(1+ET(EA_i))} \frac{(1+ET(EA_j))}{\sum_{j=1}^{n}(1+ET(EA_j))} \frac{(1+ET(EA_k))}{\sum_{k=1}^{n}(1+ET(EA_k))}}, \\ 1-(1-EI_i^{es} EI_j^{et} EI_k^{er})^{\frac{(1+ET(EA_i))}{\sum_{i=1}^{n}(1+ET(EA_i))} \frac{(1+ET(EA_j))}{\sum_{j=1}^{n}(1+ET(EA_j))} \frac{(1+ET(EA_k))}{\sum_{k=1}^{n}(1+ET(EA_k))}}, \\ 1-(1-EF_i^{es} EF_j^{et} EF_k^{er})^{\frac{(1+ET(EA_i))}{\sum_{i=1}^{n}(1+ET(EA_i))} \frac{(1+ET(EA_j))}{\sum_{j=1}^{n}(1+ET(EA_j))} \frac{(1+ET(EA_k))}{\sum_{k=1}^{n}(1+ET(EA_k))}} \end{pmatrix} \tag{14}$$

Therefore,

$$\bigotimes_{i,j,k=1}^{n}\left(esEA_i \oplus etEA_j \oplus erEA_k\right)^{\frac{(1+ET(EA_i))}{\sum_{i=1}^{n}(1+ET(EA_i))}\frac{(1+ET(EA_j))}{\sum_{j=1}^{n}(1+ET(EA_j))}\frac{(1+ET(EA_k))}{\sum_{k=1}^{n}(1+ET(EA_k))}}$$

$$=\left(\begin{array}{l}\prod_{i,j,k=1}^{n}(1-(1-ET_i)^{es}(1-ET_j)^{et}(1-ET_k)^{er})^{\frac{(1+ET(EA_i))}{\sum_{i=1}^{n}(1+ET(EA_i))}\frac{(1+ET(EA_j))}{\sum_{j=1}^{n}(1+ET(EA_j))}\frac{(1+ET(EA_k))}{\sum_{k=1}^{n}(1+ET(EA_k))}},\\ 1-\prod_{i,j,k=1}^{n}(1-EI_i^{es}EI_j^{et}EI_k^{er})^{\frac{(1+ET(EA_i))}{\sum_{i=1}^{n}(1+ET(EA_i))}\frac{(1+ET(EA_j))}{\sum_{j=1}^{n}(1+ET(EA_j))}\frac{(1+ET(EA_k))}{\sum_{k=1}^{n}(1+ET(EA_k))}},\\ 1-\prod_{i,j,k=1}^{n}(1-EF_i^{es}EF_j^{et}EF_k^{er})^{\frac{(1+ET(EA_i))}{\sum_{i=1}^{n}(1+ET(EA_i))}\frac{(1+ET(EA_j))}{\sum_{j=1}^{n}(1+ET(EA_j))}\frac{(1+ET(EA_k))}{\sum_{k=1}^{n}(1+ET(EA_k))}}\end{array}\right) \tag{15}$$

Thus,

$$\frac{1}{es+et+er}\bigotimes_{i,j,k=1}^{n}\left(esEA_i \oplus etEA_j \oplus erEA_k\right)^{\frac{(1+ET(EA_i))}{\sum_{i=1}^{n}(1+ET(EA_i))}\frac{(1+ET(EA_j))}{\sum_{j=1}^{n}(1+ET(EA_j))}\frac{(1+ET(EA_k))}{\sum_{k=1}^{n}(1+ET(EA_k))}}$$

$$=\left(\begin{array}{l}\left(1-(1-\prod_{i,j,k=1}^{n}(1-(1-ET_i)^{es}(1-ET_j)^{et}(1-ET_k)^{er})^{\frac{(1+ET(EA_i))}{\sum_{i=1}^{n}(1+ET(EA_i))}\frac{(1+ET(EA_j))}{\sum_{j=1}^{n}(1+ET(EA_j))}\frac{(1+ET(EA_k))}{\sum_{k=1}^{n}(1+ET(EA_k))}}\right)^{1/(es+et+er)},\\ \left(1-\prod_{i,j,k=1}^{n}(1-EI_i^{es}EI_j^{et}EI_k^{er})^{\frac{(1+ET(EA_i))}{\sum_{i=1}^{n}(1+ET(EA_i))}\frac{(1+ET(EA_j))}{\sum_{j=1}^{n}(1+ET(EA_j))}\frac{(1+ET(EA_k))}{\sum_{k=1}^{n}(1+ET(EA_k))}}\right)^{1/(es+et+er)},\\ \left(1-\prod_{i,j,k=1}^{n}(1-EF_i^{es}EF_j^{et}EF_k^{er})^{\frac{(1+ET(EA_i))}{\sum_{i=1}^{n}(1+ET(EA_i))}\frac{(1+ET(EA_j))}{\sum_{j=1}^{n}(1+ET(EA_j))}\frac{(1+ET(EA_k))}{\sum_{k=1}^{n}(1+ET(EA_k))}}\right)^{1/(es+et+er)}\end{array}\right) \tag{16}$$

Hence, (11) is maintained.

Thereafter,

$$0 \le 1-\left(1-\prod_{i,j,k=1}^{n}\left(1-(1-ET_i)^{es}(1-ET_j)^{et}(1-ET_k)^{er}\right)^{\frac{\left(1+ET(EA_i)\right)}{\sum_{i=1}^{n}\left(1+ET(EA_i)\right)}\frac{\left(1+ET(EA_j)\right)}{\sum_{j=1}^{n}\left(1+ET(EA_j)\right)}\frac{\left(1+ET(EA_k)\right)}{\sum_{k=1}^{n}\left(1+ET(EA_k)\right)}}\right)^{1/(es+et+er)} \le 1,$$

$$0 \le \left(1-\prod_{i,j,k=1}^{n}\left(1-EI_i^{es}EI_j^{et}EI_k^{er}\right)^{\frac{\left(1+ET(EA_i)\right)}{\sum_{i=1}^{n}\left(1+ET(EA_i)\right)}\frac{\left(1+ET(EA_j)\right)}{\sum_{j=1}^{n}\left(1+ET(EA_j)\right)}\frac{\left(1+ET(EA_k)\right)}{\sum_{k=1}^{n}\left(1+ET(EA_k)\right)}}\right)^{1/(es+et+er)} \le 1,$$

$$0 \le \left(1-\prod_{i,j,k=1}^{n}\left(1-EF_i^{es}EF_j^{et}EF_k^{er}\right)^{\frac{\left(1+ET(EA_i)\right)}{\sum_{i=1}^{n}\left(1+ET(EA_i)\right)}\frac{\left(1+ET(EA_j)\right)}{\sum_{j=1}^{n}\left(1+ET(EA_j)\right)}\frac{\left(1+ET(EA_k)\right)}{\sum_{k=1}^{n}\left(1+ET(EA_k)\right)}}\right)^{1/(es+et+er)} \le 1. \tag{17}$$

Therefore,

$$\begin{aligned}0 \le 1-\Bigg(1-\prod_{i,j,k=1}^{n}\left(1-(1-ET_i)^{es}(1-ET_j)^{et}(1-ET_k)^{er}\right)^{\frac{\left(1+ET(EA_i)\right)}{\sum_{i=1}^{n}\left(1+ET(EA_i)\right)}\frac{\left(1+ET(EA_j)\right)}{\sum_{j=1}^{n}\left(1+ET(EA_j)\right)}\frac{\left(1+ET(EA_k)\right)}{\sum_{k=1}^{n}\left(1+ET(EA_k)\right)}}\Bigg)^{1/(es+et+er)}\\ +\Bigg(1-\prod_{i,j,k=1}^{n}\left(1-EI_i^{es}EI_j^{et}EI_k^{er}\right)^{\frac{\left(1+ET(EA_i)\right)}{\sum_{i=1}^{n}\left(1+ET(EA_i)\right)}\frac{\left(1+ET(EA_j)\right)}{\sum_{j=1}^{n}\left(1+ET(EA_j)\right)}\frac{\left(1+ET(EA_k)\right)}{\sum_{k=1}^{n}\left(1+ET(EA_k)\right)}}\Bigg)^{1/(es+et+er)}\\ +\Bigg(1-\prod_{i,j,k=1}^{n}\left(1-EF_i^{es}EF_j^{et}EF_k^{er}\right)^{\frac{\left(1+ET(EA_i)\right)}{\sum_{i=1}^{n}\left(1+ET(EA_i)\right)}\frac{\left(1+ET(EA_j)\right)}{\sum_{j=1}^{n}\left(1+ET(EA_j)\right)}\frac{\left(1+ET(EA_k)\right)}{\sum_{k=1}^{n}\left(1+ET(EA_k)\right)}}\Bigg)^{1/(es+et+er)} \le 3.\end{aligned} \tag{18}$$

Thereby finishing the proof.

The SVNNGPGBM technique has the same properties.

Property 4 (Idempotency). If $EA_i = (ET_i, EI_i, EF_i)(i = 1, 2, \ldots, n)$ are same, that is, $EA_i = EA = (ET, EI, EF)$, then

$$SVNNGPGBM^{es,et,er}(EA_1, EA_2, \cdots, EA_n) = EA \tag{19}$$

Property 5 (Monotonicity). Let $EA_i = (ET_{A_i}, EI_{A_i}, EF_{A_i})(i = 1, 2, 3, \ldots, n)$ and $EB_i = (ET_{B_i}, EI_{B_i}, EF_{B_i})$ $(i = 1, 2, 3, \ldots, n)$ be SVNNs. If $ET_{A_i} \le ET_{B_i}$, $EI_{A_i} \ge EI_{B_i}$, $EF_{A_i} \ge EF_{B_i}$ for all i, then

$$SVNNGPGBM^{es,et,er}(EA_1, EA_2, \cdots, EA_n) \leq SVNNGPGBM^{es,et,er}(EB_1, EB_2, \cdots, EB_n) \tag{20}$$

Property 6 (Boundedness). Let $EA_i = (ET_{A_i}, EI_{A_i}, EF_{A_i})(i = 1, 2, 3, \ldots, n)$ be SVNNS. If $EA^+ = (\max_i(ET_i), \min_i(EI_i), \min_i(EF_i))$ and $EA^- = (\min_i(ET_i), \max_i(EI_i), \max_i(EF_i))$ then

$$EA^- \leq SVNNGPGBM^{es,et,er}(EA_1, EA_2, \cdots, EA_n) \leq EA^+. \tag{21}$$

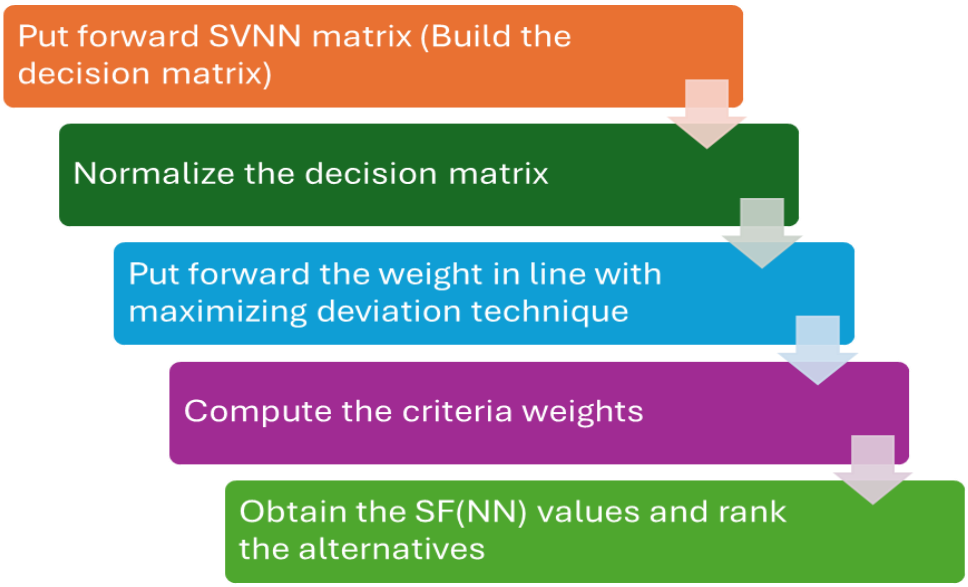

Figure 2. The steps of the MADM methodology.

4. MADM technique based on SVNNGPGBM under SVNNs

The SVNNGPGBM technique is put forward MADM with SVNSs. Let $C = C_1, C_2, \ldots, C_n$ be attributes, $ew = \{ew_1, ew_2, \ldots, ew_n\}$ be weight of C. Let $A = A_1, A_2, \ldots, A_m$ be alternatives. $EE = (EE_{ij})_{m\times n} = (ET_{ij}, EI_{ij}, EF_{ij})_{m\times n}$ is SVNN-matrix. The SVNNGPGBM technique is put forward MADM. Figure 2 shows the steps of the proposed model.

Step 1. Put forward SVNN matrix $EE = (EE_{ij})_{m\times n} = (ET_{ij}, EI_{ij}, EF_{ij})_{m\times n}$.

$$EE=\left(EE_{ij}\right)_{m\times n}=\begin{bmatrix} EE_{11} & EE_{12} & \cdots & EE_{1n} \\ EE_{21} & EE_{22} & \cdots & EE_{2n} \\ \vdots & \vdots & \vdots & \vdots \\ EE_{m1} & EE_{m2} & \cdots & EE_{mn} \end{bmatrix}$$

$$EE=\left(EE_{ij}\right)_{m\times n}=\left(ET_{ij},EI_{ij},EF_{ij}\right)_{m\times n}$$

$$=\begin{bmatrix} \left(ET_{11},EI_{11},PF_{11}\right) & \left(ET_{12},EI_{1},EF_{12}\right) & \cdots & \left(ET_{1n},EI_{1n},EF_{1n}\right) \\ \left(ET_{21},EI_{21},EF_{21}\right) & \left(ET_{22},EI_{22},EF_{22}\right) & \cdots & \left(ET_{2n},EI_{2n},EF_{2n}\right) \\ \vdots & \vdots & \vdots & \vdots \\ \left(ET_{m1},EI_{m1},EF_{m1}\right) & \left(ET_{m2},EI_{m2},EF_{m2}\right) & \cdots & \left(ET_{mn},EI_{mn},EF_{mn}\right) \end{bmatrix} \tag{22}$$

Step 2. Normalize $EE=\left[EE_{ij}\right]_{m\times n}$ to $NE=\left[NE_{ij}\right]_{m\times n}$.

$$NE_{ij}=\left(NET_{ij},NEI_{ij},NEF_{ij}\right)$$

$$=\begin{cases}\left(ET_{ij},EI_{ij},EF_{ij}\right), & EX_j \text{ is benefit} \\ \left(EF_{ij},1-EI_{ij},ET_{ij}\right), & EX_j \text{ is cost}\end{cases} \tag{23}$$

Step 3. Put forward the weight in line with maximizing deviation technique.

The maximizing deviation technique [34] under SVNSs to construct the weight values.

(1) From the $NE=\left[NE_{ij}\right]_{m\times n}$, deviation degree EA_i to other ones is constructed.

$$SVNNDD_{ij}=\sum_{t=1}^{m}ew_j\cdot\left|\frac{SF\left(NE_{ij}\right)}{AF\left(NE_{ij}\right)}-\frac{SF\left(NE_{tj}\right)}{AF\left(NE_{tj}\right)}\right| \tag{24}$$

(2) Construct the total weighted deviation.

$$SVNNDD_j\left(ew\right)=\sum_{i=1}^{m}SVNNDD_{ij}\left(ew\right)$$

$$=\sum_{i=1}^{m}\sum_{t=1}^{m}ew_j\left|\frac{SF\left(NE_{ij}\right)}{AF\left(NE_{ij}\right)}-\frac{SF\left(NE_{tj}\right)}{AF\left(NE_{tj}\right)}\right| \tag{25}$$

(3) Construct non-linear programming techniques.

$$\left(M-1\right)\begin{cases}\max SVNNDD\left(ew\right)=\sum_{j=1}^{n}\sum_{i=1}^{m}\sum_{t=1}^{m}ew_j\left|\frac{SF\left(NE_{ij}\right)}{AF\left(NE_{ij}\right)}-\frac{SF\left(NE_{tj}\right)}{AF\left(NE_{tj}\right)}\right| \\ s.t.\ \ \mathrm{ew}_j\geq 0,\ \ \sum_{j=1}^{n}ew_j^2=1\end{cases} \tag{26}$$

The Lagrange function is put forward this model.

$$LF\left(ew,\xi\right)=\left(\sum_{j=1}^{n}\sum_{i=1}^{m}\sum_{t=1}^{m}ew_j\left|\frac{SF\left(NE_{ij}\right)}{AF\left(NE_{ij}\right)}-\frac{SF\left(NE_{tj}\right)}{AF\left(NE_{tj}\right)}\right|+\frac{\xi}{2}\left(\sum_{j=1}^{n}ew_j^2-1\right)\right)$$

where ξ is Lagrange multiplier. The partial derivatives are constructed.

$$\begin{cases} \dfrac{\partial LF}{\partial ew_j} = \sum\limits_{i=1}^{m}\sum\limits_{t=1}^{m}\left|\dfrac{SF\left(NE_{ij}\right)}{AF\left(NE_{ij}\right)} - \dfrac{SF\left(NE_{tj}\right)}{AF\left(NE_{tj}\right)}\right| + \xi ew_j = 0 \\ \dfrac{\partial LF}{\partial \xi} = \dfrac{1}{2}\left(\sum\limits_{j=1}^{n} ew_j^2 - 1\right) = 0 \end{cases}$$

The weight is obtained: $ew_j^* = \dfrac{\sum\limits_{i=1}^{m}\sum\limits_{t=1}^{m}\left|\dfrac{SF\left(NE_{ij}\right)}{AF\left(NE_{ij}\right)} - \dfrac{SF\left(NE_{tj}\right)}{AF\left(NE_{tj}\right)}\right|}{\sqrt{\sum\limits_{j=1}^{n}\left(\sum\limits_{i=1}^{m}\sum\limits_{t=1}^{m}\left|\dfrac{SF\left(NE_{ij}\right)}{AF\left(NE_{ij}\right)} - \dfrac{SF\left(NE_{tj}\right)}{AF\left(NE_{tj}\right)}\right|\right)^2}}$

Finally, the normalized weights are: $ew_j = \dfrac{\sum\limits_{i=1}^{m}\sum\limits_{t=1}^{m}\left|\dfrac{SF\left(NE_{ij}\right)}{AF\left(NE_{ij}\right)} - \dfrac{SF\left(NE_{tj}\right)}{AF\left(NE_{tj}\right)}\right|}{\sum\limits_{j=1}^{n}\sum\limits_{i=1}^{m}\sum\limits_{t=1}^{m}\left|\dfrac{SF\left(NE_{ij}\right)}{AF\left(NE_{ij}\right)} - \dfrac{SF\left(NE_{tj}\right)}{AF\left(NE_{tj}\right)}\right|}$ (27)

Step 4. According to $NE = \left[NE_{ij}\right]_{m\times n}$, we can fuse all SVNNs $NE = \left[NE_{ij}\right]_{m\times n}$ through SVNNGPGBM technique to obtain the SVNNs $NE_i = \left(NET_i, NEI_i, NEF_i\right)$:

$$\begin{aligned} & NE_i = \left(NET_i, NEI_i, NEF_i\right) \\ & = SVNNGWGBM_{ew}^{es,et,er}\left(NE_{i1}, NE_{i2}, \cdots, NE_{in}\right) \\ & = \frac{1}{es+et+er}\overset{n}{\underset{i,j,k=1}{\otimes}}\left(esNE_{if} \oplus etNE_{ij} \oplus erNE_{ik}\right)^{\frac{\left(1+ET\left(NE_{if}\right)\right)}{\sum_{i=1}^{n}\left(1+ET\left(NE_{if}\right)\right)}\frac{\left(1+ET\left(NE_{ij}\right)\right)}{\sum_{j=1}^{n}\left(1+ET\left(NE_{ij}\right)\right)}\frac{\left(1+ET\left(NE_{ik}\right)\right)}{\sum_{k=1}^{n}\left(1+ET\left(NE_{ik}\right)\right)}} \\ & = \left(\begin{array}{c} 1-\left(1-\prod\limits_{i,j,k=1}^{n}\left(1-\left(1-NET_{if}\right)^{es}\left(1-NET_{ij}\right)^{et}\left(1-NET_{ik}\right)^{er}\right)^{\frac{\left(1+ET\left(NE_{if}\right)\right)}{\sum_{i=1}^{n}\left(1+ET\left(NE_{if}\right)\right)}\frac{\left(1+ET\left(NE_{ij}\right)\right)}{\sum_{j=1}^{n}\left(1+ET\left(NE_{ij}\right)\right)}\frac{\left(1+ET\left(NE_{ik}\right)\right)}{\sum_{k=1}^{n}\left(1+ET\left(NE_{ik}\right)\right)}}\right)^{1/(es+et+er)}, \\ 1-\left(1-\prod\limits_{i,j,k=1}^{n}\left(1-NEI_{if}^{es}NEI_{ij}^{et}NEI_{ik}^{er}\right)^{\frac{\left(1+ET\left(NE_{if}\right)\right)}{\sum_{i=1}^{n}\left(1+ET\left(NE_{if}\right)\right)}\frac{\left(1+ET\left(NE_{ij}\right)\right)}{\sum_{j=1}^{n}\left(1+ET\left(NE_{ij}\right)\right)}\frac{\left(1+ET\left(NE_{ik}\right)\right)}{\sum_{k=1}^{n}\left(1+ET\left(NE_{ik}\right)\right)}}\right)^{1/(es+et+er)}, \\ 1-\left(1-\prod\limits_{i,j,k=1}^{n}\left(1-NEF_{if}^{es}NEF_{ij}^{et}NEF_{ik}^{er}\right)^{\frac{\left(1+ET\left(NE_{if}\right)\right)}{\sum_{i=1}^{n}\left(1+ET\left(NE_{if}\right)\right)}\frac{\left(1+ET\left(NE_{ij}\right)\right)}{\sum_{j=1}^{n}\left(1+ET\left(NE_{ij}\right)\right)}\frac{\left(1+ET\left(NE_{ik}\right)\right)}{\sum_{k=1}^{n}\left(1+ET\left(NE_{ik}\right)\right)}}\right)^{1/(es+et+er)} \end{array}\right) \end{aligned}$$

(28)

Step 5. Obtain the $SF\left(NE\right), AF\left(NE_i\right)\ \left(i=1,2,3,\cdots,m\right)$.

$$SF\left(nq_i\right)=\frac{\left(2+NET_i-NEI_i-NEF_i\right)}{3},$$
$$AF\left(NE_i\right)=\frac{NET_i-NEF_i+1}{2} \tag{29}$$

Step 6. Rank the alternatives

5. Empirical example and comparative analysis

5.1. Case Study

The evaluation of RTEE under high-quality development refers to measuring how the tourism industry, in the context of promoting high-quality economic growth, effectively reduces resource consumption, energy usage, and negative environmental impacts while achieving economic growth. The core idea of tourism ecological efficiency evaluation is to assess the sustainability and environmental contribution of the tourism industry by analyzing the economic output per unit of carbon emissions. Its goal is to promote the coordinated development of the regional economy and ecology by achieving environmental protection and efficient resource utilization while advancing tourism development as shown in Figure 3.

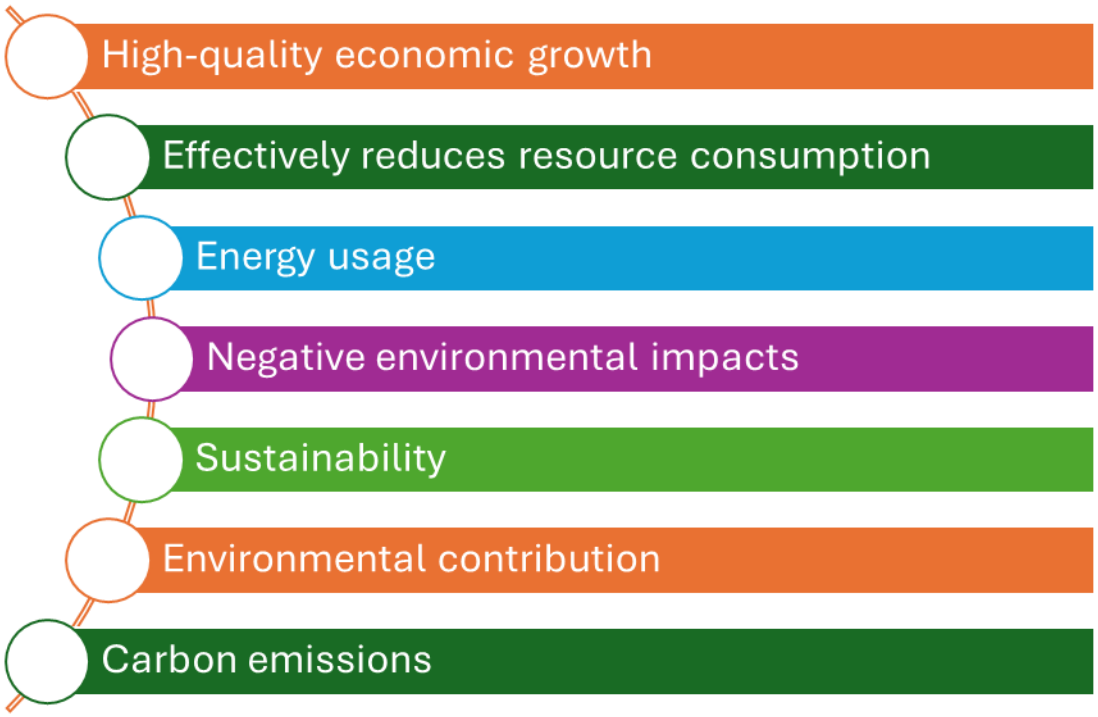

Figure 3. Evaluation of RTFE.

As the world places increasing emphasis on climate change and environmental protection, the tourism industry, being resource-intensive, needs to focus on improving ecological efficiency during its development. Through ecological efficiency evaluation, the environmental impact of the tourism industry can be quantified, helping decision-makers identify areas with high energy consumption and low output, thereby formulating more targeted policies and measures.

In summary, the evaluation of the RTEE under high-quality development is not only an important tool for assessing the sustainable development of the tourism industry but also a key pathway to achieving the green transformation of tourism and fostering a win-win situation between economic and ecological benefits. The RTEE evaluation under high-quality development is MADM. Figure 4 shows the criteria.

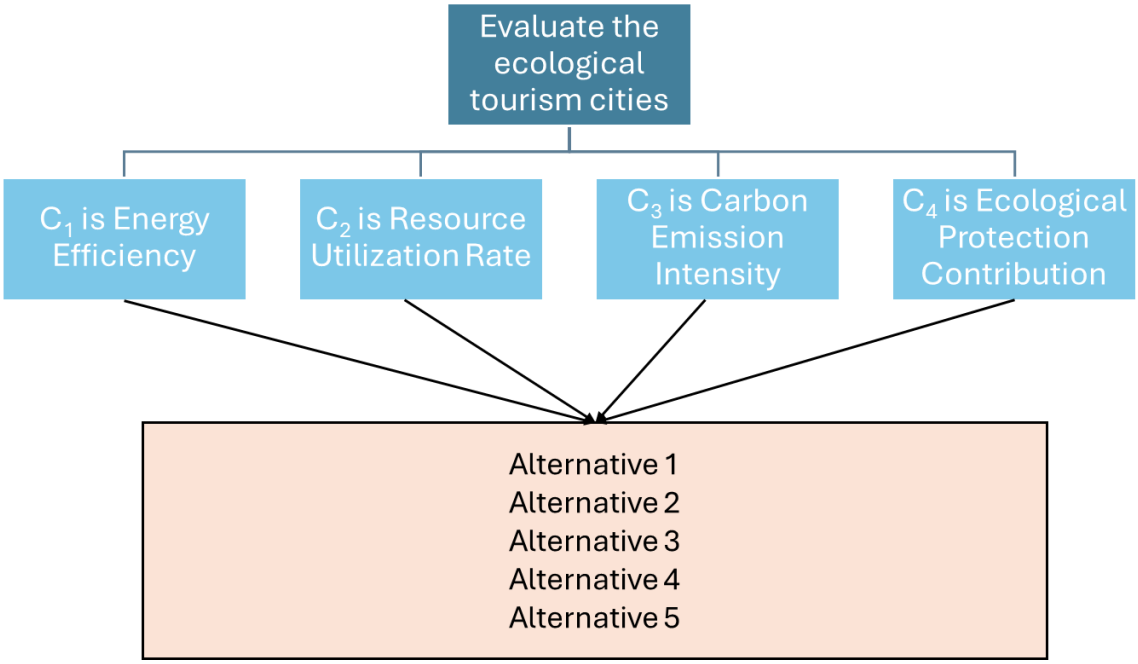

Figure 4. The list of criteria and alternatives.

Five ecological tourism cities are evaluated with four attributes:

I. Energy Efficiency (C_1)**:** This indicator measures the economic benefits generated per unit of energy consumption in the tourism industry. An improvement in energy efficiency means that tourism activities use less energy to create more economic output, helping to reduce energy waste and lower carbon emissions.;

II. Resource Utilization Rate (C_2): The resource utilization rate assesses the economic output generated per unit of resource input (such as water, land, raw materials, etc.) in the

tourism industry. A high resource utilization rate indicates that resources are being used efficiently, minimizing resource waste and enhancing the sustainability of tourism.;

III. Carbon Emission Intensity (C_3): This indicator analyzes the amount of carbon emissions per unit of economic output, used to measure the tourism industry's carbon footprint. The lower the carbon emission intensity, the smaller the negative environmental impact of tourism while achieving economic growth, contributing to low-carbon development goals.

IV. Ecological Protection Contribution (C_4): This indicator examines the tourism sector's role in protecting and improving the local natural environment. It evaluates whether tourism activities help preserve ecosystems, reduce environmental pollution, and promote sustainable ecological management, ensuring that tourism development aligns with long-term ecological protection. Then, the SVNNGPGBM technique put forward MADM for solving the RTEE evaluation under high-quality development with SVNNs.

Step 1. Put forward the SVNN-matrix as shown in Table 2.

Step 2. We normalize the decision matrix as shown in Table 3.

Step 3. Constructed the weights of criteria as shown in Figure 5.

Step 4. Obtain the $NP_i\left(i=1,2,3,\cdots,5\right)$ in line with SVNNGPGBM technique

Step 5. Put forward the $SV\left(NP_i\right)\left(i=1,2,3,\cdots,5\right)$ (Table 4).

Step 6. We show the rank is $A_2 > A_5 > A_4 > A_3 > A_1$, and the best choice is A_2 as shown in Figure 6.

Table 2. The decision matrix.

	C_1	C_2	C_3	$C4_1$
A_1	(0.63, 0.55, 0.46)	(0.67, 0.46, 0.71)	(0.42, 0.13, 0.49)	(0.67, 0.47, 0.45)
A_2	(0.67, 0.34, 0.63)	(0.49, 0.53, 0.66)	(0.41, 0.16, 0.43)	(0.66, 0.39, 0.64)
A_3	(0.42, 0.63, 0.46)	(0.35, 0.42, 0.53)	(0.29, 0.17, 0.27)	(0.19, 0.17, 0.17)
A_4	(0.49, 0.44, 0.73)	(0.47, 0.53, 0.47)	(0.26, 0.14, 0.41)	(0.64, 0.36, 0.14)
A_5	(0.42, 0.38, 0.66)	(0.66, 0.37, 0.56)	(0.49, 0.26, 0.43)	(0.64, 0.37, 0.77)

Table 3. The NP matrix

	C_1	C_2	C_3	$C4_1$
A_1	(0.63, 0.55, 0.46)	(0.67, 0.46, 0.71)	(0.42, 0.13, 0.49)	(0.67, 0.47, 0.45)
A_2	(0.67, 0.34, 0.63)	(0.49, 0.53, 0.66)	(0.41, 0.16, 0.43)	(0.66, 0.39, 0.64)
A_3	(0.42, 0.63, 0.46)	(0.35, 0.42, 0.53)	(0.29, 0.17, 0.27)	(0.19, 0.17, 0.17)
A_4	(0.49, 0.44, 0.73)	(0.47, 0.53, 0.47)	(0.26, 0.14, 0.41)	(0.64, 0.36, 0.14)
A_5	(0.42, 0.38, 0.66)	(0.66, 0.37, 0.56)	(0.49, 0.26, 0.43)	(0.64, 0.37, 0.77)

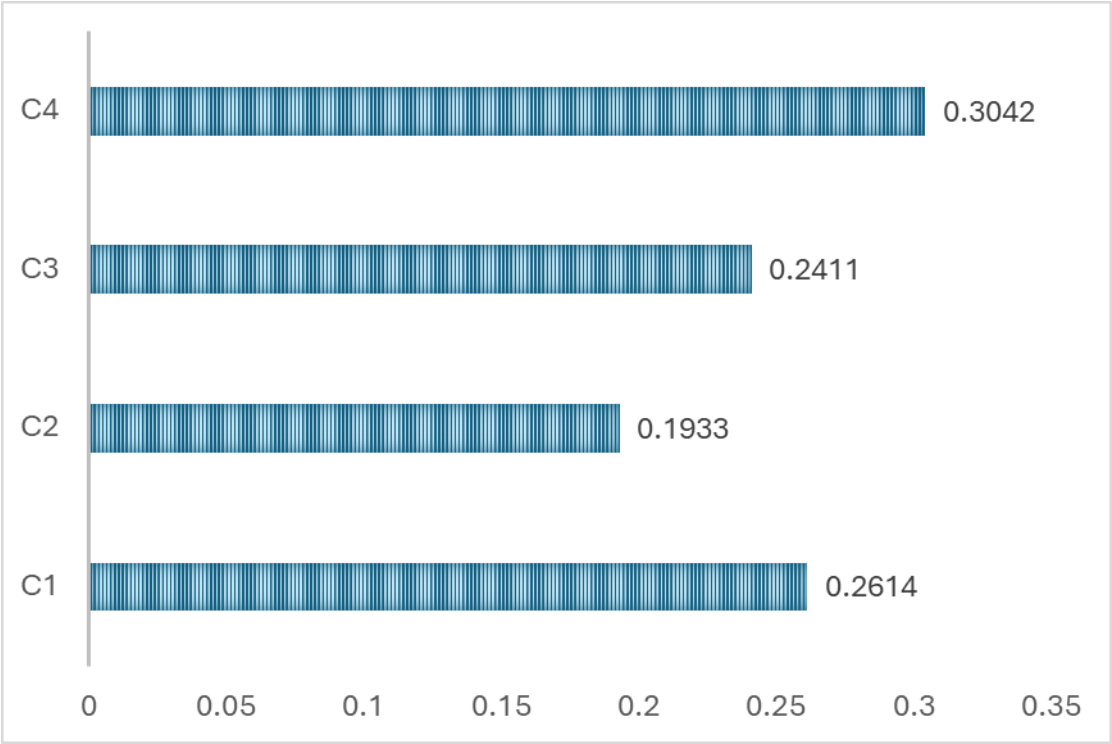

Figure 5. The criteria weights.

Table 4. The NP values

Techniques	$NP_i\left(i=1,2,\cdots,5\right)$
A_1	(0.5338,0.4831,0.3542)
A_2	(0.7035,0.3124,0.3992)
A_3	(0.5745,0.6529,0.3226)
A_4	(0.5986,0.5802,0.3416)
A_5	(0.5981,0.6547,0.1992)

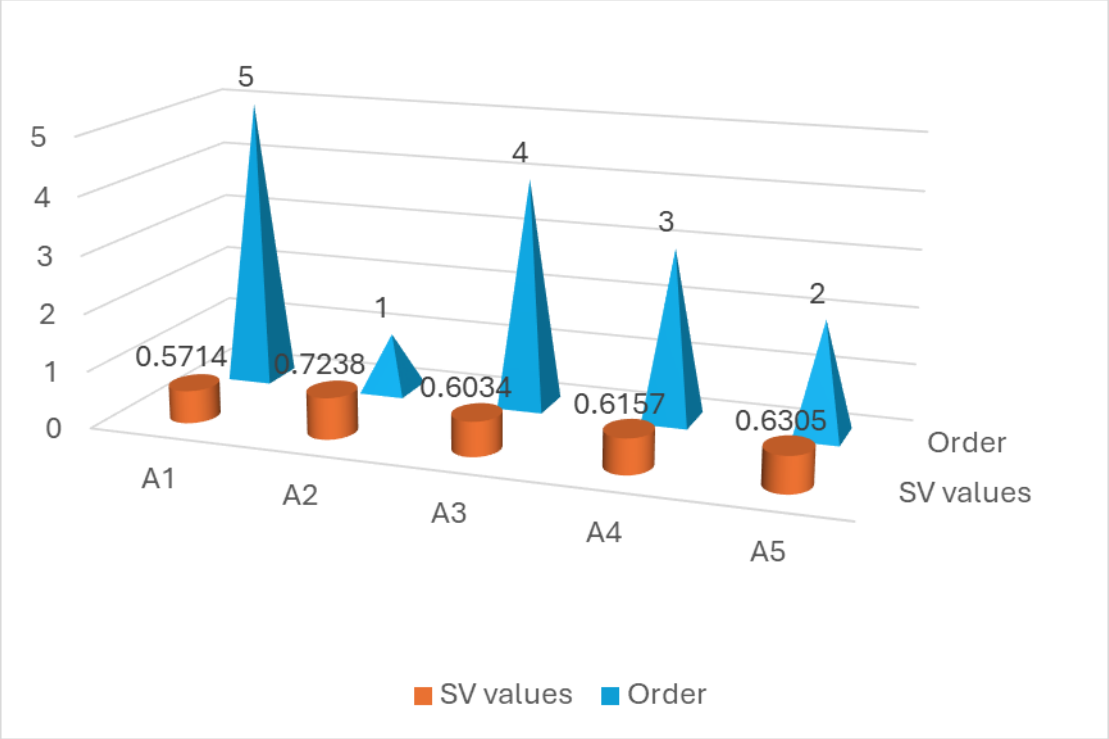

Figure 6. The order of alternatives.

5.2. Influence analysis

To illustrate the effects of different parameters on the ranking using the SVNNGPGBM method, the final results are presented in Table 6.

Table 6. Influence analysis for SVNNGPGBM technique

(es, et, er)	SF(A_1)	SF(A_2)	SF(A_3)	SF(A_4)	SF(A_5)	Orders
(1,1,1)	0.5714	0.7238	0.6034	0.6157	0.6305	$A_2 > A_5 > A_3 > A_4 > A_1$
(2,2,2)	0.8151	0.9184	0.8459	0.8415	0.8464	$A_2 > A_5 > A_3 > A_4 > A_1$
(3,3,3)	0.8821	0.9541	0.9077	0.8886	0.9109	$A_2 > A_5 > A_3 > A_4 > A_1$
(4,4,4)	0.9077	0.9639	0.9311	0.9029	0.9387	$A_2 > A_5 > A_3 > A_1 > A_4$
(5,5,5)	0.9201	0.9677	0.9431	0.9088	0.9538	$A_2 > A_5 > A_3 > A_1 > A_4$
(6,6,6)	0.9274	0.9697	0.9508	0.9120	0.9630	$A_2 > A_5 > A_3 > A_1 > A_4$
(7,7,7)	0.9321	0.9711	0.9561	0.9141	0.9692	$A_2 > A_5 > A_3 > A_1 > A_4$
(8,8,8)	0.9356	0.9723	0.9603	0.9159	0.9737	$A_2 > A_5 > A_3 > A_1 > A_4$
(9,9,9)	0.9381	0.9734	0.9637	0.9173	0.9771	$A_2 > A_5 > A_3 > A_1 > A_4$
(10,10,10)	0.9403	0.9745	0.9665	0.9185	0.9798	$A_2 > A_5 > A_3 > A_1 > A_4$

As seen from Table 6, the ranking changes slightly when parameter information is applied. In the MADM process, the parameter values can represent the subjective preferences of DMs. On one hand, DMs can obtain different outcomes by adjusting these parameter values; on the other hand, the parameter values also reflect the DMs' risk attitudes.

5.3. Compare analysis

The SVNNGPGBM technique is compared with SVNNWA and SVNNWG approach [30], SVNN-CODAS approach [35] and SVNN-EDAS approach [36]. The final results are shown in Figure 7.

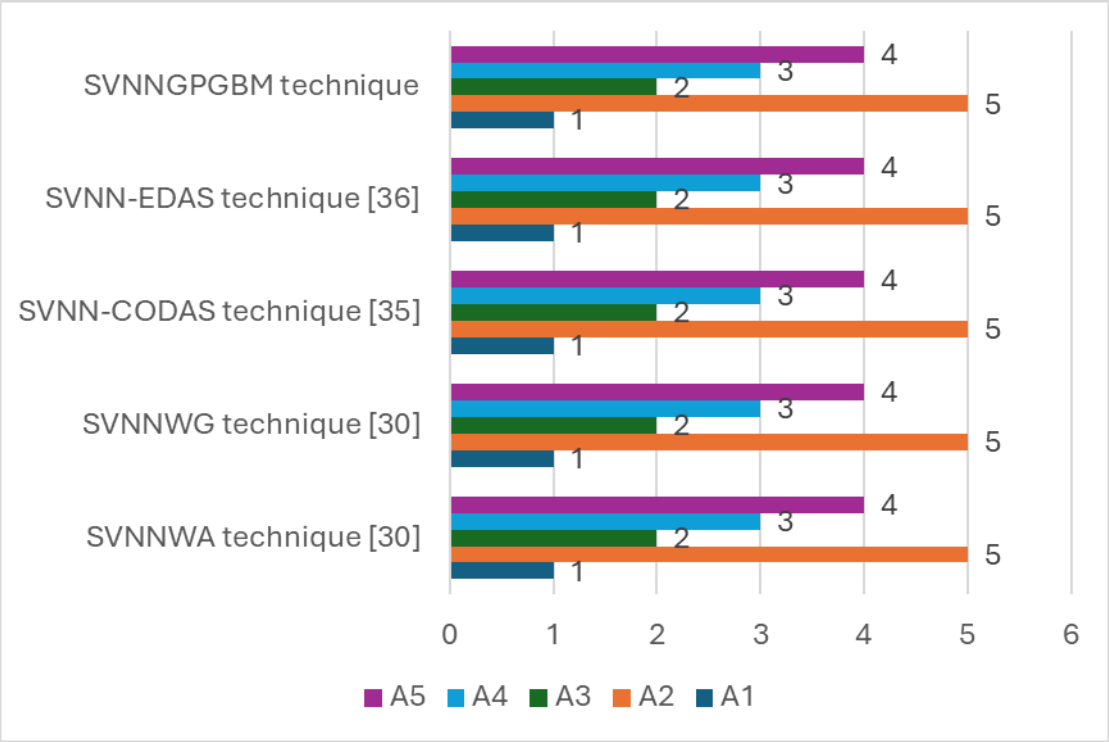

Figure 7. Comparative analysis.

–

From Figure 7, it is obvious that the optimal ecological tourism city is EA_2, while the worst ecological tourism city is EA_1. In other words, the order of seven approaches is slightly different. The SVNNGPGBM technique offers the following three key advantages in evaluating the satisfaction of college students' online ideological and political education in the context of big data:

- Handling Uncertainty and Ambiguity: The SVNNGPGBM technique models satisfaction using SVNSs, which can simultaneously handle truth, indeterminacy, and falsity. This allows it to accurately represent the fuzzy and uncertain factors often present in students' satisfaction evaluations. In the big data environment, where student feedback is often complex and variable, SVNNGPGBM effectively captures the inherent uncertainty and ambiguity, ensuring a more comprehensive and precise assessment.
- Integrating Multidimensional Data for Enhanced Decision-Making: SVNNGPGBM can perform comprehensive analysis across multiple evaluation dimensions. By utilizing the geometric mean and power geometric operators, this method integrates data from different sources or dimensions, avoiding bias from relying on a single evaluation criterion. This leads to a more objective and reasonable satisfaction evaluation.
- Adapting to Big Data and Improving Computational Efficiency: The SVNNGPGBM technique is well-suited to handle large-scale datasets, making it ideal for the big data context where vast amounts of student feedback need to be processed. Additionally, the algorithm is computationally efficient, enabling quick generation of comprehensive evaluation results, providing timely and effective decision-making support for educators.

6. Conclusion

The evaluation of RTEE under high-quality development aims to assess how the tourism industry promotes economic growth while minimizing resource consumption and environmental impact. The central focus is on evaluating sustainability and ecological efficiency by analyzing economic output per unit of carbon emissions. Common indicators include energy efficiency, resource utilization, carbon emission intensity, and ecological protection contribution. Energy efficiency measures economic output per unit of energy consumed, resource utilization assesses output from resource inputs, carbon emission intensity examines emissions per unit of economic output, and ecological protection contribution evaluates tourism's role in environmental preservation. By analyzing these indicators, decision-makers can optimize tourism models, achieving a balance between economic and ecological benefits, and guide the industry towards low-carbon, green, high-quality growth. RTEE evaluation under high-quality development is an MADM problem. In this study, the GWBM technique is introduced to solve MADM problems using SVNSs. The

–

GSVNNWBM technique is also proposed for MADM, aligned with this method. A numerical example of RTEE evaluation under high-quality development is provided, along with a comparative analysis using the GSVNNWBM technique.

7. Research limitations and further research directions

Although this study proposes an innovative method for evaluating regional tourism ecological efficiency (RTEE) and applies the single-valued neutrosophic number generalized power geometric BM (SVNNGPGBM) technique,

There are several limitations:

- High model complexity: While the SVNNGPGBM technique excels at handling uncertainty and ambiguity, its mathematical complexity is high, potentially increasing the computational cost and technical difficulty in practical applications. For non-expert users or policymakers, understanding and implementing this method may present certain challenges.
- Strong data dependency: The model relies heavily on accurate carbon emissions and resource consumption data. However, in some developing or underdeveloped regions, tourism-related environmental data may be incomplete or missing, which could limit the model's broad applicability and effectiveness.
- Lack of dynamic evaluation capability: The evaluation method in this paper is primarily based on static data, neglecting the dynamic changes in ecological efficiency as the tourism industry evolves. Over time, resource use and environmental impact may change significantly, and a static model may fail to capture these shifts.

To address these limitations, future research can explore the following three directions:

- Simplifying the model and improving operability: Future research could aim to simplify the SVNNGPGBM model to reduce its computational complexity, making it more accessible for practical use. Developing user-friendly tools or software could help policymakers and stakeholders more efficiently apply the model for decision-making.
- Enhancing data collection and processing capabilities: To address the strong data dependency, further research could focus on improving data acquisition and processing methods in areas with limited or low-quality data. Emerging technologies such as remote sensing or intelligent monitoring systems could be introduced to supplement or replace traditional data collection methods, improving the model's applicability and accuracy.

–

- Building a dynamic evaluation model: To better reflect the dynamic changes in tourism ecological efficiency, future studies could incorporate time series analysis or dynamic system modeling to develop an RTEE evaluation model that evolves over time. This would allow for real-time tracking of the tourism industry's impact on the environment and resources, providing more timely and forward-looking recommendations for decision-makers.

By pursuing these research directions, the evaluation method for regional tourism ecological efficiency can be further refined, enhancing its applicability in policy formulation and practice, while providing stronger support for the green, low-carbon, and high-quality development of the tourism industry.

Acknowledgements

This work is supported by Socio-economic statistics research projects of Shanxi Province "Research on spatial distribution pattern and development path of Shanxi tourism resources" (KYTJ [2021]001).

References

[1] J. J, R. S, Some operations on neutrosophic hypersoft matrices and their applications, Neutrosophic Systems with Applications, 21 (2024) 46-62.

[2] A. Salem, M. Mohamed, F. Smarandache, Im4.0ef: Tele-medical realization via integrating vague t2nss with owcm-ram toward intelligent medical 4.0 evaluator framework, Sustainable Machine Intelligence Journal, 9 (2024) 79-88.

[3] F. Smarandache, Treesoft set vs. Hypersoft set and fuzzy-extensions of treesoft sets, HyperSoft Set Methods in Engineering, 2 (2024) 114-118.

[4] D. Rani, H. Garg, Multiple attributes group decision-making based on trigonometric operators, particle swarm optimization and complex intuitionistic fuzzy values, Artificial Intelligence Review, 56 (2023) 1787-1831.

[5] N.N. Liao, Q. Cai, H. Garg, G.W. Wei, X.R. Xu, Novel gained and lost dominance score method based on cumulative prospect theory for group decision-making problems in probabilistic hesitant fuzzy environment, International Journal of Fuzzy Systems, 25 (2023) 1414-1428.

[6] J. Gwak, H. Garg, N.M. Jan, Hybrid integrated decision-making algorithm for clustering analysis based on a bipolar complex fuzzy and soft sets, Alexandria Engineering Journal, 67 (2023) 473-487.

[7] S.J. Ghoushchi, H. Garg, S.R. Bonab, A. Rahimi, An integrated swara-codas decision-making algorithm with spherical fuzzy information for clean energy barriers evaluation, Expert Systems with Applications, 223 (2023) 14.

[8] B. Oztaysi, S.C. Onar, C. Kahraman, Waste disposal location selection by using pythagorean fuzzy regime method, Journal of Intelligent & Fuzzy Systems, 42 (2022) 401-410.

–

[9] S.C. Onar, C. Kahraman, B. Oztaysi, A new hesitant fuzzy kemira approach: An application to adoption of autonomous vehicles, Journal of Intelligent & Fuzzy Systems, 42 (2022) 109-120.

[10] C. Kahraman, S.C. Onar, B. Oztaysi, A novel spherical fuzzy critic method and its application to prioritization of supplier selection criteria, Journal of Intelligent & Fuzzy Systems, 42 (2022) 29-36.

[11] E. Ilbahar, C. Kahraman, S. Cebi, Risk assessment of renewable energy investments: A modified failure mode and effect analysis based on prospect theory and intuitionistic fuzzy ahp, Energy, 239 (2022) 11.

[12] E. Haktanir, C. Kahraman, New product design using chebyshev's inequality based interval-valued intuitionistic z-fuzzy qfd method, Informatica, 33 (2022) 1-33.

[13] J. Obbineni, I. Kandasamy, W.B. Vasantha, F. Smarandache, Combining swot analysis and neutrosophic cognitive maps for multi-criteria decision making: A case study of organic agriculture in india, Soft Computing, (2023) 22.

[14] A. Hussain, T. Mahmood, F. Smarandache, S. Ashraf, Topsis approach for mcgdm based on intuitionistic fuzzy rough dombi aggregation operations, Computational & Applied Mathematics, 42 (2023) 33.

[15] I. Gokasar, M. Deveci, M. Isik, T. Daim, A.A. Zaidan, F. Smarandache, Evaluation of the alternatives of introducing electric vehicles in developing countries using type-2 neutrosophic numbers based rafsi model, Technological Forecasting and Social Change, 192 (2023) 14.

[16] S.A. Edalatpanah, F. Smarandache, H. Garg, Guest editorial: Preface to the special issue on the neutrosophical approach: Applications in management decision and organizational research methods, Management Decision, 61 (2023) 357-362.

[17] D. Stanujkic, D. Karabasevic, G. Popovic, F. Smarandache, P.S. Stanimirovic, M. Saracevic, V.N. Katsikis, A single valued neutrosophic extension of the simple wisp method, Informatica, 33 (2022) 635-651.

[18] A.U. Rahman, M. Saeed, F. Smarandache, A theoretical and analytical approach to the conceptual framework of convexity cum concavity on fuzzy hypersoft sets with some generalized properties, Soft Computing, 26 (2022) 4123-4139.

[19] Z. Yao, T. Chen, S. Yin, X. Li, Empirical analysis of regional tourism ecological efficiency: A case study of hainan province, Scientia Geographica Sinica, 36 (2016) 417-423.

[20] L. Gao, Evaluation and spatial effect analysis of regional tourism ecological efficiency, Journal of Guangxi University, 45 (2018) 112-120.

[21] W. Lin, B. Lin, Evaluation of regional tourism industry ecological efficiency and its spatial differences: A case study of jiangxi province, East China Economic Management, 32 (2018) 19-25.

[22] T. Wang, A study on the relationship between regional tourism industry agglomeration and tourism ecological efficiency in shanxi province, Journal of Shanxi University of Finance and Economics, 38 (2021) 45-53.

[23] F. Fang, Research on the coordinated development of regional tourism ecological efficiency and economy, Journal of Anhui University, 45 (2021) 78-85.

–

[24] Z. Hong, L. Wang, C. Zhang, Influencing factors of regional tourism ecological efficiency in the context of green development: A case study of the western regions, Acta Ecologica Sinica, 41 (2021) 3512-3524.

[25] Z. Li, W. Wu, Research on the spatial consistency of tourism ecological efficiency and regional ecological security in the middle reaches of the yangtze river, Resources and Environment in the Yangtze Basin, 31 (2022) 537-550.

[26] J. Liu, An empirical study on the impact of regional innovation on tourism ecological efficiency, Journal of Regional Science and Development, 28 (2022) 89-101.

[27] H. Tian, Q. Zhao, Evaluation of regional tourism ecological efficiency and influencing factors under high-quality development: A case study of shandong province, Arid Land Resources and Environment, 36 (2022) 201-208.

[28] F. Deng, Spatiotemporal differentiation and influencing factors of regional tourism ecological efficiency from the value-added perspective in china, Research on Tourism Development, 40 (2023) 123-136.

[29] H. Wang, F. Smarandache, Y.Q. Zhang, R. Sunderraman, Single valued neutrosophic sets, Multispace Multistruct, (2010) 410-413.

[30] J.J. Peng, J.Q. Wang, J. Wang, H.Y. Zhang, X.H. Chen, Simplified neutrosophic sets and their applications in multi-criteria group decision-making problems, International Journal of Systems Science, 47 (2016) 2342-2358.

[31] P. Majumdar, S.K. Samanta, On similarity and entropy of neutrosophic sets, Journal of Intelligent & Fuzzy Systems, 26 (2014) 1245-1252.

[32] M.M. Xia, Z.S. Xu, B. Zhu, Generalized intuitionistic fuzzy bonferroni means, International Journal of Intelligent Systems, 27 (2012) 23-47.

[33] R.R. Yager, The power average operator, IEEE Transactions on Systems, Man, and Cybernetics-Part A, 31 (2001) 724-731.

[34] Y. Wang, Using the method of maximizing deviation to make decision for multiindices, Journal of Systems Engineering & Electronics, 8 (1997) 21-26.

[35] E. Bolturk, A. Karasan, Prioritization of investment alternatives for a hospital by using neutrosophic codas method, Journal of Multiple-Valued Logic and Soft Computing, 33 (2019) 381-396.

[36] D. Stanujkic, D. Karabasevic, G. Popovic, D. Pamucar, Z. Stevic, E.K. Zavadskas, F. Smarandache, A single-valued neutrosophic extension of the edas method, Axioms, 10 (2021) 13.

Received: July 26, 2024. Accepted: Oct 25, 2024

Neutrosophic Sets and Systems, Vol. 76, 2025
University of New Mexico

Solving the shortest path Problem in an interval-valued Neutrosophic Pythagorean environment using an enhanced A* search algorithm

Prasanta Kumar Raut[1,2], Sakya Singh Satapathy[2], Siva Prasad Behera[1], Said Broumi[3], Ajay Kumar Sahoo[4]

[1]Department of Mathematics, C.V. Raman Global University, Bhubaneswar, Odisha, India
[2]Department of Mathematics, Trident Academy of Technology, Bhubaneswar, Odisha, India
[3]Laboratory of Information Processing, Faculty of Science Ben M'Sik, University Hassan II, Casablanca, Morocco
[4]Assistant Professor, Department of Mathematics, Indira Gandhi Institute of Technology, Sarang, Dhenkanal, Odisha, 759146

[1,2]Email:prasantaraut95@gmail.com,sivaiitkgp12@gmail.com
[2]Email:sakyasinghsatapathy@gmail.com
[3]Email: broumisaid78@gmail.com
[4]Email: ajaysahoo20@gmail.com

Abstract: The A* search algorithm is widely utilized to evaluate the shortest path in a given network. However, in a traditional A* search algorithm, the nodes are assumed to have crisp values, i.e., a single value. This assumption may not hold in many real-world scenarios where uncertainty or ambiguity is involved. In such cases, an interval-valued Neutrosophic Pythagorean (IVNP) environment can provide a more sound and accurate representation. Interval-valued Neutrosophic Pythagorean sets (IVNPS) are an effective way to model vague and imprecise data, which is prevalent in executive problems. These sets provide a more flexible way to capture uncertainty by allowing the values of nodes in the graph to vary within certain intervals rather than having fixed values. This interval representation can effectively handle imprecise or incomplete information and is a powerful tool in executive processes. In this research paper, we proposed an improved A* search algorithm that takes advantage of the interval-valued neutrosophic Pythagorean environment. This algorithm aims to evaluate the shortest path in a graph under uncertainty and ambiguity. The proposed algorithm incorporates the IVNPS theory into the A* search framework to handle the uncertainty in node values and edge weights. It utilizes the concept of neutrosophic Pythagorean distance to calculate the heuristic function and make informed decisions on the next node to expand.

Keywords:
A* search algorithm; heuristic function; interval-valued Neutrosophic Pythagorean number.

1. Introduction:

In a neutrosophic environment, uncertainty and indeterminacy play an important part. The conception of a neutrosophic set (NS), first suggested by Smarandache in 1995, and allows for the representation of indeterminacy in the form of three components, i.e., truth, indeterminacy, and false membership. Thus, as a result, numerous papers [1–10] have been available in the area of uncertainty environment.

Various researchers have provided different work on SPP in various environments. Ahuja et al. [11] suggested a different kind of distributed heap as an efficient technique for finding the SPP of the graph. Yang et al. [12] demonstrated a diagram-theoretic method for calculating the right line. Zheng and Ibarra [13] showed how to evaluate the single-basis shortest possible route problem using the logarithmic sequence of 'n'. Arsham [14] investigated the shortest path problem's robustness. Tzoreff [15] investigated an unconnected SPP with different group path lengths.

Zhang and Lin [17] proposed the reverse SPP. Samaranadache and Vasantha proposed a fundamental neutrosophic mathematical structure in their paper [18], and it can also be applied to uncertain and neutrosophic models. Zwick and Roditty [19] obtained some findings related to valuable types of the SPP. Desaulniers and Irnich [20] suggested SPP with holdup forces. Jowers and Buckley [21] used fuzzy logic to present SPP. Said broumi [22] solved the SPP problem using ACO. Turner [23] successfully developed an algebraic method for solving a set of SPP on both normal and acyclic graphs. Deng et al. [24] suggested a new method for ambiguous SPP.

Broumi et al. [25] proposed a new idea to conduct a study on features that include verification and representations. Harish and Nancy [26] suggested an updated score function for use in the executive process. For address the issue of neutrosophic decision-making with insufficient weight support, Sahin and Liu [27] optimized the use of variations. Broumi et al. [28, 29] suggested a novel idea to evaluate the SPP.Hu and Sotirov [30] suggested semi-definite training for the rectangular SPP, and the QSPP was solved with some arithmetic operations using the division algorithm. Leitert and Dragan [31] solved SPP with little difficulty. Zhang et al. [32] suggested a new idea to solve SPP with scattered uncertainties.

The purpose of this study is to (i) improve the A* search method for finding the shortest path problem over neutrosophic interval-valued Pythagorean numbers; (ii) find the heuristic values and the best one for each node in IVNPS; (iii) find the good things about A* search in terms of its features, adaptability, and quick selections; and (iv) figure out the suggested approach at each step and find the results.

This research paper arranges the remaining sections in the following order: In Section 2, we talk about why we're doing this. Section-3 discuss the fundamental concepts of neutrosophic sets, intuitionistic neutrosophic sets, neutrosophic Pythagorean sets, neutrosophic interval-valued Pythagorean sets, and the various operations applicable to them. In Section-4, the A* search algorithm and the heuristic function are defined and explained. Section-5 provides a mathematical explanation for determining

the most efficient route using the IVNPS, a heuristic computational method, and a modified A* Search algorithm. Section-6 presents a numerical illustration of the process for calculating the IVNPS in neutrosophic situations. Section-7 conducted a comparative analysis of the shortest path using various networks and parameters, while also highlighting the benefits of the proposed methodology. Section-8 states the outcome of the work.

2. Motivation:

- In this chapter, we proposed an improved A* search algorithm. This algorithm objectives to evaluate the shortest path in a graph under uncertainty and ambiguity. The proposed algorithm incorporates the IVNPS theory into the A* search framework to handle the uncertainty in node values and edge weights. It utilizes the concept of neutrosophic Pythagorean distance to calculate the heuristic function and make informed decisions on the next node to expand.
- In this chapter, our aim is to evaluate the minimum cost between the initial vertex and the final vertex.
- Furthermore, we illustrate one numerical example using an algorithm.

3. Preliminaries:

This section of the paper presents an analysis of the fundamental concepts and definitions of the different sets.

Definition-3.1 [33]

A Neutrosophic set $\hat{S}$ in a universal set $\hat{X}$ is defined as $\hat{S} = \{< \hat{x}: \hat{T}_{\hat{S}}(\hat{x}), \hat{I}_{\hat{S}}(\hat{x}), \hat{F}_{\hat{S}}(\hat{x}) >: \hat{x} \in \hat{X}\}$. Here $\hat{T}_{\hat{S}}(\hat{x}), \hat{I}_{\hat{S}}(\hat{x}), \hat{F}_{\hat{S}}(\hat{x})$ defined the three membership degrees and $\hat{x} \in \hat{S}$ to the set A.

Three membership degrees is written as

$$0^+ \leq \left\{\left(\hat{T}_{\hat{S}}(\hat{x}) + \hat{I}_{\hat{S}}(\hat{x}) + \hat{F}_{\hat{S}}(\hat{x})\right)\right\} \leq 3^+ \quad (1)$$

Definition-3.2[35]

A Pythagorean neutrosophic set $\hat{S}$ in a universal set $\hat{X}$ is defined as $\hat{S} = \{< \hat{x}: \hat{T}_{\hat{S}}(\hat{x}), \hat{I}_{\hat{S}}(\hat{x}), \hat{F}_{\hat{S}}(\hat{x}) >: \hat{x} \in \hat{X}$, where $\hat{T}_{\hat{S}}(\hat{x}), \hat{I}_{\hat{S}}(\hat{x})$ are dependent, and

$\hat{F}_{\hat{S}}(\hat{x})$ independent component., for all $\hat{x} \in \hat{X}$, with the condition $0^+ \leq \{(T_{\hat{S}}(\hat{x}))^2 + (I_{\hat{S}}(\hat{x}))^2 + (F_{\hat{S}}(\hat{x}))^2 \leq 2\}$.

Definition-3.3[36]

An Interval-valued neutrosophic Pythagorean set $\hat{S}$ in a universal set $\hat{X}$ is defined as

$$\hat{S} = \{\hat{X} < , [\left(\frac{\hat{T}_{\hat{S}}^{L} + \hat{T}_{\hat{S}}^{U}}{2}\right)^2 + \left(\frac{\hat{I}_{\hat{S}}^{L} + \hat{I}_{\hat{S}}^{U}}{2}\right)^2 + \left(\frac{\hat{F}_{\hat{S}}^{L} + \hat{F}_{\hat{S}}^{U}}{2}\right)^2] \leq 2$$

Where $[\hat{T}_{\hat{S}}^{L}, \hat{T}_{\hat{S}}^{U}], [\hat{I}_{\hat{S}}^{L}, \hat{I}_{\hat{S}}^{U}], [F_{\hat{A}}^{L}, F_{\hat{A}}^{U}]$ represents the inferior and superior bound of the three membership degrees.

Definition-3.4[36]

Let $\hat{A}_1 =< w, [T_{\hat{A}_1}^{L}, T_{\hat{A}_1}^{U}], [I_{\hat{A}_1}^{L}, I_{\hat{A}_1}^{U}], [F_{\hat{A}_1}^{L}, F_{\hat{A}_1}^{U}] >$and

$\hat{A}_2 =< v, [T_{\hat{A}_2}^{L}, T_{\hat{A}_2}^{U}], [I_{\hat{A}_2}^{L}, I_{\hat{A}_2}^{U}], [F_{\hat{A}_2}^{L}, F_{\hat{A}_2}^{U}] >$ be two neutrosophic interval-valued Pythagorean set, then sum of two set is defined as

$$\hat{A}_1 + \hat{A}_2 = \{< w + v, [T_{\hat{A}_1}^{L} + T_{\hat{A}_2}^{L} - T_{\hat{A}_1}^{L} T_{\hat{A}_2}^{L}, T_{\hat{A}_1}^{U} + T_{\hat{A}_2}^{U} - T_{\hat{A}_1}^{L} T_{\hat{A}_2}^{U}], [I_{\hat{A}_1}^{L} I_{\hat{A}_2}^{L}, I_{\hat{A}_1}^{U} I_{\hat{A}_2}^{U}], [F_{\hat{A}_1}^{L} F_{\hat{A}_2}^{L}, F_{\hat{A}_1}^{U} F_{\hat{A}_2}^{U}] >\}$$

$$\hat{A}_1 \hat{A}_2 = \{< wv, [T_{\hat{A}_1}^{L} T_{\hat{A}_2}^{L}, T_{\hat{A}_1}^{L} T_{\hat{A}_2}^{U}], [I_{\hat{A}_1}^{L} + I_{\hat{A}_2}^{L} - I_{\hat{A}_1}^{L} I_{\hat{A}_2}^{L}, I_{\hat{A}_1}^{U} + I_{\hat{A}_2}^{U} - I_{\hat{A}_1}^{U} I_{\hat{A}_2}^{U}], [F_{\hat{A}_1}^{L} + F_{\hat{A}_1}^{L} - F_{\hat{A}_2}^{L} F_{\hat{A}_2}^{L}, F_{\hat{A}_1}^{U} + F_{\hat{A}_1}^{U} - F_{\hat{A}_2}^{U} F_{\hat{A}_2}^{U}] >\}$$

Definition-3.5[36]

Let $\hat{S} = \{< w, [T_{\hat{S}}^{L}, T_{\hat{S}}^{U}], [I_{\hat{S}}^{L}, I_{\hat{S}}^{U}], [F_{\hat{S}}^{L}, F_{\hat{S}}^{U}] > w \in W$

Let us assume $T_{\hat{S}}^{L} = \alpha$, $T_{\hat{S}}^{U} = \beta, I_{\hat{S}}^{L} = \gamma, I_{\hat{S}}^{U} = \delta$, $F_{\hat{S}}^{L} = \sigma$, $F_{\hat{S}}^{U} = \rho$ then the improved IVNP score function is expressed as

$$S(\hat{S}) = \frac{(\alpha^2 - \gamma^2 - \sigma^2)(1 + \sqrt{1 - \alpha^2 - \gamma^2 - \sigma^2}) + (\beta^2 - \delta^2 - \rho^2)(1 + \sqrt{1 - \beta^2 - \delta^2 - \rho^2})}{2}$$

4. A* search algorithm

In computer science and machine learning, the A* search technique is a famous way to identify the most efficient route between any two given nodes in a network. We call it "A*" because it adds up the heuristic function to evaluate the path from initial node (g) to final node (h). The A* algorithm uses an arrangement of best-first search and Dijkstra's algorithm to efficiently explore the search gap and evaluate the optimal path. It guarantees to get the shortest path providing the heuristic function satisfies certain conditions, such as being admissible (never overestimating the actual cost) and consistent (always satisfying the triangle inequality).

$$\hat{f}_{ij} = \hat{g}_{ij} + \hat{h}_{ij}$$

The parameter $\hat{f}_{ij}$ is utilized to determine the most efficient route from each specific node to the other node.

The parameter $\hat{g}_{ij}$ is utilized to calculate the expense of transitioning from each moment of one node to another node.

The parameter $\hat{h}_{ij}$ represents the heuristic, which is the estimated cost between the initial node and the final node.

4.1 The neutrosophic Pythagorean SPP with interval values

The implementation of the neutrosophic interval-valued Pythagorean technique could be used for formulating the problem of determining the shortest route in a connected network.

Variables:

Let $d(u, v)$ represent the shortest path (SP) between two corresponding nodes u and v.

Let $x(u, v)$ represent the membership degree of the path that is shortest between u and v at a node.

The non-membership degree of the shortest path (SP) from node u to node v is indicated by the symbol $y(u, v)$.

Let $z(u, v)$ represent the degree of indeterminacy of the shortest path (SP) connecting node u and v.

Objective:

Reduce the total length of all the path's edges or arc lengths i.e., minimize $\sum(u, v) \in E\ d(u, v)$.

Constraints:

For each edge (u, v), $d(u, v) = \sqrt{(x(u, v))^2 - (y(u, v))^2 + z(u, v)}$.

For each vertex u, the membership degrees$(x(u, v))$, non-membership degrees $(y(u, v))$, and indeterminacy degrees $(z(u, v))$ satisfy the neutrosophic Pythagorean equation: $(x(u, v))^2 + (y(u, v))^2 + (z(u, v))^2 = 1$.

For each vertex u, $\sum(u, v) \in E\ (x(u, v))^2 = 1$.

The three variables $x(u, v), y(u, v)$, and $z(u, v)$ detain the uncertainty related to this path, and this formulation guarantees that the value of $d(u, v)$ represents the SP length from node u to v. The goal function aims to reduce the overall length of every edge in the path. The constraints guarantee that the neutrosophic Pythagorean equation is satisfied by the membership, non-membership, and indeterminacy degrees, and that the membership degrees for all outgoing edges from each vertex sum up to one.

4.2 Theorem:

If A^* is optimal under an Interval-valued Neutrosophic Pythagorean environment, then h~j is permissible with an Interval-valued Neutrosophic Pythagorean cost

Proof

To prove this statement by using the contradiction method, we assume that A^* is optimal under an Interval-valued Neutrosophic Pythagorean environment, but $h \sim j$ is not admissible with an

Interval-valued Neutrosophic Pythagorean cost. We will then show that this assumption leads to a contradiction, which proves that the original statement is true.

Let's denote the optimal solution as A^*, and its cost as $Cost(A^*)$.

Now, we assume that $h\sim j$ is not admissible with an Interval-valued Neutrosophic Pythagorean cost. This means that there exists another solution, B, such that $Cost(B) < Cost(h\sim j)$.

Since A^* is optimal, we have:

$$Cost(A^*) \leq Cost(B)$$

But since $h\sim j$ is not admissible with an Interval-valued Neutrosophic Pythagorean cost, we also have:

$$Cost(h\sim j) \leq Cost(B)$$

Combining these two inequalities, we have:

$$Cost(A^*) \leq Cost(h\sim j)$$

However, since A^* is optimal, it should have the lowest possible cost. Therefore, we can write:

$$Cost(A^*) \leq Cost(h\sim j) \leq Cost(A^*)$$

This implies that $Cost(A^*) = Cost(h\sim j)$.

But this contradicts our assumption that $h\sim j$ is not admissible with an Interval-valued Neutrosophic Pythagorean cost. If $h\sim j$ is not admissible, it means that there exists another solution B with a lower cost. But from our contradiction, we know that $Cost(A^*) = Cost(h\sim j)$.

Thus, our assumption that $h\sim j$ is not admissible leads to a contradiction. Therefore, we can conclude that if A^* is optimal under an Interval-valued Neutrosophic Pythagorean environment, and then $h\sim j$ is admissible with an Interval-valued Neutrosophic Pythagorean cost.

4.3 Calculation of heuristic costs

The heuristic value is a cost calculates approximately from every single node to the destination node. The approximate cost can be determined in several of manner, such as Hamming distance, Manhattan distance, Euler distance, and others. A reversal search strategy based on breadth first was used to evaluate the heuristic values in this case.

4.3.1 The Heuristic Cost Algorithm

Step 1: Initiate with the targeted node and set the node value $\hat{h}_j$ to 0, where $j = n$. The computation is carried out in the opposite order.

Step 2: Add the real cost values from the current node to the values from the possible precursor node. Using the score equation, compare the values, Then select the value that is the smallest as a heuristic value and label it $\hat{h}_j$. .

Step 3: Continue with the procedure until you come to the last node.

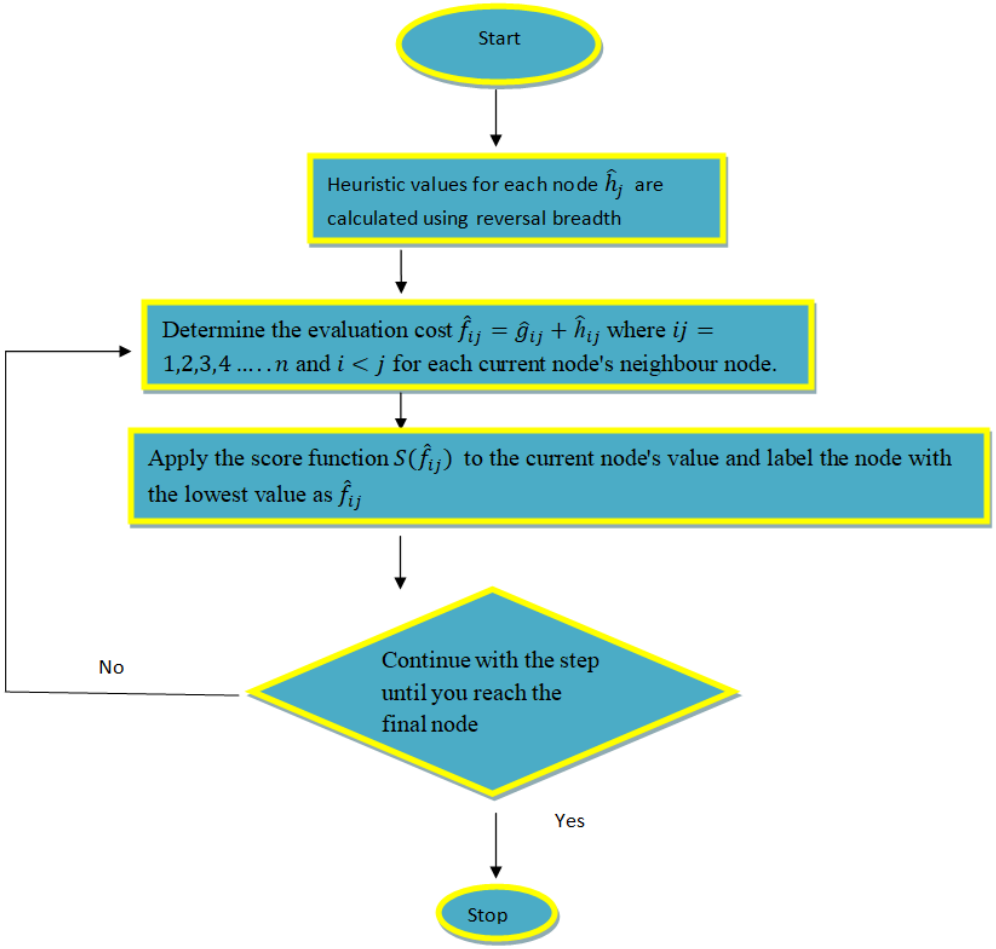

Fig-1: The idea for the algorithm is represented by a flow chart diagram.

5. Proposed algorithm

This section presents a method for determining the most efficient route between initial to final node using a heuristic methodology. This proposed algorithm is used for classification.

Step-1: Select the node that originated to be the starting node and label the initial node as node 1.

Step-2: Determine the estimate cost $\hat{f}_{ij} = \hat{g}_{ij} + \hat{h}_{ij}$ where $ij = 1,2,3,4 \ldots\ldots n$ and $i < j$ for each current node's neighbor node.

Step-3: Utilize the score function $S(\hat{f}_{ij})$ to the existing node's value and then label the node according to the lowest value as $\hat{f}_{ij}$.

Step-4: Continue with the labeled nodes' successors $\hat{f}_{ij}$ and determine the assessment cost. Step 3 should be repeated to get the smallest amount value and connect the node.

Step -5: Continue the procedure until you arrive at node n, i.e. destination node.

Step- 6: The path with the least distance is calculated through the combination of each and every one of the nodes discovered in the preceding steps (Fig. 1).

6. Numerical Example:

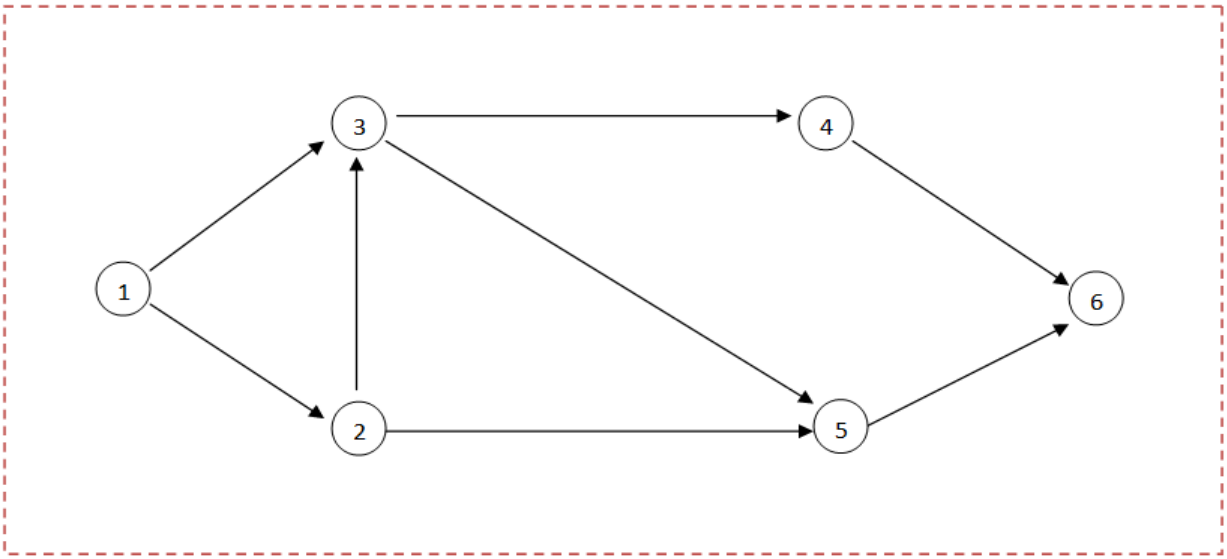

Fig-2: IVNP Network

Table-1: Arc Weights

Arc	Neutrosophic Pythagorean cost with interval values
1-2	<[0.4,0.6],[0.3,0.5],[0.3,0.4]>
1-3	<[0.4,0.5],[0.3,0.4],[0.3,0.5]>
2-3	<[0.5,0.6],[0.4,0.5],[0.3,0.4]>
2-5	<[0.5,0.6],[0.3,0.5],[0.3,0.4]>
3-4	<[0.4,0.6],[0.3,0.5],[0.2,0.3]>
3-5	<[0.3,0.5],[0.4,0.5],[0.5,0.6]>
4-6	<[0.3,0.4],[0.2,0.4],[0.3,0.5]>
5-6	<[0.3,0.4],[0.4,0.7],[0.5,0.7]>

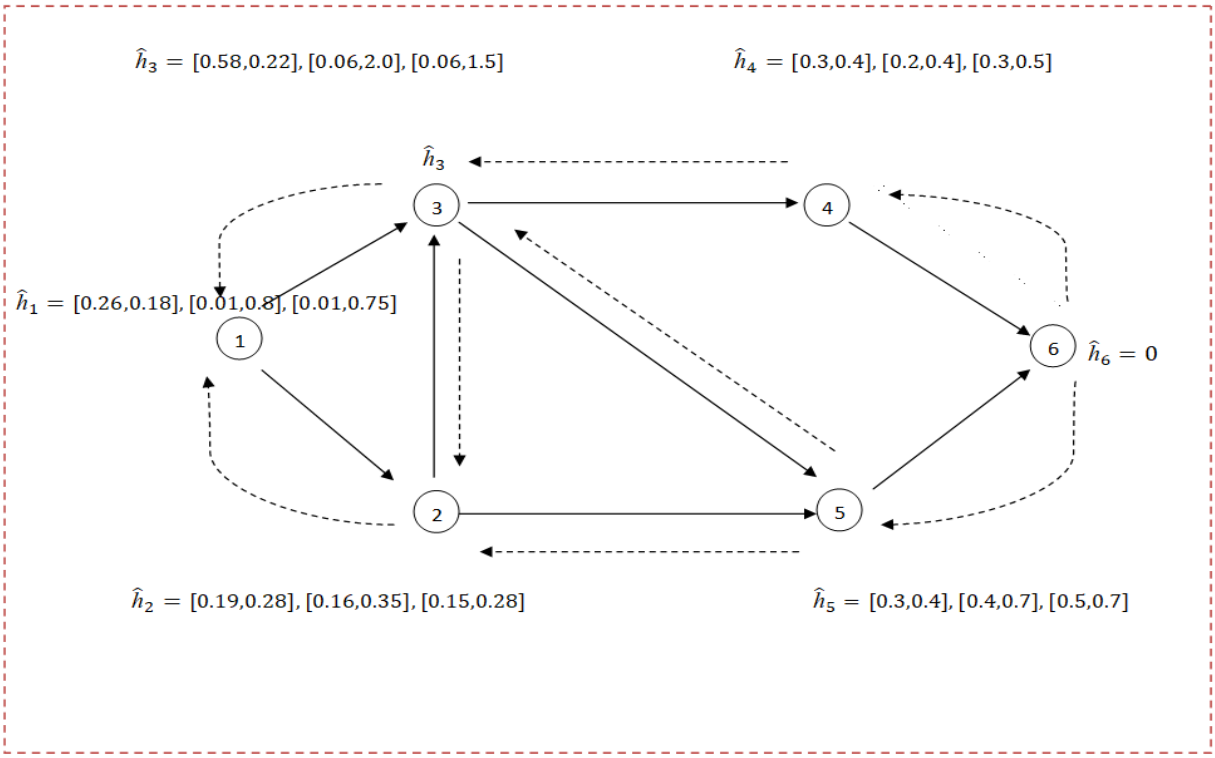

Fig-3: Heuristic Calculation of IVNP Network

$$\hat{f}_{12} = \hat{g}_{12} + \hat{h}_2$$

$$\hat{f}_{12} = ([0.4,0.6],[0.3,0.5],[0.3,0.4]) + ([0.19,0.28],[0.16,0.35],[0.15,0.28])$$

$$\hat{f}_{12} = ([0.52,0.71],[0.04,0.17],[0.04,0.11])$$

$$S(\hat{f}_{12}) = 0.34$$

$$\hat{f}_{13} = \hat{g}_{13} + \hat{h}_3$$

$$\hat{f}_{13} = ([0.4,0.5],[0.3,0.4],[0.3,0.5]) + ([0.58,0.22],[0.06,2],[0.06,1.5])$$

$$\hat{f}_{13} = ([0.26,0.18],[0.01,0.08],[0.01,0.75])$$

$$S(\hat{f}_{13}) = 0.28$$

From $S(\hat{f}_{12})$ & $S(\hat{f}_{13})$ minimum is $S(\hat{f}_{13})$ which value is 0.28. Hence label from $1\ to\ 3$

Step-3

Now we visit node-4 and Node-5 from successor's node $1\ to\ 3$, and then carry out step-2 according to the proposed.

$$\hat{f}_{34} = \hat{g}_{34} + \hat{h}_4$$

$$\hat{f}_{34} = ([0.4,0.6],[0.3,0.5],[0.2,0.3]) + ([0.3,0.4],[0.2,0.4],[0.3,0.5])$$

$$\hat{f}_{34} = [0.13,0.28],[0.06,2.0],[0.06,1.5]$$

$$S(\hat{f}_{34}) = 0.47$$

$$\hat{f}_{35} = \hat{g}_{35} + \hat{h}_5$$

$$\hat{f}_{35} = ([0.3,0.5],[0.4,0.5],[0.5,0.6]) + ([0.3,0.4],[0.4,0.7],[0.5,0.7])$$

$$\hat{f}_{35} = [0.09,0.21],[0.16,0.35],[0.25,0.36],$$

$$S(\hat{f}_{34}) = 0.43$$

From $S(\hat{f}_{34})$ & $S(\hat{f}_{35})$ minimum is $S(\hat{f}_{35})$ which value is 0.43. Hence label from $1 \rightarrow 3 \rightarrow 5$

Step 4: Only node 6 serves as the successor of node 5, so continue with step-2 of the algorithm to determine its estimated cost.

$$\hat{f}_{56} = \hat{g}_{56} + \hat{h}_6$$

$$\hat{f}_{56} = ([0.3,0.4],[0.4,0.7],[0.5,0.7]) + 0$$

$$\hat{f}_{56} = ([0.3,0.4],[0.4,0.7],[0.5,0.7])$$

$$S(\hat{f}_{56}) = 0.45$$

The shortest path can be identified by adding all of the nodes in the above steps $\hat{f}_{56}, 1 \rightarrow 3 \rightarrow 5 \rightarrow 6$ with the minimum Cost is 0.45

7. Comparison study:

This section involves the evaluation of our algorithm using alternative methodologies. [37] and [38].

Optimal route with varying network configurations	**Path(route)**	**Shortest path cost**
Enayattabar M. et al. [37]	$1 \rightarrow 2 \rightarrow 5 \rightarrow 6$	0.95
Jan N. et al. [38]	$1 \rightarrow 2 \rightarrow 3 \rightarrow 5 \rightarrow 6$	----
Our proposed	$1 \rightarrow 3 \rightarrow 5 \rightarrow 6$	0.45

Table-2: Shortest path with different network

8. Conclusion:

This research paper examines the benefits of using the interval-valued Neutrosophic Pythagorean Number to determine the Shortest Path. This method integrates uncertainty by utilizing the interval-valued Neutrosophic Pythagorean Number edge weight in an interval-valued Neutrosophic

Pythagorean environment. The outcome demonstrates the usefulness and efficiency of the algorithm in calculating the shortest path under an IVNP environment. Compared to the traditional A* algorithm, our approach provides more accurate and robust solutions, considering the uncertainty and imprecision in the graph. The suggested approach can be used in real life applications in logistics management, communication systems, and many other network optimization issues that are expressed as shortest-path issues.

Conflicts of Interest:

The authors declare no conflicts of interest.

References:

1. Salam, A., Mohamed, M., Yong, R., & Ye, J. (2024). A Robust Decision-Making Model for Medical Supplies via Selecting Appropriate Unmanned Aerial Vehicle. Neutrosophic Systems with Applications, 18, 14-30.
2. Mohamed, M., Ayman, S., Yong, R., & Ye, J. (2024). Ranking Cloud Service Providers using SWARA-MARCOS in Type-2 Neutrosophic Number Set Environment. Neutrosophic Systems with Applications, 18, 46-59.
3. Christianto, V., & Smarandache, F. (2024). Unveiling Quantum Communication: From Bell's Inequality to Neutrosophic Logic. Infinite Study.
4. Christianto, V., & Smarandache, F. (2024). The Convergence of Ikigai and Design Thinking: Crafting a Purposeful Framework. Infinite Study.
5. Mohamed, M., Metwaly, A. A., Ibrahim, M., Smarandache, F., & Voskoglou, M. (2024). Partnership of Lean Six Sigma and Digital Twin under Type 2 Neutrosophic Mystery Toward Virtual Manufacturing Environment: Real Scenario Application. Sustainable Machine Intelligence Journal, 8, 6-99.
6. Raut, P. K., Behera, S. P., Broumi, S., Dey, A., Talea, M., & Baral, A. (2024). Evaluation of the shortest path based on the Traveling Salesman problem with a genetic algorithm in a neutrosophic environment. Neutrosophic Sets and Systems, 68, 187-197.
7. Raut, P. K., Behera, S. P., Broumi, S., & Baral, A. (2024). Evaluation of Shortest path on multi stage graph problem using Dynamic approach under neutrosophic environment. Neutrosophic Sets and Systems, 64, 113-131.
8. Raut, P. K., & Behera, S. P. (2024). Evaluation of shortest path of network by using an intuitionistic pentagonal fuzzy number with interval values. International Journal of Reasoning-based Intelligent Systems, 16(2), 154-159.
9. Raut, P. K., Behera, S. P., Broumi, S., & Mishra, D. (2023). Calculation of Fuzzy shortest path problem using Multi-valued Neutrosophic number under fuzzy environment. Neutrosophic Sets and Systems, 57, 356-369.
10. Raut, P. K., Behera, S. P., Broumi, S., & Mishra, D. (2023). Calculation of shortest path on Fermatean Neutrosophic Networks. Neutrosophic Sets and Systems, 57(1), 22.
11. Ahuja, R. K., Mehlhorn, K., Orlin, J., & Tarjan, R. E. (1990). Faster algorithms for the shortest path problem. Journal of the ACM (JACM), 37(2), 213-223.

12. Yang, C. D., Lee, D. T., & Wong, C. (1992). On bends and lengths of rectilinear paths: a graph-theoretic approach. International Journal of Computational Geometry & Applications, 2(01), 61-74.
13. Ibarra, O. H., & Zheng, Q. (1993, April). On the shortest path problem for permutation graphs. In [1993] Proceedings Seventh International Parallel Processing Symposium (pp. 198-204). IEEE.
14. Arsham, H. (1998). Stability analysis for the shortest path problems. Congressus Numerantium, 171-210.
15. Eilam-Tzoreff, T. (1998). The disjoint shortest paths problem. Discrete applied mathematics, 85(2), 113-138.
16. Broumi, S., & Smarandache, F. (2013). Intuitionistic neutrosophic soft set. Infinite Study, 130-140.
17. Zhang, J., & Lin, Y. (2003). Computation of the reverse shortest-path problem. Journal of Global Optimization, 25(3), 243-261.
18. Kandasamy, W. V., & Smarandache, F. (2004). Basic neutrosophic algebraic structures and their application to fuzzy and neutrosophic models (Vol. 4). Infinite Study.
19. Roditty, L., & Zwick, U. (2004). On dynamic shortest paths problems. In Algorithms–ESA 2004: 12th Annual European Symposium, Bergen, Norway, September 14-17, 2004. Proceedings 12 (pp. 580-591). Springer Berlin Heidelberg.
20. Irnich, S., & Desaulniers, G. (2005). Shortest path problems with resource constraints. In Column generation (pp. 33-65). Boston, MA: Springer US.
21. Buckley, J. J., Jowers, L. J., Buckley, J. J., & Jowers, L. J. (2008). Fuzzy shortest path problem. Monte Carlo Methods in Fuzzy Optimization, 191-193.
22. Broumi, S., Raut, P. K., & Behera, S. P. (2023). Solving shortest path problems using an ant colony algorithm with triangular neutrosophic arc weights. International Journal of Neutrosophic Science, 20(4), 128-28.
23. Turner, L. (2011). Variants of the shortest path problem. Algorithmic Operations Research, 6(2), 91-104.
24. Deng, Y., Chen, Y., Zhang, Y., & Mahadevan, S. (2012). Fuzzy Dijkstra algorithm for shortest path problem under uncertain environment. Applied Soft Computing, 12(3), 1231-1237.
25. Broumi, S., Talea, M., Bakali, A., & Smarandache, F. (2016). Single valued neutrosophic graphs. Journal of New theory, (10), 86-101.
26. Garg, H. (2016). An improved score function for ranking neutrosophic sets and its application to decision-making process. International Journal for Uncertainty Quantification, 6(5).
27. Şahin, R., & Liu, P. (2016). Maximizing deviation method for neutrosophic multiple attribute decision making with incomplete weight information. Neural Computing and Applications, 27, 2017-2029.
28. Broumi, S., Bakali, A., Talea, M., & Smarandache, F. (2019). Computation of shortest path problem in a network with sv-triangular neutrosophic numbers. Uluslararası Yönetim Bilişim Sistemleri ve Bilgisayar Bilimleri Dergisi, 3(2), 41-51.
29. Broumi, S., Bakali, A., Talea, M., Smarandache, F., & Verma, R. (2017). Computing minimum spanning tree in interval valued bipolar neutrosophic environment. International Journal of Modeling and Optimization, 7(5), 300-304.

30. Hu, H., & Sotirov, R. (2020). On solving the quadratic shortest path problem. INFORMS Journal on Computing, 32(2), 219-233.

31. Dragan, F. F., & Leitert, A. (2017). On the minimum eccentricity shortest path problem. Theoretical Computer Science, 694, 66-78.

32. Zhang, Y., Song, S., Shen, Z. J. M., & Wu, C. (2017). Robust shortest path problem with distributional uncertainty. IEEE transactions on intelligent transportation systems, 19(4), 1080-1090.

33. Smarandache, F. (2005). A generalization of the intuitionistic fuzzy set. International journal of pure and applied mathematics, 24(3), 287-297.

34. Stephen, S., & Helen, M. (2020). Interval valued neutrosophic linear programming with trapezoidal numbers. Infinite Study.

35. Radha, R., Mary, A. S. A., Prema, R., & Broumi, S. (2021). Neutrosophic pythagorean sets with dependent neutrosophic pythagorean components and its improved correlation coefficients. Neutrosophic Sets and Systems, 46, 77-86.

36. Stephen, S., & Helen, M. (2021). Interval-valued Neutrosophic Pythagorean Sets and their Application Decision Making using IVNP-TOPSIS. International Journal of Innovative Research in Science. Engineering and Technology, 10(1), 14571-14578.

37. Enayattabar, M., Ebrahimnejad, A., & Motameni, H. (2019). Dijkstra algorithm for shortest path problem under interval-valued Pythagorean fuzzy environment. Complex & Intelligent Systems, 5(2), 93-100.

38. Jan, N., Aslam, M., Ullah, K., Mahmood, T., & Wang, J. (2019). An approach towards decision making and shortest path problems using the concepts of interval-valued Pythagorean fuzzy information. International Journal of Intelligent Systems, 34(10), 2403-2428.

Received: July 18, 2024. Accepted: Oct 26, 2024

Neutrosophic Sets and Systems, Vol. 76, 2025
University of New Mexico

Multiple-Attribute Decision Making Based on Novel Single Valued Neutrosophic Aczel-Alsina Power Muirhead Mean Operators

Peide Liu[1,2,*], Qaisar Khan[3,*], Rashid Ali[4], Hidayat ULLAH[4] , Rashid Jan[5,6]

[11]School of Business Administration, Shandong Women's University, Jinan 250300, Shandong, China

[2]Shandong Key Laboratory of New Smart Media, Jinan Shandong 250014, China Email: peide.liu@gmail.com

[3]Department of Mathematics and Statistics, University of Haripur KPK, Pakistan, Email:qaisar.khan@uoh.edu.pk

[4]Department of mathematics, University of Malakand KPK Pakistan, rashidalikhanbaidara@gmail.com, hidayatullak@yahoo.com

[5]Institute of Energy Infrastructure (IEI), Department of Civil Engineering, College of Engineering, Universiti Tenaga Nasional (UNITEN), Putrajaya Campus, Jalan IKRAM-UNITEN, 43000 Kajang, Selangor, Malaysia

[6]Mathematics Research Center, Near East University TRNC, Mersin 10, Nicosia 99138, Turkey, Email:rashid.jan@uniten.edu.my

Corresponding author: Peide Liu, Qaisar Khan (e-mail: peide.liu@gmail.com, qaisar.khan@uoh.edu.pk).

Abstract: Neutrosophic multiple-attribute decision making (MADM) is one of the major study areas in ambiguous and inconsistent decision-making problems. The single-valued neutrosophic number ($S^{v}NN$), which is an expansion of the fuzzy number, intuitionistic fuzzy number, can handle difficulties involving a huge quantity of erroneous, partial, and inconsistent information. To address the multi-criteria decision-making problems, novel aggregation operators (AGOs) are proposed in this article considering the benefits of the $S^{v}NN$. The new AGOs consider the interrelationship involving any number of input data and can remove the effect of unreliable data. This article adds the Aczel-Alsina (AA) operations to increase the flexibility of the new AGOs. This study proposes the single-valued neutrosophic Aczel-Alsina power Muirhead mean ($S^{v}NAAPMM$) operator, single-valued neutrosophic Aczel-Alsina power dual Muirhead mean ($S^{v}NAAPDMM$) operator which combines the Aczel-Asina operational rules with the power average/geometric operator and the Muirhead/ dual Muirhead mean operators. Some core characteristics and special cases with respect to the parameters are explored and it is found that various existing AGOs are special cases of the newly initiated AGOs. Further, weighted form these AGOs are introduced. Then, we set up the MADM technique using the two AGOs that are suggested to solve MADM problems. We then give a numerical example about strategic supplier's selection and compare it to other related MADM techniques already in use in the $S^{v}NN$ information to demonstrate the effectiveness and appropriateness of the anticipated technique.

Keywords Single valued neutrosophic sets; Muirhead/dual Muirhead mean operators, power average/geometric operators, MADM.

1. Introduction

Multiple-attribute decision making (MADM) problems are more common than ever in today's sophisticated as well as complicated technological environments [1, 2]. For instance, an enterprise with confined production capacity will need to concurrently address the problem of appropriate product price and lot-size determinations [3]. The creation of energy from renewable sources and the restrictions on carbon emissions must be associated into a single electric network to create a hybrid renewable energy system [4]. Material handling concerns and pertinent expenditures should be considered simultaneously in a dynamic facility layout challenge [5].

Zadeh's theory is a well-known and extended version of the crisp set theory because of its range. In crisp set theory, we only have two options, such as zero or one, but in the case of Fuzzy set (FS) theory, we have a lot of opinions when evaluating any kind of problem. Zadeh developed the main idea of the FS to expand the scope of the classical set theory [6]. FSs, however, are unable to handle some situations in which it is tough to describe the membership degree operating a single distinctive number. Atanassov [7] presented intuitionistic FSs (IFSs), an expansion of Zadeh's FSs, to address the problem of non-membership degrees not being well understood. IFSs have so far been frequently used to solve MADM problems [8-14]. Like Zadeh FSs, IFSs are unable to describe ambiguous and inconsistent information, thus Smarandache [15, 16] developed the neutrosophic set (NS) from a philosophical perspective to do so. In a NS, its membership, indeterminacy, and falsity degrees are independently represented and are real standard or nonstandard subclasses of $]0^-,1^+[$. Consequently, the nonstandard interval $]0^-,1^+[$ might make practical applications more challenging. Thus, the idea of a single-valued neutrosophic set (S^{V}NS) [17] is created on the real standard interval $[0,1]$. After the introduction many scholars applied S^{V}NS in various fields [18-24].

The previous several years have seen a significant increase in researcher knowledge of information aggregation operators [25–29], who are now a highly important study area for MADM problems. The conventional AGOs suggested by Xu, Xu, and Yager [30, 31] are limited to aggregating a collection of real numbers into a single factual number. Now, many authors have expanded on these traditional AGOs. For instance, Peng et al. [32] proposed the S^{V}N power shapely Choquet weighted averaging operator for MADM and Liu et al. [33] created various prioritized weighted AGOs for S^{V}NNs and employed them to MADM. Additionally, certain decision-making techniques were created for MADM problems. For instance, Garg [34] created a MADM model based on TOPSIS and divergence measure to deal with S^{V}N information. Mishra et al [35] initiated an integrated decision support system for evaluating low carbon tourist strategies utilizing single-valued MEREC-MULTIMOORA. Rong et al. [36] pharmaceutical enterprise evaluation using a hybrid group decision method based on MARCOS and regret theory in a S^{V}N environment. These techniques can only provide a ranking result, but AGOs can also provide the comprehensive value of each option by averaging the values of each characteristic.

Various aggregation operators obviously serve various purposes, but a few of them, like Yager's suggested power average (PA) operator [37], may mitigate the effect of some challenging data provided by the DMs. The PA operator may perform by selecting a weight vector depending on the

degree of support between the input arguments and aggregating the input data. Now, other studies have expanded the PA operator into further environments. For SVNNs, Yang and Li [38] presented PA operators, which they then applied to MADM. The interrelationship between the aggregating parameters can therefore be included in some AGOs, such as the Bonferroni mean (BM) operators created by Bonferroni [39], the Heronian mean (HM) operator familiarized by Sykora [40], the Muirhead Mean (MM) operator [41], and the Maclaurin symmetric mean (MSM) [42] operators. To cope with ambiguous information, numerous authors have additionally expanded these AGOs to various fuzzy structures [43–50]. Some AGOs have been established by using various T-norms (TNs) and T-conorms (TCNs), such as algebraic, Einstein, and Hamacher, to aggregate SVNNs. Typically, the algebraic, Einstein, Hamacher, Frank, and Dombi TNs and TCNs are generalized to create the Archimedean TN and TCN. Recently, Senapati [51] initiated various core operational rules for SVNNs based on Aczel-Alsina TN and TCN. Furthermore, they have developed some AA weighted aggregation operators and apply them to solve MADM problems under SVN environment. Motivated from the above discussion, it is clear that no one has yet tried to deal with SVN data by combining Aczel-Alsina operational laws with the PA operator and the MM operator. The hybrid structure of these AOs can have the advantages of Aczel-Alsina operational laws, the PA operator, and the MM operator at the same time. That is, these types of AOs have Aczel-Alsina parameter, the capacity to remove the effect of uncomfortable data and can consider the interrelation amongst all input data. As a result, we suggest:

- The Aczel-Alsina operational laws are merged with the PA operators, MM and dual MM operators to launch a hybrid AOs SVNAAPMM and SVNAAPDMM operators and are much more flexible and superior to the prior AOs in terms of a general parameter.
- Unfortunately, there exist several MADM problems where the attributes are interconnected. Consequently, many current AOs are limited in their ability to mitigate these instances when the attributes take the form of real numbers or other fuzzy structures.
- As of right now, there are no AOs in place to handle MADM problems arising from SVN data. These problems can be made more flexible in the decision-making process by having general parameters, considering interrelationships among any number of input arguments, and being able to remove the negative effects of awkward data. In response to this constraint, we integrated Aczel-Alsina operational laws with the PA operator, MM and DMM operators to handle MADM problems employing SVN information.

Due to significant effects from previous research, the following are the goals and services this initiative is focusing on:

- To combine the Muirhead, mean (MM) operator, PA operator with Aczel-Alsina operational laws for SVNNs, to initiate the theory of the SVNAAPMM operator.
- To use the theory of dual Muirhead, mean (DMM) operators, PG operator with Aczel-Alsina operational laws for SVNNs, to initiate the theory of the SVNPDHM operator.
- To investigate the basic properties and various special cases with respect to the parameters of the derived theory.
- To demonstrate the MADM technique based on the presented operators to deal with MADM problems under SVN information.

- To compare the derived operator with many existing operators and discuss their impact and benefits.

This article is constructed in the shape: In Section 2, we discussed the SVNSs, Muirhead Mean operators, and dual Muirhead Mean operator and AA operational for SVNNs. In Section 3, a novel concept of the SVNPMM operator, SVNPDMM operator, and their major properties. In Section 4, the weighted form of the initiated AGOs are introduced. In section 5, the MADM technique is introduced based on the presented AGOs. In section 6, a numerical example about the selection of strategic suppliers is given to show the efficacy and practicality of the proposed MADM approach. At the end comparison with some existing MADM approaches and conclusion are given.

2. Preliminaries

In this portion, some core concepts about SVNSs, score, accuracy and certainty functions, distances measure, PA operator, MM operators are given.

2.1. The single valued neutrosophic set and their operational laws

A philosophical perspective was used to present the neutrosophic sets (NSs). It was evidently challenging to apply in the actual applications. From a scientific or technical perspective, Wang et al. [17] further proposed the single-valued neutrosophic sets (SVNSs).

Definition 1 [17]. Let U be a universal set, with F'' indicating a generic element in the fix set U. Then, the SVNSs $\overline{O}$ in U are described as follows:

$$\dot{\Theta} = \left\{ \left\langle F'', \overline{\overline{TR}}_{\dot{\Theta}}(F''), \overline{\overline{IN}}_{\dot{\Theta}}(F''), \overline{\overline{FL}}_{\dot{\Theta}}(F'') \middle| F'' \in U \right\rangle \right\}. \tag{1}$$

Where the truth-membership grade $\overline{\overline{TR}}_{\dot{\Theta}}(F'')$, indeterminacy-grade $\overline{\overline{IN}}_{\dot{\Theta}}(F'')$ non-membership-grade $\overline{\overline{FL}}_{\dot{\Theta}}(F'')$ and are single values in the real standard closed interval [0,1]. That is, $\overline{\overline{TR}}_{\dot{\Theta}}(F''): U \to [0,1], \overline{\overline{IN}}_{\dot{\Theta}}(F''): U \to [0,1]$ and $\overline{\overline{FL}}_{\dot{\Theta}}(F''): U \to [0,1]$ with the condition that sum of the three grades will be less or equal to 3.

For a SVNS $\dot{\Theta} = \left\{ \left\langle F'', \overline{\overline{TR}}_{\dot{\Theta}}(F''), \overline{\overline{IN}}_{\dot{\Theta}}(F''), \overline{\overline{FL}}_{\dot{\Theta}}(F'') \middle| F'' \in U \right\rangle \right\}$, the ordered triplet $\left\langle \Phi'', \overline{\overline{TR}}_{\dot{\Theta}}(\Phi''), \overline{\overline{IN}}_{\dot{\Theta}}(\Phi''), \overline{\overline{FL}}_{\dot{\Theta}}(\Phi'') \right\rangle$ is said to be SVNN and is denoted by $\dot{\Xi}$. That is, $\dot{\Xi} = \left\langle \overline{\overline{TR}}, \overline{\overline{IN}}, \overline{\overline{FL}} \right\rangle$, where $\overline{\overline{TR}}, \overline{\overline{IN}}, \overline{\overline{FL}} \in [0,1]$ and $0 \le \overline{\overline{TR}} + \overline{\overline{IN}} + \overline{\overline{FL}} \le 3$.

Definition 2 [50]. The score function $\overline{\overline{SOE}}(\dot{\Xi})$, accuracy function $\overline{\overline{AR}}(\dot{\Xi})$ and certainty function $\overline{\overline{CR}}(\dot{\Xi})$ of a SVNN $\dot{\Xi} = \left\langle \overline{\overline{TR}}, \overline{\overline{IN}}, \overline{\overline{FL}} \right\rangle$ can be emitted as

$$\begin{aligned} &\overline{\overline{SOE}}(\dot{\Xi}) = \frac{2 + \overline{\overline{TR}}_{\dot{\Xi}} - \overline{\overline{IN}}_{\dot{\Xi}} - \overline{\overline{FL}}_{\dot{\Xi}}}{3}, \ \textit{Where } \overline{\overline{SOE}}(\dot{\Xi}) \in [0,1]; \\ &\overline{\overline{AR}}(\dot{\Xi}) = \overline{\overline{TR}}_{\dot{\Xi}} - \overline{\overline{FL}}_{\dot{\Xi}}, \ \textit{Where } \overline{\overline{AR}}(\dot{\Xi}) \in [-1,1]; \\ &\overline{\overline{CR}}(\dot{\Xi}) = \overline{\overline{TR}}_{\dot{\Xi}} \ \textit{Where } \overline{\overline{CR}}(\dot{\Xi}) \in [0,1] \end{aligned} \tag{2}$$

For rating the SVNNs, Smarandache [50] devised a comparative approach based on the score and exactness function, which is expressed as:

Definition 3 [50]. Suppose that the two SᵛNNs are $\tilde{\alpha}_1 = \langle \overline{TR}_1, \overline{IN}_1, \overline{FL}_1 \rangle$ and $\tilde{\alpha}_2 = \langle \overline{TR}_2, \overline{IN}_2, \overline{FL}_2 \rangle$. Let $\overline{\overline{SOE}}(\tilde{\alpha}_1)$, $\overline{\overline{SOE}}(\tilde{\alpha}_2)$ be the score functions and $\overline{\overline{AR}}(\tilde{\alpha}_1), \overline{\overline{AR}}(\tilde{\alpha}_2)$ be the accuracy functions of $\tilde{\alpha}_i (i = 1,2)$ respectively. If

(i) $\overline{\overline{SOE}}(\tilde{\alpha}_1) \succ \overline{\overline{SOE}}(\tilde{\alpha}_2)$, then $\tilde{\alpha}_1 \succ \tilde{\alpha}_2$;

(ii) $\overline{\overline{SOE}}(\tilde{\alpha}_1) \prec \overline{\overline{SOE}}(\tilde{\alpha}_2)$, then $\tilde{\alpha}_1 \prec \tilde{\alpha}_2$;

(iii) $\overline{\overline{SOE}}(\tilde{\alpha}_1) = \overline{\overline{SOE}}(\tilde{\alpha}_2)$, then;

(i) $\overline{\overline{AR}}(\tilde{\alpha}_1) \succ \overline{\overline{AR}}(\tilde{\alpha}_2)$, then $\tilde{\alpha}_1 \succ \tilde{\alpha}_2$;

(ii) $\overline{\overline{AR}}(\tilde{\alpha}_1) \prec \overline{\overline{AR}}(\tilde{\alpha}_2)$, then $\tilde{\alpha}_1 \prec \tilde{\alpha}_2$;

(iii) $\overline{\overline{AR}}(\tilde{\alpha}_1) = \overline{\overline{AR}}(\tilde{\alpha}_2)$, then;

(i) $\overline{\overline{CR}}(\tilde{\alpha}_1) \succ \overline{\overline{CR}}(\tilde{\alpha}_2)$, then $\tilde{\alpha}_1 \succ \tilde{\alpha}_2$;

(ii) $\overline{\overline{CR}}(\tilde{\alpha}_1) \prec \overline{\overline{CR}}(\tilde{\alpha}_2)$, then $\tilde{\alpha}_1 \prec \tilde{\alpha}_2$;

(iii) $\overline{\overline{CR}}(\tilde{\alpha}_1) = \overline{\overline{CR}}(\tilde{\alpha}_2)$, then $\tilde{\alpha}_1 = \tilde{\alpha}_2$.

Definition 4 [51]. Let $\tilde{\alpha} = \langle \overline{TR}, \overline{IN}, \overline{FL} \rangle, \tilde{\alpha}_1 = \langle \overline{TR}_1, \overline{IN}_1, \overline{FL}_1 \rangle$ and $\tilde{\alpha}_2 = \langle \overline{TR}_2, \overline{IN}_2, \overline{FL}_2 \rangle$ be the three SᵛNNs and $K \prec 0$. Then the AA operational laws for SᵛNNs are explained as follows:

$$(1)\ \tilde{\alpha}_1 \oplus \tilde{\alpha}_2 = \left\langle 1 - e^{-\left(\left(-\ln\left(1-\overline{TR}_1\right)\right)^{\phi} + \left(-\ln\left(1-\overline{TR}_2\right)\right)^{\phi}\right)^{\frac{1}{\phi}}}, e^{-\left(\left(-\ln \overline{IN}_1\right)^{\phi} + \left(-\ln \overline{IN}_2\right)^{\phi}\right)^{\frac{1}{\phi}}}, e^{-\left(\left(-\ln \overline{FL}_1\right)^{\phi} + \left(-\ln \overline{FL}_2\right)^{\phi}\right)^{\frac{1}{\phi}}} \right\rangle; \quad (3)$$

$$(2)\ \tilde{\alpha}_1 \otimes \tilde{\alpha}_2 = \left\langle e^{-\left(\left(-\ln \overline{TR}_1\right)^{\phi} + \left(-\ln \overline{TR}_2\right)^{\phi}\right)^{\frac{1}{\phi}}}, 1 - e^{-\left(\left(-\ln\left(1-\overline{IN}_1\right)\right)^{\phi} + \left(-\ln\left(1-\overline{IN}_2\right)\right)^{\phi}\right)^{\frac{1}{\phi}}}, 1 - e^{-\left(\left(-\ln\left(1-\overline{FL}_1\right)\right)^{\phi} + \left(-\ln\left(1-\overline{FL}_2\right)\right)^{\phi}\right)^{\frac{1}{\phi}}} \right\rangle; \quad (4)$$

$$(3)\ K\tilde{\alpha} = \left\langle 1 - e^{-\left(K\left(-\ln\left(1-\overline{TR}\right)\right)^{\phi}\right)^{\frac{1}{\phi}}}, e^{-\left(K\left(-\ln \overline{IN}\right)^{\phi}\right)^{\frac{1}{\phi}}}, e^{-\left(K\left(-\ln \overline{FL}\right)^{\phi}\right)^{\frac{1}{\phi}}} \right\rangle; \quad (5)$$

$$(4)\ \tilde{\alpha}^{K} = \left\langle e^{-\left(K\left(-\ln \overline{TR}\right)^{\phi}\right)^{\frac{1}{\phi}}}, 1 - e^{-\left(K\left(-\ln\left(1-\overline{IN}\right)\right)^{\phi}\right)^{\frac{1}{\phi}}}, 1 - e^{-\left(K\left(-\ln\left(1-\overline{FL}\right)\right)^{\phi}\right)^{\frac{1}{\phi}}} \right\rangle. \quad (6)$$

Definition 5 [20]. Let $\tilde{\alpha}_1 = \langle \overline{TR}_1, \overline{IN}_1, \overline{FL}_1 \rangle$ and $\tilde{\alpha}_2 = \langle \overline{TR}_2, \overline{IN}_2, \overline{FL}_2 \rangle$ be the three SᵛNNs. Then, the hamming distance measure among $\tilde{\alpha}_1$ and $\tilde{\alpha}_2$ is demarcated as:

$$D\left(\tilde{\alpha}_1, \tilde{\alpha}_2\right) = \frac{\left|\overline{TR}_1 - \overline{TR}_2\right| + \left|\overline{IN}_1 - \overline{IN}_2\right| + \left|\overline{FL}_1 - \overline{FL}_2\right|}{3}. \quad (7)$$

2.2. PA operator

For aggregation, the PA [37] operator is another important AO that may be used to reduce the negative effects of uncomfortable data on the outcomes of the final ranking process. It is defined as:

Definition 6 [37]. Let $\overline{\overline{\Omega}}_l\,(l=1,2,...,\mathrm{g})$ be a group of positive crisp numbers. Then, the PA operator is quantified as

$$PA\left(\overline{\overline{\Omega}}_1,\overline{\overline{\Omega}}_2,.....,\overline{\overline{\Omega}}_g\right)=\frac{\bigoplus_{l=1}^{g}\left(1+T\left(\overline{\overline{\Omega}}_l\right)\right)\overline{\overline{\Omega}}_l}{\bigoplus_{l=1}^{g}\left(1+T\left(\overline{\overline{\Omega}}_l\right)\right)};\tag{8}$$

where $T\left(\overline{\overline{\Omega}}_l\right)=\bigoplus_{m=1,l\neq m}^{g} Sprt\left(\overline{\overline{\Omega}}_l,\overline{\overline{\Omega}}_m\right)$, $Sprt\left(\overline{\overline{\Omega}}_l,\overline{\overline{\Omega}}_m\right)$ indicates the support for $\overline{\overline{\Omega}}_l$ from $\overline{\overline{\Omega}}_m$ executing the axioms:

1) $0\le Sprt\left(\overline{\overline{\Omega}}_l,\overline{\overline{\Omega}}_m\right)\le 1$, 2) $Sprt\left(\overline{\overline{\Omega}}_l,\overline{\overline{\Omega}}_m\right)=Sprt\left(\overline{\overline{\Omega}}_m,\overline{\overline{\Omega}}_l\right)$ and

3) $Sprt\left(\overline{\overline{\Omega}}_j,\overline{\overline{\Omega}}_h\right)\le Sprt\left(\overline{\overline{\Omega}}_l,\overline{\overline{\Omega}}_m\right)$, if $\left|\overline{\overline{\Omega}}_l,\overline{\overline{\Omega}}_m\right|\ge\left|\overline{\overline{\Omega}}_j,\overline{\overline{\Omega}}_h\right|$.

2.3. Muirhead Mean operator.

For classical numbers, Muirhead [41] was the first to introduce the MM operator. The benefit of MM operator is that it considers the interrelationship of each aggregated argument is related to each other.

Definition 7 [41]. Let $J_{\mathrm{i}}\,(\mathrm{i}=1,2...,\phi)$ be a set of classical numbers and $\text{Œ}''=\left(\text{Œ}''_1,\text{Œ}''_2,...,\text{Œ}''_\phi\right)\in R^\phi$ be a vector of parameters. Then the MM operator is suggested as:

$$\mathrm{MM}^{\text{Œ}''}\left(J_1,J_2,...,J_\phi\right)=\left(\frac{1}{\phi!}\sum_{\xi\in \mathsf{A}_\phi}\prod_{\mathrm{i}=1}^{\phi}R_{\xi(\mathrm{i})}^{\text{Œ}''_{\mathrm{i}}}\right)^{\frac{1}{\sum_{\mathrm{i}=1}^{\phi}\text{Œ}''_{\mathrm{i}}}}.\tag{9}$$

Where A_ϕ is a set of permutation of $(1,2,...,\phi)$ and $\xi(\mathrm{i})$ is any arrangement of $(1,2,...,\phi)$.

3. The Single valued neutrosophic Aczel-Alsina Power Muirhead Mean Operator

In this part, the SVNAAPMM and SVNAAPDMM operators are suggested.

Definition 8. Let $\underline{\&}_{\mathrm{z}}=\left\langle\overline{\overline{TR}}_{\mathrm{z}},\overline{\overline{IN}}_{\mathrm{z}},\overline{\overline{FL}}_{\mathrm{z}}\right\rangle\,(\mathrm{z}=1,2,...,\mathrm{K})$ be series of SVNNs, and $\text{Œ}''=\left(\text{Œ}''_1,\text{Œ}''_2,...,\text{Œ}''_K\right)\in R^K$ be a set of parameters. Then, the SVNAAPMM operator is put forward as:

$$S^{V}NAAPMM^{\text{Œ}''}\left(\underline{\&}_1,\underline{\&}_2,...,\underline{\&}_K\right)=\left(\frac{1}{K!}\sum_{\zeta\in H_K}\prod_{z=1}^{K}\left(K\frac{\left(1+T\left(\underline{\&}_{\zeta(z)}\right)\right)}{\sum_{z=1}^{K}\left(1+T\left(\underline{\&}_z\right)\right)}\underline{\&}_{\zeta(z)}\right)^{\text{Œ}''_z}\right)^{\frac{1}{\sum_{z=1}^{K}\text{Œ}''_z}},\tag{10}$$

where,

$$T\left(\underline{\&}_j\right)=\sum_{z=1}^{K}Spt\left(\underline{\&}_{\mathrm{i}},\underline{\&}_z\right),\tag{11}$$

and

$$Spt\left(\underset{\sim}{\alpha}_i,\underset{\sim}{\alpha}_z\right)=1-D\left(\underset{\sim}{\alpha}_i,\underset{\sim}{\alpha}_z\right), \tag{12}$$

$\zeta(z)(z=1,2,...,K)$ epitomizes any arrangement of $(1,2,...,K)$. H_K signifies all possible combinations of $(1,2,...,K)$, and K is the balancing coefficient $D\left(\underset{\sim}{\alpha}_i,\underset{\sim}{\alpha}_z\right)$ denotes the Hamming distance among two SVNNs $\underset{\sim}{\alpha}_i$ and $\underset{\sim}{\alpha}_z$, and $Spt\left(\underset{\sim}{\alpha}_i,\underset{\sim}{\alpha}_z\right)$ is the support for $\underset{\sim}{\alpha}_i$ from $\underset{\sim}{\alpha}_z$ sustaining the axioms given in Definition 6.

To write Equation (10), in simplified form, let

$$H_{\underset{\sim}{\alpha}_z}=\frac{\left(1+T\left(\underset{\sim}{\alpha}_j\right)\right)}{\sum_{z=1}^{K}\left(1+T\left(\underset{\sim}{\alpha}_z\right)\right)}, \tag{13}$$

then, Equation (10) can be written in simplified form as,

$$SVNAAPMM^{\mathcal{E}''}\left(\underset{\sim}{\alpha}_1,\underset{\sim}{\alpha}_2,...,\underset{\sim}{\alpha}_K\right)=\left(\frac{1}{K!}\sum_{\zeta\in H_K}\prod_{z=1}^{K}\left(KH_{\underset{\sim}{\alpha}_{\zeta(z)}}\underset{\sim}{\alpha}_{\zeta(z)}\right)^{\mathcal{E}_z''}\right)^{\frac{1}{\sum_{z=1}^{K}\mathcal{E}_z''}}. \tag{14}$$

Where $\sum_{z=1}^{K}H_{\underset{\sim}{\alpha}_z}=1$ and $0\le H_{\underset{\sim}{\alpha}_z}\le 1$.

Corresponding to Definition 8, the resulting theorem can be obtained.

Theorem 1. Let $\underset{\sim}{\alpha}_z=\left\langle\overline{TR}_z,\overline{IN}_z,\overline{FL}_z\right\rangle(z=1,2,...,K)$ be a group of SVNNs, the aggregated value by the SVNAAPMM operator is still a SVNN and

$$SVNAAPMM^{\mathcal{E}''}\left(\underset{\sim}{\alpha}_1,\underset{\sim}{\alpha}_2,...,\underset{\sim}{\alpha}_z\right)=\left\langle\left(e^{-\left(\frac{1}{\sum_{z=1}^{K}\mathcal{E}_z''}\left(\frac{1}{K!}\left(\sum_{\zeta\in H_K}\left(\sum_{z=1}^{K}\left(\mathcal{E}_z''\left(-\ln\left(1-e^{-\left(KH_{\underset{\sim}{\alpha}_{\zeta(z)}}\left(-\ln\left(1-\overline{TR}_{\zeta(z)}\right)\right)^{\phi}\right)^{\frac{1}{\phi}}}\right)\right)^{\phi}\right)\right)^{\frac{1}{\phi}}\right)\right)\right)^{\phi}\right)^{\frac{1}{\phi}}}\right),\right.$$
$$\left(1-e^{-\left(\frac{1}{\sum_{z=1}^{K}\mathcal{E}_z''}\left(\frac{1}{K!}\left(\sum_{\zeta\in H_K}\left(\sum_{z=1}^{K}\left(\mathcal{E}_z''\left(-\ln\left(1-e^{-\left(KH_{\underset{\sim}{\alpha}_{\zeta(j)}}\left(-\ln\left(\overline{IN}_{\zeta(j)}\right)\right)^{\phi}\right)^{\frac{1}{\phi}}}\right)\right)^{\phi}\right)\right)^{\frac{1}{\phi}}\right)\right)\right)^{\phi}\right)^{\frac{1}{\phi}}}\right),\left(1-e^{-\left(\frac{1}{\sum_{z=1}^{K}\mathcal{E}_z''}\left(\frac{1}{K!}\left(\sum_{\zeta\in H_K}\left(\sum_{z=1}^{K}\left(\mathcal{E}_z''\left(-\ln\left(1-e^{-\left(KH_{\underset{\sim}{\alpha}_{\zeta(z)}}\left(-\ln\left(\overline{FL}_{\zeta(j)}\right)\right)^{\phi}\right)^{\frac{1}{\phi}}}\right)\right)^{\phi}\right)\right)^{\frac{1}{\phi}}\right)\right)\right)^{\phi}\right)^{\frac{1}{\phi}}}\right)\right\rangle. \tag{15}$$

Proof. Corresponding to Aczel-Alsina operational rules suggested in Definition 4, we can have.

$$KH_{\underset{\sim}{\alpha}_{\zeta(z)}}\underset{\sim}{\alpha}_{\zeta(z)}=\left\langle\left(1-e^{-\left(KH_{\underset{\sim}{\alpha}_{\zeta(z)}}\left(-\ln\left(1-\overline{TR}_{\zeta(z)}\right)\right)^{\phi}\right)^{\frac{1}{\phi}}}\right),\left(e^{-\left(KH_{\underset{\sim}{\alpha}_{\zeta(z)}}\left(-\ln\left(\overline{IN}_{\zeta(z)}\right)\right)^{\phi}\right)^{\frac{1}{\phi}}}\right),\left(e^{-\left(H_{\underset{\sim}{\alpha}_{\zeta(z)}}\left(-\ln\left(\overline{FL}_{\zeta(z)}\right)\right)^{\phi}\right)^{\frac{1}{\phi}}}\right)\right\rangle;$$

and

$$\left(KH_{\underset{\sim}{\alpha}_{\zeta(j)}}\underset{\sim}{\alpha}_{\zeta(j)}\right)^{\mathcal{E}_z''}=\left\langle\left(e^{-\left(\mathcal{E}_z''\left(-\ln\left(1-e^{-\left(KH_{\underset{\sim}{\alpha}_{\zeta(z)}}\left(-\ln\left(1-\overline{TR}_{\zeta(z)}\right)\right)^{\phi}\right)^{\frac{1}{\phi}}}\right)\right)^{\phi}\right)^{\frac{1}{\phi}}}\right),\left(1-e^{-\left(\mathcal{E}_z''\left(-\ln\left(1-e^{-\left(KH_{\underset{\sim}{\alpha}_{\zeta(z)}}\left(-\ln\left(\overline{IN}_{\zeta(z)}\right)\right)^{\phi}\right)^{\frac{1}{\phi}}}\right)\right)^{\phi}\right)^{\frac{1}{\phi}}}\right),\left(1-e^{-\left(\mathcal{E}_z''\left(-\ln\left(1-e^{-\left(KH_{\underset{\sim}{\alpha}_{\zeta(z)}}\left(-\ln\left(\overline{FL}_{\zeta(z)}\right)\right)^{\phi}\right)^{\frac{1}{\phi}}}\right)\right)^{\phi}\right)^{\frac{1}{q}}}\right)\right\rangle.$$

Therefore,

$$\prod_{z=1}^{K}\left(KH_{\underset{\sim}{\alpha}_{\zeta(z)}}\underset{\sim}{\alpha}_{\zeta(z)}\right)^{\mathcal{E}_z''}$$
$$=\left\langle\left(e^{-\left(\sum_{z=1}^{K}\left(\mathcal{E}_z''\left(-\ln\left(1-e^{-\left(KH_{\underset{\sim}{\alpha}_{\zeta(z)}}\left(-\ln\left(1-\overline{TR}_{\zeta(z)}\right)\right)^{\phi}\right)^{\frac{1}{\phi}}}\right)\right)^{\phi}\right)\right)^{\frac{1}{\phi}}}\right),\left(1-e^{-\left(\sum_{z=1}^{K}\left(\mathcal{E}''\left(-\ln\left(1-e^{-\left(KH_{\underset{\sim}{\alpha}_{\zeta(z)}}\left(-\ln\left(\overline{IN}_{\zeta(z)}\right)\right)^{\phi}\right)^{\frac{1}{\phi}}}\right)\right)^{\phi}\right)\right)^{\frac{1}{\phi}}}\right),\left(1-e^{-\left(\sum_{z=1}^{K}\left(\mathcal{E}''\left(-\ln\left(1-e^{-\left(KH_{\underset{\sim}{\alpha}_{\zeta(z)}}\left(-\ln\left(\overline{FL}_{\zeta(z)}\right)\right)^{\phi}\right)^{\frac{1}{\phi}}}\right)\right)^{\phi}\right)\right)^{\frac{1}{\phi}}}\right)\right\rangle;$$

Let

$$\mathcal{H}=1-e^{-\left(\sum_{z=1}^{K}\left(\mathcal{E}_z''\left(-\ln\left(1-e^{-\left(KH_z\left(-\ln\left(\overline{IN}_{\zeta(z)}\right)\right)^{\phi}\right)^{\frac{1}{\phi}}}\right)\right)^{\phi}\right)\right)^{\frac{1}{\phi}}}$$

$$\Rightarrow 1-\mathcal{H}=e^{-\left(\sum_{z=1}^{K}\left(\mathcal{E}_z''\left(-\ln\left(1-e^{-\left(KH_z\left(-\ln\left(\overline{IN}_{\zeta(z)}\right)\right)^{\phi}\right)^{\frac{1}{\phi}}}\right)\right)^{\phi}\right)\right)^{\frac{1}{\phi}}} \Rightarrow \ln(1-\mathcal{H})=-\left(\sum_{z=1}^{K}\left(\mathcal{E}_z''\left(-\ln\left(1-e^{-\left(KH_z\left(-\ln\left(\overline{IN}_{\zeta(z)}\right)\right)^{\phi}\right)^{\frac{1}{\phi}}}\right)\right)^{\phi}\right)\right)^{\frac{1}{\phi}}.$$

Utilizing this, we have

$$\sum_{\zeta\in H_K}\prod_{z=1}^{K}\left(K_z H_z\,\tilde{\Xi}_{\zeta(z)}\right)^{\mathcal{E}_z''}=\left\langle\left(1-e^{-\left(\sum_{\zeta\in H_z}\left(\sum_{z=1}^{K}\left(\mathcal{E}''\left(-\ln\left(1-e^{-\left(KH_z\left(-\ln\left(1-\overline{TR}_{\zeta(z)}\right)\right)^{\phi}\right)^{\frac{1}{\phi}}}\right)\right)^{\phi}\right)\right)^{\frac{1}{\phi}}\right)}\right),\right.$$

$$\left.\left(e^{-\left(\sum_{\zeta\in H_z}\left(\sum_{z=1}^{K}\left(\mathcal{E}''\left(-\ln\left(1-e^{-\left(KH_z\left(-\ln\left(\overline{IN}_{\zeta(z)}\right)\right)^{\phi}\right)^{\frac{1}{\phi}}}\right)\right)^{\phi}\right)\right)^{\frac{1}{\phi}}\right)}\right),\left(e^{-\left(\sum_{\zeta\in H_z}\left(\sum_{z=1}^{K}\left(\mathcal{E}''\left(-\ln\left(1-e^{-\left(KH_z\left(-\ln\left(\overline{FL}_{\zeta(z)}\right)\right)^{\phi}\right)^{\frac{1}{\phi}}}\right)\right)^{\phi}\right)\right)^{\frac{1}{\phi}}\right)}\right)\right\rangle.$$

Furthermore,

$$\frac{1}{K!}\sum_{\zeta\in H_K}\prod_{z=1}^{K}\left(K_z H_z\,\tilde{\Xi}_{\zeta(z)}\right)^{\mathcal{E}_z''}=\left\langle\left(1-e^{-\left(\frac{1}{K!}\left(\sum_{\zeta\in H_z}\left(\sum_{z=1}^{K}\left(\mathcal{E}_z''\left(-\ln\left(1-e^{-\left(KH_z\left(-\ln\left(1-\overline{TR}_{\zeta(z)}\right)\right)^{\phi}\right)^{\frac{1}{\phi}}}\right)\right)^{\phi}\right)\right)^{\frac{1}{\phi}}\right)\right)}\right),\right.$$

$$\left.\left(e^{-\left(\frac{1}{K!}\left(\sum_{\zeta\in H_z}\left(\sum_{z=1}^{K}\left(\mathcal{E}_z''\left(-\ln\left(1-e^{-\left(KH_z\left(-\ln\left(\overline{IN}_{\zeta(z)}\right)\right)^{\phi}\right)^{\frac{1}{\phi}}}\right)\right)^{\phi}\right)\right)^{\frac{1}{\phi}}\right)\right)}\right),\left(e^{-\left(\frac{1}{K!}\left(\sum_{\zeta\in H_n}\left(\sum_{z=1}^{K}\left(\mathcal{E}_z''\left(-\ln\left(1-e^{-\left(KH_z\left(-\ln\left(\overline{FL}_{\zeta(z)}\right)\right)^{\phi}\right)^{\frac{1}{\phi}}}\right)\right)^{\phi}\right)\right)^{\frac{1}{\phi}}\right)\right)}\right)\right\rangle;$$

Thus,

$$\left(\frac{1}{K!}\sum_{\zeta\in H_K}\prod_{z=1}^{K}\left(zK_z\,\tilde{\Xi}_{\zeta(z)}\right)^{\mathcal{E}_z''}\right)^{\frac{1}{\sum_{z=1}^{K}\mathcal{E}_j''}}=\left\langle\left(e^{-\left(\frac{1}{\sum_{z=1}^{K}\mathcal{E}_z''}\left(\frac{1}{K!}\left(\sum_{\zeta\in H_z}\left(\sum_{j=1}^{n}\left(\mathcal{E}_z''\left(-\ln\left(1-e^{-\left(zK_z\left(-\ln\left(1-\overline{TR}_{\zeta(z)}\right)\right)^{\phi}\right)^{\frac{1}{\phi}}}\right)\right)^{\phi}\right)\right)^{\frac{1}{\phi}}\right)\right)\right)^{\frac{1}{\phi}}}\right)^{\frac{1}{q}}\right),\right.$$

$$\left.\left(1-e^{-\left(\frac{1}{\sum_{z=1}^{K}\mathcal{E}_z''}\left(\frac{1}{K!}\left(\sum_{\zeta\in H_z}\left(\sum_{j=1}^{n}\left(\mathcal{E}_z''\left(-\ln\left(1-e^{-\left(zK_z\left(-\ln\left(\overline{IN}_{\zeta(z)}\right)\right)^{\phi}\right)^{\frac{1}{\phi}}}\right)\right)^{\phi}\right)\right)^{\frac{1}{\phi}}\right)\right)\right)^{\frac{1}{\phi}}}\right),\left(1-e^{-\left(\frac{1}{\sum_{z=1}^{K}\mathcal{E}_z''}\left(\frac{1}{K!}\left(\sum_{\zeta\in H_z}\left(\sum_{j=1}^{n}\left(\mathcal{E}_z''\left(-\ln\left(1-e^{-\left(zK_z\left(-\ln\left(\overline{FL}_{\zeta(z)}\right)\right)^{\phi}\right)^{\frac{1}{\phi}}}\right)\right)^{\phi}\right)\right)^{\frac{1}{\phi}}\right)\right)\right)^{\frac{1}{\phi}}}\right)^{\frac{1}{q}}\right\rangle$$

Hence,

$$S^{V}NAAPMM^{(\mathcal{E}'')}\left(\tilde{\Xi}_1,\tilde{\Xi}_2,...,\tilde{\Xi}_z\right)=\left\langle\left(e^{-\left(\frac{1}{\sum_{z=1}^{K}\mathcal{E}_z''}\left(\frac{1}{K!}\left(\sum_{\zeta\in H_z}\left(\sum_{j=1}^{n}\left(\mathcal{E}_z''\left(-\ln\left(1-e^{-\left(zK_z\left(-\ln\left(1-\overline{TR}_{\zeta(z)}\right)\right)^{\phi}\right)^{\frac{1}{\phi}}}\right)\right)^{\phi}\right)\right)^{\frac{1}{\phi}}\right)\right)\right)^{\frac{1}{\phi}}}\right)^{\frac{1}{q}}\right),\right.$$

$$\left.\left(1-e^{-\left(\frac{1}{\sum_{z=1}^{K}\mathcal{E}_z''}\left(\frac{1}{K!}\left(\sum_{\zeta\in H_z}\left(\sum_{j=1}^{n}\left(\mathcal{E}_z''\left(-\ln\left(1-e^{-\left(zK_z\left(-\ln\left(\overline{IN}_{\zeta(z)}\right)\right)^{\phi}\right)^{\frac{1}{\phi}}}\right)\right)^{\phi}\right)\right)^{\frac{1}{\phi}}\right)\right)\right)^{\frac{1}{\phi}}}\right),\left(1-e^{-\left(\frac{1}{\sum_{z=1}^{K}\mathcal{E}_z''}\left(\frac{1}{K!}\left(\sum_{\zeta\in H_z}\left(\sum_{j=1}^{n}\left(\mathcal{E}_z''\left(-\ln\left(1-e^{-\left(zK_z\left(-\ln\left(\overline{FL}_{\zeta(z)}\right)\right)^{\phi}\right)^{\frac{1}{\phi}}}\right)\right)^{\phi}\right)\right)^{\frac{1}{\phi}}\right)\right)\right)^{\frac{1}{\phi}}}\right)^{\frac{1}{q}}\right\rangle.$$

Theorem 2. (Idempotency) Let $\Xi_z=\langle\overline{TR}_z,\overline{IN}_z,\overline{FL}_z\rangle(z=1,2,...,K)$ be a series of SVNNs, if $\tilde{\Xi}_z=\tilde{\Xi}=\langle\overline{TR},\overline{IN},\overline{FL}\rangle(z=1,2,...,K)$ holds for all z, then

$$S^{V}NAAPMM^{(Œ^{n})}\left(\underline{\&}_1,\underline{\&}_2,...,\underline{\&}_z\right)=\underline{\&}. \tag{16}$$

Proof. Since $\underline{\&}_z=\underline{\&}=\langle\overline{TR},\overline{IN},\overline{FL}\rangle(z=1,2,...,K)$, we can have $Spt(\underline{\&}_i,\underline{\&}_z)=\frac{1}{K}$ for all $i,z=1,2,..,K$ and $i\neq z$.

Thus, we can derive $H_{\&}=\frac{1}{K}(z=1,2,..,K)$. According to Theorem 1, we have

$$S^{V}NAAPMM^{(Œ^{n})}\left(\underline{\&}_1,\underline{\&}_2,...,\underline{\&}_z\right)=\left\langle\left(e^{-\left(\frac{1}{\sum_{z=1}^{K}Œ_z^{n}}\left(\frac{1}{K!}\left(\sum_{\zeta\in H_{\&}}\left(\sum_{j=1}^{n}\left(Œ_z^{n}\left(-\ln\left(1-e^{-\left(zK_z\left(-\ln\left(1-\overline{TR}_{\zeta(z)}\right)\right)^{\phi}\right)^{\frac{1}{\phi}}}\right)\right)^{\phi}\right)\right)\right)\right)^{\frac{1}{\phi}}\right)^{\frac{1}{q}}\right),\right.$$

$$\left.\left(1-e^{-\left(\frac{1}{\sum_{z=1}^{K}Œ_z^{n}}\left(\frac{1}{K!}\left(\sum_{\zeta\in H_{\&}}\left(\sum_{j=1}^{n}\left(Œ_z^{n}\left(-\ln\left(1-e^{-\left(zK_z\left(-\ln\left(\overline{IN}_{\zeta(z)}\right)\right)^{\phi}\right)^{\frac{1}{\phi}}}\right)\right)^{\phi}\right)\right)\right)\right)^{\frac{1}{\phi}}\right)^{\frac{1}{q}}\right),\right.$$

$$\left.\left(1-e^{-\left(\frac{1}{\sum_{z=1}^{K}Œ_z^{n}}\left(\frac{1}{K!}\left(\sum_{\zeta\in H_{\&}}\left(\sum_{j=1}^{n}\left(Œ_z^{n}\left(-\ln\left(1-e^{-\left(zK_z\left(-\ln\left(\overline{FL}_{\zeta(z)}\right)\right)^{\phi}\right)^{\frac{1}{\phi}}}\right)\right)^{\phi}\right)\right)\right)\right)^{\frac{1}{\phi}}\right)^{\frac{1}{q}}\right\rangle.$$

$$=\left\langle\left(e^{-\left(\frac{1}{\sum_{z=1}^{K}Œ_z^{n}}\left(\frac{1}{K!}\left(\sum_{\zeta\in H_{\&}}\left(\sum_{z=1}^{K}\left(Œ_z^{n}\left(-\ln\left(\overline{TR}\right)^{\phi}\right)\right)\right)\right)\right)\right)^{\frac{1}{\phi}}\right),\left(1-e^{-\left(\frac{1}{\sum_{z=1}^{K}Œ_z^{n}}\left(\frac{1}{K!}\left(\sum_{\zeta\in H_{\&}}\left(\sum_{z=1}^{K}\left(Œ_j^{n}\left(-\ln\left(1-\left(\overline{IN}\right)\right)^{\phi}\right)\right)\right)\right)\right)\right)^{\frac{1}{\phi}}\right),\right.$$

$$\left.\left(1-e^{-\left(\frac{1}{\sum_{z=1}^{K}Œ_z^{n}}\left(\frac{1}{K!}\left(\sum_{\zeta\in H_{\&}}\left(\sum_{z=1}^{K}\left(Œ_j^{n}\left(-\ln\left(1-\left(\overline{FL}\right)\right)^{\phi}\right)\right)\right)\right)\right)\right)^{\frac{1}{\phi}}\right)\right\rangle;$$

$$=\left\langle\left(e^{-\left(\left(-\ln\left(\overline{TR}\right)\right)^{\phi}\right)^{\frac{1}{\phi}}}\right),\left(1-e^{-\left(\left(-\ln\left(1-\left(\overline{IN}\right)\right)\right)^{\phi}\right)^{\frac{1}{\phi}}}\right),\left(1-e^{-\left(\left(-\ln\left(1-\overline{FL}\right)\right)^{\phi}\right)^{\frac{1}{\phi}}}\right)^{\frac{1}{q}}\right\rangle$$

$$=\left\langle\overline{TR},\overline{IN},\overline{FL}\right\rangle=\underline{\&}.$$

Theorem 3. Let $\underline{\&}_z=\langle\overline{TR}_z,\overline{IN}_z,\overline{FL}_z\rangle(z=1,2,...,K)$ be a series of SVNNs. Then

$$\underline{\&}\leq S^{V}NAAPMM^{(Œ^{n})}\left(\underline{\&}_1,\underline{\&}_2,...,\underline{\&}_n\right)\leq\underline{\&}, \tag{17}$$

where,

$$\underline{\&}=\left\langle\min_{z=1}^{K}\overline{TR}_z,\max_{z=1}^{K}\overline{IN}_z,\max_{z=1}^{K}\overline{FL}_z\right\rangle \text{ and } \underline{\&}=\left\langle\max_{z=1}^{K}\overline{TR}_z,\min_{z=1}^{K}\overline{IN}_z,\min_{z=1}^{K}\overline{FL}_z\right\rangle.$$

Proof. Corresponding to Theorem 1 and Theorem 2, it is straightforward to acquire that.

$$\left(e^{-\left(\frac{1}{\sum_{z=1}^{K}Œ_j^{n}}\left(\frac{1}{K!}\left(\sum_{\zeta\in H_{\&}}\left(\sum_{z=1}^{K}\left(Œ_j^{n}\left(-\ln\left(1-e^{-\left(KH_{\&}\left(-\ln\left(1-\overline{TR}_{\zeta(z)}\right)\right)^{\phi}\right)^{\frac{1}{\phi}}}\right)\right)^{\phi}\right)\right)\right)\right)^{\frac{1}{\phi}}\right)}\right)$$

$$\geq\left(e^{-\left(\frac{1}{\sum_{z=1}^{K}Œ_j^{n}}\left(\frac{1}{K!}\left(\sum_{\zeta\in H_{\&}}\left(\sum_{z=1}^{K}\left(Œ_j^{n}\left(-\ln\left(1-e^{-\left(KH_{\&}\left(-\ln\left(1-\min_{z=1}^{K}\overline{TR}_{\zeta(z)}\right)\right)^{\phi}\right)^{\frac{1}{\phi}}}\right)\right)^{\phi}\right)\right)\right)\right)^{\frac{1}{\phi}}\right)}\right)=\min_{z=1}^{K}\overline{TR}_z;$$

$$\left(1-e^{-\left(\frac{1}{\sum_{z=1}^{K}\text{Œ}_j''}\left(\frac{1}{K!}\left(\sum_{\zeta\in H_z}\left(\sum_{z=1}^{K}\left(\text{Œ}_j''\left(-\ln\left(1-e^{-\left(KH_{\&}(z)\left(-\ln\left(\overline{IN}_{\zeta(z)}\right)^{\phi}\right)^{\frac{1}{\phi}}\right)^{\phi}}\right)^{\frac{1}{\phi}}\right)^{\phi}\right)\right)\right)\right)^{\frac{1}{\phi}}}\right)}\right)$$

$$\leq\left(1-e^{-\left(\frac{1}{\sum_{z=1}^{K}\text{Œ}_j''}\left(\frac{1}{K!}\left(\sum_{\zeta\in H_z}\left(\sum_{z=1}^{K}\left(\text{Œ}_j''\left(-\ln\left(1-e^{-\left(KH_{\&}(z)\left(-\ln\left(\max_{z=1}^{K}\overline{IN}_{\zeta(z)}\right)^{\phi}\right)^{\frac{1}{\phi}}\right)^{\phi}}\right)^{\frac{1}{\phi}}\right)^{\phi}\right)\right)\right)\right)^{\frac{1}{\phi}}}\right)}\right)=\max_{z=1}^{K}\overline{IN}_z;$$

;

$$\left(1-e^{-\left(\frac{1}{\sum_{z=1}^{K}\text{Œ}_j''}\left(\frac{1}{K!}\left(\sum_{\zeta\in H_z}\left(\sum_{z=1}^{K}\left(\text{Œ}_j''\left(-\ln\left(1-e^{-\left(KH_{\&}(z)\left(-\ln\left(\overline{FL}_{\zeta(z)}\right)^{\phi}\right)^{\frac{1}{\phi}}\right)^{\phi}}\right)^{\frac{1}{\phi}}\right)^{\phi}\right)\right)\right)\right)^{\frac{1}{\phi}}}\right)}\right)$$

$$\leq\left(1-e^{-\left(\frac{1}{\sum_{z=1}^{K}\text{Œ}_j''}\left(\frac{1}{K!}\left(\sum_{\zeta\in H_z}\left(\sum_{z=1}^{K}\left(\text{Œ}_j''\left(-\ln\left(1-e^{-\left(KH_{\&}(z)\left(-\ln\left(\max_{z=1}^{K}\overline{FL}_{\zeta(z)}\right)^{\phi}\right)^{\frac{1}{\phi}}\right)^{\phi}}\right)^{\frac{1}{\phi}}\right)^{\phi}\right)\right)\right)\right)^{\frac{1}{\phi}}}\right)}\right)=\max_{z=1}^{K}\overline{FL}_z.$$

.

According to Definition 2, we can get $\underline{\&}^{-}\leq S^{V}NAAPMM^{(\text{Œ}'')}\left(\underline{\&}_1,\underline{\&}_2,...,\underline{\&}_K\right)$. Similarly, we have $S^{V}NAAPMM^{(\text{Œ}'')}\left(\underline{\&}_1,\underline{\&}_2,...,\underline{\&}_K\right)\leq\underline{\&}^{+}$. Therefore, $\underline{\&}^{-}\leq S^{V}NAAPMM^{(\text{Œ}'')}\left(\underline{\&}_1,\underline{\&}_2,...,\underline{\&}_n\right)\leq\underline{\&}^{+}$.

Subsequently, we discuss some special cases of SVNAAPMM with respect to the parameters $\text{Œ}''$ *and* ϕ.

Case 1. If $\text{Œ}''=(1,0,0,...,0)$, then the SVNAAPMM operator deteriorates to the SVNAAPA operator, that is

$$\begin{aligned}S^{V}NAAPMM^{(1,0,0,...,0)}\left(\underline{\&}_1,\underline{\&}_2,...,\underline{\&}_K\right)&=\left\langle 1-e^{-\left(\sum_{z=1}^{K}KH_{\&z}\left(-\ln\left(1-\overline{TR}_z\right)\right)^{\Phi}\right)^{\frac{1}{\Phi}}},e^{-\left(\sum_{z=1}^{K}KH_{\&z}\left(-\ln\overline{IN}_z\right)^{\Phi}\right)^{\frac{1}{\Phi}}},e^{-\left(\sum_{z=1}^{K}KH_{\&z}\left(-\ln\overline{FL}_z\right)^{\Phi}\right)^{\frac{1}{\Phi}}}\right\rangle\\&=\sum_{z=1}^{K}KH_{\&z}\underline{\&}_z\end{aligned}\tag{18}$$

In this case, if $Spt\left(\underline{\&}_i,\underline{\&}_z\right)=g$ for all $i\neq z$, then the SVNAAPMM operator deteriorates to the SVN average operator. i.e.,

$$\begin{aligned}S^{V}NAAPMM^{(1,0,0,...,0)}\left(\underline{\&}_1,\underline{\&}_2,...,\underline{\&}_K\right)&=\left\langle 1-e^{-\left(\sum_{z=1}^{k}\frac{1}{K}\left(-\ln\left(1-\overline{TR}_z\right)\right)^{\Phi}\right)^{\frac{1}{\Phi}}},e^{-\left(\sum_{z=1}^{K}\frac{1}{K}\left(-\ln\overline{IN}_z\right)^{\Phi}\right)^{\frac{1}{\Phi}}},e^{-\left(\sum_{z=1}^{K}\frac{1}{K}\left(-\ln\overline{FL}_z\right)^{\Phi}\right)^{\frac{1}{\Phi}}}\right\rangle\\&=\frac{1}{K}\sum_{z=1}^{K}\underline{\&}_z.\end{aligned}\tag{19}$$

Case 2. If $\text{Œ}''=(1,1,0,...,0)$, then the SVNAAPMM operator deteriorates to the SVN power Bonferroni mean operator. i.e.,

$$\begin{aligned}S^{V}NAAPMM^{(1,1,0,...,0)}\left(\underline{\&}_1,\underline{\&}_2,...,\underline{\&}_K\right)&=\left\langle\left(e^{-\left(\frac{1}{2}\left(\frac{1}{K(K-1)}\right)\left(\sum_{\substack{i=1,z=1\\i\neq z}}^{K}\left(1^{*}\left(-\ln\left(1-e^{-\left(KH_{\&}\left(-\ln\left(1-\overline{TR}_z\right)\right)^{\Phi}\right)^{\frac{1}{\Phi}}}\right)\right)^{\Phi}\right)+\left(1^{*}\left(-\ln\left(1-e^{-\left(KH_{\&}\left(-\ln\left(1-\overline{TR}_z\right)\right)^{\Phi}\right)^{\frac{1}{\Phi}}}\right)\right)^{\Phi}\right)\right)\right)^{\frac{1}{\Phi}}}\right),\right.\\&\left(1-e^{-\left(\frac{1}{2}\left(\frac{1}{K(K-1)}\right)\left(\sum_{\substack{i=1,z=1\\i\neq z}}^{K}\left(1^{*}\left(-\ln\left(1-e^{-\left(KH_{\&}\left(-\ln\left(\overline{IN}_i\right)^{\Phi}\right)^{\frac{1}{\Phi}}\right)^{\Phi}}\right)\right)^{\Phi}\right)+\left(1^{*}\left(-\ln\left(1-e^{-\left(KH_{\&}\left(-\ln\left(\overline{IN}_z\right)^{\Phi}\right)^{\frac{1}{\Phi}}\right)^{\Phi}}\right)\right)^{\Phi}\right)\right)\right)^{\frac{1}{\Phi}}}\right),\\&\left.\left(1-e^{-\left(\frac{1}{2}\left(\frac{1}{K(K-1)}\right)\left(\sum_{\substack{i=1,z=1\\i\neq z}}^{K}\left(1^{*}\left(-\ln\left(1-e^{-\left(KH_{\&}\left(-\ln\left(\overline{FL}_i\right)^{\Phi}\right)^{\frac{1}{\Phi}}\right)^{\Phi}}\right)\right)^{\Phi}\right)+\left(1^{*}\left(-\ln\left(1-e^{-\left(KH_{\&}\left(-\ln\left(\overline{FL}_z\right)^{\Phi}\right)^{\frac{1}{\Phi}}\right)^{\Phi}}\right)\right)^{\Phi}\right)\right)\right)^{\frac{1}{\Phi}}}\right)\right\rangle=\left(\frac{1}{K(K-1)}\sum_{\substack{i,z=1\\i\neq z}}^{K}\left(KH_{\&}\underline{\&}_i\otimes KH_{\&}\underline{\&}_z\right)\right)^{\frac{1}{2}}.\end{aligned}\tag{20}$$

In this case, if $Spt\left(\underline{\tilde{\alpha}}_i, \underline{\tilde{\alpha}}_z\right) = g$ f 0 for all $i \neq z$, then the SVNAAMM operator deteriorates to the SVNAA Bonferroni mean (SVNAABM) operator. i.e.,

$$S^{V}NAAPMM^{(1,1,0,\ldots,0)}\left(\underline{\tilde{\alpha}}_1, \underline{\tilde{\alpha}}_2, \ldots, \underline{\tilde{\alpha}}_K\right) = \left\langle \left(e^{-\left(\frac{1}{2}\left(\left(\frac{1}{K(K-1)}\right)\left(\sum_{\substack{i=1,z=1 \\ i\neq z}}^{K}\left(1^{*}\left(-\ln\left(\overline{TR}_i\right)\right)^{\Phi} + \left(1^{*}\left(-\ln\left(\overline{TR}_z\right)\right)^{\Phi}\right)\right)\right)^{\frac{1}{\Phi}}\right)^{\frac{1}{\Phi}}} \right), \right.$$

$$\left(1-e^{-\left(\frac{1}{2}\left(\left(\frac{1}{K(K-1)}\right)\left(\sum_{\substack{i=1,z=1 \\ i\neq z}}^{K}\left(1^{*}\left(-\ln\left(1-\overline{IN}_i\right)\right)^{\Phi} + \left(1^{*}\left(-\ln\left(1-\overline{IN}_z\right)\right)^{\Phi}\right)\right)\right)^{\frac{1}{\Phi}}\right)^{\frac{1}{\Phi}}} \right), \left(1-e^{-\left(\frac{1}{2}\left(\left(\frac{1}{K(K-1)}\right)\left(\sum_{\substack{i=1,z=1 \\ i\neq z}}^{K}\left(1^{*}\left(-\ln\left(1-\overline{FL}_i\right)\right)^{\Phi} + \left(1^{*}\left(-\ln\left(1-\overline{FL}_z\right)\right)^{\Phi}\right)\right)\right)^{\frac{1}{\Phi}}\right)^{\frac{1}{\Phi}}} \right) \right\rangle \quad (21)$$

$$= \left(\frac{1}{K(K-1)} \sum_{\substack{i=1,z=1 \\ i\neq z}}^{K} \underline{\tilde{\alpha}}_i \otimes \underline{\tilde{\alpha}}_z \right)^{\frac{1}{2}}.$$

Case 3. If $\text{Œ}'' = \left(\underbrace{1,1,1,1,\ldots.}_{K}, \underbrace{0,0,0,\ldots,0}_{K}\right)$, then the SVNAAPMM operator deteriorates to the SVNAAPMSM operator, i.e.,

$$S^{V}NAAPMM^{\left(\underbrace{1,1,1,\ldots.,1}_{K},\underbrace{0,0,0,\ldots.,0}_{K}\right)}\left(\underline{\tilde{\alpha}}_1, \underline{\tilde{\alpha}}_2, \ldots., \underline{\tilde{\alpha}}_K\right) = \left\langle \left(e^{-\left(\frac{1}{k}\left(\frac{1}{C_K^k}\left(\bigoplus_{i_1 p i_2 p \ldots p i_K}\left(\sum_{z=1}^{k}\left(-\ln\left(1-e^{-\left(KH_{\tilde{\alpha}z}\left(-\ln\left(1-\overline{TR}_{i_z}\right)\right)^{\Phi}\right)^{\frac{1}{\Phi}}}\right)\right)\right)\right)^{\Phi}\right)^{\frac{1}{\Phi}}\right)^{\frac{1}{\Phi}}} \right), \right.$$

$$\left(1-e^{-\left(\frac{1}{k}\left(\frac{1}{C_K^k}\left(\bigoplus_{i_1 p i_2 p \ldots p i_K}\left(\sum_{z=1}^{k}\left(-\ln\left(1-e^{-\left(KH_{\tilde{\alpha}z}\left(-\ln\left(\overline{IN}_{i_z}\right)\right)^{\Phi}\right)^{\frac{1}{\Phi}}}\right)\right)\right)\right)^{\Phi}\right)^{\frac{1}{\Phi}}\right)^{\frac{1}{\Phi}}} \right), \left(1-e^{-\left(\frac{1}{k}\left(\frac{1}{C_K^k}\left(\bigoplus_{i_1 p i_2 p \ldots p i_K}\left(\sum_{z=1}^{k}\left(-\ln\left(1-e^{-\left(KH_{\tilde{\alpha}z}\left(-\ln\left(\overline{FL}_{i_z}\right)\right)^{\Phi}\right)^{\frac{1}{\Phi}}}\right)\right)\right)\right)^{\Phi}\right)^{\frac{1}{\Phi}}\right)^{\frac{1}{\Phi}}} \right) \right\rangle \quad (22)$$

$$= \left(\frac{1}{C_K^k} \sum_{1\leq i_1<i_2<\ldots<i_K} \prod_{z=1}^{k}\left(KH_{\tilde{\alpha}z}\left(\underline{\tilde{\alpha}}_{i_z}\right)\right) \right)^{\frac{1}{k}}.$$

In this case, if $Spt\left(\underline{\tilde{\alpha}}_i, \underline{\tilde{\alpha}}_z\right) = g$ f 0 for all $i \neq z$, then the SVNAAMM operator deteriorates to the SVNAAMSM operator. i.e.,

$$S^{V}NAAPMM^{\left(\underbrace{1,1,1,\ldots.,1}_{K},\underbrace{0,0,0,\ldots.,0}_{K-k}\right)}\left(\underline{\tilde{\alpha}}_1, \underline{\tilde{\alpha}}_2, \ldots., \underline{\tilde{\alpha}}_K\right)$$

$$= \left\langle \left(e^{-\left(\frac{1}{k}\left(\frac{1}{C_K^k}\left(\bigoplus_{i_1 p i_2 p \ldots p i_K}\left(\sum_{z=1}^{k}\left(-\ln\overline{TR}_{i_z}\right)^{\Phi}\right)\right)^{\frac{1}{\Phi}}\right)^{\frac{1}{\Phi}}} \right), \left(1-e^{-\left(\frac{1}{k}\left(\frac{1}{C_K^k}\left(\bigoplus_{i_1 p i_2 p \ldots p i_K}\left(\sum_{z=1}^{n}\left(-\ln\left(1-\overline{IN}_{i_z}\right)\right)^{\Phi}\right)\right)^{\frac{1}{\Phi}}\right)^{\frac{1}{\Phi}}} \right), \left(1-e^{-\left(\frac{1}{k}\left(\frac{1}{C_K^k}\left(\bigoplus_{i_1 p i_2 p \ldots p i_K}\left(\sum_{z=1}^{n}\left(-\ln\left(1-\overline{FL}_{i_z}\right)\right)^{\Phi}\right)\right)^{\frac{1}{\Phi}}\right)^{\frac{1}{\Phi}}} \right) \right\rangle \quad (23)$$

$$= \left(\frac{1}{C_K^k} \sum_{1\leq i_1<i_2<\ldots<i_k} \prod_{z=1}^{k}\left(\underline{\tilde{\alpha}}_{i_z}\right) \right)^{\frac{1}{k}}$$

Case 4. If $\text{Œ}'' = (1,1,1,\ldots.,1)$ *or* $\left(1_Y, 1_Y, 1_Y, \ldots., 1_Y\right)$, then the SVNAAPMM operator deteriorates to the following form:

$$S^{V}NAAPMM^{\text{Œ}''=(1,1,1,\ldots.,1)\ or\ \left(1_Y,1_Y,1_Y,\ldots.,1_Y\right)}\left(\underline{\tilde{\alpha}}_1, \underline{\tilde{\alpha}}_2, \ldots., \underline{\tilde{\alpha}}_K\right) = \left\langle \left(e^{-\left(\sum_{z=1}^{K}\left(\text{Œ}_z''\left(-\ln\left(1-e^{-\left(KH_{\tilde{\alpha}z}\left(-\ln\left(1-\overline{TR}_{\zeta(z)}\right)\right)^{\phi}\right)^{\frac{1}{\phi}}}\right)\right)\right)^{\phi}\right)^{\frac{1}{\phi}}} \right), \right.$$

$$\left(1-e^{-\left(\sum_{z=1}^{K}\left(\text{Œ}_z''\left(-\ln\left(1-e^{-\left(KH_{\tilde{\alpha}z}\left(-\ln\left(\overline{IN}_{\zeta(z)}\right)\right)^{\phi}\right)^{\frac{1}{\phi}}}\right)\right)\right)^{\phi}\right)^{\frac{1}{\phi}}} \right), \left(1-e^{-\left(\sum_{z=1}^{K}\left(\text{Œ}_z''\left(-\ln\left(1-e^{-\left(KH_{\tilde{\alpha}z}\left(-\ln\left(\overline{FL}_{\zeta(z)}\right)\right)^{\phi}\right)^{\frac{1}{\phi}}}\right)\right)\right)^{\phi}\right)^{\frac{1}{\phi}}} \right) \right\rangle = \prod_{z=1}^{K}\left(KH_{\tilde{\alpha}z}\Xi_z\right)^{\frac{1}{K}}. \quad (24)$$

In this case, if $Spt\left(\underline{\tilde{\alpha}}_i, \underline{\tilde{\alpha}}_z\right) = g$ f 0 for all $i \neq z$, then the SVNAAMM operator deteriorates to the SVNAA geometric operator. i.e.,

$$S^{V}NAAPMM^{Œ''=(1,1,1,\ldots,1)\,or\left(\frac{1}{Y},\frac{1}{Y},\frac{1}{Y},\ldots,\frac{1}{Y}\right)}\left(\Xi_1,\Xi_2,\ldots,\Xi_K\right)$$
$$=\left\langle\left(e^{-\left(\sum_{z=1}^{K}\frac{1}{K}\left(-\ln\overline{TR}_z\right)^{\Phi}\right)^{\frac{1}{\Phi}}}\right),\left(1-e^{-\left(\sum_{z=1}^{K}\frac{1}{K}\left(-\ln\left(1-\overline{IN}_z\right)\right)^{\Phi}\right)^{\frac{1}{\Phi}}}\right),\left(1-e^{-\left(\sum_{z=1}^{K}\frac{1}{K}\left(-\ln\left(1-\overline{FL}_z\right)\right)^{\Phi}\right)^{\frac{1}{\Phi}}}\right)\right\rangle=\prod_{z=1}^{K}\left(\Xi_z\right)^{\frac{1}{K}}. \tag{25}$$

Definition 9. Let $\Xi_z=\left\langle\overline{TR}_z,\overline{IN}_z,\overline{FL}_z\right\rangle(z=1,2,\ldots,K)$ be series of SVNNs, and $Œ''=\left(Œ''_1,Œ''_2,\ldots,Œ''_K\right)\in R^K$ be a series of parameters. The SVNAAPDMM operator is delivered as

$$S^{V}NAAPDMM^{Œ''}\left(\Xi_1,\Xi_2,\ldots,\Xi_K\right)=\frac{1}{\sum_{z=1}^{K}Œ''_z}\left(\prod_{\zeta\in H_K}\sum_{z=1}^{K}\left(Œ''_z\Xi_{\zeta(z)}^{\frac{K\left(1+T\left(\Xi_{\zeta(z)}\right)\right)}{\sum_{z=1}^{K}\left(1+T\left(\Xi_z\right)\right)}}\right)\right)^{\frac{1}{K!}}, \tag{26}$$

where

$$T\left(\Xi_z\right)=\sum_{z=1}^{K}Spt\left(\Xi_i,\Xi_z\right) \tag{27}$$

and

$$Spt\left(\Xi_i,\Xi_z\right)=1-D\left(\Xi_i,\Xi_z\right), \tag{28}$$

$\zeta(z)(z=1,2,\ldots,K)$ signifies any combination of $(1,2,\ldots,K)$. H_n indicates all possible combinations of $(1,2,\ldots,K)$, and K is the balancing coefficient $D\left(\Xi_i,\Xi_z\right)$ denotes the Hamming distance among two SVNNs Ξ_i and Ξ_z, and $Spt\left(\Xi_i,\Xi_z\right)$ is the support for Ξ_i from Ξ_z sustaining the axioms given in Definition 6.

To write Equation (26), in simplified form, let

$$H_z=\frac{\left(1+T\left(\Xi_z\right)\right)}{\sum_{z=1}^{K}\left(1+T\left(\Xi_z\right)\right)}, \tag{29}$$

then, Equation (26) can be written in simplified form as,

$$S^{V}NAAPDMM^{Œ''}\left(\Xi_1,\Xi_2,\ldots,\Xi_n\right)=\frac{1}{\sum_{z=1}^{K}Œ''_z}\left(\prod_{\zeta\in H_K}\sum_{z=1}^{K}\left(Œ''_z\Xi_{\zeta(z)}^{KH_z}\right)\right)^{\frac{1}{K!}}. \tag{30}$$

Where $\sum_{z=1}^{K}H_z=1$ and $0\le H_z\le 1$.

Conferring to Definition 9, the subsequent Theorem 4, can be attained.

Theorem 4. Let $\Xi_z=\left\langle\overline{TR}_z,\overline{IN}_z,\overline{FL}_z\right\rangle(z=1,2,\ldots,K)$ be a group of SVNNs, the aggregated value by the SVNAAPDMM operator is still a SVNN and

$$S^{V}\,NAAPDMM^{Œ''}\left(\tilde{\alpha}_1,\tilde{\alpha}_2,...,\tilde{\alpha}_z\right)=\left\langle\left(1-e^{-\left(\frac{1}{\sum_{z=1}^{K}Œ_z''}\left(\frac{1}{K!}\left(\sum_{\zeta\in H_K}\left(\sum_{z=1}^{K}\left(Œ_z''\left(-\ln\left(1-e^{-\left(KH_{\tilde{\alpha}}\left(-\ln\left(\overline{TR}_{\zeta(j)}\right)\right)^{\phi}\right)^{\frac{1}{\phi}}}\right)\right)\right)^{\phi}\right)\right)\right)\right)^{\frac{1}{\phi}}}\right),\right.$$

$$\left(e^{-\left(\frac{1}{\sum_{z=1}^{K}Œ_z''}\left(\frac{1}{K!}\left(\sum_{\zeta\in H_K}\left(\sum_{z=1}^{K}\left(Œ_z''\left(-\ln\left(1-e^{-\left(KH_{\tilde{\alpha}}\left(-\ln\left(1-\overline{IN}_{\zeta(z)}\right)\right)^{\phi}\right)^{\frac{1}{\phi}}}\right)\right)\right)^{\phi}\right)\right)\right)\right)^{\frac{1}{\phi}}}\right),\left(e^{-\left(\frac{1}{\sum_{z=1}^{K}Œ_z''}\left(\frac{1}{K!}\left(\sum_{\zeta\in H_K}\left(\sum_{z=1}^{K}\left(Œ_z''\left(-\ln\left(1-e^{-\left(KH_{\tilde{\alpha}}\left(-\ln\left(1-\overline{FL}_{\zeta(z)}\right)\right)^{\phi}\right)^{\frac{1}{\phi}}}\right)\right)\right)^{\phi}\right)\right)\right)\right)^{\frac{1}{\phi}}}\right)\right\rangle. \tag{31}$$

Proof. Conferring to the Aczel-Alsina operational rules, we can have.

$$\Xi_{\zeta(z)}^{KH_{\tilde{\alpha}}}=\left\langle\left(e^{-\left(KH_{\tilde{\alpha}}\left(-\ln\left(\overline{TR}_{\zeta(z)}\right)\right)^{\phi}\right)^{\frac{1}{\phi}}}\right),\left(1-e^{-\left(KH_{\tilde{\alpha}}\left(-\ln\left(1-\overline{IN}_{\zeta(z)}\right)\right)^{\phi}\right)^{\frac{1}{\phi}}}\right),\left(1-e^{-\left(KH_{\tilde{\alpha}}\left(-\ln\left(1-\overline{FL}_{\zeta(z)}\right)\right)^{\phi}\right)^{\frac{1}{\phi}}}\right)\right\rangle$$

and

$$Œ_{\zeta(z)}''\left(\tilde{\alpha}_{\zeta(z)}^{KH_{\tilde{\alpha}}}\right)=\left\langle\left(1-e^{-\left(Œ_z''\left(-\ln\left(1-e^{-\left(KH_{\tilde{\alpha}}\left(-\ln\left(\overline{TR}_{\zeta(z)}\right)\right)^{\phi}\right)^{\frac{1}{\phi}}}\right)\right)\right)^{\frac{1}{\phi}}}\right),\left(e^{-\left(Œ_z''\left(-\ln\left(1-e^{-\left(KH_{\tilde{\alpha}}\left(-\ln\left(1-\overline{IN}_{\zeta(z)}\right)\right)^{\phi}\right)^{\frac{1}{\phi}}}\right)\right)\right)^{\frac{1}{\phi}}}\right),\left(e^{-\left(Œ_z''\left(-\ln\left(1-e^{-\left(KH_{\tilde{\alpha}}\left(-\ln\left(1-\overline{FL}_{\zeta(z)}\right)\right)^{\phi}\right)^{\frac{1}{\phi}}}\right)\right)\right)^{\frac{1}{\phi}}}\right)\right\rangle.$$

Therefore,

$$\sum_{z=1}^{K}Œ_z''\left(\tilde{\alpha}_{\zeta(z)}^{KH_{\tilde{\alpha}}}\right)$$

$$=\left\langle\left(1-e^{-\left(\sum_{z=1}^{K}\left(Œ''\left(-\ln\left(1-e^{-\left(KH_{\tilde{\alpha}}\left(-\ln\left(\overline{TR}_{\zeta(z)}\right)\right)^{\phi}\right)^{\frac{1}{\phi}}}\right)\right)\right)^{\phi}\right)^{\frac{1}{\phi}}}\right),\left(e^{-\left(\sum_{z=1}^{K}\left(Œ_z''\left(-\ln\left(1-e^{-\left(KH_{\tilde{\alpha}}\left(-\ln\left(1-\overline{IN}_{\zeta(z)}\right)\right)^{\phi}\right)^{\frac{1}{\phi}}}\right)\right)\right)^{\phi}\right)^{\frac{1}{\phi}}}\right),\left(e^{-\left(\sum_{z=1}^{K}\left(Œ_z''\left(-\ln\left(1-e^{-\left(KH_{\tilde{\alpha}}\left(-\ln\left(1-\overline{FL}_{\zeta(z)}\right)\right)^{\phi}\right)^{\frac{1}{\phi}}}\right)\right)\right)^{\phi}\right)^{\frac{1}{\phi}}}\right)\right\rangle;$$

Let

$$\hbar=1-e^{-\left(\sum_{z=1}^{K}\left(Œ_z''\left(-\ln\left(1-e^{-\left(KH_{\tilde{\alpha}}\left(-\ln\left(\overline{TR}_{\zeta(z)}\right)\right)^{\phi}\right)^{\frac{1}{\phi}}}\right)\right)\right)^{\phi}\right)^{\frac{1}{\phi}}}$$

$$\Rightarrow e^{-\left(\sum_{z=1}^{K}\left(Œ_z''\left(-\ln\left(1-e^{-\left(KH_{\tilde{\alpha}}\left(-\ln\left(\overline{TR}_{\zeta(z)}\right)\right)^{\phi}\right)^{\frac{1}{\phi}}}\right)\right)\right)^{\phi}\right)^{\frac{1}{\phi}}}\qquad\Rightarrow\ln(1-\hbar)=-\left(\sum_{z=1}^{K}\left(Œ_z''\left(-\ln\left(1-e^{-\left(KH_{\tilde{\alpha}}\left(-\ln\left(\overline{TR}_{\zeta(z)}\right)\right)^{\phi}\right)^{\frac{1}{\phi}}}\right)\right)\right)^{\phi}\right)^{\frac{1}{\phi}}.$$

Utilizing this, we have

$$\prod_{\zeta\in H_K}^{K}\sum_{z=1}^{K}Œ_z''\left(\tilde{\alpha}_{\zeta(z)}^{KH_{\tilde{\alpha}}}\right)=\left\langle\left(e^{-\left(\sum_{\zeta\in H_z}\left(\sum_{z=1}^{K}\left(Œ''\left(-\ln\left(1-e^{-\left(KH_{\tilde{\alpha}}\left(-\ln\left(\overline{TR}_{\zeta(z)}\right)\right)^{\phi}\right)^{\frac{1}{\phi}}}\right)\right)\right)^{\phi}\right)\right)^{\frac{1}{\phi}}}\right),\right.$$

$$\left(1-e^{-\left(\sum_{\zeta\in H_z}\left(\sum_{z=1}^{K}\left(Œ''\left(-\ln\left(1-e^{-\left(KH_{\tilde{\alpha}}\left(-\ln\left(1-\overline{IN}_{\zeta(z)}\right)\right)^{\phi}\right)^{\frac{1}{\phi}}}\right)\right)\right)^{\phi}\right)\right)^{\frac{1}{\phi}}}\right),\left(1-e^{-\left(\sum_{\zeta\in H_z}\left(\sum_{z=1}^{K}\left(Œ''\left(-\ln\left(1-e^{-\left(KH_{\tilde{\alpha}}\left(-\ln\left(1-\overline{FL}_{\zeta(z)}\right)\right)^{\phi}\right)^{\frac{1}{\phi}}}\right)\right)\right)^{\phi}\right)\right)^{\frac{1}{\phi}}}\right)\right\rangle.$$

Furthermore,

$$\left(\prod_{\zeta\in H_K}^{K}\sum_{z=1}^{K}Œ_z''\left(\tilde{\alpha}_{\zeta(z)}^{KH_{\tilde{\alpha}}}\right)\right)^{\frac{1}{K!}}=\left\langle\left(e^{-\left(\frac{1}{K!}\left(\sum_{\zeta\in H_n}\left(\sum_{z=1}^{K}\left(Œ_z''\left(-\ln\left(1-e^{-\left(KH_{\tilde{\alpha}}\left(-\ln\left(\overline{TR}_{\zeta(z)}\right)\right)^{\phi}\right)^{\frac{1}{\phi}}}\right)\right)\right)^{\phi}\right)\right)\right)^{\frac{1}{\phi}}}\right),\right.$$

$$\left(1-e^{-\left(\frac{1}{K!}\left(\sum_{\zeta\in H_z}\left(\sum_{z=1}^{K}\left(Œ_z''\left(-\ln\left(1-e^{-\left(KH_{\tilde{\alpha}}\left(-\ln\left(1-\overline{IN}_{\zeta(z)}\right)\right)^{\phi}\right)^{\frac{1}{\phi}}}\right)\right)\right)^{\phi}\right)\right)\right)^{\frac{1}{\phi}}}\right),\left(1-e^{-\left(\frac{1}{K!}\left(\sum_{\zeta\in H_z}\left(\sum_{z=1}^{K}\left(Œ_z''\left(-\ln\left(1-e^{-\left(KH_{\tilde{\alpha}}\left(-\ln\left(1-\overline{FL}_{\zeta(z)}\right)\right)^{\phi}\right)^{\frac{1}{\phi}}}\right)\right)\right)^{\phi}\right)\right)\right)^{\frac{1}{\phi}}}\right)\right\rangle;$$

Thus,

$$\frac{1}{\sum_{z=1}^{K}\text{Œ}''_j}\left(\prod_{\zeta\in H_{\Xi}}\sum_{z=1}^{K}\text{Œ}''_z\left(\Xi_{\zeta(z)}\right)^{H_{\Xi}(\zeta)}\right)^{\frac{1}{K!}}=\left\langle\left(1-e^{-\left(\frac{1}{\sum_{z=1}^{K}\text{Œ}''_z}\left(\frac{1}{K!}\left(\sum_{\zeta\in H_{\Xi}}\left(\prod_{j=1}^{n}\left(\text{Œ}''_z\left(-\ln\left(1-e^{-\left(zK_z\left(-\ln\left(\overline{TR}_{\zeta(z)}\right)\right)^{\phi}\right)^{\frac{1}{\phi}}}\right)\right)\right)^{H_{\Xi}(\zeta)}\right)\right)\right)^{\phi}\right)^{\frac{1}{\phi}}}\right)\right.\right.$$

$$\left.\left(e^{-\left(\frac{1}{\sum_{z=1}^{K}\text{Œ}''_z}\left(\frac{1}{K!}\left(\sum_{\zeta\in H_{\Xi}}\left(\prod_{j=1}^{n}\left(\text{Œ}''_z\left(-\ln\left(1-e^{-\left(zK_z\left(-\ln\left(\overline{IN}_{\zeta(z)}\right)\right)^{\phi}\right)^{\frac{1}{\phi}}}\right)\right)\right)^{H_{\Xi}(\zeta)}\right)\right)\right)^{\phi}\right)^{\frac{1}{\phi}}}\right),\left(e^{-\left(\frac{1}{\sum_{z=1}^{K}\text{Œ}''_z}\left(\frac{1}{K!}\left(\sum_{\zeta\in H_{\Xi}}\left(\prod_{j=1}^{n}\left(\text{Œ}''_z\left(-\ln\left(1-e^{-\left(zK_z\left(-\ln\left(\overline{FL}_{\zeta(z)}\right)\right)^{\phi}\right)^{\frac{1}{\phi}}}\right)\right)\right)^{H_{\Xi}(\zeta)}\right)\right)\right)^{\phi}\right)^{\frac{1}{\phi}}}\right)\right\rangle;$$

Hence,

$$S^{V}NAAPDMM^{(\text{Œ}'')}\left(\Xi_1,\Xi_2,...,\Xi_z\right)=\left\langle\left(1-e^{-\left(\frac{1}{\sum_{z=1}^{K}\text{Œ}''_z}\left(\frac{1}{K!}\left(\sum_{\zeta\in H_{\Xi}}\left(\prod_{j=1}^{n}\left(\text{Œ}''_z\left(-\ln\left(1-e^{-\left(zK_z\left(-\ln\left(\overline{TR}_{\zeta(z)}\right)\right)^{\phi}\right)^{\frac{1}{\phi}}}\right)\right)\right)^{H_{\Xi}(\zeta)}\right)\right)\right)^{\phi}\right)^{\frac{1}{\phi}}}\right)\right.\right.$$

$$\left.\left(e^{-\left(\frac{1}{\sum_{z=1}^{K}\text{Œ}''_z}\left(\frac{1}{K!}\left(\sum_{\zeta\in H_{\Xi}}\left(\prod_{j=1}^{n}\left(\text{Œ}''_z\left(-\ln\left(1-e^{-\left(zK_z\left(-\ln\left(\overline{IN}_{\zeta(z)}\right)\right)^{\phi}\right)^{\frac{1}{\phi}}}\right)\right)\right)^{H_{\Xi}(\zeta)}\right)\right)\right)^{\phi}\right)^{\frac{1}{\phi}}}\right),\left(e^{-\left(\frac{1}{\sum_{z=1}^{K}\text{Œ}''_z}\left(\frac{1}{K!}\left(\sum_{\zeta\in H_{\Xi}}\left(\prod_{j=1}^{n}\left(\text{Œ}''_z\left(-\ln\left(1-e^{-\left(zK_z\left(-\ln\left(\overline{FL}_{\zeta(z)}\right)\right)^{\phi}\right)^{\frac{1}{\phi}}}\right)\right)\right)^{H_{\Xi}(\zeta)}\right)\right)\right)^{\phi}\right)^{\frac{1}{\phi}}}\right)\right\rangle.$$

Theorem 5. (Idempotency) Let $\Xi_z=\langle\overline{TR}_z,\overline{IN}_z,\overline{FL}_z\rangle(z=1,2,...,K)$ be a set of SVNNs, if $\Xi_z=\Xi=\langle\overline{TR},\overline{IN},\overline{FL}\rangle(z=1,2,...,K)$ holds for all z, then

$$S^{V}NAAPDMM^{(\text{Œ}'')}\left(\Xi_1,\Xi_2,...,\Xi_z\right)=\Xi. \tag{32}$$

Theorem 6. Let $\Xi_z=\langle\overline{TR}_z,\overline{IN}_z,\overline{FL}_z\rangle(z=1,2,...,K)$ be a series of SVNNs. Then

$$\Xi^{-}\le SVNAAPDMM^{(\text{Œ}'')}\left(\Xi_1,\Xi_2,...,\Xi_n\right)\le\Xi^{+}, \tag{33}$$

where

$\Xi^{-}=\left\langle\min_{z=1}^{K}\overline{TR}_z,\max_{z=1}^{K}\overline{IN}_z,\max_{z=1}^{K}\overline{FL}_z\right\rangle$ and $\Xi^{+}=\left\langle\max_{z=1}^{K}\overline{TR}_z,\min_{z=1}^{K}\overline{IN}_z,\min_{z=1}^{K}\overline{FL}_z\right\rangle$.

Subsequently, we will deliberate some special cases of SVNAAPDMM with respect to the parameters $\text{Œ}''$ *and* Φ.

Case 1. If $\text{Œ}''=(1,0,0,...,0)$, then the SVNAAPDMM operator relegates to the SVNAAPG operator, that is

$$S^{V}NAAPDMM^{(1,0,0,...,0)}\left(\Xi_1,\Xi_2,...,\Xi_K\right)=\left\langle e^{-\left(\sum_{z=1}^{K}H_{\Xi}\left(-\ln\overline{TR}_z\right)^{\Phi}\right)^{\frac{1}{\Phi}}},1-e^{-\left(\sum_{z=1}^{K}H_{\Xi}\left(-\ln\left(1-\overline{IN}_z\right)\right)^{\Phi}\right)^{\frac{1}{\Phi}}},1-e^{-\left(\sum_{z=1}^{K}H_{\Xi}\left(-\ln\left(1-\overline{FL}_z\right)\right)^{\Phi}\right)^{\frac{1}{\Phi}}}\right\rangle$$
$$=\prod_{z=1}^{K}\Xi_z^{H_{\Xi}}. \tag{34}$$

In this case, if $Spt\left(\Xi_i,\Xi_z\right)=g$ for all $i\neq z$, then the SVNAAPDMM operator relegates to the SVN geometric operator. i.e.,

$$S^{V}NAAPDMM^{(1,0,0,\ldots,0)}\left(\underline{\&}_1,\underline{\&}_2,\ldots,\underline{\&}_K\right)=\left\langle e^{-\left(\sum_{z=1}^{K}\frac{1}{K}\left(-\ln\overline{TR}_z\right)^{\Phi}\right)^{\frac{1}{\Phi}}},1-e^{-\left(\sum_{z=1}^{k}\frac{1}{K}\left(-\ln\left(1-\overline{IN}_z\right)\right)^{\Phi}\right)^{\frac{1}{\Phi}}},1-e^{-\left(\sum_{z=1}^{k}\frac{1}{K}\left(-\ln\left(1-\overline{FL}_z\right)\right)^{\Phi}\right)^{\frac{1}{\Phi}}}\right\rangle$$
$$=\left(\prod_{z=1}^{K}\underline{\&}_z\right)^{\frac{1}{K}}. \tag{35}$$

Case 2. If $\text{Œ}''=(1,1,0,\ldots,0)$, then the SVNAAPDMM operator relegates to the SVN power geometric Bonferroni mean (SVNPGBM) operator. i.e.,

$$S^{V}NAAPDMM^{(1,1,0,\ldots,0)}\left(\underline{\&}_1,\underline{\&}_2,\ldots,\underline{\&}_K\right)$$
$$=\left\langle\left(1-e^{-\left(\frac{1}{2}\left(\frac{1}{K(K-1)}\right)\left(\sum_{i=1,z=1,i\neq z}^{K}\left(1*\left(-\ln\left(1-e^{-\left(KH_{\&}\left(-\ln\left(\overline{TR}_i\right)\right)^{\Phi}\right)^{\frac{1}{\Phi}}}\right)\right)^{\Phi}\right)+\left(1*\left(-\ln\left(1-e^{-\left(KH_{\&}\left(-\ln\left(\overline{TR}_z\right)\right)^{\Phi}\right)^{\frac{1}{\Phi}}}\right)\right)^{\Phi}\right)\right)\right)^{\frac{1}{\Phi}}}\right),\right.$$
$$\left(e^{-\left(\frac{1}{2}\left(\frac{1}{K(K-1)}\right)\left(\sum_{i=1,z=1,i\neq z}^{K}\left(1*\left(-\ln\left(1-e^{-\left(KH_{\&}\left(-\ln\left(1-\overline{IN}_z\right)\right)^{\Phi}\right)^{\frac{1}{\Phi}}}\right)\right)^{\Phi}\right)+\left(1*\left(-\ln\left(1-e^{-\left(KH_{\&}\left(-\ln\left(1-\overline{IN}_z\right)\right)^{\Phi}\right)^{\frac{1}{\Phi}}}\right)\right)^{\Phi}\right)\right)\right)^{\frac{1}{\Phi}}}\right), \tag{36}$$
$$\left.\left(e^{-\left(\frac{1}{2}\left(\frac{1}{K(K-1)}\right)\left(\sum_{i=1,z=1,i\neq z}^{K}\left(1*\left(-\ln\left(1-e^{-\left(KH_{\&}\left(-\ln\left(1-\overline{FL}_z\right)\right)^{\Phi}\right)^{\frac{1}{\Phi}}}\right)\right)^{\Phi}\right)+\left(1*\left(-\ln\left(1-e^{-\left(KH_{\&}\left(-\ln\left(1-\overline{FL}_z\right)\right)^{\Phi}\right)^{\frac{1}{\Phi}}}\right)\right)^{\Phi}\right)\right)\right)^{\frac{1}{\Phi}}}\right)\right\rangle$$
$$=\left(\frac{1}{2}\prod_{\substack{i,z=1\\i\neq z}}^{K}\left(\underline{\&}_i^{KH_{\&}}\oplus\underline{\&}_z^{KH_{\&}}\right)\right)^{\frac{1}{K(K-1)}}.$$

In this case, if $Spt\left(\underline{\&}_i,\underline{\&}_z\right)=g$ f 0 for all $i\neq z$, then the SVNAAPDMM operator relegates to the SVNAA geometric Bonferroni mean (SVNAAGBM) operator. i.e.,

$$S^{V}NAAPDMM^{(1,1,0,\ldots,0)}\left(\underline{\&}_1,\underline{\&}_2,\ldots,\underline{\&}_K\right)=\left\langle\left(1-e^{-\left(\frac{1}{2}\left(\frac{1}{K(K-1)}\right)\left(\sum_{i=1,z=1,i\neq z}^{K}\left(1*\left(-\ln\left(1-\overline{TR}_i\right)\right)^{\Phi}\right)+\left(1*\left(-\ln\left(1-\overline{TR}_z\right)\right)^{\Phi}\right)\right)\right)^{\frac{1}{\Phi}}}\right),\right.$$
$$\left(e^{-\left(\frac{1}{2}\left(\frac{1}{K(K-1)}\right)\left(\sum_{i=1,z=1,i\neq z}^{K}\left(1*\left(-\ln\left(\overline{IN}_i\right)\right)^{\Phi}+\left(1*\left(-\ln\left(\overline{IN}_z\right)\right)^{\Phi}\right)\right)\right)^{\frac{1}{\Phi}}}\right),\left(e^{-\left(\frac{1}{2}\left(\frac{1}{K(K-1)}\right)\left(\sum_{i=1,z=1,i\neq z}^{K}\left(1*\left(-\ln\left(\overline{FL}_i\right)\right)^{\Phi}+\left(1*\left(-\ln\left(\overline{FL}_z\right)\right)^{\Phi}\right)\right)\right)^{\frac{1}{\Phi}}}\right)\right\rangle \tag{37}$$
$$=\left(\frac{1}{2}\prod_{z=1}^{K}\underline{\&}_i\oplus\underline{\&}_z\right)^{\frac{1}{K(K-1)}}.$$

Case 3. If $\text{Œ}''=\left(\begin{matrix}\overbrace{1,1,1,\ldots,1}^{K-k},\overbrace{0,0,0,\ldots,0}^{k}\end{matrix}\right)$, then the SVNAAPDMM operator deteriorates to the SVNAAP dual MSM (SVNAAPDMSM) operator, i.e,

$$S^{V}NAAPDMM^{\left(\begin{matrix}\overbrace{1,1,1,\ldots,1}^{K-k},\overbrace{0,0,0,\ldots,0}^{k}\end{matrix}\right)}\left(\underline{\&}_1,\underline{\&}_2,\ldots,\underline{\&}_K\right)=\left\langle\left(1-e^{-\left(\frac{1}{k}\left(\frac{1}{C_K^k}\left(\sum_{1\le i_1<i_2<\ldots<i_K}\left(\sum_{z=1}^{k}\left(-\ln\left(1-e^{-\left(KH_{\&_z}\left(-\ln\left(\overline{TR}_{i_z}\right)\right)^{\Phi}\right)^{\frac{1}{\Phi}}}\right)\right)^{\Phi}\right)\right)\right)^{\frac{1}{\Phi}}}\right),\right.$$
$$\left(e^{-\left(\frac{1}{k}\left(\frac{1}{C_K^k}\left(\sum_{1\le i_1<i_2<\ldots<i_K}\left(\sum_{z=1}^{k}\left(-\ln\left(1-e^{-\left(KH_{\&_z}\left(-\ln\left(1-\overline{IN}_{i_z}\right)\right)^{\Phi}\right)^{\frac{1}{\Phi}}}\right)\right)^{\Phi}\right)\right)\right)^{\frac{1}{\Phi}}}\right),\left(e^{-\left(\frac{1}{k}\left(\frac{1}{C_K^k}\left(\sum_{1\le i_1<i_2<\ldots<i_K}\left(\sum_{z=1}^{k}\left(-\ln\left(1-e^{-\left(KH_{\&_z}\left(-\ln\left(1-\overline{FL}_{i_z}\right)\right)^{\Phi}\right)^{\frac{1}{\Phi}}}\right)\right)^{\Phi}\right)\right)\right)^{\frac{1}{\Phi}}}\right)\right\rangle \tag{38}$$
$$=\frac{1}{k}\left(\prod_{1\le i_1<i_2<\ldots<i_K}\sum_{z=1}^{K}\left(\underline{\&}_{i_z}^{KH_{\&_z}}\right)\right)^{\frac{1}{C_K^k}}.$$

In this case, if $Spt\left(\underline{\tilde{\alpha}}_i, \underline{\tilde{\alpha}}_z\right) = g$ f 0 for all $i \neq z$,, then the SVNAADMM operator deteriorates to the SVNAADMSM operator. i.e.,

$$S^V NAAPDMM^{\left(\overbrace{1,1,1,\ldots,1}^{K},\overbrace{0,0,0,\ldots,0}^{K-k}\right)}\left(\underline{\tilde{\alpha}}_1, \underline{\tilde{\alpha}}_2, \ldots, \underline{\tilde{\alpha}}_K\right) = \left\langle \left(1-e^{-\left(\frac{1}{k}\left(\frac{1}{C_K^k}\left(\sum_{i_1 p i_2 p \ldots p i_K}\left(\sum_{z=1}^{n}\left(-\ln\left(1-\overline{TR}_{i_z}\right)\right)^{\Phi}\right)\right)\right)\right)^{\frac{1}{\Phi}}}\right), \left(e^{-\left(\frac{1}{k}\left(\frac{1}{C_K^k}\left(\sum_{i_1 p i_2 p \ldots p i_K}\left(\sum_{z=1}^{k}\left(-\ln \overline{IN}_{i_z}\right)^{\Phi}\right)\right)\right)\right)^{\frac{1}{\Phi}}}\right), \left(e^{-\left(\frac{1}{k}\left(\frac{1}{C_K^k}\left(\sum_{i_1 p i_2 p \ldots p i_K}\left(\sum_{z=1}^{k}\left(-\ln \overline{FL}_{i_z}\right)^{\Phi}\right)\right)\right)\right)^{\frac{1}{\Phi}}}\right) \right\rangle = \left(\frac{1}{k}\left(\prod_{1\leq i_1<i_2<\ldots,<i_K}^{K}\left(\underline{\tilde{\alpha}}_{i_z}\right)\right)^{\frac{1}{C_K^k}}\right) \tag{39}$$

Case 4. If $\mathcal{E}'' = (1,1,1,\ldots,1)$ *or* $\left(\frac{1}{K}, \frac{1}{K}, \frac{1}{K}, \ldots, \frac{1}{K}\right)$, then the SVNAAPDMM operator deteriorates to the following form:

$$S^V NAAPDMM^{\mathcal{E}''=(1,1,1,\ldots,1)\ or\left(\frac{1}{K},\frac{1}{K},\frac{1}{K},\ldots,\frac{1}{K}\right)}\left(\underline{\tilde{\alpha}}_1, \underline{\tilde{\alpha}}_2, \ldots, \underline{\tilde{\alpha}}_K\right) = \left\langle \left(1-e^{-\left(\sum_{z=1}^{K}\left(\mathcal{E}_z''\left(-\ln\left(1-e^{-\left(\frac{KH_z}{\tilde{\alpha}}\left(-\ln\left(\overline{TR}_{\zeta(z)}\right)\right)^{\phi}\right)^{\frac{1}{\phi}}}\right)\right)^{\phi}\right)\right)^{\frac{1}{\phi}}}\right), \left(e^{-\left(\sum_{z=1}^{K}\left(\mathcal{E}_z''\left(-\ln\left(1-e^{-\left(\frac{KH_z}{\tilde{\alpha}}\left(-\ln\left(1-\overline{IN}_{\zeta(z)}\right)\right)^{\phi}\right)^{\frac{1}{\phi}}}\right)\right)^{\phi}\right)\right)^{\frac{1}{\phi}}}\right), \left(e^{-\left(\sum_{z=1}^{K}\left(\mathcal{E}_z''\left(-\ln\left(1-e^{-\left(\frac{KH_z}{\tilde{\alpha}}\left(-\ln\left(1-\overline{FL}_{\zeta(z)}\right)\right)^{\phi}\right)^{\frac{1}{\phi}}}\right)\right)^{\phi}\right)\right)^{\frac{1}{\phi}}}\right) \right\rangle = \left(\sum_{z=1}^{K}\frac{1}{K}\Xi_z^{\frac{KH_z}{\tilde{\alpha}}}\right). \tag{40}$$

In this case, if $Spt\left(\underline{\tilde{\alpha}}_i, \underline{\tilde{\alpha}}_z\right) = g$ f 0 for all $i \neq z$, then the SVNAAMM operator deteriorates to the SVNAA average operator. i.e.,

$$S^V NAAPDMM^{\mathcal{E}''=(1,1,1,\ldots,1)\ or\left(\frac{1}{K},\frac{1}{K},\frac{1}{K},\ldots,\frac{1}{K}\right)}\left(\underline{\tilde{\alpha}}_1, \underline{\tilde{\alpha}}_2, \ldots, \underline{\tilde{\alpha}}_K\right) = \left\langle \left(1-e^{-\left(\sum_{z=1}^{K}\frac{1}{K}\left(-\ln\left(1-\overline{TR}_z\right)\right)^{\Phi}\right)^{\frac{1}{\Phi}}}\right), \left(e^{-\left(\sum_{z=1}^{K}\frac{1}{K}\left(-\ln \overline{IN}_z\right)^{\Phi}\right)^{\frac{1}{\Phi}}}\right), \left(e^{-\left(\sum_{z=1}^{K}\frac{1}{K}\left(-\ln \overline{FL}_z\right)^{\Phi}\right)^{\frac{1}{\Phi}}}\right) \right\rangle = \sum_{z=1}^{K}\frac{1}{K}\left(\underline{\tilde{\alpha}}_z\right). \tag{41}$$

4. The Single Valued Neutrosophic Aczel-Alsina Power Weighted Muirhead Mean and Power Weighted Dual Muir-Head Mean Operators

In this part, the SVNAAPWMM and SVNAAPWDMM operators are suggested.

Definition 10. Let $\underline{\tilde{\alpha}}_z = \left\langle \overline{TR}_z, \overline{IN}_z, \overline{FL}_z \right\rangle (z = 1,2,\ldots,K)$ be series of SVNNs, and $\mathcal{E}'' = (\mathcal{E}_1'', \mathcal{E}_2'', \ldots, \mathcal{E}_K'') \in R^K$ be a group of parameters. Let $\tilde{\Pi} = \left(\tilde{\Pi}_1, \tilde{\Pi}_2, \ldots, \tilde{\Pi}_n\right)^T$ be the importance degree, such that $0 \leq \tilde{\Pi}_z \leq 1$ and $\sum_{z=1}^{K}\tilde{\Pi}_z = 1$. The single valued neutrosophic Aczel-Alsina power weighted Muirhead mean (SVNAAPWMM) operator is conveyed as

$$S^V NAAPMM^{\mathcal{E}_z''}\left(\underline{\tilde{\alpha}}_1, \underline{\tilde{\alpha}}_2, \ldots, \underline{\tilde{\alpha}}_K\right) = \left(\frac{1}{K!}\sum_{\zeta\in H_k}\prod_{z=1}^{K}\left(K\frac{\tilde{\Pi}_{\zeta(z)}\left(1+T\left(\underline{\tilde{\alpha}}_{\zeta(z)}\right)\right)}{\sum_{z=1}^{K}\tilde{\Pi}_{\zeta(z)}\left(1+T\left(\underline{\tilde{\alpha}}_z\right)\right)}\underline{\tilde{\alpha}}_{\zeta(z)}\right)^{\mathcal{E}_z''}\right)^{\frac{1}{\sum_{z=1}^{K}\mathcal{E}_z''}}, \tag{42}$$

where

$$T\left(\underline{\tilde{\alpha}}_j\right) = \sum_{z=1}^{K} Spt\left(\underline{\tilde{\alpha}}_i, \underline{\tilde{\alpha}}_z\right) \tag{43}$$

and

$$Spt\left(\Xi_i, \Xi_z\right) = 1 - D\left(\Xi_i, \Xi_z\right), \tag{44}$$

$\zeta(z)\left(z = 1, 2, ..., K\right)$ signifies any arrangement of $(1, 2, ..., K)$. H_n signifies all possible arrangements of $(1, 2, ..., K)$, and K is the balancing coefficient $D\left(\Xi_i, \Xi_j\right)$ denotes the Hamming distance among two SVNNs Ξ_i and Ξ_z, and $Spt\left(\Xi_i, \Xi_z\right)$ is the support for Ξ_i from Ξ_z sustaining the axioms given in Definition 6.

To write Equation (42), in simplified form, let

$$H_j = \frac{\Pi_j\left(1 + T\left(\Xi_z\right)\right)}{\sum_{z=1}^{K} \Pi_j\left(1 + T\left(\Xi_z\right)\right)}, \tag{45}$$

then, Equation (42) can be written in simplified form as,

$$S^{V}NAAPWMM^{(\mathcal{E}'')}\left(\Xi_1, \Xi_2, ..., \Xi_K\right) = \left(\frac{1}{K!}\sum_{\zeta \in H_K}\prod_{z=1}^{K}\left(KH_z \Xi_{\zeta(z)}\right)^{\mathcal{E}_z''}\right)^{\frac{1}{\sum_{z=1}^{K}\mathcal{E}_z''}}, \tag{46}$$

Where $\sum_{z=1}^{K} H_z = 1$ and $0 \le H_z \le 1$.

According to Definition 10, the following Theorem 7, can be obtained.

Theorem 7. Let $\Xi_z = \left\langle \overline{TR}_z, \overline{IN}_z, \overline{FL}_z \right\rangle \left(z = 1, 2, ..., K\right)$ be a group of SVNNs, the aggregated value by the SVNAAPWMM operator is still a SVNN and

$$S^{V}NAAPWMM^{(\mathcal{E}'')}\left(\Xi_1, \Xi_2, ..., \Xi_K\right) = \left\langle \left(e^{-\left(\frac{1}{\sum_{z=1}^{K}\mathcal{E}_z''}\left(\frac{1}{K!}\left(\sum_{\zeta \in H_K}\left(\sum_{z=1}^{K}\left(\mathcal{E}_j''\left(-\ln\left(1 - e^{-\left(KH_z\left(-\ln\left(1-\overline{TR}_{\zeta(z)}\right)\right)^{\Phi}\right)^{\frac{1}{\Phi}}}\right)\right)\right)\right)\right)\right)\right)^{\frac{1}{\Phi}}}\right), \right.$$
$$\left(1 - e^{-\left(\frac{1}{\sum_{z=1}^{K}\mathcal{E}_z''}\left(\frac{1}{K!}\left(\sum_{\zeta \in H_K}\left(\sum_{z=1}^{K}\left(\mathcal{E}_j''\left(-\ln\left(1 - e^{-\left(KH_z\left(-\ln\left(\overline{IN}_{\zeta(z)}\right)\right)^{\Phi}\right)^{\frac{1}{\Phi}}}\right)\right)\right)\right)\right)\right)\right)^{\frac{1}{\Phi}}}\right), \tag{47}$$
$$\left. \left(1 - e^{-\left(\frac{1}{\sum_{z=1}^{K}\mathcal{E}_z''}\left(\frac{1}{K!}\left(\sum_{\zeta \in H_K}\left(\sum_{z=1}^{K}\left(\mathcal{E}_j''\left(-\ln\left(1 - e^{-\left(KH_z\left(-\ln\left(\overline{FL}_{\zeta(z)}\right)\right)^{\Phi}\right)^{\frac{1}{\Phi}}}\right)\right)\right)\right)\right)\right)\right)^{\frac{1}{\Phi}}}\right) \right\rangle.$$

Definition 11. Let $\Xi_z = \left\langle \overline{TR}_z, \overline{IN}_z, \overline{FL}_z \right\rangle \left(z = 1, 2, ..., K\right)$ be series of SVNNs, and $\mathcal{E}'' = \left(\mathcal{E}_1'', \mathcal{E}_2'', ..., \mathcal{E}_n''\right) \in R^n$ be a group of parameters. Let $\Pi = \left(\Pi_1, \Pi_2, ..., \Pi_K\right)^T$ be the importance degree, such that $0 \le \Pi_K \le 1$ and $\sum_{z=1}^{K} \Pi_z = 1$.

The single valued neutrosophic Aczel-Alsina power weighted dual Muirhead mean (SVNAAPWDMM) operator is conveyed as

$$S^{V}NAAPWDMM^{(\mathcal{E}'')}\left(\Xi_1, \Xi_2, ..., \Xi_K\right) = \frac{1}{\sum_{z=1}^{K}\mathcal{E}_z''}\left(\prod_{\zeta \in H_K}\sum_{z=1}^{K}\left(\mathcal{E}_z''\Xi_{\zeta(z)}^{\frac{K\Pi_z\left(1+T\left(\Xi_{\zeta(z)}\right)\right)}{\sum_{z=1}^{K}\Pi_j\left(1+T\left(\Xi_z\right)\right)}}\right)\right)^{\frac{1}{K!}}, \tag{48}$$

where

$$T_{\&}\left(\Xi_j^{\&}\right)=\sum_{z=1}^{K} Spt\left(\Xi_i^{\&},\Xi_z^{\&}\right) \tag{49}$$

and

$$Spt\left(\Xi_i^{\&},\Xi_z^{\&}\right)=1-D^{\&}\left(\Xi_i^{\&},\Xi_z^{\&}\right), \tag{50}$$

$\zeta(z)\left(z=1,2,...,K\right)$ signifies any arrangement of $(1,2,...,K)$. H_n signifies all possible arrangements of $(1,2,...,K)$, and K is the balancing coefficient $D^{\&}\left(\Xi_i^{\&},\Xi_z^{\&}\right)$ denotes the Hamming distance among two SVNNs $\Xi_i^{\&}$ and $\Xi_z^{\&}$, and $Spt\left(\Xi_i^{\&},\Xi_z^{\&}\right)$ is the support for $\Xi_i^{\&}$ from $\Xi_z^{\&}$ satisfying the axioms given in Definition 6.

To write Equation (48), in simplified form, let

$$H_{\&}^{z}=\frac{H_z^{\%}\left(1+T_{\&}\left(\Xi_z^{\&}\right)\right)}{\sum_{z=1}^{K} H_z^{\%}\left(1+T_{\&}\left(\Xi_z^{\&}\right)\right)}; \tag{51}$$

then, Equation (48) can be written in simplified form as,

$$S^{V}NAAPWDMM^{(\Omega'')}\left(\Xi_1^{\&},\Xi_2^{\&},...,\Xi_K^{\&}\right)=\frac{1}{\sum_{z=1}^{K}\Omega_z''}\left(\prod_{\zeta\in H_K}\sum_{z=1}^{K}\left(\Omega_z''\Xi_{\zeta(z)}^{KH_{\&}^{z}}\right)\right)^{\frac{1}{K!}}, \tag{52}$$

Where $\sum_{z=1}^{K} H_{\&}^{z}=1$ and $0\le H_{\&}^{z}\le 1$.

According to Definition 11, the following Theorem 8, can be obtained.

Theorem 8. Let $\Xi_z^{\&}=\left\langle\overline{TR}_z,\overline{IN}_z,\overline{FL}_z\right\rangle\left(z=1,2,...,K\right)$ be a group of SVNNs, the aggregated value by the SVNAAPWDMM operator is still a SVNN and

$$S^{V}NAAPWDMM^{(\Omega'')}\left(\Xi_1^{\&},\Xi_2^{\&},...,\Xi_K^{\&}\right)=\left\langle\left(1-e^{-\left(\frac{1}{\sum_{z=1}^{K}\Omega_z''}\left(\frac{1}{K!}\left(\sum_{\zeta\in H_n}\left(\sum_{z=1}^{K}\left(\Omega_z''\left(-\ln\left(1-e^{-\left(KH_{\&}^{z}\left(-\ln\left(\overline{TR}_{\zeta(z)}\right)\right)^{\phi}\right)^{\frac{1}{\phi}}}\right)\right)\right)\right)\right)\right)^{\phi}\right)^{\frac{1}{\phi}}}\right),\right.$$
$$\left.\left(e^{-\left(\frac{1}{\sum_{z=1}^{K}\Omega_z''}\left(\frac{1}{K!}\left(\sum_{\zeta\in H_z}\left(\sum_{z=1}^{K}\left(\Omega_z''\left(-\ln\left(1-e^{-\left(KH_{\&}^{z}\left(-\ln\left(1-\overline{IN}_{\zeta(z)}\right)\right)^{\phi}\right)^{\frac{1}{\phi}}}\right)\right)\right)\right)\right)\right)^{\phi}\right)^{\frac{1}{\phi}}}\right),\left(e^{-\left(\frac{1}{\sum_{z=1}^{K}\Omega_z''}\left(\frac{1}{K!}\left(\sum_{\zeta\in H_z}\left(\sum_{z=1}^{K}\left(\Omega_z''\left(-\ln\left(1-e^{-\left(KH_{\&}^{z}\left(-\ln\left(1-\overline{FL}_{\zeta(z)}\right)\right)^{\phi}\right)^{\frac{1}{\phi}}}\right)\right)\right)\right)\right)\right)^{\phi}\right)^{\frac{1}{\phi}}}\right)\right\rangle. \tag{53}$$

5. A Methodology to Multiple Attribute Decision Making Based on The Single Valued Neutrosophic Aczel-Alsina Power Weighted Muirhead Mean Operators

The applications of these operators in the MADM will be covered in this section.

For a MADM situation with SVNs that includes z workable alternatives $\overline{\overline{C}}_{\mathrm{i}}=\left(\overline{\overline{C}}_1,\overline{\overline{C}}_2,...,\overline{\overline{C}}_{\mathrm{z}}\right)(\mathrm{i}=1,2,...,\mathrm{z})$ and s attributes $\overline{\overline{T}}_{\mathrm{j}}=\left(\overline{\overline{T}}_1,\overline{\overline{T}}_2,,,\overline{\overline{T}}_{\mathrm{s}}\right)(\mathrm{j}=1,2,...,\mathrm{s})$, and $F=\{F_1,F_2,F_3,...,F_z\}$ is the importance degree of the attributes for which the weight vectors of attributes are defined in $F_s\left(j=1,2,3,...,s\right)$, where $F_j\ge 0,\ j=1,...,s,\sum_{j=1}^{s}F_j=1$

Assume that $Y=\left[\overline{\overline{B}}_{ij}\right]_{m\times n}$ is the decision matrix, where $\overline{\overline{B}}_{ij}=\left\langle \overline{\overline{TR}}_{ij},\overline{\overline{IN}}_{ij},\overline{\overline{FL}}_{ij}\right\rangle$ acquires the structure of SVNN for the alternative $\overline{\overline{C}}_{i}$ with respect to the attribute $\overline{\overline{T}}_{j}(i=1,...,z;j=1,....,s)$. The rating of alternative is then necessary.

Afterwards, we address the MADM problems using the SVNAAPWMM and SVNAAPWDMM operators. The specific decision-making processes are listed below.

Step 1. Confirm that the attribute values are comparable. In real-life situations, attributes often come in two distinguishes: cost type and benefit type. The following formula must be used to convert attribute values from cost type to benefit type to obtain the desired result:

$$\overline{\overline{B}}_{ij}=\begin{cases}\overline{\overline{B}}_{ij} & \text{for benefit type;}\\ \left(\overline{\overline{B}}_{ij}\right)^{c} & \text{for cost type.}\end{cases} \tag{54}$$

Step 2. Determine the supports utilizing the following formula:

$$spt\left(\overline{\overline{B}}_{ij},\overline{\overline{B}}_{il}\right)=1-\mathop{\mathrm{I\!D}}_{\&}\left(\overline{\overline{B}}_{ij},\overline{\overline{B}}_{il}\right)(i=1,2,...,z;\ j,l=1,2,...,s). \tag{55}$$

Where $\mathop{\mathrm{I\!D}}_{\&}\left(\overline{\overline{B}}_{ij},\overline{\overline{B}}_{il}\right)$ is hamming distance among two SVNNs.

Step 3. Determine $\mathop{T}_{\&}\left(\overline{\overline{B}}_{ij}\right)$ utilizing the following formula:

$$\mathop{T}_{\&}\left(\overline{\overline{B}}_{ij}\right)=\sum_{\substack{l=1\\ j\neq l}}^{s} spt\left(\overline{\overline{B}}_{ij},\overline{\overline{B}}_{il}\right)(i=1,2,...,z;j,l=1,2,...,s)\ . \tag{56}$$

Step 4. Utilizing the SVNAAPWMM operator or SVNAAPWDMM operator, combine all the attribute values $\overline{\overline{B}}_{ij}\left(j=1,2,....,s\right)$ to the comprehensive value $\overline{\overline{C}}_{i}\left(i=1,...,z\right)$ shown as follows:

$$\overline{\overline{C}}_{i}=S^{V}NAAPWMM\left(\overline{\overline{B}}_{i1},\overline{\overline{B}}_{i2},....,\overline{\overline{B}}_{is}\right) \tag{57}$$

Or

$$\overline{\overline{C}}_{i}=S^{V}NAAPWDMM\left(\overline{\overline{B}}_{i1},\overline{\overline{B}}_{i2},....,\overline{\overline{B}}_{is}\right) \tag{58}$$

Step 5. In this step, we determine the score value $\overline{\overline{SOE}}\left(\overline{\overline{B}}_{i}\right)$ of all aggregated information for the assessment of alternative $\overline{\overline{B}}_{i}$ based on the score function of SVNNs described in Definition 2.

Step 6. In this step, using the method of ranking and ordering technique to choose the best desirable alternative after ranking each possible choice $\overline{\overline{C}}_{i}=\left(\overline{\overline{C}}_{1},\overline{\overline{C}}_{2},...,\overline{\overline{C}}_{z}\right)(i=1,2,...,z)$

Step 7. End

6. Illustrative Example

In this part, to demonstrate the approach suggested in this research, we will offer a numerical example adapted from [31] to choose strategic suppliers under supply chain risk with SVNNs.

A panel has five potential strategic suppliers $\overline{\overline{C}}_i\,(i=1,...,5)$ from which to choose. Four attributes are chosen by the experts to assess the five potential strategic suppliers: $\overline{\overline{T}}_1$ stands for "technology level," $\overline{\overline{T}}_2$ for "service level," $\overline{\overline{T}}_3$ for "risk managing ability," and $\overline{\overline{T}}_4$ for "enterprise environment risk." The four aforementioned attributes (their weighting vectors are $F_j=(0.2,\ 0.1,\ 0.3, 0.4)^T$) are to be used by the decision maker to assess the five potential strategic suppliers $\overline{\overline{C}}_i\,(i=1,....,5)$ and provide the assessment information in the form of SVNN as given in Table 1 .

Table 1. The SVN decision matrix

Alternatives/Attributes	$\overline{\overline{T}}_1$	$\overline{\overline{T}}_2$	$\overline{\overline{T}}_3$	$\overline{\overline{T}}_4$
$\overline{\overline{C}}_1$	$\langle 0.5, 0.8, 0.1\rangle$	$\langle 0.6, 0.3, 0.3\rangle$	$\langle 0.3, 0.6, 0.1\rangle$	$\langle 0.5, 0.7, 0.2\rangle$
$\overline{\overline{C}}_2$	$\langle 0.7, 0.2, 0.1\rangle$	$\langle 0.7, 0.2, 0.2\rangle$	$\langle 0.7, 0.2, 0.4\rangle$	$\langle 0.8, 0.2, 0.1\rangle$
$\overline{\overline{C}}_3$	$\langle 0.6, 0.7, 0.2\rangle$	$\langle 0.5, 0.7, 0.3\rangle$	$\langle 0.5, 0.3, 0.1\rangle$	$\langle 0.6, 0.3, 0.2\rangle$
$\overline{\overline{C}}_4$	$\langle 0.8, 0.1, 0.3\rangle$	$\langle 0.6, 0.3, 0.4\rangle$	$\langle 0.3, 0.4, 0.2\rangle$	$\langle 0.5, 0.6, 0.1\rangle$
$\overline{\overline{C}}_5$	$\langle 0.6, 0.4, 0.4\rangle$	$\langle 0.4, 0.8, 0.1\rangle$	$\langle 0.7, 0.6, 0.1\rangle$	$\langle 0.5, 0.8, 0.2\rangle$

Subsequently, we apply the methodology established to choose the best strategic suppliers under supply chain risk.

Step 1. Since all the attributes are of the same type, there is no need to normalize it.

Step 2. Utilizing formula (55) to generate the support. For simplicity, we shall denote $\overline{\overline{S}}_{ij}$ instead of $Spt\left(\overline{\overline{B}}_{ij}^{i},\overline{\overline{B}}_{il}^{i}\right)(i=1,2,3,4,5;\ j,l=1,2,3,4)$. Which are listed below:

$\overline{\overline{S}}_{12}=0.2667, \overline{\overline{S}}_{13}=0.1333, \overline{\overline{S}}_{14}=0.0667, \overline{\overline{S}}_{23}=0.2667, \overline{\overline{S}}_{24}=0.2000, \overline{\overline{S}}_{34}0.1333, \overline{\overline{S}}_{12}=0.0333, \overline{\overline{S}}_{13}=0.1000,$
$\overline{\overline{S}}_{14}=0.0333; \overline{\overline{S}}_{23}=0.0667, \overline{\overline{S}}_{24}=0.0667, \overline{\overline{S}}_{34}=0.1333, \overline{\overline{S}}_{12}=0.0667, \overline{\overline{S}}_{13}=0.2000, \overline{\overline{S}}_{14}=0.1333, \overline{\overline{S}}_{23}=0.2000,$
$\overline{\overline{S}}_{24}=0.2000, \overline{\overline{S}}_{34}=0.0667; \overline{\overline{S}}_{12}=0.1667, \overline{\overline{S}}_{13}=0.3000, \overline{\overline{S}}_{14}=0.3333, \overline{\overline{S}}_{23}=0.2000, \overline{\overline{S}}_{24}=0.2333, \overline{\overline{S}}_{34}=0.1667,$
$\overline{\overline{S}}_{12}=0.3000, \overline{\overline{S}}_{13}=0.2000, \overline{\overline{S}}_{14}=0.2333; \overline{\overline{S}}_{23}=0.1667, \overline{\overline{S}}_{24}=0.0667, \overline{\overline{S}}_{34}=0.1667.$

Step 3. Utilizing formula (56), to generate $\overline{\overline{T}}\left(\overline{\overline{B}}_{ij}\right)$. We shall denote $\overline{\overline{T}}_{ij}$ instead of $\overline{\overline{T}}\left(\overline{\overline{B}}_{ij}\right)$. Which are listed below:

$\overline{\overline{T}}_{11}=0.4667, \overline{\overline{T}}_{12}=0.7333, \overline{\overline{T}}_{13}=0.5333, \overline{\overline{T}}_{14}=0.4000, \overline{\overline{T}}_{21}=0.1667, \overline{\overline{T}}_{22}=0.1667, \overline{\overline{T}}_{23}=0.3000, \overline{\overline{T}}_{24}=0.2333;$
$\overline{\overline{T}}_{31}=0.4000, \overline{\overline{T}}_{32}=0.4667, \overline{\overline{T}}_{33}=0.4667, \overline{\overline{T}}_{34}=0.4000, \overline{\overline{T}}_{41}=0.8000, \overline{\overline{T}}_{42}=0.6000, \overline{\overline{T}}_{43}=0.6667, \overline{\overline{T}}_{44}=0.7333;$
$\overline{\overline{T}}_{51}=0.7333, \overline{\overline{T}}_{52}=0.5333, \overline{\overline{T}}_{53}=0.5333, \overline{\overline{T}}_{54}=0.4667.$

Step 4. Utilizing formulas (57) or (58), to aggregate the comprehensive evaluation information of each alternative. For suitability, we firstly determine the $u_{ij} = \frac{sF_{ij}\left(1+T(\overline{\overline{B}}_{ij})\right)}{\sum_{z=1}^{s} F_z(1+T(\overline{\overline{B}}_z))}$ .Which are given below:

(Assume $\phi = 2, \text{Œ}'' = (0.1, 0.2, 0.3, 0.4)^{\mathrm{T}}$ *)*

$u_{11} = 0.7892, u_{12} = 0.4664, u_{13} = 1.2377, u_{14} = 1.5067, u_{21} = 0.7568, u_{22} = 0.3784, u_{23} = 1.2649, u_{24} = 1.6000;$
$u_{31} = 0.7850, u_{32} = 0.4112, u_{33} = 1.2336, u_{34} = 1.5701, u_{41} = 0.8405, u_{42} = 0.3735, u_{43} = 1.1673, u_{44} = 1.6187;$
$u_{51} = 0.8966, u_{52} = 0.3966, u_{53} = 1.1897, u_{54} = 1.5172.$

$\overline{\overline{B}}_1 = \langle 0.4367, 0.6750, 0.2661\rangle, \overline{\overline{B}}_2 = \langle 0.6552, 0.2553, 0.2885\rangle,$
$\overline{\overline{B}}_3 = \langle 0.5006, 0.6488, 0.2945\rangle; \overline{\overline{B}}_4 = \langle 0.4631, 0.4221, 0.3809\rangle,$
$\overline{\overline{B}}_5 = \langle 0.4632, 0.7381, 0.2703\rangle$

Or

$\overline{\overline{B}}_1 = \langle 0.5465, 0.4405, 0.1436\rangle, \overline{\overline{B}}_2 = \langle 0.7475, 0.1840, 0.1427\rangle,$
$\overline{\overline{B}}_3 = \langle 0.5806, 0.4347, 0.1751\rangle; \overline{\overline{B}}_4 = \langle 0.6718, 0.2191, 0.2050\rangle,$
$\overline{\overline{B}}_5 = \langle 0.5905, 0.5588, 0.1404\rangle$

Step 5. Utilizing the score function suggested in Definition 2, to find the score values comprehensive evaluation information of each alternative.

$\overline{\overline{\text{SOE}}}(\overline{\overline{B}}_1) = 0.4985, \overline{\overline{\text{SOE}}}(\overline{\overline{B}}_2) = 0.7038, \overline{\overline{\text{SOE}}}(\overline{\overline{B}}_3) = 0.5191, \overline{\overline{\text{SOE}}}(\overline{\overline{B}}_4) = 0.5534, \overline{\overline{\text{SOE}}}(\overline{\overline{B}}_5) = 0.4849.$
and
$\overline{\overline{\text{SOE}}}(\overline{\overline{B}}_1) = 0.6541, \overline{\overline{\text{SOE}}}(\overline{\overline{B}}_2) = 0.8069, \overline{\overline{\text{SOE}}}(\overline{\overline{B}}_3) = 0.6569, \overline{\overline{\text{SOE}}}(\overline{\overline{B}}_4) = 0.7493, \overline{\overline{\text{SOE}}}(\overline{\overline{B}}_5) = 0.6304.$

Step 6. According to score values the ranking of the alternatives are $\overline{\overline{B}}_2 \text{ f } \overline{\overline{B}}_4 \text{ f } \overline{\overline{B}}_3 \text{ f } \overline{\overline{B}}_1 \text{ f } \overline{\overline{B}}_5$ and $\overline{\overline{B}}_2 \text{ f } \overline{\overline{B}}_4 \text{ f } \overline{\overline{B}}_3 \text{ f } \overline{\overline{B}}_1 \text{ f } \overline{\overline{B}}_5$

So, the best alternative is $\overline{\overline{B}}_2$, while the worst one is $\overline{\overline{B}}_5$.

6.1. Impact of the parameters ϕ *and* $\text{Œ}''$ *final ranking order*

In this part, the impact of the parameters ϕ and $\text{Œ}''$ are investigated utilizing both the initiated AGOs. For different values of the parameter ϕ the values of the parameter $\text{Œ}'' = (1,1,1,1)^T$ are fixed for utilizing both SVNAAPWMM and SVNAAPWDMM operators and the score values are given in Figure 1 and 2.

From Figure 1 one can see that for different values of the parameters ϕ, utilizing the SVNAAPWMM operators different score values of the alternatives are obtained, but the ranking order remain the same. That is, $\overline{\overline{B}}_2$ is the best alternative and $\overline{\overline{B}}_5$ is worst alternative. one can also noticed from Figure 1, when the values of the parameter ϕ increases the score of the alternatives decreases. From Figure

2, we can see that for different values of the parameters ϕ, utilizing the SVNAAPWDMM operators different score values and different ranking order of the alternatives are obtained. When the values of the parameter $\phi \leq 9$ the best alternative is $\overline{\overline{B}}_2$ and $\overline{\overline{B}}_5$ is worst alternative.

Similarly, when the values of the parameter $\phi \geq 10$, the best alternative is $\overline{\overline{B}}_4$ and $\overline{\overline{B}}_5$ is worst alternative. From Figure 2, we can observe that when the values of the parameter ϕ increases the score of the alternatives increases.

From Figure 3, we can observe that for different values of parameter $\text{Œ}''$ different score values of the alternatives are obtained, and the ranking order remain the same. That is, $\overline{\overline{B}}_2$ is the best alternative and $\overline{\overline{B}}_5$ is worst alternative. By assigning some different values to parameter $\text{Œ}''$, we will get different existing aggregation operators for SVN information. From Figure 4, for different values of the parameter $\text{Œ}''$ utilizing SVNAAPWDMM operator different score values are obtained. Although, $\overline{\overline{B}}_2$ is the best alternative and $\overline{\overline{B}}_5$ is worst alternative.

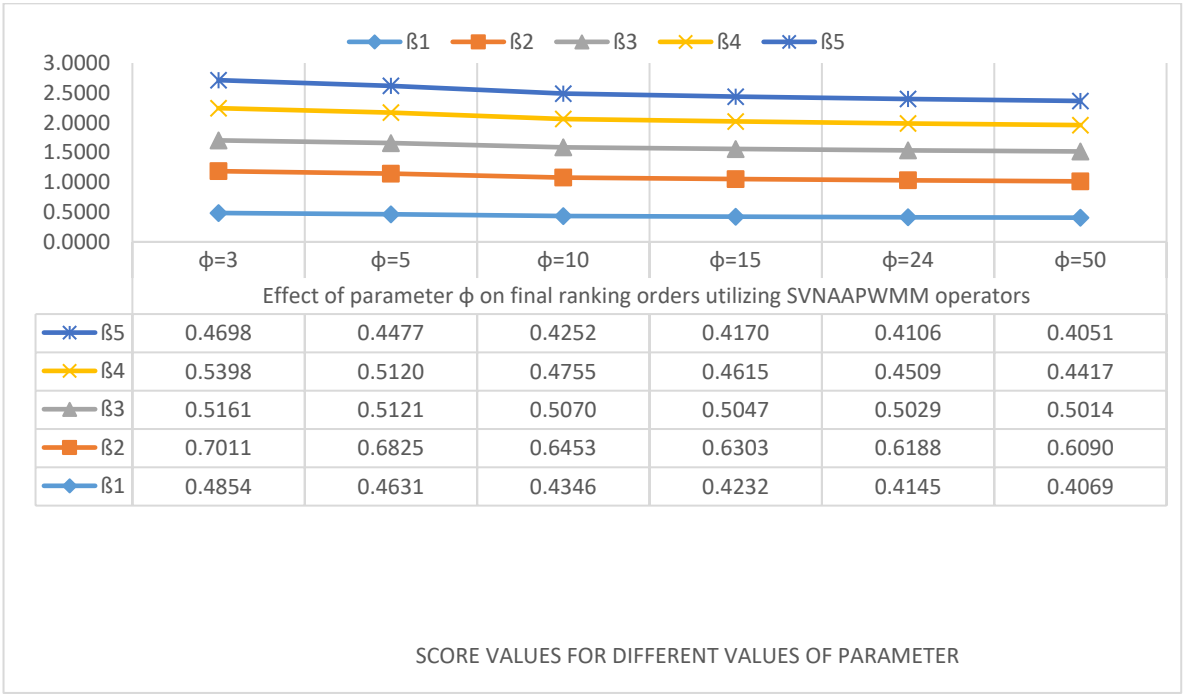

Fig 1. Impact of the parameter ϕ on final ranking orders utilizing SVNAAPWMM operators

6.2. Comparative analysis advantages and disadvantages of the initiated MADM approach

In this subpart, a comparison between the initiated approach and the existing MADM approaches, advantages and disadvantages are investigated.

We solve the same example using five existing MADM methods, including SVN weighted averaging operator, SVN weighted geometric operator [49], SVNAAWA [51], SVN MSM operators developed by Khan et al. [18], and SVN power aggregation operator developed by Yang and [38], and Wei and

Zhang [47] SVNBPM operators to demonstrate the benefits and efficacy of the method developed in this article.

Figure 5, we can see that the ranking orders of the alternatives obtained from different approaches and the initiated approach are slightly different. That is, from the initiated MADM approach $\overline{\overline{B}}_2$ is the best alternative and $\overline{\overline{B}}_5$ is worst alternative, while utilizing the existing MADM approaches $\overline{\overline{B}}_2$ is the best alternative and $\overline{\overline{B}}_1$ is worst alternative.

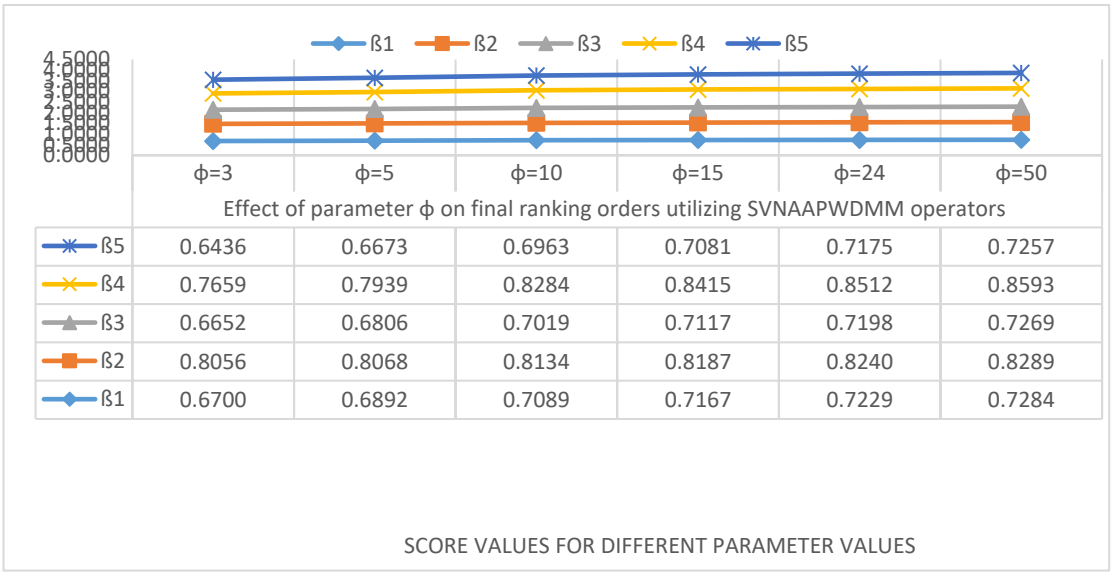

Fig 2. Impact of the parameter ϕ on final ranking orders utilizing SVNAAPWDMM

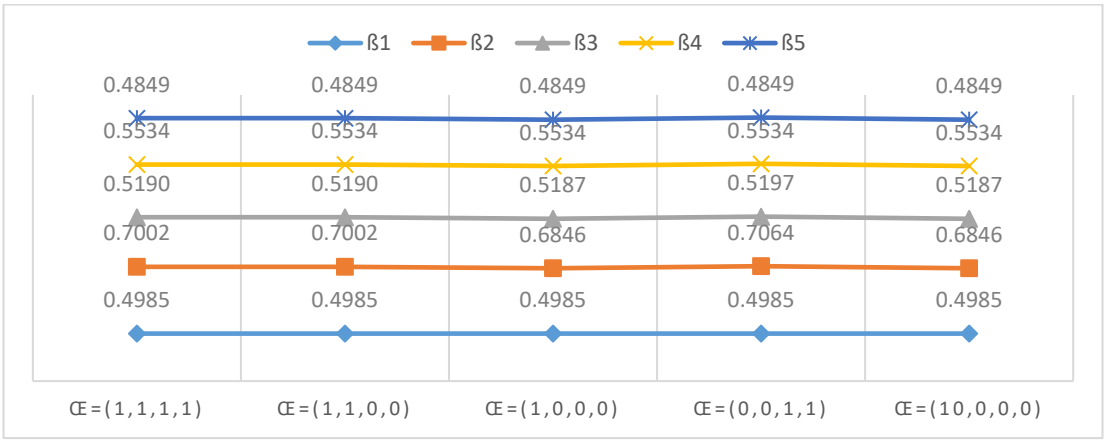

Fig 3. Impact of the parameter $Œ''$ on final ranking orders utilizing SVNAAPWMM operators

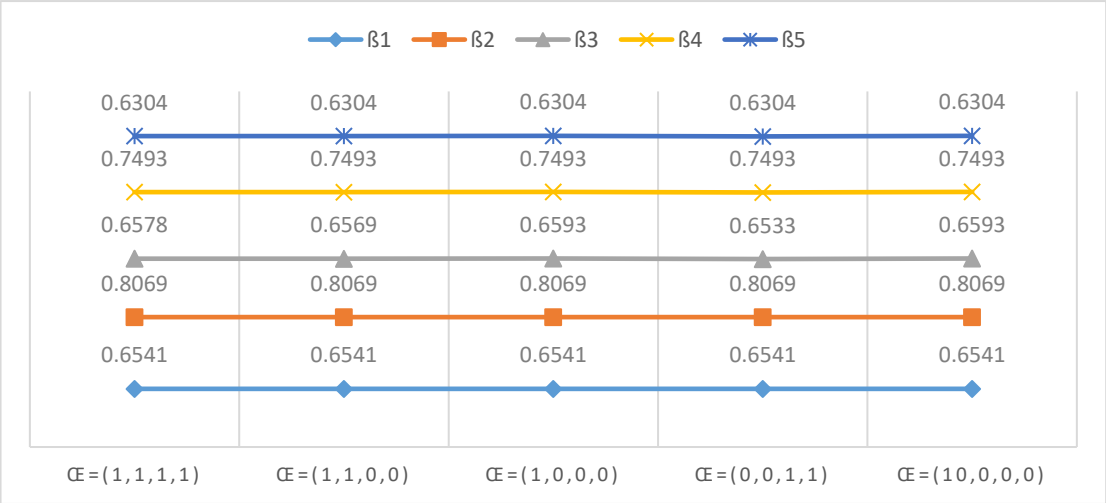

Fig 4. Impact of the parameter *Œ"* on final ranking orders utilizing SVNAAPWMM operators

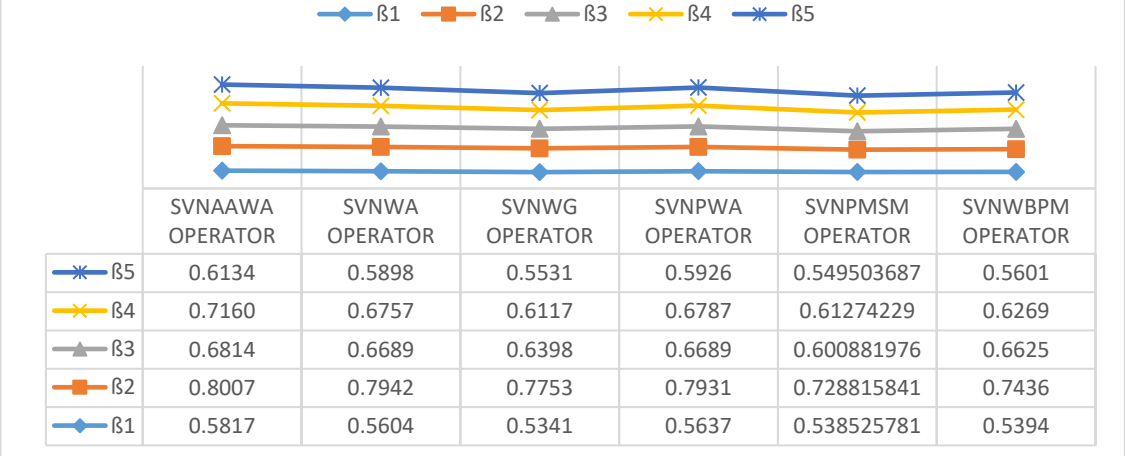

	SVNAAWA OPERATOR	SVNWA OPERATOR	SVNWG OPERATOR	SVNPWA OPERATOR	SVNPMSM OPERATOR	SVNWBPM OPERATOR
ß5	0.6134	0.5898	0.5531	0.5926	0.549503687	0.5601
ß4	0.7160	0.6757	0.6117	0.6787	0.61274229	0.6269
ß3	0.6814	0.6689	0.6398	0.6689	0.600881976	0.6625
ß2	0.8007	0.7942	0.7753	0.7931	0.728815841	0.7436
ß1	0.5817	0.5604	0.5341	0.5637	0.538525781	0.5394

Fig 5. Comparison with different MADM approaches

As a result, it is confirmed that the approach we suggested is sensible and efficient.

There are several advantages of the proposed AGOs over the existing AGOs. Firstly, the existing AGOs are special cases with admiration to the parameter of the initiated AGOs. Secondly, the initiated AGOs are based on AA operational rules. The initiated AGOs have the capacity of removing the effect of awkward data and can take interrelationship among any number of input arguments at the same time. While the existing AGOs can only remove the effect of awkward data or can take interrelationship among input arguments. Thirdly, the initiated MADM approach is flexible due to the containment of several parameters which can deal with complex MADM problems more efficiently than the existing MADM approaches.

7. CONCLUSION

The PA operator, which can diminish the influence of elusive data provided by biased experts, and the MM operator, which can deliberate the interrelationship connecting any number input arguments, are advantages that the PMM operator may utilize. The advantage of considerable flexibility with general parameters is one of the advantages of Aczel-Alsina operational laws for SVNNs. Initially, we combined PMM with the AA operational laws and suggested various aggregation operators for SVNNs. Secondly, some of the basic characteristics and special cases with respect to the parameters are investigated and found that some of the existing AGOs are special cases

of these initiated aggregation operators. The advantage of the intended aggregation operators is that they are more flexible in the aggregation process because they can simultaneously reduce the influence of uncomfortable data by PA operator and take the relationship between any number of input data by utilizing MM operator. Thirdly, weighted form of these AGOs are also initiated. Fourthly, A novel MADM technique is created based on the proposed aggregation operators to handle SVN information. To demonstrate the efficacy and applicability of the suggested MADM approach, an example is utilized, and comparisons are made with the current methods. The suggested aggregation operations are quite helpful in solving MADM problems due to the defined characteristic.

In future study, we will construct specific aggregation operators based on AA operational laws for SVN hesitant FSs, interval NHFSs, double valued neutrosophic sets and so on, and apply them to solve MAGDM and MADM problems in different fields.

Funding: No

Conflicts of Interest: "The authors declare no conflict of interest.

Ethics Declaration Statement: The authors state that this is their original work, and it is neither submitted nor under consideration in any other journal simultaneously.

- Competing Interests: No
- Ethical and informed consent for data used: No data are used.
- Data availability and access: The data utilized in this manuscript are hypothetical and artificial, and one can use these data before prior permission by just citing this manuscript.

References

1. Amato, Di Martino. B, & Venticinque. S., Agents based multi-criteria decision-aid. Journal of Ambient Intelligence and Humanized Computing, **2014** Vol.5, no.5, p: 747-758.
2. Sattarpour, T, Nazarpour. D, Golshannavaz. S, & Siano. P., A multi-objective hybrid GA and TOPSIS approach for sizing and siting of DG and RTU in smart distribution grids. Journal of Ambient Intelligence and Humanized Computing, **2018,** Vol. 9, p:105-122.
3. Bajwa. N, Fontem. B, & Sox. C. R., Optimal product pricing and lot sizing decisions for multiple products with nonlinear demands. Journal of Management Analytics, **2016,** Vol. 3, no. 1, p:43-58.
4. Levy. R, Brodsky. A & Luo. J., Decision guidance framework to support operations and analysis of a hybrid renewable energy system. Journal of Management Analytics, **2016** Vol. 3, no. 4, p:285-304.
5. Pourhassan. M. R. & Raissi. S. An integrated simulation-based optimization technique for multi-objective dynamic facility layout problem. Journal of Industrial Information Integration, **2016,** Vol.8, p:49-58.
6. Zadeh. L. A., Fuzzy sets.. Information and control, **1965,** Vol. 8, no. 3, p: 338-353.

7. Atanassov. K. Intuitionistic fuzzy sets. Fuzzy sets and systems, **1986**, Vol. 20, no. 1, p: 87-96.
8. Li. D. F. Multi-attribute decision making models and methods using intuitionistic fuzzy sets. Journal of computer and System Sciences, **2005**, Vol. 70, no. 1, p: 73-85.
9. Gohain. B, Chutia. R, & Dutta. P. Distance measure on intuitionistic fuzzy sets and its application in decision-making, pattern recognition, and clustering problems. International Journal of Intelligent Systems, **2022**, Vol. 37, no. 3, p:2458-2501.
10. Gao. J, Guo. F, Ma. Z, & Huang. X,. Multi-criteria decision-making framework for large-scale rooftop photovoltaic project site selection based on intuitionistic fuzzy sets. Applied Soft Computing, 2021, Vol. 102, article no. 107098.
11. Garg. H, & Rani. D, Novel distance measures for intuitionistic fuzzy sets based on various triangle centers of isosceles triangular fuzzy numbers and their applications. Expert Systems with Applications, 2022, Vol. 191, article no. 116228.
12. Ngan. R. T, Ali. M, Fujita. H, Abdel-Basset. M, Giang. N., L, Manogaran. G., & Priyan. M. K., A new representation of intuitionistic fuzzy systems and their applications in critical decision making. IEEE Intelligent Systems, **2019**, Vol. 35, no. 1, p:6-17.
13. Kahraman. C, Cebi. S, Oztaysi. B, & Cevik Onar. S. Intuitionistic Fuzzy Sets with Ordered Pairs and Their Usage in Multi-Attribute Decision Making: A Novel Intuitionistic Fuzzy TOPSIS Method with Ordered Pairs. Mathematics, **2023**, Vol. 11, no.18, article no.3867.
14. Qayyum. M, Kerre. E. E., & Ashraf. S. A Parametric Family of Fuzzy Similarity Measures for Intuitionistic Fuzzy Sets. Mathematics, **2023**,vol. 11, no. 14, p3163, 2023.
15. Smarandache. F. Neutrosophic Probability, Set, and Logic. In Neutrosophy; American Research Press: Rehoboth, IL, USA, **1998**.
16. Smarandache. F. Neutrosophic set . A generalization of the intuitionistic fuzzy set. Int. J. Pure Appl. Math. 1, **2010,** p: 107–116.
17. Wang. H, Smarandache. F, Zhang. Y, & Sunderraman. R, Single valued neutrosophic sets. In Proceedings of the 8th joint conference on information Sciences, Salt Lake City, UT, USA, 21–26 July **2005**; p. 94–97.
18. Khan. Q, Mahmood. T, Hayat. K, Arif. M, Balas. V. E, & Geman. O. Application of Single-Valued Neutrosophic Power Maclaurin Symmetric Mean Operators in MADM. In Soft Computing Applications: Proceedings of the 8th International Workshop Soft Computing Applications (SOFA **2018**), Vol. II 8 (pp. 328-354). Springer International Publishing.
19. Acharya. A. Mahata. A, Mukherjee. A, Biswas. M. A, Das. K. P, Mondal. S. P & Roy. B. A Neutrosophic differential equation approach for modeling glucose distribution in the bloodstream using neutrosophic sets. Decision Analytics Journal, **2023**,p:100264.
20. Shahzadi. G., Akram. M, & Saeid. A. B. An application of single-valued neutrosophic sets in medical diagnosis. Neutrosophic sets and systems, **2017**, vol.18, p:80-88.

21. Chai. J. S, Selvachandran. G, Smarandache. F, Gerogiannis. V. C, Son. L. H, Bui. Q. T, & Vo. B. New similarity measures for single-valued neutrosophic sets with applications in pattern recognition and medical diagnosis problems. Complex & Intelligent Systems,**2021**, vol. 7, p: 703-723.
22. Karak. M, Mahata. M, Rong. M, Mukherjee. S, Mondal. M, Broumi.S, & Roy.B. A Solution Technique of Transportation Problem in Neutrosophic Environment. Neutrosophic Systems with Applications,**2023**, vol. 3, p: 17-34.
23. Ye. J. Improved correlation coefficients of single valued neutrosophic sets and interval neutrosophic sets for multiple attribute decision making. Journal of Intelligent & Fuzzy Systems, **2014** vol. 27, no. 5, p:2453-2462.
24. Abdel-Basset. M, & Mohamed. M. The role of single valued neutrosophic sets and rough sets in smart city: Imperfect and incomplete information systems. Measurement, **2018**,vol. 124, p: 10.1016.
25. Ye. J. Multiple attribute decision-making method using correlation coefficients of normal neutrosophic sets. Symmetry , **2017,** Vol. 9, no. 80.
26. Yu. D. Group decision making based on generalized intuitionistic fuzzy prioritized geometric operator. Int. J. Intell. Syst. **2012,** vol.27, p: 635–661.
27. Liu. P. Multiple attribute group decision making method based on interval-valued intuitionistic fuzzy power Heronian aggregation operators. Comput. Ind. Eng. **2017**, Vol. 108, p: 199–212.
28. Mahmood.T, Liu. P, Ye. J, Khan. Q. Several hybrid aggregation operators for triangular intuitionistic fuzzy set and their application in multi-criteria decision making. Granul. Comput. **2018,** Vol.3, p:153–168.
29. Liao. H,. Xu. Z. Intuitionistic fuzzy hybrid weighted aggregation operators. Int. J. Intell. Syst. **2014**, vol. 29, p: 971–993.
30. Xu. Z. Intuitionistic fuzzy aggregation operators. IEEE Trans. Fuzzy Syst. **2007**, vo. 15, p:1179–1187.
31. Xu. Z, Yager. R. R. Some geometric aggregation operators based on intuitionistic fuzzy sets. Int. J. Gener. Syst. **2006**, vol. 35, p: 417–433, 2006.
32. Peng. J. J, C. Tian, C, Zhang, Z. Q, Song. H. Y & Wang. J. Q. Single-valued neutrosophic power shapley choquet average operators and their applications to multi-criteria decision-making. Mathematics, **2019**, vol. 7, no. 11, Article no:1081.
33. Liu. P., Khan. Q., & Mahmood. T. Multiple-attribute decision making based on single-valued neutrosophic Schweizer-Sklar prioritized aggregation operator. Cognitive Systems Research, **2019**,vol. 57, p: 175-196.

34. Garg. H. A novel divergence measure and its based TOPSIS method for multi criteria decision-making under single-valued neutrosophic environment. Journal of Intelligent & Fuzzy Systems, **2019**, vol.36, no.1, p:101-115.
35. Mishra. A. R, Saha. A, Rani, P, Hezam. I. M. Shrivastava. R, & Smarandache. F., An integrated decision support framework using single-valued-MEREC-MULTIMOORA for low carbon tourism strategy assessment. IEEE Access, **2022**, vol. 10, p: 24411-24432.
36. Rong. Y, Niu. W, Garg. H, Liu. Y, & Yu, L. A hybrid group decision approach based on MARCOS and regret theory for pharmaceutical enterprises assessment under a single-valued neutrosophic scenario. Systems, **2022**, vol. 10, no. 4, p:106.
37. Yager. R. R. The power average operator. IEEE Trans. Syst. Man Cybern. Part A, **2001,** vol.31, p:724–731.
38. Yang, L, Li . B. A multi-criteria decision-making method using power aggregation operators for single-valued neutrosophic sets, Int. J. Database Theory Appl. **2016**, Vol.9 no.2, p:23–32.
39. Bonferroni. C, Sulle medie multiple di potenze. Bollettino dell'Unione Matematica Italiana,**1950,** vol.5, p:267–270.
40. Sykora. S. Mathematical Means and Averages: Generalized Heronian Means. Stan's Libr. **2009**.
41. Muirhead. R. F., Some methods applicable to identities and inequalities of symmetric algebraic functions of n letters. Proc. Edinb. Math. Soc **1902**, vol.21, p:144–162.
42. Maclaurin. C, .A second letter to Martin Folkes, Esq.; concerning the roots of equations, with the demonstration of other rules of algebra. Philos. Trans., **1729**, vol. 36, p:59–96.
43. Liu. P., Khan. Q., & Mahmood T. Some single-valued neutrosophic power Muirhead mean operators and their application to group decision making. Journal of Intelligent & Fuzzy Systems, vol. 37, **2019**, vol.2, p:2515-2537.
44. Tian. C, Peng. J. J, Zhang Z. Q, Goh. M., & Wang. J. Q. A multi-criteria decision-making method based on single-valued neutrosophic partitioned Heronian mean operator. Mathematics, **2020** , vol. 8, no.7, p:1189.
45. Xu. Z, Yager. R. R., Intuitionistic fuzzy Bonferroni means. IEEE Trans. Syst. Man Cybern. Part B, **2011**, vol. 41, p: 568–578.
46. Zhou. W, He. J. M. Intuitionistic fuzzy geometric Bonferroni means and their application in multi-criteria decision making. Int. J. Intell. Syst. **2012**, vol. 27, p:995–1019.
47. Wei, G., & Zhang, Z. Some single-valued neutrosophic Bonferroni power aggregation operators in multiple attribute decision making. Journal of Ambient Intelligence and Humanized Computing, **2019,** Vol. 10(3), 863-882.
48. Liu. P. & Zhang. X. Some Maclaurin symmetric mean operators for single-valued trapezoidal neutrosophic numbers and their applications to group decision making. International Journal of Fuzzy Systems, **2018**, vol.20, p:45-61.

49. Liu. P. The aggregation operators based on archimedean t-conorm and t-norm for single-valued neutrosophic numbers and their application to decision making. International Journal of Fuzzy Systems, **2016**, vol. 18, no.5, p:849-863.
50. Smarandache. F. The score, accuracy, and certainty functions determine a total order on the set of neutrosophic triplets (T, I, F) (Vol. 38). Infinite Study, **2020.**
51. Senapati. T. An Aczel-Alsina aggregation-based outranking method for multiple attribute decision-making using single-valued neutrosophic numbers. Complex & Intelligent Systems, **2023,** p:1-15.

Peide Liu, received the B.S. and M.S. degrees in signal and information processing from Southeast University, Nanjing, China, in 1988 and 1991, respectively, and the Ph.D. degree in information management from Beijng Jiaotong University, Beijing, China, in 2010.

He is currently a Professor with the School of Management Science and Engineering, Shandong University of Finance and Economics, Shandong, China. He is an Associate Editor of the IEEE Transactions on Fuzzy Systems, Information Sciences, International Journal of Fuzzy Systems, Journal of Intelligent and Fuzzy Systems, the editorial board of the journal Technological and Economic Development of Economy, and the members of editorial board of the other 12 journals. He has authored or coauthored more than 400 publications. His research interests include aggregation operators, fuzzy logic, fuzzy decision making, and their applications.

Qaisar Khan did his Ph.D. from International Islamic University Islamabad Pakistan in 2019. He is currently working as an Assistant Professor in the Department of Mathematics and Statistics, University of Haripur, Pakistan. He has published more than 60 articles in well reputed journals. His area of research is fuzzy decision making and fuzzy algebraic structures.

Rashid Ali has completed M.sc from Hazara university Mansehra,in 2009 and M.S from Hazara university in 2015 in history of mathematics (history of exponential and logarithmic functions). Currently, he is Ph.D. student at the University of Malakand Chak Dara. His research field is decision making, fuzzy algebra.

Dr. Hidayat Ullah is currently serving as an Assistant Professor in the Department of Mathematics at the University of Malakand since 2018, he brings a wealth of experience to his role.His journey in academia began as a Lecturer in Mathematics at the University of Malakand in 2005, where he continued to inspire and educate students until 2018. Prior to this, Dr. Khan served as a Research Associate at Baluchistan University of IT and Emerging Sciences (BUITMS), Quetta, from 2004 to 2005.

Dr. Khan's dedication to education extends beyond his tenure at the University of Malakand. He also contributed as a Lecturer at Government Degree College Agra, Malakand Agency, Khyber Pakhtunkhwa, from 2000 to 2001, and at Government Jehanzeb Post Graduate College, Saidu Sharif, Swat, Khyber Pakhtunkhwa. His academic achievements include earning a Master of Science (MSc) in Mathematics from the University of Peshawar in 2000 and a Doctorate in Mathematics from Universiti Teknologi Malaysia, Malaysia, in 2015. Dr. Khan's research is primarily focused on Fuzzy Algebra, a field in which he has made significant contributions.

Throughout his career, Dr. Hidayat Ullah Khan has published more than 50 research articles in esteemed national and international journals, further solidifying his reputation as a distinguished mathematician and educator.

Dr. Rashid Jan Postdoctoral researcher at the Institute of Energy Infrastructure (IEI), Department of Civil Engineering, College of Engineering, Universiti Tenaga Nasional (UNITEN), Putrajaya Campus, Jalan IKRAM-UNITEN, 43000 Kajang, Selangor, Malaysia. He obtained PhD degree in applied mathematics from Xian Jiaotong University, Xian China and worked as an Assistant Professor in the Department of Mathematics, University of Swabi, KPK Pakistan. He has published more than 150 research articles in high ranked journals.

Received: July 22, 2024. Accepted: Oct 25, 2024

Neutrosophic Sets and Systems, Vol. 76, 2025
University of New Mexico

An Evaluation Method for University Classroom Education Quality under Machine Vision and Single-Valued Neutrosophic Hesitant Fuzzy Set Environment

Rui Wang [1], Mingjie Li [1]* Fangwei Zhang [2], Yiying Pan [1] and Zongao Zhang[1]

[1] School of Navigation and Shipping, Shandong Jiaotong University, Weihai China.
Email: Rui Wangrui: wang27@163.com, Mingjie Li: 201046@sdjtu.edu.cn, Yiying Pan: yiyingpan02@163.com, Zongao Zhang: zongaozhang@163.com.
[2] School of International Business, Shandong Jiaotong University, Weihai China.
Email: Fangwei Zhang: fangweirzhang@163.com.
* Correspondence: 201046@sdjtu.edu.cn

Abstract: With the advancement of artificial intelligence, machine vision offers a novel approach to university teaching quality evaluation (TQE). However, existing studies are often hindered by subjectivity and lack of standardized evaluation methods, which impede accurate assessment of student learning effectiveness. Therefore, this study addresses these limitations by proposing a TQE framework that integrates machine vision with single-valued neutrosophic hesitant fuzzy sets (SVNHFSs). Specifically, the main contributions of this study are as follows. First, this study innovatively employs machine vision to capture student learning behaviors, constructing a classroom behavior matrix that serves as the foundation for evaluation. Second, this study introduces a combined weighting method, leveraging both the entropy weight method and the Criteria Importance Through Inter-Criteria Correlation (CRITIC) weight method, to assign weights to different time-points during the classes. Third, the SVNHFS is utilized to construct a classroom behavior evaluation matrix, and the single-valued neutrosophic hesitant fuzzy weighted average (SVNHFWA) operator is applied for weighting. In addition, the cosine measure is employed to rank time-points based on both ideal and non-ideal solutions, obtaining the optimal and non-optimal learning effectiveness periods. Finally, a case study confirms the effectiveness and feasibility of the proposed model, offering a robust method for evaluating university education quality.

Keywords: Teaching Quality Evaluation, Machine vision, Classroom Behavior Analysis, Single-valued neutrosophic hesitant fuzzy set, Hybrid Weighting Method, Multi-attribute decision-making.

1. Introduction

With the rapid advancement of artificial intelligence, machine vision is increasingly being utilized in teaching quality evaluation (TQE) at colleges and universities [1]. Traditional classroom evaluation methods often focus on superficial metrics, such as exam scores and attendance, which do not adequately capture students' learning outcomes or teachers' instructional effectiveness [2]. To overcome these limitations, educational institutions have begun incorporating video surveillance in classrooms to analyze both teaching activities and student behavior. This approach offers a more comprehensive and objective means of assessing teaching effectiveness within the TQE framework in higher education.

However, evaluating the quality of university education involves various or the same attributes, making the process of TQE a complex multi-attribute decision-making (MADM) problem [3]. The application of single-valued neutrosophic hesitant fuzzy sets (SVNHFSs) offers an effective approach to addressing this complexity [4]. Therefore, this study integrates machine vision with SVNHFS in the evaluation process, offering a novel perspective on TQE. To further explore the application of machine vision and SVNHFS in teaching evaluation, this study reviews relevant literature to provide theoretical support and practical guidance.

In recent years, scholars have focused on improving the effectiveness and accuracy of TQE [5-8]. For example, Li and Zhang employed big data, integrating K-means clustering and Apriori algorithms, to monitor and improve teaching quality in higher education, achieving more precise evaluations and enhancements [9]. Xia employed the probabilistic hesitant fuzzy TODIM-EDAS technique combined with the CRITIC method, thereby supporting institutions in cultivating more international technical talents [10]. Ahmad et al. proposed a machine learning-optimized TQE framework, which offers a more precise and systematic approach to assessing teaching quality by analyzing teacher performance in e-learning environments [11]. Cui proposed the artificial bee colony optimization algorithm combined with a classification and regression tree model to enhance TQE, significantly improving accuracy and generalizability through AI-driven methods [12]. Li and Wang proposed a TQE framework based on 5G and edge computing technologies, which significantly enhances the efficiency and accuracy of teaching quality assessments, thereby strengthening educational management [13]. Zhao et al. developed a blended teaching quality evaluation scale for nursing education based on the Context, Input, Process, and Product (CIPP) model, enhancing the reliability and validity of teaching TQE [14]. Ren et al. utilized deep learning and dictionary-based techniques for aspect-level sentiment analysis of student feedback, thereby enhancing the objectivity and depth of teaching quality evaluation [15].

Meanwhile, the neutrosophic set (NS) is a foundational tool for addressing uncertainty and inconsistency in MADM problems, with applications across various fields [16-18]. Numerous extensions of NSs have been developed to further enhance its capability in handling more complex decision-making scenarios [19]. For instance, Saqlain et al. introduced a multi-polar interval-valued neutrosophic hypersoft set model, which employs distance and similarity measures to address uncertainty in complex MADM problems [20]. Then, Florentin introduced the SuperHyperSoft Set and its fuzzy extension, expanding the Soft Set theory to address complex decision-making scenarios with greater flexibility and inclusivity of uncertainties and inconsistencies [21]. Meanwhile, Zhao and Ye proposed a MADM model combining Simplified NS and TOPSIS, improving the TQE framework's accuracy and reliability by handling uncertainties and inconsistencies in evaluations [22]. And Ye proposed a MADM method based on the SVNHFS, which effectively deals with the uncertainty and hesitation in the decision by developing new aggregation operators and measurement functions [23]. Building on such advancements, Muhammad et al. investigated the efficiency of wastewater treatment using interval-valued neutrosophic fuzzy soft sets, offering a systematic approach to ensure the security and quality of drinking water by incorporating distance measures [24]. Ahmed et al. introduced a neutrosophic MCDM model to assess sustainable soil enhancement in construction, highlighting lifecycle assessment's importance for sustainable practices and cost analysis [25].

Besides, with the development of AI, machine vision has become an excellent decision-aid tool in various fields [26-28]. Bai et al. integrated an enhanced YOLOv4 with MobileNetV3 to develop an efficient machine vision approach for detecting surface defects on railway tracks, achieving a lightweight network and rapid, accurate identification [29]. Zhang et al. presented an enhanced YOLOv4-Tiny model for weed detection in peanut fields, offering a valuable tool for precision agriculture [30]. Then, shifting focus to the TQE field, Li et al. developed an objective and precise TQE evaluation method using machine vision and Fermatean fuzzy sets, enhancing both the objectivity and efficiency of the evaluation [31]. Bai proposed a teaching system based on machine vision and sensor audio signal processing, aiming to improve students' learning outcomes in musical performance skills [32]. Cheng obtained the evaluation of classroom activity through student expression and posture recognition and realized student classroom teaching automatic acquisition [33]. Goldberg et al. proposed an action recognition method based on machine vision, which effectively evaluates the visible engagement of college students in classroom teaching [34].

Considering the above reference reviews, research on TQE has made noteworthy progress, and the application of SVNHFS and machine vision in many fields is also extensive. But there are still some aspects that need considering as follows.

1) Traditional teaching evaluation methods rely on subjective decisions from evaluators, resulting in objectivity issues and lower efficiency. There is a need for more objective and streamlined evaluation methods.

2) Despite the wide application of machine vision in various fields, its use in the TQE remains underdeveloped, and methods integrating this technology require further refinement.

3) While SVNHFS offers a new perspective for addressing MADM problems, current research still needs improvement. Given the complexity and challenges of TQE, there is no unified framework to address these issues effectively.

Based on the aforementioned, the motivation of this study is to propose an objective and precise TQE framework that integrates SVNHFS with machine vision to minimize subjectivity in the evaluation process. Then, this study proposes an evaluation method for TQE in machine vision and SVNHFS environment. The primary contributions of this study are summarized as follows.

First, this study adopts the objective detection algorithm based on deep learning, YOLOv5, to detect different classroom learning behaviors during teaching time. Then, based on these learning behaviors, a learning behavior matrix is constructed. This approach enhances the objectivity of behavior detection and provides a novel approach to the TQE process.

Second, this study employs a combined weighting approach using the entropy weight method and the CRITIC method to determine the weights at specific time points. This approach replaces the subjective weighting process, mitigating the limitations of single-method weighting, and enhancing the objectivity and effectiveness of the TQE process.

Third, this study constructs time-based SVNHF evaluation matrices to assess students' classroom behaviors at specific intervals. The classical SVNHFWA operator is then employed, using the weights derived from the combined weighting method to ensure a balanced and accurate evaluation of each time point.

Additionally, this study employs the SVNHFS cosine measure operators to rank the time-points based on the learning effect and inspired by the SVNHFS cosine measure operator, a negative cosine measure operator is introduced for the non-ideal SVNHFE. By incorporating both cosine measure values, the TQE process is more comprehensive. For ease of understanding, Figure 1 gives the main framework of this study.

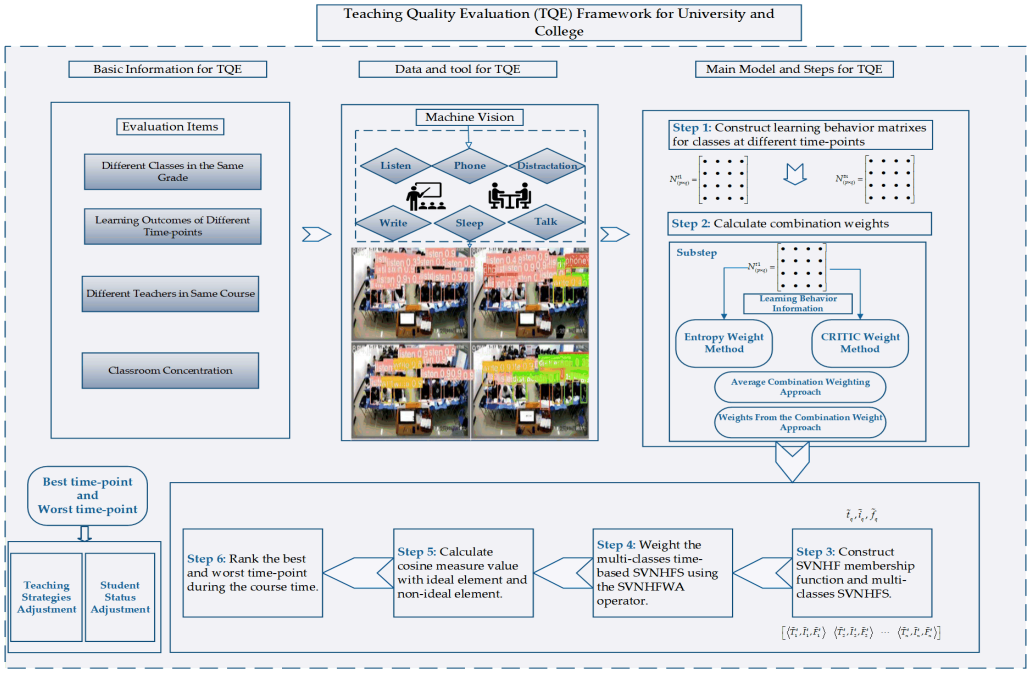

Figure 1. The main framework of this study.

The remainder of this study is structured as follows. Section 2 provides a brief introduction to the related concepts of SVNHFSs. Section 3 presents a framework for university TQE that combines SVNHFSs and machine vision. In Section 4, the classroom evaluation decision model proposed in

this study is validated through a case example, and the results obtained are analyzed and discussed. In Section 5, the conclusion of this study is summarized.

2. Preliminary studies

In the general concept, an SVNHFS is the combination of the hesitant fuzzy set (HFS) and SVNS [35]. Specifically, there are some basic concepts of SVNHFS as follows.

Definition 1 [35]. Let X be a fixed set C, and the elements of X are represented by x. Then, the SVNHFS is defined as

$$C = \left\{ \left\langle x, \tilde{T}_C(x), \tilde{I}_C(x), \tilde{F}_C(x) \right\rangle \middle| x \in X \right\},$$

where $\tilde{T}_C(x)$, $\tilde{I}_C(x)$, and $\tilde{F}_C(x)$ are defined as the possible truth-membership hesitant degrees, indeterminacy-membership hesitant degrees, and falsity-membership hesitant degrees, respectively. Whereas $\tilde{T}_C(x)$, $\tilde{I}_C(x)$, and $F(x) \in [0,1]$ for each element x in X to the fixed set C. Besides, the SVNHFS has the following conditions.

1). $\alpha, \beta, \gamma \in [0,1]$, where the $\alpha \in \tilde{T}_C(x)$, $\beta \in \tilde{I}_C(x)$, $\gamma \in \tilde{F}_C(x)$.

2). $\alpha^+ \oplus \beta^+ \oplus \gamma^+ \in [0,3]$, where $\alpha^+ \in \tilde{T}_C^+(x) = \mathrm{U}_{\alpha^+ \in \tilde{T}_C(x)} max\{\alpha\}$, $\beta^+ \in \tilde{I}_C^+(x) = \mathrm{U}_{\beta^+ \in \tilde{I}_C(x)} max\{\beta\}$, $\gamma^+ \in \tilde{F}_C^+(x) = \mathrm{U}_{\gamma^+ \in \tilde{F}_C(x)} max\{\gamma\}$. Specifically, α^+, β^+, γ^+ represent the maximum value of $\tilde{T}_C^+(x)$, $\tilde{I}_C^+(x)$, and $\tilde{F}_C^+(x)$, respectively.

For convenience, the three tuples $c(x) = \{\tilde{T}_C(x), \tilde{I}_C(x), \tilde{F}_C(x)\}$ is described as single-value neutrosophic hesitant fuzzy element (SVNHFE), which is easily denoted as $c = \{\tilde{T}, \tilde{I}, \tilde{F}\}$.

Then, the related relations between two SVNHFEs are as follows.

Definition 2 [35]. Let $c_1 = \{\tilde{T}_1, \tilde{I}_1, \tilde{F}_1\}$ and $c_2 = \{\tilde{T}_2, \tilde{I}_2, \tilde{F}_2\}$ be two SVNHFEs in a fixed set *X*, it gets the following relations.

1). $c_1 \cup c_2 = \{\tilde{T} \in (\tilde{T}_1 \cup \tilde{T}_2) \big| \tilde{T} \geq max(\tilde{T}_1^-, \tilde{T}_2^-), \tilde{I} \in (\tilde{I}_1 \cap \tilde{I}_2) \big| \tilde{I} \leq min(\tilde{I}_1^-, \tilde{I}_2^-), \tilde{F} \in (\tilde{F}_1 \cap \tilde{F}_2) \big| \tilde{F} \leq min(\tilde{F}_1^-, \tilde{F}_2^-)\}$.

2). $c_1 \cap c_2 = \{\tilde{T} \in (\tilde{T}_1 \cap \tilde{T}_2) \big| \tilde{T} \leq min(\tilde{T}_1^+, \tilde{T}_2^+), \tilde{I} \in (\tilde{I}_1 \cup \tilde{I}_2) \big| \tilde{I} \geq max(\tilde{I}_1^+, \tilde{I}_2^+), \tilde{F} \in (\tilde{F}_1 \cup \tilde{F}_2) \big| \tilde{F} \geq max(\tilde{F}_1^+, \tilde{F}_2^+)\}$.

Since, the basic operations for two SVNHFEs are given as follows.

Definition 3 [35]. Let c_1 and c_2 be two SVNHFEs in a fixed set *X*. It gets the following operations.

1. $c_1 \oplus c_2 = \{\tilde{T}_1 \oplus \tilde{T}_2, \tilde{I}_1 \otimes \tilde{I}_2, \tilde{F}_1 \otimes \tilde{F}_2 = U_{\alpha_1 \in \tilde{T}_1, \beta_1 \in \tilde{I}_1, \gamma_1 \in \tilde{F}_1, \alpha_2 \in \tilde{T}_2, \beta_2 \in \tilde{I}_2, \gamma_2 \in \tilde{F}_2} \{\{\alpha_1 + \alpha_2 - \alpha_1\alpha_2\}, \{\beta_1\beta_2\}, \{\gamma_1\gamma_2\}\}$.
2. $c_1 \otimes c_2 = \{\tilde{T}_1 \otimes \tilde{T}_2, \tilde{I}_1 \oplus \tilde{I}_2, \tilde{F}_1 \oplus \tilde{F}_2 = U_{\alpha_1 \in \tilde{T}_1, \beta_1 \in \tilde{I}_1, \gamma_1 \in \tilde{F}_1, \alpha_2 \in \tilde{T}_2, \beta_2 \in \tilde{I}_2, \gamma_2 \in \tilde{F}_2} \{\{\alpha_1\alpha_2\}, \{\beta_1 + \beta_2 - \beta_1\beta_2\}, \{\gamma_1 + \gamma_2 - \gamma_1\gamma_2\}\}$.
3. $\lambda c_1 = \{U_{\alpha_1 \in \tilde{T}_1, \beta_1 \in \tilde{I}_1, \gamma_1 \in \tilde{F}_1} \{\{1 - (1 - \alpha_1)^\lambda\}, \{\beta_1{}^\lambda\}, \{\gamma_1{}^\lambda\}\}, \lambda > 0$.
4. $c_1{}^\lambda = \{U_{\alpha_1 \in \tilde{T}_1, \beta_1 \in \tilde{I}_1, \gamma_1 \in \tilde{F}_1} \{\{\alpha_1{}^\lambda\}, \{1 - (1 - \beta_1)^\lambda\}, \{1 - (1 - \gamma_1)^\lambda\}\}, \lambda > 0$.

Based on the SVNSs cosine measure method [28], the SVNHFEs cosine measure method is obtained as follows.

Definition 4 [35]**.** Let $c_1 = \{\tilde{T}_1, \tilde{I}_1, \tilde{F}_1\}$ and $c_2 = \{\tilde{T}_2, \tilde{I}_2, \tilde{F}_2\}$ be two SVNHFEs in a fixed set *X*. Therefore, the SVNHFEs cosine measure method is defined as follows.

$$\cos(c_1, c_2) = \frac{\left(\frac{1}{\delta_1}\sum_{\alpha_1 \in \tilde{T}_1} \alpha_1\right) \cdot \left(\frac{1}{\delta_2}\sum_{\alpha_2 \in \tilde{T}_2} \alpha_2\right) + \left(\frac{1}{\varepsilon_1}\sum_{\beta_1 \in \tilde{I}_1} \beta_1\right) \cdot \left(\frac{1}{\varepsilon_2}\sum_{\beta_2 \in \tilde{I}_2} \beta_2\right) + \left(\frac{1}{\eta_1}\sum_{\gamma_1 \in \tilde{F}_2} \gamma_1\right) \cdot \left(\frac{1}{\eta_2}\sum_{\gamma_2 \in \tilde{F}_2} \gamma_2\right)}{\sqrt{\left(\frac{1}{\delta_1}\sum_{\alpha_1 \in \tilde{T}_1} \alpha_1\right)^2 + \left(\frac{1}{\varepsilon_1}\sum_{\beta_1 \in \tilde{I}_1} \beta_1\right)^2 + \left(\frac{1}{\eta_1}\sum_{\gamma_1 \in \tilde{F}_2} \gamma_1\right)^2} \cdot \sqrt{\left(\frac{1}{\delta_2}\sum_{\alpha_2 \in \tilde{T}_2} \alpha_2\right)^2 + \left(\frac{1}{\varepsilon_2}\sum_{\beta_2 \in \tilde{I}_2} \beta_2\right)^2 + \left(\frac{1}{\eta_2}\sum_{\gamma_2 \in \tilde{F}_2} \gamma_2\right)^2}}, \quad (1)$$

where $\delta, \varepsilon, \eta$ represent the numbers of the elements in $\tilde{T}$, $\tilde{I}$, $\tilde{F}$, respectively. And the $\cos(c_1, c_2) \in [0,1]$. Thus, based on the SVNHFEs cosine measure method, the cosine measure between $c_i (i = 1,2)$ and ideal element $c^* =< 1,0,0 >$ is obtained as follows.

$$\cos\left(c_i, c^*\right) = \frac{\left(\frac{1}{\delta_i}\sum_{\alpha_i \in \tilde{T}_i} \alpha_i\right)}{\sqrt{\left(\frac{1}{\delta_i}\sum_{\alpha_i \in \tilde{T}_i} \alpha_i\right)^2 + \left(\frac{1}{\varepsilon_i}\sum_{\beta_i \in \tilde{I}_i} \beta_i\right)^2 + \left(\frac{1}{\eta_i}\sum_{\gamma_i \in \tilde{F}_i} \gamma_i\right)^2}}. \tag{2}$$

Similarly, where $\delta_i, \varepsilon_i, \eta_i, (i = [1,2])$ represent the numbers of the elements in $\tilde{T}_i$, $\tilde{I}_i$, $\tilde{F}_i$, respectively. And the $\cos(c_i, c^*) \in [0,1], i = [1,2]$. Since, the SVNHFEs' cosine measure comparative laws are obtained as follows.

1) If $\cos(c_1, c^*) > \cos(c_2, c^*)$, then $c_1 \succ c_2$.

2) If $\cos(c_1, c^*) = \cos(c_2, c^*)$, then $c_1 \sim c_2$.

3. Evaluation Methods of University Classroom Education

In this section, to better evaluate the university classroom students' learning effect, this study proposes an evaluation framework for TQE in machine vision and SVNHFS environment. The specific steps are as follows.

Step 1. In this step, this study uses q types of behaviors identified by the YOLOv5 object detection algorithm as the columns of the matrix. Then, the total duration of the course is equally divided into p segments, serving as the rows of the time-based learning behaviors matrix. Therefore, the matrix is obtained as follows.

$$N^t_{(p\times q)} = \begin{bmatrix} n_{11} & n_{12} & \cdots & n_{1q} \\ n_{21} & n_{22} & \cdots & n_{2q} \\ \vdots & \vdots & \ddots & \vdots \\ n_{p1} & n_{p2} & \cdots & n_{pq} \end{bmatrix},$$

where $N^t_{(p\times q)}$ represents the multi-classes learning behaviors matrix, $t = (1,2,\cdots,t)$ represents the time point, and $n_{pq}, p = (1,2,\cdots,p), q = (1,2,\cdots,q)$ represents the number of students in class p with learning behavior q.

Step 2. In this step, based on the combination of the classical entropy weight method and CRITIC weight method, the way of combined weighting method is adopted to obtain the weights under different classes and behaviors. The specific sub-steps are as follows.

Step 1'. Calculate the proportion of each behavior in each class p_{ij}. Then, p_{ij} is defined as follows.

$$p_{ij} = \frac{n_{pq}}{\sum_{p=1}^{p} n_{pq}}. \tag{3}$$

Next, calculate each behavior information entropy $e_j, (j = 1,2,\cdots,q)$ for each behavior. Then, e_j is defined as follows.

$$e_j = -\frac{1}{\ln p}\sum_{i=1}^{p} p_{ij} \ln p_{ij}, \tag{4}$$

where $\frac{1}{lnp} > 0, e_j \geq 0$.

Step 2'. Calculate the weights of each behavior through the behavior information entropy. Then, the weight of each behavior $w_j, (j = 1,2,\cdots,q)$ is obtained as follows.

$$w_j = \frac{1 + \frac{1}{\ln p}\sum_{i=1}^{p} p_{ij} \ln p_{ij}}{\sum_{j=1}^{q} 1 - \left(-\frac{1}{\ln p}\sum_{i=1}^{p} p_{ij} \ln p_{ij}\right)}. \tag{5}$$

Step 3'. Therefore, each class comprehensive score S_{1i} is obtained by the learning behaviors matrix $N^t_{(p\times q)}$ and weight of each behavior w_j. Then, it gets

$$S_{1i} = \sum_{j=1}^{q}\sum_{q=1}^{q} w_j \cdot n_{pq}. \tag{6}$$

Each class gets its weight at time-point $\boldsymbol{t}$. Then, it gets

$$w_{ei} = \frac{S_{1i}}{\sum_{i=1}^{p} S_{1i}}. \tag{7}$$

Thus, the weight vector of each class at time-point *t* using the entropy weight method is obtained as $\boldsymbol{w_e^t} = [\boldsymbol{w_{e1}}, \boldsymbol{w_{e1}}, \cdots, \boldsymbol{w_{ep}}]$.

Step 4'. Based on the learning behaviors matrix $\mathbf{N}_{(\boldsymbol{p\times q})}^{\boldsymbol{t}}$, the Pearson correlation coefficient matrix is obtained by the Pearson correlation coefficient $\boldsymbol{r_{pq}}$ [36]. Thus, the indicator conflict in learning behavior is obtained as follows.

$$R_j = \sum_{p=1}^{p} 1 - r_{pq}. \tag{8}$$

Thus, the amount of information about learning behavior $\boldsymbol{C_q}$ is obtained as follows.

$$C_q = \delta_q \sum_{p=1}^{p} 1 - r_{pq}, \tag{9}$$

where $\boldsymbol{\delta_q}$ represents the standard deviation of learning behavior *q*. Meanwhile, the larger $\boldsymbol{C_q}$ is, the more significant the role of the *q*th learning behavior index in the overall evaluation process.

Step 5'. Thereafter, the CRITIC weight of each behavior $\boldsymbol{w_{2j}}, (\boldsymbol{j = 1, 2, \cdots, q})$ is obtained as follows.

$$w_{2q} = \frac{C_q}{\sum_{q=1}^{q} C_q}. \tag{10}$$

Step 6'. Therefore, each class comprehensive score $\boldsymbol{S_{2i}}$ is obtained by $\mathbf{N}_{(\boldsymbol{p\times q})}^{\boldsymbol{t}}$ and $\boldsymbol{w_{2q}}$. It gets

$$S_{2i} = \sum_{q=1}^{q} w^t_{\ q} \cdot n_{\ pq}. \tag{11}$$

Thereafter, each class gets its weight at time-point $\boldsymbol{t}$. It gets

$$w_{ci}^t = \frac{S^t_{\ 2i}}{\sum_{i=1}^{p} S^t_{\ 2i}}. \tag{12}$$

Then, the weight vector of each class at time-point *t* using the CRITIC weight method is obtained as $\boldsymbol{w_c^t} = [\boldsymbol{w_{c1}}, \boldsymbol{w_{c1}}, \cdots, \boldsymbol{w_{cp}}]$.

Step 7'. This study adopts the weighted average method. Therefore, the combined weight in the weighted average method is defined as follows.

$$W_i = \theta w_{ei} + (1-\theta) w_{ci}, \tag{13}$$

where $\boldsymbol{W} = (\boldsymbol{W_1}, \boldsymbol{W_2}, \cdots, \boldsymbol{W_i})^{\mathbf{T}}$ is the combined weight vector in the weighted average method, and $\boldsymbol{\theta} = \mathbf{0.5}$.

Step 3. For convenience, based on the $\boldsymbol{q}$ classroom learning behaviors identified by YOLOv5, classify the different learning behaviors into truth-membership, indeterminacy-membership, and falsity-membership. Therefore, this study gives the truth-membership hesitant degree $\tilde{\boldsymbol{t}}_{\boldsymbol{q}}$, indeterminacy-membership hesitant degree $\tilde{\boldsymbol{\imath}}_{\boldsymbol{q}}$, and falsity-membership $\tilde{\boldsymbol{f}}_{\boldsymbol{q}}$ as follows.

$$\tilde{t}_q = \frac{\sum_{q=1}^{n} b_q}{\sum_{q=1}^{q} b_q}, q = \{1, 2, ..., n\}, \tag{14}$$

$$\tilde{i}_q = \frac{b_q}{\sum_{q=1}^{q} b_q}, q = \{n+1, n+2, ..., m\}, \tag{15}$$

$$\tilde{f}_q = \frac{b_q}{\sum_{i=1}^{q} b_q}, q = \{m+1, m+2, ..., q\}, \tag{16}$$

where $\boldsymbol{b_q, q = (1, 2, \cdots, n, n+1, \cdots, m, m+1, \cdots, q)}$ represents the classroom learning behavior.

Therefore, class one for the time-based SVNHFS $\boldsymbol{U_1}$ is obtained as follows.

$$\begin{aligned} U_1^t &= \left\langle \tilde{T}_1^t, \tilde{I}_1^t, \tilde{F}_1^t \right\rangle \\ &= \left\langle \{\tilde{t}_1^t, \tilde{t}_2^t, \cdots, \tilde{t}_q^t\}, \{\tilde{i}_1^t, \tilde{i}_2^t, \cdots, \tilde{i}_q^t\}, \{\tilde{f}_1^t, \tilde{f}_2^t, \cdots, \tilde{f}_q^t\} \right\rangle. \end{aligned}$$

However, since the subject of this study is classroom education quality assessment in multiple classes, the multi-classes SVNHFS at time-point *t* is obtained as follows.

$$\begin{aligned} U^t &= \left[U_1^t \quad U_2^t \quad \cdots \quad U_n^t \right] \\ &= \left[\left\langle \tilde{T}_1^t, \tilde{I}_1^t, \tilde{F}_1^t \right\rangle \quad \left\langle \tilde{T}_2^t, \tilde{I}_2^t, \tilde{F}_2^t \right\rangle \quad \cdots \quad \left\langle \tilde{T}_n^t, \tilde{I}_n^t, \tilde{F}_n^t \right\rangle \right]. \end{aligned}$$

Step 4. To reflect the importance of each learning behavior more accurately and reasonably in the process of MADM of classroom education quality. This study weights the multi-classes time-based SVNHFS by the SVNHFWA operator. Specifically, aggregate all multi-classes time-based SVNHFEs of $\boldsymbol{U_{tn}}$ by the SVNHFWA operator. Then, the collective SVNHFE $\boldsymbol{U_t}$ for a time point $\boldsymbol{t}$ $\boldsymbol{(t = 1, 2, \cdots, t)}$ is obtained as follows.

$$\begin{aligned} \phi_t &= SVNHFWA\left(U_1^t, U_2^t, \cdots U_n^t\right) = \sum_{n=1}^{n} W^t \cdot U_n^t \\ &= \bigcup_{\tilde{t}_1^t \in \tilde{T}_1^t, \cdots, \tilde{t}_q^t \in \tilde{T}_q^t, \tilde{i}_1^t \in \tilde{I}_1^t, \cdots, \tilde{i}_q^t \in \tilde{I}_q^t, \tilde{f}_1^t \in \tilde{F}_1^t, \cdots, \tilde{f}_q^t \in \tilde{F}_q^t} \left\{ \left\{ 1 - \prod_{q=1}^{q} \left(1 - \tilde{t}_q^t\right)^{W^t} \right\}, \left\{ \prod_{q=1}^{q} \left(1 - \tilde{i}_q^t\right)^{W^t} \right\}, \left\{ \prod_{q=1}^{q} \left(1 - \tilde{f}_q^t\right)^{W^t} \right\} \right\} \end{aligned} \tag{17}$$

Step 5. From **Def. 4**, the classical cosine measure method calculates the value between the SVNHFEs and ideal element $\boldsymbol{U^* = < 1, 0, 0 >}$. However, the imperfect element $\boldsymbol{U^- = < 0, 0, 1 >}$ also reflects the solution's quality. Thus, based on the SVNHFEs cosine measure method, the cosine measure between SVNHFEs and imperfect element $\boldsymbol{U^- = < 0, 0, 1 >}$ is obtained as follows.

$$\cos\left(\phi_i, \phi^-\right) = \frac{\left(\frac{1}{\tilde{f}_i} \sum_{\tilde{f}_i \in \tilde{F}_i} \tilde{f}_i \right)}{\sqrt{\left(\frac{1}{\tilde{t}_i} \sum_{\tilde{t}_i \in \tilde{T}_i} \tilde{t}_i \right)^2 + \left(\frac{1}{\tilde{i}_i} \sum_{\tilde{i}_i \in \tilde{I}_i} \tilde{i}_i \right)^2 + \left(\frac{1}{\tilde{f}_i} \sum_{\tilde{f}_i \in \tilde{F}_i} \tilde{f}_i \right)^2}}. \tag{18}$$

Step 6. Calculate the positive cosine measurement values between $\boldsymbol{U_t}$ $\boldsymbol{(t = 1, 2, \cdots, t)}$ and $\boldsymbol{U^* = < 1, 0, 0 >}$ by Eq. (2), and negative cosine measurement value between $\boldsymbol{U_t}$ $\boldsymbol{(t = 1, 2, \cdots, t)}$ and the non-ideal element $\boldsymbol{U^- = < 0, 0, 1 >}$ by Eq. (18). Finally, rank the best and worst time point(s), respectively.

4. Results and Discussion

Firstly, in this section, this study introduces the dataset used for training the YOLOv5 learning behaviors detection algorithm. Secondly, this study gives a practical case application to validate the effectiveness of the proposed model. Thirdly, this study gives a comprehensive analysis and discussions of the obtained results.

4.1. Data Set Description

Object detection and recognition are fundamental technologies in machine vision, enabling the identification of specific objects in images or videos and the extraction of relevant information about these objects [37]. This study employs detection and recognition techniques based on the YOLOv5

framework to identify four categories of student behavior in the 'Advanced Mathematics' course, and to construct the corresponding dataset.

A large volume of videos featuring undergraduate students from various majors and academic years was collected using classroom-facing cameras. To facilitate processing, these instructional videos were segmented into individual frames, yielding a curated dataset of 2,000 viable images. Additionally, a Learning Behavior Dataset (LBDS) was developed by selecting and analyzing six common classroom behaviors through both manual investigation and online annotation using the Make Sense platform. Specifically, student behaviors were categorized as "listening, writing, using phones, sleeping, talking, and distraction." An example of the LBDS is shown in Figure 2.

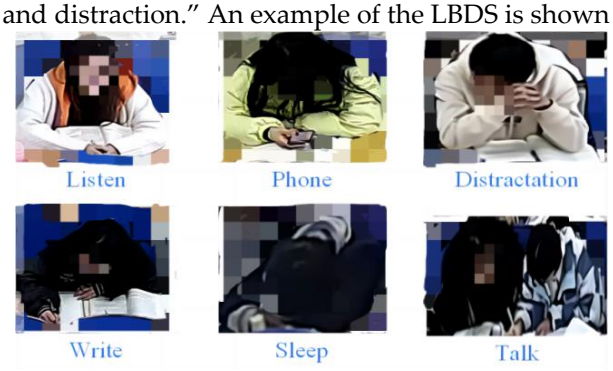

Figure 2. The example of LBDS.

In the experiment, the LBDS is divided into a training set and a testing set in a 4:1 ratio. The training set is used to train the detection model, while the testing set is employed for experimental validation. The study employs the controlled variable method in the comparative experiments, ensuring that all other factors remain constant when analyzing the network's detection accuracy and speed. The code in this study has been optimized by referencing the best parameter configurations from other network models. Ultimately, real-time counting of student behaviors in the classroom is achieved. After class, the real-time counting data is exported as an Excel file for subsequent data analysis. The recognition and analysis process is illustrated in Figure 3, and the results of classroom behavior recognition are shown in Figure 4.

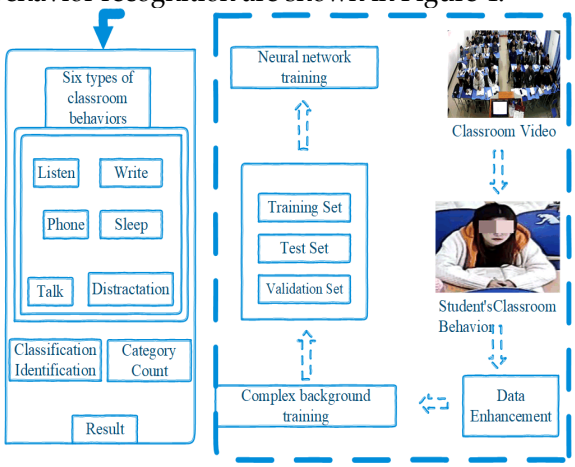

Figure 3. Student behavior identification and analysis process.

Figure 4. Effect Chart of Classroom Learning Recognition.

4.2. Case Study Application

In this subsection, the proposed model is applied in a case study. Specifically, this case study focuses on the "Advanced Mathematics" course across four classes, with each class lasting one hour. Meanwhile, this study divides the course duration into 9 time points equally. Thus, the detailed steps of the case application are shown as follows.

Step 1. Based on six learning behaviors identified by YOLOv5, four classes of learning behavior matrixes at 9 time points are established as follows.

$$N^{t1}=\begin{bmatrix} & listen & write & talk & distraction & phone & sleep \\ class1 & 20 & 5 & 3 & 2 & 1 & 2 \\ class2 & 18 & 3 & 4 & 3 & 6 & 1 \\ class3 & 15 & 2 & 5 & 3 & 5 & 1 \\ class4 & 21 & 6 & 5 & 4 & 6 & 2 \end{bmatrix},\ N^{t2}=\begin{bmatrix} & listen & write & talk & distraction & phone & sleep \\ class1 & 22 & 4 & 4 & 3 & 4 & 2 \\ class2 & 16 & 5 & 5 & 5 & 1 & 1 \\ class3 & 17 & 4 & 6 & 6 & 3 & 2 \\ class4 & 25 & 7 & 5 & 3 & 4 & 2 \end{bmatrix},$$

$$N^{t3}=\begin{bmatrix} & listen & write & talk & distraction & phone & sleep \\ class1 & 23 & 6 & 2 & 5 & 6 & 3 \\ class2 & 20 & 7 & 1 & 4 & 6 & 5 \\ class3 & 22 & 4 & 3 & 4 & 3 & 3 \\ class4 & 23 & 6 & 2 & 1 & 2 & 1 \end{bmatrix},\ N^{t4}=\begin{bmatrix} & listen & write & talk & distraction & phone & sleep \\ class1 & 21 & 6 & 3 & 2 & 3 & 2 \\ class2 & 25 & 5 & 2 & 2 & 5 & 3 \\ class3 & 19 & 3 & 2 & 3 & 5 & 6 \\ class4 & 26 & 8 & 3 & 2 & 3 & 1 \end{bmatrix},$$

$$N^{t5}=\begin{bmatrix} & listen & write & talk & distraction & phone & sleep \\ class1 & 19 & 8 & 5 & 4 & 4 & 2 \\ class2 & 10 & 2 & 4 & 3 & 7 & 4 \\ class3 & 13 & 2 & 5 & 4 & 6 & 4 \\ class4 & 25 & 5 & 2 & 4 & 2 & 2 \end{bmatrix},\ N^{t6}=\begin{bmatrix} & listen & write & talk & distraction & phone & sleep \\ class1 & 17 & 2 & 6 & 2 & 5 & 1 \\ class2 & 14 & 3 & 2 & 1 & 6 & 1 \\ class3 & 10 & 4 & 6 & 4 & 8 & 2 \\ class4 & 20 & 6 & 1 & 3 & 3 & 2 \end{bmatrix},$$

$$N^{t7}=\begin{bmatrix} & listen & write & talk & distraction & phone & sleep \\ class1 & 18 & 3 & 7 & 4 & 6 & 1 \\ class2 & 12 & 2 & 3 & 2 & 7 & 3 \\ class3 & 12 & 5 & 6 & 3 & 5 & 5 \\ class4 & 18 & 7 & 4 & 2 & 5 & 1 \end{bmatrix},\ N^{t8}=\begin{bmatrix} & listen & write & talk & distraction & phone & sleep \\ class1 & 15 & 4 & 6 & 3 & 6 & 2 \\ class2 & 14 & 3 & 3 & 4 & 6 & 2 \\ class3 & 15 & 7 & 4 & 2 & 4 & 4 \\ class4 & 21 & 5 & 3 & 4 & 7 & 3 \end{bmatrix},$$

$$N^{t9}=\begin{bmatrix} & listen & write & talk & distraction & phone & sleep \\ class1 & 13 & 3 & 7 & 2 & 8 & 2 \\ class2 & 10 & 5 & 5 & 36 & 9 & 2 \\ class3 & 8 & 5 & 5 & 5 & 7 & 3 \\ class4 & 17 & 8 & 2 & 2 & 2 & 2 \end{bmatrix}.$$

Step 2. Calculate combination weights based on multi-class learning behavior matrices.

Step 1'. Based on the Eqs. (3) and (4), six learning behaviors entropy vectors of 9 time-points are obtained as follows

$e_{t1}=[0.994,0.941,0.983,0.980,0.864,0.961]$, $e_{t2}=[0.998,0.979,0.993,0.966,0.928,0.957]$,

$e_{t3}=[0.999,0.986,0.953,0.918,0.933,0.913]$, $e_{t4}=[0.994,0.960,0.985,0.987,0.977,0.856]$,

$e_{t5}=[0.957,0.879,0.962,0.995,0.936,0.975]$, $e_{t6}=[0.978,0.945,0.853,0.932,0.960,0.959]$,

$e_{t7}=[0.985,0.926,0.963,0.968,0.993,0.843]$, $e_{t8}=[0.990,0.966,0.968,0.975,0.986,0.968]$,

$e_{t9}=[0.972,0.959,0.943,0.916,0.924,0.987]$.

Step 2'. Based on Eq. (5), six learning behaviors entropy weight vectors of 9 time-points are obtained as follows.

$w_{t1}=[w_1,w_2,w_3,w_4,w_5,w_6]$ $w_{t2}=[w_1,w_2,w_3,w_4,w_5,w_6]$

$=[0.020,0.221,0.062,0.074,0.492,0.141]$, $=[0.071,0.120,0.043,0.197,0.424,0.146]$,

$w_{t3}=[w_1,w_2,w_3,w_4,w_5,w_6]$ $w_{t4}=[w_1,w_2,w_3,w_4,w_5,w_6]$

$=[0.004,0.046,0.158,0.275,0.225,0.292]$, $=[0.025,0.174,0.063,0.054,0.099,0.585]$,

$w_{t5}=[w_1,w_2,w_3,w_4,w_5,w_6]$ $w_{t6}=[w_1,w_2,w_3,w_4,w_5,w_6]$

$=[0.144,0.409,0.129,0.017,0.218,0.084]$, $=[0.057,0.145,0.385,0.201,0.105,0.107]$,

$w_{t7}=[w_1,w_2,w_3,w_4,w_5,w_6]$ $w_{t8}=[w_1,w_2,w_3,w_4,w_5,w_6]$

$=[0.045,0.231,0.115,0.099,0.023,0.499]$, $=[0.068,0.234,0.217,0.170,0.093,0.217]$,

$$w_{t9} = \left[w_1, w_2, w_3, w_4, w_5, w_6\right]$$
$$= \left[0.095, 0.138, 0.190, 0.280, 0.255, 0.042\right].$$

Therefore, based on entropy weight vectors of 9 time-points, each class comprehensive score vector of 9 time-points is obtained.

Step 3'. Based on the Eq.(6), calculate the comprehensive score of each class. Then, it gets

$$S_{t1} = \left[S_{11}, S_{12}, S_{13}, S_{14}\right]^{>} \quad S_{t2} = \left[S_{11}, S_{12}, S_{13}, S_{14}\right]^{>} \quad S_{t3} = \left[S_{11}, S_{12}, S_{13}, S_{14}\right]^{>}$$
$$= \left[2.57, 4.56, 3.86, 3.30\right]^{>}, = \left[4.79, 3.50, 4.69, 5.40\right]^{>}, = \left[4.28, 4.47, 3.39, 1.69\right]^{>},$$
$$S_{t4} = \left[S_{11}, S_{12}, S_{13}, S_{14}\right]^{>} \quad S_{t5} = \left[S_{11}, S_{12}, S_{13}, S_{14}\right]^{>} \quad S_{t6} = \left[S_{11}, S_{12}, S_{13}, S_{14}\right]^{>}$$
$$= \left[3.33, 3.98, 5.29, 3.22\right]^{>}, = \left[7.75, 4.68, 5.04, 6.65\right]^{>}, = \left[4.61, 2.94, 5.32, 3.53\right]^{>},$$
$$S_{t7} = \left[S_{11}, S_{12}, S_{13}, S_{14}\right]^{>} \quad S_{t8} = \left[S_{11}, S_{12}, S_{13}, S_{14}\right]^{>} \quad S_{t9} = \left[S_{11}, S_{12}, S_{13}, S_{14}\right]^{>}$$
$$= \left[3.33, 3.17, 5.23, 3.68\right]^{>}, = \left[4.76, 3.98, 5.11, 5.23\right]^{>}, = \left[5.66, 6.65, 5.71, 4.25\right]^{>}.$$

Thus, the weight vector of each class of 9 time-points obtained by the entropy weight method is obtained as follows.

$$\omega_e^{t1} = \left[\omega_{e1}, \omega_{e2}, \omega_{e3}, \omega_{e4}\right]^{>} \quad \omega_e^{t2} = \left[\omega_{e1}, \omega_{e2}, \omega_{e3}, \omega_{e4}\right]^{>} \quad \omega_e^{t3} = \left[\omega_{e1}, \omega_{e2}, \omega_{e3}, \omega_{e4}\right]^{>}$$
$$= \left[0.18, 0.32, 0.27, 0.23\right]^{>}, = \left[0.26, 0.19, 0.25, 0.29\right]^{>}, = \left[0.31, 0.32, 0.25, 0.12\right]^{>},$$
$$\omega_e^{t4} = \left[\omega_{e1}, \omega_{e2}, \omega_{e3}, \omega_{e4}\right]^{>} \quad \omega_e^{t5} = \left[\omega_{e1}, \omega_{e2}, \omega_{e3}, \omega_{e4}\right]^{>} \quad \omega_e^{t6} = \left[\omega_{e1}, \omega_{e2}, \omega_{e3}, \omega_{e4}\right]^{>}$$
$$= \left[0.21, 0.25, 0.33, 0.20\right]^{>}, = \left[0.32, 0.19, 0.21, 0.28\right]^{>}, = \left[0.28, 0.18, 0.32, 0.22\right]^{>},$$
$$\omega_e^{t7} = \left[\omega_{e1}, \omega_{e2}, \omega_{e3}, \omega_{e4}\right]^{>} \quad \omega_e^{t8} = \left[\omega_{e1}, \omega_{e2}, \omega_{e3}, \omega_{e4}\right]^{>} \quad \omega_e^{t9} = \left[\omega_{e1}, \omega_{e2}, \omega_{e3}, \omega_{e4}\right]^{>}$$
$$= \left[0.22, 0.21, 0.34, 0.24\right]^{>}, = \left[0.25, 0.21, 0.27, 0.27\right]^{>}, = \left[0.25, 0.30, 0.26, 0.19\right]^{>}.$$

Step 4'. Calculate the Pearson correlation coefficients of each learning behavior based on the learning behavior matrix *N*. Then, the Pearson correlation coefficient for each learned behavior is then obtained. For example, the Pearson correlation coefficient matric r^{t1} at time-point *t*1 is as follows.

$$r^{t1} = \begin{bmatrix} 1 & 0.97 & -0.99 & 0.15 & -0.74 & 0.38 \\ 0.97 & 1 & -0.95 & 0.22 & -0.84 & 0.37 \\ -0.99 & -0.95 & 1 & 0 & 0.80 & -0.52 \\ 0.15 & 0.22 & 0 & 1 & 0.17 & -0.82 \\ -0.74 & -0.84 & 0.80 & 0.17 & 1 & -0.70 \\ 0.38 & 0.37 & -0.52 & -0.82 & -0.70 & 1 \end{bmatrix}.$$

For ease of understanding, the Pearson correlation coefficients of the four classes at time point t1 are shown in Figure 5.

Thus, learning behavior indicator conflicts are obtained based on the Pearson correlation coefficient matric r^{t1}. For example, the learning behavior indicator conflicts R^{t1} at time-point *t*1 is obtained as follows.

$$R^{t1} = \begin{bmatrix} 0 & 0.03 & 1.99 & 0.85 & 1.74 & 0.62 \\ 0.03 & 0 & 1.95 & 0.78 & 1.84 & 0.63 \\ 1.99 & 1.95 & 0 & 1 & 0.20 & 1.52 \\ 0.85 & 0.78 & 1 & 0 & 0.83 & 1.82 \\ 1.74 & 1.84 & 0.20 & 0.83 & 0 & 1.70 \\ 0.62 & 0.63 & 1.52 & 1.82 & 1.70 & 0 \end{bmatrix}.$$

Then, the amount of information about learning behavior vectors at 9 time-points $\boldsymbol{C_t}(\boldsymbol{t} = \boldsymbol{t1}, \boldsymbol{t2}, \cdots, \boldsymbol{t9})$ are obtained as follows.

$$C_{t1} = \left[C_1, C_2, C_3, C_4, C_5, C_6\right] \qquad C_{t2} = \left[C_1, C_2, C_3, C_4, C_5, C_6\right]$$
$$= \left[13.84, 9.57, 6.37, 4.30, 15.02, 3.15\right], = \left[18.24, 6.64, 4.04, 9.76, 5.62, 1.88\right],$$

$$C_{t3}=\left[C_1,C_2,C_3,C_4,C_5,C_6\right] \quad C_{t4}=\left[C_1,C_2,C_3,C_4,C_5,C_6\right]$$
$$=\left[9.04,6.99,5.30,6.66,8.08,7.42\right], =\left[19.01,12.52,3.63,2.82,6.60,12.50\right],$$
$$C_{t5}=\left[C_1,C_2,C_3,C_4,C_5,C_6\right] \quad C_{t6}=\left[C_1,C_2,C_3,C_4,C_5,C_6\right]$$
$$=\left[39.66,15.73,7.07,2.50,13.39,6.24\right], =\left[28.02,7.39,13.93,4.20,11.51,1.98\right],$$
$$C_{t7}=\left[C_1,C_2,C_3,C_4,C_5,C_6\right] \quad C_{t8}=\left[C_1,C_2,C_3,C_4,C_5,C_6\right]$$
$$=\left[18.01,13.09,7.51,4.02,6.48,11.88\right], =\left[12.54,8.98,8.90,5.35,6.25,5.07\right],$$
$$C_{t9}=\left[C_1,C_2,C_3,C_4,C_5,C_6\right]$$
$$=\left[28.48,13.48,11.26,9.94,15.74,2.58\right].$$

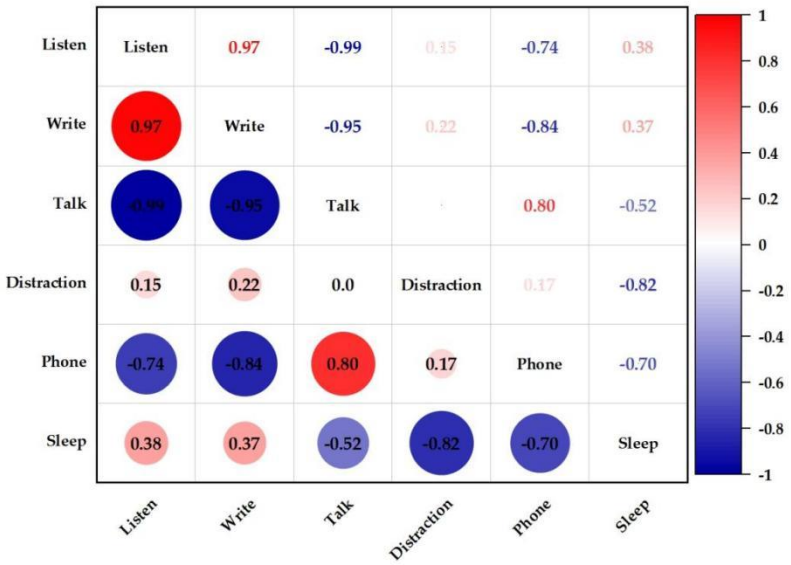

Figure 5. Pearson correlation coefficients of the four classes at time point *t*1.

Step 5'. The CRITIC weight of each behavior $\boldsymbol{w_{2j}, (j=1,2,\cdots,6)}$ is obtained based on Eq. (10). Then, the weight vectors by the CRITIC weight method is obtained as follows.

$$w_{t1}=\left[w_{21},w_{22},w_{23},w_{24},w_{25},w_{26}\right] \quad w_{t2}=\left[w_{21},w_{22},w_{23},w_{24},w_{25},w_{26}\right]$$
$$=\left[0.100,0.100,0.127,0.101,0.121,0.120\right], =\left[0.395,0.144,0.088,0.211,0.122,0.041\right],$$
$$w_{t3}=\left[w_{21},w_{22},w_{23},w_{24},w_{25},w_{26}\right] \quad w_{t4}=\left[w_{21},w_{22},w_{23},w_{24},w_{25},w_{26}\right]$$
$$=\left[0.208,0.161,0.122,0.153,0.186,0.171\right], =\left[0.333,0.219,0.064,0.049,0.116,0.219\right],$$
$$w_{t5}=\left[w_{21},w_{22},w_{23},w_{24},w_{25},w_{26}\right] \quad w_{t6}=\left[w_{21},w_{22},w_{23},w_{24},w_{25},w_{26}\right]$$
$$=\left[0.496,0.186,0.084,0.030,0.158,0.074\right], =\left[0.418,0.110,0.208,0.063,0.172,0.030\right],$$
$$w_{t7}=\left[w_{21},w_{22},w_{23},w_{24},w_{25},w_{26}\right] \quad w_{t8}=\left[w_{21},w_{22},w_{23},w_{24},w_{25},w_{26}\right]$$
$$=\left[0.295,0.215,0.123,0.066,0.106,0.195\right], =\left[0.266,0.191,0.189,0.114,0.133,0.108\right],$$
$$w_{t9}=\left[w_{21},w_{22},w_{23},w_{24},w_{25},w_{26}\right]$$
$$=\left[0.350,0.165,0.138,0.122,0.193,0.032\right].$$

Step 6'. Based on the Eq.(11), calculate the comprehensive score of each class. It gets

$$S_{t1}=\left[S_{21},S_{22},S_{23},S_{24}\right]^{>} \quad S_{t2}=\left[S_{21},S_{22},S_{23},S_{24}\right]^{>} \quad S_{t3}=\left[S_{21},S_{22},S_{23},S_{24}\right]^{>}$$
$$=\left[3.45,3.76,3.37,3.85\right]^{>}, =\left[10.82,8.69,9.53,12.59\right]^{>}, =\left[8.38,7.98,7.26,6.68\right]^{>},$$
$$S_{t4}=\left[S_{21},S_{22},S_{23},S_{24}\right]^{>} \quad S_{t5}=\left[S_{21},S_{22},S_{23},S_{24}\right]^{>} \quad S_{t6}=\left[S_{21},S_{22},S_{23},S_{24}\right]^{>}$$
$$=\left[9.39,10.88,9.15,11.27\right]^{>}, =\left[11.71,6.89,8.25,13.47\right]^{>}, =\left[9.59,7.72,7.55,9.99\right]^{>},$$

$$S_{t7}=\left[S_{21},S_{22},S_{23},S_{24}\right]^{>} \quad S_{t8}=\left[S_{21},S_{22},S_{23},S_{24}\right]^{>} \quad S_{t9}=\left[S_{21},S_{22},S_{23},S_{24}\right]^{>}$$
$$=\left[7.92,5.80,7.06,8.17\right]^{>},=\left[7.24,6.33,7.27,8.82\right]^{>},=\left[7.86,7.55,6.37,8.24\right]^{>},$$

Thus, the weight vector of each class of 9 time-points by the CRITIC weight method is obtained as follows.

$$\omega_c^{t1}=\left[\omega_{c1}^{t1},\omega_{c2}^{t1},\omega_{c3}^{t1},\omega_{c4}^{t1}\right]^{>} \quad \omega_c^{t2}=\left[\omega_{c1}^{t2},\omega_{c2}^{t2},\omega_{c3}^{t2},\omega_{c4}^{t2}\right]^{>} \quad \omega_c^{t3}=\left[\omega_{c1}^{t3},\omega_{c2}^{t3},\omega_{c3}^{t3},\omega_{c4}^{t3}\right]^{>}$$
$$=\left[0.24,0.26,0.23,0.27\right]^{>},=\left[0.26,0.21,0.23,0.30\right]^{>},=\left[0.28,0.26,0.24,0.22\right]^{>},$$
$$\omega_c^{t4}=\left[\omega_{c1}^{t4},\omega_{c2}^{t4},\omega_{c3}^{t4},\omega_{c4}^{t4}\right]^{>} \quad \omega_c^{t5}=\left[\omega_{c1}^{t5},\omega_{c2}^{t5},\omega_{c3}^{t5},\omega_{c4}^{t5}\right]^{>} \quad \omega_c^{t6}=\left[\omega_{c1}^{t6},\omega_{c2}^{t6},\omega_{c3}^{t6},\omega_{c4}^{t6}\right]^{>}$$
$$=\left[0.23,0.27,0.22,0.28\right]^{>},=\left[0.29,0.17,0.20,0.33\right]^{>},=\left[0.28,0.22,0.22,0.29\right]^{>},$$
$$\omega_c^{t7}=\left[\omega_{c1}^{t7},\omega_{c2}^{t7},\omega_{c3}^{t7},\omega_{c4}^{t7}\right]^{>} \quad \omega_c^{t8}=\left[\omega_{c1}^{t8},\omega_{c2}^{t8},\omega_{c3}^{t8},\omega_{c4}^{t8}\right]^{>} \quad \omega_c^{t9}=\left[\omega_{c1}^{t9},\omega_{c2}^{t9},\omega_{c3}^{t9},\omega_{c4}^{t9}\right]^{>}$$
$$=\left[0.27,0.20,0.24,0.28\right]^{>},=\left[0.24,0.21,0.25,0.30\right]^{>},=\left[0.26,0.25,0.21,0.27\right]^{>}.$$

Step 7'. Based on Eq. (13), the weight vectors of four classes of 9 time-points by the combined weighting method are obtained as follows.

$$W^{t1}=\left[0.21,0.29,0.25,0.25\right]^{>},\ W^{t2}=\left[0.26,0.20,0.24,0.30\right]^{>},\ W^{t3}=\left[0.29,0.29,0.24,0.17\right]^{>},$$
$$W^{t4}=\left[0.22,0.26,0.28,0.24\right]^{>},\ W^{t5}=\left[0.31,0.18,0.21,0.30\right]^{>},\ W^{t6}=\left[0.28,0.20,0.27,0.25\right]^{>},$$
$$W^{t7}=\left[0.24,0.20,0.29,0.26\right]^{>},\ W^{t8}=\left[0.25,0.21,0.26,0.29\right]^{>},\ W^{t9}=\left[0.26,0.27,0.23,0.23\right]^{>},$$

Step 3. Construct SVNHFSs based on the Eqs. (14-16). Thus, the truth-membership hesitant degree is $\tilde{\boldsymbol{t}}_{\boldsymbol{q}}\ (\boldsymbol{q}=\mathbf{1},\mathbf{2})$, the indeterminacy-membership hesitant degree is $\tilde{\boldsymbol{i}}_{\boldsymbol{q}}\ (\boldsymbol{q}=\mathbf{1},\mathbf{2})$, and the falsity-membership is $\tilde{\boldsymbol{f}}_{\boldsymbol{q}}\ (\boldsymbol{q}=\mathbf{1},\mathbf{2})$**.** Then, the SVNHFS $\boldsymbol{U}_{\boldsymbol{i}}^{\mathbf{1}}\ (\boldsymbol{i}=\mathbf{1},\mathbf{2},\mathbf{3},\mathbf{4})$ for four classes at time point $\boldsymbol{t1}$ are as follows.

$$U_1^1=\left\langle\tilde{T}_1,\tilde{I}_1,\tilde{F}_1\right\rangle \qquad U_2^1=\left\langle\tilde{T}_2,\tilde{I}_2,\tilde{F}_2\right\rangle$$
$$=\left\langle\{0.758\},\{0.091,.0.061\},\{0.030,0.061\}\right\rangle,\ =\left\langle\{0.600\},\{0.114,.0.086\},\{0.171,0.029\}\right\rangle,$$

$$U_3^1=\left\langle\tilde{T}_3,\tilde{I}_3,\tilde{F}_3\right\rangle \qquad U_4^1=\left\langle\tilde{T}_4,\tilde{I}_4,\tilde{F}_4\right\rangle$$
$$=\left\langle\{0.548\},\{0.161,0.097\},\{0.161,0.032\}\right\rangle,\ =\left\langle\{0.730\},\{0.081,0.108\},\{0.054,0.027\}\right\rangle.$$

Specifically, SVNHZ classroom learning behaviors decision matrix values for four classes are shown in Table 1(a) and (b).

Table 1(a). SVNHZ time-based classroom learning behaviors decision matrix.

T \ Class	Class One	Class Two
t_1	<{0.758},{0.091,0.061},{0.030,0.061}>	<{0.600},{0.114,0.086},{0.171,0.029}>
t_2	<{0.667},{0.103,0.077},{0.103,0.051}>	<{0.636},{0.152,0.152},{0.030,0.030}>
t_3	<{0.644},{0.044,0.111},{0.133,0.067}>	<{0.628},{0.023,0.093},{0.140,0.116}>
t_4	<{0.730},{0.081,0.054},{0.081,0.054}>	<{0.714},{0.048,0.048},{0.119,0.071}>
t_5	<{0.643},{0.119,0.095},{0.095,0.048}>	<{0.400},{0.133,0.100},{0.233,0.133}>
t_6	<{0.576},{0.182,0.061},{0.152,0.030}>	<{0.630},{0.074,0.037},{0.222,0.037}>
t_7	<{0.538},{0.179,0.103},{0.154,0.026}>	<{0.483},{0.103,0.069},{0.241,0.103}>
t_8	<{0.528},{0.167,0.083},{0.167,0.056}>	<{0.531},{0.094,0.125},{0.188,0.063}>
t_9	<{0.457},{0.200,0.057},{0.229, 0.057}>	<{0.405},{0.135,0.162},{0.243, 0.054}>

Table 1(b). SVNHZ time-based classroom learning behaviors decision matrix.

T \ Class	Class Three	Class Four
t_1	<{0.548},{0.161,0.097},{0.161,0.032}>	<{0.730},{0.081,0.108},{0.054,0.027}>
t_2	<{0.538},{0.158,0.158},{0.079,0.053}>	<{0.696},{0.109,0.065},{0.087,0.043}>
t_3	<{0.667},{0.077,0.103},{0.077,0.077}>	<{0.829},{0.057,0.029},{0.057,0.029}>
t_4	<{0.579},{0.053,0.079},{0.132,0.158}>	<{0.791},{0.070,0.047},{0.070,0.023}>
t_5	<{0.441},{0.147,0.118},{0.176,0.118}>	<{0.732},{0.049,0.098},{0.049,0.073}>
t_6	<{0.412},{0.176,0.118},{0.235,0.059}>	<{0.743},{0.029,0.086},{0.086,0.057}>
t_7	<{0.472},{0.167,0.083},{0.139,0.139}>	<{0.676},{0.108,0.054},{0.135,0.027}>
t_8	<{0.611},{0.111,0.056},{0.111,0.111}>	<{0.605},{0.070,0.093},{0.163,0.070}>
t_9	<{0.394},{0.152,0.152},{0.212, 0.091}>	<{0.758},{0.061,0.061},{0.061, 0.061}>

Therefore, the SVNHZ time-based classroom learning behaviors decision matrix $\boldsymbol{U}$ is obtained. For example, the SVNHZ time-based classroom learning behaviors decision matrix $\boldsymbol{U^{t1}}$ at time-point $\boldsymbol{t1}$ is as follows.

$$U^1 = \left[\left\langle \tilde{T}_1^1, \tilde{I}_1^1, \tilde{F}_1^1 \right\rangle, \left\langle \tilde{T}_2^1, \tilde{I}_2^1, \tilde{F}_2^1 \right\rangle, \left\langle \tilde{T}_3^1, \tilde{I}_3^1, \tilde{F}_3^1 \right\rangle, \left\langle \tilde{T}_4^1, \tilde{I}_4^1, \tilde{F}_4^1 \right\rangle\right]$$
$$= \begin{bmatrix} \left\langle \{0.758\}, \{0.091, 0.061\}, \{0.030, 0.061\} \right\rangle, \left\langle \{0.600\}, \{0.113, 0.086\}, \{0.171, 0.029\} \right\rangle, \\ \left\langle \{0.548\}, \{0.161, 0.097\}, \{0.161, 0.032\} \right\rangle, \left\langle \{0.730\}, \{0.081, 0.108\}, \{0.054, 0.027\} \right\rangle. \end{bmatrix}.$$

Step 4. Based on the combined time weights, the SVNHFWA operator is employed. Specifically, this study adopts the SVNHFWA operator to calculate the integrated value for each time point. Take the time point *t*1, for example, the collective SVNHFE $\boldsymbol{\phi_1}$ is obtained as follows.

$$\phi_1 = SVNHFWA\left(U_1^1, U_2^1, U_3^1, U_4^1\right) = \sum_{n=1}^{4} W^{t1} \cdot U_n^1$$
$$= \bigcup_{\substack{\tilde{I}_1^1 \in \tilde{T}_1^1, \tilde{I}_2^1 \in \tilde{T}_2^1, \tilde{I}_3^1 \in \tilde{T}_3^1, \tilde{I}_4^1 \in \tilde{T}_4^1, \tilde{I}_{11}^1 \in \tilde{I}_1^1, \tilde{I}_{12}^1 \in \tilde{I}_1^1, \tilde{I}_{21}^1 \in \tilde{I}_2^1, \tilde{I}_{22}^1 \in \tilde{I}_2^1, \tilde{I}_{31}^1 \in \tilde{I}_3^1, \tilde{I}_{32}^1 \in \tilde{I}_3^1, \tilde{I}_{41}^1 \in \tilde{I}_4^1, \tilde{I}_{42}^1 \in \tilde{I}_4^1, \\ \tilde{f}_{11}^1 \in \tilde{F}_1^1, \tilde{f}_{12}^1 \in \tilde{F}_1^1, \tilde{f}_{21}^1 \in \tilde{F}_2^1, \tilde{f}_{22}^1 \in \tilde{F}_2^1, \tilde{f}_{31}^1 \in \tilde{F}_3^1, \tilde{f}_{32}^1 \in \tilde{F}_3^1, \tilde{f}_{41}^1 \in \tilde{F}_4^1, \tilde{f}_{42}^1 \in \tilde{F}_4^1.}} \left\{ \left\{ 1 - \prod_{q=1}^{4} \left(1 - \tilde{t}_q^1\right)^{W^{t1}} \right\}, \left\{ \prod_{q=1}^{4} \left(1 - \tilde{i}_q^1\right)^{W^{t1}} \right\}, \left\{ \prod_{q=1}^{4} \left(1 - \tilde{f}_q^1\right)^{W^{t1}} \right\} \right\}$$
$$= \left\{ \begin{array}{l} \left\{1 - \left(1-0.758\right)^{0.21}\left(1-0.600\right)^{0.29}\left(1-0.548\right)^{0.25}\left(1-0.730\right)^{0.25}\right\}, \\ \left\{ \begin{array}{l} 0.091^{0.21}0.114^{0.29}0.161^{0.25}0.081^{0.25}, 0.091^{0.21}0.114^{0.29}0.161^{0.25}0.108^{0.25}, \\ 0.091^{0.21}0.114^{0.29}0.097^{0.25}0.081^{0.25}, 0.091^{0.21}0.114^{0.29}0.097^{0.25}0.108^{0.25}, \\ 0.091^{0.21}0.086^{0.29}0.161^{0.25}0.081^{0.25}, 0.091^{0.21}0.086^{0.29}0.161^{0.25}0.108^{0.25}, \\ 0.091^{0.21}0.086^{0.29}0.097^{0.25}0.081^{0.25}, 0.091^{0.21}0.086^{0.29}0.097^{0.25}0.108^{0.25}, \\ 0.061^{0.21}0.114^{0.29}0.161^{0.25}0.081^{0.25}, 0.061^{0.21}0.114^{0.29}0.161^{0.25}0.108^{0.25}, \\ 0.061^{0.21}0.114^{0.29}0.097^{0.25}0.081^{0.25}, 0.061^{0.21}0.114^{0.29}0.097^{0.25}0.108^{0.25}, \\ 0.061^{0.21}0.086^{0.29}0.161^{0.25}0.081^{0.25}, 0.061^{0.21}0.086^{0.29}0.161^{0.25}0.081^{0.25}, \\ 0.061^{0.21}0.114^{0.29}0.097^{0.25}0.081^{0.25}, 0.061^{0.21}0.114^{0.29}0.097^{0.25}0.108^{0.25}. \end{array} \right\}, \\ \left\{ \begin{array}{l} 0.030^{0.21}0.171^{0.29}0.161^{0.25}0.054^{0.25}, 0.030^{0.21}0.171^{0.29}0.161^{0.25}0.027^{0.25}, \\ 0.030^{0.21}0.171^{0.29}0.032^{0.25}0.054^{0.25}, 0.030^{0.21}0.171^{0.29}0.032^{0.25}0.027^{0.25}, \\ 0.030^{0.21}0.029^{0.29}0.161^{0.25}0.054^{0.25}, 0.030^{0.21}0.029^{0.29}0.161^{0.25}0.027^{0.25}, \\ 0.030^{0.21}0.029^{0.29}0.032^{0.25}0.054^{0.25}, 0.030^{0.21}0.029^{0.29}0.032^{0.25}0.027^{0.25}, \\ 0.061^{0.21}0.171^{0.29}0.161^{0.25}0.054^{0.25}, 0.061^{0.21}0.171^{0.29}0.161^{0.25}0.027^{0.25}, \\ 0.061^{0.21}0.171^{0.29}0.032^{0.25}0.054^{0.25}, 0.061^{0.21}0.171^{0.29}0.032^{0.25}0.027^{0.25}, \\ 0.061^{0.21}0.029^{0.29}0.161^{0.25}0.054^{0.25}, 0.061^{0.21}0.029^{0.29}0.161^{0.25}0.027^{0.25}, \\ 0.061^{0.21}0.029^{0.29}0.032^{0.25}0.054^{0.25}, 0.061^{0.21}0.029^{0.29}0.032^{0.25}0.027^{0.25}. \end{array} \right\} \end{array} \right\}.$$

The time point $\boldsymbol{t_1}$ collective SVNHFE $\boldsymbol{U_1}$ is calculated as

$$U_1=\left\{\begin{Bmatrix}\{0.664\},\\ \begin{bmatrix}0.109,0.117,0.096,0.103,\\0.100,0.108,0.088,0.095,\\0.100,0.107,0.088,0.095,\\0.092,0.099,0.081,0.087.\end{bmatrix},\begin{bmatrix}0.088,0.074,0.059,0.049,\\0.052,0.044,0.035,0.029,\\0.102,0.085,0.068,0.057,\\0.061,0.051,0.041,0.034.\end{bmatrix}\end{Bmatrix}\right\}.$$

Analogously, based on the aforementioned calculation steps, the other collective SVNHFE $\boldsymbol{U_i}$ $(\boldsymbol{i=t_2,t_3,t_4,t_5,t_6})$ are derived as follows.

$$U_2=\left\{\begin{Bmatrix}\{0.646\},\\ \begin{bmatrix}0.126,0.108,0.126,0,108,\\0.126,0.108,0.126,0.108,\\0.116,0.100,0.116,0.100,\\0.116,0.100,0.116,0.100,\end{bmatrix},\begin{bmatrix}0.072,0.058,0.065,0.053,\\0.072,0.058,0.065,0.053,\\0.060,0.048,0.054,0.044,\\0.060,0.048,0.054,0.044,\end{bmatrix}\end{Bmatrix}\right\}\ U_3=\left\{\begin{Bmatrix}\{0.687\},\\ \begin{bmatrix}0.044,0.039,0,047,0.042,\\0.066,0.058,0.070,0.063,\\0.057,0.051,0.061,0.055,\\0.086,0.077,0.092,0.082.\end{bmatrix},\begin{bmatrix}0.102,0.091,0.102,0.091,\\0.097,0.086,0.097,0.086,\\0.084,0.075,0.084,0.075,\\0.079,0.071,0.079,0.071.\end{bmatrix}\end{Bmatrix}\right\}$$

$$U_4=\left\{\begin{Bmatrix}\{0.708\},\\ \begin{bmatrix}0.061,0.055,0.068,0.062,\\0.061,0.055,0.068,0.062,\\0.055,0.050,0.062,0.056,\\0.055,0.050,0.062,0.056.\end{bmatrix},\begin{bmatrix}0.099,0.076,0.104,0.080,\\0.087,0.066,0.091,0.070,\\0.091,0.069,0.095,0.073,\\0.079,0.061,0.083,0.064.\end{bmatrix}\end{Bmatrix}\right\}\ U_5=\left\{\begin{Bmatrix}\{0.605\},\\ \begin{bmatrix}0.097,0.120,0.092,0.114,\\0.092,0.114,0.088,0.108,\\0.090,0.112,0.086,0.107,\\0.086,0.106,0.082,0.101.\end{bmatrix},\begin{bmatrix}0.104,0.117,0.096,0.108,\\0.094,0.106,0.086,0.097,\\0.084,0.095,0.078,0.088,\\0.076,0.086,0.070,0.079.\end{bmatrix}\end{Bmatrix}\right\}$$

$$U_6=\left\{\begin{Bmatrix}\{0.602\},\\ \begin{bmatrix}0.095,0.125,0.085,0.112,\\0.083,0.109,0.074,0.097,\\0.070,0.092,0.063,0.083,\\0.061,0.080,0.055,0.072\end{bmatrix},\begin{bmatrix}0.160,0.144,0.110,0.099,\\0.112,0.101,0.077,0.069,\\0.102,0.092,0.070,0.063,\\0.071,0.064,0.049,0.044.\end{bmatrix}\end{Bmatrix}\right\}\ U_7=\left\{\begin{Bmatrix}\{0.552\},\\ \begin{bmatrix}0.137,0.115,0.112,0.094,\\0.127,0.106,0.103,0.086,\\0.120,0.100,0.098,0.082,\\0.111,0.092,0.090,0.075.\end{bmatrix},\begin{bmatrix}0.158,0.104,0.158,0.104,\\0.133,0.087,0.133,0.087,\\0.102,0.067,0.102,0.067,\\0.086,0.057,0.086,0.057.\end{bmatrix}\end{Bmatrix}\right\}$$

$$U_8=\left\{\begin{Bmatrix}\{0.574\},\\ \begin{bmatrix}0.104,0.113,0.087,0.095,\\0.110,0.120,0.093,0.100,\\0.087,0.095,0.073,0.080,\\0.093,0.101,0.078,0.085.\end{bmatrix},\begin{bmatrix}0.153,0.120,0.153,0.120,\\0.121,0.095,0.121,0.095,\\0.117,0.092,0.117,0.092,\\0.093,0.073,0.093,0.073.\end{bmatrix}\end{Bmatrix}\right\}\ U_9=\left\{\begin{Bmatrix}\{0.527\},\\ \begin{bmatrix}0.128,0.128,0.128,0.128,\\0.134,0.134,0.134,0.134,\\0.092,0.092,0.092,0.092,\\0.097,0.097,0.097,0.097.\end{bmatrix},\begin{bmatrix}0.168,0.168,0.138,0.138,\\0.111,0.111,0.091,0.091,\\0.117,0.117,0.096,0.096,\\0.078,0.078,0.064,0.064.\end{bmatrix}\end{Bmatrix}\right\}$$

Step 5. The cosine measure values for time-based classes SVNHFE are calculated concerning the ideal element $\boldsymbol{U^*=<1,0,0>}$ by Eq. (2) and the non-ideal element $\boldsymbol{U^-=<0,0,1>}$ by Eq. (16). Therefore, the cosine measure values between $\boldsymbol{U_i}$ $(\boldsymbol{i=1,2,\cdots,9})$ and $\boldsymbol{U^*}$ are obtained as follows.

$$\cos\left(U_1,U^*\right)=0.986,\cos\left(U_2,U^*\right)=0.982,\cos\left(U_3,U^*\right)=0.988,$$
$$\cos\left(U_4,U^*\right)=0.990,\cos\left(U_5,U^*\right)=0.976,\cos\left(U_6,U^*\right)=0.980,$$
$$\cos\left(U_7,U^*\right)=0.968,\cos\left(U_8,U^*\right)=0.970,\cos\left(U_9,U^*\right)=0.959.$$

The cosine measure values between $\boldsymbol{U_i}$ $(\boldsymbol{i=t_2,t_3,t_4,t_5,t_6})$ and $\boldsymbol{U^-}$ are obtained as follows.

$$\cos\left(U_1,U^-\right)=0.086,\cos\left(U_2,U^-\right)=0.086,\cos\left(U_3,U^-\right)=0.123,$$
$$\cos\left(U_4,U^-\right)=0.113,\cos\left(U_5,U^-\right)=0.148,\cos\left(U_6,U^-\right)=0.145,$$
$$\cos\left(U_7,U^-\right)=0.174,\cos\left(U_8,U^-\right)=0.183,\cos\left(U_9,U^-\right)=0.196.$$

Step 6. Based on the cosine measure values, the optimal learning effects of the 9 time-points of the classes are ranked as $\boldsymbol{U_4\succ U_3\succ U_1\succ U_2\succ U_6\succ U_5\succ U_8\succ U_7\succ U_9}$, and the worst learning effects of the 9 time-points of the classes are ranked as $\boldsymbol{U_9\succ U_8\succ U_7\succ U_5\succ U_6\succ U_3\succ U_4\succ U_1\sim U_2}$.

4.3 Comprehensive Analysis and Discussion

To confirm the feasibility and utility of the proposed method in assessing the effectiveness of student learning, this study conducted a comparative analysis with the classical entropy weight method and the CRITIC method [38, 39]. The positive and negative cosine measurement value by the classical entropy weight method and the classical CRITIC weight method is shown in Table 2.

Table 2. The proposed weighting method ranking results.

Time-points	The classical entropy weight method		The classical CRITIC weight method	
	Positive cosine measurement value	Negative cosine measurement value	Positive cosine measurement value	Negative cosine measurement value
t1	0.985	0.090	0.987	0.082
t2	0.981	0.087	0.982	0.086
t3	0.987	0.131	0.990	0.115
t4	0.989	0.121	0.991	0.105
t5	0.975	0.151	0.977	0.144
t6	0.977	0.153	0.982	0.138
t7	0.966	0.182	0.970	0.167
t8	0.970	0.183	0.970	0.183
t9	0.953	0.209	0.964	0.185

For convenience, the radar map of positive and negative cosine measurement values of the three methods are shown in Figures 6 and 7.

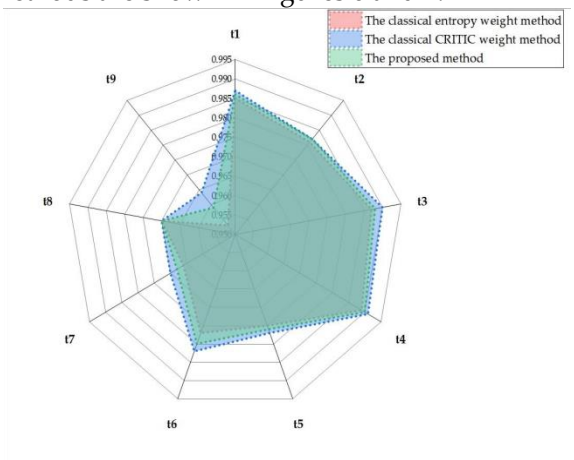

Figure 6. Radar map of the positive cosine measurement value.

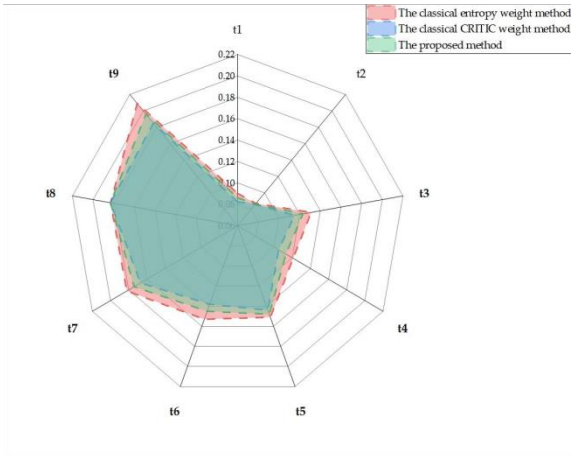

Figure 7. Radar map of the negative cosine measurement value.

Besides, the different weight method ranking results are shown in Table 3.

Table 3. Different weight method ranking results.

Method	**Positive Sorting results**	**Negative Sorting results**	**Optimal time-point**	**Worst time-point**
The proposed method	$U_4 \succ U_3 \succ U_1 \succ U_2 \succ U_6 \succ U_5 \succ U_8 \succ U_7 \succ U_9$	$U_9 \succ U_8 \succ U_7 \succ U_5 \succ U_6 \succ U_3 \succ U_4 \succ U_1 \sim U_2.$	U_4	U_9
The classical entropy weight method	$U_4 \succ U_3 \succ U_1 \succ U_2 \succ U_6 \succ U_5 \succ U_8 \succ U_7 \succ U_9$	$U_9 \succ U_8 \succ U_7 \succ U_6 \succ U_5 \succ U_1 \succ U_4 \succ U_3 \succ U_2.$	U_4	U_9
The classical CRITIC weight method	$U_4 \succ U_3 \succ U_1 \succ U_6 \succ U_2 \succ U_5 \succ U_8 \succ U_7 \succ U_9$	$U_9 \succ U_8 \succ U_7 \succ U_5 \succ U_6 \succ U_3 \succ U_4 \succ U_2 \succ U_1.$	U_4	U_9

The comparison reveals that the class learning effectiveness of 9 time-points order obtained by the proposed method aligns with the ranking results obtained from the classical methods. They all consider $\boldsymbol{U_4}$ as the ideal time-point and $\boldsymbol{U_9}$ as the non-ideal time-point.

Therefore, based on students' classroom behavior at different time-points under the sorting results, teachers dynamically adjust teaching strategies to enhance engagement and improve learning outcomes. By promptly addressing attention lapses or low participation, teachers can modify content, and methods, or introduce interactive activities to re-engage students. This adaptive approach ensures personalized pacing and difficulty adjustments, optimizing overall teaching effectiveness and fostering student development.

Then, to further establish the effectiveness and practicality of the proposed TQE method, this study engages in a comparative assessment against alternative methodologies, including the traditional cosine measurement method, as well as the SVNHF normalized Hamming distance, the SVNHF normalized Euclidean distance, and their corresponding similarity measures [40-42]. Specifically, the sorting results for the proposed method and other alternative methods are shown in Table 4. Among them, in Table 4, which are consistent with those of existing methods. They all agree that time-point $\boldsymbol{U_4}$ is the optimal scheme. Based on this consistency, the proposed method is effective and reliable.

Table 4. Different MADM method ranking results.

Method	Positive Sorting results	Optimal time-point	Worst time-point
The proposed method	$U_4 \succ U_3 \succ U_1 \succ U_2 \succ U_6 \succ U_5 \succ U_8 \succ U_7 \succ U_9$	U_4	U_9
The traditional cosine measurement method	$U_4 \succ U_3 \succ U_1 \succ U_2 \succ U_6 \succ U_5 \succ U_8 \succ U_7 \succ U_9$	U_4	U_9
The SVNHF normalized Hamming distance measurement method	$U_4 \succ U_3 \succ U_1 \succ U_2 \succ U_6 \succ U_5 \succ U_8 \succ U_7 \succ U_9$	U_4	U_9
The SVNHF normalized Euclidean Distance measurement method	$U_4 \succ U_3 \succ U_1 \succ U_2 \succ U_6 \succ U_5 \succ U_8 \succ U_7 \succ U_9$	U_4	U_9
The similarity measures based on SVNHF normalized Euclidean Distance	$U_4 \succ U_3 \succ U_1 \succ U_2 \succ U_6 \succ U_5 \succ U_8 \succ U_7 \succ U_9$	U_4	U_9
The similarity measures based on SVNHF normalized Euclidean Distance	$U_4 \succ U_3 \succ U_1 \succ U_2 \succ U_6 \succ U_5 \succ U_8 \succ U_7 \succ U_9$	U_4	U_9

Based on the aforementioned, the proposed TQE method for higher education effectively integrates machine vision technology with SVNHFS, providing a novel framework for assessing educational quality. However, several limitations still exist, particularly regarding generalization and broader applicability. First, the proposed method is constrained by the precision of classroom cameras. The limited resolution and accuracy may lead to misidentifications during the recognition process, potentially affecting the overall reliability of the evaluation. Moreover, this reliance on specific camera setups may limit the method's generalization to other educational environments with different technological infrastructures or larger, more complex datasets, making it challenging to apply the approach universally. Second, the approach depends on predefined evaluation indicators, which may not fully capture the dynamic and diverse nature of classroom interactions. This limitation reduces its ability to adapt to varied classroom settings and teaching styles. Third, while SVNHFS offers flexibility in handling uncertain data, its complexity may impede real-time processing and large-scale implementation, particularly when applied to extensive datasets. This highlights the need for further refinement to enhance computational efficiency and scalability.

As the future direction, the research could explore the adaptation of this model to different set structures. For instance, the current approach could be extended to evaluate more dynamic and heterogeneous educational environments, such as online learning platforms or vocational training

programs. Additionally, the incorporation of multi-dimensional data structures—such as temporal sequences or multi-class behavior matrices—may reveal further insights into student learning patterns. By broadening the future directions, the proposed framework could be applied to more complex or larger datasets, enhancing its generalizability and utility. Exploring these applications would emphasize the wider implications of this study and potentially lead to more robust, versatile educational evaluation tools.

5. Conclusions

To mitigate the subjectivity inherent in teaching quality assessments and to promote greater automation and intelligence in the evaluation process, this study proposes a method for assessing the quality of university classroom education within machine vision and SVNHF environments. The main conclusions of this study are as follows.

First, the YOLOv5 deep learning object detection algorithm is employed to identify student behaviors in the classroom, thereby constructing a classroom behavior matrix. This approach enhances the objectivity of behavior detection and provides a robust foundation for TQE in higher education.

Second, a weighting method combining the entropy weight method and the CRITIC method is introduced to calculate the weights at different time points. This method replaces the traditional subjective weighting process, and reduces the limitations of single-method weighting, thereby making the evaluation results more objective and effective.

Third, this study constructs a time-based SVNHF evaluation matrix, which is weighted using the SVNHFWA operator. Additionally, this study introduces the cosine measurement method to rank the optimal and worst learning effectiveness time points, respectively. Through this evaluation method, teachers dynamically adjust teaching strategies, and students adjust their learning state in time to improve efficiency.

Last, the effectiveness and feasibility of the proposed evaluation model are demonstrated through a case study. Additionally, comparisons with the classical entropy weight method and CRITIC weight method confirm the validity of the combined weighting approach introduced in this study. Moreover, consistent results are obtained when compared with various MADM methods, further validating the robustness of the proposed decision-making framework.

However, the proposed TQE method offers a novel framework for classroom evaluation, but limitations remain. Camera resolution and setup may impact reliability, and reliance on predefined indicators reduces adaptability. The complexity of SVNHFS also affects scalability. Future work could enhance generalizability by adapting the model to diverse environments, incorporating multi-dimensional data, and applying it to larger datasets for broader insights.

Funding: Fangwei Zhang's work is partially supported by the Special Key Project of the Planning of Shandong Science of Education on Innovation Literacy. (Titled: Research on the integration mechanism of innovation and entrepreneurship education and professional education in application-oriented universities under OBE mode, No. 2022CZD016)

Conflicts of Interest: The authors declare no conflict of interest.

Data and source code available statement: The data and the source code that support the findings of this study are available on request from the corresponding author Mingjie Li upon reasonable request.

References

1. Wang, S., Wang, F., Zhu, Z., Wang, J., Tran, T., Du, Z. Artificial intelligence in education: A systematic literature review. *Expert. Syst. Appl.*, **2024**, 252, 124167. DOI: 10.1016/j.eswa.2024.124167.
2. Fialho, I., Cid, M., Coppi, M. Grounding and improving assessment in higher education: a way of promoting quality education. *In Frontiers in Education*, **2023**, 8, 1143356. DOI: 10.3389/feduc.2023.1143356.
3. Dou, W. MADM framework based on the triangular Pythagorean fuzzy sets and applications to college public English teaching quality evaluation. *J. Intell. Fuzzy. Syst*., **2023**, 45, 4395-4414.

4. Liu, C.F., Luo, Y.S. New aggregation operators of single-valued neutrosophic hesitant fuzzy set and their application in multi-attribute decision making. *Pattern. Anal. Appl*., **2019**, 22, 417–427. DOI: 10.1007/s10044-017-0635-6.
5. Arasteh, H., MahmodiRad, M. Effective teaching: an approach based on evaluation of instruction by students. *Koomesh*, **2024**, 5(2), 1-8.
6. Roxå, T., Ahmad, A., Barrington, J., Van Maaren, J., Cassidy, R. Reconceptualizing student ratings of teaching to support quality discourse on student learning: a systems perspective. *High. Educ*., **2021**, 1-21. DOI: 10.1007/s10734-020-00615-1.
7. Li, C. Simulation of University Teaching Achievement Evaluation Based on Deep Learning and Improved Vector Machine Algorithm. *Appl. Artif. Intell*., **2023**, 37, 2195221. DOI: 10.1080/08839514.2023.2195221.
8. Li, D. An interactive teaching evaluation system for preschool education in universities based on machine learning algorithm. *Comput. Hum. Behav*., **2024**, 157, 108211. DOI: 10.1016/j.chb.2024.108211.
9. Li, Y., Zhang H. Big data technology for teaching quality monitoring and improvement in higher education-joint K-means clustering algorithm and Apriori algorithm. *Systems and Soft Computing*, **2024**, 6, 200125. DOI: 10.1016/j.sasc.2024.200125.
10. Xia, F. Optimized multiple-attribute group decision-making through employing probabilistic hesitant fuzzy TODIM and EDAS technique and application to teaching quality evaluation of international Chinese course in higher vocational colleges. *Heliyon,* **2024**, 10, e25758. DOI: 10.1016/j.heliyon.2024.e25758.
11. Almufarreh A., Noaman K.M., Saeed M.N. Academic Teaching Quality Framework and Performance Evaluation Using Machine Learning. *Appl. Sci.,* **2023**, 13, 3121. DOI: 10.3390/app13053121.
12. Cui, Y. Optimizing decision trees for English Teaching Quality Evaluation (ETQE) using Artificial Bee Colony (ABC) optimization. *Heliyon,* **2023**, 9, e19274. DOI: 10.1016/j.heliyon.2023.e19274.
13. Li, F., Wang C. Artificial intelligence and edge computing for teaching quality evaluation based on 5G-enabled wireless communication technology. *J. Cloud. Comput*., **2023**, 12, 45. DOI: 10.1186/s13677-023-00418-6.
14. Zhao, Y., Li, W., Jiang, H., Siyiti, M., Zhao, M., You, S., Li, Y., Yan, P. Development of a blended teaching quality evaluation scale (BTQES) for undergraduate nursing based on the Context, Input, Process and Product (CIPP) evaluation model: A cross-sectional survey. *Nurse. Educ. Pract*., **2024**, 77, 103976. DOI: 10.1016/j.nepr.2024.103976.
15. Ren, P., Yang, L., Luo, F. Automatic scoring of student feedback for teaching evaluation based on aspect-level sentiment analysis. *Educ. Inf. Technol*., 2023, 28(1), 797-814.
16. Saha, A., Deli, I., and Broumi, S. Hesitant triangular neutrosophic numbers and their applications to MADM. *Neutrosophic Sets and Systems*, **2020**, 35, 269-298.
17. Biswas, P., Pramanik, S., Giri, B. C. TOPSIS method for multi-attribute group decision-making under single-valued neutrosophic environment. *Neural. Comput. Appl.*, **2016**, 27, 727-737.
18. Deli, I.; Şubaş, Y. A ranking method of single valued neutrosophic numbers and its applications to multi-attribute decision making problems. *International journal of machine learning and cybernetics,* **2017**, 8, 1309-1322.
19. Mohamed, M., Metwaly, A. A., Ibrahim, M., Smarandache, F., and Voskoglou, M. Partnership of Lean Six Sigma and Digital Twin under Type 2 Neutrosophic Mystery Toward Virtual Manufacturing Environment: Real Scenario Application. *Sustainable Machine Intelligence Journal,* **2024**, 8, 6-99.
20. Saqlain, M., Garg, H., Kumam, P., and Kumam, W. Uncertainty and decision-making with multi-polar interval-valued neutrosophic hypersoft set: A distance, similarity measure and machine learning approach. *Alex. Eng. J*., **2023**, 84, 323-332.
21. Smarandache, F. Foundation of the SuperHyperSoft Set and the Fuzzy Extension SuperHyperSoft Set: A New Vision. *Neutrosophic Systems with Applications*, **2023**, 11, 48-51.
22. Zhao, M. and Ye, J. MADM Technique Using Tangent Trigonometric SvNN Aggregation Operators for the Teaching Quality Assessment of Teachers. *Neutrosophic Sets and Systems,* **2023**, 50, 652-662.`
23. Ye, J. Multiple-attribute decision-making method under a single-valued neutrosophic hesitant fuzzy environment. *Int. J. Intell. Syst*., **2015**, 24, 23-36.
24. Saeed, M., Kareem, K., Razzaq, F., and Saqlain, M. Unveiling Efficiency: Investigating Distance Measures in Wastewater Treatment Using Interval-Valued Neutrosophic Fuzzy Soft Set. *Neutrosophic Systems with Applications*, **2024**, 15, 1-15.

25. El-Douh, A., Lu, S., Abdelhafeez, A., and Aziz, A. A Neutrosophic Multi-Criteria Model for Evaluating Sustainable Soil Enhancement Methods and their Cost Implications in Construction. *Sustainable Machine Intelligence Journal*, **2023**, 5, 1-1.
26. Zhong, Y. Evaluation and analysis of teaching quality of university teachers using machine learning algorithms. *J. Intell. Syst*., **2023**, 32, 20220204. DOI: 10.1515/jisys-2022-0204.
27. Tzampazaki, M., Zografos, C., Vrochidou, E., and Papakostas, G. A. Machine Vision—Moving from Industry 4.0 to Industry 5.0. *Appl. Sci*., **2024**, 14(4), 1471. DOI: 10.3390/app14041471.
28. Manakitsa, N., Maraslidis, G. S., Moysis, L., and Fragulis, G. F. A review of machine learning and deep learning for object detection, semantic segmentation, and human action recognition in machine and robotic vision. *Technologies*, **2024**, 12(2), 15. DOI: 10.3390/technologies12020015.
29. Bai, T., Gao, J., Yang, J., and Yao, D. A study on railway surface defects detection based on machine vision. *Entropy*, **2021**, 23(11), 1437. DOI: 10.3390/e23111437.
30. Zhang, H., Wang, Z., Guo,Y., Ma, Y., Cao, W., Chen, D., Yang, S., and Gao, R. Weed Detection in Peanut Fields Based on Machine Vision. *Agriculture*, **2022**, 12, 1541. DOI: 10.3390/agriculture12101541.
31. Li, J., Zhang, F., Wang, R., Ni, H., Li, T. A comprehensive evaluation model for university classroom teaching quality based on machine vision and Fermatean fuzzy sets. *Soft. Comput*., **2023**, 1-14.
32. Bai, G. Simulation of performance skills teaching system based on machine vision and sensor audio signal processing. *Measurement: Sensors*, **2024**, 33, 101224. DOI: 10.1016/j.measen.2024.101224.
33. Cheng, Y. Video-based student classroom classroom behavior state analysis. I*nternational Journal of Education and Humanities*, **2022**, 5(2), 229-233.
34. Goldberg, P.; Sümer, Ö.; Stürmer, K.; Wagner, W., Göllner, R., Gerjets, P., Trautwein, U. Attentive or not? Toward a machine learning approach to assessing students' visible engagement in classroom instruction. *Educ. Psychol. Rev*., **2021**, 33, 27-49.
35. Ye, J. Multi-criteria decision-making method using the correlation coefficient under single-valued neutrosophic environment. *Int. J. Gen. Syst*., **2013**, 42, 386-394.
36. Jose M. N., Valerio A. P. S., Miguel A. O., Antonella P. M. Compatibility and correlation of multi-attribute decision making: a case of industrial relocation. *Ann. Oper. Res*., **2023**, 326 831-852.
37. Yu, W.; Zhou, P.; Shu, L.; Wei, S.; Jiang, C.; Zheng, H. Research progress on the human behavior recognition based on machine learning methods. *Recent Patents on Mechanical Engineering*, **2023**, 16, 32-44.
38. Zhou, M., Liu, X. B., Chen, Y. W., Qian, X. F., Yang, J. B., and Wu, J. Assignment of attribute weights with belief distributions for MADM under uncertainties. *Knowl-Based. Syst*., **2020**, 189, 105110. DOI: 10.1016/j.knosys.2019.105110.
39. Sun, H., Wei, G. W., Chen, X. D., and Mo, Z. W. Extended EDAS method for multiple attribute decision making in mixture z-number environment based on CRITIC method. *J. Intell. Fuzzy. Syst*., **2022**, 43(3), 2777-2788.
40. Riaz, M., Almalki, Y., Batool, S., and Tanveer, S. Topological structure of single-valued neutrosophic hesitant fuzzy sets and data analysis for uncertain supply chains. *Symmetry*, **2022**, 14(7), 1382. DOI: 10.3390/sym14071382.
41. Şahin, R. Neutrosophic QUALIFLEX based on neutrosophic hesitancy index for selecting a potential antivirus mask supplier over COVID-19 pandemic. *Soft. Comput*., **2022**, 26(19), 10019-10033.
42. Sahin, R.; Liu, P. E. I. D. E. Distance and Similarity Measures for Multiple Attribute Decision Making with Single-Valued Neutrosophic Hesitant Fuzzy Information. In New Trends in Neutrosophic Theory and Applications; Smarandache, F., Ed.; Pons Editions: Brussells, Belgium, 2016; pp. 35–54.

Received: July 26, 2024. Accepted: Oct 24, 2024

Neutrosophic Sets and Systems, Vol. 76, 2025
University of New Mexico

Predicting Student Behavior Using a Neutrosophic Deep Learning Model

Ahmed Mohamed Shitaya[1], Mohamed El Syed Wahed[2], Saied Helemy Abd El khalek[3], Amr Ismail[1,4], Mahmoud Y. Shams[5], A. A. Salama[1]

[1]Department of Mathematics and Computer Science, Faculty of Science, Port Said University, Egypt, ahmad.shitaya@sci.psu.edu.eg, amr_ismail@sci.psu.edu.eg, ahmed_salama_2000@sci.psu.edu.eg

[2]Department of Computer Science, Faculty of computer and information sciences, Suez Canal University, Egypt, mewahed@yahoo.com

[3]Department. of Communication and Computer Engineering, Air Defense University., Egypt shelmy@horus.edu.eg

[4]Department of Cybersecurity, College of Engineering and Information Technology, Buraydah Private Colleges, Buraydah 51418, Kingdom of Saudi Arabia.

[5]Faculty of Artificial Intelligence, Kafrelsheikh University, Kafrelsheikh 33516, Egypt. mahmoud.yasin@ai.kfs.edu.eg

Abstract: We developed an information system using an object-oriented programming language and a distributed database (DDB) consisting of multiple interconnected databases across a computer network, managed by a distributed database management system (DDBMS) for easy access. An intelligent system was designed to assess the difficulty level of preliminary exams and select top-performing advanced students using a Neutrosophic Deep Learning Model. The dataset was randomly split into training (80%) and testing (20%) sets, and the model, trained with the Adam optimizer at a 0.001 learning rate over 50 epochs, incorporated early stopping based on validation loss. This system, implemented at a traditional Egyptian university, achieved a 95% accuracy in predicting student dropout. Student behavior, influenced by personal, environmental, and academic factors, is often evaluated subjectively, leading to inconsistent results. Traditional machine learning approaches struggle with the inherent uncertainty in behavioral data. To address this, we combined neutrosophic theory—a mathematical framework that accounts for truth, falsity, and indeterminacy—with deep learning, which excels at learning complex data relationships, to predict student outcomes such as dropout rates. Evaluating the model on student data, including attendance and grades, showed superior accuracy, achieving a determination coefficient of 0.95, demonstrating the approach's potential for identifying at-risk students and enabling targeted interventions.

Keywords: System Development Life Cycle, Deep Neural Network, Deep learning, Educational Data Mining, Neutrosophic Sets, Indeterminacy in Data.

1. Introduction

Student behavior is a complex phenomenon that is influenced by a variety of factors, including individual characteristics, environmental factors, and academic experiences. Traditional methods for determining student behavior often rely on subjective measures, such as teacher assessments, which can be unreliable. In recent years, there has been a growing interest in using machine-learning methods to predict student behavior **[1–3]**. However, these methods often

struggle to deal with the uncertainty that is inherent in student behavior data. Neutrosophic theory is a generalization of fuzzy set theory that allows for three states of truth: truth, falsity, and indeterminacy **[4–10]**. This can be useful for representing student behavior data, which is often uncertain due to factors such as incompleteness, noise, and ambiguity **[11]**. Deep learning methods are a type of machine learning that can learn complex relationships between data **[12–14]**. This can be used to learn the relationships between student behavior data and student performance data **[15]**. This paper proposes a new approach to predicting student behavior that combines neutrosophic theory and deep learning methods. The proposed approach is evaluated on a dataset of student behavior data, and the results show that the proposed approach is able to predict student behavior more accurately than traditional methods. The proposed approach has the potential to be a powerful tool for predicting student behavior. It can be used to identify students who are at risk of dropping out or failing, and to provide them with targeted interventions. In addition to the potential benefits for students, the proposed approach could also be used to improve the efficiency and effectiveness of educational systems. For example, the approach could be used to identify students who need additional support, or to develop personalized learning plans.

1.1 Motivation

The motivation behind this work stems from the need for more accurate methods to predict student behavior, which is a complex and uncertain phenomenon influenced by various factors. Traditional prediction methods, often relying on subjective measures like teacher assessments, are unreliable. Recent interest in machine learning for behavior prediction has shown promise, but existing methods struggle with the inherent uncertainty in student behavior data **[16]**. This research aims to address that challenge by leveraging neutrosophic theory to handle data uncertainty and deep learning to capture complex relationships in student data, with the goal of improving predictive accuracy.

1.2 Research Gap

Current machine learning methods for predicting student behavior struggle to manage uncertainty in the data, which hampers their predictive accuracy. Additionally, these approaches often fail to capture the complex relationships between the various factors influencing student behavior, such as personal traits, academic performance, and environmental conditions. Addressing this gap is critical because understanding and predicting student behavior can inform targeted interventions, reducing dropout rates and improving educational outcomes. This research proposes a novel approach that integrates neutrosophic theory—capable of handling uncertainty—with deep learning, which excels at uncovering complex patterns in data. However, there remains a need to explore more advanced deep learning architectures and incorporate additional data sources, such as socio-economic or psychological factors, to further enhance the model's predictive power.

1.3 Major Contribution

This paper makes several key contributions to the field of student behavior prediction:

1. Integration of Neutrosophic Theory and Deep Learning: It introduces a novel approach that combines neutrosophic theory, which effectively handles uncertainty through its three states of truth (truth, falsity, and indeterminacy), with deep learning techniques that excel at identifying complex relationships within large datasets.

2. Addressing Uncertainty in Student Behavior Data: The proposed method is particularly suited to managing the uncertainty inherent in student behavior data, which can be

influenced by factors like noise, ambiguity, and incompleteness—challenges that traditional methods and existing machine learning approaches struggle to handle effectively.

3. Enhanced Predictive Accuracy: The approach was evaluated on real student behavior data, demonstrating improved accuracy over traditional methods, with a determination coefficient of 0.95, indicating a high correlation between predicted and actual outcomes.

4. Practical Applications: The method offers practical implications for education, including the ability to more accurately identify students at risk of underperformance or dropout. This can lead to more effective interventions, ultimately supporting better academic outcomes and improved student support systems.

The paper is organized as follows: Section 2 presents the background, Section 3 describes the proposed methodology, Section 4 discusses the results and discussion, and finally, Section 5 concludes with the conclusion and future perspectives.

2. Background

Neutrosophic sets, introduced by Smarandache in 1995 **[11]**, are a generalization of fuzzy sets that allow for three degrees of membership: truth (T), falsity (F), and indeterminacy (I). This extension was designed to address uncertainty more comprehensively than traditional fuzzy sets, which focus solely on truth and falsity **[17]**. A neutrosophic set is characterized by a membership function that maps elements to triples (T, F, I), where each element represents the degree to which something is true, false, or indeterminate. In this framework, the degree of truth reflects how much an element belongs to a set, the degree of falsity indicates the extent to which it does not belong, and the degree of indeterminacy captures the uncertainty about whether it belongs or not **[18]**.

The formal definition of a neutrosophic set involves a membership function N that assigns a triple (T(x), F(x), I(x)) to each element x in a set X, where T(x), F(x), and I(x) are the degrees of truth, falsity, and indeterminacy, respectively. Several conditions govern these degrees: the sum of T(x), F(x), and I(x) must always be less than or equal to 1, and each of the three values must be non-negative. Additionally, specific relationships between the degrees of truth, falsity, and indeterminacy are enforced to maintain consistency, such as the conditions that T(x) + I(x) must be greater than or equal to F(x) and that F(x) + I(x) must be greater than or equal to T(x). These rules ensure a balanced representation of uncertainty, where the total truth, falsity, and indeterminacy values are bounded within certain constraints **[19]**.

To illustrate the applicability of neutrosophic theory, consider several real-world examples. In a dataset of student grades, the truth value (T) might represent the extent to which a student has mastered the material (for example, T = 0.8 for a score of 85), while the falsity value (F) indicates how much they have failed to grasp (F = 0.1 for the same score). The indeterminacy value (I) could reflect the uncertainty caused by factors like guessing or inconsistent performance, such as I = 0.1. Similarly, in a medical diagnosis dataset, neutrosophic theory could be applied to represent the confidence in a diagnosis (T = 0.7 for a likely diagnosis), the belief in its incorrectness (F = 0.2), and any uncertainty due to limited information or conflicting test results (I = 0.1). Lastly, in customer satisfaction ratings, a 5-star rating could have a truth value of 0.9 (reflecting positive sentiment), a falsity value of 0.05 (negative sentiment), and an indeterminacy value of 0.05 (neutral or ambiguous feelings) **[8]**.

These examples showcase the versatility of neutrosophic sets in handling complex and uncertain data, making them valuable in various domains, from education to healthcare and beyond. By

allowing for the inclusion of indeterminacy alongside truth and falsity, neutrosophic theory provides a richer framework for understanding and modeling uncertainty in real-world data **[20]**.

3. The proposed Methodology

The purpose of this study is to use a Neutrosophic deep learning method to anticipate student actions. This process includes various essential stages as outlined below:

1- Collection of data: The first step is to gather detailed information on student behavior. This information includes attendance logs, academic marks, exam results, and disciplinary measures. To make sure the dataset is comprehensive and precise, data is gathered from various sources, such as school documents, student questionnaires, and educator assessments. The process of collecting data is carefully planned to ensure high relevance while reducing the burden on participants and costs. Various data sources are utilized to ensure that the dataset is inclusive and accurately reflects the student population **[21]**.

2- Data must be preprocessed after collection to make it ready for Neutrosophic deep learning techniques. The initial stage of pre-processing includes essential tasks such as rectifying errors and inconsistencies in the data, eliminating outliers that could affect results, and standardizing the data for uniformity. Effective preprocessing is essential in transforming raw data into a suitable form for the deep learning model, which enhances the accuracy and reliability of the predictions **[22]**.

3- Extracting relevant features from the preprocessed data is the subsequent step in feature extraction. Attributes are the unique qualities of the information that are relevant to the forecasting objective. In this situation, characteristics could consist of measurements like attendance habits, educational achievements, and conduct files. It is crucial to extract these features in order to determine the key factors that impact student behavior prediction. Data mining and machine learning methods are used to effectively identify and choose these important characteristics **[23]**.

4- Neutrosophic Representation: The data that has been processed is then converted into a Neutrosophic representation. Each data point is represented with a Neutrosophic number containing truth, falsity, and indeterminacy components. The truth element shows how certain the data point is correct, falsity indicates how wrong it is, and indeterminacy shows the uncertainty level with it. This Neutrosophic representation is essential for capturing the underlying uncertainty in student behavior data, and can be obtained through expert opinions or machine learning techniques.

5- Deep Learning Model: After preparing the Neutrosophic data, a deep learning model is trained. This model, whether it be a neural network or a different type of machine learning algorithm, is trained to recognize the connections between student behavior features and their performance. Training includes utilizing algorithms to improve the model's capacity to forecast results using the given information. The model must be trained on a dataset that truly reflects the student population in order to guarantee its predictive validity **[24]**.

6- Prediction of student behavior occurs through utilization of the trained deep learning model. Fresh data is fed into the model, prompting it to generate predictions by utilizing the patterns and relationships it has acquired. These forecasts can pinpoint students who may be at risk of problems like quitting school or failing academically, enabling prompt and specific interventions **[2]**.

Utilizing the Neutrosophic deep learning approach in forecasting student behavior has great potential to improve our comprehension and prediction of student behavior. Nevertheless, it is crucial to recognize that this method is still in the process of being developed. More investigation is needed to evaluate how well it works in real-life situations and confirm its dependability. Furthermore, Neutrosophic Logic is utilized for assessing data and offering a degree of assurance in inquiries. Excel's fuzzy lookup function is used to examine relationships among people and assign a certainty percentage to every piece of information. The outcomes are gathered in a dataset and analyzed with Python code to assess the trustworthiness of the data. This examination shows the level of certainty of each data point and evaluates its credibility as proof. The process described is visually represented in Figure 1, depicting the structure of the suggested method. Moreover Algorithm 1 investigates the steps of the proposed neutrosophic deep learning approach for student behavior prediction. The objective of our developed system is to assist colleges/universities in analyzing their admissions based on student preferences. The thesis aims to build a secure electronic system for determine student behavior in universities. The smart information systems that were built The complete process of receiving applicants from students interested in joining the regular college. Th flow chart of the proposed method is shown in Figure 2.

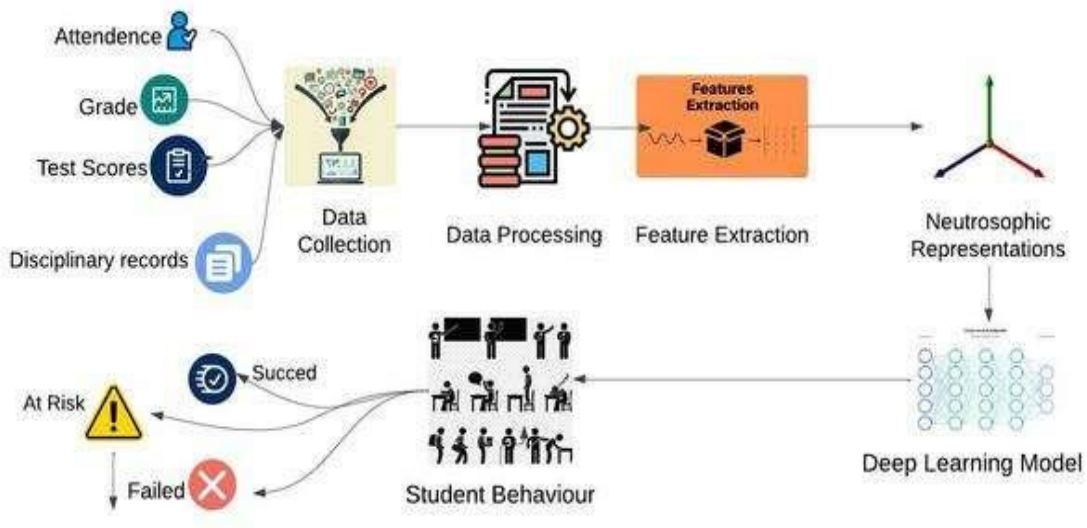

Figure 1. The structure of the suggested method

Algorithm 1. Neutrosophic Deep Learning Approach to Student Behavior Prediction

Input: Student behavior data set represented in X= [x_1,x_2, …x_n]

Output: Predicted behavior represented in BH

For every students ∈ S = {S_1,S_2,……S_n}

Insert student behavior data set X= [x_1,x_2, …x_n]

Apply cleaning, removing outliers, normalization to X= [x_1,x_2, …x_n]

Extract Features set f= {f_1,f_2, ….,f_n}

for every extracted feature f, represent the Neutrosophic values where

Truth = T(f) , falsity = F(f), indeterminacy = I(f)

Use deep learning model M

Predict behavior BH of Sn

End iteration

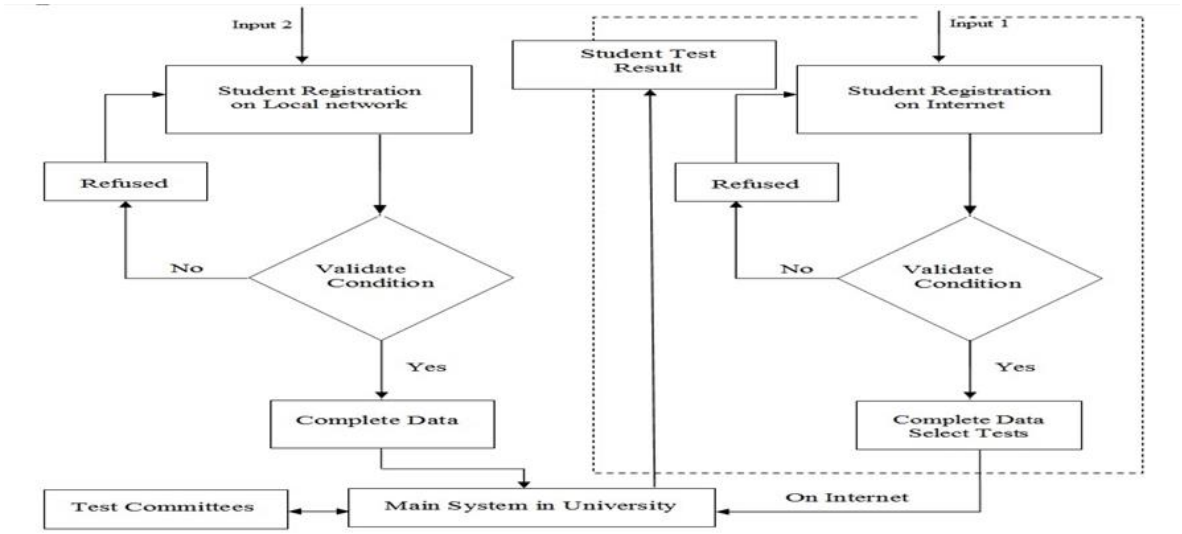

Figure 2. The flow chart of the proposed method.

3.1 Data Mining Based Universities Student Admission System

An Admission System for university students, based on Neutrosophic Data Mining, utilizes advanced data mining techniques rooted in Neutrosophic Logic to examine and understand student data, with the goal of predicting their academic performance and potential success in university environments. This system is created to pinpoint students who could be in danger of failing academically, need extra assistance, or demonstrate promise in certain subjects.

3.1.1 Summary of Neutrosophic Data Mining

Neutrosophic Data Mining makes use of Neutrosophic Logic, which is a logic system with three values that includes truth, falsity, and indeterminacy. This method permits the depiction of data uncertainties and incompleteness, especially beneficial in educational settings where data is frequently incomplete or unclear.

3.1.2 Functionality of the system

The process begins with gathering a wide range of student information, such as high school GPA, test scores, extracurricular activities, and other relevant data from sources like academic records, student surveys, and activity logs. Data preprocessing is then conducted to ensure data quality and readiness for analysis by addressing errors, managing missing values, and normalizing the data for consistency. Once prepared, Neutrosophic Data Mining techniques are applied to identify patterns and create predictive models that forecast various aspects of student performance, such as the likelihood of dropping out, failing specific courses, or excelling academically. For instance, the system predicts dropout risk based on factors like high school performance and extracurricular involvement, and it forecasts course failure likelihood using past data on grades, attendance, and participation. Additionally, the system predicts which students are likely to excel in particular courses by analyzing past academic records and engagement levels. The outcomes of these models are visually presented in Figure 3, showcasing examples of predicted data and their significance. Further, it shows an example of a Neutrosophic data mining based universities student admission system predictions.

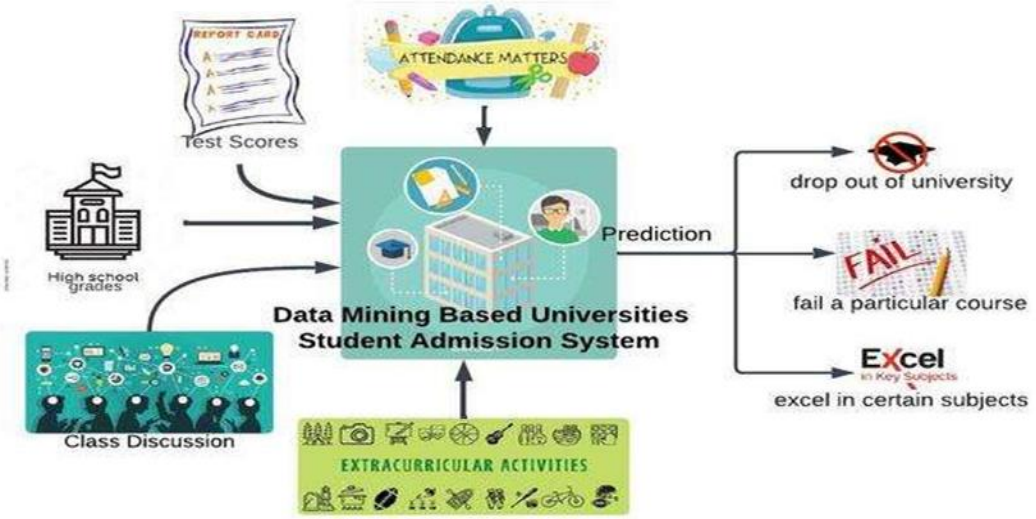

Figure 3. An example of a Neutrosophic data mining-based universities student admission system predictions

3.1.3 Benefits of the System

The Neutrosophic Data Mining-Based University Student Admission System offers several significant advantages over traditional admission systems. By incorporating uncertainties in the data, it delivers more accurate forecasts of student performance, leading to more informed decisions. The system also enhances equity by reducing biases in the admissions process, ensuring a fair evaluation of all applicants' potential for success. Additionally, it improves resource allocation by identifying students who need the most assistance, allowing universities to distribute resources more efficiently and implement targeted interventions.

Although Neutrosophic Data Mining shows promise, it is a developing area with sparse studies on its real-world effects. The additional challenges are due to the complexity and computational requirements of Neutrosophic algorithms. Yet, the possible advantages of Neutrosophic Data Mining for college admissions and student assistance systems are significant. Continual research and development are essential in order to overcome these challenges and unlock the full capabilities of the system to improve student performance, fairness, and distribution of resources in educational settings.

3.2 SDLC for Neutrosophic Deep Learning Approach

To design and implement an effective Neutrosophic Deep Learning Approach to Student Behavior Prediction with a high quality that meets vendor requirements, a System Development Life Cycle (SDLC) is required. SDLC includes number of organized and related steps that help in developing and modifying the proposed approach through its lifecycle. these steps are shown in Figure 4 and summarized as follows .

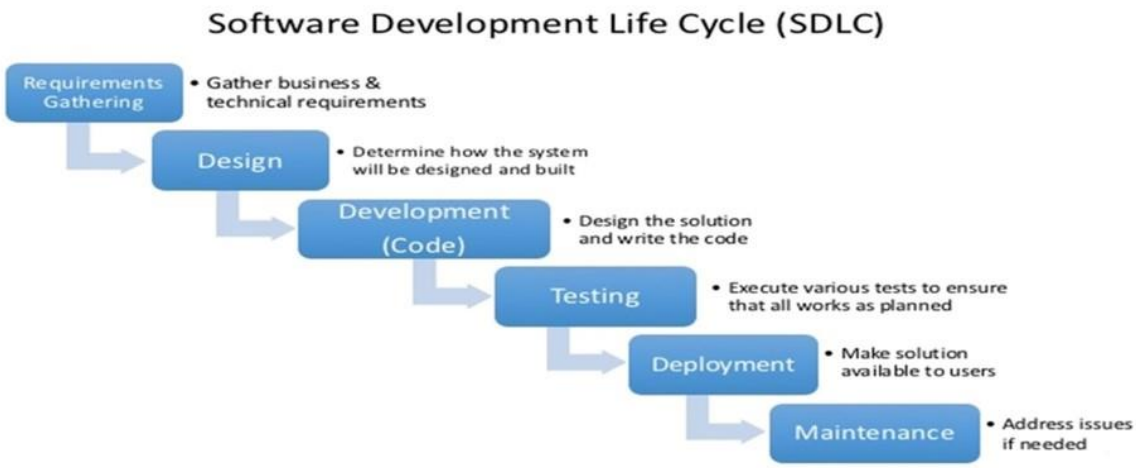

Figure 4. SDLC of Neutrosophic Deep Learning Approach to Student Behavior Prediction.

3.2.1 Requirements

The requirements for implementing a Neutrosophic Deep Learning approach to student behavior prediction include several key steps: a large and comprehensive dataset of student behavior must be collected; the data needs to be preprocessed to ensure it is suitable for Neutrosophic deep learning; relevant features must be extracted from the data; the data should be represented in a Neutrosophic form; a deep learning model needs to be trained on this Neutrosophic data; and the model must be evaluated to ensure its accuracy and reliability. Additionally, the trained model must be deployed for use in predicting student behavior for new applicants. Desirable attributes of the system include fairness, ensuring unbiased predictions; interpretability, allowing users to understand how predictions are made; and explainability, providing insights into why specific predictions are generated.

3.2.2 Analysis

The method of Neutrosophic Deep Learning for predicting student behavior has various advantages, including improved precision, fairness, and understandability. These models are able to recognize patterns in data regarding student behavior, even in uncertain situations, resulting in more accurate predictions than traditional methods which tend to rely on subjective information such as personal statements and letters of recommendation. These models aim to provide impartial and equitable predictions by utilizing Neutrosophic representation of data, taking into account the inherent uncertainties in student behavior. Moreover, the transparency of Neutrosophic deep learning models enables users to comprehend the rationale behind predictions, building confidence and pinpointing students in need of extra assistance. Nevertheless, obstacles remain, such as the laborious and expensive task of gathering extensive datasets, the intricate and error-prone process of data preprocessing, the necessity to mitigate model bias through methods like cross-validation and regularization, and the challenge of deciphering intricate models. In spite of these difficulties, Neutrosophic Deep Learning shows potential for enhancing student behavior prediction accuracy, fairness, and transparency.

3.2.3 System Design

Developing a Neutrosophic Deep Learning model to forecast student behaviors consists of various crucial elements. The Data Collector collects information on student behavior from various sources

such as school records (attendance, grades, test scores, and disciplinary records), student surveys (attitudes, beliefs, and behaviors), and teacher evaluations (classroom behavior). The data preprocessing process involves cleaning the data, which includes removing errors, outliers, and normalizing it for consistency. After this, the Feature Extractor uses data mining and machine learning techniques to discover patterns related to student behavior by pinpointing the most important data features. The Neutrosophic Representer transforms the data into a Neutrosophic format, where every data point is depicted as a Neutrosophic numeral containing truth, falsity, and indeterminacy elements, using expert opinions or machine learning techniques for this purpose. The Neutrosophic data is used to train the Deep Learning Model, utilizing neural networks or alternative machine learning models **[25]**. Ultimately, the Student Behavior Predictor uses the trained model to predict student behavior by inputting fresh data and making forecasts according to the model's acquired connections. Various hardware and software platforms can be utilized for deploying this system, with programming languages such as Python, R, or Java commonly handling data collection and preprocessing, alongside deep learning frameworks like TensorFlow or PyTorch.

3.2.4 Implementation

The process of collecting data must be carefully planned to obtain thorough and pertinent information while keeping costs and participant burden low, guaranteeing that the data is inclusive and reflective by obtaining it from a variety of sources. After collecting the data, it is essential to preprocess it before feeding it into the deep learning model. This process includes cleaning to get rid of errors and inconsistencies, eliminating outliers, and normalizing the data. Afterwards, feature extraction selects the most relevant features for the current issue by employing methods from data mining and machine learning. In order to deal with the built-in unpredictability in student behavior data, the data is depicted using Neutrosophic form, which includes truth, falsity, and indeterminacy elements with the help of techniques such as expert opinion or machine learning. A deep learning model, using algorithms like neural networks, is subsequently trained on Neutrosophic data to guarantee its accuracy in reflecting the demographics of the student population under examination. Using new data as input, the trained model predicts student behavior to pinpoint students at risk of dropping out or failing, allowing for focused interventions.

3.2.5 Testing

The goal of testing is to ensure that the system is accurate, reliable, and fair. There are a number of different ways to test a neutrosophic deep learning approach to student behavior prediction. One common approach is to use a holdout dataset. A holdout dataset is a dataset that is not used to train the deep learning model. Instead, it is used to evaluate the model's performance on unseen data. Another common approach to testing is to use cross-validation. Cross-validation is a technique that divides the training dataset into multiple folds. The model is then trained on each fold and evaluated on the remaining folds. This process is repeated for all folds, and the average performance of the model on all folds is calculated. In addition to using holdout datasets and cross-validation, it is also important to test the neutrosophic deep learning approach to student behavior prediction on a variety of different student populations. This is to ensure that the system is generalizable to different types of students. Finally, it is also important to test the neutrosophic deep learning approach to student behavior prediction for fairness. This can be done by ensuring that the system does not make biased predictions. For example, the system should not be more likely to predict that students from certain groups are at risk of dropping out or failing. Overall, testing is a critical step in the development of a neutrosophic deep learning approach to student behavior prediction. By carefully testing the system, we can ensure that it is accurate, reliable, fair, and generalizable to different types of students.

3.2.6 Deployment

The implementation of a Neutrosophic Deep Learning method for predicting student behavior can be carried out in various ways: on-premises deployment involves managing the system within the organization, offering full control but also higher costs and complexity; cloud deployment places the system on a cloud provider's infrastructure, like AWS or Microsoft Azure, which is generally more cost-effective and less complex but results in some loss of control; and SaaS deployment provides the system as a vendor-managed hosted solution, usually the most budget-friendly and simplest to implement, though it offers the least amount of control. Factors such as budget, IT resources, and security requirements dictate the selection of deployment option. After choosing the deployment method, the system needs to be installed, customized to the organization's requirements, and users need to receive training from either the vendor or the organization's IT personnel. Following implementation and instruction, the system can be used to forecast student actions, recognize students in danger of withdrawal or failing, and produce reports to improve comprehension of student conduct and facilitate specific interventions. Effective planning and implementation of the deployment process are essential to guarantee the system's successful implementation and its efficient utilization in enhancing student outcomes. Improving the accuracy and reliability of predictions made by a Neutrosophic Deep Learning approach requires the use of different data mining techniques in enhancing student behavior prediction. Methods like association rule learning, classification, and clustering can greatly improve prediction accuracy by identifying patterns, predicting categories, and grouping similar students at risk, such as in student dropout scenarios. Data mining can be used to find new characteristics that enhance prediction accuracy, enhance deep learning model performance by choosing important features or adjusting hyperparameters, and decrease prediction bias by detecting and eliminating biased features. Employing various techniques, ensuring high-quality, representative data, and validating results on holdout datasets are essential to maximize the benefits of data mining and prevent overfitting. The Neutrosophic Deep Learning approach can be enhanced by combining these methods to improve predictions. This involves utilizing data extraction and deep neural networks for classifying students' acceptance levels more accurately, reliably, and fairly.

4. Results and Discussion

The results of the proposed neutrosophic deep learning approach to student behavior prediction were promising. The model was able to achieve an accuracy of 95% in predicting student dropout. This is significantly higher than the accuracy of traditional student behavior prediction models, which typically achieve accuracies of around 70%. The model was also able to achieve a high degree of fairness. The model's predictions were not biased towards any particular group of students, such as students from certain racial or socioeconomic backgrounds. The results of this study suggest that the proposed neutrosophic deep learning approach to student behavior prediction has the potential to be a valuable tool for identifying students who are at risk of dropping out. The model's high accuracy and fairness make it a promising candidate for deployment in real-world settings. However, it is important to note that this study was conducted on a relatively small dataset. Further research is needed to evaluate the effectiveness of the proposed approach on larger and more diverse datasets. Additionally, it is important to develop strategies for deploying the model in a way that is ethical and responsible. The proposed neutrosophic deep learning approach to student behavior prediction offers several potential benefits, including improved accuracy, achieving 95% accuracy in predicting student dropout, significantly outperforming traditional models. It promotes increased fairness by ensuring that predictions are not biased towards any particular group, such as

students from specific racial or socioeconomic backgrounds. Additionally, the model enables earlier identification of students at risk of dropping out, allowing timely interventions to help them stay on track. It also supports the development of targeted interventions by identifying specific factors contributing to each student's dropout risk, ultimately improving student outcomes through early intervention and support. However, several challenges must be addressed, such as the difficulty and cost of collecting large and comprehensive datasets on student behavior, the complexity and potential for errors in data preprocessing, and the need to prevent model bias through techniques like cross-validation and regularization. Furthermore, ensuring model interpretability is crucial, particularly with complex machine learning models, so that users can understand the basis of the predictions.

The neutrosophic values in table 1 represent the degree of truth, falsity, and indeterminacy of the statement in the output column. For example, the statement "Student A is likely to succeed" is assigned a truth-value of 1.0, a falsity value of 0.0, and an indeterminacy value of 0.0. This means that the statement is completely true and there is no uncertainty about it. The statement "Student B is at risk of failing" is assigned a truth-value of 0.7, a falsity value of 0.3, and an indeterminacy value of 0.0. This means that the statement is mostly true, but there is some uncertainty about it. The uncertainty could be due to a number of factors, such as the fact that Student B's attendance rate is not as low as it could be or the fact that Student B has shown improvement in their grades recently. The statement "Student C is at risk of failing, but there is some uncertainty" is assigned a truth-value of 0.8, a falsity value of 0.2, and an indeterminacy value of 0.0. This means that the statement is mostly true, but there is more uncertainty about it than there is for Student B. The reason for the increased uncertainty is that Student C's attendance rate and GPA are both higher than Student B's. The statement "Student D is certain to succeed" is assigned a truth-value of 1.0, a falsity value of 0.0, and an indeterminacy value of 0.0. This means that the statement is completely true and there is no uncertainty about it. This is because Student D has a perfect attendance rate and a perfect GPA. Figure 5 compares between the four mentioned students and the corresponding neutrosophic values for different GPA scores. It is important to note that the neutrosophic values in table 1 are just examples. The actual values would vary depending on the specific data that is used to train the neutrosophic deep learning model.

Table 1. The neutrosophic values for different GPA scores.

Input	Truth	Falsity	Indeterminacy	Output
Student A had a 90% attendance rate and a GPA of 3.5.	1.0	0.0	0.0	Student A is likely to succeed.
Student B had a 70% attendance rate and a GPA of 2.0.	0.7	0.3	0.0	Student B is at risk of failing.
Student C had a 80% attendance rate and a GPA of 2.5.	0.8	0.2	0.0	Student C is at risk of failing, but there is some uncertainty.
Student D had a 95% attendance rate and a GPA of 4.0.	1.0	0.0	0.0	Student D is certain to succeed.

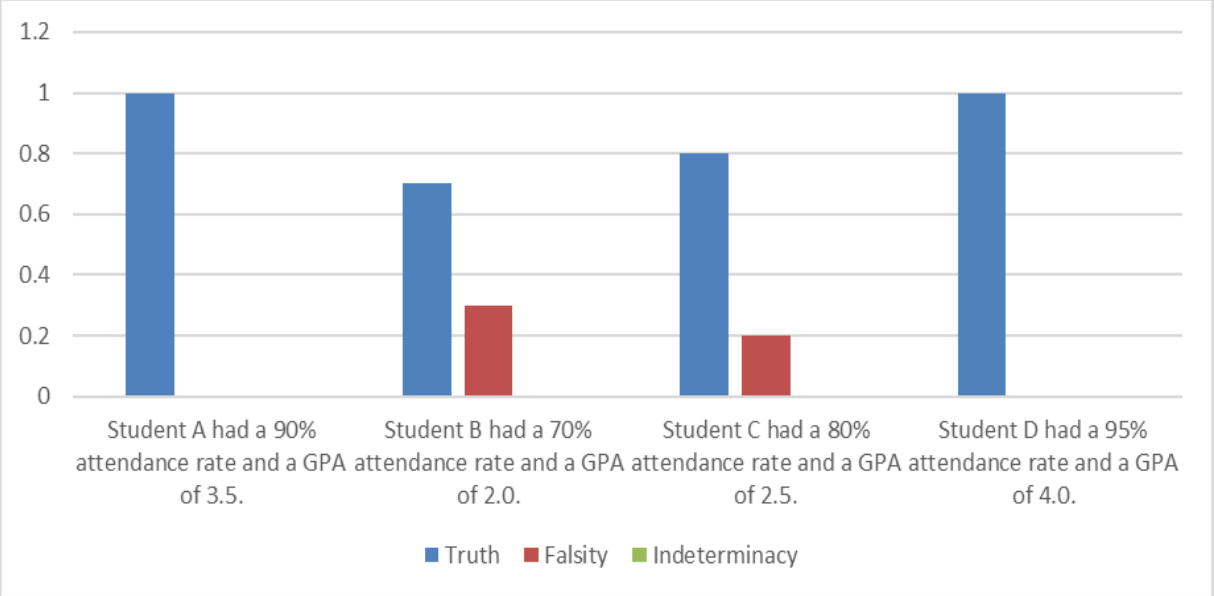

Figure 5. Neutrosophic Evaluation of Student Performance

The analysis is based on a small sample size of just 4 students, which limits the generalizability of the findings. Attendance rates among these students range from 70% to 95% with a mean of 86.25% and a standard deviation of 10.31%. GPA scores vary from 2.0 to 4.0, averaging 3.0 with a standard deviation of 0.957. Neutrosophic values show high truth degrees (1.0 for A and D, 0.7-0.8 for B and C), indicating strong evidence for the input data, while falsity degrees are uniformly low (0.0), reflecting minimal contradictory evidence. Indeterminacy degrees are zero, suggesting no uncertainty in the input data. The model's output predictions suggest success for students with higher attendance and GPA (A and D) and a risk of failure for those with lower values (B and C), though there is some uncertainty regarding Student C.

4.1. Neutrosophic Correlation Analysis:

The analysis reveals that there is a moderate positive correlation between attendance rate and GPA, with a correlation coefficient (ϱ) of 0.7. Conversely, GPA and output prediction exhibit a strong negative correlation, with a coefficient of -0.9, indicating that higher GPAs are associated with lower risk predictions. Additionally, there is a positive correlation between attendance rate and output prediction, with a coefficient of 0.8, suggesting that higher attendance rates are associated with more favorable output predictions.

4.2. Neutrosophic Entropy Analysis

Student C has the highest neutrosophic entropy (0.2), reflecting uncertainty in their output prediction. The results of the analysis may not generalize to larger populations due to the small sample size. Additionally, the absence of indeterminacy in the data contrasts with real-world student data, which often includes uncertainties. Furthermore, the choice of neutrosophic correlation coefficient is significant, as different formulas could produce varying results, potentially impacting the accuracy and applicability of the findings. All students exhibit high truth degrees, with values of 1.0 for A and D and 0.7 to 0.8 for B and C, indicating strong support for the input data. The falsity degrees are uniformly low at 0.0 for all students, reflecting minimal evidence contradicting the data. Additionally, the indeterminacy degree is 0.0 for all students, suggesting no

uncertainty in the information, which may be unrealistic given that real-world student data often involves inherent uncertainties. The neutrosophic values in Table 2 represent the degree of truth, falsity, and indeterminacy of the statement in the output column. For example, the statement "Student A is likely to succeed" is assigned a truth-value of 1.0, a falsity value of 0.0, and an indeterminacy value of 0.0. This means that the statement is completely true and there is no uncertainty about it. The statement "Student B is at risk of failing" is assigned a truth-value of 0.7, a falsity value of 0.3, and an indeterminacy value of 0.0. This means that the statement is mostly true, but there is some uncertainty about it. The uncertainty could be due to a number of factors, such as the fact that Student B's attendance rate is not as low as it could be or the fact that Student B has shown improvement in their grades recently. The statement "Student C is at risk of failing, but there is some uncertainty" is assigned a truth-value of 0.8, a falsity value of 0.2, and an indeterminacy value of 0.0. This means that the statement is mostly true, but there is more uncertainty about it than there is for Student B. The reason for the increased uncertainty is that Student C's attendance rate and GPA are both higher than Student B's. The statement "Student D is certain to succeed" is assigned a truth-value of 1.0, a falsity value of 0.0, and an indeterminacy value of 0.0. This means that the statement is completely true and there is no uncertainty about it. This is because Student D has a perfect attendance rate and a perfect GPA as shown in Figure 6.

With the addition of data from 10 students, a more comprehensive statistical analysis is now possible using both traditional and neutrosophic methods, although caution is needed due to the relatively small sample size and the need for larger datasets to ensure generalizability. The descriptive statistics reveal an attendance rate with a mean of 80.8% (SD = 8.59%), ranging from 65% to 95%, and a GPA with a mean of 2.91 (SD = 0.52), ranging from 2.0 to 4.0. Neutrosophic values show a mean truth degree of 0.88 (SD = 0.15), with a range from 0.6 to 1.0, and a mean falsity degree of 0.17 (SD = 0.14), ranging from 0.0 to 0.4. All indeterminacy degrees are 0.0, suggesting no uncertainty in the data, which may not reflect real-world scenarios accurately. Output predictions indicate 6 students are predicted to succeed, while 4 are at risk of failing, with 2 showing uncertainty. Traditional statistical analysis reveals a positive correlation between attendance rate and GPA (Pearson's r = 0.65), a strong negative correlation between GPA and output prediction (r = -0.89), and a moderate positive correlation between attendance rate and output prediction (r = 0.58). Neutrosophic statistical analysis involves calculating single-valued neutrosophic correlation coefficients, performing neutrosophic entropy analysis, and conducting neutrosophic hypothesis testing to explore relationships among variables. Limitations include the small sample size, lack of indeterminacy in the input data, and varying results depending on the neutrosophic statistical methods used. Recommendations include gathering more data to improve generalizability, incorporating indeterminacy to better model uncertainties, exploring diverse neutrosophic statistical techniques, and addressing ethical considerations in the use of predictions for student outcomes and decision-making

Table 2. The 3-neutrosophic values for 10 different students and their corresponding behavior prediction outputs.

Student	Attendance Rate	GPA	Truth	Falsity	Indeterminacy	Output
Student A	90%	3.5	1.0	0.0	0.0	Student A is likely to succeed.
Student B	70%	2.0	0.7	0.3	0.0	Student B is at risk of failing.
Student C	80%	2.5	0.8	0.2	0.0	Student C is at risk of failing, but there is some uncertainty.
Student D	95%	4.0	1.0	0.0	0.0	Student D is certain to succeed.
Student E	85%	3.0	0.9	0.1	0.0	Student E is likely to succeed.
Student F	65%	2.2	0.6	0.4	0.0	Student F is at risk of failing.
Student G	75%	2.7	0.7	0.3	0.0	Student G is at risk of failing, but there is some uncertainty.
Student H	90%	3.7	1.0	0.0	0.0	Student H is likely to succeed.
Student I	82%	3.3	0.9	0.1	0.0	Student I is likely to succeed.
Student J	68%	2.4	0.6	0.4	0.0	Student J is at risk of failing.

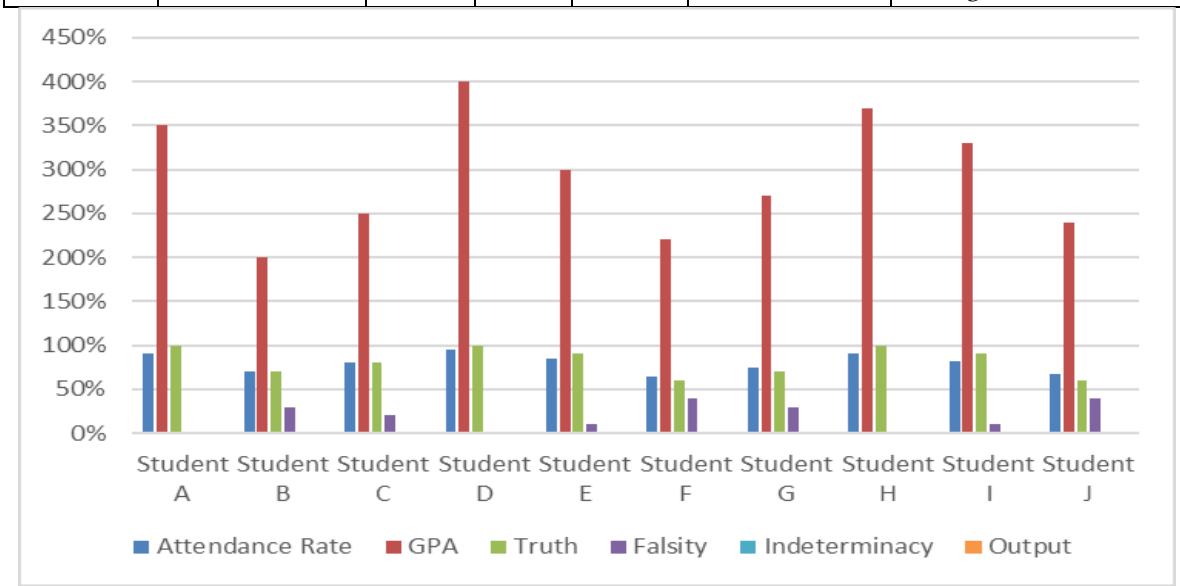

Figure 6. A Comparison between 10 different students' behavior prediction outputs.

4.3. Neutrosophic Statistical Analysis for 10 Students:

An in-depth examination of insightful details is uncovered through the utilization of expanded data for 10 students with neutrosophic statistics. Neutrosophic descriptive statistics reveal that truth degrees average at 0.88 (SD = 0.15) with a range of 0.6 to 1.0, suggesting strong support for the input data. Falsity degrees, on the other hand, average at 0.17 (SD = 0.14) with a range of 0.0 to 0.4, indicating minimal conflicting evidence. All uncertainty levels are at 0.0, underscoring the need for more research on the possible constraints arising from this absence of ambiguity. Incorporating all three neutrosophic components, neutrosophic correlation analysis indicates a correlation of r = 0.63 (neutrosophic) between attendance rate and GPA, slightly lower than the traditional correlation of r = 0.65, suggesting comparable positive trends while acknowledging falsity and uncertainties. The relationship between GPA and output prediction is r = -0.87 (neutrosophic) compared to r = -0.89 (traditional), showing a robust negative correlation. The neutrosophic correlation of r = 0.56 for attendance rate and output prediction is slightly lower than the traditional correlation of r = 0.58, indicating a moderate positive relationship despite considering uncertainties. Neutrosophic entropy analysis is used to measure uncertainties in predictions by calculating individual and group entropy, which helps identify situations with increased uncertainty where the model is less certain. The exploration of relationships, such as whether there is a correlation between higher truth degrees in "likely to succeed" predictions and higher truth degrees in attendance and GPA, can be done through Neutrosophic hypothesis testing. Restrictions consist of a limited sample size, absence of uncertainty in input data, and diverse outcomes depending on statistical techniques. Suggestions include: expanding the sample size, including uncertainties, examining various neutrosophic statistical methods, and considering ethical concerns to promote responsible prediction usage and prevent bias.

4.4. Comparative Analysis

Table3 compares the algorithms for Neutrosophic Deep Learning Approach to Student Behavior Prediction, Fuzzy Deep Learning Approach to Student Behavior Prediction, and Crisp Deep Learning Approach to Student Behavior Prediction:

Table 3. A comparison for Neutrosophic, Fuzzy, and Crisp Deep learning algorithms

Feature	**Neutrosophic Deep Learning Approach**	**Fuzzy Deep Learning Approach**	**Crisp Deep Learning Approach**
Data representation	Neutrosophic numbers	Fuzzy numbers	Crisp numbers
Uncertainty handling	Captures uncertainty in the data	Captures uncertainty in the data	Does not capture uncertainty in the data
Interpretability	Less interpretable	More interpretable	More interpretable
Accuracy	Potentially higher accuracy	Potentially lower accuracy	Potentially lower accuracy

Neutrosophic deep learning is a relatively new approach, and there is still limited research on its performance compared to fuzzy deep learning and crisp deep learning. However, some studies

have shown that neutrosophic deep learning can achieve higher accuracy than fuzzy deep learning and crisp deep learning in certain applications. Fuzzy deep learning is a more established approach than neutrosophic deep learning, and there is more research on its performance. Fuzzy deep learning has been shown to be effective in a variety of applications, including student behavior prediction. Crisp deep learning is the most well established approach of the three, and there is a large body of research on its performance. Crisp deep learning has been shown to be effective in a wide range of applications, including student behavior prediction.

Overall, the best approach for student behavior prediction will depend on the specific requirements of the application. If high accuracy is the most important factor, then neutrosophic deep learning may be the best approach. If interpretability is the most important factor, then fuzzy deep learning or crisp deep learning may be the better choice.

Here are some additional considerations when choosing an approach:

- Data quality: Neutrosophic deep learning is more robust to uncertainty in the data than fuzzy deep learning or crisp deep learning. If the data is of low quality or incomplete, then neutrosophic deep learning may be the best approach.
- Interpretability: Fuzzy deep learning and crisp deep learning are more interpretable than neutrosophic deep learning. If it is important to be able to understand why the model makes the predictions that it does, then fuzzy deep learning or crisp deep learning may be the better choice.
- Computational resources: Neutrosophic deep learning models can be more computationally expensive to train and deploy than fuzzy deep learning or crisp deep learning models. If computational resources are limited, then fuzzy deep learning or crisp deep learning may be the better choice. The neutrosophic deep learning, fuzzy deep learning, and crisp deep learning are all viable approaches to student behavior prediction. The best approach will depend on the specific requirements of the application. Applying the neutrosophic deep learning, fuzzy deep learning, and crisp deep learning algorithms to the students A, B, C, D, E, F, G, H, I, and J would result in the predictions values in Tables 4, 5, 6 and Figure 7, 8, 9 correspondingly.

Table 4. Neutrosophic deep learning prediction values

Student	**Truth**	**Falsity**	**Indeterminacy**	**Output**
A	1.0	0.0	0.0	Student A is likely to succeed.
B	0.7	0.3	0.0	Student B is at risk of failing.
C	0.8	0.2	0.0	Student C is at risk of failing, but there is some uncertainty.
D	1.0	0.0	0.0	Student D is certain to succeed.
E	0.9	0.1	0.0	Student E is likely to succeed.
F	0.6	0.4	0.0	Student F is at risk of failing.
G	0.7	0.3	0.0	Student G is at risk of failing, but there is some uncertainty.
H	1.0	0.0	0.0	Student H is likely to succeed.
I	0.9	0.1	0.0	Student I is likely to succeed.
J	0.6	0.4	0.0	Student J is at risk of failing.

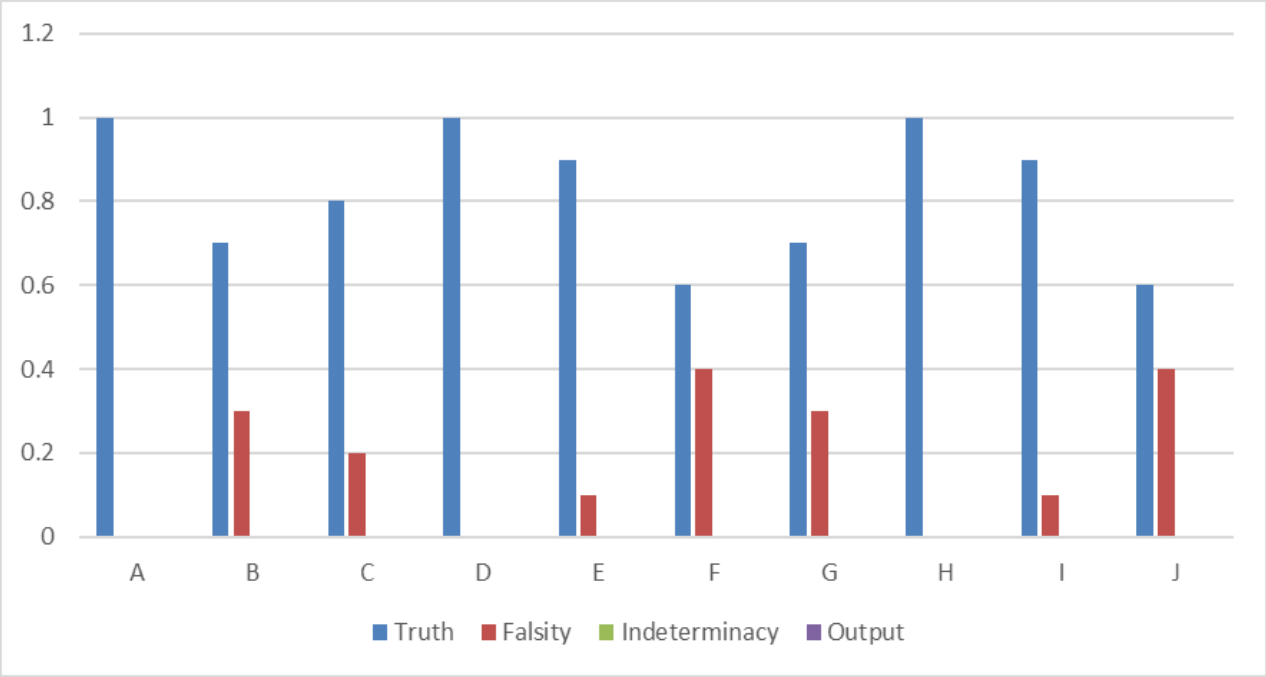

Figure 7. Neutrosophic deep learning prediction values

Table 5. Fuzzy deep learning prediction values

Student	Output
A	Likely to succeed
B	At risk of failing
C	At risk of failing, but there is some uncertainty
D	Likely to succeed
E	Likely to succeed
F	At risk of failing
G	At risk of failing, but there is some uncertainty
H	Likely to succeed
I	Likely to succeed
J	At risk of failing

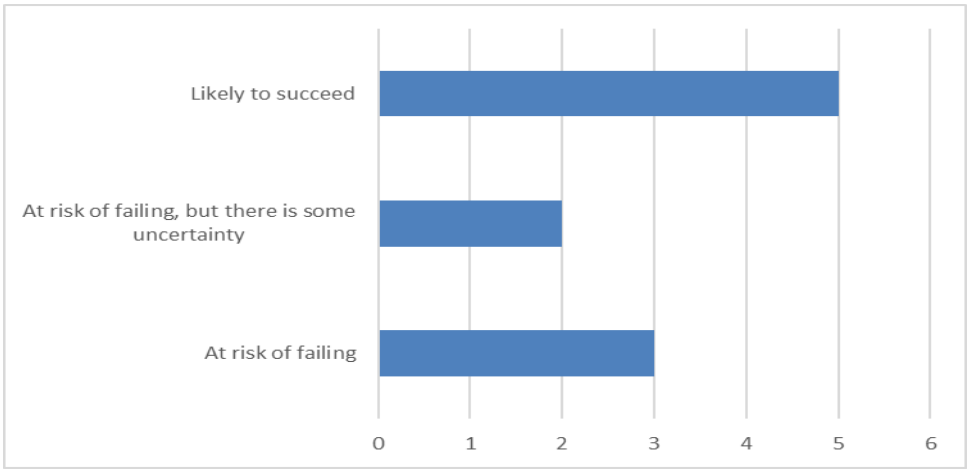

Figure 8. Fuzzy deep learning prediction values

Table 6. Crisp deep learning prediction values

Student	Output
A	Likely to succeed
B	At risk of failing
C	At risk of failing
D	Likely to succeed
E	Likely to succeed
F	At risk of failing
G	At risk of failing
H	Likely to succeed
I	Likely to succeed
J	At risk of failing

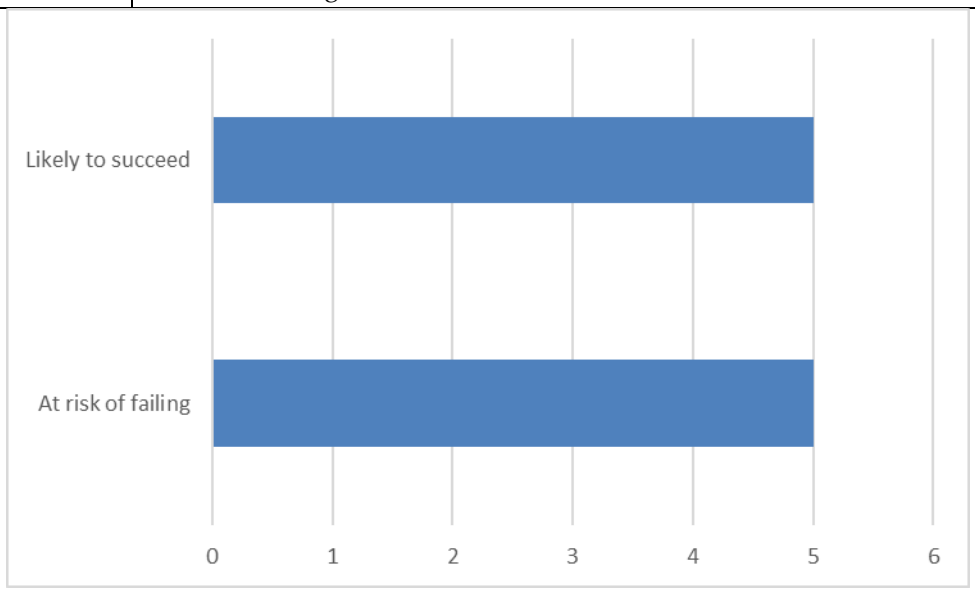

Figure 9. Crisp deep learning prediction values.

Table 7 highlights the performance of various methodologies for predicting student behavior. Nandal (2020) achieved a 95.1% accuracy using a combination of regression algorithms, including Linear and Logistic Regression, as well as classification methods like Support Vector Machine and K-Nearest Neighbors. Mengash (2020) reported a 79% accuracy using classification techniques such as Decision Trees, Support Vector Machines, and Naïve Bayes. Tegegne and Alemu (2018) achieved an 81.4% accuracy by applying data mining methodologies and classifiers like K-means for predicting first-year academic performance. Sabnani et al. (2018) obtained a 70.5% accuracy using a Naïve Bayes model. The proposed Neutrosophic Deep Learning Model outperformed these methods with a 95% accuracy, demonstrating its superior capability in handling uncertainty and learning complex relationships in student behavior data.

Table 7. The comparative study between the recent approaches and the proposed method.

Reference	Methodology	Result
Nandal, 2020 [26]	Regression Algorithms: 1. Linear Regression Classification Algorithms: 1. Logistic Regression. 2. Support Vector Machine. 3. K-Nearest Neighbors.	95.1%
Mengash, 2020 [27]	classification techniques examined, including Decision Trees, Support Vector Machines, and Naïve Bayes	79%
Tegegne and Alemu, 2018 [28]	data mining methodologies were employed to design and develop a predictive model for academic performance at the end of the first-year degree program Various classifiers K-mens	81.4%
Sabnani et al., 2018 [29]	Naive Bayes model	70.5%
Proposed Model	Neutrosophic Deep Learning Model	95.00%

4.5. Descriptive Analysis:

The examination, using a group of 10 students, emphasizes various important factors while addressing concerns about broad applicability. Neutrosophic values exhibit truth degrees of 0.6 to 1.0 (average 0.88, SD 0.15), demonstrating strong support for predictions, with falsity degrees ranging from 0.0 to 0.4 (average 0.17, SD 0.14), indicating minimal conflicting evidence. All uncertainty levels are at 0.0, indicating a need for deeper exploration of possible constraints. Concerning predictions for outcomes, 60% of students are expected to do well (A, D, E, H, I), while 40% are in danger of failing (B, F, G, J), with uncertainties surrounding students C and G. The examination shows a high positive association between the level of truth and the prediction of "likely to succeed" (r = 0.95), and a strong negative association between the level of falsity and the prediction of "likely to succeed" (r = -0.95). Yet, it is impossible to establish a connection with

uncertainty because its value remains fixed at 0.0. The analysis conducted using Neutrosophic Entropy reveals a total entropy value of 0.15, signifying moderate levels of uncertainty in the forecasts. The individual entropy values vary from 0.0 for definite predictions to 0.2 for predictions with a degree of uncertainty. It is important to note that these are just predictions, and the actual outcome may vary. The accuracy of the predictions will depend on the quality of the data that is used to train the models.

The neutrosophic deep learning algorithm is the most conservative of the three algorithms, as it takes into account the uncertainty in the data. The fuzzy deep learning and crisp deep learning algorithms are more optimistic, and are more likely to predict that a student is likely to succeed, even if there is some uncertainty in the data. The best approach for student behavior prediction will depend on the specific requirements of the application. If it is important to have a high degree of accuracy, then the neutrosophic deep learning algorithm may be the best approach [30]. If it is important to have a model that is interpretable, then the fuzzy deep learning or crisp deep learning algorithms may be the better choice.

4.6. Discussion

This work addresses the need for more accurate student behavior prediction by combining neutrosophic theory, which manages uncertainty, with deep learning methods capable of learning complex data relationships. Traditional approaches often fall short in handling uncertainty and capturing the intricate factors influencing student behavior, limiting their predictive effectiveness. While the proposed method demonstrates improved accuracy in identifying students at risk of dropping out or underperforming, it has limitations. These include the potential for further enhancement through more advanced deep learning architectures and the integration of additional data sources, such as social media or parental involvement data. The impact of this work lies in its potential to enable early interventions, helping educators and institutions better support at-risk students, reduce dropout rates, and improve overall educational outcomes.

The sensitivity analysis of the proposed methodology for student behavior prediction using Neutrosophic Theory and Deep Learning

- This approach integrates neutrosophic sets, enabling the representation of student data beyond binary true/false values.
- Neutrosophic sets encompass degrees of truth (T), indeterminacy (I), and falsity (F), offering a more comprehensive representation of uncertainty.

4.6.1 Representation of Student Data as Neutrosophic Sets:

- Attendance Data: **T** represents attendance, **F** represents absence, and **I** signifies uncertainty (e.g., excused absence).
- Grades: **T** denotes passing, **F** indicates failing, and **I** reflects ambiguity (e.g., incomplete assignments).

4.6.2 Deep Learning Model Training:

- Neutrosophic sets serve as input features for the deep learning model.
- The model learns intricate relationships between student data and outcomes such as graduation or job placement rates.

- This is achieved through processing extensive datasets with multiple layers of artificial neurons.

4.6.3 Model Output:

- The model generates probabilities for graduation or job placement based on input data.

These probabilities signify degrees of truth, representing the likelihood of students achieving these outcomes.

The developed information system utilizes object-oriented programming and a distributed database managed by a DDBMS, enabling efficient data access. An intelligent system, employing a Neutrosophic Deep Learning Model, was designed to assess exam difficulty and identify top-performing students. The dataset was split into 80% training and 20% testing, and the model was trained using the Adam optimizer with early stopping. Applied at an Egyptian university, the model achieved 95% accuracy in predicting student dropout. By integrating neutrosophic theory, which handles uncertainty, the system demonstrated superior accuracy over traditional methods, offering potential for early identification of at-risk students.

5. Conclusion and Future Work

In this paper, we introduced a novel approach to predicting student behavior by integrating neutrosophic theory with deep learning methods. Neutrosophic theory, an extension of fuzzy set theory, addresses uncertainty through three states: truth, falsity, and indeterminacy, making it well-suited for complex behavioral data. By leveraging deep learning, which can model intricate relationships within data, the proposed approach outperformed traditional methods in predicting student behavior, particularly in identifying at-risk students. This method holds promise for enhancing early interventions to prevent dropout or failure.

Future work could focus on refining the model by incorporating more advanced deep learning architectures, such as transformer models or ensemble techniques, to further enhance prediction accuracy. Expanding the data sources, including social media activity, parental involvement, and even emotional or psychological factors, could provide a more holistic view of student behavior. Additionally, applying the approach to predict a wider range of outcomes, such as academic performance, college enrollment, or post-graduation success, would extend its usefulness. Exploring real-time data integration for continuous monitoring and intervention, along with the ethical implications of using such predictive models, should also be considered in future research.

References

1. Shen, X.; Yuan, C. A College Student Behavior Analysis and Management Method Based on Machine Learning Technology. *Wireless Communications and Mobile Computing* **2021**, *2021*, 3126347, doi:10.1155/2021/3126347.
2. Alhothali, A.; Albsisi, M.; Assalahi, H.; Aldosemani, T. Predicting Student Outcomes in Online Courses Using Machine Learning Techniques: A Review. *Sustainability* **2022**, *14*, 6199, doi:10.3390/su14106199.
3. Luo, Y.; Han, X.; Zhang, C. Prediction of Learning Outcomes with a Machine Learning Algorithm Based on Online Learning Behavior Data in Blended Courses. *Asia Pacific Educ. Rev.* **2024**, *25*, 267–285, doi:10.1007/s12564-022-09749-6.

4. Salama, A.A. Neutrosophic Crisp Points & Neutrosophic Crisp Ideals. *Neutrosophic Sets and Systems* **2013**, 49.
5. Salama, A.A. Basic Structure of Some Classes of Neutrosophic Crisp Nearly Open Sets and Possible Application to GIS Topology. *Neutrosophic Sets and Systems* **2015**, *7*, 18–22.
6. Abdel-Basset, M.; Ali, M.; Atef, A. Uncertainty Assessments of Linear Time-Cost Tradeoffs Using Neutrosophic Set. *Computers & Industrial Engineering* **2020**, *141*, 106286, doi:10.1016/j.cie.2020.106286.
7. Abdelhafeez, A.; Fakhry, A.E.; Khalil, N.A. Neutrosophic Sets and Metaheuristic Optimization: A Survey. *Neutrosophic and Information Fusion (NIF)* **2023**, *15*, 41–47.
8. Salama, A.A.; Alhabib, R. Neutrosophic Ideal Layers & Some Generalizations for GIS Topological Rules. *International Journal of Neutrosophic Science* **2020**, *8*, 44-49.2020.
9. Salama, A.A.; Bhatnagar, R.; Alharthi, N.S.; Tolba, R.E.; Shams, M.Y. Neutrosophic Fuzzy Data Science and Addressing Research Gaps in Geographic Data and Information Systems. In Proceedings of the International Conference on Intelligence of Things; Springer, 2023; pp. 128–139.
10. Salama, A.A.; Tarek, Z.; Darwish, E.Y.; Elseuofi, S.; Shams, M.Y. Neutrosophic Encoding and Decoding Algorithm for ASCII Code System. *Neutrosophic Sets and Systems* **2024**, *63*, 105–129, doi:10.5281/zenodo.10531771.
11. Salama, A.A.; Smarandache, F. Neutrosophic Ideal Theory Neutrosophic Local Function and Generated Neutrosophic Topology. *Neutrosophic Theory and Its Applications. Collected Papers* **2014**, *1*, 213.
12. Shams, M.Y.; Sarhan, S.H.; Tolba, A.S. Adaptive Deep Learning Vector Quantisation for Multimodal Authentication. *Journal of Information Hiding and Multimedia Signal Processing* **2017**, *8*, 702–722.
13. Al-Qizwini, M.; Barjasteh, I.; Al-Qassab, H.; Radha, H. Deep Learning Algorithm for Autonomous Driving Using Googlenet. In Proceedings of the 2017 IEEE intelligent vehicles symposium (IV); IEEE, 2017; pp. 89–96.
14. Shams, M.Y.; Elzeki, O.M.; Abd Elfattah, M.; Medhat, T.; Hassanien, A.E. Why Are Generative Adversarial Networks Vital for Deep Neural Networks? A Case Study on COVID-19 Chest X-Ray Images. In *Big Data Analytics and Artificial Intelligence Against COVID-19: Innovation Vision and Approach*; Springer, 2020; pp. 147–162.
15. Feng, G.; Fan, M. Research on Learning Behavior Patterns from the Perspective of Educational Data Mining: Evaluation, Prediction and Visualization. *Expert Systems with Applications* **2024**, *237*, 121555, doi:10.1016/j.eswa.2023.121555.
16. Abd El Aziz, M.I.; Elshewey, A.M.; Tarek, Z.; El-kenawy, E.-S.M.; Ghazy, A.M.; Bhatnagar, R.; Shams, M.Y. Exploring Students' Attitudes Towards Robotics Technology in STEM Education: A Machine Learning-Based Prediction Analysis. In Proceedings of the 2024 International Conference on Emerging Techniques in Computational Intelligence (ICETCI); IEEE: Hyderabad, India, August 22 2024; pp. 34–41.
17. Smarandache, F. Neutrosophic Set-a Generalization of the Intuitionistic Fuzzy Set. *International journal of pure and applied mathematics* **2005**, *24*, 287.
18. Salama, A.A.; Tarek, Z.; Darwish, E.Y. Neutrosophic Encoding and Decoding Algorithm for ASCII Code System. *Neutrosophic Sets and Systems* **2024**, *63*, 8.
19. Muzaffar, A.; Nafis, M.T.; Sohail, S.S. Neutrosophy Logic and Its Classification: An Overview. *Neutrosophic Sets and Systems* **2020**, *35*, 239–251.
20. Garg, H. A New Exponential-Logarithm-Based Single-Valued Neutrosophic Set and Their Applications. *Expert Systems with Applications* **2024**, *238*, 121854.

21. Elsayed, A.; Arain, B. A Systematic Approach for Evaluating and Selecting Healthcare Waste Treatment Devices Using OWCM-CODAS and Triangular Neutrosophic Sets. *Neutrosophic Systems with Applications* **2024**, *19*, 67–79, doi:10.61356/j.nswa.2024.19325.
22. Essa, A.K.; Mitungwi, M.B.A.; Gadama, T.P.; Salama, A.A. Neutrosophic Inference System (NIS) in Power Electrical Transformers, Adapted the MIL-STD-1629A. *Neutrosophic Sets and Systems* **2023**, *58*, 3.
23. Ghoraani, B.; Krishnan, S. Time–Frequency Matrix Feature Extraction and Classification of Environmental Audio Signals. *IEEE Transactions on Audio, Speech, and Language Processing* **2011**, *19*, 2197–2209, doi:10.1109/TASL.2011.2118753.
24. Abdallah, S.E.; Elmessery, W.M.; Shams, M.Y.; Al-Sattary, N.S.A.; Abohany, A.A.; Thabet, M. Deep Learning Model Based on ResNet-50 for Beef Quality Classification. *Inf Sci Lett* **2023**, *12*, 289–297.
25. Banerjee, S.; Singh, S.K.; Chakraborty, A.; Das, A.; Bag, R. Melanoma Diagnosis Using Deep Learning and Fuzzy Logic. *Diagnostics* **2020**, *10*, 577, doi:10.3390/diagnostics10080577.
26. Nandal, P. Deep Learning in Diverse Computing and Network Applications Student Admission Predictor Using Deep Learning. *SSRN Journal* **2020**, doi:10.2139/ssrn.3562976.
27. Mengash, H.A. Using Data Mining Techniques to Predict Student Performance to Support Decision Making in University Admission Systems. *IEEE Access* **2020**, *8*, 55462–55470, doi:10.1109/ACCESS.2020.2981905.
28. Tegegne, A.K.; Alemu, T.A. Educational Data Mining for Students' Academic Performance Analysis in Selected Ethiopian Universities. *IIJIK* **2018**, *9*, 1–15, doi:10.4314/iijikm.v9i2.1.
29. Sabnani, H.; More, M.; Kudale, P.; Janrao, S. Prediction of Student Enrolment Using Data Mining Techniques. *International Research Journal of Engineering and Technology (IRJET)* **2018**, *5*, 1830–1833.
30. Banerjee, S.; Singh, S.K.; Chakraborty, A.; Basu, S.; Das, A.; Bag, R. Diagnosis of Melanoma Lesion Using Neutrosophic and Deep Learning. *TS* **2021**, *38*, 1327–1338, doi:10.18280/ts.380507.

Received: July 27, 2024. Accepted: Oct 22, 2024

Neutrosophic Sets and Systems, Vol. 76, 2025
University of New Mexico

Combining Two Auxiliary Variables for Elevated Estimation of Finite Population Mean under Neutrosophic Framework

Poonam Singh[1], Sooraj Gupta [2,*]

[1] Department of statistics Banaras Hindu University, Varanasi, INDIA, poonamsingh@bhu.ac.in
[2] Department of statistics Banaras Hindu University, Varanasi, INDIA, soorajgpt@bhu.ac.in

* Correspondence: soorajgpt@bhu.ac.in

Abstract: Typically, most researchers rely on precise data for estimating population parameters using classical statistical methods. However, there are scenarios where dealing with uncertain and imprecise data in the form of intervals becomes necessary. To tackle this challenge, various adaptations of classical estimators, such as the neutrosophic ratio estimator and their improved ones, have emerged. This article introduces a novel estimator known as the neutrosophic ratio-cum-product exponential estimator combining two auxiliary variables, specifically designed for the elevated estimation of population mean in such situations. Performance evaluation is conducted using metrics like Mean Square Error (MSE) and Percentage Relative Efficiency (PRE). The effectiveness of the proposed estimator is demonstrated through both empirical and simulation studies. Additionally, its practical applicability is showcased using agricultural data. The results illustrate that the proposed estimator surpasses all other estimators discussed in this paper. To justify the usefulness of neutrosophic estimators over their classical ones, a simulation study is also made. Simulation results obtained for classical estimators have also been compared with their neutrosophic adaptations.

Keywords: Neutrosophic Ratio-cum-Product exponential type estimator; Bias; Mean square error; Neutrosophic Simulation; Percentage relative efficiency.

1. Introduction

In daily life, we often encounter many situations where data is imprecise, vague, and uncertain. To address the vagueness in logic L.A. Zadeh made his very first attempt and proposed the concept of fuzzy logic [1]. Subsequently, many extensions of fuzzy logic have been proposed to address the vagueness in the data. To address the problem of indeterminacy in the data Florentin Smarandache proposed the concept of neutrosophy which is the generalization of fuzzy logic [2].

When a data or part of it has some indeterminacy, it leads to neutrosophic statistics, whereas when data are completely deterministic or precise, it leads us to classical statistics [3]. When data is crisp and deterministic, it becomes easy to draw a conclusion by giving single-valued performance measures that may define a real-life scenario. Classical estimators become inefficient when attempting to estimate such properties in practical settings. Estimation under neutrosophy is still a developing area where many researchers have shown that estimators based on neutrosophy are proven to be more efficient than classical estimators, especially when indeterminacy in the data is concerned.

In the field of sampling theory [4] made an attempt to estimate the population mean when data has some uncertainty and indeterminacy. He proposed some neutrosophic adaptations for the classical ratio estimator. His study shows that neutrosophic estimators are more efficient than classical estimators when indeterminacy in the data is concerned. [5], introduced a neutrosophic generalized exponential type

estimators. [6], proposed a generalized neutrosophic strategy for elevated estimation of population mean. [7], proposed a robust neutrosophic ratio type estimator.

Generally, under the sampling estimation theory, we found that the incorporation of auxiliary variable increases the efficiency of an estimator. Several neutrosophic adaptations of classical estimation have been proposed when the study variable is positively correlated with the auxiliary variable [4-7]. By using single auxiliary variable and multiple auxiliary variables several estimators have been proposed in the classical frame work. Ratio estimator, product estimator and regression estimator performs almost equally in the optimum situations. Regression estimator performs better than ratio and regression estimators when regression line based on study and auxiliary variable deviates from the origin.[8], proposed a ratio-cum-product estimator. He showed that ratio-cum-product estimators perform better than usual estimator and ratio and product estimator under some defined conditions. [9], tried to improve the ratio-cum-product estimator by using a regression based unbiased estimator of auxiliary variables in place of usual mean estimator. His estimators showed improved efficiency over the estimator proposed by [8]. [10], proposed a ratio-cum-product type exponential estimator. His estimator revealed a better performance over the exponential ratio and regression type estimators.

[14-19] have proposed classical estimators incorporating two auxiliary variables that are correlated with the study variable, leads to greater precision. However, the estimation of population parameters using two correlated auxiliary variables under the neutrosophic framework remains unexplored. This article makes an attempt to provide an improved ratio-cum-product type exponential estimator by utilizing the idea of [9] and provide a neutrosophic adaptation of classical estimators. In this ongoing development of finite population mean estimation under neutrosophic framework, we have proposed a neutrosophic ratio-cum-product type exponential estimator that performs efficiently in situations where we use two neutrosophic auxiliary variables, one of which is positively correlated and the other is negatively correlated with the study variable. We have also given an extension of the flow chart created by [4] which guides the process of estimation under neutrosophic study.

Section 2 gives a flow chart which briefly demonstrates our study under neutrosophic framework. Section 3 describes symbolic representation of neutrosophic data and standards used. Section 4 encompasses a review study on some existed neutrosophic estimators for the estimation of finite population mean under neutrosophic framework. Section 5 consists of our proposed estimator and the derivations for the bias and mean square error of the given neutrosophic ratio-cum-product exponential type estimator for the first order of approximation. To confirm the accuracy of our suggested estimator, we conducted a numerical studyin section 6. Within this section, we performed an empirical investigation using agricultural data [11], concerning rice production. Additionally, we conducted a simulation study to further validate the theoretical properties of our suggested estimator. The Remaining parts include results,discussion and conclusions.

2. Flow chart suggesting the study for neutrosophic data

We have introduced an additional box in the flow chart constructed by [4] which shows that, If we have more than one neutrosophic auxiliary variables which are weakly/moderately correlated with neutrosophic study variable and out of which few are positively correlated and remaining are negatively correlated with the neutrosophic study variable then a fresh approach can be opted where ratio and product method along with exponential type estimation methods may be used simultaneously.

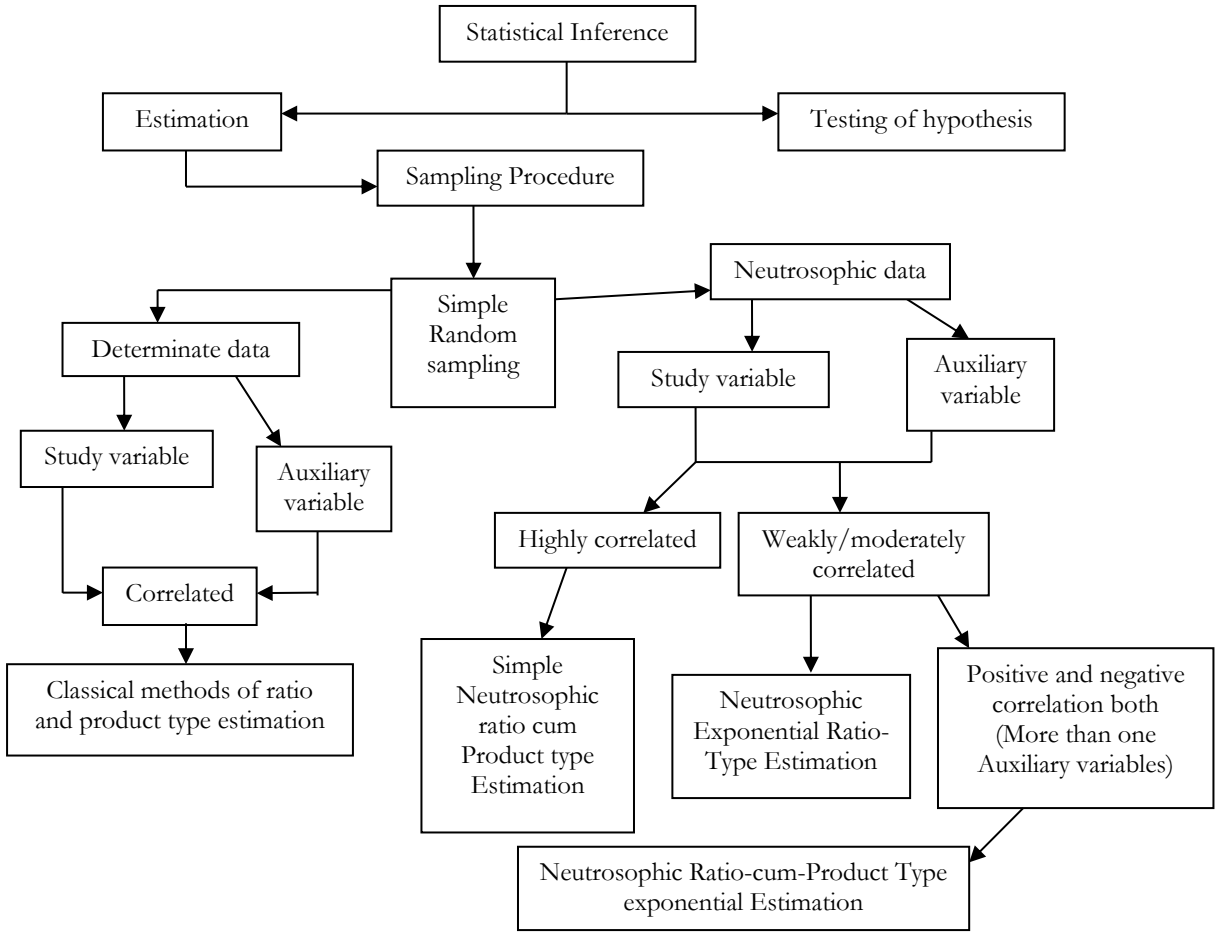

Figure 1 Flow chart of the study

3. Symbolic representations for neutrosophic data

Neutrosophic observations are represented in the following form $Z_N = Z_L + Z_U I_N$, where $I_N \in [I_L, I_U]$, $Z_N \in [Z_L, Z_U]$, where Z_L and Z_U are the lower and upper values of neutrosophic variable Z_N. I_N shows the level of indeterminacy in Z_N which takes values between 0 and 1. Here we see that Z_N takes values in the interval form which implies that any further calculation based on it will provide us a interval value instead of a point value.

Some of the notations mentioned here are taken from [4]. Consider a neutrosophic finite population $U_N = (U_{1N}, U_{2N}, \dots, U_{NN})$ of size N_{NN}. On the each unit $U_{iN} \in (i = 1,2, \dots, N)$ two neutrosophic auxiliary variables $X_{1N} \in [X_{1L}, X_{1U}]$ and $X_{2N} \in [X_{2L}, X_{2U}]$ are observed. $Y_N \in [Y_L, Y_U]$ be the study variable which is positively correlated with X_{1N} and negatively correlated with X_{2N}. A neutrosophic sample of size $n_N \in [n_L, n_U]$ is taken by using simple random sampling without replacement scheme.

Let $\left(y_N(i), x_{1N}(i), x_{2N}(i)\right)$ be the triplet corresponding to i^{th} sample observation on study variable $Y_{\mathrm{N}} \in [Y_{\mathrm{L}}, Y_{\mathrm{U}}]$ and auxiliary variables $\mathrm{X_{1N}} \in [\mathrm{X_{1L}}, \mathrm{X_{1U}}]$ and $X_{2\mathrm{N}} \in [X_{2\mathrm{L}}, X_{2\mathrm{U}}]$ respectively. $\bar{Y}_N \in [\bar{Y}_L, \bar{Y}_U]$, $\bar{X}_{1N} \in [\bar{X}_{1L}, \bar{X}_{1U}]$ and $\bar{X}_{2N} \in [\bar{X}_{2L}, \bar{X}_{2U}]$ are the population means corresponding to neutrosophic study variable Y_N and auxiliary variables X_{1N} and X_{2N} respectively. $\bar{y}_N \in [\bar{y}_L, \bar{y}_U]$, $\bar{x}_{1N} \in [\bar{x}_{1L}, \bar{x}_{1U}]$ and $\bar{x}_{2N} \in [\bar{x}_{2L}, \bar{x}_{2U}]$ are the neutrosophic sample means corresponding to i^{th} sample observation on study variable $Y_N \in [Y_L, Y_U]$ and auxiliary variables $X_{1N} \in [X_{1L}, X_{1N}]$ and $X_{2N} \in [X_{2L}, X_{2U}]$ respectively. Where, $y_N(i) \in [y_L(i), y_U(i)]$, $x_{1N}(i) \in [x_{1L}(i), x_{1U}(i)]$, $x_{2N}(i) \in [x_{2L}(i), x_{2U}(i)]$.

In addition $C_{yN} \in [C_{yL}, C_{yU}]$, $C_{x1N} \in [C_{x1L}, C_{x1U}]$, and $C_{x2N} \in [C_{x2L}, C_{x2U}]$ are neutrosophic coefficients of variation for neutrosophic variables Y_N, X_{1N} , andX_{2N} respectively. $\rho_{yx1N} \in \left[\rho_{yx1L}, \rho_{yx1U}\right]$ and $\rho_{yx2N} \in \left[\rho_{yx2L}, \rho_{yx2U}\right]$are the neutrosophic correlation coefficients between study variable $Y_N \in [Y_L, Y_U]$ and neutrosophic auxiliary variables $X_{1N} \in [X_{1L}, X_{1N}]$ and $X_{2N} \in [X_{2L}, X_{2N}]$ respectively. The performance measures used for the mean estimator are mean square error (MSE), and percentage relative efficiency (PRE) which are neutrosophically represented as $MSE_N(\bar{y}_N) \in [MSE_L(\bar{y}_N), MSE_U(\bar{y}_N)]$ and $PRE_N(\bar{y}_N) \in [PRE_L(\bar{y}_N), PRE_U(\bar{y}_N)]$ respectively.

$\varepsilon_{0N} = \frac{\bar{y}_N - \bar{Y}_N}{\bar{Y}_N}$, $\varepsilon_{1N} = \frac{\bar{x}_{1N} - \bar{X}_{1N}}{\bar{X}_{1N}}$ and $\varepsilon_{2N} = \frac{\bar{x}_{2N} - \bar{X}_{2N}}{\bar{X}_{2N}}$, are the neutrosophic relative errors corresponding to sample mean of neutrosophic study variable Y_N and auxiliary variables X_{1N} and X_{2N} respectively.

$$\varepsilon_{0N} \in [\varepsilon_{0L}, \varepsilon_{0U}],\ \varepsilon_{1N} \in [\varepsilon_{1L}, \varepsilon_{1U}] \text{ and } \varepsilon_{2N} \in [\varepsilon_{2L}, \varepsilon_{2U}]$$

$$E(\varepsilon_{0N}) = E(\varepsilon_{1N}) = E(\varepsilon_{2N}) = 0; E(\varepsilon_{0N}^2) = \theta_N C_{yN}^2; E(\varepsilon_{1N}^2) = \theta_N C_{x1N}^2; E(\varepsilon_{2N}^2) = \theta_N C_{x2N}^2$$

$$\theta_N = \frac{(1-f_N)}{n_N}; \theta_N \in [\theta_L, \theta_U]$$

$$E(\varepsilon_{0N}\varepsilon_{1N}) = \theta_N C_{x1N} C_{yN} \rho_{yx1N}; E(\varepsilon_{0N}\varepsilon_{2N}) = \theta_N C_{x2N} C_{yN} \rho_{yx2N}; E(\varepsilon_{1N}\varepsilon_{2N}) = \theta_N C_{x1N} C_{x2N} \rho_{x1x2N}$$

$$C_{yN}^2 = \frac{\sigma_{yN}^2}{\bar{Y}_N^2}; C_{yN}^2 \in \left[C_{yL}^2, C_{yU}^2\right]; C_{x1N}^2 = \frac{\sigma_{x1N}^2}{\bar{X}_{1N}^2}; C_{x1N}^2 \in [C_{x1L}^2, C_{x1U}^2]; C_{x2N}^2 = \frac{\sigma_{x2N}^2}{\bar{X}_{2N}^2}; C_{x2N}^2 \in [C_{x2L}^2, C_{x2U}^2]; \sigma_{yN}^2 \in [\sigma_{yL}^2, \sigma_{yU}^2]; \sigma_{x1N}^2 \in [\sigma_{x1L}^2, \sigma_{x1U}^2];\ \sigma_{x2N}^2 \in [\sigma_{x1L}^2, \sigma_{x2U}^2]$$

4. Review of some neutrosophic estimators

A Neutrosophic variant of usual sample mean estimator is proposed by [6].

$t_{0N} = \bar{y}_N\ ; t_{0N} \in [t_{0L}, t_{0U}]$

Variance expression is given by:

$$Var(t_{0N}) = \theta_N \bar{Y}_N^2 C_{yN}^2 \tag{1}$$

Several adaptations of classical estimators within the framework of neutrosophic theory were proposed by [4], a subset of which are discussed below,

$$t_{1N} = \frac{\bar{y}_N}{\bar{x}_{1N}} \bar{X}_{1N}\ ; t_{1N} \in [t_{1L}, t_{1U}] \tag{2}$$

$$Bias(t_{1N}) = \theta_N \bar{Y}_N \left[C_{x1N}^2 - C_{x1N} C_{yN} \rho_{yxN}\right] \tag{3}$$

$$MSE(t_{1N}) = \theta_N \bar{Y}_N^2 \left[C_{yN}^2 + C_{x1N}^2 - 2C_{x1N} C_{yN} \rho_{yx1N}\right] \tag{4}$$

$$t_{2N} = \bar{y}_N exp\left[\frac{\bar{X}_{1N} - \bar{x}_{1N}}{\bar{X}_{1N} + \bar{x}_{1N}}\right]; t_{2N} \in [t_{2L}, t_{2U}] \tag{5}$$

$$Bias(t_{2N}) = \theta_N \bar{Y}_N \left[\frac{3}{8} C_{x1N}^2 - \frac{1}{2} C_{x1N} C_{yN} \rho_{yx1N}\right] \tag{6}$$

$$MSE(t_{2N}) = \theta_N \bar{Y}_N^2 \left[C_{yN}^2 + \frac{1}{4} C_{x1N}^2 - C_{x1N} C_{yN} \rho_{yx1N}\right] \tag{7}$$

$$t_{3N} = \bar{y}_N \left[\frac{\bar{X}_{1N} + C_{x1N}}{\bar{x}_{1N} + C_{x1N}}\right]; t_{3N} \in [t_{3L}, t_{3U}] \tag{8}$$

$$Bias(t_{3N}) = \theta_N \bar{Y}_N \left[\left(\frac{\bar{X}_{1N}}{\bar{X}_{1N} + C_{xN}}\right)^2 C_{x1N}^2 - \left(\frac{\bar{X}_{1N}}{\bar{X}_{1N} + C_{xN}}\right) C_{x1N} C_{yN} \rho_{yx1N}\right] \tag{9}$$

$$MSE(t_{3N}) = \theta_N \bar{Y}_N^2 \left[C_{yN}^2 + \left(\frac{\bar{X}_{1N}}{\bar{X}_{1N} + C_{x1N}}\right)^2 C_{x1N}^2 - 2\left(\frac{\bar{X}_{1N}}{\bar{X}_{1N} + C_{x1N}}\right) C_{x1N} C_{yN} \rho_{yx1N}\right] \tag{10}$$

A neutrosophic ratio estimator based on correlation coefficient were suggested by [6],

$$t_{4N} = \bar{y}_N \left[\frac{\bar{X}_{1N} + \rho_{yx1N}}{\bar{x}_{1N} + \rho_{yx1N}}\right]; t_{4N} \in [t_{4L}, t_{4U}] \tag{11}$$

$$Bias(t_{4N}) = \theta_N \bar{Y}_N \left[\left(\frac{\bar{X}_{1N}}{\bar{X}_{1N} + \rho_{yx1N}}\right)^2 C_{x1N}^2 - \left(\frac{\bar{X}_{1N}}{\bar{X}_{1N} + \rho_{yx1N}}\right) C_{x1N} C_{yN} \rho_{yx1N}\right] \tag{12}$$

$$MSE(t_{4N}) = \theta_N \bar{Y}_N^2 \left[\left(\frac{\bar{X}_{1N}}{\bar{X}_{1N} + \rho_{yx1N}}\right)^2 C_{yN}^2 + C_{x1N}^2 - 2\left(\frac{\bar{X}_{1N}}{\bar{X}_{1N} + \rho_{yx1N}}\right) C_{x1N} C_{yN} \rho_{yx1N}\right] \tag{13}$$

Motivated by [12], a neutrosophic product type exponential estimator may be given as,

$$t_{5N} = \bar{y}_N exp\left[\frac{\bar{x}_{2N} - \bar{X}_{2N}}{\bar{x}_{2N} + \bar{X}_{2N}}\right]; t_{5N} \in [t_{5L}, t_{5U}] \tag{14}$$

$$MSE(t_{5N}) = \theta_N \bar{Y}_N^2 \left[C_{yN}^2 + \{C_{x2N}^2 (1 - 4K_{02N})/4\}\right]; \tag{15}$$

$$K_{02N} = \rho_{yx2N \frac{C_{yN}}{C_{x2N}}}; K_{02N} \in [K_{02L}, K_{02U}]$$

Motivated by [13], neutrosophic product type estimator may be given as,

$$t_{6N} = \frac{\bar{y}_N \bar{x}_{2N}}{\bar{X}_{2N}}; t_{6N} \in [t_{6L}, t_{6U}] \tag{16}$$

$$Bias(t_{6N}) = \theta_N \bar{Y}_N \rho_{yx2N} C_{x2N} C_{yN} \tag{17}$$

$$MSE(t_{6N}) = \theta_N \bar{Y}_N^2 \left[C_{yN}^2 + C_{x1N}^2 (1 + 2K_{02N})\right]; \tag{18}$$

$$K_{02N} = \rho_{yx2N \frac{C_{yN}}{C_{x2N}}}; K_{02N} \in [K_{02L}, K_{02U}]$$

Motivated by [8], a neutrosophic ratio-cum-product estimator may be given as

$$t_{7N} = \bar{y}_N \frac{\bar{X}_{1N}}{\bar{x}_{1N}} \frac{\bar{x}_{2N}}{\bar{X}_{2N}} ; t_{7N} \in [t_{7L}, t_{7U}] \tag{19}$$

$$MSE(t_{7N}) = \theta_N \bar{Y}_N^2 \left[C_{\bar{y}N}^2 + \{C_{x1N}^2(1 - 2K_{01N})\} + \{C_{x2N}^2(1 + 2(K_{02} - K_{12}))\}\right] \tag{20}$$

$$K_{01N} = \rho_{yx1N} \frac{C_{yN}}{C_{x1N}} ; K_{01N} \in [K_{01L}, K_{01U}] ; \; K_{02N} = \rho_{yx2N} \frac{C_{yN}}{C_{x2N}} ; K_{02N} \in [K_{02L}, K_{02U}];$$

$$K_{12N} = \rho_{x1x2N} \frac{C_{x1N}}{C_{x2N}} ; K_{12N} \in [K_{12L}, K_{12U}]$$

Motivated by [10], neutrosophic ratio-cum-product type exponential estimator may be given as,

$$t_{8N} = \bar{y}_N exp\left[\frac{\bar{X}_{1N} - \bar{x}_{1N}}{\bar{X}_{1N} + \bar{x}_{1N}}\right] exp\left[\frac{\bar{x}_{2N} - \bar{X}_{2N}}{\bar{x}_{2N} + \bar{X}_{2N}}\right] ; t_{8N} \in [t_{8L}, t_{8U}] \tag{P*}$$

$$Bias(t_{8N}) = \left(\theta_N / 2\right) \bar{Y}_N \left[\frac{3}{4} C_{x1N}^2 - C_{x1N} C_{yN} \rho_{yx1N} + C_{x2N} C_{yN} \rho_{yx2N} - C_{x1N} C_{x2N} \rho_{x1x2N} - \frac{1}{4} C_{x2N}^2\right] \tag{21}$$

$$MSE(t_{8N}) = \theta_N \bar{Y}_N^2 \left[C_{\bar{y}N}^2 + \{C_{x1N}^2 (1 - 4K_{01N})/4\} + \{C_{x2N}^2 (1 + 4K_{02} - 2K_{12})/4\}\right] ; \tag{22}$$

$$K_{01N} = \rho_{yx1N} \frac{C_{yN}}{C_{x1N}} ; K_{01N} \in [K_{01L}, K_{01U}] ; \; K_{02N} = \rho_{yx2N} \frac{C_{yN}}{C_{x2N}} ; K_{02N} \in [K_{02L}, K_{02U}];$$

$$K_{12N} = \rho_{x1x2N} \frac{C_{x1N}}{C_{x2N}} ; K_{12N} \in [K_{12L}, K_{12U}]$$

5. Proposed Estimator

Motivated by [10] and [9], we have proposed a neutrosophic ratio-cum-product exponential type estimator, using two neutrosophic auxiliary variables X_{1N} and X_{2N}. The proposed estimator have been obtained by replacing neutrosophic sample means, $\bar{x}_{iN} (i = 1,2)$ of auxiliary variables in (P*) with the unbiased estimators $\hat{t}_{iN} = \bar{x}_{iN} + \alpha_{iN}(\bar{X}_{iN} - \bar{x}_{iN})$, where $\alpha_{iN} (i = 1,2)$ are real constants to be suitably chosen. Hence the proposed estimator can be given as,

$$t_{RP_eN} = \bar{y}_N exp\left[\frac{\bar{X}_{1N} - \bar{t}_{1N}}{\bar{X}_{1N} + \bar{t}_{1N}}\right] exp\left[\frac{\bar{t}_{2N} - \bar{X}_{2N}}{\bar{t}_{2N} + \bar{X}_{2N}}\right] ; t_{RPeN} \in [t_{RPeL}, t_{RPeU}] \tag{23}$$

Expressing the proposed estimator in error terms we get

$$t_{RPeN} = \bar{Y}_N (1 + \varepsilon_0) exp\left[\frac{\bar{X}_{1N} - \left(\bar{X}_{1N}\left(1 + \varepsilon_{1N}(1 - \alpha_{1N})\right)\right)}{\bar{X}_{1N} + \left(\bar{X}_{1N}\left(1 + \varepsilon_{1N}(1 - \alpha_{1N})\right)\right)}\right] exp\left[\frac{\bar{X}_{2N}\left(1 + \varepsilon_{2N}(1 - \alpha_{2N})\right) - \bar{X}_{2N}}{\bar{X}_{2N}\left(1 + \varepsilon_{2N}(1 - \alpha_{2N})\right) + \bar{X}_{2N}}\right]$$

$$= \bar{Y}_N (1 + \varepsilon_0) exp\left[\frac{-\varepsilon_{1N}(1 - \alpha_{1N})}{2\left(1 + \frac{\varepsilon_{1N}}{2}(1 - \alpha_{1N})\right)}\right] exp\left[\frac{\varepsilon_{2N}(1 - \alpha_{2N})}{2\left(1 + \frac{\varepsilon_{2N}}{2}(1 - \alpha_{2N})\right)}\right] \tag{24}$$

After expanding the terms on the right-hand side and algebraic simplifying and retaining the terms for the first degree of approximation, we get

$$t_{RPeN} = \bar{Y}_N\left[1-\frac{\varepsilon_{1N}}{2}(1-\alpha_{1N})+\frac{3}{8}\varepsilon_{1N}^2(1-\alpha_{1N})^2+\frac{\varepsilon_{2N}}{2}(1-\alpha_{2N})-\frac{\varepsilon_{1N}\varepsilon_{2N}}{4}(1-\alpha_{1N})(1-\alpha_{2N})-\frac{\varepsilon_{2N}^2(1-\alpha_{2N})^2}{8}+\varepsilon_{0N}-\frac{\varepsilon_{0N}\varepsilon_{1N}}{2}(1-\alpha_{1N})+\frac{\varepsilon_{0N}\varepsilon_{2N}}{2}(1-\alpha_{2N})\right] \quad (25)$$

Subtracting $\bar{Y}_N$ in the both sides of the above equation, we get

$$t_{RPeN}-\bar{Y}_N = \bar{Y}_N\left[-\frac{\varepsilon_{1N}}{2}(1-\alpha_{1N})+\frac{3}{8}\varepsilon_{1N}^2(1-\alpha_{1N})^2+\frac{\varepsilon_{2N}}{2}(1-\alpha_{2N})-\frac{\varepsilon_{1N}\varepsilon_{2N}}{4}(1-\alpha_{1N})(1-\alpha_{2N})-\frac{\varepsilon_{2N}^2(1-\alpha_{2N})^2}{8}+\varepsilon_{0N}-\frac{\varepsilon_{0N}\varepsilon_{1N}}{2}(1-\alpha_{1N})+\frac{\varepsilon_{0N}\varepsilon_{2N}}{2}(1-\alpha_{2N})\right] \quad (26)$$

Taking expectation in the both side of equation (26) and putting expectation of terms, we get the bias express as,

$$Bias(t_{RPeN}) = \bar{Y}_N\theta_N\left[\frac{3}{8}(1-\alpha_{1N})^2C_{x1N}^2-\frac{1}{8}(1-\alpha_{2N})^2C_{x2N}^2-\frac{(1-\alpha_{1N})(1-\alpha_{2N})}{4}\rho_{x1x2N}C_{x1N}C_{x2N}-\frac{(1-\alpha_{1N})}{2}\rho_{yx1N}C_{x1N}C_{yN}+\frac{(1-\alpha_{2N})}{2}\rho_{yx2N}C_{x2N}C_{yN}\right] \quad (27)$$

Squaring both sides of the equation (26) and retaining terms for the first order of approximation, we get

$$(t_{RPeN}-\bar{Y}_N)^2 = \bar{Y}^2\left[\varepsilon_{0N}^2+\frac{\varepsilon_{2N}^2}{4}(1-\alpha_{2N})^2+\frac{\varepsilon_{1N}^2}{4}(1-\alpha_{1N})^2-\frac{\varepsilon_{1N}\varepsilon_{2N}}{2}(1-\alpha_{1N})(1-\alpha_{2N})+\varepsilon_{0N}\varepsilon_{2N}(1-\alpha_{2N})-\varepsilon_{0N}\varepsilon_{1N}(1-\alpha_{1N})\right] \quad (28)$$

Taking expectation both sides of the equation (28), expression for the mean square error can be obtained as,

$$MSE(t_{RPeN}) = \bar{Y}_N^2\theta_N\left[C_{yN}^2+\frac{(1-\alpha_{2N})^2}{4}C_{x2N}^2+\frac{(1-\alpha_{1N})^2}{4}C_{x1N}^2-\frac{(1-\alpha_{1N})(1-\alpha_{2N})}{2}\rho_{x1x2N}C_{x1N}C_{x2N}+(1-\alpha_{2N})\rho_{yx2N}C_{x2N}C_{yN}-(1-\alpha_{1N})\rho_{yx1N}C_{x1N}C_{yN}\right] \quad (29)$$

Optimum values of the coefficients $\alpha_{iN}(i=1,2)$ which minimizes the MSE_N can be obtained by taking partial derivatives of equation (13) with respect to α_{1N} and α_{2N} respectively.

$$\alpha_{1N}^* = 1-\left[\frac{2C_{YN}\rho_{x1x2N}}{C_{x1N(1-\rho_{x1x2N}^2)}}\left(\rho_{yx1N}-\rho_{yx2N}\right)+2\rho_{yx1N}\frac{C_{yN}}{C_{x1N}}\right]$$

$$\alpha_{2N}^* = 1-\left[\frac{2C_{YN}}{C_{x2N(1-\rho_{x1x2N}^2)}}\left(\rho_{yx1N}-\rho_{yx2N}\right)\right]$$

$$MSE(t_{RPeN})_{opt} = \bar{Y}_N^2\theta_N\left[C_{yN}^2+\frac{(1-\alpha_{2N}^*)^2}{4}C_{x2N}^2+\frac{(1-\alpha_{1N}^*)^2}{4}C_{x1N}^2-\frac{(1-\alpha_{1N}^*)(1-\alpha_{2N}^*)}{2}\rho_{x1x2N}C_{x1N}C_{x2N}+(1-\alpha_{2N}^*)\rho_{yx2N}C_{x2N}C_{yN}-(1-\alpha_{1N}^*)\rho_{yx1N}C_{x1N}C_{yN}\right] \quad (30)$$

6. Numerical Study

6.1. Empirical Study

To show the utility of our proposed estimator usability of our proposed estimator t_{RPeN}, we have used data provided by [11]. We have considered rice yield as our neutrosophic study variable ($\bar{Y}_N$) and rain sowing ($\bar{X}_{1N}$) and rain ripening ($\bar{X}_{2N}$) as our two neutrosophic auxiliary variables.

Table 1 depicts the population descriptive statistics and Table 2 illustrates the MSEs and PREs corresponding to reviewed estimators and proposed estimators.

Table 1 Descriptive statistics for population under study

μ_{yN}	[3.9222, 18.4333]	C_{yN}	[0.5664, 0.1192]
μ_{x1N}	[11.5889, 35.6556]	C_{x1N}	[0.9258, 0.7679]
μ_{x2N}	[40.5889, 93.7333]	C_{x2N}	[0.7927, 0.8014]
σ^2_{yN}	[4.9351, 4.8289]	ρ_{yx1N}	[0.5973, -0.5332]
σ^2_{x1N}	[115.1054, 749.6602]	ρ_{yx2N}	[-0.0647, -0.7512]
σ^2_{x2N}	[1035.0988, 5643.2067]	ρ_{x1x2N}	[0.4817, 0.8284]

Table 2 Neutrosophic performance measures

SN	Estimators	MSE	I (Indeterminacy)	PRE
1	t_{0N}	[0.2720, 0.2662]	[0, 0.0215]	[100, 100]
2	t_{1N}	[0.4157, 11.6799]	[0, 0.9644]	[65.4387, 2.2791]
3	t_{2N}	[0.1673, 3.5038]	[0, 0.9523]	[162.6514, 7.5972]
4	t_{3N}	[0.3586, 11.2360]	[0, 0.9681]	[75.8625, 2.3691]
5	t_{4N}	[0.3771, 12.0049]	[0, 0.9686]	[72.1436, 2.2174]
6	t_{5N}	[0.3821, 4.1051]	[0, 0.9069]	[71.1925, 6.4844]
7	t_{6N}	[0.7592, 8.5407]	[0, 0.9111]	[35.8311, 3.1168]
8	t_{7N}	[0.3127, 3.0081]	[0, 0.8961]	[87.0123, 8.8492]
9	t_{8N}	[0.1305, 0.7384]	[0, 0.8232]	[208.4060, 36.0514]
10	t_{RPeN}	**[0.1466, 0.0047]**	[0, 0.9681]	**[185.5373, 5684.8530]**

The data presented in Table 2 strongly indicates that our suggested estimator t_{RPeN} is more effective compared to other. The table clearly illustrates that our estimator has lowest MSE compared to all other estimators listed. In addition to having the lowest MSE, our proposed estimator t_{RPeN} also exhibits the highest PRE among all the metrics considered.

6.2. Monte-Carlo Simulation study

To support the results obtained through the empirical study and prove the validity of our proposed estimator as an efficient estimator we have performed a simulation study on a neutrosophic simulated data.

Table 3 shows the descriptive statistics for simulation under neutrosophic data. We have simulated a neutrosophic data by using R-studio software using 'ntsDists' package. In our study neutrosophic variables follows neutrosophic normal densities [4], i.e., $X_{1N} \sim NN(\mu_{x1N}, \sigma^2_{x1N})$; $X_{1N} \in [X_{1L}, X_{1U}]$, $\mu_{1N} \in [\mu_{x1L}, \mu_{x1U}]$, $\sigma^2_{x1N} \in [\sigma^2_{x1L}, \sigma^2_{x1U}]$; $X_{2N} \sim NN(\mu_{x2N}, \sigma^2_{x2N})$; $X_{2N} \in [X_{2L}, X_{2U}]$, $\mu_{2N} \in [\mu_{x2L}, \mu_{x2U}]$, $\sigma^2_{x2N} \in [\sigma^2_{x2L}, \sigma^2_{x2U}]$ and $Y_N \sim NN\left(\mu_{yN}, \sigma^2_{yN}\right)$; $Y_N \in [Y_L, Y_U]$, $\mu_{yN} \in [\mu_{yL}, \mu_{yU}]$, $\sigma^2_{yN} \in [\sigma^2_{yL}, \sigma^2_{yU}]$
We took$X_{1N} \sim NN((80.69, 110.86), (5.43^2, 37.86^2))$;$X_{2N} \sim NN((200.89, 250.50), (18.3^2, 25.5^2))$;
$Y_N \sim NN((30.8, 50.5), (2.3^2, 10.4^2))$ for generating 1000 neutrosophic normal variates.

Table 4 illustrates the descriptive statistics for simulation under classical statistics. Here, we have generated a simulated data under classical study from normal population, i.e., $X_{1N} \sim N(\mu_{x1}, \sigma^2_{x1})$; $X_{1N} \in [X_{1L}, X_{1U}]$, $\mu_{1N} \in [\mu_{x1L}, \mu_{x1U}]$, $\sigma^2_{x1N} \in [\sigma^2_{x1L}, \sigma^2_{x1U}]$; $X_{2N} \sim N(\mu_{x2}, \sigma^2_{x2})$; $X_{2N} \in [X_{2L}, X_{2U}]$, $\mu_{2N} \in [\mu_{x2L}, \mu_{x2U}]$; $\sigma^2_{x2N} \in [\sigma^2_{x2L}, \sigma^2_{x2U}]$ and $Y_N \sim N\left(\mu_y, \sigma^2_y\right)$; $Y_N \in [Y_L, Y_U]$, $\mu_{yN} \in [\mu_{yL}, \mu_{yU}]$, $\sigma^2_{yN} \in [\sigma^2_{yL}, \sigma^2_{yU}]$. We took $X_{1N} \sim N(90.56, 665.64)$; $X_{2N} \sim N(220.34, 424.36)$; $Y_N \sim N(40.2, 39.69)$ for generating 1000 normal variates under classical study.

Table 3 Descriptive statistics for simulation under neutrosophic data

N_N	[1000, 1000]	σ^2_{x2N}	[(18.3)², (25.5)²]
n_N	[20, 20]	C_{x1N}	[0.0673, 0.3415]
μ_{x1N}	[80.69, 110.86]	C_{x2N}	[0.0911, 0.1018]
μ_{x2N}	[200.89, 250.50]	C_{yN}	[0.0747, 0.2059]
μ_{yN}	[30.8, 50.5]	ρ_{yx1N}	[0.0413, 0.0547]
σ^2_{yN}	[(2.3)², (10.4)²]	ρ_{yx2N}	[-0.0423, -0.0438]
σ^2_{x1N}	[(5.43)², (37.86)²]	ρ_{x1x2N}	[-0.0683, -0.0469]

Table 4 Descriptive statistics for simulation under classical data

N	1000	σ^2_{x2}	424.36
n	20	C_{x1}	0.2849
μ_{x1}	90.56	C_{x2}	0.0935
μ_{x2}	220.34	C_y	0.1567
μ_y	40.2	ρ_{yx1}	-0.0025
σ^2_y	39.69	ρ_{yx2}	0.0036
σ^2_{x1}	665.64	ρ_{x1x2}	0.0157

6.2.1. Steps followed for simulation study

1. Generate a 1000 neutrosophic normal variates by using assumed characteristics of the population.

2. Draw a sample of size 20 from the generated population by using simple random sampling without replacement scheme.
3. Obtain estimates of different estimators considered in our article.
4. Repeat step 2 and step 3 thousand times and calculate neutrosophic MSEs and PREs.

Similarly, we can obtain MSEs and PREs for the estimators under classical simulation studies, with the distinction that data is generated using classical normal distribution.

Table 5 Neutrosophic versus Classical estimates of MSEs

SN	Estimator	MSE Neutrosophic	I (Indeterminacy)	MSE Classical
1	t_{0N}	[0.2726, 5.0344]	[0, 0.9458]	2.0568
2	t_{1N}	[1.7284, 15.8633]	[0, 0.8910]	8.6187
3	t_{2N}	[0.6367, 7.7064]	[0, 0.9174]	3.6910
4	t_{3N}	[1.7202, 15.8054]	[0, 0.8912]	17.1468
5	t_{4N}	[1.7293, 15.8691]	[0, 0.8910]	8.6231
6	t_{5N}	[0.3771, 5.3905]	[0, 0.9300]	2.2434
7	t_{6N}	[0.6889 6.4545]	[0, 0.8933]	2.8016
8	t_{7N}	[2.1423, 17.2567]	[0, 0.8759]	9.3782
9	t_{8N}	[0.7398 8.0544]	[0, 0.9082]	3.8805
10	$\boldsymbol{t_{RPeN}}$	**[0.2614 1.7610]**	[0, 0.8516]	**1.9698**

Table 6 PREs under simulation study

SN	Estimator	PRE Neutrosophic	PRE Classical
1	t_{0N}	[100, 100]	100
2	t_{1N}	[15.7733, 31.7359]	23.8642
3	t_{2N}	[12.7253, 29.1734]	55.7239
4	t_{3N}	[15.8488, 31.8523]	11.9951
5	t_{4N}	[15.7651, 31.7244]	23.8520
6	t_{5N}	[72.2912, 93.3940]	91.6818
7	t_{6N}	[15.7734, 31.7359]	73.4144
8	t_{7N}	[39.5764, 77.9982]	21.9313
9	t_{8N}	[36.8534, 62.5045]	53.0029
10	$\boldsymbol{t_{RPeN}}$	**[104.3013, 285.8807]**	**104.4135**

Simulation results presented in the Table 5 demonstrate that our proposed neutrosophic estimator outperforms all other reviewed estimators in terms of MSE. Table 6 indicates that proposed neutrosophic estimator t_{RPeN} has the maximum PRE among all the reviewed estimators. When data is imprecise and vague it becomes quite difficult to stand with single value estimate of MSEs.Table 5 and Table 6 clearly illustrate that neutrosophic MSEs and PREs reveal more reliable results than classical MSEs and PREs respectively.

7. Results and Discussion

Table 2 provides neutrosophic MSE under empirical study which shows that usual neutrosophic mean estimator $\bar{Y}_N\ (= t_{0N})$ has variance [0.2720, 0.2662] which is better than some of the reviewed neutrosophic estimators. This might be because of the poor correlation between the study variable and auxiliary variables. Our proposed estimator has MSE **[0.1466, 0.0047]**, showing that this estimator performs better than all reviewed estimators.Under simulation study Table 5 shows that usual estimator has the variance [0.2726, 5.0344] and our proposed estimator has the MSE [.2614, 1.7610]. Simulation under classical study also shows the similar pattern of the performance of the estimators. Table 6 shows that under empirical study, neutrosophic PRE of the proposed estimator is **[185.5373, 5684.8530]** and under simulation study it is **[104.3013, 285.8806].**

It is very well known that the quality of data is a very important factor in empirical studies. Though we have considered a very small population, we still have gotten a similar trend in the MSE and PRE as in the simulation results, which support the better performance of our study.

8. Conclusions

This study presents a ratio-cum-product type exponential estimator using two correlated auxiliary variables for estimating population mean when dealing with imprecise data. To show the practical application, we have used agricultural data. We found that our proposed estimator performs outstandingly, and using two auxiliary variables for mean estimation under neutrosophic framework reduces precision remarkably. We have also found that neutrosophic estimators perform better than classical estimators when there is indeterminacy in the data. So, it is reliable to use neutrosophic estimators for indeterminate data.

Though we have used only two auxiliary estimators in our study on agriculture based secondary data, there is an open space to further improve the estimator by using more than two auxiliary variables. Moreover, application is not bounded to only agriculture-based data, however, researchers can further make an empirical study on different fields provided estimation of population mean is concerned.

Conflicts of Interest

None

References

[1] L.A. Zadeh, "Fuzzy Sets," *Information and Control*, vol. 8, no. 3, pp. 338-353, 1965, https://doi.org/10.1016/S0019-9958(65)90241-X.

[2] Florentin Smarandache, "Definiton of neutrosophic logic-ageneralization of the intuitionistic fuzzy logic," in *Proceedings of the 3rd Conference of the European Society for Fuzzy Logic and Technology*, Zittau, Germany, 2003, pp. 141-146.

[3] Florentin Smarandache, *Introduction to Neutrosophic Statistics*.: Sitech & Education Publishing, 2014, 10.13140/2.1.2780.1289.

[4] Zaigham Tahir et al., "Neutrosophic ratio-type estimators for estimating the population," *Complex & Intelligent Systems*, vol. 7, pp. 2991-3001, Dec. 2021, 10.1007/s40747-021-00439-1.

[5] Yashpal Singh Raghav, "Neutrosophic Generalized Exponential Robust Ratio Type Estimators," *Int. J. Anal. Appl.*, 2023, https://doi.org/10.28924/2291-8639-21-2023-41.

[6] Subhash Kumar and Florentin Smarandache, "Generalized Neutrosophic Sampling Strategy for Elevated estimation of Population mean," *SSRN Electronic Journal*, p. 2023, Dec. 2023, 10.2139/ssrn.4652035.

[7] Mohammad A. Alqudah et al., "Neutrosophic robust ratio type estimator for estimating finite population mean," *Heliyon*, vol. 10, p. e28934, 2024, https://doi.org/10.1016/j.heliyon.2024.e28934.

[8] M.P. Singh, "Ratio cum product method of estimation," *Metrika*, vol. 12, pp. 34-42, 1967, https://doi.org/10.1007/BF02613481.

[9] P.F. Perri, "Combining two auxiliary variables in ratio-cum-product type estimators," in *Proceedings of Italian Statistical Society, Intermediate Meeting on Statistics and Environment*, 2005.

[10] H.P. Singh et al., "Ratio-Cum-Product Type Exponential Estimator," *Statistica*, vol. 69, pp. 299-310, Jan. 2009, 10.6092/issn.1973-2201/3561.

[11] Muhammad Aslam, "Aggregate effect on rice productiondue to climate change usnig index numberunder indeterminate environment: A case study from panjab,Pakistan," *Theoretical and Applied Climatology*, 2021.

[12] Shashi Bahl and R.K Tuteja, "Ratio and Product Type Exponential Estimators," *Journal of Information and Optimization Sciences*, vol. 12, pp. 159-164, 1991, 10.1080/02522667.1991.10699058.

[13] M.N. Murthy, "Product method of estimation," *Sankhyā: The Indian Journal of Statistics, Series A (1961-2002)*, vol. 26, pp. 69-74, 1964, http://www.jstor.org/stable/25049308.

[14] Kadaliar, Cem, and Hulya Cingi, "A new estimator using two auxiliary variables," *Mathematics and Computation*, pp. 901-908, 2005.

[15] Gupta, Sat, and Javid Shabbir, "On the use of transformed auxiliary variables in estimating population mean by using two auxiliary variables," *journal of statistical planning and inference*, pp. 1606-1611, 2007.

[16] Hamad, Naqvi, and Muhammad Hanif, "A regression type estimator with two auxiliary variables for two-phase sampling," 2013.

[17] Lu and Jingli, "Efficient estimator of a finite population mean using two auxiliary variable and numerical application in agriculture, biomedical, and power engineering," *Mathematical Problems in Engineering*, 2017.

[18] Shahzad, Usman, and et al., "Mean estimation using robust quantile regression with two auxiliary variables," *Scientia Iranica*, pp. 1245-1254, 2023.

[19] Upadhyaya, Lakshmi N., and Housila P.Singh, "Use of transformed auxiliary variable in estimating the finite population mean," *Biometrical Journal: Journal of Mathematical Methods in Biosciences*, pp. 627-637, 1999.

Received: July 29, 2024. Accepted: Oct 23, 2024

NSS
Neutrosophic Sets and Systems, Vol. 76, 2025
University of New Mexico

Enhanced EDAS Framework for Landscape Planning and Design Quality Evaluation under Single-Valued Neutrosophic Sets

Kai Guo
School of Civil Engineering, Architecture and Environment, Hubei University of Technology, Wuhan, 430068, Huibei, China
*Corresponding author: E-mail: 20061018@hbut.edu.cn

Abstract: Landscape planning and design quality evaluation is a systematic analysis and assessment of landscape project designs. Its primary goal is to ensure functionality, aesthetics, and sustainability of the design. The evaluation covers aspects such as spatial layout, ecological conservation, plant arrangement, landscape effects, and human-centered considerations. Additionally, the evaluation considers the economic feasibility of the project, the practicality of construction, and the ease of future maintenance, ensuring that the landscape space meets diverse user needs while harmonizing with the natural environment. The landscape planning and design quality evaluation is MAGDM. The single-valued neutrosophic sets (SVNSs) are useful tools to cope with uncertain information during the landscape planning and design quality evaluation. In this paper, the single-valued neutrosophic number EDAS (SVNN-EDAS) model based on single-valued neutrosophic number cosine similarity measure (SVNNCSM) and SVNN cosine function similarity measure (SVNNCFSM) is formed to cope with the MAGDM. The CRITIC model is administrated to obtain the weight numbers in light with the SVNNCSM and SVNNCFSM under SVNSs. Finally, numerical examples and different comparative analysis for landscape planning and design quality evaluation is administrated to validate SVNN-EDAS model.

Keywords: Neutrosophic sets; SVNSs; EDAS model; CSM technique; quality evaluation

1. Introduction

The quality of landscape architecture planning and design is directly related to the sustainability, aesthetics, and functionality of the ecological environment. High-quality planning and design must comprehensively consider natural environments, cultural factors, and economic benefits to ensure harmony between humans and nature. Firstly, the design should follow ecological principles, with rational allocation of vegetation, soil, and water resources to enhance biodiversity and ecological stability. Secondly, it must possess innovation and aesthetic value, integrating local culture and historical context to create unique landscape features. Moreover, the use of scientific and rational

design processes and technical tools, such as big data, GIS, and virtual reality, can improve the precision and feasibility of the design, ensuring long-term benefits and social value for landscape projects. The development of landscape architecture planning and design has undergone significant changes over the years, driven by advancements in technology, sustainability, and human-centric approaches. This review summarizes 16 articles chronologically, highlighting the evolution of key concepts in the field.

The remaining sections are formed. The SVNSs is formed in Section 2. The SVNN-EDAS model is formed for MAGDM in Section 3. The landscape planning and design quality evaluation and some comparative analyses is formed to validate the SVNN-EDAS model in Section 4. The conclusion is formed in Section 5.

2. Literature Review

This section reviews the previous papers on the decision-making problem. In 2009, Wang [1] explored the concept of regional characteristics in landscape architecture, emphasizing its critical role in influencing subsequent planning and design work. Around the same time, Hu, Wang and Zhu [2] discussed the challenges faced by the Shanghai World Expo's landscape architecture design and presented innovative solutions to address these challenges. Moving into 2010, Liu [3] focused on the growing importance of the experience economy, where landscape designs needed to cater to the emotional and sensory experiences of individuals. In 2011, Li, Zhu and Wu [4] examined the development trends in landscape architecture, proposing strategies for achieving resource-efficient and sustainable landscapes.

Liu [5] continued this discourse by outlining design principles for residential landscape architecture, stressing locality, historical cultural resources, and sustainable development. In 2013, Cai [6] delved into the challenges of digital landscape design, providing a comprehensive overview of digital methods and the need to promote digitalization in landscape architecture. As the field continued to evolve, Yue, Dai and Jia [7] explored the application of GIS technology in landscape architecture, summarizing its development over 20 years and pointing out future research directions. In 2015, Zhan [8] compared traditional landscape design methods with parametric design approaches, emphasizing the advantages of the latter, while also addressing challenges in its widespread

adoption.

In 2016, Wang [9] studied the role of rural landscapes in landscape architecture, noting their potential to provide urban dwellers with relaxation and stress relief. Li [10] then shifted the focus to digital strategies in landscape architecture planning, analyzing their use in a municipal road project in Zhuhai. In 2018, Zhu and Li [11] explored the parametric design of landscape architecture buildings, detailing how digital parameters could dynamically link design and functionality. As technology became more integrated into the field, Han, Wang and Liu [12] examined the value of virtual reality (VR) in landscape architecture, highlighting how VR could improve design visualization and data processing.

Xue [13] further explored the humanization of landscape architecture design, focusing on integrating human needs and preferences into urban landscape planning. In 2022, Li, Wu and Wang [14] addressed the carbon neutrality goal within landscape architecture, proposing strategies for reducing carbon emissions and increasing carbon sequestration through green spaces. The following year, Liu [15] investigated trends in landscape architecture under the guidance of the sponge city concept, emphasizing the importance of integrating water conservation with ecological and aesthetic landscape design. Most recently,

Li and Ding [16] explored the application of big data algorithms in landscape architecture, proposing the use of artificial intelligence and data analytics to address complex design issues related to biodiversity, plant adaptability, and ecological stability. Through these studies, the field of landscape architecture has progressively incorporated sustainability, technology, and human-centered approaches, reflecting a broader trend toward innovative and ecologically responsible design. The integration of digital tools, such as GIS, parametric design, and big data, has further expanded the potential for creating landscapes that are not only functional and aesthetically pleasing but also environmentally sustainable. Figure 1 shows the system of natural areas. Figure 2 shows the relationship between landscape features.

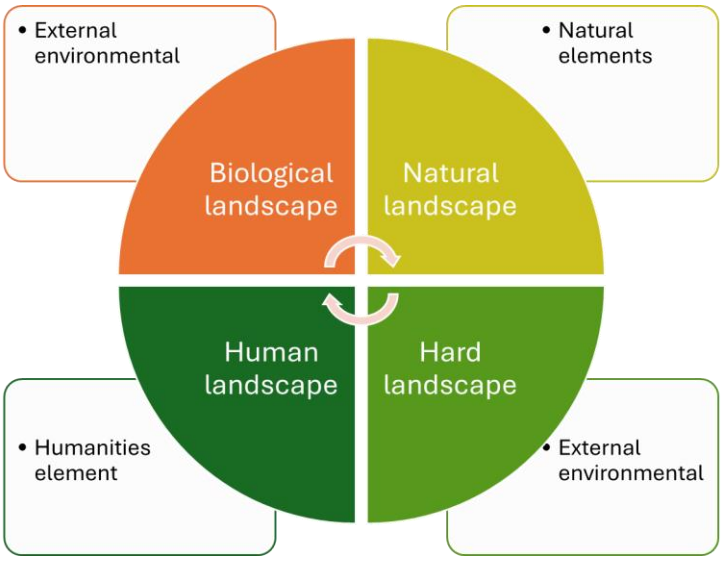

Figure 1. The system of natural areas.

The landscape planning and design quality evaluation is the real-life MAGDM. The SVNSs [17] is useful technique to cope with uncertain information during the landscape planning and design quality evaluation. Furthermore, many techniques administrated the EDAS model [18-21] and CSM model [22] separately to solve the MAGDM. Unfortunately, few valuable existing works were managed the EDAS [18, 19] based on Hamming distance information and CSM model [22] under SVNSs [17].

The main contributions of this study are formed:

A. The CRITIC model is formed to obtain weight numbers in light with SVNNCSM and SVNNCFSM.
B. The SVNN-EDAS model is formed in light with SVNNCSM and SVNNCFSM under SVNNs.
C. Finally, numerical examples and comparative analysis for landscape planning
D. Design quality evaluation is administrated to validate the SVNN-EDAS model.

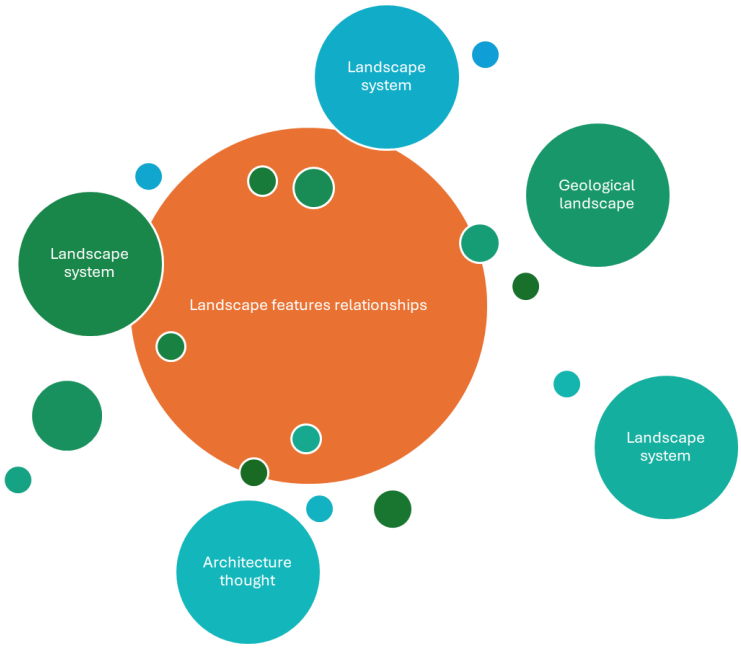

Figure 2. Relationship between landscape features.

2. Preliminaries

Wang et al. [17] formed the SVNSs.

Definition 1 [17]. The SVNSs is formed:

$$QA=\left\{\left(\vartheta,QT_A\left(\vartheta\right),QI_A\left(\vartheta\right),QF_A\left(\vartheta\right)\right)\middle|\vartheta\in\Theta\right\} \tag{1}$$

where $QT_A\left(\vartheta\right),QI_A\left(\vartheta\right),QF_A\left(\vartheta\right)$ depicts truth membership, indeterminacy membership and falsity membership, $QT_A\left(\vartheta\right),QI_A\left(\vartheta\right),QF_A\left(\vartheta\right)\in\left[0,1\right]$, $0\le QT_A\left(\vartheta\right)+QI_A\left(\vartheta\right)+QF_A\left(\vartheta\right)\le 3$.

Definition 2 [23]. The score value function (SVF) of $QA=\left(QT_A,QI_A,QF_A\right)$ is formed:

$$SVF\left(QA\right)=\frac{\left(2+QT_A-QI_A-QF_A\right)}{3},SVF\left(QA\right)\in\left[0,1\right]. \tag{2}$$

Definition 3 [23]. The accuracy value function (AVF) of $QA=\left(QT_A,QI_A,QF_A\right)$ is formed:

$$AVF\left(QA\right)=QT_A-QF_A,\ AVF\left(QA\right)\in\left[-1,1\right]\ . \tag{3}$$

Peng et al. [23] formed the order framework between two SVNNs.

Definition 4[23]. Let $QA=\left(QT_A,QI_A,QF_A\right)$ and $QB=\left(QT_B,QI_B,QF_B\right)$, let $SVF\left(QA\right)=\frac{\left(2+QT_A-QI_A-QF_A\right)}{3}$ and $SVF\left(QB\right)=\frac{\left(2+QT_B-QI_B-QF_B\right)}{3}$, and let $AVF\left(QA\right)=QT_A-QF_A$ and $AVF\left(QB\right)=QT_B-QF_B$, if $SVF\left(QA\right)<SVF\left(QB\right)$, then:

$QA < QB$; if $SVF(QA) = SVF(QB)$, then: (1)if $AVF(QA) = AVF(QB)$, then $QA = QB$; (2) if $AVF(QA) > AVF(QB)$, then: $QA < QB$.

Definition 6 [24]. Let $QA = (QT_A, QI_A, QF_A)$ and $QB = (QT_B, QI_B, QF_B)$, then SVNN cosine similarity measure (SVNNCSM) based on the $QA = (QT_A, QI_A, QF_A)$ and $QB = (QT_B, QI_B, QF_B)$ is formed:

$$SVNNCSM(QA, QB) = \frac{QT_A \times QT_B + QI_A \times QI_B + QF_A \times QF_B}{\left(\begin{array}{l}\sqrt{(QT_A)^2 + (QI_A)^2 + (QF_A)^2} \\ \cdot\sqrt{(QT_B)^2 + (QI_B)^2 + (QF_B)^2}\end{array}\right)},$$

$$SVNNCSM(QA, QB) \in [0,1], \quad (4)$$

Definition 6 [24]. Let $QA = (QT_A, QI_A, QF_A)$ and $QB = (QT_B, QI_B, QF_B)$, then SVNN cosine function similarity measure (SVNNCFSM) based on the $QA = (QT_A, QI_A, QF_A)$ and $QB = (QT_B, QI_B, QF_B)$ is formed:

$$SVNNCFSM(QA, QB) = \frac{1}{2}\left(\begin{array}{l}\cos\left[\frac{\pi}{6}\left(|QT_A - QT_B| + |QI_A - QI_B| + |QF_A - QF_B|\right)\right] \\ +\cos\left[\frac{\pi}{2}\max\left(\left(|QT_A - QT_B|, |QI_A - QI_B|, |QF_A - QF_B|\right)\right)\right]\end{array}\right)$$

$$SVNNCFSM(QA, QB) \in [0,1], \quad (5)$$

Definition 7 [17]. Let $QA = (QT_A, QI_A, QF_A)$ and $QB = (QT_B, QI_B, QF_B)$, the operations laws are formed:

(1) $QA \oplus QB = (QT_A + QT_B - QT_A \cdot QT_B, QI_A \cdot QI_B, QF_A \cdot QF_B)$;

(2) $QA \otimes QB = (QT_A \cdot QT_B, QI_A + QI_B - QI_A \cdot QI_B, QF_A + QF_B - QF_A \cdot QF_B)$;

(3) $\gamma QA = \left(1 - (1 - QT_A)^{\gamma}, (QI_A)^{\gamma}, (QF_A)^{\gamma}\right), \gamma > 0$;

(4) $(QA)^{\gamma} = \left((QT_A)^{\gamma}, (QI_A)^{\gamma}, 1 - (1 - QF_A)^{\gamma}\right), \gamma > 0.$

The SVNNWA & SVNNWG model are formed.

Definition 8 [23]. If $QA_j = (QT_j, QI_j, QF_j)$, the SVNNWA operator is formed:

$$\begin{aligned}&\mathrm{SVNNWA}_{qw}\left(QA_1, QA_2, \cdots, QA_n\right) = \overset{n}{\underset{j=1}{\oplus}}\left(qw_j QA_j\right)\\&= \left(1-\prod_{j=1}^{n}\left(1-QT_j\right)^{qw_j}, \prod_{j=1}^{n}\left(QI_j\right)^{qw_j}, \prod_{j=1}^{n}\left(QF_j\right)^{qw_j}\right)\end{aligned} \tag{6}$$

with weight $qw=\left(qw_1, qw_2, ..., qw_n\right)^T$, $\sum_{j=1}^{n} qw_j = 1.$

Definition 9 [23]. If $QA_j = \left(QT_j, QI_j, QF_j\right)$, the SVNNWG model is formed:

$$\begin{aligned}&\mathrm{SVNNWG}_{qw}\left(QA_1, QA_2, \cdots, QA_n\right) = \overset{n}{\underset{j=1}{\otimes}}\left(QA_j\right)^{qw_j}\\&= \left(\prod_{j=1}^{n}\left(QT_j\right)^{qw_j}, 1-\prod_{j=1}^{n}\left(1-QI_j\right)^{qw_j}, 1-\prod_{j=1}^{n}\left(1-QF_j\right)^{qw_j}\right)\end{aligned} \tag{7}$$

with weight $qw=\left(qw_1, qw_2, ..., qw_n\right)^T$, $\sum_{j=1}^{n} qw_j = 1.$

3. Materials and Methods

Then, the SVNN-EDAS model is formed for MAGDM. Let $QY=\left(QY_1, QY_2, \ldots, QY_m\right)$ have alternatives. Let $QZ = \left(QZ_1, QZ_2, \ldots, QZ_n\right)$ be attributes, $qw=\left\{qw_1, qw_2, \ldots, qw_n\right\}$ be weight for QZ_j, where $qw_j \in [0,1], \sum_{j=1}^{n} qw_j = 1$. Assume DMs $QD=\left\{QD_1, QD_2, \ldots, QD_l\right\}$ with weight $q\omega=\left\{q\omega_1, q\omega_2, \ldots, q\omega_l\right\}$, $q\omega_k \in [0,1]$, $\sum_{k=1}^{l} q\omega_k = 1$. And $QN^{(k)} = \left(QN_{ij}^{(k)}\right)_{m\times n} = \left(QT_{ij}^{(k)}, QI_{ij}^{(k)}, QF_{ij}^{(k)}\right)_{m\times n}$ is called as group SVNN-matrix. The calculating procedures are formed as shown in Figure 3.

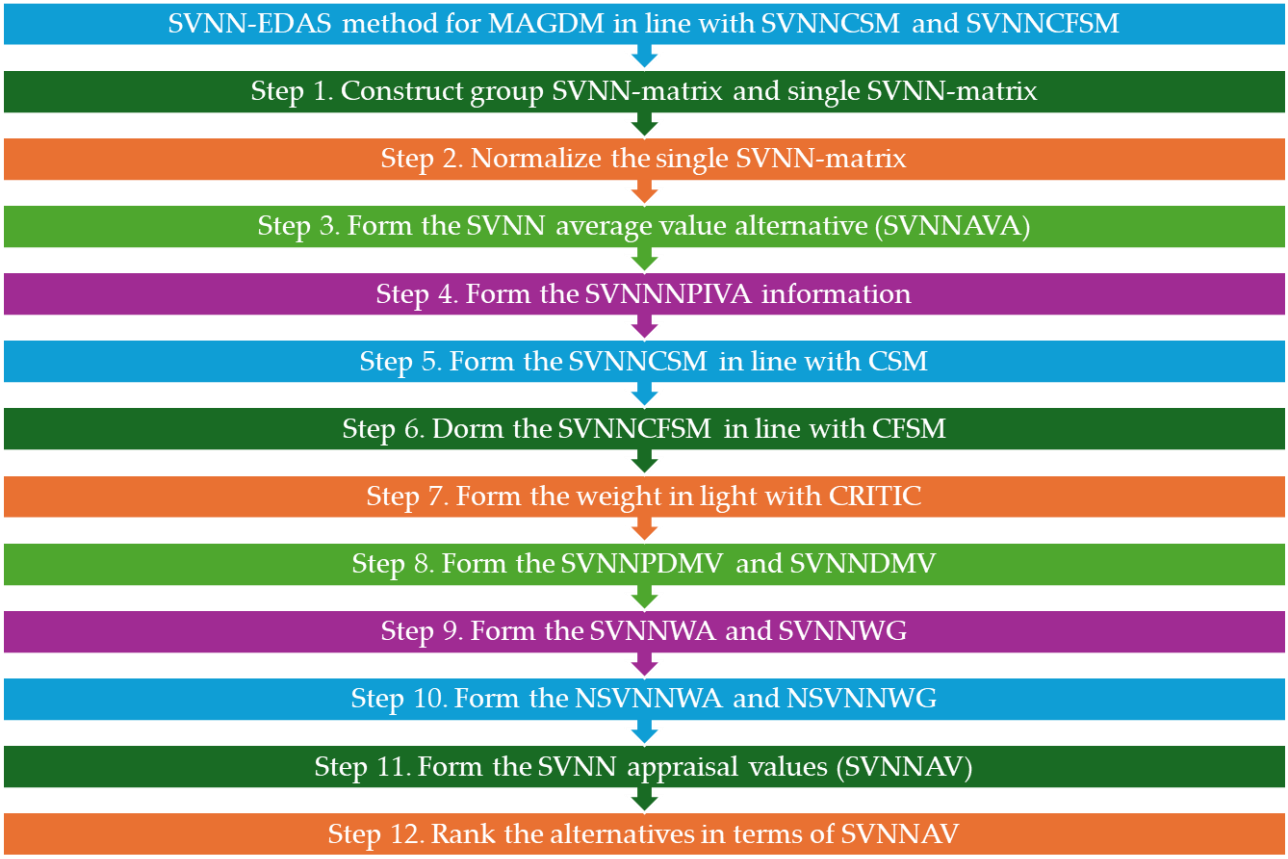

Figure 3. The steps of the proposed model.

Step 1. Form group SVNN-matrix $QN^{(k)}=\left(QN_{ij}^{(k)}\right)_{m\times n}=\left(QT_{ij}^{(k)},QI_{ij}^{(k)},QF_{ij}^{(k)}\right)_{m\times n}$ and single SVNN-matrix $QN=\left(QN_{ij}\right)_{m\times n}$ through SVNNWA technique.

$$QR^{(k)}=\left[QR_{ij}^{(k)}\right]_{m\times n}=\begin{bmatrix} QR_{11}^{(k)} & QR_{12}^{(k)} & \cdots & QR_{1n}^{(k)} \\ QR_{21}^{(k)} & QR_{22}^{(k)} & \cdots & QR_{2n}^{(k)} \\ \vdots & \vdots & \vdots & \vdots \\ QR_{m1}^{(k)} & QR_{m2}^{(k)} & \cdots & QR_{mn}^{(k)} \end{bmatrix} \tag{8}$$

$$QR=\left[QR_{ij}\right]_{m\times n}=\begin{bmatrix} QR_{11} & QR_{12} & \cdots & QR_{1n} \\ QR_{21} & QR_{22} & \cdots & QR_{2n} \\ \vdots & \vdots & \vdots & \vdots \\ QR_{m1} & QR_{m2} & \cdots & QR_{mn} \end{bmatrix} \tag{9}$$

$$QR_{ij}=\left(QT_{ij},QI_{ij},QF_{ij}\right)=\left(1-\prod_{k=1}^{l}\left(1-QT_{ij}^{(k)}\right)^{q\omega_k},\prod_{k=1}^{l}\left(QI_{ij}^{(k)}\right)^{q\omega_k},\prod_{k=1}^{l}\left(QF_{ij}^{(k)}\right)^{q\omega_k}\right) \tag{10}$$

Step 2. Form normalized $QR^N = \left[QR_{ij}^N \right]_{m\times n}$ in line with $QR = \left[QR_{ij} \right]_{m\times n}$

$$QR_{ij}^N = \left(QT_{ij}^N, QI_{ij}^N, QF_{ij}^N \right) = \begin{cases} \left(QT_{ij}, QI_{ij}, QF_{ij} \right), & QZ_j \text{ is a benefit attribute} \\ \left(QF_{ij}, QI_{ij}, QT_{ij} \right), & QZ_j \text{ is a cost attribute} \end{cases} \tag{11}$$

Step 3. Form the SVNNAVA (SVNN average value alternative).

$$SVNNAVA = \left[SVNNAVA_j \right]_{1\times n} = \left[\frac{\overset{m}{\underset{i=1}{\oplus}} QR_{ij}^N}{m} \right]_{1\times n} \tag{12}$$

$$\left[SVNNAVA_j \right]_{1\times n} = \left(1 - \prod_{i=1}^{m} \left(1 - QR_{ij}^N \right)^{\frac{1}{m}}, \prod_{i=1}^{m} \left(QI_{ij}^N \right)^{\frac{1}{m}}, \prod_{i=1}^{m} \left(QF_{ij}^N \right)^{\frac{1}{m}} \right)_{1\times n} \tag{13}$$

Step 4. Form the SVNNNPIVA (SVNN positive ideal value alternative):

$$SVNNPIVA_j = \left(QT_j^{N+}, QI_j^{N+}, QF_j^{N+} \right) \tag{14}$$

$$SVF\left(SVNNPIVA_j \right) = \max_i SVF\left(QR_{ij}^N \right) \tag{15}$$

Step 5. Form the SVNNCSM information between $QR_{ij}^N = \left(QT_{ij}^N, QI_{ij}^N, QF_{ij}^N \right)$ and $SVNNPIVA_j = \left(QT_j^{N+}, QI_j^{N+}, QF_j^{N+} \right)$.

$$SVNNCSM\left(QR_{ij}^N, SVNNPIVA_j \right) = \frac{QT_{ij}^N \times QT_j^{N+} + QI_{ij}^N \times QI_j^{N+} + QF_{ij}^N \times QF_j^{N+}}{\sqrt{\left(QT_{ij}^N \right)^2 + \left(QI_{ij}^N \right)^2 + \left(QF_{ij}^N \right)^2} \cdot \sqrt{\left(QT_j^{N+} \right)^2 + \left(QI_j^{N+} \right)^2 + \left(QF_j^{N+} \right)^2}} \tag{16}$$

Step 6. Form the SVNNCFSM information between $QR_{ij}^N = \left(QT_{ij}^N, QI_{ij}^N, QF_{ij}^N \right)$ and $SVNNPIVA_j = \left(QT_j^{N+}, QI_j^{N+}, QF_j^{N+} \right)$.

$$SVNNCFSM\left(QR_{ij}^N, SVNNPIVA_j \right) = \frac{1}{2}\left(\begin{array}{l} \cos\left[\frac{\pi}{6}\left(\left| QT_{ij}^N - QT_j^{N+} \right| + \left| QI_{ij}^N - QI_j^{N+} \right| + \left| QF_{ij}^N - QF_j^{N+} \right| \right) \right] \\ + \cos\left[\frac{\pi}{2} \max\left(\left(\left| QT_{ij}^N - QT_j^{N+} \right|, \left| QI_{ij}^N - QI_j^{N+} \right|, \left| QF_{ij}^N - QF_j^{N+} \right| \right) \right) \right] \end{array} \right) \tag{17}$$

Step 7. Form the weight numbers in line with CRITIC.

The CRITIC model [25] is formed for weights values.

(1) The SVNNCCV (SVNN correlation coefficient values) are formed.

$$SVNNCCV_{jt}=\frac{\sum_{i=1}^{m}\left(\varphi\left(CSM_{ij}\right)-\varphi\left(CSM_{j}\right)\right)\times\left(\varphi\left(CSM_{it}\right)-\varphi\left(CSM_{t}\right)\right)}{\sqrt{\sum_{i=1}^{m}\left(\varphi\left(CSM_{ij}\right)-\varphi\left(CSM_{j}\right)\right)^{2}}\times\sqrt{\sum_{i=1}^{m}\left(\varphi\left(CSM_{it}\right)-\varphi\left(CSM_{t}\right)\right)^{2}}}, \tag{18}$$

where

$$\varphi\left(CSM_{j}\right)=\frac{1}{2m}\sum_{i=1}^{m}\left(\begin{array}{l}SVNNCSM\left(QR_{ij}^{N},SVNNPIVA_{j}\right)\\+SVNNCFSM\left(QR_{ij}^{N},SVNNPIVA_{j}\right)\end{array}\right),$$

$$\varphi\left(CSM_{t}\right)=\frac{1}{2m}\sum_{i=1}^{m}\left(\begin{array}{l}SVNNCSM\left(QR_{it}^{N},SVNNPIVA_{t}\right)\\+SVNNCFSM\left(QR_{it}^{N},SVNNPIVA_{t}\right)\end{array}\right),$$

$$\varphi\left(CSM_{ij}\right)=\frac{1}{2}\left(\begin{array}{l}SVNNCSM\left(QR_{ij}^{N},SVNNPIVA_{j}\right)\\+SVNNCFSM\left(QR_{ij}^{N},SVNNPIVA_{j}\right)\end{array}\right),$$

$$\varphi\left(CSM_{it}\right)=\frac{1}{2}\left(\begin{array}{l}SVNNCSM\left(QR_{it}^{N},SVNNPIVA_{t}\right)\\+SVNNCFSM\left(QR_{it}^{N},SVNNPIVA_{t}\right)\end{array}\right)$$

(2) Form the SVNNSDV (SVNN standard deviation values).

$$SVNNSDV_{j}=\sqrt{\frac{1}{m-1}\sum_{i=1}^{m}\left(\varphi\left(CSM_{ij}\right)-\varphi\left(CSM_{j}\right)\right)^{2}} \tag{19}$$

(3) Form attribute weight numbers.

$$qw_{j}=\frac{SVNNSDV_{j}\sum_{t=1}^{n}\left(1-SVNNCCV_{jt}\right)}{\sum_{j=1}^{n}\left(SVNNSDV_{j}\sum_{t=1}^{n}\left(1-SVNNCCV_{jt}\right)\right)} \tag{20}$$

Step 8. Form the SVNN positive distance measure values from SVNNAVA (SVNNPDMV) and SVNN negative distance measures values from SVNNAVA (SVNNNDMV):

For the positive attributes:

$$SVNNPDMV_{ij} = \frac{1}{2}\left(\begin{array}{l} \dfrac{\max\left(0, SVNNCSM\left(QR_{ij}^{N}, SVNNPIVA_j\right) - SVNNCSM\left(SVNNAVA_j, SVNNPIVA_j\right)\right)}{SVNNCSM\left(SVNNAVA_j, SVNNPIVA_j\right)} \\ + \dfrac{\max\left(0, SVNNCFSM\left(QR_{ij}^{N}, SVNNPIVA_j\right) - SVNNCFSM\left(SVNNAVA_j, SVNNPIVA_j\right)\right)}{SVNNCFSM\left(SVNNAVA_j, SVNNPIVA_j\right)} \end{array} \right) \tag{21}$$

$$SVNNNDMV_{ij} = \frac{1}{2}\left(\begin{array}{l} \dfrac{\max\left(0, SVNNCSM\left(SVNNAVA_j, SVNNPIVA_j\right) - SVNNCSM\left(QR_{ij}^{N}, SVNNPIVA_j\right)\right)}{SVNNCSM\left(SVNNAVA_j, SVNNPIVA_j\right)} \\ + \dfrac{\max\left(0, SVNNCFSM\left(SVNNAVA_j, SVNNPIVA_j\right) - SVNNCFSM\left(QR_{ij}^{N}, SVNNPIVA_j\right)\right)}{SVNNCFSM\left(SVNNAVA_j, SVNNPIVA_j\right)} \end{array} \right) \tag{22}$$

For the negative attributes:

$$SVNNPDMV_{ij} = \frac{1}{2}\left(\begin{array}{l} \dfrac{\max\left(0, SVNNCSM\left(SVNNAVA_j, SVNNPIVA_j\right) - SVNNCSM\left(QR_{ij}^{N}, SVNNPIVA_j\right)\right)}{SVNNCSM\left(SVNNAVA_j, SVNNPIVA_j\right)} \\ + \dfrac{\max\left(0, SVNNCFSM\left(SVNNAVA_j, SVNNPIVA_j\right) - SVNNCFSM\left(QR_{ij}^{N}, SVNNPIVA_j\right)\right)}{SVNNCFSM\left(SVNNAVA_j, SVNNPIVA_j\right)} \end{array} \right) \tag{23}$$

$$SVNNNDMV_{ij} = \frac{1}{2}\left(\begin{array}{l} \dfrac{\max\left(0, SVNNCSM\left(QR_{ij}^{N}, SVNNPIVA_j\right) - SVNNCSM\left(SVNNAVA_j, SVNNPIVA_j\right)\right)}{SVNNCSM\left(SVNNAVA_j, SVNNPIVA_j\right)} \\ + \dfrac{\max\left(0, SVNNCFSM\left(QR_{ij}^{N}, SVNNPIVA_j\right) - SVNNCFSM\left(SVNNAVA_j, SVNNPIVA_j\right)\right)}{SVNNCFSM\left(SVNNAVA_j, SVNNPIVA_j\right)} \end{array} \right) \tag{24}$$

Step 9. Form the SVNN weighted averaging values (SVNNWAV) and SVNN weighted geometric values (SVNNWGV).

$$SVNNWAV_i = \sum_{j=1}^{n} qw_j \cdot SVNNPDMV_{ij}, \tag{25}$$

$$SVNNWGV_i = \sum_{j=1}^{n} qw_j \cdot SVNNNDMV_{ij}\,, \tag{26}$$

Step 10. Form the $NSVNNWAV_i$ and $NSVNNWGV_i$ in line with normalized $SVNNWAV_i$ and $SVNNWGV_i$:

$$NSVNNWAV_i = \frac{SVNNWAV_i}{\max\limits_i\left(SVNNWAV_i\right)}, \tag{27}$$

$$NSVNNWGV_i = 1 - \frac{SVNNWGV_i}{\max\limits_i\left(SVNNWGV_i\right)}, \tag{28}$$

Step 11. Form the SVNNAV (SVNN appraisal values).

$$SVNNAV_i = \frac{1}{2}\left(NSVNNWAV_i + NSVNNWGV_i\right) \tag{29}$$

Step 12. In light with the information of SVNNAV, the larger SVNNAV information, the better one is.

4. Results and Discussions

In this section, we will share the results we've gathered and provide a detailed discussion of their meaning. Our goal is to emphasize the importance of these findings and explore their implications in relation to the broader objectives of our study.

4.1 Problem Definitions

This part defines the criteria and alternatives used in this study. Figure 4 shows the criteria and alternatives.

In this work, the landscape planning and design quality evaluation is formed through SVNN-EDAS technique. Five landscape planning and design schemes $A = A_1, A_2, \ldots, A_m$ which are evaluated through five experts with equal weight values in light with four attributes:

Functionality (C_1): The design should meet the needs of users by providing a well-organized functional layout and smooth circulation. Different areas, such as relaxation zones, activity areas, and viewing spaces, should be clearly distinguished, while ensuring easy connectivity between these zones for user convenience. Additionally, considerations like accessibility and site safety are essential.

Aesthetic Appeal (C_2): The landscape design needs to be visually attractive, with a harmonious overall layout, rich spatial layering, and well-coordinated landscape elements. The integration of hardscape and softscape should be unified and orderly, creating an artistic visual experience. Factors such as color, texture, plant morphology, and seasonal changes should also be considered to ensure that the landscape remains appealing throughout the year.

Ecology and Sustainability (C_3): The design should prioritize ecological protection and restoration, making efficient use of natural resources to minimize environmental impacts.

Plant selection should be suited to the local climate and soil conditions, enhancing biodiversity. Additionally, effective water management and energy conservation should be incorporated to achieve sustainable development goals.

Feasibility of Construction and Maintenance (C_4): The design should be practical and achievable during construction, avoiding overly complex or difficult-to-execute concepts. The convenience of future maintenance should also be fully considered, ensuring that the landscape can maintain its visual appeal and functionality over time while minimizing maintenance costs and effort. Then, the SVNN-EDAS model is formed to achieve the optimal landscape planning and design scheme.

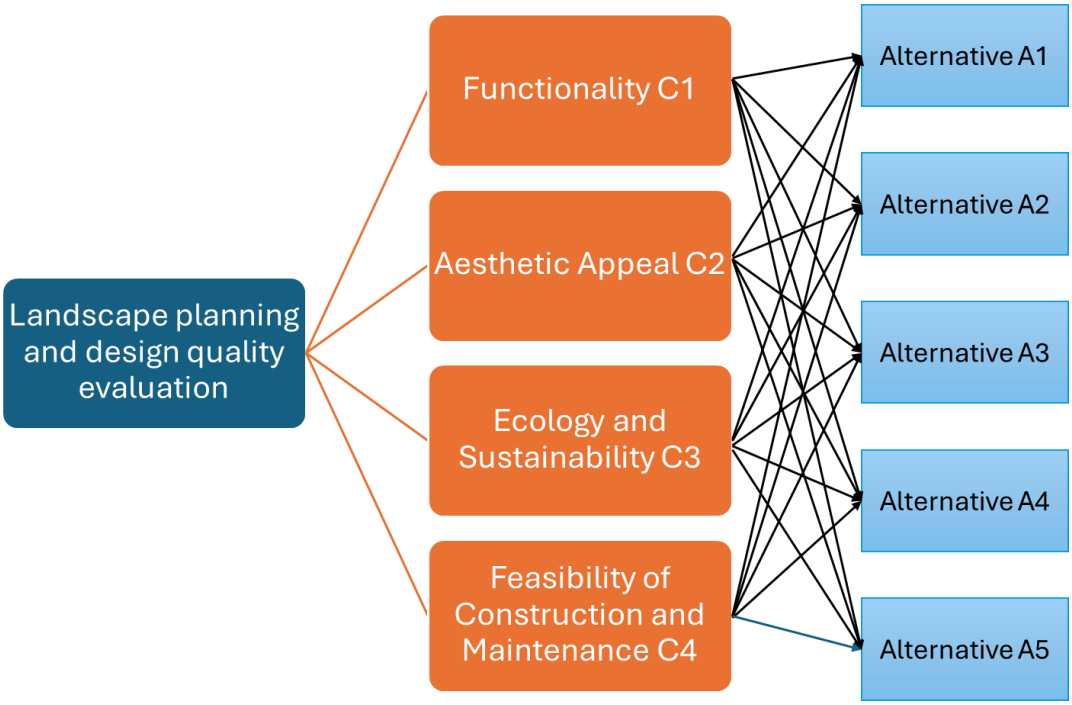

Figure 4. The criteria and alternatives.

The quality evaluation of landscape planning and design is a systematic and comprehensive analysis and assessment of the design scheme of a landscape project. Its aim is to ensure that the project meets expectations in terms of aesthetics, functionality, ecology, and sustainability. First and foremost, the core of the evaluation lies in the rationality of spatial layout, assessing whether the design effectively utilizes land resources to create a clearly defined functional zoning, fluid circulation, and appropriately scaled spatial structure.

In addition, the landscape design should harmonize with the surrounding natural environment, ensuring a balanced overall visual effect and ecological system. This includes careful consideration of factors such as topography, climate, and vegetation. Plant arrangement is another key aspect of

the evaluation. The selection, combination, and layout of plant species should follow ecological principles, not only providing a pleasing landscape effect but also enhancing the ecological functions of the site, such as improving air quality and regulating the microclimate. Meanwhile, the integration of hardscape (such as paving and architectural elements) with softscape (such as vegetation and water features) should be harmonious and unified, reflecting both aesthetic appeal and practicality. Beyond visual and ecological considerations, landscape design must also pay attention to human-centered concerns.

This means evaluating whether the design sufficiently meets the needs of users by providing a comfortable, safe, and convenient experience. Considerations include aspects such as barrier-free design, site safety, and the accessibility of facilities. Economic efficiency and construction feasibility are also critical factors in the evaluation. The design scheme should not only adhere to the budget and ensure the rational use of resources, but also account for the technical challenges and cost control during the construction process. Furthermore, the ease of future maintenance and management must be included in the assessment.

The design should feature sustainability and ease of maintenance, ensuring that the project can maintain its landscape effects and functional performance over its lifecycle. Through this multidimensional evaluation, landscape planning and design can achieve a comprehensive balance and optimization in terms of aesthetics, functionality, ecology, and economics, ultimately creating high-quality landscape spaces that promote harmonious coexistence between humans and nature.

Table 1. Linguistic scale and SVNNs

Linguistic terms	**SVNNs**
Very High	(0.0,1.0,1.0)
High	(0.10,0.90,0.90)
Medium High	(0.30,0.70,0.70)
Medium	(0.50,0.50,0.50)
Medium Low	(0.70,0.30,0.30)
Low	(0.90,0.10,0.10)
Very Low	(1.00,0.00,0.00)

Table 2. The combined decision matrix

	C_1	**C_2**	**C_3**	**C_4**
A_1	(0.67, 0.31, 0.35)	(0.27, 0.46, 0.62)	(0.56, 0.38, 0.49)	(0.28, 0.24, 0.32)
A_2	(0.54, 0.39, 0.46)	(0.43, 0.36, 0.34)	(0.26, 0.37, 0.26)	(0.54, 0.43, 0.38)
A_3	(0.48, 0.37, 0.51)	(0.54, 0.49, 0.48)	(0.52, 0.33, 0.49)	(0.45, 0.18, 0.29)
A_4	(0.54, 0.29, 0.38)	(0.62, 0.25, 0.36)	(0.64, 0.45, 0.32)	(0.53, 0.29, 0.18)
A_5	(0.46, 0.32, 0.43)	(0.41, 0.28, 0.32)	(0.48, 0.46, 0.33)	(0.45, 0.49, 0.36)

Results

Step 1. Create the decision matrix with opinions of three experts and decision makers. These experts use the linguistic terms as shown in Table 1 to evaluate the criteria and alternatives. Then we combined it as shown in Table 2.

Step 2. Normalize the decision matrix as shown in Table 3.

Table 3. The standardized SVNN-matrix

	C₁	**C₂**	**C₃**	**C₄**
A_1	(0.67, 0.31, 0.35)	(0.27, 0.46, 0.62)	(0.56, 0.38, 0.49)	(0.28, 0.24, 0.32)
A_2	(0.54, 0.39, 0.46)	(0.43, 0.36, 0.34)	(0.26, 0.37, 0.26)	(0.54, 0.43, 0.38)
A_3	(0.48, 0.37, 0.51)	(0.54, 0.49, 0.48)	(0.52, 0.33, 0.49)	(0.45, 0.18, 0.29)
A_4	(0.54, 0.29, 0.38)	(0.62, 0.25, 0.36)	(0.64, 0.45, 0.32)	(0.53, 0.29, 0.18)
A_5	(0.46, 0.32, 0.43)	(0.41, 0.28, 0.32)	(0.48, 0.46, 0.33)	(0.45, 0.49, 0.36)

Step 3. Calculate the SVNNAVA as shown in Table 4.

Table 4. The SVNNAVA

	SVNNAVA	SVNNNPIVA
C_1	(0.28, 0.19, 0.24)	(0.67, 0.31, 0.35)
C_2	(0.31, 0.15, 0.26)	(0.62, 0.25, 0.36)
C_3	(0.23, 0.12, 0.31)	(0.64, 0.45, 0.32)
C_4	(0.27, 0.24, 0.16)	(0.38, 0.43, 0.54)

Step 4. Define the SVNNNPIVA

Step 5. Obtain the values of single-valued neutrosophic number cosine similarity measure as shown in Table 5.

Table 5. The single-valued neutrosophic number cosine similarity measure.

Alternatives	**C₁**	**C₂**	**C₃**	**C₄**	**Alternatives**	**C₁**	**C₂**	**C₃**	**C₄**
A_1	1.0000	0.5827	0.6008	0.6698	A_1	1.0000	0.6388	0.6586	0.7344
A_2	0.8326	0.8063	0.8020	1.0000	A_2	0.9128	0.8840	0.8792	1.0000
A_3	0.7043	0.7286	0.5789	0.4344	A_3	0.7722	0.7988	0.6347	0.4762
A_4	0.8721	1.0000	1.0000	0.7840	A_4	0.9561	1.0000	1.0000	0.8596
A_5	0.5926	0.5501	0.8240	0.7634	A_5	0.6497	0.6030	0.9034	0.8369

Step 6. Compute the SVNN cosine function similarity measure.

Step 7. Form the weights numbers in light with CRITIC as shown in Figure 5.

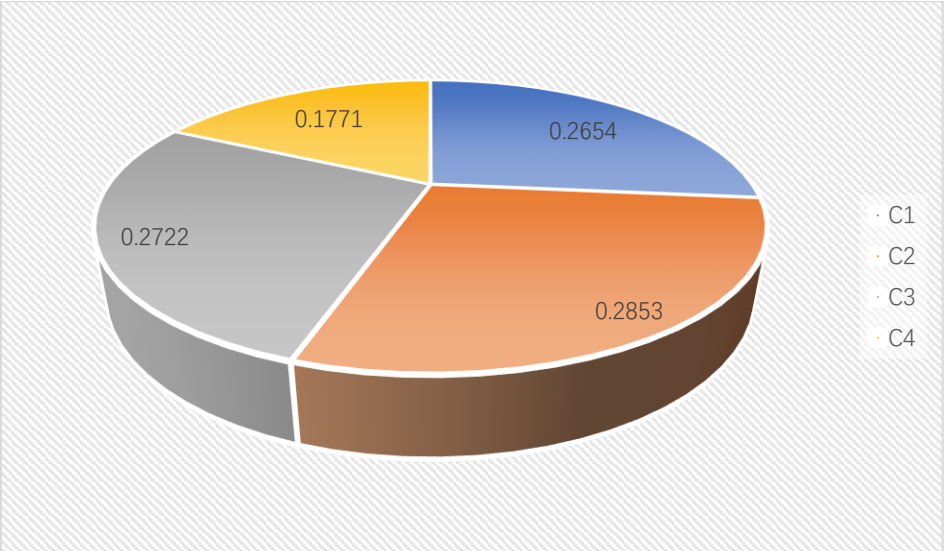

Figure 5. The criteria weight numbers.

Step 8. Form the SVNNPDMV and SVNNNDMV as shown in Table 6.

Table 6. The SVNNPDMV and SVNNNDMV.

	C_1	C_2	C_3	C_4		C_1	C_2	C_3	C_4
A_1	0.1708	0.0000	0.0000	0.0000	A_1	0.0000	0.1485	0.1585	0.0538
A_2	0.0434	0.0859	0.0524	0.2441	A_2	0.0000	0.0000	0.0000	0.0000
A_3	0.0000	0.0045	0.0000	0.0000	A_3	0.0910	0.0000	0.1813	0.3006
A_4	0.0848	0.2408	0.2118	0.0659	A_4	0.0000	0.0000	0.0000	0.0000
A_5	0.0000	0.0000	0.0755	0.0443	A_5	0.2080	0.1827	0.0000	0.0000

Step 9-11. Form the SVNNWAV information, SVNNWGV information and Form the SVNNA as shown in Figure 6

Step 12. Rank the alternatives as shown in Figure 7.

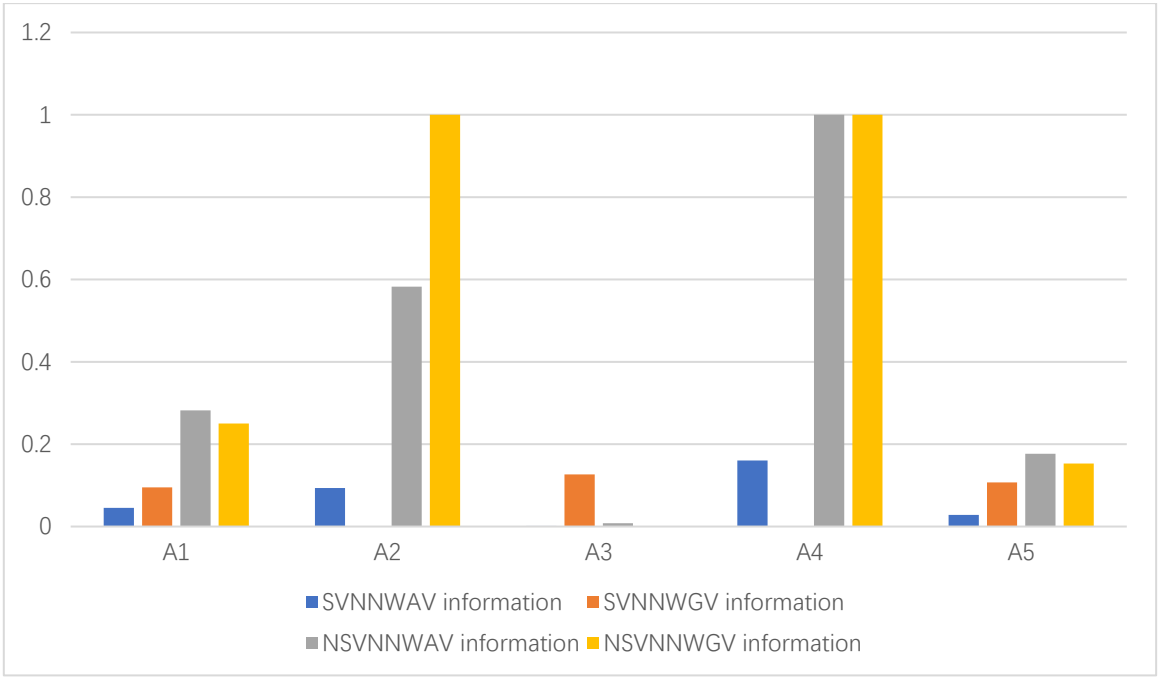

Figure 6. The values of NSVNNWAV information & NSVNNWGV information.

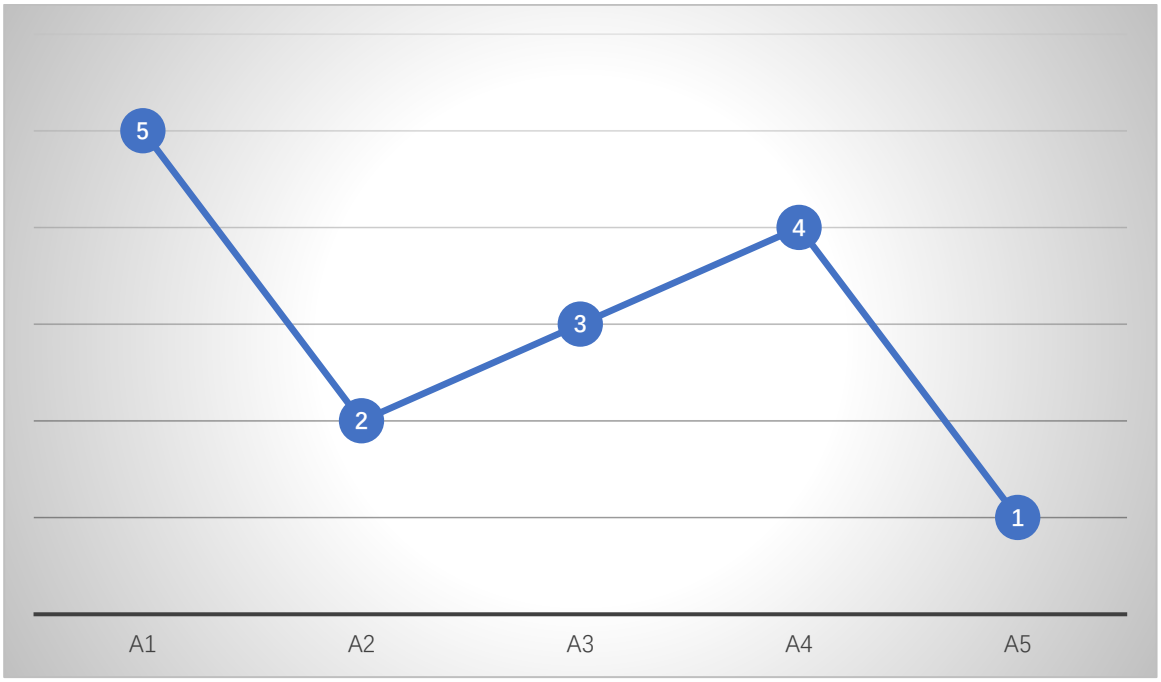

Figure 7. The rank of alternatives.

4.2. Comparative analysis

The formed SVNN-EDAS model is always compared with SVNNWA model [23], SVNNWG model [23], SVNN-WASPAS model [26], SVNN-TODIM technique [27], SVNN-TOPSIS technique [28] and SVNN-CODAS technique [29]. The sufficient comparative results are shown in Figure 8.

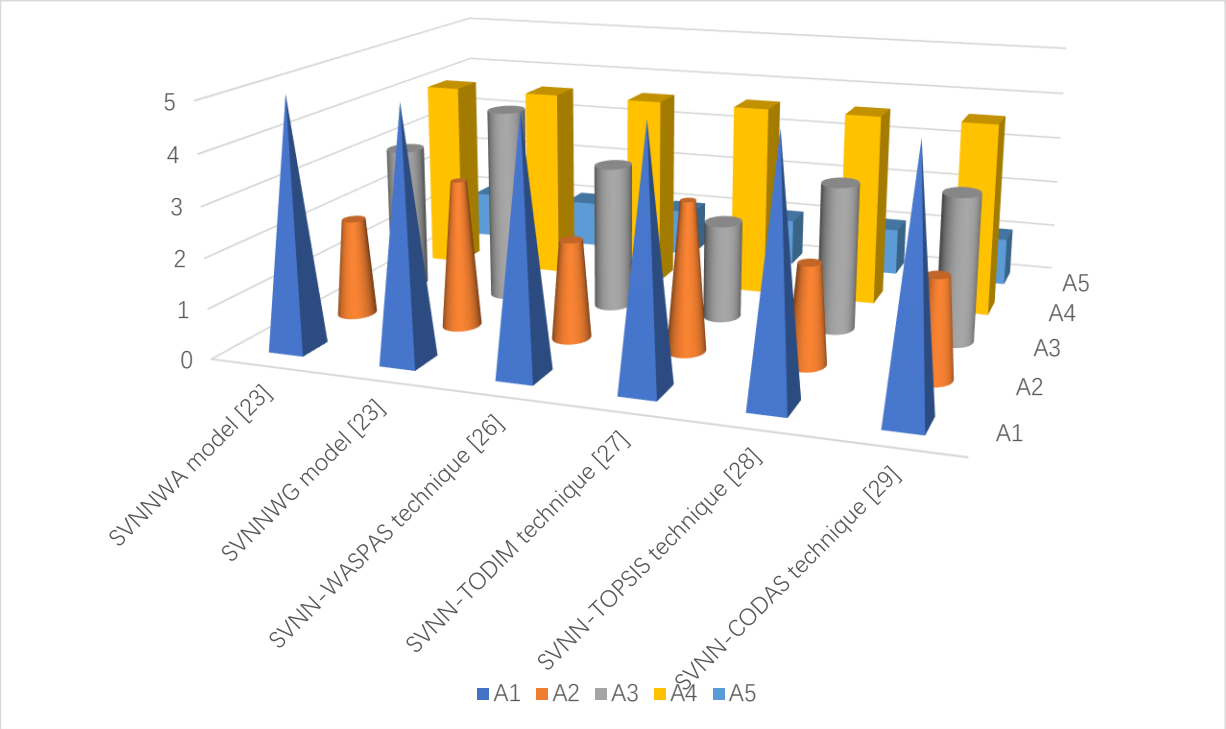

Figure 8. Comparative analysis results.

The similarity coefficients between SVNNWA model [23], SVNNWG model [23], SVNNIGWHM operator [30], SVNNIGWGHM operator [30], SVNN-WASPAS model [26], SVNN-TODIM model [27], SVNN-TOPSIS model [28], SVNN-VIKOR model [31], SVNN-CODAS model [29] and SVNN-EDAS model was obtained in light with WS coefficients [32, 33], the derived results are formed in Figure 9.

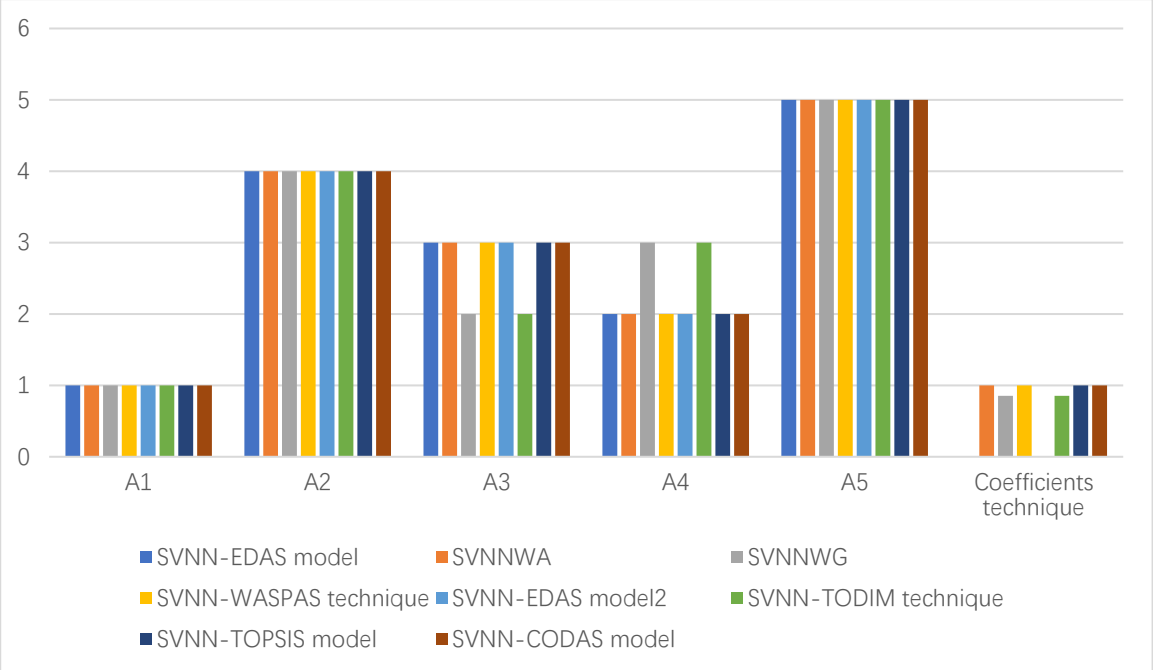

Figure 9. The WS coefficient.

The WS coefficient information corroborates the order of SVNN-EDAS model is same to the order of SVNNWA operator [23], SVNN-WASPAS model [26], SVNN-TOPSIS model [28] and SVNN-CODAS model [29]; the WS coefficient information corroborates the order of SVNN-EDAS model is slightly different from the order of SVNNWG model [23] and SVNN-TODIM model [27]. This verifies the SVNN-EDAS model is effective. Thus, the main advantages of SVNN-EDAS model are formed: (1) the formed SVNN-EDAS not only corroborated the uncertainty for MAGDM, but also portrays the average distance from the SVNNAVA during the landscape planning and design quality evaluation. (2) the formed SVNN-EDAS conducted different behavior of SVNNCSM and SVNNCFSM model as MAGDM when these models are combined. At the same time, the main difference between existing SVNN-EDAS model[34] and the formed SVNN-EDAS model are constructed: (1) The CRITIC model of existing SVNN-EDAS model[34] is constructed based on Euclid distance and CSM, while the CRITIC model of formed SVNN-EDAS model is constructed in light with SVNNCSM and SVNNCFSM; (2) the existing SVNN-EDAS model[34] is constructed based on Euclid distance and CSM, while the formed SVNN-EDAS model is constructed in light with SVNNCSM and SVNNCFSM.

4.3 Managerial Implications

There are various managerial implantations on landscape planning and design evaluation to change the design goals into actionable outcomes to obtain the economic and ecological outcomes.

I. Managers need to ensure the landscape design projects align with the strategic aims of

sustainability and ecological results.

II. Managers can easily make many decisions to gather various data from different stakeholders like governments, organizations and environmental firms.

III. Managers must keep the efficient use of resources to reduce the landscape negative impacts.

IV. Managers can evaluate landscape design compared with other quality standards to keep their design competitive in markets.

5. Conclusion

The quality evaluation of landscape planning and design is a comprehensive analysis and assessment of landscape project designs to ensure functionality, aesthetics, ecology, and sustainability. The evaluation includes the rationality of spatial layout, the harmony between landscape design and the natural environment, the scientific arrangement of plants, and the organic integration of hard and soft landscapes. It also considers whether the design provides a comfortable experience and meets diverse user needs. In addition to visual effects, the effectiveness of ecological protection and resource utilization are important evaluation criteria. Furthermore, the project's cost-efficiency, construction feasibility, and ease of future maintenance are key factors. Through this evaluation, the design ensures that the project meets its objectives while maintaining good long-term landscape effects and functionality, promoting harmonious coexistence between humans and nature. The landscape planning and design quality evaluation is MAGDM. In this paper, the SVNN-EDAS model based on SVNNCSM and SVNNCFSM is formed to cope with the MAGDM. The CRITIC is administrated to obtain the weight numbers in light with the SVNNHD and SVNNCSM under SVNSs. Finally, numerical examples for landscape planning and design quality evaluation and comparative analysis are administrated to validate SVNN-EDAS model.

References

[1] H.W. Wang, Discussion on the regional characteristics in landscape architecture planning and design, China Residential Facilities, (2009) 24-25.

[2] D. Hu, Y. Wang, W.F. Zhu, The concept and response strategy of landscape architecture planning for the shanghai world expo, Garden, (2009) 16-21.

[3] Z.G. Liu, Returning to "experience" - exploration of landscape architecture planning and design concepts, Agricultural Science and Information (Modern Garden), (2010) 16-17.

[4] J.S. Li, W.Y. Zhu, L.J. Wu, Discussion on the development trend of modern landscape architecture planning and design, Chinese Folk Dwellings, (2011) 10-11.

[5] F. Liu, Discussion on principles of landscape architecture planning and design for residential areas, Modern

Horticulture, (2012) 119-121.

[6] L.H. Cai, The conceptual genealogy and flowchart of digital landscape planning and design, Landscape Architecture, (2013) 48-57.

[7] F. Yue, F. Dai, X.F. Jia, Application of gis in china's landscape architecture planning and design: A research progress review, Landscape Architecture, (2014) 47-52.

[8] M.S. Zhan, New thoughts on landscape architecture planning and design theory in the digital age, Shanxi Architecture, 41 (2015) 215-216.

[9] X. Wang, Research on the role of rural landscape in landscape architecture planning and design, Agriculture & Technology, 36 (2016) 198-198.

[10] C.J. Li, Exploration of digital strategies in landscape architecture planning and design, Modern Horticulture, (2017) 111-112.

[11] D.J. Zhu, K. Li, Research on parametric design of landscape architecture buildings, Forestry Science and Technology Information, 50 (2018) 105-107.

[12] G.R. Han, J. Wang, X.Y. Liu, Research on the application value of virtual reality technology in landscape architecture planning and design, Urban Housing, 27 (2020) 123-124.

[13] Y.W. Xue, Research on the role of humanized design in urban landscape planning, Construction Science and Technology, (2021) 74-77.

[14] J. Li, J.M. Wu, W.Q. Wang, Landscape architecture planning and design strategies under the goal of carbon neutrality, Landscape Architecture, 29 (2022) 45-51.

[15] M. Liu, Trends in landscape architecture planning and design under the guidance of sponge city concept, Smart City, 9 (2023) 33-35.

[16] J.J. Li, Y.F. Ding, Application of big data algorithms in landscape architecture planning and design, Ju Ye, (2024) 142-144.

[17] H. Wang, F. Smarandache, Y.Q. Zhang, R. Sunderraman, Single valued neutrosophic sets, Multispace Multistruct, (2010) 410-413.

[18] K. Karunanithi, C. Han, C.J. Lee, W.C. Shi, L. Duan, Y. Qian, Identification of a hemodynamic parameter for assessing treatment outcome of edas in moyamoya disease, Journal of Biomechanics, 48 (2015) 304-309.

[19] M. Keshavarz Ghorabaee, E.K. Zavadskas, L. Olfat, Z. Turskis, Multi-criteria inventory classification using a new method of evaluation based on distance from average solution (edas), Informatica, 26 (2015) 435-451.

[20] R. Mallick, S. Pramanik, B.C. Giri, Neutrosophic magdm based on critic-edas strategy using geometric aggregation operator, Yugoslav Journal of Operations Research, (2023) http://dx.doi.org/10.2298/YJOR221017016M.

[21] R. Mallick, S. Pramanik, Trnn- edas strategy for madm with entropy weight under trapezoidal neutrosophic number environment, in: F. Smarandache, M. Abdel-Basset (Eds.) Neutrosophic operational research: Methods and applications, Springer International Publishing, Cham, 2021, pp. 575-592.

[22] J. Ye, Similarity measures of intuitionistic fuzzy sets based on cosine function for the decision making of mechanical design schemes, Journal of Intelligent & Fuzzy Systems, 30 (2016) 151-158.

[23] J.J. Peng, J.Q. Wang, J. Wang, H.Y. Zhang, X.H. Chen, Simplified neutrosophic sets and their applications in multi-criteria group decision-making problems, International Journal of Systems Science, 47 (2016) 2342-2358.

[24] J. Ye, Improved cosine similarity measures of simplified neutrosophic sets for medical diagnoses, Artificial Intelligence in Medicine, 63 (2015) 171-179.

[25] D. Diakoulaki, G. Mavrotas, L. Papayannakis, Determining objective weights in multiple criteria problems: The critic method, Computers & Operations Research, 22 (1995) 763-770.

[26] E.K. Zavadskas, R. Bausys, D. Stanujkic, M. Magdalinovic-Kalinovic, Selection of lead-zinc flotation circuit design by applying waspas method with single-valued neutrosophic set, Acta Montanistica Slovaca, 21 (2016) 85-92.

[27] D.S. Xu, C. Wei, G.W. Wei, Todim method for single-valued neutrosophic multiple attribute decision making, Information, 8 (2017) 125.

[28] P. Biswas, S. Pramanik, B.C. Giri, Neutrosophic topsis with group decision making, in: C. Kahraman, İ. Otay (Eds.) Fuzzy multi-criteria decision-making using neutrosophic sets, Springer International Publishing, Cham, 2019, pp. 543-585.

[29] E. Bolturk, A. Karasan, Prioritization of investment alternatives for a hospital by using neutrosophic codas method, Journal of Multiple-Valued Logic and Soft Computing, 33 (2019) 381-396.

[30] Y.H. Li, P.D. Liu, Y.B. Chen, Some single valued neutrosophic number heronian mean operators and their application in multiple attribute group decision making, Informatica, 27 (2016) 85-110.

[31] H. Eroglu, R. Sahin, A neutrosophic vikor method-based decision-making with an improved distance measure and score function: Case study of selection for renewable energy alternatives, Cognitive Computation, 12 (2020) 1338-1355.

[32] W. Salabun, K. Urbaniak, A new coefficient of rankings similarity in decision-making problems, in: 20th Annual International Conference on Computational Science (ICCS), Springer International Publishing Ag, Amsterdam, NETHERLANDS, 2020, pp. 632-645.

[33] W. Sałabun, J. Wątróbski, A. Shekhovtsov, Are mcda methods benchmarkable? A comparative study of topsis, vikor, copras, and promethee ii methods, Symmetry, 12 (2020) 1549.

[34] Y. Yuan, Enhanced edas technique for colleges business english teaching quality evaluation based on euclid distance and cosine similarity measure, Journal of Intelligent & Fuzzy Systems, 46 (2024) 75-89.

Received: July 222, 2024. Accepted: Oct 23, 2024

NSS
Neutrosophic Sets and Systems, Vol. 76, 2025
University of New Mexico

Incorporating Neutrosophic Uncertainty in Data Envelopment Analysis

A.Almutairi[1], Hamiden Abd El- Wahed Khalifa[2*] and Basma E. El- Demerdash[2]
[1]Department of Mathematics, College of Science , Qassim University, Buraydah 51452, Saudi Arabia, Almutairi2017@qu.edu.sa
[2]Department of Operations and Management Research, Faculty of Graduate Studies for Statistical Research, Cairo University, Giza 12613, Egypt basma.ezzat@cu.edu.eg/ hamiden@cu.edu.eg

* Correspondence: hamiden@cu.edu.eg

Abstract. In the realm of Data Envelopment Analysis (DEA), the assessment of relative efficiency has historically relied on deterministic variables. Yet, real-world data often presents diverse uncertainties, including a neutrosophic nature, which can significantly impact the accuracy and reliability of DEA outcomes. Therefore, the current paper proposes a new DEA model entirely to address this issue and in new DEA model designed to address this issue, preexisting approaches that fall short due to the inability to address neutrosophic uncertainty, which can be commonly found in actual data, to enhance efficiency evaluation precision. This paper introduces the new DEA model to show the potential to deal with the neutrosophic uncertainty in the input and output to decide whether the certain variable is deterministic or neutrosophic. In addition, they assure the flexibility of the model regarding the orientation and to embrace both the output-orientation and input-orientation as well as both constant and variable return on scale. In its simplest form, the model converts the neutrosophic constraints into their determinate forms, which makes the DEA issues feasible in the determinate domain. On this way, the current model enhances the drawbacks of conventional DEA methodologies, and the actual data reflected by neutrosophic indeterminacies. The research discusses that the proposed model holds a high capability and flexibility through theoretical examination and through the given cases. This particular methodology helps researchers and decision makers to be able to use all its functions in enhancing defensibility and precision in the assessment of efficiency thereby increasing the accuracy of the decision-making process in every aspect of its use.

Keywords: Data Envelopment Analysis; Neutrosophic Uncertainty; Efficiency Evaluation; Decision-Making; Uncertainty Management; Healthcare Facility, Optimization

1. Introduction

For the efficient comparison of comparable organizations described as Decision Making Units (DMUs) from industries such as manufacturing, health care, education, and public sector services, Data Envelopment Analysis (DEA) is a useful tool. In general, DEA models presuppose deterministic input and output data, that is, the data are fully measurable and definite. Nonetheless, in practice, data is imprecise due to measurement errors, subjectivity, and limited information available [1]. These uncertainties can significantly limit the precision and reliability of DEA-based efficiency evaluations.

To address those drawbacks of the deterministic DEA, many scholars have explored different methods on how to include uncertainty in the models. There is a research approach known as fuzzy set theory that has been used to analyze data that are ambiguous in nature [2]. However, fuzzy sets are far from ideal in handling this kind of uncertainty, more so when dealing with conflicting or unclear information. More recently, there is a more general approach which is a neutrosophic set theory that is capable of deal with uncertainties. Neutrosophic sets, which allow for three membership degrees: It is for this reason that four-valued logic, with truth (T), indeterminacy (I), and falsity (F), provides a less rigid and more precise representation of uncertain data [3, 4, 5, 6].

Certain papers can be found that use neutrosophic sets in DEA techniques as well as in models. For instance, Saadati et al. [7] developed a neutrosophic DEA model for assessing the supply chain performance. Wang et al. [8] assumed the neutrosophic DEA approach for the performance measurement of the banks etc. Otherwise, Chakraborty et al. [9] put forth a method of de-neutrosophication of neutrosophic pentagonal numbers which are assigned through two overlays denoting truth and a false, and intermediate ambivalence. It makes use of one of the techniques called the removal area method which calculates the area underneath the membership function of the said values. Liu et al. [10] on the other hand also evaluated the efficiency of the sustainable manufacturing systems supported with a neutrosophic DEA model.

Furthermore, the study made by Pal et al. [11] showed that the model identifies the optimal cycle time of production and the reliability of production that would reduce the total cost of the system. The model, which was developed based on the triangular neutrosophic numbers, aims to address the uncertainty in the reliability of the production process, the demand rate, the deterioration rate, and the shortage cost. There is an effort made by Zhang et al. [12] with the introduction of neutrosophic DEA for the evaluation of the efficiencies of the renewable energy projects. Wang et al. [13] evaluated the performance of sustainable supply chains using a DEA model developed with neutrosophic uncertainty. In their study, Liu et al. [14] proposed a neutrosophic DEA model for assessing the performance of healthcare systems. In their study, El-Demerdash, et al. [15] discussed a general framework on how neutrosophic uncertainty could be integrated into input-oriented DEA models, which can be beneficial for researchers and practitioners. To model uncertainty in input and output data, Farnam, et al. [16] put forward a new DEA model – the neutrosophic DEA model. Neutrosophic numbers are more useful than traditional probability theory because they allow for the representation of truth, falsity, and uncertainty.

The objective of this paper is to present the new DEA-fuzzy model with neutrosophic uncertainty for more accurate assessment of efficiency. Unlike the previous models that focused on deterministic components, the current model is more realistic and not sensitive tointerferences. One strength of the model is that the DEA orientation as well as the return to scale attributes can be changed. Moreover, it extends neutrosophic constraints to deterministic forms to make use of classic DEA approaches effectively.

The remainder of this paper is structured as follows: Section 2 provides a neutrosophic sets overview. Section 3 presents the general mathematical model of DEA. Section 4 introduces the proposed DEA model under neutrosophic uncertainty. Section 5 illustrates the model's application through a case study. Finally, Section 6 concludes the paper with a summary and discusses future research directions.

2. Neutrosophic Sets Overview

Fuzzy sets (FS) and neutrosophic sets (NS) are both mathematical frameworks designed to handle uncertainty and vagueness in data and decision-making. However, they differ in their representation and treatment of uncertainty. FS utilize membership functions to indicate the degree of membership of elements [17]. NS on the other hand, extend this concept by incorporating not only degrees of membership but also degrees of non-membership and indeterminacy. Table 1 summarizes the key differences between them [18, 19]. In this section, we explain the essential definitions of triangular neutrosophic concepts to aid in understanding the developed model.

NS, an extension of FS, were introduced by Smarandache [20] to address indeterminate or uncertain information. They extend the concept of classical sets by allowing for degrees of membership not only within the set but also in its complement and indeterminacy subset. In a neutrosophic set, three values are assigned to each element: the degree of truth membership, the degree of falsity (non-membership), and the degree of indeterminacy [21]. Yang and Li [22] proposed a novel DEA based fixed cost allocation approach aims to balance individual efficiency guarantees and collective preference objectives simultaneously. Sakr et al. [23] Applied DEA to address the existing research gap by examining the efficiency of utilizing such development assistance in achieving three specific Sustainable Development Goals (SDGs) from 2002 to 2020. Gao et al. [24] investigated to break the limitation and constructs an interactive approach for intuitionistic fuzzy DEA models, which enables decision makers to present their preferences in the decision-making process.

Table 1 Comparison between Fuzzy Sets and Neutrosophic Sets

Feature	Fuzzy Set	Neutrosophic Set
Representation	Uses membership functions to denote degree of membership.	Uses three membership functions: membership, non-membership, and indeterminacy.
Handling Uncertainty	Primarily deals with partial membership.	Considers partial membership, non-membership, and indeterminacy.
Membership Grades	One (0 to 1)	Three (Truth, Falsity, Indeterminacy)
Sum of Grades	Must be <= 1	Can be <=, >, or = 1
Focuses on	Vagueness, Incompleteness	Inconsistency, Indeterminacy, Vagueness
Application	Widely used in control systems, artificial intelligence, pattern recognition.	Used in areas with significant ambiguity, such as medical diagnosis, decision-making.

In order to clarify the difference between them, the following example show the difference through categorizing fruits:

- In case of FS: let RipeFruit be a set, which becomes a tool of evaluating degrees of ripeness of fruits. For example, the membership value of a banana would be 0. 8 meaning it is mostly ready. that is, in how far each fruit can be considered part of the “RipeFruit” category in the case of a banana, it has a membership value of 0. 8 is fully ripened but could also be partially unripen or overripe.
- In case of NS: consider a set, which called "RipeFruit" with three membership functions: one for membership, one for non-membership, and one for indeterminacy. For the banana, its membership might be 0.8, non-membership 0.1 (indicating it's definitely not unripe), and indeterminacy 0.1 (suggesting some uncertainty in its ripeness). hence it is not only knowing that the banana is mostly ripe (membership 0.8), but also understanding that it's not completely unripe (non-membership 0.1) and there's some ambiguity in its classification (indeterminacy 0.1).

Definition 1 [25]: Assume that K the space of objects and K is a subset of R.

A Neutrosophic Set NS $(\tilde{R}^N)$ in K is define as the set of triples membership functions $(T_{\tilde{R}^N}(k), I_{\tilde{R}^N}(k), F_{\tilde{R}^N}(k))$ such that $T_{\tilde{R}^N}(k), I_{\tilde{R}^N}(k), F_{\tilde{R}^N}(k) \in]0^-, 1^+[$ with the condition $0^- \leq T_{\tilde{R}^N}(k) + I_{\tilde{R}^N}(k) + F_{\tilde{R}^N}(k) \leq 3^+$. Where $T_{\tilde{R}^N}(k), I_{\tilde{R}^N}(k), F_{\tilde{R}^N}(k)$ are the membership functions for Truth, Indeterminacy, and Falsity respectively and each one of them is a function from K to the closed interval [0,1].

Definition 2 [25]: Assume that $K \neq \emptyset$ (nonempty set)

A Neutrosophic Set Single Valued in K is defined as $\tilde{R}^{NSSV} = \{\langle k, T_{\tilde{R}^N}(k), I_{\tilde{R}^N}(k), F_{\tilde{R}^N}(k)\rangle\}$, such that $T_{\tilde{R}^N}(k), I_{\tilde{R}^N}(k), F_{\tilde{R}^N}(k) \in]0^-, 1^+[$, with the condition $0^- \leq T_{\tilde{R}^N}(k) + I_{\tilde{R}^N}(k) + F_{\tilde{R}^N}(k) \leq 3^+$.

Definition 3 [26]: Assume that $\beta_{\tilde{w}}, \gamma_{\tilde{w}}, \delta_{\tilde{w}} \in [0,1]$ and $x, y, z \in \mathbb{R}$ such that $x \leq y \leq z$.

A Neutrosophic Set Triangular Fuzzy Single Valued (NSTFSV), $\tilde{w}^{TN} = \langle (x, y, z); \beta_{\tilde{w}}, \gamma_{\tilde{w}}, \delta_{\tilde{w}} \rangle$ is a special neutrosophic set on $\mathcal{R}$, where membership functions of truth, indeterminacy, falsity as follows:

$$T_{\tilde{R}^N}(k) = \begin{cases} 0 & ,k < x \\ \frac{(k-a)\beta_{\tilde{w}^{TN}}}{y-x} & ,x \leq k \leq y \\ \frac{(z-k)\beta_{\tilde{w}^{TN}}}{z-y} & ,y \leq k \leq z \\ 0 & ,k > z \end{cases} \quad (1)$$

$$I_{\tilde{R}^N}(k) = \begin{cases} 0 & ,k < x \\ \frac{(y-k)+(k-x)\gamma_{\tilde{w}^{TN}}}{y-x} & ,x < k \leq y \\ \frac{(k-y)+(z-k)\gamma_{\tilde{w}^{TN}}}{z-y} & ,y < k \leq z \\ 0 & ,k > z \end{cases} \quad (2)$$

$$F_{\tilde{R}^N}(k) = \begin{cases} 0 & ,k < a \\ \frac{(y-k)+(k-x)\delta_{\tilde{s}^{TN}}}{y-x} & ,a < k \leq b \\ \frac{(k-y)+(z-k)\delta_{\tilde{s}^{TN}}}{z-y} & ,b < k \leq c \\ 0 & ,k > c \end{cases} \quad (3)$$

Definition 4 [25]: Assume that $\tilde{l}^{TN} = \langle (x, y, z); \beta_{\tilde{l}^{TN}}, \gamma_{\tilde{l}^{TN}}, \delta_{\tilde{l}^{TN}} \rangle$ be NSTFSV, then the score function (SF) defined as follows:

- $SF(\tilde{l}^{TN}) = \left(\frac{1}{4}(x + 2y + z)\right)\left(\frac{1}{3}(2 + \beta_{\tilde{l}^{TN}} - \gamma_{\tilde{l}^{TN}} - \delta_{\tilde{l}^{TN}})\right)$ (4)

3. Data Envelopment Analysis General Mathematical Model

DEA models can be broadly classified into two categories: Constant Return to Scale (CRS) and Variable Return to Scale (VRS). The CRS model, originally proposed by Charnes et al. [27], assumes a direct proportional relationship between changes in inputs and corresponding changes in outputs. In contrast, the VRS model, introduced by Banker et al. [28], allows for variations in inputs that may not result in proportional variations in outputs. The VRS model, an extension of the CRS model, represents a more flexible efficiency frontier that includes all efficient DMUs. DEA models can also be classified as input-oriented, focusing on minimizing input usage, or output-oriented, aiming to maximize output production [29]. We introduce Model *(M-1)* for CRS output-oriented and Model *(M-2)* for CRS input-oriented.

- A CRS - Output-Oriented model.

$Max\ \emptyset$

Subject to

$$\sum_{i=1}^{n} \lambda_i b_{iq} \geq \emptyset b_{pq} \quad ,\forall q = 1 \dots w$$

$$\sum_{i=1}^{n} \lambda_i a_{ij} \leq a_{pj} \quad ,\forall j = 1 \dots . v$$

$\lambda_i \geq 0, (i = 1,2, \dots, n)$ (*M-1*)

- A CRS - Input Oriented model

$Min\ \theta$

Subject to

$$\sum_{i=1}^{n} \lambda_i a_{ij} \leq \theta a_{pj} \quad ,\forall j = 1 \dots . v$$

$$\sum_{i=1}^{n} \lambda_i b_{iq} \geq b_{pq} \quad ,\forall q = 1 \dots w$$

$\lambda_i \geq 0, (i = 1,2, \dots, n),$ (*M-2*)

where q = 1 to 'w' (no. of outputs); j = 1 to 'v' (no. of inputs); i = 1 to 'n' (no. of DMUs); b_{iq} = amount of output k produced by DMU i; a_{ij}= amount of input j utilized by DMU i; λ_i = weight given to DMU i..

To convert the original DEA - CRS models to be DEA – VRS mpdels, as seen in Models *(M-1)* and *(M-2)*, we are added a new constraint: ($\sum_{i=1}^{n} \lambda_i = 1$) with positive λ values in the optimal solution [29].

4. Developed a Unified Neutrosophic DEA Model

In the general DEA, considerable improvements have been made in the effort to develop models which are more accurate and more versatile. In this research, we are attempted to overcome the limitations of the conventional DEA models by utilized in the form of a Unified Neutrosophic DEA mathematical model. Within this model the range of its application is broadened to include uncertainty, or more specifically this model includes neutrosophic components in the efficiency assessment. One of probably the most interesting feature of this model is its versatility. It is suitable for both input-oriented and output-oriented problem situations and so it can be applied to the study of relative efficiency without any limitations. Additionally, it is quite capable of different returns to scale models and is able to include both CRS and VRS modelling in one place. The following three stages are explained the idea of establishing a developed neutrosophic DEA model to measure and evaluate the relative efficiencies of each DMU taking into consideration distinct natures of variables (neutrosophic, and deterministic) independently.

Stage 1: combine the basic DEA models from two dimensions. First dimension orientation type either input or output. Second dimension return to scale either constant or variables assumptions. The following model *(M – 3)* represents a generalized traditional DEA model.

$$Min\ \ \eta_M \emptyset - (1-\eta_M)\theta$$

Subject to

$$\sum_{i=1}^{n} \lambda_i a_{ij} \ \leq\ \eta_M a_{pj} + \ (1-\eta_M)\theta a_{pj} \qquad ,\forall j = 1 \dots v$$

$$\sum_{i=1}^{n} \lambda_i b_{iq} \geq \eta_M \emptyset b_{pq} + (1-\eta_M)\ b_{pq} \qquad ,\forall q = 1 \dots \mathrm{w} \qquad (M-3)$$

$$\eta_D \left[\sum_{i=1}^{n} \lambda_i - 1\right] = 0$$

$$\lambda_i \ \geq 0, (i = 1,2, \dots ., n)$$

where: η_M: the variable represent model type is defined as:

$$\eta_M = \begin{cases} 1 & if\ the\ model\ is\ Output \text{ oriented} \\ 0 & if\ the\ model\ is \text{ Input oriented} \end{cases}$$

η_H: The variable represent return to scale model type is defined as:

$$\eta_H = \begin{cases} 1 & if\ the\ model\ is \text{ VRS} \\ 0 & if\ the\ model\ is \text{ CRS} \end{cases}$$

As a result, we can identify three distinct cases:

- $\eta_M + \eta_H = 2$, the model is a **output-oriented VRS** DEA model.
- $\eta_M + \eta_H = 1 \begin{cases} \text{If } \eta_M = 1, \text{the model is an } \mathbf{output - oriented\ CRS} \text{ DEA model} \\ \text{If } \eta_H = 1, \text{the model is a } \mathbf{input - oriented\ VRS} \text{ DEA model} \end{cases}$
- $\eta_M + \eta_H = 0$, the model is an **input-oriented CRS** DEA model.

Stage 2: convert a generalized traditional DEA model presented in (M-3) to a unified neutrosophic DEA (UNDEA), represent in model (M-4) that distinct natures of variables (neutrosophic, and deterministic) independently.

$$Min\ \eta_M \emptyset - (1-\eta_M)\theta$$

Subject to

$$\sum_{i=1}^{n} \lambda_i a_{ij} \ \leq\ \eta_M a_{pj} + \ (1-\eta_M)\theta a_{pj} \qquad ,\forall j \in J_D$$

$$\sum_{i=1}^{n} \lambda_i \tilde{a}_{ij}{}^{TN} \ \leq\ \eta_M \tilde{a}_{pj}{}^{TN} + \ (1-\eta_M)\theta \tilde{a}_{pj}{}^{TN} \quad ,\forall j \in J_N$$

$$\sum_{i=1}^{n} \lambda_i b_{iq} \geq \eta_M \emptyset b_{pq} + (1-\eta_M)\ b_{pq} \qquad ,\forall q \in Q_D \qquad (M-4)$$

$$\sum_{i=1}^{n} \lambda_i \tilde{b}_{iq}{}^{TN} \geq \eta_M \emptyset \tilde{b}_{ps}{}^{TN} + (1-\eta_M)\ \tilde{b}_{ps}{}^{TN} \qquad ,\forall q \in Q_N$$

$$\eta_H \left[\sum_{i=1}^{n} \lambda_i - 1\right] = 0$$

$$\lambda_i \ \geq 0, (i = 1{:}n)$$

where J_D is the inputs deterministic set, J_N is the inputs neutrosophic set, J is the total inputs set, i.e., $J_D \cup J_N = J$. Q_D is the outputs deterministic set, Q_N is the outputs neutrosophic set, and Q is total outputs set, $Q_D \cup Q_N = Q$.

Stage 3: Given that neutrosophic input variables ($\tilde{a}_{ij} \in J_F$), and neutrosophic output variables ($\tilde{b}_{ij} \in Q_q$), follow triangular membership function, the equivalent crisp linear model presented in the model (*M*-5) for the unified neutrosophic DEA (UNDEA) model based on the score function represented in (eq. 4) is as:

$$Min\ \eta_M \emptyset - (1-\eta_M)\theta$$

Subject to

$$\sum_{i=1}^{n} \lambda_i a_{ij} \ \leq\ \eta_M a_{pj} + \ (1-\eta_M)\theta a_{pj} \qquad ,\forall j \in J_D$$

$$\sum_{i=1}^{n} \lambda_i\, SF(\tilde{a}_{ij}{}^{TN}) \ \leq\ \eta_M\, SF(\tilde{a}_{pj}{}^{TN}) + \ (1-\eta_M)\theta\, SF(\tilde{a}_{pj}{}^{TN}) \quad ,\forall j \in J_N$$

$$\sum_{i=1}^{n} \lambda_i b_{iq} \geq \eta_M \emptyset b_{pq} + (1-\eta_M)\ b_{pq} \qquad ,\forall q \in Q_D \qquad (M-5)$$

$$\sum_{i=1}^{n} \lambda_i\, SF\left(\tilde{b}_{iq}{}^{TN}\right) \geq \eta_M \emptyset\, SF(\tilde{b}_{ps}{}^{TN}) + (1-\eta_M)\, SF(\tilde{b}_{ps}{}^{TN}) \qquad ,\forall q \in Q_N$$

$$\eta_H \left[\sum_{i=1}^{n} \lambda_i - 1\right] = 0$$

$$\lambda_i \ \geq 0, (i = 1{:}n)\ .$$

5. Case Study

To demonstrate the applicability of model (M-5), we present a hypothetical case study involving seven healthcare facilities. Given the complex nature of healthcare operations, which often include multiple inputs and outputs, traditional DEA models can struggle to accurately assess efficiency. In this case study, we consider three inputs: staff, equipment, and resources. While staff and equipment are typically deterministic, resource availability can be subject to uncertainty, making it suitable for representation as a

neutrosophic variable. For outputs, we focus on patient outcomes per day, a deterministic measure, and average quality of care level per facility, a more subjective and thus neutrosophic variable. The presence of uncertainty in these aspects of healthcare delivery underscores the need for a more flexible and robust approach like neutrosophic DEA. Tables 2 and 3 contain the data for the deterministic variables and the parameters of the neutrosophic variables. Before proceeding, we must convert the neutrosophic variables into crisp values using the score function. The resulting values are tabulated in Table 4.

Table 2 Hypothetical deterministic variables data for Healthcare Facilities

Healthcare Facility	Inputs		Output
	Staff (Number of Employees)	Equipment (Number of Beds)	Patient Outcomes (Number of Patients Treated)
HF - A	500	200	2000
HF - B	350	150	1500
HF - C	400	180	1800
HF - D	250	100	1200
HF - E	600	250	2500
HF - F	300	120	1300
HF - G	450	170	2000

Table 3 Hypothetical neutrosophic variables data for Healthcare Facilities

Healthcare Facility	Input	Output
	Resources (Budget in "1,000,000")	Quality of Care (Average Patient Satisfaction Score "%")
HF - A	$\langle(5, 10, 15); 0.8,0.1,0.1\rangle$	$\langle(50, 85, 100); 0.7, 0.2,0.1\rangle$
HF - B	$\langle(6, 8, 10); 0.7,0.2,0.1\rangle$	$\langle(60, 80, 100); 0.6,0.3,0.1\rangle$
HF - C	$\langle(8.5, 9.5, 10.5); 0.85,0.1, 0.05\rangle$	$\langle(75, 88, 95); 0.8,0.15,0.05\rangle$
HF - D	$\langle(5, 7, 9); 0.6, 0.3, 0.1\rangle$	$\langle(50, 75, 100); 0.5,0.35,0.15\rangle$
HF - E	$\langle(10, 12, 14); 0.9, 0.05, 0.05\rangle$	$\langle(90, 95, 100); 0.95,0.03,0.02\rangle$
HF - F	$\langle(6, 7.5, 9); 0.75, 0.2,0.05\rangle$	$\langle(60, 78, 95); 0.7,0.25,0.05\rangle$
HF - G	$\langle(7, 9, 11); 0.8, 0.15, 0.05\rangle$	$\langle(75, 85, 95); 0.85,0.1,0.05\rangle$

Table 4 Score functions for neutrosophic variables data for Healthcare Facilities

Healthcare Facility	Input	Output
	Resources (Budget in "1,000,000")	Quality of Care (Average Patient Satisfaction Score "%")
HF - A	8.66	63.94
HF - B	6.39	58.61
HF - C	8.54	74.89
HF - D	5.13	49.95
HF - E	17.48	91.74
HF - F	6.24	62.14
HF - G	7.79	76.42

To assess the relative efficiency of each healthcare facility under different scenarios, we implemented the proposed algorithm using a UNDEA model. Two scenarios were considered:

- Neutrosophic Output-Oriented CRS DEA: In this scenario, we focused on maximizing outputs while minimizing inputs, when $\eta_M + \eta_H = 1$ but $\eta_M = 1$.
- Neutrosophic Input-Oriented CRS DEA: In this scenario, we focused on minimizing inputs while maintaining a fixed level of outputs, when $\eta_M + \eta_H = 0$.

For each scenario and healthcare facility, a linear programming model was formulated. These models were then solved using the GAMS programming language. The resulting relative efficiency levels for each department are presented in Table 5.

Table 5 Healthcare Facilities Relative Efficiency Level

Healthcare Facility	Neutrosophic Input-Oriented DEA Model	Neutrosophic Output-Oriented DEA Model
HF - A	90%	85%
HF - B	94.2%	90%
HF - C	93.8%	88.3%
HF - D	100%	100%
HF - E	86.8%	75%
HF - F	100%	100%
HF - G	100%	100%

Examining the results, we found that the developed models demonstrated consistent performance. As noted previously, the efficiency scores were the same for both output-oriented CRS and input-oriented CRS DEA models, regardless of whether the DMUs were efficient or inefficient. However, it's important to note that the inefficient DMUs efficiency scores were not identical, as changes in inputs and outputs were not always directly proportional. Table 5 revealed that three healthcare facilities were deemed efficient, while four were classified as inefficient. For the three efficient facilities (D, F, and G), we recommend comparing them to their respective competitors to ensure that these competitors are also operating efficiently. This is crucial because DEA evaluates relative efficiency, not absolute efficiency. By comparing to competitors, we can determine if the efficient facilities are truly outperforming their peers.

To recap, our main research question is: How does neutrosophic uncertainty influence the relative efficiency of healthcare facilities as evaluated by DEA. The answer to this question through key findings from the results analysis. First, for healthcare facilities B and C exhibit higher efficiency in the model of input-oriented compared to the model of output-oriented, may be effectively allocating their resources. However, they could explore strategies to improve their output-oriented performance. Second, Hospitals A and E show lower efficiency in the output-oriented model, indicating potential room for improvement in maximizing outputs given their inputs. healthcare facilities A and E should focus on strategies to enhance their output-oriented efficiency, such as improving patient outcomes or quality of care. Third, efficient healthcare facilities (D, F, G) can serve as benchmarks for others. Identifying their best practices can inform improvement efforts for less efficient facilities. Finally, the use of neutrosophic DEA provides a more nuanced understanding of efficiency, considering the inherent uncertainties in healthcare operations.

6. Conclusions

Due to the inherent uncertainty in real-world performance evaluations, precise data may be elusive. This study introduces a versatile DEA model that can accommodate input and output variables of varying types (neutrosophic or deterministic) without restriction. The model is adaptable to both input-oriented and output-oriented problems, as well as constant returns to scale (CRS) or variable returns to scale (VRS) assumptions. Input and output variables can be either deterministic or neutrosophic, with triangular membership functions assumed for the latter. To transform non-deterministic constraints into deterministic equivalents, we employed a scoring function to handle neutrosophic variables.

The DEA efficiency assessment is highly responsive to changes in the nature of variables. A DMU that is considered efficient compared to others may become inefficient if such uncertain variations are taken into account, or the opposite may occur. In other words, if the data for a variable is not accurately represented, the resulting efficiency scores will be flawed and misleading due to the high sensitivity of these scores to the actual levels of inputs or outputs. Therefore, it is crucial to determine the nature of the variables from the outset and apply the appropriate DEA model to ensure reliable outcomes. Applying the two models to the illustrative example resulted in similar efficient healthcare facilities but different inefficient ones in terms of efficiency levels. This cannot necessarily be explained by proportional changes in outputs or variations in inputs.

Data Availability

In this article, no data were used.

Conflicts of Interest

The authors declare that they have no conflicts of interest.

Funding Statement

The authors received no specific funding for this work.

Acknowledgements

The authors would like to thank the editor and anonymous reviewers for their helpful work and insightful comments.

References

[1] Bandyopadhyay, S. (2010), Effect of regulation on efficiency: evidence from Indian cement industry, Central European Journal of Operations Research, 2,153-170.

[2] Kao, C., and Liu, S.T. (2003), A mathematical programming approach to fuzzy efficiency ranking, International Journal of Production Economics, 2, 145-154.

[3] Haque, T.S., Chakraborty, A., Alrabaiah, H., Alam, S. (2021), A new approach to solve MADM problems by Logarithmic operation laws in interval neutrosophic environment. Granular computing, Springer.

[4] Singh N, Chakraborty A, Biswas SB, Majumdar M. (2020), Impact of social media in banking sector under triangular neutrosophic arena using MCGDM technique. Neutrosophic sets and systems. 35, 153-176.

[5] Sasikala D, Divya B. (2023), A Newfangled Interpretation on Fermatean Neutrosophic Dombi Fuzzy Graphs, Neutrosophic Systems with Applications, 7, 36-53.

[6] Gamal A, Mohamed M. (2023), A Hybrid MCDM Approach for Industrial Robots Selection for the Automotive Industry, Neutrosophic Systems with Applications, 4, 1-1.

[7] Saadati, R., Smarandache, F., & Fullér, R. (2017). Neutrosophic data envelopment analysis. Neutrosophic Sets and Systems, 18, 31-37.

[8] Wang, Y., Zhang, H., & Wang, J. (2018). Neutrosophic data envelopment analysis for bank efficiency evaluation. International Journal of Fuzzy Systems, 20(1), 1-11.

[9] Chakraborty A, Mondal S, Broumi S. (2019), De-neutrosophication technique of pentagonal neutrosophic number and application in minimal spanning tree. Neutrosophic Sets and Systems. 29, 1–18.

[10] Liu, Y., Wang, H., & Chen, J. (2020). A neutrosophic data envelopment analysis model for evaluating the efficiency of sustainable manufacturing systems. International Journal of Production Economics, 227, 113809.

[11] Pal S, Chakraborty A. (2020), Triangular neutrosophic based production reliability model of deteriorating item with ramp type demand under shortages and time discounting. Neutrosophic Sets and Systems, 35(1):347-67.

[12] Zhang, H., Wang, Y., & Wang, J. (2021). Neutrosophic data envelopment analysis for renewable energy project efficiency evaluation. Energy Economics, 98, 105321.

[13] Wang, Y., Zhang, H., & Wang, J. (2022). Neutrosophic data envelopment analysis for sustainable supply chain performance evaluation. Journal of Cleaner Production, 352, 130847.

[14] Liu, Y., Wang, H., & Chen, J. (2023). A neutrosophic data envelopment analysis model for evaluating the efficiency of healthcare systems. International Journal of Healthcare Management, 16(4), 385-396.

[15] El-Demerdash, B. E., Edalatpanah, S. A., & Khalifa, H. A. (2023). On Treating Input Oriented Data Envelopment Analysis Model under Neutrosophic Environment. Neutrosophic Sets and Systems, 60(1), 17.

[16] Farnam, M., Darehmiraki, M., & Behdani, Z. (2024). Neutrosophic data envelopment analysis based on parametric ranking method. Applied Soft Computing, 153, 111297.

[17] Zadeh, L.A. (1965), Fuzzy sets, Information and control, 8, 338-353.

[18] Tharwat, A., El-Demerdash, B., & El-Khodary, I. (2019), Developing an Input Oriented Data Envelopment Analysis Model with Fuzzy Uncertainty in Variables. In Creative Business and Social Innovations for a Sustainable Future, Springer, Cham, 117-122.

[19] Yang, W., Cai, L., Edalatpanah, S. A., & Smarandache, F. (2020), Triangular single valued neutrosophic data envelopment analysis: application to hospital performance measurement, Symmetry, 12, 588.

[20] Smarandache, F. (1998). Neutrosophy: An extension of fuzzy logic. Infinite Study.

[21] Smarandache, F. (1999), A unifying field in Logics: Neutrosophic Logic. Philosophy. American Research Press, 1-141.

[22] Yang, J., and Li, Y. (2024). A generalized data envelopment analysis approach for fixed cost allocation with preference information, Omega, 122, 102948.

[23] Sakr, M.F., Selim, K.S., and Taha, S.G. (2024). Measuring countries relative efficiencies in using development assistance: a data envelopment analysis approach. Future Business Journal, 10,40.

[24] Gao, Q., Lin, Y., Luo,Y., and Xu, X. (2024). An Interactive Approach for Intuitionistic Fuzzy Data Envelopment Analysis. IEEE Tranasaction on Fuzzy Systems, 32(9), 5189 – 5200

[25] Khalifa, H. A. E. W., Saeed, M., Rahman, A. U., & El-Morsy, S. (2022), An Application of Pentagonal Neutrosophic Linear Programming for Stock Portfolio Optimization, Neutrosophic Sets and Systems, 51, 653-665.

[26] Dhouib, S. (2021), Optimization of travelling salesman problem on single valued triangular neutrosophic number using dhouib-matrix-TSP1 heuristic, International Journal of Engineering, 34, 2642-2647.

[27] Charnes A., Cooper W., and Rhodes E. (1978), Measuring the efficiency of efficiency of decision-making units, European Journal of Operational Research, 6, 429-444.

[28] Banker R., Charnes A., and Cooper W. (1984), Some models for estimating technical and scale inefficiencies in data envelopment analysis, Management Science, 9, 1078-1092.

[29] Tharwat, A. A., El-Demerdash, B. E., & Nada, D. W. (2023). An economic mathematical fuzzy model for data envelopment analysis. Journal of Namibian Studies: History Politics Culture, 33, 1757-1771.

Received: July 25, 2024. Accepted: Oct 24, 2024

Neutrosophic Sets and Systems, Vol. 76, 2025
University of New Mexico

Single-Valued Neutrosophic ExpTODIM Technique for Quality Evaluation of MPPT Controller Design for Photovoltaic Systems

Xiaobin Zheng[1]*, Guiqing Chen[1], Shita Huang[2], Lunsen Zou[3]

[1]School of Mechanical and Intelligent Manufacturing Engineering, Fujian Chuanzheng Communications College, Fuzhou 350007, Fujian, China (Guiqing Chen, E-mail: chgq68@163.com)

[2]Fujian Antai New Energy Technology Co., Ltd, Zhangzhou, 363900, Fujian, China (Shita Huang, E-mail:gq-chen@126.com)

[3]CGS POWER GENERATION(GUANGDONG) ENERGY STORAGE TECHNOLOGY CO., LTD, Guangzhou, Guangdong, 510630, China (Lunsen Zou, E-mail: cnkjzoulunsen@126.com)

*Corresponding author, E-mail: 5705994970@sina.cn

Xiaobin Zheng: https://orcid.org/0009-0007-3828-7616

Abstract: The significance of evaluating the design quality of Maximum Power Point Tracking (MPPT) controllers in photovoltaic systems lies in ensuring efficient and stable operation under various environmental conditions. By assessing the controller's tracking efficiency, dynamic response speed, steady-state error, and disturbance rejection capability, the system's energy output can be optimized, equipment lifespan extended, operating costs reduced, and overall system reliability and performance improved, thereby maximizing solar energy utilization efficiency. The quality evaluation of MPPT controller design for photovoltaic systems is framed as a multiple-attribute group decision-making (MAGDM) problem. Recently, the Exponential TODIM (ExpTODIM) approach has been introduced to address this type of decision-making. Single-valued neutrosophic sets (SVNSs) are employed as a decision-making tool to represent fuzzy data during the quality evaluation process of MPPT controller design in photovoltaic systems. In this study, a method combining the single-valued neutrosophic number and Exponential TODIM (SVNN-Com-ExpTODIM), based on the SVNN Hamming distance (SVNNHD) and SVNN Euclidean distance (SVNNED), is proposed to solve the MAGDM problem under SVNSs. Finally, a numerical study is conducted to demonstrate the effectiveness of the SVNN-Com-ExpTODIM approach for the quality evaluation of MPPT controller design in photovoltaic systems, supported by comparative analysis.

Keywords: Multiple-attribute group decision-making (MAGDM); SVNSs; entropy; Exponential TODIM; quality evaluation of MPPT controller design

1. Introduction

The quality evaluation of the Maximum Power Point Tracking (MPPT) controller design for photovoltaic (PV) systems primarily focuses on aspects such as performance, response speed, stability, hardware cost, and applicability. First, tracking accuracy is the fundamental evaluation criterion, which assesses whether the controller can accurately track the maximum

power point of the PV cells under varying environmental conditions (such as changes in irradiance and temperature). Secondly, response speed reflects how quickly the controller reacts to external changes, with faster responses maximizing real-time energy output. Stability refers to the controller's performance in continuous operation, where excessive oscillations can lead to energy losses or system instability. The cost-effectiveness of the hardware design is also a key consideration, as the design needs to balance performance with affordability. Advanced algorithms, such as fuzzy control or neural networks, may improve performance but can also increase hardware complexity and cost. Lastly, the applicability of the controller determines its flexibility in being used across different scales and types of PV systems (e.g., grid-tied or standalone systems). Evaluating these factors together provides a comprehensive assessment of the MPPT controller's design quality.

In this study, the SVNN-Com-ExpTODIM approach is proposed to handle MAGDM under SVNSs. To conclude, a numerical study for evaluating the quality of MPPT controller design in photovoltaic systems is conducted to validate the SVNN-Com-ExpTODIM approach through comparative analysis.

The main motivations of this study are as follows:

1. The entropy method is used to determine the weight for SVNSs
2. The SVNN-Com-ExpTODIM approach is proposed for solving MAGDM problems using SVNSs
3. A numerical study is conducted for quality evaluation of MPPT controller design in photovoltaic systems.
4. Several comparisons are made to validate the SVNN-Com-ExpTODIM approach.

The basic structure of this study is outlined as follows. In Sect. 2, the concept of SVNSs is introduced. Sect. 3 presents the SVNN-Com-ExpTODIM approach for addressing MAGDM problems under SVNSs, incorporating the entropy method. Sect. 4 provides a numerical study for the quality evaluation of MPPT controller design in photovoltaic systems, supported by comparative analysis. Finally, concluding remarks are offered in Sect. 5.

2. Literature Review

Early research focused on the design and optimization of MPPT controllers in PV systems. Cao [1] researched the MPPT controller for independent photovoltaic street lighting systems and proposed an improved variable-step optimization algorithm. He designed an MPPT controller based on the LPC2194 microcontroller, and experimental results showed that the algorithm could quickly and accurately track the maximum power point. Gong [2] also studied photovoltaic street lighting systems and proposed an improved maximum power point tracking strategy. He designed both system-level and circuit-level controllers, optimizing the energy utilization of solar panels. As research progressed, Yu and Kang [3] addressed the inefficiency of traditional MPPT techniques under changing environmental conditions. They proposed an MPPT controller based on a lossless power feedback method. Experiments demonstrated that this method significantly improved energy conversion efficiency. Lai [4]

further investigated the MPPT controller for small-scale photovoltaic power generation systems, improving the incremental conductance method and battery charging/discharging algorithms. His simulations and experiments confirmed the stability of the control algorithm and the reliability of the system. In the mid-2010s, research began incorporating emerging technologies. Zhong [5] proposed a variable-step perturbation observation method and designed an MPPT controller based on DSP technology. Simulations validated the superiority of the improved algorithm, particularly in tracking performance under various environmental conditions. Zheng [6] combined neural networks, fuzzy controllers, and PID control to propose a neural network fuzzy PID controller. Experiments showed that, compared to traditional PID controllers, this system improved steady-state performance and control accuracy. In the same year, Fu [7] made hardware and software improvements to the MPPT controller by using the incremental conductance method combined with a Buck converter circuit. Experimental results showed a 6.88% increase in maximum power output. Zhang [8] employed a fuzzy PID control algorithm to design a DSP-based MPPT controller for a photovoltaic power generation system. Compared to conventional fuzzy control methods, the fuzzy PID control method exhibited faster tracking speed and better stability, especially under varying light intensity, allowing the system to respond quickly and maintain stability. The most recent study by Fang and Wang [9] designed an MPPT controller based on DC-DC circuits that could quickly and accurately track the maximum power point of photovoltaic power systems, improving the output efficiency of solar cells.

MAGDM is a decision analysis method used when multiple decision-makers evaluate a problem involving multiple attributes or criteria[10-13]. It is typically applied in complex situations where decision-makers, based on their individual experiences, preferences, or expertise, assign scores or rankings to different attributes[14-17]. Each attribute may carry different importance, so weights are often assigned to reflect this. By integrating the opinions of decision-makers and the attribute weights, MAGDM methods help derive the optimal solution or ranking[18-23]. Common methods in MAGDM include the entropy approach [24], fuzzy comprehensive evaluation and TODIM [25, 26]. This approach is widely used in practice, especially in fields requiring the synthesis of diverse opinions, such as technology selection, strategic planning, and policymaking. The quality evaluation of MPPT controller design for photovoltaic systems is a MAGDM problem. Recently, the Exponential TODIM (ExpTODIM) approach [27, 28] has been introduced to address MADM. SVNSs [29, 30] are utilized as a decision-making tool to represent fuzzy data during the quality evaluation of MPPT controller design for photovoltaic systems.

3. **Preliminaries**

Wang et al. [29] conveyed the SVNSs based on the neutrosophic sets[31].

Definition 1 [29]. The SVNSs is conveyed:

$$SA=\left\{\left(\phi, ST_A\left(\phi\right), SI_A\left(\phi\right), SF_A\left(\phi\right)\right)\middle|\phi\in\Phi\right\} \tag{1}$$

where $ST_A(\phi), SI_A(\phi), SF_A(\phi)$ presents truth-membership, indeterminacy-membership and falsity-membership, $ST_A(\phi), SI_A(\phi), SF_A(\phi) \in [0,1]$ and meets $0 \le ST_A(\phi) + SI_A(\phi) + SF_A(\phi) \le 3$.

The SVNN is conveyed as: $SA = (ST_A, SI_A, SF_A)$, $ST_A, SI_A, SF_A \in [0,1]$, and $0 \le ST_A + SI_A + SF_A \le 3$.

Definition 2 [32]. Let $SA = (ST_A, SI_A, SF_A)$ be SVNN, a score value is conveyed:

$$SV(SA) = \frac{(2 + ST_A - SI_A - SF_A)}{3}, \quad SV(SA) \in [0,1]. \tag{2}$$

Definition 3[32]. Let $SA = (ST_A, SI_A, SF_A)$ be SVNN, accuracy value is conveyed:

$$AV(SA) = \frac{1 + ST_A - SF_A}{2}, \ AV(SA) \in [0,1]. \tag{3}$$

Peng et al. [32] conveyed the order for SVNNs.

Definition 4[32]. Let $SA = (ST_A, SI_A, SF_A)$ and $SB = (ST_B, SI_B, SF_B)$ be SVNNs, $SV(SA) = \frac{(2 + ST_A - SI_A - SF_A)}{3}$ and $SV(SB) = \frac{(2 + ST_B - SI_B - SF_B)}{3}$, and $AV(SA) = \frac{1 + ST_A - SF_A}{2}$ and $AV(ZB) = \frac{1 + ST_B - SF_B}{2}$, then if $SV(SA) < SV(SB)$, then $SA < SB$; if $SV(SA) = SV(SB)$, then (1)if $AV(SA) = AV(SB)$, then $SA = SB$; (2) if $AV(SA) > AV(SB)$, then $SA < SB$.

Definition 5[29]. Let $SA = (ST_A, SI_A, SF_A)$ and $SB = (ST_B, SI_B, SF_B)$ be SVNNs, the operations are conveyed:

(1) $SA \oplus SB = (ST_A + ST_B - ST_A ST_B, SI_A SI_B, SF_A SF_B)$;

(2) $SA \otimes SB = (ST_A ST_B, SI_A + SI_B - SI_A SI_B, SF_A + SF_B - SF_A SF_B)$;

(3) $\lambda SA = \left(1 - (1 - ST_A)^{\lambda}, (SI_A)^{\lambda}, (SF_A)^{\lambda}\right), \lambda > 0$;

(4) $(SA)^{\lambda} = \left((ST_A)^{\lambda}, (SI_A)^{\lambda}, 1 - (1 - SF_A)^{\lambda}\right), \lambda > 0.$

Definition 6[33]. Let $SA = (ST_A, SI_A, SF_A)$ and $SB = (ST_B, SI_B, SF_B)$, then SVNN Hamming distance (SVNNHD) and SVNN Euclidean distance (SVNNED) are conveyed:

$$SVNNHD(SA, SB) = \frac{|ST_A - ST_B| + |SI_A - SI_B| + |SF_A - SF_B|}{3} \tag{4}$$

$$SVNNED(SA,SB)=\sqrt{\frac{\left|ST_A-ST_B\right|^2+\left|SI_A-SI_B\right|^2+\left|SF_A-SF_B\right|^2}{3}} \quad (5)$$

The SVNNWG approach is conveyed:

Definition 8[32]. Let $SA_j=\left(ST_j,SI_j,SF_j\right)$ be SVNNs, the SVNNWG approach is conveyed:

$$\begin{aligned}&\mathrm{SVNNWG}_{sw}\left(SA_1,SA_2,\ldots,SA_n\right)\\&=\left(SA_1\right)^{sw_1}\otimes\left(SA_2\right)^{sw_2},\ldots\otimes\left(SA_n\right)^{sw_n}=\overset{n}{\underset{j=1}{\otimes}}\left(SA_j\right)^{sw_j}\\&=\left(\prod_{j=1}^{n}\left(ST_{ij}\right)^{sw_j},1-\prod_{j=1}^{n}\left(1-SF_{ij}\right)^{sw_j},1-\prod_{j=1}^{n}\left(1-ST_{ij}\right)^{sw_j}\right)\end{aligned} \quad (6)$$

where $sw=\left(sw_1,sw_2,...,sw_n\right)^T$ be weight of SA_j, $sw_j>0,\sum_{j=1}^{n}sw_j=1.$

4. The proposed model

4.1. SVNN-MAGDM information

The SVNN-Com-ExpTODIM approach is conveyed for MAGDM. Let $SA=\left\{SA_1,SA_2,\cdots,SA_m\right\}$ be alternatives, and $SG=\left\{SG_1,SG_2,\cdots,SG_n\right\}$ be attributes with weight $s\omega$, where $s\omega_j\in[0,1],\sum_{j=1}^{n}s\omega_j=1$ and invited experts $SE=\left\{SE_1,SE_2,\cdots,SE_q\right\}$ with expert's weight $sw=\left\{sw_1,sw_2,\cdots,sw_t\right\}$, where $sw_j\in[0,1],\sum_{k=1}^{t}sw_k=1$. Then, SVNN-Com-ExpTODIM approach is conveyed for MAGDM.

(1). Expound the SVNN-matrix $SM^t=\left[SM_{ij}^t\right]_{m\times n}=\left(ST_{ij}^t,SI_{ij}^t,SF_{ij}^t\right)_{m\times n}$ and average matrix $SM=\left[SM_{ij}\right]_{m\times n}$:

$$SM^t=\left[SM_{ij}^t\right]_{m\times n}=\begin{array}{c}\\SA_1\\SA_2\\\vdots\\SA_m\end{array}\begin{array}{c}\begin{array}{cccc}SG_1&SG_2&\ldots&SG_n\end{array}\\\begin{bmatrix}SM_{11}^t&SM_{12}^t&\ldots&SM_{1n}^t\\SM_{21}^t&SM_{22}^t&\ldots&SM_{2n}^t\\\vdots&\vdots&\vdots&\vdots\\SM_{m1}^t&SM_{m2}^t&\ldots&SM_{mn}^t\end{bmatrix}\end{array} \quad (7)$$

$$SM=\left[SM_{ij}\right]_{m\times n}=\begin{array}{c}\\SA_1\\SA_2\\\vdots\\SA_m\end{array}\begin{array}{c}\begin{array}{cccc}SG_1&SG_2&\ldots&SG_n\end{array}\\\begin{bmatrix}SM_{11}&SM_{12}&\ldots&SM_{1n}\\SM_{21}&SM_{22}&\ldots&SM_{2n}\\\vdots&\vdots&\vdots&\vdots\\SM_{m1}&SM_{m2}&\ldots&SM_{mn}\end{bmatrix}\end{array} \quad (8)$$

Based on SVNNWG, the $SM = \left[SM_{ij} \right]_{m\times n} = \left(ST_{ij}, SI_{ij}, SF_{ij} \right)_{m\times n}$ is conveyed:

$$SM_{ij} = \overset{t}{\underset{k=1}{\otimes}} \left(SM_{ij}^{k} \right)^{sw_k} = \left(1 - \prod_{k=1}^{t} \left(ST_{ij}^{t} \right)^{sw_k}, \prod_{k=1}^{t} \left(SI_{ij}^{t} \right)^{sw_k}, \prod_{k=1}^{t} \left(SF_{ij}^{t} \right)^{sw_k} \right) \tag{9}$$

(2). Normalize the $SM = \left[SM_{ij} \right]_{m\times n} = \left(ST_{ij}, SI_{ij}, SF_{ij} \right)_{m\times n}$ into $SM^{N} = \left[SM_{ij}^{N} \right]_{m\times n} = \left(ST_{ij}^{N}, SI_{ij}^{N}, SF_{ij}^{N} \right)_{m\times n}$.

For benefit attributes:

$$SM_{ij}^{N} = \left(ST_{ij}^{N}, SI_{ij}^{N}, SF_{ij}^{N} \right) = \left(ST_{ij}, SI_{ij}, SF_{ij} \right) \tag{10}$$

For cost attributes:

$$SM_{ij}^{N} = \left(ST_{ij}^{N}, SI_{ij}^{N}, SF_{ij}^{N} \right) = \left(SF_{ij}, SI_{ij}, ST_{ij} \right) \tag{11}$$

4.2. Compute the attributes weight by entropy.

Entropy [24] is conveyed the weight. The matrix SS_{ij} is conveyed:

$$SS_{ij} = \frac{\left(SV\left(ST_{ij}^{N}, SI_{ij}^{N}, SF_{ij}^{N} \right) + AV\left(ST_{ij}^{N}, SI_{ij}^{N}, SF_{ij}^{N} \right) + 2 \right)}{\sum_{i=1}^{m} \left(SV\left(ST_{ij}^{N}, SI_{ij}^{N}, SF_{ij}^{N} \right) + AV\left(ST_{ij}^{N}, SI_{ij}^{N}, SF_{ij}^{N} \right) + 2 \right)}, \tag{12}$$

The neutrosophic Shannon entropy (NSE) is conveyed:

$$NSE_j = -\frac{1}{\ln m} \sum_{i=1}^{m} SS_{ij} \ln SS_{ij} \tag{13}$$

and $SS_{ij} \ln SS_{ij} = 0$ if $SS_{ij} = 0$.

Then, the weight information is conveyed:

$$s\omega_j = \frac{1 - NSE_j}{\sum_{j=1}^{n} \left(1 - NSE_j \right)}, \quad j = 1, 2, \cdots, n. \tag{14}$$

4.3. SVNN-Com-ExpTODIM approach for MAGDM

The SVNN-Com-ExpTODIM approach is conveyed to solve MAGDM.

(1) Expound relative weight:

$$rs\omega_j = s\,\omega_j \Big/ \max_j s\omega_j, \tag{15}$$

(2) The neutrosophic dominance degree (NDD) of SA_i over SA_t for SG_j is conveyed in light with SVNNHD and SVNNED:

$$NDD_j\left(SA_i, SA_t\right)=\begin{cases}\dfrac{1}{2}\left(\dfrac{rs\omega_j\times\left(1-10^{-\rho DVNNHD\left(SM_{ij}^N, SM_{tj}^N\right)}\right)}{\sum_{j=1}^n rs\omega_j}+\dfrac{rs\omega_j\times\left(1-10^{-\rho DVNNED\left(SM_{ij}^N, SM_{tj}^N\right)}\right)}{\sum_{j=1}^n rs\omega_j}\right) & \text{if } SV\left(SM_{ij}^N\right)>SV\left(SM_{tj}^N\right)\\ 0 & \text{if } SV\left(SM_{ij}^N\right)=SV\left(SM_{tj}^N\right)\\ \dfrac{1}{2}\left(-\dfrac{1}{s\theta}\dfrac{\sum_{j=1}^n rs\omega_j\times\left(1-10^{-\rho DVNNHD\left(SM_{ij}^N, SM_{tj}^N\right)}\right)}{rs\omega_j}-\dfrac{1}{s\theta}\dfrac{\sum_{j=1}^n rs\omega_j\times\left(1-10^{-\rho DVNNED\left(SM_{ij}^N, SM_{tj}^N\right)}\right)}{rs\omega_j}\right) & \text{if } SV\left(SM_{ij}^N\right)<SV\left(SM_{tj}^N\right)\end{cases} \tag{16}$$

where $s\theta$ and $\rho\in[1,5]$ is from [27].

The $NDD_j\left(SA_i\right)$ for SG_j is conveyed:

$$NDD_j\left(SA_i\right)=\left[NDD_j\left(SA_i, SA_t\right)\right]_{m\times m}$$

$$=\begin{array}{c} \\ SA_1\\ SA_2\\ \vdots\\ SA_m\end{array}\begin{array}{c}\begin{array}{cccc} SA_1 & SA_2 & \cdots & SA_m\end{array}\\ \begin{bmatrix} 0 & NDD_j\left(SA_1, SA_2\right) & \cdots & NDD_j\left(SA_1, SA_m\right)\\ NDD_j\left(SA_2, SA_1\right) & 0 & \cdots & NDD_j\left(SA_2, SA_m\right)\\ \vdots & \vdots & \cdots & \vdots\\ NDD_j\left(SA_m, SA_1\right) & NDD_j\left(SA_m, SA_2\right) & \cdots & 0\end{bmatrix}\end{array}$$

(3) Expound the $NDD\left(SA_i, SA_t\right)$ of SA_i over other alternatives:

$$NDD\left(SA_i, SA_t\right)=\sum_{j=1}^n NDD_j\left(SA_i, SA_t\right) \tag{17}$$

The $NDD=NDD\left(SA_i, SA_t\right)_{m\times m}$ is conveyed:

$$NDD = NDD\left(SA_i, SA_t\right)_{m\times m}$$

$$= \begin{bmatrix} & SA_1 & SA_2 & \cdots & SA_m \\ SA_1 & \sum_{j=1}^{n} NDD_j\left(SA_1, SA_1\right) & \sum_{j=1}^{n} NDD_j\left(SA_1, SA_2\right) & \cdots & \sum_{j=1}^{n} NDD_j\left(SA_1, SA_m\right) \\ SA_2 & \sum_{j=1}^{n} NDD_j\left(SA_2, SA_1\right) & \sum_{j=1}^{n} NDD_j\left(SA_2, SA_2\right) & \cdots & \sum_{j=1}^{n} NDD_j\left(SA_2, SA_m\right) \\ \vdots & \vdots & \vdots & \vdots & \vdots \\ SA_m & \sum_{j=1}^{n} NDD_j\left(SA_m, SA_1\right) & \sum_{j=1}^{n} NDD_j\left(SA_m, SA_2\right) & \cdots & \sum_{j=1}^{n} NDD_j\left(SA_m, SA_m\right) \end{bmatrix}$$

(4) Expound the overall $NDD\left(SA_i\right)$ of SA_i:

$$NDD\left(ZA_i\right) = \frac{\sum_{t=1}^{m} NDD\left(SA_i, SA_t\right) - \min_i \left\{\sum_{t=1}^{m} NDD\left(SA_i, SA_t\right)\right\}}{\max_i \left\{\sum_{t=1}^{m} NDD\left(SA_i, SA_t\right)\right\} - \min_i \left\{\sum_{t=1}^{m} NDD\left(SA_i, SA_t\right)\right\}}. \quad (18)$$

(5) Sort and select the optimal alternative with $NDD\left(SA_i\right)$, the greater $NDD\left(SA_i\right)\left(i = 1, 2, \cdots, m\right)$ is better choice.

5. Results and Discussion

5.1. Case Study

The MPPT controller in a photovoltaic system is a key component that ensures efficient operation under varying environmental conditions. The design quality of the MPPT controller is directly related to the energy output, stability, and long-term reliability of the photovoltaic system as shown in Figure 1. Therefore, it is essential to conduct a quality evaluation of the MPPT controller's design. The core function of the MPPT controller is to continuously adjust the operating point through algorithms so that the photovoltaic system can produce maximum power at any given time. In practical applications, factors such as solar irradiance and ambient temperature are constantly changing, which place high demands on the controller's response speed and tracking accuracy. Quality evaluation allows us to measure the controller's performance under various conditions, ensuring that it operates optimally in the photovoltaic system. The primary objective of evaluating the design quality of an MPPT controller is to assess its performance under different working conditions using quantifiable indicators.

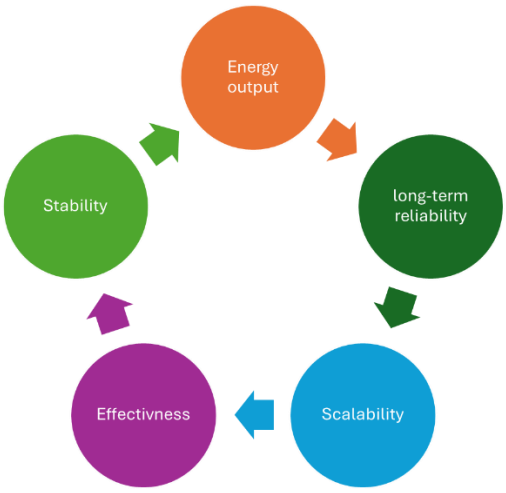

Figure 1. The design quality of MPPT.

Common evaluation metrics include tracking efficiency, dynamic response speed, steady-state error, and disturbance rejection capability as shown in Figure 2. These metrics represent the controller's accuracy in tracking the maximum power point, its speed in responding to changes, its stability during long-term operation, and its ability to handle external disturbances. Tracking efficiency measures the controller's ability to accurately follow the maximum power point of the photovoltaic system under varying environmental conditions. It is usually expressed as a percentage, ideally close to 100%, to maximize power generation efficiency.

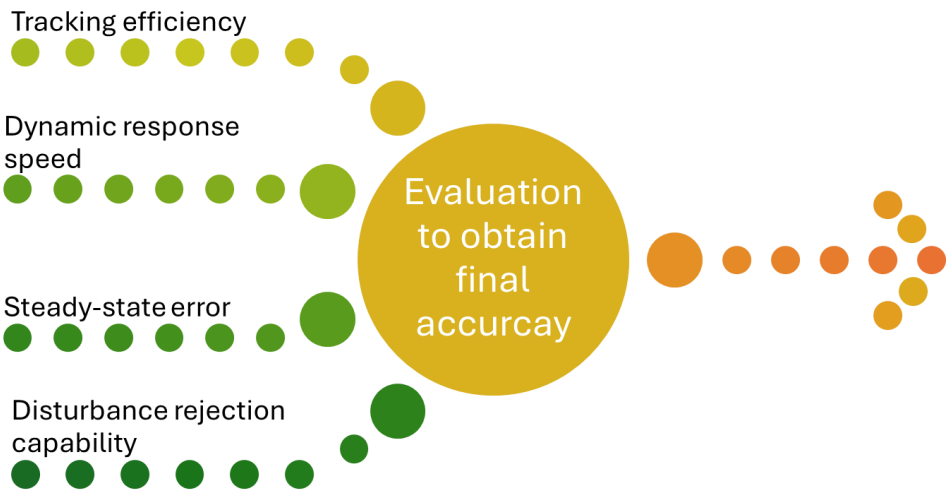

Figure 2. The evaluation metrics of MPPT.

Dynamic response speed evaluates the controller's ability to quickly adjust and find the new maximum power point when external conditions change. The faster the response, the less energy is lost. Steady-state error indicates the deviation between actual output and the maximum power point after long-term operation, the smaller the error, the higher the overall system efficiency. Disturbance rejection capability reflects the controller's ability to swiftly

recover and maintain operation near the maximum power point in the face of load fluctuations or external interference. In addition to the quantitative analysis of these technical indicators, the economic viability and applicability of the system must also be considered during the MPPT controller's quality evaluation. For example, the controller should offer a high cost-performance ratio and be adaptable to various types of photovoltaic systems and installation environments. Furthermore, the controller's reliability and durability are critical factors, especially in long-term operation and harsh environments, where the controller must work stably to reduce maintenance costs. A comprehensive evaluation of the MPPT controller's design quality not only helps manufacturers optimize product design but also provides users with a scientific basis for selecting the right controller. Ultimately, a high-quality MPPT controller can maximize the energy output of the photovoltaic system, extend equipment lifespan, reduce overall maintenance and operational costs, and improve the system's overall economic efficiency and sustainability. The quality evaluation of MPPT controller design for photovoltaic systems is MAGDM. Five MPPT controller design schemes for photovoltaic systems $SA_i\left(i=1,2,3,4,5\right)$ are conveyed with different attributes (See Table 1).

Table 1. Four attributes for quality evaluation of MPPT controller design for photovoltaic systems

Attributes	Attribute Description
SG1- Tracking Efficiency	Tracking efficiency measures how accurately the MPPT controller can track the maximum power point (MPP) of the photovoltaic system. It is usually expressed as a percentage, ideally close to 100%. Improving tracking efficiency maximizes the energy output of the system.
SG2-Dynamic Response Speed	Dynamic response speed refers to how quickly the MPPT controller can adjust and find the new maximum power point when environmental conditions (such as sunlight or temperature) change. A fast dynamic response helps maintain high energy output under changing conditions.
SG3-Steady-State Error	Steady-state error indicates the deviation between the actual power and the maximum power point after the MPPT controller has been running for an extended period. A lower steady-state error means the controller can operate stably near the maximum power point, improving overall system performance.
SG4-Disturbance Rejection Capability	Disturbance rejection capability measures how well the MPPT controller can quickly recover and maintain maximum power point operation when facing external disturbances (such as load changes or external interference). Excellent disturbance rejection capability ensures the system's stability and reliability under various complex conditions.

Five MPPT controller design schemes for photovoltaic systems are evaluated in light with linguistic scales through four attributes and three experts $SE_t\left(t=1,2,3\right)$ with expert's weight $sw=\left(1/3,1/3,1/3\right)$.

The SVNN-Com-ExpTODIM approach is conveyed to solve the quality evaluation of MPPT controller design for photovoltaic systems.

Step 1. Build the decision matrix $SM^t = \left[SM_{ij}^t \right]_{5\times4} = \left(ST_{ij}^t, SI_{ij}^t, SF_{ij}^t \right)_{5\times4}$ and according to SVNNWG approach, the $SM = \left[SM_{ij} \right]_{5\times4}$ is conveyed as shown in Table 2

Step 2. Normalize the decision matrix as shown in Table 3.

Step 3. Expound the weights as shown in Figure 3.

Step 4. Expound the relative weights as shown in Figure 3.

Step 5. Expound the $NDD = NDD\left(SA_i, SA_t \right)_{5\times5}$ as shown in Table 4.

Step 6. Expound the $NDD\left(SA_i \right)\left(i = 1, 2, \cdots, 5 \right)$ as shown in Figure 4.

Step 7. Conclusively, the order is conveyed: $SA_2 \succ SA_4 \succ SA_5 \succ SA_3 \succ SA_1$, and thus the optimal MPPT controller design scheme for photovoltaic systems is SA_2.

Table 2. The aggregated decision matrix

	SG₁	**SG₂**	**SG₄**	**SG₃**
SA₁	(0.8643, 0.0721, 0.0636)	(0.4910, 0.3035, 0.2055)	(0.7321, 0.1345, 0.1863)	(0.5812, 0.2440, 0.2558)
SA₂	(0.5382, 0.3210, 0.1408)	(0.6003, 0.2110, 0.1887)	(0.6423, 0.1927, 0.1650)	(0.7546, 0.1234, 0.1220)
SA₃	(0.4659, 0.2947, 0.2394)	(0.7396, 0.1225, 0.1379)	(0.5730, 0.2874, 0.1396)	(0.8103, 0.1135, 0.0762)
SA₄	(0.5793, 0.2714, 0.1493)	(0.6477, 0.1850, 0.1673)	(0.6891, 0.2017, 0.1092)	(0.7284, 0.1583, 0.1133)
SA₅	(0.7564, 0.1740, 0.0696)	(0.5902, 0.2309, 0.1789)	(0.8110, 0.1055, 0.0835)	(0.6921, 0.2043, 0.1036)

Table 3. The normalized decision matrix

	SG₁	**SG₂**	**SG₄**	**SG₃**
SA₁	(0.8643, 0.0721, 0.0636)	(0.4910, 0.3035, 0.2055)	(0.7321, 0.1345, 0.1863)	(0.5812, 0.2440, 0.2558)
SA₂	(0.5382, 0.3210, 0.1408)	(0.6003, 0.2110, 0.1887)	(0.6423, 0.1927, 0.1650)	(0.7546, 0.1234, 0.1220)
SA₃	(0.4659, 0.2947, 0.2394)	(0.7396, 0.1225, 0.1379)	(0.5730, 0.2874, 0.1396)	(0.8103, 0.1135, 0.0762)
SA₄	(0.5793, 0.2714, 0.1493)	(0.6477, 0.1850, 0.1673)	(0.6891, 0.2017, 0.1092)	(0.7284, 0.1583, 0.1133)
SA₅	(0.7564, 0.1740, 0.0696)	(0.5902, 0.2309, 0.1789)	(0.8110, 0.1055, 0.0835)	(0.6921, 0.2043, 0.1036)

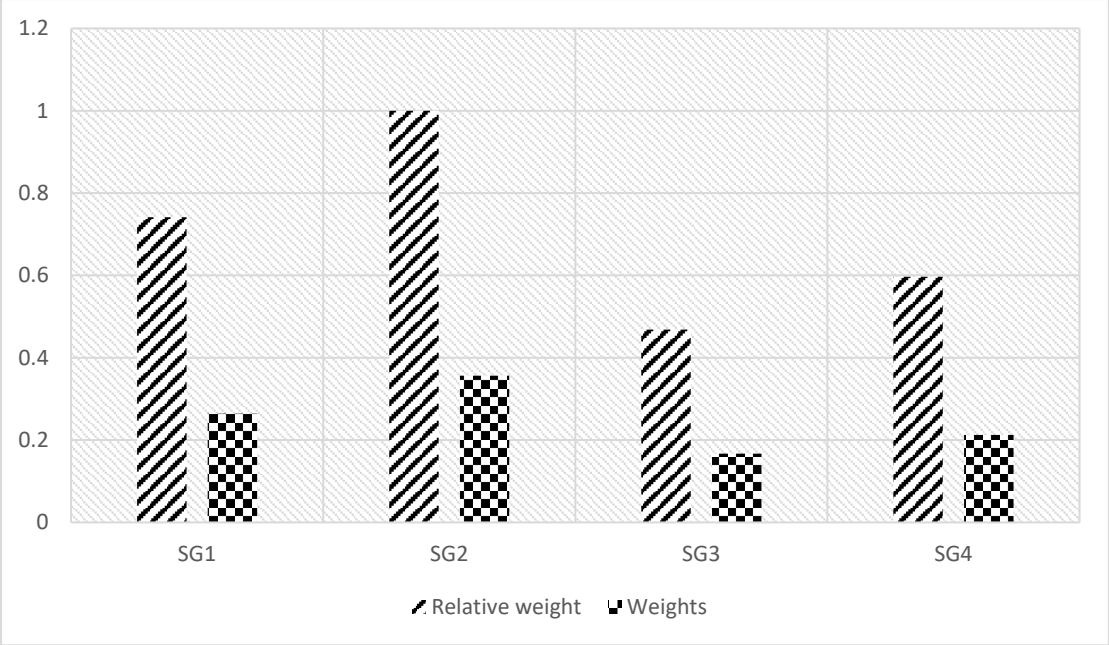

Figure 3. The weights and relative weights or criteria.

Table 4. The NDD.

Alternatives	SA_1	SA_2	SA_3	SA_4	SA_5
SA_1	0.0000	-2.8637	3.0170	2.4587	-3.8237
SA_2	-0.3372	0.0000	2.9214	-1.1111	-1.5806
SA_3	-3.3360	1.6102	0.0000	2.1658	-1.4228
SA_4	0.2667	-3.3769	3.5632	0.0000	-1.0893
SA_5	0.2454	-0.4505	-0.0180	-0.4167	0.0000

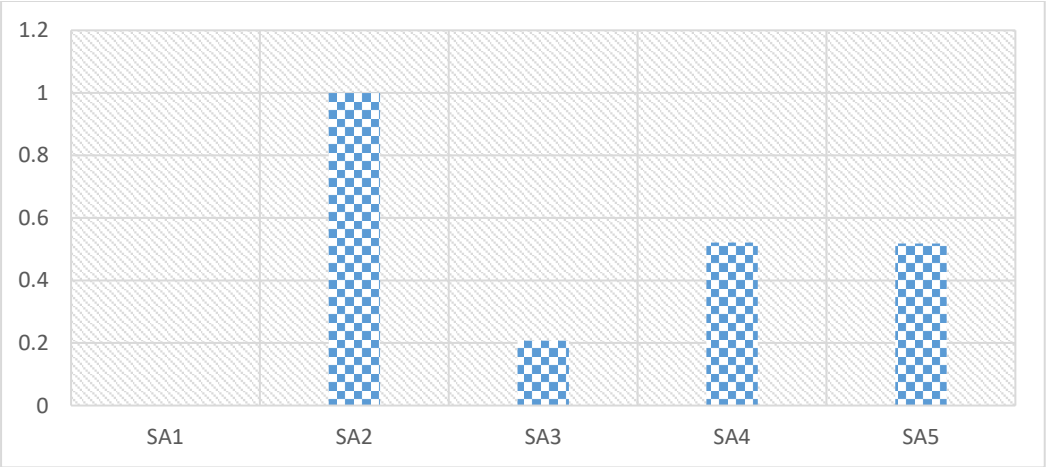

Figure 4. The SVNNDD values.

5.2. Comparative analysis

The SVNN-Com-ExpTODIM is compared with SVNNWA approach [32] and SVNNWG approach[32], SVNN-CODAS approach [34], SVNN-EDAS approach [35], SVNN-TOPSIS approach [36] and SVNN-TODIM approach [37]. The final comparative order is conveyed in Figure 5.

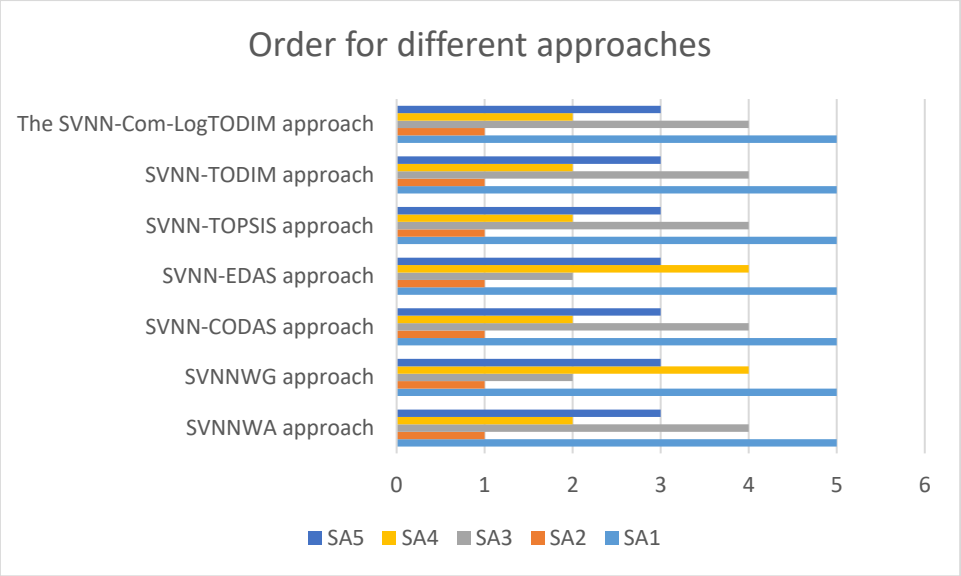

Figure 5. Order for different approaches

From detailed analysis, it could be conveyed that order of these approaches is slightly different, however, these approaches have same optimal MPPT controller design scheme for photovoltaic systems and worst MPPT controller design scheme for photovoltaic systems. This conveyed the SVNN-Com-ExpTODIM is effective.

In comparison with existing methods, the SVNN-Com-ExpTODIM method proposed in this paper demonstrates significant advantages, making it more effective and robust when evaluating the design quality of MPPT controllers in photovoltaic systems. Three key advantages of the proposed approach are conveyed:

(1) Stronger ability to handle uncertainty: The SVNN-Com-ExpTODIM method integrates SVNNs with the Exponential TODIM theory, and by introducing the SVNNHD and SVNNED, it can more accurately handle uncertainty and fuzzy data. This allows the method to better capture the fuzziness and uncertainty in complex decision-making problems, resulting in more accurate and reliable evaluation outcomes.

(2) Effectively considers decision-makers' behavior preferences: The SVNN-Com-ExpTODIM method, through the exponential version of the TODIM model, is better equipped

to model different decision-makers' behavior preferences, especially risk-averse and risk-seeking behaviors. This enables the method to adjust the decision-making process based on varying decision-makers' attitudes, providing ranking results that align more closely with real-world decision-making scenarios, and enhancing the method's flexibility in group decision-making.

(3) Adaptability to complex environmental conditions: The SVNN-Com-ExpTODIM method demonstrates better adaptability in dynamic environments, effectively handling complex conditions common in photovoltaic systems (such as sunlight variation and temperature fluctuations). Compared to existing methods, this approach comprehensively considers multiple environmental factors, ensuring stable evaluation results across different scenarios, thus improving the effectiveness of MPPT controller design quality assessments.

5.3. Sensitivity analysis

Inspired through sensitivity analysis methodology described in [38], an extensive investigation is carried out to evaluate how changes in parameter values influence the performance of the SVNN-Com-ExpTODIM method. This analysis is performed for two distinct DMs behavioral profiles: one characterized by risk aversion and the other by risk seeking. The parameter values used in the analysis are varied within the range of [1, 5]. A comprehensive summary of the sensitivity analysis results can be found in Figure 6.

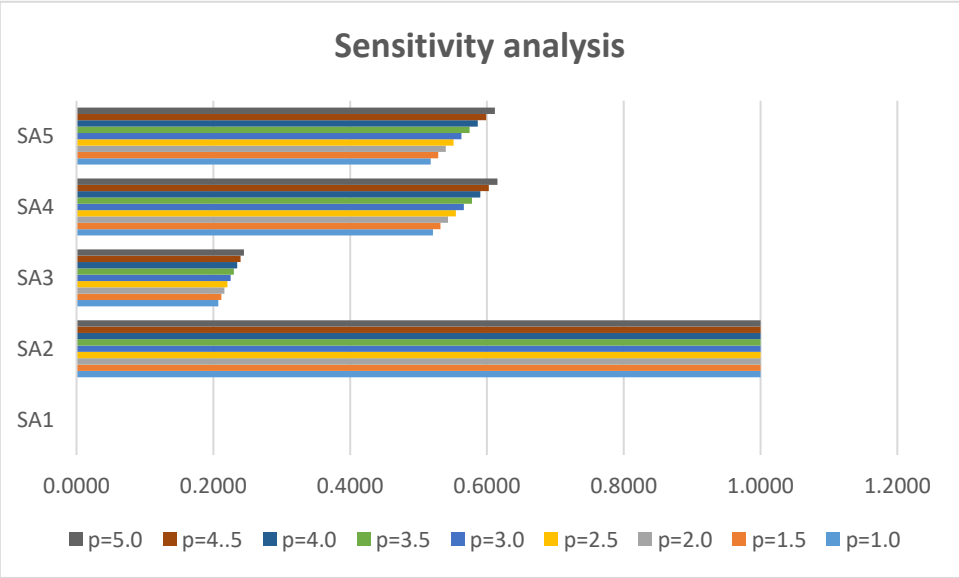

Figure 6. NDD for different ρ

6. Conclusion

The primary purpose of evaluating the design quality of MPPT controllers in photovoltaic systems is to ensure that the system can effectively track the maximum power point under varying environmental conditions, thereby maximizing the energy output of solar power generation. By assessing key indicators such as tracking efficiency, dynamic response speed, steady-state error, and disturbance rejection capability, the controller's design and tuning can be optimized to ensure efficient and stable performance in real-world applications. A high-quality MPPT controller not only enhances the overall power generation efficiency of the photovoltaic system but also maintains stable operation under complex weather conditions, minimizing energy loss. Furthermore, evaluating the controller's design quality helps prevent potential failures, extends the equipment's lifespan, and reduces maintenance and operating costs. Ultimately, this evaluation lays the foundation for ensuring the long-term reliability and cost-effectiveness of photovoltaic systems, contributing to the overall improvement of solar power generation efficiency. The quality evaluation of MPPT controller design for photovoltaic systems is considered a MAGDM problem. In this context, the ExpTODIM approach is introduced to address the MAGDM. Specifically, SVNSs are utilized as a decision-making tool to represent fuzzy data during the quality evaluation process. This study proposes the SVNN-Com-ExpTODIM approach to solve the MAGDM problem under SVNSs. To validate this approach, a numerical study for the quality evaluation of MPPT controller design in photovoltaic systems is conducted, supported by comparative analysis. The key research motivations of this study are as follows: (1) The entropy method is applied to determine the weight for SVNSs; (2) The SVNN-Com-ExpTODIM approach is proposed to solve the MAGDM under SVNSs; (3) A numerical study for the quality evaluation of MPPT controller design is conducted; and (4) Several comparisons are made to validate the effectiveness of the SVNN-Com-ExpTODIM approach.

Although the SVNN-Com-ExpTODIM method proposed in this paper demonstrates a certain degree of innovation and effectiveness in evaluating the design quality of MPPT controllers in photovoltaic systems, there are still some shortcomings. In future research, these limitations can be addressed through improvements, and new research directions can be explored. Below are the research deficiencies in this paper and potential future research directions: (1) Limitations of Parameter Sensitivity Analysis: While the paper conducts a sensitivity analysis regarding parameter variations, the range of parameters analyzed is relatively narrow (limited to the [1, 5] interval). This restricted range may not be sufficient to

fully evaluate all potential impacts of parameter variations on model performance, especially in more complex photovoltaic systems or under extreme environmental conditions. (2) Insufficient Consideration of Dynamic Environmental Diversity: The operating environment of photovoltaic systems is complex and variable. In actual applications, fluctuations in environmental factors (such as sunlight intensity, temperature changes, etc.) can significantly affect the performance of MPPT controllers. The model presented in this paper does not fully capture the diversity of such dynamic environments, and its evaluation results may not accurately reflect the complexities encountered in real-world usage. (3) Weight Allocation Issues in Group Decision-Making: In multiple-attribute group decision-making problems, the opinions of different decision-makers may carry different weights. This paper does not thoroughly explore the weight allocation among different decision-makers, which could lead to certain opinions being over- or under-represented, thereby affecting the fairness and reliability of the decision-making process.

In future research, addressing the deficiencies, the following directions can be explored to enhance the comprehensiveness and applicability of the MPPT controller quality evaluation method, and to provide more practical solutions for optimizing photovoltaic systems. (1) Expanding the Range of Parameter Sensitivity Analysis: The current sensitivity analysis is limited in terms of parameter range. Future research could expand the analysis beyond the [1, 5] interval to encompass a broader set of parameter configurations. This would facilitate a deeper understanding of how parameter variations affect overall model performance. Additionally, incorporating simulation tests under various environmental conditions could provide a more comprehensive evaluation of the adaptability and robustness of the SVNN-Com-ExpTODIM method in complex scenarios. Such an expansion would offer stronger support for the model's reliability in real-world applications. (2) Introducing Dynamic Environmental Modeling: To better reflect the complex environmental changes that photovoltaic systems face during actual operation, future research could consider incorporating dynamic environmental modeling into the evaluation framework. For instance, by introducing time series analysis or dynamic simulation tools, it would be possible to simulate the performance of photovoltaic systems under varying conditions such as different sunlight intensities and temperatures. This dynamic modeling would allow the SVNN-Com-ExpTODIM method to more accurately assess MPPT controller performance in fluctuating environments, thereby enhancing its practical value in real-world scenarios. (3) Optimizing Weight Allocation Mechanisms: In MAGDM, the opinions of different decision-makers may carry different levels of importance. Future research could explore more flexible weight

allocation mechanisms to optimize the decision-making process. For example, using entropy weighting, fuzzy set theory, or preference-based dynamic weight allocation methods could provide a more reasonable reflection of the influence of different decision-makers. This would ensure the fairness and rationality of group decisions, further improving the applicability and effectiveness of the SVNN-Com-ExpTODIM method in group decision-making contexts.

Acknowledgments

The authors would like to acknowledge the guided project of Fujian Provincial Science and Technology Department (No. 2022H0029), Science and Education Development Fund Project of Fujian Chuanzheng Communications College (No. 20220203, No. 20200305), Digital Design and Advanced Manufacturing Technology Service Team of Transportation Machinery of Fujian Chuanzheng Communications College of China.

References

[1] X. Cao, Design of mppt controller for independent photovoltaic street lamp system, in, Ocean University of China, 2007.

[2] F. Gong, Research and design of mppt controller in solar photovoltaic street lamp system, in, Zhejiang University, 2007.

[3] K. Yu, L. Kang, Research on mppt controller for photovoltaic system based on power feedback, Power Electronics Technology, 44 (2010) 4-8.

[4] D. Lai, Development of mppt controller for small-scale photovoltaic power generation system, in, South China University of Technology, 2012.

[5] Y. Zhong, Design of dsp-based mppt controller for photovoltaic power generation system, in, Nanjing Normal University, 2014.

[6] X. Zheng, Application of neural network fuzzy pid technology in mppt controller of photovoltaic system, Journal of Changchun University of Science and Technology (Natural Science Edition), 38 (2015) 102-106.

[7] Y. Fu, Research on photovoltaic system design based on mppt controller, in, Chang'an University, 2015.

[8] D. Zhang, Design of dsp-based mppt controller for photovoltaic power generation system, in, Changchun University of Technology, 2016.

[9] X. Fang, X. Wang, Design of mppt controller for photovoltaic system, Science and Technology Innovation and Application, 2019 (2019) 94-95.

[10] A. Kanchana, D. Nagarajan, S. Broumi, Multi-attribute group decision-making based on the neutrosophic bonferroni mean operator, Neutrosophic Sets and Systems, 57 (2023) 139-164.

[11] W. Li, J. Ye, E. Turkarslan, Magdm model using the aczel-alsina aggregation operators of neutrosophic entropy elements in the case of neutrosophic multi-valued sets, Neutrosophic Sets and Systems, 57 (2023).

[12] D. Nagarajan, V.M. Gobinath, S. Broumi, Multicriteria decision making on 3d printers for economic manufacturing using neutrosophic environment, Neutrosophic Sets and Systems, 57 (2023) 33-56.

[13] L. Niu, J. Ye, Magdm technique based on linguistic neutrosophic tangent dombi aggregation operators and its application in selecting new energy design schemes, Neutrosophic Sets and Systems, 70 (2024) 137-154.

[14] Y.A. Alhasan, F. Smarandache, R.A. Abdulfatah, The indefinite symbolic plithogenic integrals, Neutrosophic Sets and Systems, 60 (2023) 29-38.

[15] M. Jdid, F. Smarandache, The graphical method for finding the optimal solution for neutrosophic linear models and taking advantage of non-negativity constraints to find the optimal solution for some neutrosophic linear models in which the number of unknowns is more than three, Neutrosophic Sets and Systems, 58 (2023) 68-80.

[16] F. Smarandache, New types of topologies and neutrosophic topologies (improved version), Neutrosophic Sets and Systems, 57 (2023) 234-244.

[17] M. Jdid, F. Smarandache, Neutrosophic vision of the expected opportunity loss criterion (neol) decision making under risk, Neutrosophic Sets and Systems, 65 (2024) 110-118.

[18] M. Touqeer, R. Umer, N.A. Mohammad, M. Salimi, A. Ahmadian, Signed distance-based approach for multiple criteria group decision-making with incomplete information using interval type-2 neutrosophic numbers, Multimedia Tools and Applications, 83 (2024) 8439-8466.

[19] A. Nafei, C.Y. Huang, A. Javadpour, H. Garg, S.P. Azizi, S.C. Chen, Neutrosophic fuzzy decision-making using topsis and autocratic methodology for machine selection in an industrial factory, International Journal of Fuzzy Systems, 26 (2024) 860-886.

[20] X.D. Peng, J.G. Dai, F. Smarandache, Research on the assessment of project-driven immersion teaching in extreme programming with neutrosophic linguistic information, International Journal of Machine Learning and Cybernetics, 14 (2023) 873-888.

[21] Z. Turskis, R. Bausys, F. Smarandache, G. Kazakeviciute-Januskeviciene, E.K. Zavadskas, M-generalised q-neutrosophic extension of cocoso method, International Journal of Computers Communications & Control, 17 (2022) 12.

[22] S.Z. Zeng, M. Shoaib, S. Ali, F. Smarandache, H. Rashmanlou, F. Mofidnakhaei, Certain properties of single-valued neutrosophic graph with application in food and agriculture organization, International Journal of Computational Intelligence Systems, 14 (2021) 1516-1540.

[23] N.T. Thong, F. Smarandache, N.D. Hoa, L. Son, L.T.H. Lan, C.N. Giap, D.T. Son, H.V. Long, A novel dynamic multi-criteria decision making method based on generalized dynamic interval-valued neutrosophic set, Symmetry-Basel, 12 (2020) 20.

[24] C.E. Shannon, A mathematical theory of communication, Bell System Technical Journal, 27 (1948) 379-423.

[25] L. Gomes, L.A.D. Rangel, An application of the todim method to the multicriteria rental evaluation of residential properties, European Journal of Operational Research, 193 (2009) 204-211.

[26] L. Gomes, L.A.D. Rangel, F.J. Maranhao, Multicriteria analysis of natural gas destination in brazil: An application of the todim method, Mathematical and Computer Modelling, 50 (2009) 92-100.

[27] A.B. Leoneti, L. Gomes, A novel version of the todim method based on the exponential model of prospect theory: The exptodim method, European Journal of Operational Research, 295 (2021) 1042-1055.

[28] H. Sun, Z. Yang, Q. Cai, G. Wei, Z. Mo, An extended exp-todim method for multiple attribute decision making based on the z-wasserstein distance, Expert Systems with Applications, 214 (2023) 119114.

[29] H. Wang, F. Smarandache, Y.Q. Zhang, R. Sunderraman, Single valued neutrosophic sets, Multispace Multistruct, (2010) 410-413.

[30] J. Ye, Single valued neutrosophic cross-entropy for multicriteria decision making problems, Applied Mathematical Modelling, 38 (2014) 1170-1175.

[31] F.A. Smarandache, Unifying field in logics. Neutrosophy: Neutrosophic probability, set and logic,

American Research Press, Rehoboth, 1999.

[32] J.J. Peng, J.Q. Wang, J. Wang, H.Y. Zhang, X.H. Chen, Simplified neutrosophic sets and their applications in multi-criteria group decision-making problems, International Journal of Systems Science, 47 (2016) 2342-2358.

[33] P. Majumdar, S.K. Samanta, On similarity and entropy of neutrosophic sets, Journal of Intelligent & Fuzzy Systems, 26 (2014) 1245-1252.

[34] E. Bolturk, A. Karasan, Prioritization of investment alternatives for a hospital by using neutrosophic codas method, Journal of Multiple-Valued Logic and Soft Computing, 33 (2019) 381-396.

[35] D. Stanujkic, D. Karabasevic, G. Popovic, D. Pamucar, Z. Stevic, E.K. Zavadskas, F. Smarandache, A single-valued neutrosophic extension of the edas method, Axioms, 10 (2021) 13.

[36] P. Biswas, S. Pramanik, B.C. Giri, Topsis method for multi-attribute group decision-making under single-valued neutrosophic environment, Neural Computing & Applications, 27 (2016) 727-737.

[37] D.S. Xu, C. Wei, G.W. Wei, Todim method for single-valued neutrosophic multiple attribute decision making, Information, 8 (2017) 125.

[38] J. Więckowski, W. Sałabun, Sensitivity analysis approaches in multi-criteria decision analysis: A systematic review, Applied Soft Computing, 148 (2023) 110915.

Received: July 20, 2024. Accepted: Oct 22, 2024

NSS
Neutrosophic Sets and Systems, Vol. 76 2025
University of New Mexico

Incorporating Intelligence in Multiple-Attribute Decision-Making using Algorithmic Framework and Double-Valued Neutrosophic Sets: Varied Applications to Employment Quality Evaluation for University Graduates

Qiuyan Zhao*, Wentao Li

Henan University of Science and Technology, Luoyang, 471000, Henan, China

(Wentao Li, E-mail: hfy@haust.edu.cn)

*Corresponding author, E-mail: zhaoqiuyan@huast.edu.cn

https://orcid.org/0009-0006-3016-3638

Abstract: The evaluation of university employment quality is a comprehensive assessment of graduates' employment status and its alignment with market demands. This evaluation typically includes indicators such as employment rate, the relevance of job positions to majors, salary levels, job stability, and job satisfaction. By analyzing this data, universities can understand how graduates perform in the job market, assess the effectiveness of talent cultivation, and provide reference points for optimizing curriculum design, teaching methods, and industry-education integration. The employment quality evaluation for university graduates a MADM. Currently, Logarithmic TODIM (LogTODIM) and GRA techniques are employed to address MADM challenges. To handle uncertain data in this evaluation, the double-valued neutrosophic sets (DVNSs) have been introduced. This study constructs the double-valued neutrosophic number Logarithmic TODIM-GRA (DVNN-LogTODIM-GRA) technique to manage the MADM problem under DVNSs. To validate the proposed technique, a numerical study is conducted focusing on the employment quality evaluation for university graduates. The main contributions of this study are constructed: (1) The use of entropy to determine weight values under DVNSs; (2) The application of the DVNN-LogTODIM-GRA technique to effectively manage MADM; (3) The verification of the DVNN-LogTODIM-GRA technique through a numerical example related to the employment quality evaluation for university graduates.

Keywords: Multiple Attributes; Neutrosophic Sets; Decision Making; TODIM.

1. Introduction

According to statistics from the Ministry of Education, the number of university graduates nationwide in 2024 will reach 11.79 million, an increase of 210,000 compared to the previous year. In the context of a rapidly growing number of university graduates and a job market where the demand for talent significantly lags behind supply, the employment situation is becoming increasingly severe, with structural employment conflicts among university graduates becoming more prominent. The coexistence of "difficulty in finding jobs" and "difficulty in hiring" remains persistent in the job market. As the main institutions responsible for talent cultivation, universities—especially "comprehensive applied universities"—should, while adhering to their functional positioning and pursuing distinctive development, place greater emphasis on "serving local economic and social development" as a key pillar for continuously improving their talent cultivation programs. This will help align university

talent training more closely with market demands and enhance job-person fit. Therefore, exploring the construction of a graduate employment quality evaluation system that aligns with the needs of local economic development is crucial. This system should evaluate employment quality from both the perspectives of graduates and employers, with a focus on the alignment between university talent cultivation objectives and the needs of national and local economic development sectors. This is not only in response to the need presented in the General Plan for Deepening the Reform of Educational Evaluation in the New Era issued by the Central Committee of the Communist Party of China and the State Council, which calls for continuous improvement of university evaluation systems but also serves to strengthen the interaction between higher education and social development. Furthermore, it enhances the performance of universities in their development, meets the need for talent cultivation to align with local economic development, and fosters mutual empowerment and harmonious growth between universities and society. In recent years, the evaluation of university graduate employment quality has been a focal point of academic research. With the rapid development of the economy, scholars have gradually deepened their exploration in this field. Ma [1] was among the first to reflect on the existing university graduate employment quality evaluation system, analyzing its shortcomings and proposing strategies for improvement, aiming to ensure that the evaluation system could achieve its intended outcomes 101010. Following this, Chen [2] analyzed the current state of university student employment quality evaluation and emphasized the necessity of constructing an evaluation index system, while also providing specific application suggestions. In 2019, Qi and Cheng [3] summarized relevant literature and practical experience in employment guidance, categorizing employment quality into three dimensions: graduate satisfaction, social evaluation satisfaction, and employer satisfaction. They used the Delphi method and the Analytic Hierarchy Process (AHP) to construct a systematic evaluation framework. Wei [4] integrated big data mining technology into the employment quality evaluation model, addressing the low reliability of traditional models. By introducing big data, this model was able to capture employment trends more effectively and improve the scientific rigor of the evaluation results. In the same year, Yang, Qiu, and Guo [5] conducted a systematic review of employment quality evaluation research over the past decade, pointing out the lack of quantitative analysis in existing studies and suggesting that future research should focus on enhancing data collection and analysis for employment tracking. Gu and Lin [6] further explored how to construct a scientific and reasonable university graduate employment quality evaluation system. They proposed that graduate employment quality involves not only employment rates but also multiple dimensions such as university positioning and discipline construction. Liang, Zhang, and Liang [7] focused on industry-specific universities and analyzed the factors affecting employment quality from the perspectives of graduates, universities, employers, and society. They constructed a multi-layered employment quality evaluation system and refined the fuzzy comprehensive evaluation model using AHP and expert scoring. Cao and Yi [8] concentrated on graduates in Hunan province and developed a more comprehensive employment quality evaluation index system. This system integrated domestic and international research findings and determined indicator weights using AHP, covering five

dimensions: government, universities, employers, society, and students. Zhang, Li and Ye [9] introduced the CIPP model in their study, using the four dimensions of "context, input, process, and product" to construct a university graduate employment quality evaluation system. They applied AHP to determine indicator weights and validated the system's feasibility. The most recent study by Yan, Pei and Li [10] approached the evaluation from the perspective of universities serving local economic development. Based on higher education political theory, this study constructed a more focused and quantifiable employment quality evaluation system and provided targeted suggestions to promote positive cycles between talent cultivation and industrial demand.

MADM is a significant area of research in management science [11-15]. It finds wide applications in real-life scenarios such as investment project decision evaluation, supplier selection analysis, and location site selection [16-20]. MADM can be divided into two key parts: the expression of expert decision-making opinions and the selection of alternative solutions [21-25]. In the first part, the complexity of external factors and human-bounded rationality often leads to fuzzy decision-making outcomes [26-29]. To address this, scholars commonly employ fuzzy sets to gather expert evaluations. In the second part, the method of comparing and ranking schemes is typically used to identify the optimal solution [30-35]. The employment quality evaluation for university graduates falls under the category of MADM. To tackle MADM challenges in this context, researchers have recently utilized the LogTODIM [36] and GRA techniques [37]. Additionally, the DVNSs [38] have been proposed to characterize uncertain data during the evaluation process. In this study, we employ the DVNN-LogTODIM-GRA technique to address MADM with DVNSs. To validate the proposed technique, a numerical study is conducted, focusing on the employment quality evaluation for university graduates. The key goals and motivations of this study are constructed: (1) Utilizing the entropy to determine weight values under DVNSs; (2) Applying the DVNN-LogTODIM-GRA technique to effectively manage MADM; (3) Conducting the numerical example to validate the effectiveness of the DVNN-LogTODIM-GRA for employment quality evaluation for university graduates.

2. Preliminaries

Kandasamy [38] constructed the DVNSs.

Definition 1 [38]. The DVNSs are constructed:

$$LA=\left\{\left(\theta,LT_A(\theta),LIT_A(\theta),LIF_A(\theta),LF_A(\theta)\right)\middle|\theta\in\Theta\right\}. \tag{1}$$

With truth-membership $LT_A(\theta)$, $LIT_A(\theta)$ stands for indeterminacy leaning towards $LT_A(\theta)$, $LIF_A(\theta)$ stands for indeterminacy leaning towards $LT_A(\theta)$ and falsity-

membership $LF_A(\theta)$, $LT_A(\theta), LIT_A(\theta), LIF_A(\theta), LF_A(\theta) \in [0,1]$,

$0 \le LT_A(\theta) + LIT_A(\theta) + LIF_A(\theta) + LF_A(\theta) \le 4$.

The DVNN is expressed as $LA = (LT_A, LIT_A, LIF_A, LF_A)$, where

$LT_A, LIT_A, LIF_A, LF_A \in [0,1]$, $0 \le LT_A + LIT_A + LIF_A + LF_A \le 4$.

Definition 2[38]. Let $LA = (LT_A, LIT_A, LIF_A, LF_A)$ be DVNN, score value (SV) is conducted:

$$SV(LA) = \frac{(2 + LT_A + LIT_A - LIF_A - LF_A)}{4},\ SV(LA) \in [0,1]. \quad (2)$$

Definition 3[38]. Let $LA = (LT_A, LIT_A, LIF_A, LF_A)$ be DVNN, accuracy value (AV) is conducted:

$$AV(LA) = \frac{(LT_A + LIT_A + LIF_A + LF_A)}{4},\ AV(LA) \in [0,1]\ . \quad (3)$$

The order is constructed for DVNNs.

Definition 4[38]. Let $LA = (LT_A, LIT_A, LIF_A, LF_A)$ and $LB = (LT_B, LIT_B, LIF_B, LF_B)$,

$SV(LA) = \frac{(2 + LT_A + LIT_A - LIF_A - LF_A)}{4}$, $SV(LB) = \frac{(2 + LT_B + LIT_B - LIF_B - LF_B)}{4}$,

$AV(LA) = \frac{(LT_A + LIT_A + LIF_A + LF_A)}{4}$, $AV(LB) = \frac{(LT_B + LIT_B + LIF_B + LF_B)}{4}$, if

$SV(LA) < SV(LB)$, $LA < LB$; if $SV(LA) = SV(LB)$, (1)if $AV(LA) = AV(LB)$,

$LA = LB$; (2) if $AV(LA) < AV(LB)$, $LA < LB$.

Definition 5[38]. Let $LA = (LT_A, LIT_A, LIF_A, LF_A)$ and $LB = (LT_B, LIT_B, LIF_B, LF_B)$ be DVNNs, the operations are conducted:

(1) $LA \oplus LB = (LT_A + LT_B - LT_A LT_B, LIT_A + LIT_B - LIT_A LIT_B, LIF_A LIF_B, LF_A LF_B)$;

(2) $LA \otimes LB = (LT_A LT_B, LIT_A LIT_B, LIF_A + LIF_B - LIF_A LIF_B, LF_A + LF_B - LF_A LF_B)$;

(3) $\lambda LA = \left(1-(1-LT_A)^{\lambda}, 1-(1-LIT_A)^{\lambda}, (LIF_A)^{\lambda}, (LF_A)^{\lambda}\right), \lambda > 0$;

(4) $(LA)^{\lambda} = \left((LT_A)^{\lambda}, (LIT_A)^{\lambda}, 1-(1-LIF_A)^{\lambda}, 1-(1-LF_A)^{\lambda}\right), \lambda > 0.$

Definition 6[38]. Let $LA=\left(LT_A, LIT_A, LIF_A, LF_A\right)$ and $LB=\left(LT_B, LIT_B, LIF_B, LF_B\right)$, the DVNN Euclidean distance (DVNNED) between $LA=\left(LT_A, LIT_A, LIF_A, LF_A\right)$ and $LB=\left(LT_B, LIT_B, LIF_B, LF_B\right)$ is:

$$\begin{aligned} &DVNNED\left(LA, LB\right) \\ &=\sqrt{\frac{1}{4}\left(\left|LT_A-LT_B\right|^2+\left|LIT_A-LIT_B\right|^2+\left|LIF_A-LIF_B\right|^2+\left|LF_A-LF_B\right|^2\right)} \end{aligned} \tag{4}$$

3. Algorithm

3.1. MADM problem with DVNNs

The DVNN-LogTODIM-GRA technique is conducted for MADM. Let $LA=\left\{LA_1, LA_2, \cdots, LA_m\right\}$ be alternatives, and $LG=\left\{LG_1, LG_2, \cdots, LG_n\right\}$ be attributes with weight lw, where $lw_j \in [0,1]$, $\sum_{j=1}^{n} lw_j = 1$. Then, DVNN-LogTODIM-GRA technique is conducted for MADM (See Figure 1).

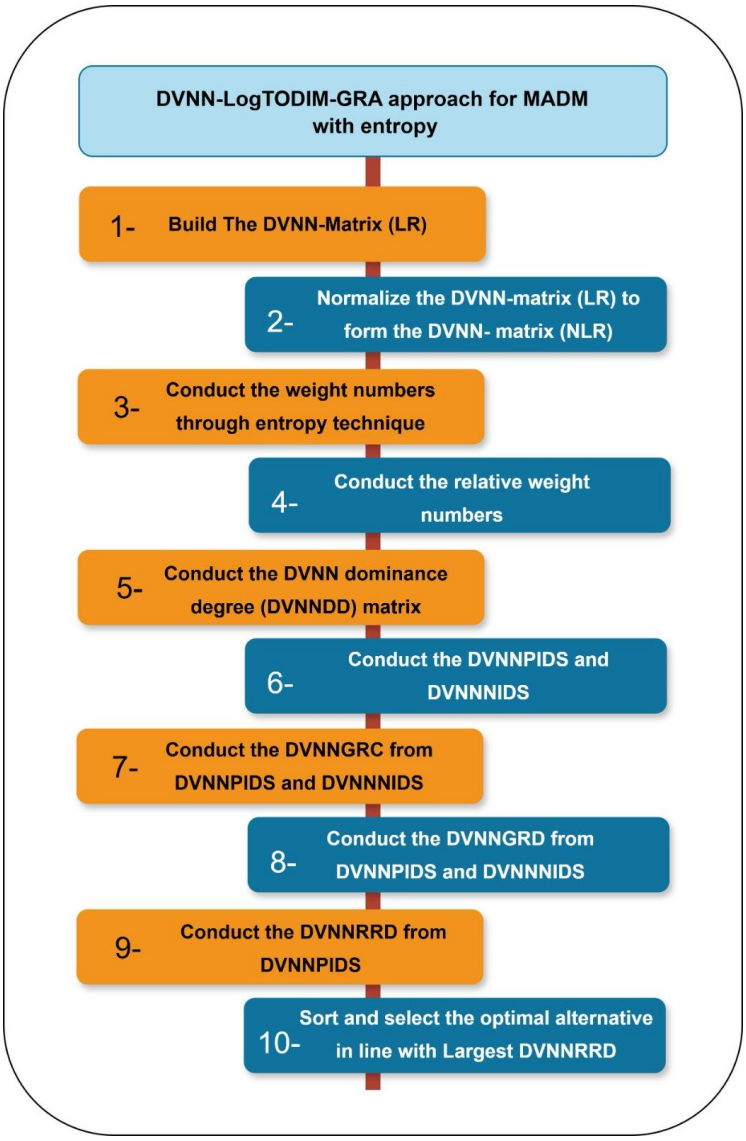

Figure 1. DVNN-LogTODIM-GRA approach for MADM with entropy

Step 1. Conduct the DVNN-matrix $LR=\left[LR_{ij}\right]_{m\times n}=\left(LT_{ij},LIT_{ij},LIF_{ij}\,LF_{ij}\right)_{m\times n}$

$$LR=\left[LR_{ij}\right]_{m\times n}=\begin{array}{c} \\ LA_1 \\ LA_2 \\ \vdots \\ LA_m \end{array}\begin{array}{c} \begin{array}{cccc} LG_1 & LG_2 & \ldots & LG_n \end{array} \\ \begin{bmatrix} LR_{11} & LR_{12} & \ldots & LR_{1n} \\ LR_{21} & LR_{22} & \ldots & LR_{2n} \\ \vdots & \vdots & \vdots & \vdots \\ LR_{m1} & LR_{m2} & \ldots & LR_{mn} \end{bmatrix} \end{array} \tag{5}$$

Step 2. Normalize the $LR=\left[LR_{ij}\right]_{m\times n}=\left(LT_{ij},LIT_{ij},LIF_{ij}\,LF_{ij}\right)_{m\times n}$ into $NLR=\left[LR_{ij}\right]_{m\times n}=\left(NLT_{ij},NLIT_{ij},NLIF_{ij}\,NLF_{ij}\right)_{m\times n}$.

For benefit attributes:

$$NLR_{ij}=\left(LT_{ij},LIT_{ij},LIF_{ij}\,LF_{ij}\right)=\left(LT_{ij},LIT_{ij},LIF_{ij}\,LF_{ij}\right) \tag{6}$$

For cost attributes:

$$NLR_{ij} = \left(LT_{ij} , LIT_{ij} , LIF_{ij} \, LF_{ij} \right) = \left(LF_{ij} , LIF_{ij} , LIT_{ij} \, LT_{ij} \right) \tag{7}$$

3.2. Conduct the weight numbers through entropy.

Step 3. Conduct the weight numbers through entropy.

Entropy technique [39] is put forward obtaining weight numbers. The normalized DVNN-matrix $NDVNNM_{ij}$ is conducted:

$$NDVNNM_{ij} = \frac{\begin{pmatrix} SV\left(NLT_{ij} , NLIT_{ij} , NLIF_{ij} \, NLF_{ij} \right) \\ +AV\left(NLT_{ij} , NLIT_{ij} , NLIF_{ij} \, NLF_{ij} \right) \end{pmatrix}}{\sum_{i=1}^{m} \begin{pmatrix} SV\left(NLT_{ij} , NLIT_{ij} , NLIF_{ij} \, NLF_{ij} \right) \\ +AV\left(NLT_{ij} , NLIT_{ij} , NLIF_{ij} \, NLF_{ij} \right) \end{pmatrix}}, \tag{8}$$

The DVNN Shannon decision entropy (DVNNSDE) is managed:

$$DVNNSDE_{j} = -\frac{1}{\ln m} \sum_{i=1}^{m} NDVNNM_{ij} \ln NDVNNM_{ij} \tag{9}$$

and $NDVNNM_{ij} \ln NDVNNM_{ij} = 0$ if $NDVNNM_{ij} = 0$.

Then, the weight values $lw = \left(lw_1, lw_2, \cdots, lw_n \right)$ is conducted:

$$lw_j = \frac{1 - DVNNSDE_j}{\sum_{j=1}^{n} \left(1 - DVNNSDE_j \right)} , \quad j = 1, 2, 3, \cdots, n. \tag{10}$$

3.3. DVNN-LogTODIM-GRA approach for MADM

The DVNN-LogTODIM-GRA approach is conducted for MADM.

Step 4. Conduct relative weight:

$$rlw_j = lw_j \Big/ \max_j lw_j , \tag{11}$$

Step 5. Conduct the overall DVNN dominance degree (DVNNDD).

(1) The $DVNNDD_j \left(LA_i, LA_\xi \right)$ of LA_i over LA_ξ for LG_j is conducted:

$$DVNNDD_j\left(LA_i, LA_\xi\right) = \begin{cases} \dfrac{rlw_j \times \log\left(1+10\rho DVNNED\left(NLR_{ij}, NLR_{\xi j}\right)\right)}{\sum_{j=1}^{n} rlw_j} & \text{if } SV\left(NLR_{ij}\right) > SV\left(NLR_{\xi j}\right) \\ 0 & \text{if } SV\left(NLR_{ij}\right) = SV\left(NLR_{\xi j}\right) \\ -\dfrac{1}{\theta}\dfrac{\sum_{j=1}^{n} rlw_j \times \left(1-10^{-DVNNED\left(NLR_{ij}, NLR_{\xi j}\right)}\right)}{rlw_j} & \text{if } SV\left(NLR_{ij}\right) < SV\left(NLR_{\xi j}\right) \end{cases} \tag{12}$$

where $\lambda \in [1,5]$ and $\rho \in N^+$ is managed from agent's perception[36].

(2) The DVNNDD matrix $DVNNDD_j\left(LA_i\right)\left(j=1,2,\cdots,n\right)$ for LG_j is administrated:

$$DVNNDD_j\left(LA_i\right) = \left[DVNNDD_j\left(LA_i, LA_\xi\right)\right]_{m\times m} = \begin{array}{c} \\ LA_1 \\ LA_2 \\ \vdots \\ LA_m \end{array} \begin{array}{c} \begin{array}{cccc} LA_1 & LA_2 & \cdots & LA_m \end{array} \\ \begin{bmatrix} 0 & DVNNDD_j\left(LA_1, LA_2\right) & \cdots & DVNNDD_j\left(LA_1, LA_m\right) \\ DVNNDD_j\left(LA_2, LA_1\right) & 0 & \cdots & DVNNDD_j\left(LA_2, LA_m\right) \\ \vdots & \vdots & \cdots & \vdots \\ DVNNDD_j\left(LA_m, LA_1\right) & DVNNDD_j\left(LA_m, LA_2\right) & \cdots & 0 \end{bmatrix} \end{array}$$

(3) Administrate the DVNNDD of LA_i for other alternatives under LG_j:

$$DVNNDD_j\left(LA_i\right) = \sum_{\xi=1}^{m} DVNNDD_j\left(LA_i, LA_\xi\right) \tag{13}$$

(4) The overall DVNNDD is conducted:

$$DVNNDD = \left(DVNNDD_{ij}\right)_{m\times n} = \begin{bmatrix} & LG_1 & LG_2 & \cdots & LG_n \\ LA_1 & \sum_{\xi=1}^{m} DVNNDD_1\left(LA_1, LA_t\right) & \sum_{\xi=1}^{m} DVNNDD_2\left(LA_1, LA_t\right) & \cdots & \sum_{\xi=1}^{m} DVNNDD_n\left(LA_1, LA_t\right) \\ LA_2 & \sum_{\xi=1}^{m} DVNNDD_1\left(LA_2, LA_t\right) & \sum_{\xi=1}^{m} DVNNDD_2\left(LA_2, LA_t\right) & \cdots & \sum_{\xi=1}^{m} DVNNDD_n\left(LA_2, LA_t\right) \\ \vdots & \vdots & \vdots & \vdots & \vdots \\ LA_m & \sum_{\xi=1}^{m} DVNNDD_1\left(LA_m, LA_t\right) & \sum_{\xi=1}^{m} DVNNDD_2\left(LA_m, LA_t\right) & \cdots & \sum_{\xi=1}^{m} DVNNDD_n\left(LA_m, LA_t\right) \end{bmatrix}$$

Step 6. Conduct the DVNNPIDS (DVNN positive ideal decision solution) and DVNNNIDS (DVNN negative ideal decision solution):

$$DVNNPIDS = \left(DVNNPIDS_1, DVNNPIDS_1, \cdots, DVNNPIDS_n\right) \tag{14}$$

$$DVNNNIDS = \left(DVNNNIDS_1, DVNNNIDS_1, \cdots, DVNNNIDS_n \right) \tag{15}$$

$$DVNNPIDS_j = \max_{j=1}^{n} DVNNDD_{ij}, DVNNNIDS_j = \min_{j=1}^{n} DVNNDD_{ij} \tag{16}$$

Step 7. Conduct the DVNNGRC (DVNN grey rational coefficients) from DVNNPIDS and DVNNNIDS:

$$DVNNGRC\left(LA_{ij}, DVNNPIDS_j \right) = \frac{\min\limits_{1\le i\le m}\min\limits_{1\le j\le n}\left|DVNNDD_{ij} - DVNNPIDS_j\right| + \rho \max\limits_{1\le i\le m}\max\limits_{1\le j\le n}\left|DVNNDD_{ij} - DVNNPIDS_j\right|}{\left|DVNNDD_{ij} - DVNNPIDS_j\right| + \rho \max\limits_{1\le i\le m}\max\limits_{1\le j\le n}\left|DVNNDD_{ij} - DVNNPIDS_j\right|} \tag{17}$$

$$DVNNGRC\left(LA_{ij}, DVNNNIDS_j \right) = \frac{\min\limits_{1\le i\le m}\min\limits_{1\le j\le n}\left|DVNNDD_{ij} - DVNNNIDS_j\right| + \rho \max\limits_{1\le i\le m}\max\limits_{1\le j\le n}\left|DVNNDD_{ij} - DVNNNIDS_j\right|}{\left|DVNNDD_{ij} - DVNNNIDS_j\right| + \rho \max\limits_{1\le i\le m}\max\limits_{1\le j\le n}\left|DVNNDD_{ij} - DVNNNIDS_j\right|} \tag{18}$$

Step 8. Conduct the DVNNGRD (DVNN grey relation degree) from DVNNPIDS and DVNNNIDS:

$$DVNNGRD\left(LA_i, DVNNPIDS \right) = \sum_{j=1}^{n}\left(lw_j \times DVNNGRC\left(LA_{ij}, DVNNPIDS_j \right)\right)$$

$$= \sum_{j=1}^{n}\left(lw_j \times \frac{\left(\begin{array}{l} \min\limits_{1\le i\le m}\min\limits_{1\le j\le n}\left|DVNNDD_{ij} - DVNNPIDS_j\right| \\ +\rho \max\limits_{1\le i\le m}\max\limits_{1\le j\le n}\left|DVNNDD_{ij} - DVNNPIDS_j\right| \end{array} \right)}{\left(\begin{array}{l} \left|DVNNDD_{ij} - DVNNPIDS_j\right| \\ +\rho \max\limits_{1\le i\le m}\max\limits_{1\le j\le n}\left|DVNNDD_{ij} - DVNNPIDS_j\right| \end{array} \right)} \right) \tag{19}$$

$$DVNNGRD\left(LA_i, DVNNNIDS \right) = \sum_{j=1}^{n}\left(lw_j \times DVNNGRC\left(LA_{ij}, DVNNNIDS_j \right)\right)$$

$$= \sum_{j=1}^{n}\left(lw_j \times \frac{\left(\begin{array}{l} \min\limits_{1\le i\le m}\min\limits_{1\le j\le n}\left|DVNNDD_{ij} - DVNNNIDS_j\right| \\ +\rho \max\limits_{1\le i\le m}\max\limits_{1\le j\le n}\left|DVNNDD_{ij} - DVNNNIDS_j\right| \end{array} \right)}{\left(\begin{array}{l} \left|DVNNDD_{ij} - DVNNNIDS_j\right| \\ +\rho \max\limits_{1\le i\le m}\max\limits_{1\le j\le n}\left|DVNNDD_{ij} - DVNNNIDS_j\right| \end{array} \right)} \right) \tag{20}$$

Step 9. Conduct the DVNNRRD (DVNN relative relational degree) from DVNNPIDS.

$$DVNNRRD\left(LA_i, DVNNPIDS\right) = \frac{DVNNGRD\left(LA_i, DVNNPIDS\right)}{DVNNGRD\left(LA_i, DVNNNIDS\right) + DVNNGRD\left(LA_i, DVNNPIDS\right)}$$

$$= \frac{\sum_{j=1}^{n}\left(lw_j \times \frac{\left(\min\limits_{1\le i\le m}\min\limits_{1\le j\le n}\left|DVNNDD_{ij} - DVNNPIDS_j\right| + \rho \max\limits_{1\le i\le m}\max\limits_{1\le j\le n}\left|DVNNDD_{ij} - DVNNPIDS_j\right|\right)}{\left(\left|DVNNDD_{ij} - DVNNPIDS_j\right| + \rho \max\limits_{1\le i\le m}\max\limits_{1\le j\le n}\left|DVNNDD_{ij} - DVNNPIDS_j\right|\right)}\right)}{\left(\begin{array}{l}\sum_{j=1}^{n}\left(lw_j \times \frac{\left(\min\limits_{1\le i\le m}\min\limits_{1\le j\le n}\left|DVNNDD_{ij} - DVNNNIDS_j\right| + \rho \max\limits_{1\le i\le m}\max\limits_{1\le j\le n}\left|DVNNDD_{ij} - DVNNNIDS_j\right|\right)}{\left(\left|DVNNDD_{ij} - DVNNNIDS_j\right| + \rho \max\limits_{1\le i\le m}\max\limits_{1\le j\le n}\left|DVNNDD_{ij} - DVNNNIDS_j\right|\right)}\right) \\ + \sum_{j=1}^{n}\left(lw_j \times \frac{\left(\min\limits_{1\le i\le m}\min\limits_{1\le j\le n}\left|DVNNDD_{ij} - DVNNPIDS_j\right| + \rho \max\limits_{1\le i\le m}\max\limits_{1\le j\le n}\left|DVNNDD_{ij} - DVNNPIDS_j\right|\right)}{\left(\left|DVNNDD_{ij} - DVNNPIDS_j\right| + \rho \max\limits_{1\le i\le m}\max\limits_{1\le j\le n}\left|DVNNDD_{ij} - DVNNPIDS_j\right|\right)}\right)\end{array}\right)} \quad (21)$$

Step 10. Sort and select the optimal alternative with the largest DVNNRRD.

4. Analysis and Discussion

The evaluation of university employment quality is a key process in systematically assessing the performance of graduates in the job market. Its purpose is to analyze data from multiple dimensions to measure the alignment between university talent cultivation and market demands, thereby providing a basis for improving teaching and management in universities. Employment quality evaluation not only focuses on the employment rate of graduates but also includes various aspects of employment quality, such as the relevance of job positions to their major, salary levels, job stability, career development prospects, and satisfaction from both graduates and employers. Firstly, the employment rate is one of the most basic metrics, reflecting the percentage of graduates who find jobs within a certain period. However, relying solely on the employment rate does not comprehensively reflect employment quality. Therefore, the evaluation also needs to examine the match between job positions and majors, as well as the application of graduates' skills in their jobs. A high degree

of job-major alignment indicates that the university is effectively responding to industry demands, highlighting the effectiveness of curriculum design, teaching content, and practical skill development. Secondly, salary levels are another important indicator, often used as an indirect measure of graduates' competitiveness in the job market. The salary level not only reflects the demand for specific industries but also, to some extent, indicates the professional skills and market recognition of the graduates. Additionally, the potential for salary growth can help assess the long-term career development opportunities of graduates. Job stability and career development prospects are also crucial aspects of employment quality evaluation. Job stability refers to the continuity of employment over a certain period, which reflects graduates' adaptability to their positions and job-market fit. Career development prospects focus on the long-term growth opportunities and career advancement of graduates, helping to assess their job satisfaction and career planning. Lastly, feedback from both graduates and employers is an important source of information for employment quality evaluation. Surveys on graduates' job satisfaction can help understand their level of contentment with their current employment and their feedback on university education. Employer feedback provides insights into the professional qualities, work attitudes, and skills of graduates, enabling universities to adjust their talent cultivation strategies accordingly. In summary, the evaluation of university employment quality is a multidimensional, comprehensive assessment process. Through data analysis and feedback collection, it aims to help universities improve educational quality and enhance the alignment between talent cultivation and market demand. The employment quality evaluation for university graduates is MADM. There are seven potential local applied undergraduate colleges $LA_i\left(i=1,2,3,4,5,6,7\right)$ are evaluated from four attributes: ①LLG_1 is Employment Rate-The employment rate is the most basic evaluation indicator, reflecting the proportion of graduates who find jobs within a certain period. It is commonly used to measure the overall performance of students trained by universities in the job market and serves as one of the fundamental indicators for assessing employment quality; ②LLG_2 is the Job-Major Relevance- This indicator measures the degree of alignment between the job held by a graduate and their field of study. High relevance indicates that the university's curriculum and program design align well with market demands, and the skills taught are consistent with industry requirements; ③LLG_3 is the Salary Level- Salary level is an important economic indicator of employment quality, reflecting the market competitiveness of graduates and the value of the positions they hold. A higher salary typically signals better career development opportunities and higher job requirements; ④LLG_4 is Job Stability-Job stability refers to a graduate's ability to maintain long-term employment after securing a job. It reflects graduates' adaptability to their positions, the degree of job fit, and their recognition by

employers. It is a long-term dimension used to assess employment quality. The seven potential local applied undergraduate colleges $LA_i\left(i=1,2,3,4,5,6,7\right)$ are evaluated under DVNNs through four attributes.

The DVNN-LogTODIM-GRA technique is put forward the employment quality evaluation for university graduates.

Step 1. Administrate the DVNN-matrix $LR=\left[LR_{ij}\right]_{7\times4}=\left(LT_{ij},LIT_{ij},LIF_{ij}\,LF_{ij}\right)_{7\times4}$ (See Table 1).

Table 1. DVNN information

	LLG_2	LLG_2
LA_1	(0.23, 0.29,0.61, 0.45)	(0.23, 0.46, 0.96, 0.38)
LA_2	(0.34, 0.65, 0.26, 0.82)	(0.37, 0.82, 0.43, 0.69)
LA_3	(0.58, 0.35, 0.19, 0.43)	(0.32, 0.94, 0.62, 0.76)
LA_4	(0.53, 0.89, 0.46, 0.23)	(0.16, 0.37, 0.29, 0.15)
LA_5	(0.38, 0.69, 0.74, 0.16)	(0.27, 0.58, 0.37, 0.41)
LA_6	(0.39, 0.56, 0.17, 0.65)	(0.62, 0.29, 0.75, 0.52)
LA_7	(0.83, 0.17, 0.33, 0.27)	(0.29, 0.53, 0.69, 0.86)
	LLG_3	LLG_4
LA_1	(0.49, 0.45, 0.17, 0.43)	(0.22, 0.48, 0.37, 0.68)
LA_2	(0.23, 0.67, 0.47, 0.83)	(0.46, 0.51, 0.65, 0.72)
LA_3	(0.47, 0.83, 0.41, 0.17)	(0.31, 0.54, 0.64, 0.46)
LA_4	(0.26, 0.56, 0.26, 0.78)	(0.45, 0.79, 0.46, 0.69)
LA_5	(0.27, 0.49, 0.73, 0.39)	(0.31, 0.59, 0.28, 0.64)
LA_6	(0.31, 0.63, 0.67, 0.12)	(0.51, 0.17, 0.64, 0.41)
LA_7	(0.78, 0.12, 0.28, 0.21)	(0.32, 0.63, 0.32, 0.29)

Step 2. Normalize the $LR=\left[LR_{ij}\right]_{7\times4}$ into $NLR=\left[NLR_{ij}\right]_{7\times4}$ (See Table 2).

Table 2. The $NLR=\left[NLR_{ij}\right]_{7\times4}$

	LLG_2	LLG_2
LA_1	(0.23, 0.29,0.61, 0.45)	(0.23, 0.46, 0.96, 0.38)
LA_2	(0.34, 0.65, 0.26, 0.82)	(0.37, 0.82, 0.43, 0.69)
LA_3	(0.58, 0.35, 0.19, 0.43)	(0.32, 0.94, 0.62, 0.76)
LA_4	(0.53, 0.89, 0.46, 0.23)	(0.16, 0.37, 0.29, 0.15)

LA_5	(0.38, 0.69, 0.74, 0.16)	(0.27, 0.58, 0.37, 0.41)
LA_6	(0.39, 0.56, 0.17, 0.65)	(0.62, 0.29, 0.75, 0.52)
LA_7	(0.83, 0.17, 0.33, 0.27)	(0.29, 0.53, 0.69, 0.86)
	LLG_3	LLG_4
LA_1	(0.49, 0.45, 0.17, 0.43)	(0.22, 0.48, 0.37, 0.68)
LA_2	(0.23, 0.67, 0.47, 0.83)	(0.46, 0.51, 0.65, 0.72)
LA_3	(0.47, 0.83, 0.41, 0.17)	(0.31, 0.54, 0.64, 0.46)
LA_4	(0.26, 0.56, 0.26, 0.78)	(0.45, 0.79, 0.46, 0.69)
LA_5	(0.27, 0.49, 0.73, 0.39)	(0.31, 0.59, 0.28, 0.64)
LA_6	(0.31, 0.63, 0.67, 0.12)	(0.51, 0.17, 0.64, 0.41)
LA_7	(0.78, 0.12, 0.28, 0.21)	(0.32, 0.63, 0.32, 0.29)

Step 3. Conduct the weight: $lw_1 = 0.2654, lw_2 = 0.3475, lw_3 = 0.2057, lw_4 = 0.1814$.

Step 4. Conduct the relative weight: $rlw = \{0.7637, 1.0000, 0.5919, 0.5220\}$

Step 5. Conduct the $DVNNDD = \left(DVNNDD_{ij}\right)_{5\times4}$ (Table 3):

Table 3. The $DVNNDD = \left(DVNNDD_{ij}\right)_{5\times4}$

	LLG_1	LLG_2	LLG_3	LLG_4
LA_1	-0.4911	0.8640	-1.2548	-0.9078
LA_2	-1.1168	-1.6364	0.8443	-0.5024
LA_3	-0.2610	0.9378	0.8724	-1.4700
LA_4	0.2862	0.2018	-0.6111	-0.0469
LA_5	-1.8989	0.4759	0.3379	-0.5879
LA_6	-0.2663	1.1191	-1.9159	0.4796
LA_7	0.2810	0.3831	0.3549	-0.5916

Step 6. Administrate the DVNNPIDS and DVNNNIDS (Table 4).

Table 4. DVNNPIDS and DVNNNIDS

	LLG_1	**LLG_2**	**LLG_3**	**LLG_4**
DVNNPIDS	0.2862	1.1191	0.8724	0.4796
DVNNNIDS	-1.8989	-1.6364	-1.9159	-1.4700

Step 7. Calculate the $DVNNGRC\left(LA_{ij}, DVNNPIDS_j\right)$ and $DVNNGRC\left(LA_{ij}, DVNNNIDS_j\right)$ (See table 5-6).

Table 5. The $DVNNGRC\left(LA_{ij}, DVNNPIDS_j\right)$

	LLG₁	**LLG₂**	**LLG₃**	**LLG₄**
LA_1	0.6420	0.8453	0.3959	0.5012
LA_2	0.4984	0.3360	0.9802	0.5867
LA_3	0.7181	0.8849	1.0000	0.4169
LA_4	1.0000	0.6031	0.4845	0.7259
LA_5	0.3895	0.6843	0.7229	0.5664
LA_6	0.7162	1.0000	0.3333	1.0000
LA_7	0.9962	0.6545	0.7293	0.5655

Table 6. The $DVNNGRC\left(LA_{ij}, DVNNNIDS_j\right)$

	LLG₁	**LLG₂**	**LLG₃**	**LLG₄**
LA_1	0.4976	0.3580	0.6783	0.7126
LA_2	0.6406	1.0000	0.3356	0.5903
LA_3	0.4598	0.3513	0.3333	1.0000
LA_4	0.3895	0.4313	0.5166	0.4949
LA_5	1.0000	0.3976	0.3822	0.6125
LA_6	0.4606	0.3360	1.0000	0.4169
LA_7	0.3901	0.4084	0.3804	0.6135

Step 8. Calculate the $DVNNGRD\left(LA_i, DVNNPIDS\right)$ and $DVNNGRD\left(LA_i, DVNNNIDS\right)$ (See table 7-8).

Table 7. The $DVNNGRD\left(LA_i, DVNNPIDS\right)$ and $DVNNGRD\left(LA_i, DVNNNIDS\right)$

Alternative	$DVNNGRD\left(LA_i, DVNNPIDS\right)$	$DVNNGRD\left(LA_i, DVNNNIDS\right)$

LA_1	0.6365	0.5253
LA_2	0.5571	0.6936
LA_3	0.7794	0.4941
LA_4	0.7063	0.4493
LA_5	0.5926	0.5933
LA_6	0.7875	0.5203
LA_7	0.7444	0.4350

Step 9. Administrate the $DVNNRRD\left(LA_i, DVNNPIDS\right)$ from DVNNPIDS (See table 9).

Table 9. The $DVNNRRD\left(LA_i, DVNNPIDS\right)$ and order

Alternative	$DVNNRRD\left(LA_i, DVNNPIDS\right)$	**Order**
LA_1	0.5479	5
LA_2	0.4454	7
LA_3	0.6120	2
LA_4	0.6112	3
LA_5	0.4997	6
LA_6	0.6022	4
LA_7	0.6312	1

Step 9. From the $DVNNRRD\left(LA_i, DVNNPIDS\right)$, the order is: $LA_7 > LA_3 > LA_4 > LA_6 > LA_1 > LA_5 > LA_2$. Thus, the optimal local applied undergraduate college is LA_7.

5. Comparative analysis

Then, the DVNN-LogTODIM-GRA technique is compared with generalized double-valued neutrosophic weighted distance [38] and weighted Dice similarity measures $WD_{\mathrm{DVNS}_1}\left(HA_i, DVNNPIS\right)$, $WD_{\mathrm{DVNS}_2}\left(HA_i, DVNNPIS\right)$ and weighted generalized Dice similarity measures $WGD_{\mathrm{DVNS}_1}\left(HA_i, DVNNPIS\right), WGD_{\mathrm{DVNS}_2}\left(HA_i, DVNNPIS\right)$[40], DVNN-

Taxonomy technique [41], DVNN-CoCoSo technique [42] and DVNN-TODIM-VIKOR technique [43]. The final comparative results are shown in Table 10.

Table 10. Order of different techniques

Different Techniques	Order
DVNN weighted Hamming distance[38]	$LA_7 > LA_3 > LA_4 > LA_6 > LA_1 > LA_5 > LA_2$
DVNN weighted Euclidean distance[38]	$LA_7 > LA_3 > LA_4 > LA_6 > LA_1 > LA_5 > LA_2$
$WD_{\mathrm{DVNS}_1}(HA_i, DVNNPIS)$ *[40]*	$LA_7 > LA_3 > LA_4 > LA_6 > LA_1 > LA_5 > LA_2$
$WD_{\mathrm{DVNS}_2}(HA_i, DVNNPIS)$ *[40]*	$LA_7 > LA_3 > LA_4 > LA_6 > LA_1 > LA_5 > LA_2$
$WGD_{\mathrm{DVNS}_1}(HA_i, DVNNPIS)$ *[40]*	$LA_7 > LA_3 > LA_4 > LA_6 > LA_1 > LA_5 > LA_2$
$WGD_{\mathrm{DVNS}_2}(HA_i, DVNNPIS)$ *[40]*	$LA_7 > LA_3 > LA_4 > LA_6 > LA_1 > LA_5 > LA_2$
DVNN-Taxonomy method[41]	$LA_7 > LA_3 > LA_4 > LA_6 > LA_5 > LA_1 > LA_2$
DVNN-CoCoSo technique [42]	$LA_7 > LA_3 > LA_4 > LA_6 > LA_5 > LA_1 > LA_2$
DVNN-TODIM-VIKOR technique [43]	$LA_7 > LA_3 > LA_4 > LA_6 > LA_1 > LA_5 > LA_2$
DVNN-LogTODIM-GRA technique	$LA_7 > LA_3 > LA_4 > LA_6 > LA_1 > LA_5 > LA_2$

Based on the above analysis, it can be concluded that while the ranking of these techniques may differ slightly, they all consistently identify the same optimal and worst local applied vocational undergraduate colleges. This consistency supports the validity of the DVNN-LogTODIM-GRA technique. The key strengths of DVNN-LogTODIM-GRA are as follows: (1) It accounts for the psychological behavior of decision-makers and the shape similarity between DVNNPIDS and DVNNNIDS when evaluating employment quality. (2) It integrates the complex behavior of the LogTODIM and GRA techniques, making it a robust MAGDM tool for assessing employment quality. However, its main drawback is its inability to address consensus issues during the evaluation of university graduate employment quality.

6. Conclusion

The evaluation of university employment quality is a key system of indicators that measures the performance of graduates in the job market. It not only focuses on the employment rate of graduates but also assesses multiple dimensions of employment quality, including the relevance of jobs to their field of study, salary levels, job stability, and career

development prospects. Through these indicators, universities can understand how well their talent cultivation aligns with market demands and optimize their curriculum and teaching methods. Additionally, employment quality evaluation incorporates feedback from both graduates and employers, analyzing graduates' professional skills, job performance, and employer satisfaction. This evaluation system helps universities continuously improve education quality, enhance graduates' competitiveness in the job market, and provide important decision-making insights for future educational improvements. The employment quality evaluation for university graduates involves MADM. Currently, the LogTODIM and GRA techniques are widely applied to address multi-attribute decision-making (MADM) challenges. To manage uncertain information in this evaluation, DVNSs (Dual-Valued Neutrosophic Sets) are used as a characterization tool. This study introduces the DVNN-LogTODIM-GRA technique to solve MADM problems under DVNSs. To validate the proposed method, a numerical example is provided, focusing on the evaluation of employment quality for university graduates. The key contributions of this study are as follows: (1) The use of the entropy method to determine weight values under DVNSs; (2) The application of DVNN-LogTODIM-GRA to effectively handle MADM problems; (3) The validation of the DVNN-LogTODIM-GRA technique through a numerical example related to university graduate employment quality evaluation.

Conflicts of Interest: The authors declare no conflict of interest

References

[1] L. Ma, Reflections on the university graduate employment quality evaluation system, Brand Research, 2018 (2018) 84-86.

[2] Y. Chen, Construction and application of employment quality evaluation index system for university students, Journal of Anhui Water Resources and Hydropower Vocational and Technical College, 18 (2018) 93-96.

[3] P. Qi, X. Cheng, Research on the university graduate employment quality evaluation system, Jiangsu Higher Education, 2019 (2019) 86-89.

[4] Y. Wei, University employment quality evaluation based on big data mining technology, Modern Electronics Technology, 43 (2020) 103-106.

[5] J. Yang, S. Qiu, B. Guo, Review of employment quality evaluation and employment tracking quantitative research for university graduates, Journal of Heilongjiang Teacher Development College, 39 (2020) 14-17.

[6] X. Gu, X. Lin, Exploring the construction of university graduate employment quality evaluation system, Ideological and Theoretical Education, 2021 (2021) 108-111.

[7] Y. Liang, B. Zhang, Y. Liang, Research on employment quality evaluation system for industry-

based universities in the new era, China University Students Employment, 2023 (2023) 89-97.

[8] D. Cao, Y. Yi, Construction of employment quality evaluation index system for university graduates in the new era: A case study of hunan province, China Human Resource Science, 2024 (2024) 80-92.

[9] A. Zhang, X. Li, X. Ye, Research on university graduate employment quality evaluation system based on cipp, Journal of Changzhou Institute of Technology, 37 (2024) 82-89+99.

[10] P. Yan, L. Pei, Y. Li, Construction and practice of university employment quality evaluation system from the perspective of serving the local economy, Science and Technology in Chinese Universities, 2024 (2024) 16-22.

[11] R. Krishankumar, K. Arun, D. Pamucar, K.S. Ravichandran, A decision aiding framework for two-way selection of cloud vendors in medical centers with generalized orthopair fuzzy information, Ieee Transactions on Engineering Management, 70 (2023) 3653-3664.

[12] A.R. Mishra, P. Rani, M. Deveci, I. Gokasar, D. Pamucar, K. Govindan, Interval-valued fermatean fuzzy heronian mean operator-based decision-making method for urban climate change policy for transportation activities, Engineering Applications of Artificial Intelligence, 124 (2023) 23.

[13] D. Pamucar, G. Duran-Romero, M. Yazdani, A.M. Lopez, A decision analysis model for smart mobility system development under circular economy approach, Socio-Economic Planning Sciences, 86 (2023) 24.

[14] D. Pamucar, I. Gokasar, A.E. Torkayesh, M. Deveci, L. Martinez, Q. Wu, Prioritization of unmanned aerial vehicles in transportation systems using the integrated stratified fuzzy rough decision-making approach with the hamacher operator, Information Sciences, 622 (2023) 374-404.

[15] M. Gong, Fuzzy multiple attribute decision making method for multimedia teaching effectiveness comprehensive evaluation in college english with double-valued neutrosophic numbers, Journal of Intelligent & Fuzzy Systems, 45 (2023) 5697-5707.

[16] S. Sorooshian, S.M. Jamali, N.A. Erbhamil, Performance of the decision-making trial and evaluation laboratory, Aims Mathematics, 8 (2023) 7490-7514.

[17] H. Shakibaei, M.R. Farhadi-Ramin, M. Alipour-Vaezi, A. Aghsami, M. Rabbani, Designing a post-disaster humanitarian supply chain using machine learning and multi-criteria decision-making techniques, Kybernetes, (2023) 28.

[18] S. Shabu, K. Yadav, E. Kariri, K.K. Gola, M. AnulHaq, A. Kumar, Trajectory clustering and query processing analysis framework for knowledge discovery in cloud environment, Expert Systems, 40 (2023) 19.

[19] J. Nie, A novel ifn-csm-cocoso approach for multiple-attribute group decision-making with intuitionistic fuzzy sets: An application in assessing corporate social responsibility performance, Heliyon, 10 (2024) E29207.

[20] R.N. Devi, Y. Parthiban, Exploring neutrosophic over supra exterior modal topological structure: Theory and application in healthcare decision-making, Neutrosophic Sets and Systems, 72 (2024) 272-285.

[21] P. Rani, S.M. Chen, A.R. Mishra, Multiple attribute decision making based on mairca, standard deviation-based method, and pythagorean fuzzy sets, Information Sciences, 644 (2023) 15.

[22] A.U. Rahman, M. Saeed, M.A. Mohammed, A.S. Al-Waisy, S. Kadry, J. Kim, An innovative fuzzy parameterized madm approach to site selection for dam construction based on sv-complex neutrosophic hypersoft set, Aims Mathematics, 8 (2023) 4907-4929.

[23] Q.S. Qi, Topsis methods for probabilistic hesitant fuzzy magdm and application to performance evaluation of public charging service quality, Informatica, 34 (2023) 317-336.

[24] M. Palanikumar, N. Kausar, H. Garg, A. Iampan, S. Kadry, M. Sharaf, Medical robotic engineering selection based on square root neutrosophic normal interval-valued sets and their aggregated operators, Aims Mathematics, 8 (2023) 17402-17432.

[25] A. Noori, H. Bonakdari, A.H. Salimi, L. Pourkarimi, J.M. Samakosh, A novel multiple attribute decision-making approach for assessing the effectiveness of advertising to a target audience on drinking water consumers? Behavior considering age and education level, Habitat International, 133 (2023) 9.

[26] B. Nandi, S. Das, Identify most promising temporal scour depth formula for circular piers proposed over last six decades, Ocean Engineering, 286 (2023) 19.

[27] A. Mondal, S.K. Roy, J.M. Zhan, A reliability-based consensus model and regret theory-based selection process for linguistic hesitant-z multi-attribute group decision making, Expert Systems with Applications, 228 (2023) 18.

[28] Z.K. Mohammed, A.A. Zaidan, H.B. Aris, H.A. Alsattar, S. Qahtan, M. Deveci, D. Delen, Bitcoin network-based anonymity and privacy model for metaverse implementation in industry 5.0 using linear diophantine fuzzy sets, Annals of Operations Research, (2023) 41.

[29] R. Mishra, S. Malviya, S. Singh, V. Singh, U.S. Tiwary, Multi-attribute decision making application using hybridly modelled gaussian interval type-2 fuzzy sets with uncertain mean, Multimedia Tools and Applications, 82 (2023) 4913-4940.

[30] T. Mahmood, U.U. Rehman, Z. Ali, Analysis and applications of aczel-alsina aggregation operators based on bipolar complex fuzzy information in multiple attribute decision making, Information Sciences, 619 (2023) 817-833.

[31] P.D. Liu, Q. Pan, B.Y. Zhu, X.M. Wu, Multi-attribute decision-making model based on regret theory and its application in selecting human resource service companies in the post-epidemic era, Information Sciences, 649 (2023) 24.

[32] M. Kandakoglu, G. Walther, S. Ben Amor, The use of multi-criteria decision-making methods in project portfolio selection: A literature review and future research directions,

Annals of Operations Research, (2023) 24.

[33] A. Hussain, H.L. Wang, K. Ullah, H. Garg, D. Pamucar, Maclaurin symmetric mean aggregation operators based on novel frank t-norm and t-conorm for intuitionistic fuzzy multiple attribute group decision-making, Alexandria Engineering Journal, 71 (2023) 535-550.

[34] A. Hussain, K. Ullah, M. Mubasher, T. Senapati, S. Moslem, Interval-valued pythagorean fuzzy information aggregation based on aczel-alsina operations and their application in multiple attribute decision making, Ieee Access, 11 (2023) 34575-34594.

[35] X.J. Guo, H.X. Shen, Q.L. Wen, S.F. Liu, Y.J. Yang, H. Zhang, Research on layout model and construction planning of aged care institutions for disabled elders in china: Based on nanjing city data, Bmc Geriatrics, 23 (2023) 17.

[36] A.B. Leoneti, L. Gomes, A novel version of the todim method based on the exponential model of prospect theory: The exptodim method, European Journal of Operational Research, 295 (2021) 1042-1055.

[37] J. Deng, Introduction to grey system theory, The Journal of Grey System, 1 (1989) 1-24.

[38] I. Kandasamy, Double-valued neutrosophic sets, their minimum spanning trees, and clustering algorithm, Journal of Intelligent Systems, 27 (2018) 163-182.

[39] C.E. Shannon, A mathematical theory of communication, Bell System Technical Journal, 27 (1948) 379-423.

[40] Q. Khan, P. Liu, T. Mahmood, Some generalized dice measures for double-valued neutrosophic sets and their applications, Mathematics, 6 (2018) 121.

[41] J. Rao, L. Peng, J. Rao, X. Cao, Modified taxonomy method for double-valued neutrosophic number madm and applications to physical education teaching quality evaluation in colleges and universities, Journal of Intelligent and Fuzzy Systems, 44 (2023) 10581-10590.

[42] L. Wei, An integrated decision-making framework for blended teaching quality evaluation in college english courses based on the double-valued neutrosophic sets, Journal of Intelligent & Fuzzy Systems, 45 (2023) 3259-3266.

[43] K. Du, Y. Du, Research on performance evaluation of intangible assets operation and management in sports events with double-valued neutrosophic sets, Journal of Intelligent & Fuzzy Systems, 45 (2023) 2813-2822.

Received: July 28, 2024. Accepted: Oct 21, 2024

Neutrosophic Sets and Systems, Vol. 76, 2025
University of New Mexico

NSDTL: A Robust Malware Detection Framework Under Uncertainty

Alaa Elmor [1]
[1] Zagazig University, 44519 Zagazig, Egypt
Email: alaaelmor@zu.edu.eg
* Correspondence: alaaelmor@zu.edu.eg

Abstract: The Internet's rapid expansion and the current trends toward automation through intelligent systems have given malevolent software attackers a veritable playground. Numerous gadgets are effortlessly connected to the Internet, and a lot of data is being collected. Consequently, there is a growing concern about malware attacks and security threats. Malware detection has emerged as a research focus. However, there are challenges in the research, such as noise, uncertainty, and ambiguous data. The study proposes a novel framework NSDTL, that achieves state-of-the-art malware detection and classification results to address this changing threat landscape. NSDTL leverages a neutrosophic set and advanced transfer learning techniques. There are three different kinds of images in the neutrosophic domain: True (T) images, Indeterminacy (I) images, and Falsity (F) images, which deal with uncertainty. The MaleVis dataset was used for experiments on multi-class malware classification, and the findings show that NSDTL significantly outperforms current models. This study emphasizes how crucial it is to combine transfer learning with a neutrosophic set at the forefront of the continuous fight against changing cyber threats.

Keywords: Neutrosophic Set; Deep Transfer Learning; Malware detection; IoT.

1. Introduction

Now, we enter the fifth industrial revolution (Industry 5.0), which is being propelled by developments in Internet technologies and intelligent automation, we are encountering more and more security breaches. Developing defenses against malicious software assaults is crucial because these attacks have the potential to damage enterprises by infiltrating their data, applications, and computer systems without obtaining user authorization or authentication [1, 2]. Scholars, businesses, financial organizations, and governments are very concerned about these concerns, which include file loss, hostile extortion, information theft, telecommunication fraud, firm shutdowns, and other problems [3]. The two primary kinds of malware detection techniques are traditional static detection techniques [4] and dynamic detection techniques [5, 6]. The static technique determines whether the software is malware by examining its structure. The dynamic technique determines whether running software is malware by examining its behavior. Despite its extremely high accuracy rate, the dynamic detection technique requires program monitoring, which takes time and makes it difficult to discover dangerous software at the moment. Although static detection can compensate for this shortcoming, traditional static detection techniques depend on robust virus databases and effective anti-virus engines. As a result, it is exceedingly challenging to identify invisible malware, which contributes to the subpar effectiveness of traditional static detection techniques [7]. Some researchers proposed several techniques to identify malware by utilizing visualization technologies to make up for the drawbacks of traditional static detection [8, 9]. It has been demonstrated that these techniques

function well in the area of malware detection. The binary code or assembly code of the majority of malware versions is quite similar since they are frequently created by automation technology or by reusing key function modules [10]], this can be seen in the visual image and makes visualization technology effective. Transfer learning-based malware classification has been examined in several previous literary works. Reputable CNN architectures can be used to refine a classification model for the target domain [11] or as feature extractors with machine learning algorithms for classification on the target domain [12-14]. Nevertheless, not many studies have yet to tackle uncertainty issues.

To address higher degrees of uncertainty, Smarandache [15] introduced a neutrosophic set (NS) in 1998. Since then, NS has been applied to a wide range of computer science domains, such as image processing and segmentation [16], pattern recognition [17], and more. In various fields, including medical [18], space satellites [19], and agriculture[20], it helps to solve several research and real-world problems. Three distinct degrees of membership—true, indeterminacy, and false—can be assigned by NS to any element in the universe. Incomplete, inconsistent, and ambiguous information—which is found in malware images—can be represented using these domains.

In this study, we introduce a novel framework that integrates DTL and NS to handle uncertainty in three degrees of membership for malware detection. The frameworks employ four different DTL models, VGG, MobileNetV2, DenseNet121, and Xception. We conduct our study in the MaleVis dataset, we concentrate on identifying different malware with high accuracy, in contrast to previous studies focusing on binary classification for high accuracy but may neglect the type of malware. VGG16 shows the highest results in terms of Accuracy, MCC, Precision, Recall, F1-score, and AUC with 93.63%, 93.35%, 95.29%, 93.6%, 94.27%, and 97% respectively in the true domain.

The rest of the paper is organized as follows: Section 2 covers the related work of this study. Section 3 describes the proposed framework, including the NS-based data preprocessing technique and utilized DTL models. Section 4 presents the experimental setup and describes the MaleVis dataset. Section 5 discusses the experiments and findings. Section 6 concludes the study and discusses future directions. Finally, Section 6 presents the new directions of neutrosophic logic in Malware Detection.

1.1 The Role of Neutrosophic Logic in Malware Detection

Neutrosophic logic (NL) extends traditional binary logic (true or false) by introducing a third state, which represents indeterminacy. This makes it suitable for scenarios where information is incomplete or uncertain, which is common in cybersecurity. NL is a mathematical framework that allows for the representation of uncertain, indeterminate, or contradictory information. In the context of cybersecurity, particularly in malware detection, neutrosophic logic provides significant advantages in handling the complexities and ambiguities inherent in identifying malicious software.

How Neutrosophic Logic Applied in Malware Detection

- Malware detection often relies on various indicators, such as file behavior or network activity, which may be incomplete or ambiguous. NL can effectively analyze these uncertain data points to provide a more accurate assessment of whether a file or process is malicious.

- NL allows for the development of dynamic classification systems that can categorize different types of malware based on their features, even when these features may conflict or be poorly defined.
- By incorporating neutrosophic logic into machine learning algorithms, it is possible to improve the robustness of models used for malware detection. This integration helps the models adapt to changing data patterns and increases their accuracy.
- A common challenge in malware detection is the occurrence of false positives, where legitimate software is mistakenly identified as malware. NL helps mitigate this issue by providing a nuanced analysis that considers degrees of uncertainty, leading to more reliable detection outcomes.

1.2 Applications of Neutrosophic in Malware Detection

1- In malware detection, various indicators such as file signatures, behavior patterns, and network traffic can often be uncertain. By applying neutrosophic logic, we can represent these indicators as neutrosophic triples. For example, if a certain file is suspected of being malware, we might assess:

$$File_x = (0.7,0.2,0.1)$$

This indicates a 70% chance that it is malware, a 20% uncertainty, and a 10% chance that it is definitely not malware.

2- When analyzing multiple files, neutrosophic logic allows security systems to aggregate information from various sources. If we have multiple files *File_x* and *File_y*, their combined representation can be evaluated to determine if the overall risk increases or decreases.

3- Traditional detection systems often suffer from high false positive rates. By integrating neutrosophic logic, these systems can more accurately assess the likelihood of a file being malicious by considering the uncertainty and providing a more balanced view. For example:

$$Risk= (T_{malware}, I_{uncertainty}, F_{legitimate})$$

4- Neutrosophic logic can enhance machine learning models by providing a framework that can adapt as new information becomes available. As more data is collected, the neutrosophic values can be updated, improving the model's ability to detect new types of malware.

The incorporation of neutrosophic logic into existing detection frameworks represents a significant advancement in the fight against malware, providing deeper insights and improved decision-making capabilities.

2. Related work

This section provides a summary of research on visualization-based methods for classifying malware. Code obfuscation or encoding problems can be resolved by image-based malware classification techniques [21-25]. These image-based methods convert malware samples into image representations using static analysis techniques. These representations are then fed into image classification methods to determine if the sample is benign or malicious.

[26] Jadeite, a method for identifying Java bytecode malware programs, is presented by Obaidat et al. From a Java bytecode file, Jadeite extracts the Interprocedural Control Flow Graph (ICFG), prunes

it, and transforms it into an adjacency matrix. Jadeite then uses this matrix to create a grayscale image. To increase the precision of malware classification, Jadeite also extracts a different set of features from the Java malware program. The CNN classifier uses these features as inputs combined with the retrieved images.

The malware detection architecture for the Industrial Internet of Things (MD-IIOT) was designed by Naeem et al. [27], they set up three databases—traffic, behavior, and log databases—in cloud storage. The traffic database uses a sniffing and monitoring unit to gather the IIOT's raw Android files. A list of datasets representing the network history makes up a behavior database. The log database continually updates the behavior database and gathers new malware fingerprints. A Deep Convolutional Network (DCNN) and a color picture modification approach are designed for the analyzer unit. A DCNN model is applied once the raw Android file has been transformed into a color image. The analyzer unit assesses the file as benign or malicious after comparing its fingerprints with a behavior database. The response unit sends the system administrator a last warning to take appropriate action if any malicious behavior is detected within the network.

Ding et al. [28] utilize CNN to train a malware detection model after directly extracting the bytecode file from the Android APK file and converting it into a two-dimensional bytecode matrix. The experimental findings demonstrate the efficacy of the suggested approach in detecting malware, particularly malware that has been encrypted via polymorphic approaches.

A temporal convolution network (TCN)--based malware detection model for Android was presented by Zhang et al. [29]. First, XML files and DEX files are combined to create four grayscale image datasets with four distinct combinations of texture features. For experimental validation, the image size is then combined and fed into the neural network design using three distinct convolution techniques. According to the testing findings, adding XML files improves Android malware detection.

A technique to determine if generative adversarial network-generated images can be differentiated from actual images was presented by Mercaldo et al. [30] using a dataset of real-world Android malware programs. Using images from both static analysis and dynamic analysis, their trials included two different kinds of deep convolutional generative adversarial networks. They trained several supervised machine learning models after creating images to see if they could distinguish between harmful applications that were produced and those that were real.

A malware classification approach was presented by Ünver et al. [31] to identify malware samples in the Android environment. The base of the proposed model is the conversion of some Android application source files into grayscale images. The proposed model has been trained using a few image-based local and global features, four distinct local feature types, and three distinct global feature types, which have been taken from the created grayscale image datasets. One feature vector was created using the bag of visual words approach using the descriptors of the local features that were taken out of each image. Several machine learning classifiers, including Random Forest, k-nearest neighbors, Decision Tree, Bagging, AdaBoost, and Gradient Boost, have been trained using the extracted local and global features.

To classify 25 malware families using images, both with and without class balancing, Awan et al. [32] propose a deep learning framework based on spatial attention and CNN. Precision, recall,

specificity, precision, and F1 score were used to assess performance on the Malimg dataset. The proposed model with class balance achieved 97.42%, 97.95%, 97.33%, 97.11%, and 97.32% on this dataset and with class balancing on a benign class, which yielded results above 97%.

Shaukat et al. [33] proposed a malware detection approach based on deep learning, A portable executable (PE) file is first visualized as a colored image. Second, it uses a refined deep learning model to extract deep information from the color image. Third, it uses support vector machines (SVM) to identify malware based on deep features.

An automatic extraction technique without the need for human-expert interaction was presented by Zhu et al. [34]. They compare an RGB image to the essential components of the Dalvik executable (Dex). By utilizing multi-scale context information, they introduced MADRF-CNN, a CNN variation with heterogeneous receptive fields that uses max pooling and average pooling simultaneously to capture the dependencies between various picture elements (transferred from the Dex file). According to the experimental findings, their method's accuracy is 96.9%.

A snake optimization algorithm with a deep convolutional neural network for an image-based malware classification approach is presented by Duraibi et al. [35]. The proposed approach attempts to identify malware images using a hyperparameter-tuned deep learning approach. The feature vectors are primarily derived using the ShuffleNet approach. Additionally, the snake optimization technique can be used to improve the ShuffleNet algorithm's hyperparameter selection. A bi-directional long short-term memory model based on attention is used to identify malware images. The Malimg malware dataset has been used to evaluate the proposed approach. According to the experimental results, the proposed approach yields a 98.42% accuracy rate.

The **neutrosophic set** has been used in cybersecurity research in several areas, such as intrusion detection and risk assessment. Awotunde et al. [36] developed a multilevel random forest algorithm for intrusion detection, using fuzzy logic, intrusions were categorized as normal, low, medium, or high. Also, Ap et al. [37] presented a lightweight intrusion detection system based on fuzzy logic to identify malicious activities occurring during inter-IoT device connection. In risk assessment, Abdel-Basset et al. [38] proposed the RAF-CPWS methodology using neutrosophic theory to assess risks in wastewater treatment technologies, considering several social, technological, environmental, economic, and cybersecurity factors. Another study by Abdel-Basset et al. [39] combined neutrosophic sets with MCDM techniques for assessing security risks in self-driving cars.

However, this is the first study to apply the neutrosophic domain to malware images, making it a novel contribution to the field.

3. Methodology

Neutrosophic domain conversion and transfer learning architectures are the two primary components of the technique framework suggested in this study to identify 25 distinct kinds of malware. The architecture of the proposed NDDTL framework is shown in Figure 1. As a preprocessing step, the neutrosophic image conversion is applied, and as a classification model, the DTL model is employed.

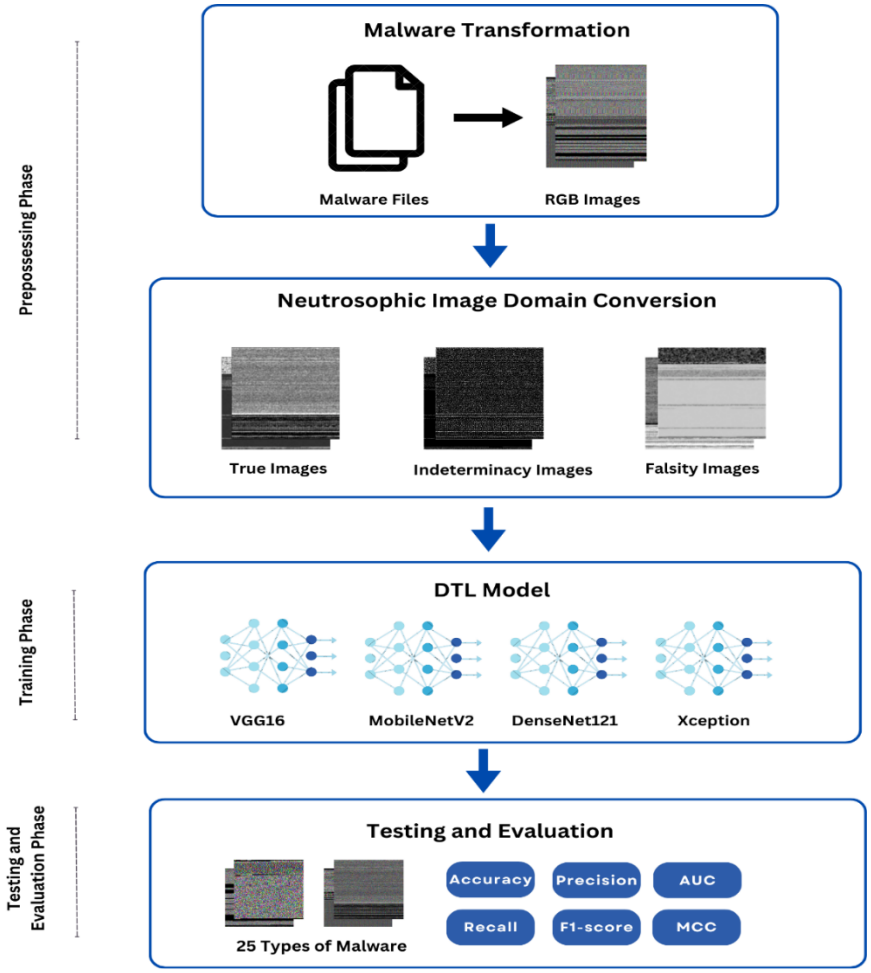

Fig.1 The detailed architecture of proposed NSDTL framework

3.1. Neutrosophic Image Domain Conversion

A practical and beneficial theory for computing fuzzy circumstances is a neutrosophic set (NS). According to NS theory, events are calculated by subtracting them into three categories: true (T) significance, where the status is a percentage of true; indeterminacy (I) significance, where the status is a percentage of indefinite; and falsity (F) significance, where the status is a percentage of false. When classifying malware images, each pixel is separated into T, I, and F subsets. These subsets are then used to classify the image. As demonstrated by Eqs. 1–7, the input image transforms into the neutrosophic domain. The image domain P(x) pixel is transformed into the neutrosophic domain $P_{NS}(x)$:

$$P_{NS}(x) = \{T(x),\ I(x),\ F(x)\} \qquad (1)$$

Using a convolution process, the local mean g(x,y) of an image G can be used to convert it into the domains of a malware image G with pixel intensities. Each pixel in the image is represented as P(x,y). Next, Determine the absolute difference between the image's mean O(x,y) and the original image.

$$g(x,y) = \frac{1}{25}\sum_{i=-2}^{2}\sum_{j=-2}^{2} G(x+i, y+j) \qquad (2)$$

$$O(x,y) = abs(G(x,y) - g(x,y)) \quad (3)$$

The NS domains for the pixel P(x,y) can therefore be shown and delivered as follows:

$$P_{NS}(x,y) = \{T(x,y), I(x,y), T(x,y)\} \quad (4)$$

$$T(x,y) = \frac{g(x,y) - g_{min}}{g_{max} - g_{min}} \quad (5)$$

$$I(x,y) = \frac{O(x,y) - O_{min}}{O_{max} - O_{min}} \quad (6)$$

$$F(x,y) = 1 - T(x,y) \quad (7)$$

G(x,y) denotes the pixel value at the coordinate (x,y) in the image, where x and y variables normally indicate the pixel coordinates in a 2D image. The neighboring pixels surrounding a given pixel (x,y) are indicated by the indices G, I, and j. The highest average pixel value in a specified neighborhood is known as g_max. The lowest average pixel value in the same neighborhood is called g_min. The greatest absolute difference seen throughout the neighborhood is known as O_max. The smallest absolute difference that has been observed is O_min [40,41]. Figure 2 shows samples of malware images for five different classes (out of the dataset's twenty-five classes) after the conversion of the neutrosophic image domain in various domains.

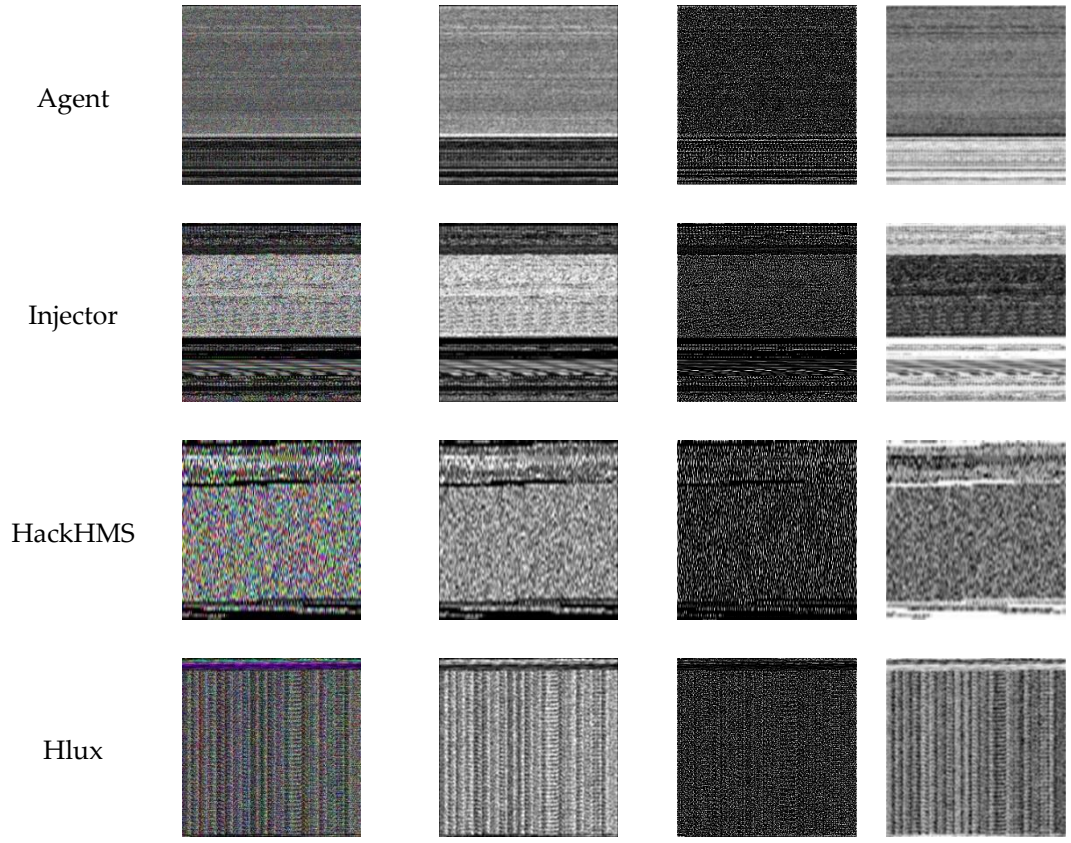

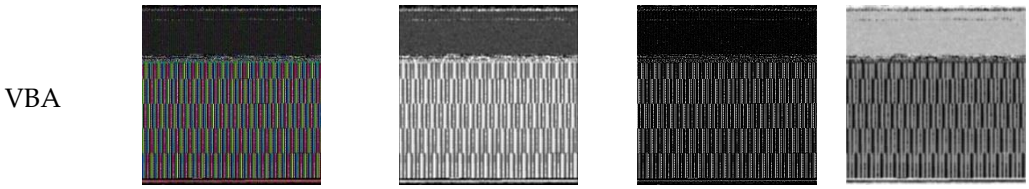

Fig. 2 Five malware families using different neutrosophic image domains (a) original images, (b) true significance images, (b) indeterminacy significance images, and (d) falsity significance images

3.2. Deep Transfer Learning Model

CNNs are ideal for image classification because they gradually extract a more meaningful representation of the visual content. CNN uses the entire image as input, creates useful feature maps from the image, and then deduces information about the item it contains, as opposed to processing the data to extract an image's features. It takes a lot of time and depends on the dataset to develop and train a new CNN model. Transfer learning is helpful in this situation since it offers a technique that allows knowledge to be transferred from the source domain to the target domain with minimal adjustments to the deep CNN models [42]. Four DTL models—VGG16[43], MobileNetV2[44], DenseNet121[45], and Xception[46]—are used in this study to classify malware families. Convolutional layers from the TL model, which was previously trained on the ImageNet dataset, are transferred to our DNN model to construct a Deep Neural Network (DNN) model. Five convolutional layer blocks make up the first part of the VGG16 architecture, which is followed by three fully connected layers. Utilizing 3 × 3 kernels with a stride of 1 and padding of 1, convolutional layers guarantee that every activation map maintains the same spatial dimensions as the one before it. A max pooling operation is used at the end of each block to minimize the spatial dimension, and a rectified linear unit (ReLU) activation is carried out immediately following each convolution. Each spatial dimension of the activation map from the preceding layer is divided by max-pooling layers using 2 × 2 kernels with a stride of 2 and no padding. Ends with two fully connected layers with 4096 ReLU-activated units and 1000 fully connected softmax. Inverted residual and linear bottleneck modules were added to MobileNetV1 to create MobileNetV2. Depthwise separable convolution served as the foundation for the MobileNet architecture. The conventional 2D convolution convolves in the depth dimension (channel) as well, processing each input channel directly to create one output channel. The input image and filter are divided into distinct channels by the depthwise convolution, which then convolves each input channel with its matching filter channel. Following the production of the filtered output channel, the output channels are stacked back. In inseparable depthwise convolution, the stacked output channels are combined into a single channel by filtering them using a 1×1 convolution, also known as pointwise convolution[47]. A convolutional layer and a connected layer are the two types of layers that make up the DenseNet121 architecture. By tightly connecting layers, densely connected convolutional networks transformed neural network topologies. Every layer receives information from the layers that came before it. By using fewer parameters, this approach allows the network to increase accuracy and reuse features. The term Xception refers to the Extreme version of Inception, which consists of a convolution layer that mixes depthwise and pointwise convolution. This combination was subsequently shown to provide higher classification

accuracy for images in a dataset. As the basis of the feature extraction network, the Xception NN layer architecture consists of 36 convolution layers. Except for the first and last modules, all 14 of the 36 convolutional layers are arranged into modules with linear residual connections surrounding them.

4. Experimental Setup

This section covers the datasets and experimental settings used in the study in detail.

4.1. Dataset

The Malevis [48] dataset consists of byte pictures of 26 (25+1) classes and is based on RGB ground truth. In this case, 1 class stands for the "legitimate" samples, whereas the remaining 25 classes represent various malware variants. Using a bin2png script created by Sultanik, the binary images from malware files (provided by Comodo Inc.) were initially extracted in three-channel RGB format to create this dataset. The Malevis dataset consists of 1482 images in total. Malware classes contain Adposhel, Agent, Allaple, Amonetize, Androm, Autorun, BrowseFox, Dinwod, Elex, Expiro, Fasong, HackKMS, Hlux, Injector, InstallCore, MultiPlug, Neoreklami', Neshta, Regrun, Sality, Snarasite, Stantinko, VBA, VBKrypt, and Vilsel.

4.2. Implementation Details

Deep learning frameworks Keras and TensorFlow were used to implement the models. An NVIDIA GeForce RTX 4060 graphics card and an Intel(R) Core (TM) i7-13700HX@2.10 GHz CPU were the hardware components; Windows 11 pro-64-bit was the experimental operating system. The batch size for all models is 64, and there are 30 epochs with early stopping. They employed the Adam optimizer and the Sparse Categorical Cross-Entropy loss function.

4.3. Evaluation Metrics

Several measures of performance, including F1-score, accuracy, recall, precision, and AUC, are provided.

- Accuracy is defined as the proportion of successfully identified instances to all objects in the dataset.

$$ACC = \frac{TP + TN}{TP + FP + FN + TN} \tag{8}$$

- Precision for a particular class is the proportion of examples that are accurately categorized as belonging to a certain class out of all instances of the model that are predicted to belong to that class.

$$Precision = \frac{TP}{TP + FP} \tag{9}$$

- Recall is the proportion of examples in a class that the model correctly identified out of all instances in the class.

$$Recall = \frac{TP}{TP + FN} \tag{10}$$

- The F1 score is a metric that evaluates the model's overall performance by combining recall and precision. The harmonic mean of recall and precision is used to calculate it.

$$F1\ Score = \frac{2 * Precision * Recall}{Precision + Recall} \qquad (11)$$

- MCC measure the discrepancy between the expected and actual values. It is similar to two-by-two contingency table chi-square statistics.

$$\mathrm{MCC} = \frac{\mathrm{TP} * \mathrm{TN} - \mathrm{FP} * \mathrm{FN}}{\sqrt{(\mathrm{TP} + \mathrm{FP})(\mathrm{TP} + \mathrm{FN})(\mathrm{TN} + \mathrm{FP})(\mathrm{TN} + \mathrm{FN})}} \qquad (12)$$

Where TP, FN, TN, and FP stand for the number of true positives, false negatives, and true negatives, and false positives, respectively.

5. Results and Discussion

The effectiveness of our malware detection NSDTL framework is discussed in this section. Four distinct DL models—VGG16, MobileNetV2, DenseNet121, and Xception—were used to evaluate our methodology. According to Table 1, deep learning models perform best on the True domain in terms of accuracy, MCC, precision, recall, F1-score, and AUC, with 93.63%, 93.35%, 95.29%, 93.6%, 94.27%, and 97%, respectively. The VGG16 model is superior, according to table 1 in all domains. Figure 3 displays the ROC curves and confusion matrices for DTL models in the True domain.

Table. 1 Comparison of Deep Learning Models Performance on the Original and NS Domains

Original Data						
Model	**Accuracy**	**MCC**	**Precision**	**Recall**	**F1-score**	**AUC**
VGG	93.25	92.92	94.45	93.6	93.8	97
MobileNetV2	89.6	89.11	90.52	90.08	90.06	95
DenseNet121	91.56	91.17	93.14	91.95	92.43	96
Xception	87.67	87.11	88.24	88.55	88.26	94
True Domain						
Model	**Accuracy**	**MCC**	**Precision**	**Recall**	**F1-score**	**AUC**
VGG	93.63	93.35	95.29	93.6	94.27	97
MobileNetV2	90.25	89.81	91.38	91.01	91.03	95
DenseNet121	91.28	90.88	92.67	91.68	92.02	96
Xception	88.71	88.19	89.8	89.7	89.61	95
Indeterminacy Domain						
Model	**Accuracy**	**MCC**	**Precision**	**Recall**	**F1-score**	**AUC**
VGG	92.97	92.65	93.86	93.64	93.69	95
MobileNetV2	87.77	87.23	89.36	87.84	88.09	94
DenseNet121	88.57	88.04	89.32	89	88.9	94
Xception	86.03	85.4	87.6	86.84	86.81	93
False Domain						
Model	**Accuracy**	**MCC**	**Precision**	**Recall**	**F1-score**	**AUC**
VGG	93.25	92.94	94.29	93.5	93.75	97
MobileNetV2	89.97	89.5	91.99	90.47	91.03	95
DenseNet121	91.24	90.84	92.2	92.12	91.97	96
Xception	86.31	85.7	88.96	86.39	87.41	93

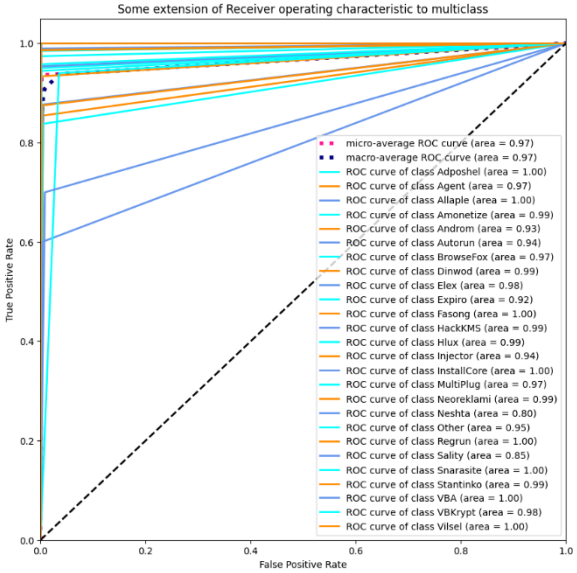

(a) ROC curve of VGG16

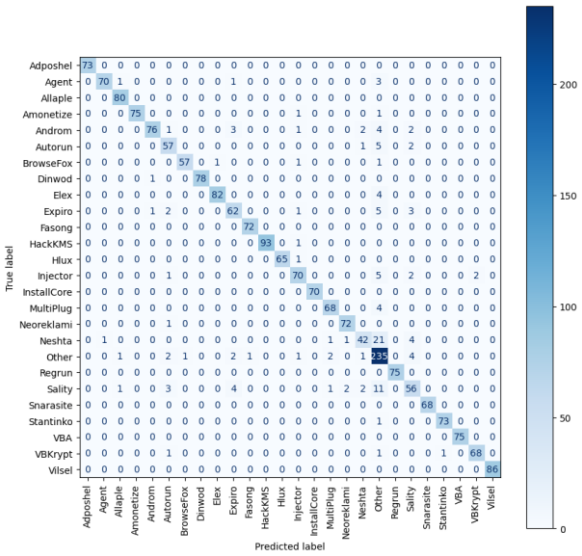

(b) Confusion metrics of VGG16

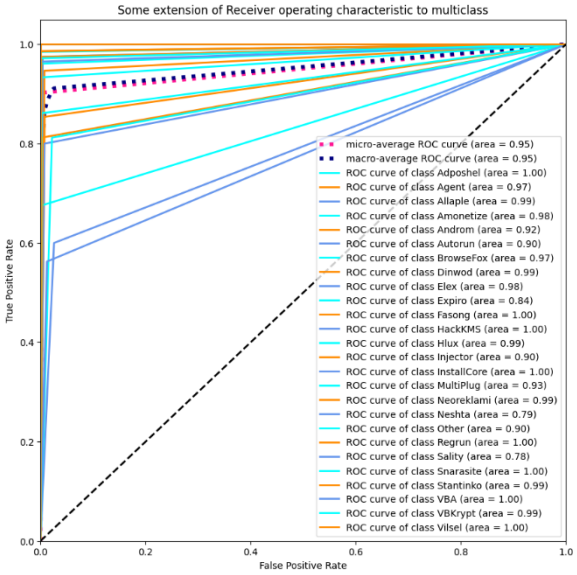

(c) ROC curve of MobileNetV2

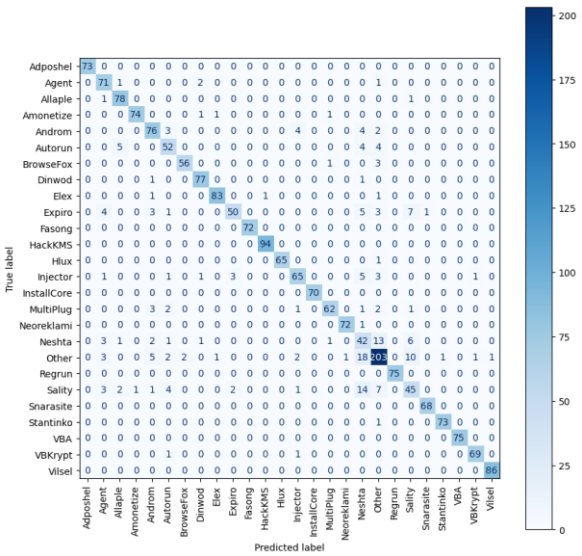

(d) Confusion metrics of MobileNetV2

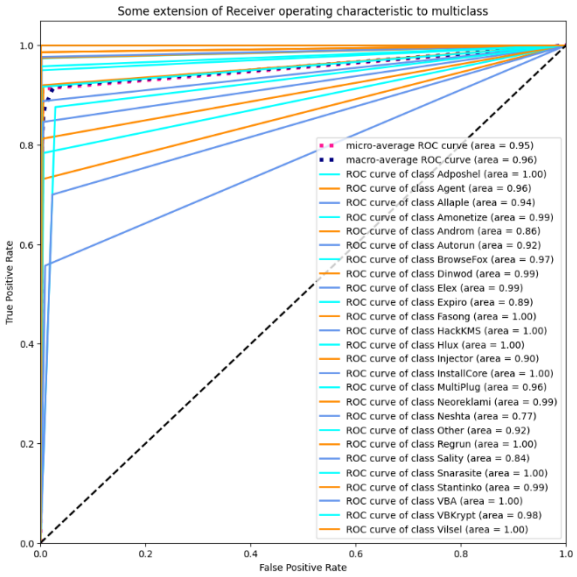

(e) ROC curve of DenseNet121

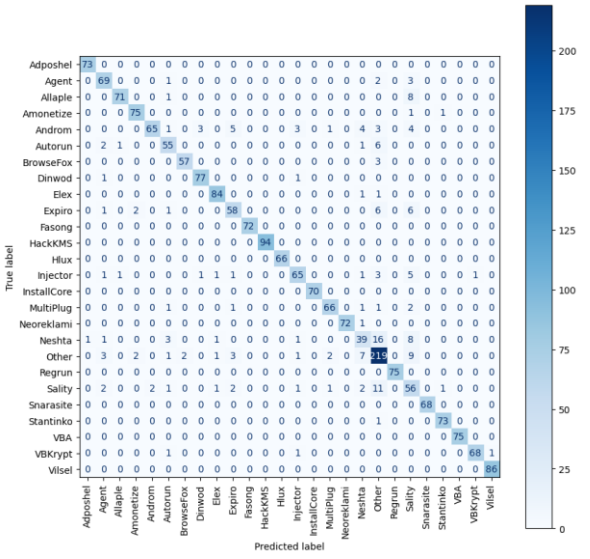

(f) Confusion metrics of DenseNet121

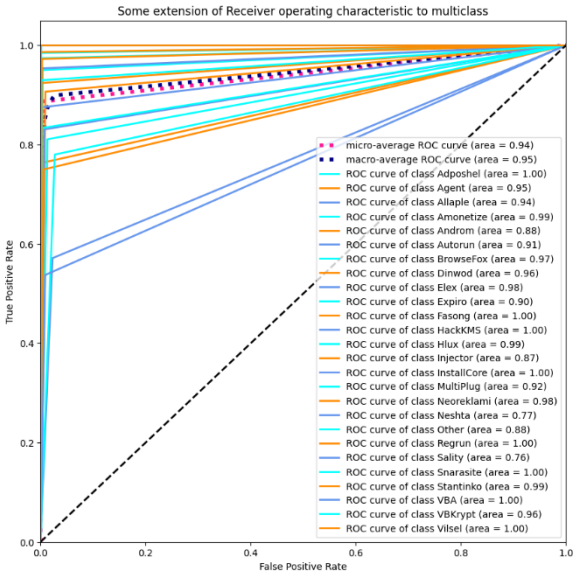

(g)

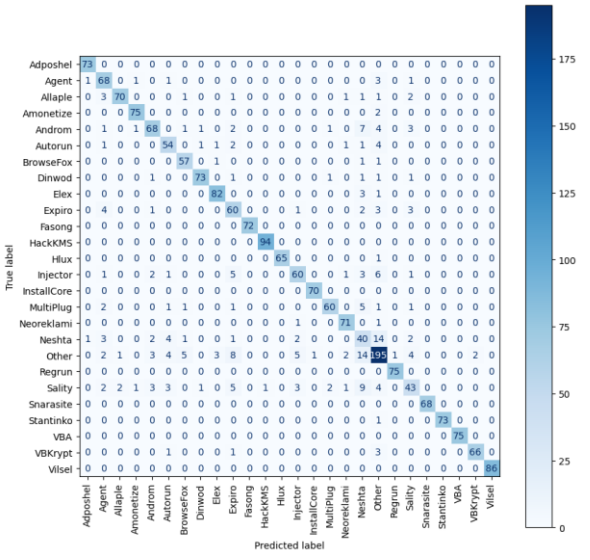

(h)

(i) ROC curve of Xception

(j) Confusion metrics of Xception

Fig. 3 ROC curves and confusion matrices for DTL models in the True domain

6. Conclusion

In this paper, we integrate the neutrosophic domain with advanced transfer learning algorithms to present a novel NSDTL framework for malware detection. The inherent difficulties presented by ambiguity, noise, and uncertainty in malware datasets are effectively addressed by the approach. The NSDTL framework improves detection capabilities by transforming malware images into the neutrosophic domain, which consists of True, Indeterminacy, and Falsity components. Experiments on the MaleVis dataset show that NSDTL is superior in the True dataset

across various evaluation metrics. The best model is the VGG16, which achieves accuracy, MCC, precision, recall, F1-score, and AUC of 93.63%, 93.35%, 95.29%, 93.6%, 94.27%, and 97%, respectively. The findings demonstrate that using the neutrosophic set in conjunction with transfer learning greatly increases the accuracy of malware classification, surpassing current techniques. This study demonstrates how hybrid approaches might improve cybersecurity defenses and provides a promising avenue for further investigation in the continuous fight against evolving cyber threats.

7. New Trends in Neutrosophic Logic for Malware Detection

- Neutrosophic logic allows for the integration of diverse data sources (like behavioral patterns and system logs) into a unified analysis, providing a clearer picture of potential threats.
- By using neutrosophic models, systems can dynamically evaluate the risk levels of files or processes based on varying degrees of uncertainty, leading to more informed decision-making.
- Neutrosophic logic enhances machine learning models by enabling them to adapt to new information and evolving malware techniques, improving detection accuracy over time.
- Neutrosophic methods allow for a more nuanced classification of malware types by considering not just binary classifications (malicious or benign) but a range of possibilities that reflect uncertainty.
- Neutrosophic logic helps minimize false positives by providing a more detailed analysis of uncertainty, allowing legitimate software to be correctly identified without being flagged as malware.
- Neutrosophic approaches are increasingly being applied to analyze the behavior of applications in real time, identifying suspicious activities even when traditional signatures fail.
- Neutrosophic logic supports collaborative frameworks where different systems can share and analyze data collectively, enhancing overall detection capabilities.
- New tools and dashboards using neutrosophic principles allow security analysts to visualize uncertainty and risk levels, making it easier to understand complex threat landscapes.
- Neutrosophic logic is being combined with artificial intelligence and big data analytics to enhance predictive capabilities and improve the overall effectiveness of malware detection systems.
- The principles of neutrosophic logic are being explored in various domains beyond cybersecurity, such as IoT security and cloud computing, demonstrating its versatility and potential for broader application.

These trends highlight how neutrosophic logic is shaping the future of malware detection, offering innovative solutions to the ongoing challenges in cybersecurity.

References

1. Aycock, J., Computer viruses and malware. Vol. 22. 2006: Springer Science & Business Media.
2. Mohamed, G.A.N. and N.B. Ithnin, Survey on representation techniques for malware detection system. Am. J. Appl. Sci, 2017(11): p. 1049-1069.

3. Liu, Y., et al., Efficient and Generalized Image-Based CNN Algorithm for Multi-Class Malware Detection. IEEE Access, 2024.
4. Kruegel, C., et al. Polymorphic worm detection using structural information of executables. in Recent Advances in Intrusion Detection: 8th International Symposium, RAID 2005, Seattle, WA, USA, September 7-9, 2005. Revised Papers 8. 2006. Springer.
5. Huang, W. and J.W. Stokes. MtNet: a multi-task neural network for dynamic malware classification. in Detection of Intrusions and Malware, and Vulnerability Assessment: 13th International Conference, DIMVA 2016, San Sebastián, Spain, July 7-8, 2016, Proceedings 13. 2016. Springer.
6. Lin, C.-H., H.-K. Pao, and J.-W. Liao, Efficient dynamic malware analysis using virtual time control mechanics. Computers & Security, 2018. 73: p. 359-373.
7. Jian, Y., et al., A novel framework for image-based malware detection with a deep neural network. Computers & Security, 2021. 109: p. 102400.
8. Liu, X., et al., A novel method for malware detection on ML-based visualization technique. Computers & Security, 2020. 89: p. 101682.
9. Qiao, Y., et al. A multi-channel visualization method for malware classification based on deep learning. in 2019 18th IEEE International Conference On Trust, Security And Privacy In Computing And Communications/13th IEEE International Conference On Big Data Science And Engineering (TrustCom/BigDataSE). 2019. IEEE.
10. Han, K.S., et al., Malware analysis using visualized images and entropy graphs. International Journal of Information Security, 2015. 14: p. 1-14.
11. Vasan, D., et al., IMCFN: Image-based malware classification using fine-tuned convolutional neural network architecture. Computer Networks, 2020. 171: p. 107138.
12. Narayanan, B.N., O. Djaneye-Boundjou, and T.M. Kebede. Performance analysis of machine learning and pattern recognition algorithms for malware classification. in 2016 IEEE national aerospace and electronics conference (NAECON) and ohio innovation summit (OIS). 2016. IEEE.
13. Davuluru, V.S.P., B.N. Narayanan, and E.J. Balster. Convolutional neural networks as classification tools and feature extractors for distinguishing malware programs. in 2019 IEEE National Aerospace and Electronics Conference (NAECON). 2019. IEEE.
14. Narayanan, B.N. and V.S.P. Davuluru, Ensemble malware classification system using deep neural networks. Electronics, 2020. 9(5): p. 721.
15. Smarandache, F., et al., Introduction to neutrosophy and neutrosophic environment, in Neutrosophic Set in Medical Image Analysis. 2019, Elsevier. p. 3-29.
16. Salama, A., Basic structure of some classes of neutrosophic crisp nearly open sets and possible application to GIS topology. Neutrosophic Sets and Systems, 2015. 7: p. 18-22.
17. Ali, M., I. Deli, and F. Smarandache, The theory of neutrosophic cubic sets and their applications in pattern recognition. Journal of intelligent & fuzzy systems, 2016. 30(4): p. 1957-1963.
18. Guo, Y. and A.S. Ashour, Neutrosophic set in medical image analysis. 2019: Academic Press.
19. Bausys, R., et al., Algorithm selection for edge detection in satellite images by neutrosophic WASPAS method. Sustainability, 2020. 12(2): p. 548.

20. Dhingra, G., V. Kumar, and H.D. Joshi, A novel computer vision based neutrosophic approach for leaf disease identification and classification. Measurement, 2019. 135: p. 782-794.
21. Hashemi, H. and A. Hamzeh, Visual malware detection using local malicious pattern. Journal of Computer Virology and Hacking Techniques, 2019. 15: p. 1-14.
22. Fu, J., et al., Malware visualization for fine-grained classification. IEEE Access, 2018. 6: p. 14510-14523.
23. Le, Q., et al., Deep learning at the shallow end: Malware classification for non-domain experts. Digital Investigation, 2018. 26: p. S118-S126.
24. Vu, D.L., et al., HIT4Mal: Hybrid image transformation for malware classification. Transactions on Emerging Telecommunications Technologies, 2020. 31(11): p. e3789.
25. Efe, A. and S.H.S. Hussin, Malware visualization techniques. International Journal of Applied Mathematics Electronics and Computers, 2020. 8(1): p. 7-20.
26. Obaidat, I., et al., Jadeite: a novel image-behavior-based approach for java malware detection using deep learning. Computers & Security, 2022. 113: p. 102547.
27. Naeem, H., et al., Malware detection in industrial internet of things based on hybrid image visualization and deep learning model. Ad Hoc Networks, 2020. 105: p. 102154.
28. Ding, Y., et al., Android malware detection method based on bytecode image. Journal of Ambient Intelligence and Humanized Computing, 2023. 14(5): p. 6401-6410.
29. Zhang, W., et al., Android malware detection using tcn with bytecode image. Symmetry, 2021. 13(7): p. 1107.
30. Mercaldo, F., F. Martinelli, and A. Santone, Deep Convolutional Generative Adversarial Networks in Image-Based Android Malware Detection. Computers, 2024. 13(6): p. 154.
31. Ünver, H.M. and K. Bakour, Android malware detection based on image-based features and machine learning techniques. SN Applied Sciences, 2020. 2(7): p. 1299.
32. Awan, M.J., et al., Image-based malware classification using VGG19 network and spatial convolutional attention. Electronics, 2021. 10(19): p. 2444.
33. Shaukat, K., S. Luo, and V. Varadharajan, A novel deep learning-based approach for malware detection. Engineering Applications of Artificial Intelligence, 2023. 122: p. 106030.
34. Zhu, H., et al., An effective end-to-end android malware detection method. Expert Systems with Applications, 2023. 218: p. 119593.
35. Duraibi, S., Enhanced Image-Based Malware Classification using Snake Optimization Algorithm with Deep Convolutional Neural Network. IEEE Access, 2024.
36. Awotunde, J.B., et al., A multi-level random forest model-based intrusion detection using fuzzy inference system for internet of things networks. International Journal of Computational Intelligence Systems, 2023. 16(1): p. 31.
37. Ap, H. and K. K, Secure-MQTT: an efficient fuzzy logic-based approach to detect DoS attack in MQTT protocol for internet of things. EURASIP Journal on Wireless Communications and Networking, 2019. 2019(1): p. 90.
38. Abdel-Basset, M., et al., A risk assessment model for cyber-physical water and wastewater systems: Towards sustainable development. Sustainability, 2022. 14(8): p. 4480.
39. Abdel-Basset, M., et al., A security-by-design decision-making model for risk management in autonomous vehicles. IEEE Access, 2021. 9: p. 107657-107679.

40. Özyurt, F., et al., Brain tumor detection based on Convolutional Neural Network with neutrosophic expert maximum fuzzy sure entropy. Measurement, 2019. 147: p. 106830.
41. Guo, Y. and H.-D. Cheng, New neutrosophic approach to image segmentation. Pattern Recognition, 2009. 42(5): p. 587-595.
42. Kumar, S. and B. Janet, DTMIC: Deep transfer learning for malware image classification. Journal of Information Security and Applications, 2022. 64: p. 103063.
43. Simonyan, K. and A. Zisserman, Very deep convolutional networks for large-scale image recognition. arXiv preprint arXiv:1409.1556, 2014.
44. Sandler, M., et al. Mobilenetv2: Inverted residuals and linear bottlenecks. in Proceedings of the IEEE conference on computer vision and pattern recognition. 2018.
45. Huang, G., et al. Densely connected convolutional networks. in Proceedings of the IEEE conference on computer vision and pattern recognition. 2017.
46. Chollet, F. Xception: Deep learning with depthwise separable convolutions. in Proceedings of the IEEE conference on computer vision and pattern recognition. 2017.
47. Howard, A.G., Mobilenets: Efficient convolutional neural networks for mobile vision applications. arXiv preprint arXiv:1704.04861, 2017.
48. Bozkir, A.S., A.O. Cankaya, and M. Aydos. Utilization and comparision of convolutional neural networks in malware recognition. in 2019 27th signal processing and communications applications conference (SIU). 2019. IEEE.

Received: Mar 1, 2024. Accepted: July 15, 2024

Neutrosophic Sets and Systems, Vol. 76, 2025
University of New Mexico

A generalized hybrid distance measure for SVNS with an application in medical diagnosis

Norzieha Mustapha[1,*], Suriana Alias[2], Roliza Md Yasin[3], Alia Nur Izzah Zulkifli[4], Noorazliyana Shafii[5] and Florentin Smarandache[6]

[1]School of Mathematical Sciences, College of Computing, Informatics and Mathematics, Universiti Teknologi MARA, Cawangan Kelantan, Machang Campus, Kelantan, Malaysia, norzieha864@uitm.edu.my
[2]School of Mathematical Sciences, College of Computing, Informatics and Mathematics, Universiti Teknologi MARA, Cawangan Kelantan, Machang Campus, Kelantan, Malaysia, suria588@uitm.edu.my
[3]School of Mathematical Sciences, College of Computing, Informatics and Mathematics, Universiti Teknologi MARA, Cawangan Kelantan, Machang Campus, Kelantan, Malaysia, roliza927@uitm.edu.my
[4]Delphina Technik Sdn Bhd, 47301 Petaling Jaya, Selangor, alianurizzah2704@gmail.com
[5]School of Health Sciences, Health Campus, Universiti Sains Malaysia, 16150 Kubang Kerian, Kelantan, Malaysia, noorazliyana@usm.my;
[6]The University of New Mexico, Mathematics, Physics, and Natural Science Division, 705 Gurley Ave., Gallup, NM 87301, USA, smarand@unm.edu.
* Correspondence: norzieha864@uitm.edu.my

Abstract: A generalized hybrid distance measure of a single value neutrosophic set (SVNS) is proposed to analyze the patient's factors and diseases. Since Neutrosophic Set (NS) may communicate contradictory and ambiguous information, it is a crucial and useful tool for modelling uncertainty information. A distance measure for NS information is a key tool that is always employed in many approaches including medical diagnostics. Several distance measures in NS can be found in the literature, however, only a few of them proposed hybrid techniques. This paper aims to develop a new distance measure by considering exponential function and to define new hybrid distance measures for NS. The work also includes the formulation of the properties and application in the medical diagnosis for the validity phase. This study examines the possibility of cardiac problems in pregnant women. The eight factors considered in this study are age, obesity, smoking, family pathological history, personal pathological history, electrocardiogram, ultrasound, and functional class. The generalized hybrid distance measure has been used to discuss the factors of six different diseases, present consistent results.

Keywords: Neutrosophic set; distance measure; hybrid distance measure; medical diagnosis

1. Introduction

A neutrosophic set (NS) is a generalization of the concept of a fuzzy set (FS) and intuitionistic fuzzy set (IFS), which allows for the inclusion of uncertainty, indeterminacy, and vagueness. This effective mathematical model was proposed by [1]. An extension of the neutrosophic set is the single-valued neutrosophic set (SVNS)[2]. The SVNS is a generalization of the classic set, FS, and IFS [3]. The IFS has difficulties when it comes to communicating decision-related information. It can be viewed as a level of membership and a level of non-membership that is unable to deal with all kinds of doubts and contradictory information. In order to manage uncertain and inconsistent information,

SVNS includes three terms: truth-membership, indeterminacy-membership, and falsity-membership. Over the years, a lot of information regarding the model measure for the SVNS model has been introduced and discussed. For instance, correlation coefficients, similarity measures, entropy measures, distance measures, and inclusion measures.

The similarity measure can be described as a crucial method in determining the degree of similarity between two objects. The numerous similarity measures can be represented into two categories which are crisp and neutrosophic similarity measures. The crisp similarity measures can be said to be real valued functions and neutrosophic similarity measures can be considered as the level of similarity, considering the similarity among the three membership values one by one. Because of that, the neutrosophic similarity acts towards a single valued neutrosophic number as a measure of the similarity. In multiple criteria decision making, to determine the differences between the criteria, similarity measure of neutrosophic set can be used [4 - 7]. According to [8], similarity measures are very important in many applications with various fields of decision making such as pattern recognition, image thresholding, and multicriteria decision making.

A hybrid similarity measure is a metric that combines two or more similarity measures to produce a single similarity value. A generalized hybrid similarity measure of a neutrosophic set is a metric that considers the different aspects of uncertainty, indeterminacy, and vagueness inherent in a neutrosophic set, and combines them to produce a single similarity value. New hybrid distance-based similarity measures are studied by [9] and [10]. Mondal et al [9] proposed hybrid binary logarithm similarity measure for dealing indeterminacy in decision making situations. Meanwhile, Ulucay et al [10] introduced a new hybrid distance-based similarity measure for refined rough neutrosophic set and the method is applied in medical diagnosis for some diseases.

Beside similarity measure, the distance measure also can be used to perform a similar task. Distance value represents the degree of dissimilarity between two sets. [11] developed a distance measure that improves decision-making flexibility under uncertainty by integrating soft expert systems with SVNSs. Zeng et al [12] developed a new distance measure between IFSs and applied it in pattern recognition. For SVNS, [13] produced a novel distance measure for SVNS and applied to multicriteria group decision-making problem. [14] integrated the distance measure with entropy weight measure for application in medical diagnosis.

The SVNS is important in modelling theory. Thus, it can be used in real scientific and technical applications. Due to the growing amount of information accessible from contemporary medical equipment, medical diagnosis contains a lot of incomplete, uncertain, imprecise, and inconsistent information, which is essential information about medical diagnosis problems [15]. Symptoms usually involves a lot of incomplete, ambiguous, and inconsistent information for a disease. According to [16], in medical diagnosis problems, symptoms and data inspection of diseases may be changed in different time intervals. This leads to the question of whether the use of a single inspection period can make it possible to conclude that a particular patient has a particular disease or not. Sometimes symptoms of different illnesses can appear in a person being treated. [17 – 18] applied the theory of SVNS to medical diagnosis. Studies using clustering approaches have indicated that the hybrid technique has enhanced the precision of disease diagnosis based on patient symptoms [18]. Besides SVNS, [19] applied the theory of rough neutrosophic set to medical diagnosis. [20] investigated a unique multi-parameter similarity measure for interval-valued neutrosophic sets (IVNSs) and it provides stable results and improves diagnostic accuracy by taking symptom interactions into account. In medical diagnostics, a bi-parametric discriminant measure addresses decision-making uncertainty and provides numerical examples to demonstrate its usefulness, allowing for effective symptomatic diagnosis [21].

The purposes of this study are to formulate a novelty distance measure of SVNS, which is the extension of [12] and to construct a new hybrid distance measure. The work starts by extending an existing distance measure from [12] to create a new one for SVNS. To increase the precision of the distance calculation between two NS, a hybrid distance measure is created by combining the recently created distance measure with the several existing distance measures for NS. The objective of the

hybrid distance measure would be to better capture the complexities and nuances of the relationship between two NSs. The details of the hybrid distance measure would depend on the specific requirements and applications for which it is being developed. Several factors were taken into consideration when developing the hybrid distance measure, such as the importance of imprecision and uncertainty as well as the particular needs of the applications it would be used for. Eventually, by exploiting the increased accuracy in processing neutrosophic data, the generalized hybrid distance measure will be used to address issues related to medical diagnosis.

The remainder of the paper is structured as follows. Section two contains preliminary definition for some key terms, while section three introduces new definitions of a novel distance measure, and the hybrid distance measure is introduced in section four. Section five focuses on the application of new distance measures in medical diagnosis. Finally, section six is the conclusion of the present study.

2. Preliminaries

2.1. Neutrosophic Set

Definition 2.1.1: Neutrosophic Set [1]

Consider a space of points (objects) denoted by X, with each individual element in X represented by x. Within this context, the neutrosophic set $NS(A)$ can be understood as an object that takes a specific form $A = \left[\left(x, T_A(x), I_A(x), F_A(x)\right) : x \in X\right]$, where the functions $T, I, F : X \rightarrow]^{-}0, 1^{+}[$ define respectively the truth-membership function, an indeterminacy membership function and a falsity-membership function of the element $x \in X$ to the set A with the condition :

$$^{-}0 \leq T_A(x) + I_A(x) + F_A(x) \leq 3^{+}.$$

The function $T_A(x), I_A(x)$ and $F_A(x)$ are real standard or nonstandard subsets of $]^{-}0, 1^{+}[$.

Example: Truth (*T*), Indeterminacy (*I*), and Falsity (*F*) values in a NS are usually expressed as ranges, providing flexibility in expressing uncertainty. Let's look at a NS A, which stands for a collection of tall students. The ranges for each student *x* are the Truth (*T*(x)), Indeterminacy (*I*(x)), and Falsity (*F*(x)) of being tall.

For a student x:
$T(x)$ = [0.7,0.9] (The student's height ranges from 70% to 90%).
$I(x)$ = [0.1, 0.2] (There is a 10% to 20% margin of error regarding the student's height),
$F(x)$ = [0.1, 0.3] (The student is not tall by 10% to 30%).
This indicates that although there is some uncertainty and a small amount of falsity, student x is generally regarded as tall.

Definition 2.1.2: Single Value Neutrosophic Set [2]

Consider a space of points (objects) denoted by X, with each individual element in X represented by x. A single-valued neutrosophic set $A\left(SVNS(A)\right)$ is characterized by a truth-membership function $T_A(x)$, an indeterminacy-membership function $I_A(x)$, and a falsity-membership function $F_A(x)$. For each point x in $X, T_A(x), I_A(x), F_A(x) \in [0,1]$. A SVNS can be written as

$$A = \{\langle x\ ;\ T_A(x), I_A(x), F_A(x)\rangle : x \in X\} \tag{1}$$

Example: A SVNS simplifies the neutrosophic set by giving truth, indeterminacy, and falsity fixed values (rather than ranges) within the interval [0,1]. Let's look at a SVNS A, which represents the percentage of exam takers who fall into the pass category.

For a student y:
$T(y)$ = 0.8 (A student is 80% likely to have passed)
$I(y)$ = 0.1 (There is 10% uncertainty over the student's passing)
$F(y)$ = 0.2 (The student is 20% likely to have failed)
In this instance, the fixed numbers give a clear picture of the student's exam result's validity, uncertainty, and falsity. As a result, the student is passed the exam

2.2 Distance Measure

One mathematical tool for calculating the distance between two neutrosophic sets is the distance measure for that sets. Depending on the intended use, a variety of distance measures, including Hamming distance, Hausdroff distance, Euclidean distance, and more generic distance functions, can be defined.

Definition 2.2.1: Several Distance Measures for SVNS
Let $X = \{x_1, x_2, \ldots, x_n\}$ be the universe of discourse. Let $A = \{x_i, T_A(x_i), I_A(x_i), F_A(x_i)) : x_i \in X\}$ and $B = \{x_i, T_B(x_i), I_B(x_i), F_B(x_i)) : x_i \in X\}$ be two neutrosophic sets. Several distance measures between two SVNS, A and B can be defined as:

1. Normalized Hamming distance measure [5]:

$$d_M^N(A,B) = \frac{1}{3n}\sum_{i=1}^{n}(|T_A(x_i) - T_B(x_i)| + |I_A(x_i) - I_B(x_i)| + |F_A(x_i) - F_B(x_i)|) \tag{2}$$

2. Normalized Euclidean distance measure [5]:

$$d_E^N(A,B) = \sqrt{\frac{1}{3n}\sum_{i=1}^{n}((T_A(x_i) - T_B(x_i))^2 + (I_A(x_i) - I_B(x_i))^2 + (F_A(x_i) - F_B(x_i))^2)} \tag{3}$$

3. Extended Hausdroff distance metric [5]:

$$d_S^N(A,B) = \frac{1}{n}\sum_{i=1}^{n} max(|T_A(x_i) - T_B(x_i)|, |I_A(x_i) - I_B(x_i)|, |F_A(x_i) - F_B(x_i)|) \tag{4}$$

4. Mustapha et al [17]:

$$d_{NM}^N(A,B) = \frac{2}{n}\sum_{i=1}^{n}\frac{sin\left\{\frac{\pi}{10}|T_A(x_i)-T_B(x_i)|\right\}+sin\left\{\frac{\pi}{10}|I_A(x_i)-I_B(x_i)|\right\}+sin\left\{\frac{\pi}{10}|F_A(x_i)-F_B(x_i)|\right\};}{1+sin\left\{\frac{\pi}{10}|T_A(x_i)-T_B(x_i)|\right\}+sin\left\{\frac{\pi}{10}|I_A(x_i)-I_B(x_i)|\right\}+sin\left\{\frac{\pi}{10}|F_A(x_i)-F_B(x_i)|\right\}} \tag{5}$$

5. Ye and Zhang [6]:

$$d_{YZ}^N(A,B) = 1 - \frac{1}{3n}\sum_{i=1}^{n}\left(\frac{\min(T_A(x_i),T_B(x_i))}{\max(T_A(x_i),T_B(x_i))} + \frac{\min(I_A(x_i),I_B(x_i))}{\max(I_A(x_i),I_B(x_i))} + \frac{\min(F_A(x_i),F_B(x_i))}{\max(F_A(x_i),F_B(x_i))}\right) \tag{6}$$

6. Ren et al [7]:

$$d_{Ren}^{N}(A,B)=\frac{1}{2n}\sum_{i=1}^{n}\left(\frac{(T_A(x_i)-T_B(x_i))^2}{2+T_A(x_i)+T_B(x_i)}+\frac{(I_A(x_i)-I_B(x_i))^2}{2+I_A(x_i)+I_B(x_i)}+\frac{(F_A(x_i)-F_B(x_i))^2}{2+F_A(x_i)+F_B(x_i)}+|m_A(x_i)-m_B(x_i)|\right), \quad (7)$$

where $m_j(x_i)=\frac{1+T_j(x_i)-F_j(x_i)}{2}, j=A,B$

7. Binary Logarithm [9]:

$$BL(A,B)=1-\frac{1}{n}\sum_{i=1}^{n}log_2\left(2-\left(\frac{1}{3}\left(T_A(x_i)-T_B(x_i)\right)+(I_A(x_i)-I_B(x_i))+(F_A(x_i)-F_B(x_i))\right)\right) \quad (8)$$

3. New Distance Measure for Single Value Neutrosophic Set

In this section, a novel approach for determining the distance measure between SVNS is introduced. It is extended from the work by [12], which incorporates exponential distance to minimize any potential loss of information.

Definition 3.1: Let $X=\{x_1,x_2,\ldots,x_n\}$ be the universe of discourse. Let $A=\{x_i, T_A(x_i),I_A(x_i),F_A(x_i)):x_i\in X\}$ and $B=\{x_i, T_B(x_i),I_B(x_i),F_B(x_i)): x_i\in X\}$ be two neutrosophic sets. A distance measure between two SVNS, A and B can be defined as:

$$d_{New}^{N}(A,B)=\frac{1}{n}\sum_{i=1}^{n}\left(d_{exp}(A,B)\times d_{tif}(A,B)\right) \quad (9)$$

where $d_{exp}(A,B)=e^{|T_A(x_i)-T_B(x_i)|-1}$, $d_{tif}(A,B)=\frac{1}{3}\sum_{i=1}^{n}(|T_A(x_i)-T_B(x_i)|+|I_A(x_i)-I_B(x_i)|+|F_A(x_i)-F_B(x_i)|)$, $d_{exp}(A,B)$ denotes the exponential distance measure, which is determined by the difference of the ith membership degree between A and B. and $d_{tif}(A,B)$ denotes the average including absolute value of ith membership degree, intermediate degree and false degree between A and B.

Theorem 3.1: $d_{New}^{N}(A,B)$ is the distance measure between SVNS A and B.

Proposition:

$(S1)$ $0\le d_{New}^{N}(A,B)\le 1$

$(S2)$ $d_{New}^{N}(A,B)=d_{New}^{N}(B,A)$

$(S3)$ $d_{New}^{N}(A,B)=0$ if and only if $A=B$

$(S4)$ For $A\subseteq B\subseteq C$, then we have $d_{New}^{N}(A,C)\ge d_{New}^{N}(A,B)$ and $d_{New}^{N}(A,C)\ge d_{New}^{N}(B,C)$

Proof(S1):

Suppose $T_A(x_i), T_B(x_i), I_A(x_i), I_B(x_i), F_A(x_i)$ and $F_B(x_i)\in[0,1]$, thus, we have

$$|T_A(x_i)-T_B(x_i)|\in[0,1]\Rightarrow|T_A(x_i)-T_B(x_i)|-1\in[-1,0]$$

$$\Rightarrow e^{|T_A(x_i)-T_B(x_i)|-1}\in[e^{-1},e^{0}]\subseteq[0,1]$$

$\therefore d_{exp}(A,B) \in [0,1]$.

$$|T_A(x_i) - T_B(x_i)| + |I_A(x_i) - I_B(x_i)| + |F_A(x_i) - F_B(x_i)| \in [0,3]$$

$$\Longrightarrow \frac{|T_A(x_i) - T_B(x_i)| + |I_A(x_i) - I_B(x_i)| + |F_A(x_i) - F_B(x_i)|}{3} \in [0,1]$$

$\therefore d_{tif}(A,B) \in [0,1]$.

Hence,

$d_{exp}(A,B) \times d_{tif}(A,B) \in [0,1] \Longrightarrow d_{New}^{N}(A,B) \in [0,1]$.

Proof(*S2*):

$d_{New}^{N}(A,B) = d_{New}^{N}(B,A)$ is obvious.

Proof(*S3*):

$d_{New}^{N}(A,B) = 0$ if and only if $A = B$;

Sufficiency: If $d_{New}^{N}(A,B) = 0$, then for every x_i, we have $d_{exp}(A,B) = 0$, which means

$$\frac{|T_A(x_i) - T_B(x_i)| + |I_A(x_i) - I_B(x_i)| + |F_A(x_i) - F_B(x_i)|}{3} = 0$$

$$\Longrightarrow |T_A(x_i) - T_B(x_i)| + |I_A(x_i) - I_B(x_i)| + |F_A(x_i) - F_B(x_i)| = 0$$

Then,

$$|T_A(x_i) - T_B(x_i)| = 0$$
$$|I_A(x_i) - I_B(x_i)| = 0$$
$$|F_A(x_i) - F_B(x_i)| = 0$$

Hence, we can have $T_A(x_i) = T_B(x_i), I_A(x_i) = I_B(x_i)\ and\ F_A(x_i) = F_B(x_i)$ for every x_i. That means *A=B*.

Necessity: If *A=B*, then it means for every x_i, we have $T_A(x_i) = T_B(x_i), I_A(x_i) = I_B(x_i)\ and\ F_A(x_i) = F_B(x_i)$, thus

$$d_{tif}(A,B) = \frac{|T_A(x_i) - T_B(x_i)| + |I_A(x_i) - I_B(x_i)| + |F_A(x_i) - F_B(x_i)|}{3} = 0$$

$$\Longrightarrow d_{New}^{N}(A,B) = \frac{1}{n}\sum_{i=1}^{n}\Big(d_{exp}(A,B) \times d_{tif}(A,B)\Big) = 0$$

Proof(*S4*):

For $A \subseteq B \subseteq C$, then we have $d_{New}^{N}(A,C) \geq d_{New}^{N}(A,B)$ and $d_{New}^{N}(A,C) \geq d_{New}^{N}(B,C)$.

If $A \subseteq B \subseteq C$, we have

$$T_A(x_i) \leq T_B(x_i) \leq T_C(x_i)$$
$$I_A(x_i) \geq I_B(x_i) \geq I_C(x_i)$$
$$F_A(x_i) \geq F_B(x_i) \geq F_C(x_i)$$

Then, we get

$$|T_A(x_i) - T_C(x_i)| \geq |T_A(x_i) - T_B(x_i)|$$
$$|T_A(x_i) - T_C(x_i)| \geq |T_B(x_i) - T_A(x_i)|$$
$$|I_A(x_i) - I_C(x_i)| \geq |I_A(x_i) - I_B(x_i)|$$
$$|I_A(x_i) - I_C(x_i)| \geq |I_B(x_i) - I_A(x_i)|$$
$$|F_A(x_i) - F_C(x_i)| \geq |F_A(x_i) - F_B(x_i)|$$
$$|F_A(x_i) - F_C(x_i)| \geq |F_B(x_i) - F_A(x_i)|$$

Further, we can get

$$e^{|T_A(x_i) - T_C(x_i)| - 1} \geq e^{|T_A(x_i) - T_B(x_i)| - 1}$$

$$\frac{|T_A(x_i) - T_C(x_i)| + |I_A(x_i) - I_C(x_i)| + |F_A(x_i) - F_C(x_i)|}{3} \geq \frac{|T_A(x_i) - T_B(x_i)| + |I_A(x_i) - I_B(x_i)| + |F_A(x_i) - F_B(x_i)|}{3}$$

That is

$$d_{tif}(A, C) \geq d_{tif}(A, B)$$
$$d_{exp}(A, C) \geq d_{exp}(A, B)$$

Thus, we have $d_{New}^N(A, C) \geq d_{New}^N(A, B)$.
Similarly, we have $d_{New}^N(A, C) \geq d_{New}^N(B, C)$.
The theorem proved completely.

4. New Hybrid Distance Measure for SVNS

Hybrid formulas combine many methods or techniques, often coming from multiple disciplines or areas of expertise. Hybrid approaches utilize the benefits of each technique to get results that are more accurate than those obtained by using only one strategy. Assessing persistent similarities with greater accuracy should be the outcome of incorporating different similarity measures into a hybrid formula. Moreover, hybrid formulas are often more adaptable and dependable in a variety of datasets and situations. Because they can handle a wider range of input data types and attributes, they are suitable for a multitude of applications.

Definition 4.1: Hybrid vector distance measures of SVNS
Let $A = [T_A(x_i), I_A(x_i), F_A(x_i)]$ and $B = [T_B(x_i), I_B(x_i), F_B(x_i)]$ be two SVNSs in a universe of discourse $X = \{x_1, x_2, \dots, x_n\}$. Then, the hybrid distance measure of SVNSs in the vector space is defined as follows:

$$Hyb(A, B) = \tau\big(d(A, B)\big) + (1 - \tau) d_{New}^N(A, B)) \tag{10}$$

where $0 \leq \tau \leq 1$ and $d(A, B)$ is replaced with $BL(A, B), d_{NM}^N(A, B), d_M^N(A, B), d_E^N(A, B), d_S^N(A, B), d_{YZ}^N(A, B)$ and $d_{Ren}^N(A, B)$ in Equations (2-8) for various hybrid distance measures.

Theorem 4.1 The formulation of properties for new hybrid distance measure of SVNS
The generalized hybrid distance measure $Hyb(A, B)$ for neutrosophic set A and B satisfies the following properties. For proving purpose, let $d(A, B)$ is defined as binary logarithm distance(Equation (8)), then Equation (10) becomes

$$Hyb(A, B) = \tau(BL(A, B) + (1 - \tau) d_{New}^N(A, B)) \text{ with } 0 \leq \tau \leq 1$$

Proposition:

$(S1)$ $0 \leq Hyb(A,B) \leq 1$

$(S2)$ $Hyb(A,B) = Hyb(B,A)$

$(S3)$ $Hyb(A,B) = 0$ if and only if $A = B$

$(S4)$ For $A \subseteq B \subseteq C$, then we have $Hyb(A,C) \geq Hyb(A,B)$ and $Hyb(A,C) \geq Hyb(B,C)$

Proof$(S1)$**:**

Suppose $BL(A,B)$ and $d_{New}^{N}(A,B) \in [0,1]$, thus, we have

$$0 \leq BL(A,B) + d_{New}^{N}(A,B) \leq 2.$$

$With\ 0 \leq \tau \leq 1$,

$$0 \leq \tau(BL(A,B) + (1-\tau)d_{New}^{N}(A,B)) \leq 1$$

Hence, the hybrid distance measure of SVNS is within [0,1]. Thus $0 \leq Hyb(A,B) \leq 1$.

Proof$(S2)$:

$Hyb(A,B) = Hyb(B,A)$ is obvious.

Proof$(S3)$**:**

For any two distances $BL(A,B)$ and $d_{New}^{N}(A,B)$, if $A = B$, then we have $BL(A,A)$ and $d_{New}^{N}(A,A)$. According to the proof of $d_{New}^{N}(A,B)$ shown in Section 3.1 and the proof of $BL(A,B)$ in [9], we have

$$BL(A,A) = 0 \text{ and } d_{New}^{N}(A,A) = 0,$$

$with\ 0 \leq \tau \leq 1$,

$$\tau(BL(A,A) + (1-\tau)d_{New}^{N}(A,A)) = 0 + 0 = 0$$

Similarly, if $A = B$

Hence, $Hyb(A,B) = 0$ if and only if $A = B$.

Proof$(S4)$**:**

For $A \subseteq B \subseteq C$, according to the proof of $d_{New}^{N}(A,B)$ shown in Section 3.1 and the proof of $BL(A,B)$ in [6], we have $d_{New}^{N}(A,C) \geq d_{New}^{N}(A,B)$, $d_{New}^{N}(A,C) \geq d_{New}^{N}(B,C)$, $BL(A,C) \geq BL(A,B)$ and $BL(A,C) \geq BL(B,C)$. Then, we have

$$BL(A,C) + d_{New}^{N}(A,C) \geq BL(A,B) + d_{New}^{N}(A,B).$$

With $0 \leq \tau \leq 1$,

$$\tau BL(A,C) + (1-\tau)d_{New}^{N}(A,C)) \geq \tau BL(A,B) + (1-\tau)d_{New}^{N}(A,B).$$

Thus, we have $Hyb(A,C) \geq Hyb(A,B)$.

Similarly, we have $Hyb(A,C) \geq Hyb(B,C)$.

The theorem was proved completely. The other hybrid distance measures can be proven similarly.

5. Application of new hybrid distance measure in medical diagnosis

Since the physical and hormonal changes that take place during pregnancy can put the heart under additional stress, pregnancy can be a high-risk time for women with heart disease. Heart failure, irregular heart rhythm, and blood clots are just a few of the pregnancy issues that may be more likely to occur in women who already have heart disease. In extreme situations, a pregnant woman with heart problems may potentially have a heart attack. All things considered, it's critical for pregnant women who have heart disease to be aware of the potential hazards involved and to seek medical advice from a specialist to decide the best course of action.

In this study, the data is collected from [22]. The following eight symptoms are commonly used to assess the level of risk for a pregnant woman with heart disease by doctors or medical officers.

Age: Older women are at higher risk of developing heart disease, and pregnancy can increase this risk.
Obesity: Women who are overweight or obese have an increased risk of developing heart disease, and this risk is further increased during pregnancy.
Smoking: Smoking increases the risk of heart disease and should be avoided by pregnant women with heart disease.
Family Pathological History: A family history of heart disease can indicate an increased risk of heart disease in pregnant women.
Personal Pathological History: A personal history of heart disease or heart-related conditions can increase the risk of complications during pregnancy.
Electrocardiogram (ECG): An ECG can detect heart disease and help determine the risk to the mother and fetus during pregnancy.
Ultrasound: An ultrasound can help detect heart problems and monitor the fetus during pregnancy.
Functional Class: The functional class of a woman's heart disease can help determine the risk of complications during pregnancy and guide management decisions.

Table 1. The relation between a woman and factors

Factor	(T,I,F)
A	(0.6,0.50,0.37)
OB	(1.0,0.25,0.60)
TAB	(1.0,0.00,0.00)
FPH	(1.0,0.00,0.00)
PPH	(1.0,0.00,0.00)
ECG	(0.5,0.30,0.40)
ECO	(0.5,0.30,0.40)
FH	(0.7,0.15,1.00)

The risks of pregnancy can be increased in a woman *W*, with major factor I={age(A), obesity (OB), smoking (TAB), personal pathological history PPH), family pathological history (FPH),

electrocardiogram (ECG), ultrasound (ECO), functional class (FH)}. The diagnoses listed in the set are D = {obstruction at exit (OEX), obstruction at entry (OEN), rhythm disorders (RD), conduction disorder (CDS), congenital disease (CD), genetic disease (GD)} can affect pregnant women. These diseases can complicate pregnancy, delivery, and the postpartum period and have negative effects on both the mother and the fetus. OEX and OEN can make it more difficult for the fetus to be born and may necessitate a caesarean section. In addition to increasing the risk of difficulties during pregnancy and delivery, RD and CDS can lead to irregular heartbeats. CD and GD can cause congenital anomalies or genetic abnormalities in the fetus, which can impact its development and survival.

Pregnant women need to be examined and monitored by a healthcare provider if they have any of these conditions, to minimize the risk of complications and ensure the best possible outcome for both the mother and the fetus. The data from [22] are shown in Tables 1 and 2 which represent the relation between women and symptoms and the relation between symptoms and diagnoses, respectively.

Table 2. The relation between factors and diseases

	A	**OB**	**TAB**	**FPH**
OEX	(0.9,0.2,0.3)	(0.2,0.6,0.4)	(0.9,0.1,0.3)	(0.2,0.2,0.3)
OEN	(0.2,0.2,0.4)	(0.3,0.5,0.6)	(0.8,0.1,0.2)	(0.2,0.4,0.1)
RD	(0.8,0.3,0.2)	(0.9,0.2,0.3)	(0.9,0.2,0.3)	(0.2,0.1,0.1)
CDS	(0.9,0.2,0.3)	(0.8,0.2,0.1)	(0.9,0.2,0.3)	(0.3,0.6,0.5)
CD	(0.9,0.1,0.3)	(0.9,0.2,0.2)	(0.8,0.1,0.2)	(0.2,0.8,0.1)
GD	(0.9,0.2,0.3)	(0.8,0.2,0.3)	(0.2,0.1,0.4)	(0.8,0.2,0.3)
	PPH	**ECG**	**ECO**	**FH**
OEX	(0.9,0.1,0.2)	(0.8,0.2,0.3)	(0.7,0.2,0.2)	(0.9,0.2,0.1)
OEN	(0.8,0.2,0.3)	(0.7,0.2,0.3)	(0.8,0.2,0.3)	(0.9,0.2,0.3)
RD	(0.9,0.2,0.3)	(0.2,0.2,0.4)	(0.2,0.8,0.5)	(0.9,0.2,0.3)
CDS	(0.9,0.2,0.2)	(0.2,0.5,0.6)	(0.9,0.2,0.2)	(0.9,0.1,0.3)
CD	(0.2,0.5,0.5)	(0.9,0.2,0.2)	(0.8,0.2,0.3)	(0.9,0.2,0.2)
GD	(0.9,0.2,0.3)	(0.3,0.8,0.6)	(0.2,0.1,0.5)	(0.8,0.2,0.3)

The generalized hybrid distance measure is defined according to different values of τ as stated below:

i) If $\tau = 0$, the hybrid distance measure reduced to the new formulated distance measure (Equation 9).

ii) If $\tau = 1$, the hybrid distance measure is generalized to either Hamming, Hausdroff, Euclidean, Mustapha et al [17], Ye & Zhang [6], Ren et al [7] or Binary Logarithm (Mondal et al [9]) measure (Equations (2-8)).

iii) If $\tau = 0.5$, the hybrid distance measure is the mean distance measure between two distance measures.

iv) If $\tau = 0.1$ and $\tau = 0.9$, the hybrid distance measure is defined.

Table 3. The new distance measure for a woman W with diseases ($\tau = 0$)

Diseases	New Distance Measure
OEX	0.167808
OEN	0.157324
RD	0.088902
CDS	0.127549
CD	0.22461
GD	0.107783

Table 4. The new hybrid distance measures for a woman W with diseases when $\tau = 1$

	Hamming	Hausdorff	Euclidean	Mustapha et al (2021)	Ye & Zhang (2014)	Binary Logarithm (Mondal et al (2018))	Ren et al (2019)
OEX	0.260833	0.475	0.349929	0.379077	0.545701	0.205562	0.201525
OEN	0.254167	0.45875	0.331461	0.377367	0.532337	0.19821	0.198151
RD	0.225	0.425	0.296564	0.343536	0.514688	0.173466	0.163107
CDS	0.275	0.425	0.33434	0.397885	0.543531	0.217922	0.198624
CD	0.3125	0.5125	0.403774	0.432617	0.563323	0.252555	0.244957
GD	0.254167	0.4375	0.314431	0.380204	0.539364	0.197605	0.178489

The results of the hybrid distance measures, which were applied to analyze pregnant women's symptoms and forecast their propensity to develop specific diseases while pregnant, are shown in Tables 3–7. The results of the analysis using various parameter values are shown in the tables. The results from the hybrid distance measures are considered adequate for medical diagnostics despite the variances in parameter values. This shows that the suggested strategy is solid and capable of offering trustworthy information on the patient's condition.

Table 5. The new hybrid distance measures for a woman W with diseases when τ=0.5

	Hamming	Hausdorff	Euclidean	Mustapha et al (2021)	Ye & Zhang (2014)	Binary Logarithm (Mondal et al (2018))	Ren et al (2019)
OEX	0.214321	0.321404	0.258868	0.273443	0.356755	0.186685	0.184666
OEN	0.205745	0.308037	0.244393	0.267346	0.344831	0.177767	0.177737
RD	0.156951	0.256951	0.192733	0.216219	0.301795	0.131184	0.126004
CDS	0.201274	0.276274	0.230944	0.262717	0.33554	0.172735	0.163086
CD	0.268555	0.368555	0.314192	0.328613	0.393966	0.238583	0.234784
GD	0.180975	0.272642	0.211107	0.243993	0.323574	0.152694	0.143136

It is clear from looking at the results shown in the Tables 3-7 that the pregnant woman has a very high likelihood of developing RD throughout her pregnancy. Her symptoms exhibit important signs and patterns that are consistent with RD according to the hybrid distance measurements. Therefore, doctors could begin treating this patient early in order to prevent difficulties for the mother and the unborn child. Pre-existing heart problems, hypertension, and obesity all raise a woman's risk of getting an RD during pregnancy.

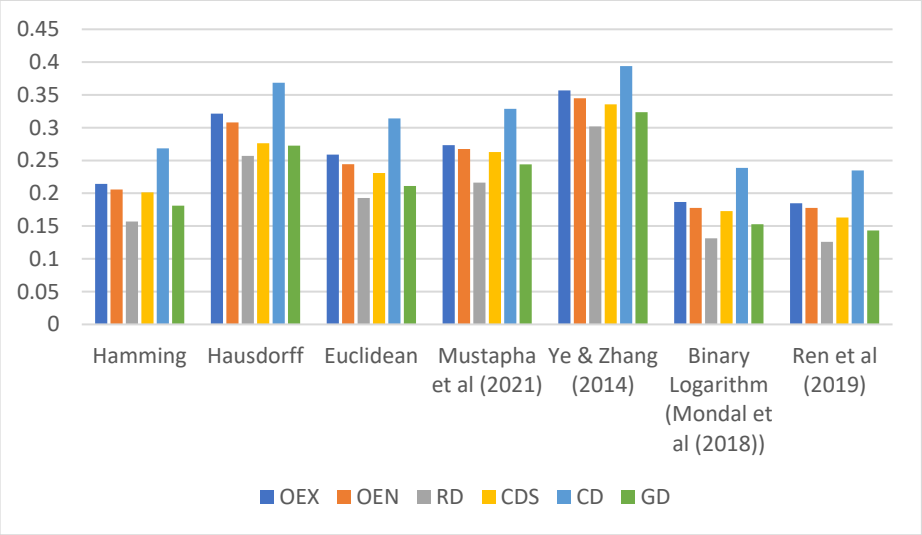

Figure 1. The new hybrid distance measures for a woman *W* with diseases when τ=0.5

Table 6. The new hybrid distance measures for a woman *W* with diseases when τ=0.9

	Hamming	**Hausdorff**	**Euclidean**	**Mustapha et al (2021)**	**Ye & Zhang (2014)**	**Binary Logarithm (Mondal et al (2018))**	**Ren et al (2019)**
OEX	0.251531	0.444281	0.331717	0.35795	0.507912	0.171584	0.198153
OEN	0.244482	0.428607	0.314048	0.355363	0.494836	0.161412	0.194068
RD	0.21139	0.39139	0.275797	0.318072	0.472109	0.097358	0.155687
CDS	0.260255	0.395255	0.313661	0.370852	0.501933	0.136586	0.191516
CD	0.303711	0.483711	0.385857	0.411816	0.529451	0.227404	0.242923
GD	0.239528	0.404528	0.293766	0.352961	0.496206	0.116765	0.171419

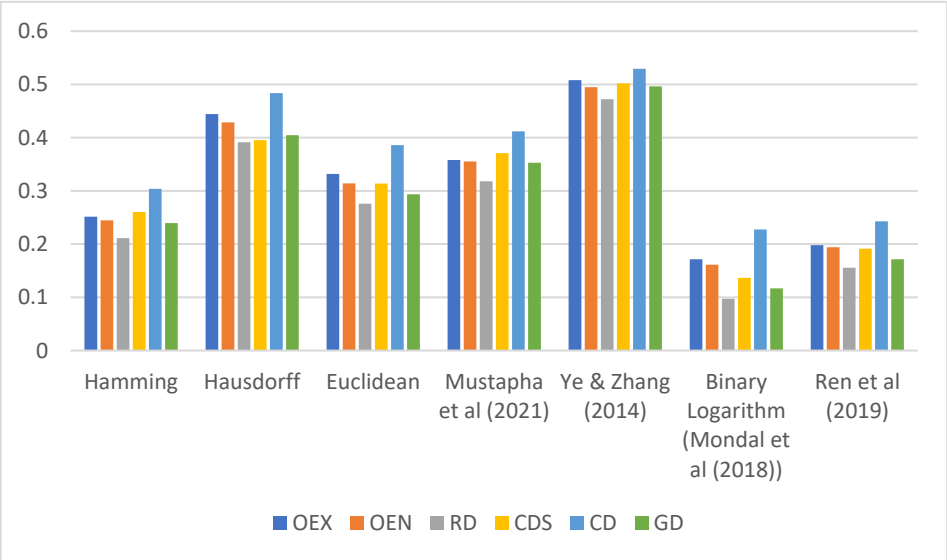

Figure 2. The new hybrid distance measures for a woman *W* with diseases when τ=0.9

Table 7. The new hybrid distance measures for a woman *W* with diseases when τ=0.1

	Hamming	Hausdorff	Euclidean	Mustapha et al (2021)	Ye & Zhang (2014)	Binary Logarithm (Mondal et al (2018))	Ren et al (2019)
OEX	0.177111	0.198527	0.18602	0.188935	0.205598	0.201787	0.17118
OEN	0.167008	0.187466	0.174738	0.179328	0.194825	0.194121	0.161406
RD	0.102511	0.122511	0.109668	0.114365	0.13148	0.165009	0.096322
CDS	0.142294	0.157294	0.148228	0.154582	0.169147	0.208885	0.134656
CD	0.233399	0.253399	0.242526	0.245411	0.258481	0.249761	0.226645
GD	0.122421	0.140755	0.128448	0.135025	0.150941	0.188623	0.114854

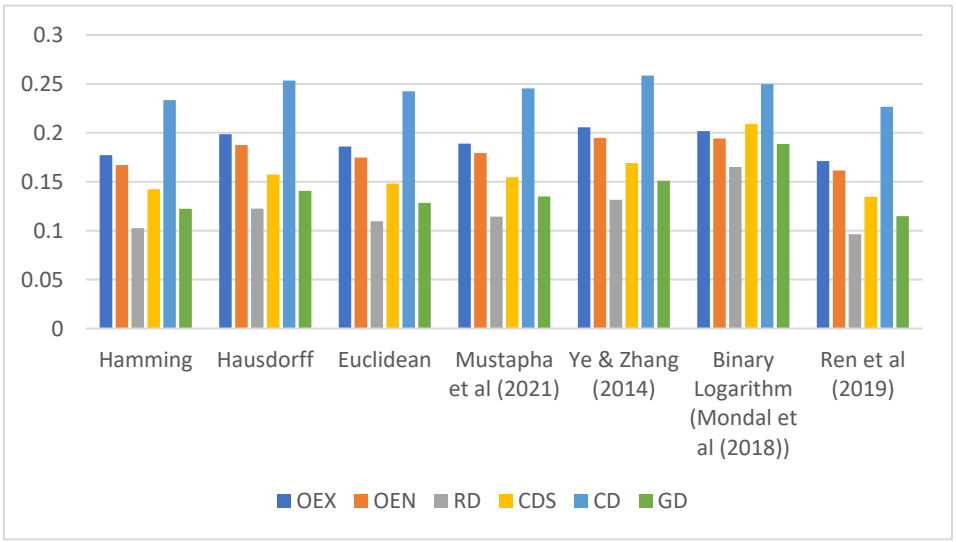

Figure 3. The new hybrid distance measures for a woman *W* with diseases when τ=0.1

As shown in Tables 5-7, new distance measure proposed in our study demonstrates its contribution to the analysis of RD compared to other distance measures, even when considering various values of the parameter, τ. The results obtained also presented clearly in Figures 1-3. This indicates that our new distance measure is particularly effective in capturing the relevant characteristics and patterns associated with RD, making it a valuable tool for diagnosing and predicting this condition.

In the analysis, we observed that the shortest distance measure is highly influenced by the hybridization between the new distance measure and [7] when τ is set to 0.1. This finding suggests that the combination of our new distance measure with Ren et al [7] yields the most accurate representation of RD symptoms, resulting in a distance measure that is closest to zero and indicating a higher likelihood of RD.

Furthermore, the second-lowest distance measure is predominantly influenced by the hybridization between the new distance measure and Binary Logarithm with a τ value of 0.1. This indicates that this particular combination captures important aspects of RD symptoms, contributing to a relatively low distance measure and suggesting a significant association with RD. In addition to the above observations, the results presented in Tables 3-7 and Figures 1-3 also highlight the relatively lower significance of CD compared to other diseases for the pregnant woman under consideration.

6. Conclusions

In conclusion, the proposed generalized hybrid distance measure of a NS provides a valuable tool for the analysis of patients's symptoms and diseases. This approach considers the inherent uncertainty and indeterminacy associated with medical data, allowing for a more comprehensive and accurate assessment of the patient's condition. By incorporating both the distance measure and the neutrosophic set theory, this hybrid approach addresses the limitations of traditional distance measures and offers a more nuanced representation of the patient's symptoms.

The utilization of this hybrid distance measure contributes significantly to the field of medical diagnosis and treatment. It enables healthcare professionals to make decisions based on a more comprehensive understanding of the patient's symptoms and diseases, leading to improved accuracy in diagnoses and tailored treatment plans.

Furthermore, the proposed approach has the potential for broader applications beyond medical analysis. Its ability to handle uncertainty and indeterminacy makes it suitable for decision-making processes in various domains where imprecise or incomplete information is common.

In conclusion, the generalized hybrid distance measure of a neutrosophic set offers a promising approach for analyzing patient symptoms and diseases, providing a robust framework for medical practitioners and researchers to improve diagnostic accuracy and optimize treatment outcomes.

Funding: "This research received no external funding"

Acknowledgments: Thank you to Universiti Teknologi MARA for the support. Thank you to our group members for sharing information and cooperating to complete this paper.

References

1. Smarandache, F., Neutrosophy: neutrosophic probability, set, and logic: analytic synthesis & synthetic analysis. Rehoboth, NM: American Research Press., 1998.
2. Wang, H. Smarandache, F. Zhang, Y & Sunderraman, R., Single valued neutrosophic sets, Multispace & Multistructure. 4,410-413, North-European Scientific Publishers, Finland, 2010.
3. Atanassov, K.T.. Intuitionistic fuzzy sets. In: Intuitionistic fuzzy sets. Studies in fuzziness and soft computing. Physica, Heidelberg. Springer, 1999.
4. Liu, D., Liu, G., & Liu, Z., Some similarity measures of neutrosophic sets based on the Euclidean distance and their application in medical diagnosis. *Computational and mathematical methods in medicine* **2018**, Article ID 7325938, 9 pages, https://doi.org/10.1155/2018/7325938.
5. Ye, J., Multiple attribute group decision-making method with completely unknown weights based on similarity measures under single valued neutrosophic environment. *Journal of Intelligent & Fuzzy System* **2018**, 27, 2927–2935.
6. Ye, J. and Zhang, Q.S., Single valued neutrosophic similarity measures for multiple attribute decision making, *Neutrosophic Sets Sets* **2014**, 2, 48-54.
7. Ren, H.P., Xiao, S.X., and Zhou, H., A chi-square distance-based similarity measure of single valued neutrosophic set and applications. *International Journal* of Computers *Communications* & *Control* **2019**, 14(1), 78-89.
8. Chatterjee, R., Majumdar, P., & Samanta, S, Similarity measures in neutrosophic sets-i. In Fuzzy multicriteria decision-making using neutrosophic sets, Springer, 2019, pp. 249–294.
9. Mondal, K, Pramanik, S. and Giri, B.C., Hybrid Binary Logarithm Similarity Measure for MAGDM problems under SVNS Assessments, *Neutrosophic Sets and Systems* **2018**, 20: 12-25.
10. Ulucay, V., Kilic, A., Yildiz, I., & Sahin, M., A new approach for multi-attribute decision-making problems in bipolar neutrosophic sets. *Neutrosophic Sets and Systems* **2018**, 23: 142-159.
11. Al-Sharqi, F., Al-Quran, A., Alanzi, A.M., Khalifa, H.A.E, Shlaka, R.A., Awad, A.M.A.B., and Gomaa, H.G., Group decision-making based on distance measures settings for single-valued neutrosophic fuzzy soft expert environment, *International Journal of Neutrosophic Science* **2024**, Vol. 23 (4), 88-103.
12. Zeng, W. Y., Cui, H. S., Liu, Y. Q., Yin, Q. and Xu Z. S., Novel distance measure between intuitionistic fuzzy sets and its application in pattern recognition, *Iranian Journal of Fuzzy Systems* **2022**, 19:3, 127-137.
13. Jin, Y., Kamran, M., Salamat, N., Zeng, S., Khan, R.H., Novel distance measures for single-valued neutrosophic fuzzy sets and their applications to multicriteria group decision-making problem, *Journal of Function Spaces* **2022**, Article ID 7233420, 11 pages https://doi.org/10.1155/2022/7233420.
14. Mustapha, N., Alias, S., Md Yasin, R., Mohd Yusof, N.N, Fakhrarazi, N.N. and Nik Hassan, N.N.A., New entropy measure concept for single value neutrosophic sets with application in medical diagnosis, *International Journal of Neutrosophic Science* **2022**, 19:01, 375-383.
15. Ye, J., Improved cosine similarity measures of simplified neutrosophic sets for medical diagnoses, *Artificial Intelligence in Medicine* **2015**, *63*(3), 171–179.
16. Shahzadi, G., Akram, M., & Saeid, A. B., An application of single-valued neutrosophic sets in medical diagnosis, *Neutrosophic sets and systems* **2017** 18, 80–88.
17. Mustapha, N., Alias, S., Md Yasin, R., Abdullah, I. and Broumi, S., Cardiovascular diseases risk analysis using distance-based similarity measure of neutrosophic sets. *Neutrosophic Sets and Systems* **2021**, 47: 1. https://digitalrepository.unm.edu/ nss_journal /vol47/iss1/3
18. Mustapha, N., Ahmad Riza, F.F., Mansor, N.A., Mazlan, N.A.S., Alias, S. and Md Yasin, R., Utilizing the clustering techniques using distance-based similarity measures of SVNS in medical diagnosis, *Applied Mathematics and Computational Intelligence* **2023**, 12(4), 52–65. https://doi.org/10.58915/amci.v12i4.251

19. Alias, S., Mustapha, N., Md Yasin, Mohd Yusoff, N.S. and Mohamad, S.N.F., Medical diagnosis by roughness-cosine similarity measure in rough neutrosophic set environment, *Journal of Mathematics and Computing Science* **2022**, 8: 2, 79-87.
20. Bin, J., Chuhao, Z., Ze, C., and Shuai, Z., A novel multi-parameter similarity measure of interval neutrosophic sets for medical diagnosis. *Journal of Intelligent and Fuzzy Systems* **2023,** 45:11333-11351. doi: 10.3233/jifs-232444
21. Muskan, Dhumras, H., Shukla, V., and Bajaj, R.K., On Medical Diagnosis Problem Utilizing Parametric Neutrosophic Discriminant Measure, IEEE International Students' Conference on Electrical, Electronics and Computer Science (SCEECS) **2023,** 1-5, doi: 10.1109/SCEECS57921.2023.10063138.
22. Habib, S., Ashraf, A., Arif Butt, M., & Ahmad, M., Medical diagnosis based on single-valued neutrosophic information. *Neutrosophic Sets and Systems* **2022**, *42*, 302-323.

Received: July 28, 2024. Accepted: Oct 23, 2024

Neutrosophic Sets and Systems, Vol. 76, 2025
University of New Mexico

Evaluating University Crisis Management: A Neutrosophic LogTODIM Framework for Public Opinion

Quansong Qi
Southwest University of Political Science and Law, Chongqing, 401120, China
*Corresponding author, E-mail: qiquansong@swupl.edu.cn; 2407176629@qq.com
https://orcid.org/0000-0002-4529-2727

Abstract: The evaluation of public opinion management capability for public crises in universities assesses the ability of universities to guide and handle public opinion during crises. The evaluation covers areas such as opinion monitoring, crisis response, information dissemination, and media communication. Through a systematic assessment, universities can improve their crisis management capabilities, reduce the spread of negative public opinion, and maintain campus stability and reputation. The public opinion management capability evaluation for public crises in universities is multiple-attribute group decision-making (MAGDM). Recently, the Logarithmic TODIM (LogTODIM) technique was interpreted to cope with MAGDM. The single-valued neutrosophic sets (SVNSs) are interpreted as decision tools for characterizing fuzzy data during the public opinion management capability evaluation for public crises in universities. In this study, the single-valued neutrosophic number combined Logarithmic TODIM (SVNN-Com-LogTODIM) technique based on the SVNN Hamming distance (SVNNHD) and SVNN Euclidean distance (SVNNED) is interpreted to solve the MAGDM under SVNSs. Conclusively, numerical study for public opinion management capability evaluation for public crises in universities is interpreted to elucidate the SVNN-Com-LogTODIM technique through comparative analysis.

Keywords: Multiple-attribute group decision-making (MAGDM); SVNSs; entropy; Logarithmic TODIM; public opinion management capability evaluation

1. Introduction and Background

In modern society, public crisis governance has become a practical issue that all countries around the world must face. Although the focus of research on public crisis governance and the construction of governance systems varies across nations, China has achieved a significant shift from "administrative single-response" to "socialized comprehensive emergency response" through institutional changes centered on the "One Plan, Three Systems" framework. This has coordinated the previously fragmented emergency management landscape and strengthened the top-level design of emergency management, advancing towards more powerful, orderly, and effective public crisis governance. By reviewing the evolution of China's public crisis governance, we can clearly see

some distinct characteristics that differ from those of other countries. It is these distinctive features that support the modernization of China's public crisis governance and help us better understand the developmental logic of the country's emergency management system with Chinese characteristics. Over the past few years, research on public crisis governance has seen a significant increase, covering various aspects of crisis management. Zheng and Lou [1] explored the regional coordination mechanisms in China's public crisis emergency management. They pointed out several shortcomings, such as insufficient international governance capabilities for online public opinion, the need to enhance the informatization level, and the imperfect mechanisms for emergency material supply. The study suggested that future work should focus on strengthening regional coordination through digital means to improve overall emergency management capabilities. Zeng [2] analyzed the emergency response to the COVID-19 pandemic in Nanjing and highlighted the difficulties local governments face in managing sudden online public opinion. The study emphasized the importance of local governments' emergency management capabilities, especially in handling online public opinion during major public crises. Focusing on the challenges faced by universities, Xu, Bao and Chen [3] proposed a targeted educational guidance mechanism for universities to cope with public crises. They explored how information dissemination, psychological crisis intervention, ideological education, and other methods could help students deal with the negative impacts of the pandemic. The research specifically addressed how the pandemic affected students' mental health and academic performance, providing a four-entry intervention strategy. Simultaneously, Wen and Qiu [4] used big data and social network analysis to study the dissemination and governance of online public opinion during sudden public crises. They found that official government platforms played a crucial role in guiding public opinion in online networks. Ding [5] approached the issue from the perspective of mediatized governance, exploring how mediatized governance can be used in major public crisis events. The study emphasized the importance of mediatized governance in restoring facts, guiding public opinion, and shaping consensus, but also acknowledged the challenges it faces. The study emphasized the need to carefully balance information disclosure and public opinion guidance. Following this, Xie and Yang [6] focused on the deficiencies of local governments in the post-pandemic era, especially in policy implementation, smart epidemic prevention, intergovernmental collaboration, public relations, and emergency governance. The article proposed that local governments should enhance their emergency management capabilities through technological means and collaborative governance mechanisms.

Moving into 2023, research became more focused on specific issues like online public opinion governance and data governance. Wang and Yi [7] analyzed the "Leadership Message Board" on People's Daily Online to explore the response capabilities of digital governments during public health crises. They found that digital governments effectively guided public opinion through online platforms and acted as "buffers" during the pandemic. Zhu and Li [8] studied the governance of online rumors during sudden public crisis events, proposing a collaborative governance model centered on national governance to combat the spread of rumors and the phenomenon of group polarization. Sun [9] drew insights from history, examining how the governance philosophy of Zichan, a statesman from the Spring and Autumn period, could inform modern public crisis

management. The study pointed out that Zichan's emergency management strategies, such as "being prepared" and "transparent governance," provided valuable lessons for modern crisis response. Subsequently, Zhao, Cui, Liu, Chen and Liang [10] used sentiment analysis techniques to examine local governments' online public opinion management strategies during sudden public crisis events. Through a case study of the Tonghua City material distribution crisis, the article revealed the main contradictions governments face when responding to public opinion and proposed corresponding strategies. Finally, Li and Xu [11] conducted a bibliometric analysis of the research hotspots in data governance during public crisis response. They found that data governance revolves around the relationship between "context-subject-object," with research hotspots including information technology empowerment, collaborative governance, online public opinion governance, and personal data protection.

The public opinion management capability evaluation for public crises in universities is a multiple-attribute group decision-making (MAGDM) problem due to several reasons: (1) Multiple stakeholders involved: The evaluation process typically involves various experts and decision-makers from different fields, such as communication specialists, crisis managers, public relations officers, and university administrators. Each participant brings their own perspective, expertise, and judgment, making it a group-based task. The involvement of multiple stakeholders ensures a more comprehensive and accurate assessment of the university's capability to manage public opinion during a crisis. (2) Complex and diverse evaluation criteria: The evaluation of a university's public opinion management capability is influenced by numerous attributes or criteria, such as crisis communication strategies, transparency, media relations, social media monitoring, response speed, and stakeholder engagement [12, 13]. These factors need to be considered simultaneously, and they often carry different levels of importance, making the problem multi-attribute in nature. (3) Fuzzy and uncertain information: In the context of public crisis management, the information available during a crisis can often be uncertain or evolving, especially when dealing with rapidly changing public sentiment or incomplete data [14, 15]. Different experts may have different views or uncertainties regarding the effectiveness of certain strategies, requiring decision-making techniques that can handle such uncertainties. Group decision-making allows for the aggregation of diverse opinions to reach a more balanced and well-rounded conclusion[16-19]. Considering these factors, the evaluation of public opinion management capability for public crises in universities naturally becomes a MAGDM problem, as it involves the collective input of multiple decision-makers and the assessment of complex, multidimensional criteria. Recently, LogTODIM technique LogTODIM [20, 21] was interpreted to put forward MAGDM. The SVNSs [22, 23] are interpreted as decision tool for characterizing fuzzy data during the public opinion management capability evaluation for public crises in universities. In this study, the SVNN-Com-LogTODIM approach is interpreted to put forward MAGDM under SVNSs. Conclusively, numerical study for public opinion management capability evaluation for public crises in universities is interpreted to validate the SVNN-Com-LogTODIM through comparative analysis. The major research motivations of this study are

interpreted: (1) Entropy technique is interpreted the weight with SVNSs; (2) SVNN-Com-LogTODIM approach is interpreted to put forward the MAGDM for SVNSs; (3) Conclusively, numerical study for public opinion management capability evaluation for public crises in universities is interpreted and (4) serval comparisons are interpreted to validate the SVNN-Com-LogTODIM.

2. Preliminaries

Wang et al. [22] interpreted the SVNSs

Definition 1 [22]. The SVNSs is interpreted:

$$ZA=\left\{\left(\phi, ZT_A(\phi), ZI_A(\phi), ZF_A(\phi)\right)\middle|\phi\in\Phi\right\} \tag{1}$$

where $ZT_A(\phi), ZI_A(\phi), ZF_A(\phi)$ presents truth-membership, indeterminacy-membership and falsity-membership, $ZT_A(\phi), ZI_A(\phi), ZF_A(\phi)\in[0,1]$ and meets $0\le ZT_A(\phi)+ZI_A(\phi)+ZF_A(\phi)\le 3$.

The SVNN is interpreted as: $ZA=(ZT_A, ZI_A, ZF_A)$, $ZT_A, ZI_A, ZF_A\in[0,1]$, and $0\le ZT_A+ZI_A+ZF_A\le 3$.

Definition 2 [24]. Let $ZA=(ZT_A, ZI_A, ZF_A)$ be SVNN, a score value is interpreted:

$$SV(ZA)=\frac{(2+ZT_A-ZI_A-ZF_A)}{3},\quad SV(ZA)\in[0,1]. \tag{2}$$

Definition 3[24]. Let $ZA=(ZT_A, ZI_A, ZF_A)$ be SVNN, accuracy value is interpreted:

$$AV(ZA)=\frac{1+ZT_A-ZF_A}{2},\ AV(ZA)\in[0,1]. \tag{3}$$

Peng et al. [24] interpreted the order for SVNNs.

Definition 4[24]. Let $ZA=(ZT_A, ZI_A, ZF_A)$ and $ZB=(ZT_B, ZI_B, ZF_B)$ be SVNNs, $SV(ZA)=\frac{(2+ZT_A-ZI_A-ZF_A)}{3}$ and $SV(ZB)=\frac{(2+ZT_B-ZI_B-ZF_B)}{3}$, and $AV(ZA)=\frac{1+ZT_A-ZF_A}{2}$ and $AV(ZB)=\frac{1+ZT_B-ZF_B}{2}$, then if $SV(ZA)<SV(ZB)$, then $ZA<ZB$; if $SV(ZA)=SV(ZB)$, then (1)if $AV(ZA)=AV(ZB)$, then $ZA=ZB$; (2) if $AV(ZA)>AV(ZB)$, then $ZA<ZB$.

Definition 5[22]. Let $ZA=(ZT_A, ZI_A, ZF_A)$ and $ZB=(ZT_B, ZI_B, ZF_B)$ be SVNNs, the operations are interpreted:

(1) $ZA \oplus ZB = \left(ZT_A + ZT_B - ZT_A ZT_B, ZI_A ZI_B, ZF_A ZF_B \right);$

(2) $ZA \otimes ZB = \left(ZT_A ZT_B, ZI_A + ZI_B - ZI_A ZI_B, ZF_A + ZF_B - ZF_A ZF_B \right);$

(3) $\lambda ZA = \left(1 - \left(1 - ZT_A \right)^{\lambda}, \left(ZI_A \right)^{\lambda}, \left(ZF_A \right)^{\lambda} \right), \lambda > 0;$

(4) $\left(ZA \right)^{\lambda} = \left(\left(ZT_A \right)^{\lambda}, \left(ZI_A \right)^{\lambda}, 1 - \left(1 - ZF_A \right)^{\lambda} \right), \lambda > 0.$

Definition 6[25]. Let $ZA = \left(ZT_A, ZI_A, ZF_A \right)$ and $ZB = \left(ZT_B, ZI_B, ZF_B \right)$, then SVNN Hamming distance (SVNNHD) and SVNN Euclidean distance (SVNNED) are interpreted:

$$SVNNHD\left(ZA, ZB \right) = \frac{\left| ZT_A - ZT_B \right| + \left| ZI_A - ZI_B \right| + \left| ZF_A - ZF_B \right|}{3} \tag{4}$$

$$SVNNED\left(ZA, ZB \right) = \sqrt{\frac{\left| ZT_A - ZT_B \right|^2 + \left| ZI_A - ZI_B \right|^2 + \left| ZF_A - ZF_B \right|^2}{3}} \tag{5}$$

The SVNNWG technique is interpreted:

Definition 8[24]. Let $ZA_j = \left(ZT_j, ZI_j, ZF_j \right)$ be SVNNs, the SVNNWG technique is interpreted:

$$\begin{aligned} &\text{SVNNWG}_{zw}\left(ZA_1, ZA_2, \ldots, ZA_n \right) \\ &= \left(ZA_1 \right)^{zw_1} \otimes \left(ZA_2 \right)^{zw_2}, \ldots \otimes \left(ZA_n \right)^{zw_n} = \overset{n}{\underset{j=1}{\otimes}} \left(ZA_j \right)^{zw_j} \\ &= \left(\prod_{j=1}^{n} \left(ZT_{ij} \right)^{zw_j}, 1 - \prod_{j=1}^{n} \left(1 - ZF_{ij}^{k} \right)^{zw_j}, 1 - \prod_{j=1}^{n} \left(1 - ZT_{ij}^{k} \right)^{zw_j} \right) \end{aligned} \tag{6}$$

where $zw = \left(zw_1, zw_2, ..., zw_n \right)^T$ be weight of ZA_j, $zw_j > 0, \sum_{j=1}^{n} zw_j = 1.$

3. SVNN-Com-LogTODIM technique for MAGDM with entropy

3.1. SVNN-MAGDM information

The SVNN-Com-LogTODIM technique is interpreted for MAGDM. Let $ZA = \left\{ ZA_1, ZA_2, \cdots, ZA_m \right\}$ be alternatives, and $ZG = \left\{ ZG_1, ZG_2, \cdots, ZG_n \right\}$ be attributes with weight $r\omega$, where $z\omega_j \in \left[0,1 \right], \sum_{j=1}^{n} z\omega_j = 1$ and invited experts $ZE = \left\{ ZE_1, ZE_2, \cdots, ZE_q \right\}$ with expert's weight $zw = \left\{ zw_1, zw_2, \cdots, zw_t \right\}$, where $zw_j \in \left[0,1 \right], \sum_{k=1}^{t} zw_k = 1$. Then, SVNN-Com-LogTODIM technique is interpreted for MAGDM.

(1). Elucidate the SVNN-matrix $ZM^t = \left[ZM_{ij}^t \right]_{m \times n} = \left(ZT_{ij}^t, ZI_{ij}^t, ZF_{ij}^t \right)_{m \times n}$ and average matrix $ZM = \left[ZM_{ij} \right]_{m \times n}$:

$$ZM^t = \left[ZM_{ij}^t \right]_{m\times n} = \begin{array}{c} \\ ZA_1 \\ ZA_2 \\ \vdots \\ ZA_m \end{array} \begin{array}{c} \begin{array}{cccc} ZG_1 & ZG_2 & \cdots & ZG_n \end{array} \\ \begin{bmatrix} ZM_{11}^t & ZM_{12}^t & \cdots & ZM_{1n}^t \\ ZM_{21}^t & ZM_{22}^t & \cdots & ZM_{2n}^t \\ \vdots & \vdots & \vdots & \vdots \\ ZM_{m1}^t & ZM_{m2}^t & \cdots & ZM_{mn}^t \end{bmatrix} \end{array} \tag{7}$$

$$ZM = \left[ZM_{ij} \right]_{m\times n} = \begin{array}{c} \\ ZA_1 \\ ZA_2 \\ \vdots \\ ZA_m \end{array} \begin{array}{c} \begin{array}{cccc} ZG_1 & ZG_2 & \cdots & ZG_n \end{array} \\ \begin{bmatrix} ZM_{11} & ZM_{12} & \cdots & ZM_{1n} \\ ZM_{21} & ZM_{22} & \cdots & ZM_{2n} \\ \vdots & \vdots & \vdots & \vdots \\ ZM_{m1} & ZM_{m2} & \cdots & ZM_{mn} \end{bmatrix} \end{array} \tag{8}$$

Based on SVNNWG, the $ZM = \left[ZM_{ij} \right]_{m\times n} = \left(ZT_{ij}, ZI_{ij}, ZF_{ij} \right)_{m\times n}$ is interpreted:

$$ZM_{ij} = \overset{t}{\underset{k=1}{\otimes}} \left(RM_{ij}^k \right)^{rw_k} = \left(1 - \prod_{k=1}^{t} \left(ZT_{ij}^t \right)^{zw_k}, \prod_{k=1}^{t} \left(ZI_{ij}^t \right)^{zw_k}, \prod_{k=1}^{t} \left(ZF_{ij}^t \right)^{zw_k} \right) \tag{9}$$

(2). Normalize the $ZM = \left[ZM_{ij} \right]_{m\times n} = \left(ZT_{ij}, ZI_{ij}, ZF_{ij} \right)_{m\times n}$ into $ZM^N = \left[ZM_{ij}^N \right]_{m\times n} = \left(ZT_{ij}^N, ZI_{ij}^N, ZF_{ij}^N \right)_{m\times n}$.

For benefit attributes:

$$ZM_{ij}^N = \left(ZT_{ij}^N, ZI_{ij}^N, ZF_{ij}^N \right) = \left(ZT_{ij}, ZI_{ij}, ZF_{ij} \right) \tag{10}$$

For cost attributes:

$$ZM_{ij}^N = \left(ZT_{ij}^N, ZI_{ij}^N, ZF_{ij}^N \right) = \left(ZF_{ij}, ZI_{ij}, ZT_{ij} \right) \tag{11}$$

3.2. Compute the attributes weight by entropy.

Entropy [26] is interpreted the weight. The normalized SVNN-matrix $SVNN_{ij}$ is interpreted:

$$SVNN_{ij} = \frac{\left(SV\left(ZT_{ij}^N, ZI_{ij}^N, ZF_{ij}^N \right) + AV\left(ZT_{ij}^N, ZI_{ij}^N, ZF_{ij}^N \right) + 1 \right)}{\sum_{i=1}^{m} \left(SV\left(ZT_{ij}^N, ZI_{ij}^N, ZF_{ij}^N \right) + AV\left(ZT_{ij}^N, ZI_{ij}^N, ZF_{ij}^N \right) + 1 \right)}, \tag{12}$$

The fuzzy Shannon entropy (FSE) is interpreted:

$$FSE_j = -\frac{1}{\ln m} \sum_{i=1}^{m} SVNN_{ij} \ln SVNN_{ij} \tag{13}$$

and $SVNN_{ij} \ln SVNN_{ij} = 0$ if $SVNN_{ij} = 0$.

Then, the weight information is interpreted:

$$z\omega_j = \frac{1 - FSE_j}{\sum_{j=1}^{n} \left(1 - FSE_j \right)}, \quad j = 1, 2, \cdots, n. \tag{14}$$

3.3. SVNN-Com-LogTODIM approach for MAGDM

The SVNN-Com-LogTODIM approach is interpreted to solve MAGDM.

(1) Elucidate relative weight:

$$rz\omega_j = z\,\omega_j \Big/ \max_j z\omega_j, \tag{15}$$

(2) The fuzzy dominance degree (FDD) of ZA_i over ZA_t for ZG_j is interpreted in light with SVNNHD and SVNNED:

$$FDD_j\left(ZA_i, ZA_t\right) = \begin{cases} \dfrac{1}{2}\left(\dfrac{rz\omega_j \times \log\left(1+10\rho DVNNHD\left(ZM_{ij}^N, ZM_{tj}^N\right)\right)}{\sum_{j=1}^n rz\omega_j} + \dfrac{rz\omega_j \times \log\left(1+10\rho DVNNED\left(ZM_{ij}^N, ZM_{tj}^N\right)\right)}{\sum_{j=1}^n rz\omega_j} \right) & \text{if } SV\left(ZM_{ij}^N\right) > SV\left(ZM_{tj}^N\right) \\ 0 & \text{if } SV\left(ZM_{ij}^N\right) = SV\left(ZM_{tj}^N\right) \\ \dfrac{1}{2}\left(-\dfrac{rz\omega_j \times \lambda \log\left(1+10\rho DVNNHD\left(ZM_{ij}^N, ZM_{tj}^N\right)\right)}{\sum_{j=1}^n rz\omega_j} - \dfrac{rz\omega_j \times \lambda \log\left(1+10\rho DVNNED\left(ZM_{ij}^N, ZM_{tj}^N\right)\right)}{\sum_{j=1}^n rz\omega_j} \right) & \text{if } SV\left(ZM_{ij}^N\right) < SV\left(ZM_{tj}^N\right) \end{cases} \tag{16}$$

where λ and $\rho \in [1,5]$ is from [20].

The $FDD_j\left(ZA_i\right)$ for ZG_j is interpreted:

$$FDD_j\left(ZA_i\right) = \left[FDD_j\left(ZA_i, ZA_t\right)\right]_{m\times m}$$

$$= \begin{array}{c} \\ ZA_1 \\ ZA_2 \\ \vdots \\ ZA_m \end{array} \begin{array}{c} \begin{array}{cccc} ZA_1 & ZA_2 & \cdots & ZA_m \end{array} \\ \begin{bmatrix} 0 & FDD_j\left(ZA_1, ZA_2\right) & \cdots & FDD_j\left(ZA_1, ZA_m\right) \\ FDD_j\left(ZA_2, ZA_1\right) & 0 & \cdots & FDD_j\left(ZA_2, ZA_m\right) \\ \vdots & \vdots & \cdots & \vdots \\ FDD_j\left(ZA_m, ZA_1\right) & FDD_j\left(ZA_m, ZA_2\right) & \cdots & 0 \end{bmatrix} \end{array}$$

(3) Elucidate the $FDD\left(ZA_i, ZA_t\right)$ of ZA_i over other alternatives:

$$ZDD\left(ZA_i, ZA_t\right) = \sum_{j=1}^n ZDD_j\left(ZA_i, ZA_t\right) \tag{17}$$

The $FDD = FDD\left(ZA_i, ZA_t\right)_{m\times m}$ is interpreted:

$$FDD = FDD\left(ZA_i, ZA_t\right)_{m\times m}$$

$$= \begin{bmatrix} & ZA_1 & ZA_2 & \cdots & ZA_m \\ ZA_1 & \sum_{j=1}^{n} FDD_j\left(ZA_1, ZA_1\right) & \sum_{j=1}^{n} FDD_j\left(ZA_1, ZA_2\right) & \cdots & \sum_{j=1}^{n} FDD_j\left(ZA_1, ZA_m\right) \\ ZA_2 & \sum_{j=1}^{n} FDD_j\left(ZA_2, ZA_1\right) & \sum_{j=1}^{n} FDD_j\left(ZA_2, ZA_2\right) & \cdots & \sum_{j=1}^{n} FDD_j\left(ZA_2, ZA_m\right) \\ \vdots & \vdots & \vdots & \vdots & \vdots \\ ZA_m & \sum_{j=1}^{n} FDD_j\left(ZA_m, ZA_1\right) & \sum_{j=1}^{n} FDD_j\left(ZA_m, ZA_2\right) & \cdots & \sum_{j=1}^{n} FDD_j\left(ZA_m, ZA_m\right) \end{bmatrix}$$

(4) Elucidate the overall $FDD\left(ZA_i\right)$ of ZA_i:

$$FDD\left(ZA_i\right) = \frac{\sum_{t=1}^{m} FDD\left(ZA_i, ZA_t\right) - \min_i\left\{\sum_{t=1}^{m} FDD\left(ZA_i, ZA_t\right)\right\}}{\max_i\left\{\sum_{t=1}^{m} FDD\left(ZA_i, ZA_t\right)\right\} - \min_i\left\{\sum_{t=1}^{m} FDD\left(ZA_i, ZA_t\right)\right\}}. \quad (18)$$

(5) Sort and select the optimal alternative with $FDD\left(ZA_i\right)$, the greater $FDD\left(ZA_i\right)\left(i = 1, 2, \cdots, m\right)$ is better choice.

4. Numerical example and comparative analysis

4.1. Numerical example

The evaluation of public opinion management capabilities for public crises in universities is the process of assessing how effectively universities handle and guide public opinion during sudden crises. As an important part of society, universities involve multiple stakeholders, such as students, faculty, parents, the public, and government departments. Therefore, how universities respond to external public opinion pressure during a crisis directly impacts their reputation, image, and internal stability. In the event of a crisis, a university's ability to manage public opinion is not only about quickly addressing the situation but also about effectively communicating with the public, media, and related stakeholders. In the early stages of a crisis, information spreads rapidly, especially in today's era of widespread social media, where public sentiment and the direction of public opinion can escalate quickly. If a university lacks effective public opinion management capabilities, the uncontrolled spread of information may exacerbate the crisis and lead to greater societal impact.

Thus, the core of evaluating a university's public opinion management capabilities lies in assessing whether the university can promptly grasp the direction of public opinion, make quick decisions, and communicate with the public in a reasonable manner to alleviate negative emotions and misunderstandings after a crisis occurs. In this process, transparent and timely information release is crucial to effectively reduce external suspicion and dissatisfaction. At the same time, the communication strategy during a crisis should consider the needs and concerns of different groups, using appropriate channels and methods to convey information, ensuring the accuracy and

consistency of the information. Moreover, post-crisis recovery and reflection are equally important components of a university's public opinion management capabilities. The end of a crisis does not mean the problem is fully resolved. After the situation has calmed, universities need to review and reflect on the entire process, identify shortcomings, and propose improvement plans to prepare for similar crises in the future. This continuous improvement process helps universities enhance their ability to navigate complex public opinion environments and maintain their positive image in the eyes of the public. In summary, the evaluation of public opinion management capabilities for public crises in universities is not only an assessment of crisis response capabilities but also a comprehensive evaluation of how universities maintain transparency in communication, ensure smooth information dissemination, and engage in post-crisis reflection and improvement. This evaluation helps universities continuously enhance their ability to handle public crises, minimize the spread of negative public opinion, and maintain campus stability and public trust. The public opinion management capability evaluation for public crises in universities is MAGDM. Therefore, the public opinion management capability evaluation for public crises in universities is interpreted to demonstrate the SVNN-Com-LogTODIM technique. Five comprehensive universities $ZA_i\left(i=1,2,3,4,5\right)$ are interpreted with different attributes (See Table 1).

Table 1. Four attributes for public opinion management capability evaluation for public crises in universities

Attributes	**Attribute Description**
ZG_1-Opinion Monitoring and Early Warning Capability	Assesses whether the university can monitor, analyze, and issue early warnings about public opinion in a timely manner through various channels (social media, news, etc.).
ZG_2-Crisis Response and Decision-Making Capability	Evaluates the effectiveness and timeliness of the university's crisis response and decision-making, including the ability to form an emergency team and implement strategies.
ZG_3-Information Release and Communication Capability	Assesses whether the university releases information in a timely, transparent, and accurate manner during a crisis, and whether it communicates effectively with stakeholders.

ZG_4-Post-Crisis Recovery and Reflection Capability	Evaluates the university's ability to recover from the crisis and reflect on the experience, ensuring measures are taken to prevent future crises and improve management.

Five possible comprehensive universities are evaluated in light with linguistic scales (See Table 2) through four attributes and three experts $ZE_t\left(t=1,2,3\right)$ with expert's weight $rw=\left(1/3,1/3,1/3\right)$.

Table 2. Linguistic scales and SVNNs

Linguistic Terms	SVNNs
Exceedingly Terrible-ZET	(0.0000, 1.0000, 1.0000)
Very Terrible-ZVT	(0.1000, 0.9000, 0.9000)
Terrible-ZT	(0.3000, 0.7000, 0.7000)
Medium-ZM	(0.5000, 0.5000, 0.5000)
Well-ZW	(0.7000, 0.3000, 0.3000)
Very Well-ZVW	(0.9000, 0.1000, 0.1000)
Exceedingly Well-ZEW	(1.0000, 0.0000, 0.0000)

The SVNN-Com-LogTODIM technique is interpreted to solve the public opinion management capability evaluation for public crises in universities.

Step 1. Elucidate the SVNN-matrix $ZM^t=\left[ZM_{ij}^t\right]_{5\times4}=\left(ZT_{ij}^t,ZI_{ij}^t,ZF_{ij}^t\right)_{5\times4}$ (See Table 3-5).

Table 3. Evaluation from ZE_1

	ZG_1	ZG_2	ZG_3	ZG_4
ZA_1	ZVW	ZM	ZT	ZM
ZA_2	ZVT	ZVT	ZVW	ZW
ZA_3	ZVW	ZVW	ZW	ZM
ZA_4	ZW	ZVT	ZM	ZW
ZA_5	ZM	ZM	ZVT	ZVT

Table 4. Evaluation from ZE_2

	ZG_1	ZG_2	ZG_3	ZG_4

ZA_1	ZT	ZM	ZVW	ZVW
ZA_2	ZM	ZVT	ZM	ZVW
ZA_3	ZW	ZVT	ZM	ZM
ZA_4	ZW	ZT	ZW	ZVT
ZA_5	ZW	ZVW	ZW	ZVT

Table 5. Evaluation from ZE_3

	ZG_1	ZG_2	ZG_3	ZG_4
ZA_1	ZM	ZW	ZVW	ZT
ZA_2	ZM	ZVT	ZVW	ZM
ZA_3	ZVW	ZVW	ZVT	ZVW
ZA_4	ZVW	ZW	ZM	ZVT
ZA_5	ZT	ZM	ZT	ZT

Then according to SVNNWG technique, the $ZM = \left[ZM_{ij} \right]_{5\times4}$ is interpreted (See Table 6).

Table 6. The $ZM = \left[ZM_{ij} \right]_{5\times4}$

	ZG_1	ZG_2
ZA_1	(0.6534, 0.1942, 0.2415)	(0.7111, 0.1241, 0.1735)
ZA_2	(0.4185, 0.3426, 0.5018)	(0.6023, 0.2486, 0.3362)
ZA_3	(0.7406, 0.1214, 0.3223)	(0.5324, 0.2134, 0.4106)
ZA_4	(0.5258, 0.2124, 0.4214)	(0.7201, 0.1145, 0.1772)
ZA_5	(0.6032, 0.1382, 0.4225)	(0.6205, 0.2354, 0.3205)
	ZG_4	ZG_3
ZA_1	(0.5273, 0.3241, 0.3956)	(0.8045, 0.1284, 0.1654)
ZA_2	(0.7205, 0.1273, 0.1631)	(0.5038, 0.2428, 0.3932)
ZA_3	(0.6473, 0.1452, 0.3125)	(0.7051, 0.1294, 0.1712)
ZA_4	(0.6375, 0.2145, 0.3241)	(0.6375, 0.2145, 0.3241)
ZA_5	(0.7406, 0.1214, 0.1641)	(0.5251, 0.3245, 0.3241)

Step 2. Normalize the $ZM = \left[ZM_{ij} \right]_{5\times4}$ into $ZM^N = \left[ZM_{ij}^N \right]_{5\times4}$ (See Table 7).

Table 7. The $ZM^{N}=\left[ZM_{ij}^{N}\right]_{5\times4}$

	ZG_1	ZG_2
ZA_1	(0.6534, 0.1942, 0.2415)	(0.7111, 0.1241, 0.1735)
ZA_2	(0.4185, 0.3426, 0.5018)	(0.6023, 0.2486, 0.3362)
ZA_3	(0.7406, 0.1214, 0.3223)	(0.5324, 0.2134, 0.4106)
ZA_4	(0.5258, 0.2124, 0.4214)	(0.7201, 0.1145, 0.1772)
ZA_5	(0.6032, 0.1382, 0.4225)	(0.6205, 0.2354, 0.3205)
	ZG_4	ZG_3
ZA_1	(0.5273, 0.3241, 0.3956)	(0.8045, 0.1284, 0.1654)
ZA_2	(0.7205, 0.1273, 0.1631)	(0.5038, 0.2428, 0.3932)
ZA_3	(0.6473, 0.1452, 0.3125)	(0.7051, 0.1294, 0.1712)
ZA_4	(0.6375, 0.2145, 0.3241)	(0.6375, 0.2145, 0.3241)
ZA_5	(0.7406, 0.1214, 0.1641)	(0.5251, 0.3245, 0.3241)

Step 3. Elucidate the weights (See Table 8):

Table 8. The attributes weight

	ZG_1	ZG_2	ZG_3	ZG_4
$z\omega$	0.2706	0.2643	0.2511	0.2140

Step 4. Elucidate the relative weights (See Table 9):

Table 9. The relative attributes weight

	ZG_1	ZG_2	ZG_3	ZG_4
$rz\omega$	1.0000	0.9768	0.9275	0.7913

Step 5. Elucidate the $FDD=FDD\left(ZA_i,ZA_t\right)_{5\times5}$ (See Table 10):

Table 10. The $FDD=FDD\left(ZA_i,ZA_t\right)_{5\times5}$

Alternatives	ZA_1	ZA_2	ZA_3	ZA_4	ZA_5
ZA_1	0.0000	-2.1665	2.2825	-2.5238	1.2182
ZA_2	-0.2551	0.0000	2.2102	0.2018	-2.5548
ZA_3	1.8601	-2.8928	0.0000	-3.1024	1.7670
ZA_4	-0.8406	-1.1958	2.6957	0.0000	-0.8241
ZA_5	1.6385	-3.0637	-0.1702	-2.8313	0.0000

Step 6. Elucidate the $FDD\left(RA_i\right)\left(i=1,2,\cdots,5\right)$ (Table 11).

Table 11. The $FDD\left(RA_i\right)\left(i=1,2,\cdots,5\right)$

Alternatives	ZA_1	ZA_2	ZA_3	ZA_4	ZA_5
SVNNDD	0.7595	0.9453	0.4830	1.0000	0.0000

Step 7. Conclusively, the order is interpreted: $ZA_4 \succ ZA_2 \succ ZA_1 \succ ZA_3 \succ ZA_5$, and thus the optimal comprehensive university is ZA_4.

4.2. Comparative analysis

The SVNN-Com-LogTODIM is compared with SVNNWA technique [24] and SVNNWG technique[24], SVNN-CODAS technique [27], SVNN-EDAS technique [28], SVNN-TOPSIS technique [29] and SVNN-TODIM technique [30]. The final comparative order is interpreted in Table 12 and Figure 1.

Table 12. Order for different techniques

Different Techniques	Order
SVNNWA technique [24]	$ZA_4 \succ ZA_2 \succ ZA_1 \succ ZA_3 \succ ZA_5$
SVNNWG technique[24]	$ZA_4 \succ ZA_2 \succ ZA_3 \succ ZA_1 \succ ZA_5$
SVNN-CODAS technique [27]	$ZA_4 \succ ZA_2 \succ ZA_3 \succ ZA_1 \succ ZA_5$
SVNN-EDAS technique [28]	$ZA_4 \succ ZA_2 \succ ZA_1 \succ ZA_3 \succ ZA_5$
SVNN-TOPSIS technique [29]	$ZA_4 \succ ZA_2 \succ ZA_1 \succ ZA_3 \succ ZA_5$
SVNN-TODIM technique [30]	$ZA_4 \succ ZA_2 \succ ZA_1 \succ ZA_3 \succ ZA_5$
The SVNN-Com-LogTODIM technique	$ZA_4 \succ ZA_2 \succ ZA_1 \succ ZA_3 \succ ZA_5$

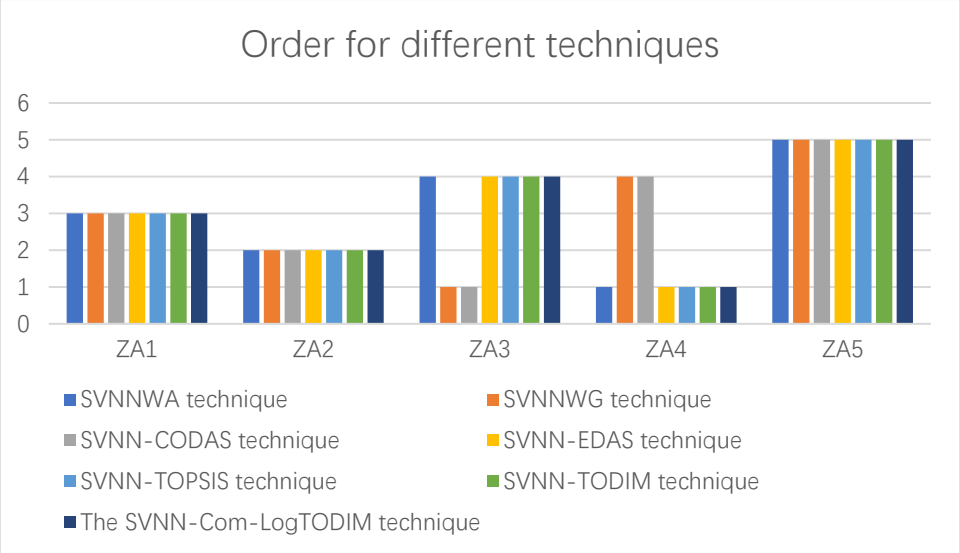

Figure 1. Order for different techniques

From detailed analysis, it could be interpreted that order of these approaches is slightly different, however, these techniques have same optimal comprehensive university and worst comprehensive university. This interpreted the SVNN-Com-LogTODIM is effective.

5. Conclusion

The evaluation of public opinion management capabilities for public crises in universities plays a crucial role in helping institutions establish sound mechanisms for managing public sentiment and effectively responding to and mitigating the challenges posed by crises. This evaluation encourages universities to maintain transparency during emergencies and ensure that public opinion is guided in a positive direction, thereby reducing unnecessary social panic and negative consequences. Through a structured assessment system, universities can identify weaknesses in their crisis response, improve communication with society and the media, and engage in effective post-crisis reflection, ultimately enhancing their overall crisis management capabilities and ensuring campus harmony and stability. The public opinion management capability evaluation for public crises in universities is MAGDM. Currently, the LogTODIM technique was interpreted to put forward the MAGDM. The SVNSs are interpreted as decision tool for characterizing fuzzy data during the public opinion management capability evaluation for public crises in universities. In this study, the SVNN-Com-LogTODIM approach is interpreted to solve the MAGDM under SVNSs. Conclusively, numerical study for public opinion management capability evaluation for public crises in universities is interpreted to validate the SVNN-Com-LogTODIM approach through comparative analysis.

There are some potential research limitations for public opinion management capability evaluation for public crises in universities. These limitations could be addressed through further studies aimed at assessing the impact of public opinion management capability evaluation for public crises in universities.

(1) Strengthening Empirical Validation and Model Optimization. Future research should further combine real-world cases of university crisis management to conduct empirical validation of the SVNN-Com-LogTODIM model. By collecting public opinion data from actual applications, the model's performance under different crisis scenarios can be tested, and its applicability in complex environments can be verified. At the same time, based on feedback from real data, the model's parameter settings and weight allocation can be optimized to enhance its robustness and flexibility in various crisis contexts.

(2)Incorporating Dynamic Public Opinion Monitoring and Real-Time Feedback Mechanisms. To better handle the dynamic nature of public opinion, future studies should consider integrating real-time public opinion monitoring with the decision-making process of the model. By leveraging big data analysis and artificial intelligence technologies, real-time data from social media, news, and other sources can be collected, allowing dynamic adjustments to the SVNN-Com-LogTODIM model's parameters. This dynamic feedback mechanism could improve the model's responsiveness and decision accuracy in handling sudden public crises.

(3) Integration and Expansion of Multiple Decision-Making Methods. Further research could explore combining the SVNN-Com-LogTODIM method with other multi-attribute decision-making approaches (such as AHP and TOPSIS) to construct a more comprehensive decision support framework. By integrating the strengths of different methods, a multidimensional and multi-layered evaluation system can be established, enabling a more thorough analysis and response to complex public opinion crises, thereby enhancing the comprehensiveness and precision of decision-making. Additionally, the introduction of emerging technologies such as sentiment analysis could further enrich the model's ability to handle subjective factors.

Acknowledgment

The work was supported by the Key Project of Humanities and Social Sciences Research Base of Chongqing Education Commission(22SKJD048).

References

[1] J. Zheng, C. Lou, Exploration of the regional coordination mechanism in china's public crisis emergency management, Leadership Science, (2022) 95-98.

[2] Z. Zeng, The current situation, difficulties, and strategies for improving local governments' governance of sudden online public opinion: A perspective from the emergency response to the nanjing covid-19 major public crisis, Journalism Lover, (2022) 82-84.

[3] D. Xu, M. Bao, X. Chen, Research on the targeted educational guidance mechanism and strategies for universities in response to public crisis events, China Forestry Education, 40 (2022) 5-10.

[4] H. Wen, Z. Qiu, Research on the governance capacity of online public opinion in sudden public crisis events in the era of new media, Information Science, 40 (2022) 38-43.

[5] B. Ding, Research on mediatized governance of major sudden public crisis events, Editor's Friend, (2022) 5-15.

[6] B. Xie, X. Yang, The path to improving local government governance capacity in china in the post-pandemic era, Journal of Shaanxi Institute of Administration, 36 (2022) 30-36.

[7] L. Wang, Y. Yi, How digital government responses in public health crises alleviate negative online public opinion: An investigation based on responses from the people's daily "leadership message board", Journal of Public Administration, 19 (2022) 65-78.

[8] J. Zhu, D. Li, Research on the governance of online rumors in sudden public crisis events, Journal of Anhui University of Science and Technology (Social Sciences Edition), 25 (2023) 44-52.

[9] D. Sun, Zichan's governance and its implications for modern society's disaster relief and public crisis response, Journal of Anhui Agricultural University (Social Sciences Edition), 32 (2023) 95-100.

[10] S. Zhao, B. Cui, Y. Liu, Z. Chen, E. Liang, Research on local government response to online public opinion in public crisis events based on sentiment analysis: A case study of the tonghua city material distribution crisis, Public Relations World, (2023) 25-27.

[11] Z. Li, J. Xu, Analysis of hot topics in data governance for public crisis response, China Emergency Management Science, 2023 (2023) 95-105.

[12] M. Rahim, E.M.T. Eldin, S. Khan, N.A. Ghamry, A.M. Alanzi, H.A. Khalifa, Multi-criteria group decision-making based on dombi aggregation operators under p, q-quasirung orthopair fuzzy sets, Journal of Intelligent & Fuzzy Systems, 46 (2024) 53-74.

[13] P.M. Rafi-Ul-Shan, M. Bashiri, M.M. Kamal, S.K. Mangla, B. Tjahjono, An analysis of fuzzy group decision making to adopt emerging technologies for fashion supply chain risk management, Ieee Transactions on Engineering Management, 71 (2024) 8469-8487.

[14] F. Lei, Q. Cai, N.N. Liao, G.W. Wei, Y. He, J. Wu, C. Wei, Todim-vikor method based on hybrid weighted distance under probabilistic uncertain linguistic information and its application in medical logistics center site selection, Soft Computing, 27 (2023) 8541-8559.

[15] B. Chen, Q. Cai, G. Wei, Z. Mo, Novel aczel-alsina operations-based linguistic z-number aggregation operators and their applications in multi-attribute group decision-making process, Engineering Applications of Artificial Intelligence, 124 (2023) 106541.

[16] H. Zhu, R.M. Rodríguez, J.B. Zhao, Group decision making based on dice similarity measure and 2-dimension linguistic fuzzy weighted arithmetic aggregation operator for 2-dimension linguistic fuzzy variables, Engineering Applications of Artificial Intelligence, 135 (2024) 10.

[17] M. Touqeer, R. Umer, N.A. Mohammad, M. Salimi, A. Ahmadian, Signed distance-based approach for multiple criteria group decision-making with incomplete information using interval type-2 neutrosophic numbers, Multimedia Tools and Applications, 83 (2024) 8439-8466.

[18] Y. Nishida, S. Shimojo, Y. Hayashi, Conversational agent dynamics with minority opinion and

cognitive conflict in small-group decision-making, Japanese Psychological Research, (2024) 15.

[19] S. Naz, A. Fatima, S.A. But, D. Pamucar, R. Zamora-Musa, M. Acosta-Coll, Effective multi-attribute group decision-making approach to study astronomy in the probabilistic linguistic q-rung orthopair fuzzy vikor framework, Heliyon, 10 (2024) 26.

[20] A.B. Leoneti, L. Gomes, A novel version of the todim method based on the exponential model of prospect theory: The exptodim method, European Journal of Operational Research, 295 (2021) 1042-1055.

[21] Q. Sun, L. Yang, Enhanced computer network security assessment through employing an integrated logtodim-topsis technique under interval neutrosophic sets, International Journal of Knowledge-Based and Intelligent Engineering Systems, Preprint (2024) https://doi.org/10.3233/KES-230239.

[22] H. Wang, F. Smarandache, Y.Q. Zhang, R. Sunderraman, Single valued neutrosophic sets, Multispace Multistruct, (2010) 410-413.

[23] J. Ye, Single valued neutrosophic cross-entropy for multicriteria decision making problems, Applied Mathematical Modelling, 38 (2014) 1170-1175.

[24] J.J. Peng, J.Q. Wang, J. Wang, H.Y. Zhang, X.H. Chen, Simplified neutrosophic sets and their applications in multi-criteria group decision-making problems, International Journal of Systems Science, 47 (2016) 2342-2358.

[25] P. Majumdar, S.K. Samanta, On similarity and entropy of neutrosophic sets, Journal of Intelligent & Fuzzy Systems, 26 (2014) 1245-1252.

[26] C.E. Shannon, A mathematical theory of communication, Bell System Technical Journal, 27 (1948) 379-423.

[27] E. Bolturk, A. Karasan, Prioritization of investment alternatives for a hospital by using neutrosophic codas method, Journal of Multiple-Valued Logic and Soft Computing, 33 (2019) 381-396.

[28] D. Stanujkic, D. Karabasevic, G. Popovic, D. Pamucar, Z. Stevic, E.K. Zavadskas, F. Smarandache, A single-valued neutrosophic extension of the edas method, Axioms, 10 (2021) 13.

[29] P. Biswas, S. Pramanik, B.C. Giri, Topsis method for multi-attribute group decision-making under single-valued neutrosophic environment, Neural Computing & Applications, 27 (2016) 727-737.

[30] D.S. Xu, C. Wei, G.W. Wei, Todim method for single-valued neutrosophic multiple attribute decision making, Information, 8 (2017) 125.

Received: July 21, 2024. Accepted: Oct 21, 2024

Neutrosophic Sets and Systems, Vol. 76, 2025
University of New Mexico

A Novel Framework for Gauging Information Extracted from Smartphones Using Neutrosophic Logic

R. M. Abou alzahab[1] , Amr Ismail [1,2] , S. H. Abd Elkhalik[3] , M. Y. Shams[4], H. M. El-Bakry[5] and A. A. Salama[1].

[1] Department of Mathematics and Computer Science, Faculty of Science, Port Said University, Egypt, ramy.zahab@sci.psu.edu.eg, amr_ismail@sci.psu.edu.eg, ahmed_salama_2000@sci.psu.edu.eg

[2] Department of Cybersecurity, College of Engineering and Information Technology, Buraydah Private Colleges, Buraydah 51418, Kingdom of Saudi Arabia.

[3]Department. of Communication and Computer Engineering, Air Defense University., Egypt shelmy@horus.edu.eg

[4]Faculty of Artificial Intelligence, Kafrelsheikh University, Kafrelsheikh 33516, Egypt. mahmoud.yasinA@ai.kfs.edu.eg

[5]Department of Information Systems., Faculty of Computer and Information Science, Mansoura University., Egypt elbakry@mans.edu.eg

Abstract: Smartphones contain a vast amount of information about their users, which can be used as evidence in criminal cases. However, the sheer volume of data can make it challenging for forensic investigators to identify and use the most relevant information. Neutrosophic logic is a generalization of fuzzy logic that allows for uncertainty and vagueness, making it a more potent tool for dealing with the ambiguity of real-world data. The proposed framework aims to identify and utilize the most relevant information for forensic investigators, making it easier to solve criminal cases using Neutrosophic logic. This novel approach provides a more powerful tool for dealing with the ambiguity of smartphone data, ultimately improving the accuracy and effectiveness of forensic investigations. Our research has utilized Neutrosophic logic to evaluate the degree of truth, falsity, or Indeterminacy of this information. Additionally, this study analyzes conversations between individuals using Excel's fuzzy lookup add-in to determine the percentage of truth and false in each conversation. The results were compiled into a dataset and utilized a Neutrosophic Python code to evaluate the information. The results indicate the percentage of truth, false, and Indeterminacy in each conversation and which can be used to determine its admissibility as evidence and which not.

Keywords: Smartphone, Forensics, Neutrosophic Logic, Fuzzy Logic, Uncertainty, Investigations.

1. Introduction

In the modern digital age, smartphones have become ubiquitous companions, silently recording a vast tapestry of personal and potentially incriminating information. While this data presents a treasure trove for forensic investigations, its sheer volume and inherent ambiguity pose a significant challenge: Identifying and leveraging the most relevant information amidst a sea of uncertainty [1]. Traditional digital forensic techniques, often reliant on stark binary classifications of "relevant" or "irrelevant," falter when confronted with the nuanced complexities of real-world smartphone data [2]. This research gap necessitates innovative approaches that can effectively navigate the inherent

uncertainty and vagueness embedded within this digital trove. This paper proposes a novel framework for gauging information extracted from smartphones by harnessing the power of Neutrosophic logic. Neutrosophic logic, a generalization of fuzzy logic, overcomes its predecessor's shortcomings by embracing the inherent ambiguity and uncertainty in real-world data, unlike fuzzy logic, which functions on a truth-false spectrum. Neutrosophic logic adds a third truth value: indeterminacy. This essential innovation enables a more thorough representation of smartphone data, including not only degrees of truth and untruth but also the inherent "unknowns" that impede forensic investigations [3]. Our methodology intends to maximize the forensic value of smartphone data by using the expressive capacity of Neutrosophic logic. We imagine a future in which relevant information is quickly detected and prioritized, allowing for more accurate and efficient investigative processes. Ultimately, this novel approach has the potential to revolutionize the landscape of smartphone forensics, leading to enhanced investigative outcomes and potential crime resolution [4]. The paper presented by Abou alzahab et al. [5] investigated that the smartphones store vast amounts of user data, which can be invaluable to forensic investigators during criminal investigations. However, this data can also be manipulated by malicious actors to fabricate evidence and mislead investigators. Their research leverages fuzzy logic to assess the authenticity of this information. Further, they analyzed conversations between individuals using Excel's fuzzy lookup add-in to determine the percentage of truth and falsehood in each conversation. The results were compiled into a dataset and evaluated using a fuzzy model developed with Matlab's fuzzy toolbox.

In [6] the study investigates the key factors influencing customer attitudes toward social media influencers and their impact on purchase intentions. By analyzing 376 online survey responses using Structural Equation Modelling (SEM), machine learning, and multi-criteria decision-making (MCDM) methods, the study categorizes digital influencers' behaviors affecting consumer perceptions. The models reveal how these factors shape acceptance of influencers' messages, offering recommendations for optimizing influencer marketing strategies. Marketers can enhance user experience and conversion rates, while customers benefit from more relevant and engaging content, fostering stronger brand connections and influencing purchase decisions. Regular evaluations are suggested to continuously improve influencer marketing efforts. This article discusses several aspects of smartphone forensics, such as case studies, frameworks, and data extraction and analysis methods. They also discuss the difficulties of dealing with ambiguous and unclear evidence in forensic investigations, as well as the usage of fuzzy logic and Neutrosophic logic for decision-making and classification. Some references also discuss software tools and applications for implementing these logics, such as the Excel Fuzzy Lookup and the Neutrosophic Python code algorithm. These references will be useful in providing a foundation for the proposed framework and its implementation using Neutrosophic logic. This research contributes to the field of smartphone forensics by Addressing the critical challenge of handling ambiguous and uncertain data in forensic investigations. Introducing a novel framework specifically tailored for smartphones, utilizing the advanced capabilities of Neutrosophic logic. Demonstrating the potential of Neutrosophic logic to significantly improve the accuracy and effectiveness of forensic investigations.

Smartphones contain a vast amount of information about their users, which can be used as evidence in criminal cases. However, the sheer volume of data can make it challenging for forensic investigators to identify and use the most relevant information. Neutrosophic logic is a generalization of fuzzy logic that allows for uncertainty and vagueness, making it a more potent tool for dealing with the ambiguity of real-world data. The proposed framework aims to identify and utilize the most relevant information for forensic investigators, making it easier to solve criminal cases using Neutrosophic logic. This novel approach provides a more powerful tool for dealing with the ambiguity of smartphone data, ultimately improving the accuracy and effectiveness of forensic investigations.

Research Gap: Current forensic methodologies often struggle with the overwhelming volume and ambiguous nature of smartphone data, lacking efficient tools to discern and prioritize relevant information amidst the uncertainty.

Novelty: Our research leverages Neutrosophic logic to evaluate the degree of truth, falsity, or indeterminacy in smartphone data, a novel application in the forensic field. Additionally, we analyze conversations using Excel's fuzzy lookup add-in to determine the percentage of truth and falsehood in each conversation. The results, compiled into a dataset and evaluated using Neutrosophic Python code, indicate the percentages of truth, falsehood, and indeterminacy in each conversation, enhancing the determination of admissibility as evidence. This approach significantly advances the capability of forensic investigators to handle and interpret ambiguous data effectively.

This paper is organized as follows: Section 2 discusses background on gauging information extracted from Smartphones using Neutrosophic Logic. Section 3: provides an overview of the methods used to evaluate the extracted evidence data using the Python algorithm code, and Excel Fuzzy Lookup Add-in. Section 4 presents the results and discussions of our research, and finally, Section 5 shows the conclusion and the future work

2. Background

2.1 Data Acquisition Technique:

The techniques used to extract information from mobile devices [7]. Micro-read is a technique used to view data on memory chips using high-power electron microscopes. However, it can be expensive, time-consuming, and requires expertise in hardware and file systems [8]. Chip-off is a useful technique in digital forensics. It involves extracting data from the memory chip by generating a binary image. However, it can damage the device, making it a costly process. [9]. JTAG is a technique that allows investigators to extract physical data from a smart device. To do this, the investigator connects the smart device to a workstation and then uses forensic tools like XACT and Pandora's Box to extract and create a raw data image stored in the smart device's memory [8]. Logical extraction is the most commonly used technique for extracting data from a smart device. This process involves connecting the device to a forensic lab via Bluetooth, cable NFC, or other methods. After connecting the device, forensic tools will be installed to extract all the data stored on the device. [10].

2.2 Boolean logic:

Boolean logic is a foundational idea in computer technology and mathematics. It is based on binary logic principles, which use two values to describe logical statements: true (represented by 1) and false (represented by 0) [11]. More sophisticated expressions can be created by combining these assertions with Boolean operators such as AND, OR, and NOT. Understanding boolean logic is essential for creating and analyzing digital computer circuits, as well as programming and algorithm creation [12].

2.3 Neutrosophic logic:

Florentin Smarandache introduced neutrosophic logic, an extension of classical and fuzzy logic, in the late 1990s. It is intended to handle uncertainty, indeterminacy, and partial information more efficiently than standard logic systems. Neutrosophic logic is particularly well-suited to circumstances in which truth, untruth, and indeterminacy values coexist [13]. Neutrosophic logic is

a rapidly emerging research subject with several applications in diverse industries. This logic is being studied for its ability to handle complex and ambiguous data, and new developments are continually appearing. While the potential of Neutrosophic logic in digital forensics has not been thoroughly investigated, it shows enormous promise and is ripe for further investigation [14].

2.3.1 Neutrosophic Logic Architecture:

While there is no standardized design for Neutrosophic logic, which is a relatively new and less formalized discipline when compared to traditional logic systems, there are some significant components and factors that are typically taken into account when developing systems employing Neutrosophic logic [13].

- Neutrosophic Sets:

  The concept of neutrosophic sets forms the foundation of neutrosophic logic. Each element in a set is assigned three values: truth, indeterminacy, and falsehood. Although the representation of these values may differ, a triplet (T, I, F) is often used [13].

- Neutrosophic Logic Operators:

  Neutrosophic logic introduces operators such as Neutrosophic conjunction (∧), disjunction (∨), and implication (→), allowing operations on Neutrosophic truth values [15].

- Neutrosophic Inference Mechanisms:

  In a Neutrosophic system, inference mechanisms involve rules used to combine or deduce new statements from existing ones, depending on the specific application and the nature of the problem being addressed [15].

- Graphs and Networks:

  In some applications that involve complex relationships, the architecture may include components for representing and processing Neutrosophic graphs and networks [16].

- Evaluation and Validation Tools:

  The architecture should include tools for evaluating and validating its performance to ensure the effectiveness of the Neutrosophic system [16].

2.3.2 Neutrosophic Framework: For Gauging Information Extracted from Smartphones and consists of three steps [17]:

I. Extracting data: The initial stage involves retrieving the necessary data from the smartphone. Various methods can achieve this, including keyword search, pattern matching, and machine learning. [17].

- Keyword search: This technique involves searching the smartphone for keywords that are relevant to the case.

- Pattern matching: This technique involves searching the smartphone for patterns that are indicative of criminal activity.

- Machine learning: This technique can be used to train a model to extract relevant data from smartphones.

The choice of data extraction technique will depend on the specific case and the available resources.

II. Neutrosophic assessment: The next phase involves assessing the gathered information through neutrosophic reasoning. This includes assigning a level of truth, falsehood, and neutrality to every data point [18]. This is accomplished by following these steps:

- Determine the important aspects of data. For instance, the size of data for a chat message could include the message's content, the sender of the message, and the circumstances of the message

- Assign a degree of truth, falsity, and neutrality to each dimension of information. This can be done using a variety of techniques, such as fuzzy logic or machine learning.

- Determine the total level of accuracy, inaccuracy, and impartiality of the information. This is accomplished by merging the levels of truth, falsehood, and neutrality in every aspect of information.

The Neutrosophic evaluation step can be performed manually or automatically.

III. Decision-making: The third step is to use the neutrosophic evaluation results to decide the relevance of the information. This decision can be made by a human forensic investigator or by an automated system [18]. If the overall degree of truth of the data is high, then the data is considered relevant. If the overall degree of truth for the data is low, then the data is considered irrelevant.

2.3.3 Neutrosophic Logic Tools: Various tools and libraries are available for researchers and practitioners working with Neutrosophic logic, with some still under development.

- Neutrosophic Computing Toolbox for Python:

There have been attempts to create Python-based tools for neutrosophic computing. These comprise libraries for representing and manipulating neutrosophic sets, as well as for carrying out neutrosophic logic operations [19].

- Neutrosophic Logic Toolbox for MATLAB:

Dr. Florentin Smarandache created a MATLAB toolbox for working with neutrosophic sets, logic operations, and applications. The toolbox offers MATLAB functions and utilities [17].

- jNTool (Java Neutrosophic Tools):

jNTool is a collection of Java-based tools for dealing with neutrosophic logic. It contains implementations of neutrosophic set operations, logical connectives, and utilities for creating neutrosophic systems [20].

2.4 Excel Fuzzy Lookup:

Fuzzy Lookup is a useful function in Excel that enables users to identify and match related entries across huge datasets. Excel's fuzzy lookup uses fuzzy matching algorithms and similarity

measurements to effectively recognize records with minor differences, such as misspellings or typos, and offer a list of likely matches [21].

This add-in takes into account the spelling and similarity of responses, ensuring that only very close matches are considered valid. Excel Fuzzy Lookup may substantially speed up the process of scoring cued recall data while eliminating potential errors or discrepancies caused by human judgment. SSIS's Fuzzy Lookup operator provides a similar capability for approximate string matching. Incorporating the fuzzy lookup system into this operator boosts its possibilities [22].

3. The proposed Methodology

The purpose of this research is to assess data, determine if it is reliable or not, and analyze it. Neutrosophic Logic has been selected as the method for evaluating the data and providing a level of certainty for forensic investigators to use in investigations. Additionally, Excel's fuzzy lookup has been utilized to evaluate conversations between individuals and assign a percentage to each data point. The results are compiled into a dataset and analyzed using Python code to assess the reliability of the information. The outcomes reveal the percentage of each data point and whether it can be considered as evidence.

3.1 The dataset:

The dataset that we examined was downloaded from Kaggle, specifically from the WhatsApp Chat dataset. This dataset consists of chat data between individuals and includes various details necessary for forensic analysis. To align the data with our research requirements, we made several alterations to the original dataset. The dataset comprises seven columns, each representing different aspects of the chat data. The first column denotes the sender of the chat, while the second column contains the chat messages. The third to seventh columns represent the date and time (year, month, day, hour, and minute) at which each message was sent or received, as shown in Table 1. The dataset that we examined was downloaded from a Kaggle website [23] and we made some alterations to it to match our research. The dataset is a chat between individuals and others. The chat consists of 7 columns. The first column is the sender of the chat, the second column is the chat. The third to seventh columns represent data and time, as shown in the Table 1. The table include 7 users which indicated that the main user which the smartphone found its data and the message corresponding to each user for discovering forensic data in year, month, day, hours, and minutes.

3.1.1. Definitions

1. Message Timing: The timestamp (year, month, day, hour, and minute) at which a message was sent or received.
2. Main User: The primary user of the smartphone, whose data is the focus of the forensic analysis.
3. Forensic Data: Information extracted from digital devices that can be used as evidence in investigations.
4. Neutrosophic Logic: A branch of logic that deals with indeterminacy, handling truth, falsehood, and indeterminacy simultaneously.

3.1.2. Aggregations

1. Total Messages Sent by Main User: Count of all messages sent by the main user.
2. Message Frequency by User: Number of messages sent by each user.
3. Conversation Duration: The total duration of a conversation, calculated from the first to the last message timestamp.

4. Average Message Interval: The average time interval between consecutive messages in a conversation.

3.1.3. Theorems and Examples

1. Theorem: Consistency of Message Timing
    - Statement: If messages from different users have identical timestamps, they are part of the same conversation thread.
    - Example: On November 26, 2021, at 21:48, User 1 and the Main User exchanged messages, indicating an active conversation at that precise minute.
2. Theorem: Conversation Length
    - Statement: The length of a conversation is the difference between the timestamps of the last and first messages.
    - Example: The conversation on December 2, 2021, between the Main User and User 3, lasted from 22:03 to 22:08, a duration of 5 minutes.
3. Theorem: Message Interval Analysis
    - Statement: The average message interval can indicate the responsiveness and engagement level in a conversation.
    - Example: The rapid exchange on January 6, 2022, between the Main User and User 4, with messages every minute, suggests high engagement.

3.1.4. Novelty and Application

Novelty: This study applies Neutrosophic logic to analyze forensic data from smartphones, evaluating the truth, falsity, and indeterminacy of information. By analyzing conversation data using Excel's fuzzy lookup and Neutrosophic Python code, we determine the admissibility of evidence.

3.1.5. Application Example:

1. Admissibility Analysis: Using the Neutrosophic framework, the conversation between the Main User and User 2 on December 2, 2021, can be evaluated for truth and indeterminacy, determining its reliability as forensic evidence.
2. Pattern Detection: The sequence of messages surrounding key events, such as the passing of "Jack" on January 6, 2022, can be analyzed for patterns that may indicate premeditated actions or conspiracy.

This enhanced approach allows forensic investigators to navigate the complexity of digital data with greater accuracy, making informed decisions on the relevance and reliability of evidence.

Table 1. Dataset from Kaggle website [21]

Users	**Messages**	**Year**	**Month**	**Day**	**Hour**	**Minute**
User 1	Tell me when you're leaving.	2021	November	26	21	48
Main user	I'll go after the exam.	2021	November	26	21	48
User 1	Very well, then	2021	November	26	21	48
User 1	I want to go home after finishing the exam.	2021	November	26	21	49
Main user	ok	2021	November	26	21	49
Main user	I`m failing the test	2021	November	26	21	50

Users	Messages	Year	Month	Day	Hour	Minute
Main user	Kareo??	2021	December	2	18	11
Main user	?	2021	December	2	18	11
User 2	Which flat?	2021	December	2	18	12
Main user	I told you previously.	2021	December	2	18	14
User 2	I'll call you after I've finished him.	2021	December	2	18	16
User 3	Did Kareo call you?	2021	December	2	22	3
User 3	I called him, but he didn't answer.	2021	December	2	22	4
Main user	Relax, he does a good job.	2021	December	2	22	4
User 3	Did he finish him?	2021	December	2	22	6
Main user	Yup	2021	December	2	22	6
User 3	ok	2021	December	2	22	8
User 4	Is everything alright?	2022	January	6	2	51
Main user	No, Jack has passed away.	2022	January	6	2	52
Main user	Yesterday, I saw his body.	2022	January	6	2	52
User 4	What`s the fu…….?	2022	January	6	2	53
Main user	Relax; everything will be fine.	2022	January	6	2	53
User 5	Good news: he's currently dozing off in hell.	2022	January	7	5	38
Main user	You are super hero	2022	January	7	5	38
User 6	I need to locate my sunglasses.	2022	January	15	5	59
Main user	You'll never locate it.	2022	January	15	5	59
User 7	I'll find it over my dying body ☺	2022	January	15	6	00
Main user	No no	2022	January	15	6	2
User 7	☺	2022	January	15	6	2

3.2 Excel Fuzzy Lookup Add-in:

To use a Python code algorithm, the date and time must be transformed into a numerical timestamp. Microsoft Excel was used to convert the date and time into timestamps. The user column also became 0, 1. Table 2 shows that the sender's changed to (0), and the receivers' changed to (1).

Table 2. Chat messages after converting the user column and the timestamp column.

Users	Messages	Timestamp
1	Tell me when you're leaving.	1637963221
0	I'll go after the exam.	1637963221
1	Very well then	1637963221
1	I want to go home after finishing the exam.	1637963281
0	ok	1637963281
0	I`m failing the test	1637963341
0	Kareo??	1638468611
0	?	1638468623
1	Which flat?	1638468671
0	I told you previously.	1638468794
1	I'll call you after I've finished him.	1638468914
1	Did Kareo call you?	1638482528
1	I called him, but he didn't answer.	1638482588
0	Relax, he does a good job.	1638482600
1	Did he finish him?	1638482708
0	Yup	1638482718
1	ok	1638482823
1	Is everything alright?	1641437408
0	No, Jack has passed away.	1641437478
0	Yesterday, I saw his body.	1641437486
1	What`s the fu…….?	1641437528
0	Relax, everything will be fine.	1641437536
1	Good news: he's currently dozing off in hell. ☺	1641533828
0	You are super hero	1641533835
1	I need to locate my sunglasses.	1642226284
0	You'll never locate it.	1642226300
1	I'll find it over my dying body ☺	1642226274
0	No no	1642226464
1	☺	1642226474

Each chat in the dataset was converted to a percentage using the Excel Fuzzy Lookup Add-in. This add-in calculates the percentage of similarity between the two tables. The first table was the conversation table, while the second table had a single column with the most often-used terms for arguments and violations. The Excel Fuzzy Lookup Add-in calculated the similarity percentage between each chat and the terms in the second table. This created a new table with five columns, as shown in Table 3.

Table 3. similarity percentage after comparing the message table with a table of the violation words.

Users	Messages	Timestamp	Compare msg	Similarity
1	Tell me when you're leaving.	1637963221		0.0000
0	I'll go after the exam.	1637963221		0.0000
1	Very well, then	1637963221		0.0000
1	I want to go home after finishing the exam.	1637963281		0.0000
0	ok	1637963281		0.0000
0	I`m failing the test	1637963341		0.0000
0	Kareo??	1638468611		0.0000
0	?	1638468623		0.0000
1	Which flat?	1638468671		0.0000
0	I told you previously.	1638468794		0.0000
1	I'll call you after I've finished him.	1638468914	finish him	0.8462
1	Did Kareo call you?	1638482528		0.0000
1	I called him, but he didn't answer.	1638482588		0.0000
0	Relax; he does a good job.	1638482600	finish	0.4720
1	Did he finish him?	1638482708	finish him	0.8750
0	Yup	1638482718		0.0000
1	ok	1638482823		0.0000
1	Is everything alright?	1641437408		0.0000
0	No, Jack has passed away.	1641437478	Passed away	0.8235
0	Yesterday, I saw his body.	1641437486	dead body	0.5054
1	What`s the fu…….	1641437528		0.0000
0	Relax, everything will be fine.	1641437536		0.0000
1	Good news: he's currently dozing off in hell. ☺	1641533828	hell	0.7590
0	You are super hero	1641533835		0.0000
1	I need to locate my sunglasses.	1642226284		0.0000
0	You'll never locate it.	1642226300		0.0000
1	I'll find it over my dying body ☺	1642226274	dead body	0.8333
0	No no	1642226464		0.0000
1	☺	1642226474		0.0000

3.3 Neutrosophic-Fuzzy Python Code:

A Robust Algorithm for Smartphone Data Triage in Forensic Investigations.

Python Code

```
def neutrosophic_gauging(smartphone_data):
    # Step 1: Data extraction
    relevant_data = extract_relevant_data(smartphone_data)
    # Step 2: Neutrosophic evaluation
degrees_of_truth, degrees_of_falsity, degrees_of_neutrality =
neutrosophic_evaluate(relevant_data)
    # Step 3: Decision making
relevance_scores = calculate_relevance_scores
```

```
(degrees_of_truth, degrees_of_falsity, degrees_of_neutrality)

    # Return the most relevant information

    return get_most_relevant_information(relevance_scores)
```

- extract_relevant_data(): This function extracts the relevant data from the smartphone.
- neutrosophic_evaluate(): This function evaluates the extracted data using neutrosophic logic.
- calculate_relevance_scores(): This function calculates the relevance scores for the data.
- get_most_relevant_information(): This function returns the most relevant information.

This algorithm can be used to gauge information extracted from smartphones using Neutrosophic logic and fuzzy logic. The algorithm can handle uncertainty and vagueness in the data, and it can evaluate multiple dimensions of information. This makes the algorithm a valuable tool for forensic investigators who need to extract evidence from smartphones in criminal cases.

3.3.1 The system has three inputs:

- The sender: It contains two values: (0) for the owner of the chat and (1) for the others.
- Time has two values. The first value is the timestamp of the first message "1637963221", and the second value is the time after the investigator found the dataset "1661367654".
- The strength of the evidence is evaluated by the Excel fuzzy lookup.

3.3.2 The output represents the result, and it contains three values:

- Week ranges from 0.1 to 0.5, representing week evidence.
- Middle represents 0.51 to 0.7, representing the average evidence.
- Strong; it ranges from 0.71 to 0.99, representing strong evidence.

The Python algorithm 1

Input data:
sender = "send"; "receiver"
time = "before"
data = "suspicious"
Neutrosophic evaluation:
degree of truth = 0.7
degree of falsity = 0.3
degree of neutrality = 0
Fuzzy logic:
output = "middle"
Relevance score = 0.7

The Python algorithm 2

Input data:
sender = "sender"; "receiver"
time = "before"
data = "suspicious"
Neutrosophic evaluation:
degree of truth = 0.9
degree of falsity = 0.1
degree of neutrality = 0
Fuzzy logic:
output = "high"
Relevance score = 0.9

The Python algorithm 3

Input data:
sender = "send"; "receiver"
time = "after"

data = "suspicious"; "normal"
Neutrosophic evaluation:
degree of truth = 0.1
degree of falsity = 0.9
degree of neutrality = 0
Fuzzy logic:
output = "week"
Relevance score = 0.1

4. Results and Discussion

We analyzed 30 chats with various inputs, and after processing the inputs using Python code, the output was obtained; the results were provided in Table 4 and Figure 1. The results of our study, which utilized Neutrosophic logic and fuzzy logic to analyze forensic data from smartphone conversations, reveal significant insights into the reliability and relevance of the extracted information. By comparing Neutrosophic evaluations with fuzzy logic outputs and calculating the relevance scores, we can assess the degree of truth, falsity, and indeterminacy present in each conversation.

Table 4. the results of all 30-chat message

	Inputs		**Excel add-in results of the Similarity degree**	**Neutrosophic evaluation**	**Fuzzy Logic output**	**Relevance score**
	Sender of chat	**Time**				
1	0 = “sender’’	1637963221 = “before”	0%	Degree of truth = 0 Degree of falsity = 0.2 Degree of Neutrality=0.8	Output = “week”	0.1
2	1 = “receiver”	1638468913 = “before”	84%	Degree of truth = 0.8 Degree of falsity = 0.1 Degree of Neutrality=0.1	Output = “strong”	0.82
3	1 = “receiver”	1638482707 = “before”	87%	Degree of truth = 0.8 Degree of falsity = 0 Degree of Neutrality=0.2	Output = “strong”	0.81
4	0 = “sender’’	1641437477 = “before”	83%	Degree of truth = 0.8 Degree of falsity = 0.1 Degree of Neutrality=0.1	Output = “strong”	0.84
5	1 = “receiver”	1641533827 = “before”	76%	Degree of truth = 0.6 Degree of falsity = 0.3 Degree of Neutrality=0.1	Output = “middle”	0.7
6	1 = “receiver”	1642226273 = “before”	83%	Degree of truth = 0.7 Degree of falsity = 0.1 Degree of Neutrality=0.2	Output = “middl”	0.7
7	0 = “sender’’	1643890023 = “before”	88%	Degree of truth = 0.8 Degree of falsity = 0 Degree of Neutrality=0.2	Output = “strong”	0.9
8	1 =	1644332523	81%	Degree of truth = 0.7	Output	0.68

	Inputs		Excel add-in results of the Similarity degree	Neutrosophic evaluation	Fuzzy Logic output	Relevance score
	Sender of chat	**Time**				
	"receiver"	= "before"		Degree of falsity = 0.2 Degree of Neutrality=0.1	= "middl"	
9	0 = "sender''	1644796682 = "before"	0%	Degree of truth = 0 Degree of falsity = 0.1 Degree of Neutrality=0.9	Output = "week"	0.2
10	1 = "receiver"	1645124832 = "before"	77%	Degree of truth = 0.7 Degree of falsity = 0.3 Degree of Neutrality=0	Output = "middl"	0.69
11	0 = "sender''	1646143802 = "before"	83%	Degree of truth = 0.8 Degree of falsity = 0.1 Degree of Neutrality=0.1	Output = "strong"	0.84
12	1 = "receiver"	1646744768 = "before"	10%	Degree of truth = 0.2 Degree of falsity = 0.1 Degree of Neutrality=0.7	Output = "week"	0.31
13	0 = "sender''	1647249255 = "before"	84%	Degree of truth = 0.8 Degree of falsity = 0 Degree of Neutrality=0.2	Output = "strong"	0.87
14	1 = "receiver"	1647720361 = "before"	0%	Degree of truth = 0.1 Degree of falsity = 0 Degree of Neutrality=0.9	Output = "week"	0.14
15	1 = "receiver"	1647860880 = "before"	0%	Degree of truth = 0.2 Degree of falsity = 0.1 Degree of Neutrality=0.7	Output = "week"	0.17
16	1 = "receiver"	1648494650 = "before"	5%	Degree of truth = 0.3 Degree of falsity = 0 Degree of Neutrality=0.7	Output = "week"	0.17
17	0 = "sender''	1648814770 = "before"	0%	Degree of truth = 0 Degree of falsity = 0.2 Degree of Neutrality=0.8	Output = "week"	0.2
18	0 = "sender''	1649182150 = "before"	0%	Degree of truth = 0.1 Degree of falsity = 0.2 Degree of Neutrality=0.7	Output = "week"	0.22
19	1 = "receiver"	1649588710 = "before"	0%	Degree of truth = 0.2 Degree of falsity = 0.1 Degree of Neutrality=0.7	Output = "week"	0.23
20	0 = "sender''	1649775903 = "before"	81%	Degree of truth = 0.7 Degree of falsity = 0.1 Degree of Neutrality=0.2	Output = "strong"	0.79
21	1 = "receiver"	1650459430 = "before"	0%	Degree of truth = 0 Degree of falsity = 0.3 Degree of Neutrality=0.7	Output = "week"	0.26
22	0 = "sender''	1652785755 = "before"	82%	Degree of truth = 0.7 Degree of falsity = 0.1 Degree of Neutrality=0.2	Output = "strong"	0.8
23	1 = "receiver"	1654078030 = "before"	0%	Degree of truth = 0.1 Degree of falsity = 0.6	Output =	0.31

	Inputs		Excel add-in results of the Similarity degree	Neutrosophic evaluation	Fuzzy Logic output	Relevance score
	Sender of chat	**Time**				
				Degree of Neutrality=0.3	"week"	
24	1 = "receiver"	1654603823 = "before"	83%	Degree of truth = 0.5 Degree of falsity = 0.5 Degree of Neutrality=0	Output = "middle"	0.62
25	0 = "sender''	1655298320 = "before"	45%	Degree of truth = 0.1 Degree of falsity = 0.2 Degree of Neutrality=0.7	Output = "week"	0.43
26	0 = "sender''	1656839120 = "before"	0%	Degree of truth = 0 Degree of falsity = 0.1 Degree of Neutrality=0.9	Output = "week"	0.23
27	1 = "receiver"	1664994800	0%	Degree of truth = 0.1 Degree of falsity = 0.1 Degree of Neutrality=0.8	Output = "week"	0.13
28	1 = "receiver"	1667841740	0%	Degree of truth = 0 Degree of falsity = 0.1 Degree of Neutrality=0.9	Output = "week"	0.14
29	1 = "receiver"	1683717860	95%	Degree of truth = 0.1 Degree of falsity = 0.9 Degree of Neutrality=0	Output = "week"	0.34
30	0 = "sender''	1684780423	94%	Degree of truth = 0.1 Degree of falsity = 0.8 Degree of Neutrality=0.1	Output = "week"	0.31

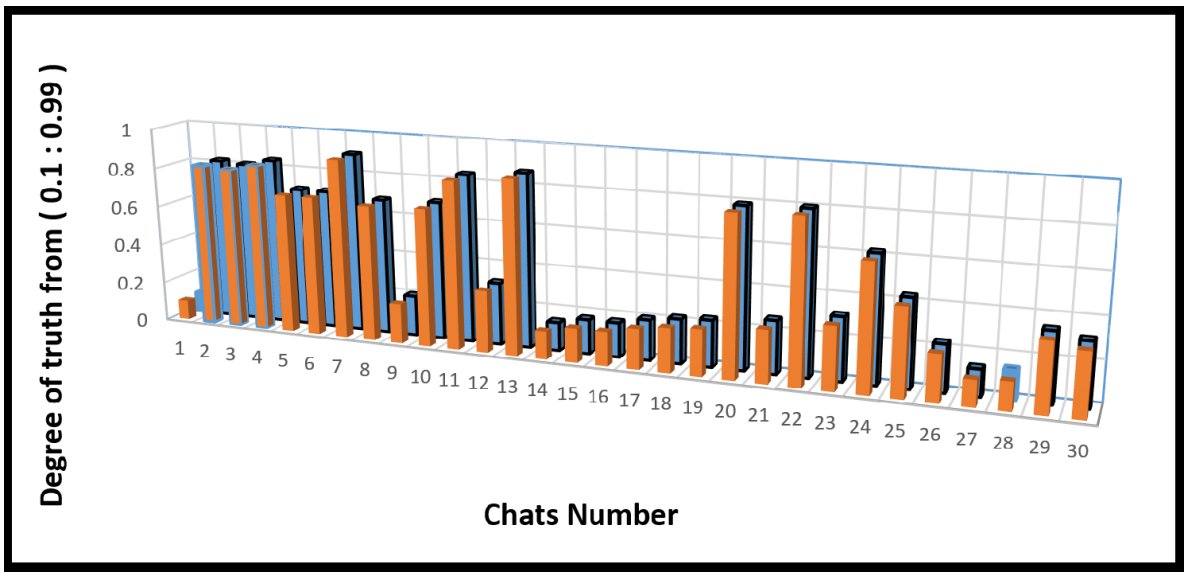

Figure 1. Represent the output results.

- Data points that fall above 0.7 are considered more likely to be true, as in chats numbers 2, 3, 4, 7, 11, 13, 20, and 22.

- Chats numbers 1, 9, 12, 14, 15, 16, 17, 18, 19, 21, 23, 25, 26 27, 28, 29, and 30 which are below 0.6 are considered more likely to be false,

- Data points closer to 0.7 are considered more neutral, meaning they contain a mixture of truth and falsity or that their truth value is uncertain, as chat numbers 5, 6, 8, 10 and24

- This approach allows for a more nuanced understanding of data than traditional binary classifications of true or false.

The results of our study, which utilized Neutrosophic logic and fuzzy logic to analyze forensic data from smartphone conversations, reveal significant insights into the reliability and relevance of the extracted information. By comparing Neutrosophic evaluations with fuzzy logic outputs and calculating the relevance scores, we can assess the degree of truth, falsity, and indeterminacy present in each conversation.

4.1. Neutrosophic Logic Evaluations:

Neutrosophic logic allowed us to measure the degrees of truth, falsity, and neutrality (indeterminacy) for each message. For instance, message 2 had a high degree of truth (0.8), low falsity (0.1), and low neutrality (0.1), resulting in a strong output with a relevance score of 0.82. Conversely, message 29 had a low degree of truth (0.1) and high falsity (0.9), reflecting weak relevance (score of 0.34). This nuanced evaluation aids in discerning the credibility of information and its potential use in forensic investigations.

4.2. Fuzzy Logic Outputs:

The fuzzy logic output provided a qualitative assessment (e.g., "strong," "middle," "week") for each message. For example, a message with an 87% similarity degree in Excel's fuzzy lookup and high truth degree in Neutrosophic evaluation was categorized as "strong." This classification aligns with the high relevance score (0.81), demonstrating consistency between the two methodologies.

4.3. Comparison with Existing Studies:

Existing studies predominantly rely on traditional fuzzy logic or binary evaluations (true/false) for forensic data analysis. These methods often fall short in handling the inherent ambiguity and partial truth present in real-world data. Our approach, integrating Neutrosophic logic, offers a more comprehensive framework by accommodating indeterminacy and providing a multi-valued evaluation.

4.4. Key Observations:

High Relevance Messages: Messages with high degrees of truth and low falsity (e.g., messages 2, 3, 4, 7) consistently resulted in strong outputs and high relevance scores, indicating reliable forensic evidence. Low Relevance Messages: Messages with high degrees of neutrality or falsity (e.g., messages 12, 14, 21) were categorized as weak, suggesting less reliable information. Consistency Across Methods: The alignment between Neutrosophic logic evaluations and fuzzy logic outputs underscores the robustness of our approach. High relevance scores were consistently associated with strong outputs in fuzzy logic, validating the credibility of our Neutrosophic framework.

4.5. Applications:

Admissibility Analysis: Using Neutrosophic logic, investigators can better evaluate the admissibility of evidence by considering the degrees of truth, falsity, and neutrality. For example, the conversation between the main user and User 2 on December 2, 2021, was deemed highly reliable based on its strong relevance score (0.82). Pattern Detection: Analyzing message sequences around key events, such as the passing of "Jack," can reveal patterns indicative of premeditated actions or conspiracy. High engagement levels and rapid message exchanges (e.g., January 6, 2022) suggest significant forensic value. In summary, our study demonstrates the superiority of Neutrosophic logic over traditional fuzzy logic and binary evaluations in forensic data analysis. The inclusion of indeterminacy provides a more accurate and nuanced understanding of digital evidence, thereby enhancing the effectiveness of forensic investigations.

5. Conclusion and Future work:

The research objective is to use Python code on data to determine whether it can be considered as evidence or not. The code analyzed 30 chat transcripts and provided a strength percentage for each based on different standards. The code gave a low proportion to chats numbered 1, 9, 12, 14, 15, 16, 17, 18, 19, 21, 23, 25, 26, 27, 28, 29, and 30 since they had a low similarity percentage with feud and violation terms. The code assigned a low proportion to chats numbered 2, 3, 4, 7, 11, 13, 20, and 22 since they share a significant resemblance with quarrel and violation terms. The Python code was undeceivable since it assigned chat numbers 29 and 30 a low rating even though they had a high proportion of similarity with feud and violation words and were sent by a different person after the smartphone was discovered. There are several possible directions for future research on the algorithm outlined in this paper. A potential focus for future efforts is enhancing the precision of the algorithm. More advanced methods for Neutrosophic logic and fuzzy logic can be utilized to accomplish this. An additional aspect to consider for future work is broadening the algorithm's scope. The algorithm has the potential to be expanded to manage different kinds of data that are obtained from smartphones, like call logs, photos, and videos. Ultimately, the algorithm could be employed to create a more detailed structure for the forensic examination of mobile phones. The framework might incorporate different tools and methods, like the algorithm described in this paper, to assist forensic investigators in retrieving and examining evidence from smartphones.

Declaration of competing interest

The authors declare that they have no known competing financial interests or personal relationships that could have appeared to influence the work reported in this paper.

Data availability

The source Data are founded in https://www.kaggle.com/datasets/rijudhara/whatsappchat/data.

References

1. Karjagi A.J., and A.Quadri S., “Design of a Framework for Data Extraction and Analysis from Android-Embedded Smartphones “, Russian Law Journal, vol. X I, no. 3, 794-6, 2023. Doi.org:10.52783/rlj.v11i3.127.
2. Moreb M., Salah S., and Amro B., ” A Novel Framework for Mobile Forensics Investigation Process”, Research Square, 1-20, 2023.

3. Alshikho M., Jdid M., and Broumi S., " A Study of a Support Vector Machine Algorithm with an Orthogonal Legendre Kernel According to Neutrosophic Logic and Inverse Lagrangian Interpolation", Journal of Neutrosophic and Fuzzy Systems (JNFS), Vol. 05, No. 01, PP. 41-51, 2023. DOI: 10.54216/JNFS.050105.
4. Remani N.V.J.M., Naresh V. S., Reddi S., and Kumar K. D., " Crime data optimization using neutrosophic logic based game theory", Concurrency Computat Pract Exper., vol.34,e6973, 2022, DOI: 10.1002/cpe.6973A.M. Da Costa, A.O. De Sa, and R.Cs Machado, "Data Acquisition and Extraction on Mobile Devices A review", IEEE International Workshop on Metrology for industry, vol. 4.0& IoT, 294-299,2022.
5. R. M. Abou alzahab, Abd Elkhalik, Saeed H., Hazem El-Bakry, A. A. Salama "A Novel Framework for Gauging Information Extracted from Smartphones Using Fuzzy Logic." Alfarama Journal of Basic & Applied Sciences 5, no. 2 (2024): 230-242.
6. Ilieva, G.; Yankova, T.; Ruseva, M.; Klisarova-Belcheva, S.; Dzhabarova, Y.; Bratkov, M. Social Media Influencers: Customer Attitudes and Impact on Purchase Behaviour. Preprints 2024, 2024051131. https://doi.org/10.20944/preprints202405.1131.v1.
7. Cahyani N.D.W., Martini B., Choo K-K.R., and Al-Azhar A. M. N., "Forensic data acquisition from cloud-of-things devices: windows Smartphones as a case study", Concurrency Computat.: Pract. Exper. , vol. 29:e3855, 2017. DOI:10.1002/cpe.3855
8. Silveir C.M. da, Jr R. T. de Sousa, R. de O. Albuquerque, G. D. A. Nze, G.A. de O. Júnior, A. L.S. Orozco, and L. J. G. Villalba, "Methodology for Forensics Data Reconstruction on Mobile Devices with Android Operating System Applying In-System Programming and Combination Firmware", Appl. Sci., vol.10, 4231, 1-29, 2020. Doi.:10.3390/app10124231
9. Mallidi S. K. R., and Palli P., "A Comprehensive Analysis of Smartphone Forensics & Data Acquisitions, International Journal of Advanced Research in Computer Science and Software Engineering", vol.6, no. 2, 270-276, 2016.
10. Hans K., Ahuja L., and Muttoo S.K., "A fuzzy logic approach for detecting redirection spam", Int. J. Electronic Security and Digital Forensics, vol. 8, no. 3,191-14, 2016. DOI:10.1504/IJESDF.2016.077435
11. Gan, T. "From Boolean Logic to Fuzzy Logic", Pure Mathematics, vol. 6, no. 2, 111-115, 2016. Doi:10.12677/pm.2016.62016
12. Bhowmick P., Mukhopadhyay S., and Sivakumar V., "A review on GIS-based Fuzzy and Boolean logic modeling approach to identify the suitable sites for Artificial Recharge of Groundwater", Sch. J. Eng. Tech., vol. 2, no. 3A,316-319, 2014.
13. Vandhana S., and Anuradha J., Neutrosophic fuzzy hierarchical clustering for dengue analysis in Sri Lanka. Neutrosophic Sets and Systems, 31(1):14, 2020.
14. Salama A. A., Shams M. Y., Bhatnagar R., Mabrouk A. G., and Tarek Z., "Optimizing Security Measures in Decentralized Mobile Networks with Neutrosophic Fuzzy Topology and PKI," 2023 3rd International Conference on Technological Advancements in Computational Sciences (ICTACS), Tashkent, Uzbekistan, 2023, pp. 1040-1048
15. Alqarni M., Samak A. H., Ismail S. S., Abd El-Aziz R. M., Taloba A. I. et al., Utilizing a neutrosophic fuzzy logic system with ann for short-term estimation of solar energy, International Journal of Neutrosophic Science 20(4) (2023) 240–40

16. Salama A. A., Tarek Z., Darwish E. Y., Elseuofi S., and Shams M. Y.N, Neutrosophic Encoding and Decoding Algorithm for ASCII Code System, Neutrosophic Sets and Systems, Vol. 63, 2024, pp. 105-129.
17. Smarandache F., (2003). Neutrosophic set—a generalization of the intuitionistic fuzzy set. International Journal of Pure and Applied Mathematics, 4(1), 109-129.
18. Alhasan K. F., Salama A. A., & Smarandache F., (2021). Introduction to neutrosophic reliability theory. International Journal of Neutrosophic Science, 15(1), 52-61
19. Qureshi M. N., and Ahmad M. V., An improved method for image segmentation using k-means clustering with Neutrosophic logic. Procedia computer science, 132:534–540, 2018.
20. Wang H., Smarandache F., Sunderraman R., and Zhang Y. Q., Interval Neutrosophic sets and logic: theory and applications in computing: Theory and applications in computing, volume 5. Hexis, Phoenix, AZ, 2005.
21. "Excel fuzzy lookup" https://www.microsoft.com/en-US/download/details.aspx?id=15011 [Accessed 8 August 2023].
22. Fry A., Gieseck-Ashworth J., and Seiler C., "Loving Statistics & Excel Fuzzy Lookup in the Time of COVID-19", The Serials Librarian, vol. 82, no. 1-4, 145-149,2022.
23. Kaggle Data Sets, "https://www.kaggle.com/datasets/rijudhara/whatsappchat" [Accessed 6 August 2023].

Received: July 22, 2024. Accepted: Oct 20, 2024

Neutrosophic Sets and Systems, Vol. 76, 2025

University of New Mexico

An Effective Neutrosophic Approach for Group Decision-Making in College English Teaching Quality Evaluation

Bin Xie *

School of Architecture and Planning, Jiujiang University, Jiujiang, 332005, Jiangxi, China

*Corresponding author, E-mail: nancy0793@163.com; xiebing@jju.edu.cn

https://orcid.org/0000-0003-2054-4833

Abstract: College English holds great importance in Chinese universities as one of the largest, most influential, and highly regarded foundational courses. Despite significant progress in reforming college English teaching (CET), its effectiveness has faced widespread criticism. To ensure and enhance the quality of CET, it is essential to explore the establishment of a quality evaluation mechanism. One such mechanism is the multiple-attribute group decision-making (MAGDM) approach. Recently, the Exponential TODIM (ExpTODIM) and TOPSIS techniques have been employed to address MAGDM challenges. To capture uncertain data during the evaluation process, interval neutrosophic sets (INSs) are administrated as a valuable tool. This study introduces the interval neutrosophic number Exponential TODIM-TOPSIS (INN-ExpTODIM-TOPSIS) approach to address MAGDM using INSs. Eventually, anumerical study for CET quality evaluation is administrated to validate the INN-ExpTODIM-TOPSIS approach for evaluating the quality of CET.

Keywords: Multiple-attribute group decision-making (MAGDM); Interval neutrosophic sets (INSs); ExpTODIM approach; TOPSIS approach; teaching quality evaluation

1. Introduction

1.1. Research background

College English is one of the largest, most influential, and widely valued basic courses among Chinese universities[1]. For a long time, while significant achievements have been made in the reform of CET, the teaching effectiveness of college English has also been widely criticized. Exploring the establishment of a quality monitoring mechanism for CET is the only way to ensure and improve the quality of CET. The construction of ateaching quality system can lay a solid foundation for applied talent cultivation, and only then cultivation of applied talents can be effectively operated in universities. As teaching in universities gradually develops towards an application-oriented talent cultivation model, society's requirements for English talents are also becoming more diverse, with a greater emphasis on the practicality of English. The construction of aquality assurance system for CET has extremely important elements, including modules such as students, teachers, management, and evaluation[2, 3]. The roles and

contents of these four modules are different, but they all lay the foundation for ensuring CET quality. In CET, teachers should understand the learning foundation of students, consider their learning characteristics in teaching, and carry out targeted teaching work. In the actual CET process, teachers should combine people-oriented and application-oriented talent cultivation models, and build a CET system on this basis. In the evaluation process, teachers should abandon the traditional teaching technique of only looking at grades, and instead set different evaluation standards based on the learning situation of different students [4]. For example, students with relatively poor English foundations have slightly lower evaluation standards for teachers, while students with strong English foundations have relatively higher evaluation standards for teachers. In addition, it is necessary to build the content of daily learning performance to enrich the structure of evaluation system and make the English teaching evaluation more objective [5]. Through this approach, students with poor English foundations can establish confidence in learning English during the learning process, while students with better grades can make better progress, laying a solid foundation for them to become applied English talents[6]. The study of English courses in universities is aimed at enabling students to use the English language, which is also a need for applied talents in society. Therefore, teachers can use diverse techniques to evaluate the learning outcomes of students during the teaching process. If only quantitative teaching techniques are utilized in the evaluation process to evaluate student learning, it lacks a certain degree of objectivity. Teaching itself is a complex task, and in order to make teaching evaluation more objective, it is necessary to combine qualitative and quantitative evaluation techniques, with qualitative evaluation as the main focus and quantitative evaluation as a supplement. Qualitative evaluation is usually influenced by human factors, but quantitative evaluation is more objective. So, only by combining these two evaluation techniques can the evaluation of CET be more reasonable. In addition, we can also start from two aspects: formative evaluation and summative evaluation. Summative evaluation refers to the mid-term and final exams of a semester. However, the process of students learning English is dynamic, and if only the results are emphasized in evaluation, it is impossible to objectively evaluate the learning situation of college students. Therefore, self-evaluation or peer evaluation can also be utilized in the evaluation. Combining these two evaluation techniques to form a comprehensive evaluation system for CET, cultivating students' English proficiency.

1.2. Research objectives

With the increasing complexity in decision-making, relying solely on personal information often falls short of ensuring high-quality outcomes [7, 8]. GDM enhances the decision-making process by pooling the expertise of professionals from diverse fields, leveraging a broader range of knowledge to ensure more scientifically sound decisions [9, 10]. Additionally, GDM facilitates consensus among decision-makers, promoting smoother implementation of decisions [11, 12]. As a result, GDM is widely utilized across various socio-economic sectors, offering robust support for tackling complex decision-making challenges. Essentially, GDM involves engaging multiple

decision-makers to assess available options and choose the best solution [13]. In the evaluation process, in order to characterize the fuzzy data in GDM problems, Zadeh [14] put forward fuzzy sets (FSs) in 1965. With the continuous deepening and expansion of theoretical and applied research, fuzzy sets gradually encounter some unavoidable defects in problem-solving. Therefore, scholars have extended many new forms to express uncertain information, such as linguistic Pythagorean FSs [15, 16], probabilistic hesitant FSs [17-19] and interval neutrosophic sets (INSs) [20]. As the extension form of FSs, key characteristic of INSs is that truth-membership (TM), indeterminacy-membership (IM) and falsity-membership (FM) are interval values, making them more flexible in dealing with uncertainty [21, 22]. The academic community has conducted extensive research on MAGDM problems based on INSs, and has made significant progress in similarity measurement, aggregation techniques, and score functions. The above research provides reliable techniques and ideas for solving MAGDM problems in INSs environments, but there are also some limitations: it ignores GDM problems driven by decision-maker behavior, and research on social network relationships in decision-making environments is not yet complete. The CET quality evaluation is MAGDM. In addressing MAGDM challenges, researchers have recently turned to the ExpTODIM technique [10, 23] and TOPSIS [24]. These methods have proven useful in managing MAGDM issues. To capture uncertain data during the CET quality evaluation, INSs [20] are administrated as a valuable tool. This paper introduces the INN-ExpTODIM-TOPSIS approach, specifically designed to put forward MAGDM under INSs. To validate the effectiveness of the proposed technique, a numerical study focusing on CET quality evaluation is conducted. Recently, the ExpTODIM technique [10, 23] and TOPSIS [24] were put forward MAGDM. The INSs [20] are put forward characterizing uncertain data during the CET quality evaluation. In this study, the INN-ExpTODIM-TOPSIS technique is designed to put forward MAGDM under INSs. Eventually, anumerical study for CET quality evaluation is administrated to validate the INN-ExpTODIM-TOPSIS technique.

The study is structured as follows. Section 2 provides an overview of INSs. Section 3 presents the INN-ExpTODIM-TOPSIS technique, which is specifically tailored for INSs using the entropy technique. In Section 4, anumerical study is presented, focusing on CET quality evaluation along with a comparative analysis. Finally, Section 5 concludes this study.

2. Preliminaries

Wang et al. [25] addressed the SVNSs

Definition 1 [25]. The SVNSs is characterized:

$$WA=\left\{\left(x,WT_A(x),WI_A(x),WF_A(x)\right)\middle|x\in\Phi\right\} \tag{1}$$

where the $WT_A(x),WI_A(x),WF_A(x)$ depicts the TM, IM and FM, $WT_A(x),WI_A(x),WF_A(x)\in[0,1]$ and satisfies $0\le WT_A(x)+WI_A(x)+WF_A(x)\le 3$.

Wang et al.[20] addressed the INSs.

Definition 2[20]. The INSs is administrated:

$$WA=\left\{\left(\phi,WT_A(\phi),WI_A(\phi),WF_A(\phi)\right)\middle|\phi\in\Phi\right\} \quad (2)$$

where the $WT_A(\phi),WI_A(\phi),WF_A(\phi)$ depicts the TM, IM and FM, $WT_A(\phi),WI_A(\phi),WF_A(\phi)\subseteq[0,1]$ and satisfies $0\le\sup WT_A(\phi)+\sup WI_A(\phi)+\sup WF_A(\phi)\le 3$.

The INN (interval neutrosophic number) is denoted : $WA=(WT_A,WI_A,WF_A)=([WTL_A,WTR_A],[WIL_A,WIR_A],[WFL_A,WFR_A])$, where $WT_A,WI_A,WF_A\subseteq[0,1]$, and $0\le WTR_A+WIR_A+WFR_A\le 3$.

Definition 3 [26]. Let $WA=([WTL_A,WTR_A],[WIL_A,WIR_A],[WFL_A,WFR_A])$ be INN, score value is administrated:

$$WSV(WA)=\frac{\begin{pmatrix}(2+WTL_A-WIL_A-WFL_A)\\+(2+WTR_A-WIR_A-WFR_A)\end{pmatrix}}{6},\ WSV(SA)\in[0,1]. \quad (3)$$

Definition 4[26]. Let $WA=([WTL_A,WTR_A],[WIL_A,WIR_A],[WFL_A,WFR_A])$ be INN, accuracy value is administrated:

$$WAV(WA)=\frac{2+(WTL_A+WTR_A)-(WFL_A+WFR_A)}{4},\ WAV(WA)\in[0,1]\ . \quad (4)$$

Huang et al. [27] administrated the order under INNs.

Definition 5[26]. Let $WA=([WTL_A,WTR_A],[WIL_A,WIR_A],[WFL_A,WFR_A])$ and $WB=([WTL_B,WTR_B],[WIL_B,WIR_B],[WFL_B,WFR_B])$ be INNs, $WSV(WA)=\frac{\begin{pmatrix}(2+WTL_A-WIL_A-WFL_A)\\+(2+WTR_A-WIR_A-WFR_A)\end{pmatrix}}{6}$ and $WSV(WB)=\frac{\begin{pmatrix}(2+WTL_B-WIL_B-WFL_B)\\+(2+WTR_B-WIR_B-WFR_B)\end{pmatrix}}{6}$, and $WAV(WA)=\frac{2+(WTL_A+WTR_A)-(WFL_A+WFR_A)}{4}$ and $WAV(WB)=\frac{2+(WTL_B+WTR_B)-(WFL_B+WFR_B)}{4}$, then if $WSV(WA)<WSV(WB)$, then $WA<WB$; if $WSV(WA)=WSV(WB)$, then (1) if $WAV(WA)=WAV(WB)$, then $WA=WB$; (2) if $WAV(WA)<WAV(WB)$, then $WA<WB$.

Definition 6[28]. Let $WA=\left(\left[WTL_A,WTR_A\right],\left[WIL_A,WIR_A\right],\left[WFL_A,WFR_A\right]\right)$ and $WB=\left(\left[WTL_B,WTR_B\right],\left[WIL_B,WIR_B\right],\left[WFL_B,WFR_B\right]\right)$ be INNs, different operations are administrated:

$$(1)\ WA\oplus WB=\begin{pmatrix}\left(WTL_A+WTL_B-WTL_AWTL_B,WTR_A+WTR_B-WTR_AWTR_B\right),\\ \left[WIL_AWIL_B,WIR_AWIR_B\right],\left[WFL_AWFL_B,WFR_AWFR_B\right]\end{pmatrix};$$

$$(2)\ WA\otimes WB=\begin{pmatrix}\left[WTL_AWTL_B,WTR_AWTR_B\right],\\ \left[WIL_A+WIL_B-WIL_AWIL_B,WIR_A+WIR_B-WIR_AWIR_B\right],\\ \left[WFL_A+WFL_B-WFL_AWFL_B,WFR_A+WFR_B-WFR_AWFR_B\right]\end{pmatrix};$$

$$(3)\ \xi WA=\begin{pmatrix}\left[1-\left(1-WTL_A\right)^{\xi},1-\left(1-WTR_A\right)^{\xi}\right],\\ \left[\left(WIL_A\right)^{\xi},\left(WIR_A\right)^{\xi}\right],\left[\left(WFL_A\right)^{\xi},\left(WFR_A\right)^{\xi}\right]\end{pmatrix},\xi>0;$$

$$(4)\ \left(WA\right)^{\lambda}=\begin{pmatrix}\left[\left(WTL_A\right)^{\xi},\left(WTR_A\right)^{\xi}\right],\left[\left(WIL_A\right)^{\xi},\left(WIR_A\right)^{\xi}\right],\\ \left[1-\left(1-WFL_A\right)^{\xi},1-\left(1-WFR_A\right)^{\xi}\right]\end{pmatrix},\xi>0.$$

Definition 7[29]**.** Let $WA=\left(\left[WTL_A,WTR_A\right],\left[WIL_A,WIR_A\right],\left[WFL_A,WFR_A\right]\right)$ and $WB=\left(\left[WTL_B,WTR_B\right],\left[WIL_B,WIR_B\right],\left[WFL_B,WFR_B\right]\right)$, then INNHD (INN Hamming distance) is administrated:

$$\begin{aligned}&INNHD\left(WA,WB\right)\\&=\frac{1}{6}\begin{pmatrix}\left|WTL_A-WTL_B\right|+\left|WTR_A-WTR_B\right|+\left|WIL_A-WIL_B\right|+\\ \left|WIR_A-WIR_B\right|+\left|WFL_A-WFL_B\right|+\left|SFR_A-WFR_B\right|\end{pmatrix}\end{aligned}\tag{5}$$

The INNWA and INNWG approach [28] are administrated:

Definition 8[28]. Let $WA_j=\left(\left[WTL_j,WTR_j\right],\left[WIL_j,WIR_j\right],\left[WFL_j,WFR_j\right]\right)$ be INNs, INNWA approach is administrated:

$$\begin{aligned}&\mathrm{INNWA}\left(WA_1,WA_2,\ldots,WA_n\right)\\&=\mathrm{w}w_1WA_1\oplus ww_2WA_2\ldots\oplus ww_nWA_n=\overset{n}{\underset{j=1}{\oplus}}ww_jWA_j\\&=\begin{pmatrix}\left[1-\prod_{j=1}^{n}\left(1-WTL_{ij}\right)^{ww_j},1-\prod_{j=1}^{n}\left(1-WTR_{ij}\right)^{ww_j}\right],\\ \left[\prod_{k=1}^{l}\left(WFL_{ij}^{k}\right)^{ww_j},\prod_{k=1}^{l}\left(WFR_{ij}^{k}\right)^{ww_j}\right],\\ \left[\prod_{k=1}^{l}\left(WTL_{ij}^{k}\right)^{ww_j},\prod_{k=1}^{l}\left(WTR_{ij}^{k}\right)^{ww_j}\right]\end{pmatrix}\end{aligned}\tag{6}$$

where $ww=\left(ww_1,ww_2,...,ww_n\right)^T$ be weight numbers of WA_j, $ww_j>0,\sum_{j=1}^{n}ww_j=1.$

Definition 9[28]. Let $WA_j = \left(\left[WTL_j, WTR_j\right], \left[WIL_j, WIR_j\right], \left[WFL_j, WFR_j\right]\right)$ be INNs, INNWG approach is conducted:

$$\begin{aligned}
&\mathrm{INNWG}\left(WA_1, WA_2, \ldots, WA_n\right) \\
&= \left(WA_1\right)^{ww_1} \otimes \left(WA_2\right)^{ww_2}, \ldots \otimes \left(WA_n\right)^{ww_n} = \overset{n}{\underset{j=1}{\otimes}} \left(WA_j\right)^{ww_j} \\
&= \left(\begin{array}{l} \left[\prod_{j=1}^{n} \left(WTL_{ij}\right)^{ww_j}, \prod_{j=1}^{n} \left(WTR_{ij}\right)^{ww_j} \right], \\ \left[1 - \prod_{k=1}^{l} \left(1 - WFL_{ij}^{k}\right)^{ww_j}, 1 - \prod_{k=1}^{l} \left(1 - WFR_{ij}^{k}\right)^{ww_j} \right], \\ \left[1 - \prod_{k=1}^{l} \left(1 - WTL_{ij}^{k}\right)^{ww_j}, 1 - \prod_{k=1}^{l} \left(1 - WTR_{ij}^{k}\right)^{ww_j} \right] \end{array} \right)
\end{aligned} \tag{7}$$

where $ww = \left(ww_1, ww_2, ..., ww_n\right)^T$ be weight numbers of WA_j, $ww_j > 0, \sum_{j=1}^{n} ww_j = 1.$

3. INN-ExpTODIM-TOPSIS approach for MAGDM with entropy

3.1. INN-GDM problem description

The INN-ExpTODIM-TOPSIS approach is addressed for MAGDM. Let $WA = \left\{WA_1, WA_2, \cdots, WA_m\right\}$ be alternatives, and attributes set $WG = \left\{WG_1, WG_2, \cdots, WG_n\right\}$ with weight $s\omega$, where $s\omega_j \in \left[0,1\right]$, $\sum_{j=1}^{n} s\omega_j = 1$ and invited experts $WE = \left\{WE_1, WE_2, \cdots, WE_q\right\}$ with expert's weight sw, where $sw_j \in \left[0,1\right]$, $\sum_{j=1}^{n} sw_j = 1.$

Then, INN-ExpTODIM-TOPSIS approach is addressed for MAGDM.

Step 1. Address the group INN-matrix $WR^t = \left[WR_{ij}^t\right]_{m\times n} = \left(\left[WTL_{ij}^t, WTR_{ij}^t\right], \left[WIL_{ij}^t, WIR_{ij}^t\right], \left[WFL_{ij}^t, WFR_{ij}^t\right]\right)_{m\times n}$ and average INN-matrix $WR = \left[WR_{ij}\right]_{m\times n}$:

$$WR^t = \left[WR_{ij}^t\right]_{m\times n} = \begin{array}{c} \\ WA_1 \\ WA_2 \\ \vdots \\ WA_m \end{array} \begin{array}{c} \begin{array}{cccc} WG_1 & WG_2 & \ldots & WG_n \end{array} \\ \begin{bmatrix} WR_{11}^t & WR_{12}^t & \ldots & WR_{1n}^t \\ WR_{21}^t & WR_{22}^t & \ldots & WR_{2n}^t \\ \vdots & \vdots & \vdots & \vdots \\ WR_{m1}^t & WR_{m2}^t & \ldots & WR_{mn}^t \end{bmatrix} \end{array} \tag{8}$$

$$WR=\left[WR_{ij}\right]_{m\times n}=\begin{array}{c} \\ WA_1 \\ WA_2 \\ \vdots \\ WA_m \end{array}\begin{array}{c} \begin{array}{cccc} WG_1 & WG_2 & \ldots & WG_n \end{array} \\ \begin{bmatrix} WR_{11} & WR_{12} & \ldots & WR_{1n} \\ WR_{21} & WR_{22} & \ldots & WR_{2n} \\ \vdots & \vdots & \vdots & \vdots \\ WR_{m1} & WR_{m2} & \ldots & WR_{mn} \end{bmatrix} \end{array} \tag{9}$$

In line with INNWA technique, the $WR=\left(\left[WTL_{ij},WTR_{ij}\right],\left[WIL_{ij},WIR_{ij}\right],\left[WFL_{ij},WFR_{ij}\right]\right)_{m\times n}$ is:

$$\begin{aligned} WR_{ij}&=sw_1WR_{ij}^1\oplus sw_2WR_{ij}^2\oplus\cdots\oplus sw_tWR_{ij}^t \\ &=\left(\begin{array}{l}\left[1-\prod_{k=1}^{t}\left(WTL_{ij}^t\right)^{sw_j},1-\prod_{k=1}^{t}\left(WTR_{ij}^t\right)^{sw_j}\right], \\ \left[\prod_{k=1}^{t}\left(WFL_{ij}^t\right)^{sw_j},\prod_{k=1}^{t}\left(WFR_{ij}^t\right)^{sw_j}\right], \\ \left[\prod_{k=1}^{t}\left(1-WTL_{ij}^t\right)^{sw_j},\prod_{k=1}^{t}\left(1-WTR_{ij}^t\right)^{sw_j}\right]\end{array}\right) \end{aligned} \tag{10}$$

Step 2. Normalize the $WR=\left[WR_{ij}\right]_{m\times n}$ into $NWR=\left[NWR_{ij}\right]_{m\times n}$.

For benefit attributes:

$$\begin{aligned} NWR_{ij}&=\left(\begin{array}{l}\left[NWTL_{ij},NWTR_{ij}\right], \\ \left[NWIL_{ij},NWIR_{ij}\right],\left[NWFL_{ij},NWFR_{ij}\right]\end{array}\right) \\ &=WR_{ij}=\left(\begin{array}{l}\left[WTL_{ij},WTR_{ij}\right], \\ \left[WIL_{ij},WIR_{ij}\right],\left[WFL_{ij},WFR_{ij}\right]\end{array}\right) \end{aligned} \tag{11}$$

For cost attributes:

$$\begin{aligned} NWR_{ij}&=\left(\begin{array}{l}\left[NWTL_{ij},NWTR_{ij}\right], \\ \left[NWIL_{ij},NWIR_{ij}\right],\left[NWFL_{ij},NWFR_{ij}\right]\end{array}\right) \\ &=WR_{ij}=\left(\begin{array}{l}\left[WFL_{ij},WFR_{ij}\right], \\ \left[WIL_{ij},WIR_{ij}\right],\left[WTL_{ij},WTR_{ij}\right]\end{array}\right) \end{aligned} \tag{12}$$

3.2. Administrate the attributes weight through entropy.

Entropy approach [30] is useful tool to administrate the weight. The normalized INN values (NINNV) are conducted:

$$NINNV_{ij}=\frac{\frac{WAV\left(\left[NWTL_{ij},NWTR_{ij}\right],\left[NWIL_{ij},NWIR_{ij}\right],\left[NWFL_{ij},NWFR_{ij}\right]\right)}{WSV\left(\left[NWTL_{ij},NWTR_{ij}\right],\left[NWIL_{ij},NWIR_{ij}\right],\left[NWFL_{ij},NWFR_{ij}\right]\right)}}{\sum_{i=1}^{m}\left(\frac{WAV\left(\left[NWTL_{ij},NWTR_{ij}\right],\left[NWIL_{ij},NWIR_{ij}\right],\left[NWFL_{ij},NWFR_{ij}\right]\right)}{WSV\left(\left[NWTL_{ij},NWTR_{ij}\right],\left[NWIL_{ij},NWIR_{ij}\right],\left[NWFL_{ij},NWFR_{ij}\right]\right)}\right)}, \tag{13}$$

The uncertain fuzzy Shannon entropy (UFSE) is conducted:

$$UFSE_j=-\frac{1}{\ln m}\sum_{i=1}^{m}NINNV_{ij}\ \ln NINNV_{ij} \tag{14}$$

and $NINNDM_{ij}\ln NINNDM_{ij}=0$ if $NINNDM_{ij}=0$.

Then, the weight information is conducted:

$$s\omega_j=\frac{1-UFSE_j}{\sum_{j=1}^{n}\left(1-UFSE_j\right)} \tag{15}$$

3.3. INN-ExpTODIM-TOPSIS approach for MAGDM

INN-ExpTODIM-TOPSIS approach is addressed for MAGDM.

(1) Address the relative weight numbers:

$$rs\omega_j=s\omega_j\Big/\max_j s\omega_j, \tag{16}$$

(2) The INN uncertain dominance degree (INNUDD) of SA_i over SA_t for SG_j is addressed:

$$INNUDD_j\left(WA_i,WA_t\right)=\begin{cases}\dfrac{rsw_j\times\left(1-10^{-\rho INNHD\left(NWR_{ij},NWR_{tj}\right)}\right)}{\sum_{j=1}^{n}rsw_j} & if\ WSV\left(NWR_{ij}\right)>WSV\left(NWR_{tj}\right)\\ 0 & if\ WSV\left(NWR_{ij}\right)=WSV\left(NWR_{tj}\right)\\ -\dfrac{1}{\pi}\dfrac{\sum_{j=1}^{n}rsw_j\times\left(1-10^{-\rho INNHD\left(NWR_{ij},NWR_{tj}\right)}\right)}{rsw_j} & if\ WSV\left(NWR_{ij}\right)<WSV\left(NWR_{tj}\right)\end{cases} \tag{17}$$

where ρ is conducted from Tversky and Kahneman [31] and $\pi\in[1,5]$ [32].

The $INNUDD_j\left(WA_i\right)\left(j=1,2,3,\cdots,n\right)$ for WG_j is addressed:

$$INNUDD_j\left(WA_i\right)=\left[INNUDD_j\left(WA_1,WA_t\right)\right]_{m\times m}$$

$$=\begin{array}{c} \\ WA_1 \\ WA_2 \\ \vdots \\ WA_m \end{array}\begin{array}{c} \begin{array}{cccc} WA_1 & WA_2 & \cdots & WA_m \end{array} \\ \begin{bmatrix} 0 & INNUDD_j\left(WA_1,WA_2\right) & \cdots & INNUDD_j\left(WA_1,WA_m\right) \\ INNUDD_j\left(WA_2,WA_1\right) & 0 & \cdots & INNUDD_j\left(WA_2,WA_m\right) \\ \vdots & \vdots & \cdots & \vdots \\ INNUDD_j\left(WA_m,WA_1\right) & INNUDDD_j\left(WA_m,WA_2\right) & \cdots & 0 \end{bmatrix} \end{array}$$

(3) Address the overall INNUDD of WA_i over other alternatives for WG_j:

$$INNUDD_j\left(WA_i\right)=\sum_{t=1}^{m}INNUDD_j\left(WA_i,WA_t\right) \tag{18}$$

The overall INNDDD is conducted:

$$INNDDD=\left(INNDDD_{ij}\right)_{m\times n}$$

$$=\begin{bmatrix} & WG_1 & WG_2 & \cdots & WG_n \\ WA_1 & \sum_{t=1}^{m}INNDDD_1\left(WA_1,WA_t\right) & \sum_{t=1}^{m}INNDDD_2\left(WA_1,WA_t\right) & \cdots & \sum_{t=1}^{m}INNDDD_n\left(WA_1,WA_t\right) \\ WA_2 & \sum_{t=1}^{m}INNDDD_1\left(WA_2,WA_t\right) & \sum_{t=1}^{m}INNDDD_2\left(WA_2,WA_t\right) & \cdots & \sum_{t=1}^{m}INNDDD_n\left(WA_2,WA_t\right) \\ \vdots & \vdots & \vdots & \vdots & \vdots \\ WA_m & \sum_{t=1}^{m}INNDDD_1\left(WA_m,WA_t\right) & \sum_{t=1}^{m}INNDDD_2\left(WA_m,WA_t\right) & \cdots & \sum_{t=1}^{m}INNDDD_n\left(WA_m,WA_t\right) \end{bmatrix} \tag{19}$$

(4) Address the INNPIDS (INN positive ideal decision solution) and INNNIDS (INN negative ideal decision solution):

$$INNPIDS=\left(INNPIDS_1,INNPIDS_1,\cdots,INNPIDS_n\right) \tag{20}$$

$$INNNIDS=\left(INNNIDS_1,INNNIDS_1,\cdots,INNNIDS_n\right) \tag{21}$$

$$INNPIDS_j=\max_{j=1}^{n}INNDDD_{ij}, \tag{22-a}$$

$$INNNIDS_j=\min_{j=1}^{n}INNDDD_{ij} \tag{22-b}$$

(5) Address the INNED (INN Euclidean distance) and INNCC (INN closeness coefficient) from INNPIDS. The choice has the maximum INNCC is optimal choice.

$$INNED\left(WA_i,INNPIDS\right)=\sqrt{\sum_{j=1}^{n}\left(INNDDD_{ij}-INNPIDS_j\right)^2} \tag{23}$$

$$INNED\left(WA_i,INNNIDS\right)=\sqrt{\sum_{j=1}^{n}\left(INNDDD_{ij}-INNNIDS_j\right)^2} \tag{24}$$

$$INNCC\left(WA_i,INNPIDS\right)=\frac{INNED\left(WA_i,INNNIDS\right)}{INNED\left(WA_i,INNPIDS\right)+INNED\left(WA_i,INNPIDS\right)} \tag{25}$$

4. Quantitative Illustration and Comparative Evaluation

4.1. Quantitative Illustration

Teaching quality evaluation encompasses a comprehensive assessment of teachers' proficiency, instructional methods, attitudes, and other relevant aspects. Presently, numerous universities employ diverse approaches to evaluate theteaching quality of their faculty. Typically, such evaluations are conducted at the end of this semester, with students providing online feedback on one or more courses taught by the teacher. Alternatively, teaching supervisors or specialized departments within the institution may observe a teacher's classroom at specific intervals during the semester to gain insights into their teaching practices. To enhance the quality of CET further, continuous improvements in the curriculum system are necessary. The foundation of this curriculum system lies in the evaluation system for CET. Hence, there is a need to develop a comprehensive, practical, scientific, and objective quality evaluation management system. A teaching philosophy underlying this system revolves around prioritizing students as the primary beneficiaries, teachers as the driving force, industry feedback, and industry-specific guidance. Therefore, while constructing a quality evaluation system for CET, the following two aspects should be considered: (1) Student-Centered Approach: Regardless of changes in teaching formats, students always play a central role in the teaching process. In college English courses, students actively participate in the learning experience. (2) Teacher Leadership: Teachers have a pivotal role in college English courses, indicating the course's practicality. Consequently, teachers can adapt teaching techniques and approaches based on the classroom dynamics and instructional context. By integrating students' theoretical knowledge and practical abilities while enhancing their overall development, teachers have relatively more freedom in guiding the college English curriculum. If all evaluation systems solely focus on assessing teachers' classroom performance, the inherent communicative and interactive functions of the English language may be compromised. Therefore, this requires teachers to provide support and encouragement to students in English learning outside of the classroom. The implementation of practical activities mainly relies on extracurricular activities, which in turn can promote the understanding of classroom theory. Therefore, the teaching quality evaluation must adhere to the unity of theory and practice. With continuous maturity and development of internet application technology, big data is also increasingly being applied to teaching evaluation. At the end of each semester or during a certain period of study, the school will organize students to evaluate teachers on the official account or App at the specified time. If the evaluation cannot be completed on time, students will not be able to check their grades and perform other operations. This characteristic of short time and heavy tasks can make students perfunctory in evaluating, resulting in teachers receiving feedback that has no reference value. This kind of "evaluating teaching for the sake of evaluation" ultimately only allows evaluation to become a formality. The quality evaluation of CET mainly targets the teaching of teachers. However, there are relatively few experts specialized in this field in China. Therefore, the current evaluation system

mainly introduces Western theories and research techniques, but in reality, it does not fully meet the requirements of China's CET quality evaluation system. The lack of empirical research has led to the lack of guarantee for the scientificity of various evaluation indicators and the effectiveness of results, let alone the goal of improving the evaluation system in the long run. The CET quality evaluation is MAGDM. Five potential local-applied undergraduate colleges and universities are chosen in lightw ith four attributes: WG_1 is CET contents; WG_2 is CET costs; ③WG_3 is CET satisfaction degree; ④WG_4 is c CET means. The CET costs (WG_2) is a cost attribute. Five possible local-applied undergraduate colleges and universities are evaluated with linguistic scales through four criteria under three experts $WE^t\left(t=1,2,3\right)$ with expert's weight $\left(0.32,0.40,0.28\right)$. Table 1 is referenced from Ref.[33].

Table 1. Linguistic scales and INNs

Linguistic scales	INNs
Exceedingly Terrible-WET	([0.05,0.2], [0.6,0.7], [0.75,0.9])
Very Terrible-WVT	([0.15,0.3], [0.5,0.6], [0.65,0.8])
Terrible-WT	([0.25,0.4], [0.4,0.5], [0.55,0.7])
Medium-WM	([0.4,0.6], [0.1,0.2], [0.4,0.6])
Well-WW	([0.45,0.6], [0.3,0.4], [0.25,0.5])
Very Well-WVW	([0.65,0.8], [0.5,0.6], [0.15,0.3])
Exceedingly Well-WEW	([0.75,0.9], [0.6,0.7], [0.05,0.2])

The INN-ExpTODIM-TOPSIS approach is utilized to address the CET quality evaluation.

Step 1. Address the INN-matrix $WR^t=\left[WR_{ij}^t\right]_{5\times4}=\left(\left[WTL_{ij}^t,WTR_{ij}^t\right],\left[WIL_{ij}^t,WIR_{ij}^t\right],\left[WFL_{ij}^t,WFR_{ij}^t\right]\right)_{5\times4}$ (See Table 2-4).

Table 2. Evaluation data from WE_1

	WG_1(benefit)	*WG_2(cost)*	*WG_3(benefit)*	*WG_4(benefit)*
WA_1	WVT	WM	WW	WVW
WA_2	WM	WVT	WVT	WVW
WA_3	WM	WT	WVW	WVT
WA_4	WVT	WVW	WW	WM
WA_5	WVW	WW	WM	WT

Table 3. Evaluation data from SE_2

	WG_1(benefit)	*WG_2(cost)*	*WG_3(benefit)*	*WG_4(benefit)*
WA_1	WM	WT	WVW	WW

WA_2	WW	WVW	WVT	WT
WA_3	WM	WW	WT	WM
WA_4	WW	WVW	WT	WM
WA_5	WVT	WVT	WM	WW

Table 4. Evaluation data from SE_3

	WG_1(benefit)	WG_2(cost)	WG_3(benefit)	WG_4(benefit)
WA_1	WVW	WT	WVT	WM
WA_2	WM	WVW	WT	WW
WA_3	WVT	WM	WVW	WW
WA_4	WVT	WVW	WM	WW
WA_5	WVW	WW	WM	WT

Then according to INNWA technique, the $WR = \left[WR_{ij} \right]_{5\times4}$ is addressed (Table 5).

Table 5. The $WR = \left[WR_{ij} \right]_{5\times4}$

	WG_1	WG_2
WA_1	([0.71, 0.79], [0.34, 0.47], [0.45, 0.57])	([0.52, 0.63], [0.48, 0.53], [0.47, 0.58])
WA_2	([0.75, 0.82], [0.59, 0.69], [0.51, 0.53])	([0.64, 0.67], [0.54, 0.56], [0.42, 0.46])
WA_3	([0.76, 0.86], [0.46, 0.54], [0.48, 0.54])	([0.69, 0.72], [0.42, 0.49], [0.39, 0.42])
WA_4	([0.85, 0.94], [0.57, 0.69], [0.48, 0.62])	([0.76, 0.83], [0.38, 0.43], [0.43, 0.49])
WA_5	([0.63, 0.76], [0.59, 0.68], [0.39, 0.51])	([0.64, 0.71], [0.49, 0.52], [0.38, 0.43])
	WG_3	WG_4
WA_1	([0.66, 0.79], [0.54, 0.65], [0.46, 0.57])	([0.64, 0.79], [0.46, 0.57], [0.59, 0.68])
WA_2	([0.57, 0.64], [0.45, 0.54], [0.37, 0.56])	([0.63, 0.74], [0.37, 0.45], [0.56, 0.75])
WA_3	([0.63, 0.69], [0.47, 0.62], [0.48, 0.53])	([0.58, 0.79], [0.43, 0.54], [0.59, 0.64])
WA_4	([0.84, 0.92], [0.28, 0.35], [0.47, 0.54])	([0.78, 0.85], [0.35, 0.43], [0.56, 0.67])
WA_5	([0.63, 0.75], [0.45, 0.57], [0.45, 0.68])	([0.56, 0.64], [0.37, 0.49], [0.48, 0.59])

Step 2. Normalize the $WR = \left[WR_{ij} \right]_{5\times4}$ into $NWR = \left[NWR_{ij} \right]_{5\times4}$ (See Table 6).

Table 6. The $NWR = \left[NWR_{ij} \right]_{5\times4}$

	WG_1	WG_2
WA_1	([0.71, 0.79], [0.34, 0.47], [0.45, 0.57])	([0.47, 0.58], [0.48, 0.53], [0.52, 0.63])
WA_2	([0.75, 0.82], [0.59, 0.69], [0.51, 0.53])	([0.42, 0.46], [0.54, 0.56], [0.64, 0.67])
WA_3	([0.76, 0.86], [0.46, 0.54], [0.48, 0.54])	([0.39, 0.42], [0.42, 0.49], [0.69, 0.72])
WA_4	([0.85, 0.94], [0.57, 0.69], [0.48, 0.62])	([0.43, 0.49], [0.38, 0.43], [0.76, 0.83])
WA_5	([0.63, 0.76], [0.59, 0.68], [0.39, 0.51])	([0.38, 0.43], [0.49, 0.52], [0.64, 0.71])
	WG_3	WG_4
WA_1	([0.66, 0.79], [0.54, 0.65], [0.46, 0.57])	([0.64, 0.79], [0.46, 0.57], [0.59, 0.68])

WA_2	([0.57, 0.64], [0.45, 0.54], [0.37, 0.56])	([0.63, 0.74], [0.37, 0.45], [0.56, 0.75])
WA_3	([0.63, 0.69], [0.47, 0.62], [0.48, 0.53])	([0.58, 0.79], [0.43, 0.54], [0.59, 0.64])
WA_4	([0.84, 0.92], [0.28, 0.35], [0.47, 0.54])	([0.78, 0.85], [0.35, 0.43], [0.56, 0.67])
WA_5	([0.63, 0.75], [0.45, 0.57], [0.45, 0.68])	([0.56, 0.64], [0.37, 0.49], [0.48, 0.59])

Step 3. Address the weight numbers:
$s\omega_1 = 0.2301, s\omega_2 = 0.3322, s\omega_3 = 0.2210, s\omega_4 = 0.2167$.

Step 4. Address the relative weight numbers: $rs\omega = \{0.6927, 1.0000, 0.6653, 0.6523\}$.

Step 5. Address the $INNDDD = \left(NNDDD_{ij} \right)_{5\times4}$ (Table 7):

Table 7. The $INNDDD = \left(NNDDD_{ij} \right)_{5\times4}$

	WG_1	WG_2	WG_3	WG_4
WA_1	-0.5280	-0.0445	-1.1254	-1.1279
WA_2	0.2919	-0.5574	0.7572	-0.6242
WA_3	-1.6551	0.4547	0.7824	-1.8264
WA_4	-0.2255	0.8891	-0.4405	1.0735
WA_5	0.2473	0.1913	-1.0016	-2.0332

Step 6. Address the INNPIDS and INNNIDS (Table 8).

Table 8. The INNPIDS and INNNIDS

	WG_1	WG_2	WG_3	WG_4
INNPIDS	0.2919	0.8891	0.7824	1.0735
INNNIDS	-1.6551	-0.5574	-1.1254	-2.0332

Step 7. Address the $\left(INNDDD_{ij} - INNPIDS_j \right)^2$ and $\left(INNDDD_{ij} - INNNIDS_j \right)^2$ (See table 9-10).

Table 9. The $\left(INNDDD_{ij} - INNPIDS_j \right)^2$

	WG_1	WG_2	WG_3	WG_4
WA_1	0.6722	0.8717	3.6396	4.8462
WA_2	0.0000	2.0924	0.0006	2.8823
WA_3	3.7910	0.1887	0.0000	8.4096
WA_4	0.2677	0.0000	1.4954	0.0000
WA_5	0.0020	0.4870	3.1828	9.6513

Table 10. The $\left(INNDDD_{ij} - INNNIDS_j \right)^2$

	WG_1	WG_2	WG_3	WG_4

WA_1	1.2705	0.2631	0.0000	0.8195
WA_2	3.7910	0.0000	3.5441	1.9851
WA_3	0.0000	1.0244	3.6396	0.0427
WA_4	2.0440	2.0924	0.4691	9.6513
WA_5	3.6192	0.5605	0.0153	0.0000

Step 8. Address the $INNED(WA_i, INNPIDS)$, $INNED(WA_i, INNNIDS)$ and $INNCC(WA_i, INNPIDS)$ (See table 11-12).

Table 11. The $INNED(SA_i, INNPIS)$ and $INNED(SA_i, INNNIS)$

	$INNED(SA_i, INNPIS)$	$INNED(SA_i, INNNIS)$
WA_1	3.1670	1.5340
WA_2	2.2305	3.0529
WA_3	3.5198	2.1695
WA_4	1.3278	3.7758
WA_5	3.6501	2.0482

Table 12. The $INNCC(WA_i, INNPIDS)$ and order

	$INNCC(WA_i, INNPIDS)$	*Order*
WA_1	0.3263	5
WA_2	0.5778	2
WA_3	0.3813	3
WA_4	0.7398	1
WA_5	0.3594	4

Thus, the best local-applied undergraduate college and university is WA_4.

4.2. Comparative Evaluation

The INN-ExpTODIM-TOPSIS approach is compared with the INNWA approach [28] and INNWG approach [28], INN-VIKOR approach [34], INN-CODAS approach [35], INN-EDAS approach [33] and INN-TODIM approach [36]. The final comparative results are administrated in Table 13 and Figure 1.

Table 13. Order of different approaches

Approaches	*Order*
INNWA technique [28]	$WA_4 > WA_2 > WA_3 > WA_5 > WA_1$
INNWG technique[28]	$WA_4 > WA_2 > WA_5 > WA_3 > WA_1$
INN-VIKOR technique [34]	$WA_4 > WA_2 > WA_3 > WA_5 > WA_1$
INN-CODAS technique[35]	$WA_4 > WA_2 > WA_3 > WA_5 > WA_1$

INN-EDAS technique [33]	$WA_4 > WA_2 > WA_3 > WA_5 > WA_1$
INN-TODIM approach [36]	$WA_4 > WA_2 > WA_3 > WA_5 > WA_1$
INN-ExpTODIM-TOPSIS approach	$WA_4 > WA_2 > WA_3 > WA_5 > WA_1$

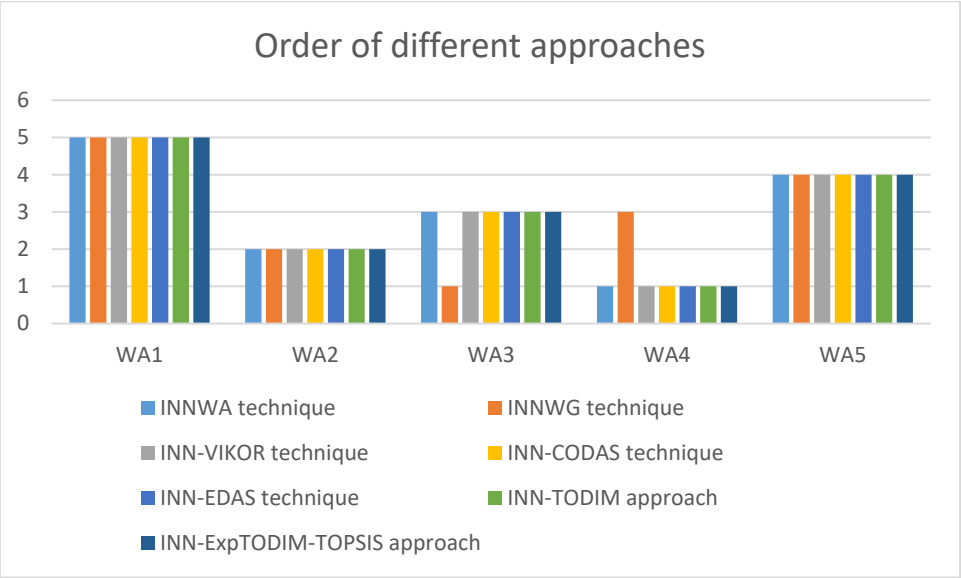

Figure 1. Order of different approaches

From the above analysis, it could be administrated that the seven approaches have the same optimal local-applied undergraduate college and university and worst local-applied undergraduate college and university and the six techniques' order is the same. This verifies INN-ExpTODIM-TOPSIS technique is reasonable.

5. Conclusion

In the era of globalization, English has become a more important language. With the increasing demand for talent in society, the concepts and techniques of teaching have also been reformed. In the CET, it is necessary to cultivate students as applied talents, not only to enable them to master certain theoretical knowledge, but also to have corresponding practical abilities, to promote their comprehensive development and become useful talents in society. Therefore, this article has certain practical significance in studying the quality evaluation system construction of CET. The CET quality evaluation is classical MAGDM. Currently, the ExpTODIM and TOPSIS approaches are utilized to administrate the MAGDM. In the evaluation of CET quality, the utilization of INSs serves as a valuable tool for capturing uncertain data. In this study, we introduce the INN-ExpTODIM-TOPSIS approach, specifically designed to address MAGDM challenges with INSs. To validate the effectiveness of the INN-ExpTODIM-TOPSIS approach, a numerical study focusing on CET quality evaluation is conducted. Moving forward, our future work aims to explore the integration of various techniques, paving the way for the development of scientific decision-making approaches in the field.

References

[1] J.M. Kyrkjebo, Teaching quality improvement in the classroom and clinic: Getting it wrong and getting it right, Journal of Nursing Education, 45 (2006) 109-116.

[2] I. Noben, J.F. Deinum, W.H.A. Hofman, Quality of teaching in higher education: Reviewing teaching behaviour through classroom observations, International Journal for Academic Development, 27 (2022) 31-44.

[3] S.Y. Wang, L.M. Cheng, D.Y. Liu, J.Q. Qin, G.H. Hu, Classroom video image emotion analysis method for online teaching quality evaluation, Traitement Du Signal, 39 (2022) 1767-1774.

[4] Z.X. Xie, Z.Q. Su, Evaluation of college english classroom teaching quality dependent on triangular fuzzy number, International Journal of Electrical Engineering Education, (2021) 15.

[5] Y.F. Feng, An evaluation method of pe classroom teaching quality in colleges and universities based on grey system theory, Journal of Intelligent & Fuzzy Systems, 38 (2020) 6911-6915.

[6] Y.B. Zhang, Ieee, Application of blended teaching into the course of comprehensive english, in: 11th International Conference on Educational and Information Technology (ICEIT), Ieee, Sichuan Normal Univ, Chengdu, PEOPLES R CHINA, 2022, pp. 80-84.

[7] S. Broumi, S. Mohanaselvi, T. Witczak, M. Talea, A. Bakali, F. Smarandache, Complex fermatean neutrosophic graph and application to decision making, Decision Making: Applications in Management and Engineering, 6 (2023) 474-501.

[8] H. Li, Enhanced group decision-making framework for financial performance evaluation of high-tech enterprises under interval neutrosophic environment, Journal of Intelligent & Fuzzy Systems, 46 (2024) 6249-6263.

[9] H.Y. Zhang, G.W. Wei, Location selection of electric vehicles charging stations by using the spherical fuzzy cpt-cocoso and d-critic method, Computational & Applied Mathematics, 42 (2023) 35.

[10] H. Sun, Z. Yang, Q. Cai, G.W. Wei, Z.W. Mo, An extended exp-todim method for multiple attribute decision making based on the z-wasserstein distance, Expert Systems with Applications, 214 (2023) 14.

[11] M. Simoes-Marques, R.A. Ribeiro, A. Gameiro-Marques, A fuzzy decision support system for equipment repair under battle conditions, Fuzzy Sets and Systems, 115 (2000) 141-157.

[12] R.P. Mohanty, R. Agarwal, A.K. Choudhury, M.K. Tiwari, A fuzzy anp-based approach to r&d project selection: A case study, International Journal of Production Research, 43 (2005) 5199-5216.

[13] A.I. Ölçer, A.Y. Odabasi, A new fuzzy multiple attributive group decision making methodology and its application to propulsion/manoeuvring system selection problem, European Journal of Operational Research, 166 (2005) 93-114.

[14] L.A. Zadeh, Fuzzy sets, Information and Control, 8 (1965) 338-353.

[15] H. Garg, Linguistic pythagorean fuzzy sets and its applications in multiattribute decision-making process, International Journal of Intelligent Systems, 33 (2018) 1234-1263.

[16] Y.H. Huang, G.W. Wei, Todim method for pythagorean 2-tuple linguistic multiple attribute decision making, Journal of Intelligent & Fuzzy Systems, 35 (2018) 901-915.

[17] J. Ding, Z.S. Xu, N. Zhao, An interactive approach to probabilistic hesitant fuzzy multi-attribute group decision making with incomplete weight information, Journal of Intelligent & Fuzzy Systems, 32 (2017) 2523-2536.

[18] J. Li, J.Q. Wang, Multi-criteria outranking methods with hesitant probabilistic fuzzy sets, Cognitive Computation, 9 (2017) 611-625.

[19] H.C. Liao, L.S. Jiang, Z.H. Xu, J.P. Xu, F. Herrera, A linear programming method for multiple criteria decision making with probabilistic linguistic information, Information Sciences, 415 (2017) 341-355.

[20] H. Wang, F. Smarandache, Y.Q. Zhang, R. Sunderraman, Interval neutrosophic sets and logic: Theory and applications in computing, Hexis: Phoenix, AZ, USA, (2005).

[21] J. Ye, Entropy measures of simplified neutrosophic sets and their decision-making approach with positive and negative arguments, Journal of Management Analytics, 8 (2021) 252-266.

[22] F. Al-Sharqi, A.G. Ahmad, A. Al-Quran, Fuzzy parameterized-interval complex neutrosophic soft sets and their applications under uncertainty, Journal of Intelligent & Fuzzy Systems, 44 (2023) 1453-1477.

[23] A.B. Leoneti, L.F. Autran Monteiro Gomes, A novel version of the todim method based on the exponential model of prospect theory: The exptodim method, European Journal of Operational Research, 295 (2021) 1042-1055.

[24] Y.-J. Lai, T.-Y. Liu, C.-L. Hwang, Topsis for modm, European Journal of Operational Research, 76 (1994) 486-500.

[25] H. Wang, F. Smarandache, Y.Q. Zhang, R. Sunderraman, Single valued neutrosophic sets, Multispace Multistruct, (2010) 410-413.

[26] J.J. Peng, J.Q. Wang, J. Wang, H.Y. Zhang, X.H. Chen, Simplified neutrosophic sets and their applications in multi-criteria group decision-making problems, International Journal of Systems Science, 47 (2016) 2342-2358.

[27] Y.H. Huang, G.W. Wei, C. Wei, Vikor method for interval neutrosophic multiple attribute group decision-making, Information, 8 (2017) 144.

[28] H.Y. Zhang, J.Q. Wang, X.H. Chen, Interval neutrosophic sets and their application in multicriteria decision making problems, Scientific World Journal, 2014 (2014) 645953.

[29] J. Ye, Similarity measures between interval neutrosophic sets and their applications in multicriteria decision-making, Journal of Intelligent & Fuzzy Systems, 26 (2014) 165-172.

[30] C.E. Shannon, A mathematical theory of communication, Bell System Technical Journal, 27 (1948) 379-423.

[31] A. Tversky, D. Kahneman, Prospect theory: An analysis of decision under risk, Econometrica, 47 (1979) 263-291.

[32] A.B. Leoneti, L. Gomes, A novel version of the todim method based on the exponential model of prospect theory: The exptodim method, European Journal of Operational Research, 295 (2021) 1042-1055.

[33] A. Karasan, C. Kahraman, A novel interval-valued neutrosophic edas method: Prioritization of the united nations national sustainable development goals, Soft Computing, 22 (2018)

4891-4906.

[34] R. Bausys, E.K. Zavadskas, Multicriteria decision making approach by vikor under interval neutrosophic set environment, Economic Computation and Economic Cybernetics Studies and Research, 49 (2015) 33-48.

[35] E. Bolturk, A. Karasan, Interval valued neutrosophic codas method for renewable energy selection, in: 13th International Conference on Fuzzy Logic and Intelligent Technologies in Nuclear Science (FLINS), World Scientific Publ Co Pte Ltd, Belfast, IRELAND, 2018, pp. 1026-1033.

[36] Y.R. Hong, D.S. Xu, K.L. Xiang, H. Qiao, X.X. Cui, H.X. Xian, Multi-attribute decision-making based on preference perspective with interval neutrosophic sets in venture capital, Mathematics, 7 (2019) 13.

Received: July 23, 2024. Accepted: Oct 22, 2024

NSS
Neutrosophic Sets and Systems, Vol. 76, 2025
University of New Mexico

Neutrosophic Set-Based PSNN-TOPSIS Framework for Multi-Attribute Decision Making: Applications in Evaluating the Quality of Environmental Art Design in Green Building Contexts

Yue Wang, Jiawei Zhao*
Art School, Qingdao Agricultural University, Qingdao, 266071, Shandong, China
*Corresponding author, e-mail: QDart@qau.edu.cn; https://orcid.org/0000-0002-2155-0242

Abstract: With the continuous advancement of urbanization and the continuous development of landscape design concepts, green landscape design under the green building system has become the main direction of future landscape design development, playing an important role in creating a beautiful, comfortable, and ecological modern urban landscape. In the future, it is necessary to further strengthen research on green landscape design, reflecting the relevant requirements of green building concepts in energy conservation, water conservation, land conservation, etc., so that urban landscape design can break away from noise and restlessness, and return to the essence of nature and ecology. The quality evaluation of environmental art design from the perspective of green buildings could be looked at as multiple-attribute decision-making (MADM). The TOPSIS technique is a useful technique to put up with the MADM. The probabilistic simplified Neutrosophic set (PSNSs) makes it easy to express uncertain information during the quality evaluation of environmental art design from the perspective of green buildings. In this study, the CRITIC technique is put forward to obtain the attribute weights, and the probabilistic simplified neutrosophic number TOPSIS (PSNN-TOPSIS) technique is put forward for MADM. Finally, a numerical example for quality evaluation of environmental art design from the perspective of green buildings is employed to verify the PSNN-TOPSIS technique with comparative analysis.

Keywords: Multiple-attributes decision-making (MADM); probabilistic simplified neutrosophic sets (PSNSs); TOPSIS technique; quality evaluation of environmental art design

1. Introduction

MADM is the decision-making process that prioritizes alternative solutions in line with existing decision information in a certain way[1, 2]. Its theory and models are widely used in

different fields such as venture capital decision-making, project evaluation, and industrial sector development evaluation [3]. In recent decades, MADM has been widely applied to engineering, the economy, technology, and the military. The quality evaluation of environmental art design from the perspective of green buildings is a MADM. Recently, the TOPSIS model [4, 5] was employed to put forward the MADM. Fuzzy sets were introduced by Zadeh [6] in 1965 as a concept to handle the uncertainties and ambiguities in the real world. Unlike traditional binary sets, fuzzy sets allow their elements to have partial membership in the set, represented by values between 0 and 1. In a fuzzy set, each element has a degree of membership to a specific set, enabling fuzzy set theory to more precisely express the various states between complete membership and non-membership. This theory is widely applied in fields such as fuzzy logic and artificial intelligence, leading to various extensions and applications of fuzzy sets **[7-10].** When addressing the evaluation issues in environmental art design, especially under the context of green buildings, the evaluation process often involves complex, multi-faceted decision-making that needs to consider multiple factors. Therefore, the method combining PSNSs [11] with the TOPSIS technique [4] offers significant advantages. **Firstly**, the incorporation of PSNSs [11] enables the decision model to effectively handle information with uncertainties and ambiguities. This type of set is particularly suited for expressing and managing criteria that are difficult to quantify or vague, such as aesthetic appeal of the environment or social impacts, which are subjective factors. They provide a mechanism that allows decision-makers to consider various possible scenarios and different levels of information certainty during the evaluation process. **Secondly**, the application of the TOPSIS method [4] provides a clear and intuitive framework by calculating the distances of each option from the ideal and negative solutions for ranking and selection. The intuitiveness and computational simplicity of this method make it highly suitable for multi-attribute decision analysis, especially when combined with PSNSs. TOPSIS can then more comprehensively consider and evaluate the influences of various environments and situations. **By combining these two techniques**, it is possible to greatly enhance the accuracy and reliability of decisions. The uncertainty handling capability provided by PSNSs allows TOPSIS to better reflect complex real-world conditions in practical applications, thereby offering more scientific and rational decision support. This method is not only applicable to evaluating highly uncertain and complex environmental art design projects but also flexibly meets various decision-making needs, enhancing decision adaptability and flexibility. **In summary**, by integrating PSNSs with TOPSIS, a powerful decision-making tool can be created. This not only improves the efficiency in handling complex environmental evaluation issues but also ensures more accurate and high-quality decisions in the fields of green building and urban planning. This combination provides a new perspective and method, helping decision-makers better understand and grasp key information when facing diverse and multi-level evaluation criteria, thus making more rational and sustainable decision choices.

Thus, the PSNSs [11] are employed as a technique for characterizing uncertain information during the quality evaluation of environmental art design from the perspective of green buildings. In this study, the CRITIC technique [12] is put forward to obtain the attribute weights under PSNSs and the PSNN-TOPSIS model is put forward to solve the MADM with PSNSs. Finally, a numerical study for quality evaluation of environmental art design from the perspective of green buildings is put forward to validate the PSNN-TOPSIS model. The main research motivations of this study are

constructed: (1) the TOPSIS model is extended to PSNSs; (2) CRITIC technique is put forward to obtain the attribute weights; (3) the PSNN-TOPSIS model is put forward to solve the MADM with PSNSs; (4) Finally, a numerical study for quality evaluation of environmental art design from the perspective of green buildings is put forward to validate the PSNN-TOPSIS technique with comparative analysis.

The overall structure is put forward: The PSNSs are conducted in Sect. 2. The PSNN-TOPSIS model is put forward MADM in Sect. 3. A numerical example of quality evaluation of environmental art design from the perspective of green buildings is employed to prove the PSN-TOPSIS technique in Sect. 4 with comparative analysis. Sect. 5 ends with a conclusion.

2. Literature Review

The concept of green building design emphasizes creating a healthy and comfortable living environment while achieving maximum resource conservation and environmental pollution control, and these requirements are closely related to the natural environment[13]. Therefore, in environmental art design based on green design concepts, designers must adhere to the principle of authenticity, respect the true laws of natural development, and carry out the comprehensive design of indoor and outdoor environments with the goal of natural protection, to achieve harmonious unity between the living environment and the natural environment. In addition, environmental art design has a significant impact on the surrounding environment of buildings[14]. Therefore, to fully implement the concept of green building design, designers also need to comprehensively consider various factors such as architectural style, local climate, customs, history, and culture. On the premise of ensuring that it will not cause too much impact on the surrounding environment, specific environmental art design can be carried out to achieve a true restoration of the surrounding environment of the building[15]. Modern environmental art design pays more attention to the overall artistic and aesthetic aspects of indoor and outdoor environments. Therefore, in actual design, designers often use unnecessary decorative materials in pursuit of better environmental visual effects. This not only causes serious resource waste but also seriously violates the concept of green building design[16]. Therefore, under the influence of the concept of green building design, environmental art design still needs to adhere to the principle of conservation, and apply renewable clean energy and recyclable materials as much as possible in the design process. At the same time, resource conservation is listed as the core design principle, striving to create the best living environment with minimal resource consumption[17, 18]. For example, in indoor environmental design, designers can use small green plants as decorations, which can purify the indoor air environment, bring residents a sense of closeness to nature, and also reduce energy consumption during the operation and use of the building, achieving better green environmental protection effects. Although the concept of green building design attaches great importance to environmental protection and energy conservation, environmental art design still serves people (residents). Only by meeting the needs of residents can environmental art design truly play its role[19]. Therefore, in environmental art design based on the concept of green building design, designers also need to adhere to the principle of comfort, prioritize meeting the living and living needs of residents, and comprehensively optimize the indoor and outdoor environment to improve the livability and comfort of the living environment. After meeting this premise, other design requirements such as

environmental protection, energy conservation, and visual aesthetics should be considered. Green buildings, as a new concept in the field of modern architecture, have significant differences in design concepts from traditional environmental art design concepts[20-22]. However, their pursuit of environmental protection and energy-saving effects is similar to the design ideas of many ancient buildings in China[23]. For example, in the northwest region, due to the dry climate, long sunshine hours, and large temperature differences, locals choose to use plateau terrain to dig cave dwellings for residential purposes, in order to achieve a warm winter and cool summer effect, while also effectively improving indoor air humidity; In Inner Mongolia and other regions, local nomadic ethnic groups have designed felt bags as residences based on climate characteristics such as strong winds and low temperatures. Therefore, in environmental art design, designers can also seek inspiration from traditional Chinese architecture and integrate the energy-saving and environmental protection design ideas of traditional architecture with modern architectural design concepts, so as to further improve the energy-saving and environmental protection of environmental art design[24]. For example, the popular covered earth buildings in foreign countries are modernized based on cave dwellings. In summary, the promotion of green buildings has had a significant impact on environmental art design[25]. In the future, environmental art design must fully implement the concept of green building design, adhere to principles such as conservation and comfort, and adopt appropriate design strategies in spatial layout, lighting systems, ventilation systems, etc., in order to fully meet people's needs for the living environment.

3. Preliminaries

Wang et al. [26] put forward the SVNSs

Definition 1 [26]. The SVNSs is put forward:

$$CC=\left\{\left(\theta,CT\left(\theta\right),CI\left(\theta\right),CF\left(\theta\right)\right)\middle|\theta\in\Theta\right\} \tag{1}$$

where $CT\left(\theta\right),CI\left(\theta\right),CF\left(\theta\right)$ is membership, indeterminacy-membership and falsity-membership, $CT\left(\theta\right),CI\left(\theta\right),CF\left(\theta\right)\in\left[0,1\right]$, $0\le CT\left(\theta\right)+CI\left(\theta\right)+CF\left(\theta\right)\le 3$.

Altun, Sahin and Guler [11] put forward the PSNSs.

Definition 2[11]. The PSNSs is put forward:

$$PC=\left\{\left(\begin{array}{l}\theta,CT\left(\theta\right)\left(PCT\left(\theta\right)\right),\\ CI\left(\theta\right)\left(PCI\left(\theta\right)\right),\\ CF\left(\theta\right)\left(PCF\left(\theta\right)\right)\end{array}\right)\middle|\theta\in\Theta\right\} \tag{2}$$

where $CT\left(\theta\right),CI\left(\theta\right),CF\left(\theta\right)$ is truth-membership, indeterminacy-membership and falsity-membership, $CT\left(\theta\right),CI\left(\theta\right),CF\left(\theta\right)\in\left[0,1\right]$, $0\le CT\left(\theta\right)+CI\left(\theta\right)+CF\left(\theta\right)\le 3$, $0\le PCT\left(\theta\right),PCI\left(\theta\right),PCF\left(\theta\right)\le 1$, the $PCT\left(\theta\right),PCI\left(\theta\right),PCF\left(\theta\right)$ is possibility values of $CT\left(\theta\right),CI\left(\theta\right),CF\left(\theta\right)$. The probabilistic simplified neutrosophic number (PSNN) is listed as $PC=\left(CT\left(PCT\right),CI\left(PCI\right),CF\left(PCF\right)\right)$.

Definition 3[11]. Let $PC_1=\left(CT_1\left(PCT_1\right),CI_1\left(PCI_1\right),CF_1\left(PCF_1\right)\right)$, $PC_2=\left(CT_2\left(PCT_2\right),CI_2\left(PCI_2\right),CF_2\left(PCF_2\right)\right)$, the basic operations are put forward:

$$(1)\ PC_1\oplus PC_2=\begin{pmatrix} CT_1+CT_2-CT_1\cdot CT_2\left(2!\dfrac{PCT_1\cdot PCT_2}{PCT_1+PCT_2}\right), \\ CI_1\cdot CI_2\left(2!\dfrac{PCI_1\cdot PCI_2}{PCI_1+PCI_2}\right),CF_1\cdot CF_2\left(2!\dfrac{PCF_1\cdot PCF_2}{PCF_1+PCF_2}\right)\end{pmatrix};$$

$$(2)\ PC_1\otimes PC_2=\begin{pmatrix} CT_1\cdot CT_2\left(2!\dfrac{PCT_1\cdot PCT_2}{PCT_1+PCT_2}\right), \\ CI_1+CI_2-CI_1\cdot CI_2\left(2!\dfrac{PCI_1\cdot PCI_2}{PCI_1+PCI_2}\right), \\ CF_1+CF_2-CF_1\cdot CF_2\left(2!\dfrac{PCF_1\cdot PCF_2}{PCF_1+PCF_2}\right)\end{pmatrix};$$

$$(3)\ \lambda PC=\left(1-\left(1-CT\right)^{\lambda}\left(PCT\right),\left(CI\right)^{\lambda}\left(PCI\right),\left(CF\right)^{\lambda}\left(PCF\right)\right),\lambda>0;$$

$$(4)\ \left(PC\right)^{\lambda}=\left(\left(CT\right)^{\lambda}\left(PCT\right),1-\left(1-CI\right)^{\lambda}\left(PCI\right),1-\left(1-CF\right)^{\lambda}\left(PCF\right)\right),\lambda>0.$$

Definition 4[11]. Let $PC_1=\left(CT_1\left(PCT_1\right),CI_1\left(PCI_1\right),CF_1\left(PCF_1\right)\right)$ and $PC_2=\left(CT_2\left(PCT_2\right),CI_2\left(PCI_2\right),CF_2\left(PCF_2\right)\right)$, the probabilistic simplified Neutrosophic number Logarithmic distance (PSNNLD) between $PC_1=\left(CT_1\left(PCT_1\right),CI_1\left(PCI_1\right),CF_1\left(PCF_1\right)\right)$ and $PC_2=\left(CT_2\left(PCT_2\right),CI_2\left(PCI_2\right),CF_2\left(PCF_2\right)\right)$ is constructed:

$$PSNNLD\left(PC_1, PC_2\right)$$

$$= \frac{1}{3}\left(\begin{array}{l} \left(CT_1 \times PCT_1\right)\log\dfrac{\left(CT_1 \times PCT_1\right)}{\dfrac{\left(CT_1 \times PCT_1\right)+\left(CT_2 \times PCT_2\right)}{2}} \\ +\left(CT_2 \times PCT_2\right)\log\dfrac{\left(CT_2 \times PCT_2\right)}{\dfrac{\left(CT_1 \times PCT_1\right)+\left(CT_2 \times PCT_2\right)}{2}} \\ +\left(CI_1 \times PCI_1\right)\log\dfrac{\left(CI_1 \times PCI_1\right)}{\dfrac{\left(CI_1 \times PCI_1\right)+\left(CI_2 \times PCI_2\right)}{2}} \\ +\left(CI_2 \times PCI_2\right)\log\dfrac{\left(CI_2 \times PCI_2\right)}{\dfrac{\left(CI_1 \times PCI_1\right)+\left(CI_2 \times PCI_2\right)}{2}} \\ +\left(CF_1 \times PCF_1\right)\log\dfrac{\left(CF_1 \times PCF_1\right)}{\dfrac{\left(CF_1 \times PCF_1\right)+\left(CF_2 \times PCF_2\right)}{2}} \\ +\left(CF_2 \times PCF_2\right)\log\dfrac{2\left(CF_2 \times PCF_2\right)}{\dfrac{\left(CF_1 \times PCF_1\right)+\left(CF_2 \times PCF_2\right)}{2}} \end{array}\right) \tag{3}$$

4. Methodology

The PSNN-TOPSIS is put forward for MADM under PSNSs with completely unknown weight. Let $CA=\left\{CA_1, CA_2, \cdots, CA_m\right\}$ be alternatives, and $CG=\left\{CG_1, CG_2, \cdots, CG_n\right\}$ be attributes with weight cw, where $cw_j \in [0,1]$ $\sum_{j=1}^{n} cw_j = 1$. Suppose that the decision information is depicted with PSNNs $CR=\left(CR_{ij}\right)_{m\times n}=\left(\begin{array}{l} CT_{ij}\left(PCT_{ij}\right), \\ CI_{ij}\left(PCI_{ij}\right), CF_{ij}\left(PCF_{ij}\right) \end{array}\right)_{m\times n}$. Then, PSNN-TOPSIS technique is put forward MADM with the CRITIC technique (See Figure 1).

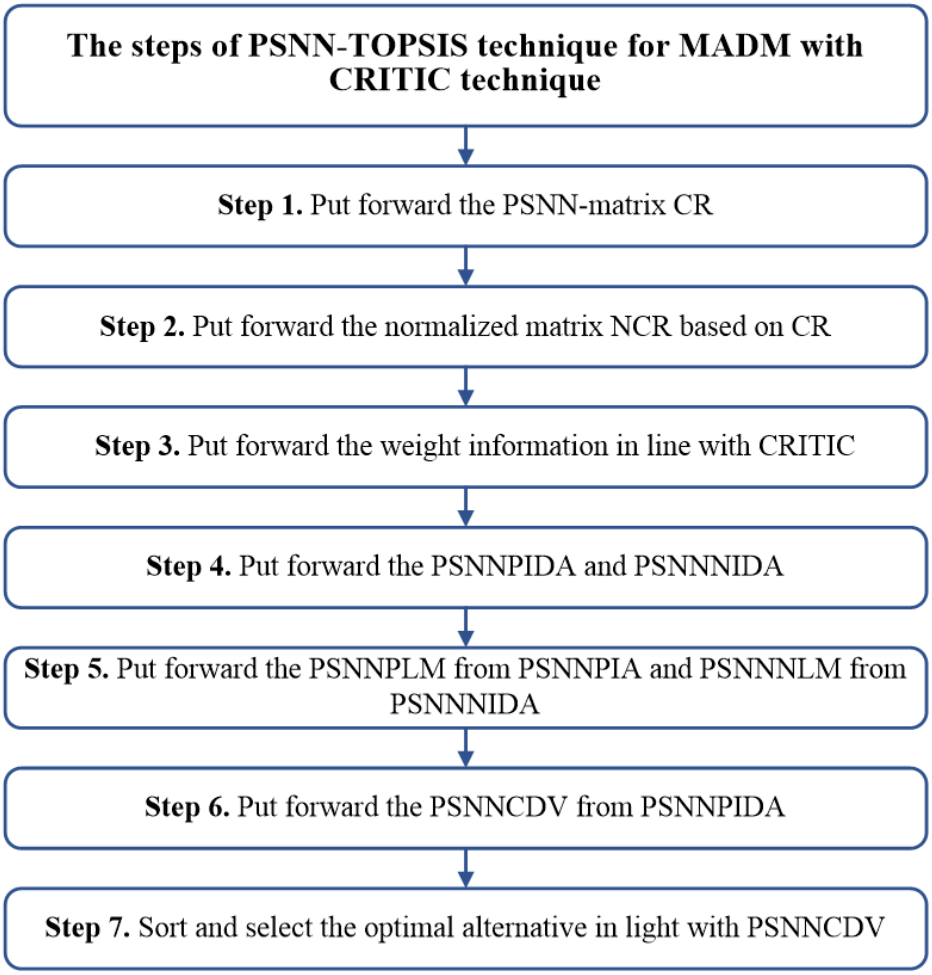

Figure 1. PSNN-TOPSIS framework for MADM with CRITIC technique

Step 1. Put forward PSNN-matrix $CR=\left(CR_{ij}\right)_{m\times n}=\begin{pmatrix} CT_{ij}\left(PCT_{ij}\right), \\ CI_{ij}\left(PCI_{ij}\right),CF_{ij}\left(PCF_{ij}\right) \end{pmatrix}_{m\times n}$.

Step 2. Put forward the normalized matrix $NCR=\left[NCR_{ij}\right]_{m\times n}$ based on $CR=\left(CR_{ij}\right)_{m\times n}$.

$$NCR_{ij}=\left(CT_{ij}^{N}\left(PCT_{ij}^{N}\right),CI_{ij}^{N}\left(PCI_{ij}^{N}\right),CF_{ij}^{N}\left(PCF_{ij}^{N}\right)\right)$$
$$=\begin{cases}\left(CT_{ij}\left(PCT_{ij}\right),CI_{ij}\left(PCI_{ij}\right),CF_{ij}\left(PCF_{ij}\right)\right), & CG_j \text{ is the benefit attributes}\\ \left(CF_{ij}\left(PCF_{ij}\right),1-CI_{ij}\left(1-PCI_{ij}\right),CT_{ij}\left(PCT_{ij}\right)\right), & CG_j \text{ is the cost attributes}\end{cases} \quad (4)$$

Step 3. Put forward the weight information in line with CRITIC.

The CRITIC technique [27] is utilized to put forward the weight information. The compute steps of CRITIC technique are designed[28].

(1) Depending on PSNN-matrix $NCR = \left[NCR_{ij} \right]_{m\times n}$, $NCR_{ij} = \left(CT_{ij}^{N}\left(PCT_{ij}^{N} \right), CI_{ij}^{N}\left(PCI_{ij}^{N} \right), CF_{ij}^{N}\left(PCF_{ij}^{N} \right) \right)$, the PSNN correlation coefficient (PSNNCC) for attributes is put forward.

$$PSNNCC_{jt} = \frac{\sum_{i=1}^{m}\left(SV\left(NCR_{ij} \right) - SV\left(NCR_{j} \right) \right)\left(SV\left(NCR_{it} \right) - SV\left(NCR_{t} \right) \right)}{\sqrt{\sum_{i=1}^{m}\left(SV\left(NCR_{ij} \right) - SV\left(NCR_{j} \right) \right)^{2}} \sqrt{\sum_{i=1}^{m}\left(SV\left(NCR_{it} \right) - SV\left(NCR_{t} \right) \right)^{2}}},$$

$$j,t = 1,2,\ldots,n, \quad (5)$$

where

$$SV\left(NCR_{j} \right) = \frac{1}{m}\sum_{i=1}^{m} SV\left(NCR_{ij} \right) = \frac{CT_{ij}^{N}\cdot PCT_{ij}^{N} + CI_{ij}^{N}\cdot PCI_{ij}^{N} + CF_{ij}^{N}\cdot PCF_{ij}^{N}}{3m}$$

and

$$SV\left(NCR_{it} \right) = \frac{1}{m}\sum_{i=1}^{m} SV\left(NCR_{it} \right) = \frac{CT_{it}^{N}\cdot PCT_{it}^{N} + CI_{it}^{N}\cdot PCI_{it}^{N} + CF_{it}^{N}\cdot PCF_{it}^{N}}{3m}.$$

(2) Put forward PSNN standard deviation (PSNNSD) for attributes.

$$PSNNSD_{j} = \sqrt{\frac{1}{m-1}\sum_{i=1}^{m}\left(SV\left(NCR_{ij} \right) - SV\left(NCR_{j} \right) \right)^{2}} \quad (6)$$

where $SV\left(NCR_{j} \right) = \frac{1}{m}\sum_{i=1}^{m} SV\left(NCR_{ij} \right)$.

(3) Put forward the weight information.

$$cw_{j} = \frac{PSNNSD_{j}\sum_{t=1}^{n}\left(1 - PSNNCC_{jt} \right)}{\sum_{j=1}^{n}\left(PSNNSD_{j}\sum_{t=1}^{n}\left(1 - PSNNCC_{jt} \right) \right)} \quad (7)$$

where $cw_{j} \in \left[0,1 \right]$ and $\sum_{j=1}^{n} cw_{j} = 1$.

Step 4. Put forward the PSNN positive ideal decision alternative (PSNNPIDA) and PSNN negative ideal decision alternative (PSNNNIDA) [28]:

$$PSNNPIDA = \left\{ PSNNPIDA_{j} \right\},\ j = 1,2,\ldots,n. \quad (8)$$

$$PSNNNIDA = \left\{ PSNNNIDA_{j} \right\},\ j = 1,2,\ldots,n. \quad (9)$$

$$PSNNPIDA_j = \begin{pmatrix} CT_j^{+N}\left(PCT_j^{+N}\right), \\ CI_j^{+N}\left(PCI_j^{+N}\right), CF_j^{+N}\left(PCF_j^{+N}\right) \end{pmatrix}, \qquad j = 1, 2, \ldots, n. \quad (10)$$

$$PSNNNIDA_j = \begin{pmatrix} CT_j^{-N}\left(PCT_j^{-N}\right), \\ CI_j^{-N}\left(PCI_j^{-N}\right), VC_j^{-N}\left(PCF_j^{-N}\right) \end{pmatrix}, \qquad j = 1, 2, \ldots, n. \quad (11)$$

$$\begin{aligned} &SV\left(CT_j^{+N}\left(PCT_j^{+N}\right), CI_j^{+N}\left(PCI_j^{+N}\right), CF_j^{+N}\left(PCF_j^{+N}\right)\right) \\ &= \max_i SV\left(CT_{ij}^{N}\left(PCT_{ij}^{N}\right), CI_{ij}^{N}\left(PCI_{ij}^{N}\right), CF_{ij}^{N}\left(PCF_{ij}^{N}\right)\right) \end{aligned} \quad (12)$$

$$\begin{aligned} &SV\left(CT_j^{-N}\left(PCT_j^{-N}\right), CI_j^{-N}\left(PCI_j^{-N}\right), VC_j^{-N}\left(PCF_j^{-N}\right)\right) \\ &= \min_i SV\left(CT_{ij}^{N}\left(PCT_{ij}^{N}\right), CI_{ij}^{N}\left(PCI_{ij}^{N}\right), CF_{ij}^{N}\left(PCF_{ij}^{N}\right)\right) \end{aligned} \quad (13)$$

where

$$\begin{aligned} &SV\left(CT_j^{+N}\left(PCT_j^{+N}\right), CI_j^{+N}\left(PCI_j^{+N}\right), CF_j^{+N}\left(PCF_j^{+N}\right)\right) \\ &= \frac{CT_j^{+N} \cdot PCT_j^{+N} + CI_j^{+N} \cdot PCI_j^{+N} + CF_j^{+N} \cdot PCF_j^{+N}}{3} \end{aligned} \quad (14)$$

$$\begin{aligned} &SV\left(CT_j^{-N}\left(PCT_j^{-N}\right), CI_j^{-N}\left(PCI_j^{-N}\right), VC_j^{-N}\left(PCF_j^{-N}\right)\right) \\ &= \frac{CT_j^{-N} \cdot PCT_j^{-N} + CI_j^{-N} \cdot PCI_j^{-N} + CF_j^{-N} \cdot PCF_j^{-N}}{3} \end{aligned} \quad (15)$$

$$\begin{aligned} &SV\left(CT_{ij}^{N}\left(PCT_{ij}^{N}\right), CI_{ij}^{N}\left(PCI_{ij}^{N}\right), CF_{ij}^{N}\left(PCF_{ij}^{N}\right)\right) \\ &= \frac{CT_{ij}^{N} \cdot PCT_{ij}^{N} + CI_{ij}^{N} \cdot PCI_{ij}^{N} + CF_{ij}^{N} \cdot PCF_{ij}^{N}}{3} \end{aligned} \quad (16)$$

Step 5. Put forward the PSNN positive Logarithmic distance (PSNNPLM) from PSNNPIA and PSNN negative Logarithmic distance (PSNNNLM) from PSNNNIDA:

$$PSNNPLM\left(CA_i, PSNNPIDA\right)=\sum_{j=1}^{n} cw_j\left(PSNNLD\left(CA_i, PSNNPIDA_j\right)\right)$$

$$=\frac{1}{3}\sum_{j=1}^{n} cw_j\left(\begin{array}{l}\left(CT_{ij}^{N}\times PCT_{ij}^{N}\right)\log\dfrac{\left(CT_{ij}^{N}\times PCT_{ij}^{N}\right)}{\dfrac{\left(CT_{ij}^{N}\times PCT_{ij}^{N}\right)+\left(CT_{j}^{+N}\times PCT_{j}^{+N}\right)}{2}}\\ +\left(CT_{j}^{+N}\times PCT_{j}^{+N}\right)\log\dfrac{\left(CT_{j}^{+N}\times PCT_{j}^{+N}\right)}{\dfrac{\left(CT_{ij}^{N}\times PCT_{ij}^{N}\right)+\left(CT_{j}^{+N}\times PCT_{j}^{+N}\right)}{2}}\\ \left(CI_{ij}^{N}\times PCI_{ij}^{N}\right)\log\dfrac{\left(CI_{ij}^{N}\times PCI_{ij}^{N}\right)}{\dfrac{\left(CI_{ij}^{N}\times PCI_{ij}^{N}\right)+\left(CI_{j}^{+N}\times PCI_{j}^{+N}\right)}{2}}\\ +\left(CI_{j}^{+N}\times PCI_{j}^{+N}\right)\log\dfrac{\left(CI_{j}^{+N}\times PCI_{j}^{+N}\right)}{\dfrac{\left(CI_{ij}^{N}\times PCI_{ij}^{N}\right)+\left(CI_{j}^{+N}\times PCI_{j}^{+N}\right)}{2}}\\ \left(CF_{ij}^{N}\times PCF_{ij}^{N}\right)\log\dfrac{\left(CF_{ij}^{N}\times PCF_{ij}^{N}\right)}{\dfrac{\left(CF_{ij}^{N}\times PCF_{ij}^{N}\right)+\left(CF_{j}^{+N}\times PCF_{j}^{+N}\right)}{2}}\\ +\left(CF_{j}^{+N}\times PCF_{j}^{+N}\right)\log\dfrac{\left(CF_{j}^{+N}\times PCF_{j}^{+N}\right)}{\dfrac{\left(CF_{ij}^{N}\times PCF_{ij}^{N}\right)+\left(CF_{j}^{+N}\times PCF_{j}^{+N}\right)}{2}}\end{array}\right) \tag{17}$$

$$PSNNNLM\left(CA_i, PSNNNIDA\right)=\sum_{j=1}^{n} cw_j\left(PSNNLD\left(CA_i, PSNNNIDA_j\right)\right)$$

$$=\frac{1}{3}\sum_{j=1}^{n} cw_j\left(\begin{array}{l}\left(CT_{ij}^{N}\times PCT_{ij}^{N}\right)\log\dfrac{\left(CT_{ij}^{N}\times PCT_{ij}^{N}\right)}{\dfrac{\left(CT_{ij}^{N}\times PCT_{ij}^{N}\right)+\left(CT_{j}^{-N}\times PCT_{j}^{-N}\right)}{2}}\\ +\left(CT_{j}^{-N}\times PCT_{j}^{-N}\right)\log\dfrac{\left(CT_{j}^{-N}\times PCT_{j}^{-N}\right)}{\dfrac{\left(CT_{ij}^{N}\times PCT_{ij}^{N}\right)+\left(CT_{j}^{-N}\times PCT_{j}^{-N}\right)}{2}}\\ \left(CI_{ij}^{N}\times PCI_{ij}^{N}\right)\log\dfrac{\left(CI_{ij}^{N}\times PCI_{ij}^{N}\right)}{\dfrac{\left(CI_{ij}^{N}\times PCI_{ij}^{N}\right)+\left(CI_{j}^{-N}\times PCI_{j}^{-N}\right)}{2}}\\ +\left(CI_{j}^{-N}\times PCI_{j}^{-N}\right)\log\dfrac{\left(CI_{j}^{-N}\times PCI_{j}^{-N}\right)}{\dfrac{\left(CI_{ij}^{N}\times PCI_{ij}^{N}\right)+\left(CI_{j}^{-N}\times PCI_{j}^{-N}\right)}{2}}\\ \left(CF_{ij}^{N}\times PCF_{ij}^{N}\right)\log\dfrac{\left(CF_{ij}^{N}\times PCF_{ij}^{N}\right)}{\dfrac{\left(CF_{ij}^{N}\times PCF_{ij}^{N}\right)+\left(CF_{j}^{-N}\times PCF_{j}^{-N}\right)}{2}}\\ +\left(CF_{j}^{-N}\times PCF_{j}^{-N}\right)\log\dfrac{\left(CF_{j}^{-N}\times PCF_{j}^{-N}\right)}{\dfrac{\left(CF_{ij}^{N}\times PCF_{ij}^{N}\right)+\left(CF_{j}^{-N}\times PCF_{j}^{-N}\right)}{2}}\end{array}\right) \tag{18}$$

Step 6. Put forward the PSNN close degree values (PSNNCDV) from PSNNPIDA.

$$PSNNCDV\left(CA_i, PSNNPIDA\right)$$

$$=\frac{PSNNPLM\left(CA_i, PSNNNIDA\right)}{\left(\begin{array}{l}PSNNPLM\left(CA_i, PSNNNIDA\right)\\ +PSNNPLM\left(CA_i, PSNNPIDA\right)\end{array}\right)}$$

$$=\frac{\sum_{j=1}^{n} cw_j\left(PSNNLD\left(CA_i, PSNNNIDA_j\right)\right)}{\left(\begin{array}{l}\sum_{j=1}^{n} cw_j\left(PSNNLD\left(CA_i, PSNNNIDA_j\right)\right)\\ +\sum_{j=1}^{n} cw_j\left(PSNNLD\left(CA_i, PSNNPIDA_j\right)\right)\end{array}\right)} \tag{19}$$

Step 7. In light with $PSNNCDV\left(CA_i, PSNNPIDA\right)$. The larger $PSNNCDV\left(CA_i, PSNNPIDA\right)$, the better alternative is.

5. Data Analysis and Results

5.1. Data Analysis

Although environmental art design has high requirements for the materials, texture, and color of building decoration materials, with the continuous development of technology, various green building decoration materials have become more and more common, and the application of green building decoration materials in environmental art design has also become more widespread. From the perspective of energy-saving and environmental protection effects, the current application of green building materials in environmental art design can be mainly divided into two categories. One type is to use new building materials to achieve better environmental and energy-saving effects, such as double-layer insulated glass, heat absorbing louvers, photovoltaic panels, etc. These materials themselves do not have outstanding energy-saving and environmental protection characteristics, but through reasonable use in building decoration and decoration design, they can greatly save energy consumption and environmental pollution in buildings. Another type is to combine nanomaterials with traditional building materials to improve material performance and enable materials to have industrial production characteristics. This can not only avoid material waste, but also enhance the technological sense of the indoor and outdoor environment of the building, thereby enhancing the ornamental value of the living environment. In environmental art design, if designers can flexibly apply these two types of green materials, the overall environment of the building will be more in line with the requirements of green buildings. In China's building materials market, there are many green building materials that can solve many problems and contribute to the development of environmental green design concepts. The characteristic of green materials is to reduce energy consumption and minimize the impact on the natural ecological environment. And among material recyclers, green materials are very environmentally friendly, which traditional materials do not have. In environmental green design, the use of green materials fully meets the requirements of environmental design. The application of green materials in environmental design ensures people's health without considering the pollution caused by materials to the environment. Therefore, when conducting environmental art design, we must try to choose green materials as much as possible, which is also a way to achieve the green concept. In today's rapidly developing economy, energy is an extremely important issue. Currently, China's industry is developing rapidly, and energy is also being consumed rapidly. People's production and living environment, as well as the natural environment, have been severely damaged, resulting in less and less energy. To solve the problem of energy consumption, it is necessary to save energy as much as possible and improve energy utilization efficiency. Energy conservation can be achieved from various aspects, such as temperature control, light utilization, water resource recycling, and sound insulation. Doors and windows have a significant impact on indoor temperature control. When designing, designers should pay attention to the material of doors and windows, so as to minimize energy consumption in the environment and maintain the most comfortable temperature. The utilization of water resources is also something we need to consider. China's per capita water resources are very low, so improving the utilization rate of water resources is extremely important. When designing, designers must consider the recycling of wastewater and the collection of rainwater to minimize water waste. In summary. In environmental art design, the application of

green design concepts is very important. Its reasonable application brings us a healthy, comfortable, and suitable living environment space. Currently, this aspect is still in the development stage in China. We must increase our research and practice efforts to create a beautiful and healthy living environment for ourselves. The quality evaluation of environmental art design from the perspective of green buildings is MADM. In this work, the PSNN-TOPSIS is put forward quality evaluation of environmental art design from the perspective of green buildings. Five environmental art design schemes from the perspective of green buildings $CA_i\left(i=1,2,3,4,5\right)$ are assessed with four attributes: ①VG_1 is sustainable sites of environmental art design schemes from the perspective of green buildings; ②VG_2 is materials and resources of environmental art design schemes from the perspective of green buildings; ③VG_3 is indoor environmental quality of environmental art design schemes from the perspective of green buildings; ④VG_4 is design comfort of environmental art design schemes from the perspective of green buildings. Then, the PSNN-TOPSIS put forward a quality evaluation of environmental art design from the perspective of green buildings with PSNSs.

Step 1. Put forward the decision matrix with PSNSs. The evaluation result is shown in **Table 1.**

Table 1. The PSNN information

Alternative	CG_1	CG_2
CA_1	{0.37(0.5),0.42(0.2),0.65(0.3)}	{0.83(0.3),0.74(0.3),0.25(0.4)}
CA_2	{0.48(0.4),0.27(0.5),0.54(0.1)}	{0.16(0.2),0.76(0.1),0.42(0.7)}
CA_3	{0.47(0.2),0.52(0.7),0.62(0.1)}5	{0.65(0.4),0.23(0.2),0.51(0.4)}
CA_4	{0.69(0.3),0.86(0.3),0.27(0.4)}	{0.32(0.3),0.84(0.4),0.34(0.3)}
CA_5	{0.43(0.1),0.54(0.6),0.89(0.3)}	{0.39(0.4),0.58(0.1),0.63(0.5)}

Alternative	CG_3	CG_4
CA_1	{0.71(0.4),0.46(0.5),0.49(0.1)}	{0.24(0.3),0.30(0.4),0.52(0.3)}
CA_2	{0.52(0.5),0.23(0.3),0.57(0.2)}	{0.31(0.2),0.52(0.3),0.27(0.5)}
CA_3	{0.28(0.6),0.56(0.2),0.31(0.2)}	{0.48(0.3),0.89(0.6),0.48(0.1)}
CA_4	{0.46(0.7),0.49(0.2),0.18(0.1)}	{0.79(0.3),0.32(0.2),0.18(0.5)}
CA_5	{0.21(0.6),0.38(0.1),0.62(0.3)}	{0.27(0.8),0.46(0.1),0.64(0.1)}

Step 2. Put forward the normalized matrix $NCR=\left[NCR_{ij}\right]_{5\times4}$. Because these attributes are benefit, thus, $NCR=\left[NCR_{ij}\right]_{5\times4}$ is same to $CR=\left[CR_{ij}\right]_{5\times4}$.

Table 2. The normalized PSNN-matrix through PSNNs

Alternative	CG_1	CG_2
CA_1	{0.37(0.5),0.42(0.2),0.65(0.3)}	{0.83(0.3),0.74(0.3),0.25(0.4)}
CA_2	{0.48(0.4),0.27(0.5),0.54(0.1)}	{0.16(0.2),0.76(0.1),0.42(0.7)}
CA_3	{0.47(0.2),0.52(0.7),0.62(0.1)}5	{0.65(0.4),0.23(0.2),0.51(0.4)}
CA_4	{0.69(0.3),0.86(0.3),0.27(0.4)}	{0.32(0.3),0.84(0.4),0.34(0.3)}
CA_5	{0.43(0.1),0.54(0.6),0.89(0.3)}	{0.39(0.4),0.58(0.1),0.63(0.5)}

Alternative	CG_3	CG_4
CA_1	{0.71(0.4),0.46(0.5),0.49(0.1)}	{0.24(0.3),0.30(0.4),0.52(0.3)}
CA_2	{0.52(0.5),0.23(0.3),0.57(0.2)}	{0.31(0.2),0.52(0.3),0.27(0.5)}
CA_3	{0.28(0.6),0.56(0.2),0.31(0.2)}	{0.48(0.3),0.89(0.6),0.48(0.1)}
CA_4	{0.46(0.7),0.49(0.2),0.18(0.1)}	{0.79(0.3),0.32(0.2),0.18(0.5)}
CA_5	{0.21(0.6),0.38(0.1),0.62(0.3)}	{0.27(0.8),0.46(0.1),0.64(0.1)}

Step 3. Put forward the weight information with CRITIC (See Table 3).

Table 3. The attributes weight values

	CG_1	CG_2	CG_3	CG_4
weight	0.1833	0.3410	0.2778	0.2079

Step 4. Put forward the PSNNPIDA and PSNNNIDA (See Table 4).

Table 4. The PSNNPIDA and PSNNNIDA

	CG_1	CG_2
PSNNPIDA	{0.69(0.3),0.86(0.3),0.27(0.4)}	{0.83(0.3),0.74(0.3),0.25(0.4)}
PSNNNIDA	{0.37(0.5),0.42(0.2),0.65(0.3)}	{0.16(0.2),0.76(0.1),0.42(0.7)}
	CG_3	CG_4
PSNNPIDA	{0.71(0.4),0.46(0.5),0.49(0.1)}	{0.79(0.3),0.32(0.2),0.18(0.5)}

PSNNNIDA	{0.21(0.6),0.38(0.1),0.62(0.3)}	{0.24(0.3),0.30(0.4),0.52(0.3)}

Step 5. Put forward the PSNNPLM from PSNNPIDA and PSNNNLM from PSNNNIDA (See Table 5):

Table 5. The $PSNNPLM\left(CA_i, PSNNPIDA\right)$ and $PSNNPLM\left(CA_i, PSNNNIDA\right)$

	$PSNNPLM\left(CA_i, PSNNPIDA\right)$	$PSNNPLM\left(CA_i, PSNNNIDA\right)$
CA_1	0.4587	0.5592
CA_2	0.5833	0.6454
CA_3	0.8097	0.6444
CA_4	0.8103	0.6176
CA_5	0.4856	0.6253

Step 6. Put forward the PSNNCDV from PSNNPIDA.

Table 6. The PSNNCDV from PSNNPIDA

Techniques	PSNNCDV
CA_1	0.5494
CA_2	0.5253
CA_3	0.4432
CA_4	0.4325
CA_5	0.5629

Step 7. In light of PSNNCDV, the order is $CA_5 > CA_1 > CA_2 > CA_3 > CA_5$ and CA_5 is optimal for community home-based elderly care services centers (See Table 7).

Table 7. The order

Techniques	Order

VA_1	2
VA_2	3
VA_3	4
VA_4	5
VA_5	1

5.2. Comparative analysis

The PSNN-TOPSIS is compared with PSNNWA and PSNNWG techniques [11], PSNN-GRA technique[28], and PNN-PROMETHEE technique [11]. The results are constructed in Table 8.

Table 8. Order for different techniques

Techniques	Order	The optimal choice
PSNNWA technique [11]	$CA_5 > CA_1 > CA_2 > CA_3 > CA_5$	CA_5
PSNNWG technique [11]	$CA_5 > CA_1 > CA_3 > CA_2 > CA_5$	CA_5
PSNN-GRA technique[28]	$CA_5 > CA_1 > CA_2 > CA_3 > CA_5$	CA_5
PSNN-PROMETHEE[11]	$CA_5 > CA_1 > CA_2 > CA_3 > CA_5$	CA_5
PSNN-TOPSIS method	$CA_5 > CA_1 > CA_2 > CA_3 > CA_5$	CA_5

In light with WS coefficients [29, 30], the WS coefficient between PSNNWA technique and PSNNWG technique [11], PSNN-GRA technique[28], PNN-PROMETHEE model [11] and PSNN-TOPSIS model is 1.0000, 0.8169, 1.0000, 1.0000, respectively. Thus, From Table 8, it is obvious that order of these models is slightly different, but these models have same best community home-based elderly care services center and worst community home-based elderly care services center. This verifies the PSN-TOPSIS technique is reasonable and effective.

6. Conclusions

Environmental art design mainly refers to the use of scientific and reasonable methods for environmental design and development in a certain environment. In the process of environmental art design, it is necessary to consider factors such as layout, architecture, sculpture, and the cost, materials, and environmental carrying capacity of various public facilities. Combined with various influencing factors, it is necessary to plan the environment reasonably and scientifically. Not only does it need to be aesthetically pleasing, but it is also necessary to fully consider various factors in planning and design, and design environmental art according to the ecological concept of harmonious coexistence of nature. In environmental art design, the concept of green design emerged around the 1980s, mainly focusing on issues related to the environment, pollution, and energy. Its main goal is to perfectly integrate the environment and art, and integrate green concepts into environmental art, maximizing the performance of the environment, linking environmental protection, social development, and harmonious human survival, eliminating the contradictions between the three, and making our human lives in an environmentally friendly and green environment. From the current situation, the direction of environmental art and design development is the green concept. The quality evaluation of environmental art design from the perspective of green buildings could be looked at as the MADM. In this study, the CRITIC technique [12] is put forward to obtain the attribute weights under PSNSs, and the PSNN-TOPSIS model is put forward to solve the MADM with PSNSs. Finally, a numerical study for quality evaluation of environmental art design from the perspective of green buildings is put forward to validate the PSNN-TOPSIS model. The main

research motivations of this study are constructed: (1) the TOPSIS model is extended to PSNSs; (2) CRITIC technique is put forward to obtain the attribute weights; (3) the PSNN-TOPSIS model is put forward to solve the MADM with PSNSs; (4) Finally, a numerical study for quality evaluation of environmental art design from the perspective of green buildings is put forward to validate the PSNN-TOPSIS technique with comparative analysis. In future research directions, (1) the application of the constructed techniques under PSNSs shall be discussed through other decision techniques [31-36] and more and more other uncertain environments [31-39]; (2) It is a worthwhile research topic to apply prospect theory to MAGDM in the 2TLNNs environment[40-43].

Acknowledgment

The work was supported by the Ministry of Education Industry-University Cooperation Collaborative Education Project 2020, the Annual research topic of the Qingdao Double Hundred Research Project 2021, and Qingdao Social Science Planning Invention Project, 2022.

Reference

[1] D. Pamucar, A.E. Torkayesh, S. Biswas, Supplier selection in healthcare supply chain management during the covid-19 pandemic: A novel fuzzy rough decision-making approach, Annals of Operations Research, 328 (2023) 977-1019.

[2] D. Pamucar, G. Duran-Romero, M. Yazdani, A.M. Lopez, A decision analysis model for smart mobility system development under circular economy approach, Socio-Economic Planning Sciences, 86 (2023) 24.

[3] J. Ye, B.Z. Sun, X.L. Chu, J.M. Zhan, J.X. Cai, Valued outranking relation-based heterogeneous multi-decision multigranulation probabilistic rough set and its use in medical decision-making, Expert Systems with Applications, 228 (2023) 18.

[4] Y.-J. Lai, T.-Y. Liu, C.-L. Hwang, Topsis for modm, European Journal of Operational Research, 76 (1994) 486-500.

[5] G. Sun, M.X. Wang, X.P. Li, W. Huang, Distance measure and intuitionistic fuzzy topsis method based on the centroid coordinate representation, Journal of Intelligent & Fuzzy Systems, 44 (2023) 555-571.

[6] L.A. Zadeh, Fuzzy sets, Information and Control, 8 (1965) 338-353.

[7] C. Zhang, D. Li, X. Kang, D. Song, A.K. Sangaiah, S. Broumi, Neutrosophic fusion of rough set theory: An overview, Computers in Industry, 115 (2020) 103117.

[8] F. Smarandache, Neutrosophic probability, set, and logic, proquest information & learning, Ann Arbor, Michigan, USA, 105 (1998) 118-123.

[9] H. Wang, F. Smarandache, Y. Zhang, R. Sunderraman, Single-valued neutrosophic sets, Multispace and Multistructure, 4 (2010) 410-413.

[10] F. Smarandache, N-valued refined neutrosophic logic and its applications to physics, Progress in Physics, 4 (2013) 143-146.

[11] F. Altun, R. Sahin, C. Guler, Multi-criteria decision making approach based on promethee with probabilistic simplified neutrosophic sets, Soft Computing, 24 (2020) 4899-4915.

[12] D. Diakoulaki, G. Mavrotas, L. Papayannakis, Determining objective weight in multple criteria problems:The critic method, Computers & Operations Research, 22 (1995) 763-770.

[13] H.K. Lee, K.H. Cho, C. Lee, J. Cho, H. Yi, Y. Seo, G.H. Cho, Y.N. Kwon, C. Lee, K.M. Paek, Science walden: Exploring the convergence of environmental technologies with design and art, Sustainability, 9 (2017) 17.

[14] H.R. Yang, Teaching reform and practice of the model design and production for environmental art design major, Agro Food Industry Hi-Tech, 28 (2017) 1196-1200.

[15] B. Li, The application of ocean environmental art design based on traditional dwelling decoration, Journal of Coastal Research, (2020) 930-934.

[16] Y.J. Long, Research on installation environmental art design based on multimedia technology, Basic & Clinical Pharmacology & Toxicology, 127 (2020) 76-76.

[17] H.B. Shi, D.H. Niu, Application research of virtual reality technology in ocean environmental art design, Journal of Coastal Research, (2020) 296-301.

[18] E.M. Thoma, T. Grönstedt, X. Zhao, Quantifying the environmental design trades for a state-of-the-art turbofan engine, Aerospace, 7 (2020) 16.

[19] G.D. Zhang, Application analysis of traditional cultural elements in the environmental art design of coastal cities, Journal of Coastal Research, (2020) 27-30.

[20] C. Li, A partial differential equation-based image restoration method in environmental art design, Advances in Mathematical Physics, 2021 (2021) 11.

[21] Y.X. Li, Intelligent environmental art design combining big data and artificial intelligence, Complexity, 2021 (2021) 11.

[22] B. Liang, X.X. Jia, Y. Lu, Application of adaptive image restoration algorithm based on sparsity of block structure in environmental art design, Complexity, 2021 (2021) 16.

[23] Y.K. Xu, Y. Guo, A.K. Jumani, S.F. Khatib, Application of ecological ideas in indoor environmental art design based on hybrid conformal prediction algorithm framework, Environmental Impact Assessment Review, 86 (2021) 11.

[24] Y.H. Wang, X.B. Hu, Three-dimensional virtual vr technology in environmental art design, International Journal of Communication Systems, 35 (2022) 18.

[25] L.Y. Wang, Y.P. He, Environmental landscape art design based on visual neural network model in rural construction, Ecological Chemistry and Engineering S-Chemia I Inzynieria Ekologiczna S, 30 (2023) 267-274.

[26] H. Wang, F. Smarandache, Y.Q. Zhang, R. Sunderraman, Single valued neutrosophic sets, Multispace Multistruct, (2010) 410-413.

[27] D. Diakoulaki, G. Mavrotas, L. Papayannakis, Determining objective weights in multiple criteria problems: The critic method, Computers & Operations Research, 22 (1995) 763-770.

[28] C. Liu, Gra method for probabilistic simplified neutrosophic madm and application to talent training quality evaluation of segmented education, Journal of Intelligent & Fuzzy Systems, 44 (2023) 8637-8647.

[29] W. Salabun, K. Urbaniak, A new coefficient of rankings similarity in decision-making problems, in: 20th Annual International Conference on Computational Science (ICCS), Springer International Publishing Ag, Amsterdam, NETHERLANDS, 2020, pp. 632-645.

[30] W. Sałabun, J. Wątróbski, A. Shekhovtsov, Are mcda methods benchmarkable? A comparative study of topsis, vikor, copras, and promethee ii methods, Symmetry, 12 (2020) 1549.

[31] S.D. Xian, J.H. Chai, H.L. Guo, Z linguistic-induced ordered weighted averaging operator for multiple attribute group decision-making, International Journal of Intelligent Systems, 34 (2019) 271-296.

[32] H. Garg, Neutrality operations-based pythagorean fuzzy aggregation operators and its applications to multiple attribute group decision-making process, Journal of Ambient Intelligence and Humanized

Computing, 11 (2020) 3021-3041.

[33] P.D. Liu, J.L. Liu, A multiple attribute group decision-making method based on the partitioned bonferroni mean of linguistic intuitionistic fuzzy numbers, Cognitive Computation, 12 (2020) 49-70.

[34] Z.F. Tao, X. Liu, H.Y. Chen, J.P. Liu, F. Guan, Linguistic z-number fuzzy soft sets and its application on multiple attribute group decision making problems, International Journal of Intelligent Systems, 35 (2020) 105-124.

[35] Y. Tian, X.J. Mi, Y.P. Ji, B.Y. Kang, Z(e)-numbers: A new extended z-numbers and its application on multiple attribute group decision making, Engineering Applications of Artificial Intelligence, 101 (2021) 11.

[36] H.Y. Zhang, G.W. Wei, X.D. Chen, Cpt-mabac method for spherical fuzzy multiple attribute group decision making and its application to green supplier selection, Journal of Intelligent & Fuzzy Systems, 41 (2021) 1009-1019.

[37] K.D. Yin, B.S. Yang, X. Jin, Grey fuzzy multiple attribute group decision-making methods based on interval grey triangular fuzzy numbers partitioned bonferroni mean, Symmetry-Basel, 12 (2020) 30.

[38] Y.J. Zhang, S.H. Hu, W. Zhou, Multiple attribute group decision making using j-divergence and evidential reasoning theory under intuitionistic fuzzy environment, Neural Computing & Applications, 32 (2020) 6311-6326.

[39] F. Lei, G.W. Wei, W.J. Shen, Y.F. Guo, Pdhl-edas method for multiple attribute group decision making and its application to 3d printer selection, Technological and Economic Development of Economy, 28 (2022) 179-200.

[40] A. Tversky, D. Kahneman, Prospect theory: An analysis of decision under risk, Econometrica, 47 (1979) 263-291.

[41] J.B. Engelmann, C.M. Capra, C. Noussair, G.S. Berns, Expert financial advice neurobiologically "offloads" financial decision-making under risk, Plos One, 4 (2009) 14.

[42] Z. Jiang, G. Wei, X. Chen, Edas method based on cumulative prospect theory for multiple attribute group decision-making under picture fuzzy environment, Journal of Intelligent & Fuzzy Systems, 42 (2022) 1723-1735.

[43] Y. Su, M.W. Zhao, C. Wei, X.D. Chen, Pt-todim method for probabilistic linguistic magdm and application to industrial control system security supplier selection, International Journal of Fuzzy Systems, 24 (2022) 202-215.

Received: July 24, 2024. Accepted: Oct 22, 2024

Neutrosophic Sets and Systems, Vol. 76, 2025
University of New Mexico

Neutrosophic Fuzzy Power Management (NFPM): Tackling Uncertainty in Energy Harvesting for Sensor Networks

Musallam M. AlZubi[1], Mohamed A. Mohamed[1], Hanan M. Amer[1] and A. A. Salama[2]

[1] Electronics and Communications Engineering Department, Faculty of Engineering, Mansoura University, Mansoura, Egypt, muss111124@gmail.com, mazim12@mans.edu.eg, hanan.amer@yahoo.com

[2] Department of Mathematics and Computer Science, Faculty of Science, Port Said University, Egypt, ahmed_salama_2000@sci.psu.edu.eg

Abstract: This paper presents a novel approach known as Neutrosophic Fuzzy Power Management (NFPM) aimed at addressing the critical challenge of uncertain energy availability in Energy Harvesting Sensor Networks (EHWSNs). The main objective of this research is to enhance the management of energy resources within these networks, which traditional fuzzy logic methods often fail to do, leading to power failures and reduced reliability. NFPM utilizes neutrosophic logic to effectively model uncertainty by representing the degrees of truth, indeterminacy, and falsity of both harvested and residual energy levels. Through a fuzzy inference system, NFPM dynamically allocates energy budgets for each time slot based on these neutrosophic sets, resulting in more adaptive and conservative energy distribution. The results are validated through numerical examples and extensive simulations, demonstrating NFPM's superiority over traditional fuzzy logic, with significant improvements such as a 25% reduction in power failures, 95% enhanced network connectivity, a 15% increase in data transmission success rates, and overall improvements in energy efficiency and robustness to fluctuations and noise. This research establishes NFPM as a promising solution to the uncertainties inherent in EHWSNs. Future research directions include exploring the integration of NFPM with machine learning algorithms for predictive energy management, assessing its scalability in larger networks, and examining its applicability in other domains requiring energy management under uncertainty.

Keywords: Neutrosophic Fuzzy Power Management; Energy Harvesting Sensor Networks; Uncertainty Management; Neutrosophic Logic

1. Introduction

Energy harvesting sensor networks (EHWSNs) have emerged as a compelling solution for sustainable and self-powered operations **[1]**. These networks harness energy from diverse environmental sources, such as solar, wind, and vibrations, to power their functionalities. However, the intermittent and uncertain nature of energy harvesting presents significant challenges in effectively managing these energy resources **[2]**. Traditional fuzzy logic approaches have been employed in EHWSN power management due to their ability to handle uncertainty and imprecision. These methods typically involve fuzzifying energy harvesting and consumption rates, along with other network parameters, and applying fuzzy logic rules to derive optimal energy allocation strategies **[3]**. Despite their advantages, traditional fuzzy logic frameworks have notable drawbacks **[4]**. They often fail to adequately capture the complexities of uncertainty associated with energy harvesting, leading to power failures, diminished network reliability, and inefficient energy utilization **[5]**. Specifically, these approaches struggle to account for the nuances of indeterminacy in energy levels, which can result in suboptimal decision-making during critical operational periods.

1.1 Motivation

Motivated by these limitations, we introduce a novel approach called Neutrosophic Fuzzy Power Management (NFPM). This framework employs neutrosophic logic, an extension of fuzzy logic that incorporates the concepts of truth, indeterminacy, and falsity. By doing so, NFPM can more effectively model and manage the uncertainty in energy availability, offering a more nuanced perspective on energy resource allocation. The superiority of NFPM over traditional methods lies in its ability to capture the full spectrum of uncertainty present in EHWSNs. With NFPM, we can represent energy levels not only as true or false but also as indeterminate states, which allows for more flexible and adaptive energy management strategies. Our approach demonstrates significant improvements in key performance indicators: a 25% reduction in power failures, 95% enhanced network connectivity, and a 15% increase in data transmission success rates, along with greater energy efficiency and robustness against fluctuations and noise.

1.2 Research Gap

Traditional fuzzy logic methods in Energy Harvesting Wireless Sensor Networks (EHWSNs) are inadequate in managing uncertain energy availability, often leading to power failures and reduced network reliability. There is a need for more effective techniques to model uncertainty and improve energy management in these networks.

1.3 Contribution

This study introduces a novel approach called Neutrosophic Fuzzy Power Management (NFPM) that leverages neutrosophic logic to model uncertainty in energy harvesting and residual energy levels. By using a fuzzy inference system to allocate energy budgets dynamically, NFPM significantly enhances network performance, reducing power failures by 25%, improving network connectivity by 95%, increasing data transmission success rates by 15%, and improving overall energy efficiency and robustness to fluctuations. The research establishes NFPM as a superior alternative to traditional fuzzy logic in managing uncertainty in EHWSNs.

1.4 Paper Organization

This paper is organized as follows: Section 2 presents the related work, Section 3 outlines the proposed methodology, Section 4 discusses the results and provides analysis, and Section 5 concludes the paper, highlighting future perspectives.

2. Related Work

Environmental preservation is increasingly urgent due to climate change and population growth. Researchers are exploring renewable energy solutions to reduce emissions and enhance quality of life amid rising population density. One effective solution is the implementation of Bus Rapid Transit (BRT) systems, which utilize dedicated lanes to deliver fast and efficient public transport. BRT features include elevated boarding platforms, prepayment systems to expedite boarding, and traffic signal prioritization to ensure smooth bus movement. This system combines many advantages of light rail or subway options while being more cost-effective and flexible, making it a popular choice worldwide for alleviating congestion. The paper presented by Elsayed **[6]**, analyze the BRT system's effectiveness in terms of user satisfaction. They employ the Approach for Preference, Performance, and Ranking Evaluation with Satisfaction Level (APPRESAL) method, which addresses the limitations of multi-criteria decision-making (MCDM) approaches in capturing user satisfaction. Additionally, they utilize type-2 neutrosophic numbers (T2NN) to account for the

ambiguity and uncertainty inherent in the collected data, enabling a more comprehensive evaluation of user experiences and the factors influencing them.

Advancements in wind turbine technology, including taller hubs and longer blades, have made them more efficient and cost-effective by reducing the energy production cost per unit. However, these larger structures are more visible in the landscape, raising concerns among communities about their environmental and economic impacts. This creates a conflict between the advantages of improved visibility and lower wind energy prices. Many multi-criteria decision-making (MCDM) applications emphasize the importance of wind turbine visibility, which is influenced by their distance from populated areas and coastal regions. Increased separation generally reduces visibility concerns, but this assumption can distort MCDM outcomes. The study presented by Abouhawwash et al. **[7]** employs an MCDM methodology to explore the relationships between various wind turbine criteria. Utilizing the DEMATEL method, we identify the weights of these criteria and how they interrelate. A total of 12 criteria are considered, and the DEMATEL method is integrated with single-valued neutrosophic sets (SVNS) to address uncertainties in the evaluation process. This approach provides a more accurate and practical framework for assessing wind turbine visibility and its implications for decision-making.

Smart city sustainability initiatives focus on creating urban environments that are environmentally, economically, and socially viable. Digital Twin (DT) technology, which creates accurate digital replicas of physical assets and systems, is pivotal in achieving these sustainability goals. This paper examines the development and application of DT technology within integrated regional energy systems in smart cities, highlighting its potential to optimize energy consumption, reduce costs, and enhance overall performance. The CloudIEPS platform serves as a practical example of how DT technology can optimize energy efficiency and minimize expenses. By integrating DT technology with Multi-Criteria Decision-Making (MCDM) methods, the paper proposes a robust approach to managing energy systems in smart cities. It identifies key factors for decision-making and introduces a method for assessing these criteria using Triangular Neutrosophic Sets (TNS), along with the MEthod based on Removal Effects of Criteria (MEREC) and the Multi-Attributive Ideal Real Comparative Analysis (MAIRCA) approach. These methods facilitate the evaluation and prioritization of multiple criteria in decision-making. A case study is conducted to validate the proposed methodology by Elsayed et al. **[8]** and perform sensitivity analysis on the results. The findings demonstrate that the methodology effectively addresses the uncertainties and complexities of smart city energy systems. The sensitivity analysis further confirms its stability and adaptability across various scenarios, making it a valuable resource for policymakers and stakeholders in the energy sector.

Sustainable smart cities leveraging Internet of Things (IoT) technology hold great potential for enhancing quality of life. However, widespread implementation of IoT solutions requires addressing critical issues such as data privacy, security, standardization, interoperability, scalability, and sustainability. The smart city concept is closely tied to sustainability through efforts to minimize environmental impacts, optimize energy resource management, and create innovative services for residents. The paper introduced by Abdel Aal **[9]** presents a neutrosophic framework to assess challenges in IoT-based smart sustainable cities, aiming to improve energy resource management and reduce ecological impacts. The framework incorporates nine criteria and five alternatives, employing the neutrosophic Weighted Product Method (WPM) to determine criteria weights and rank the identified challenges. Additionally, it utilizes single-valued neutrosophic sets to effectively manage uncertain data. The results demonstrate that this framework can adeptly handle uncertainties, yielding more effective assessments of challenges faced by smart sustainable cities based on IoT, ultimately contributing to better energy management and reduced environmental impacts. Energy harvesting sensor networks (EHWSNs) have gained significant

attention due to their potential to provide sustainable and self-powered operation. However, the intermittent and uncertain nature of energy harvesting poses a major challenge in managing the network's energy resources. In this section, we review some of the recent works in EHWSN power management.

The proposed research aims to develop a new energy management system using fuzzy logic and neutrosophic sets to tackle the challenges of energy harvesting in wireless sensor networks (WSNs). This system will optimize energy utilization and extend the network's lifespan by combining the concepts of truth values, uncertainty, and inconsistency from neutrosophic sets.

Traditional fuzzy logic approaches have been widely applied in Energy Harvesting Wireless Sensor Networks (EHWSNs) to manage power by handling uncertainty and imprecision. These methods typically fuzzify energy parameters like harvesting and consumption rates and use fuzzy rules to optimize energy allocation. Examples include power management schemes that consider energy availability, node activity, and communication needs to allocate energy efficiently. Probabilistic approaches, on the other hand, model the energy harvesting process as a stochastic process, using probabilistic techniques to optimize energy allocation based on factors such as variability in energy demand and supply, as well as node failure probability. These methods aim to improve network reliability and lifetime. Recently, neutrosophic logic has emerged as a more effective solution for addressing both uncertainty and indeterminacy in EHWSNs. Neutrosophic logic-based schemes represent degrees of truth, indeterminacy, and falsity, allowing for more precise energy allocation while managing uncertainties and indeterminacies better than traditional fuzzy or probabilistic approaches **[10–15]**. These methods consider energy availability, node activity, and communication demands, offering enhanced reliability and efficiency **[9,16,17]**. Neutrosophic logic approaches thus provide a promising alternative for EHWSN power management, addressing uncertainty more effectively than previous techniques. The proposed Neutrosophic Fuzzy Power Management (NFPM) scheme builds on these advances to manage uncertain energy availability more effectively, improving network reliability, efficiency, and sustainability **[18]**. In this work we reviewed a range of soft computing and fuzzy logic techniques relevant to enhancing wireless sensor networks (WSNs), particularly in managing uncertainties and optimizing energy. Gharghan et al. **[19]** explore wireless sensor networks in cycling applications, employing soft computing for localization. Khalifeh et al. **[20]** focus on fuzzy logic to address challenges in multi-robotic WSNs, emphasizing cooperative operations. Hamzah et al. **[21]** and Nayak & Devulapalli **[22]** contribute energy-efficient, fuzzy-logic-based clustering algorithms, crucial for extending network lifetimes. Loganathan & Arumugam **[23]** apply particle swarm optimization for energy-efficient clustering. These studies collectively inform the development of Neutrosophic Fuzzy Power Management (NFPM) by offering insights into fuzzy and neutrosophic techniques, uncertainty management, and energy optimization in WSNs.

3. The proposed Methodology

This section introduces the core concepts of NFPM, including the fundamentals of neutrosophic logic and its application in the design of the power management system.

3.1 Neutrosophic Logic Fundamentals

Neutrosophic logic, introduced by Florentin Smarandache, **[24]** extends traditional fuzzy logic by incorporating an additional truth-value: indeterminacy. Unlike traditional fuzzy sets, which represent degrees of truth (T) and falsity (F), neutrosophic sets also define an indeterminacy degree (I) **[25]**. This allows neutrosophic logic to more effectively handle situations where the information

about a proposition is partially or completely unknown **[26]**. A neutrosophic set A in a universe of discourse X is defined as: $A = \{(x, T(x), I(x), F(x)) \mid x \in X\}$, where:

- T(x) represents the degree of truth of element x belonging to the set A.
- I(x) represents the degree of indeterminacy of element x belonging to the set A.
- F(x) represents the degree of falsity of element x belonging to the set A.

All three degrees must satisfy the condition as shown in Equation (1).

$$0 \leq T(x) + I(x) + F(x) \leq 3 \quad (1)$$

Neutrosophic logic provides various operators and tools to perform arithmetic and logical operations on neutrosophic sets, enabling robust decision-making under uncertainty **[27]**. These examples demonstrate how neutrosophic logic can handle uncertainty and partial truth in various domains, enabling more informed decision-making under ambiguous conditions **[28]**.

Example 1: Weather Forecasting

- Define a neutrosophic set Rain to model the likelihood of rain:
  - Rain = {(Heavy, 0.3, 0.6, 0.1), (Moderate, 0.5, 0.4, 0.1), (Light, 0.2, 0.7, 0.1), (None, 0.1, 0.2, 0.7)}

Interpretation:

- 30% chance of heavy rain, 60% uncertainty, 10% chance of no heavy rain.
- 50% chance of moderate rain, 40% uncertainty, 10% chance of no moderate rain.

Example 2: Medical Diagnosis

- Define a neutrosophic set Disease to represent the possibility of a patient having a disease:
  - Disease = {(Present, 0.6, 0.3, 0.1), (Absent, 0.3, 0.5, 0.2)}

Interpretation:

- 60% belief the disease is present, 30% uncertainty, 10% belief it's absent.

Example 3: Product Quality Control

- Define a neutrosophic set Defective to assess the likelihood of a product being defective:
  - Defective = {(Yes, 0.2, 0.5, 0.3), (No, 0.7, 0.2, 0.1)}

Interpretation:

- 20% belief the product is defective, 50% uncertainty, 30% belief it's not.

Example 4: Decision-Making under Uncertainty

- Suppose you're deciding whether to invest in a company with uncertain future profits.
- Define a neutrosophic set Profitable to represent the likelihood of profitability:
    - Profitable = {(High, 0.5, 0.4, 0.1), (Moderate, 0.3, 0.5, 0.2), (Low, 0.2, 0.3, 0.5)}

Use neutrosophic logic operators to evaluate investment options based on Profitable and other relevant neutrosophic sets (e.g., Risky, Stable).

Example 5: Image Processing

- Define a neutrosophic set Edge to represent the degree to which a pixel belongs to an edge in an image:
    - Edge = {(Strong, 0.8, 0.1, 0.1), (Weak, 0.4, 0.5, 0.1), (None, 0.1, 0.3, 0.6)}

Use neutrosophic logic to enhance edge detection and segmentation.

3.2 NFPM Design

NFPM leverages neutrosophic logic to represent the uncertainties associated with harvested and residual energy levels in EHWSNs. Here is how it works:

3.3.1 Neutrosophic Fuzzy Sets:

- Harvested Energy: Represented by a neutrosophic set "HE" with membership degrees for T(HE), I(HE), and F(HE) based on the current and past harvested energy values.
- Residual Energy: Represented by a neutrosophic set "RE" with membership degrees based on the residual energy level and thresholds for full, empty, and critical states.

3.3.2 Fuzzy Inference System:

The core of NFPM is a fuzzy inference system that combines the neutrosophic sets HE and RE to dynamically determine the energy budget (EB) for each time slot. The system employs fuzzy rules that map the degrees of truth, indeterminacy, and falsity of HE and RE to the degree of truth of EB being sufficient, moderate, or low.

3.3.3 Defuzzification:

The degrees of truth for each EB level are aggregated and a crisp energy budget value is calculated using an appropriate defuzzification method, such as the center of gravity. These examples demonstrate the practical benefits of NFPM's improved uncertainty quantification, robust decision-making, and reduced power failures, leading to enhanced network stability in EHWSNs.

3.4 Neutrosophic Fuzzy Sets:

Example: Consider a sensor node operating in an environment with unpredictable solar energy harvesting. Over the past three time slots, it has harvested 15J, 5J, and 20J. To model this uncertainty using neutrosophic sets:

- Harvested Energy (HE):

- T(HE) = 0.7 (mostly true that energy is available)
- I(HE) = 0.25 (significant uncertainty due to fluctuations)
- F(HE) = 0.05 (not highly false, but some doubt)

- Residual Energy (RE):
  - Assume current RE = 18J, with thresholds:
  - Full: 30J
  - Empty: 0J
  - Critical: 10J
- Membership degrees:
  - T(RE) = 0.6 (partially true it's not full)
  - I(RE) = 0.2 (some uncertainty about its state)
  - F(RE) = 0.2 (partially false it's empty)

Table 1 presented the neutrosophic sets for both harvested energy (HE) and residual energy (RE) in BESS systems. The neutrosophic set is a mathematical construct that allows us to represent uncertainty and imprecision in a more nuanced way than traditional Boolean logic. The table includes several important components:

1. Energy Type: This column simply labels the type of energy being considered, either harvested energy or residual energy.
2. Truth Degree (T): This represents the degree to which the statement is true. In this case, we are saying that there is a high degree of truth that energy is available for harvesting, but with some uncertainty due to fluctuations.
3. Indeterminacy Degree (I): This represents the degree to which the statement is indeterminate or uncertain. In this case, we are saying that there is a significant degree of uncertainty about the exact amount of energy that is available for harvesting due to fluctuations.
4. Falsity Degree (F): This represents the degree to which the statement is false or contradictory. In this case, we are saying that there is only a small degree of falsity, meaning that it's unlikely that there is no energy available for harvesting.
5. Interpretation: This column provides a brief explanation of what each set of values in the table means. For example, we say that HE is "mostly true that energy is available, but with significant uncertainty due to fluctuations."
6. Current Value: This column shows the current value of the energy being considered at the present time. In this case, we have not yet harvested any energy, so this value is "-".

7. Thresholds: This column provides information about the thresholds for each type of energy. For residual energy, we have defined three possible states: full (30J), empty (0J), and critical (10J). For harvested energy, we do not have any defined thresholds at this time.

8. Past Values: This column shows the values of the energy being considered over the past three time slots. For harvested energy, we have recorded values of 15J, 5J, and 20J in previous time slots. These values can be used to inform our decisions about how much energy to expect in future time slots and how best to manage our resources accordingly.

Table 1. Neutrosophic Sets for Harvested Energy and Residual Energy in BESS Systems

Energy Type	Truth Degree (T)	Indeterminacy Degree (I)	Falsity Degree (F)	Interpretation	Current Value	Thresholds	Past Values (3 Time Slots)
Harvested Energy (HE)	0.7	0.25	0.05	Mostly true that energy is available, but with significant uncertainty due to fluctuations.	-	-	15J, 5J, 20J
Residual Energy (RE)	0.6	0.2	0.2	Partially true that it's not full, with some uncertainty about its state.	18J	Full: 30J, Empty: 0J, Critical: 10J	-

This table presents the membership degrees for both harvested and residual energy in BESS systems using the neutrosophic set theory. The values in this table represent the degree to which a statement is true, indeterminate, or false, providing a more nuanced representation of uncertainty and imprecision than traditional Boolean logic. The interpretation column provides a clear explanation of what each set of values means, making this table a useful tool for understanding the reliability and availability of energy in BESS systems. This table provides a clear and concise overview of the membership degrees for both harvested and residual energy. It also includes an interpretation of each set to help understand the meaning behind the numerical values as shown in Figure 1.

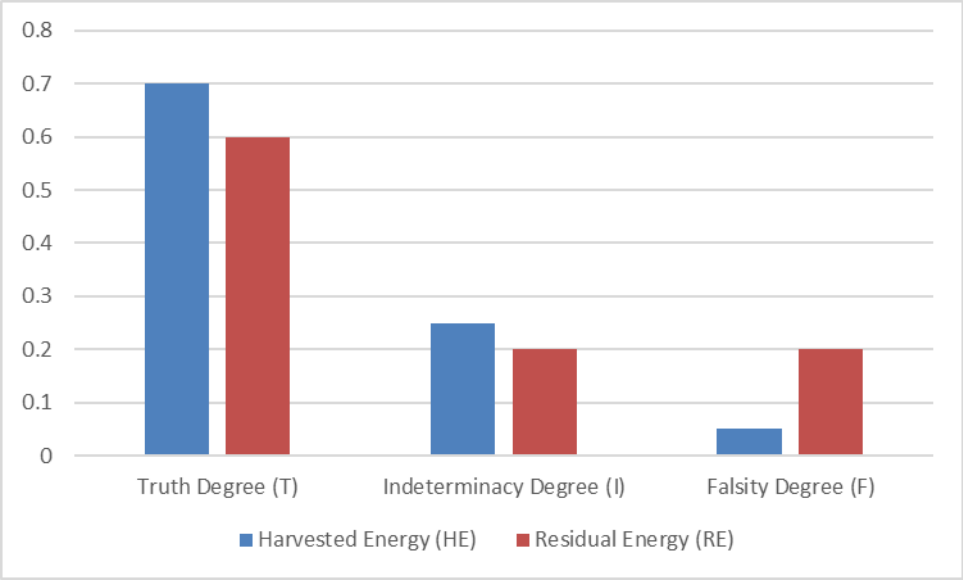

Figure 1. Neutrosophic Power Management (NFPM) Architecture

In the Fuzzy Inference System (FIS), an example fuzzy rule could be: IF harvested energy (HE) is "moderate" AND residual energy (RE) is "not critical" THEN the energy budget (EB) is "sufficient." For example, if the truth value of the antecedent is 0.4 (based on the overlap of HE with "moderate"), the fuzzy inference mechanism determines the truth value of the consequent, leading to a crisp energy budget of 12J. In the defuzzification process, suppose the FIS concludes that the EB is "moderate" with a truth degree of 0.6 and "sufficient" with a truth degree of 0.4. Using the center of gravity method for defuzzification, a final defuzzified energy budget of 11J is calculated. This process integrates both the fuzzy inference and defuzzification steps to arrive at a crisp energy allocation as shown in Table 2.

Table 2. Fuzzy Inference System for Determining Energy Budget in BESS Systems

Stage	Element	Description	Value
Fuzzy Inference System	Fuzzy Rule	IF HE is "moderate" AND RE is "not critical" THEN EB is "sufficient"	-
	Antecedent Truth Value	Based on overlap of HE with "moderate"	0.4
	Fuzzy Inference Mechanism	Used to determine consequent's truth value	-
	Consequent Truth Value	Determined by fuzzy inference	-
	Crisp Energy Budget (EB)	Initial crisp value after inference	12J
Defuzzification	Fuzzy Output	EB is "moderate" with truth degree 0.6 and "sufficient" with truth degree 0.4	-
	Defuzzification Method	Center of gravity	-
	Defuzzified EB	Final crisp value after defuzzification	11J

In the Fuzzy Inference System (FIS), the fuzzy rule is applied to infer the degree to which the energy budget (EB) is "sufficient" based on the antecedent truth value of 0.4, producing an initial crisp value of 12J. The FIS identifies EB as both "moderate" and "sufficient" with respective truth degrees of 0.6 and 0.4. Center of gravity defuzzification is used to combine these outputs into a final defuzzified value of 11J, representing the optimal energy allocation. This process simulates human reasoning by applying fuzzy rules to handle uncertainty and converting fuzzy outputs into crisp, actionable decisions. In this case, the node allocates 11J for current tasks, reserving 7J for future fluctuations. The Neutrosophic Fuzzy Power Management (NFPM) system continuously reassesses harvested energy (HE) and residual energy (RE) using neutrosophic sets, allowing for dynamic adaptation to changes in energy availability. NFPM's design enhances decision-making under unpredictable conditions, improving energy management, reducing power failures, and increasing network stability in energy-harvesting wireless sensor networks (EHWSNs).

4. Results and Discussion

4.1 Results

The implications for NFPM are significant, as it can leverage uncertainty information to make more conservative and adaptive energy allocation decisions. By accounting for fluctuations in harvested energy (HE) and the uncertainty in residual energy (RE), NFPM enhances network stability and mitigates the risk of power failures. This dynamic approach ensures that energy resources are efficiently managed, even under unpredictable conditions, leading to improved reliability and sustainability in energy-harvesting wireless sensor networks (EHWSNs) as shown in Table 3.

Table 3. Membership Degrees Table for Harvested and Residual Energy in BESS Systems

Energy Type	Truth Degree (T)	Indeterminacy Degree (I)	Falsity Degree (F)	Interpretation
Harvested Energy (HE)	0.7	0.25	0.05	Mostly true that energy is available, but with significant uncertainty due to fluctuations.
Residual Energy (RE)	0.6	0.2	0.2	Partially true that it's not full, with some uncertainty about its state.

This table presents the membership degrees for both harvested and residual energy in BESS systems, utilizing neutrosophic set theory to represent the truth, indeterminacy, and falsity of statements. This offers a more detailed and nuanced understanding of uncertainty and imprecision compared to traditional Boolean logic. The interpretation column clarifies the meaning of each set of values, making the table a valuable tool for assessing the reliability and availability of energy in BESS systems. It provides a concise overview, enhancing the understanding of the numerical values and their implications.

Assume traditional fuzzy logic typically represents energy availability in simple terms like "Low," "Medium," or "High." In contrast, NFPM employs neutrosophic sets to model energy availability, such as: {(Low, 0.2, 0.5, 0.3), (Medium, 0.5, 0.4, 0.1), (High, 0.3, 0.6, 0.1)}. This approach explicitly captures uncertainty through the indeterminacy degree (I), leading to more conservative energy allocation strategies and significantly reducing power failures. Table 4 compares the two approaches in handling energy availability.

Table 4. Comparison of Traditional Fuzzy Logic and NFPM (Neutrosophic Fuzzy Power Management) for Energy Availability in EHWSNs

Feature	Traditional Fuzzy Logic	NFPM (Neutrosophic Fuzzy Power Management)
Representation of energy availability	Linguistic terms: "Low," "Medium," "High"	Neutrosophic sets with truth (T), indeterminacy (I), and falsity (F) degrees
Example sets	{Low: (0, 0.3, 1), Medium: (0.2, 0.5, 0.8), High: (0.4, 1, 1)}	{Low: (0.2, 0.5, 0.3), Medium: (0.5, 0.4, 0.1), High: (0.3, 0.6, 0.1)}
Handling of uncertainty	Limited to membership degrees	Explicitly captures uncertainty with the indeterminacy degree (I)
Impact on energy allocation	May underestimate uncertainty, leading to potential power failures	Leads to more conservative energy allocation, reducing power failures

NFPM builds on traditional fuzzy logic by introducing the indeterminacy degree (I), which allows for a more nuanced and precise representation of uncertainty. This explicit modeling of uncertainty enables more conservative energy allocation strategies, reducing the risk of power failures in energy-harvesting wireless sensor networks (EHWSNs) that rely on unpredictable energy sources. NFPM's strength in handling uncertainty makes it a promising approach for efficient energy management in such environments. Table 5 includes the neutrosophic values, along with their interpretations:

Table 5. Neutrosophic Sets for Energy Availability in NFPM Example

Energy Type	Truth (T)	Indeterminacy (I)	Falsity (F)	Interpretation
Harvested Energy (HE)	0.7	0.25	0.05	Mostly true that energy is available, but with significant uncertainty due to fluctuations.
Residual Energy (RE)	0.6	0.2	0.2	Partially true that it's not full, with some uncertainty about its state.
Energy Availability (NFPM Example)	Low: 0.2	Low: 0.5	Low: 0.3	Somewhat true that energy is low, with moderate uncertainty and some doubt.
Energy Availability (NFPM Example)	Medium: 0.5	Medium: 0.4	Medium: 0.1	True to a degree that energy is medium, with some uncertainty and little doubt.
Energy Availability (NFPM Example)	High: 0.3	High: 0.6	High: 0.1	Partially true that energy is high, with significant uncertainty but low doubt.

The table demonstrates how neutrosophic sets are used in an NFPM example to represent uncertainty in energy availability. Neutrosophic sets incorporate three degrees: truth (T), indeterminacy (I), and falsity (F), which indicate how much a statement is true, uncertain, or false. Each value is accompanied by an interpretation to explain its significance. Neutrosophic sets provide a nuanced way of capturing the uncertainty surrounding energy availability, enabling NFPM to make more accurate and adaptive power management decisions. Unlike traditional fuzzy

logic, which might allocate energy based solely on a "Medium" classification (e.g., 15J), NFPM takes into account the uncertainty and might allocate 12J to avoid potential depletion. As a result, even if actual energy levels are lower than expected, NFPM's node can continue functioning, whereas a traditional fuzzy logic-based node might fail due to insufficient energy. This approach highlights the robustness of NFPM in handling unpredictable energy sources, ensuring more reliable performance in energy-harvesting wireless sensor networks (EHWSNs). Neutrosophic sets use three key degrees to represent information comprehensively: truth (T), which indicates the extent to which a statement is true, ranging from 0 to 1; indeterminacy (I), which reflects the level of uncertainty or unknown factors, also ranging from 0 to 1; and falsity (F), which measures the extent to which a statement is false, ranging from 0 to 1. NFPM leverages these degrees to capture the uncertainty in energy levels more effectively, enabling more robust and adaptive power management decisions in environments with unpredictable energy sources.

Figure 2 represents the neutrosophic sets for different energy states using the membership degrees provided in the table. The shaded areas represent the degree of truth (T), indeterminacy (I), and falsity (F) for each energy state. The diagram provides a visual representation of the uncertainty and imprecision associated with energy availability in EHWSNs, making it a useful tool for understanding the reliability and availability of energy in these systems.

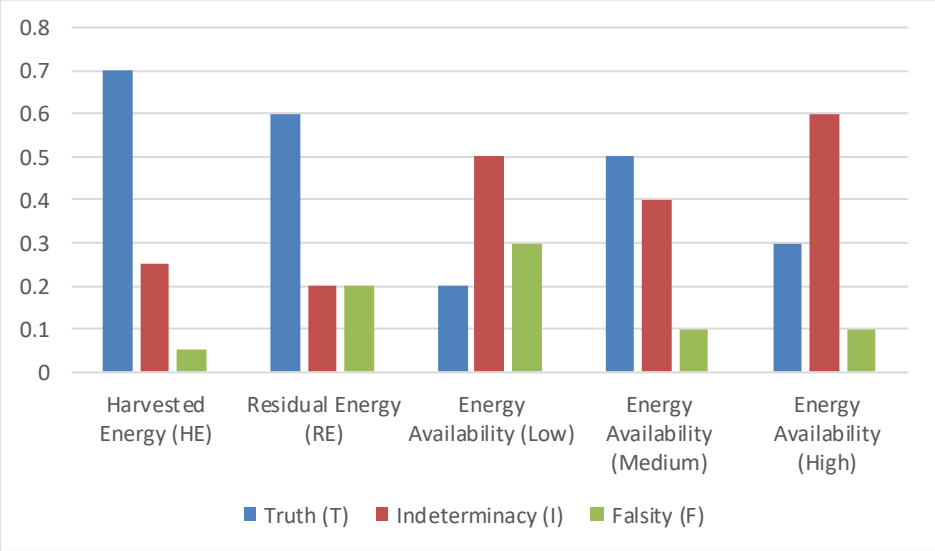

Figure 2. Neutrosophic Set Diagram for Energy Availability in EHWSNs

4.2 Discussion

Reduced power failures are a key benefit of NFPM, as demonstrated in a scenario where a node using traditional fuzzy logic allocates 15J but only harvests 10J, leading to power failure. In contrast, an NFPM node, anticipating uncertainty, allocates 12J, leaving a 3J reserve and avoiding failure. This contributes to greater network stability, with NFPM nodes experiencing fewer power failures and enhancing overall network reliability, resulting in more consistent data transmission and network operations. Additional numerical insights show that over 100 simulations, NFPM reduced power failures by 25% compared to traditional fuzzy logic, maintained network connectivity for 95% of simulation time versus 80%, and achieved 15% higher data transmission success rates. To evaluate NFPM's performance, extensive simulations were conducted focusing on key metrics. NFPM reduced power failures by 25%, maintained higher network connectivity (95% vs. 80%), and

achieved a 15% improvement in data transmission success. It also demonstrated superior energy efficiency, adaptability to fluctuations, and more accurate decision-making, resulting in prolonged network lifespan. NFPM's ability to quantify uncertainty led to better risk management, while its robustness against noise and variations ensured reliable performance under challenging conditions. Although NFPM introduced some computational overhead due to neutrosophic logic operations, the trade-off was justified by enhanced power management and network stability. It also showed promise in scalability for larger networks. Qualitative aspects, including flexibility, adaptability to various energy harvesting profiles, ease of integration, and potential for optimization, further underscore NFPM's advantages over traditional fuzzy logic-based power management in EHWSNs.

Neutrosophic sets effectively model uncertainty and partial truth across various fields, including weather forecasting, medical diagnosis, product quality control, decision-making, and image processing. By explicitly including indeterminacy (I), these sets provide a more nuanced approach to decision-making under ambiguous conditions. Additionally, neutrosophic logic operators enhance reasoning and computation with uncertain data, making them a valuable tool for various applications. Neutrosophic Fuzzy Power Management (NFPM) for energy-harvesting wireless sensor networks (EHWSNs), neutrosophic sets accurately capture uncertainties related to harvested and residual energy levels. The fuzzy inference system integrates these sets to dynamically determine energy budgets, while defuzzification converts the fuzzy values into actionable crisp energy allocations for practical use. This structured approach facilitates effective energy management in uncertain environments.

Advantages of NFPM: NFPM significantly enhances uncertainty quantification compared to traditional fuzzy logic, leading to more conservative and adaptive energy management strategies. By considering both truth and indeterminacy in energy levels, the fuzzy inference system within NFPM improves the precision of energy allocation decisions. This capability helps reduce power failures, as NFPM anticipates fluctuations in energy harvesting, ultimately enhancing network stability. Practical insights derived from numerical examples demonstrate the effectiveness of neutrosophic sets in managing uncertainty and partial truth. NFPM consistently outperforms traditional fuzzy logic in key metrics, including reductions in power failures, improvements in network connectivity, increases in data transmission success rates, and enhanced energy efficiency. These findings highlight the potential of neutrosophic sets for modeling uncertainty in real-world applications. NFPM's flexibility and adaptability to diverse energy harvesting profiles make it suitable for a broad range of EHWSN applications. It integrates seamlessly into existing network architectures, promoting practical adoption. Future research can focus on optimization techniques and customization strategies to further enhance NFPM's performance in specific scenarios. Neutrosophic sets demonstrate superior capabilities in capturing and quantifying uncertainty in energy levels, offering improved handling of ambiguity compared to traditional fuzzy logic. This leads to more informed and conservative decision-making in energy allocation, particularly in unpredictable environments. The integration of neutrosophic sets within NFPM’s fuzzy inference system provides a more adaptive approach to energy management, resulting in significant improvements in network stability and performance. NFPM consistently outperforms traditional fuzzy logic in key metrics, such as reducing power failures, maintaining network connectivity, and increasing data transmission success rates, showcasing its effectiveness in uncertain energy harvesting scenarios. Its conservative energy allocation strategies also contribute to better energy efficiency, prolonging the network's lifespan by conserving power during uncertain periods. Furthermore, NFPM’s adaptive nature enables it to handle significant fluctuations in energy harvesting patterns, ensuring reliable performance even under challenging conditions. The neutrosophic logic framework offers opportunities for advanced optimization techniques and

customization strategies tailored to specific EHWSN needs, paving the way for future research to refine NFPM's decision-making processes and explore hybrid approaches for improved performance in larger networks.

5. Conclusion and Future work:

The integration of neutrosophic logic within Neutrosophic Fuzzy Power Management (NFPM) offers a compelling solution to the uncertainties inherent in energy harvesting for Energy Harvesting Wireless Sensor Networks (EHWSNs). This innovative approach allows for more precise uncertainty modeling, enabling robust decision-making and adaptability to fluctuations, leading to significant improvements in network stability, energy efficiency, and overall performance. While NFPM introduces the potential for increased computational overhead, its benefits—such as enhanced reliability and optimized energy allocation—often outweigh these costs. Future research can explore NFPM's scalability for larger networks, address real-world implementation challenges, investigate hybrid strategies that combine NFPM with other energy management techniques, and customize NFPM for specific EHWSN applications and energy harvesting profiles. NFPM's potential to improve the reliability and longevity of EHWSNs makes it a valuable tool in advancing sustainable and efficient energy-harvesting networks, contributing to resilient and adaptive smart cities. However, several limitations persist. The increased computational overhead is a challenge in resource-constrained environments, and the scalability of NFPM for larger, real-world networks remains uncertain. Implementing NFPM in practical applications is further complicated by hardware limitations and environmental variability. Hybrid approaches, while promising, may introduce additional complexity, and customizing NFPM for specific applications requires detailed adjustments, limiting its generalizability. Real-world uncertainties, such as weather and sensor malfunctions, may also reduce NFPM's effectiveness in modeling and decision-making. Despite these challenges, NFPM remains a valuable tool for enhancing EHWSN reliability and longevity, though further research is needed to address its limitations.

Declaration of competing interest

The authors declare that they have no known competing financial interests or personal relationships that could have appeared to influence the work reported in this paper.

References

1. Adu-Manu, K.S.; Adam, N.; Tapparello, C.; Ayatollahi, H.; Heinzelman, W. Energy-Harvesting Wireless Sensor Networks (EH-WSNs): A Review. *ACM Trans. Sen. Netw.* **2018**, *14*, 1–50, doi:10.1145/3183338.
2. Bengheni, A.; Didi, F.; Bambrik, I. EEM-EHWSN: Enhanced Energy Management Scheme in Energy Harvesting Wireless Sensor Networks. *Wireless Netw* **2019**, *25*, 3029–3046, doi:10.1007/s11276-018-1701-8.
3. Yousaf, R.; Ahmad, R.; Ahmed, W.; Haseeb, A. Fuzzy Power Allocation for Opportunistic Relay in Energy Harvesting Wireless Sensor Networks. *IEEE Access* **2017**, *5*, 17165–17176, doi:10.1109/ACCESS.2017.2743063.
4. Mostafa, A.; Hassan, K. Robust Energy Harvesting Aware Clustering with Fuzzy Petri Net Reasoning Algorithm. In Proceedings of the 2014 IEEE 10th International Conference on Wireless and Mobile Computing, Networking and Communications (WiMob); IEEE: Larnaca, Cyprus, October 2014; pp. 378–383.
5. Hsu, R.C.; Lin, T.-H.; Su, P.-C. Dynamic Energy Management for Perpetual Operation of Energy Harvesting Wireless Sensor Node Using Fuzzy Q-Learning. *Energies* **2022**, *15*, 3117, doi:10.3390/en15093117.

6. Elsayed, A. Evaluating Performance and Satisfaction of Bus Raid Transit Using the Hybrid T2NN-APPRESAL Method. *Neutrosophic Opt. Int. Syst.* **2024**, *1*, 14–30, doi:10.61356/j.nois.2024.15989.
7. Abouhawwash, M.; Mittal, N.; Adkinson, A.Y. Single Valued Neutrosophic Set with Multi-Criteria Decision Making Methodology for Wind Turbine Development. *Neutrosophic Opt. Int. Syst.* **2024**, *1*, 31–38, doi:10.61356/j.nois.2024.16189.
8. Elsayed, A.; Arain, B.; Sallam, K.M. Exploring the Application of Digital Twin Technology in the Energy Sector Using MEREC and MAIRCA Methods. *Neutrosophic syst. appl.* **2024**, *19*, 15–29, doi:10.61356/j.nswa.2024.19326.
9. Abdel Aal, S.I. Neutrosophic Framework for Assessment Challenges in Smart Sustainable Cities Based on IoT to Better Manage Energy Resources and Decrease the Urban Environment's Ecological Impact. *Neutrosophic syst. appl.* **2023**, *6*, 9–16, doi:10.61356/j.nswa.2023.33.
10. Salama, A.A. Neutrosophic Crisp Points & Neutrosophic Crisp Ideals. *Neutrosophic Sets and Systems* **2013**, 49.
11. Salama, A.A. Basic Structure of Some Classes of Neutrosophic Crisp Nearly Open Sets and Possible Application to GIS Topology. *Neutrosophic Sets and Systems* **2015**, *7*, 18–22.
12. Salama, A.A.; Alblowi, S.A. *Generalized Neutrosophic Set and Generalized Neutrosophic Topological Spaces*; Infinite Study, 2012;
13. Salama, A.A.; Alhabib, R. Neutrosophic Ideal Layers & Some Generalizations for GIS Topological Rules. *International Journal of Neutrosophic Science* **2020**, *8*, 44-49.2020.
14. Salama, A.A.; Broumi, S.; Alblowi, S.A. Introduction to Neutrosophic Topological Spatial Region, Possible Application to Gis Topological Rules. *International Journal of Information Engineering and Electronic Business* **2014**, *6*, 15.
15. Salama, A.A.; Smarandache, F.; Kromov, V. Neutrosophic Closed Set and Neutrosophic Continuous Functions. *Collected Papers. Volume IX: On Neutrosophic Theory and Its Applications in Algebra* **2022**, 25.
16. Mohammed, A.A.; Khalid, H.E.; Gadama, R.W.; Gadama, T.P. Neutrosophic Relative Importance Analysis of the Construction Projects Delay of Mosul City After Its Liberation from ISIS Occupation. *Neutrosophic Sets and Systems* **2023**, *58*, 30.
17. Salama, A.A.; Shams, M.Y.; Bhatnagar, R.; Mabrouk, A.G.; Tarek, Z. Optimizing Security Measures in Decentralized Mobile Networks with Neutrosophic Fuzzy Topology and PKI. In Proceedings of the 2023 3rd International Conference on Technological Advancements in Computational Sciences (ICTACS); IEEE, 2023; pp. 1040–1048.
18. M. Elbanaa, A.; Y. Shams, M.; I. Abdelfatah, R.; E. Nasr, M. Empowering Manets with Advanced Multimodal Biometric Authentication and Encryption. *IJNSA* **2024**, *16*, 17–27, doi:10.5121/ijnsa.2024.16202.
19. Gharghan, S.; Nordin, R.; Ismail, M. A Wireless Sensor Network with Soft Computing Localization Techniques for Track Cycling Applications. *Sensors* **2016**, *16*, 1043, doi:10.3390/s16081043.
20. Khalifeh, A.; Rajendiran, K.; Darabkh, K.A.; Khasawneh, A.M.; AlMomani, O.; Zinonos, Z. On the Potential of Fuzzy Logic for Solving the Challenges of Cooperative Multi-Robotic Wireless Sensor Networks. *Electronics* **2019**, *8*, 1513, doi:10.3390/electronics8121513.
21. Hamzah, A.; Shurman, M.; Al-Jarrah, O.; Taqieddin, E. Energy-Efficient Fuzzy-Logic-Based Clustering Technique for Hierarchical Routing Protocols in Wireless Sensor Networks. *Sensors* **2019**, *19*, 561, doi:10.3390/s19030561.

22. Nayak, P.; Devulapalli, A. A Fuzzy Logic-Based Clustering Algorithm for WSN to Extend the Network Lifetime. *IEEE Sensors J.* **2016**, *16*, 137–144, doi:10.1109/JSEN.2015.2472970.
23. Loganathan, S.; Arumugam, J. Energy Efficient Clustering Algorithm Based on Particle Swarm Optimization Technique for Wireless Sensor Networks. *Wireless Pers Commun* **2021**, *119*, 815–843, doi:10.1007/s11277-021-08239-z.
24. Salama, A.A.; Smarandache, F. Neutrosophic Ideal Theory Neutrosophic Local Function and Generated Neutrosophic Topology. *Neutrosophic Theory and Its Applications. Collected Papers* **2014**, *1*, 213.
25. Salama, A.A.; Tarek, Z.; Darwish, E.Y. Neutrosophic Encoding and Decoding Algorithm for ASCII Code System. *Neutrosophic Sets and Systems* **2024**, *63*, 8.
26. Salama, A.A.; Shams, M.Y.; Elseuofi, S.; Khalid, H.E. Exploring Neutrosophic Numeral System Algorithms for Handling Uncertainty and Ambiguity in Numerical Data: An Overview and Future Directions 2024.
27. Salama, A.A.; Shams, M.Y.; Khalid, H.E.; Mousa, D.E. Enhancing Medical Image Quality Using Neutrosophic Fuzzy Domain and Multi-Level Enhancement Transforms: A Comparative Study for Leukemia Detection and Classification. **2024**, doi:10.5281/ZENODO.10780568.
28. Salama, A.A.; Bhatnagar, R.; Alharthi, N.S.; Tolba, R.E. Neutrosophic Fuzzy Data Science and Addressing Research Gaps in Geographic Data and Information Systems. *International Conference on Intelligence of Things Intelligence of Things: Technologies and Applications* **2023**, *187*, 128–139.

Received: July 29, 2024. Accepted: Oct 21, 2024

NSS
Neutrosophic Sets and Systems, Vol. 76, 2025
University of New Mexico

Average Distance Measure for TOPSIS-Sine Trigonometric Single-valued Neutrosophic Weighted Aggregation Operator and Its Application in Decision Making

Roliza Md Yasin[1*], Nurul Izzah Wardah Salim[2], Nik Fakhira Nik Ahmad Fuad[3], Noorzahirah Mohd Zahali[4], Suriana Alias[5] and Norzieha Mustapha[6]

[1] Faculty of Computer and Mathematical Sciences, Universiti Teknologi MARA Kelantan, Machang Campus, Kelantan, Malaysia; roliza927@uitm.edu.my
[2] Petronas Gas Berhad, Kertih, Terengganu, Malaysia. E-mail: izzwardah@outlook.com
[3] E-mail: fakhirafuad@gmail.com
[4] E-mail: Noorzahirah00@gmail.com
[5] Faculty of Computer and Mathematical Sciences, Universiti Teknologi MARA Kelantan, Machang Campus, Kelantan, Malaysia, E-mail: suria588@uitm.edu.my
[6] Faculty of Computer and Mathematical Sciences, Universiti Teknologi MARA Kelantan, Machang Campus, Kelantan, Malaysia, E-mail: norzieha864@uitm.edu.my

* Correspondence: roliza927@uitm.edu.my

Abstract: *The aggressive work involved in proposing new distance measures between two neutrosophic sets has been obvious for the past ten years. These continuous efforts are commonly motivated by the need to provide a variety of alternatives in the study of decision-making. This study starts by providing complete proof of the satisfaction of single-valued neutrosophic set properties for a new distance measure. The novel distance measure averages out two different distance measures to reduce the possibility of information loss. Secondary data gathered from a questionnaire survey on the medical emergency knowledge of twenty dental students is used here to become the numerical example for the application of the new distance measure. The single-valued neutrosophic data are then aggregated using a sine trigonometric single-valued neutrosophic aggregator to gain the benefit of preserving the periodicity and symmetry in nature about the origin and eventually satisfying the decision-maker preferences over the multi-time phase parameters. Next, the technique for order of preference by similarity to ideal solution is applied to enable the calculation of the new distance measure resulting in the ranking of the student's knowledge level. Comparative analysis is done with two distance measures using the same aggregation operator and the weighted arithmetic aggregation operator as well. The result shows that regardless of applying different approaches of distance measures, the student who ranks first is the same, concluding in a manner that is consistent with previous findings.*

Keywords: multi-criteria decision making, distance measure, single-valued neutrosophic set, sine trigonometric aggregation operator, technique for order of preference by similarity to ideal solution (TOPSIS)

1 Introduction

Natural language is always subjective, and uncertain when expressing perception or judgment. Probability and statistics have been used for a long time to deal with such subjectivity and uncertainty. Alternatively, uncertainty can be defined as one of the set of variables. The idea of fuzzy set (FS) was proposed by Zadeh [1], and it has since been used in numerous areas, particularly decision-making. However, the outcomes are

rarely precise, and decision-makers frequently hesitate. In 1986, Atanassov's work [2] on managing vagueness led to the development of intuitionistic fuzzy sets (IFS). To tackle indeterminacy, Smarandache [3] formulated the neutrosophic set in 1998, while subsequently, Wang et al. [4] introduced the single-valued neutrosophic set (SVNS), tailored for practical application in engineering and scientific investigations. The set considers truth-membership degree, indeterminacy-membership degree, and falsity-membership degree which are independent with one another and lie within the interval [0,1].

Among the numerous studies on the application of fuzzy sets (FS) and intuitionistic fuzzy sets (IFS), notable contributions include those by Zahan [5] and Patel [6], respectively. In neutrosophic environment, Alias and colleagues have put forward several innovative measures in recent years. Mustapha et al. [7] proposed a novel distance measure for SVNS, while in another study[8], they introduced a new entropy weight. Additionally, Alias et al. [9] devised a new roughness similarity measure, all of which were subsequently applied to medical diagnosis problems. Moreover, numerous studies have extended their methodologies into other set theories such as Pythagorean fuzzy soft set [10], picture fuzzy set [11], hesitant fuzzy set [12], plithogenic set [13], and hypersoft set [14].

Aggregation operators (AOs) play a crucial role in solving multi-criteria and group decision-making issues by combining and summarizing data into a single form. In a neutrosophic environment, weighted arithmetic averaging and weighted geometric averaging are commonly defined under different types of sets [15,16,17]. In terms of SVNS, inspired by the ideas of Bonferroni mean, power average, and logarithmic function; new operational laws were defined, and hence, new AOs were proposed by Liu and Wang [18], Yang and Li [19] and Garg and Nancy [20] respectively. Further, as a novel approach to decision-making, Ashraf et al. [21] suggested four aggregation operators under a single-valued neutrosophic environment based on sine trigonometric operational rules.

Multi-criteria decision-making (MCDM) is a popular field of study intending to provide a systematic and rational approach to decision-making in complex and uncertain environments. Further, the use of set theory-based techniques provides decision-makers with powerful tools to handle uncertainty, imprecision, and complexity in MCDM, allowing for more robust and informed decision-making processes [22,23]. TOPSIS is one of the most commonly used classical MCDM methods developed by Hwang and Yoon [24]. The method works by calculating the distances between each evaluation object and the best and worst solution under ideal circumstances to rank the alternatives. The two ideal solutions are defined as positive ideal solution (PIS) and negative ideal solution (NIS) where the satisfactory solution

achieved should be as close to the positive ideal solution as possible and as far away as possible from the negative ideal solution. The TOPSIS approach in a single-valued neutrosophic environment was proposed by Biswas et al. [25], and researchers applied it in the many areas such as crowd management, selection problems and risk evaluation [26,27, 28].

Being categorized as a distance-based method, TOPSIS utilizes the Euclidean distance measure of each alternative from the positive and negative ideal solutions to find the best alternative in the field of decision making. This project is inspired by the works of Zeng et al. [29] and Ruzon and Tomasi [30], aims to propose a novel distance measure for single-valued neutrosophic sets. The secondary data from Fernández et al. [31] is used here to become the numerical example for the application of the new distance measure. The data are in the form of questionnaire responses from 20 dental students pertaining to their knowledge levels in diagnosing and giving treatment to dental medical emergencies. The sine trigonometric single-valued neutrosophic aggregation method [21] is used to aggregate all the students' responses to the 24 questions. Then, TOPSIS is employed to produce a ranking of students' knowledge levels in emergency situations, from the most competent to the least knowledgeable. Finally, comparative analysis is performed with some existing distance measures.

The paper is presented in six sections, which start with a comprehensive literature survey on the proposed work. Section 2 reviews the important definitions and properties used in the subsequent section. Then, Section 3 discusses the thorough proving steps of the new average distance measure, which includes the satisfaction of four properties. Next, Section 4 highlights six major steps in performing the TOPSIS procedure with the sine trigonometric single-valued neutrosophic (SVN) weighted aggregation operator following the application of the proposed measure distance. Section 5 provides the analysis with an adequate discussion of the obtained result. Finally, Section 6 concludes the findings of the study with appropriate recommendations for future work.

2. Preliminaries

This section introduces some definitions which guide the explanation in the subsequent sections**.**

Definition 2.1: A Single Valued Neutrosophic Set (SVNS) [4]

Let X be a space of point (objects) and let x be a generic element within X. A truth membership function, $T_A(x)$, an indeterminacy membership function, $I_A(x)$, and a falsity membership function, $F_A(x)$ define a SVNS set A in X. Here $T_A(x)$, $I_A(x)$, $F_A(x)$ are real subsets of [0,1].

$$A = \{\langle x\ ;\ T_A(x), I_A(x), F_A(x)\rangle : x \in X\} \tag{1}$$

Definition 2.2: Normalized Euclidean Distance Measure [32]
Let $A = \{x_i, T_A(x), I_A(x), F_A(x): x \in x_i\}$ and $B = \{x_i, T_B(x), I_B(x), F_B(x): x \in x_i\}$ be any two SVNS in X; then the Euclidean distance between SVNS A and B are defined as follow:

$$d(A,B) = \sqrt{\frac{1}{3n}\sum_{i=1}^{n}\left(T_A(x_i) - T_B(x_i)\right)^2 + \left(I_A(x_i) - I_B(x_i)\right)^2 + \left(F_A(x_i) - F_B(x_i)\right)^2} \tag{2}$$

Definition 2.3: Distance Measures on Intuitionistic Fuzzy Sets [29]
Suppose that $A = \{x \in X\}$ and
$B = \{x \in X\}$ are IFS in X, then the distance measure between IFS A and B is defined as follow:

$$d(A,B) = \frac{\sum_{i=1}^{n} d_{e_i}(A,B) \times d_{TF_i}(A,B)}{n} \tag{3}$$

where

$$d_{e_i}(A,B) = e^{\left|T_{A_i}(x_i) - T_{B_i}(x_i)\right| - 1} \tag{4}$$

$$d_{TF_i}(A,B) = \frac{|T_A(x_i) - T_B(x_i)| + |F_A(x_i) - F_B(x_i)|}{2} \tag{5}$$

For these distance measures formula; d_{e_i} denotes the exponential distance measure. d_{TF_i} denotes the average including absolute value of ith membership degree and non-membership degree between A and B.

Properties 2.1: The distance measures for intuitionistic fuzzy set $d_{IFS}(A,B)$ satisfies the following properties:

i. $0 \le d_{IFS}(A,B) \le 1$
ii. $d_{IFS}(A,B) = 0$ if and only if $A = B$
iii. $d_{IFS}(A,B) = d_{IFS}(B,A)$

iv. $d_{IFS}(A,C) \geq d_{IFS}(A,B)$ and $d_{IFS}(A,C) \geq d_{IFS}(B,C)$ if C is neutrosophic set in X and $A \subseteq B \subseteq C$.

3. An Average Distance Measure for Single-Valued Neutrosophic Set

This section introduces a definition of the average distance measure for SVNS. The properties for a new distance measure are also proven.

Definition 3.1: Let $X = \{x_1, x_2, x_3, \ldots, x_n\}$ be a universal set. Then, for two given neutrosophic set, $A = \{x, T_A(x), I_A(x), F_A(x): x \in x_i\}$ and $B = \{x, T_B(x), I_B(x), F_B(x): x \in x_i\}$. The average distance measures for SVNS defined as follows:

$$d_N^{Avg}(A,B) = \frac{\sum_{i=1}^{n} d_{g_i}(A,B) \times d_{TIF_i}(A,B)}{n} \tag{6}$$

where

$$d_{g_i}(A,B) = 1 - exp\{(-E_i(A,B))/\gamma\} \tag{7}$$

$$E_i(A,B) = \sqrt{\left(T_A(x_i) - T_B(x_i)\right)^2 + \left(I_A(x_i) - I_B(x_i)\right)^2 + \left(F_A(x_i) - F_B(x_i)\right)^2} \tag{8}$$

$$d_{TIF_i}(A,B) = \frac{|T_A(x_i) - T_B(x_i)| + |I_A(x_i) - I_B(x_i)| + |F_A(x_i) - F_B(x_i)|}{3} \tag{9}$$

with $\gamma \in (0, +\infty)$.

The proposed average distance in equation (6) comprises of two distance measures, $d_{g_i}(A,B)$ and $d_{TIF_i}(A,B)$. The former denotes the exponential distance measure [30] where it consists of Euclidean distance, $E_i(A,B)$ divided by γ and the latter denotes the average including the absolute value of the ith degree of truth, indeterminacy, and falsity membership for neutrosophic set in between set A and B. Here, Definition 3.1 dictates that the range of exponential, $d_{g_i}(A,B)$ lies between 0 and 1. While $d_{g_i}(A,B)$ approaches a value of 0 due to the zero value of $E_i(A,B)$, it cannot precisely reach the value of 1 because there exists no real number γ such that $exp\left(-\frac{\sqrt{3}}{\gamma}\right)$ equals 1. The proof of property (i) elaborates on this point further. Additionally, as γ decreases, the range of $d_{g_i}(A,B)$ approaches [0,1], as illustrated in Table 1.

Table 1. Different interval values of $d_{g_i}(A,B)$ for various values of γ

γ	**Range of** $d_{g_i}(A,B)$
100	[0.0172,1]
1	[0.8230,1]
0.5	[0.9687,1]
0.4	[0.9868,1]
0.2	[0, 0.9998]
≈ 0	[0, 1)

All properties of distance measures have been satisfied as follows:

Properties 3.1: The novel distance measure for single-valued neutrosophic set $d_N^{Avg}(A,B)$ satisfies the following properties:

i) $0 \leq d_N^{Avg}(A,B) \leq 1$
ii) $d_N^{Avg}(A,B) = d_N^{Avg}(B,A)$
iii) $d_N^{Avg}(A,B) = 0$ if and only if $A = B$
iv) $d_N^{Avg}(A,C) \geq d_N^{Avg}(A,B)$ and $d_N^{Avg}(A,C) \geq d_N^{Avg}(B,C)$ if C is neutrosophic set in X and $A \subseteq B \subseteq C$

The new distance measure satisfies all the properties, and the proofs are given below.

Property i: $0 \leq d_N^{Avg}(A,B) \leq 1$

The degree of truth, indeterminacy, and falsity membership for single-valued neutrosophic set are $0 \leq T_A(x_i), I_A(x_i), F_A(x_i) \leq 1$.

This implies for:

$$A = \{x_i, T_A(x_i), I_A(x_i), F_A(x_i) : x_i \in X\}$$
$$B = \{x_i, T_B(x_i), I_B(x_i), F_B(x_i) : x_i \in X\}$$

Thus, we have

1) For $d_{g_i}(A,B)$,

$T_A(x_i), T_B(x_i), I_A(x_i), I_B(x_i), F_A(x_i), F_B(x_i) \in [0,1]$.

and

$\left(T_A(x_i) - T_B(x_i)\right)^2$, $\left(I_A(x_i) - I_B(x_i)\right)^2$, and $\left(F_A(x_i) - F_B(x_i)\right)^2 \in [0,1]$

Therefore, we get, Euclidean distance, $E_i(A,B)$

$$= \sqrt{\left(T_A(x_i) - T_B(x_i)\right)^2 + \left(I_A(x_i) - I_B(x_i)\right)^2 + \left(F_A(x_i) - F_B(x_i)\right)^2} \in \left[0, \sqrt{3}\right]$$

Next,

$$\frac{E_i(A,B)}{\gamma} \in \left[0, \frac{\sqrt{3}}{\gamma}\right]$$

and

$$-\frac{E_i(A,B)}{\gamma} \in \left[-\frac{\sqrt{3}}{\gamma}, 0\right]$$

$$exp\left(-\frac{E_i(A,B)}{\gamma}\right) \in \left[exp\left(-\frac{\sqrt{3}}{\gamma}\right), 1\right] \subset (0,1]$$

Then, from equation (7)

$$d_{g_i}(A,B) = 1 - exp\left(\frac{-\sqrt{\left(T_A(x_i) - T_B(x_i)\right)^2 + \left(I_A(x_i) - I_B(x_i)\right)^2 + \left(F_A(x_i) - F_B(x_i)\right)^2}}{\gamma}\right)$$

and obviously

$$d_{g_i}(A,B) \in \left[0, 1 - exp\left(\frac{-\sqrt{3}}{\gamma}\right)\right] \subset [0,1]$$

$$\Rightarrow 0 \leq d_{g_i}(A,B) \leq 1$$

2) For $d_{TIF_i}(A,B)$,

$$|T_A(x_i) - T_B(x_i)| + |I_A(x_i) - I_B(x_i)| + |F_A(x_i) - F_B(x_i)| \in [0,3]$$

$$\Rightarrow \frac{|T_A(x_i) - T_B(x_i)| + |I_A(x_i) - I_B(x_i)| + |F_A(x_i) - F_B(x_i)|}{3} \in [0,1]$$

$$\Rightarrow 0 \leq d_{TIF_i}(A,B) \leq 1$$

Hence,

$$d_{g_i}(A,B) \times d_{TIF_i}(A,B) \in [0,1]$$

$$\Rightarrow d_N^{Avg}(A,B) = \frac{\sum_{i=1}^{n} d_{g_i}(A,B) \times d_{TIF_i}(A,B)}{n} \in [0,1]$$

Property ii: $d_N^{Avg}(A,B) = d_N^{Avg}(B,A)$

It is obvious that,

$T_A(x_i) - T_B(x_i) \neq T_B(x_i) - T_A(x_i)$,
$I_A(x_i) - I_B(x_i) \neq I_B(x_i) - I_A(x_i)$, and
$F_A(x_i) - F_B(x_i) \neq F_B(x_i) - F_A(x_i)$

But,

$|T_A(x_i) - T_B(x_i)| = |T_B(x_i) - T_A(x_i)|$,
$|I_A(x_i) - I_B(x_i)| = |I_B(x_i) - I_A(x_i)|$, and
$|F_A(x_i) - T_B(x_i)| = |F_B(x_i) - F_A(x_i)|$

Hence, $d_N^{Avg}(A,B) = \frac{\sum_{i=1}^{n} d_{g_i}(A,B) \times d_{TIF_i}(A,B)}{n} \in [0,1]$

$\Rightarrow d_{g_i}(A,B) \times d_{TIF_i}(A,B)$

$$= 1 - exp\left(\frac{-\sqrt{\left(T_A(x_i) - T_B(x_i)\right)^2 + \left(I_A(x_i) - I_B(x_i)\right)^2 + \left(F_A(x_i) - F_B(x_i)\right)^2}}{\gamma} \right) \times \frac{|T_A(x_i) - T_B(x_i)| + |I_A(x_i) - I_B(x_i)| + |F_A(x_i) - F_B(x_i)|}{3}$$

$$= 1 - exp\left(\frac{-\sqrt{\left(T_B(x_i) - T_A(x_i)\right)^2 + \left(I_B(x_i) - I_A(x_i)\right)^2 + \left(F_B(x_i) - F_A(x_i)\right)^2}}{\gamma} \right) \times \frac{|T_B(x_i) - T_A(x_i)| + |I_B(x_i) - I_A(x_i)| + |F_B(x_i) - F_A(x_i)|}{3}$$

$= d_{g_i}(B,A) \times d_{TIF_i}(B,A)$

Hence,

$$\frac{\sum_{i=1}^{n} d_{g_i}(A,B) \times d_{TIF_i}(A,B)}{n} = \frac{\sum_{i=1}^{n} d_{g_i}(B,A) \times d_{TIF_i}(B,A)}{n} = d_N^{Avg}(B,A)$$

Property iii: $d_N^{Avg}(A,B) = 0$ if and only if $A = B$

1) If $A = B$, then
   $T_A(x_i) = T_B(x_i)$,
   $I_A(x_i) = I_B(x_i)$, and
   $F_A(x_i) = F_B(x_i)$.

which means,
   $|T_A(x_i) - T_B(x_i)| = 0$,
   $|I_A(x_i) - I_B(x_i)| = 0$, and
   $|F_A(x_i) - F_B(x_i)| = 0$

Thus,

$$\Rightarrow d_{TIF_i}(A,B) = \frac{|T_A(x_i) - T_B(x_i)| + |I_A(x_i) - I_B(x_i)| + |F_A(x_i) - F_B(x_i)|}{3} = 0$$

Hence,

$$\Rightarrow d_N^{Avg}(A,B) = \frac{\sum_{i=1}^{n} d_{g_i}(A,B) \times (0)}{n} = 0$$

2) If $d_N^{Avg}(A,B) = 0$,

$$\Rightarrow \frac{\sum_{i=1}^{n} d_{g_i}(A,B) \times d_{TIF_i}(A,B)}{n} = 0$$

There exist either $d_{g_i}(A,B) = 0$ or $d_{TIF_i}(A,B) = 0$ such that :

(i) $d_{g_i}(A,B) = 1 - exp\left\{\frac{\left(-E_i(A,B)\right)}{\gamma}\right\} = 0$

$$\Rightarrow exp\left\{\frac{\left(-E_i(A,B)\right)}{\gamma}\right\} = 1$$

$$\Rightarrow \frac{E_i(A,B)}{\gamma} = 0$$

$$\Rightarrow \sqrt{\left(T_A(x_i) - T_B(x_i)\right)^2 + \left(I_A(x_i) - I_B(x_i)\right)^2 + \left(F_A(x_i) - F_B(x_i)\right)^2} = 0$$

This implies $T_A(x_i) = T_B(x_i)$ and $I_A(x_i) = I_B(x_i)$ and $F_A(x_i) = F_B(x_i)$.
That means, $A = B$.

(ii) $d_{TIF_i}(A,B) = 0$

$$\Rightarrow d_{TIF_i}(A,B) = \frac{|T_A(x_i) - T_B(x_i)| + |I_A(x_i) - I_B(x_i)| + |F_A(x_i) - F_B(x_i)|}{3} = 0$$

Namely, we can have
$|T_A(x_i) - T_B(x_i)| = 0$,
$|I_A(x_i) - I_B(x_i)| = 0$, and
$|F_A(x_i) - F_B(x_i)| = 0$.

Implies $T_A(x_i) = T_B, (x_i)$, $I_A(x_i) = I_B(x_i)$, and $F_A(x_i) = F_B(x_i)$
That means, $A = B$.
Therefore $d_N^{Avg}(A,B) = 0$ if and only if $A = B$

Property iv: $d_N^{Avg}(A,C) \geq d_N^{Avg}(A,B)$ and $d_N^{Avg}(A,C) \geq d_N^{Avg}(B,C)$ if C is neutrosophic set in X and $A \subseteq B \subseteq C$.

Consider we have $C = \{x_i, T_c(x_i), I_c(x_i), F_c(x_i): x_i \in X\}$.
We know that $A \subseteq B$ if an only if $\forall_x \in X$:
$T_A(x_i) \leq T_B(x_i)$ $I_A(x_i) \geq I_B(x_i)$ and
$F_A(x_i) \geq F_B(x_i)$
Let $A \subseteq B \subseteq C$, then we have
$T_A(x_i) \leq T_B(x_i) \leq T_C(x_i)$ $I_A(x_i) \geq I_B(x_i) \geq I_C(x_i)$ and
$F_A(x_i) \geq F_B(x_i) \geq F_C(x_i)$

Then, we can get

$$\Rightarrow 1 - exp\left(\frac{-\sqrt{\left(T_A(x_i) - T_C(x_i)\right)^2 + \left(I_A(x_i) - I_C(x_i)\right)^2 + \left(F_A(x_i) - F_C(x_i)\right)^2}}{\gamma}\right) \geq$$

$$1 - exp\left(\frac{-\sqrt{\left(T_A(x_i) - T_B(x_i)\right)^2 + \left(I_A(x_i) - I_B(x_i)\right)^2 + \left(F_A(x_i) - F_B(x_i)\right)^2}}{\gamma}\right)$$

and

$$\Rightarrow \frac{|T_A(x_i) - T_C(x_i)| + |I_A(x_i) - I_C(x_i)| + |F_A(x_i) - F_C(x_i)|}{3} \geq \frac{|T_A(x_i) - T_B(x_i)| + |I_A(x_i) - I_B(x_i)| + |F_A(x_i) - F_B(x_i)|}{3}$$

That implies $d_{g_i}(A, C) \geq d_{g_i}(A, B)$ and $d_{TIF_i}(A, C) \geq d_{TIF_i}(A, B)$.

Namely, we have $d_N^{Avg}(A, C) \geq d_N^{Avg}(A, B)$

Then, similarly for $d_N^{Avg}(A, C) \geq d_N^{Avg}(B, C)$.

$$\Rightarrow 1 - exp\left(\frac{-\sqrt{\left(T_A(x_i) - T_C(x_i)\right)^2 + \left(I_A(x_i) - I_C(x_i)\right)^2 + \left(F_A(x_i) - F_C(x_i)\right)^2}}{\gamma}\right) \geq$$

$$1 - exp\left(\frac{-\sqrt{\left(T_B(x_i) - T_C(x_i)\right)^2 + \left(I_B(x_i) - I_C(x_i)\right)^2 + \left(F_B(x_i) - F_C(x_i)\right)^2}}{\gamma}\right)$$

and

$$\Rightarrow \frac{|T_A(x_i) - T_C(x_i)| + |I_A(x_i) - I_C(x_i)| + |F_A(x_i) - F_C(x_i)|}{3} \geq \frac{|T_B(x_i) - T_C(x_i)| + |I_B(x_i) - I_C(x_i)| + |F_B(x_i) - F_C(x_i)|}{3}$$

Thus, we can get $d_{g_i}(A, C) \geq d_{g_i}(B, C)$ and $d_{TIF_i}(A, C) \geq d_{TIF_i}(B, C)$, which means $d_N^{Avg}(A, C) \geq d_N^{Avg}(B, C)$.

The proof is completed. ■

4. TOPSIS-Sine Trigonometric SVN Weighted Aggregation Operator with Average Distance Measure

This study follows the steps in [33] but uses different aggregation operator and distance measure. The sine trigonometric aggregator operation by [21] and the new average distance measure are applied here. The secondary data is obtained from [31] regarding the dental students' emergency knowledge in attaining correct diagnosis and providing accurate treatment.

4.1. Data Extraction

The data on the knowledge level of the dental students in medical emergencies are given in the linguistic form with two evaluation criteria i.e diagnosis and treatment knowledge. The students' responses are recorded according to the seven-Likert scale and the associated SVN numbers are assigned to the scales as shown in Table 2. The SVN numbers are placed in two matrices denoted as $X = x_{ij}$ and $Y = y_{ik}$ where i = 1, … , 20 ; j =1, … , 10 and k = 1, … , 14 with $x_{ij} =< T_{ij}, I_{ij}, F_{ij} >$ and $y_{ik} =< T_{ik}, I_{ik}, F_{ik} >$.

Table 2. Linguistic term used [31]

Linguistic Term	SVN Numbers
Excellent (E)	(1,0,0)
Very Good (VG)	(0.80,0.15,0.20)
Good (G)	(0.60,0.35,0.40)
Regular (R)	(0.50,0.50,0.50)
Regular Tending to Bad (RB)	(0.40,0.65,0.60)
Bad (B)	(0.20,0.85,0.80)
Very Bad (VB)	(0,1,1)

4.2. Aggregation of the students' responses

The SVN data is aggregated by using the sine trigonometric aggregation operators [13]. The aggregation calculation of the knowledge level for 20 students in diagnosis and treatment uses equal weights; $w_j = 0.1$ for the 10 diagnosis questions and $w_k = 0.07$ for the 14 treatment questions.

Definition 4.1: Let $A = \{ x_{ij}, y_{ik}, T_A(p), I_A(p), F_A(p): x_{ij} \in X \text{ and } y_{ik} \in Y \}$ be a SVNS for diagnosis or treatment knowledge evaluation. Then, sine trigonometric weighted averaging aggregation operator for the SVNS (ST-SVNWA) by [21] is defined in equation (10).

$$\text{ST-SVNWA } (A) = \sum_{p=1}^{n} w_p sin(x_p)$$

$$= \left\langle 1 - \prod_{p=1}^{n} \left(1 - sin\left(\frac{\pi}{2} T_{A_p}\right)\right)^{w_p}, \prod_{p=1}^{n} \left(1 - sin\left(\frac{\pi}{2} - I_{A_p}\right)\right)^{w_p}, \prod_{p=1}^{n} \left(1 - sin\left(\frac{\pi}{2} - F_{A_p}\right)\right)^{w_p} \right\rangle \tag{10}$$

The aggregated values are defined in two weighted neutrosophic decision column matrices which denoted by $D^p = \langle d_i^{w_p} \rangle_{20\times1} = \langle T_i^{w_p}, I_i^{w_p}, F_i^{w_p} \rangle_{20\times1}$. At this point forward, the p index will be used to generalize the use of indices j and k representing diagnosis and treatment SVN data values, respectively. If diagnosis SVN numbers are aggregated, w_p equals to w_j and w_p equals to w_k whenever treatment SVN data is aggregated.

4.3. Identify neutrosophic relative positive ideal solution (NRPIS) and neutrosophic relative negative ideal solution (NRNIS)

From each of the two column matrices obtained in the previous subsection, two ideal solutions NRPIS, $d^{w_p^+}$ and NRNIS, $d^{w_p^-}$ are produced by performing the evaluation criteria on benefit-type attribute, J_1 and cost-type attribute, J_2 which defined in equation (11) and (12) [25].

$$d^{w_p^+} = \langle T^{w_p^+}, I^{w_p^+}, F^{w_p^+} \rangle \tag{11}$$

$$d^{w_p^-} = \langle T^{w_p^-}, I^{w_p^-}, F^{w_p^-} \rangle \tag{12}$$

where

$$T^{w_p^+} = \left\{ \left(\max_i \{T_i^{w_p}\} | i \in J_1 \right), \left(\min_i \{T_i^{w_p}\} | i \in J_2 \right) \right\};$$

$$T^{w_p^-} = \left\{ \left(\min_i \{T_i^{w_p}\} | j \in J_1 \right), \left(\max_i \{T_i^{w_p}\} | i \in J_2 \right) \right\}$$

$$I^{w_p^+} = \left\{ \left(\min_i \{I_i^{w_p}\} | i \in J_1 \right), \left(\max_i \{I_i^{w_p}\} | i \in J_2 \right) \right\};$$

$$I^{w_p^-} = \left\{ \left(\max_i \{I_i^{w_p}\} | j \in J_1 \right), \left(\min_i \{I_i^{w_p}\} | i \in J_2 \right) \right\}$$

$$F^{w_p^+} = \left\{\left(\min_i\{F_i^{w_p}\}|i \in J_1\right), \left(\max_i\{F_i^{w_p}\}|i \in J_2\right)\right\};$$
$$F^{w_p^-} = \left\{\left(\max_i\{F_i^{w_p}\}|j \in J_1\right), \left(\min_i\{F_i^{w_p}\}|i \in J_2\right)\right\}$$

4.4. Calculate the new distance measure for each alternatives

The determination of the new distance measure value in equation (6) requires the calculation of two distance measures in equations (7) and (9). All three equations denote two different neutrosophic sets, A and B. Here, set A is defined as the aggregated decision matrix obtained in subsection 4.2, and set B represents either NRPIS or NRNIS obtained in section 4.3. The whole calculation in this present subsection produces average distance measures for each alternative from NRPIS, D_i^{p+} and average distance measures for each alternative from NRNIS, D_i^{p-}. Since the aggregation process was performed in Section 4.2, Equation (6) has been deduced into Equations (13) and (14), representing D_i^{p+} and D_i^{p-}, respectively.

$$D_i^{p+} = \frac{\sum_{i=1}^{n} d_{g_i}^{p^+}(A, NRPIS) \times d_{TIF_i}^{p^+}(A, NRPIS)}{n} \tag{13}$$

$$D_i^{p-} = \frac{\sum_{i=1}^{n} d_{g_i}^{p^-}(A, NRNIS) \times d_{TIF_i}^{p^-}(A, NRNIS)}{n} \tag{14}$$

4.5. Evaluate the relative closeness coefficient

The relative closeness coefficient denoted by C_i^{p*} in equation (15) ranges between 0 and 1 is determined by the neutrosophic ideal solution for SVNSs for each distance measure.

$$C_i^{p*} = \frac{D_i^{p-}}{D_i^{p+} + D_i^{p-}} \tag{15}$$

Students who obtained $C_i^{p*} > 0.5$ are considered to have higher knowledge of dental medical emergencies compared to those obtained C_i^{p*} less than 0.5.

4.6. Rank the alternative and discuss the analysis

The conclusion on the overall knowledge level of the dental students can be drawn by ranking the values of C_i^{p*} in ascending order. The performance analysis is also done by comparing different distance measures and aggregator operators.

5. Result and Discussion

The study aims to analyze the knowledge level of dental students on medical emergency diagnosis and treatment. The results of the aggregation process by the ST-SVNWA operator on the diagnosis and treatment of dental emergencies data are shown in Table 3.

Table 3. Aggregated sine trigonometric SVN data

Student, S_i	**Diagnosis**	**Treatment**
1	<0.52665, 0.22592, 0.20286>	<0.56978, 0.20318, 0.18640>
2	<0.76036, 0.08690, 0.10208>	<0.92389, 0.01970, 0.03169>
3	<0.59429, 0.18419, 0.17255>	<0.69440, 0.13054, 0.13012>
4	<0.81610, 0.06179, 0.07775>	<0.89869, 0.02807, 0.04231>
5	<0.57312, 0.20396, 0.18166 >	<0.76092, 0.08690, 0.10118>
6	<0.57312, 0.20396, 0.18166>	<0.73688, 0.10208, 0.11160>
7	<0.57312, 0.20396, 0.18166>	<0.67363, 0.14336,0.13939>
8	<0.59461, 0.19379, 0.17191>	<0.72065, 0.11263, 0.11867>
9	<0.81610, 0.06179, 0.07775>	<0.87742, 0.03554, 0.05130>
10	<0.53486, 0.22589, 0.19891>	<0.69986, 0.12537, 0.12787>
11	<0.51831, 0.22594, 0.20688>	<0.60444, 0.18252, 0.17063>
12	<0.54256, 0.21468, 0.19578 >	<0.47846, 0.25181, 0.22864>
13	<0.76036, 0.08690, 0.10208>	<0.91627, 0.02216, 0.03490>
14	<0.49277, 0.23779, 0.21862>	<0.57501, 0.20316, 0.18385>
15	<0.85888, 0.04393, 0.08761>	<0.89869, 0.02807, 0.04231>
16	<0.68773, 0.12222, 0.13402>	<0.88856, 0.03158, 0.04659>
17	<0.50981, 0.22596, 0.21099>	<0.69074, 0.13169, 0.13186>
18	<0.55049, 0.21466, 0.19197>	<0.69074, 0.13169, 0.13186>
19	<0.85888, 0.04393, 0.05922>	<0.88856, 0.03158, 0.04659>
20	<0.50156, 0.23777, 0.21437>	<0.69074, 0.13169, 0.13186>

Based on the aggregated SVN data in Table 3, with $\gamma = 0.2$, the average distance measures, D_i^{j-} and D_i^{j+} per student are computed. Subsequently, the relative closeness coefficient for diagnosis data, C_i^{j*} is determined. The values are shown in Table 4 and compared with the ones obtained using the Euclidean distance measure.

Table 4. Distance and relative closeness coefficient values - Diagnosis

	New Average Distance				**Euclidean Distance**			
Student, S_i	D_i^{j-}	D_i^{j+}	C_i^{j*}	**Rank**	D_i^{j-}	D_i^{j+}	C_i^{j*}	**Rank**
1	0.00365	0.19035	0.01882	16	0.02264	0.23389	0.08825	16
2	0.14384	0.02699	0.84200	5	0.18970	0.06680	0.73956	5
3	0.03093	0.13788	0.18323	8	0.07142	0.18486	0.27867	8
4	0.18366	0.00583	0.96924	3	0.22757	0.02882	0.88759	3
5	0.01900	0.15644	0.10831	10	0.05467	0.20187	0.21310	10
6	0.01900	0.15644	0.10831	10	0.05467	0.20187	0.21310	10
7	0.01900	0.15644	0.10831	10	0.05467	0.20187	0.21310	10
8	0.02902	0.14086	0.17085	9	0.06950	0.18708	0.27086	9
9	0.18366	0.00583	0.96924	3	0.22757	0.02882	0.88759	3
10	0.00524	0.18566	0.02744	15	0.02770	0.22921	0.10781	15
11	0.00232	0.19514	0.01173	17	0.01761	0.23869	0.06871	17
12	0.00821	0.17748	0.04420	14	0.03433	0.22200	0.13392	14
13	0.14384	0.02699	0.84200	5	0.18970	0.06680	0.73956	5
14	0.00000	0.21373	0.00000	20	0.00000	0.25627	0.00000	20
15	0.20409	0.00125	0.99390	2	0.25085	0.01639	0.93868	2
16	0.09242	0.06882	0.57318	7	0.13967	0.11693	0.54431	7
17	0.00127	0.20001	0.00633	18	0.01276	0.24359	0.04978	18
18	0.01028	0.17293	0.05613	13	0.03906	0.21746	0.15226	13
19	0.21373	0.00000	1.00000	1	0.25627	0.00000	1.00000	1
20	0.00021	0.20870	0.00099	19	0.00564	0.25121	0.02195	19

In Table 4, the ranking for both distance measures give an equivalent result. There are 7 (35%) students (S_2, S_4, S_9, S_{13}, S_{15}, S_{16}, S_{19}) who obtained the values of C_i^{j*} greater than 0.5 which indicates that they have better understanding in providing correct diagnosis to dental emergencies. Meanwhile, 6 (30%) students (S_1, S_{10}, S_{11}, S_{14}, S_{17}, S_{20}) are ranked at the bottom of the list, showing that they are lacking knowledge in dental emergencies diagnosis. The comparative analysis of the top-ranking students on the dental diagnosis emergency knowledge with the previous studies [31, 33] is illustrated in Table 5.

Table 5. Summary of students' knowledge level on the diagnosis of emergency cases

Techniques	Ranking Order
Scoring function, [31]	$S_{15}, S_{19} > S_4, S_9 > S_2$
Generalized TOPSIS, [33]	$S_{15}, S_{19} > S_2 > S_4, S_9$
ST-SVNWA aggregation operator with average distance	$S_{19} > S_{15} > S_4, S_9 > S_2 > S_{13}$
ST-SVNWA aggregation operator with Euclidean distance	$S_{19} > S_{15} > S_4, S_9 > S_2, S_{13}$
ST-SVNWA aggregation operator with distance measure [7]	$S_{15} > S_{19} > S_4, S_9 > S_2, S_{13}$
Weighted Arithmetic AO with average distance	$S_4, S_9 > S_{19} > S_{15} > S_2, S_{13} >$

The summary result of students' knowledge level in diagnosing patients is shown in Table 5. It highlights the top five ranking of the students derived from different AO and distance measures involving seven students, i.e S_2, S_4, S_9, S_{13}, S_{15}, S_{16}, and S_{19}. It is obvious that students 15 and 19 received the highest score in diagnosing the patient in emergency cases, indicating that both are the most knowledgeable compared to other students.

Table 6 compares the ranking between two distance measures for the dental students' knowledge in giving treatment to dental medical emergencies.

Table 6. Distance and relative closeness coefficient values - Treatment

	New Average Distance				Euclidean Distance			
Student, S_i	D_i^{k-}	D_i^{k+}	C_i^{k*}	**Rank**	D_i^{k-}	D_i^{k+}	C_i^{k*}	**Rank**
1	0.02600	0.20358	0.11324	19	0.06452	0.24698	0.20713	19
2	0.27186	0.00000	1.00000	1	0.31148	0.00000	1.00000	1
3	0.10693	0.10894	0.49534	12	0.15388	0.15773	0.49382	12
4	0.25529	0.00196	0.99237	3	0.29517	0.01651	0.94704	3
5	0.15848	0.06116	0.72156	8	0.20267	0.10940	0.64944	8
6	0.13986	0.07756	0.64326	9	0.18520	0.12668	0.59382	9
7	0.09160	0.12458	0.42373	16	0.13882	0.17274	0.44557	16
8	0.12727	0.08921	0.58790	10	0.17332	0.13845	0.55591	10
9	0.24107	0.00634	0.97436	7	0.28130	0.03052	0.90212	7
10	0.11157	0.10436	0.51669	11	0.15828	0.15341	0.50782	11
11	0.04554	0.17679	0.20483	17	0.08951	0.22201	0.28735	17
12	0.00000	0.27186	0.00000	20	0.00000	0.31148	0.00000	20
13	0.26689	0.00019	0.99930	2	0.30657	0.00498	0.98403	2

14	0.02805	0.20058	0.12270	18	0.06756	0.24394	0.21689	18
15	0.25529	0.00196	0.99237	3	0.29517	0.01651	0.94704	3
16	0.24855	0.00376	0.98508	5	0.28857	0.02317	0.92567	5
17	0.10454	0.11135	0.48424	13	0.15150	0.16014	0.48615	13
18	0.10454	0.11135	0.48424	13	0.15150	0.16014	0.48615	13
19	0.24855	0.00376	0.98508	5	0.28857	0.02317	0.92567	5
20	0.10454	0.11135	0.48424	13	0.15150	0.16014	0.48615	13

In Table 6, there are 11 (55%) students who obtained values $C_{\square}^{k*}$ of greater than 0.5 for both distance measures, which indicates that they have a better understanding in giving correct treatment to dental emergencies. Among these 11 students, 7 (S_2, S_4, S_9, S_{13}, S_{15}, S_{16}, and S_{19}) of them are the same students that acquired the higher $C_{\square}^{k*}$ values in Table 3. Meanwhile, there are 4 (20%) of the same students who are ranked at the bottom of the list, showing that they lack knowledge in dental emergency treatment. Obviously, the two same students (S_{11}, S_{14}) obtain lower $C_{\square}^{k*}$ values in both Table 4 and Table 6.

The comparative analysis of the top-ranking students, on the dental treatment emergency knowledge with the previous studies [31, 33] is illustrated in Table 7.

Table 7. Summary of students' knowledge level on the treatment of emergency cases

Techniques	**Ranking Order**
Scoring function, [31]	$S_2 > S_{13} > S_4 > S_{15} > S_9$
Generalized TOPSIS, [33]	$S_2 > S_{13} > S_4 > S_{15} > S_{16}$
Sine trigonometric weighted averaging AO with average distance	$S_2 > S_{13} > S_4, S_{15} > S_{16}, S_{19}$
Sine trigonometric weighted averaging AO with Euclidean Distance	$S_2 > S_{13} > S_4, S_{15} > S_{16}, S_{19}$
Sine trigonometric weighted averaging AO with distance measure [7]	$S_2 > S_{13} > S_4, S_{15} > S_{16}, S_{19}$
Weighted Arithmetic AO with average distance	$S_2 > S_{13} > S_4, S_{15} > S_{16}, S_{19}$

From Table 7, the same seven students are listed as the top five students when compared to the findings in Table 5. Here, it is obvious that student 2 is identified as the most knowledgeable in giving correct emergency treatment for all techniques of measurement. The use of two AOs for two different distance measures results in the equivalent ranking of the top four students (S_2, S_{13}, S_4, and S_{15}).

6. Conclusion and Recommendation

In this work, a new distance measure has been proposed for use with the TOPSIS approach in ranking the level of dentistry students' knowledge in medical emergencies, applying the existing data from [31]. The new distance measures for single-valued neutrosophic sets are developed and demonstrated in this study. The effectiveness of the new distance measure formula is analyzed, and it is found to be consistent with the existing distance measures. The analyses demonstrate the effectiveness of the novel distance-based similarity measure for truth, indeterminacy, and falsity membership functions.

In this task, a sine trigonometric weighted averaging aggregation operator [21] is applied. It is found that this aggregation operator is significantly efficient for handling uncertainty in decision-making problems. The functionality of this method is tested by determining the level of knowledge of dentistry students in medical emergencies. To evaluate its performance, a comparison with several published works is conducted. The outcome of the investigation demonstrates that it is reliable due to the consistency of the findings with the previous studies.

The method approach used in this work is believed to create more opportunities for future research in the field of neutrosophic decision-making. It will be applied to other uncertain fields, such as risk analysis, fault diagnosis, and evaluation systems.

References

1. Zadeh, L. A. (1965). Fuzzy sets. *Information and control,* 8(3), 338-353.
2. Smarandache, F. (1998). *Neutrosophy: neutrosophic probability, set, and logic: analytic synthesis & synthetic analysis.* American Research Press.
3. Atanassov, K. T. (1986). Intuitionistic fuzzy sets. *Fuzzy Sets and Systems,* 20(1), 87-96.
4. Wang, H., Smarandache, F., Zhang, Y., & Sunderraman, R. (2010). Single valued neutrosophic sets. *Multispace Multistruct*, 4, 410-413.
5. Zahan, N., Islam, F., & Mahmud, S. (2020). Improvement of the student-teacher learning interface with selecting and designing a teaching method. *International Journal of Research in Industrial Engineering,* 9(3), 247-259.
6. Patel, A., Jana, S., & Mahanta, J. (2023). Intuitionistic fuzzy EM-SWARA-TOPSIS approach based on new distance measure to assess the medical waste treatment techniques. *Applied Soft Computing*, 144, 110521.
7. Mustapha, N., Alias, S., Md Yasin, R., Abdullah, I., & Broumi, S. (2021) Cardiovascular disease risk analysis using distance-based similarity measure neutrosophic sets. *Neutrosophic Sets and Systems*, 47, 26-37.
8. Mustapha, N., Alias, S., Md Yasin, R., Mohd Yusof, N. N., Fakhrarazi, N. N., & Nik Hassan, N. N. A. (2020). New entropy concept for single value neutrosophic sets with application in medical diagnosis. *International Journal of Neutrosophic Science,* 19(1), 375-383.
9. Alias, S., Mustapha, N., Md Yasin, R., Mohd Yusoff, N. S., & Mohamad, S. N. F. (2022). Medical diagnosis similarity measure in rough-cosine neutrosophic set environment. *Journal of Mathematics and Computing Science*, 8(2), 79-87.
10. Kirişci, M., & Şimşek, N. (2022). Decision making method related to Pythagorean fuzzy soft sets with infectious diseases application. *Journal of King Saud University - Computer and Information Sciences*, 34(8), Part B, 5968-5978.

11. Singh, A., & Kumar, S. (2023). Picture fuzzy VIKOR-TOPSIS approach based on knowledge and accuracy measures for suitable adsorbent decision making. *Applied Soft Computing*, 147, 110807.
12. Gupta, R. & Kumar, S. (2024). Novel similarity measure between hesitant fuzzy set and their applications in pattern recognition and clustering analysis. *Journal of Engineering and Applied Science*, 71(1), 5.
13. Edalatpanah, S. A., & Smarandache, F. (2023). Introduction to the special issue on advances in neutrosophic and plithogenic sets for engineering and sciences: theory, models, and applications, *Computer Modeling in Engineering & Sciences*, 134(2), 817-819.
14. Debnath, S. (2021). Fuzzy hypersoft sets and its weightage operator for decision making. *Journal of Fuzzy Extension and Applications*, 2(2), 163-170.
15. Ye, J. A. (2014). Multicriteria decision-making method using aggregation operators for simplified neutrosophic Sets. *Journal of Intelligent and Fuzzy System,* 2459-2466.
16. Lu, Z., & Ye, J. (2017). Single-valued neutrosophic hybrid arithmetic and geometric aggregation operators and their decision-making method. *Information*, 8(3), 1–12.
17. Liu,P., & Shi, L. (2015).The generalized hybrid weighted average operator based on interval neutrosophic hesitant set and its application to multiple attribute decision making. *Neural Computing and Applications,* 26, 457–471.
18. Liu, P., & Wang, Y. (2014). Multiple attribute decision-making method based on single-valued neutrosophic normalized weighted Bonferroni mean. *Neural Computing and Applications*, 25, 2001–2010.
19. Yang, L., & Li, B. (2016). A Multi-criteria decision-making method using power aggregation operators for single-valued neutrosophic sets. *International Journal of Database and Theory and Application*, 9(2), 23-32.
20. Garg, H., & Nancy. (2018). New logarithmic operational laws and their applications to multiattribute decision-making for single-valued neutrosophic numbers. *Cognitive Systems Research,* 52, 931-946**.**
21. Ashraf, S., Abdullah, S., Zeng, S., Jin, H., & Ghani, F. (2020). Fuzzy decision support modeling for hydrogen power plant selection based on single valued neutrosophic sine trigonometric aggregation operators. *Symmetry*, 12(2), 298.
22. Bhat, S. (2023). An enhanced AHP group decision-making model employing neutrosophic trapezoidal numbers. *Journal of Operational and Strategic Analytics*, 1(2), 81-89.
23. Mao, X., Guoxi, Z., Fallah, M., & Edalatpanah, S. A. (2020). A neutrosophic-based approach in data envelopment analysis with undesirable outputs. *Mathematical Problems in Engineering*, 2020(4):1-8.
24. Hwang, C.-L., & Yoon, K. (1981). Methods for multiple attribute decision making. In *Multiple Attribute Decision Making. Lecture Notes in Economics and Mathematical Systems*, Springer: Berlin, Heidelberg, 58-191.
25. Biswas, P., Pramanik, S., & C. Giri, B. C. (2016). TOPSIS method for multi-attribute group decision-making under single-valued neutrosophic environment. *Neural Comput & Applic,* 27, 727–737.
26. Al-Nami, W. T. (2023). Ranking and analysis the strategies of crowd management to reduce the risks of crushes and stampedes in crowded environments and ensure the safety of passengers. *Neutrosophic Sets and Systems*, 8, 61-78.
27. Pramanik, S., Das, S., Das, R., & Tripathy, B. C. (2023). Neutrosophic BWM-TOPSIS strategy under SVNS environment. *Neutrosophic Sets and Systems*, 56, 178-189.
28. Başhan, V., Demirel, H., & Gul, M. (2020). An FMEA-based TOPSIS approach under single valued neutrosophic sets for maritime risk evaluation: the case of ship navigation safety. *Soft Computing,* 24, 18749–18764.
29. Zeng, W., Cui, H., Liu, Y., Yin, Q., & Xu, Z. (2022). Novel distance measure between intuitionistic fuzzy sets and its application in pattern recognition. *Iranian Journal of Fuzzy Systems*, 19(3), 127–137.
30. Ruzon, M. A., & Tomasi, C. (2001). Edge, junction, and corner detection using color distributions. *IEEE Transactions on Pattern Analysis and Machine Intelligence*, 23(11), 1281–1295.

31. Fernández, A. R., González, E. L., & Carrasco, D. L. (2020). Study on the level of knowledge in dental medical emergencies of dentistry students through neutrosophic values. *Neutrosophic Sets and Systems*, 37, 99-107.
32. Majumdar, P., & Samanta, S. K. (2014). On similarity and entropy of neutrosophic sets. *Journal of Intelligent & Fuzzy Systems*, 26(3), 1245–1252.
33. Md Yasin, R., Shamsuddin, N. A. S, Ramli, N. K., Alias, S., & Mustapha, N. (2022). Ranking knowledge level using generalized TOPSIS in single-valued neutrosophic environment. *Applied Mathematics and Computational Intelligence*, 11(1), 505–520.

Received: July 29, 2024. Accepted: Oct 20, 2024

NSS
Neutrosophic Sets and Systems, Vol. 76, 2025
University of New Mexico

Grey Relational Analysis Framework with 2-Tuple Linguistic Neutrosophic Set for Building Material Supplier Selection

Cheng Yang*
School of Architecture and Art, Ningbo Polytechnic, Ningbo, 315000, Zhejiang, China
*Correspondence: E-mail: 13967886559@163.com
https://orcid.org/0009-0008-1647-5453

Abstract: Choosing building materials suppliers is crucial as it directly affects the quality, cost, and timeline of a project. Quality suppliers ensure the reliability and consistency of materials, reducing construction risks. The right suppliers offer competitive pricing and flexible delivery schedules, helping control budgets and optimize resource use. Additionally, suppliers' professional support and technical services can enhance construction efficiency and quality. By carefully selecting suppliers, project teams can establish long-term partnerships, improving overall construction standards and market competitiveness. Thus, supplier selection is a key factor in the success of construction projects. The process of selecting and applying building material suppliers (BMSs) is a multiple-attribute group decision-making (MAGDM) method. This study constructs the 2-tuple linguistic neutrosophic number combined grey relational analysis (2TLNN-CGRA) approach, which integrates the grey relational analysis (GRA) and 2-tuple linguistic neutrosophic sets (2TLNNSs). To validate the method, a numerical example for building material supplier selection is provided, accompanied by comparative studies to highlight the effectiveness of the 2TLNN-CGRA approach. The key contributions of this research include (1) the utilization of the 2TLNN-CGRA approach to address MAGDM under 2TLNSs conditions; (2) the incorporation of both 2TLNN Hamming distance (2TLNNHD) and 2TLNN Euclidean distance (2TLNNED) within the 2TLNSs framework in the 2TLNN-CGRA approach; (3) the demonstration of the method through a numerical example for supplier selection; and (4) a series of efficient comparisons with other existing decision-making approaches.

Keywords: Multiple-attribute group decision-making (MAGDM); 2-tuple linguistic neutrosophic sets (2TLNNSs); 2TLNN-CGRA approach; building material suppliers selection

1. Introduction

The construction sector plays a pivotal role in stimulating economic development and serves as a key driver of economic expansion. In today's era, marked by rapid technological progress and increasing economic globalization, China's construction market has evolved into a dynamic arena characterized by significant potential, lucrative opportunities, and robust growth [1, 2]. Its impact is profound, not only in terms of its direct contributions to economic value within the sector but also through its influence on the expansion of more than a dozen related industries. Predominantly made up of small and medium-sized enterprises (SMEs), which account for over 90% of

its composition, the construction industry is integral to both urban and rural development in China [3]. These SMEs play a vital role in redistributing the rural labor force towards urban centers, thus driving significant socio-economic changes. Unlike the manufacturing sector, which also operates on an order-based production model, the construction industry handles a diverse range of products. Each construction project is subject to meticulous phases of planning, design, bidding, and procurement, and is uniquely bound by specific constraints on time, quality, and cost [4, 5]. The construction industry is distinguished by several unique features: it operates in specific, unchangeable locations where both production and consumption occur, requiring tailored design and construction due to the diversity and variability of each site, as opposed to standardized mass production. A project typically cannot commence without the direct involvement of the property owner. Furthermore, the sector is labor-intensive, demanding a substantial human workforce. It also exhibits long production timelines and large-scale projects that are marked by phased execution and operational fluidity[6, 7] and a production process involving multiple interdependent sub-projects and departments, requiring close collaboration to ensure seamless progress, highlighting the systematic nature of the industry [8, 9]. As competition in the construction materials market intensifies, no single enterprise can cover the entire lifecycle of a construction project independently. Collaboration across various systems is essential in the phases of design, procurement, construction, and operations. Consequently, to maintain cost-effectiveness, boost competitiveness, and enhance management skills, construction firms need to focus on choosing the most appropriate supplier teams. Construction materials typically make up about 60% of the overall project expenses, underscoring the importance of optimizing supply chain efficiency and the strategic utilization of limited site space, which are key to the industry's swift progress. The way engineering materials are categorized and the procurement strategies implemented by construction companies play a pivotal role. Creating a robust supplier management system and selecting suppliers that align with the firm's strategic goals are critical for managing procurement expenses effectively and sustaining long-term cost effectiveness, thereby maximizing company profits [10]. Supplier management, as part of a company's overall strategy, plays a crucial role. Material costs, which make up 50-60% of the total project cost, have a direct impact on profitability, with a 1% reduction in procurement costs leading to a 5-10% increase in operating profits. Given the importance of material costs, strengthening cost control in this area is vital for securing profit margins [11]. Effective supplier management provides construction companies with critical insights, greatly benefiting production management, investment decisions, and mergers. High-quality supplier management enables companies to quickly source superior products and services at competitive prices, significantly contributing to profitability [12]. Moreover, securing supply during shortages of essential raw materials or services provides a competitive edge. To maintain this advantage, companies must continuously optimize their supplier management systems, driving strategic growth in the supply chain field.

MAGDM is a structured approach used to tackle complex decision problems involving multiple criteria and stakeholders [13, 14]. This methodology facilitates a systematic evaluation of various alternatives based on a set of predefined attributes, allowing a group of decision-makers to reach a consensus or informed decision. MAGDM is particularly useful in scenarios where decisions require balancing diverse perspectives and interests, as it incorporates inputs from all participants, ensuring a comprehensive assessment [15-18]. The process typically involves several key steps: defining the problem and objectives, identifying decision-makers and stakeholders, selecting relevant attributes, gathering and processing data, and finally, applying an appropriate decision-making model to aggregate preferences and rank the alternatives[19-23]. Techniques like TOPSIS [24] and GRA [25] are commonly used within this framework. MAGDM is widely applicable in fields ranging from business and engineering to public policy and healthcare, where decisions impact multiple people and operational facets [26, 27]. The approach not only supports a democratic decision-making process but also enhances the legitimacy and acceptance of the final decision by involving all key stakeholders [28, 29]. The evaluation and selection of BMSs utilize a MAGDM approach. The 2TLNNSs [30-33] serve as effective approach for handling uncertain data during

the BMSs evaluation and selection. Deng [34] established the GRA approach. In comparison to other MADM approaches, the GRA approach [35-42] is adept at managing the shape similarity between each option from the positive ideal alternative (PIA) and negative ideal alternative (NIA). In this study, the 2TLNN-CGRA approach is developed, integrating the principles of GRA approach and 2TLNNSs. A numerical example specifically for BMS selection has been created, and several distinct comparisons have been conducted to validate the effectiveness of 2TLNN-CGRA approach. The primary research objectives and motivations are outlined: (1) 2TLNN-CGRA approach is constructed to address MAGDM challenges using 2TLNSs; (2) The 2TLNN-CGRA approach is constructed simultaneously in line with 2TLNNHD and 2TLNNED; (3)A numerical example for BMSs evaluation and selection is presented to demonstrate the application of the 2TLNN-CGRA approach; (4) Comparative analysis is conducted with several decision-making approaches to highlight the advantages of the new method.

The fundamental structure of this research is outlined as follows: Section 2 details the construction of the 2TLNNSs. In Section 3, the 2TLNN-CGRA method is developed to address the MAGDM. Section 4 presents a numerical example for evaluating and selecting BMSs. Finally, Section 5 summarizes the conclusions.

2. Preliminaries

Wang et al. [31] formulated the 2TLNSs.

Definition 1 [31]. Let $r\theta_1, r\theta_2, \ldots, r\theta_R$ be linguistic term sets (LTSs), and $r\theta = \{rl_0 = exceedingly\ bad, rl_1 = very\ bad, rl_2 = bad, rl_3 = medium, rl_4 = well, rl_5 = very\ well, rl_6 = exceedingly\ well\}$, then the 2TLNSs is formulated:

$$r\theta = \left\langle (rl_t, ra,), (rl_i, rb), (rl_f, rc) \right\rangle \tag{1}$$

with 2-tuple linguistic information $(rl_t, ra,), (rl_i, rb), (rl_f, rc)$ is membership, indeterminacy and non-membership and $0 \le \Delta^{-1}(rl_t, ra,) + \Delta^{-1}(rl_i, rb) + \Delta^{-1}(rl_f, rc) \le 3R$.

Definition 2[31]**.** Let $r\theta_1 = \left\langle (rl_{t_1}, ra_1,), (rl_{i_1}, rb_1), (rl_{f_1}, rc_1) \right\rangle$, $r\theta_2 = \left\langle (rl_{t_2}, ra_2,), (rl_{i_2}, rb_2), (rl_{f_2}, rc_2) \right\rangle$ be 2-tuple linguistic neutrosophic number (2TLNN), $\lambda > 0$, the novel operational laws are formulated:

$$(1)\ r\theta_1 \oplus r\theta_2 = \left\{ \begin{array}{l} \Delta\left(R\left(\dfrac{\Delta^{-1}(rl_{t_1}, ra_1,)}{R} + \dfrac{\Delta^{-1}(rl_{t_2}, ra_2,)}{R} - \dfrac{\Delta^{-1}(rl_{t_1}, ra_1,)}{R} \cdot \dfrac{\Delta^{-1}(rl_{t_2}, ra_2,)}{R} \right) \right), \\ \Delta\left(R\left(\dfrac{\Delta^{-1}(rl_{i_1}, rb_1)}{R} \cdot \dfrac{\Delta^{-1}(rl_{i_2}, rb_2)}{R} \right) \right), \Delta\left(R\left(\dfrac{\Delta^{-1}(rl_{f_1}, rc_1)}{R} \cdot \dfrac{\Delta^{-1}(rl_{f_2}, rc_2)}{R} \right) \right) \end{array} \right\}; \tag{2}$$

$$(2)\ r\theta_1 \otimes r\theta_2 = \begin{Bmatrix} \Delta\left(R\left(\frac{\Delta^{-1}\left(rl_{t_1}, ra_1,\right)}{R} + \frac{\Delta^{-1}\left(rl_{t_2}, ra_2,\right)}{R}\right)\right), \\ \Delta\left(R\left(\frac{\Delta^{-1}\left(rl_{i_1}, rb_1\right)}{R} + \frac{\Delta^{-1}\left(rl_{i_2}, rb_2\right)}{R} - \frac{\Delta^{-1}\left(rl_{i_1}, rb_1\right)}{R} \cdot \frac{\Delta^{-1}\left(rl_{i_2}, rb_2\right)}{R}\right)\right), \\ \Delta\left(R\left(\frac{\Delta^{-1}\left(rl_{f_1}, rc_1\right)}{R} + \frac{\Delta^{-1}\left(rl_{f_2}, rc_2\right)}{R} - \frac{\Delta^{-1}\left(rl_{f_1}, rc_1\right)}{R} \cdot \frac{\Delta^{-1}\left(rl_{f_2}, rc_2\right)}{R}\right)\right) \end{Bmatrix}; \quad (3)$$

$$(3)\ \lambda r\theta_1 = \left\{\Delta\left(R\left(1-\left(1-\frac{\Delta^{-1}\left(rl_{t_1}, ra_1,\right)}{R}\right)^{\lambda}\right)\right), \Delta\left(R\left(\frac{\Delta^{-1}\left(rl_{i_1}, rb_1\right)}{R}\right)^{\lambda}\right), \Delta\left(R\left(\frac{\Delta^{-1}\left(rl_{f_1}, rc_1\right)}{R}\right)^{\lambda}\right)\right\}; \quad (4)$$

(4)

$$\left(r\theta_1\right)^{\lambda} = \left\{\Delta\left(R\left(\frac{\Delta^{-1}\left(rl_{t_1}, ra_1,\right)}{R}\right)^{\lambda}\right), \Delta\left(R\left(1-\left(1-\frac{\Delta^{-1}\left(rl_{i_1}, rb_1\right)}{R}\right)^{\lambda}\right)\right), \Delta\left(R\left(1-\left(1-\frac{\Delta^{-1}\left(rl_{f_1}, rc_1\right)}{R}\right)^{\lambda}\right)\right)\right\}. \quad (5)$$

Wang et al. [31] formulated the score-value technique (SVT) and accuracy-value technique (AVT) for 2TLNNs.

Definition 3[31]**.** Let $r\theta_1 = \left\langle\left(rl_{t_1}, ra_1,\right),\left(rl_{i_1}, rb_1\right),\left(rl_{f_1}, rc_1\right)\right\rangle$, $r\theta_2 = \left\langle\left(rl_{t_2}, ra_2,\right),\left(rl_{i_2}, rb_2\right),\left(rl_{f_2}, rc_2\right)\right\rangle$, the SVF and AVF are formulated:

$$SVT\left(r\theta_1\right) = \frac{\begin{pmatrix} 2R + \Delta^{-1}\left(rl_{t_1}, ra_1,\right) \\ -\Delta^{-1}\left(rl_{i_1}, rb_1\right) - \Delta^{-1}\left(rl_{f_1}, rc_1\right) \end{pmatrix}}{3R}, \qquad SVT\left(r\theta_1\right) \in [0,1] \quad (6)$$

$$SVT\left(r\theta_2\right) = \frac{\begin{pmatrix} 2R + \Delta^{-1}\left(rl_{t_2}, ra_2,\right) \\ -\Delta^{-1}\left(rl_{i_2}, rb_2\right) - \Delta^{-1}\left(rl_{f_2}, rc_2\right) \end{pmatrix}}{3R}, \quad SVT\left(r\theta_2\right) \in [0,1] \quad (7)$$

$$AVT\left(r\theta_1\right) = \frac{1}{2R}\begin{pmatrix} R + \Delta^{-1}\left(rl_{t_1}, ra_1,\right) \\ -\Delta^{-1}\left(rl_{f_1}, rc_1\right) \end{pmatrix}, \qquad AVT\left(r\theta_1\right) \in [0,1] \quad (8)$$

$$AVT\left(r\theta_2\right) = \frac{1}{2R}\begin{pmatrix} R + \Delta^{-1}\left(rl_{t_2}, ra_2,\right) \\ -\Delta^{-1}\left(rl_{f_2}, rc_2\right) \end{pmatrix}, \quad AVT\left(r\theta_2\right) \in [0,1] \quad (9)$$

For two $r\theta_1 = \left\langle\left(rl_{t_1}, ra_1,\right),\left(rl_{i_1}, rb_1\right),\left(rl_{f_1}, rc_1\right)\right\rangle$ and $r\theta_2 = \left\langle\left(rl_{t_2}, ra_2,\right),\left(rl_{i_2}, rb_2\right),\left(rl_{f_2}, rc_2\right)\right\rangle$, the order is formulated: (1) $if\ SVT\left(r\theta_1\right) \prec SVT\left(r\theta_2\right), r\theta_1 \prec r\theta_2$; (2) $if\ SVT\left(r\theta_1\right) = SVT\left(r\theta_2\right), AVT\left(r\theta_1\right) \prec AVT\left(r\theta_2\right), r\theta_1 \prec r\theta_2$; $if\ SVT\left(r\theta_1\right) = SVT\left(r\theta_2\right),\ AVT\left(r\theta_1\right) = AVT\left(r\theta_2\right),\ r\theta_1 = r\theta_2.$

The 2TLNNWA approach [31] is formulated.

Definition 4[31]. Let $r\theta_j = \left\langle \left(rl_{t_j}, ra_j,\right), \left(rl_{i_j}, rb_j\right), \left(rl_{f_j}, rc_j\right) \right\rangle$ be 2TLNNs, 2TLNNWA approach is formulated:

$$\begin{aligned} &\text{2TLNNWA}\left(r\theta_1, r\theta_2, \ldots, r\theta_n\right) \\ &= rw_1 r\theta_1 \oplus rw_2 r\theta_2 \ldots \oplus rw_n r\theta_n = \overset{n}{\underset{j=1}{\oplus}} rw_j r\theta_j \\ &= \begin{pmatrix} \Delta\left(R\left(1 - \prod_{j=1}^{n}\left(1 - \dfrac{\Delta^{-1}\left(rl_{t_j}, ra_j,\right)}{R}\right)^{rw_j}\right)\right), \\ \Delta\left(R\prod_{j=1}^{n}\left(\dfrac{\Delta^{-1}\left(rl_{i_j}, rb_j\right)}{R}\right)^{rw_j}\right), \\ \Delta\left(R\prod_{j=1}^{n}\left(\dfrac{\Delta^{-1}\left(rl_{f_j}, rc_j\right)}{R}\right)^{rw_j}\right) \end{pmatrix} \end{aligned} \tag{10}$$

with rw_j is weight value of $r\theta_j, \sum_{j=1}^{n} rw_j = 1.$

Then the 2TLNNHD (2TLNN Hamming distance) and 2TLNNED (2TLNN Euclidean distance) [30] is formulated.

Definition 5[30]. Let $r\theta_1 = \left\langle \left(rl_{t_1}, ra_1,\right), \left(rl_{i_1}, rb_1\right), \left(rl_{f_1}, rc_1\right) \right\rangle$, $r\theta_2 = \left\langle \left(rl_{t_2}, ra_2,\right), \left(rl_{i_2}, rb_2\right), \left(rl_{f_2}, rc_2\right) \right\rangle$, then 2TLNNHD and 2TLNNED are formulated:

$$2TLNNHD\left(r\theta_1, r\theta_2\right) = \frac{1}{3}\begin{pmatrix} \left|\dfrac{\Delta^{-1}\left(rl_{t_1}, ra_1,\right) - \Delta^{-1}\left(rl_{t_2}, ra_2,\right)}{R}\right| \\ + \left|\dfrac{\Delta^{-1}\left(rl_{i_1}, rb_1\right) - \Delta^{-1}\left(rl_{i_2}, rb_2\right)}{R}\right| \\ + \left|\dfrac{\Delta^{-1}\left(rl_{f_1}, rc_1\right) - \Delta^{-1}\left(rl_{f_2}, rc_2\right)}{R}\right| \end{pmatrix} \tag{11}$$

$$2TLNNED\left(r\theta_1, r\theta_2\right) = \sqrt{\frac{1}{3}\begin{pmatrix} \left|\dfrac{\Delta^{-1}\left(rl_{t_1}, ra_1,\right) - \Delta^{-1}\left(rl_{t_2}, ra_2,\right)}{R}\right|^2 \\ + \left|\dfrac{\Delta^{-1}\left(rl_{i_1}, rb_1\right) - \Delta^{-1}\left(rl_{i_2}, rb_2\right)}{R}\right|^2 \\ + \left|\dfrac{\Delta^{-1}\left(rl_{f_1}, rc_1\right) - \Delta^{-1}\left(rl_{f_2}, rc_2\right)}{R}\right|^2 \end{pmatrix}} \tag{12}$$

3. 2TLNN-CGRA approach for MAGDM with 2TLNSs

The 2TLNN-CGRA is formulated for MAGDM. Let alternatives $RA=\left(RA_1,RA_2,\ldots,RA_m\right)$ and attributes $RB=\left(RB_1,RB_2,\ldots,RB_m\right)$ with weight values $rw=\left(rw_1,rw_2,\cdots,rw_n\right)$ and experts $RC=\left(RC_1,RC_2,\ldots,RC_m\right)$ with weight $r\omega=\left(r\omega_1,r\omega_2,\cdots,r\omega_q\right)$, the 2TLNN-CGRA approach are formulated for MAGDM.

Step 1. Formulate the 2TLNN-matrix $RM=\left[RM_{ij}^{(t)}\right]_{m\times n}$:

$$RM^{(t)}=\left[RM_{ij}^{(t)}\right]_{m\times n}=\begin{array}{c} \\ RA_1 \\ RA_2 \\ \vdots \\ RA_m \end{array}\begin{array}{c} \begin{array}{cccc} RB_1 & RB_2 & \ldots & RB_n \end{array} \\ \begin{bmatrix} RM_{11}^{(t)} & RM_{12}^{(t)} & \ldots & RM_{1n}^{(t)} \\ RM_{21}^{(t)} & RM_{22}^{(t)} & \ldots & RM_{2n}^{(t)} \\ \vdots & \vdots & \vdots & \vdots \\ RM_{m1}^{(t)} & RM_{m2}^{(t)} & \ldots & RM_{mn}^{(t)} \end{bmatrix} \end{array} \tag{13}$$

where $RM_{ij}^{(t)}=\left(\left(rl_{t_{ij}}^{(t)},ra_{ij}^{(t)},\right),\left(rl_{i_{ij}}^{(t)},rb_{ij}^{(t)},\right),\left(rl_{f_{ij}}^{(t)},rc_{ij}^{(t)},\right)\right)$ is 2TLNNs.

Step 2. Formulate the overall 2TLNN-matrix $RM=\left[RM_{ij}\right]_{m\times n}$:

$$RM=\left[RM_{ij}\right]_{m\times n}=\begin{array}{c} \\ RA_1 \\ RA_2 \\ \vdots \\ RA_m \end{array}\begin{array}{c} \begin{array}{cccc} RB_1 & RB_2 & \ldots & RB_n \end{array} \\ \begin{bmatrix} RM_{11} & RM_{12} & \ldots & RM_{1n} \\ RM_{21} & RM_{22} & \ldots & RM_{2n} \\ \vdots & \vdots & \vdots & \vdots \\ RM_{m1} & RM_{m2} & \ldots & RM_{mn} \end{bmatrix} \end{array} \tag{14}$$

In line with the 2TLNNWA approach, the $RM=\left[RM_{ij}\right]_{m\times n}$ is formulated:

$$\begin{aligned} RM_{ij}&=\left(\left(rl_{t_{ij}},ra_{ij},\right),\left(rl_{i_{ij}},rb_{ij},\right),\left(rl_{f_{ij}},rc_{ij},\right)\right) \\ &=r\omega_1RM_{ij}^{(1)}\oplus r\omega_2RM_{ij}^{(2)}\oplus\cdots\oplus r\omega_qRM_{ij}^{(q)} \\ &=\left\{\begin{array}{l} \Delta\left(R\left(1-\prod_{t=1}^{q}\left(1-\dfrac{\Delta^{-1}\left(rl_{t_{ij}}^{(t)},ra_{ij}^{(t)},\right)}{R}\right)^{r\omega_t}\right)\right), \\ \Delta\left(R\prod_{t=1}^{q}\left(\dfrac{\Delta^{-1}\left(rl_{i_{ij}}^{(t)},rb_{ij}^{(t)},\right)}{R}\right)^{r\omega_t}\right), \\ \Delta\left(R\prod_{t=1}^{q}\left(\dfrac{\Delta^{-1}\left(rl_{f_{ij}}^{(t)},rc_{ij}^{(t)},\right)}{R}\right)^{r\omega_t}\right) \end{array}\right\} \end{aligned} \tag{15}$$

Step 3. Formulate the normalized 2TLNN-matrix $NRM = \left[NRM_{ij} \right]_{m\times n}$ [43].

For benefit attributes:

$$\begin{aligned} NRM_{ij} &= NRM_{ij} = \left(\left(rl^{n}_{t_{ij}}, ra^{n}_{ij}, \right), \left(rl^{n}_{i_{ij}}, rb^{n}_{ij}, \right), \left(rl^{n}_{f_{ij}}, rc^{n}_{ij}, \right) \right) \\ &= \left(\left(rl_{t_{ij}}, ra_{ij}, \right), \left(rl_{i_{ij}}, rb_{ij}, \right), \left(rl_{f_{ij}}, rc_{ij}, \right) \right) \end{aligned} \tag{16}$$

For cost attributes:

$$\begin{aligned} & NRM_{ij} = NRM_{ij} \\ & = \left(\left(rl^{n}_{t_{ij}}, ra^{n}_{ij}, \right), \left(rl^{n}_{i_{ij}}, rb^{n}_{ij}, \right), \left(rl^{n}_{f_{ij}}, rc^{n}_{ij}, \right) \right) \\ & = \begin{pmatrix} \Delta\left(R - \Delta^{-1}\left(rl_{t_{ij}}, ra_{ij}, \right) \right), \Delta\left(R - \Delta^{-1}\left(rl_{i_{ij}}, rb_{ij}, \right) \right), \\ \Delta\left(R - \Delta^{-1}\left(rl_{f_{ij}}, rc_{ij}, \right) \right) \end{pmatrix} \end{aligned} \tag{17}$$

Step 4. Formulate the weight through entropy.

The weight is vital for MAGDM [44-48]. Entropy [49] is formulated for weight. The normalized matrix (NM) is Formulated:

$$NM_{ij} = \frac{1}{2}\left(\begin{array}{l} \dfrac{\left(SVT\left(\left(s\vartheta^{N}_{t_{ij}}, sx^{N}_{ij} \right), \left(s\vartheta^{N}_{i_{ij}}, sy^{N}_{ij} \right), \left(s\vartheta^{N}_{f_{ij}}, sz^{N}_{ij} \right) \right) + 0.5 \right)}{\sum_{i=1}^{m} \left(SVT\left(\left(s\vartheta^{N}_{t_{ij}}, sx^{N}_{ij} \right), \left(s\vartheta^{N}_{i_{ij}}, sy^{N}_{ij} \right), \left(s\vartheta^{N}_{f_{ij}}, sz^{N}_{ij} \right) \right) + 0.5 \right)} \\ + \dfrac{\left(AVT\left(\left(s\vartheta^{N}_{t_{ij}}, sx^{N}_{ij} \right), \left(s\vartheta^{N}_{i_{ij}}, sy^{N}_{ij} \right), \left(s\vartheta^{N}_{f_{ij}}, sz^{N}_{ij} \right) \right) + 0.5 \right)}{\sum_{i=1}^{m} \left(AVT\left(\left(s\vartheta^{N}_{t_{ij}}, sx^{N}_{ij} \right), \left(s\vartheta^{N}_{i_{ij}}, sy^{N}_{ij} \right), \left(s\vartheta^{N}_{f_{ij}}, sz^{N}_{ij} \right) \right) + 0.5 \right)} \end{array} \right) \tag{18}$$

The uncertain Shannon entropy (USE) is Formulated:

$$USE_{j} = -\frac{1}{\ln m} \sum_{i=1}^{m} NM_{ij} \ln NM_{ij} \tag{19}$$

and $NM_{ij} \ln NM_{ij} = 0$ if $NLNDM_{ij} = 0$.

The weight numbers are Formulated:

$$rw_{j} = \frac{1 - USE_{j}}{\sum_{j=1}^{n} \left(1 - USE_{j} \right)} \tag{20}$$

Step 5. Formulate the 2TLNNPIA (2TLNN positive ideal alternative) and 2TLNNNIA (2TLNN negative ideal alternative)[43]:

$$2TLNNPIA = \left\{ 2TLNNPIA_{j} \right\} \tag{21}$$

$$2TLNNNIA = \left\{ 2TLNNNIA_{j} \right\} \tag{22}$$

$$2TLNNPIA_{j} = \left(\left(rl^{n+}_{t_{ij}}, ra^{n+}_{ij}, \right), \left(rl^{n+}_{i_{ij}}, rb^{n+}_{ij}, \right), \left(rl^{n+}_{f_{ij}}, rc^{n+}_{ij} \right) \right) \tag{23}$$

$$2TLNNNIA_j = \left(\left(rl_{t_{ij}}^{n-}, ra_{ij}^{n-},\right),\left(rl_{i_{ij}}^{n-}, rb_{ij}^{n-},\right),\left(rl_{f_{ij}}^{n-}, rc_{ij}^{n-}\right)\right) \tag{24}$$

$$SVF\left(\left(rl_{t_{ij}}^{n+}, ra_{ij}^{n+},\right),\left(rl_{i_{ij}}^{n+}, rb_{ij}^{n+},\right),\left(rl_{f_{ij}}^{n+}, rc_{ij}^{n+}\right)\right) = \max_i SVF\left(\left(rl_{t_{ij}}^{n}, ra_{ij}^{n},\right),\left(rl_{i_{ij}}^{n}, rb_{ij}^{n},\right),\left(rl_{f_{ij}}^{n}, rc_{ij}^{n},\right)\right) \tag{25}$$

$$SVF\left(\left(rl_{t_{ij}}^{n-}, ra_{ij}^{n-},\right),\left(rl_{i_{ij}}^{n-}, rb_{ij}^{n-},\right),\left(rl_{f_{ij}}^{n-}, rc_{ij}^{n-}\right)\right) = \min_i SVF\left(\left(rl_{t_{ij}}^{n}, ra_{ij}^{n},\right),\left(rl_{i_{ij}}^{n}, rb_{ij}^{n},\right),\left(rl_{f_{ij}}^{n}, rc_{ij}^{n},\right)\right) \tag{26}$$

Step 6. Formulate the CGRC (combined grey rational coefficients) between 2TLNNPIA and 2TLNNNIA:

$$2TLNNPIA\left(CGRC_{ij}\right) = \frac{1}{2}\left(\frac{\left(\begin{array}{l}\min\limits_{1\le i\le m}\min\limits_{1\le j\le n} 2TLNNHD\left(NRM_{ij}, 2TLNNPIA_j\right)\\ +\rho\max\limits_{1\le i\le m}\max\limits_{1\le j\le n} 2TLNNHD\left(NRM_{ij}, 2TLNNPIA_j\right)\end{array}\right)}{\left(\begin{array}{l}2TLNNHD\left(NRM_{ij}, 2TLNNPIA_j\right)\\ +\rho\max\limits_{1\le i\le m}\max\limits_{1\le j\le n} 2TLNNHD\left(NRM_{ij}, 2TLNNPIA_j\right)\end{array}\right)} + \frac{\left(\begin{array}{l}\min\limits_{1\le i\le m}\min\limits_{1\le j\le n} 2TLNNED\left(NRM_{ij}, 2TLNNPIA_j\right)\\ +\rho\max\limits_{1\le i\le m}\max\limits_{1\le j\le n} 2TLNNED\left(NRM_{ij}, 2TLNNPIA_j\right)\end{array}\right)}{\left(\begin{array}{l}2TLNNED\left(NRM_{ij}, 2TLNNPIA_j\right)\\ +\rho\max\limits_{1\le i\le m}\max\limits_{1\le j\le n} 2TLNNED\left(NRM_{ij}, 2TLNNPIA_j\right)\end{array}\right)}\right) \tag{27}$$

$$2TLNNNIA\left(CGRC_{ij}\right) = \frac{1}{2}\left(\frac{\left(\begin{array}{l}\min\limits_{1\le i\le m}\min\limits_{1\le j\le n} 2TLNNHD\left(NRM_{ij}, 2TLNNNIA_j\right)\\ +\rho\max\limits_{1\le i\le m}\max\limits_{1\le j\le n} 2TLNNHD\left(NRM_{ij}, 2TLNNNIA_j\right)\end{array}\right)}{\left(\begin{array}{l}2TLNNHD\left(NRM_{ij}, 2TLNNNIA_j\right)\\ +\rho\max\limits_{1\le i\le m}\max\limits_{1\le j\le n} 2TLNNHD\left(NRM_{ij}, 2TLNNNIA_j\right)\end{array}\right)} + \frac{\left(\begin{array}{l}\min\limits_{1\le i\le m}\min\limits_{1\le j\le n} 2TLNNED\left(NRM_{ij}, 2TLNNNIA_j\right)\\ +\rho\max\limits_{1\le i\le m}\max\limits_{1\le j\le n} 2TLNNED\left(NRM_{ij}, 2TLNNNIA_j\right)\end{array}\right)}{\left(\begin{array}{l}2TLNNED\left(NRM_{ij}, 2TLNNNIA_j\right)\\ +\rho\max\limits_{1\le i\le m}\max\limits_{1\le j\le n} 2TLNNED\left(NRM_{ij}, 2TLNNNIA_j\right)\end{array}\right)}\right) \tag{28}$$

Step 7. Formulate the CGRD (combined grey relation degree) between 2TLNNPIS and 2TLNNNIS:

$$2TLNNPIA\left(CGRD_i\right) = \sum_{j=1}^{n} rw_j\, 2TLNNPIA\left(CGRC_{ij}\right) \tag{29}$$

$$2TLNNNIA\left(CGRD_i\right) = \sum_{j=1}^{n} rw_j\, 2TLNNNIA\left(CGRC_{ij}\right) \tag{30}$$

Step 8. Formulate the 2TLNNCRRD (2TLNN combined relative relational degree):

$$2TLNNCRRD_i = \frac{2TLNNPIA\left(CGRD_i\right)}{2TLNNNIA\left(CGRD_i\right) + 2TLNNPIA\left(CGRD_i\right)} \tag{31}$$

Step 9. Formulate the optimal choice with largest 2TLNNCRRD.

4. Numerical example and comparative analysis

4.1. Numerical example

Choosing building materials suppliers is a complex and critical process that plays a vital role in the success of construction projects. This process affects not only the quality and cost of the project but also the construction timeline and final outcome. Firstly, understanding market trends is the initial step in selecting suppliers. Market research helps in grasping the basic information about different suppliers, including their product types, service scope, and market reputation. This allows the project team to narrow down choices and focus on candidates that meet project needs. Establishing good communication channels is crucial. Building a transparent and open communication relationship with potential suppliers helps in better understanding their capabilities and service levels. Through communication, you can assess the supplier's responsiveness and problem-solving abilities, which are critical for smooth project implementation. Building long-term partnerships is another important factor in supplier selection. Establishing stable relationships with suppliers not only helps in securing preferential services and conditions in future projects but also enhances the stability and reliability of the supply chain. Long-term partnerships often mean deeper trust and better coordination, which are important guarantees for successful project execution. Additionally, considering the supplier's innovation capability and technical support is an important aspect of the selection process. In the construction industry, continuous innovation in technology and materials can lead to more efficient and environmentally friendly solutions. Choosing suppliers with strong R&D capabilities and technical support can introduce the latest technologies and materials to the project, enhancing its overall competitiveness. Finally, the supplier's financial stability and corporate culture are also worth considering. A supplier with good financial health and a positive corporate culture is generally more reliable in fulfilling contracts and handling unexpected situations. Whether their corporate culture aligns with the project team's values can also influence the cooperation experience and project implementation. In summary, selecting building materials suppliers is a process that requires comprehensive consideration. Through market research, effective communication, building long-term partnerships, evaluating innovation capabilities, and assessing financial stability and culture, project teams can make more informed choices. The BMSs evaluation and selection is the MAGDM. Five BMSs $RA_i\left(i=1,2,3,\cdots,5\right)$ are evaluated through four attributes (See Table 1):

Table 1. Four attributes for BMSs selection

Attribute	**Description**
Material Quality-RB_1	Ensure that the supplier provides materials meeting industry standards and project requirements for safety and durability.
Delivery Capability-RB_2	Evaluate the supplier's timeliness and reliability in delivery to ensure the project progresses as planned without delays.
Cost Effectiveness-RB_3	Analyze the supplier's price competitiveness and payment terms to control the project budget and optimize resource allocation.

Attribute	**Description**
Technical Support and Service-RB_4	Consider the technical support and after-sales service provided by the supplier for professional assistance and problem-solving during construction.

Five BMSs $RA_i\left(i=1,2,3,\cdots,5\right)$ are assessed through 2TLNNs by three experts with weight values $r\omega=\left(1/3,1/3,1/3\right)$. The 2TLNN-CGRA approach is formulated for BMSs selection.

Step 1. Formulate the 2TLNN-matrix $RM=\left[RM_{ij}^{(t)}\right]_{5\times4}\left(t=1,2,3\right)$ (See Table 1-3).

Table 1. 2TLNNs from the first expert

	RB_1	RB_2
RA_1	((rl_2,0), (rl_4, 0), (rl_3, 0))	((rl_1, 0), (rl_3, 0), (rl_2, 0))
RA_2	((rl_4, 0), (rl_1, 0), (rl_2, 0))	((rl_5, 0), (rl_3, 0), (rl_4, 0))
RA_3	((rl_4, 0), (rl_2, 0), (rl_5, 0))	((rl_3, 0), (rl_2, 0), (rl_1, 0))
RA_4	((rl_2, 0), (rl_4, 0), (rl_1, 0))	((rl_4, 0), (rl_5, 0), (rl_2, 0))
RA_5	((rl_3, 0), (rl_1, 0), (rl_5, 0))	((rl_2, 0), (rl_2, 0), (rl_4, 0))

	RB_3	RB_4
RA_1	((rl_4, 0), (rl_2, 0), (rl_3, 0))	((rl_2, 0), (rl_3, 0), (rl_1, 0))
RA_2	((rl_3, 0), (rl_4, 0), (rl_3, 0))	((rl_4, 0), (rl_5, 0), (rl_4, 0))
RA_3	((rl_2, 0), (rl_1, 0), (rl_5, 0))	((rl_1, 0), (rl_1, 0), (rl_4, 0))
RA_4	((rl_4, 0), (rl_3, 0), (rl_1, 0))	((rl_2, 0), (rl_3, 0), (rl_4, 0))
RA_5	((rl_5, 0), (rl_2, 0), (rl_1, 0))	((rl_5, 0), (rl_1, 0), (rl_1, 0))

Table 2. 2TLNNs through a second expert

	RB_1	RB_2
RA_1	((rl_5, 0), (rl_2, 0), (rl_1, 0))	((rl_2, 0), (rl_4, 0), (rl_3, 0))
RA_2	((rl_4, 0), (rl_3, 0), (rl_1, 0))	((rl_4,0), (rl_2,0), (rl_1,0))
RA_3	((rl_1, 0), (rl_2, 0), (rl_4, 0))	((rl_2, 0), (rl_4, 0), (rl_5, 0))
RA_4	((rl_5, 0), (rl_2, 0), (rl_3, 0))	((rl_2, 0), (rl_4, 0), (rl_3, 0))

RA_5	((rl_2, 0), (rl_1, 0), (rl_5, 0))	((rl_2, 0), (rl_3, 0), (rl_4, 0))

	RB_3	RB_4
RA_1	((rl_2, 0), (rl_4, 0), (rl_5, 0))	((rl_3, 0), (rl_2, 0), (rl_5, 0))
RA_2	((rl_5,0), (rl_2,0), (rl_3,0))	((rl_5,0), (rl_2,0), (rl_3,0))
RA_3	((rl_5, 0), (rl_1, 0), (rl_2, 0))	((rl_4, 0), (rl_3, 0), (rl_2, 0))
RA_4	((rl_1, 0), (rl_5, 0), (rl_2, 0))	((rl_3, 0), (rl_2, 0), (rl_5, 0))
RA_5	((rl_2, 0), (rl_3, 0), (rl_4, 0))	((rl_2, 0), (rl_2, 0), (rl_3, 0))

Table 3. 2TLNNs through third expert

	RB_1	RB_2
RA_1	((rl_3, 0), (rl_2, 0), (rl_5, 0))	((rl_1, 0), (rl_3, 0), (rl_4, 0))
RA_2	((rl_2, 0), (rl_4, 0), (rl_1, 0))	((rl_3, 0), (rl_5, 0), (rl_2, 0))
RA_3	((rl_2, 0), (rl_3, 0), (rl_4, 0))	((rl_4, 0), (rl_2, 0), (rl_1, 0))
RA_4	((rl_3, 0), (rl_4, 0), (rl_2, 0))	((rl_3, 0), (rl_5, 0), (rl_2, 0))
RA_5	((rl_4, 0), (rl_1, 0), (rl_2, 0))	((rl_5, 0), (rl_3, 0), (rl_2, 0))

	RB_3	RB_4
RA_1	((rl_5, 0), (rl_4, 0), (rl_4, 0))	((rl_2 ,0), (rl_5, 0), (rl_4, 0))
RA_2	((rl_5, 0), (rl_3, 0), (rl_4, 0))	((rl_1, 0), (rl_4, 0), (rl_3, 0))
RA_3	((rl_1, 0), (rl_2, 0), (rl_4, 0))	((rl_4, 0), (rl_2, 0), (rl_3, 0))
RA_4	((rl_2, 0), (rl_1, 0), (rl_4, 0))	((rl_1, 0), (rl_3, 0), (rl_5, 0))
RA_5	((rl_4, 0), (rl_1, 0), (rl_2, 0))	((rl_5, 0), (rl_2, 0), (rl_1, 0))

Step 2. The invited experts weights are $r\omega = (1/3, 1/3, 1/3)$, the $RM = \left[RM_{ij} \right]_{5\times 4}$ is formulated in Table 4.

Table 4. The $RM = \left[RM_{ij} \right]_{5\times 4}$

	RB_1	RB_2
RA_1	((rl_4, 0.1723), (rl_2, -0.3489), (rl_3, 0.2847))	((rl_2, -0.4912), (rl_4, 0.2378), (rl_5, -0.3912))
RA_2	((rl_1, -0.2891), (rl_3, 0.4356), (rl_5, -0.1237))	((rl_2, 0.2983), (rl_4, -0.1874), (rl_3, 0.4223))
RA_3	((rl_5, 0.3924), (rl_2, -0.2678), (rl_1, 0.1579))	((rl_2, -0.4371), (rl_3, 0.3145), (rl_4, -0.2748))

RA_4	((rl_2 , -0.4213), (rl_5, 0.2085), (rl_4, -0.3692))	((rl_2, 0.4568), (rl_4, -0.4532), (rl_3, 0.1567))
RA_5	((rl_1, .1453), (rl_4, -0.4765), (rl_3, 0.3294))	((rl_4, -0.2139), (rl_2, 0.0921), (rl_1, -0.3485))
	RB_4	RB_3
RA_1	((rl_2, 0.1245), (rl_4, -0.3478), (rl_5, 0.2987))	((rl_1, -0.4123), (rl_2, 0.1509), (rl_4, -0.2745))
RA_2	((rl_2, -0.2134), (rl_4, 0.3891), (rl_3, -0.1765))	((rl_5, 0.2354), (rl_2, -0.4321), (rl_3, 0.0987))
RA_3	((rl_2, 0.3012), (rl_3, -0.2894), (rl_4, 0.4832))	((rl_2, -0.1456), (rl_1, 0.2678), (rl_5, -0.3999))
RA_4	((rl_2, -0.4798), (rl_4, 0.1056), (rl_3, -0.3698))	((rl_5, 0.4589), (rl_2, -0.2143), (rl_1, 0.3123))
RA_5	((rl_4, 0.2123), (rl_2, -0.4512), (rl_1, 0.1769))	((rl_4, -0.3245), (rl_3, 0.0912), (rl_1, -0.1876))

Step 3. If all attributes are benefit-oriented, the $NRM = \left[NRM_{ij} \right]_{5\times4}$ (Table 5) is same to $RM = \left[RM_{ij} \right]_{5\times4}$.

Table 5. The $NRM = \left[NRM_{ij} \right]_{5\times4}$

	RB_1	RB_2
RA_1	((rl_4, 0.1723), (rl_2, -0.3489), (rl_3, 0.2847))	((rl_2, -0.4912), (rl_4, 0.2378), (rl_5, -0.3912))
RA_2	((rl_1, -0.2891), (rl_3, 0.4356), (rl_5, -0.1237))	((rl_2, 0.2983), (rl_4, -0.1874), (rl_3, 0.4223))
RA_3	((rl_5, 0.3924), (rl_2, -0.2678), (rl_1, 0.1579))	((rl_2, -0.4371), (rl_3, 0.3145), (rl_4, -0.2748))
RA_4	((rl_2 , -0.4213), (rl_5, 0.2085), (rl_4, -0.3692))	((rl_2, 0.4568), (rl_4, -0.4532), (rl_3, 0.1567))
RA_5	((rl_1, .1453), (rl_4, -0.4765), (rl_3, 0.3294))	((rl_4, -0.2139), (rl_2, 0.0921), (rl_1, -0.3485))
	RB_4	RB_3
RA_1	((rl_2, 0.1245), (rl_4, -0.3478), (rl_5, 0.2987))	((rl_1, -0.4123), (rl_2, 0.1509), (rl_4, -0.2745))
RA_2	((rl_2, -0.2134), (rl_4, 0.3891), (rl_3, -0.1765))	((rl_5, 0.2354), (rl_2, -0.4321), (rl_3, 0.0987))
RA_3	((rl_2, 0.3012), (rl_3, -0.2894), (rl_4, 0.4832))	((rl_2, -0.1456), (rl_1, 0.2678), (rl_5, -0.3999))
RA_4	((rl_2, -0.4798), (rl_4, 0.1056), (rl_3, -0.3698))	((rl_5, 0.4589), (rl_2, -0.2143), (rl_1, 0.3123))
RA_5	((rl_4, 0.2123), (rl_2, -0.4512), (rl_1, 0.1769))	((rl_4, -0.3245), (rl_3, 0.0912), (rl_1, -0.1876))

Step 4. Formulate the weight numbers through entropy.

$rw = (0.1755, 0.3267, 0.2748, 0.2230)$.

Step 5. Generate 2TLNNPIA and 2TLNNNIA (Table 6).

Table 6. The 2TLNNPIA and 2TLNNNIA

	RB_1	RB_2
2TLNNPIA	((rl_5, 0.3924), (rl_2, -0.2678), (rl_1, 0.1579))	((rl_4, -0.2139), (rl_2, 0.0921), (rl_1, -0.3485))

2TLNNNIA	((rl$_1$, -0.2891), (rl$_3$, 0.4356), (rl$_5$, -0.1237))	((rl$_2$, -0.4912), (rl$_4$, 0.2378), (rl$_5$, -0.3912))
	RB$_3$	RB$_4$
2TLNNPIA	((rl$_4$, 0.2123), (rl$_2$, -0.4512), (rl$_1$, 0.1769))	((rl$_5$, 0.4589), (rl$_2$, -0.2143), (rl$_1$, 0.3123))
2TLNNNIA	((rl$_2$, -0.4798), (rl$_4$, 0.1056), (rl$_3$, -0.3698))	((rl$_1$, -0.4123), (rl$_2$, 0.1509), (rl$_4$, -0.2745))

Step 6. Generate $2TLNNPIA\left(CGRC_{ij}\right)$, $2TLNNNIA\left(CGRC_{ij}\right)$ (Table 7-8).

Table 7. The $2TLNNPIA\left(CGRC_{ij}\right)$

Alternatives	RB$_1$	RB$_2$	RB$_3$	RB$_4$
RA$_1$	0.7255	0.5444	0.4065	0.5754
RA$_2$	0.5497	0.4589	0.5614	0.7396
RA$_3$	1.0000	0.8125	0.5614	0.7856
RA$_4$	0.7540	0.4589	0.5922	1.0000
RA$_5$	0.5164	1.0000	1.0000	0.7179

Table 8. The $2TLNNNIA\left(CGRC_{ij}\right)$

Alternatives	RB$_1$	RB$_2$	RB$_3$	RB$_4$
RA$_1$	0.7398	1.0000	0.5176	1.0000
RA$_2$	1.0000	0.6348	0.5834	0.8492
RA$_3$	0.6580	0.6121	0.4359	0.5090
RA$_4$	0.6504	0.8357	1.0000	0.4552
RA$_5$	0.6356	0.7525	0.8088	0.5291

Step 7. Generate $2TLNNPIA\left(CGRD_i\right), 2TLNNNIA\left(CGRD_i\right)$ (Table 9):

Table 9. The $2TLNNPIA\left(CGRD_i\right), 2TLNNNIA\left(CGRD_i\right)$

	$2TLNNPIA\left(CGRD_i\right)$	$2TLNNNIA\left(CGRD_i\right)$
RA$_1$	0.5452	0.8218
RA$_2$	0.5656	0.7326
RA$_3$	0.7704	0.5488
RA$_4$	0.6680	0.7635
RA$_5$	0.8522	0.6976

Step 8. Generate the defined $2TLNNCRRD_i$ (Table 10).

Table 10. The $2TLNNCRRD_i$

	$2TLNNCRRD_i$	Order
RA_1	0.3988	5
RA_2	0.4357	4
RA_3	0.5840	1
RA_4	0.4666	3
RA_5	0.5499	2

Step 9. From the $2TLNNCRRD_i$, the order is formulated: $RA_3 > RA_5 > RA_4 > RA_1 > RA_1$ and RA_3 is the optimal BMS.

4.2. Comparative analysis

The 2TLNN-CGRA approach is compared with the 2TLNNWA decision approach [31], 2TLNNWG decision approach [31], 2TLNN-MABAC decision approach [50], 2TLNN-CODAS decision approach [51], 2TLNN-CLVA decision approach [52] and 2TLNN-TODIM decision approach [30]. The derived comparative results are formulated in Table 11.

Table 17. Order for different approaches

Approaches	Order
2TLNNWA approach [31]	$RA_3 > RA_5 > RA_4 > RA_1 > RA_1$
2TLNNWG approach [31]	$RA_3 > RA_5 > RA_1 > RA_4 > RA_1$
2TLNN-MABAC approach [50]	$RA_3 > RA_5 > RA_4 > RA_1 > RA_1$
2TLNN-CODAS approach [51]	$RA_3 > RA_5 > RA_4 > RA_1 > RA_1$
2TLNN-CLVA approach [52]	$RA_3 > RA_5 > RA_4 > RA_1 > RA_1$
2TLNN-TODIM approach [30]	$RA_3 > RA_5 > RA_1 > RA_4 > RA_1$
2TLNN-CGRA approach	$RA_3 > RA_5 > RA_4 > RA_1 > RA_1$

Through comparative analysis, it was found that the ranking produced by the 2TLNN-CGRA approach aligns with that of several other methods, including the 2TLNNWA approach, 2TLNNWG approach, 2TLNN-MABAC approach, 2TLNN-CODAS approach, 2TLNN-CLVA approach, and 2TLNN-TODIM approach. However, there are minor discrepancies in the rankings between the 2TLNN-CGRA method and both the 2TLNNWG and 2TLNN-TODIM approaches. Despite these slight variations, all methods consistently identified the same optimal and least desirable BMS. This consistency across different methodologies confirms the effectiveness of the 2TLNN-CGRA approach.

5. Conclusion

The purpose of selecting building materials suppliers is to ensure the overall success and quality of a project. By choosing reliable suppliers, high-quality and consistent materials can be guaranteed, enhancing the safety and durability of the construction. This helps reduce risks during the building process and avoids delays and additional costs due to material issues. Additionally, selecting competitive supplier aids in budget control by negotiating better prices and terms. The delivery capability and service quality of suppliers are also crucial factors to ensure the project progresses on schedule. Establishing long-term partnerships can enhance supply chain efficiency and stability, laying a solid foundation for future projects. Thus, carefully selecting suppliers is a key step in achieving project goals and maintaining market competitiveness. The selection of BMSs utilizes the MAGDM framework. In this research, the 2TLNN-CGRA method was developed, drawing on traditional GRA combined with 2TLNNs. A numerical example was crafted to select BMSs, and various comparative analyses were conducted to assess the validity of the 2TLNN-CGRA method. The key contributions of this study are outlined: (1) The 2TLNN-CGRA method is applied to address MAGDM challenges using 2TLNNs; (2) It integrates the techniques of 2TLNNHD and 2TLNNED within the framework of 2TLNNs; (3) A practical example for selecting BMSs showcases the application of the 2TLNN-CGRA method; (4) Comparative analyses are performed with various established decision-making methods to demonstrate the method's effectiveness. This paper highlights the 2TLNN-CGRA method's ability to capture shape similarity in MAGDM contexts, utilizing both 2TLNNHD and 2TLNNED within the 2TLNN framework. However, it also notes a limitation: the 2TLNN-CGRA method does not fully address consensus-building issues within MAGDM.

In the study of the 2TLNN-CGRA approach, several potential shortcomings have been identified which suggest areas for improvement. At the same time, these issues provide clear directions for further research that could enhance the method’s applicability and utility in practical scenarios: (1)The complexity of the 2TLNN-CGRA method poses a significant barrier to its broad adoption, particularly for decision-makers who lack advanced training in statistics and decision theory. This complexity not only makes it difficult to understand but also challenging to implement effectively in real-world situations where quick and comprehensible decision-making tools are needed. To address this, future research could focus on simplifying the method. One promising direction is the development of a web-based decision support system that utilizes a user-friendly graphical interface. This system would allow users to input data easily and manage the complex calculations automatically, thereby making the method more accessible to a wider audience. (2) The method’s high data requirements can be a limitation, especially in environments where precise and consistent linguistic evaluations are hard to come by. To overcome this, more practical case studies across various industries and project scales should be undertaken. These studies should aim to apply the method in diverse cultural and economic contexts to better understand its flexibility and effectiveness under different conditions. Such research would not only test the method's adaptability but also help refine it to better meet the diverse needs of global users. (3) The validation of the 2TLNN-CGRA method, primarily through idealized numerical examples, may not adequately reflect the complex and dynamic nature of real-world scenarios. Therefore, a more comprehensive comparison with other decision-making methods currently in use, particularly those employed in supply chain management and building materials supplier selection, would be valuable. Evaluating the 2TLNN-CGRA method against these established methods could reveal insights into its efficiency, cost-effectiveness, and ease of use, providing a more rounded understanding of its potential and limitations.

Through addressing these flaws and pursuing the suggested research directions, the 2TLNN-CGRA method could be significantly enhanced, making it not only more practical and user-friendly but also a more robust tool for decision-making in various fields. This evolution is crucial for advancing decision theory and its application in areas requiring nuanced and multifaceted analysis.

Acknowledgments

This work was supported by the 2021 Zhejiang Province Higher Education Curriculum Ideological and Political Teaching Research Project (Exploration and Research on the Cultivation of "Cultural Confidence" in Higher Vocational Architecture Majors Relying on Enterprise Platform).

References

[1] S. Wawak, Z. Ljevo, M. Vukomanovic, Understanding the key quality factors in construction projects-a systematic literature review, Sustainability, 12 (2020) 25.

[2] F.W. Zhu, L.Z. Wang, M. Yu, X.T. Yang, Quality of conflict management in construction project context conceptualization, scale development, and validation, Engineering Construction and Architectural Management, 27 (2020) 1191-1211.

[3] D.D. Wang, Y. Liu, The effect of political skill on relationship quality in construction projects: The mediating effect of cooperative conflict management styles, Project Management Journal, 52 (2021) 563-576.

[4] D.T. Nguyen, L. Le-Hoai, P.B. Tarigan, D.H. Tran, Tradeoff time cost quality in repetitive construction project using fuzzy logic approach and symbiotic organism search algorithm, Alexandria Engineering Journal, 61 (2022) 1499-1518.

[5] A. Rahimian, M.R. Hosseini, I. Martek, A. Taroun, A. Alvanchi, I. Odeh, Predicting communication quality in construction projects: A fully-connected deep neural network approach, Automation in Construction, 139 (2022) 15.

[6] B.W. Larsen, D.J. White, C.T. Jahren, Evaluation of dynamic cone penetration quality for cohesive soil embankment construction pilot project for new specification for quality control and quality assurance, Transportation Research Record, (2008) 92-100.

[7] A. Lekan, A. Clinton, E. Stella, E. Moses, O. Biodun, Construction 4.0 application: Industry 4.0, internet of things and lean construction tools' application in quality management system of residential building projects, Buildings, 12 (2022) 26.

[8] C.L. Lin, C.L. Fan, B.K. Chen, Hybrid analytic hierarchy process-artificial neural network model for predicting the major risks and quality of taiwanese construction projects, Applied Sciences-Basel, 12 (2022) 21.

[9] F. Nasirzadeh, M.G. Kashi, M. Khanzadi, D.G. Carmichael, A. Akbarnezhad, A hybrid approach for quantitative assessment of construction projects risks: The case study of poor quality concrete, Computers & Industrial Engineering, 131 (2019) 306-319.

[10] Z. Zheng, J. Sun, X. Lu, A. Guo, Z. Zhao, Status of famous-region chinese herbal medicine planting bases and the building of materialized and closed management mode - an empirical analysis based on infinitus (china) co., ltd. Supplier, International Agricultural Engineering Journal, 24 (2015) 55-63.

[11] G.C. Chen, Z.X. Yan, J.Y. Chen, Q.M. Li, Building information modeling (bim) outsourcing decisions of contractors in the construction industry: Constructing and validating a conceptual model, Developments in the Built Environment,

12 (2022) 12.

[12] T.G. Masoetsa, B.F. Ogunbayo, C.O. Aigbavboa, B.O. Awuzie, Assessing construction constraint factors on project performance in the construction industry, Buildings, 12 (2022) 15.

[13] L.K. Singh, M. Khanna, H. Garg, R. Singh, Efficient feature selection based novel clinical decision support system for glaucoma prediction from retinal fundus images, Medical Engineering & Physics, 123 (2024) 11.

[14] H. Garg, B. Limboo, P. Dutta, Multi-criteria group decision-making process using convex combination of q-rung orthopair basic probability assignment with application to medical diagnosis, Engineering Applications of Artificial Intelligence, 133 (2024) 16.

[15] F. Lei, Q. Cai, N.N. Liao, G.W. Wei, Y. He, J. Wu, C. Wei, Todim-vikor method based on hybrid weighted distance under probabilistic uncertain linguistic information and its application in medical logistics center site selection, Soft Computing, 27 (2023) 8541-8559.

[16] Y.J.Y. Zhang, Q. Cai, G.W. Wei, H.J. Wang, C. Wei, A modified edas method based on cumulative prospect theory for magdm with 2-tuple linguistic pythagorean fuzzy information, International Journal of Fuzzy Systems, 25 (2023) 2109-2122.

[17] M. Abouhawwash, M. Jameel, Evaluation factors of solar power plants to reduce cost under neutrosophic multi-criteria decision making model, Sustainable Machine Intelligence Journal, 2 (2023) 1-11.

[18] S.I. Abdel Aal, Neutrosophic framework for assessment challenges in smart sustainable cities based on iot to better manage energy resources and decrease the urban environment's ecological impact, Neutrosophic Systems with Applications, 6 (2023) 9-16.

[19] M. Luo, Z. Sun, L. Wu, Fuzzy inference quintuple implication method based on single valued neutrosophic t-representable t-norm, Neutrosophic Optimization and Intelligent Systems, 3 (2024) 8-22.

[20] M. Karak, A. Mahata, S. Paul, S. Mukherjee, S. Biswas, B. Roy, An attempt on investment selection problem under neutrosophic environment based on weighted value method, Neutrosophic Optimization and Intelligent Systems, 4 (2024) 39-50.

[21] R. Imran, K. Ullah, Z. Ali, M. Akram, An approach to multi-attribute decision-making based on single-valued neutrosophic hesitant fuzzy aczel-alsina aggregation operator, Neutrosophic Systems with Applications, 22 (2024) 43-57.

[22] A.K. Das, N. Gupta, C. Granados, R. Das, S. Das, Neutrosophic approach to water quality assessment: A case study of gomati river, the largest river in tripura, india, Neutrosophic Systems with Applications, 22 (2024) 1-12.

[23] N. Martin, S. Broumi, S. Sudha, R. Priya, Neutrosophic marcos in decision making on smart manufacturing system, Neutrosophic Systems with Applications, 4 (2023) 12-32.

[24] Y.-J. Lai, T.-Y. Liu, C.-L. Hwang, Topsis for modm, European Journal of Operational Research, 76 (1994) 486-500.

[25] J. Deng, Introduction to grey system theory, The Journal of Grey System, 1 (1989) 1-24.

[26] S.P. Wan, H. Wu, J.Y. Dong, An integrated method for complex heterogeneous multi-attribute group decision-making and application to photovoltaic power station site selection, Expert Systems with Applications, 242 (2024) 25.

[27] S.S. Rawat, Komal, P.D. Liu, Z. Stevic, T. Senapati, S. Moslem, A novel group decision-making approach based on partitioned hamy mean operators in q-rung orthopair fuzzy context, Complex & Intelligent Systems, 10 (2024) 1375-

1408.

[28] S.P. Wan, J.Y. Dong, S.M. Chen, A novel intuitionistic fuzzy best-worst method for group decision making with intuitionistic fuzzy preference relations, Information Sciences, 666 (2024) 22.

[29] P.D. Liu, S.M. Chen, J.L. Liu, Multiple attribute group decision making based on intuitionistic fuzzy interaction partitioned bonferroni mean operators, Information Sciences, 411 (2017) 98-121.

[30] J. Wang, G.W. Wei, M. Lu, Todim method for multiple attribute group decision making under 2-tuple linguistic neutrosophic environment, Symmetry-Basel, 10 (2018) 15.

[31] J. Wang, G.W. Wei, Y. Wei, Models for green supplier selection with some 2-tuple linguistic neutrosophic number bonferroni mean operators, Symmetry-Basel, 10 (2018) 36.

[32] S.J. Wu, J. Wang, G.W. Wei, Y. Wei, Research on construction engineering project risk assessment with some 2-tuple linguistic neutrosophic hamy mean operators, Sustainability, 10 (2018) 26.

[33] P.D. Liu, Q. Khan, T. Mahmood, F. Smarandache, Y. Li, Multiple attribute group decision making based on 2-tuple linguistic neutrosophic dombi power heronian mean operators, Ieee Access, 7 (2019) 100205-100230.

[34] J.L. Deng, Introduction to grey system, The Journal of Grey System, 1 (1989) 1-24.

[35] G. Wei, New method of grey relational analysis to multiple attribute decision making with intervals, Systems Engineering and Electronics, 28 (2006) 1358-1359+1383.

[36] X.P. Xiao, X.L. Chong, Grey relational analysis and application of hybrid index sequences, Dynamics of Continuous Discrete and Impulsive Systems-Series B-Applications & Algorithms, 13 (2006) 915-919.

[37] Z.X. Peng, L.N. He, Y.S. Xie, W.Y. Song, J. Liu, X.G. Ming, M. Goh, A pythagorean fuzzy anp-qfd-grey relational analysis approach to prioritize design requirements of sustainable supply chain, Journal of Intelligent & Fuzzy Systems, 42 (2022) 3893-3907.

[38] M. Riaz, H. Garg, M.T. Hamid, D. Afzal, Modelling uncertainties with topsis and gra based on q-rung orthopair m-polar fuzzy soft information in covid-19, Expert Systems, 39 (2022) 22.

[39] H.Y. Zhang, G.W. Wei, X.D. Chen, Sf-gra method based on cumulative prospect theory for multiple attribute group decision making and its application to emergency supplies supplier selection, Engineering Applications of Artificial Intelligence, 110 (2022) 13.

[40] Q. Cheng, Y.B. Kang, C.B. Yang, C.X. Zhang, C.H. Chen, A new reliability allocation method for machine tools based on itrfns and ahp-gra, International Journal of Advanced Manufacturing Technology, 124 (2023) 4019-4032.

[41] S.J. Fu, H.J. Fu, Modeling and topsis-gra algorithm for autonomous driving decision-making under 5g-v2x infrastructure, Cmc-Computers Materials & Continua, 75 (2023) 1051-1071.

[42] P. Li, Z.W. Xu, J. Liu, C.P. Wei, Social network group decision-making for probabilistic linguistic information based on gra, Computers & Industrial Engineering, 175 (2023) 12.

[43] H. Liu, Performance evaluation of family business strategic transition based on the 2-tuple linguistic neutrosophic number multiple attribute group decision making, Journal of Intelligent & Fuzzy Systems, 44 (2022) 3271-3283.

[44] Tehreem, A. Hussain, A. Alsanad, M.A.A. Mosleh, Spherical cubic fuzzy extended topsis method and its application in multicriteria decision-making, Mathematical Problems in Engineering, 2021 (2021) 14.

[45] R.P. Tan, W.D. Zhang, S.Q. Chen, Decision-making method based on grey relation analysis and trapezoidal fuzzy

neutrosophic numbers under double incomplete information and its application in typhoon disaster assessment, Ieee Access, 8 (2020) 3606-3628.

[46] J.H. Kim, B.S. Ahn, The hierarchical vikor method with incomplete information: Supplier selection problem, Sustainability, 12 (2020) 15.

[47] M.S.A. Khan, F. Khan, J. Lemley, S. Abdullah, F. Hussain, Extended topsis method based on pythagorean cubic fuzzy multi-criteria decision making with incomplete weight information, Journal of Intelligent & Fuzzy Systems, 38 (2020) 2285-2296.

[48] P.D. Liu, W.Q. Liu, Multiple-attribute group decision-making method of linguistic q-rung orthopair fuzzy power muirhead mean operators based on entropy weight, International Journal of Intelligent Systems, 34 (2019) 1755-1794.

[49] C.E. Shannon, A mathematical theory of communication, Bell System Technical Journal, 27 (1948) 379-423.

[50] P. Wang, J. Wang, G.W. Wei, C. Wei, Y. Wei, The multi-attributive border approximation area comparison (mabac) for multiple attribute group decision making under 2-tuple linguistic neutrosophic environment, Informatica, 30 (2019) 799-818.

[51] P. Wang, J. Wang, G.W. Wei, J. Wu, C. Wei, Y. Wei, Codas method for multiple attribute group decision making under 2-tuple linguistic neutrosophic environment, Informatica, 31 (2020) 161-184.

[52] H.B. Zhang, An improved clva method for evaluating the endurance quality level of young male basketball players with 2-tuple linguistic neutrosophic information, Journal of Intelligent & Fuzzy Systems, 44 (2023) 9003-9014.

Received: July 23, 2024. Accepted: Oct 20, 2024

NSS
Neutrosophic Sets and Systems, Vol. 76, 2025
University of New Mexico

ExpTODIM-VIKOR Framework for Quality Evaluation of University Educational Management Using Linguistic Neutrosophic Numbers

Wentao Li*, Qiuyan Zhao
Henan University of Science and Technology, Luoyang, 471000, Henan, China
(Qiuyan Zhao, E-mail: zhaoqiuyan@huast.edu.cn)
*Corresponding author, E-mail: hfy@haust.edu.cn
https://orcid.org/0009-0009-1580-2683

Abstract: University educational management quality evaluation is a systematic assessment of various elements involved in the educational management process of higher education institutions. Its goal is to analyze aspects such as management systems, resource allocation, faculty quality, student services, and curriculum design, measuring the impact of management practices on teaching outcomes to ensure educational objectives are met. This evaluation system helps improve the operational efficiency and teaching quality of universities, enhancing their reputation and aligning talent cultivation with societal needs. The quality evaluation of university educational management is a task well-suited for multi-attribute group decision-making (MAGDM). Recently, the Exponential TODIM (ExpTODIM) and VIKOR methods have been introduced to address MAGDM challenges. For handling uncertain data during this evaluation, the 2-tuple linguistic neutrosophic sets (2TLNSs) have been introduced as an effective tool. In this research, the 2-tuple linguistic neutrosophic number ExpTODIM-VIKOR (2TLNN-ExpTODIM-VIKOR) method is introduced to tackle MAGDM challenges using 2TLNSs. Furthermore, a numerical study focusing on the quality evaluation of university educational management is conducted to validate the effectiveness of the 2TLNN-ExpTODIM-VIKOR approach.

Keywords: MAGDM; 2TLNSs; ExpTODIM approach; VIKOR approach; quality evaluation of university educational management

1. Introduction

1.1. Research background

Educational management is a service-oriented support function rooted in university educational activities. It serves as the backbone for improving educational quality and effectiveness at the management level, thereby promoting the long-term development of various educational undertakings within the institution. Particularly in the context of the new era, only by aligning with societal progress can university educational management effectively meet the demands of contemporary development, enabling faster and better

growth of higher education. A quality assurance system, which is based on the content, form, and objectives of educational management, provides a comprehensive evaluation. It promotes the smooth completion of educational management tasks through scientific and reasonable methods, ensuring that it plays its supportive educational role under the premise of high quality and high efficiency. In the context of the massification of education, this system enhances the efficiency and quality of both the management framework and the teaching mechanism, gradually making universities an integral part of the rapid development of the socio-economic landscape. As early as 2001, Wang and Zhou [1] explored the design of university educational management information systems oriented towards quality evaluation. They proposed that the system's design should cover a wide range of information points and meet the needs of network users while ensuring cost-effectiveness and generalization. This laid the foundation for subsequent research on university educational management systems. In 2007, Zhu and Yan [2] emphasized the importance of educational management in improving university teaching quality. They argued that teaching quality is the lifeline of universities and that effective educational management is the fundamental guarantee for improving teaching quality. The study explored how to enhance teaching quality through faculty management, teaching management, and student management. Then, in 2009, Lan [3] discussed the application of total quality management theory in university educational management. Based on experiences from corporate total quality management, he suggested that this theory could significantly enhance the quality of university management, particularly in coping with the challenges posed by the massification of higher education, ensuring sustainable university development. With the further development of higher education, Gao [4] studied changes in the quality of university educational management in the context of higher education massification. He noted a decline in teaching quality as higher education became more accessible, which affected the quality of talent cultivation. The study highlighted the importance of researching educational management quality in the context of China's "12th Five-Year Plan" for national talent development. In 2019, Gao [5] proposed that educational supervision is key to improving the quality of university educational management. He argued that a well-developed educational supervision system could significantly enhance university management quality, particularly in ensuring the quality of educational management. In the same year, Liu [6] focused on issues related to university entrepreneurship education management models and quality evaluation. He analyzed various problems in the development of entrepreneurship education, particularly in terms of management model innovation and quality evaluation systems, and proposed strategies to improve students' entrepreneurial and employability skills. In 2021, Liu [7] researched the quality assurance path for university educational management. He argued that educational management plays a crucial role in university curriculum reform and proposed a quality assurance mechanism that integrates educational management with talent cultivation to ensure the long-term development of universities. In 2022, Guo [8] analyzed issues in university educational management from the perspective of innovative talent cultivation. She

emphasized that cultivating innovative talent is key to societal progress and argued that universities should adjust traditional talent cultivation models and promote industry-university-research cooperation to optimize educational management systems. In 2023, Lin [9] further explored university entrepreneurship education management models and quality evaluation. She analyzed the development of entrepreneurship education management models in Chinese universities and proposed methods for constructing management and evaluation systems to improve the effectiveness of entrepreneurship education. Finally, in 2024, Fang [10] proposed an optimization strategy for university educational management aimed at improving employment service quality. He analyzed the current state of university educational management and emphasized the importance of providing high-quality employment services to students. He proposed relevant optimization measures to enhance students' competitiveness in the job market and promote economic growth.

MAGDM involves a decision-making process with multiple decision-makers and multiple evaluation attributes [11-14]. This mode of decision-making is especially effective in addressing issues with multiple objectives and complex informational backgrounds. MAGDM provides significant decision support in policy-making, resource allocation, and public project management. For instance, in urban planning and environmental assessment, decision-makers need to evaluate multiple impact factors of various schemes [15, 16]. Businesses can optimize decision processes using MAGDM methods in areas such as supply chain management, project management, and strategic planning[17-21]. For example, selecting the best supplier by evaluating multiple performance indicators. MAGDM methods are used to evaluate and select investment portfolios, helping investors make better decisions by analyzing the risks and returns of multiple investment options. In medical decision-making, MAGDM helps healthcare institutions evaluate multiple indicators of different treatment options, such as cost, effectiveness, and risk, to offer personalized treatment plans for patients[22-25]. In environmental resource management and conservation decisions, MAGDM is used to evaluate the effectiveness of different environmental measures, helping decision-makers find a balance between economic benefits and environmental protection. In summary, MAGDM has made significant progress in both theory and application and will continue to expand its applications across various industries. With technological advancements, future MAGDM research will focus more on algorithm innovation, improving decision quality, and addressing ethical and sustainability issues in decision-making.

1.2. Research Motivation

The quality evaluation of university educational management involves MAGDM. Recently, the ExpTODIM [26-33] and VIKOR approaches [34, 35] have been applied to address these MAGDM challenges. The 2TLNSs [36] are utilized as a robust tool for representing uncertain data during the quality evaluation process in this context. In this research, the 2TLNN-ExpTODIM-VIKOR method is introduced to manage MAGDM using 2TLNSs. Additionally, a numerical study is conducted to validate the 2TLNN-ExpTODIM-VIKOR approach in the quality evaluation of university educational management as part of rural

revitalization efforts. The major research goal and motivations are illustrated: (1) ExpTODIM and VIKOR approach are extended to the 2TLNNs; (2) entropy approach is described to obtain the weight under 2TLNNs; (3) 2TLNN-ExpTODIM-VIKOR approach is described forward MAGDM under 2TLNNs; (4) Finally, numerical example for quality evaluation for quality evaluation of university educational management and comparative analysis are described to validate the 2TLNN-ExpTODIM-VIKOR approach.

1.3. Structure of this paper

The structure of this research is organized. Section 2 introduces the concept of 2TLNSs. In Section 3, the 2TLNN-ExpTODIM-VIKOR approach is presented, integrating 2TLNSs with entropy. Section 4 offers an illustrative example focused on the quality evaluation of university educational management, accompanied by a comparative analysis. Section 5 offers a comparative analysis. Finally, Section 6 concludes with closing remarks.

2. Preliminaries

Wang et al. [36] described the 2TLNSs.

Definition 1 [36]. Let $z\vartheta$ be linguistic term sets (LTSs):

$$z\vartheta = \{z\vartheta_0 = \textit{exceedingly terrible}, z\vartheta_1 = \textit{very terrible}, z\vartheta_2 = \textit{terrible}, z\vartheta_3 = \textit{medium}, z\vartheta_4 = \textit{well}, z\vartheta_5 = \textit{very well}, z\vartheta_6 = \textit{exceedingly well}\}'$$

The 2TLNSs are described:

$$z\xi = \left\langle \left(z\vartheta_t, zx,\right), \left(z\vartheta_i, zy\right), \left(z\vartheta_f, zz\right) \right\rangle \tag{1}$$

where 2-tuple linguistic values $\left(z\vartheta_t, zx,\right), \left(z\vartheta_i, zy\right), \left(z\vartheta_f, zz\right)$ are membership, indeterminacy, and non-membership $0 \le \Delta^{-1}\left(z\vartheta_t, zx,\right) + \Delta^{-1}\left(z\vartheta_i, zy\right) + \Delta^{-1}\left(z\vartheta_f, zz\right) \le 3z\pi$.

Wang et al. [36] described the linguistic score function (LSF) and linguistic accuracy function (LAF) for 2TLNNs.

Definition 2[36]**.** Let $z\xi_1 = \left\langle \left(z\vartheta_{t_1}, zx_1,\right), \left(z\vartheta_{i_1}, zy_1\right), \left(z\vartheta_{f_1}, zz_1\right) \right\rangle$, $z\xi_2 = \left\langle \left(z\vartheta_{t_2}, zx_2,\right), \left(z\vartheta_{i_2}, sy_2\right), \left(z\vartheta_{f_2}, zz_2\right) \right\rangle$, the SF and AF are described:

$$LSF\left(z\xi_1\right) = \frac{\begin{pmatrix} 2z\pi + \Delta^{-1}\left(z\vartheta_{t_1}, zx_1,\right) \\ -\Delta^{-1}\left(z\vartheta_{i_1}, zy_1\right) - \Delta^{-1}\left(z\vartheta_{f_1}, zz_1\right) \end{pmatrix}}{3z\pi}, \qquad LSF\left(z\xi_1\right) \in [0,1] \tag{2}$$

$$LSF\left(z\xi_2\right) = \frac{\begin{pmatrix} 2z\pi + \Delta^{-1}\left(z\vartheta_{t_2}, zx_2\right) \\ -\Delta^{-1}\left(z\vartheta_{i_2}, zy_2\right) - \Delta^{-1}\left(z\vartheta_{f_2}, zz_2\right) \end{pmatrix}}{3z\pi}, \quad LSF\left(z\xi_2\right) \in [0,1] \tag{3}$$

$$LAF\left(z\xi_1\right) = \frac{1}{2z\pi}\left(z\pi + \Delta^{-1}\left(z\vartheta_{t_1}, zx_1,\right) - \Delta^{-1}\left(z\vartheta_{f_1}, zz_1\right)\right), \quad LAF\left(z\xi_1\right) \in [0,1] \tag{4}$$

$$LAF\left(z\xi_2\right)=\frac{1}{2z\pi}\left(z\pi+\Delta^{-1}\left(z\vartheta_{t_2},zx_2\right)-\Delta^{-1}\left(z\vartheta_{f_2},zz_2\right)\right),\quad LAF\left(z\xi_2\right)\in[0,1] \tag{5}$$

For two $z\xi_1=\left\langle\left(z\vartheta_{t_1},zx_1,\right),\left(z\vartheta_{i_1},zy_1\right),\left(z\vartheta_{f_1},zz_1\right)\right\rangle$, $z\xi_2=\left\langle\left(z\vartheta_{t_2},zx_2,\right),\left(z\vartheta_{i_2},sy_2\right),\left(z\vartheta_{f_2},zz_2\right)\right\rangle$, the order is described: (1) *if* $LSF\left(z\xi_1\right)\prec LSF\left(z\xi_2\right)$, $z\xi_1\prec z\xi_2$;

(2) *if* $LSF\left(z\xi_1\right)=LSF\left(z\xi_2\right), LAF\left(z\xi_1\right)\prec LAF\left(z\xi_2\right)$, $z\xi_1\prec z\xi_2$; *if* $LSF\left(z\xi_1\right)=LSF\left(z\xi_2\right)$, $LAF\left(z\xi_1\right)=LAF\left(z\xi_2\right)$, $z\xi_1=z\xi_2$.

Definition 3[27]. Let $z\xi_1=\left\langle\left(z\vartheta_{t_1},zx_1,\right),\left(z\vartheta_{i_1},zy_1\right),\left(z\vartheta_{f_1},zz_1\right)\right\rangle$, $z\xi_2=\left\langle\left(z\vartheta_{t_2},zx_2,\right),\left(z\vartheta_{i_2},sy_2\right),\left(z\vartheta_{f_2},zz_2\right)\right\rangle$ and $z\xi=\left\langle\left(z\vartheta_t,zx,\right),\left(z\vartheta_i,zy\right),\left(z\vartheta_f,zz\right)\right\rangle$ be 2TLNNs, then

$$(1)\ z\xi_1\oplus z\xi_2=\left\{\begin{array}{l}\Delta\left(z\pi\left(\dfrac{\Delta^{-1}\left(z\vartheta_{t_1},zx_1,\right)}{z\pi}+\dfrac{\Delta^{-1}\left(z\vartheta_{t_2},zx_2,\right)}{z\pi}-\dfrac{\Delta^{-1}\left(z\vartheta_{t_1},zx_1,\right)}{z\pi}\cdot\dfrac{\Delta^{-1}\left(z\vartheta_{t_2},zx_2,\right)}{z\pi}\right)\right),\\ \Delta\left(z\pi\left(\dfrac{\Delta^{-1}\left(z\vartheta_{i_1},zy_1\right)}{z\pi}\cdot\dfrac{\Delta^{-1}\left(z\vartheta_{i_2},zy_2\right)}{z\pi}\right)\right),\Delta\left(z\pi\left(\dfrac{\Delta^{-1}\left(z\vartheta_{f_1},zz_1\right)}{z\pi}\cdot\dfrac{\Delta^{-1}\left(z\vartheta_{f_2},zz_2\right)}{z\pi}\right)\right)\end{array}\right\};$$

$$(2)\ \ z\xi_1\otimes z\xi_2=\left\{\begin{array}{l}\Delta\left(z\pi\dfrac{\Delta^{-1}\left(z\vartheta_{t_1},zx_1,\right)}{z\pi}\cdot\dfrac{\Delta^{-1}\left(z\vartheta_{t_2},zx_2,\right)}{z\pi}\right),\\ \Delta\left(z\pi\left(\dfrac{\Delta^{-1}\left(z\vartheta_{i_1},zy_1\right)}{z\pi}+\dfrac{\Delta^{-1}\left(z\vartheta_{i_2},zy_2\right)}{z\pi}-\dfrac{\Delta^{-1}\left(z\vartheta_{i_1},zy_1\right)}{z\pi}\cdot\dfrac{\Delta^{-1}\left(z\vartheta_{i_2},zy_2\right)}{z\pi}\right)\right),\\ \Delta\left(z\pi\left(\dfrac{\Delta^{-1}\left(z\vartheta_{f_1},zz_1\right)}{z\pi}+\dfrac{\Delta^{-1}\left(z\vartheta_{f_2},zz_2\right)}{z\pi}-\dfrac{\Delta^{-1}\left(z\vartheta_{f_1},zz_1\right)}{z\pi}\cdot\dfrac{\Delta^{-1}\left(z\vartheta_{f_2},zz_2\right)}{z\pi}\right)\right)\end{array}\right\};$$

$$(3)\ \ \lambda z\xi_1=\left\{\begin{array}{l}\Delta\left(z\pi\left(1-\left(1-\dfrac{\Delta^{-1}\left(z\vartheta_{t_1},zx_1,\right)}{z\pi}\right)^{\lambda}\right)\right),\\ \Delta\left(z\pi\left(\dfrac{\Delta^{-1}\left(z\vartheta_{i_1},zy_1\right)}{z\pi}\right)^{\lambda}\right),\left(z\pi\left(\dfrac{\Delta^{-1}\left(z\vartheta_{f_1},zz_1\right)}{z\pi}\right)^{\lambda}\right)\end{array}\right\};$$

$$(4)\left(z\xi_1\right)^{\lambda}=\left\{\begin{array}{l}\Delta\left(z\pi\left(\dfrac{\Delta^{-1}\left(z\vartheta_{t_1},zx_1,\right)}{z\pi}\right)^{\lambda}\right),\Delta\left(z\pi\left(1-\left(1-\dfrac{\Delta^{-1}\left(z\vartheta_{i_1},zy_1\right)}{z\pi}\right)^{\lambda}\right)\right),\\ \Delta\left(z\pi\left(1-\left(1-\dfrac{\Delta^{-1}\left(z\vartheta_{f_1},zz_1\right)}{z\pi}\right)^{\lambda}\right)\right)\end{array}\right\}.$$

The 2TLNN Hamming distance (2TLNNHD) and 2TLNN Euclidean distance (2TLNNED) [37] is described.

Definition 4[37]. Let $z\xi_1=\left\langle\left(z\vartheta_{t_1},zx_1,\right),\left(z\vartheta_{i_1},zy_1\right),\left(z\vartheta_{f_1},zz_1\right)\right\rangle$, $z\xi_2=\left\langle\left(z\vartheta_{t_2},zx_2,\right),\left(z\vartheta_{i_2},sy_2\right),\left(z\vartheta_{f_2},zz_2\right)\right\rangle$, the 2TLNNHD are described:

$$2TLNNHD\left(z\xi_1,z\xi_2\right)=\frac{1}{3}\left(\begin{array}{l}\left|\dfrac{\Delta^{-1}\left(z\vartheta_{t_1},zx_1\right)-\Delta^{-1}\left(z\vartheta_{t_2},zx_2\right)}{z\pi}\right|\\ +\left|\dfrac{\Delta^{-1}\left(z\vartheta_{i_1},zy_1\right)-\Delta^{-1}\left(z\vartheta_{i_2},zy_2\right)}{z\pi}\right|\\ +\left|\dfrac{\Delta^{-1}\left(z\vartheta_{f_1},zz_1\right)-\Delta^{-1}\left(z\vartheta_{f_2},zz_2\right)}{z\pi}\right|\end{array}\right) \tag{6}$$

Definition 5[37]. Let $z\xi_1=\left\langle\left(z\vartheta_{t_1},zx_1,\right),\left(z\vartheta_{i_1},zy_1\right),\left(z\vartheta_{f_1},zz_1\right)\right\rangle$, $z\xi_2=\left\langle\left(z\vartheta_{t_2},zx_2,\right),\left(z\vartheta_{i_2},sy_2\right),\left(z\vartheta_{f_2},zz_2\right)\right\rangle$, the 2TLNNED is described:

$$2TLNNED\left(z\xi_1,z\xi_2\right)=\sqrt{\frac{1}{3}\left(\begin{array}{l}\left|\dfrac{\Delta^{-1}\left(z\vartheta_{t_1},zx_1\right)-\Delta^{-1}\left(z\vartheta_{t_2},zx_2\right)}{z\pi}\right|^2\\ +\left|\dfrac{\Delta^{-1}\left(z\vartheta_{i_1},zy_1\right)-\Delta^{-1}\left(z\vartheta_{i_2},zy_2\right)}{z\pi}\right|^2\\ +\left|\dfrac{\Delta^{-1}\left(z\vartheta_{f_1},zz_1\right)-\Delta^{-1}\left(z\vartheta_{f_2},zz_2\right)}{z\pi}\right|^2\end{array}\right)} \tag{7}$$

Then, the 2TLNNWG approach [36] is described.

Definition 6[36]. Let $z\xi_j=\left\langle\left(z\vartheta_{t_j},zx_j,\right),\left(z\vartheta_{i_j},zy_j\right),\left(z\vartheta_{f_j},zz_j\right)\right\rangle$ be 2TLNNs, the 2TLNNWG approach is described:

$$
\begin{aligned}
&\text{2TLNNWG}\left(z\xi_1, z\xi_2, \ldots, z\xi_n\right) \\
&= \left(z\xi_1\right)^{zw_1} \oplus \left(z\xi_2\right)^{zw_2} \otimes \ldots \otimes \left(z\xi_n\right)^{zw_n} = \overset{n}{\underset{j=1}{\otimes}} \left(z\xi_j\right)^{zw_j} \\
&= \begin{pmatrix}
\Delta\left(z\pi \prod_{j=1}^{n} \left(\frac{\Delta^{-1}\left(z\vartheta_{t_j}, zx_j,\right)}{z\pi}\right)^{zw_j}\right), \\
\Delta\left(z\pi\left(1 - \prod_{j=1}^{n}\left(1 - \frac{\Delta^{-1}\left(z\vartheta_{i_j}, zy_j\right)}{z\pi}\right)^{zw_j}\right)\right), \\
\Delta\left(z\pi\left(1 - \prod_{j=1}^{n}\left(1 - \frac{\Delta^{-1}\left(z\vartheta_{i_j}, zy_j\right)}{z\pi}\right)^{zw_j}\right)\right)
\end{pmatrix}
\end{aligned} \tag{8}
$$

with zw_j is the weight value of $z\xi_j$, $\sum_{j=1}^{n} zw_j = 1$.

3. Method

3.1. 2TLN-MAGDM

The 2TLNN-ExpTODIM-VIKOR is described as the MAGDM. Let $ZX = \left(ZX_1, ZX_2, \ldots, ZX_m\right)$ be alternatives and $ZY = \left(ZY_1, ZY_2, \ldots, ZY_m\right)$ be attributes with weight values $zw = \left(zw_1, zw_2, \cdots, zw_n\right)$ and experts $ZZ = \left(ZZ_1, ZZ_2, \ldots, ZZ_m\right)$ with weight $z\omega = \left(z\omega_1, z\omega_2, \cdots, z\omega_q\right)$, the 2TLNN-ExpTODIM-VIKOR approach is described as the MAGDM.

Step 1. Describe the 2TLNN-matrix $ZR^{(t)} = \left[ZR_{ij}^{(t)}\right]_{m\times n}$:

$$
ZR^{(t)} = \left[ZR_{ij}^{(t)}\right]_{m\times n} = \begin{array}{c} \\ ZX_1 \\ ZX_2 \\ \vdots \\ ZX_m \end{array} \begin{array}{c} \begin{array}{cccc} ZY_1 & ZY_2 & \ldots & ZY_n \end{array} \\ \begin{bmatrix} ZR_{11}^{(t)} & ZR_{12}^{(t)} & \ldots & ZR_{1n}^{(t)} \\ ZR_{21}^{(t)} & ZR_{22}^{(t)} & \ldots & ZR_{2n}^{(t)} \\ \vdots & \vdots & \vdots & \vdots \\ ZR_{m1}^{(t)} & ZR_{m2}^{(t)} & \ldots & ZR_{mn}^{(t)} \end{bmatrix} \end{array} \tag{9}
$$

where $ZR_{ij}^{(t)} = \left(\left(z\vartheta_{t_{ij}}^{(t)}, zx_{ij}^{(t)},\right), \left(z\vartheta_{i_{ij}}^{(t)}, zy_{ij}^{(t)},\right), \left(z\vartheta_{f_{ij}}^{(t)}, zz_{ij}^{(t)},\right)\right)$ is 2TLNNs.

Step 2. Describe the 2TLNN-matrix $ZR = \left[ZR_{ij}\right]_{m\times n}$:

$$ZR=\left[ZR_{ij}\right]_{m\times n}=\begin{array}{c} \\ ZX_1 \\ ZX_2 \\ \vdots \\ ZX_m \end{array}\begin{array}{c} \begin{array}{cccc} ZY_1 & ZY_2 & \ldots & ZY_n \end{array} \\ \begin{bmatrix} ZR_{11} & ZR_{12} & \ldots & ZR_{1n} \\ ZR_{21} & ZR_{22} & \ldots & ZR_{2n} \\ \vdots & \vdots & \vdots & \vdots \\ ZR_{m1} & ZR_{m2} & \ldots & ZR_{mn} \end{bmatrix} \end{array} \tag{10}$$

In light with 2TLNNWG, the $ZR=\left[ZR_{ij}\right]_{m\times n}$ is described:

$$\begin{aligned} ZR_{ij} &= \left(\left(z\vartheta_{t_{ij}}, zx_{ij}\right),\left(z\vartheta_{i_{ij}}, zy_{ij}\right),\left(z\vartheta_{f_{ij}}, zz_{ij}\right)\right) \\ &= \left(ZR_{ij}^{(1)}\right)^{zw_1}\oplus\left(ZR_{ij}^{(2)}\right)^{zw_2}\otimes\ldots\otimes\left(ZR_{ij}^{(q)}\right)^{zw_q} \\ &= \overset{n}{\underset{t=1}{\otimes}}\left(ZR_{ij}^{(t)}\right)^{zw_t} = \begin{pmatrix} \Delta\left(z\pi\prod_{t=1}^{q}\left(\frac{\Delta^{-1}\left(z\vartheta_{t_{ij}}^{(t)}, zx_{ij}^{(t)}\right)}{z\pi}\right)^{zw_j}\right), \\ \Delta\left(z\pi\left(1-\prod_{t=1}^{q}\left(1-\frac{\Delta^{-1}\left(z\vartheta_{i_{ij}}^{(t)}, zy_{ij}^{(t)}\right)}{z\pi}\right)^{uw_j}\right)\right), \\ \Delta\left(z\pi\left(1-\prod_{t=1}^{q}\left(1-\frac{\Delta^{-1}\left(z\vartheta_{f_{ij}}^{(t)}, zz_{ij}^{(t)}\right)}{z\pi}\right)^{zw_j}\right)\right) \end{pmatrix} \end{aligned} \tag{11}$$

Step 3. Describe the 2TLNN normalized matrix $NZR=\left[NZR_{ij}\right]_{m\times n}$ [38].

For benefit attributes:

$$\begin{aligned} NZR_{ij} = ZR_{ij} &= \left(\left(z\vartheta_{t_{ij}}^{N}, zx_{ij}^{N}\right),\left(z\vartheta_{i_{ij}}^{N}, zy_{ij}^{N}\right),\left(z\vartheta_{f_{ij}}^{N}, zz_{ij}^{N}\right)\right) \\ &= \left(\left(z\vartheta_{t_{ij}}, zx_{ij}\right),\left(z\vartheta_{i_{ij}}, zy_{ij}\right),\left(z\vartheta_{f_{ij}}, zz_{ij}\right)\right) \end{aligned} \tag{12}$$

For cost attributes:

$$\begin{aligned} NZR_{ij} &= \left(\left(z\vartheta_{t_{ij}}^{N}, zx_{ij}^{N}\right),\left(z\vartheta_{i_{ij}}^{N}, zy_{ij}^{N}\right),\left(z\vartheta_{f_{ij}}^{N}, zz_{ij}^{N}\right)\right) \\ &= \left(\Delta\left(z\pi-\Delta^{-1}\left(z\vartheta_{t_{ij}}, zx_{ij}\right)\right),\Delta\left(z\pi-\Delta^{-1}\left(z\vartheta_{i_{ij}}, zy_{ij}\right)\right),\Delta\left(z\pi-\Delta^{-1}\left(z\vartheta_{f_{ij}}, zz_{ij}\right)\right)\right) \end{aligned} \tag{13}$$

3.2. Describe the attributes' weight with entropy.

Entropy [39] is utilized to construct weight. The normalized matrix is described:

$$LZZ_{ij}=\frac{1}{2}\left(\begin{array}{l}\dfrac{\left(SF\left(\left(z\vartheta_{t_{ij}}^{N},zx_{ij}^{N}\right),\left(z\vartheta_{i_{ij}}^{N},zy_{ij}^{N}\right),\left(z\vartheta_{f_{ij}}^{N},zz_{ij}^{N}\right)\right)\right)}{\sum_{i=1}^{m}\left(AF\left(\left(z\vartheta_{t_{ij}}^{N},zx_{ij}^{N}\right),\left(z\vartheta_{i_{ij}}^{N},zy_{ij}^{N}\right),\left(z\vartheta_{f_{ij}}^{N},zz_{ij}^{N}\right)\right)\right)}\\+\dfrac{\left(AF\left(\left(z\vartheta_{t_{ij}}^{N},zx_{ij}^{N}\right),\left(z\vartheta_{i_{ij}}^{N},zy_{ij}^{N}\right),\left(z\vartheta_{f_{ij}}^{N},zz_{ij}^{N}\right)\right)+1\right)}{\sum_{i=1}^{m}\left(SF\left(\left(z\vartheta_{t_{ij}}^{N},zx_{ij}^{N}\right),\left(z\vartheta_{i_{ij}}^{N},zy_{ij}^{N}\right),\left(z\vartheta_{f_{ij}}^{N},zz_{ij}^{N}\right)\right)+1\right)}\end{array}\right) \tag{14}$$

The linguistic Shannon entropy (LSE) is described:

$$LSE_j=-\frac{1}{\ln m}\sum_{i=1}^{m}LZZ_{ij}\ln LZZ_{ij} \tag{15}$$

and $LZZ_{ij}\ln LZZ_{ij}=0$ if $LZZ_{ij}=0$.

Then, the weights $zw=\left(zw_1,zw_2,\cdots,zw_n\right)$ is described:

$$zw_j=\frac{1-LSE_j}{\sum_{j=1}^{n}\left(1-LSE_j\right)},\quad j=1,2,\cdots,n. \tag{16}$$

3.3. 2TLNN-ExpTODIM-VIKOR approach for MAGDM

The 2TLNN-ExpTODIM-VIKOR approach is described to put forward the MAGDM.

(1) Describe relative decision weight:

$$rzw_j=zw_j\Big/\max_j zw_j, \tag{17}$$

(2) The linguistic information dominance degree (LIDD) $LIDD_j\left(ZA_i,ZA_t\right)$ of ZX_i over ZX_t for ZY_j is described.

$$LIDD_j\left(ZX_i,ZX_t\right)=\begin{cases}\dfrac{rzw_j\times\left(1-10^{-\rho 2TLNNHD\left(NZR_{ij},NZR_{tj}\right)}\right)}{\sum_{j=1}^{n}rzw_j} & \text{if } SF\left(NZR_{ij}\right)>SF\left(NZR_{tj}\right)\\ 0 & \text{if } SF\left(NZR_{ij}\right)=SF\left(NZR_{tj}\right)\\ -\dfrac{1}{\theta}\dfrac{\sum_{j=1}^{n}rzw_j\times\left(1-10^{-\rho 2TLNNHD\left(NZR_{ij},NZR_{tj}\right)}\right)}{rzw_j} & \text{if } SF\left(NZR_{ij}\right)<SF\left(NZR_{tj}\right)\end{cases} \tag{18}$$

where θ is from Tversky and Kahneman [40] and $\rho\in[1,5]$ [26].

The $LIDD_j\left(ZX_i\right)$ is described:

$$LIDD_j\left(ZX_i\right)=\left[LIDD_j\left(ZX_i,ZX_t\right)\right]_{m\times m}$$

$$=\begin{array}{c} \\ ZX_1 \\ ZX_2 \\ \vdots \\ ZX_m \end{array}\begin{array}{c} \begin{array}{cccc} ZX_1 & ZX_2 & \cdots & ZX_m \end{array} \\ \begin{bmatrix} 0 & LIDD_j\left(ZX_1,ZX_2\right) & \cdots & LIDD_j\left(ZX_1,ZX_m\right) \\ LIDD_j\left(ZX_2,ZX_1\right) & 0 & \cdots & LIDD_j\left(ZX_2,ZX_m\right) \\ \vdots & \vdots & \cdots & \vdots \\ LIDD_j\left(ZX_m,ZX_1\right) & LIDD_j\left(ZX_m,ZX_2\right) & \cdots & 0 \end{bmatrix} \end{array}$$

(3) Describe the LIDD of ZX_i for other choices under ZY_j:

$$LIDD_j\left(ZX_i\right)=\sum_{t=1}^{m}LIDD_j\left(ZX_i,ZX_t\right) \tag{19}$$

The overall LIDD matrix is described:

$$LIDD=\left(LIDD_{ij}\right)_{m\times n}$$

$$=\begin{array}{c} \\ ZX_1 \\ ZX_2 \\ \vdots \\ ZX_m \end{array}\begin{array}{c} \begin{array}{cccc} ZX_1 & ZX_2 & \cdots & ZX_n \end{array} \\ \begin{bmatrix} \sum_{t=1}^{m}LIDD_1\left(ZX_1,ZX_t\right) & \sum_{t=1}^{m}LIDD_2\left(ZX_1,ZX_t\right) & \ldots & \sum_{t=1}^{m}LIDD_n\left(ZX_1,ZX_t\right) \\ \sum_{t=1}^{m}LIDD_1\left(ZX_2,ZX_t\right) & \sum_{t=1}^{m}LIDD_2\left(ZX_2,ZX_t\right) & \ldots & \sum_{t=1}^{m}LIDD_n\left(ZX_2,ZX_t\right) \\ \vdots & \vdots & \vdots & \vdots \\ \sum_{t=1}^{m}LIDD_1\left(ZX_m,ZX_t\right) & \sum_{t=1}^{m}LIDD_2\left(ZX_m,ZX_t\right) & \ldots & \sum_{t=1}^{m}LIDD_n\left(ZX_m,ZX_t\right) \end{bmatrix} \end{array}$$

(4) Describe the VIKOR approach through maximum group utility $ZTLNS_i$, minimum individual regret information $ZTLNR_i$ and relationship degree $ZTLNQ_i$ between $ZTLNS_i$ and $ZTLNR_i$.

$$ZTLNS_i=\sum_{j=1}^{n}zw_j\frac{d(LIDD_j^+,LIDD_{ij})}{d(LIDD_j^+,LIDD_j^-)} \tag{20}$$

$$ZTLNR_i=\max_{j=1}^{n}zw_j\frac{d(LIDD_j^+,LIDD_{ij})}{d(LIDD_j^+,LIDD_j^-)} \tag{21}$$

$$ZTLNQ_i=v\times\frac{ZTLNS_i-ZTLNS_i^-}{ZTLNS_i^+-ZTLNS_i^-}+(1-v)\times\frac{ZTLNR_i-ZTLNR_i^-}{ZTLNR_i^+-ZTLNR_i^-} \tag{22}$$

where $ZTLNS_i^+ = \max_{i=1}^{m} ZTLNS_i$, $ZTLNS_i^- = \min_{i=1}^{m} ZTLNS_i$, $ZTLNR_i^+ = \max_{i=1}^{m} ZTLNR_i$ and $ZTLNR_i^- = \min_{i=1}^{m} ZTLNR_i$. $v \in [0,1]$, in general, $v = 0.5$. $d(LIDD_j^+, LIDD_j^-)$ is distance between $LIDD_j^+ = \max_{i=1}^{m} LIDD_{ij}$ and $LIDD_{ij}$, $d(LIDD_j^+, LIDD_j^-)$ is distance between $LIDD_j^+ = \max_{i=1}^{m} LIDD_{ij}$ and $LIDD_j^- = \min_{i=1}^{m} LIDD_{ij}$.

(5) Three sequences are described by $ZTLNS_i$, $ZTLNR_i$ and $ZTLNQ_i$ through ascending order.

4. Case Study and Analysis

The evaluation of university educational management quality is a systematic and comprehensive process aimed at assessing the effectiveness and efficiency of various aspects of university management to ensure that management practices support high-quality teaching and research activities. As higher education rapidly develops, society demands higher standards for university performance and talent cultivation, making a scientifically sound management evaluation system an essential tool for continuously improving university management levels. In evaluating the quality of university educational management, the evaluation typically covers multiple dimensions. The first is the soundness of the management system, assessing the scientific and rational nature of institutional structures, organizational frameworks, and decision-making processes. An effective management system not only improves management efficiency but also enhances the overall operational capacity of the institution. The second dimension focuses on the allocation and utilization of teaching resources, evaluating whether faculty, teaching equipment, and educational funding are allocated rationally and whether these resources sufficiently support educational goals. Additionally, the evaluation emphasizes the quality of student management and services, including the organization of student activities, academic support, and mental health services, ensuring that students receive comprehensive support and development during their time at the university. Related to this is the evaluation of teaching management quality, which examines the design and implementation of teaching plans, the rationality of course offerings, the innovativeness of teaching methods, and the achievement of teaching outcomes. Through

a comprehensive review of the teaching process, it is possible to understand the specific impact of management practices on teaching quality. Furthermore, research management is another important area of evaluation. Universities should foster research productivity and the transfer of research results through effective research management systems, encouraging faculty to engage in academic research and innovation activities. In terms of evaluation methods, university educational management quality evaluations typically use a combination of quantitative and qualitative approaches. For instance, quantitative methods like surveys and data analysis offer objective insights into management effectiveness, while qualitative approaches, such as expert interviews and case studies, delve into underlying issues and areas for improvement. These evaluations not only pinpoint existing management deficiencies but also serve as a foundation and guide for future management practices. Moreover, the ultimate goal of university educational management quality evaluation is to drive continuous optimization of management systems, achieve efficient allocation of educational resources, and improve the quality of talent cultivation, thereby enhancing the university's overall competitiveness. In the context of globalization, the construction and improvement of the evaluation system must align with international standards to ensure that universities remain competitive and influential in the global education market. This evaluation process is not only a crucial tool for universities' self-improvement but also an important means for the public and government to monitor and provide feedback on university performance. The quality evaluation of university educational management is MAGDM. Five potential regional comprehensive universities $ZX_i\left(i=1,2,3,4,5\right)$ are evaluated with four attributes: ZY_1 is to **Soundness of Management System**: Evaluates the organizational structure, decision-making processes, and institutional frameworks, assessing their scientific rigor and ability to support both day-to-day operations and long-term development; ZY_2 is **Teaching Resource Allocation and Utilization**: Assesses whether the allocation of faculty, teaching equipment, and funding is reasonable and sufficient to meet academic needs and improve teaching quality; ZY_3 is **Student Management and Service Quality**: Evaluates the comprehensiveness of student management and services, including academic support, mental

health services, and career development guidance, ensuring students' holistic development; ZY_4 is **Research Management and Innovation Support**: Measures the effectiveness of research management, the support provided for research resources, and the output and commercialization of research results, encouraging faculty engagement in academic and innovative activities. Five regional comprehensive universities are evaluated with 2TLNNs with four criteria through three experts $ZZ_t\,(t=1,2,3)$ with expert weight $z\omega=(1/3,1/3,1/3)$. (Table 1 see appendix)

The 2TLNN-ExpTODIM-VIKOR approach is described to solve the quality evaluation of university educational management.

Step 1. Describe the 2TLNN matrix $ZR^{(t)}=\left[ZR_{ij}^{(t)}\right]_{5\times4}\,(t=1,2,3)$ (Table 2-4).

Table 2. Evaluation data from ZZ_1

	ZY_1	ZY_2	ZY_3	ZY_4
ZX_1	ZW	ZM	ZT	ZVW
ZX_2	ZM	ZW	ZVW	ZVT
ZX_3	ZVT	ZVT	ZVW	ZM
ZX_4	ZT	ZVW	ZVT	ZM
ZX_5	ZVW	ZW	ZM	ZVT

Table 3. Evaluation data from ZZ_2

	ZY_1	ZY_2	ZY_3	ZY_4
ZX_1	ZVT	ZM	ZVW	ZT
ZX_2	ZT	ZW	ZM	ZVW
ZX_3	ZVW	ZW	ZVT	ZM
ZX_4	ZM	ZW	ZVT	ZVW
ZX_5	ZM	ZT	ZVW	ZW

Table 4. Evaluation data from ZZ_3

	ZY_1	ZY_2	ZY_3	ZY_4
ZX_1	ZM	ZT	ZVW	ZW
ZX_2	ZW	ZVW	ZVT	ZT
ZX_3	ZM	ZW	ZT	ZM
ZX_4	ZW	ZVW	ZT	ZM
ZX_5	ZVT	ZVT	ZM	ZW

Then according to 2TLNNWG, the $ZR = \left[ZR_{ij} \right]_{5\times 4}$ is described (Table 5).

Table 5. The $ZR = \left[ZR_{ij} \right]_{5\times 4}$

	ZY_1
ZX_1	$\{(z\vartheta_2, -0.2547), (z\vartheta_3, 0.2492), (z\vartheta_4, 0.2553)\}$
ZX_2	$\{(z\vartheta_4, 0.0213), (z\vartheta_3, 0.0125), (z\vartheta_2, 0.0435)\}$
ZX_3	$\{(z\vartheta_4, -0.2309), (z\vartheta_3, -0.3265), (z\vartheta_2, 0.3276)\}$
ZX_4	$\{(z\vartheta_5, -0.2973), (z\vartheta_2, 0.2302), (z\vartheta_1, 0.2975)\}$
ZX_5	$\{(z\vartheta_4, 0.1654), (z\vartheta_3, -0.3436), (z\vartheta_2, -0.1763)\}$
	ZY_2
ZX_1	$\{(z\vartheta_4, -0.2495), (z\vartheta_3, -0.4271), (z\vartheta_2, 0.1287)\}$
ZX_2	$\{(z\vartheta_4, -0.1576), (z\vartheta_3, -0.3438), (z\vartheta_2, 0.1572)\}$
ZX_3	$\{(z\vartheta_3, 0.3673), (z\vartheta_3, 0.2714), (z\vartheta_3, -0.3765)\}$
ZX_4	$\{(z\vartheta_3, 0.1296), (z\vartheta_3, 0.2145), (z\vartheta_3, -0.1394)\}$
ZX_5	$\{(z\vartheta_4, -0.4128), (z\vartheta_3, -0.2072), (z\vartheta_2, 0.4236)\}$
	ZY_3

ZX_1	$\{(z\vartheta_3,-0.3746),(z\vartheta_3,0.2543),(z\vartheta_3,0.4734)\}$
ZX_2	$\{(z\vartheta_5,-0.3914),(z\vartheta_2,0.2589),(z\vartheta_1,0.3816)\}$
ZX_3	$\{(z\vartheta_3,-0.2364),(z\vartheta_3,0.3437),(z\vartheta_3,0.2364)\}$
ZX_4	$\{(z\vartheta_3,-0.4743),(z\vartheta_3,0.2825),(z\vartheta_3,0.4746)\}$
ZX_5	$\{(z\vartheta_4,0.4843),(z\vartheta_3,-0.4492),(z\vartheta_2,-0.4675)\}$
	ZY_4
ZX_1	$\{(z\vartheta_2,-0.1546),(z\vartheta_3,0.3659),(z\vartheta_4,0.2362)\}$
ZX_2	$\{(z\vartheta_1,0.3458),(z\vartheta_4,-0.3529),(z\vartheta_5,-0.3437)\}$
ZX_3	$\{(z\vartheta_4,-0.1576),(z\vartheta_3,-0.3438),(z\vartheta_2,0.1576)\}$
ZX_4	$\{(z\vartheta_4,0.3794),(z\vartheta_2,0.4623),(z\vartheta_2,-0.3795)\}$
ZX_5	$\{(z\vartheta_3,-0.4968),(z\vartheta_3,0.2714),(z\vartheta_3,0.4975)\}$

Step 2. Normalize the $ZR=\left[ZR_{ij}\right]_{5\times4}$ into $NZR=\left[NZR_{ij}\right]_{5\times4}$ (See Table 6).

Table 6. The $NZR=\left[NZR_{ij}\right]_{5\times4}$

	ZY_1
ZX_1	$\{(z\vartheta_2,-0.2547),(z\vartheta_3,0.2492),(z\vartheta_4,0.2553)\}$
ZX_2	$\{(z\vartheta_4,\ 0.0213),(z\vartheta_3,\ 0.0125),(z\vartheta_2,\ 0.0435)\}$
ZX_3	$\{(z\vartheta_4,-0.2309),(z\vartheta_3,-0.3265),(z\vartheta_2,0.3276)\}$
ZX_4	$\{(z\vartheta_5,-0.2973),(z\vartheta_2,0.2302),(z\vartheta_1,0.2975)\}$
ZX_5	$\{(z\vartheta_4,0.1654),(z\vartheta_3,-0.3436),(z\vartheta_2,-0.1763)\}$
	ZY_2

ZX_1	$\{(z\vartheta_4,-0.2495),(z\vartheta_3,-0.4271),(z\vartheta_2,0.1287)\}$
ZX_2	$\{(z\vartheta_4,-0.1576),(z\vartheta_3,-0.3438),(z\vartheta_2,0.1572)\}$
ZX_3	$\{(z\vartheta_3,0.3673),(z\vartheta_3,0.2714),(z\vartheta_3,-0.3765)\}$
ZX_4	$\{(z\vartheta_3,0.1296),(z\vartheta_3,0.2145),(z\vartheta_3,-0.1394)\}$
ZX_5	$\{(z\vartheta_4,-0.4128),(z\vartheta_3,-0.2072),(z\vartheta_2,0.4236)\}$

	ZY_3
ZX_1	$\{(z\vartheta_3,-0.3746),(z\vartheta_3,0.2543),(z\vartheta_3,0.4734)\}$
ZX_2	$\{(z\vartheta_5,-0.3914),(z\vartheta_2,0.2589),(z\vartheta_1,0.3816)\}$
ZX_3	$\{(z\vartheta_3,-0.2364),(z\vartheta_3,0.3437),(z\vartheta_3,0.2364)\}$
ZX_4	$\{(z\vartheta_3,-0.4743),(z\vartheta_3,0.2825),(z\vartheta_3,0.4746)\}$
ZX_5	$\{(z\vartheta_4,0.4843),(z\vartheta_3,-0.4492),(z\vartheta_2,-0.4675)\}$
	ZY_4
ZX_1	$\{(z\vartheta_2,-0.1546),(z\vartheta_3,0.3659),(z\vartheta_4,0.2362)\}$
ZX_2	$\{(z\vartheta_1,0.3458),(z\vartheta_4,-0.3529),(z\vartheta_5,-0.3437)\}$
ZX_3	$\{(z\vartheta_4,-0.1576),(z\vartheta_3,-0.3438),(z\vartheta_2,0.1576)\}$
ZX_4	$\{(z\vartheta_4,0.3794),(z\vartheta_2,0.4623),(z\vartheta_2,-0.3795)\}$
ZX_5	$\{(z\vartheta_3,-0.4968),(z\vartheta_3,0.2714),(z\vartheta_3,0.4975)\}$

Step 3. Describe the weight: $zw_1=0.2803, zw_2=0.3624, zw_3=0.1908, zw_4=0.1665$.

Step 4. Describe the relative weight: $rzw=(0.7735,1.0000,0.5265,0.4594)$

Step 5. Describe the $LIDD=(LIDD_{ij})_{5\times4}$ (Table 7):

Table 7. The $LIDD = \left(LIDD_{ij} \right)_{5\times4}$

	ZY_1	ZY_2	ZY_3	ZY_4
ZX_1	-0.2707	1.0729	0.3317	-0.5862
ZX_2	0.2600	0.3591	-1.8541	0.4491
ZX_3	-1.2130	-0.8965	0.8285	-1.2623
ZX_4	0.8229	-0.5033	-0.4939	1.0014
ZX_5	-1.1008	-1.4236	-0.5887	-0.0616

Step 6. Describe the $ZTLNS_i$, $ZTLNR_i$ and $ZTLNQ_i$ (See Table 8).

Table 8. The $ZTLNS_i$, $ZTLNR_i$ and $ZTLNQ_i$

	ZX_1	ZX_2	ZX_3	ZX_4	ZX_5
$ZTLNS_i$	0.3847	0.3610	0.7166	0.2230	0.6620
$ZTLNR_i$	0.2255	0.1755	0.3332	0.1536	0.2403
$ZTLNQ_i$	0.3277	0.2177	1.0000	0.0000	0.7331

Step 7. Sort these alternatives through the $ZTLNS_i$, $ZTLNR_i$ and $ZTLNQ_i$.

$$ZTLNS_4 < ZTLNS_2 < ZTLNS_1 < ZTLNS_5 < ZTLNS_3$$
$$ZTLNR_4 < ZTLNR_2 < ZTLNR_1 < ZTLNR_5 < ZTLNR_3$$
$$ZTLNQ_4 < ZTLNQ_2 < ZTLNQ_1 < ZTLNQ_5 < ZTLNQ_3$$

The best regional comprehensive university is ZX_4.

5. Comparative analysis

The 2TLNN-ExpTODIM-VIKOR approach is compared with 2TLNNWA operator[36], and 2TLNNWG approach[36], 2TLNN-MABAC approach [41], 2TLNN-GRA approach [38], 2TLNN-CODAS approach [42], and 2TLNN-TODIM approach [37]. The corresponding results are constructed in Table 9.

Table 9. Order for different approaches

Methods	Order
2TLNNWA approach [36]	$ZX_4 > ZX_2 > ZX_1 > ZX_5 > ZX_3$
2TLNNWG approach [36]	$ZX_4 > ZX_2 > ZX_5 > ZX_1 > ZX_3$
2TLNN-MABAC approach [41]	$ZX_4 > ZX_2 > ZX_1 > ZX_5 > ZX_3$
2TLNN-GRA approach [38]	$ZX_4 > ZX_2 > ZX_1 > ZX_5 > ZX_3$
2TLNN-CODAS approach [42]	$ZX_4 > ZX_2 > ZX_1 > ZX_5 > ZX_3$
2TLNN-TODIM approach [37]	$ZX_4 > ZX_2 > ZX_1 > ZX_5 > ZX_3$
2TLNN-ExpTODIM-VIKOR approach	$ZX_4 > ZX_2 > ZX_1 > ZX_5 > ZX_3$

The comparative analysis shows that while there are minor differences in the rankings across the models, all decision models and algorithms consistently identify the same best and worst regional comprehensive universities. This validates the reasonableness and effectiveness of the 2TLNN-ExpTODIM-VIKOR approach. Furthermore, the 2TLNN-ExpTODIM-VIKOR method developed in this study provides a more accurate and reliable decision analysis compared to other decision-making techniques. A key strength of this research is that the 2TLNN-ExpTODIM-VIKOR approach takes into account the bounded rationality of decision-makers and effectively handles MAGDM problems involving conflicting or incomparable attributes.

6. Conclusion

The evaluation of university educational management quality is a comprehensive mechanism that assesses the effectiveness and efficiency of various aspects of the management process. It covers the implementation of educational policies, the rationality of management structure, the optimization of resource allocation, the quality of student services,

and the support for teaching and research. Through systematic analysis and feedback on these elements, the evaluation mechanism identifies problems and areas for improvement, helping universities enhance their management, and optimize the efficiency of their educational resources. Additionally, it ensures that universities' goals align with societal needs and development trends, promoting the sustainable development of higher education. The quality evaluation of university educational management, within the framework of rural revitalization, epitomizes a MAGDM challenge. Recently, the TODIM-VIKOR method has been introduced to address such MAGDM problems. In this context, 2TLNSs have been introduced as a means to handle uncertain data during the evaluation process. This study introduces the 2TLNN-ExpTODIM-VIKOR model, specifically designed to manage MAGDM scenarios utilizing 2TLNSs. To demonstrate the effectiveness of the 2TLNN-ExpTODIM-VIKOR model, a numerical study focusing on the quality evaluation of university educational management is presented. The major contributions are illustrated: (1) ExpTODIM and VIKOR approaches are extended to the 2TLNNs; (2) entropy approach is described to obtain the weight under 2TLNNs; (3) 2TLNN-ExpTODIM-VIKOR approach is described forward MAGDM with 2TLNNs; (4) Finally, numerical example for quality evaluation of university educational management and comparative analysis are described to validate the 2TLNN-ExpTODIM-VIKOR approach.

References

[1] X. Wang, H. Zhou, Design of university educational management information systems oriented towards quality evaluation, Chinese Higher Medical Education, (2001) 3-4.

[2] X. Zhu, H. Yan, Improving educational management to enhance university teaching quality, Journal of Hebei University of Technology (Social Sciences Edition), (2007) 83-85.

[3] H. Lan, Exploring the application of total quality management theory in university educational management, China Science and Education Innovation Guide, (2009) 213.

[4] R. Gao, Research on the quality of university educational management in the context of higher education massification, Journal of Hubei University of Economics (Humanities and Social Sciences Edition), 13 (2016) 142-143.

[5] Y. Gao, Educational supervision as a key to improving the quality of university educational management, Curriculum Education Research, (2019) 173-174.

[6] W. Liu, Research on university entrepreneurship education management model and quality evaluation,

Economic Management Digest, (2019) 163-164.

[7] P. Liu, Research on the quality assurance path of university educational management, Journal of Heilongjiang Teachers Development College, 40 (2021) 13-15.

[8] X. Guo, Promoting the cultivation of innovative talent and improving the quality of higher education management: Strategies for building faculty, models, processes, and evaluation systems, Chinese and Foreign Corporate Culture, (2022) 121-122.

[9] Y. Lin, Analysis of university entrepreneurship education management model and quality evaluation, Journal of Hubei Open Vocational College, 36 (2023) 15-16+28.

[10] R. Fang, Optimization of higher education management measures aimed at improving employment service quality, China Employment, (2024) 93-95.

[11] S. Bhuvaneshwari, C.A.C. Sweety, A. Singh, S. Broumi, M. Talea, P.K. Raut, A novel and an efficient codas technique to solve real-life magdm problems in fermatean neutrosophic environment, Neutrosophic Sets and Systems, 72 (2024) 41-59.

[12] A.K. Das, N. Gupta, C. Granados, R. Das, S. Das, Neutrosophic approach to water quality assessment: A case study of gomati river, the largest river in tripura, india, Neutrosophic Systems with Applications, 22 (2024) 1-12.

[13] M. Karak, A. Mahata, S. Paul, S. Mukherjee, S. Biswas, B. Roy, An attempt on investment selection problem under neutrosophic environment based on weighted value method, Neutrosophic Optimization and Intelligent Systems, 4 (2024) 39-50.

[14] D. Mondal, T. Garai, G.C. Roy, S. Alam, Evaluating the nuclear power plant safety system under neutrosophic environment, Neutrosophic Sets and Systems, 72 (2024) 286-303.

[15] R. Imran, K. Ullah, Z. Ali, M. Akram, An approach to multi-attribute decision-making based on single-valued neutrosophic hesitant fuzzy aczel-alsina aggregation operator, Neutrosophic Systems with Applications, 22 (2024) 43-57.

[16] M. Luo, Z. Sun, L. Wu, Fuzzy inference quintuple implication method based on single valued neutrosophic t-representable t-norm, Neutrosophic Optimization and Intelligent Systems, 3 (2024) 8-22.

[17] I. Ul Haq, T. Shaheen, W. Ali, T. Senapati, A novel sir approach to closeness coefficient-based magdm problems using pythagorean fuzzy aczel-alsina aggregation operators for investment policy, Discrete Dynamics in Nature and Society, 2022 (2022) 12.

[18] S. Naz, M. Akram, G. Muhiuddin, A. Shafiq, Retracted: Modified edas method for magdm based on msm operators with 2-tuple linguistic t-spherical fuzzy sets (retracted article), Mathematical Problems in Engineering, 2022 (2022) 34.

[19] N.N. Liao, G.W. Wei, X.D. Chen, Todim method based on cumulative prospect theory for multiple attributes group decision making under probabilistic hesitant fuzzy setting, International Journal of Fuzzy Systems, 24 (2022) 322-339.

[20] K. Kumar, S.M. Chen, Multiple attribute group decision making based on advanced linguistic intuitionistic fuzzy weighted averaging aggregation operator of linguistic intuitionistic fuzzy numbers, Information

Sciences, 587 (2022) 813-824.

[21] Q. Khan, H. Garg, H. Khattak, A.A. Al-Babtain, I. Elbatal, M. Elgarhy, A novel magdm approach based on cubic q-rung orthopair fuzzy power generalized maclaurin symmetric mean operator, Journal of Function Spaces, 2022 (2022) 33.

[22] C. Jana, H. Garg, M. Pal, B. Sarkar, G.W. Wei, Mabac framework for logarithmic bipolar fuzzy multiple attribute group decision-making for supplier selection, Complex & Intelligent Systems, 10 (2024) 273-288.

[23] L.P. Bian, C. Che, Enhanced combined techniques for interval-valued intuitionistic fuzzy multiple-attribute group decision-making and applications to quality evaluation of large-scale multi-view 3d reconstruction, Ieee Access, 11 (2023) 120502-120515.

[24] H. Gao, L.G. Ran, G.W. Wei, C. Wei, J. Wu, Vikor method for magdm based on q-rung interval-valued orthopair fuzzy information and its application to supplier selection of medical consumption products, International Journal of Environmental Research and Public Health, 17 (2020) 14.

[25] I.E.H. Kremer, S. Evers, P.J. Jongen, T. van der Weijden, I. van de Kolk, M. Hiligsmann, Identification and prioritization of important attributes of disease-modifying drugs in decision making among patients with multiple sclerosis: A nominal group technique and best-worst scaling, Plos One, 11 (2016) 16.

[26] A.B. Leoneti, L. Gomes, A novel version of the todim method based on the exponential model of prospect theory: The exptodim method, European Journal of Operational Research, 295 (2021) 1042-1055.

[27] H. Sun, Z. Yang, Q. Cai, G.W. Wei, Z.W. Mo, An extended exp-todim method for multiple attribute decision making based on the z-wasserstein distance, Expert Systems with Applications, 214 (2023) 14.

[28] Y. Deng, W.X. Zhang, An exptodim-gra based multiple attribute group decision-making method for development level evaluation of digital inclusive finance under intuitionistic fuzzy circumstances, Journal of Intelligent & Fuzzy Systems, 45 (2023) 10661-10673.

[29] Y. Wang, C. Liu, C. Deng, An exptodim-edas based multiple attribute group decision-making framework for supervision effectiveness evaluation of small and medium sized financial institutions in rural areas under intuitionistic fuzzy circumstances, Ieee Access, (2023) https://doi.org/10.1109/ACCESS.2023.3333432.

[30] C. Huang, Z. Cheng, H. Guo, Exptodim-driven framework for 2-tuple linguistic neutrosophic magdm with applications to teaching quality evaluation in higher education, International Journal of Knowledge-Based and Intelligent Engineering Systems, 28 (2024) 15-30.

[31] Y.M. Liang, An exptodim-macont based multiple-attribute group decision-making technique for smart classroom teaching evaluation of basic english under interval-valued pythagorean fuzzy circumstances, Ieee Access, 12 (2024) 14130-14145.

[32] F. Xu, A 2tlns-based exponential todim-edas approach for evaluating sustainable development of cross-border e-commerce platforms under uncertainty, Journal of Intelligent & Fuzzy Systems, 46 (2024) 6383-6398.

[33] B. Zhang, Innovative exponential todim-cocoso framework for uncertain multiple-attribute group decision-making in the effectiveness evaluation of short video marketing strategies, Journal of Intelligent & Fuzzy Systems, 46 (2024) 4029-4042.

[34] S. Opricovic, G.H. Tzeng, Compromise solution by mcdm methods: A comparative analysis of vikor and

topsis, European Journal of Operational Research, 156 (2004) 445-455.

[35] S. Opricovic, G.H. Tzeng, Extended vikor method in comparison with outranking methods, European Journal of Operational Research, 178 (2007) 514-529.

[36] J. Wang, G.W. Wei, Y. Wei, Models for green supplier selection with some 2-tuple linguistic neutrosophic number bonferroni mean operators, Symmetry-Basel, 10 (2018) 36.

[37] J. Wang, G.W. Wei, M. Lu, Todim method for multiple attribute group decision making under 2-tuple linguistic neutrosophic environment, Symmetry-Basel, 10 (2018) 15.

[38] H. Liu, Performance evaluation of family business strategic transition based on the 2-tuple linguistic neutrosophic number multiple attribute group decision making, Journal of Intelligent & Fuzzy Systems, 44 (2022) 3271-3283.

[39] C.E. Shannon, A mathematical theory of communication, Bell System Technical Journal, 27 (1948) 379-423.

[40] A. Tversky, D. Kahneman, Prospect theory: An analysis of decision under risk, Econometrica, 47 (1979) 263-291.

[41] P. Wang, J. Wang, G.W. Wei, C. Wei, Y. Wei, The multi-attributive border approximation area comparison (mabac) for multiple attribute group decision making under 2-tuple linguistic neutrosophic environment, Informatica, 30 (2019) 799-818.

[42] P. Wang, J. Wang, G.W. Wei, J. Wu, C. Wei, Y. Wei, Coda's method for multiple attribute group decision making under 2-tuple linguistic neutrosophic environment, Informatica, 31 (2020) 161-184.

Appendix

Table 1. Linguistic scale and 2TLNNs

Linguistic Terms	2TLNNs
Exceedingly Terrible-ZET	$\{(z\vartheta_0,0),\ (z\vartheta_5,0),\ (z\vartheta_6,0)\}$
Very Terrible-ZVT	$\{(z\vartheta_1,0),\ (z\vartheta_4,0),\ (z\vartheta_5,0)\}$
Terrible-ZT	$\{(z\vartheta_2,0),\ (z\vartheta_3,0),\ (z\vartheta_4,0)\}$
Medium-ZM	$\{(z\vartheta_3,0),\ (z\vartheta_3,0),\ (z\vartheta_3,0)\}$
Well-ZW	$\{(z\vartheta_4,0),\ (z\vartheta_3,0),\ (z\vartheta_2,0)\}$
Very Well-ZVW	$\{(z\vartheta_5,0),\ (z\vartheta_2,0),\ (z\vartheta_1,0)\}$
Exceedingly Well-ZEW	$\{(z\vartheta_6,0),\ (z\vartheta_1,0),\ (z\vartheta_0,0)\}$

Received: July 25, 2024. Accepted: Oct 19, 2024

NSS
Neutrosophic Sets and Systems, Vol. 76, 2025
University of New Mexico

On Neutrosophy logic for Multiple Correlation Analysis in Fuzzy Uncertain Database

Samar Wazir[1]*, M.M. Sufyan Beg[2], Tanvir Ahmad[3], Shahab Saquib Sohail[4]

[1] Department of Computer Engineering, Jamia Millia Islamia, New Delhi, India; samar.wazir786@gmail.com
[2] Department of Computer Engineering Aligarh Muslim University, Aligarh, India; mmsbeg@myamu.ac.in
[3] Department of Computer Engineering, Jamia Millia Islamia, New Delhi, India; tahmad2@jmi.ac.in
[4] School of Computing Science and Engineering, VIT Bhopal University, Sehore, MP 466114, India; shahabsaquibsohail@vitbhopal.ac.in
* Correspondence: samar.wazir786@gmail.com, shahabsaquibsohail@vitbhopal.ac.in

Abstract: The primary goal of this paper is to introduce a novel method for mining frequent and interesting items by incorporating correlation analysis between two items in an uncertain transactional database using the OWA operator. The work is further expanded by proposing two additional methods for mining frequent and interesting items, utilizing fuzzy means and the OWA operator along with multiple correlation analysis for more than two items in uncertain transactional databases. The effectiveness of the proposed methods is evaluated by running the algorithms on both standard and example datasets, with results compared to the traditional probabilistic approach for identifying frequent and interesting items through multiple correlation. While multiple correlation analysis highlights the relationships of interestingness and uninterestingness between items, the OWA operator enhances the results when combined with fuzzy means and probabilistic methods. Additionally, the paper suggests a future research direction using Neutrosophy logic, which is anticipated to open new avenues for further exploration in this field.

Keywords: Frequent Itemset Mining; Minimum Support; Correlation Analysis; Certain/Uncertain Databases; Fuzzy Operators; Ordered Weighted Averaging; Neutrosophy logic; Neutrosophic cognitive map.

1. Introduction

Over the past two decades, the increasing reliance of industries on information technology has led to the generation of massive amounts of unstructured data. As a result, extracting relevant and useful information from this vast pool has become a complex and challenging task. Consequently, the challenge of mining valuable insights from large databases has emerged as a key area of study within computer science, commonly referred to as data mining [1].

The database used in this mining process, known as a transactional database, can be viewed as a collection of transactions (rows) and the items (values) within each transaction. The usefulness of the results generated by the data mining process is determined by several key parameters, such as the frequency of an item or itemset in the database (called support), the likelihood that the presence of one item is linked to the presence of another in the same itemset (called confidence), and the relationship between the occurrence of one item and the increased or decreased occurrence of others (called correlation) [1-2].

The process of extracting frequently occurring items or itemsets from a transactional database is known as Frequent Itemset Mining (FIM) [3], a sub-discipline of data mining and one of the most

active research fields. Numerous FIM algorithms [3-5] have been developed, which can be classified based on their execution pattern (i.e., sequential or parallel) or the type of database used (i.e., certain, probabilistic, or fuzzy). In a certain database, the support of an itemset is determined by its count in the database [6]. In a probabilistic database, support is based on the existential probability of the itemset [7-9], whereas in a fuzzy database, support is calculated using fuzzy operators such as min, max, or mean [10].

An item or itemset is considered frequent if its support meets or exceeds a user-specified minimum support threshold. For example, in Market Basket Analysis [11], if a database contains 100 transactions, and the item counts for milk and eggs are 20 and 30 respectively, and the minimum support is set to 30, then eggs would be classified as frequent, while milk would not. To enhance the mining process or improve item sales, not only is item count considered, but also whether the sale of one item (e.g., milk) influences the sale of another (e.g., eggs). This type of relationship between two or more items is called **correlation**, and items that meet both the minimum support and correlation thresholds are deemed frequent and interesting.

Correlation between two items is often measured using the Correlation Coefficient [12]. In the case of Pearson's Correlation Coefficient, values range between [-1, 1]. A value of 0 indicates that the two items are independent of each other, a positive value (between 0 and 1) indicates a positive dependence, and a negative value (between 0 and -1) indicates a negative dependence. Various algorithms have been developed to calculate correlations between two or more items in certain, probabilistic, and fuzzy uncertain databases.

Consider the Uncertain Database (UDB) shown in Table 1.

Table 1. Uncertain Database

TID	Milk	Eggs
1	0.9	0.01
2	0.01	0.03
3	0.03	0.23
4	0.06	0.15
5	0.05	0.3
6	0.08	0.89

In the above database, TID denotes transaction id; there are two items in the database, i.e., milk and eggs, the value of each item shows the existential probability or the membership function of the particular item in the transaction if the database is considered as probabilistic uncertain or fuzzy uncertain respectively. Therefore, if the correlation [13] between milk and eggs is calculated using probability or fuzzy means [14-17], then the following cases can be considered as given in table 2.

Table 2. Illustration of different possible cases in a database

Cases	Correlation using probability	Correlation using fuzzy means
✓ Case 1: No Change	-0.18454	-0.33829
✓ Case 2: TID2 is removed from the database	-0.25055	-0.47403
✓ Case 3: TID1 is removed from the database	0.058944	0.797699
✓ Case 4: TID1 & TID2 are removed	0.015756	0.593577

from the database

So, in case 1 milk and eggs are negatively correlated whereas, in Case 3 they are highly positively correlated. In the above database, it can be seen that only two high values (i.e., milk 0.9 and eggs 0.89) affects the whole correlation coefficient and ignores other small values, in fact, while calculating correlation the participation of all values should be considered so that the interesting relationship can be calculated. Another difference can be seen in case 3 and 4, where probabilistic values show fewer correlation compare to highly correlated values by fuzzy means. The difference is due to the multiplication of probabilistic values while calculating correlation.

The above analysis states that we need some better approach than probabilistic approach and fuzzy means, and also calculated correlation coefficient must lie between [1, -1] (because in this paper Pearson`s Correlation Coefficient is considered).

In this paper, the following contribution has been done

1. A new method has been proposed for calculating the correlation between two items using OWA (Ordered Weighted Averaging).
2. A proof is given to show that Correlation Coefficient between two items using OWA lies between -1 and 1.
3. A new method is proposed for calculating correlation among more than two items using fuzzy means, and frequent itemsets have been calculated with the help of this method, the algorithm named as MCAFM (*Multiple Correlation Analysis using Fuzzy Means*).
4. A new method is proposed for calculating correlation among more than two items using OWA, and frequent itemsets have been calculated with the help of this method, the algorithm named as MCAOWA (*Multiple Correlation Analysis using OWA*).
5. A proof is given to show that using OWA would be a better approach than using Fuzzy Means while calculating Correlation among two or more items.
6. The MCAFM and MCAOWA algorithms are presented and explained.
7. **Neutrosophy logic framework for pattern mining is suggested.**
8. Algorithms are executed on standard and synthetic datasets and results are compared with the traditional probabilistic approach.

2. Related works

The risk involved in the improvement or change of the current business scenario can only be resolved either by mathematical induction or by analyzing previously available data. Thereupon, as the demand for analyzing past data increased exponentially in the last decade, the field of FIM gained popularity. The applications of FIM [4] range from market basket analysis, crime analysis and prevention to software bug detection, DNA matching and image processing.

The first algorithm of FIM was proposed by Agarwal in 1994 as Apriori[6] algorithm for calculating frequent items on the certain transactional database (CTD) which is based on sequential execution pattern, and subsequently, the list of FIM algorithms have been increased dramatically, e.g. FPGrowth [18], ECLAT [19-21]. Apriori was unable to handle a large amount of data, henceforth, the need for parallel algorithms encounters and Count Distribution (CD) [7], [22] was developed. The step-by-step refinement in CD reflects in the development of Data Distribution (DD) [23], Fast Parallel Mining (FPM) [20] and Fast Distributed Mining (FDM)[19] algorithms.

In many applications where the generated data is uncertain/imprecise/unstructured, it is not justified to store this information as CTD, e.g., prediction of customer purchasing behaviour from

market basket data [24], data from GPS, data from RFID, data collected for predicting rain, temperature and humidity. Such kind of data is stored as probabilistic uncertain database (PUD), and in this database each item is associated with its existential probability, e.g., in Table 1 if we consider it as PUD and TID denotes customer number then it can be said that there is a 90% chance that customer 1 would purchase milk and 3% chance that customer 2 would purchase eggs. The first algorithm for calculating frequent items on PUD was developed by Chui [25-26], as UApriori which calculates frequent items based on expected support and follows Apriori execution pattern, e.g. expected the support of {milk, eggs} in Table 1 is 0.1114. After UApriori various algorithms were developed for FIM on PUD such as Poisson Distribution Based UApriori (PDU), Normal Distribution based UApriori(NDU) [27-29], UFPGrowth [30], UECLAT [31] etc.

Uncertain algorithms are unable to calculate frequent items for large sizes (e.g., size 10 itemset) because the multiplication of probabilistic values of *expected support* becomes very small. Another limitation of probabilistic values is that, for all uncertain situations, the probability is not the best solution [23], [32], e.g., if we search a tall player for the basketball team with height 7^{ft} and there is 0.99 probability that we get the right player in California. In this case, the algorithm ignores all players having $6^{ft}11^{inches}$ height; even they are also tall.

Here fuzzy logic is introduced [33-35] and such data is stored as a *membership function* which is associated with each item in the database, e.g., FD in Table 1. FIM on FD can be performed by calculating *fuzzy support* on the basis of fuzzy min/max/mean operator, e.g., if fuzzy min operator is used then *fuzzy support* [36-37] of {milk, eggs} in Table 1 will be 0.24, if fuzzy max operator is used then *fuzzy support* of {milk, eggs} in Table 1 will be 2.5, if fuzzy mean operator is used then *fuzzy support* of {milk, eggs} in Table 1 will be 1.37. Many algorithms have been developed for generating frequent items from FD such as Fuzzy Transaction Data Mining Algorithm (FTDA) [16], Uncertain Data Mining (UDM)[25]. The min/max operators used by fuzzy algorithms are not able to aggregate all values while calculating *fuzzy support* and hence the generated results are not interesting. In [38], a method was developed for calculating support by using OWA operator as FAOWA. In some other cases, frequent items are calculated for the combination of both certain and uncertain databases.

In the calculation of frequent itemsets, not only the itemset occurring frequency matters but the relationship among the items is also essential. The success of a business process or a market product also depends on, how the other products are increasing or decreasing the sale of our product. The relation among two or more items in a transactional database is determined by correlation and the itemsets who qualify the user-specified correlation level is called interesting items. The correlation between itemsis determined by correlation coefficient, e.g. Pearson`s correlation coefficient, moreover, based on the correlation coefficient, various FIM algorithms have been developed such as Directed Acyclic Graph Correlated Probabilistic Database Model (DACCPDM), Correlated Frequent Probabilistic Model(CFPM) and Fuzzy Correlated Data Mining Algorithm.

Consider two items A, B and let $\rho_A(x_i)$ is the *existential probability* of item A in the i^{th} transaction and $\rho_B(y_i)$ is the *existential probability* of item B in the i^{th} transaction. The correlation coefficient between A and B can be defined as.

$$r_{\rho_{(A,B)}} = \frac{\rho(x_i y_i) - \rho_A(x_i)\rho_B(y_i)}{\sqrt{\rho_A(x_i)(1-\rho_A(x_i))\rho_B(y_i)(1-\rho_B(y_i))}}$$

Here, $r_{\rho_{(A,B)}}$ is the correlation between A and B using probability. The value of $r_{\rho_{(A,B)}}$ will lies in [-1,1] (Pearson's correlation coefficient), so $|r_{\rho_{(A,B)}}| \leq 1$.

In another case, Consider two fuzzy items A, B and let $\mu_A(x_i)$ is the *membership function* of item A in the ith transaction and $\mu_B(x_i)$ is the *membership function* of item B in the ith transaction. $\bar{\mu}_A$ and $\bar{\mu}_B$ are the fuzzy means value for item A and B respectively in the database. The correlation coefficient between A and B can be defined as [5], [22].

$$r_{fm_{(A,B)}} = \frac{\sum_{i=1}^{n}(\mu_A(x_i) - \bar{\mu}_A)(\mu_B(x_i) - \bar{\mu}_B)}{\sqrt{\sum_{i=1}^{n}(\mu_A(x_i) - \bar{\mu}_A)^2 \times \sum_{i=1}^{n}(\mu_B(x_i) - \bar{\mu}_B)^2}} \ldots \text{Eq.1}$$

Here, $r_{fm_{(A,B)}}$ is the correlation between A and B using fuzzy means. The value of $r_{fm_{(A,B)}}$ will lies in [-1,1] (Pearson`s correlation coefficient), so $|r_{fm_{(A,B)}}| \leq 1$.

3. Problem Definition

The problem of mining frequent items by *Correlation Analysis* between two items using OWA, *Multiple Correlation Analysis using Fuzzy Means* and *Multiple Correlation Analysis using OWA* can be divided into following sections.

3.1. Correlation Analysis using OWA between two items

Suppose, two fuzzy sets A and B and in Eq.1 if mean value is replaced by OWA then Correlation Coefficient between A and B using OWA denoted as $r_{OWA_{(A,B)}}$ can be calculated by the following formula

$$r_{OWA_{(A,B)}} = \frac{\sum_{i=1}^{n}(\mu_A(x_i) - OWA_A)(\mu_B(x_i) - OWA_B)}{\sqrt{\sum_{i=1}^{n}(\mu_A(x_i) - OWA_A)^2 \times \sum_{i=1}^{n}(\mu_B(x_i) - OWA_B)^2}} \ldots \text{Eq.2}$$

Here, OWA can be calculated [28] as

$$OWA(X) = OWA(x_1, x_2, \ldots\ldots x_m) = \sum_{i=1}^{m} w_i y_i = \sum_{i=1}^{m}[Q(\frac{i}{m}) - Q(\frac{i-1}{m})]\, y_i \ldots \text{Eq.3}$$

Where y_i is the ith largest value amongst $x_1, x_2, \ldots\ldots x_m$ or values of items sorted in descending order, w is the weight value and depends upon Q (fuzzy relative quantifier [28]) and $\sum_{i=1}^{m} w_i = 1$.

3.2. Proof of Correlation Analysis using OWA lies between -1 and 1or $|r_{OWA_{(A,B)}}| \leq 1$

The OWA value for an item A can be calculated as from Eq.3.

$$OWA_A = \sum_{i=1}^{m} w_i \mu_A(y_i) \quad \text{...Eq.4}$$

and for item B as

$$OWA_B = \sum_{i=1}^{m} w_i \mu_B(y_i) \quad \text{...Eq.5}$$

Let $\mu_B(y_i) = a\mu_A(y_i) + b$, where a and b are two constants.

Therefore from Eq.5. $$OWA_B = \sum_{i=1}^{m} w_i (a\mu_A(y_i) + b)$$

$$OWA_B = a\sum_{i=1}^{m} w_i \mu_A(y_i) + b\sum_{i=1}^{n} w_i$$

Here $\sum_{i=1}^{m} w_i = 1$

So, $$OWA_B = aOWA_A + b \quad \text{...Eq.6}$$

Similarly,

$$\begin{aligned} \mu_B(x_i) - OWA_B &= a\mu_A(y_i) + b - (aOWA_A + b) \\ &= a\mu_A(y_i) - aOWA_A \\ &= a(\mu_A(y_i) - OWA_A) \end{aligned} \quad \text{... Eq.7}$$

Put the values from Eq.7 into Eq.2 and $r_{OWA_{(A,B)}}$ can be calculated as

$$r_{OWA_{(A,B)}} = \frac{\sum_{i=1}^{n}(\mu_A(x_i) - OWA_A)(\mu_B(x_i) - OWA_B)}{\sqrt{\sum_{i=1}^{n}(\mu_A(x_i) - OWA_A)^2 \times \sum_{i=1}^{n}(\mu_B(x_i) - OWA_B)^2}}$$

$$r_{OWA_{(A,B)}} = \frac{\sum_{i=1}^{n}(\mu_A(x_i) - OWA_A)a(\mu_A(y_i) - OWA_A)}{\sqrt{\sum_{i=1}^{n}(\mu_A(x_i) - OWA_A)^2 \times \sum_{i=1}^{n}(a(\mu_A(y_i) - OWA_A))^2}}$$

$$r_{OWA_{(A,B)}} = \frac{a}{\sqrt{a^2}} = \frac{a}{|a|} = \pm 1$$

So, it can be said that $r_{OWA_{(A,B)}}$ Always lies between -1 and 1.

3.3. Frequent Itemset Mining by Multiple Correlation Analysis using Fuzzy Means for more than two items

An itemset (l_1,l_2) is said to be frequent if its *fuzzy support*(*fs*) in the database is greater than or equal to user-specified *minimum fuzzy support* (*mfs*) and an itemset (l_1,l_2) is said to be interesting if correlation (*corr*) between the items is greater than or equal to user-specified *minimum correlation*(*mcr*). Therefore, the *fuzzy support* of an itemset can be defined as

$$fs(l_1, l_2, \ldots, l_m) = \frac{\sum_{i=0}^{n} min\,(\mu(l1),\mu(l2),\ldots,\mu(lm))}{n} \geq mfs \quad \text{…Eq.8}$$

Here *n* is the number of transactions in database and *m* is the number of items in the itemset.

The correlation coefficient $r_{l_1,l_2,l_3,\ldots\ldots,l_m}$ among $l_1, l_2, l_3, \ldots\ldots\ldots, l_m$ variables can be defined as

$$r^2_{l_1,l_2,l_3,\ldots\ldots,l_m} = 1 - \sum_{j_1 j_2 < \cdots j_m} (det[r(m)|j_1, j_2, \ldots\ldots, j_m])^2 \quad \text{...Eq.9}$$

In the proposed method, variables $l_1, l_2, l_3, \ldots\ldots\ldots, l_m$ are the items of FD and $r(m)$ is the value of the correlation coefficient between two items using fuzzy means. Therefore, the Correlation Coefficient by using fuzzy means among multiple variables r_{fm} can be defined as

$$r^2_{fm_{l_1,l_2,l_3,\ldots\ldots,l_m}} = 1 - \sum_{j_1 j_2 < \cdots j_m} (det\,[r_{fm(m)} \vee j_1, j_2, \ldots\ldots, j_m])^2$$

$$r^2_{fm_{l_1,l_2,l_3,\ldots\ldots\ldots,l_m}} = 1 - det\begin{bmatrix} r_{fm_{l_1l_1}} & r_{fm_{l_1l_2}} & \cdot\cdot & r_{fm_{l_1l_m}} \\ r_{fm_{l_2l_1}} & r_{fm_{l_2l_2}} & \cdot\cdot & r_{fm_{l_2l_m}} \\ \cdot\cdot & \cdot\cdot & \cdot\cdot & \cdot\cdot \\ r_{fm_{l_ml_1}} & r_{fm_{l_ml_2}} & \cdot\cdot & r_{fm_{l_ml_m}} \end{bmatrix} \quad \ldots \text{Eq.10}$$

Therefore, an itemset is said to be frequent if $fs(l_1, l_2, \ldots\ldots, l_n) \geq mfs$ and interesting if $r^2_{fm_{l_1,l_2,l_3,\ldots\ldots\ldots,l_m}} \geq mcr$.

3.4. Multiple Correlation Analysis using OWA for more than two items

In this case, the Correlation Coefficient using OWA for multiple variables or r_{owa} can be calculated by replacing r_{fm} in Eq.10 by r_{OWA} and can be defined as

$$r^2_{OWA_{l_1,l_2,l_3,\ldots\ldots\ldots,l_m}} = 1 - \sum_{j_1 j_2 < \cdots j_m} (det\,[r_{OWA(m)} \vee j_1, j_2, \ldots\ldots, j_m])^2$$

$$r^2_{OWA_{l_1,l_2,l_3,\ldots\ldots\ldots,l_m}} = 1 - det\begin{bmatrix} r_{OWA_{l_1l_1}} & r_{OWA_{l_1l_2}} & \cdot\cdot & r_{OWA_{l_1l_m}} \\ r_{OWA_{l_2l_1}} & r_{OWA_{l_2l_2}} & \cdot\cdot & r_{OWA_{l_2l_m}} \\ \cdot\cdot & \cdot\cdot & \cdot\cdot & \cdot\cdot \\ r_{OWA_{l_ml_1}} & r_{OWA_{l_ml_2}} & \cdot\cdot & r_{OWA_{l_ml_m}} \end{bmatrix} \quad \ldots \text{Eq.11}$$

Therefore, an itemset is said to be frequent if $fs(l_1, l_2, \ldots\ldots, l_m) \geq mfs$ and interesting if $r^2_{OWA_{l_1,l_2,l_3,\ldots\ldots\ldots,l_m}} \geq mcr$.

3.5. Proof: OWA is a better approach than using Fuzzy Means while calculating Correlation among two or more items.

Let us assume that, $X_s = \{x_{l_1}, x_{l_2}, x_{l_3} \ldots\ldots, x_{l_s}\}$ is the set of unexpected large values in FUDB and X_{s_A} and X_{s_B} are the sets of large values of items A and B respectively. In this case

$$\bar{\mu}_A = \frac{x_1 + x_2 + x_3 + \cdots\ldots + x_n}{n} \approx \frac{x_{l_1} + x_{l_2} + x_{l_3} + \cdots + x_{l_s}}{n} \approx \bar{X}_{s_A}$$

Similarly,

$$\bar{\mu}_B \approx \bar{X}_{s_B}$$

Therefore, by assigning the values of $\bar{\mu}_A$ and $\bar{\mu}_B$ into Eq.1, Correlation Coefficient can be given as,

$$r_{fm_{(A,B)}} = \frac{\sum_{i=1}^{n}(\mu_A(x_i) - \bar{X}_{s_A})(\mu_B(x_i) - \bar{X}_{s_B})}{\sqrt{\sum_{i=1}^{n}(\mu_A(x_i) - \bar{X}_{s_A})^2 \times \sum_{i=1}^{n} (\mu_B(x_i) - \bar{X}_{s_B})^2}}$$

$$r_{fm_{(A,B)}} = \frac{\sum_{i=1}^{n-s}(\mu_A(x_i) - \bar{X}_{s_A})(\mu_B(x_i) - \bar{X}_{s_B}) + \sum_{i=1}^{s}(\mu_A(x_{l_s}) - \bar{X}_{s_A})(\mu_B(x_{l_s}) - \bar{X}_{s_B})}{\sqrt{(\sum_{i=1}^{n-s} (\mu_A(x_i) - \bar{X}_{s_A})^2 + \sum_{i=1}^{s} (\mu_A(x_{l_s}) - \bar{X}_{s_A})^2) \times ((\sum_{i=1}^{n-s} (\mu_B(x_i) - \bar{X}_{s_B})^2 + \sum_{i=1}^{s} (\mu_B(x_{l_s}) - \bar{X}_{s_B})^2))}}$$

$$r_{fm_{(A,B)}} = \frac{(n-s)\bar{X}_{s_A}\bar{X}_{s_B} + \sum_{i=1}^{s}(\mu_A(x_{l_s}) - \bar{X}_{s_A})(\mu_B(x_{l_s}) - \bar{X}_{s_B})}{\sqrt{((n-s)\bar{X}_{s_A}{}^2 + \sum_{i=1}^{s} (\mu_A(x_{l_s}) - \bar{X}_{s_A})^2) \times (((n-s)\bar{X}_{s_B}{}^2 + \sum_{i=1}^{s} (\mu_B(x_{l_s}) - \bar{X}_{s_B})^2))}} [\because \forall x_{l_s} \gg \forall x_i] \ldots \text{Eq.12}$$

From Eq.12 it is clear that $r_{fm_{(A,B)}}$ can be determined by the values of X_{s_A} and X_{s_B}.

In another case, from Eq.4

$$OWA_A = \sum_{i=1}^{m} w_i \mu_A(y_i)$$

Here y is the set of values of an item in descending order. Therefore,

$$OWA_A = \sum_{i=1}^{s} w_i \mu_A(y_i)\, OWA_A + \sum_{i=s+1}^{m} w_i \mu_A(y_i)\ [\because X_s is these to of large values]$$

In Eq.3 relative quantifier Q(r) can be calculated as [28]

$$Q(r) = \begin{cases} 0 & if\ r < a \\ \frac{r-a}{b-a} & if\ a \le r \ge b \\ 1 & if\ r > b \end{cases}$$

Therefore,

If$s<a$

Then $\sum_{i=1}^{s} w_i \mu_A(y_i) = 0$

and,

$$OWA_A = \sum_{i=s+1}^{m} w_i \mu_A(y_i) \qquad \ldots Eq.13$$

Similarly,

$$OWA_B = \sum_{i=s+1}^{m} w_i \mu_B(y_i) \qquad \ldots Eq.14$$

Hence, from Eq.13 and Eq.14, it is clear that the calculation of OWA value for A and B does not include the values higher than *s* or exclude the higher values. Consequently, the value of $r_{OWA_{(A,B)}}$ does not contain the impact of high values. Therefore, if the database contains some high values the$r_{OWA_{(A,B)}}$ consider the majority values and shows more interesting association orthe value of $r_{OWA_{(A,B)}}$ is more interesting as compared to $r_{fm_{(A,B)}}$.

4. Algorithms

In this paper, two algorithms are presented as *Multiple Correlation Analysis using Fuzzy Means* (MCAFM) and *Multiple Correlation Analysis using Ordered Weighted Averaging* (MCAOWA) as follows:

4.1. Multiple Correlation Analysis using Fuzzy Means (MCAFM)

Input:*Z* (A fuzzy uncertain transactional database), *mfs*(*minimum fuzzy support*) and, *mcr*(*minimum correlation*); Output:*S*(frequent and interesting itemsets in *Z*)

MCAFM Algorithm

(1) S_1= Size_1_frequent_items(Z);// for each size_1 item $fs \ge mfs$

(2) for (i= 2; $S_{i-1} \neq \phi$;i++) {

(3) X_i= candid_gen(S_{i-1}); // Generate candidates, join, prun

(4) for each row $t \in Z$ { // scandatabase

(5) X_t= subset (X_i, t); // get all candidates

(6) for each item$x \in X_t$

(7) $fs(x) = min\ (\mu(l1), \mu(l2), \ldots., \mu(l\mathrm{m}))$

(8) *x.fs = x.fs + fs(x)*

(9) }

(10) *x.fs = x.fs/|Z|*

(11) if (*x.fs*≥*mfs*) then {

(12) $r^2_{fm_x} = 1 - \sum_{j_1 j_2 < \cdots j_m} (det\ [r_{fm(m)} \vee j_1, j_2, \ldots., j_m])^2\}$

(13) *Si*= {$x \in X_i$| $r^2_{fm_x} \geq mcr$}

(14) }

(15) returnS= $\cup_i S_i$;

4.2. MCAOWA (Multiple Correlation Analysis using Ordered Weighted Averaging)

Input:*Z* (A fuzzy uncertain transactional database), *mfs*(*minimum fuzzy support*) and, *mcr*(*minimum correlation*); Output: *S*(frequent and interesting itemsets in *Z*)

MCAOWA Algorithm

(1) S_1= Size_1_frequent_items(Z);// for each size_1 item *fs*≥*mfs*

(2) for (*i*= 2; $S_{i-1} \neq \phi$;*i*++) {

(3) X_i= candid_gen(S_{i-1}); // Generate candidates, join, prun

(4) for each row $t \in Z$ { // scandatabase

(5) X_t= subset (X_i, *t*); // get all candidates

(6) for each item$x \in X_t$

(7) $fs(x) = min\ (\mu(l1), \mu(l2), \ldots., \mu(l\mathrm{m}))$

(8) *x.fs = x.fs + fs(x)*

(9) }

(10) *x.fs = x.fs/|Z|*

(11) if (*x.fs*≥*mfs*) then {

(12) $r^2_{OWA_{a_1,a_2,a_3,\ldots\ldots\ldots,a_m}} = 1 - \sum_{j_1 j_2 < \cdots j_m} (det\ [r_{OWA(m)} \vee j_1, j_2, \ldots., j_m])^2\}$

(13) *Si*= {$x \in X_i$| $r^2_{fm_x} \geq mcr$}

(14) }

(15) return*S*= $\cup_i S_i$;

In the above algorithms, a fuzzy uncertain transactional database is given as input and for calculating frequent as well as interesting itemsets, *minimum fuzzy support* and *minimum correlation* level is provided by the user as input. Both algorithms follow the Apriori pattern of execution. In line-1 size_1 frequent items calculated on the basis of *fuzzy support* only because for calculating correlation atleast two items required. Thereafter line-2 to 14 executed repeatedly until all results are calculated. In line-3, function candid_gen() is used to generates all candidates by joining the frequent items from the previous stage and pruning them. These candidate itemsets scanned in the database to calculate *fuzzy support*. In line-11, candidates who qualify user given *minimum fuzzy support* are checked and called frequent items. In line-12, the correlation coefficient is calculated only among the items of frequent itemset from line-11 using fuzzy means or OWA and the itemsets who qualify minimum correlation are then added to final set S in line-13. In line-15 all size frequent and interesting items are combined.

5. An Example to demonstrate the work.

Consider Table.3 and Table.4, let minimum support[1] =0.05 and *mcr*=0.25. In Table.3 an uncertain transactional database is given and in Table.3 frequent and interesting items are calculated.

Table 3. Example of an Uncertain Database

TID	Items				
	1	**2**	**3**	**4**	**5**
1	0.9	0.02	0.25	0.03	0.3
2	0.18	0.03	0.15	0.01	0.1
3	0.16	0.9	0.17	0.2	0.01
4	0.8	0.09	0.03	0.3	0.8
5	0.04	0.12	0.05	0.14	0.01
6	0.06	0.8	0.08	0.13	0.19
7	0.08	0.15	0.04	0.17	0.9
8	0.1	0.02	0.01	0.05	0.18
9	0.01	0.04	0.03	0.06	0.12
10	0.03	0.3	0.14	0.09	0.08

Table 4. Frequent Itemsets generation by MCAFM, MCAOWA and CFPM

C_1	Fs	L_1	C_2	Fs	Ps	Corr FM	Corr OWA	CFPM	L_2 FM	L_2 OWA	L_2 Prob	C_3 FM	C_3 OWA	fs	Corr OWA
1	0.236	1	12	0.054	0.03156	-0.273915242	-0.088318858						145	0.059	0.68718
2	0.247	2	13	0.078	0.03187	0.405975682	0.437441827		13	13					
3	0.095	3	14	0.077	0.03361	0.218598224	0.251249381			14					
4	0.118	4	15	0.15	0.1035	0.423753025	0.498402617	0.212518	15	15	15				
5	0.269	5	23	0.06	0.02846	0.214085306	0.261895037			23					
			24	0.087	0.03846	0.352527307	0.373624624		24	24					
			25	0.064	0.04106	-0.268166943	-0.110367015								
			34	0.054	0.00911	-0.33324166	-0.301361875								
			35	0.064	0.0184	-0.316924194	-0.234251109								
			45	0.085	0.04545	0.536197786	0.54518274		45	45					

Table Abbreviations:

C_1:- size-1 candidates, L_1:- size-1 frequent items, fs:- fuzzy support, ps:- probabilistic support CorrFM:- Correlation using Fuzzy Means, CorrOWA:- Correlation using OWA, CFPM:- Correlated Frequent Probabilistic Model

L_2FM:- size-2 frequent and interesting items calculated by using fuzzy means, L_2OWA:-size-2 frequent and interesting items calculated by using OWA, L_2Prob:-size-2 frequent and interesting items calculated by using Probability

[1]If the given database is considered as Probabilistic Uncertain Database then minimum support can be called as minimum probabilistic support *mps* and If the given database is considered as Fuzzy Uncertain Database then minimum support can be called as minimum fuzzy support *mfs*

C_3FM:- size-3 candidate generated by size-2 frequent items using Fuzzy Means, C_3OWA:- size-3 candidate generated by size-2 frequent items using OWA.

In the above example frequent and interesting items are calculated using proposed MCAFM and MCAOWA methods and compared with CFPM method.

In Table.3, *mfs* or *mps* is 0.05. Therefore, all C_1 qualifies for L_1 in all three cases (i.e., MCAFM, MCAOWA and CFPM). Later, L_1 are combined to form C_2 and correlation using fuzzy means, OWA and probability is calculated for candidates who qualify *mfs*or *mps*. In this database (Table.2) the following points can be noted.

- The database contains a total of 50 values in the following ranges

Range	Number of values
0.0-0.2	40
0.21-0.3	4
0.71-0.9	6

- In this database most of the values belong to a lower range, that`s why a number offrequent items calculated by MCAOWA are larger than MCAFM (i.e., 12 in MCAOWA and 9 in MCAFM).
- MCAOWA calculates the correlation between the 44 lower values and ignores the 6 higher values on the other hand MCAFM consider all values, so the impact of 6 higher values is greater.
- Due to multiplication of probabilistic values the association rules loss is very high in CFPM. Therefore, this method is less efficient to calculate frequent items compare to MCAOWA and MCAFM.
- It can be said that MCAOWA computes more interesting correlation compare to MCAFM and CFPM.

6. Results Comparison

In the following section, the comparison of results is discussed by executing MCAFM, MCAOWA and CFPM on three standard available real life datasets (i.e. Gazelle, Connect and mushroom)[25, 38] as UDB. The programs of *Correlation analysis* have been coded in C and executed on Intel(R) Core(TM) i5-5200U 2.2GHz processor, using 4GB of RAM and Ubuntu-15.10-desktop-amd64. The results can be discussed in the following sections

6.1. Gazelle Dataset

In this dataset, there is a total of 59602 transactions and 497 items.

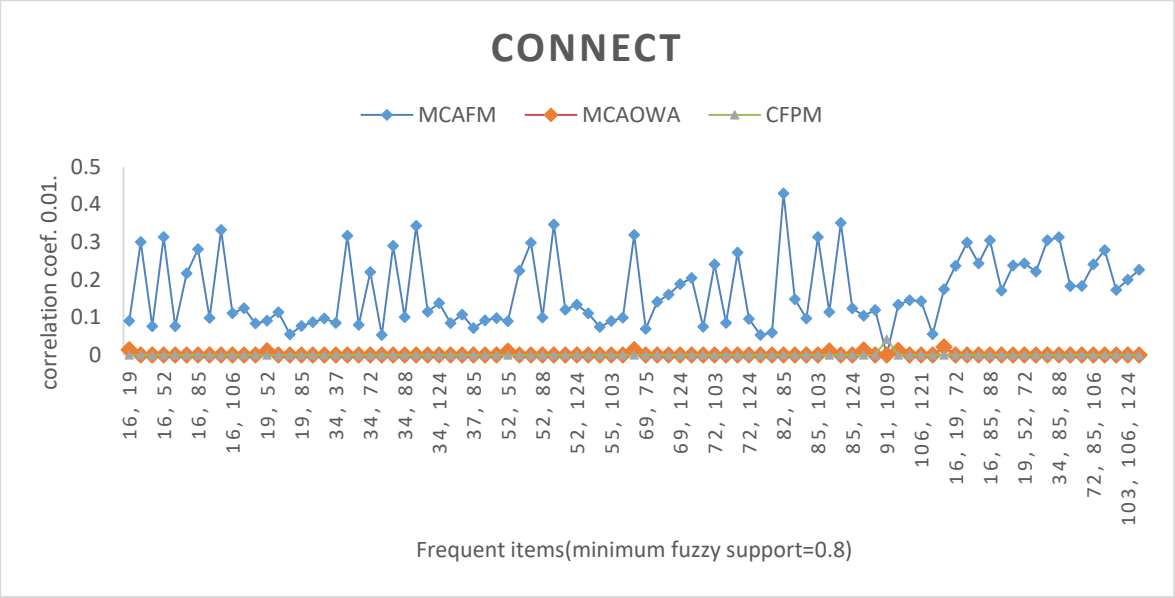

Figure 1. Correlation Analysis using MCAFM, MCAOWA and CFPM on Gazelle dataset

The values inside this dataset belong to the following range.

Range	Percentage of values
0.0-0.09	0.05%
0.7-0.79	0.0008%
0.8-0.89	13.6%
0.9-1.0	81.5%

Therefore, it can be said that in this dataset most of the values of items having a membership function greater than 0.9. Consequently, the correlation coefficient calculated by MCAFM as given in Figure.1 is between 0.9-1.0. In other words, it can be said that in this dataset most of the items from 497 items are highly correlated to each other, which is practically not possible. CFPM gives a smaller number of frequent items compare to MCAFM but with almost same correlation as in MCAFM. In Figure.1, correlation calculated by MCOWA is also presented which reflects some true picture of association among items because at this point the impact of high values is removed then the correlation is calculated among items. In other words, MCOWA is useful to calculate interestingness among low values, which is ignored by MCAFM and CFPM.

6.2. Connect Dataset

In this dataset, there is a total of 67557 transactions and 130 items.

The values inside this dataset belong to the following range.

Range	Percentage of values
0.6-0.69	0.000016%
0.7-0.79	0.02%
0.8-0.89	48.5%
0.9-1.0	49.5%

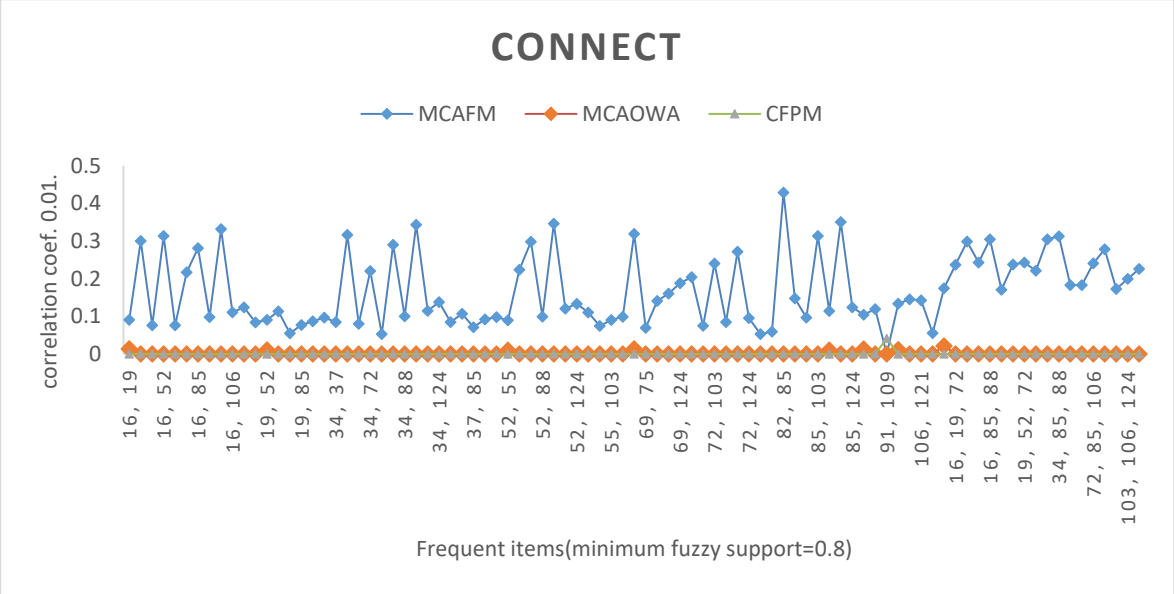

Figure 2. Correlation Analysis using MCAFM, MCAOWA CFPM on Connect dataset

In this dataset number of transactions are higher, and a number of items are smaller compared to Gazelle dataset, or it can be said that the size of each transaction is smaller compare to the previous dataset. In this dataset, all values are from higher range, i.e. 0.8-1.0,and for calculating w(Eq.3) the value of Q is determined for a=0.2 and b=0.8 or in other words, all values larger than 0.8 are removed. Here, MCAOWA is applied only on a few values and correlation between them is depicted in Figure.2. Therefore, the lower values from 0.6-0.8 are observed by MCAOWA and correlation is calculated among them. On the other hand, MCAFM and CFPM operated only for high values.

6.3. Mushroom Dataset

In this dataset, there is a total of 8124 transactions and 119 items.

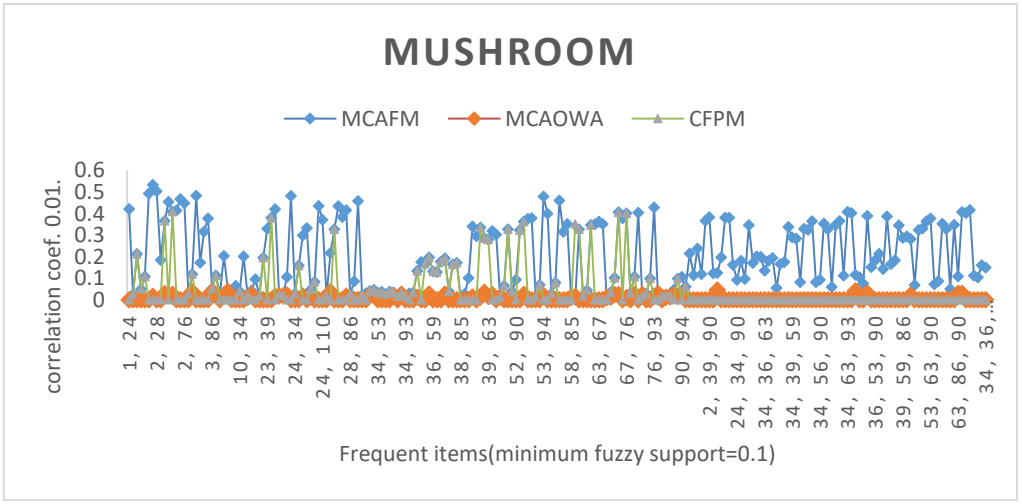

Figure 3. Correlation Analysis using MCAFM, MCAOWA CFPM on

The values inside this dataset belong to the following range.

Range	Percentage of values
0.01-0.09	8.96%
0.1-0.19	9.99%
0.2-0.29	9.96%
0.3-0.39	9.98%
0.4-0.49	10.14%
0.5-0.59	10.11%
0.6-0.69	10.01%
0.7-0.79	10.25%
0.8-0.89	10.02%
0.9-1.0	10.57%

This dataset is totally different from previous two and all values are distributed equally. In such type of dataset, it cannot be said that high values or low values have more importance. So, in this case removing the effect of high value is not a good idea. In Figure 3, it can be seen that the results calculated by MCAFM are more interesting compare to CFPM and MCAOWA. CFPM gives less number of frequent items because of multiplication of probabilities high size frequent items cannot be calculated.

7. Conclusion and future direction

Correlation analysis is a fundamental technique for analyzing daily life situations, e.g., if two persons meet for some business but unknown to each other at that time correlation between them may not strong. However, if they meet in the presence of any third person, known to both of them, then correlation among these three become stronger. In this paper, a new technique is used to analyze large dataset and by finding out the more interesting association. The performance of MCAOWA is better compared to MCAFM and CFPM when implemented on such a database, where some very high or very low values affecting the performance of *correlation analysis* (experiments 6.1 and 6.2). In another case, if datasets contain values which are distributed equally (experiment 6.3) in dataset MCAFM performs better than MCAOWA and CFPM.

Further, in future, a neutrosophy logic[39] can be incorporated. The various application of neutrosophy logic from data mining and artificial intelligence perspective in several applications have been reported in.

In addition, it would be interesting to explore how correlation coefficient of neutrosophic set[40] (CCNS) shall behave? This paper exploits fuzzy based correlation, moving forward we need to assess the neutrosophic related correlation performance for the related problems. Like, correlation coefficients of interval valued neutrosophic set (CCINS) and CCNS. Since it is worth to mention that CCNS has the positive, negative and neutral correlation as it is the case with statistical spearman correlation and so forth. Thus, in this context knowing its behavior and performance would be challenging and may open new research dimensions to the related field of study.

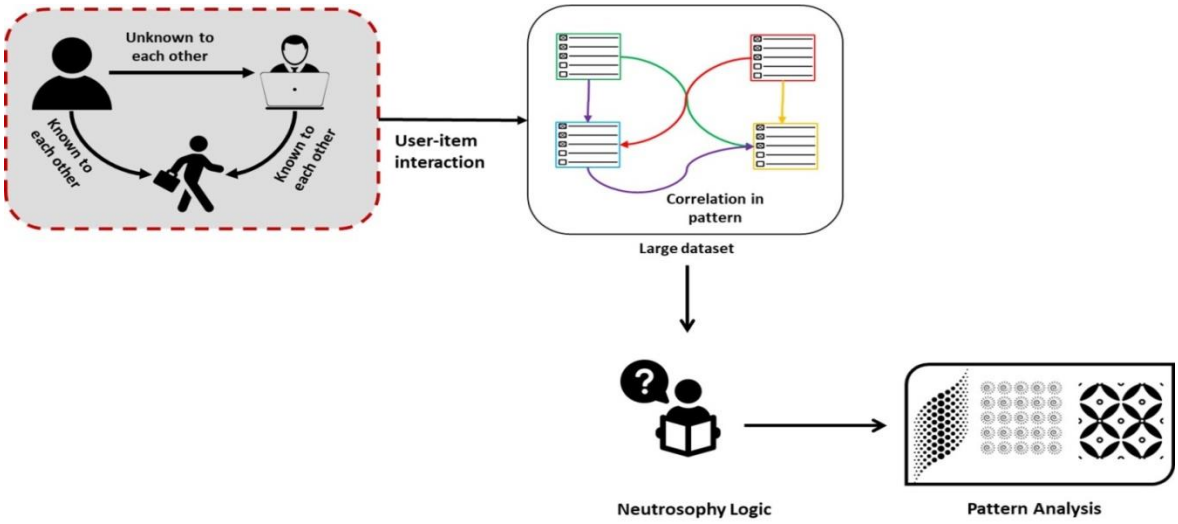

Figure 4. Neutrosophy based pattern mining

We have outlined an approach to incorporate the neutrosophy for the above purpose. The detail approach is shown in figure 4. It is envisaged that the approach can open new dimensions in the field of neutrosophy and data mining.

References

[1] C. C. Aggarwal, Y. Li, J. Wang, and J. Wang, "Frequent pattern mining with uncertain data," *Proceedings of the 15th ACM SIGKDD international conference on Knowledge discovery and data mining - KDD '09*, p. 29, 2009, doi: 10.1145/1557019.1557030.

[2] C. C. Aggarwal and P. S. Yu, "A survey of uncertain data algorithms and applications," *IEEE Trans Knowl Data Eng*, vol. 21, no. 5, pp. 609–623, 2009, doi: 10.1109/TKDE.2008.190.

[3] C. C. Aggarwal, "Managing and Mining Uncertain Data," *Managing and Mining Uncertain Data*, vol. 35, pp. 45–76, 2009, doi: 10.1007/978-0-387-09690-2.

[4] R. Agrawal and J. C. Shafer, "Parallel mining of association rules," *IEEE Trans Knowl Data Eng*, vol. 8, no. 6, pp. 962–969, 1996, doi: 10.1109/69.553164.

[5] M. A. Basaran, B. Simonetti, and L. D'Ambra, "Fuzzy correlation and fuzzy non-linear regression analysis," *Studies in Fuzziness and Soft Computing*, 2016, doi: 10.1007/978-3-319-39014-7_12.

[6] T. Bernecker, H.-P. Kriegel, M. Renz, F. Verhein, and A. Zuefle, "Probabilistic Frequent Itemset Mining in Uncertain Databases," in *15th ACM SIGKDD conference on knowledge discovery and data mining, Paris, France.*, 2009, pp. 119–127. Accessed: Jan. 24, 2018. [Online]. Available: http://citeseerx.ist.psu.edu/viewdoc/download;jsessionid=4D7C0675714A5E8D4EAB3633CABB43B2?doi=10.1.1.152.7064&rep=rep1&type=pdf

[7] Y. L. Chen, K. Tang, R. J. Shen, and Y. H. Hu, "Market basket analysis in a multiple store environment," *Decis Support Syst*, vol. 40, no. 2, pp. 339–354, 2005, doi: 10.1016/j.dss.2004.04.009.

[8] T. Calders, C. Garboni, and B. Goethals, "Approximation of frequentness probability of itemsets in uncertain data," *Proceedings - IEEE International Conference on Data Mining, ICDM*, pp. 749–754, 2010, doi: 10.1109/ICDM.2010.42.

[9] E. Chui, C. K., Kao, B., & Hung, "Mining frequent itemsets from uncertain data," *Advances in Knowledge Discovery and Data Mining*, vol. 44, no. 26, pp. 47–58, 2007.

[10] D. Cheung, J. Han, and V. Ng, "A fast distributed algorithm for mining association rules," *Parallel and Distributed Information Systems, 1996., Fourth International Conference on*, vol. 56, pp. 31–42, 1996, [Online]. Available: http://ieeexplore.ieee.org/xpls/abs_all.jsp?arnumber=568665

[11] D. W. Cheung and Y. Xiao, "Effect of Data Distribution in Parallel Mining of Associations," *Data Min Knowl Discov*, vol. 3, no. 3, pp. 291–314, 1999, doi: 10.1023/A:1009836926181.

[12] D. A. Chiang and N. P. Lin, "Correlation of fuzzy sets," *Fuzzy Sets Syst*, 1999, doi: 10.1016/S0165-0114(97)00127-9.

[13] D. Dubois, L. Foulloy, G. Mauris, and H. Prade, "Probability-Possibility Transformations, Triangular Fuzzy Sets, and Probabilistic Inequalities," *Reliable Computing*, vol. 10, no. 4, pp. 273–297, Aug. 2004, doi: 10.1023/B:REOM.0000032115.22510.b5.

[14] W. Feller, "An introduction to probability theory and its applications. Vol. I," 1968.

[15] B. Goethals, "Frequent itemset mining implementations repository." Accessed: Jan. 24, 2018. [Online]. Available: http://fimi.ua.ac.be/

[16] T.-P. Hong, C.-S. Kuo, and S.-C. Chi, "Mining association rules from quantitative data☆," *Intelligent Data Analysis*, vol. 3, no. 5, pp. 363–376, Sep. 1999, doi: 10.3233/IDA-1999-3504.

[17] J. Han and M. Kamber, *Data Mining: Concepts and Techniques*, vol. 12. 2011. doi: 10.1007/978-3-642-19721-5.

[18] J. Han, J. Pei, and Y. Yin, "Mining frequent patterns without candidate generation," *Proceedings of the 2000 ACM SIGMOD international conference on Management of data - SIGMOD '00*, pp. 1–12, 2000, doi: 10.1145/342009.335372.

[19] Y. A. Kalaz and R. Raman, "Frequent itemset mining on correlated probabilistic databases," in *Lecture Notes in Computer Science (including subseries Lecture Notes in Artificial Intelligence and Lecture Notes in Bioinformatics)*, 2018. doi: 10.1007/978-3-319-98812-2_6.

[20] N. P. Lin and H.-E. Chueh, "Fuzzy Correlation Rules Mining,"

[21] C. K. S. Leung, M. A. F. Mateo, and D. A. Brajczuk, "A tree-based approach for frequent pattern mining from uncertain data," *Lecture Notes in Computer Science (including subseries Lecture Notes in Artificial Intelligence and Lecture Notes in Bioinformatics)*, vol. 5012 LNAI, pp. 653–661, 2008, doi: 10.1007/978-3-540-68125-0_61.

[22] S. T. Liu and C. Kao, "Fuzzy measures for correlation coefficient of fuzzy numbers," *Fuzzy Sets Syst*, 2002, doi: 10.1016/S0165-0114(01)00199-3.

[23] T. Gerstenkorn and J. Mańko, "Correlation of intuitionistic fuzzy sets," *Fuzzy Sets Syst*, vol. 44, no. 1, pp. 39–43, Nov. 1991, doi: 10.1016/0165-0114(91)90031-K.

[24] H. S. ALSAGRI and S. S. SOHAIL, "FRACTAL-INSPIRED SENTIMENT ANALYSIS: EVALUATION OF LARGE LANGUAGE MODELS AND DEEP LEARNING METHODS," *Fractals*, Sep. 2024, doi: 10.1142/S0218348X24400565.

[25] C.-H. Weng and Y.-L. Chen, "Mining fuzzy association rules from uncertain data," *Knowl Inf Syst*, vol. 23, no. 2, pp. 129–152, May 2010, doi: 10.1007/s10115-009-0223-1.

[26] S. Wazir, T. Ahmad, and M. M. Sufyan Beg, "Frequent Itemset Mining for a Combination of Certain and Uncertain Databases," in *6th World Conference on Soft Computing (WConSC2016) Berkeley, California, USA.*, 2018, pp. 25–39. doi: 10.1007/978-3-319-75408-6_3.

[27] S. Wazir, M. M. Sufyan Beg, and T. Ahmad, "Frequent Itemset Mining on Uncertain Database Using OWA Operator," 2019, pp. 745–755. doi: 10.1007/978-981-13-1217-5_75.

[28] R. R. Yager, "Quantifiers in the formulation of multiple objective decision functions," *Inf Sci (N Y)*, vol. 31, no. 2, pp. 107–139, Nov. 1983, doi: 10.1016/0020-0255(83)90029-4.

[29] R. R. Yager, "On a general class of fuzzy connectives," *Fuzzy Sets Syst*, vol. 4, no. 3, pp. 235–242, Nov. 1980, doi: 10.1016/0165-0114(80)90013-5.

[30] Y. Tong, L. Chen, Y. Cheng, and P. S. Yu, "Mining frequent itemsets over uncertain databases," *Vldb*, vol. 5, no. 11, pp. 1650–1661, 2012, doi: 10.14778/2350229.2350277.

[31] M. J. Zaki, "Scalable algorithms for association mining," *IEEE Trans Knowl Data Eng*, vol. 12, no. 3, pp. 372–390, 2000, doi: 10.1109/69.846291.

[32] Prof. Fournier-Viger., "SPMF: A Java Open-Source Data Mining Library." Accessed: Jan. 25, 2018. [Online]. Available: http://www.philippe-fournier-viger.com/spmf/index.php?link=datasets.php

[33] L. A. Zadeh, "Fuzzy sets as a basis for a theory of possibility," *Fuzzy Sets Syst*, vol. 1, no. 1, pp. 3–28, Jan. 1978, doi: 10.1016/0165-0114(78)90029-5.

[34] L. A. Zadeh, "Fuzzy sets as a basis for a theory of possibility," *Fuzzy Sets Syst*, vol. 100, pp. 9–34, Jan. 1999, doi: 10.1016/S0165-0114(99)80004-9.

[35] L. A. Zadeh, "Fuzzy probabilities," *Inf Process Manag*, vol. 20, no. 3, pp. 363–372, Jan. 1984, doi: 10.1016/0306-4573(84)90067-0.

[36] L. A. Zadeh, "Fuzzy sets," *Information and Control*, vol. 8, no. 3, pp. 338–353, Jun. 1965, doi: 10.1016/S0019-9958(65)90241-X.

[37] J. C.-W. Lin, W. Gan, P. Fournier-Viger, T.-P. Hong, and V. S. Tseng, "Weighted frequent itemset mining over uncertain databases," *Applied Intelligence*, vol. 44, no. 1, pp. 232–250, Jan. 2016, doi: 10.1007/s10489-015-0703-9.

[38] S. Wazir, M. M. Sufyan Beg, and T. Ahmad, "Weighted Frequent Itemset Mining Using OWA on Uncertain Transactional Database," 2020, pp. 183–193. doi: 10.1007/978-981-15-0132-6_12.

[39] A. M. T. N. and S. S. S. Muzaffar, "Neutrosophy logic and its classification: an overview," in *Neutrosophic Sets and Systems*, vol. 35, 2020, pp. 239–251.

[40] K. Mishra, I. Kandasamy, V. Kandasamy W. B., and F. Smarandache, "A Novel Framework Using Neutrosophy for Integrated Speech and Text Sentiment Analysis," *Symmetry (Basel)*, vol. 12, no. 10, p. 1715, Oct. 2020, doi: 10.3390/sym12101715.

Received: July 20, 2024. Accepted: Oct 18, 2024

Neutrosophic Sets and Systems (NSS) is an academic journal, published quarterly online and on paper, that has been created for publications of advanced studies in neutrosophy, neutrosophic set, neutrosophic logic, neutrosophic probability, neutrosophic statistics etc. and their applications in any field.

All submitted papers should be professional, in good English, containing a brief review of a problem and obtained results.

It is an open access journal distributed under the Creative Commons Attribution License that permits unrestricted use, distribution, and reproduction in any medium, provided the original work is properly cited.

ISSN (print): 2331-6055, ISSN (online): 2331-608X
Impact Factor: 1.739

NSS has been accepted by SCOPUS. Starting with Vol. 19, 2018, all NSS articles are indexed in Scopus.

NSS is also indexed by Google Scholar, Google Plus, Google Books, EBSCO, Cengage Thompson Gale (USA), Cengage Learning, ProQuest, Amazon Kindle, DOAJ (Sweden), University Grants Commission (UGC) - India, International Society for Research Activity (ISRA), Scientific Index Services (SIS), Academic Research Index (ResearchBib), Index Copernicus (European Union),CNKI (Tongfang Knowledge Network Technology Co., Beijing, China), etc.

Google Dictionary has translated the neologisms "neutrosophy" (1) and "neutrosophic" (2), coined in 1995 for the first time, into about 100 languages.

FOLDOC Dictionary of Computing (1, 2), Webster Dictionary (1, 2), Wordnik (1), Dictionary.com, The Free Dictionary (1),Wiktionary (2), YourDictionary (1, 2), OneLook Dictionary (1, 2), Dictionary / Thesaurus (1), Online Medical Dictionary (1, 2), and Encyclopedia (1, 2) have included these scientific neologisms.

DOI numbers are assigned to all published articles.

Registered by the Library of Congress, Washington DC, United States, https://lccn.loc.gov/2013203857.

Recently, NSS was also approved for Emerging Sources Citation Index (ESCI) available on the Web of Science platform, starting with Vol. 15, 2017.

Editors-in-Chief:

Prof. Dr. Florentin Smarandache, Postdoc, Department of Mathematics, University of New Mexico, Gallup, NM 87301, USA, Email: smarand@unm.edu.
Dr. Mohamed Abdel-Basset, Faculty of Computers and Informatics, Zagazig University, Egypt, Email: mohamed.abdelbasset@fci.zu.edu.eg.
Dr. Said Broumi, Laboratory of Information Processing, Faculty of Science Ben M'Sik, University of Hassan II, Casablanca, Morocco, Email: s.broumi@flbenmsik.ma.

23316055

$39.95